TECHNICAL REPORT

OF THE

ADVISORY COMMITTEE FOR AERONAUTICS

FOR 1917-18

VOL. 2
AIRSCREWS AND
FULL-SCALE WORK

THE UNIVERSITY
OF ILLINOIS
LIBRARY

629.13
G79t
1917-18
v.2

ENGINEERING
LIBRARY

REMOTE STORAGE

AERONAUTICS.

LIBRARY
UNIVERSITY OF ILLINOIS
URBANA

TECHNICAL REPORT

OF THE

ADVISORY COMMITTEE FOR AERONAUTICS

FOR THE YEAR 1917-18.

(With APPENDICES.)

VOL. II.

Airscrews and Full Scale Work on Aeroplanes.

LONDON:
PUBLISHED BY HIS MAJESTY'S STATIONERY OFFICE.

To be purchased through any Bookseller or directly from
H.M. STATIONERY OFFICE at the following addresses:
IMPERIAL HOUSE, KINGSWAY, LONDON, W.C. 2,
28, ABINGDON STREET, LONDON, S.W. 1;
37, PETER STREET, MANCHESTER;
1, ST ANDREW'S CRESCENT, CARDIFF;
23, FORTH STREET, EDINBURGH;
or from E. PONSONBY, LTD., 116, GRAFTON STREET, DUBLIN.

1921.

Price 25*s.* 0*d. Net.*

LIBRARY
UNIVERSITY OF ILLINOIS
URBANA

629.13
G79t
1917/18
v.2
REMOTE STORAGE

CONTENTS.

LIBRARY
UNIVERSITY OF ILLINOIS
URBANA

VOL. I.

General questions, Airships and model Aeroplane research.

(Experiments on Models, etc.)

Page

Members of the Committee ... ... xiv.

Report of the Committee for the year 1917–18 1

APPENDICES TO THE REPORT.

General Questions in Aerodynamics :—

On the suggested analogy between the conduction of heat and momentum during the turbulent motion of a fluid.—By Lord Rayleigh, O.M., F.R.S., with Appendix by Dr. T. E. Stanton, F.R.S. 15

Vortex Motion. (i) Preliminary report upon an experimental method of investigating by the aid of kinematograph photography, the history of eddying flow past a model immersed in water.—By J. L. Nayler, B.A., and R. A. Frazer, B.A., B.Sc.... 18

Observations and speculations on the nature of turbulent motion.—By Major G. I. Taylor, R.F.C. Presented by Sir Napier Shaw, F.R.S. 26

Wind Channels and Methods of Test :—

Experiments on models of a " Duplex " Wind Channel :—

(i) Note on a possible method of increasing the size of wind channels beyond their present limits —By T. E. Stanton, D.Sc., F.R.S., and J. H. Hyde, A.M.Inst.C.E.,A.M.I.M.E. 33

(ii) Experiments on a model of the proposed 14′ × 7′ wind channel, with an investigation into the steadiness of the velocity and direction of the airflow compared with the corresponding effects in an existing 7-foot channel.—By J. H. Hyde, A.M.Inst.C.E.... 37

Note on the form and resistance of the spindle used by the N.P.L. for standard tests of 18″ × 3″ aerofoils.—By H. B. Irving, B.Sc., and Miss C. N. Jones 51

Description of apparatus for measurement in a wind tunnel of the performance of an airscrew or the windage torque of a rotary engine.—By A. Fage, A.R.C.Sc., H. E. Collins and T. H. Fewster 54

Experiments on Airship Models :—

Experiments on a model of the German rigid airship L.33.—By J. R. Pannell, A.M.I.M.E., and R. Jones, M.A.... 57

The resistance of certain stream-line shaped bodies.—By J. R. Pannell, A.M.I.M.E., and N. R. Campbell, Sc.D. 66

Experiments on models of Airship Sheds, and Screens :—

A study of the flow of air in the neighbourhood of an airship shed and screens, and the forces and moments brought into play.—By R. Jones, M.A., and H. Levy, M.A., B.Sc. 76

The variation in the wind above an airship shed, due to the presence of the shed.—By F. G. Woodford and G. N. Pell, B.Sc. 86

(B3828B—rB1675) Wt. 18932—555. 2375. 1/21. **Gp. 32.**

542680

Experiments on model Wind Screens :— Page

Experiments on the most efficient form and distribution of wind screens for Bessoneau hangars.—By J. L. Nayler, B.A., and F. G. Woodford 90

Ring screens for aeroplanes.—By F. G. Woodford, and G. N. Pell, B.Sc. 96

The airflow behind a screen for protecting an aeroplane in the open.—Presented by the Superintendent, Royal Aircraft Factory 102

Experiments on models of Kite Balloons :—

Model tests on bodies proposed for use as kite balloons.—By L. F. G. Simmons, B.A., A.R.C.Sc., and R. A. Frazer, B.A., B.Sc. 105

Experiments on models of Aeroplane Wings :—

I. Tests on new Wing Sections :—

(i) Tests on aerofoils, R.A.F.18, 19, 20, and a Sopwith section.—By J. L. Nayler, B.A., and F. G. Woodford 132

(ii) Tests on two aerofoils for the British and Colonial Aeroplane Co., Ltd.—By C. H. Powell, B.Sc. ... 145

(iii) Standard tests of two aerofoils of Portholme and Albatros sections, and a comparison of these with R.A.F.15 sections.—By H. B. Irving, B.Sc., and Miss C. N. Jones 149

(iv) Tests on a highly cambered aerofoil.—By W. L. Cowley, A.R.C.Sc., and H. Levy, M.A., B.Sc. ... 159

II. Special Tests on Aerofoil Sections :—

(i) Experiments with two aerofoils of high aspect ratio.—By A. Fage, A.R.C.Sc., and J. D. Coales, D.Sc. ... 162

(ii) Forces and moments on R.A.F.14 for negative angles of attack.—By W. L. Cowley, A.R.C.Sc., and H. Levy, M.A., B.Sc. 172

(iii) The effect of grooves down the face of an aerofoil.—By C. H. Powell, B.Sc. 174

(iv) The effect of rounding the wing tips of an aerofoil having a high value of maximum lift coefficient.—By H. B. Irving, B.Sc., and C. H. Powell, B.Sc. ... 177

(v) Forces and moments on a wing caused by cross winds.—By C. H. Powell, B.Sc. 180

III. Tests on Biplanes and Triplanes :—

(i) Biplane effect on R.A.F.15 wing section.—By L. W. Bryant, B.Sc., A.R.C.Sc., and Miss C. N. Jones ... 184

(ii) On the effect of cutting a hole in the top plane of a biplane.—By C. H. Powell, B.Sc. 188

(iii) Triplane investigation with R.A.F.15 section.—By W. L. Cowley, A.R.C.Sc., and H. Levy, M.A., B.Sc. 192

IV. Pressure Distribution Measurements on Biplanes :—

(i) The distribution of pressure on the upper and lower wings of a biplane.—By H. B. Irving, B.Sc., C. H. Powell, B.Sc., and Miss C. N. Jones... 198

(ii) Pressure distribution on model F.E.9 wings.—Presented by the Superintendent, Royal Aircraft Factory 218

Page

Experiments on complete models of Aeroplanes :—

Forces, moments and interferences on wings and body of a 1/12 scale model of B.E.2E with R.A.F.15 wing section.—By C. G. D. Sandison, B.Sc., and S. B. Gates, B.A. Presented by the Superintendent, Royal Aircraft Establishment... ... 229

Tests on a complete model of R.E.8.—By E. F. Relf, A.R.C.Sc., and T. Lavender 233

Tests on a model of the Grahame-White bombing machine, G.W.E.4.—By E. F. Relf, A.R.C.Sc. 241

Experiments on model Aeroplane Bodies :—

Measurements of the drag of the bodies of a model fighter and bomber machine.—By A. Fage, A.R.C.Sc., and H. E. Collins... 248

Air resistance of a model aeroplane fuselage.—By C. H. Powell, B.Sc. 252

Model Experiments on Fins and Rudders :—

Model experiments on the fin effect of balanced and unbalanced rudders when hinged freely.—Presented by the Superintendent, Royal Aircraft Factory 254

Experiments on model Struts and Aeroplane Parts :—

An investigation to determine the best shape of fairing for a circular cylinder. Part 2.—By L. F. G. Simmons, B.A., A.R.C.Sc., and R. A. Frazer, B.A., B.Sc. 255

Tests on struts suitable for the fairing of duplicate cables.—By R. A. Frazer, B.A., B.Sc., and L. F. G. Simmons, B.A., A.R.C.Sc. 263

The resistance of struts.—By C. H. Powell, B.Sc. 269

Tests on the drag of a model bomb rack fitted to R.E.8 machine.—By E. F. Relf, A.R.C.Sc., and R. Jones, M.A. 276

VOL. II.

(Airscrews and Full Scale Work on Aeroplanes).

Airscrews :—

I. Aerofoil sections for airscrew design :—

(i) Aerofoils for airscrew design.—By W. L. Cowley, A.R.C.Sc., and H. Levy, M.A., B.Sc. 277

II. Investigations relating to the airflow :—

(i) An investigation into the nature of the flow in the neighbourhood of an airscrew.—By J. R. Pannell, A.M.I.M.E., and R. Jones, M.A. 296

(ii) Exploration of the airspeed in the airscrew slipstream of a tractor machine.—Presented by the Superintendent, Royal Aircraft Factory 327

(iii) Experiments on the rotation of a propeller slipstream in a pusher aeroplane.—Presented by the Superintendent, Royal Aircraft Factory 334

(iv) Exploration of the slipstream velocity in a pusher machine.—By D. H. Pinsent. Presented by the Director-General of Aircraft Production 338

Airscrews—*cont.* Page

III. Model experiments on airscrews and aeroplane bodies :—

(i) An investigation of the mutual interference of an airscrew and body of the "Tractor" type of aeroplane.—By A. Fage, A.R.C.Sc., D.I.C., and H. E. Collins 340

(ii) An investigation of the mutual interference of the airscrew, body and wings of the tractor aeroplane, B.E.2E.—By A. Fage, A.R.C.Sc., and H. E. Collins 349

(iii) A preliminary investigation of the mutual interference of an airscrew and a tractor body, as affected by the fairing of the nose of the body.—By A. Fage, A.R.C.Sc., and H. E. Collins 363

(iv) Windage experiments with a model of the rotary engine, B.R.1.—By A. Fage, A.R.C.Sc., and H. E. Collins 376

IV. Airscrew efficiency and engine gearing :—

Dependence of the efficiency of an airscrew on the speed of rotation and the diameter, with a direct reference to the question of engine gearing.—By A. Fage, A.R.C.Sc., and H. E. Collins 388

V. Tandem airscrews :—

(i) The effect of the inflowing velocity of the air on the efficiency of an airscrew, with a special reference to the case of tandem airscrews of large machines.—By A. Fage, A.R.C.Sc., D.I.C. 400

(ii) Some experiments with tandem combinations of airscrews.—By A. Fage, A.R.C.Sc., and H. E. Collins 409

(iii) An analysis of the energy account of an airscrew, with an application to the case of the tandem airscrew. (With Appendix.)—By A. Fage, A.R.C.Sc., D.I.C. 423

VI. Lateral force on an airscrew :—

Forces on a propeller due to sideslip.—By R. G. Harris. Presented by the Superintendent, Royal Aircraft Factory 430

VII. Stresses in airscrews and airscrew shafts :—

(i) Some notes on the calculation of the working stresses of an airscrew.—By A. Fage, A.R.C.Sc., and H. E. Collins 440

(ii) The whirling and transverse vibrations of a rotating airscrew and its shaft.—By A. Fage, A.R.C.Sc. ... 458

(iii) On the shape of propeller blades.—By A. A. Griffith, M.Eng., and B. Hague, B.Sc. Presented by the Director-General of Aircraft Production 471

(iv) Preliminary report on the twisting of propeller blades. —By A. A. Griffith, M.Eng., and B. Hague, B.Sc. Presented by the Superintendent, Royal Aircraft Establishment 484

Airscrews—*cont.* Page

(v) Second report on the twisting of propeller blades. Supplementary to R. & M. 454.—By A. A. Griffith, M.Eng., and B. Hague, B.Sc. Submitted by the Superintendent, Royal Aircraft Factory 506

VIII. Variable pitch airscrews :—

(i) The variable pitch propeller. Experiments conducted at the Royal Aircraft Factory. Presented by the Superintendent, Royal Aircraft Factory ... 515

(ii) The construction of the R.A.E. experimental variable pitch airscrew.—Presented by the Controller of the Technical Department, Aircraft Production ... 518

IX. Helicopters :—

Some experiments on helicopters.—By A. Fage, A.R.C.Sc., and H. E. Collins 520

X. Scale effect in airscrew models :—

The "scale-speed" effect on a model airscrew of small diameter.—By A. Fage, A.R.C.Sc., and H. E. Collins... 530

Report of Scale Effect Sub-Committee :—

Report of the Scale Effect Sub-Committee on the relation between model tests and the full scale performance of aeroplanes ... 535

Investigations relating to Aeroplane Design :—

Prediction of the performance and longitudinal stability of an aeroplane, including the estimation of the effect of small changes in the design.—By H. Glauert and S. B. Gates. Presented by the Superintendent, Royal Aircraft Factory 576

Notes on the prediction and analysis of aeroplane performance. —By L. Bairstow, C.B.E., F.R.S., and Lieut. J. D. Coales, D.Sc. Communicated by the Technical Department, Department of Aircraft Production 592

The design of aeroplanes for use at great heights.—Presented by the Superintendent, Royal Aircraft Factory 621

Full Scale Work on Aeroplanes :—

I. Measurement of accelerations in flight :—

(i) Preliminary report on measurements of accelerations on aeroplanes in flight.—By G. F. C. Searle, D.Sc., F.R.S., and F. A. Lindemann, Ph.D. Presented by the Superintendent, Royal Aircraft Factory... 629

II. Investigations relating to the longitudinal motion of an aeroplane :—

(i) Investigation of the downwash behind a biplane.—By C. G. D. Sandison, H. Glauert, and J. H. Jones. Presented by the Superintendent, Royal Aircraft Factory... 636

(ii) The longitudinal control of an aeroplane.—By H. Glauert, of the Royal Aircraft Establishment. Presented by the Director-General of Aircraft Production 642

(iii) Full scale experiments with different shapes of tailplane.—By H. Glauert. Presented by the Superintendent, Royal Aircraft Factory 653

Full Scale Work on Aeroplanes—*cont.* Page

(iv) The full scale determination of the pitching moment of a biplane.—By S. B. Gates. Presented by the Superintendent, Royal Aircraft Factory 657

(v) Full scale experiments with elevators of different sizes.—By H. Glauert. Presented by the Superintendent, Royal Aircraft Factory 689

III. Investigations relating to the lateral motion of an aeroplane :

(i) Lateral control with different types of wing flaps.—By H. Glauert. Presented by the Superintendent, Royal Aircraft Factory 695

(ii) Lateral control of various aeroplanes.—Presented by the Superintendent, Royal Aircraft Establishment 702

IV. Other investigations :—

(i) Full scale stability experiments with R.A.F.14 wing section.—Presented by the Superintendent, Royal Aircraft Factory 706

(ii) Stresses in an aeroplane when diving steeply.—Presented by the Superintendent, Royal Aircraft Factory 710

(iii) The terminal velocity of S.E.5.—Presented by the Superintendent, Royal Aircraft Factory 712

(iv) The effect of a wind gradient on the rate of climb of an aeroplane.—Presented by the Superintendent, Royal Aircraft Factory 714

(v) The experimental and mathematical investigation of spinning.—By F. A. Lindemann, H. Glauert, and R. G. Harris. Presented by the Superintendent, Royal Aircraft Factory 716

Investigations relating to Aeroplane Design :—

The object of tabulating engine data.—By Lieut.-Col. Mervyn O'Gorman, C.B. 730

On the dissipation of heat from the surface on an air-cooled engine when running and when at rest.—By T. E. Stanton, D.Sc., F.R.S., Miss Dorothy Marshall, B.Sc., and E. Griffiths, D.Sc. 734

The variation of engine power with height.—By D. H. Pinsent and H. A. Renwick. Presented by the Superintendent, Royal Aircraft Establishment 748

VOL. III.

(Strength of Construction, etc.)

Strength of Construction :—

I. The stresses in loaded aeroplane structures :—

(i) Critical loading of struts and structures. Part I.—By W. L. Cowley, A.R.C.Sc., and H. Levy, M.A., B.Sc. 763

(ii) Critical loading of struts and structures. Part II.—By W. L. Cowley, A.R.C.Sc., and H. Levy, M.A., B.Sc. 785

Strength of Construction—*cont.* Page

(iii) Critical loading of similar structures.—By W. L. Cowley, A.R.C.Sc., and H. Levy, M.A., B.Sc. ... 796

(iv) The stresses in a loaded rigid structure, with special reference to redundancies.—By W. L. Cowley, A.R.C.Sc., and H. Levy, M.A., B.Sc. 803

(v) Report on the strength of the wings of captured German aeroplanes.—By H. B. Irving, B.Sc. ... 818

(vi) Strength test of main plane ribs. Method employed at the Royal Aircraft Establishment.—By Wm. D. Douglas, A.R.C.Sc.I. Presented by the Director-General of Aircraft Production 822

(vii) The lateral buckling of wing spars.—By J. Case and A. A. Griffith. Presented by the Superintendent, Royal Aircraft Factory 828

(viii) Short wooden struts.—By W. H. Barling, A.R.C.Sc., and H. A. Webb, M.A. Presented by the Superintendent, Royal Aircraft Factory 838

(ix) Tapered struts.—By W. H. Barling, A.R.C.Sc., and H. A. Webb, M.A. Presented by the Superintendent, Royal Aircraft Factory 852

(x) The vibration of spars.—By Lieut. A. H. Stuart, R.N.V.R. Communicated by the Director of Air Services 891

(xi) On the torsion of a fuselage.—By H. M. Garner and Arthur Berry. Communicated by the Controller of the Technical Department, Air Board 894

(xii) The determination of the torsional stiffness and strength of cylindrical bars of any shape. By A. A. Griffith, M.Eng. Presented by the Superintendent, Royal Aircraft Factory 910

II. The use of soap films for stress computation :—

(i) The use of soap films in solving torsion problems.—By G. I. Taylor, M.A., and A. A. Griffith,, M.Eng. Presented by the Superintendent, Royal Aircraft Factory 920

(ii) The application of soap films to the determination of the torsion and flexure of hollow shafts.—By A. A. Griffith, M.Eng. and G. I. Taylor, M.A.—Presented by the Superintendent, Royal Aircraft Factory ... 938

(iii) The problem of flexure and its solution by the soap film method.—By A. A. Griffith, M.Eng., and G. I. Taylor, M.A. Presented by the Superintendent, Royal Aircraft Factory 950

III. Experiments on timber :—

(i) Report on tests made on various Australian timbers to determine their suitability for use in the construction of aeroplanes.—By G. A. Hankins (National Physical Laboratory) 970

(ii) The influence of time on the breaking load and elasticity of spruce members of aeroplanes.—By W. H. Barling, A.R.C.Sc., and J. D. H. Prichard, B.Sc. Presented by the Superintendent, Royal Aircraft Factory 974

Experiments on timber—*cont.* Page

(iii) A preliminary investigation of certain elastic properties of wood.—By A. A. Griffith, M.Eng., and C. Wigley, B.A. Presented by the Superintendent, Royal Aircraft Factory 986

Seaplane Floats and Flying Boat Hulls :—

Experiments with models of seaplane floats, 12th Series.—By G. S. Baker, O.B.E., late R.C.N.C., M.Inst.N.A., and E. M. Keary 1001

Experiments with models of seaplane floats, 13th Series.—By G. S. Baker, O.B.E., late R.C.N.C., M.Inst.N.A., and E. M. Keary 1011

Some notes on floats for seaplanes of the single float type, 14th Series.—By G. S. Baker, O.B.E., late R.C.N.C., M.Inst.N.A. ... 1015

Experiments with models of seaplane floats, 11th Series. Part III. The wave formations produced by a seaplane of the single float type.—By G. H. Bottomley, A.M.Inst.N.A. 1032

Aeroplane Fabrics :—

Report on the action of sunlight on aeroplane fabric ; its nature and prevention.—By F. W. Aston, D.Sc. Presented by the Superintendent, Royal Aircraft Factory... 1038

Report on some strength tests of aeroplane fabric exposed to weather and their relation to sunlight intensity.—By F. W. Aston, D.Sc. Presented by the Superintendent, Royal Aircraft Factory 1048

Report on the suitability of cotton fabrics for covering aeroplane wings.—By A J. Turner, B.A., B.Sc. Presented by the Superintendent, Royal Aircraft Factory 1051

Report on the comparative weathering qualities of British and German doped fabric.—Presented by the Director-General of Aircraft Production... 1065

Aluminium Alloy Sheet for Aeroplane Wings :—

Memorandum on the use of aluminium alloy sheet in place of fabric for aeroplane wings, &c.—By F. W. Lanchester, M.Inst.C.E. 1068

Dopes and Varnishes :—

Report on protective varnishes for use on aeroplanes in hot climates. Part II. Experiments in sunlight. — By the Chemical Department, Royal Aircraft Factory. Presented by the Superintendent 1070

Note on a possible economy of solvent in doping aeroplane wings. —By Guy Barr, B.A., D.Sc., and Edith G. Wilson, B.A., Sc.B. 1077

Permeability of Fabrics and Dopes to Hydrogen :—

Some further notes on the hydrogen permeameter.—By Dr. G. A. Shakespear 1080

Further applications of the katharometer.—By Dr. G. A. Shakespear ; with an investigation of some sources of error in the testing of fabrics.—By H. A. Daynes... 1087

Permeability of Fabrics and Dopes to Hydrogen—*cont.*

Page

Preliminary report on the variation of the hydrogen permeability of rubber membranes with alteration in temperature.—Communication from the North British Rubber Co., Ltd., of an investigation carried out in their Research Department by B. D. Porritt, M.Sc., F.I.C., and W. S. Allen, F.I.C. 1100

On the diffusion of hydrogen along the textile of balloon fabrics, with special reference to the effect of lateral leakage at seams.—By G. A. Shakespear, D.Sc., and H. A. Daynes, M.Sc.... ... 1103

Some notes on balloon seams.—By Dr. G. A. Shakespear ... 1113

Results of some experiments on the permeability of clear Delta dope.—By Dr. G. A. Shakespear 1116

Meteorology :—

Records of temperature and altitude.—By Flight-Commander Brian C. Clayton, R.N. Comments by Sir Napier Shaw, F.R.S. 1117

Variation of temperature and humidity with altitude ; notes on the wind and other meteorological observations made at Aboukir. —Received from Major W. R. G. Atkins, O. i/c. Experiments, X.A.D., Egypt 1125

Table of temperature, pressure and density at different levels up to 20 kilometres.—By W. H. Dines, F.R.S. Communicated by Sir Napier Shaw, F.R.S. 1134

A report on high angle practice to determine the wind at various heights for comparison with simultaneous determinations by pilot balloon ascents : carried out at firing ground of H.M.S. "Excellent," 25th and 26th April, 1917.—Presented by Sir Napier Shaw, F.R.S. 1135

Variation of wind speed near the ground.—Communicated by the Director, Naval Meteorological Service, Hydrographic Department, Admiralty 1137

The variation of static pressure in a natural wind, as the velocity changes.—By J. R. Pannell, A.M.I.M.E.. 1143

Thunderstorms in the British Islands during January, February, and March, 1917.—Report by Captain C. J. P. Cave, R.E. Presented by Sir Napier Shaw, F.R.S. 1150

Special Matters :—

Economic Flight :—

Flying as affected by the Wind :—

(i) Effect of wind on the time of flight from one place to another and back again.—By Horace Darwin, F.R.S., and C. C. Mason 1154

(ii) Flying as affected by the wind.—By F. W. Lanchester, M.Inst.C.E. 1157

(iii) Flying as affected by the wind.—Communicated by Sir George Greenhill 1159

Economic flight of an aeroplane in a wind.—By W. L. Cowley, A.R.C.Sc., and H. Levy, M.A., B.Sc. 1160

Flying as affected by the Wind—*cont.* Page

On the steady flight of an aeroplane when the gradual loss of weight owing to the consumption of petrol is taken into account: with special reference to the minimum consumption of petrol.—By Arthur Berry, Fellow of King's College, Cambridge, and University Lecturer in Mathematics. With a note by H. Glauert.—Presented by the Superintendent, Royal Aircraft Factory 1163

High altitude flying.—By F. W. Lanchester, M.Inst.C.E. ... 1182

Flight by Flapping Wings :—

Flight by flapping wings.—By A. Mallock, F.R.S.... 1185

Empson Suction Tube :—

Tests on an Empson suction tube and wind gauge.—By C. H. Powell, B.Sc. 1190

GENERAL INDEX 1192

INDEX TO SERIAL NUMBERS OF THE TECHNICAL REPORTS.

	Page		Page
Report No. 311	66	Report No. 367	1103
,, ,, 324	576	,, ,, 368	894
,, ,, 330	177	,, ,, 370	105
,, ,, 331	520	,, ,, 371	296
,, ,, 332	18	,, ,, 373	785
,, ,, 333	920	,, ,, 374	535
,, ,, 334	910	,, ,, 375	149
,, ,, 338	76	,, ,, 376	629
,, ,, 343	852	,, ,, 377	145
,, ,, 344	340	,, ,, 378	276
,, ,, 345	26	,, ,, 379	714
,, ,, 346	1051	,, ,, 380	796
,, ,, 347	218	,, ,, 381	255
,, ,, 348	248	,, ,, 385	400
,, ,, 350	818	,, ,, 386	891
,, ,, 351	1143	,, ,, 388	172
,, ,, 355	198	,, ,, 389	1160
,, ,, 358	1185	,, ,, 390	530
,, ,, 359	1068	,, ,, 391	254
,, ,, 361	57	,, ,, 392	938
,, ,, 362	277	,, ,, 393	349
,, ,, 363	838	,, ,, 394	180
,, ,, 364	763	,, ,, 395	950
,, ,, 365	1032	,, ,, 396	1038
,, ,, 366	184	,, ,, 399	950

INDEX TO SERIAL NUMBERS OF THE TECHNICAL REPORTS—*cont.*

	Page		Page
Report. No 400	657	Report No. 446	1065
,, ,, 401	363	,, ,, 448	376
,, ,, 402	515	,, ,, 449	159
,, ,, 403	828	,, ,, 452	471
,, ,, 405	803	,, ,, 454	484
,, ,, 408	334	,, ,, 455	506
,, ,, 409	689	,, ,, 462	748
,, ,, 410	1011	,, ,, 470	642
,, ,, 411	716	,, ,, 471	518
,, ,, 412	1001	,, ,, 474	592
,, ,, 413	695	,, ,, 490	1190
,, ,, 414	252	,, ,, 492	712
,, ,, 415	132	,, ,, 493	621
,, ,, 416	219	,, ,, 494	710
,, ,, 417	174	,, ,, 497	15
,, ,, 418	51	,, ,, 499	1135
,, ,, 419	188	,, ,, 501	1117
,, ,, 420	440	,, ,, 502	458
,, ,, 421	409	,, ,, 503	730
,, ,, 423	86	,, ,, 505	706
,, ,, 424	96	,, ,, 507	1150
,, ,, 426	636	,, ,, 509	1134
,, ,, 427	430	,, ,, 510	974
,, ,, 428	90	,, ,, 513	1100
,, ,, 429	423	,, ,, 514	1070
,, ,, 430	1048	,, ,, 515	233
,, ,, 431	102	,, ,, 516	1080
,, ,, 432	192	,, ,, 517	1113
,, ,, 433	263	,, ,, 518	1116
,, ,, 434	241	,, ,, 520	734
,, ,, 435	1087	,, ,, 521	1154
,, ,, 436	1125	,, ,, 522	33
,, ,, 437	1015	,, ,, 527	1163
,, ,, 438	327	,, ,, 528	986
,, ,, 439	162	,, ,, 531	1137
,, ,, 440	229	,, ,, 532	653
,, ,, 441	702	,, ,, 534	1182
,, ,, 442	388	,, ,, 539	1077
,, ,, 443	822	,, ,, 563	54
,, ,, 444	337		

MEMBERS OF THE COMMITTEE.

The Right Honourable Lord Rayleigh, O.M., F.R.S. (President).
Sir Richard Glazebrook, C.B., F.R.S. (Chairman).
Major-General W. S. Brancker.
Sir Dugald Clerk, K.B.E., F.R.S.
Mr. Horace Darwin, F.R.S.
Sir E. H. Tennyson d'Eyncourt, K.C.B.
Sir Henry Fowler, K.B.E.
Mr. E. C. Given.
Sir G. Greenhill, F.R.S.
Lieut.-General Sir D. Henderson, K.C.B., D.S.O.
Major B. Hopkinson, C.M.G., F.R.S.
Mr. F. W. Lanchester, M.Inst.C.E.
Mr. H. R. A. Mallock, F.R.S.
Lieut.-Colonel Mervyn O'Gorman, C.B.
Professor J. E. Petavel, F.R.S.
Sir Napier Shaw, F.R.S.
Lieut.-Colonel J. G. Weir, C.M.G.

Secretary, Mr. F. J. Selby, M.A.

Assistant Secretary, Mr. J. L. Nayler, B.A.

National Physical Laboratory,
Teddington,
Middlesex.

AEROFOILS FOR AIRSCREW DESIGN.

By W. L. Cowley, A.R.C.Sc., and H. Levy, M.A., B.Sc.

Reports and Memoranda (New Series), No. 362. November, 1917.

Summary.—(*a*) *Introductory. (Reasons for inquiry.)*—The investigations were undertaken at the urgent request of the R.A.F., Admiralty, and others, for further information on aerofoil sections suitable for airscrew design at the largest possible value of *vl*. A series of five sets of tests was asked for, and the present report refers only to the first two sets.

(*b*) *Range of the investigation.*—The first set of aerofoils tested had a circular upper surface, a chord of 6″, and cambers of ·075, ·08, ·09, ·10, ·12, ·16 and ·20. The tests were made at a wind speed of 80 ft./sec., and the first aerofoil was tested in addition at speeds from 40 to 80 ft./sec.

The second set had its maximum ordinate at ·375 of the chord from the leading edge. The distance of each ordinate from the leading edge, which was in front of the maximum ordinate, was derived from the previous set by decreasing it in the ratio of ·375/·5, and those behind the maximum ordinate by increasing them in the ratio of ·625/·5. The same range of cambers was used. The tests were made at 70 ft./sec. (80 ft./sec. in the preceding set was found to produce too great a deflection of the aerofoil), and the aerofoils of least and greatest camber were tested over a speed range from 40 to 70 ft./sec. The lift, drag and centre of pressure coefficients were found over a range including the angles of no lift and of maximum lift.

(*c*) *Conclusions.*—The force curves of the two series of aerofoils present, in general, similar characteristics; their all-round efficiency as aerofoils was low. With increase in camber the position of zero lift moves to larger negative values, while the drag increases rapidly. As the speed (value of *vl*) is increased, the position of minimum drag moves in the negative direction (corresponding with a lower angle of incidence) with a simultaneous fall in value. This effect is most marked in the aerofoils of small camber. The variation in the lift curves with change of *vl* was not very marked.

The following series of investigations were undertaken as the result of urgent requests from the R.A.F., Admiralty and others, for tests of aerofoils suitable for use in airscrew design. Five sets, each consisting of seven aerofoils, with flat undersurface, classified according to a system shortly to be described, were selected for test, to determine forces, moments and centres of pressure, and the variations of these with increased scale. At the special request of the R.A.F., where airscrews are being developed from aerofoils of circular upper surface, the first set tested consisted of such a system of chord 6-inch and cambers ·075, ·080, ·09, ·10, ·12, ·16, ·20.

The second set, in which the position of maximum ordinate was advanced from the centre to ·375 of chord from the leading edge, was derived from the previous set by decreasing the distance of each ordinate from the leading edge in the ratio of ·375/·5 in the case where these are in front of the maximum ordinate, and extending the distance from the trailing edge for those behind in the ratio of ·625/·5 (*see* Report 72, Adv. Com. Report 1912–13). For the remaining sets these ratios were ·3/·5, ·25/·5, and ·2/·5 for the corresponding leading portions.

The present report deals with the results of experiments on the first two series. The aerofoils were constructed with a metal base plate, $\frac{1}{8}$-inch thick, forming the lower surface, 6-inch by 36-inch. At the leading and trailing edges the base plate was rounded off to a radius of $\frac{1}{16}$-inch. The upper surface was formed by plasticine worked accurately into shape by means of a metal template running on two parallel guides between which the base plate was firmly fixed in position. By this method an exceedingly smooth surface accurate to the template was rapidly obtained.

Fig. 1 indicates the position of the upper surface in relation to the base plate. The leading and trailing edges A and B of the plasticine portion were rounded off to bring them tangential to the base plate at these edges at *a* and *b*.

The experiments were conducted in the seven-foot wind channel at a speed of 80 ft./sec. for the first set, and at 70 ft./sec. for the second, as it was found that the wind forces on such a large aerofoil were so great at the higher speed that the deflections of the aerofoil became excessive.

Series A.

Circular Upper Surface.

Cambers = 0·075, 0·08, 0·09, 0·10, 0·12, 0·16, 0·20.
Aerofoil Nos. = 1 , 2 , 3 , 4 , 5 , 6 , 7 .

All the aerofoils in this set were tested at a speed of 80 ft./sec., while aerofoil No. 1 was tested in addition over a range of speeds to investigate the effect of variation in scale.

In Fig. 2 (Tables 1–5) are plotted the lift coefficients against angle of incidence.

The magnitude of the maximum lift varies moderately with camber for the smaller values of the latter, and the position of maximum lift for the larger values. In the neighbourhood of 10° no systematic variation of lift with camber can be traced, although for lower angles the changes are much more consistent, increasing very rapidly with camber at given angles of attack. The curious development of a hump over the series as the camber

is increased is very apparent, and for the highest camber a second one is produced for large negative angles, so that the lift still remains positive at $-25°$. Aerofoils Nos. 3 and 4 provide curves coinciding over a wide range. To determine whether this was due to an error in angle setting these were retested, but the previous results were repeated.

With increasing camber the minimum drag (Fig. 3) increases rapidly, accompanied by a slight decrease in angular position. In all cases the maximum L/D lies between 2° and 4°, and its magnitude between 16 and 17 except for high cambers, where it falls to 13·5.

In Fig. 7 the L/D, lift coefficients and drag coefficients are plotted against angle of incidence for the case of the aerofoil No. 7, with the highest camber.

In Fig. 5 the C.P. coefficient—the ratio of the distance of the position of centre of pressure, measured from the leading edge along the lower surface, to the size of chord—is plotted against angle of attack. In the region of 1° there appears to be very little change in the position of the centre of pressure with camber, the C.P. occupying roughly a position given by a centre of pressure coefficient = 0·55. For the thickest aerofoil, at negative angles of attack, the centre of pressure curve behaves abnormally. In Fig. 6, where the moment coefficients about the leading edge (Z, Fig. 1) are plotted, a considerable effect is apparent with change in camber, showing a consistent development over the series.

For aerofoil No. 7 the centre of pressure and moment coefficients are plotted in Fig. 8 for a range of $-30°$ to $+25°$ angle of incidence.

Scale effect.—To determine the effect of change of scale within the range afforded by the channel, aerofoil No. 1 was subjected to tests for forces and moments at speeds of 40, 50, 60, 70 and 80 ft./sec. In Fig. 9 are plotted the lift coefficients at the various speeds against angles of attack. These show the recognised increase in lift coefficient at small positive and negative angles with very little change up to the maximum. The latter appears to increase slightly with *vl*, with a corresponding increase in angular position. The position of zero lift decreases from $-2°$ to $-3°$ over the complete range of *vl*.

The drag curves (Fig. 10) seem to suggest that large increases in *vl* might still give rise to considerable further changes in the magnitude and position of the minimum. Over the range covered by the tests the minimum falls from ·0115 to ·0094, and the angle from 1·5° to 0°. For such a small range of *vl* this must be considered large. Apart from this region there appears to be very little scale effect.

In Fig. 11 the L/D curves are given. Changes due to scale appear chiefly below maximum L/D. The accuracy of the

experiment does not of course warrant any definite statement being made regarding variation in magnitude and position of the maximum value.

The C.P. curves are plotted in Fig. 12, where changes with *vl* are very marked.

At an angle of 4° no shift of C.P. occurs with *vl*. At higher angles the centre of pressure moves backward with increase of wind speed, and at lower values forward.

These changes are quite consistent with the corresponding results in R. & M. 110, for tests on R.A.F. 6a, where, however, the range of positive angle is not extended appreciably beyond the point of coincidence of the *vl* curves. In Fig. 13 the moment coefficients show a consistent variation with *vl*, except in the neighbourhood of 4° where there is very little change.

Two aerofoils similar in certain respects to two included in this set have previously been tested by other experimenters, with, however, so widely different results that it is necessary to inquire more closely into the possible causes of these discrepancies. In Fig. 14, aerofoil No. 1, series A and aile No. 7 (Eiffel Résistance de l'air et l'aviation Atlas, Plate 5) are shown for comparison. In both, the upper surface is circular, but the cambers are slightly different, being 0·075 and 0·0675 respectively.

There is of course an essential difference in the shape of the leading and trailing edges, since in Eiffel's case both these are sharply pointed. Both have flat undersurfaces. The results of the tests are shown in Fig. 15, where it appears that in the case of aerofoil No. 1, series A, the lift coefficient in the N.P.L. tests is consistently much higher over the whole range, and also the drag coefficient for angles beyond 10°. The minimum drag coefficient given by Eiffel seems exceptionally low. Since the two tests were conducted at approximately equal values of *vl* this must be due, apart from possible experimental discrepancies, to the effect of the sharpness of the leading edge. It is hoped to give further consideration to this question in a later report.

In Fig. 14 are also shown the sections of aerofoil No. 4, series A, and of an aerofoil reported on in R. & M. No. 72, 1912/13.

The cambers of these two are the same, but the leading and trailing edges of the latter are again sharper than in those used for the present series, and the portion between the maximum ordinate and the leading edge is slightly more arched. The tests in the report referred to were conducted at a *vl* of 5·84, and those of the present report at a *vl* of 40. This latter difference undoubtedly accounts for a great deal of the discrepancy between the drags, Fig. 16, but the difference in the lifts must be due to the slight variation in the form of the leading portion. It is hoped to investigate the causes of these differences by further tests.

SERIES B.

$x/c = 0{\cdot}375.$

Cambers = 0·075, 0·08, 0·09, 0·10, 0·12, 0·16, 0·20.

Aerofoil Nos. = 1 , 2 , 3 , 4 , 5 , 6 , 7 .

All the aerofoils of this series were tested at a wind speed of 70 ft. per second instead of 80 ft. per second, as in series A, for reasons already stated, with the exception of Nos. 1 and 7, which were tested for *vl* effect at speeds of 40, 50, 60 and 70 ft. per second.

The lift coefficients of the series are plotted against angle of incidence in Fig. 17. The differences due to camber are not here quite so marked as in the previous series, but the "step formation" at high cambers is still noticeable, although unlike No. 7, series A, the corresponding curve does not flatten out at large negative angles until the lift reaches a negative value. Up to 10° the variation with camber is quite systematic. Generally, however, the same remarks apply as in series A.

In Fig. 18 the drag coefficients are plotted. The curves are very similar to those of the last series with the exception of No. 7, for which the minimum drag is very much smaller in value.

The L/D curves in Fig. 19 indicate that for values below the maximum the variation with camber is easily traced. The maxima lie generally somewhat lower than for the previous set.

In Fig. 20, where centre of pressure coefficients are plotted, very little difference from the last set is indicated, with the exception that there is nothing that corresponds with the abnormal behaviour of No. 7, series A. Generally the centre of pressure is slightly further forward on these aerofoils than previously, but these differences might be partially due to the different speeds. At 1° angle of incidence the centre of pressure is approximately at the centre of the aerofoil for all cambers. The moment coefficients plotted in Fig. 21 change very consistently and regularly with camber, but not so violently as in the previous series, where the moments are much higher.

Scale effect.—For the investigation of this effect aerofoils Nos. 1 and 7 were tested at speeds of 40, 50, 60 and 70 ft. per second for forces. The lift coefficients of aerofoil No. 1 are plotted in Fig. 22, where it is clear that the maximum lift increases steadily with *vl*, without any apparent change in position. It is only within this region in the neighbourhood of the maximum that a change of *vl* has any considerable effect. The contrast with the corresponding effect in Fig. 9 of No. 1, series A, is very marked. The same applies to negative angles.

In Fig. 23 the drag coefficients in the neighbourhood of the minimum once more show a very distinct change with scale. In general shape the curves are strikingly similar to those of Fig. 10. Above the minimum an increase of *vl* evidently straightens out the curve, sweeping the minimum position further towards negative angles, accompanied by a decrease in magnitude. Although the maximum speed is only 70 ft. per second for the set, the tendency in this direction is already even more marked than in the corresponding aerofoil of the previous series. At higher positive and negative angles the scale effect appears to be comparatively small.

As shown in Fig. 24, the L/D increases steadily with speed at values below the maximum, as in the aerofoil No. 1, series A, but the variation in value of the maximum itself is much greater than previously. With increased *vl* the L/D in this region rises and then falls, an effect immediately traceable to the variation in drag in this region already referred to.

The scale effect for aerofoil No. 7, that of largest camber, is shown in Figs. 25, 26 and 27. The lift curves rise and then fall slightly below 6° with increase of speed; between 6° and 14° there is a considerable decrease. The maximum appears to vary very little.

Fig. 26 shows consistent diminution of drag with speed, the minimum falling by a fair amount, accompanied by a very slight shift towards negative angles of incidence. The rapid fall in drag with increase of speed obtained in aerofoils 1, series A and B, for small positive angles of attack is not here apparent.

In Fig. 28 is plotted the drag coefficients of R.A.F. 6a (R. & M. 110) for various angles of attack on a log *vl* base. At a value of $vl = 1{\cdot}5$—approximately the greatest value reached in that report—it is evident that considerable variation of the drag coefficient with speed exists in the neighbourhood of minimum drag, an effect very similar to that obtained in the present report for thin sections.

General remarks.—The two series of aerofoils discussed in the foregoing provide curves which in general present similar characteristics. With increase in camber the position of zero lift shifts to larger negative values, while the drag increases rapidly. It must be noticed that only in the aerofoils of low camber does the shift of the position of minimum drag with *vl* in the negative direction, with a simultaneous fall in value, take place to any considerable extent.

TABLE 1.

SERIES A, $x^*/c = 0{\cdot}5$.

AEROFOIL No. 1, CAMBER = 0·075.

Size of Plane, 6-inch by 36-inch. Speed, 80 ft./sec.

Angle. Degrees.	Drag Coefficient.	Lift Coefficient.	L/D.	C.P. Coefficient.	Moment Coefficient.
− 6	0·0316	− 0·164	− 5·20	+ 0·076	− 0·0124
− 4	0·0187	− 0·065	− 3·50	− 0·335	+ 0·0217
− 3	0·0144	− 0·015	− 1·05	− 2·39	0·0365
− 2	0·0116	+ 0·034	+ 2·91	+ 1·47	0·0500
− 1	0·0102	0·081	7·85	0·768	0·0617
0	0·0095	0·119	12·5	0·592	0·0705
+ 1	0·0101	0·149	14·6	0·504	0·0760
2	0·0117	0·185	15·6	0·454	0·0840
3	0·0134	0·218	16·2	0·419	0·0915
4	0·0155	0·256	16·4	0·390	0·100
5	0·0185	0·298	16·0	0·369	0·110
6	0·0225	0·327	14·5	0·354	0·116
8	0·0342	0·392	11·5	0·329	0·129
10	0·0505	0·452	8·94	0·312	0·141
12	0·0738	0·488	6·71	0·321	0·155
14	0·1020	0·504	4·95	—	—

* For definition of x see Fig. 1.

TABLE 2.

SERIES A, $x/c = 0{\cdot}5$.

AEROFOIL No. 1, CAMBER = 0·075.

Size of Plane, 6-inch by 36-inch. Speed, 70 ft./sec.

Angle. Degrees.	Drag Coefficient.	Lift Coefficient.	L/D.	C.P. Coefficient.	Moment Coefficient.
− 6	0·0319	− 0·169	− 5·30	+ 0·098	− 0·0166
− 4	0·0188	− 0·071	− 3·76	− 0·173	+ 0·0122
− 3	0·0148	− 0·022	− 1·47	− 1·51	0·0330
− 2	0·0120	+ 0·028	+ 2·32	+ 1·68	0·0470
− 1	0·0106	0·076	7·13	0·800	0·0604
0	0·0099	0·119	11·9	0·606	0·0720
+ 1	0·0100	0·151	15·1	0·509	0·0768
2	0·0117	0·185	15·9	0·454	0·0839
3	0·0133	0·218	16·4	0·418	0·0912
4	0·0151	0·255	16·8	0·389	0·0991
5	0·0189	0·291	15·4	0·370	0·108
6	0·0223	0·324	14·5	0·354	0·115
8	0·0337	0·390	11·5	0·326	0·127
10	0·0502	0·450	8·95	0·307	0·138
12	0·0747	0·486	6·46	0·320	0·157
14	0·1025	0·495	4·82	0·347	0·176

TABLE 3.

SERIES A, $x/c = 0{\cdot}5$.

AEROFOIL No. 1, CAMBER = 0·075.

Size of Plane, 6-inch by 36-inch. Speed, 60 ft./sec.

Angle. Degrees.	Drag Coefficient.	Lift Coefficient.	L/D.	C.P. Coefficient.	Moment Coefficient.
− 6	0·0321	− 0·172	− 5·35	+ 0·101	− 0·0176
− 4	0·0191	− 0·076	− 4·00	− 0·233	+ 0·0178
− 3	0·0151	− 0·030	− 1·96	− 1·043	0·0309
− 2	0·0127	+ 0·019	+ 1·52	+ 2·32	0·0447
− 1	0·0111	0·066	5·94	0·867	0·0572
0	0·0103	0·111	10·7	0·633	0·0702
+ 1	0·0101	0·153	15·1	0·521	0·0800
2	0·0118	0·186	15·7	0·459	0·0850
3	0·0133	0·216	16·3	0·420	0·0910
4	0·0155	0·256	16·5	0·391	0·100
5	0·0190	0·290	15·2	0·369	0·107
6	0·0227	0·323	14·2	0·351	0·113
8	0·0330	0·387	11·7	0·320	0·124
10	0·0495	0·446	9·00	0·302	0·134
12	0·0762	0·485	6·40	0·319	0·156
14	0·1005	0·460	4·58	0·360	0·170

TABLE 4.

SERIES A, $x/c = 0{\cdot}5$.

AEROFOIL No. 1, CAMBER = 0·075.

Size of Plane, 6-inch by 36-inch. Speed, 50 ft./sec.

Angle. Degrees.	Drag Coefficient.	Lift Coefficient.	L/D.	C.P. Coefficient.	Moment Coefficient.
− 6	0·0322	− 0·174	− 5·4	+ 0·113	− 0·020
− 4	0·0190	− 0·0811	− 4·25	− 0·193	+ 0·0156
− 3	0·0154	− 0·0376	− 2·44	− 0·723	0·0273
− 2	0·0130	+ 0·0095	+ 0·72	+ 4·12	0·0391
− 1	0·0117	0·0532	4·54	0·952	0·0505
0	0·0136	0·099	8·70	0·644	0·0640
+ 1	0·0109	0·149	13·7	0·525	0·0780
2	0·0114	0·187	16·4	0·458	0·0860
3	0·0129	0·217	16·8	0·414	0·0900
4	0·0156	0·251	16·1	0·389	0·0975
5	0·0186	0·284	15·3	0·366	0·104
6	0·0232	0·322	13·9	0·346	0·111
8	0·0330	0·380	11·5	0·314	0·120
10	0·0495	0·442	8·96	0·299	0·132
12	0·0765	0·480	6·26	0·315	0·153
14	0·1046	0·461	4·40	0·360	0·170

TABLE 5.

SERIES A, $x/c = 0{\cdot}5$.

AEROFOIL No. 1, CAMBER = 0·075.

Size of Plane, 6-inch by 36-inch. Speed, 40 ft./sec.

Angle. Degrees.	Drag Coefficient.	Lift Coefficient.	L/D.	C.P. Coefficient.	Moment Coefficient.
− 6	0·0321	− 0·176	− 5·47	+ 0·101	− 0·0208
− 4	0·0193	− 0·084	− 4·34	− 0·187	+ 0·0156
− 3	0·0157	− 0·043	− 2·72	− 0·610	0·0260
− 2	0·0137	+ 0·001	+ 0·04	+72·8	0·0364
− 1	0·0122	0·041	3·38	1·14	0·0472
0	0·0120	0·081	6·90	0·705	0·0575
+ 1	0·0117	0·129	11·0	0·550	0·0710
2	0·0117	0·183	15·7	0·474	0·0870
3	0·0130	0·214	16·5	0·421	0·0900
4	0·0157	0·250	15·9	0·387	0·0965
5	0·0189	0·282	14·9	0·362	0·102
6	0·0235	0·317	13·5	0·344	0·109
8	0·0340	0·380	11·2	0·312	0·118
10	0·0500	0·438	8·78	0·297	0·130
12	0·0770	0·478	6·20	0·320	0·152
14	0·1017	0·448	4·40	0·358	0·162

TABLE 6.

SERIES A, $x/c = 0{\cdot}5$.

AEROFOIL No. 2, CAMBER = 0·080.

Size of Plane, 6-inch by 36-inch. Speed, 80 ft./sec.

Angle. Degrees.	Drag Coefficient.	Lift Coefficient.	L/D.	C.P. Coefficient.	Moment Coefficient.
− 6	0·0314	− 0·145	− 4·59	+ 0·038	− 0·0055
− 4	0·0182	− 0·040	− 2·18	− 0·076	+ 0·0301
− 2	0·0117	+ 0·056	+ 4·14	+ 1·12	0·0625
− 1	0·0102	0·098	9·63	0·749	0·0733
0	0·0099	0·109	13·2	0·611	0·0790
+ 1	0·0103	0·163	15·4	0·526	0·0857
2	0·0121	0·197	16·4	0·475	0·0938
3	0·0139	0·232	16·7	0·441	0·102
4	0·0162	0·265	16·3	0·416	0·110
5	0·0192	0·300	15·5	0·395	0·118
6	0·0225	0·332	14·7	0·379	0·126
8	0·0337	0·400	11·8	0·355	0·142
10	0·0480	0·457	9·52	0·339	0·155
12	0·0695	0·505	7·24	0·330	0·167
14	0·1030	0·535	5·17	0·334	0·178

TABLE 7.

SERIES A, $x/c = 0{\cdot}5$.

AEROFOIL No. 3, CAMBER = 0·090.

Size of Plane, 6-inch by 36-inch. Speed, 80 ft./sec.

Angle. Degrees.	Drag Coefficient.	Lift Coefficient.	L/D.	C.P. Coefficient.	Moment Coefficient.
− 6	0·0301	− 0·101	− 3·34	− ·127	0·0128
− 4	0·0182	− 0·006	− 0·33	− 7·50	0·0450
− 2	0·0122	+ 0·081	+ 6·71	+ 0·958	0·0770
− 1	0·0112	0·119	10·62	0·730	0·0870
0	0·0108	0·152	14·11	0·624	0·0950
+ 1	0·0111	0·180	16·18	0·546	0·0980
2	0·0128	0·211	16·8	0·492	0·104
3	0·0144	0·242	16·7	0·451	0·109
4	0·0167	0·271	16·2	0·426	0·116
5	0·0195	0·308	15·8	0·402	0·124
6	0·0228	0·344	14·8	0·385	0·132
8	0·0341	0·407	11·9	0·358	0·146
10	0·0473	0·466	9·86	0·342	0·159
12	0·0670	0·514	7·67	0·328	0·169
14	0·0954	0·544	5·70	0·333	0·180

TABLE 8.

SERIES A, $x/c = 0{\cdot}5$.

AEROFOIL No. 4, CAMBER = 0·1.

Size of Plane, 6-inch by 36-inch. Speed, 80 ft./sec.

Angle. Degrees.	Drag Coefficient.	Lift Coefficient.	L/D.	C.P. Coefficient.	Moment Coefficient.
− 6	0·0341	− 0·096	− 2·81	− 0·242	0·0232
− 4	0·0208	− 0·006	− 0·27	+ 8·47	0·0482
− 2	0·0138	+ 0·076	+ 5·51	1·07	0·0810
− 1	0·0120	0·114	9·47	0·804	0·0910
0	0·0114	0·151	13·15	0·650	0·0980
+ 1	0·0115	0·179	15·60	0·576	0·103
2	0·0126	0·210	16·55	0·512	0·108
3	0·0140	0·240	16·8	0·470	0·113
4	0·0162	0·270	16·6	0·441	0·119
5	0·0186	0·303	16·1	0·414	0·125
6	0·0217	0·335	15·4	0·396	0·133
8	0·0297	0·397	13·3	0·369	0·146
10	0·0405	0·455	11·2	0·350	0·159
12	0·0554	0·514	9·27	0·335	0·172
14	0·0748	0·552	7·35	0·332	0·184
16	0·1045	0·531	5·07	0·354	0·188

TABLE 9.

SERIES A, $x/c = 0{\cdot}5$.

AEROFOIL No. 5, CAMBER = 0·12.

Size of Plane, 6-inch by 36-inch. Speed, 80 ft./sec.

Angle. Degrees.	Drag Coefficient.	Lift Coefficient.	L/D.	C.P. Coefficient.	Moment Coefficient.
− 6	0·0275	− 0·009	− 0·34	− 5·81	0·054
− 4	0·0189	+ 0·066	+ 3·48	+ 1·38	0·090
− 2	0·0144	0·143	9·92	0·748	0·107
− 1	0·0138	0·178	12·85	0·647	0·115
0	0·0139	0·217	15·60	0·575	0·125
+ 1	0·0150	0·253	16·85	0·523	0·132
2	0·0166	0·283	17·00	0·486	0·138
3	0·0183	0·309	16·83	0·462	0·142
4	0·0200	0·326	16·38	0·434	0·142
5	0·0228	0·347	15·17	0·412	0·143
6	0·0257	0·373	14·52	0·393	0·146
8	0·0332	0·425	12·80	0·370	0·157
10	0·0440	0·479	10·88	0·352	0·168
12	0·0556	0·535	9·55	0·341	0·182
14	0·0742	0·577	7·77	0·333	0·192
16	0·0959	0·590	6·15	0·338	0·200

TABLE 10.

SERIES A, $x/c = 0{\cdot}5$.

AEROFOIL No. 6, CAMBER = 0·16.

Size of Plane, 6-inch by 36-inch. Speed, 80 ft./sec.

Angle. Degrees.	Drag Coefficient.	Lift Coefficient.	L/D.	C.P. Coefficient.	Moment Coefficient.
− 8	0·0467	0·021	0·46	—	—
− 6	0·0336	0·074	2·19	1·35	0·099
− 4	0·0240	0·145	6·19	0·874	0·125
− 2	0·0199	0·222	11·13	0·671	0·149
− 1	0·0193	0·264	13·7	0·613	0·162
0	0·0201	0·295	14·7	0·567	0·167
+ 1	0·0214	0·329	15·4	0·535	0·176
2	0·0239	0·371	15·5	0·505	0·188
3	0·0263	0·404	15·3	0·486	0·196
4	0·0292	0·436	14·9	0·466	0·203
5	0·0317	0·445	14·0	0·450	0·200
6	0·0345	0·446	12·9	0·439	0·196
8	0·0399	0·445	11·1	0·406	0·181
10	0·0470	0·462	9·85	0·387	0·178
12	0·0581	0·503	8·65	0·371	0·187
14	0·0691	0·538	7·77	0·363	0·195
16	0·0844	0·570	6·75	0·356	0·203
18	0·1000	0·600	5·97	—	—
20	0·1282	0·600	4·66	—	—
22	0·1465	0·590	4·05	—	—

Table 11.

SERIES A, $x/c = 0{\cdot}5$.

AEROFOIL No. 7, CAMBER = 0·20.

Size of Plane, 6-inch by 36-inch. Speed, 80 ft./sec.

Angle. Degrees.	Drag Coefficient.	Lift Coefficient.	L/D.	C.P. Coefficient.	Moment Coefficient.
− 30	0·1835	− 0·0615	− 0·34	− 0·037	0·0054
− 25	0·1425	+ 0·0108	+ 0·08	− 0·95	0·048
− 20	0·1110	0·062	0·56	+ 3·9	0·078
− 18	0·1000	0·080	0·80	—	—
− 16	0·0908	0·096	1·06	1·41	0·095
− 14	0·0802	0·108	1·36	—	—
− 12	0·0722	0·118	1·63	1·037	0·104
− 10	0·0626	0·119	1·91	—	—
− 8	0·0516	0·118	2·28	1·037	0·114
− 6	0·0418	0·134	3·28	1·001	0·128
− 4	0·0328	0·183	5·57	0·834	0·153
− 3	0·0299	0·219	7·34	—	—
− 2	0·0280	0·257	9·15	0·672	0·172
− 1	0·0268	0·292	10·9	0·619	0·181
0	0·0272	0·330	12·1	0·578	0·190
+ 1	0·0282	0·364	12·9	0·548	0·199
2	0·0304	0·402	13·2	0·515	0·207
3	0·0325	0·439	13·5	0·497	0·217
4	0·0365	0·466	12·8	0·483	0·225
6	0·0440	0·496	11·3	0·469	0·232
8	0·0520	0·509	9·77	0·455	0·230
10	0·0603	0·506	8·42	0·422	0·214
12	0·0687	0·506	7·40	0·401	0·203
14	0·0790	0·530	6·72	0·389	0·206
16	0·0905	0·552	6·11	0·381	0·211
18	0·1022	0·582	5·75	0·374	0·218
20	0·1130	0·589	5·30	0·371	0·222
25	0·1690	0·569	3·42	0·382	0·216

TABLE 12.

SERIES B, $x/c = 0{\cdot}375$.

AEROFOIL No. 1, CAMBER = 0·075.

Size of Plane, 6-inch by 36-inch. Speed, 70 ft./sec.

Angle. Degrees.	Drag Coefficient.	Lift Coefficient.	L/D.	C.P. Coefficient.	Moment Coefficient.
− 4	0·0190	− 0·071	− 3·77	− 0·216	0·0152
− 2	0·0123	+ 0·0185	+ 1·50	+ 2·16	0·0400
− 1	0·0104	0·0665	6·35	0·768	0·0510
0	0·0098	0·109	11·1	0·568	0·0620
+ 1	0·0100	0·147	14·8	0·476	0·0700
2	0·0120	0·186	15·4	0·423	0·0785
3	0·0139	0·218	15·7	0·390	0·0850
5	0·0197	0·286	14·4	0·350	0·100
8	0·0316	0·385	12·2	0·310	0·119
11	0·0546	0·483	8·86	0·280	0·135
14	0·102	0·497	4·87	0·325	0·161

TABLE 13.

SERIES B, $x/c = 0{\cdot}375$.

AEROFOIL No. 1, CAMBER = 0·075.

Size of Plane, 6-inch by 36-inch. Speed, 60 ft./sec.

Angle. Degrees.	Drag Coefficient.	Lift Coefficient.	L/D.
− 6	0·0318	− 0·161	− 5·10
− 4	0·0189	− 0·0712	− 3·76
− 2	0·0123	+ 0·0158	+ 1·28
− 1	0·0106	0·0634	5·95
0	0·0102	0·109	10·6
+ 1	0·0102	0·150	14·6
2	0·0116	0·185	15·9
3	0·0136	0·221	16·2
5	0·0188	0·292	15·4
8	0·0318	0·394	12·4
11	0·0567	0·483	8·51
14	0·1042	0·495	4·76

TABLE 14.

SERIES B, $x/c = 0{\cdot}375$.

AEROFOIL No. 1, CAMBER = 0·075.

Size of Plane, 6-inch by 36-inch. Speed, 50 ft./sec.

Angle. Degrees.	Drag Coefficient.	Lift Coefficient.	L/D.
− 6	0·0317	− 0·160	− 5·06
− 4	0·0188	− 0·0733	− 3·91
− 2	0·0122	+ 0·0113	+ 0·93
− 1	0·0110	0·0564	5·12
0	0·0108	0·0980	9·08
+ 1	0·0108	0·145	13·4
2	0·0113	0·181	16·0
3	0·0127	0·218	17·0
5	0·0182	0·291	16·0
8	0·0313	0·387	12·4
11	0·0565	0·478	8·45
14	0·0990	0·486	4·90
18	0·160	0·453	2·84

TABLE 15.

SERIES B, $x/c = 0{\cdot}375$.

AEROFOIL No. 1, CAMBER = 0·075.

Size of Plane, 6-inch by 36-inch. Speed, 40 ft./sec.

Angle. Degrees.	Drag Coefficient.	Lift Coefficient.	L/D.
− 11	0·0710	− 0·243	− 3·42
− 8	0·0487	− 0·222	− 4·56
− 6	0·1330	− 0·162	− 4·92
− 4	0·0199	− 0·079	− 3·96
− 2	0·0131	+ 0·0046	+ 0·353
− 1	0·0118	0·047	3·96
0	0·0120	0·0896	7·46
+ 1	0·0114	0·136	12·0
2	0·0117	0·183	15·6
3	0·0129	0·215	16·7
5	0·0194	0·286	14·8
8	0·0322	0·385	11·9
11	0·0541	0·469	8·67
14	0·1035	0·474	4·58
18	0·1450	0·435	3·00

Table 16.

SERIES B, $x/c = 0{\cdot}375$.

AEROFOIL No. 2, CAMBER = 0·08.

Size of Plane, 6-inch by 36-inch. Speed, 70 ft./sec.

Angle. Degrees.	Drag Coefficient.	Lift Coefficient.	L/D.	C.P. Coefficient.	Moment Coefficient.
− 4	0·0204	− 0·0659	− 3·22	− 0·290	0·0191
− 2	0·0125	+ 0·0310	+ 2·50	+ 1·465	0·0455
− 1	0·0109	0·0747	6·86	0·761	0·0569
0	0·0107	0·116	10·8	0·569	0·0664
+ 1	0·0118	0·151	12·7	0·487	0·0735
2	0·0137	0·187	13·7	0·438	0·0820
3	0·0158	0·223	14·1	0·397	0·0882
5	0·0208	0·290	13·9	0·351	0·102
8	0·0364	0·390	10·7	0·312	0·122
11	0·0553	0·482	8·80	0·293	0·141
14	0·1015	0·496	4·90	0·335	0·166

Table 17.

SERIES B, $x/c = 0{\cdot}375$.

AEROFOIL No. 3, CAMBER = 0·09.

Size of Plane, 6-inch by 36-inch. Speed, 70 ft./sec.

Angle. Degrees.	Drag Coefficient.	Lift Coefficient.	L/D.	C.P. Coefficient.	Moment Coefficient.
− 4	0·0192	− 0·0274	− 1·42	− 1·373	0·0032
− 2	0·0127	+ 0·064	+ 5·02	+ 0·967	0·0618
− 1	0·0113	0·107	9·60	0·675	0·0724
0	0·0111	0·146	13·1	0·556	0·0815
+ 1	0·0124	0·180	14·5	0·493	0·0888
2	0·0141	0·212	15·1	0·442	0·0935
3	0·0166	0·242	14·6	0·415	0·100
5	0·0218	0·314	14·3	0·368	0·115
8	0·0364	0·411	11·3	0·330	0·136
11	0·0556	0·498	8·95	0·302	0·150
14	0·1006	0·533	5·30	0·331	0·177
18	0·181	0·576	3·18	0·366	0·211

TABLE 18.

SERIES B, $x/c = 0{\cdot}375$.

AEROFOIL No. 4, CAMBER = 0·1.

Size of Plane, 6-inch by 36-inch. Speed, 70 ft./sec.

Angle. Degrees.	Drag Coefficient.	Lift Coefficient.	L/D.	C.P. Coefficient.	Moment Coefficient.
− 6	0·0309	− 0·0905	− 2·93	− 0·194	0·0181
− 4	0·0185	+ 0·0065	+ 0·35	+ 8·09	0·0525
− 2	0·0126	0·0911	7·25	0·805	0·0735
− 1	0·0115	0·131	11·4	0·621	0·0815
0	0·0114	0·164	14·5	0·544	0·0890
+ 1	0·0127	0·202	15·9	0·483	0·0980
2	0·0146	0·234	16·0	0·446	0·104
3	0·0170	0·268	15·7	0·415	0·111
5	0·0215	0·332	15·4	0·362	0·121
8	0·0339	0·425	12·5	0·341	0·147
11	0·0519	0·506	9·80	0·316	0·160
14	0·0805	0·561	6·96	0·312	0·176
18	0·1225	0·582	4·75	0·329	0·191
22	0·141	0·506	3·56	—	—

TABLE 19.

SERIES B, $x/c = 0{\cdot}375$.

AEROFOIL No. 5, CAMBER = 0·12.

Size of Plane, 6-inch by 36-inch. Speed, 70 ft./sec.

Angle. Degrees.	Drag Coefficient.	Lift Coefficient.	L/D.	C.P. Coefficient.	Moment Coefficient.
− 8	0·0454	− 0·1048	− 2·32	− 0·029	0·0032
− 6	0·0302	− 0·0376	− 1·25	− 1·00	0·0400
− 4	0·0197	+ 0·0476	+ 2·42	+ 1·497	0·0711
− 2	0·0146	0·1268	8·66	0·718	0·0910
− 1	0·0142	0·1642	11·5	0·603	0·100
0	0·0141	0·208	14·8	0·529	0·110
+ 1	0·0147	0·243	16·5	0·487	0·118
2	0·0171	0·281	16·4	0·455	0·127
3	0·0192	0·316	16·4	0·427	0·135
5	0·0248	0·372	15·0	0·390	0·146
8	0·0361	0·445	12·35	0·355	0·160
11	0·0514	0·511	9·96	0·332	0·170
14	0·0700	0·572	8·16	0·319	0·182
18	0·1268	0·581	4·60	0·345	0·200

Table 20.

SERIES B, $x/c = 0{\cdot}375$.

AEROFOIL No. 6, CAMBER = 0·16.

Size of Plane, 6-inch by 36-inch. Speed, 70 ft./sec.

Angle. Degrees.	Drag Coefficient.	Lift Coefficient.	L/D.	C.P. Coefficient.	Moment Coefficient.
− 8	0·0495	− 0·0025	− 0·051	− 5·23	0·047
− 6	0·0366	+ 0·0368	+ 1·00	+ 2·21	0·071
− 4	0·0266	0·112	4·20	0·908	0·102
− 2	0·0208	0·196	9·40	0·631	0·124
− 1	0·0201	0·231	11·50	0·573	0·132
0	0·0201	0·269	13·4	0·522	0·140
+ 1	0·0210	0·304	14·4	0·489	0·148
2	0·0234	0·337	14·4	0·462	0·156
3	0·0257	0·375	14·6	0·441	0·166
5	0·0314	0·439	14·0	0·414	0·182
8	0·0411	0·497	12·1	0·317	0·187
11	0·0542	0·523	9·65	0·353	0·185
14	0·0647	0·552	8·50	0·344	0·190
18	0·0844	0·598	7·10	0·342	0·204
22	0·139	0·580	4·18	0·356	0·211

Table 21.

SERIES B, $x/c = 0{\cdot}375$.

AEROFOIL No. 7, CAMBER = 0·20.

Size of Plane, 6-inch by 36-inch. Speed, 70 ft./sec.

Angle. Degrees.	Drag Coefficient.	Lift Coefficient.	L/D.	C.P. Coefficient.	Moment Coefficient.
− 10	0·0601	− 0·0123	− 0·20	− 1·52	0·0335
− 8	0·0494	− 0·0056	− 0·11	− 3·37	0·0438
− 6	0·0363	+ 0·0334	+ 0·92	+ 2·36	0·0685
− 4	0·0263	0·108	4·10	0·929	0·0980
− 2	0·0208	0·188	9·00	0·646	0·121
− 1	0·0191	0·224	11·7	0·577	0·129
0	0·0205	0·258	12·5	0·531	0·137
+ 1	0·0215	0·292	13·6	0·494	0·144
2	0·0224	0·328	14·6	0·465	0·152
3	0·0249	0·364	14·6	0·444	0·161
5	0·0308	0·430	13·9	0·413	0·178
8	0·0414	0·487	11·7	0·379	0·185
11	0·0536	0·509	9·47	0·355	0·180
14	0·0728	0·537	7·36	0·346	0·186
18	0·102	0·565	5·52	0·344	0·196
22	0·133	0·576	4·34	0·345	0·202
25	0·184	0·555	3·00	0·362	0·212

TABLE 22.

SERIES B, $x/c = 0{\cdot}375$.

AEROFOIL No. 7, CAMBER = 0·20.

Size of Plane, 6-inch by 36-inch. Speed, 60 ft./sec.

Angle. Degrees.	Drag Coefficient.	Lift Coefficient.	L/D.
− 10	0·0592	− 0·0066	− 0·11
− 8	0·0480	+ 0·0014	+ 0·33
− 6	0·0356	0·0381	1·07
− 4	0·0257	0·120	4·66
− 2	0·0211	0·196	9·30
− 1	0·0198	0·236	11·9
0	0·0205	0·272	13·1
+ 1	0·0218	0·310	14·2
2	0·0233	0·340	14·6
3	0·0265	0·372	14·1
5	0·0320	0·442	13·8
8	0·0431	0·505	11·7
11	0·0558	0·522	9·35
14	0·0740	0·536	7·24
18	0·1042	0·556	5·34
22	0·1353	0·566	4·17
25	0·196	0·537	2·74

TABLE 23.

SERIES B, $x/c = 0{\cdot}375$.

AEROFOIL No. 7, CAMBER = 0·20.

Size of Plane, 6-inch by 36-inch. Speed, 50 ft./sec.

Angle. Degrees.	Drag Coefficient.	Lift Coefficient.	L/D.
− 10	0·0603	− 0·0044	− 0·007
− 8	0·0485	+ 0·0071	+ 0·016
− 6	0·0359	0·0425	1·19
− 4	0·0258	0·122	4·75
− 2	0·0208	0·208	10·0
− 1	0·0203	0·243	12·0
0	0·0215	0·275	12·8
+ 1	0·0225	0·314	14·0
2	0·0254	0·344	13·6
3	0·0268	0·377	14·0
5	0·0323	0·446	13·8
8	0·0432	0·520	12·0
11	0·0559	0·533	9·55
14	0·0750	0·540	7·22
18	0·1035	0·557	5·40
22	0·143	0·561	3·93
25	0·201	0·498	2·48

AEROFOILS FOR AIRSCREW DESIGN.

Series A. Upper Surface Circular Arc on 6" chord along X.Y.

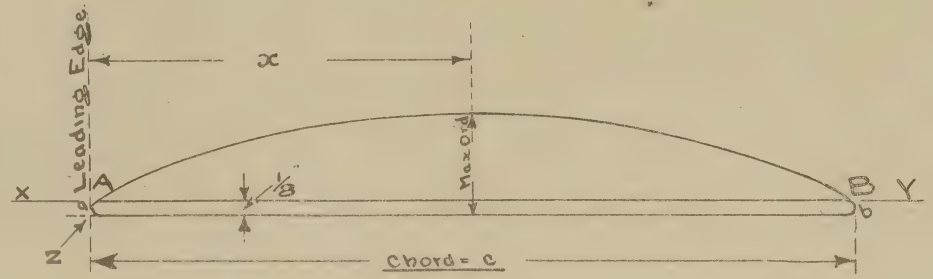

Series	A	x/c	=	0·5
"	B	"	=	0·375
"	C	"	=	0·3
"	D	"	=	0·25
"	E	"	=	0·2

REPORT No. 362.

FIG. 1.

AEROFOILS FOR AIRSCREW DESIGN.

Speed 80 ft/sec.
Size of Plane 6X36.

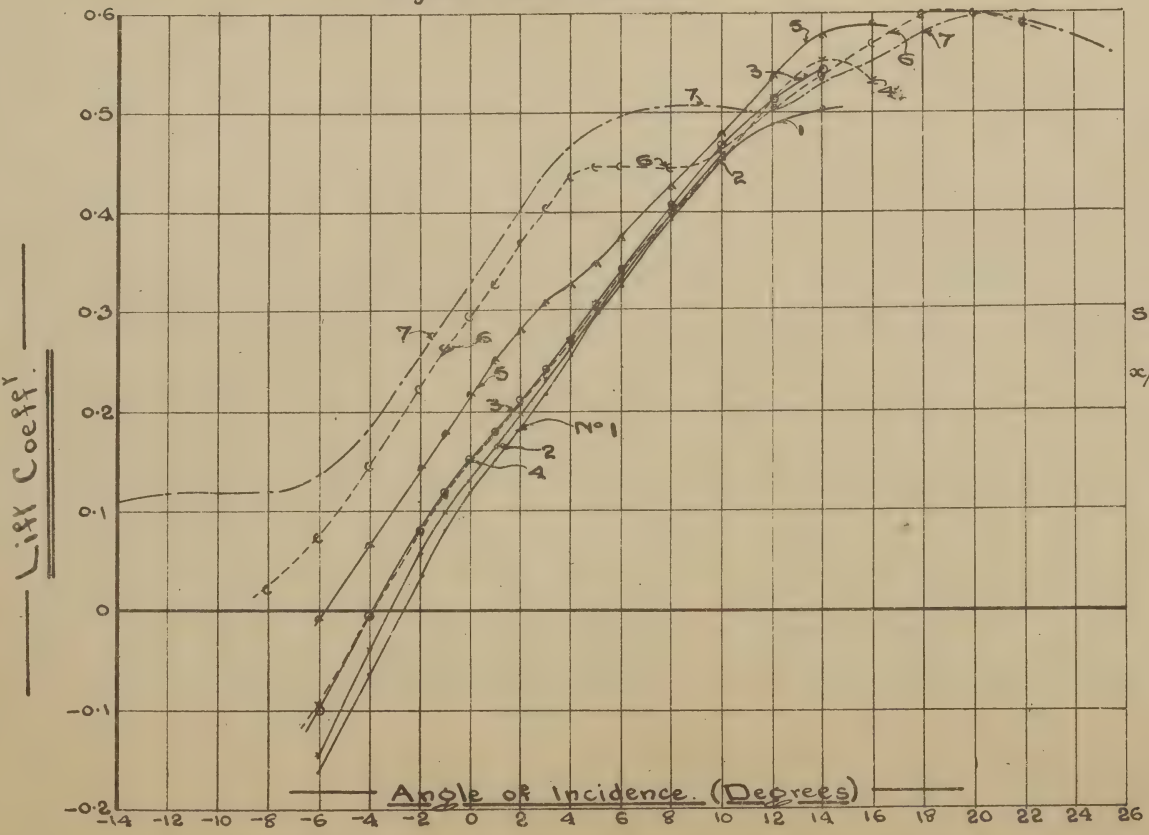

Series A
x/c = 0·3

——•——	Aerofoil. N° 1.
——x——	" N° 2.
——⊙——	" N° 3.
---V---	" N° 4.
——^——	" N° 5.
---C---	" N° 6.
——·——·——	" N° 7.

REPORT Nº 362.

FIG 2.

AEROFOILS FOR AIRSCREW DESIGN

Speed 80 ft/sec.
Size of Plane 6"X36"

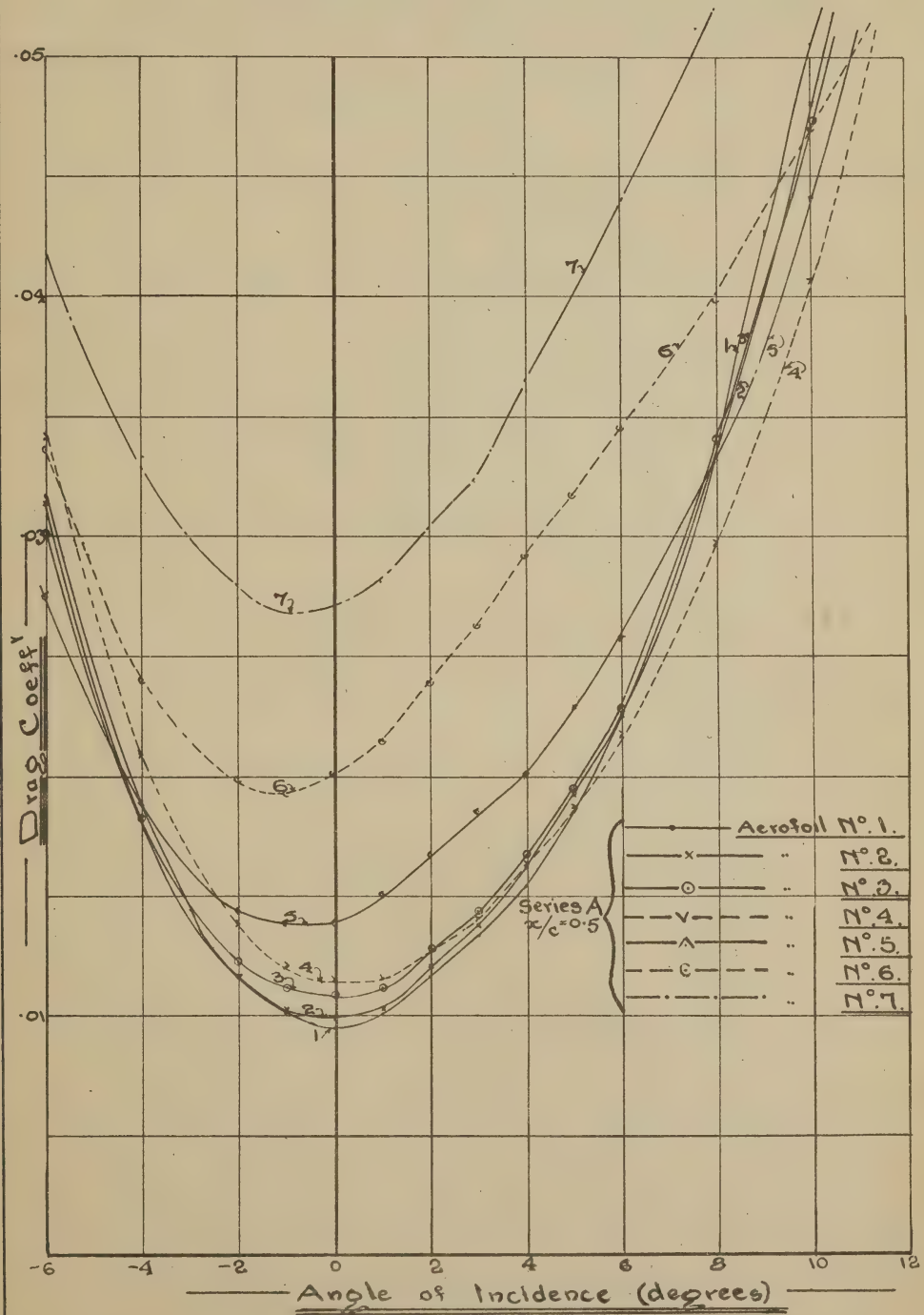

AEROFOILS FOR AIRSCREW DESIGN.

L/D against Angle of Incidence —— Wind Speed = 80 ft/sec.

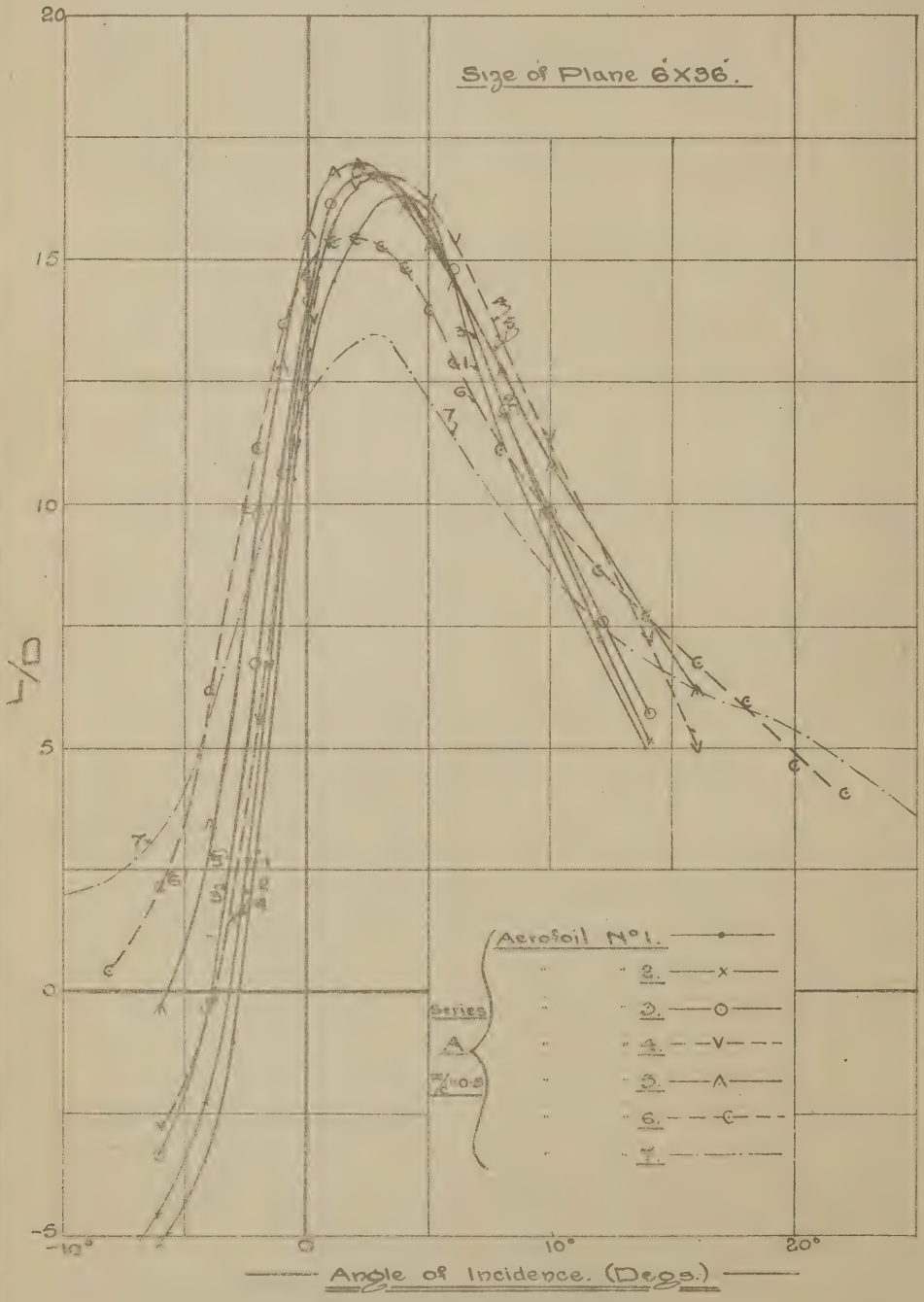

AEROFOILS FOR AIRSCREW DESIGN.

Variation of Centre of Pressure with Angle of Incidence.

Speed 80ft/sec Size of Plane 6X36

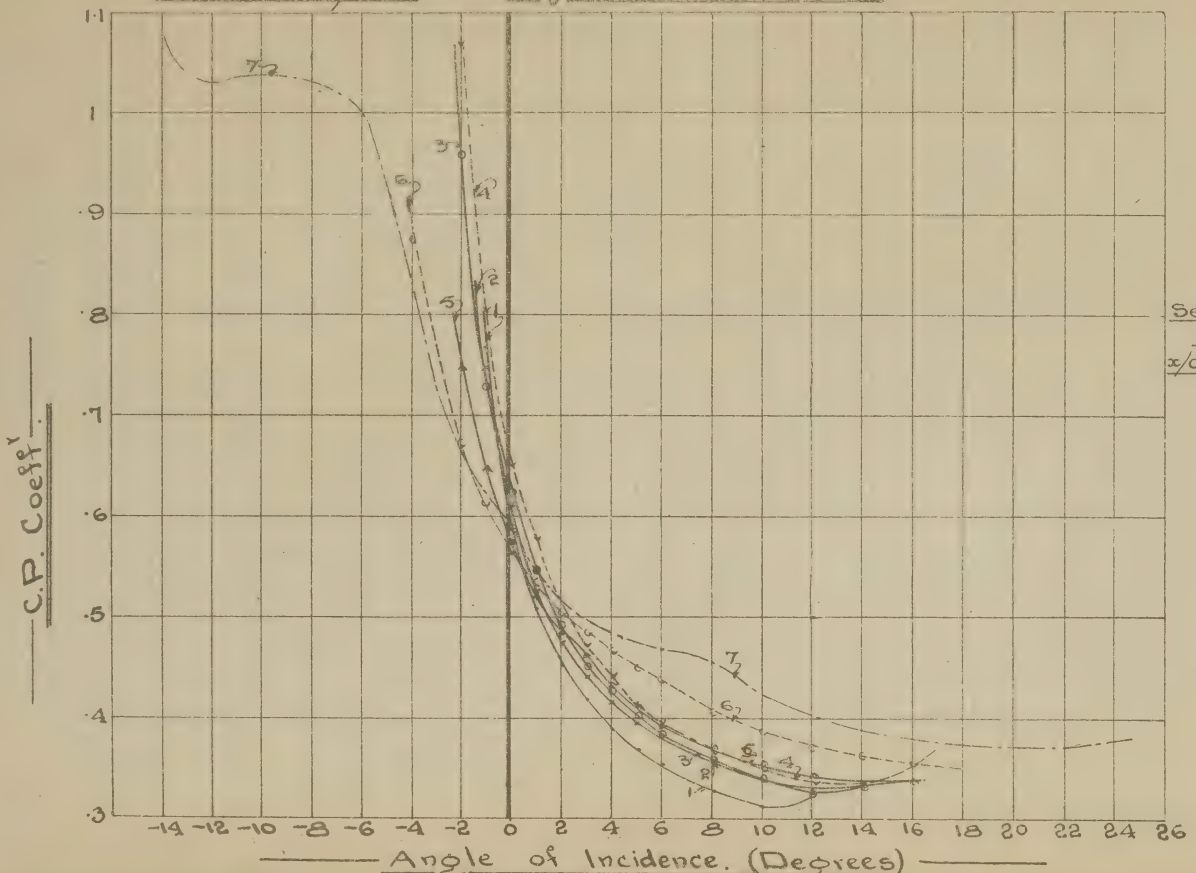

Series A x/c = 0·5

- Aerofoil N°1.
- Aerofoil N°2.
- Aerofoil N°3.
- Aerofoil N°4.
- Aerofoil N°5.
- Aerofoil N°6.
- Aerofoil N°7.

REPORT No 362.

FIG 5.

REPORT Nº 362. FIG 6.

AEROFOILS FOR AIRSCREW DESIGN.

Variation of Moment Coeff^t with Angle of Incidence.

Speed 80ft/sec Size of Plane 6"x36".

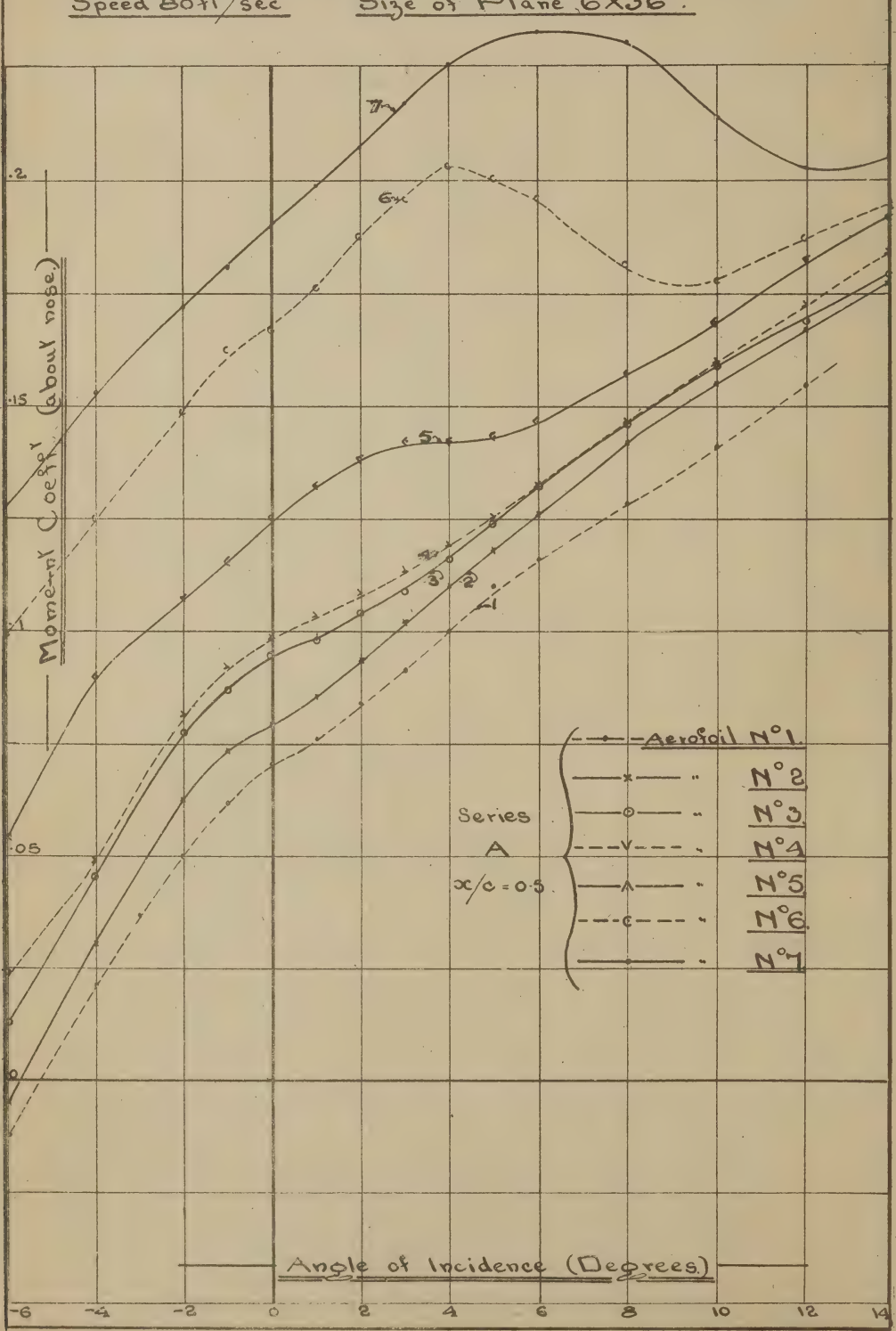

AEROFOILS FOR AIRSCREW DESIGN.

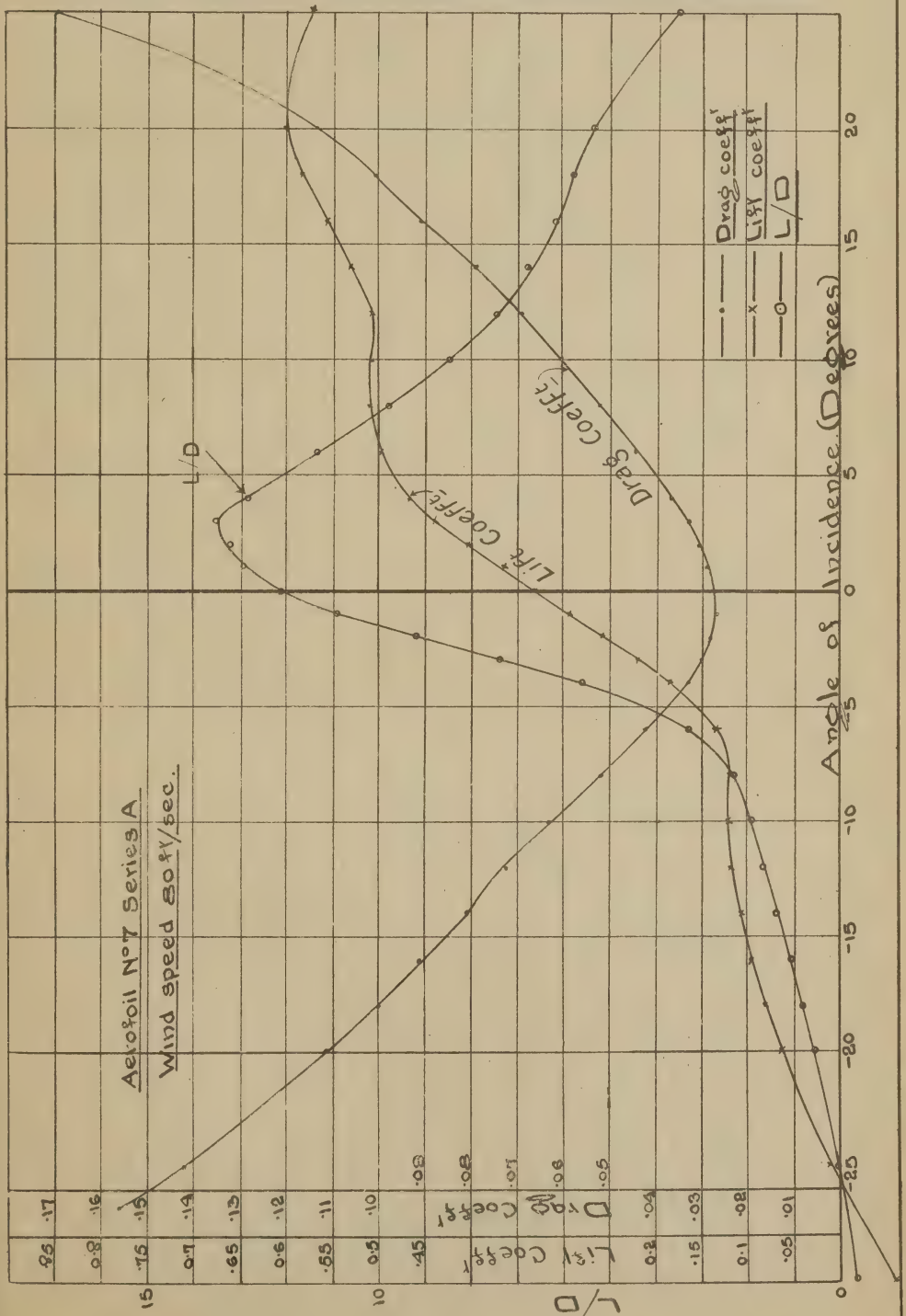

AEROFOILS FOR AIRSCREW DESIGN.

Variation of Moment Coeffᵗ and Centre of Pressure with Angle of Incidence.

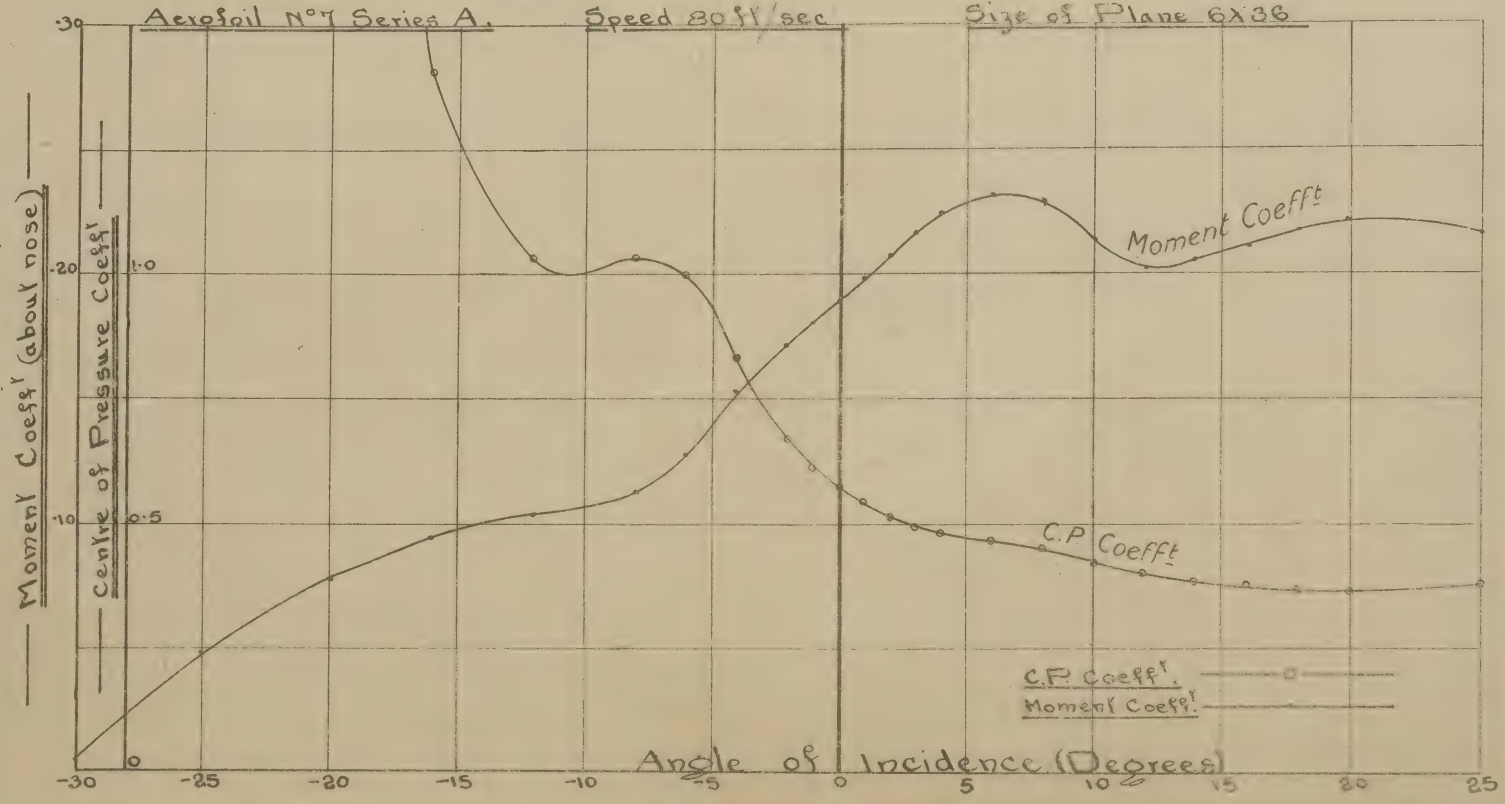

REPORT Nº 362.

FIG 8.

AEROFOILS FOR AIRSCREW DESIGN.

Aerofoil N° 1 Series A

Size of Plane 6"X36"

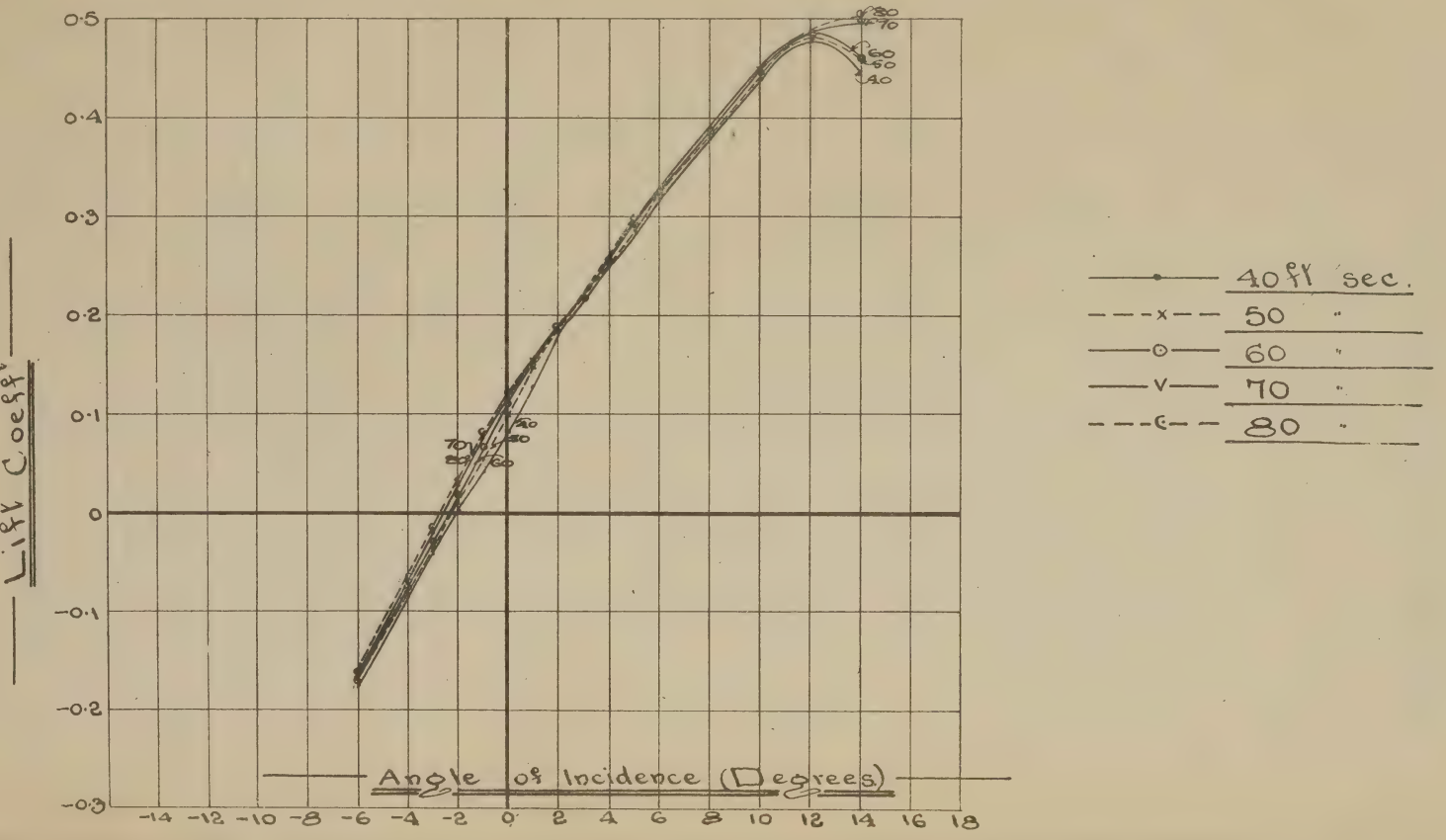

REPORT N° 362.

FIG 9.

AEROFOILS FOR AIRSCREW DESIGN

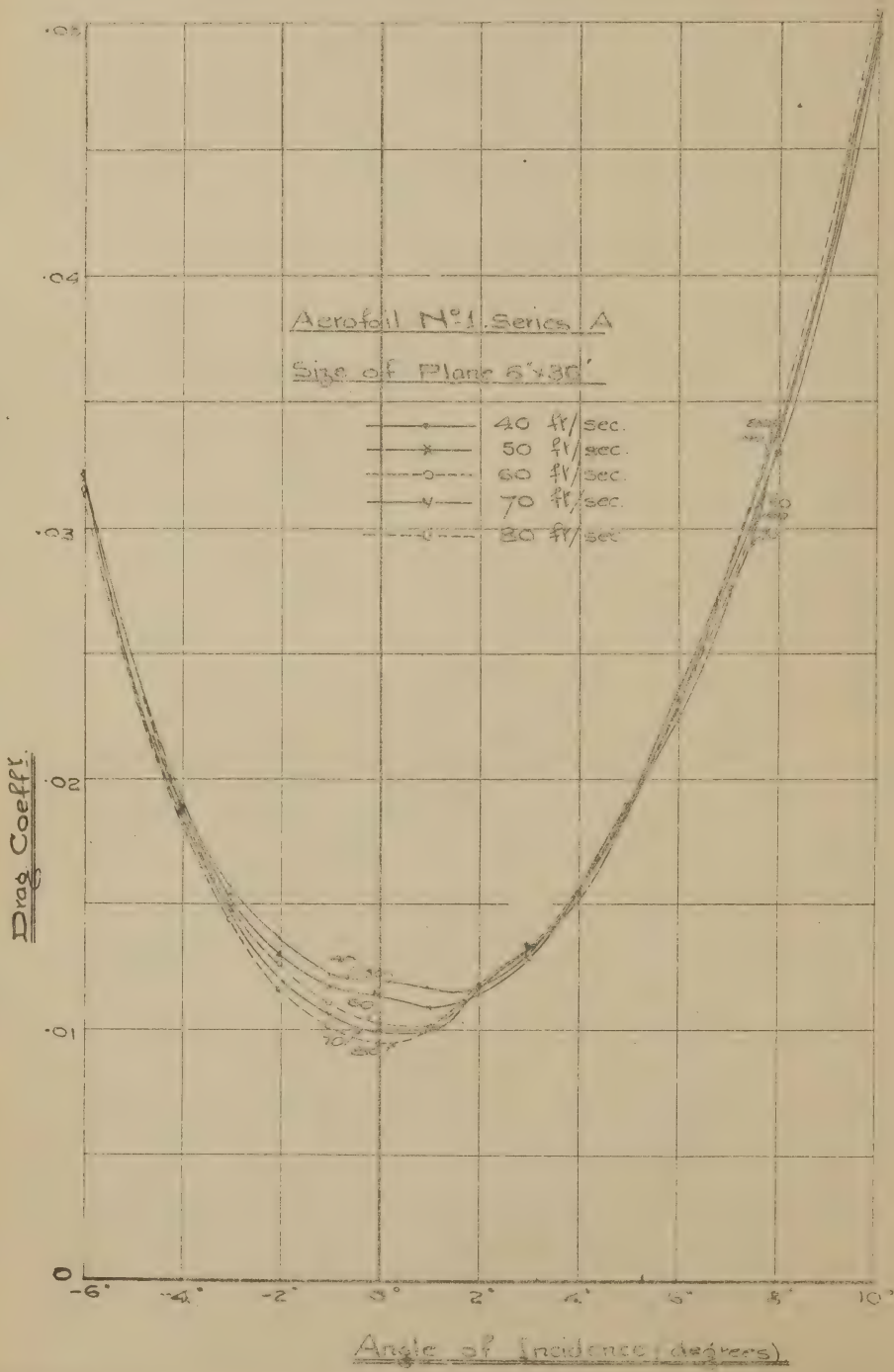

AEROFOILS FOR AIRSCREW DESIGN.

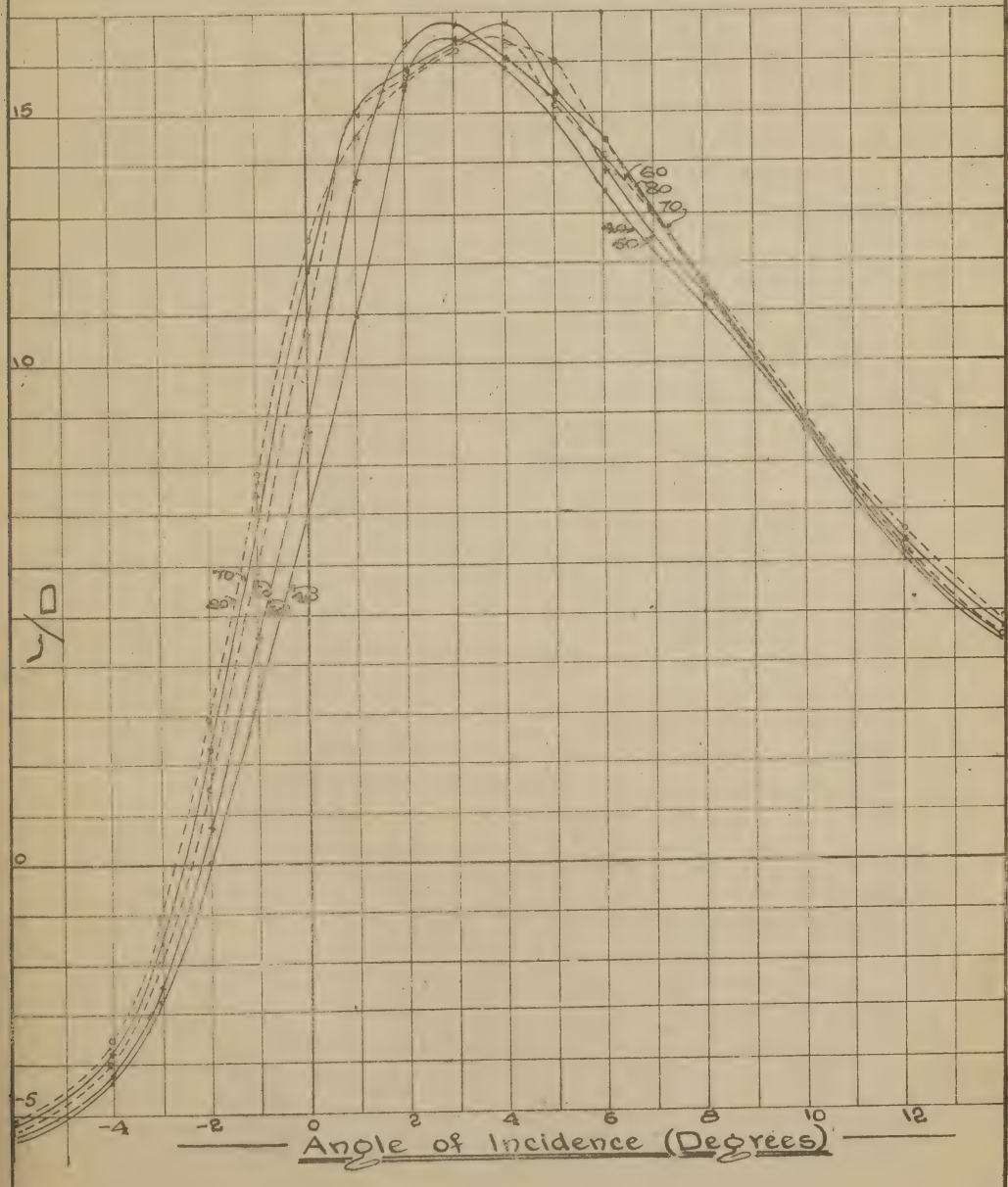

AEROFOILS FOR AIRSCREW DESIGN.

Variation of Centres of Pressure with Angle of Incidence and speed.

Aerofoil N°1 Series A Size of Plane. 6"x36"

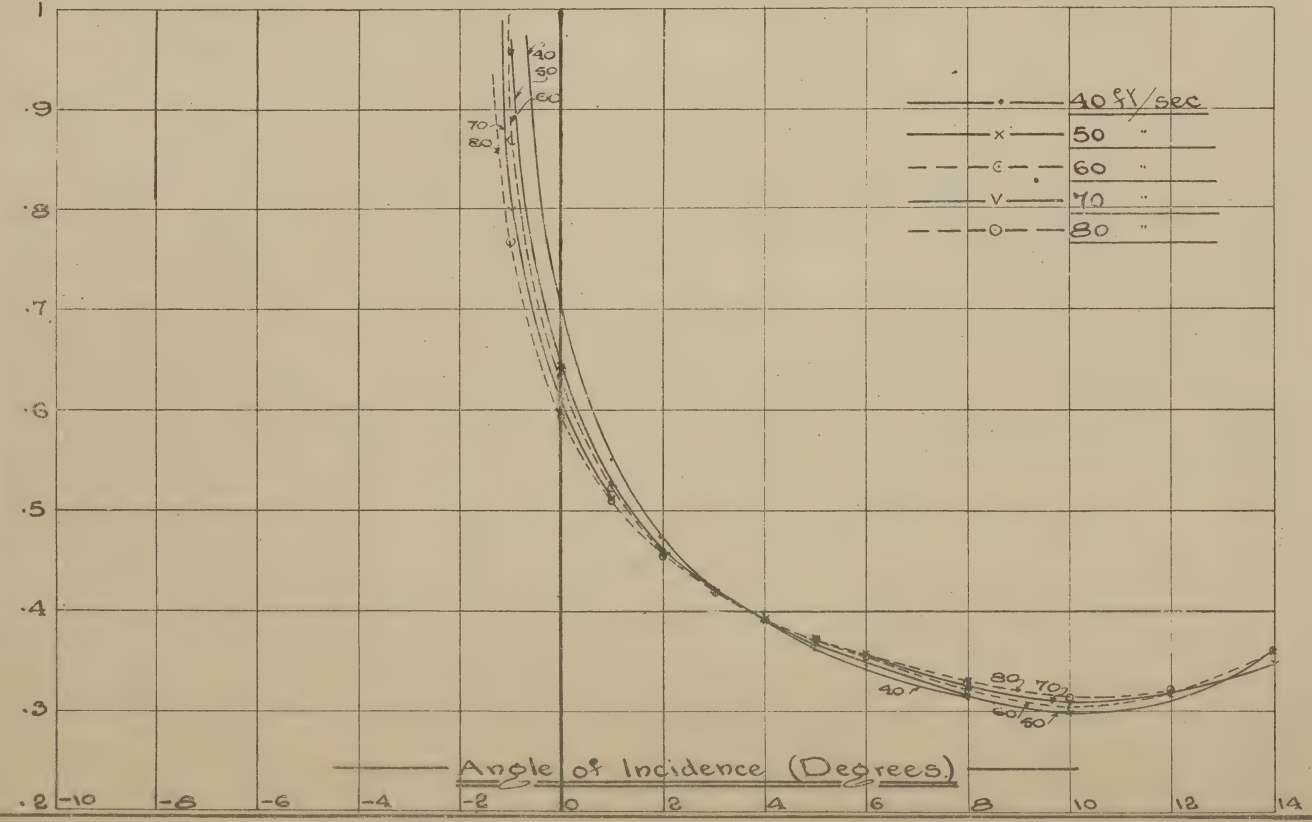

REPORT Nº 362.

FIG 12.

REPORT Nº 362. FIG 13.

AEROFOILS FOR AIRSCREW DESIGN.

Variation of Moment Coefficients with Angles of Incidence & Speed.

Aerofoil Nº 7 Series A Size of Plane 6"X36".

---o--- 40 ft/sec.
——x—— 50 ft/sec.
----c---- 60 ft/sec.
——v—— 70 ft/sec.
----o---- 80 ft/sec.

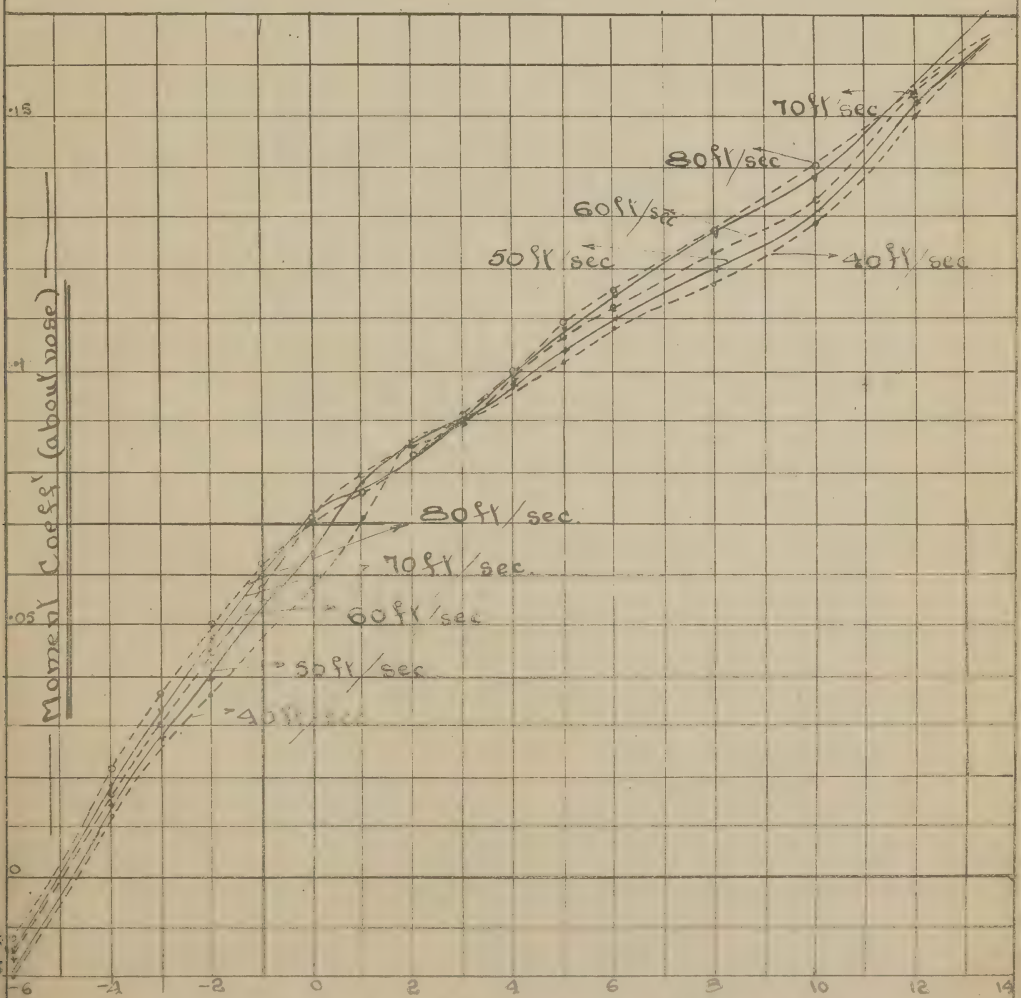

AEROFOILS FOR PROPELLER DESIGN.

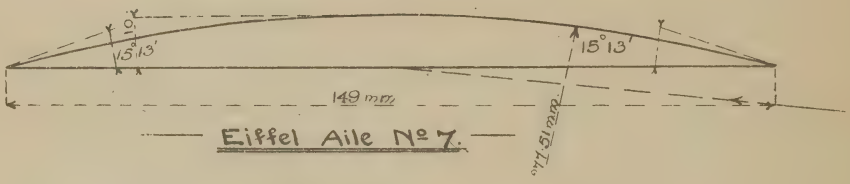

Eiffel Aile Nº 7.

Aerofoil Nº 1 Series A.

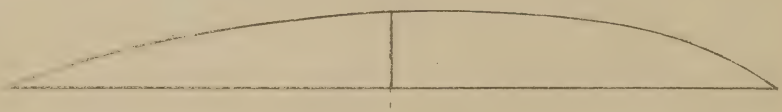

R & M. Nº 72 Design Index 0

Aerofoil Nº 4 Series A.

REPORT No. 362.

FIG 15.

AEROFOILS FOR AIRECREW DESIGN.

Comparison between two aerofoils of circular upper surface and approx equal camber. Tested by Eiffel and at the N.P.L.

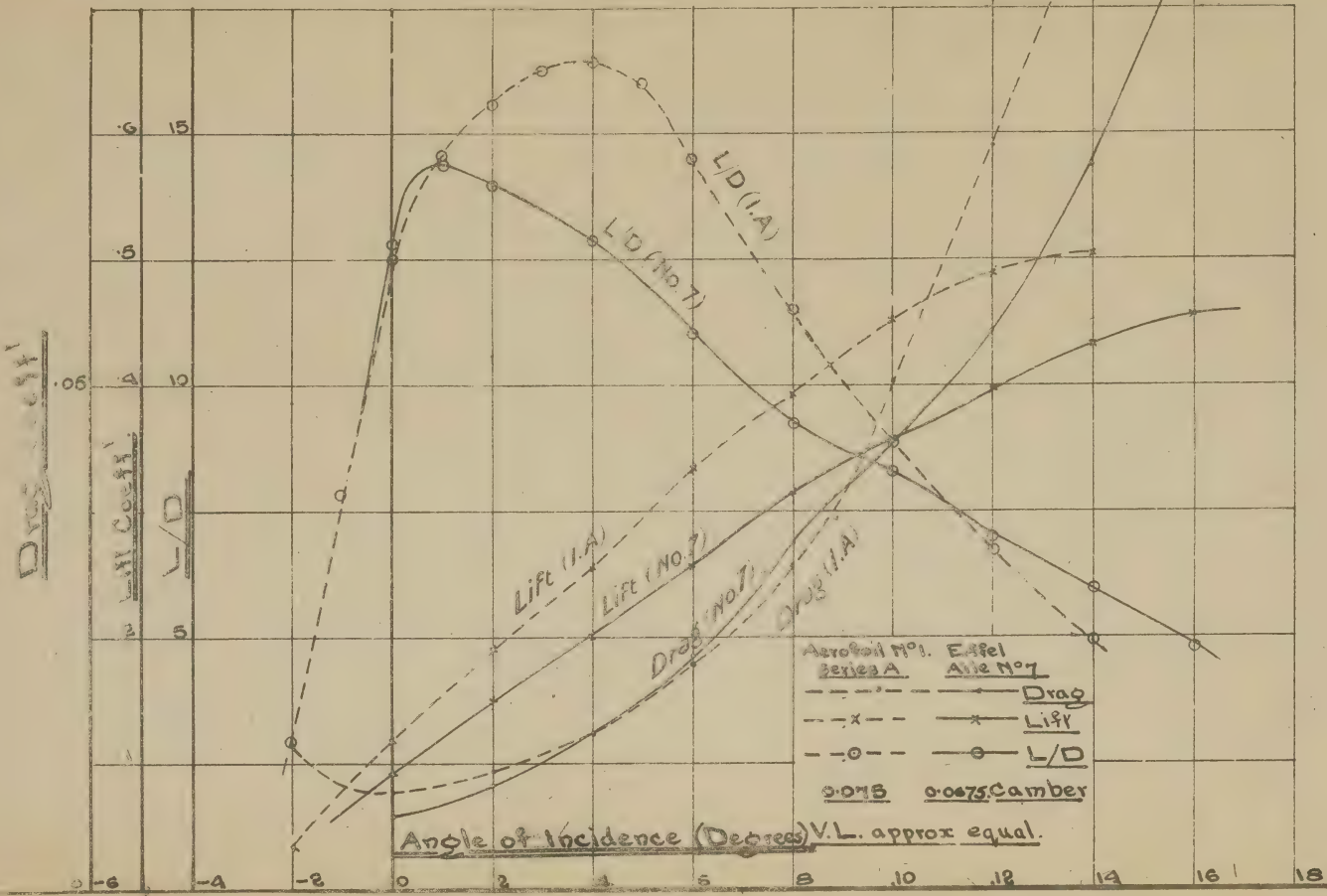

AEROFOILS FOR AIRSCREW DESIGN.

Comparison between two aerofoils, with equal camber and same position of maximum ordinate.

FIG. 16.

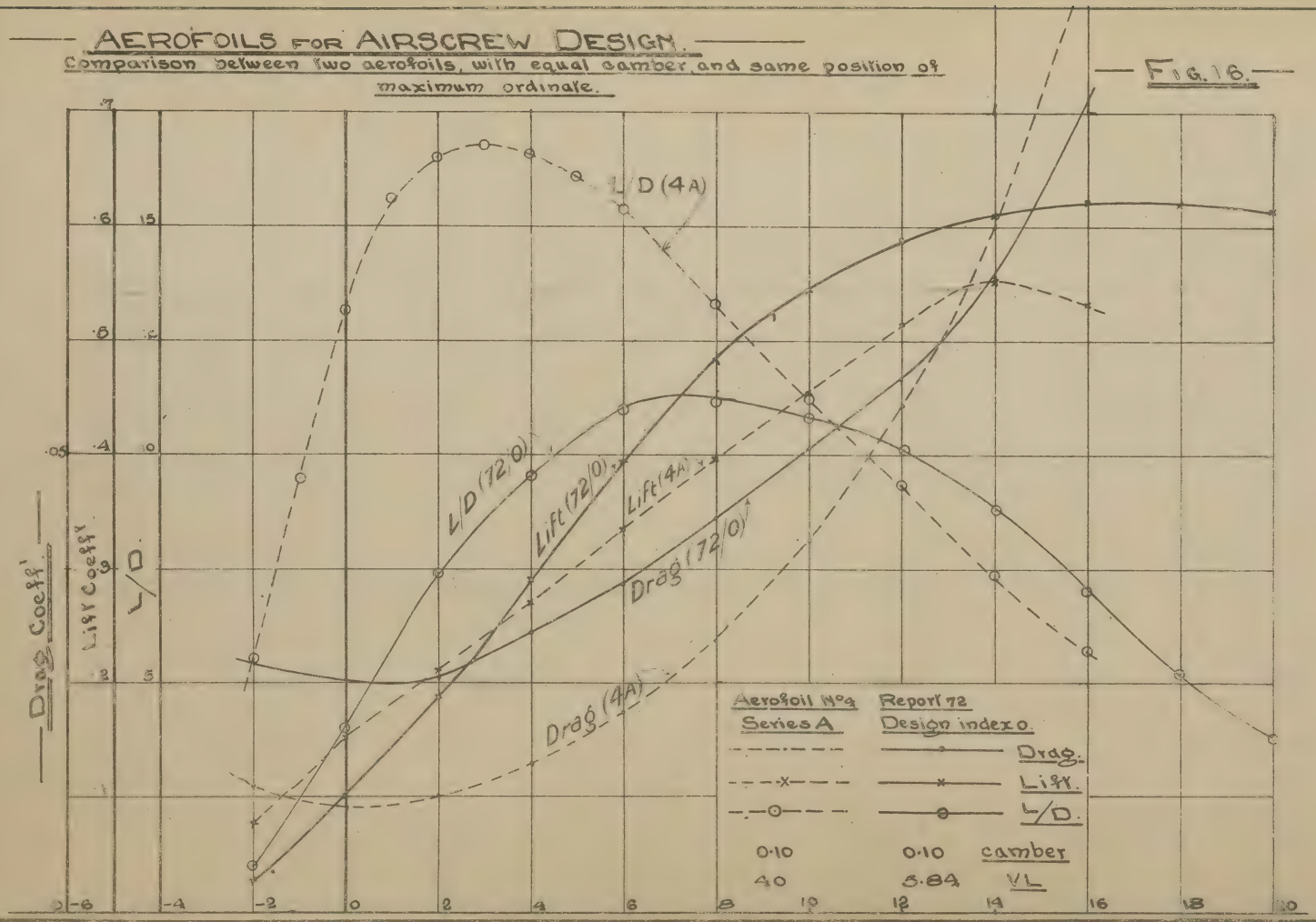

REPORT No. 362.

FIG 16.

AEROFOILS FOR AIRSCREW DESIGN.

Speed - 70 ft/sec.

Size of Plane - 6"x36".

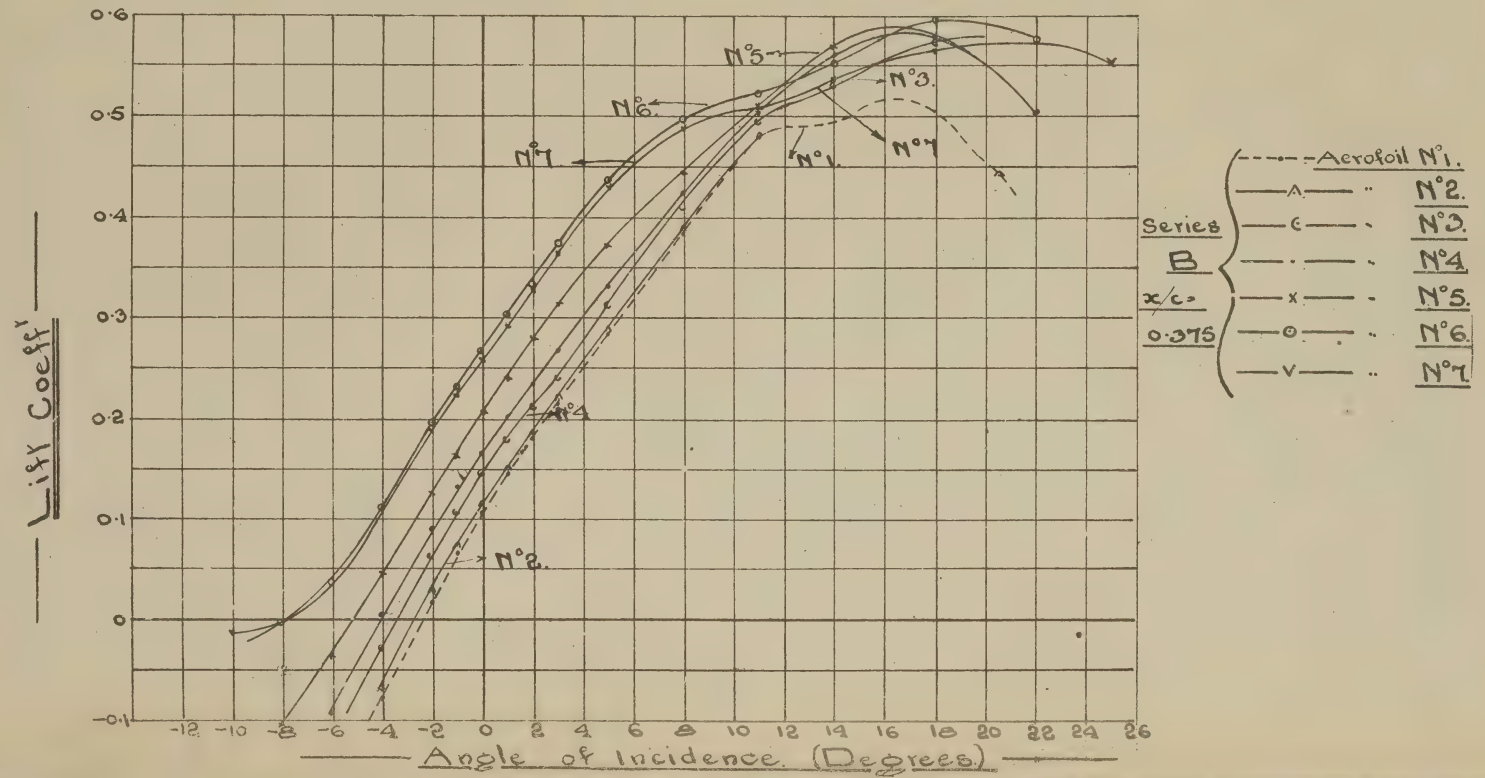

REPORT Nº 362.

FIG. 17.

REPORT Nº 362. FIG 18.

AEROFOILS FOR AIRSCREW DESIGN.

Speed = 70 ft/sec

Size of Plane = 6 x 36

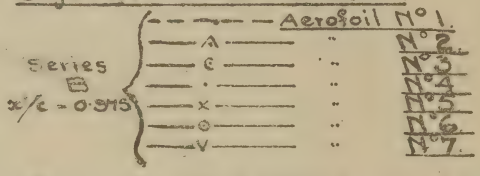

AEROFOILS FOR AIRSCREW DESIGN.

Speed = 70 ft/sec. Size of Plane = 6"X36".

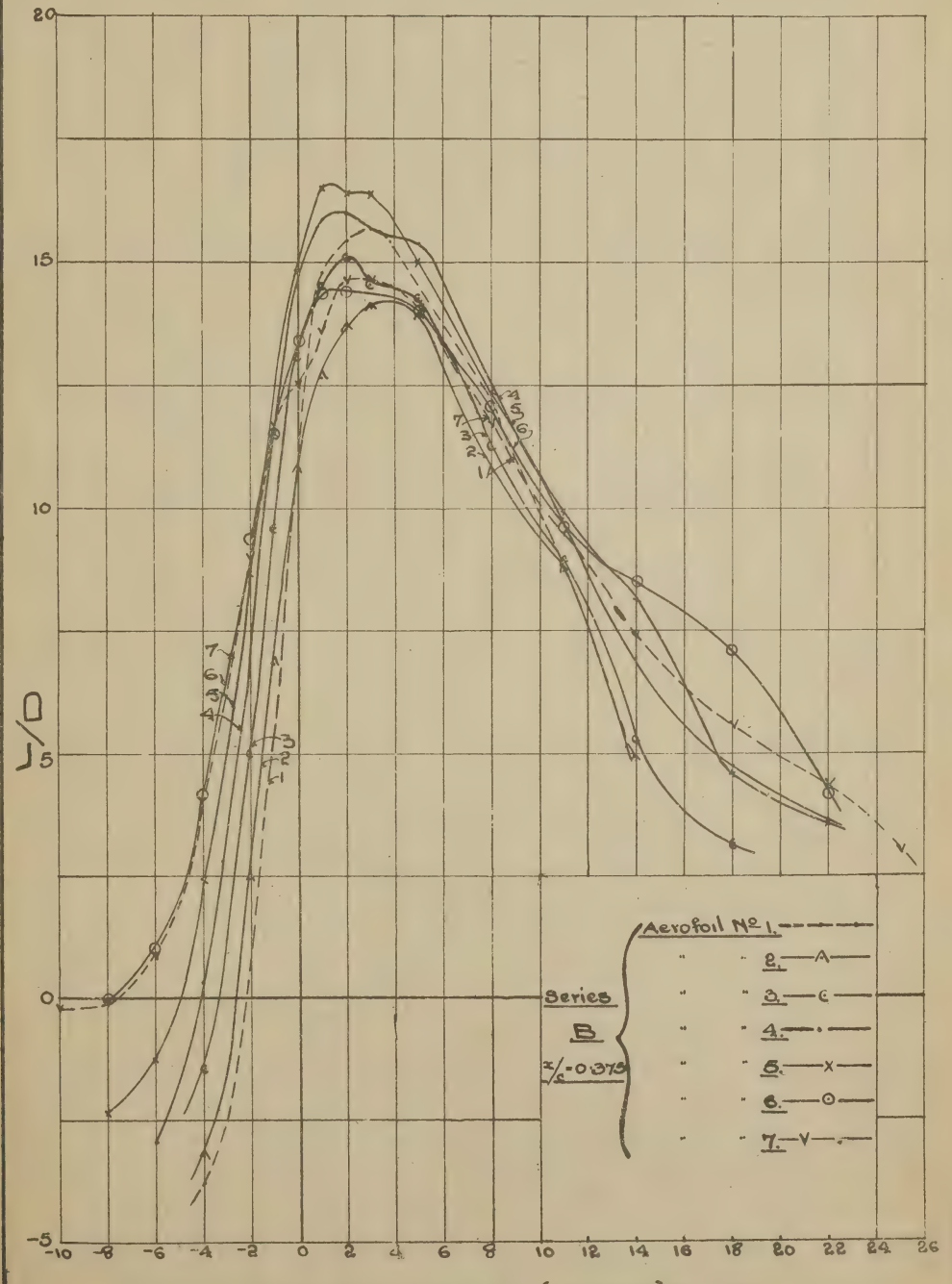

AEROFOILS FOR AIRSCREW DESIGN.

Variation of Centre of Pressure with Angle of Incidence.

Speed 70 ft/sec.

Size of Plane = 6"x36"

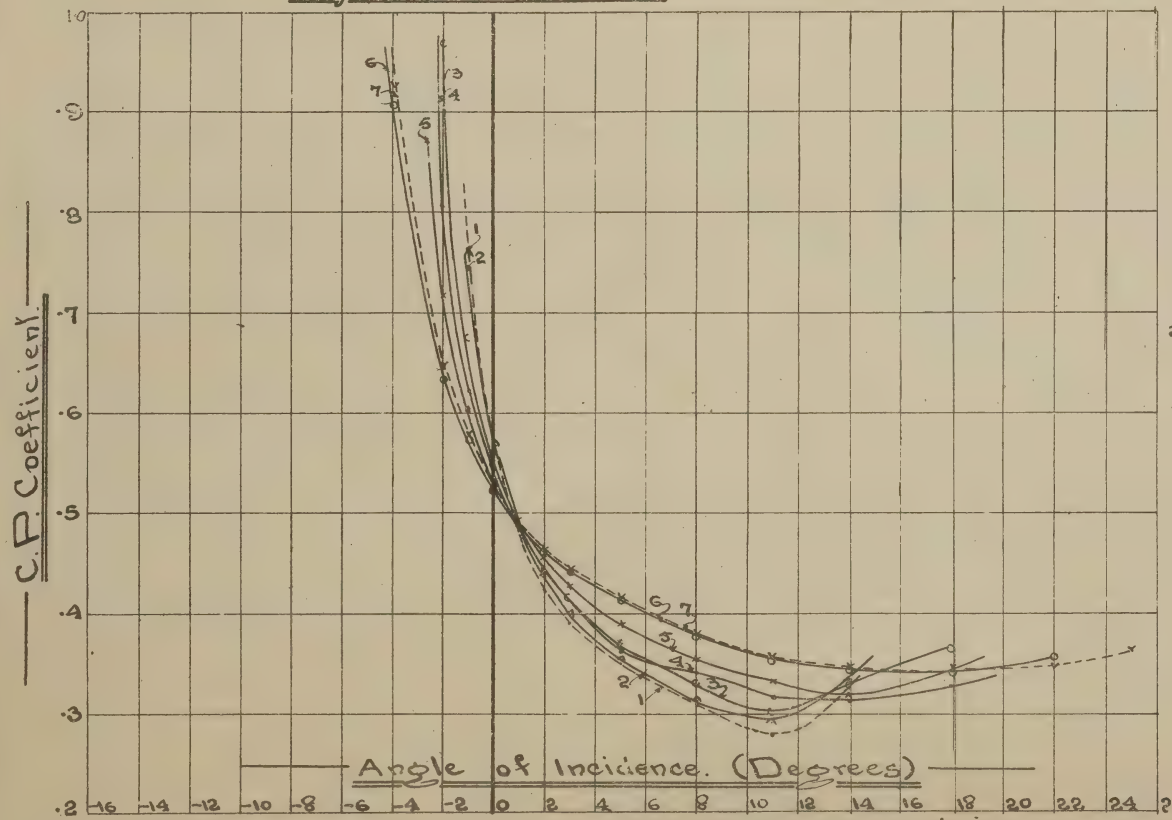

Series B x/c = 0·375

- Aerofoil N°1.
- A — N°2.
- C — N°3.
- · — N°4.
- x — N°5.
- o — N°6.
- V — N°7.

REPORT Nº 362.

FIG 20.

AEROFOILS FOR AIRSCREW DESIGN.

Variation of Moment Coefficient with Angle of Incidence.

Speed 70 ft/sec.

Size of Plane = 6"x36".

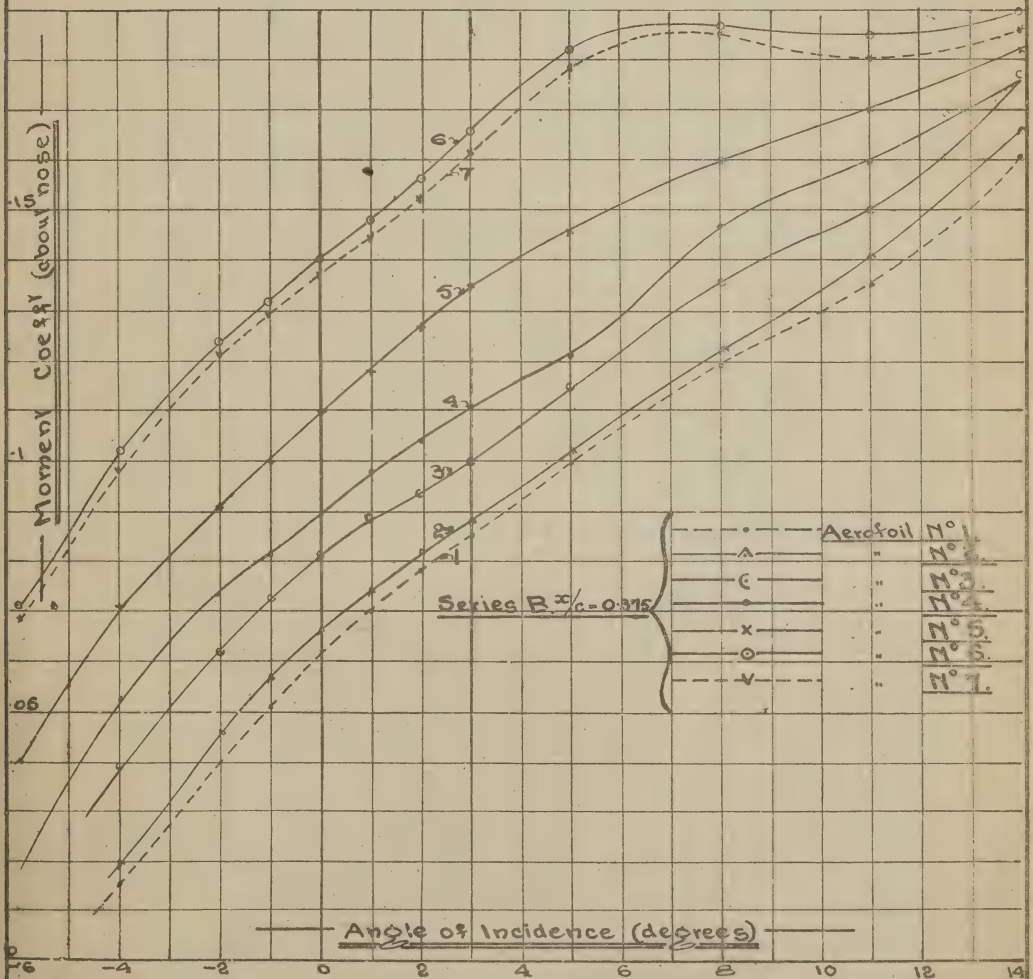

AEROFOILS FOR AIRSCREW DESIGN.

Aerofoil Nº 1 Series B

Size of Plane 6"x36".

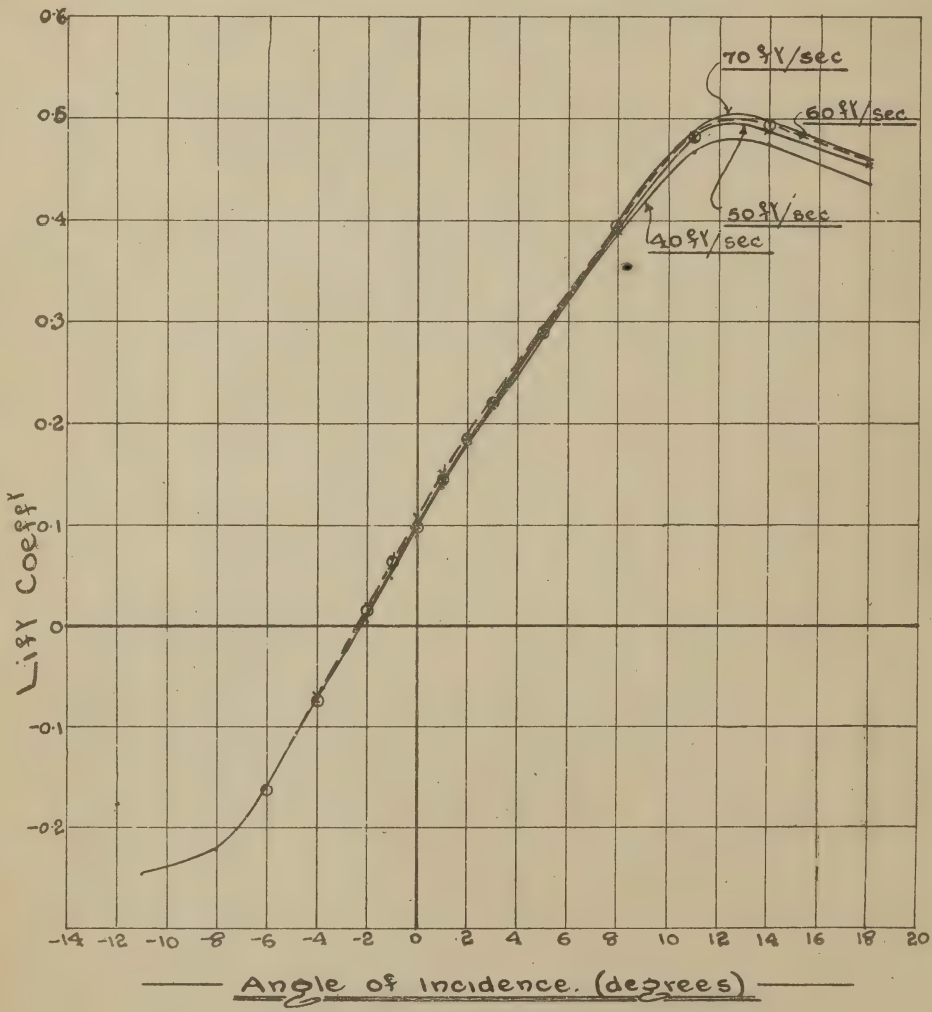

——·—— 40 ft/sec.
——×—— 50 ft/sec.
– –⊙– – – 60 ft/sec.
——v—— 70 ft/sec.

AEROFOILS FOR AIRSCREW DESIGN.

Aerofoil Nº 1 Series B. — FIG. 23.

Size of Plane 6"x36".

——·——	40 ft sec.
——x——	50 "
- - -o- - -	60 "
——v——	70 "

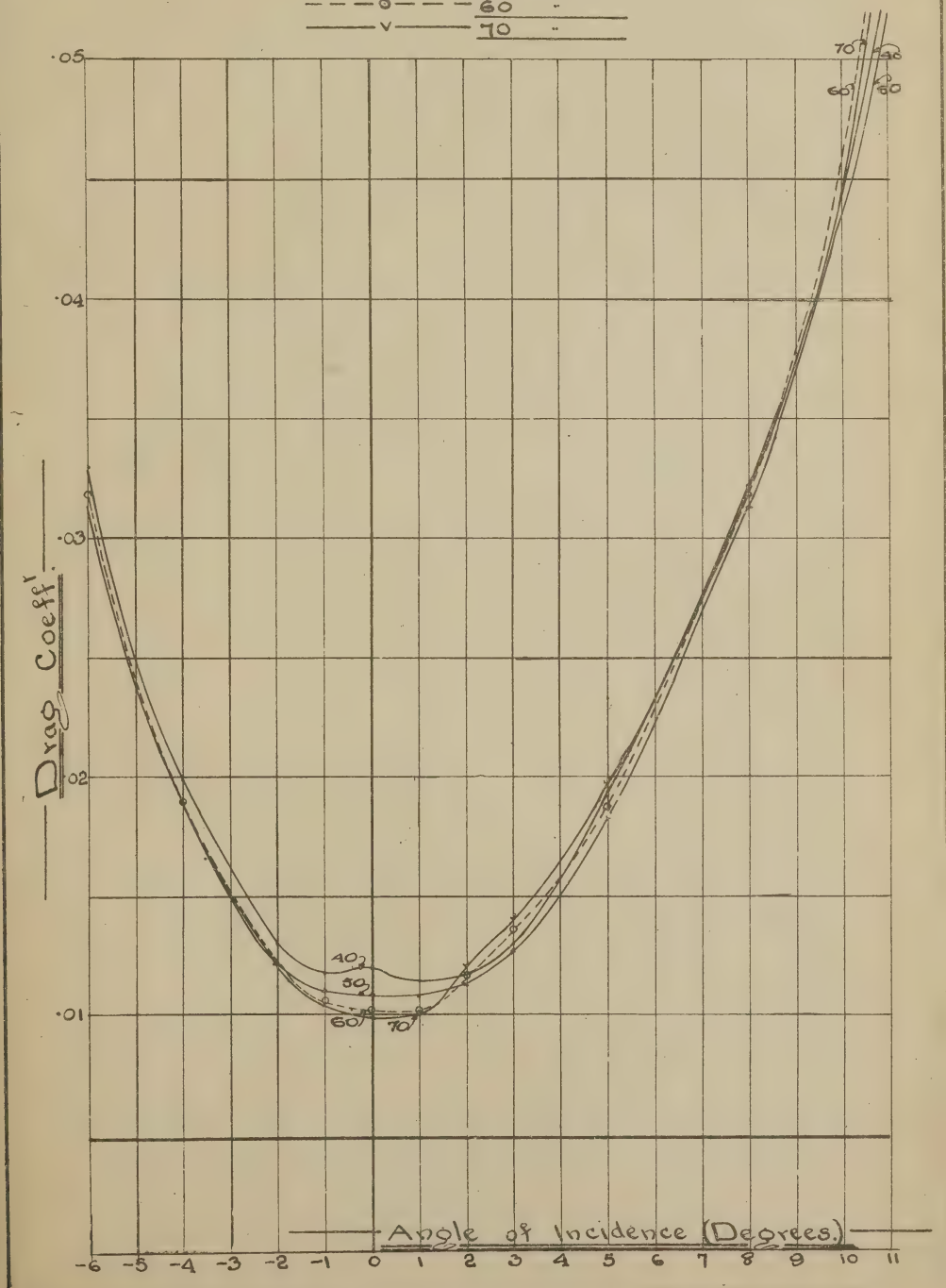

AEROFOILS FOR AIRSCREW DESIGN.

Aerofoil Nº 1 Series B.

Size of Plane 6X36

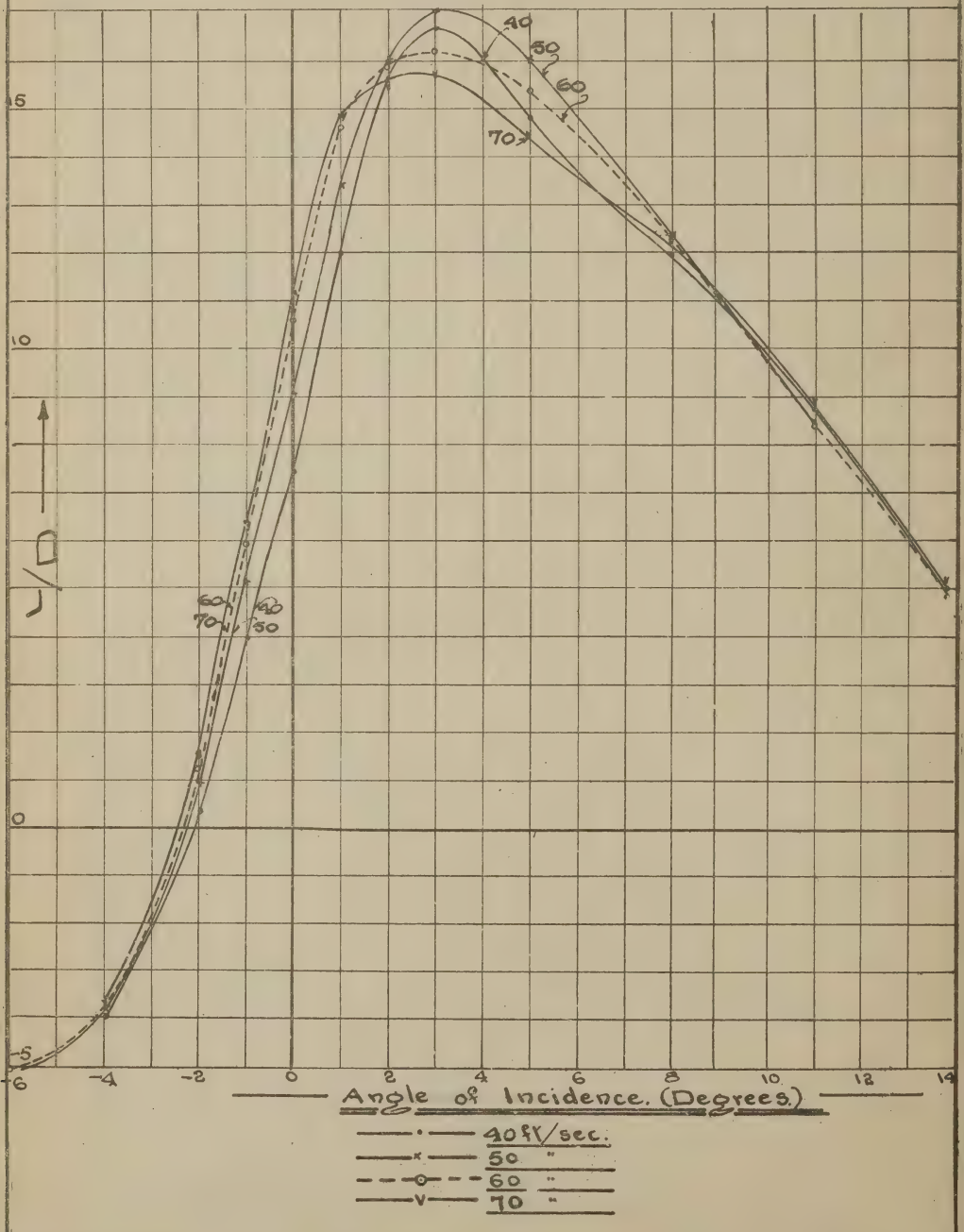

AEROFOILS FOR AIRSCREW DESIGN.

Aerofoil No 7 Series B.

Size of Plane 3 x 36

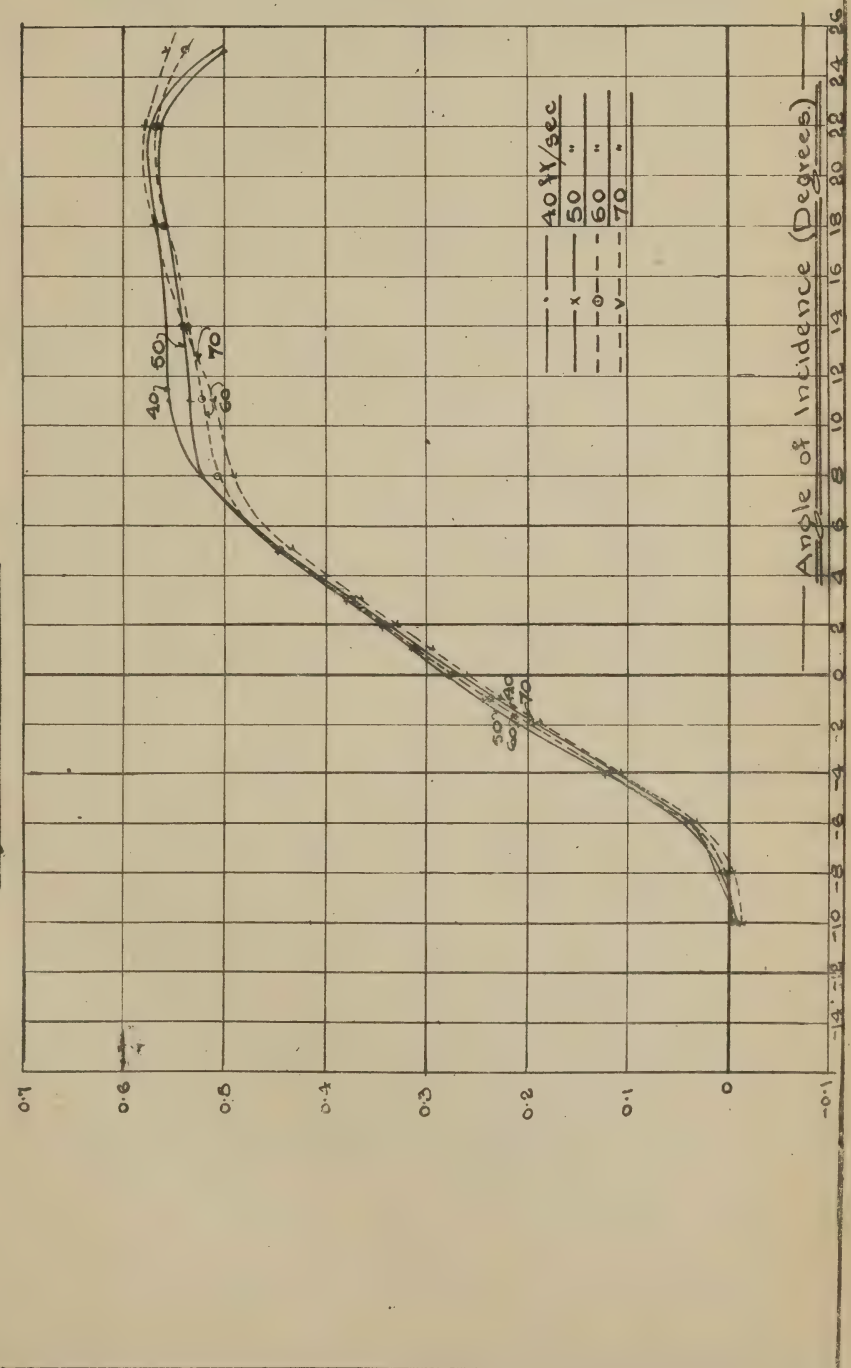

AEROFOILS FOR AIRSCREW DESIGN

Aerofoil Nº 7. Series B.

Size of Plane 6"X36".

——·—— 40 ft/sec.
——x—— 50 ft/sec.
----o---- 60 ft/sec.
——v—— 70 ft/sec.

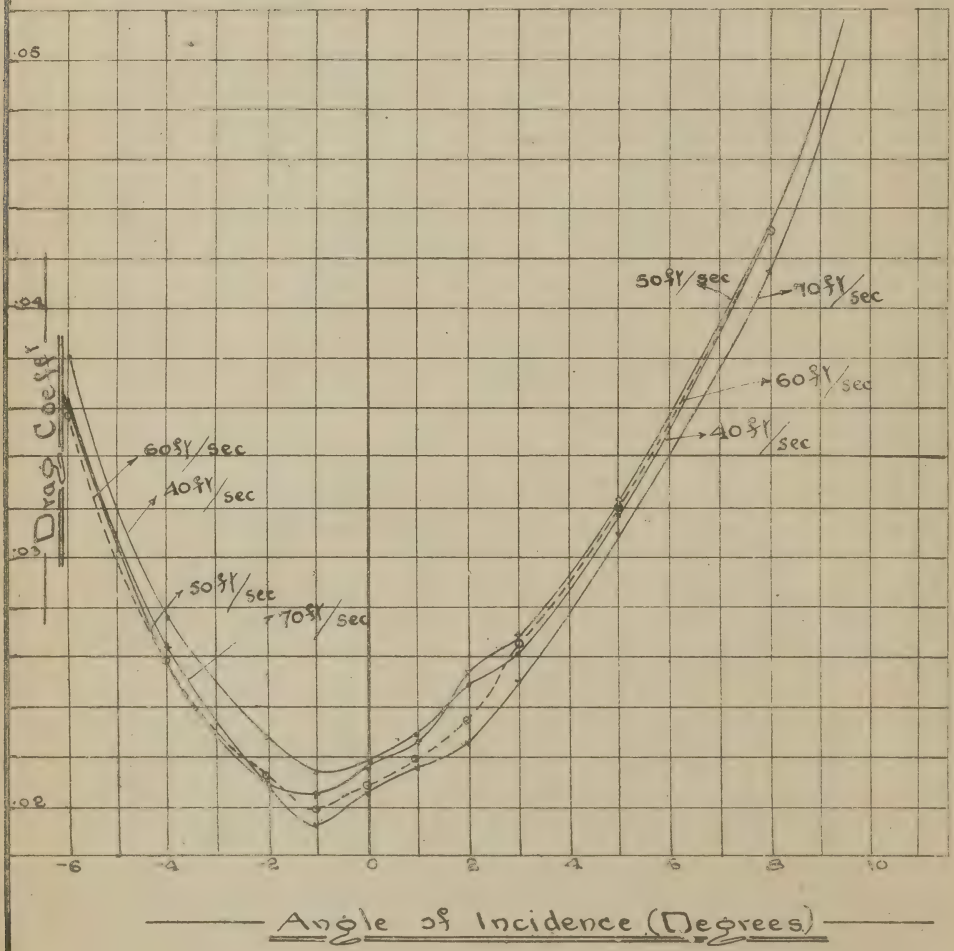

Angle of Incidence (Degrees)

AEROFOILS FOR AIRSCREW DESIGN.

Aerofoil Nº 7 Series B.

Size of Plane 6 X 36

—•— 40 ft/sec.
—x— 50 ft/sec.
- - -o- - - 60 ft/sec.
—v— 70 ft/sec.

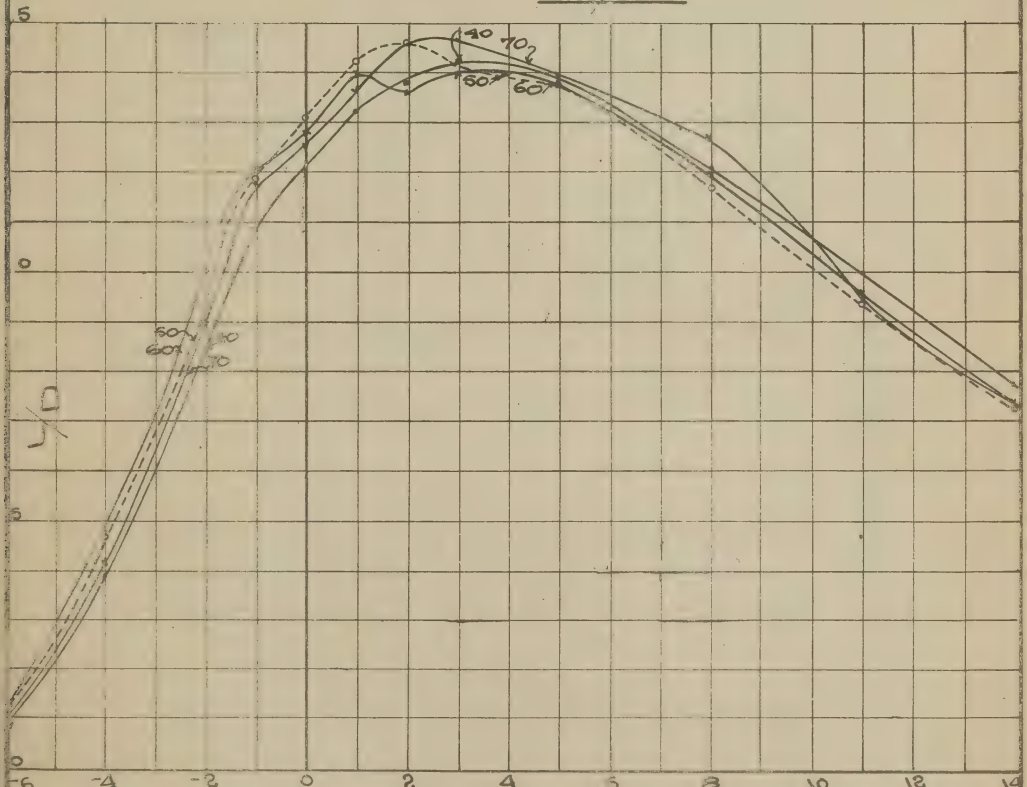

Angle of Incidence (Degrees)

AEROFOILS FOR AIRSCREW DESIGN.

R. A. F. 6A.

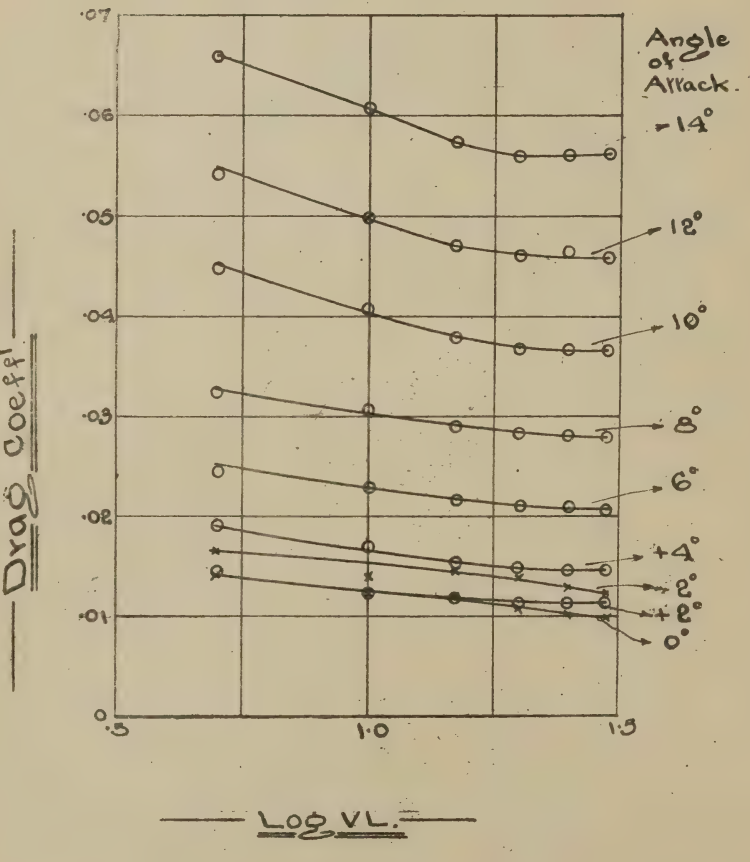

TABLE 24.

SERIES B, $x/c = 0{\cdot}375$.

AEROFOIL No. 7, CAMBER = 0·20.

Size of Plane, 6-inch by 36-inch. Speed, 40 ft./sec.

Angle. Degrees.	Drag Coefficient.	Lift Coefficient.	L/D.
− 10	0·0631	− 0·012	− 0·24
− 8	0·0511	+ 0·0102	+ 0·20
− 6	0·0380	0·0344	0·905
− 4	0·0275	0·106	3·85
− 2	0·0227	0·190	8·38
− 1	0·0213	0·232	10·9
0	0·0218	0·265	12·1
+ 1	0·0228	0·303	13·2
2	0·0248	0·338	13·7
3	0·0261	0·371	14·2
5	0·0317	0·442	13·9
8	0·0432	0·523	12·1
11	0·0558	0·554	9·94
14	0·0720	0·556	7·71
18	0·1024	0·565	5·55
22	0·1381	0·571	4·14
25	0·2040	0·508	2·49

AN INVESTIGATION INTO THE NATURE OF THE FLOW IN THE NEIGHBOURHOOD OF AN AIRSCREW.

By J. R. Pannell, A.M.I.M.E., and R. Jones, M.A.

Reports and Memoranda (*New Series*), *No.* 371. *December*, 1917.

Summary.—(*a*) *Introductory.* (*Reasons for inquiry.*)—The investigation was originally undertaken in response to a request from the R.N. Airship Station, Kingsnorth, for information as to the behaviour of the slip stream of an airscrew whose axis was inclined to the wind. The measurements were more particularly required at the same relative position behind the airscrew as the rudder occupies on the North Sea non-rigid airship. The request for the work was accompanied by the information that rudders had broken under certain circumstances, and it was suggested that the cause might be that during a turn the slip-stream from the airscrew struck the vertical stabilising surface. It was felt that the value of the investigation would be increased by observations of the structure of the slip-stream, and measurements were therefore taken, with the axis of the airscrew parallel to the wind, at varying distances from the airscrew. To define the motion completely a very large number of observations would be required, and though the observations made for this purpose occupy the greater part of the report the information is incomplete in many respects.

Diagrams showing the type of flow which occurs in the neighbourhood of an airscrew were given in the Italian Aeronautical Journal for 1912, but they were not accompanied by numerical values.

Similar investigations have also been carried out on aeroplanes at the R.A.F. and reported in R. & M. 382.

(*b*) *Range of the investigation.*—The airscrew used was a four-bladed one, 16 inches in diameter; it was mounted, with an electro-motor for driving it, on a portable framework, which could be moved about in the channel. The yawmeter was mounted on the chuck of the balance, the ends of the tubes being at the same height as the axis of the airscrew. The co-ordinates of the points at which observations were made were varied by moving the airscrew.

Experiments were carried out at wind speeds of 20 and 40 ft./sec. and rotational speeds of 1,080, 2,150 and 2,860 revs. per minute. Measurements were made in a section of the slip-stream 8 diameters behind the airscrew with the axis of the airscrew parallel to the stream and also yawed at angles of 10° and 20°. In addition, when the axis was parallel to the stream, observations were made at distances of 1, 3, 8 and 64 inches from the airscrew in the slip-stream and at 4 and 2 inches from the airscrew on the inflow side. The observations define the resultant velocity in magnitude and direction and the component velocities along the axes X, Y and Z have also been calculated; where the origin is fixed at the centre of the airscrew and the axes are drawn parallel to the channel axes, *i.e.*, the axis of X drawn down wind, &c.

The airscrew has been tested on the whirling arm and values of thrust and torque coefficients, and efficiency are given.

(*c*) *Conclusions. Axis yawed.*—Sufficient observations were obtained to define the path of the slip-stream at various values of the advance per rev., which, with a knowledge of the angular velocity of the ship, could enable the position of the slip-stream as it passes the rudders to be calculated.

Axis straight.—The minimum diameter of the slip-stream appears to lie between 0·2 and 0·5 diameter behind the airscrew and to have a value less than 0·75 of that of the airscrew. The limits of the slip-stream are very sharply defined within 0·5 airscrew diameter, but become less marked at greater distances, while the diameter of the slip-stream is greater than that of the airscrew. The boss of the airscrew has a marked effect in reducing the local velocity.

It is interesting to observe that the stream just outside the slip-stream but within 0·5 diameter of the airscrew has a velocity *less* than that of the undisturbed wind.

The spin of the air is inappreciable on the inflow side within 2 inches of the airscrew, but is very marked in the slip-stream and quite measurable at 8 diameters.

A selection of the results was compared on an advance per revolution base and showed good agreement at the overlapping points. It may be noted that the component along the direction of the channel becomes equal to the channel speed at the no thrust advance per rev. and that the spin vanishes at the no torque advance per rev.

(*d*) *Applications and further developments.*—The observations with the axis parallel to the wind should be repeated on a larger airscrew and additional sections observed, particularly between 0·5 and 3 diameters. Dr. Stanton has pointed out that useful information would be obtained from measurements of static pressure, particularly near the boundary of the slip-stream.

This investigation of the velocity and direction of the air flow behind an airscrew when the latter is either parallel to or inclined to the stream provides valuable data for the design of aeroplane and airship controls, and further measurements could usefully be made, with the axis yawed, at positions about 3 diameters behind the airscrew. Similar data should also be obtained for a more efficient airscrew.

The experiments were undertaken in response to a request from the Royal Naval Airship Station, Kingsnorth, for information as to the behaviour of the slip-stream from an airscrew, when the axis of the airscrew is inclined to the wind, the object of the investigation being to determine the position of the rudder of an airship relative to the slip-stream of the airscrew, when the ship is turning. It was thought desirable while the apparatus was erected in the channel to investigate also the structure of the slip-stream. Accordingly measurements were made with the direction and velocity meter (or yaw meter) when the airscrew axis was along the wind, at a number of positions, and values of the three velocity components u, v and w along the axes of X, Y and Z were calculated. The origin of co-ordinates is at the centre of the airscrew boss, and the positive directions of the three axes are X along the channel wind direction, Y to port

(*i.e.*, to the left when facing the wind), and Z vertically upwards. If, then, the angle between the plane ZOX and that containing the Z axis and the resultant wind (V) be α, and the angle between the direction of V and the plane XOY be β (*see* Fig. 3)

then
$$u = V \cos \alpha \cos \beta$$
$$v = V \sin \alpha \cos \beta$$
$$w = V \sin \beta.$$

The experiments were conducted in the No. 1 7-foot channel, with the airscrew rotating at three different speeds, viz., 1,080, 2,150 and 2,860 revolutions per minute.

For each of these three speeds observations were taken with the channel wind at rest, and also at wind speeds of 20 and 40 feet per second. With an airscrew of 16 inches diameter, values of U/nd ranging between 0·32 and 1·67 were thus obtained, where U is the channel speed, n the number of revolutions per minute, and d the diameter of the airscrew.

The sections of the slip-stream examined were those at 128 inches (8 diameters), 64 inches, 8 inches, 3 inches and 1 inch behind the airscrew. In the first case measurements were taken with the airscrew axis inclined at angles (Ψ) of 0°, 10° and 20° to the direction of U ; it was assumed that the rudder of an Astra Torres (North Sea type) airship, concerning which the information was required, would be about 8 diameters behind the airscrew. In addition two sections, 4 inches and 2 inches in front of the airscrew, were considered.

The investigation of any particular section consisted in taking measurements that would determine the three component speeds, at different points along the intersection of the vertical plane of the section and the horizontal plane through the airscrew axis. Observations were taken on both sides of the axis of the slip-stream, the radius being increased until the limits of the airscrew wake had been defined.

The yaw meter (which is described in detail in Rep. No. 156, 1914–15, p. 176) was mounted vertically on the balance, and could consequently be rotated about a vertical axis. The zero position (or datum relative to which subsequent angles were to be measured) for the horizontal tubes A and B was found by running the channel with only the yaw meter in place, and turning the balance until the pressures in the two tubes were equal. Having done this the direction of the plane containing the vertical and the resultant wind speed at any time, could be read off directly by turning the balance as before, until the pressures balanced. The difference between the two readings gave the angle α.

The determination of the angle β and the magnitude of V is not so straightforward. If the motion to be examined were two dimensional (*i.e.*, if β were zero), the difference of pressure between

one of the tubes A and B and the suction tube E would be exactly proportional to V^2, and a calibration at different wind speeds would suffice. But the inclination β of the wind to the horizontal plane has an appreciable effect on the pressures in A and B, and hence such a calibration will not determine the velocity in three dimensional problems. Moreover, until the magnitude of the resultant velocity V is known, the value of β cannot be determined, for the difference of pressure in the two remaining pressure tubes C and D also varies as V^2. Consequently, in order to have a complete calibration of the instrument, it was mounted horizontally on the balance so that rotation about a vertical axis was equivalent to a variation of the angle β. The difference of pressure was then observed (i) between the tubes A and E, and (ii) between the tubes C and D, at different wind speeds and various angles in the horizontal plane. A chart embodying all these observations was then prepared, in the manner devised by Mr. H. E. Collins, in which the C and D readings were plotted against the square roots of the A and E readings for particular speeds and angles (*see* Fig. 4). Values of V and β could now be read off for each position investigated. During the experiments the yaw meter was mounted vertically and the angle α determined in the manner described above ; then the C and D, and A and E observations were taken, with the yaw meter set in the position where the pressures in A and B balanced. On taking the square root of the A and E pressure difference, and finding the position on the chart corresponding to this, and the C and D difference, the values of V and β were obtained, whence on substituting in the formulæ given above u, v and w were easily calculated.

The four-bladed airscrew, details of which are given in Fig. 2 and Table 1, was mounted on a horizontal shaft, whose support was fixed to a movable frame on which also stood the motor for driving the airscrew. It is essential in experiments of this kind to support the yaw meter on the balance, and this method of support made it possible to move the airscrew about in the channel with its axis in a horizontal plane (*see* Fig. 1).

During the preliminary experiments the speed at which the airscrew rotated was measured with the aid of an electric bell and worm gear on the airscrew shaft. It was desired, however, to set the speed to a predetermined value, and as the method was unsuitable for this purpose it was rejected in favour of an electrical frequency meter. This was connected to a commutator attached to the end of the airscrew shaft. By this means it was possible to make 1, 2, 3, 4 or 5 contacts per revolution at will. The range of the frequency meter, which was only 45–55 cycles per second, was thus extended. The meter having been first calibrated by means of the bell and worm gear, a constant airscrew speed could be obtained by means of a variable resistance in the motor circuit.

Results.—The results are given in the tables* ; the magnitude of the resultant wind speed V and its direction angles α and β are given as well as the calculated components u, v and w, for all positions, and rotational and translational speeds. Most of the results have also been plotted and the curves are given in Figs. 5–16. Three methods of representing the results graphically have been resorted to.

(i) For U = 20 and 40 ft./sec. and n = 2,860 revs./min., a horizontal section of the slip-stream through the airscrew axis has been taken (*i.e.*, the plane Z = 0) and u — U has been compounded with v for all the points at which observations were taken. This gives the "*effect*" of the airscrew in this horizontal plane. The results are represented in Figs. 5 and 6. The horizontal positions of the sections x = — 4 ins., — 2 ins., 1 in. and 2 ins. are relatively correct, but those of x = 8 ins., 64 ins. and 128 ins. are purely arbitrary.

Further, to show the *effect* of the airscrew in a vertical plane perpendicular to the axis of the airscrew, the components v and w have been compounded for the same values of U and n for all the sections, viz., x = — 4 ins., — 2 ins., + 1 in., 3 ins., 8 ins., 64 ins. and 128 ins. (Fig. 7). The *heads* of the arrows give the co-ordinates of the positions in all three figures.

The results in Figs. 5, 6, 7 are shown as they would appear to an observer at rest relative to the undisturbed wind.

(ii) For the sections x = — 2 ins., 1 in., 3 ins. and 8 ins. (z = 0), the values of u/U, v/U and w/U have been plotted against U/nd for certain values of y, when the channel speed was 20 ft./sec. and 40 ft./sec. and for all three airscrew speeds (Figs. 8 and 9).

(iii) For the sections x = — 2 ins., + 1 in., 3 ins., 8 ins., 64 ins. and 128 ins., the values of u, v and w have been plotted against y ; z is, of course, = 0 throughout.

(iv) The airscrew has also been tested for thrust and torque on the whirling arm. The results are plotted against U/nd in Fig. 17, the absolute coefficients thrust and torque and the efficiency being given.

Remarks.—Mention may be made of the opportunities afforded to check the results when plotting values of u/U, v/U and w/U against U/nd (Fig. 9). The observations at 20 ft. per second were taken at values of U/nd between 0·32 and 0·84, and for those at 40 ft./sec. U/nd lay between 0·63 and 1·67. Plotting the results at the two wind speeds on a U/nd base, then, gives a curve of which the two parts determined at different wind speeds overlap. In a great majority of cases the overlapping parts coincide, the discrepancies arising when the observations were taken behind the airscrew boss, where apparently almost anything may happen (*see* especially the curves for x = + 1, Fig. 8).

* A list of the tables and figures is given on p. 305.

Figs. 5 and 6 give a clear idea of the manner in which the diameter of the slip-stream changes as the distance from the airscrew increases, the effect is, of course, most marked at 20 ft./sec. and $n = 2{,}860$ revs. per min. ; the observations made at $x = 3$ ins. and $x = 8$ ins. show the diameter to be about 0·75 of that of the airscrew at these points, though it is probably somewhat less for values of x between these two. The limits of the slip-stream are very sharply defined at $x = 3$ and $x = 8$, for while the flow is practically undisturbed at $y = 7$ ins., the velocity along the axis is increased by nearly 30 ft./sec. at $y = 6$ ins. (U = 20, $n = 2{,}860$ revs./min.). At $x = 64$ ins. the limits become less definite, the diameter being now approximately equal to that of the airscrew ; at $x = 128$ ins. the increase of velocity is still appreciable for $y = 11$ ins. The reduction of velocity due to the airscrew boss is clearly shown, particularly in Fig. 6, where at $x = 3$ ins. and $y = 0$ the velocity is reduced by 20 ft./sec. It may be noted that in Fig. 5 the observations up to $x = 8$ show that just outside the slip-stream the velocity is reduced below that of the undisturbed wind.

Fig. 7 shows the spin of the air in the slip-stream ; a striking feature of this diagram is the almost complete absence of the w component on the intake side at a distance of 2 inches from the airscrew.

Consider again Figs. 10–14 ; the curves show that v decreases rapidly (compared with w) as x increases ; w persists and decreases very slowly, and has quite an appreciable value at $x = 128$ ins. (Fig. 16) ; its maximum value there for the cases investigated is about 7·5 ft./sec. (U = 40 ft./sec.), the maximum value for that speed at $x = 1$ in. being of the order of 15 ft./sec. On the other hand, v hardly reaches 3·5 ft./sec. at $x = 8$ ins., though at $x = +1$ in. it has approximately the same maximum value as w.

On the intake side v is larger than w, and is of the same order of magnitude as in the wake ; v decreases as the distance from the boss increases. It is to be concluded from these considerations, then, that there is no appreciable spin on the intake side, but that considerable spin is set up in the wind as it passes between the airscrew blades, and persists at a fairly great distance away.

On examining the curves giving u, v and w plotted against y (Figs. 10–13), one of the first points that attract attention is the nature of the curves for u and w when U = 40 ft./ sec. and $n = 1{,}080$ revs./min., *i.e.*, $\mathrm{U}/nd = 1{\cdot}67$. u in this case never exceeds 40 ft./sec. (except to a slight extent when $x = 8$), but just reaches that limit outside the airscrew wake. Further, the sign of w is in this case for all positive values of x different from that at all the other values of U/nd considered. Moreover, the curves in Figs. 8 and 9 of w/U plotted against U/nd show that w vanishes at $\mathrm{U}/nd = 1$ approximately (taking an estimate from the curves $x = 1$ in., 3 ins. and 8 ins. for values of y not immediately behind the boss or on the

edge of the slip-stream), from which is deduced that the torque on the airscrew vanishes at $U/nd = 1$. Also, from the u/U curves, in the same figures, it is seen that $u/U = 1$ (or $u = U$) in the neighbourhood of $U/nd = 0{\cdot}95$, the deduction being that the airscrew thrust is zero at this value of U/nd. If now the curves giving the torque and thrust on the airscrew (Fig. 17) be continued to cut the horizontal axis, values of U/nd giving zero torque and thrust are obtained. These are 1·05 and 0·95 respectively, which compare with 1·0 and 0·95 deduced from the slip-stream experiments. It would thus appear that within the limits of the accuracy of the experiments the same results for these quantities are obtained, by a consideration of either of these experiments in which the methods are so widely different. The mean experimental pitch is given by the value of U/nd, for which the thrust vanishes multiplied by the diameter of the airscrew and is equal to 1·6 ft. When $U = 40$ ft./sec. and $n = 1{,}080$ revs./min., $U/nd = 1{\cdot}67$, which is greater than 0·95, and consequently under these circumstances the airscrew is running as a windmill.

If the angle between the airscrew axis and the undisturbed wind be Ψ, the effect of varying Ψ when $x = 128$ ins. can be seen from Figs. 15 and 16. In this set of experiments ($\Psi = 0$) observations were taken at equal positive and negative values of y, and the curves show that the velocity distribution is not symmetrical with regard to the axis $y = 0$, but rather with regard to $y = -1$ or $-1{\cdot}5$. This means that the central line of the slip-stream is displaced by that amount at $x = 128$ ins. This is further confirmed by the w curve ; w should vanish on the central line but in the curves w vanishes near $y = -1$ or $-1{\cdot}5$. The same " side effect " is evident at $x = 64$ ins., but in this case (as in all others except $x = 128$ ins.) the curves have all been plotted on the positive y side and a mean curve drawn. There is an apparent deviation from symmetry for small values of y, even at $x = 1$ in., 3 ins. and 8 ins., v and w do not vanish at $y = 0$, but this may be due to interference and disturbance caused by the boss.

A difficulty in drawing the curves at $\Psi = 10°$ Ψ and $= 20°$ was the paucity of observations ; this was especially the case at $\Psi = 20°$ and $n = 2{,}860$ revs./mins. It was only possible to obtain readings to define one side of the slip-stream on account of the fact that the yaw meter was mounted in the centre of the channel, and the airscrew support came into contact with the side of the channel for a value of $y = 18{\cdot}5$ ins. In drawing the curves, then, those for $\Psi = 0$ have been used as a guide as far as the introduction of maxima and minima is concerned ; the u curves in Fig. 15 show that the boss has an effect when $\Psi = 0$, and it was thought likely that the same effect would be present at $\Psi = 10°$ and 20°, particularly as in some cases (Fig. 15, $\Psi = 20°$, $U = 40$ ft./sec., $n = 1{,}080$ and 2,150 revs./min.) a curve drawn through the observed values definitely shows that a minimum exists.

Further, as w should change sign on the centre line of the slip-stream, values of y at which w vanishes in the curves of Fig. 16 have been taken as indicating the positions of the minima in the u curves. The variation of the form of the curves with changing U/nd is worthy of note. The two curves at which $U/nd = 0{\cdot}84$ (viz., those for which U = 20 ft./sec., n = 1,080 revs./min., and U = 40 ft./sec., n = 2,150 revs./min.) are similar to one another in the sets of curves for each of the three components, the ordinates of those in which U = 40 ft./sec. being, of course, twice the ordinates of those in which U = 20 ft./sec. An examination of the curves for u in Fig. 15 shows the minima displaced continuously for a variation in U/nd from (in the case of $\Psi = 20°$) about $y = 17$ ins., when $U/nd = 0{\cdot}32$ to $y = -1$ in., when $U/nd = 1{\cdot}67$.

In drawing the curves for the components on a y base, the natural tendency is to smooth out small irregularities which arise if the curves be drawn through the observations. Except, however, for a few values which appear to be mere errors of observation, the plotted points define curves the characteristics of which are faithfully reproduced at other rotational and translational speeds. A good example of this is shown in the curves for w in Fig. 11, the "kink" which appears between $y = 5$ ins. and $y = 7$ ins. being present in every one of the nine curves. The effect is also just perceptible in some of the curves for v. It is difficult to believe that the effect is due to the observations at $y = 5$ ins. and 7 ins. and $y = 6$ ins. having been made on opposite sides of the axis of the slip-stream, since the displacement required to bring the observations on a smooth curve for values of y from 5 to 7 ins. would cause appreciable discrepancies in the regions of $y = 1$ in., 2 ins. and 3 ins. Moreover, the value of y can be determined to one or two hundredths of an inch, and the slip-stream can hardly have been deflected appreciably when $x = 1$.

Experiments were carried out at the Royal Aircraft Factory on the velocity of the slip-stream behind the airscrew of an aeroplane of the pusher type (R. & M. 382). It is there concluded :

> "(*b*) That the slip-stream has a very sharp edge.
>
> "(*c*) That the shape of the stream does not change appreciably with the thrust, or with the distance behind the screw within the range of the experiment.
>
> "(*d*) That the shape of the stream is a tube with a mean outside diameter approximately equal to 0·8 times the airscrew diameter and an inside diameter of about 0·2 times the airscrew diameter."

Only measurements of the velocity along the axis of x were made, and the conditions under which these measurements were

taken differ from those of the present experiments in the presence of the aeroplane body in front of the airscrew. No strict comparison of the results can therefore be made, nor are observations available in the two reports at the same distance behind the airscrew. The shortest distance in R. & M. 382 was 0·76 airscrew diameter; the position in the present experiments nearest to this value was 0·50. If we consider the results obtained at this section we find that the "conclusion *b*" is supported, for in Fig. 5 the value of $u - U$ changes from the order of 30 ft. per second to practically zero in passing from $y = 6$ ins. to $y = 7$ ins.

"Conclusion *c*" is probably true over the range of the experiments of R. & M. 382, though the present experiments show a marked change of diameter with x. In connection with "conclusion *d*" (still referring to Fig. 5) we find the diameter of the slip-stream to lie between 0·75 and 0·85 of that of the airscrew; the limits of the low velocity region at the axis of the slip-stream are less well defined than in R. & M. 382 presumably on account of the absence of the aeroplane body in the present experiments.

List of Tables.

1. Dimensions of airscrew.
2. Results at $\Psi = 0$, $x = -4$ inches.
3. Results at $\Psi = 0$, $x = -2$ inches.
4. Results at $\Psi = 0$, $x = -1$ inch.
5. Results at $\Psi = 0$, $x = 0$ inch.
6. Results at $\Psi = 0$, $x = +1$ inch.
7. Results at $\Psi = 0$, $x = +3$ inches.
8. Results at $\Psi = 0$, $x = +8$ inches.
9. Results at $\Psi = 0$, $x = +64$ inches.
10. Results at $\Psi = 0$, $x = +128$ inches.
11. Results at $\Psi = 10°$, $x = +128$ inches.
12. Results at $\Psi = 20°$, $x = +128$ inches.

List of Figures.

1. Apparatus—Airscrew support.
2. Airscrew.
3. System of axes.
4. Calibration chart of the yaw meter.
5. Flow in a horizontal section ($z = 0$) U = 40 ft./sec., $n = 2{,}860$ revs./min.
6. Flow in a horizontal section ($z = 0$) U = 20 ft./sec., $n = 2{,}860$ revs./min.
7. Flow in vertical sections ; speeds as in Figs. 5 and 6.
8. $\frac{u}{U}$, $\frac{v}{U}$ and $\frac{w}{U}$ plotted against $\frac{U}{nd}$. $x = -2$ ins. and $+1$ in.
9. $\frac{u}{U}$, $\frac{v}{U}$ and $\frac{w}{U}$ plotted against $\frac{U}{nd}$. $x = +3$ ins. and 8 ins.
10–14. u, v and w plotted against y for $x = -2$ ins., $+1$ in., 3 ins., 8 ins., 64 ins.
15. u plotted against y, $x = 164$ ins. } Airscrew axis being inclined to the undisturbed wind at angles of 0°, 10° and 20°.
16. w plotted against y, $x = 164$ ins. }
17. Results of tests of the airscrew on the whirling arm.

Table 1.

DIMENSIONS OF AIRSCREW.

Mean Values.

Radius (inches).	Chord (inches).	Maximum thickness (fraction of chord).	Angle.
8·00	0	—	—
7·28	0·83	0·104	17° 20′
6·07	1·27	0·091	21° 30′
4·85	1·45	0·097	26° 30′
3·64	1·30	0·129	33° 53′
2·41	1·01	0·227	44° 52′
1·21	0·80	0·436	62° 0′

Table 2.

$x = -4''$, $\Psi = 0$.

U ft./sec.	n R.P.M.	V ft./sec.	α degrees.	β degrees.	u ft./sec.	v ft./sec.	w ft./sec.
			$y = 0$.				
0	1080	5·8	0	− 2·0	5·8	0	− 0·2
	2150	11·5	0	− 1·0	11·5	0	− 0·2
	2860	15·7	− 0·4	− 0·5	15·7	− 0·1	− 0·1
20	1080	18·9	0	+ 0·5	18·9	0	+ 0·2
	2150	23·5	+ 0·2	+ 0·8	23·5	0	+ 0·3
	2860	26·5	+ 0·1	+ 0·5	26·5	0	+ 0·2
40	1080	36·3	+ 0·1	+ 1·2	36·3	+ 0·1	+ 0·8
	2150	38·0	+ 0·1	+ 1·1	38·0	+ 0·1	+ 0·7
	2860	40·6	+ 0·1	+ 1·0	40·6	+ 0·1	+ 0·7
			$y = + 3''$.				
0	1080	5·6	− 12·0	− 1·0	5·5	− 1·2	+ 0·1
	2150	12·6	− 12·0	− 0·5	12·3	− 2·6	+ 0·1
	2860	17·0	− 12·0	− 0·2	16·6	− 3·5	+ 0·1
20	1080	19·8	+ 0·7	+ 0·8	19·8	+ 0·2	+ 0·3
	2150	24·6	− 1·4	+ 0·8	24·6	− 0·6	+ 0·3
	2860	27·8	− 2·8	+ 0·7	27·8	− 0·9	+ 0·3
40	1080	37·6	+ 1·3	+ 1·2	37·5	+ 0·9	+ 0·8
	2150	40·0	+ 0·7	+ 1·2	40·0	+ 0·5	+ 0·8
	2860	42·8	0	+ 0·8	42·8	0	+ 0·6

TABLE 2—*continued.*

$x = -4''$, $\Psi = 0$.

U ft./sec.	n R.P.M.	V ft./sec.	α degrees.	β degrees.	u ft./sec.	v ft./sec.	w ft./sec.
			$y = +6''$.				
0	1080	5·8	−32·0	−4·0	4·9	−3·1	−0·4
	2150	11·8	−29·5	−2·0	10·3	−5·8	−0·4
	2860	15·6	−29·0	−1·0	13·7	−7·2	−0·3
20	1080	20·6	+0·5	0	20·6	+0·2	0
	2150	24·1	−4·6	+0·3	24·1	−1·9	+0·1
	2860	26·8	−7·9	+0·4	26·7	−3·7	+0·2
40	1080	38·7	+1·8	+1·0	38·7	+1·2	+0·7
	2150	40·5	+0·4	+0·8	40·5	+0·3	+0·6
	2860	42·8	−1·4	+0·8	42·8	−1·0	+0·6
			$y = +9''$.				
0	1080	3·3	−45·0	−2·0	2·3	−2·3	−0·1
	2150	7·1	−44·0	−3·0	5·1	−4·9	−0·4
	2860	10·0	−42·0	0	7·4	−6·7	0
20	1080	20·4	+0·8	+1·1	20·4	+0·3	+0·4
	2150	21·8	−4·8	+1·0	21·6	−1·8	+0·4
	2860	22·5	−8·1	+1·5	22·3	−3·2	+0·6
40	1080	39·3	+1·8	+1·0	39·3	+1·2	+0·7
	2150	40·1	+0·2	+1·2	40·1	+0·1	+0·8
	2860	41·2	−1·7	+1·0	41·2	−1·2	+0·7
			$y = +11''$.				
0	1080	—	—	—	—	—	—
	2150	4·1	−42·0	—	—	—	—
	2860	—	−42·0	—	—	—	—
20	1080	20·3	+0·4	+0·5	20·3	+0·1	+0·2
	2150	20·5	−3·9	+0·5	20·5	−1·4	+0·2
	2860	21·0	−6·7	+0·5	20·9	−2·4	+0·2
40	1080	40·0	+1·1	+0·8	40·0	+0·8	+0·6
	2150	40·0	0	+1·1	40·0	0	+0·8
	2860	40·3	−1·3	+1·1	40·3	−0·9	+0·8

Table 3.

$x = -2''$, $\Psi = 0$.

U ft./sec.	n R.P.M.	V ft./sec.	α degrees.	β degrees.	u ft./sec.	v ft./sec.	w ft./sec.
			$y = -1{\cdot}85''$.				
0	1080	7·0	+ 2·0	+ 4·3	7·0	+ 0·2	+ 0·5
	2150	16·0	+ 2·5	− 0·2	16·0	+ 0·7	− 0·1
	2860	21·8	+ 2·8	− 0·5	21·8	+ 1·1	− 0·2
20	1080	19·0	− 3·5	+ 0·5	19·0	− 1·2	+ 0·2
	2150	24·8	− 2·6	+ 0·4	24·8	− 1·1	+ 0·2
	2860	28·9	− 1·9	+ 0·3	28·9	− 1·0	+ 0·2
40	1080	36·5	− 2·9	+ 1·8	36·5	− 1·8	+ 1·1
	2150	38·2	− 2·9	+ 1·6	38·2	− 1·9	+ 1·1
	2860	40·9	− 2·8	+ 1·3	40·8	− 2·0	+ 0·9
			$y = -5''$.				
0	1080	9·0	+ 25·0	+ 4·0	8·2	+ 3·4	+ 0·6
	2150	19·7	+ 24·5	− 0·7	17·9	+ 8·2	− 0·2
	2860	25·9	+ 24·0	− 0·8	23·7	+ 9·6	− 0·4
20	1080	20·7	− 1·1	+ 0·5	20·7	− 0·4	+ 0·2
	2150	27·9	+ 3·7	+ 0·1	27·9	+ 1·9	0
	2860	33·8	+ 8·0	+ 0·1	33·5	+ 4·6	+ 0·1
40	1080	37·2	− 2·7	+ 1·2	37·1	− 1·8	+ 0·8
	2150	40·9	− 0·9	+ 1·0	40·9	− 0·7	+ 0·7
	2860	45·5	+ 1·1	+ 1·0	45·5	+ 0·9	+ 0·8
			$y = -7{\cdot}5''$.				
0	1080	5·0	+ 50·0	− 2·0	5·2	+ 6·1	− 0·3
	2150	15·5	+ 50·0	− 1·0	9·7	+ 11·9	− 0·3
	2860	21·2	+ 48·2	− 1·2	13·9	+ 15·8	− 0·4
20	1080	20·9	0	+ 0·5	20·9	0	+ 0·2
	2150	25·1	+ 9·3	+ 0·5	24·7	+ 4·0	+ 0·2
	2860	28·7	+ 14·1	+ 0·5	27·9	+ 6·8	+ 0·2
40	1080	38·4	− 2·7	+ 1·2	38·3	− 1·8	+ 0·7
	2150	40·3	+ 0·1	+ 1·2	40·3	+ 0·1	+ 0·8
	2860	43·0	+ 3·3	+ 1·0	43·0	+ 2·5	+ 0·8

TABLE 3—*continued.*

$x = -2''$, $\Psi = 0$.

U ft./sec.	n R.P.M.	V ft./sec.	α degrees.	β degrees.	u ft./sec.	v ft./sec.	w ft./sec.
			$y = +3''$.				
0	1080	8·9	−11·0	−2·0	8·8	−1·7	−0·3
	2150	18·0	−9·7	−1·0	17·8	−2·8	−0·3
	2860	23·7	−9·7	−1·0	23·3	−4·0	−0·4
20	1080	20·0	+1·9	+0·9	20·0	+0·6	+0·4
	2150	27·2	−0·1	+0·2	27·0	0	+0·1
	2860	32·8	−1·2	+0·3	32·8	−0·7	+0·2
40	1080	37·1	+2·3	+1·0	37·1	+1·5	+0·6
	2150	40·4	+2·3	+1·1	40·4	+1·6	+0·8
	2860	44·5	+1·7	+0·9	44·5	+1·3	+0·9
			$y = +6''$.				
0	1080	8·5	−33·0	0	7·1	−4·6	0
	2150	18·1	−34·0	−0·5	15·0	−10·1	−0·2
	2860	24·3	−33·3	−1·2	20·3	−13·3	−0·5
20	1080	20·6	+0·4	+0·6	20·6	+0·2	+0·2
	2150	27·8	−7·1	+0·2	27·7	−3·4	+0·1
	2860	33·2	−11·2	+0·3	32·6	−6·4	+0·2
40	1080	37·9	+2·8	+1·2	37·8	+1·9	+0·8
	2150	40·9	+0·4	+1·0	40·9	+0·3	+0·7
	2860	45·2	−2·2	+0·9	45·2	−1·7	+0·7
			$y = +9''$.				
0	1080	5·5	−50·0	−2·0	3·5	−4·2	−0·2
	2150	10·0	−55·0	+1·0	5·7	−8·2	+0·2
	2860	13·5	−55·0	0	7·8	−11·0	0
20	1080	20·2	0	+0·5	20·2	0	+0·2
	2150	22·1	−7·7	+1·0	21·9	−3·0	+0·4
	2860	23·3	−13·4	+1·0	22·7	−5·4	+0·4
40	1080	39·6	+2·0	+1·2	39·5	+1·4	+0·8
	2150	40·4	+0·1	+0·9	40·4	+0·1	+0·7
	2860	40·9	−2·5	−1·1	40·8	−1·8	−0·8

Table 4.

$x = -1''$, $\Psi = 0$.

U ft./sec.	n R.P.M.	V ft./sec.	α degrees.	β degrees.	u ft./sec.	v ft./sec.	w ft./sec.
			$y = -7{\cdot}5''$.				
0	1080	10·4	+ 58·0	− 2·0	− 5·5	+ 8·8	− 0·4
	2150	23·0	+ 58·0	− 1·4	− 12·2	+ 19·5	− 0·6
	2860	29·6	+ 56·8	− 1·3	− 16·2	+ 24·7	− 0·7
20	1080	20·6	0	+ 0·3	20·6	0	+ 0·1
	2150	27·4	+ 13·2	+ 0·3	26·7	+ 6·1	+ 0·1
	2860	33·6	+ 21·8	− 0·3	31·1	+ 11·6	− 0·2
40	1080	39·0	− 3·5	+ 1·0	38·9	− 2·4	+ 0·7
	2150	41·1	+ 0·4	+ 1·0	41·1	+ 0·3	+ 0·7
	2860	45·1	+ 4·8	+ 0·9	44·9	+ 3·8	+ 0·7

Table 5.

$x = 0$, $\Psi = 0$.

U ft./sec.	n R.P.M.	V ft./sec.	α degrees.	β degrees.	u ft./sec.	v ft./sec.	w ft./sec.
			$y = -9''$.				
0	1080	6·0	+ 87·0	− 2·0	0·3	+ 6·0	− 0·2
	2150	12·5	+ 94·0	− 1·0	−0·9	+ 12·5	− 0·2
	2860	17·1	+ 96·0	− 1·0	−1·8	+ 17·0	− 0·2
20	1080	20·3	0	+ 0·5	20·3	0	+ 0·2
	2150	18·1	+ 12·6	+ 1·0	17·6	+ 4·0	+ 0·3
	2860	17·0	+ 20·4	+ 1·5	15·9	+ 5·9	+ 0·4
40	1080	41·2	− 3·0	+ 0·6	41·2	− 2·2	+ 0·4
	2150	40·0	+ 0·2	+ 1·3	40·0	+ 0·1	+ 0·9
	2860	38·8	+ 4·3	+ 1·5	38·6	+ 2·9	+ 1·0

Table 6.

$x = +1''$, $\Psi = 0$.

U ft./sec.	n R.P.M.	V ft./sec.	α degrees.	β degrees.	u ft./sec.	v ft./sec.	w ft./sec.
			$y = 1''$.				
0	1080	—	—	—	—	—	—
	2150	17·0	− 30·5	− 47·0	10·0	− 5·9	− 12·4
	2860	23·0	− 31·5	− 44·0	14·1	− 8·6	− 16·0
20	1080	8·5	− 14·0	− 6·0	8·2	− 2·0	− 0·9
	2150	12·0	− 23·0	− 60·0	5·5	− 2·3	− 10·4
	2860	17·0	− 28·0	− 63·0	6·8	− 3·6	− 15·2
40	1080	24·0	− 12·3	+ 10·5	23·0	− 5·0	+ 4·4
	2150	23·3	− 14·7	− 14·0	21·8	− 5·5	− 5·6
	2860	24·3	− 16·5	− 28·0	20·6	− 6·3	− 11·4
			$y = +3''$.				
0	1080	13·6	− 9·5	− 27·0	12·0	− 2·0	− 6·2
	2150	27·8	− 9·5	− 25·1	24·8	− 4·2	− 11·8
	2860	37·0	− 9·4	− 25·0	30·9	− 5·6	− 15·6
20	1080	20·2	− 3·3	− 3·0	20·0	− 1·1	− 3·0
	2150	32·4	− 4·6	− 18·1	30·6	− 2·5	− 10·1
	2860	41·7	− 5·3	− 20·2	38·8	− 3·6	− 14·4
40	1080	36·0	− 2·6	+ 10·8	35·4	− 1·6	+ 6·7
	2150	40·7	− 3·4	− 3·6	40·5	− 2·4	− 2·3
	2860	48·1	− 3·9	− 10·8	47·2	− 3·2	− 9·0
			$y = +5''$.				
0	1080	19·2	− 16·9	− 18·0	17·0	− 5·3	− 5·9
	2150	37·8	− 16·3	− 16·9	34·7	− 10·2	− 11·0
	2860	49·4	− 16·1	− 17·3	45·4	− 13·0	− 14·7
20	1080	21·9	− 2·7	− 3·4	21·7	− 1·0	− 1·3
	2150	38·2	− 7·9	− 12·4	36·9	− 5·1	− 8·2
	2860	49·2	− 9·9	− 14·9	46·7	− 8·2	− 12·6
40	1080	34·5	+ 0·8	+ 8·3	34·1	+ 0·5	+ 5·0
	2150	43·7	− 2·5	− 3·3	43·5	− 1·9	− 2·5
	2860	53·8	− 4·5	− 8·6	52·8	− 4·2	− 8·0

TABLE 6—*continued.*

$x = +1''$, $\Psi = 0$.

U ft./sec.	n R.P.M.	V ft./sec.	α degrees.	β degrees.	u ft./sec.	v ft./sec.	w ft./sec.
			$y = +7''$.				
0	1080	+ 6·6	− 1·61	− 11·5	− 6·1	− 2·2	− 1·3
	2150	10·6	− 1·61	− 16·5	− 9·5	− 3·3	− 3·0
	2860	13·6	− 1·65	− 14·5	− 12·6	− 3·4	− 3·4
20	1080	21·2	− 2·6	− 2·0	21·2	− 1·0	− 0·7
	2150	34·8	− 14·5	− 8·8	33·4	− 8·6	− 5·3
	2860	44·8	− 20·4	− 11·0	41·3	− 15·4	− 8·6
40	1080	38·5	+ 1·8	0	38·5	+ 1·2	0
	2150	42·6	− 2·3	− 1·8	42·5	− 1·7	− 1·3
	2860	50·7	− 6·9	− 5·3	50·0	− 6·0	− 4·6
			$y = -2''$.				
0	1080	11·0	+ 7·8	+ 26·0	9·8	+ 1·4	+ 4·8
	2150	24·5	+ 7·5	+ 31·0	20·8	+ 2·7	+ 12·6
	2860	31·5	+ 7·2	+ 32·0	23·7	+ 3·2	+ 16·7
20	1080	18·8	+ 6·5	+ 3·0	18·6	+ 2·1	+ 1·0
	2150	26·5	+ 4·2	+ 22·0	24·5	+ 1·8	+ 9·9
	2860	33·5	+ 5·6	+ 26·0	30·0	+ 2·9	+ 14·7
40	1080	36·1	+ 5·3	− 11·5	35·1	+ 3·3	− 7·2
	2150	38·1	+ 6·5	+ 5·5	37·6	+ 4·3	+ 3·6
	2860	42·1	+ 5·1	+ 14·2	40·5	+ 3·6	+ 10·3
			$y = -6''$.				
0	1080	19·0	+ 21·0	+ 14·5	17·0	+ 6·6	+ 4·8
	2150	37·4	+ 20·6	+ 15·0	34·8	+ 12·8	+ 9·7
	2860	49·8	+ 20·2	+ 14·8	45·0	+ 16·6	+ 12·7
20	1080	21·5	+ 1·6	+ 3·0	21·4	+ 0·6	+ 1·1
	2150	36·5	+ 9·8	+ 10·8	35·4	+ 6·1	+ 6·8
	2860	47·6	+ 12·7	+ 12·4	45·3	+ 10·2	+ 10·2
40	1080	36·0	− 2·3	− 2·8	35·9	− 1·4	− 1·8
	2150	42·5	+ 2·1	+ 3·4	42·3	+ 1·5	+ 2·5
	2860	52·3	+ 5·2	+ 7·3	51·8	+ 4·7	+ 6·7

TABLE 6—*continued.*

$x = +1''$, $\Psi = 0$.

U ft./sec.	n R.P.M.	V ft./sec.	α degrees.	β degrees.	u ft./sec.	v ft./sec.	w ft./sec.
			$y = -8''$.				
0	1080	—	—	—	—	—	—
	2150	6·0	−207	—	−5·3	+2·7	—
	2860	8·3	−227	—	−5·7	+6·1	—
20	1080	20·0	+1·7	−0·2	20·0	+0·6	+0.1
	2150	17·3	+3·6	+1·0	17·3	+1·1	+0·3
	2860	12·0	+9·2	+6·0	11·8	+1·9	+1·2
40	1080	40·0	−2·2	+3·0	39·8	−1·5	+2·1
	2150	39·7	+2·0	−0·5	39·7	+1·4	−0·4
	2860	38·2	+5·6	−0·8	38·0	+3·7	−0·5

TABLE 7.

$x = +3''$, $\Psi = 0$.

U ft./sec.	n R.P.M.	V ft./sec.	α degrees.	β degrees.	u ft./sec.	v ft./sec.	w ft./sec.
			$y = 0$.				
0	1080	10·2	−5·0	+3·5	10·1	−0·9	+0·6
	2150	15·9	−11·6	+10·0	15·3	−2·5	+2·7
	2860	24·2	−11·7	+7·4	23·4	−4·8	+3·1
20	1080	9·2	+10·0	−9·0	8·9	+1·6	−1·4
	2150	12·0	+3·0	−13·0	11·7	+0·6	−2·7
	2860	18·0	−2·0	−8·5	17·8	−0·6	−2·7
40	1080	19·8	+4·7	+5·0	19·5	+1·6	+1·7
	2150	19·6	+7·3	−11·0	19·1	+2·4	−3·7
	2860	20·3	+4·7	−12·5	19·7	+1·6	−4·4
			$y = +3''$.				
0	1080	15·3	−8·0	−23·0	13·9	−2·0	−6·0
	2150	31·9	−7·9	−23·5	28·9	−4·0	−12·7
	2860	42·3	−7·9	−22·6	38·6	−5·3	−16·2
20	1080	20·6	−2·8	−4·0	20·5	−1·0	−1·4
	2150	34·1	−5·8	−17·5	32·3	−3·3	−10·3
	2860	44·1	−6·0	−20·0	41·1	−4·3	−15·1
40	1080	36·0	−1·7	+12·5	35·1	−1·0	+7·8
	2150	40·2	−2·9	−4·2	39·9	−2·0	−2·9
	2860	48·4	−3·7	−11·9	47·1	−3·1	−10·0

TABLE 7—*continued.*

$x = +3''$, $\Psi = 0$.

U ft./sec.	n R.P.M.	V ft./sec.	α degrees.	β degrees.	u ft./sec.	v ft./sec.	w ft./sec.
			$y = +5''$.				
0	1080	20·2	− 8·6	− 18·3	18·9	− 2·8	− 6·3
	2150	40·9	− 8·9	− 16·9	38·5	− 6·1	− 11·9
	2860	53·9	− 8·8	− 17·5	49·8	− 7·7	− 16·2
20	1080	22·1	− 2·0	− 3·4	22·0	− 0·8	− 1·3
	2150	40·1	− 5·7	− 13·1	37·8	− 3·9	− 9·1
	2860	53·0	− 6·8	− 15·0	50·9	− 6·0	− 13·7
40	1080	37·8	+ 0·6	+ 5·2	37·6	+ 0·4	+ 3·4
	2150	43·8	− 1·9	− 3·6	43·7	− 1·4	− 2·8
	2860	55·0	− 3·5	− 9·2	54·3	− 3·3	− 8·8
			$y = +7''$.				
0	1080	2·6	—	− 6·5	2·6	—	− 0·3
	2150	2·7	—	− 11·5	2·6	—	− 0·5
	2860	3·6	—	—	3·6	—	—
20	1080	21·9	− 1·8	− 2·0	21·9	− 0·7	− 0·8
	2150	33·6	− 8·9	− 11·6	32·5	− 5·1	− 6·7
	2860	18·6	+ 6·1	− 14·3	17·9	+ 1·9	− 4·6
40	1080	39·0	+ 1·0	0	39·0	+ 0·7	0
	2150	43·0	− 1·6	− 2·1	42·9	− 1·2	− 1·6
	2860	51·5	− 4·2	− 5·4	51·0	− 3·7	− 4·8
			$y = -2''$.				
0	1080	13·5	+ 6·9	− 23·0	12·4	+ 1·5	− 5·3
	2150	27·3	+ 6·3	+27·5	24·0	+ 2·6	+ 12·7
	2860	36·6	+ 6·5	+ 27·0	32·4	+ 3·7	+ 16·6
20	1080	14·0	+ 5·7	+ 3·5	13·9	+ 1·4	+ 0·9
	2150	28·0	+ 8·0	+ 23·0	25·5	+ 3·6	+ 11·0
	2860	35·5	+ 6·9	+ 25·0	31·9	+ 3·9	+ 15·0
40	1080	36·0	+ 3·2	− 11·5	35·6	+ 2·0	− 7·2
	2150	39·0	+ 6·5	+ 6·2	38·5	+ 4·4	+ 4·3
	2860	43·4	+ 7·2	+ 15·1	41·6	+ 5·2	+ 11·3

TABLE 7—*continued*.

$x = +3''$, $\Psi = 0$.

U ft./sec.	n R.P.M.	V ft./sec.	α degrees.	β degrees.	u ft./sec.	v ft./sec.	w ft./sec.
			$y = -6''$.				
0	1080	14·9	+6·2	+41·0	11·2	+1·2	+9·8
	2150	34·2	+7·5	+36·0	27·3	+3·6	+20·0
	2860	45·5	+7·7	+27·0	40·2	+5·4	+20·6
20	1080	21·6	+1·0	+3·0	21·6	+0·4	+1·1
	2150	38·3	+5·7	+9·8	37·4	+3·8	+6·5
	2860	50·8	+6·8	+11·1	49·5	+5·9	+9·8
40	1080	35·1	−1·6	−4·1	34·9	−1·0	−2·5
	2150	42·9	+1·4	+3·5	42·7	+1·0	+2·6
	2860	54·0	+3·4	+7·1	53·5	+3·2	+6·7
			$y = -8''$.				
20	1080	20·1	+0·8	0	20·1	+0·3	0
	2150	18·3	+6·0	+0·5	18·1	+1·9	+0·2
	2860	16·8	+8·0	+1·0	16·8	+2·3	+0·3
40	1080	40·2	−1·1	+2·1	40·1	−0·8	+1·5
	2150	40·3	+1·1	+0·4	40·3	+0·8	+0·3
	2860	40·0	+2·8	+0·5	39·9	+2·0	+0·3

TABLE 8.

$x = +8''$, $\Psi = 0$.

U ft./sec.	n R.P.M.	V ft./sec.	α degrees.	β degrees.	u ft./sec.	v ft./sec.	w ft./sec.
			$y = 0$.				
0	1080	11·5	+1·5	+4·0	11·5	+0·3	+0·8
	2150	21·6	−1·0	−28·5	18·9	−0·3	−10·2
	2860	27·0	−7·5	−18·5	25·4	−3·3	−8·6
20	1080	15·0	+3·5	−6·0	14·8	+0·9	−1·6
	2150	22·4	+1·0	−16·0	21·6	+0·4	−6·2
	2860	28·6	−3·3	−19·0	26·9	−1·6	−8·7
40	1080	26·0	−0·7	−1·0	26·0	−0·3	−0·5
	2150	31·4	+3·2	−6·1	31·0	+1·7	−3·3
	2860	35·0	+2·0	−9·2	34·5	+1·2	−5·6

TABLE 8—*continued.*

$x = +8''$, $\Psi = 0$.

U ft./sec.	n R.P.M.	V ft./sec.	α degrees.	β degrees.	u ft./sec.	v ft./sec.	w ft./sec.
			$y = +3''$.				
0	1080	18·2	−1·5	−21·0	17·0	−0·4	−6·5
	2150	37·7	−1·5	−22·0	34·8	−0·9	−14·2
	2860	50·0	−1·7	−22·0	46·3	−1·4	−18·7
20	1080	20·9	−1·7	−3·0	20·9	−0·6	−1·1
	2150	37·6	−2·2	−16·4	35·9	−1·4	−10·6
	2860	49·8	−2·2	−18·7	47·2	−1·8	−15·9
40	1080	33·0	+0·6	+15·0	31·8	+0·3	+8·5
	2150	41·4	−1·7	−3·1	41·3	−1·2	−2·2
	2860	51·8	−1·9	−9·9	51·0	−1·7	−8·9
			$y = +6''$.				
0	1080	8·6	+1·7	−28·0	7·6	+0·2	−4·0
	2150	25·0	+2·4	−35·0	20·0	+0·8	−14·3
	2860	36·8	+0·9	−25·0	33·4	+0·5	−14·4
20	1080	22·3	−1·0	−2·7	22·3	−0·4	−1·0
	2150	39·1	−2·0	−10·3	38·4	−1·3	−7·0
	2860	49·4	−2·1	−13·0	48·1	−1·8	−11·1
40	1080	36·6	−0·4	+3·3	36·5	−0·3	+2·1
	2150	44·1	−1·2	−2·4	44·0	−0·9	−1·8
	2860	56·0	−1·7	−6·3	55·4	−1·6	−6·2
			$y = +9''$.				
20	1080	21·3	−0·9	−0·6	21·3	−0·3	−0·2
	2150	20·1	−3·0	−0·3	20·1	−1·0	−0·1
	2860	19·6	−3·4	0	19·6	−1·2	0
40	1080	41·5	−0·1	+0·5	41·5	−0·1	+0·4
	2150	40·9	−0·8	+0·7	40·9	−0·6	+0·5
	2860	40·2	−1·2	+0·6	40·2	−0·8	+0·4

TABLE 8—*continued.*

$x = +8''$, $\Psi = 0$.

U ft./sec.	n R.P.M.	V ft./sec.	α degrees.	β degrees.	u ft./sec.	v ft./sec.	w ft./sec.
			$y = -2''$.				
0	1080	16·0	+2·0	+23·0	14·7	+0·5	+6·3
	2150	30·1	+2·1	+8·5	29·6	+1·1	+4·4
	2860	43·5	+2·1	+25·2	40·3	+1·5	+14·2
20	1080	20·0	+4·8	+4·0	19·8	+1·7	+1·4
	2150	27·5	+1·1	+22·0	25·5	+0·5	+10·3
	2860	36·6	+1·8	+24·0	33·4	+1·0	+14·8
40	1080	36·0	0	−11·0	35·4	0	−6·9
	2150	39·5	+5·2	+6·2	39·0	+3·6	+4·3
	2860	39·2	+3·9	+16·4	37·3	+2·6	+11·1
			$y = -4''$.				
0	1080	21·0	+1·7	+16·0	20·2	+0·6	+5·4
	2150	41·0	+1·5	+18·4	38·9	+1·0	+13·0
	2860	54·6	+1·2	+19·2	51·8	+1·0	+18·0
20	1080	21·9	+0·8	+4·5	21·8	+0·3	+1·7
	2150	39·0	+1·3	+6·0	38·7	+0·9	+4·2
	2860	53·2	+1·4	+17·0	50·9	+1·2	+15·5
40	1080	33·1	−1·4	−13·0	32·0	−0·8	−7·5
	2150	44·7	+0·9	+13·6	43·2	+0·7	+10·5
	2860	56·4	+1·4	+11·3	55·3	+1·4	+11·1
			$y = -7''$.				
0	1080	—	—	—	—	—	—
	2150	6·0	−9·0	+33·0	4·9	−0·8	+3·3
	2860	6·5	−11·0	+58·0	3·4	−0·7	+5·5
20	1080	21·9	0	+2·1	21·9	0	+0·8
	2150	26·9	+3·0	+15·3	26·0	+1·4	+7·1
	2860	20·8	−7·2	+10·5	20·3	−2·6	+3·7
40	1080	38·2	−0·9	+1·0	38·2	−0·6	+0·7
	2150	42·6	+0·2	+2·8	42·5	+0·1	+2·1
	2860	51·1	+1·2	+6·6	50·6	+1·0	+5·8

TABLE 8—*continued.*

$x = +8''$, $\Psi = 0$.

U ft./sec.	n R.P.M.	V ft./sec.	α degrees.	β degrees.	u ft./sec.	v ft./sec.	w ft./sec.
			$y = -8''$.				
20	1080	20·7	−0·1	+1·0	20·7	0	+0·4
	2150	19·4	+1·2	+0·6	19·4	+0·4	+0·2
	2860	19·0	+1·6	+0·6	19·0	+0·6	+0·2
40	1080	40·2	−0·7	+2·1	40·2	−0·5	+1·5
	2150	40·4	0	+1·4	40·4	0	+1·0
	2860	39·4	+0·4	+1·3	39·4	+0·3	+0·9

TABLE 9.

$x = +64''$, $\Psi = 0$.

U ft./sec.	n R.P.M.	V ft./sec.	α degrees.	β degrees.	u ft./sec.	v ft./sec.	w ft./sec.
			$y = 0$.				
0	1080	11·0	−3·0	+3·0	10·9	−0·6	+0·6
	2150	22·1	−3·5	+2·2	22·0	−1·3	+0·8
	2860	29·1	−3·5	+1·9	29·0	−1·8	+1·0
20	1080	19·5	−0·8	−3·9	19·5	−0·3	−1·3
	2150	26·0	−2·2	−2·2	25·9	−1·0	−1·0
	2860	34·8	−4·0	−7·2	34·2	−2·4	−4·3
40	1080	29·9	−2·0	+8·0	29·5	−1·0	+4·2
	2150	40·2	−0·6	−9·2	39·5	−0·4	−6·4
	2860	43·4	−1·9	−7·1	42·8	−1·4	−5·3
			$y = +3''$.				
0	1080	12·0	−1·8	−13·0	11·7	−0·4	−2·7
	2150	25·1	−1·3	−12·6	24·5	−0·6	−5·5
	2860	34·1	−1·5	−12·2	33·3	−0·9	−7·2
20	1080	21·2	−1·2	−4·2	21·1	−0·4	−1·5
	2150	37·5	−1·6	−13·7	36·4	−1·0	−8·9
	2860	44·7	−2·7	−2·5	44·6	−2·1	−1·9
40	1080	31·2	−1·8	+7·4	30·7	−1·0	+4·0
	2150	42·5	−1·0	−4·6	42·3	−0·7	−3·4
	2860	53·6	−1·3	−11·5	52·5	−1·2	−10·7

TABLE 9—*continued.*

$x = +64''$, $\Psi = 0$.

U ft./sec.	n R.P.M.	V ft./sec.	α degrees.	β degrees.	u ft./sec.	v ft./sec.	w ft./sec.
			$y = +6''$.				
0	1080	11·5	+ 0·8	− 8·0	11·4	+ 0·2	− 1·6
	2150	22·3	+ 2·5	− 6·5	22·0	+ 1·0	− 2·5
	2860	29·4	+ 1·5	− 5·7	29·2	+ 0·7	− 2·9
20	1080	21·0	− 0·5	− 3·0	21·0	− 0·2	− 1·1
	2150	35·0	+ 0·2	− 7·2	34·7	+ 0·1	− 4·4
	2860	38·3	+ 0·2	− 10·0	37·7	+ 0·1	− 6·7
40	1080	36·5	− 2·0	+ 1·1	36·5	− 1·3	+ 0·7
	2150	42·4	− 0·6	− 2·6	42·3	− 0·4	− 1·9
	2860	51·2	− 0·1	− 5·0	51·0	− 0·1	− 4·5
			$y = +9''$.				
0	1080	7·0	0	− 8·0	6·9	0	− 1·0
	2150	15·2	+ 3·5	− 13·5	14·8	+ 0·9	− 3·5
	2860	19·5	+ 3·0	− 17·2	18·6	+ 1·0	− 5·8
20	1080	19·9	− 0·7	+ 8·0	19·6	− 0·2	+ 2·8
	2150	21·5	+ 1·5	− 2·0	21·5	+ 0·6	− 0·8
	2860	24·6	+ 0·2	− 12·3	24·0	+ 0·1	− 5·3
40	1080	38·4	− 0·9	+ 0·8	38·4	− 0·6	+ 0·5
	2150	38·9	− 0·4	+ 0·2	38·9	− 0·3	+ 0·1
	2860	35·8	+ 0·3	+ 0·5	35·8	+ 0·2	+ 0·3
			$y = -2''$.				
0	1080	11·5	− 2·5	+ 8·5	11·3	− 0·5	+ 1·7
	2150	23·8	− 2·3	+ 9·0	23·4	− 0·9	+ 3·7
	2860	32·3	− 1·4	+ 13·7	31·4	− 0·7	+ 7·7
20	1080	18·0	− 0·5	0	18·0	− 0·2	0
	2150	26·8	− 1·5	+ 5·6	26·6	− 0·7	+ 2·6
	2860	35·5	− 1·4	+ 12·4	34·6	− 0·8	+ 7·6
40	1080	28·7	− 2·4	− 6·0	28·4	− 1·2	− 3·0
	2150	36·8	+ 0·3	+ 0·8	36·8	+ 0·2	+ 0·5
	2860	44·2	− 0·5	+ 7·4	43·7	− 0·4	+ 5·7

TABLE 9—*continued.*

$x = +64''$, $\Psi = 0$.

U ft./sec.	n R.P.M.	V ft./sec.	α degrees.	β degrees.	u ft./sec.	v ft./sec.	w ft./sec.
			$y = -4''$.				
0	1080	12·2	−1·5	+6·0	12·1	−0·3	+1·3
	2150	24·4	−2·0	+11·0	23·8	−0·8	+4·7
	2860	33·1	−1·5	+11·0	32·3	−0·8	+6·3
20	1080	18·5	+0·1	+2·2	18·5	0	+0·7
	2150	33·2	−1·7	+15·0	31·7	−0·9	+8·6
	2860	43·7	−0·4	+17·0	41·6	−0·3	+12·6
40	1080	29·9	−1·8	−11·9	29·1	−0·9	−6·2
	2150	38·1	+0·5	+5·4	38·0	+0·3	+3·6
	2860	51·5	+0·6	+10·1	50·8	+0·5	+9·0
			$y = -8''$.				
0	1080	9·0	−3·0	+8·0	8·8	−0·5	+1·3
	2150	17·1	−4·5	+11·0	16·4	−1·3	+3·3
	2860	22·4	−3·5	+13·8	21·4	−1·3	+5·4
20	1080	20·2	−0·2	+1·0	20·2	−0·1	+0·4
	2150	31·9	−3·3	+8·6	30·8	−1·8	+4·8
	2860	33·0	−2·3	+9·4	32·2	−1·3	+5·4
40	1080	38·0	+0·2	−0·7	38·0	+0·1	−0·5
	2150	40·3	−0·4	+1·4	40·3	−0·3	+1·0
	2860	42·4	−0·2	+4·3	42·1	−0·1	+3·1

TABLE 10.

$x = 128''$, $\Psi = 0$.

U ft./sec.	n R.P.M.	V ft./sec.	α degrees.	β degrees.	u ft./sec.	v ft./sec.	w ft./sec.
			$y = 0$.				
0	1080	6·0	0	0	6·0	0	0
	2150	18·6	0	0	18·6	0	0
	2860	25·0	0	0	25·0	0	0
20	1080	20·8	−0·5	−3·4	20·6	−0·2	−1·2
	2150	29·8	0	−4·6	29·7	0	−2·4
	2860	34·0	0	−2·8	33·9	0	−1·6
40	1080	31·3	−3·0	+4·0	31·0	−1·6	+2·2
	2150	40·5	0	−4·0	40·3	0	−2·8
	2860	46·4	+1·0	−6·2	46·1	+0·8	−5·0

TABLE 10—*continued.*

$x = 128''$, $\Psi = 0$.

U ft./sec.	n R.P.M.	V ft./sec.	α degrees.	β degrees.	u ft./sec.	v ft./sec.	w ft./sec.
			$y = +4''$.				
0	1080	3·5	−0·5	−2·0	3·5	0	−0·1
	2150	17·0	+1·2	−0·7	16·9	+0·3	−0·2
	2860	23·7	+1·7	−1·4	23·7	+0·7	−0·5
20	1080	21·5	−0·3	−2·9	21·5	−0·1	−1·0
	2150	31·0	+0·3	−6·2	30·8	+0·2	−3·3
	2860	35·0	+0·5	−4·5	34·8	+0·2	−2·8
40	1080	36·0	−1·8	+2·3	35·9	−1·1	+1·4
	2150	43·4	−0·3	−3·3	43·3	−0·2	−2·5
	2860	51·8	−0·2	−6·1	51·5	−0·2	−5·5
			$y = +8''$.				
0	1080	4·8	0	−2·0	4·8	0	−0·2
	2150	15·0	+1·5	−4·0	15·0	+0·4	−1·0
	2860	19·7	+2·0	−3·3	19·7	+0·7	−1·1
20	1080	19·9	−0·5	+0·1	19·9	−0·2	0
	2150	25·1	0	−4·5	25·0	0	−2·0
	2860	28·7	−0·3	−5·2	28·6	−0·1	−2·6
40	1080	36·5	−0·7	+1·3	36·5	−0·4	+0·8
	2150	39·8	0	−0·4	39·8	0	−0·3
	2860	44·3	+0·3	−2·2	44·3	+0·2	−1·7
			$y = +10''$.				
0	1080	3·2	0	0	3·2	0	0
	2150	12·6	+1·6	−3·4	12·6	+0·4	−0·7
	2860	18·1	+2·0	−5·5	18·1	+0·6	−1·7
20	1080	19·7	−0·3	−0·3	19·7	−0·1	−0·1
	2150	23·6	+0·4	−3·1	23·6	+0·2	−1·3
	2860	25·8	−0·1	−4·7	25·8	0	−2·4
40	1080	39·6	−0·6	+0·6	39·6	−0·4	+0·4
	2150	39·5	−0·2	0	39·5	−0·2	0
	2860	40·2	+0·1	−0·1	40·2	+0·1	−0·1

TABLE 10—*continued*.

$x = 128''$, $\Psi = 0$.

U ft./sec.	n R.P.M.	V ft./sec.	α degrees.	β degrees.	u ft./sec.	v ft./sec.	w ft./sec.
			$y = +11''$.				
0	1080	0·3	+ 0·5	− 2·0	0·3	0	0
	2150	10·9	+ 1·5	− 6·0	10·9	+ 0·3	− 1·1
	2860	15·9	+ 1·5	− 7·0	15·8	+ 0·4	− 1·9
20	1080	20·0	+ 0·5	+ 0·3	20·0	+ 0·2	+ 0·1
	2150	22·0	+ 0·2	− 1·3	22·0	+ 0·1	− 0·5
	2860	23·8	− 0·1	− 3·3	23·8	0	− 1·4
40	1080	39·9	− 0·5	− 4·4	39·8	− 0·3	− 3·1
	2150	39·8	− 0·1	− 3·9	39·7	− 0·1	− 2·7
	2860	39·9	+ 0·1	− 4·2	39·8	+ 0·1	− 2·9
			$y = -4''$.				
0	1080	5·0	0	− 2·0	5·0	0	− 0·2
	2150	18·0	− 1·0	0	18·0	− 0·3	0
	2860	23·4	− 1·0	+ 1·0	23·4	− 0·4	+ 0·4
20	1080	20·1	+ 0·5	+ 2·3	20·1	+ 0·2	+ 1·2
	2150	29·8	+ 1·0	+ 6·5	29·6	+ 0·5	+ 3·3
	2860	34·4	+ 1·0	+ 5·0	34·2	+ 0·6	+ 3·0
40	1080	31·0	− 3·5	− 6·0	30·6	− 1·9	− 3·2
	2150	40·8	+ 0·8	+ 4·0	40·6	+ 0·6	+ 2·8
	2860	50·4	+ 2·2	+ 8·3	49·8	+ 1·9	+ 7·3
			$y = -8''$.				
0	1080	4·2	− 1·8	− 2·0	4·2	− 0·1	− 0·1
	2150	14·4	− 1·6	+ 3·0	14·4	− 0·4	+ 0·8
	2860	20·1	− 3·0	+ 2·1	20·0	− 1·0	+ 0·7
20	1080	20·2	− 0·5	+ 1·0	20·2	− 0·2	+ 0·4
	2150	26·3	− 0·2	+ 3·5	26·3	− 0·1	+ 1·6
	2860	30·5	− 0·5	+ 4·0	30·4	− 0·3	+ 2·1
40	1080	36·2	− 0·3	− 1·5	36·2	− 0·2	− 0·9
	2150	40·6	+ 0·1	+ 1·6	40·6	+ 0·1	+ 1·1
	2860	46·0	− 0·1	+ 3·6	46·0	− 0·1	+ 2·9

TABLE 10—*continued.*

$x = +128''$, $\Psi = 0$.

U ft./sec.	n R.P.M.	V ft./sec.	α degrees.	β degrees.	u ft./sec.	v ft./sec.	w ft./sec.
			$y = -10''$.				
0	1080	0·3	—	—	—	—	—
	2150	12·5	− 2·5	+ 3·0	12·5	− 0·5	+ 0·7
	2860	19·1	− 3·0	+ 3·0	19·1	− 1·0	+ 1·0
20	1080	20·0	0	+ 0·3	20·0	0	+ 0·1
	2150	25·2	− 0·5	+ 3·6	25·2	− 0·2	+ 1·6
	2860	27·7	0	+ 4·6	27·7	0	+ 2·2
40	1080	39·3	+ 0·1	0	39·3	+ 0·1	0
	2150	39·7	− 0·1	+ 0·6	39·7	− 0·1	+ 0·4
	2860	41·8	− 0·3	+ 2·3	41·8	− 0·2	+ 1·7
			$y = -11''$.				
0	1080	0·3	− 0·5	—	0·3	—	—
	2150	11·7	− 3·0	+ 4·4	11·7	− 0·6	+ 0·9
	2860	17·6	− 4·0	+ 3·5	17·6	− 1·2	+ 1·1
20	1080	20·2	− 0·4	+ 0·2	20·2	− 0·2	+ 0·1
	2150	23·8	− 0·4	+ 3·0	23·8	− 0·2	+ 1·2
	2860	25·8	− 0·7	+ 4·8	25·7	− 0·3	+ 2·2
40	1080	39·5	− 0·1	0	39·5	− 0·1	0
	2150	39·7	− 0·2	+ 0·4	39·7	− 0·1	+ 0·3
	2860	40·6	− 0·5	+ 1·4	40·6	− 0·4	+ 1·0

TABLE 11.

AIRSCREW YAWED.

$x = 128''$, $\Psi = 10°$.

U ft./sec.	n R.P.M.	V ft./sec.	α degrees.	β degrees.	u ft./sec.	v ft./sec.	w ft./sec.
			$y = 0$.				
20	1080	19·4	+ 1·6	+ 0·3	19·4	+ 0·5	+ 0·1
	2150	28·9	+ 2·3	+ 3·9	28·7	+ 1·2	+ 2·0
	2860	29·8	+ 2·8	+ 4·1	29·5	+ 1·4	+ 2·1
40	1080	31·9	− 1·4	+ 3·9	31·8	− 0·8	+ 2·2
	2150	40·8	+ 2·1	+ 3·9	40·6	+ 1·5	+ 2·8
	2860	49·6	+ 3·6	+ 6·8	49·2	+ 3·1	+ 5·9

TABLE 11—*continued.*

$x = 128''$, $\Psi = 10°$.

U ft./sec.	n R.P.M.	V ft./sec.	α degrees.	β degrees.	u ft./sec.	v ft./sec.	w ft./sec.
			$y = 5{\cdot}5''$.				
20	1080	21·8	+ 0·5	− 5·2	21·8	+ 0·2	− 2·0
	2150	30·3	+ 3·0	+ 1·3	30·3	+ 1·6	+ 0·7
	2860	38·1	+ 3·5	+ 3·3	38·0	+ 2·3	+ 2·2
40	1080	37·2	− 1·1	+ 1·9	37·2	− 0·7	+ 1·2
	2150	43·1	+ 0·9	− 4·7	43·0	+ 0·7	− 3·5
	2860	50·0	+ 2·7	− 7·7	49·6	+ 2·3	− 6·7
			$y = 12''$.				
20	1080	20·0	+ 0·3	− 0·1	20·0	+ 0·1	0
	2150	30·2	+ 2·9	− 5·2	30·0	+ 1·5	− 2·7
	2860	35·7	+ 2·6	− 5·1	35·5	+ 1·6	− 3·2
40	1080	39·7	− 0·6	+ 0·2	39·7	− 0·4	+ 0·1
	2150	39·7	+ 0·6	+ 0·1	39·7	+ 0·4	+ 0·1
	2860	44·7	+ 1·6	− 2·2	44·6	+ 1·2	− 1·7
			$y = 18{\cdot}5''$.				
20	1080	19·8	− 0·5	− 0·3	19·8	− 0·2	− 0·1
	2150	21·6	+ 2·0	− 2·0	21·6	+ 0·8	− 0·8
	2860	27·3	+ 3·5	− 4·2	27·1	+ 1·6	− 2·0
40	1080	39·5	− 0·4	+ 0·1	39·5	− 0·3	+ 0·1
	2150	39·5	0	− 0·1	39·5	0	− 0·1
	2860	39·2	+ 0·4	− 0·1	39·2	+ 0·3	− 0·1
			$y = 22{\cdot}5''$.				
20	1080	19·7	0	− 0·1	19·7	0	0
	2150	18·9	+ 0·4	0	18·9	+ 0·1	0
	2860	20·5	+ 2·0	− 1·7	20·5	+ 0·7	− 0·6
40	1080	39·1	− 0·4	− 0·2	39·1	− 0·3	− 0·1
	2150	39·1	− 0·1	− 0·2	39·1	− 0·1	− 0·1
	2860	39·0	+ 0·1	− 0·3	39·0	+ 0·1	− 0·2

REPORT No. 371

Fig. 1.

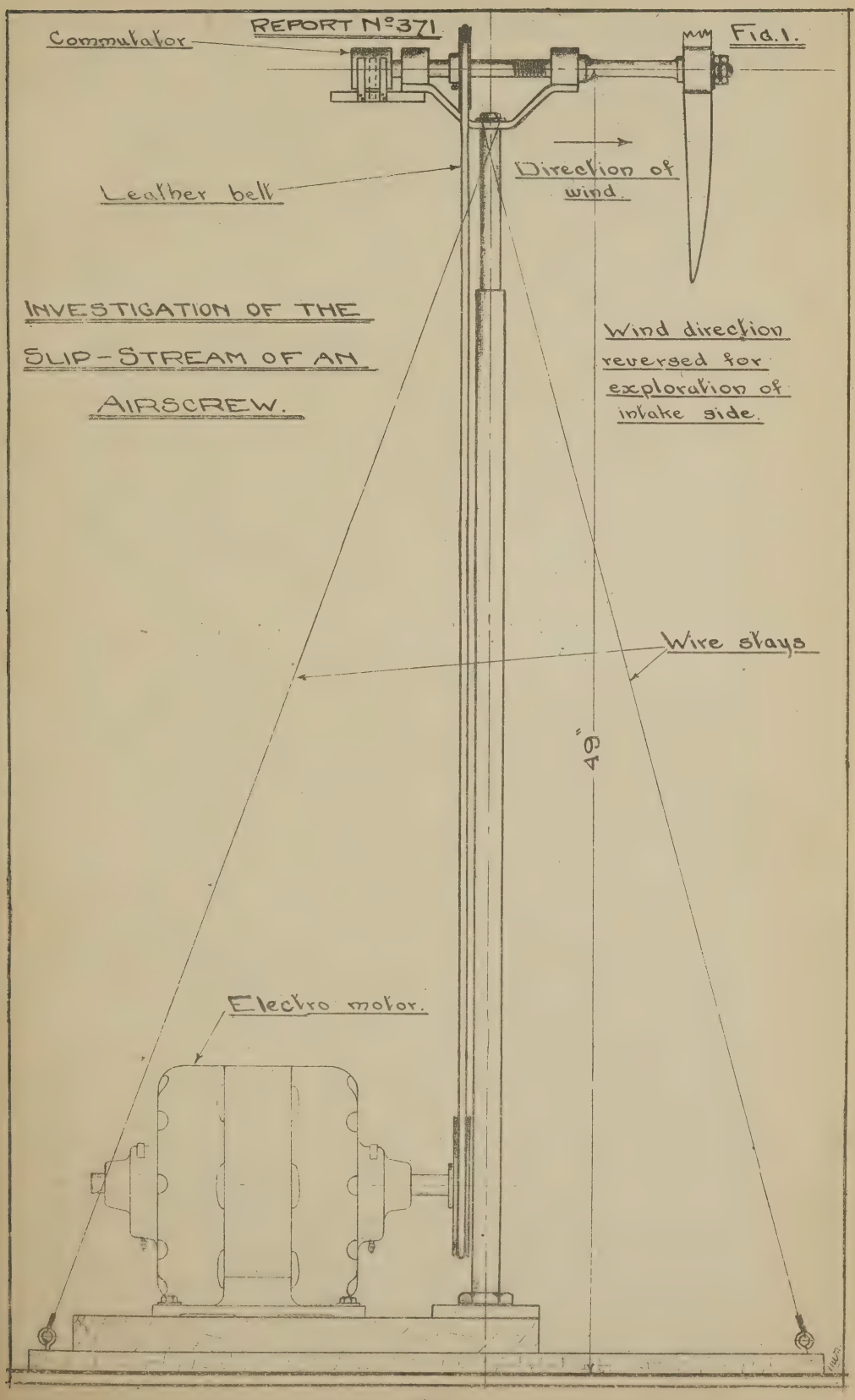

INVESTIGATION OF THE SLIP-STREAM OF AN AIRSCREW.

— INVESTIGATION OF THE SLIP-STREAM OF AN AIRSCREW —

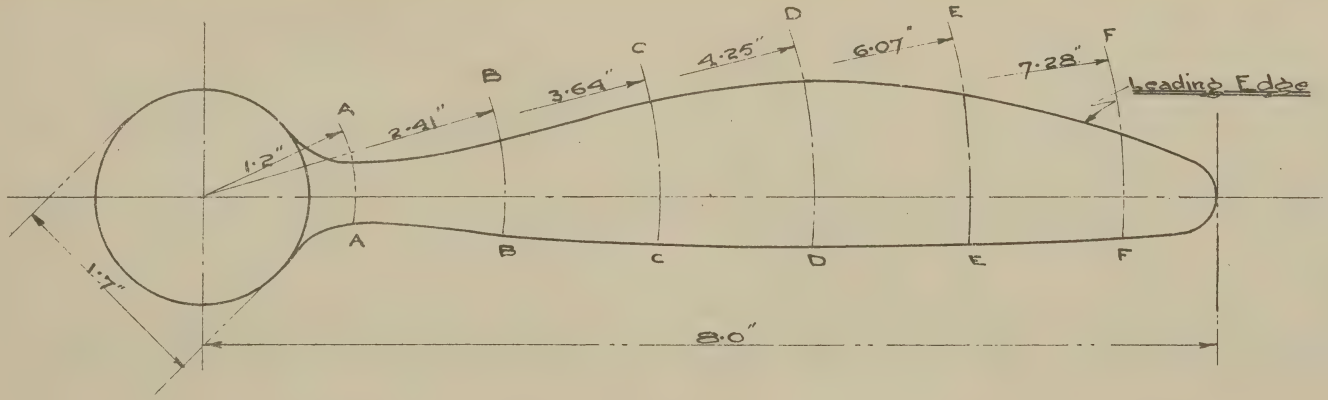

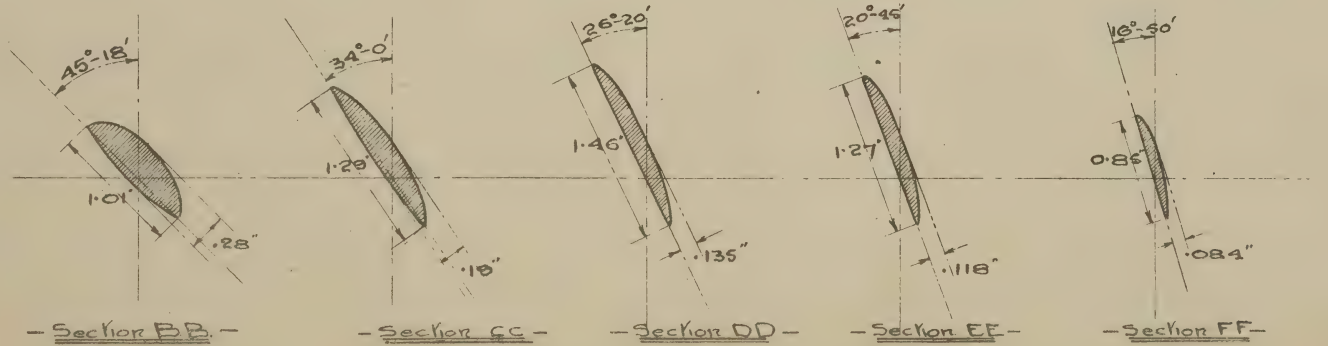

INVESTIGATION OF THE SLIP-STREAM OF AN AIRSCREW.

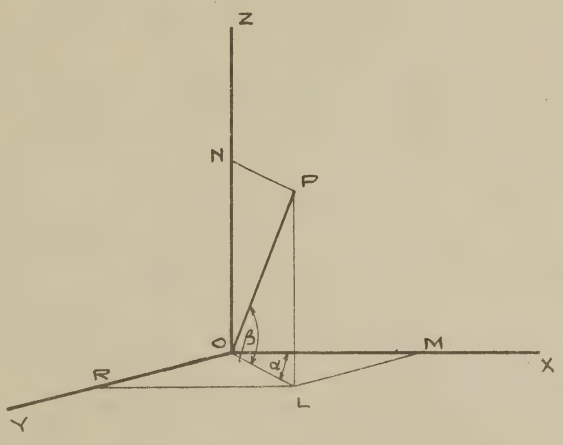

$OP = V$

$L\hat{O}M = \alpha$

$L\hat{O}P = \beta$

$OL = V\cos\beta$

$u = OM = V\cos\beta\cos\alpha$

$v = OR = V\cos\beta\sin\alpha$

$w = ON = V\sin\beta$

REPORT N°371.

– Fig 4 –

INVESTIGATION OF THE SLIP-STREAM OF AN AIRSCREW

– Chart for Reducing Yawmeter Observations –

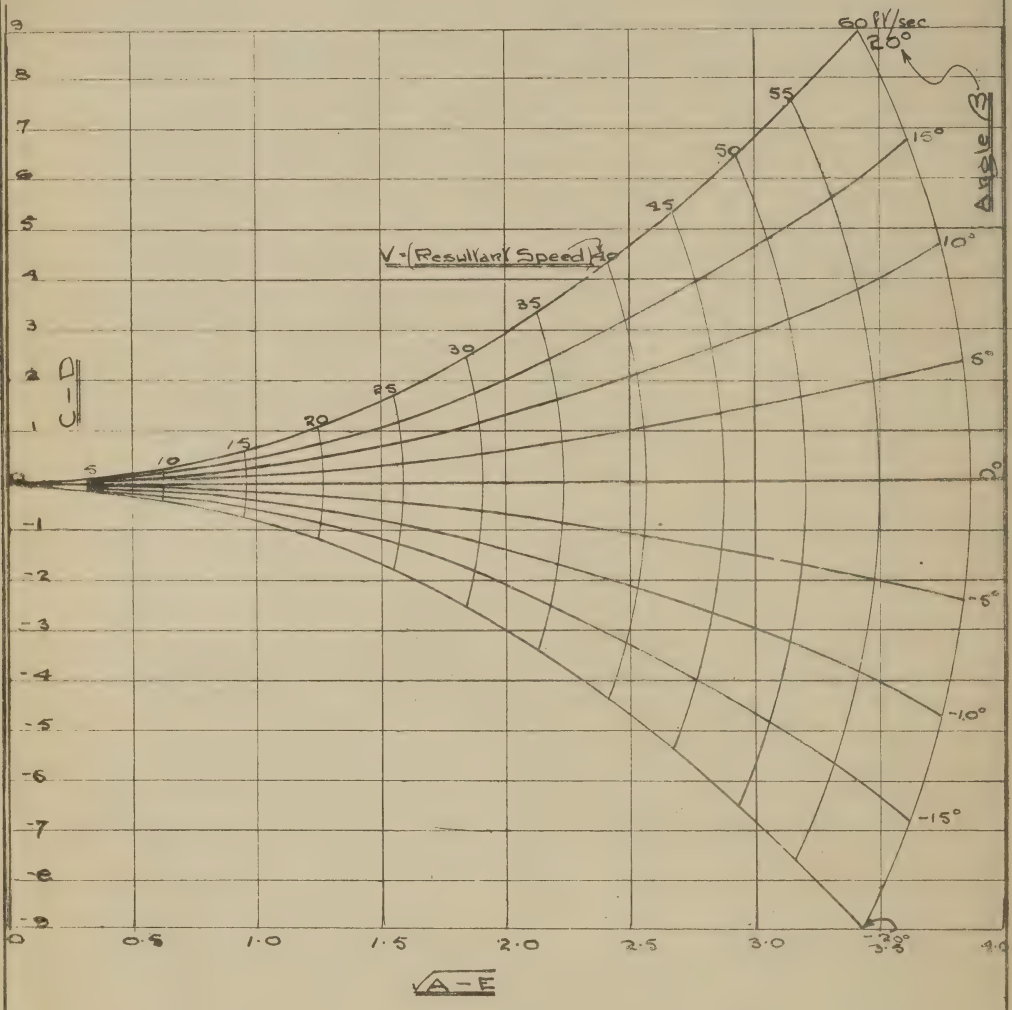

— INVESTIGATION OF THE SLIP-STREAM OF AN AIRSCREW —

REPORT No. 371.

— Longitudinal Section of Slip-Stream —

— U = 20 ft/sec R.P.M. 2860 —

— NOTE. Observations indicated thus ⟶ were taken on the opposite side of the airscrew axis & are plotted with the sign of y reversed —

— Fig 5 —

THE LIBRARY
OF THE
UNIVERSITY OF ILLINOIS

— INVESTIGATION OF THE SLIP-STREAM OF AN AIRSCREW —

— Longitudinal Section of Slip-Stream —

— R.P.M. 2860 — — U. 40 ft/sec —

— NOTE:- Observations marked thus —x— were taken on the opposite side of the airscrew axis & are plotted with the sign of y reversed. —

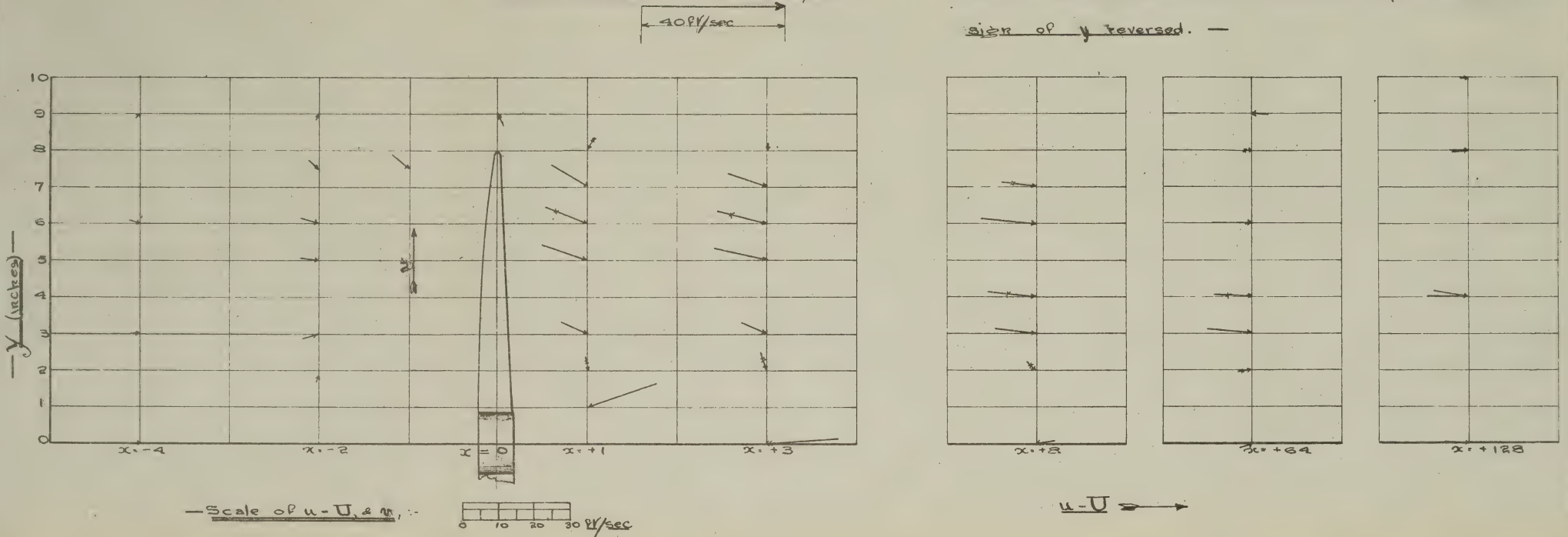

REPORT No. 371.

— Fig. 6 —

THE LIBRARY
OF THE
UNIVERSITY OF ILLINOIS

— INVESTIGATION OF THE SLIP-STREAM OF AN AIRSCREW —

REPORT No. 371.

— NOTE:- Values Marked Thus ✓ Were Observed at Negative Values of y —

— Scale of V & W —

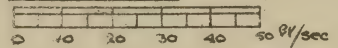

— Speed 40 ft/sec —

— R.P.M. 2860 —

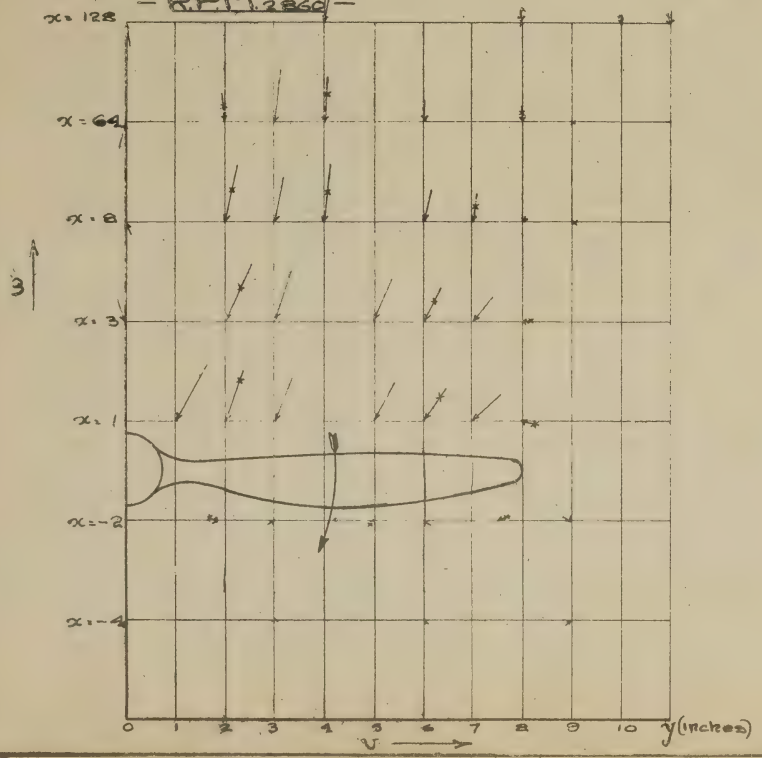

— Speed 20 ft/sec —

— R.P.M. 2860 —

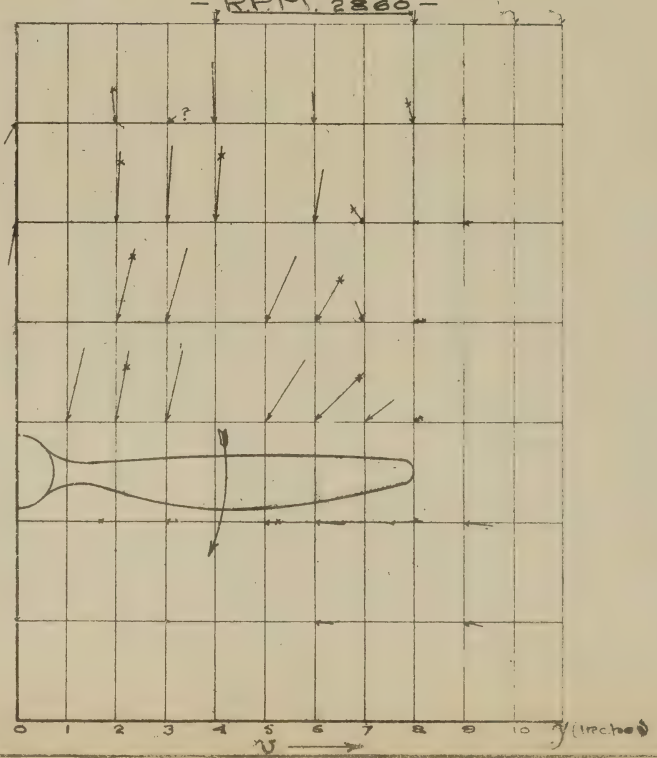

— Fig. 7 —

REPORT No. 371. — Fig. 8 —

INVESTIGATION OF THE SLIP-STREAM OF AN AIRSCREW

— Variation of u, v, and w with $\frac{U}{nd}$ —

— $x = -2$ inches —

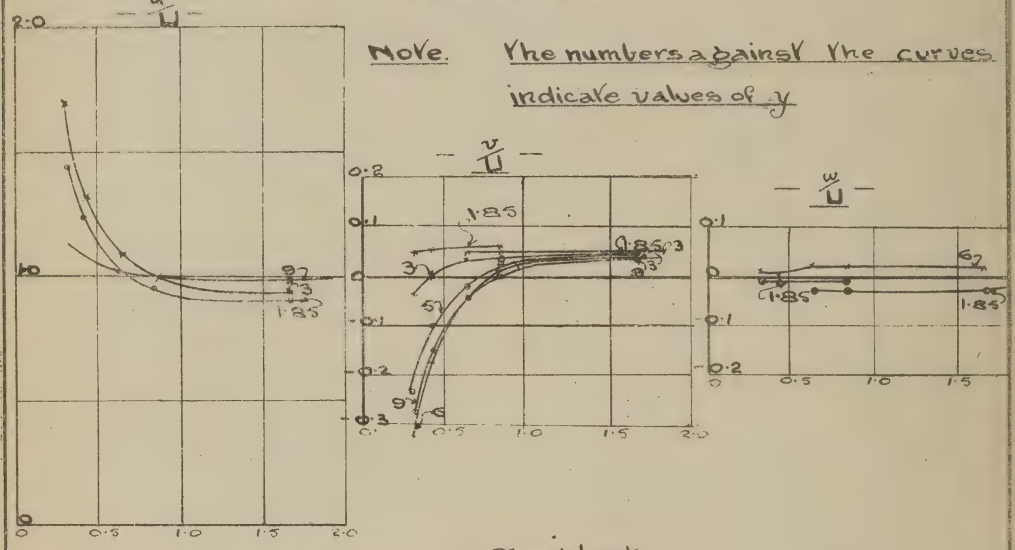

Note. The numbers against the curves indicate values of y

— $x = +1$ inch —

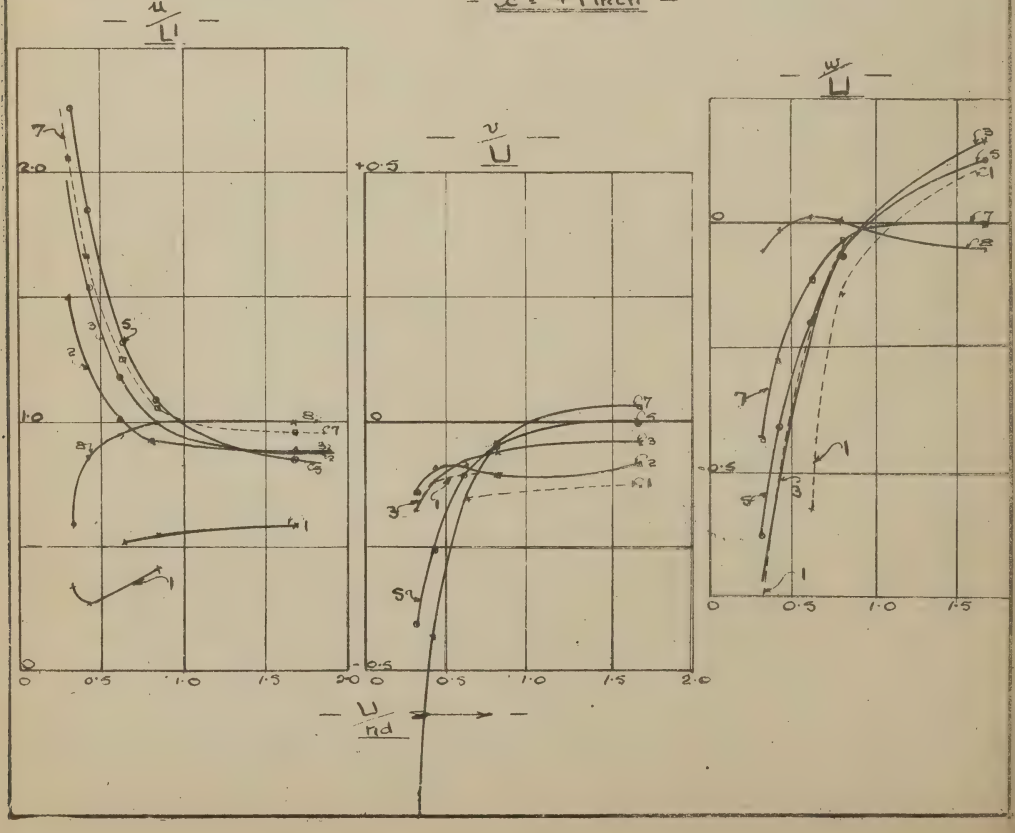

REPORT N° 371. FIG. 9.

INVESTIGATION OF THE SLIP-STREAM OF AN AIRSCREW.

Variation of u, v, & w with $\frac{U}{nd}$.

Note. The numbers against the curves indicate values of y

x = +3 inches.

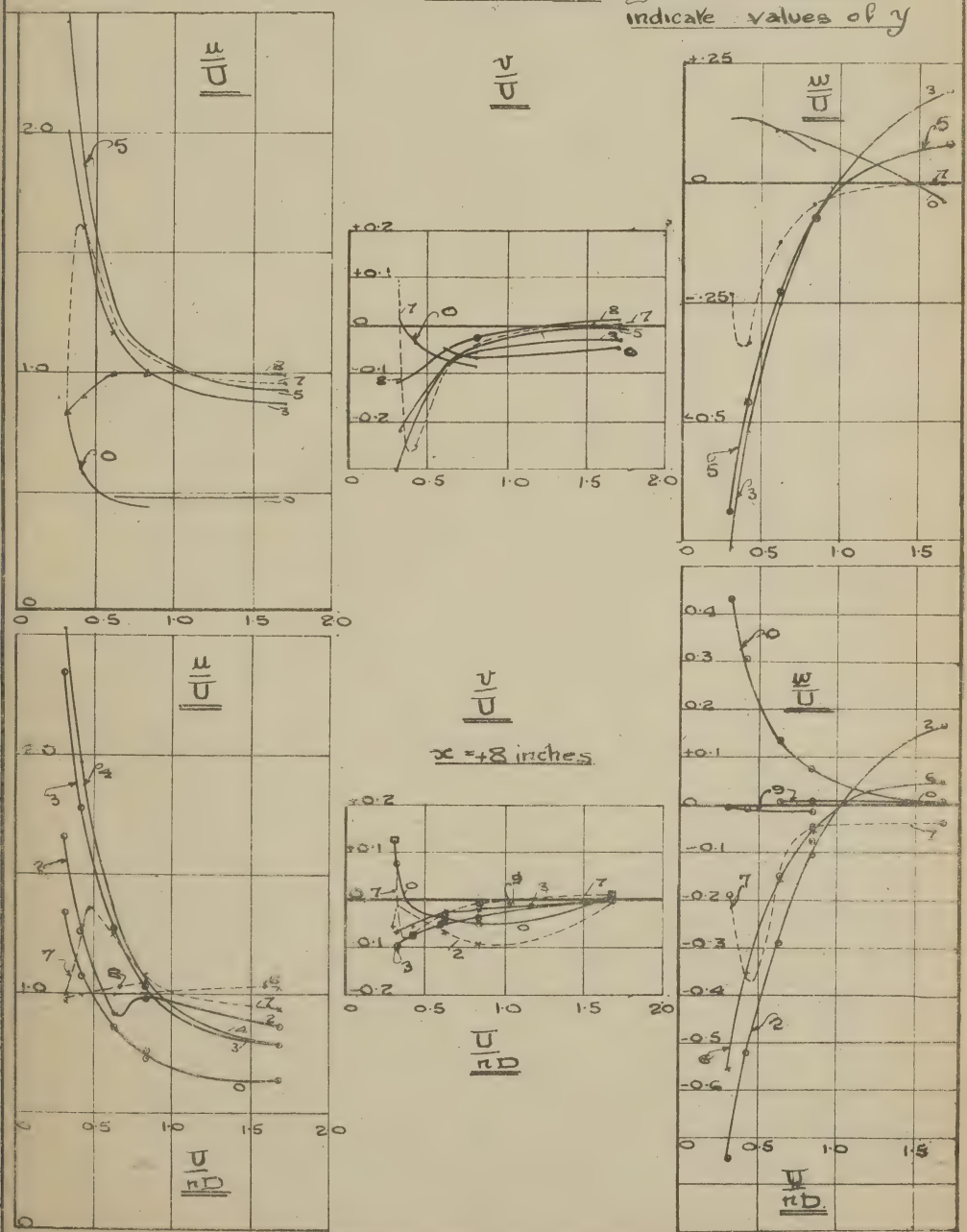

INVESTIGATION OF THE SLIP-STREAM OF AN AIRSCREW.

—o— Channel Speed 40 f/s. —x— Channel Speed 20 f/s. --- Static.

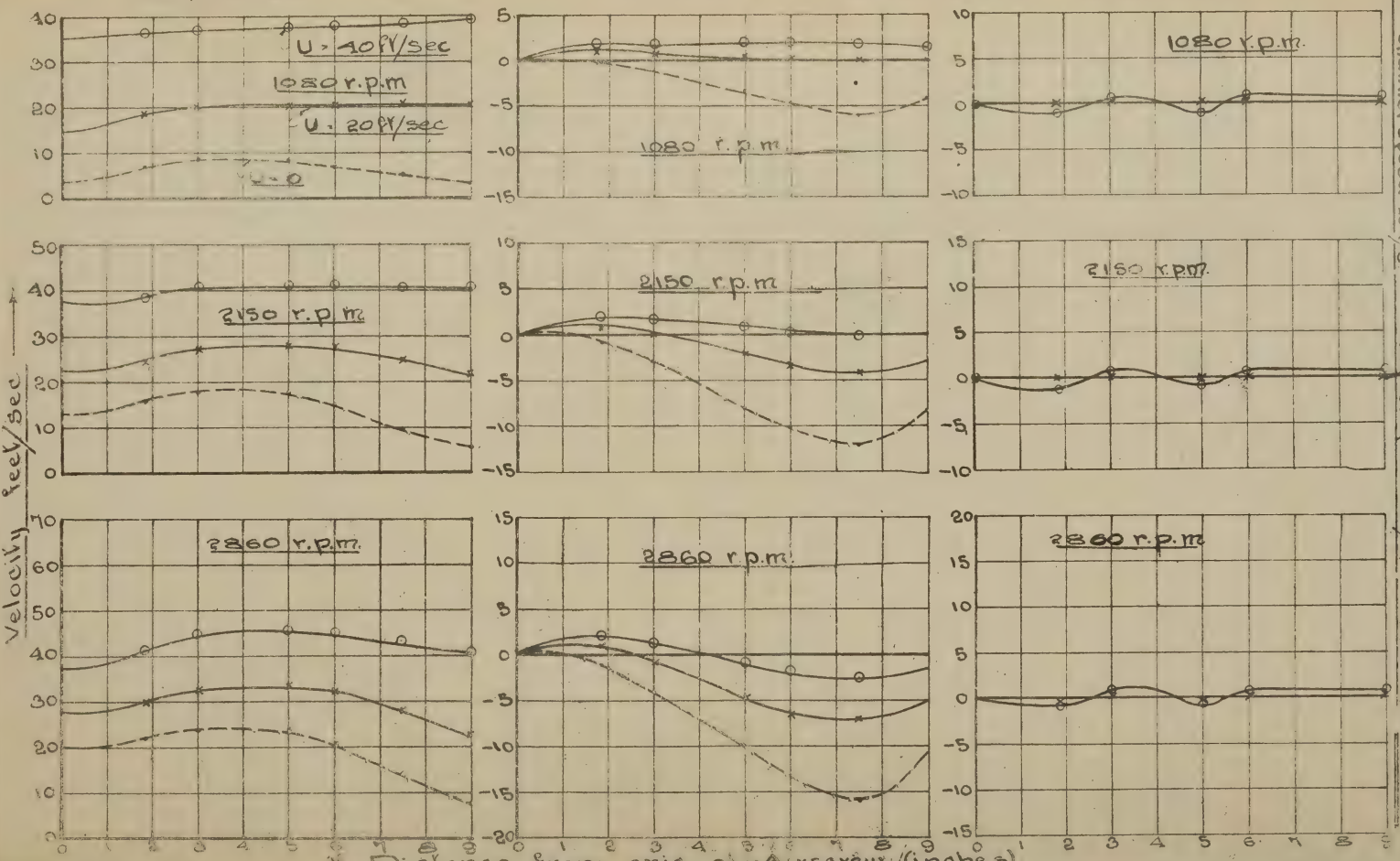

Fig 10.

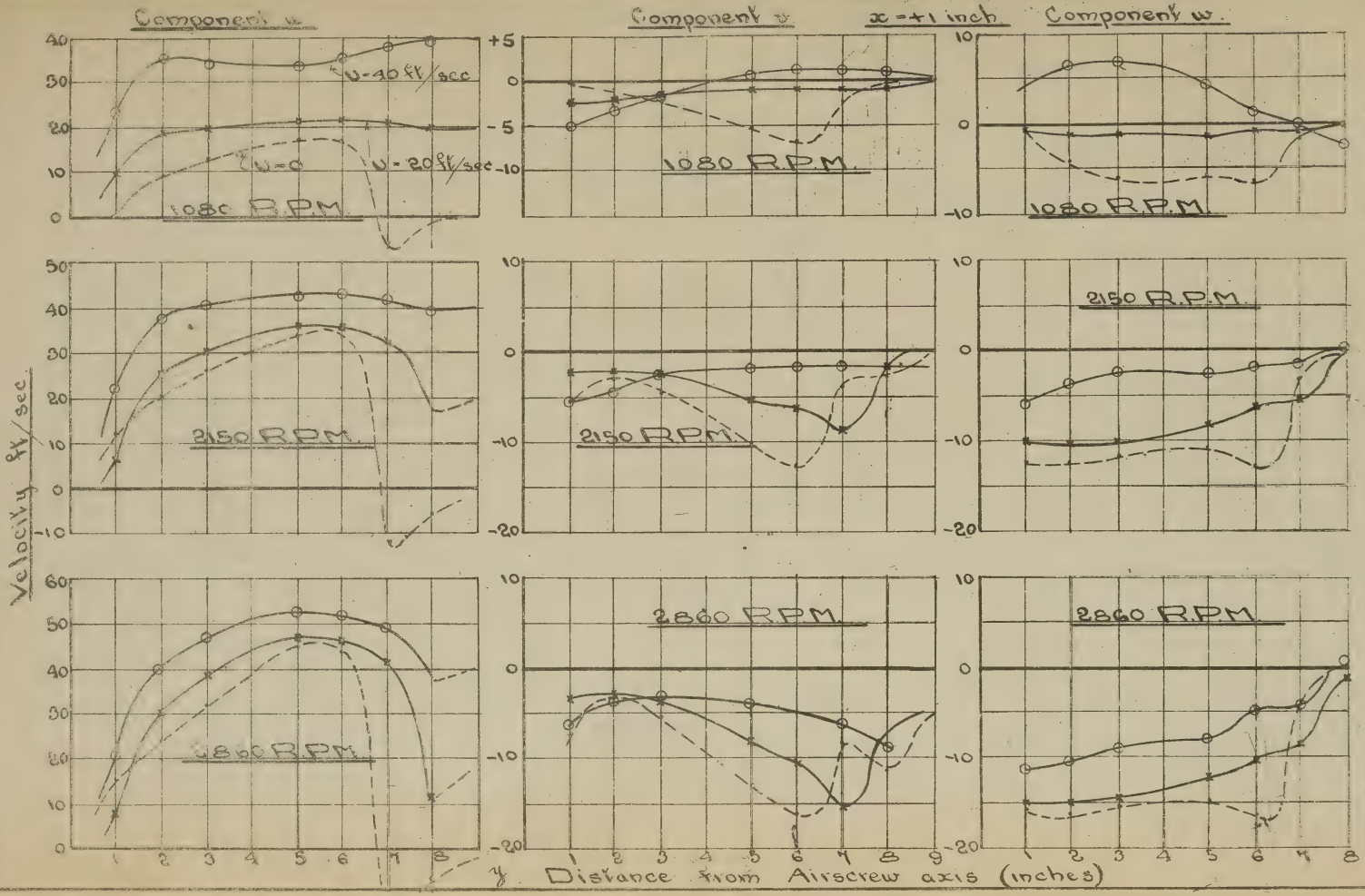

REPORT No 371
INVESTIGATION OF THE SLIP-STREAM OF AN AIRSCREW

Fig 11

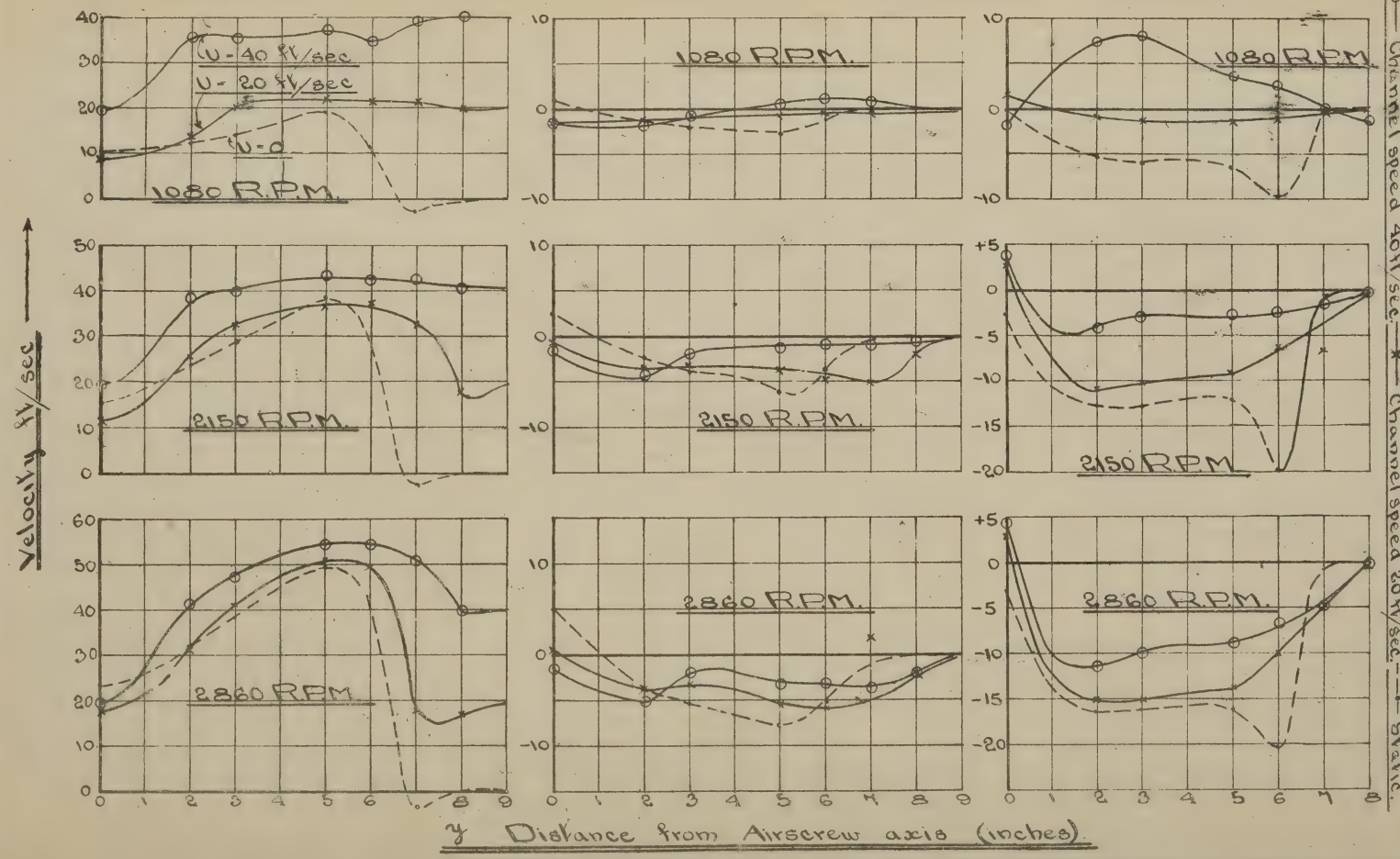

REPORT No. 371.
INVESTIGATION OF THE SLIP-STREAM OF AN AIRSCREW. Fig. 12.
—o— Channel speed 40 ft/sec. —x— Channel speed 20 ft/sec. —•— Static.

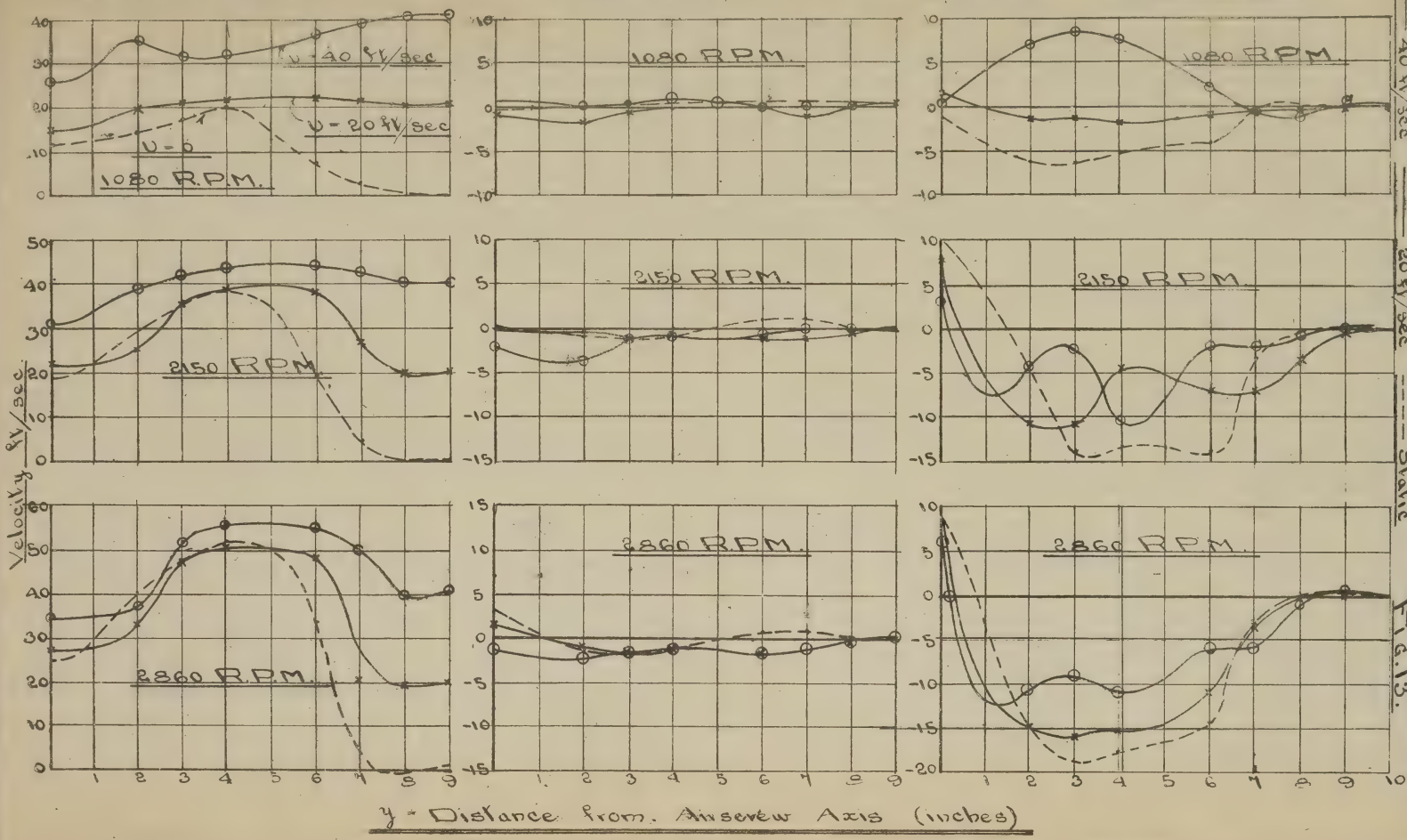
Component u
Component v
x = + 8 inches
Component w
u = 40 ft/sec
u = 20 ft/sec
u = 0
1080 R.P.M.
2150 R.P.M.
2860 R.P.M.
Velocity ft/sec
y = Distance from Airscrew Axis (inches)
Report No 371.
Investigation of the Slip-Stream of an Airscrew.
40 ft/sec
20 ft/sec
Static
Fig. 13.

REPORT N°. 371. FIG. 14.

INVESTIGATION OF THE SLIP-STREAM OF AN AIRSCREW.

—×— Channel speed 20 f/s., —o— Channel speed 40 f/s., - - - - Static.

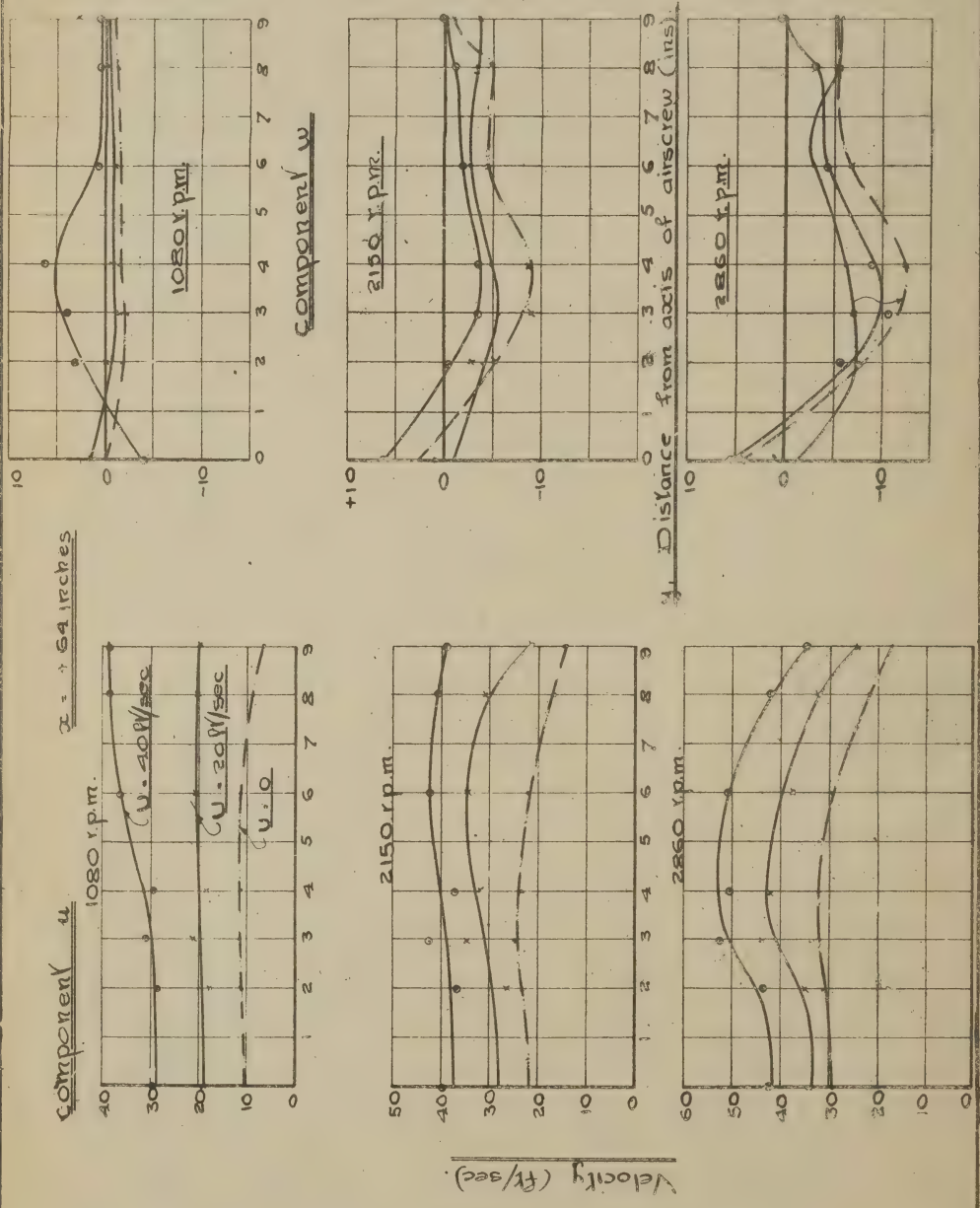

REPORT No 371.

INVESTIGATION OF THE SLIP-STREAM OF AN AIRSCREW

FIG. 15.

REPORT No. 371.

INVESTIGATION OF THE SLIP-STREAM OF AN AIRSCREW.

FIG. 16.

component w $x = 128$ inches

Angle of Yaw = $\psi = 0$ $\psi = +10°$ $\psi = +20°$

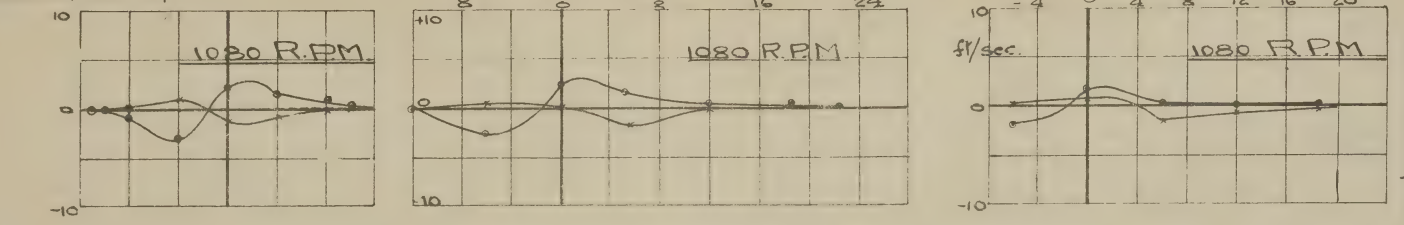

Airscrew axis yawed

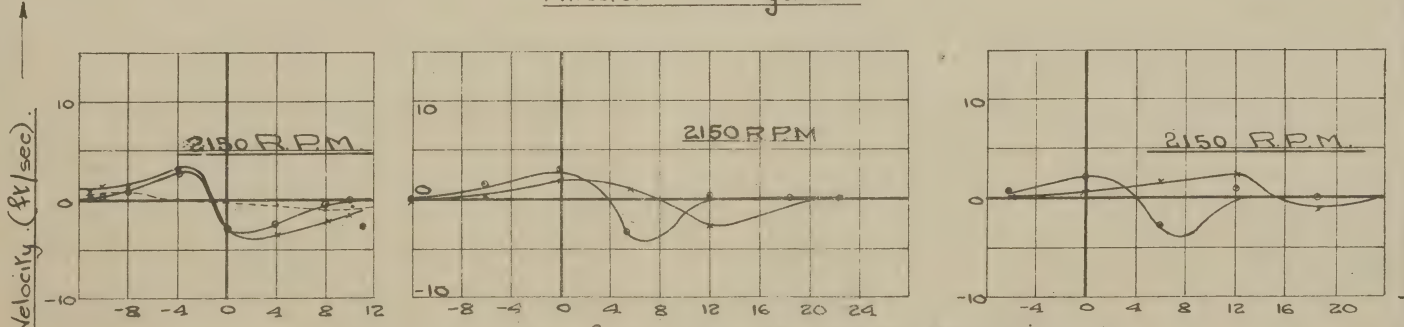

y. Distance from centre of airscrew Boss (inches)

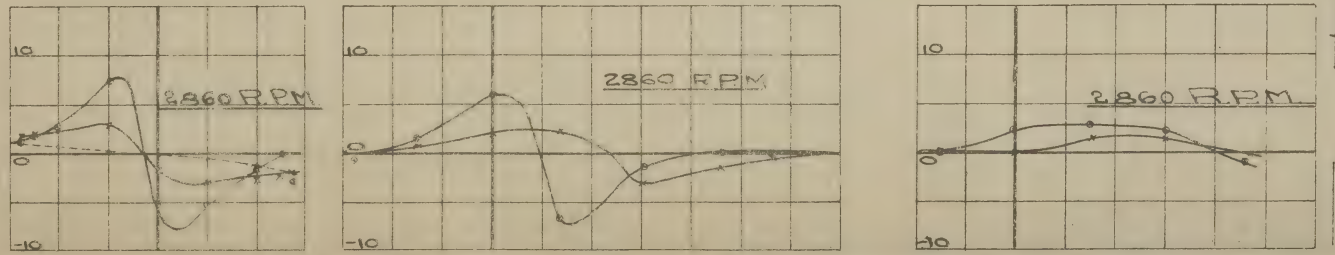

Channel speed 20 f/s. — ⊙ — Channel speed 40 f/s. - - - - Static.

FIG 17.

- INVESTIGATION OF THE SLIP-STREAM OF AN AIRSCREW -

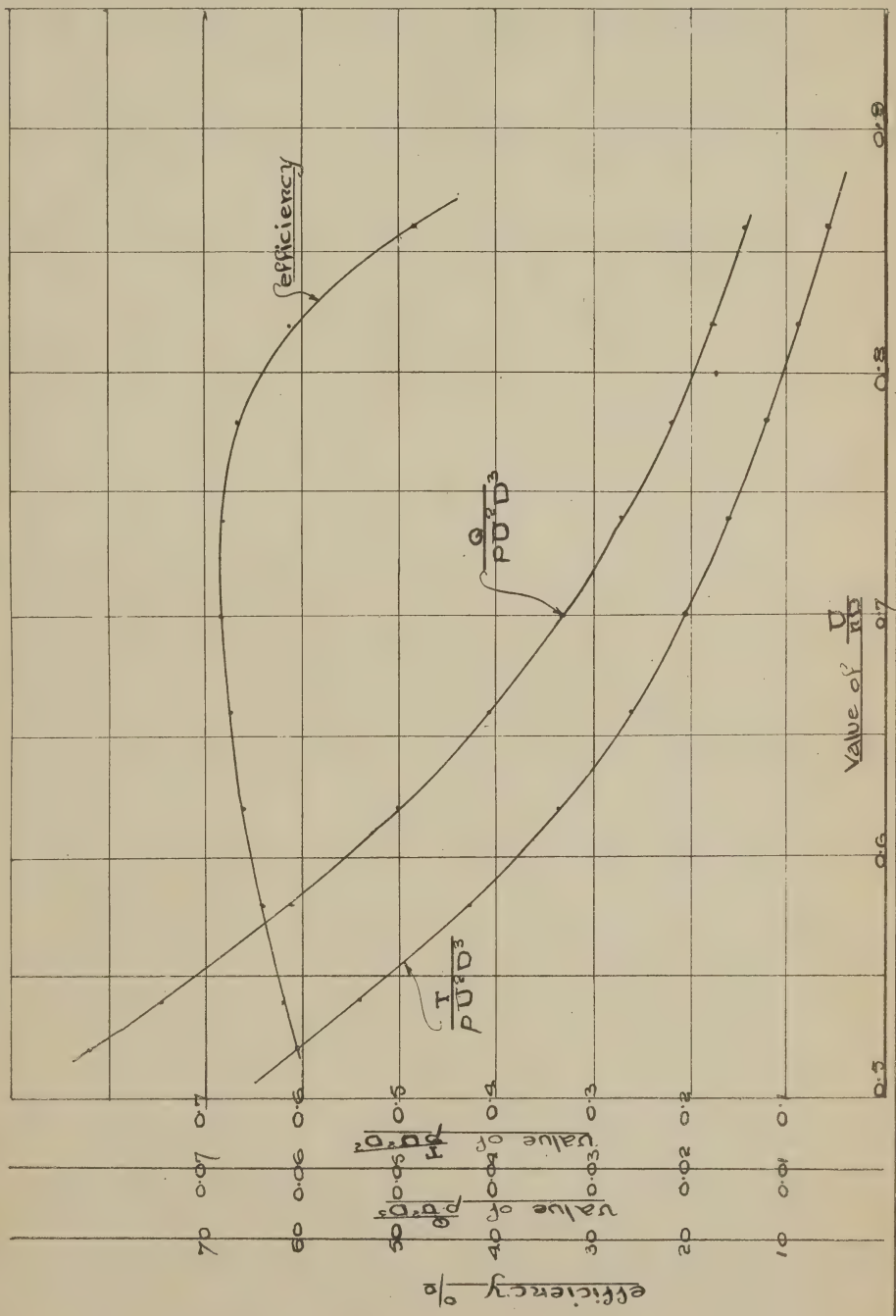

THE LIBRARY
OF THE
UNIVERSITY OF ILLINOIS

TABLE 11—*continued.*

$x = 128''$, $\Psi = 10°$.

U ft./sec.	n R.P.M.	V ft./sec.	α degrees.	β degrees.	u ft./sec.	v ft./sec.	w ft./sec.
			$y = -6''$.				
20	1080	20·2	+ 1·0	+ 1·0	20·2	+ 0·4	+ 0·4
	2150	21·0	+ 2·3	+ 1·4	21·0	+ 0·8	+ 0·5
	2860	21·2	+ 2·2	+ 2·0	21·2	+ 0·8	+ 0·7
40	1080	34·3	− 0·9	− 4·5	34·2	− 0·5	− 2·7
	2150	39·5	+ 1·0	+ 1·7	39·5	+ 0·7	+ 1·2
	2860	42·1	+ 1·0	+ 1·8	42·1	+ 0·7	+ 1·3
			$y = -12''$.				
20	1080	19·8	− 0·5	− 0·3	19·8	− 0·2	− 0·1
	2150	19·4	+ 0·7	− 0·2	19·4	+ 0·2	0
	2860	19·4	+ 0·9	0	19·4	+ 0·3	0
40	1080	39·3	− 0·2	− 0·2	39·3	− 0·1	− 0·1
	2150	39·1	0	+ 0·3	39·1	0	+ 0·2
	2860	39·2	0	− 0·2	39·2	0	− 0·1

TABLE 12.

$x = 128''$, $\Psi = 20°$.

U ft./sec.	n R.P.M.	V ft./sec.	α degrees.	β degrees.	u ft./sec.	v ft./sec.	w ft./sec.
			$y = 0$.				
20	1080	21·4	+ 2·3	+ 2·4	21·4	+ 0·9	+ 0·9
	2150	21·0	+ 3·6	+ 2·0	20·9	+ 1·3	+ 0·7
	2860	20·0	+ 3·7	+ 0·4	19·9	+ 1·3	+ 0·1
40	1080	33·7	+ 0·1	+ 2·9	33·7	+ 0·1	+ 1·7
	2150	43·2	+ 2·9	+ 3·0	43·0	+ 2·2	+ 2·2
	2860	43·8	+ 3·1	+ 3·1	43·6	+ 2·4	+ 2·4
			$y = +6''$.				
20	1080	20·1	+ 2·6	− 4·0	20·0	+ 0·9	− 1·4
	2150	28·3	+ 4·7	+ 3·0	28·0	+ 2·3	+ 1·5
	2860	24·7	+ 6·2	+ 3·0	24·4	+ 2·7	+ 1·3
40	1080	38·4	− 1·5	+ 0·2	38·4	− 1·0	+ 0·1
	2150	40·5	+ 3·4	− 4·1	40·1	+ 2·4	− 2·9
	2860	49·0	+ 5·1	+ 3·2	48·4	+ 4·3	+ 2·7

TABLE 12—*continued.*

$x = 128''$, $\Psi = 20°$.

U ft./sec.	n R.P.M.	V ft./sec.	α degrees.	β degrees.	u ft./sec.	v ft./sec.	w ft./sec.
			$y = +12''$.				
20	1080	21·2	+ 1·1	− 1·5	21·2	+ 0·4	− 0·6
	2150	30·5	+ 4·0	+ 4·4	30·3	+ 2·1	+ 2·3
	2860	34·4	+ 6·5	+ 2·2	34·2	+ 3·9	+ 1·3
40	1080	39·1	− 0·8	+ 0·2	39·1	− 0·5	+ 0·1
	2150	42·6	+ 1·7	+ 1·1	42·6	+ 1·3	+ 0·8
	2860	49·4	+ 3·6	+ 2·4	49·1	+ 3·1	+ 2·1
			$y = +18·5''$.				
20	1080	20·0	0	− 0·7	20·0	0	− 0·2
	2150	27·5	− 1·5	− 2·5	27·5	− 0·7	− 1·2
	2860	35·1	+ 6·8	− 0·5	34·8	+ 4·1	− 0·3
40	1080	39·1	− 0·6	0	39·1	− 0·4	0
	2150	39·2	+ 0·5	− 0·3	39·2	+ 0·3	− 0·2
	2860	41·0	+ 2·7	− 1·8	39·9	+ 1·9	− 1·2
			$y = -6''$.				
20	1080	20·0	+ 0·5	+ 0·5	20·0	+ 0·2	+ 0·2
	2150	20·1	+ 0·9	+ 0·2	20·1	+ 0·3	+ 0·1
	2860	20·1	+ 1·7	+ 0·3	20·1	+ 0·6	+ 0·1
40	1080	37·1	0	− 2·9	37·1	0	− 1·9
	2150	39·5	+ 1·9	+ 0·6	39·5	+ 1·3	+ 0·4
	2860	39·8	+ 1·9	− 0·2	39·8	+ 1·3	− 0·1

EXPLORATION OF THE AIRSPEED IN THE AIRSCREW SLIPSTREAM OF A TRACTOR MACHINE.

Presented by the SUPERINTENDENT, Royal Aircraft Factory.

Reports and Memoranda, No. 438. *November,* 1917.

SUMMARY.—The airspeed in the slipstream of a B.E.2c was measured over a vertical plane just in front of the tail, and from the results obtained it was possible to construct maps of the slipstream over this plane at different airspeeds and different advances per revolution of the airscrew.

The results so obtained were found to be in very close agreement with the theoretical slipstream deduced from considerations of momentum using Whirling Arm tests on the airscrew.

The results were used also to estimate the difference in tail-efficiency between a tractor and a pusher machine, due to body interference, and it was so estimated that a tractor should have a tail efficiency about 0·8 times that of a pusher; this figure agrees very well with the results of stability experiments.

1. These experiments were carried out with a B.E.2c machine, fitted with a R.A.F.1b engine and a T.7850 airscrew. The airspeed of the slipstream was measured over a vertical plane situated 33 inches in front of the leading edge of the tail plane. Pitot heads were erected at 63 different positions in this plane, being fixed to a horizontal boom, supported as illustrated in Fig. 1, which was fixed at different levels in different flights. In each flight, 8 pitot heads were used, their pressure and static sides being connected to a photographic recording instrument in the passenger's seat. This instrument was the same as that used for pressure plotting, and described in Report No. R.& M. 374. The pitot head on the wing strut was also connected to this instrument, and by this means the scale of the instrument in inches of alcohol to indicated airspeed in miles per hour was obtained—readings being taken of an airspeed indicator, also connected to the pitot head on the wing strut, at the moment of taking each photograph.

2. The experiments were made at four different air-speeds, namely, at 50, 60, 70 and 80 miles per hour, and at each air-speed photographs were taken at several different advances per revolution, ranging from the case of engine all out to that of gliding with the switch off. At the moment of taking each photograph, readings were taken of the indicated air-speed, the engine

revolutions, the height, and the temperature. From these the density, and thence the true airspeed, the advance per revolution of the airscrew, corresponding to each photograph, were deduced. In practice, 9 photographs were taken at each speed—3 with the engine all out, 3 with the engine throttled down, and 3 gliding. In all, 322 photographs were taken in this manner.

3. The height of the alcohol in the tubes was measured on the photographs, and the indicated airspeed in miles per hour at the various pitot heads deduced. If V_o be the indicated airspeed of the aeroplane (with the necessary corrections for calibration, etc.), let $(V_o + v_o)$ be the airspeed in the slipstream at any particular point in it. Let the quantity $(V_o + v_o)^2/V_o^2$ be written r/r_o. For each pitot head in the slipstream the value of this quantity r/r_o was plotted against the advance per revolution of the airscrew.

4. The mean value all over the slipstream immediately behind the airscrew (that is to say before the body and wings have begun to interfere) of $v_o(V_o + v_o)/V_o^2$ should, from considerations of momentum, be proportional to the thrust of the airscrew $/V_o^2$, and should therefore be a function of V/N — the advance per revolution only.

$$\text{Now } \frac{r}{r_o} = \frac{v_o(V_o + v_o)}{V_o^2} + \frac{V_o + v_o}{V_o} = \left(\text{a function of } \frac{V}{N}\right) + \sqrt{\frac{r}{r_o}}.$$

It follows that the mean value of r/r_o all over the slipstream immediately behind the airscrew should also be a function of V/N. It was found, on plotting r/r_o against V/N for the different pitot heads in the slipstream, that at some points the value of r/r_o at that particular point was also a function of V/N only, but that at other points it was a function both of V/N and of V_o. In Figs. 3a and 3b two curves are shown illustrating this. In Fig. 3a all the points for all airspeeds lie upon the same curve, but in Fig. 3b it will be seen that they give different but similar curves for different airspeeds. The reason of this will be shown later.

5. The positions of the pitot heads at which the airspeed was measured are shown in Fig. 2. From the curves of r/r_o against V/N for these different pitot heads it was possible to plot r/r_o along different horizontal lines across the slipstream at a given airspeed and advance per revolution. r/r_o was so plotted along five such horizontal lines, in each case for the following airspeeds and V/N, namely :—

$$50 \text{ m.p.h.} \left\{ \begin{matrix} 6{\cdot}4 \\ 7{\cdot}4 \\ 18{\cdot}0 \end{matrix} \right\} \text{Adv/Rev.}$$

$$60 \text{ m.p.h.} \left\{ \begin{matrix} 7{\cdot}6 \\ 8{\cdot}4 \\ 16{\cdot}0 \end{matrix} \right\} \text{Adv/Rev.}$$

$$70 \text{ m.p.h.} \left\{ \begin{matrix} 8{\cdot}2 \\ 9{\cdot}0 \\ 15{\cdot}4 \end{matrix} \right\} \text{Adv/Rev.}$$

$$80 \text{ m.p.h.} \left\{ \begin{matrix} 9{\cdot}0 \\ 10{\cdot}0 \\ 15{\cdot}0 \end{matrix} \right\} \text{Adv/Rev.}$$

An example of the curves so obtained is given in Fig. 4.

6. From the aggregate of these curves it was now possible, at a given airspeed and V/N, to draw illustrations in contour of the whole section of the slipstream through the plane in which the pitot heads were fixed. These contours were drawn for :—

50 m.p.h.	Adv/Rev	6·4
60 m.p.h.	Adv/Rev.	7·6
70 m.p.h.	Adv/Rev.	8·2
80 m.p.h.	Adv/Rev.	9·0

the Adv/Rev. representing roughly the case of engine all out for the various airspeeds. These contours are shown in Figs. 5, 6, 7 and 8.

7. If these contours be examined, certain characteristics stand out prominently. In the first place the slipstream attains its maximum intensity at two separate points, in the top-right and bottom-left corners. These points of maximum intensity vary in position at different airspeeds, and in general the slower the airspeed the further they have moved round in a counter clockwise direction, *i.e.*, in the direction of rotation of the airscrew. It would appear that the slipstream, immediately after leaving the airscrew, is separated by the wings and body into two distinct streams, passing between the wings on either side of the body* ; the stream on the left flowing slightly downwards, and that on the right slightly upwards, in consequence of the rotation of the airscrew. This effect of rotation appears to be greatest at a slow airspeed—this is what would be expected. Also, the centre of the slipstream, that is to say, the region in the middle where the velocity is least, is lower the greater the airspeed. This also is as would be expected, since the angle of incidence is least at high speeds, and this is partially, but only partially, compensated for by the change in downwash.

8. It is effects such as these, which are functions only of the airspeed and not of the advance per revolution, which are responsible for the sort of difference that is illustrated in Figs. 3a and 3b. Such effects are principally of two kinds—(*a*) change of incidence. This has the effect of shifting the slipstream, at a given advance/rev. but at varying airspeed, bodily up and down. It is clear that this would make very little difference at

* It is probable that there also exists a third stream, passing underneath the lower wing, but no trace of this was observed since it was impossible to rig up pitot heads very far below the body.

points in whose neighbourhood the contours are flat, but would have a marked effect elsewhere; (*b*) a difference, due to air-speed, in the amount of body and wing drag. This would have a marked effect except at points to which the slipstream has come without any interference from wings or body. The only points which satisfy the conditions for independence of V_o required both in (*a*) and (*b*), are points in the two regions of maximum intensity in the top-right and bottom-left corners of the contours, for at these points the contours are flat, and the slipstream, being at its maximum, can have been subject to very little interference from wings and body. In Fig. 2 the pitot heads where r/r_o was found to be independent of V_o are specially marked, and it will be seen that they all lie within these two regions.

9. Finally, it should be noted that the region of high velocity in the bottom left-hand corners of the contours is invariably divided into two by a line situated approximately at the level of the tail plane. This is reasonable, since it is probable that the tail plane has some retarding effect even 33 inches in front of it.

10. It is natural to assume that, when it leaves the airscrew, the slipstream is more or less symmetrical in shape—a solid cylinder with a hole in the middle—and that the intensity all over this cylinder is much the same as the maximum intensity shown in the contours. By the time that it reaches the tail, however, this slipstream will have been considerably slowed down by the drag of the body and wings, and only that part of it which has come undisturbed through the space between the wings at some distance from the body will retain its original full intensity. If the mean theoretical values of r/r_o over the slipstream as it leaves the airscrew be calculated from considerations of thrust, it is found that they agree very well with the maximum values of r/r_o shown in the contours. This mean r/r_o is of course the quantity usually called "R/R_o," being the factor necessary to allow for the increased resistance due to the slipstream of a body situated therein, and is calculated from the indicated airspeed V_o of the machine, and the value of Thrust/(Diameter of Airscrew)^2. Calculations were made on the bases of the actual observations made, the thrust being deduced from the B.H.P. of the engine, when running all out at the revolutions and density observed, and from the airscrew efficiency curve given by experiments on the Whirling Arm. A table of calculated R/R_o against maximum r/r_o shown in the contours is given below:—

Speed.	Adv/Rev.	V_o.	Observed Density.	Revs.	R/R_o.	Max. r/r_o.
50 m.p.h. all out ...	6·4	51·3	0·891	1,495	2·43	2·60–2·65
60 m.p.h. all out ...	7·6	60·8	0·800	1,575	1·86	1·80–1·90
70 m.p.h. all out ...	8·2	68·4	0·810	1,630	1·68	1·60–1·65
80 m.p.h. all out ...	9·0	81·6	0·885	1,700	1·50	1·40–1·50

11. Thus, the agreement between the theoretical R/R_o and the observed r/r_o is very good. This agreement can be illustrated in another manner, as follows. From theoretical considerations of momentum we should have :—

$$\rho_o A v_o (v_o + V_o) = T$$

where T is the thrust of the airscrew in lbs., v_o and V_o are indicated airspeeds in ft/sec., ρ_o is the standard density in slugs per cubic foot = 0·00237, and A is the area in sq. ft. of the slipstream as it leaves the airscrew. Assume, as before, that the slipstream when it leaves the airscrew is a hollow cylinder, and take the dimensions of this cylinder as 0·8 D outside diameter and 0·2 D inside diameter (where D = airscrew diameter). These are taken from slipstream experiments with a pusher machine (see Report No. R. & M. 382). In the present experiments D was = 9 ft. 2 in., and we should therefore have, theoretically, $(0{\cdot}0941)\, v_o (v_o + V_o) = T$, or

$$\frac{T}{v_o^2} \quad (10{\cdot}62) = \frac{v_o (v_o + V_o)}{V_o^2}$$

In Fig. 13 is shown the curve of (10·62) T/V_o^2 against Adv/Rev. deduced from Whirling Arm tests on a T.7850 airscrew, and also the curve of $v_o (v_o + V_o)/V_o^2$ against Adv/Rev., deduced from the observations made in the present experiments, for a pitot head approximately at the point of maximum slipstream intensity. The fact that these two curves are in substantial agreement is evidence that the momentum theory, upon which R/R_o is calculated, is correct, and is also evidence of the accuracy of the assumptions made above as to the nature and dimensions of the slipstream immediately after it has left the airscrew.

12. The experiments are therefore a direct confirmation of the theoretical methods of calculating R/R_o at present in use. They indicate, however, an error in the methods in use of employing this quantity R/R_o. Though the theoretical value of R/R_o appears to be correct for the slipstream as it leaves the airscrew, the experiments show that by the time it reaches the tail this value is, in general, much too big ; that it has been, so to speak, already considerably absorbed and used up in increasing the drag of the body and wings. This does not, of course, mean that it is incorrect to multiply the body and wing drag by the full theoretical value of R/R_o, for the small r/r_o observed are precisely the results of this increased body and wing drag, but the resistance of anything in the slipstream behind the body—for instance of the tail plane, fin, tail skid, etc.—should not be multiplied by the full theoretical R/R_o since, by the time it reaches them, R/R_o has been considerably lessened by the wings and body. In practice, however, except in one particular, the error here involved is too small to be noticeable. This one important effect is the lift of the tail plane. It is usual in

calculating the increased tail lift due to the slipstream to speak of its "effective area" being increased. Thus the lift of the tail is said to be proportional to $A'V_o^2$, where V_o is the indicated airspeed of the machine and A′ is the effective tail area. A′ is estimated as follows :—The slipstream is assumed to be a solid cylinder with its centre line along the axis of the airscrew, and with an outside diameter 0·8—and an inside diameter 0·2—of the airscrew diameter. The areas of tail plane respectively inside and outside this assumed slipstream are then measured, say A_1 sq. ft. in, and A_2 sq. ft. out. The effective area is then defined as $(A_2 + A_1 R/R_o)$. It is clear, however, that the true effective area of the tail plane should be $\int b\ r/r_o\ dy$, b being the tail chord at a distance y along the tail span, and r/r_o the value of $(v_o + V_o)^2/V_o^2$ on the level of the tail plane and at a distance y out along the span, the integration being made right along the tail span. This integration was effected graphically by means of a planimeter for a B.E.2e tail, the values of r/r_o being interpolated from the contours. The following table shows the effective area so integrated, and the effective area calculated by the standard method, at 50, 60, 70 and 80 m.p.h. engine all out :—

Speed.	Adv/Rev.	Calculated R/Ro.	Calculated effective area.	Effective area integrated from observations.	Factor.
50 m.p.h. all out.	6·4	2·43	82·7	66·6	0·805
60 m.p.h. all out.	7·6	1·86	68·2	56·0	0·821
70 m.p.h. all out.	8·2	1·68	63·7	51·9	0·815
80 m.p.h. all out.	9·0	1·50	59·1	48·5	0·821

It is seen that the error involved in the standard method of calculation is almost exactly the same at all speeds—a correcting factor of about 0·815 being invariably necessary.

13. In practice, however, this error is of academic interest only, since it has always been customary to multiply the tail lift by a factor E, called the "tail efficiency," and errors involved in estimating effective area are absorbed into this factor E. The factor E can be deduced, however, for any given machine from stability and trimming speed experiments, and it has been so found that for pusher machines E is usually of the order 0·8, and for tractor machines of the order 0·65. The discrepancy between these two values should be accounted for by the interference of the wings and body with the slipstream

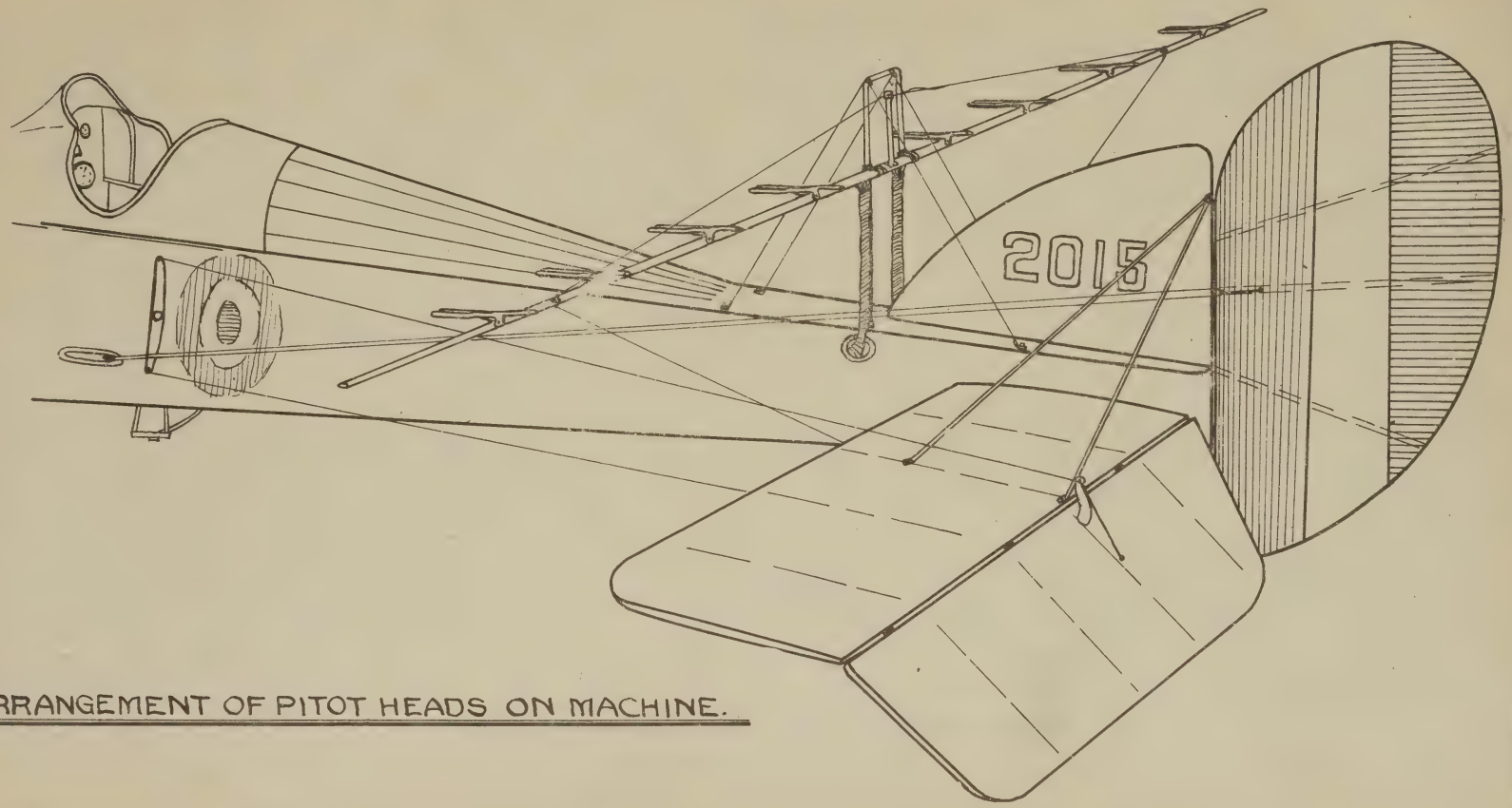

ARRANGEMENT OF PITOT HEADS ON MACHINE.

FIG. 1.

POSITION OF PITOT HEADS.

SCALE 1 INCH = 1·4 FT

◎ HEAD WHERE r/r_o WAS INDEPENDANT OF V_o.

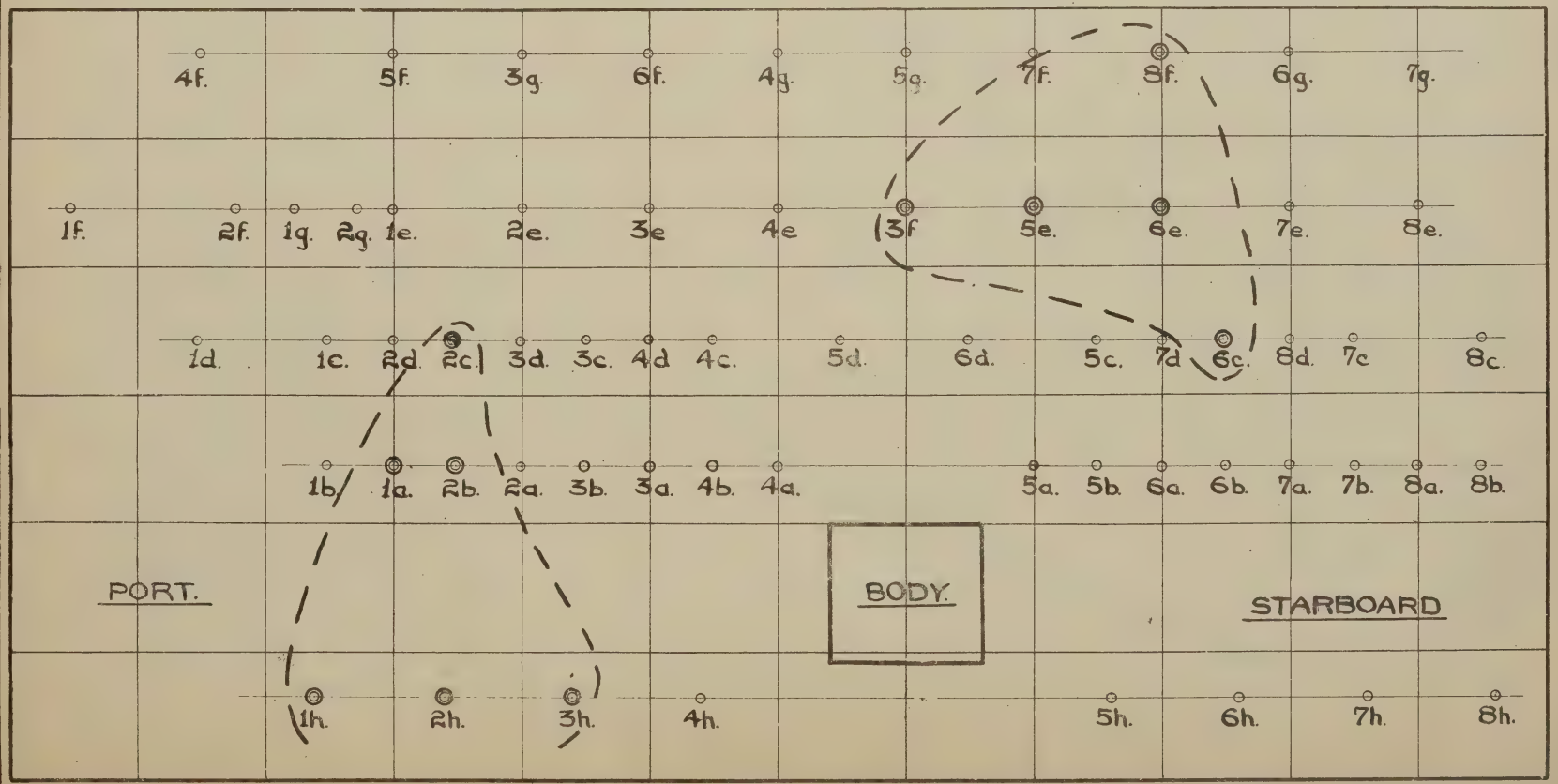

FIG. 2.

FIG. 3a.

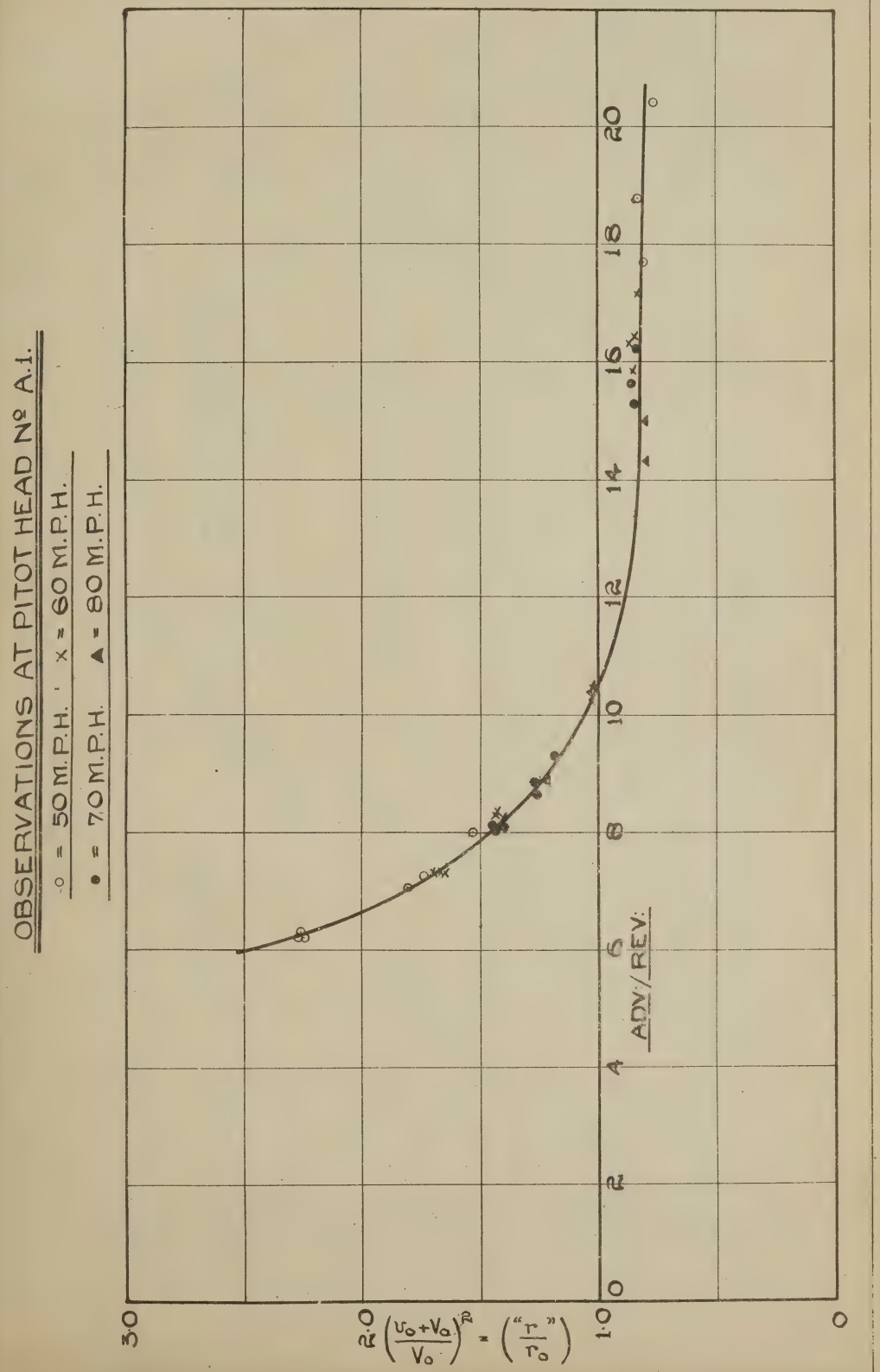
OBSERVATIONS AT PITOT HEAD Nº A.1.
○ = 50 M.P.H. × = 60 M.P.H.
● = 70 M.P.H. ▲ = 80 M.P.H.
ADV/REV:
0
2
4
6
8
10
12
14
16
18
20
3.0
2.0
1.0
0
$\left(\frac{V_o+V_a}{V_o}\right)^2 = \left(\frac{"r"}{r_o}\right)$

REPORT No 438.

OBSERVATIONS AT PITOT HEAD No. H.4.

—o— = 50 M.P.H.

—x— = 60 M.P.H.

—·—⊕—·— = 70 M.P.H.

—·—▲—·— = 80 M.P.H.

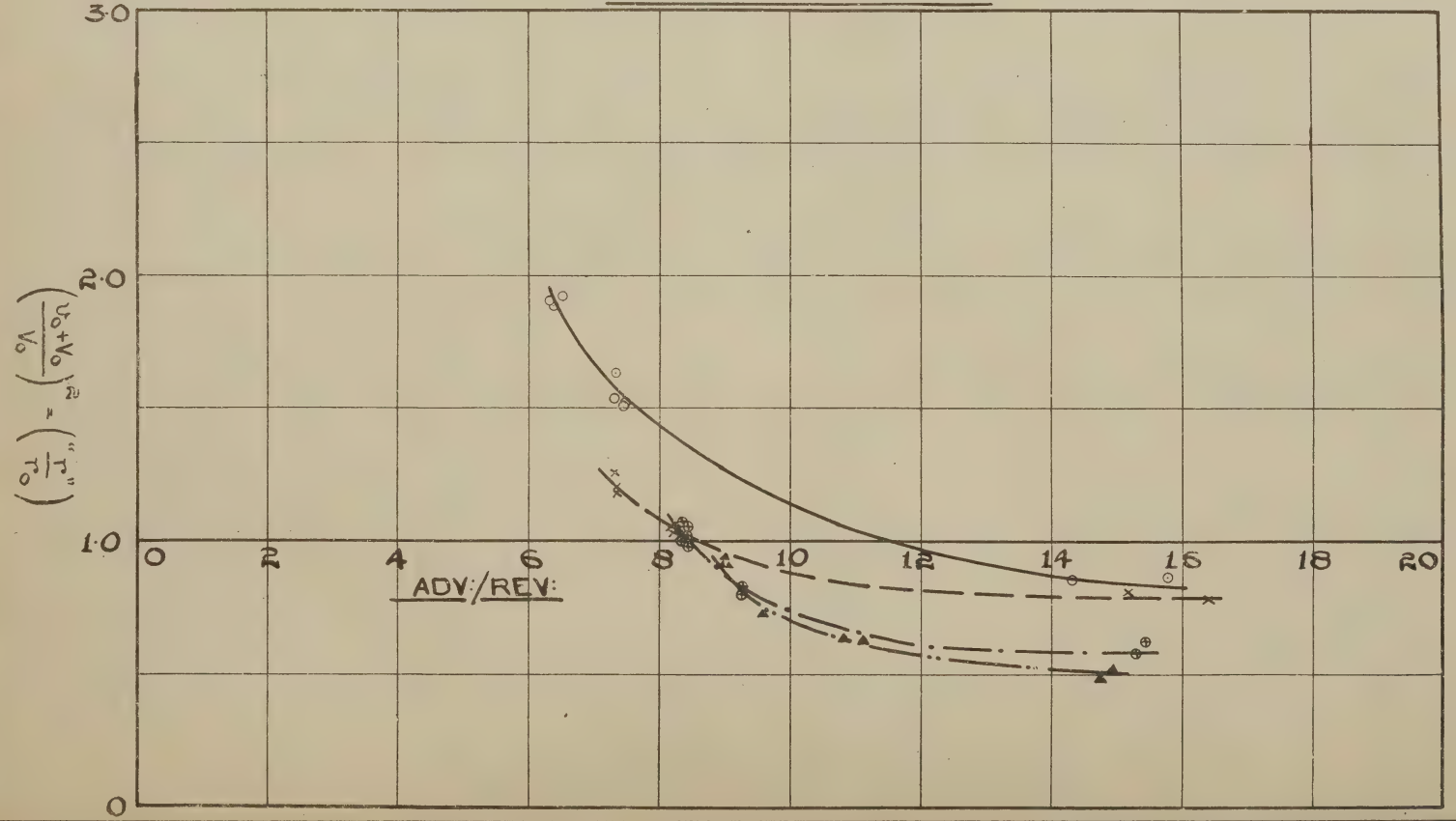

FIG.3b.

SLIP STREAM AT A LEVEL 29" ABOVE BODY, TOP SURFACE.

50 M.P.H. { x = 6·4 / o = 7·4 / + = 18·0 } ADV./REV.

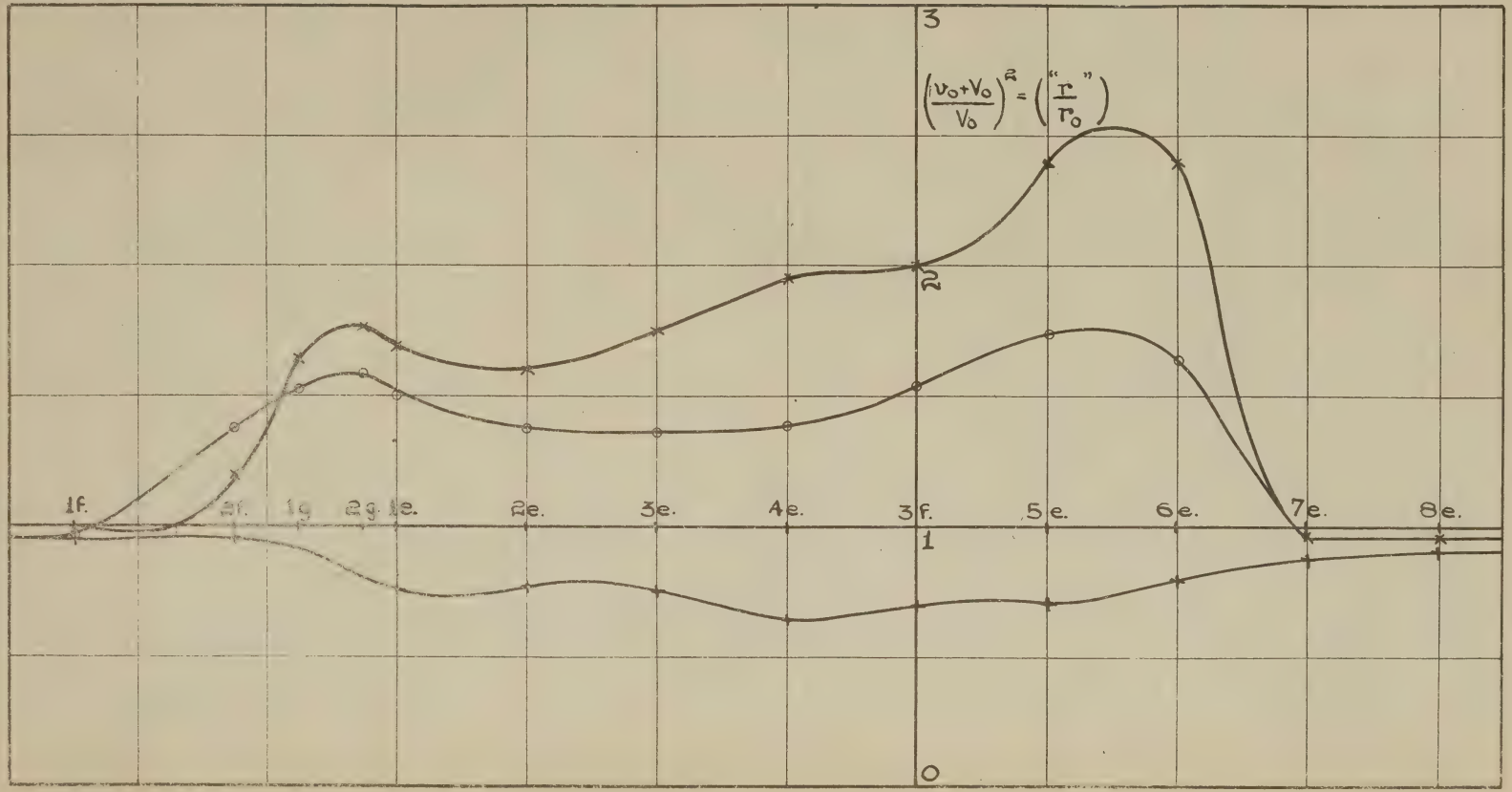

REPORT Nº 438.

FIG 4

50 M.P.H. FULL THROTTLE. CONTOURS OF THE SLIP STREAM. ADVANCE PER REV. = 6·4'

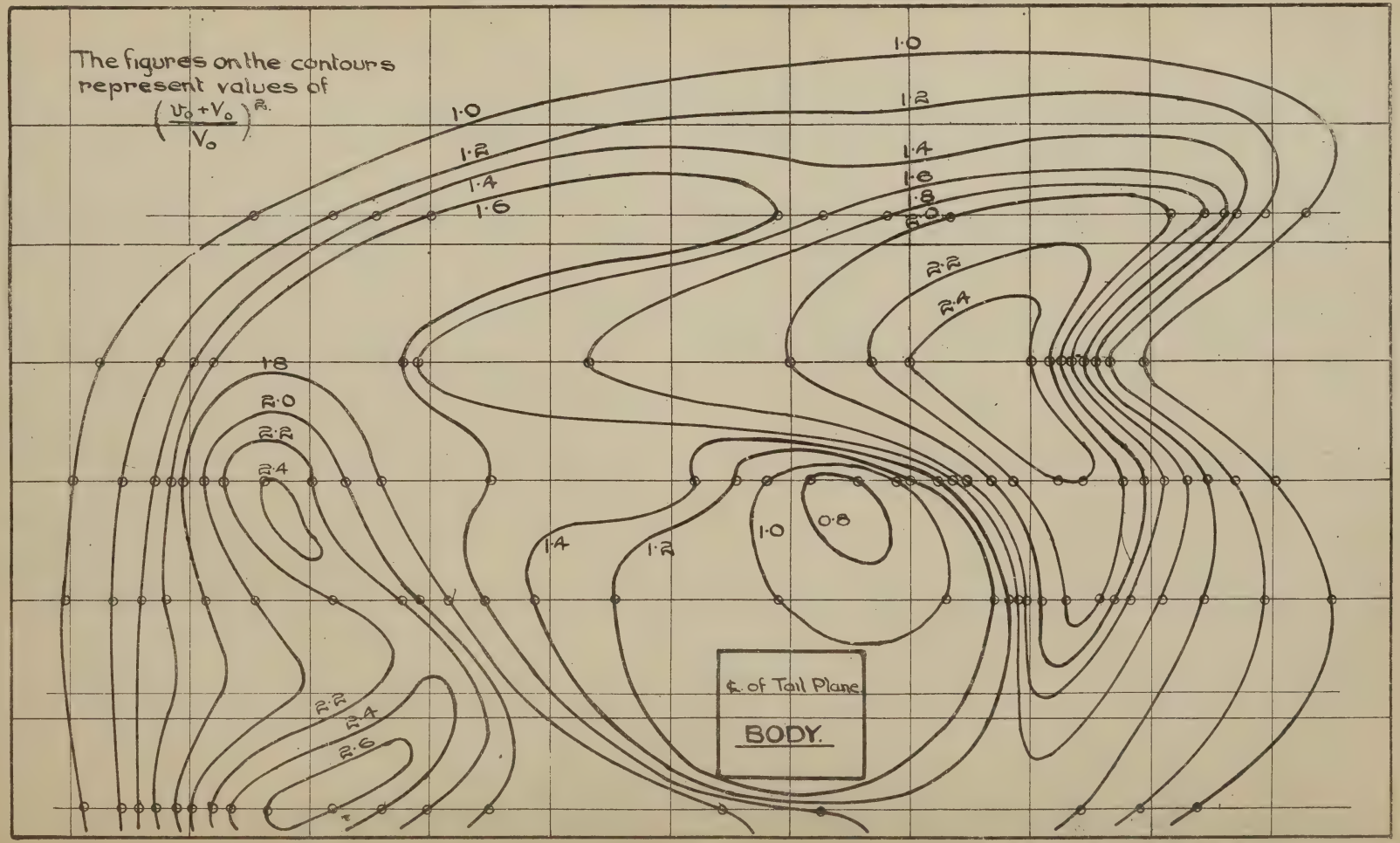

REPORT No 438.

FIG 5.

CONTOURS OF THE SLIP STREAM.

60 M.P.H. FULL THROTTLE.
ADVANCE PER REV. = 7·6'.

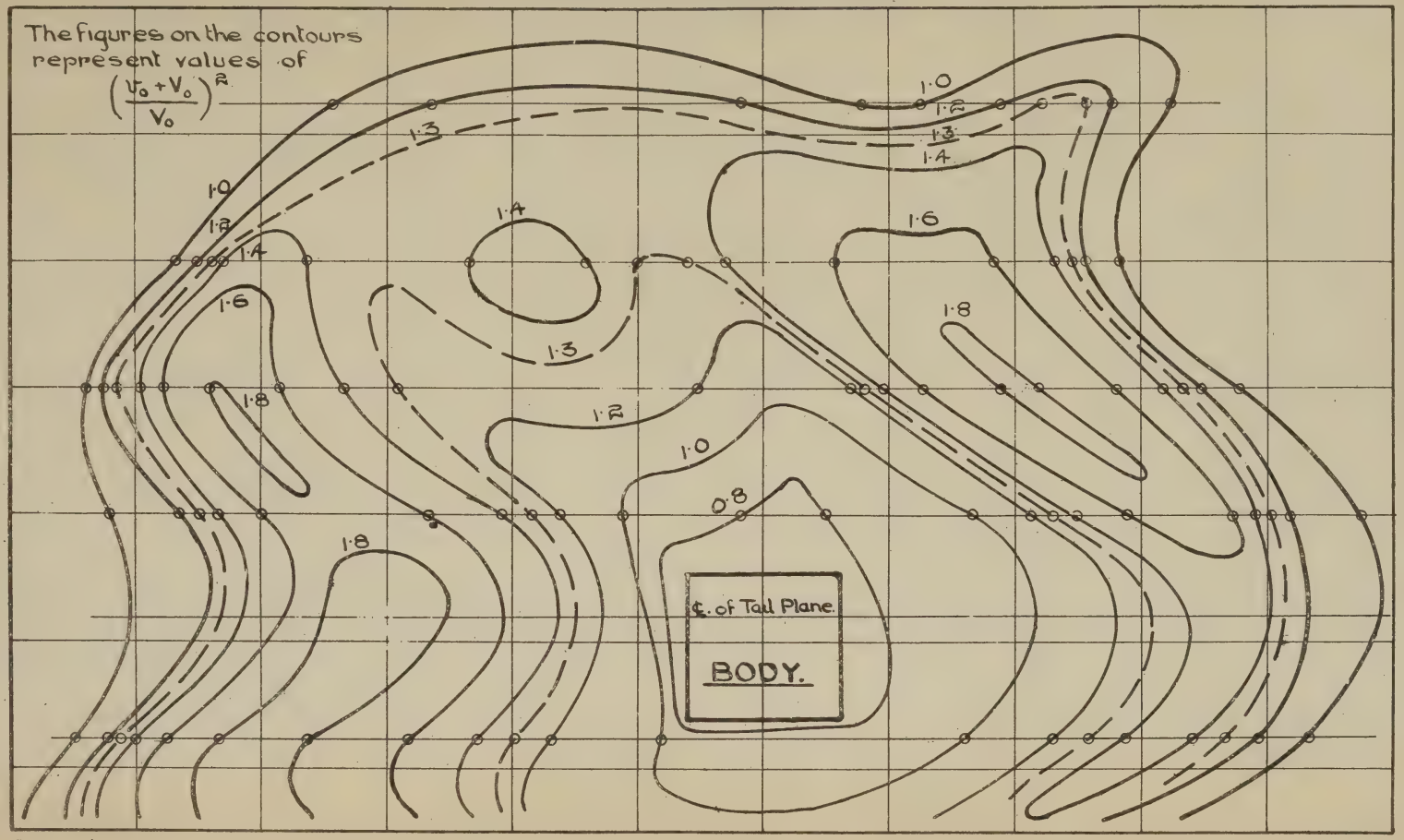

REPORT No 438.

FIG.6.

CONTOURS OF THE SLIP STREAM.

70 M.P.H. FULL THROTTLE.

ADVANCE PER REV. = 8·2'.

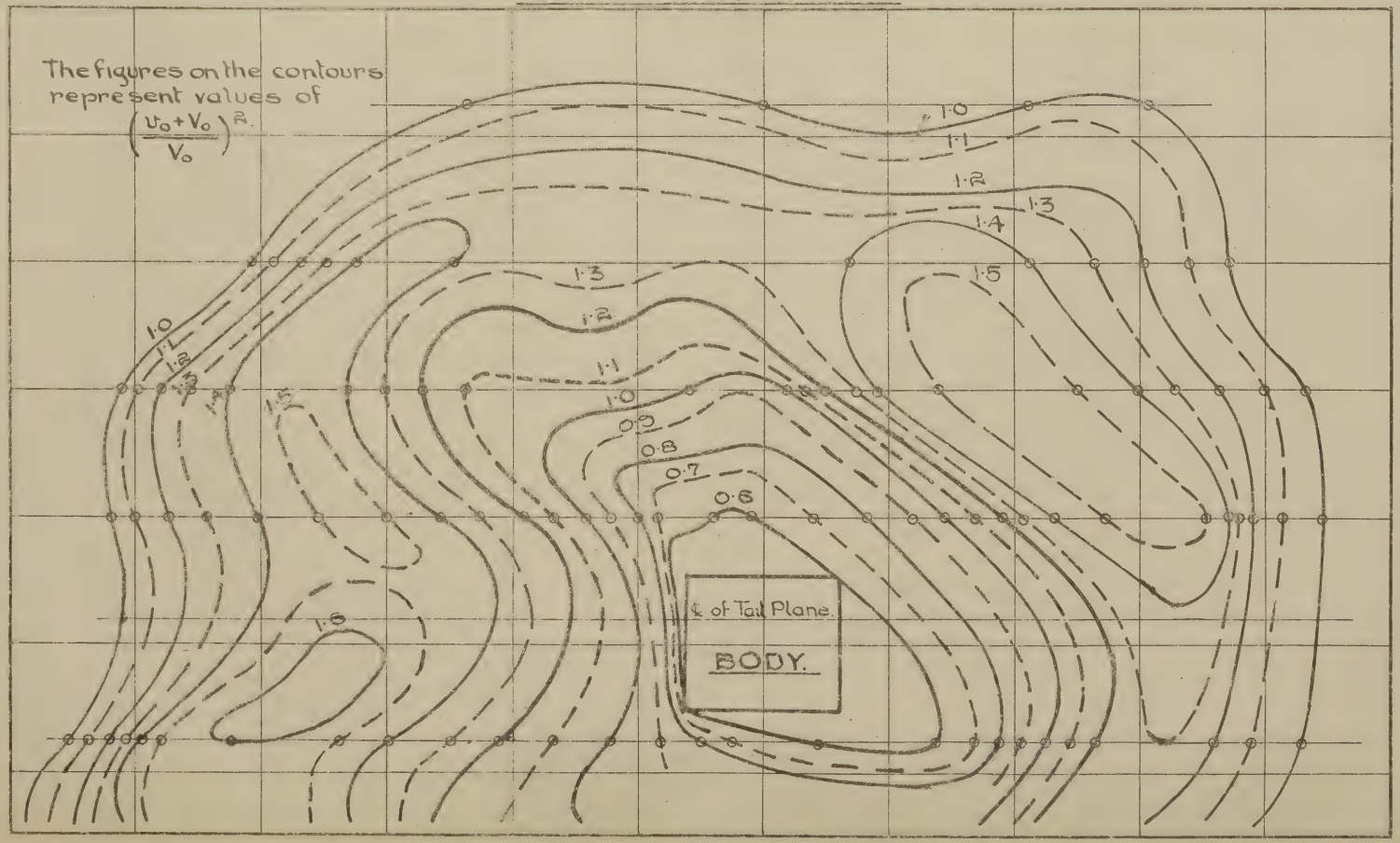

REPORT No. 438.

FIG. 7.

CONTOURS OF THE SLIP STREAM.

80 M.P.H. FULL THROTTLE.

ADVANCE PER REV. = 9·0'.

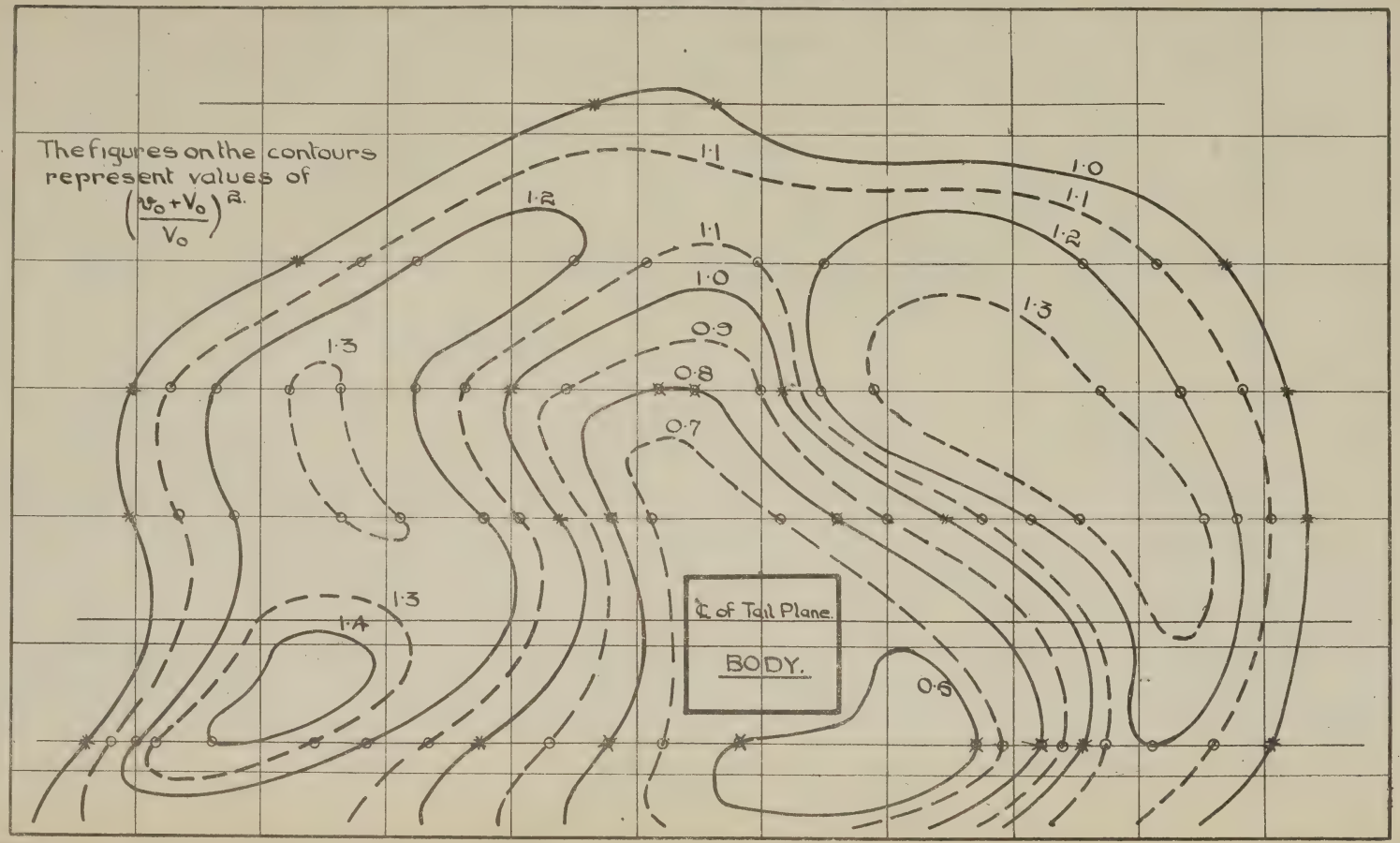

REPORT No. 438.

FIG 8.

CONTOURS OF THE SLIP STREAM.
50 M.P.H. HALF THROTTLE
ADVANCE PER REV. = 7·4'

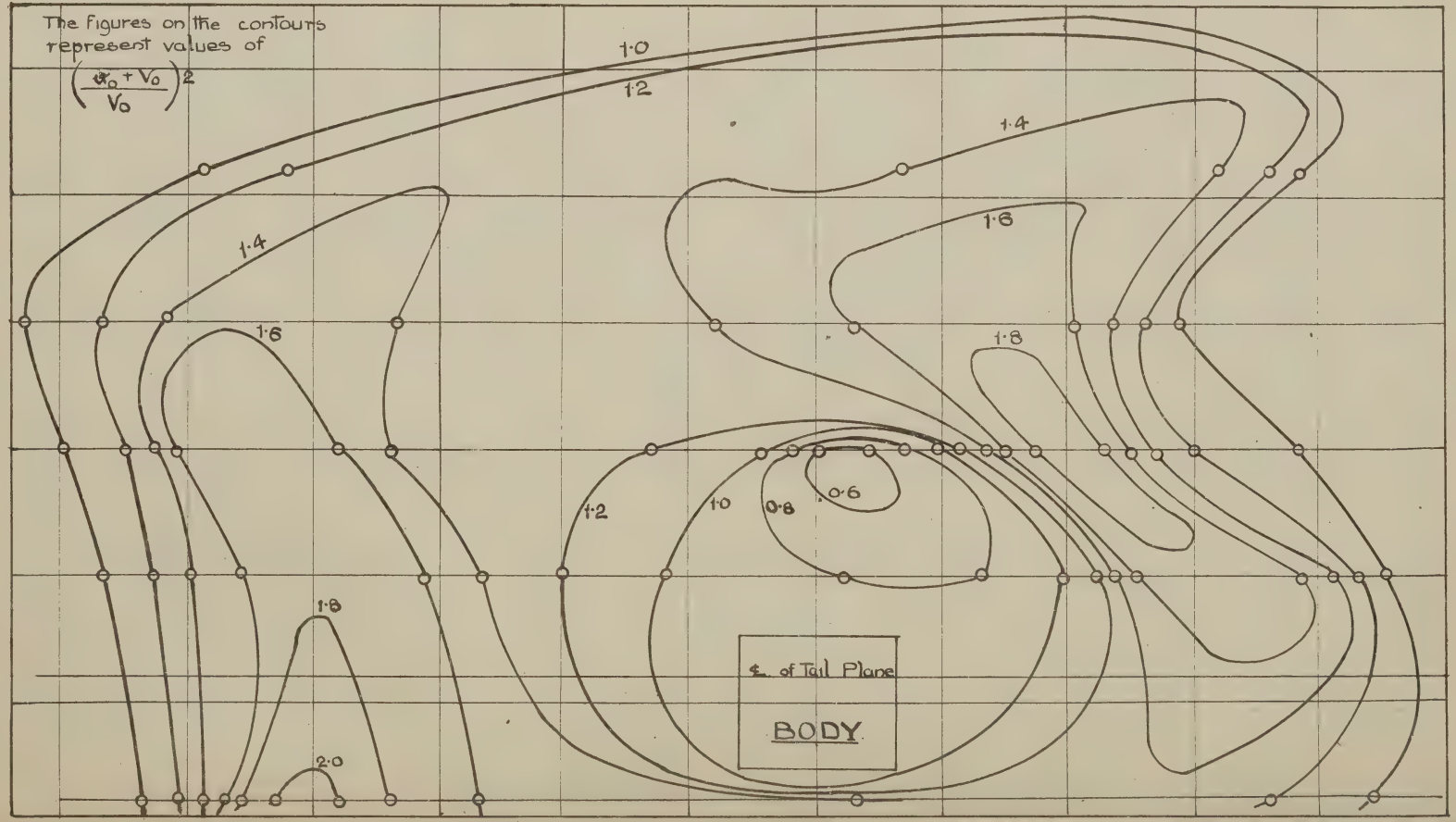

REPORT No 438.

FIG. 9.

CONTOURS OF THE SLIP STREAM

60 M.P.H. HALF THROTTLE

ADVANCE PER REV. = 8·4'.

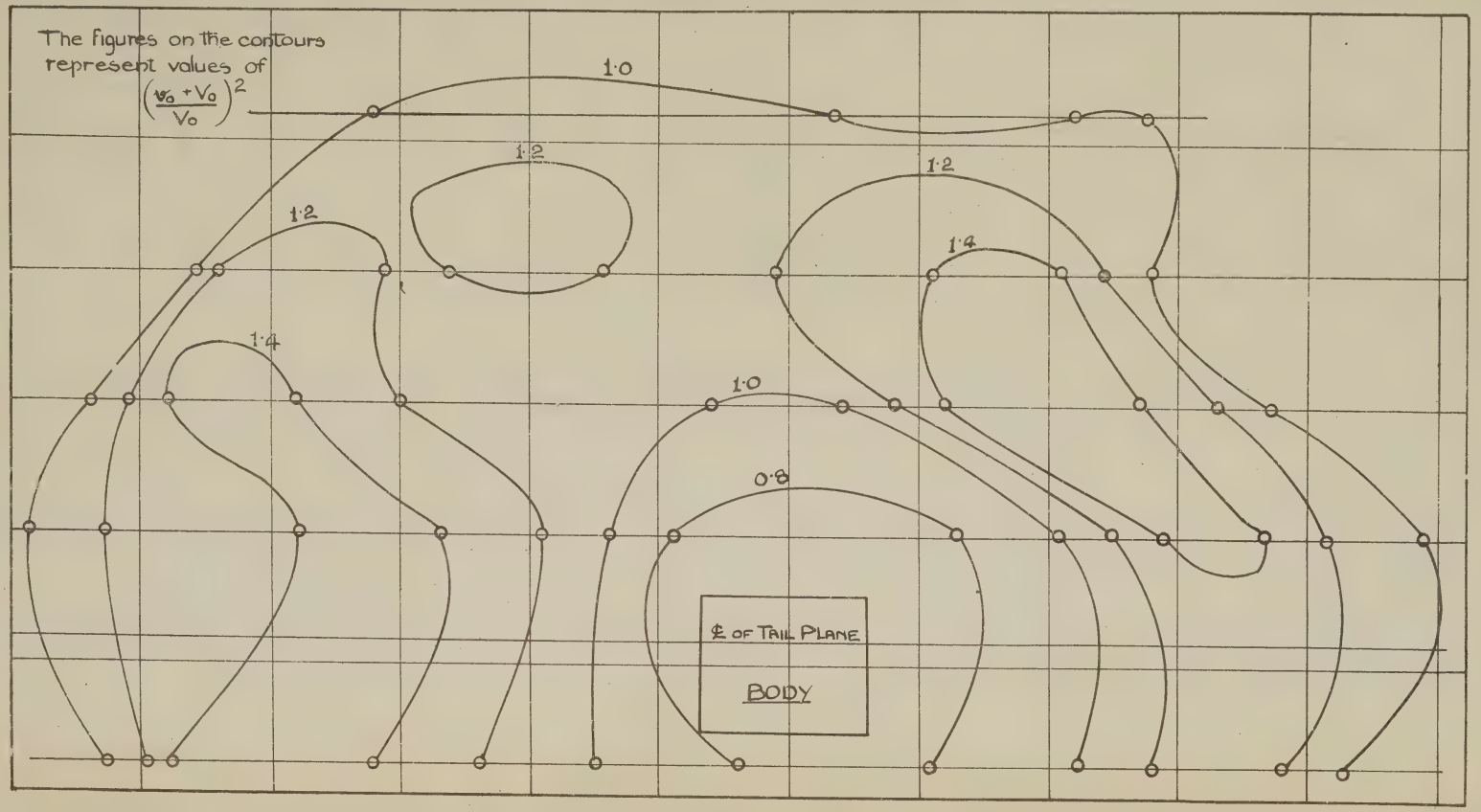

REPORT Nº 438.

FIG.10

CONTOURS OF THE SLIP STREAM

70 M.P.H. HALF THROTTLE

ADVANCE PER REV. = 9·0'.

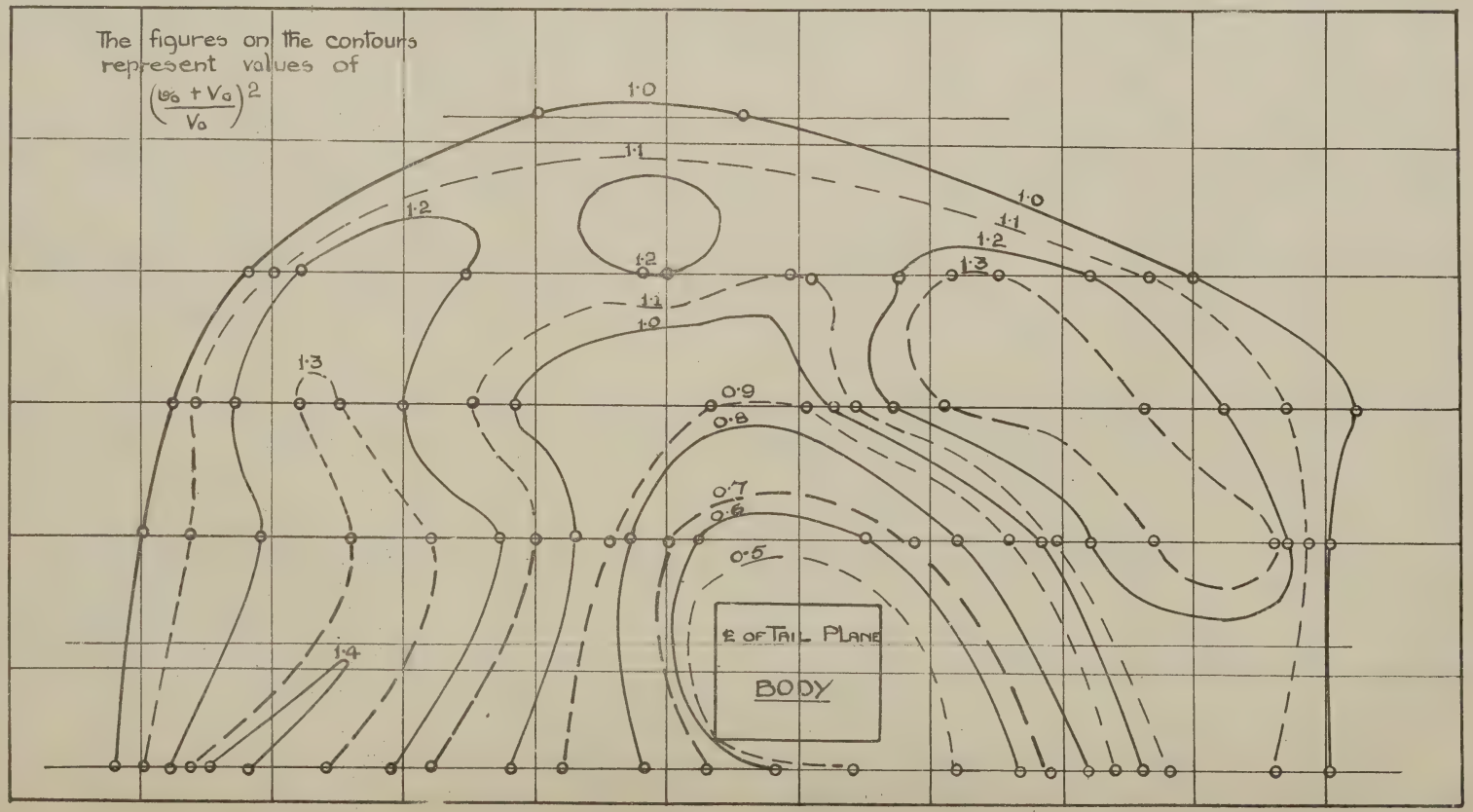

REPORT No 438.

Fig. 11.

CONTOURS OF THE SLIP STREAM

80 M.P.H. HALF THROTTLE

ADVANCE PER REV. = 10·0'

The figures on the contours represent values of $\left(\frac{V_s + V_o}{V_o}\right)^2$

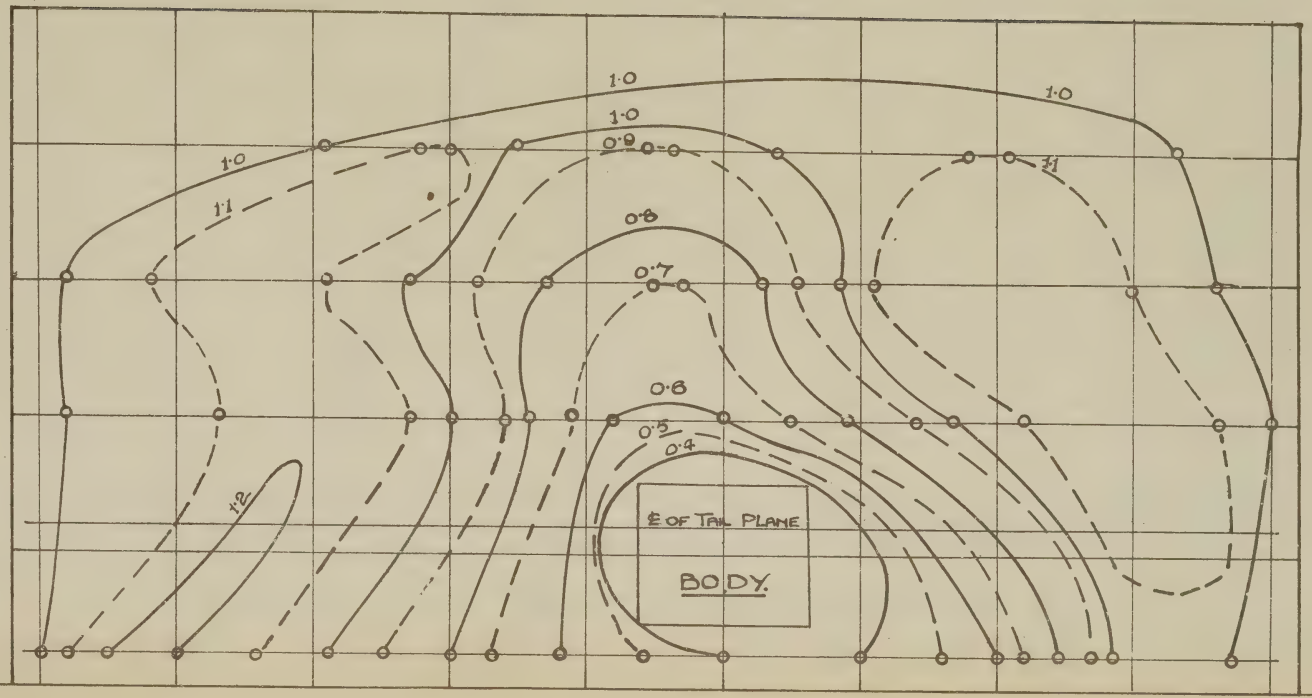

FIG. 12.

REPORT No. 438

COMPARISON OF $\frac{v_o(v_o+V_o)}{V_o^2}$ WITH THE $T/\rho A V_o^2$ GIVEN BY WHIRLING ARM TESTS.

——— = CURVE OF $\left[T/V_o^2 \times 1/\rho_o A\right]$ FOR T.7850 FROM WHIRLING ARM TESTS.

– – – = CURVE OF $\frac{v_o(v_o+V_o)}{V_o^2}$ FROM OBSERVATIONS AT PITOT HEAD No. H.1.

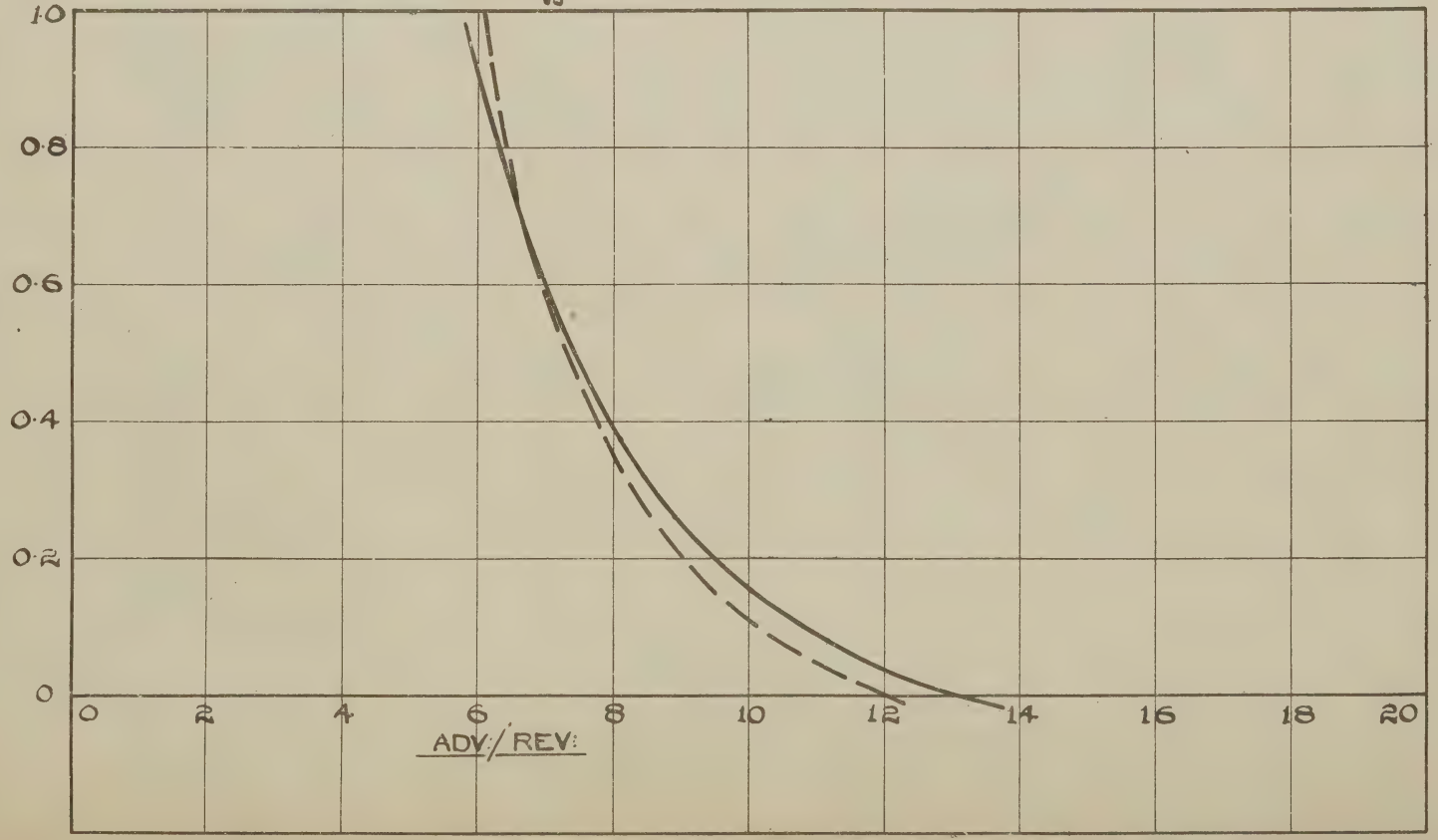

FIG. 13.

which exists in a tractor machine but not in a pusher ; in other words, this discrepancy should be identical with the error in estimating the effective tail area of a tractor described above. That error, as has been shown, necessitates a correcting factor of 0·815, and it follows that the efficiency of a tractor tail should be about 0·815 that of a pusher tail, which agrees very well with the values deduced from stability experiments. The experiments described in this report therefore confirm the stability experiments with reference to tail efficiency.

EXPERIMENTS ON THE ROTATION OF A PROPELLER SLIPSTREAM IN A PUSHER AEROPLANE.

Presented by the SUPERINTENDENT, Royal Aircraft Factory.

Reports and Memoranda (*New Series*), *No.* 408. *November*, 1917.

SUMMARY.—(*a*) *Introductory.* (*Reasons for inquiry.*)—It was found that F.E. 9, a recently designed pusher aeroplane, had a considerable turning tendency with the engine on.

(*b*) *Range of the investigation.*—Experiments were carried out to determine the angle of yaw and the position of the centre of the slipstream in the neighbourhood of the fin and rudder. The exploration was made just in front of the fin position by means of a small double vane which would indicate the direction of flow of the air. To avoid interference the fin was removed.

The angle of yaw of the slipstream was measured over a distance of 2 feet above and below the centre of the tail plane.

(*c*) *Conclusions.*—The centre of the slipstream was found to be considerably below the position estimated from previous data, due apparently to a rapid change of downwash between the propeller and the tail plane. The angle of yaw at any point of the slipstream was found to be roughly proportional to the inverse of the speed and to the inverse of the distance from the axis of the slipstream, reaching its maximum of 18° about 10″ below the tail plane.

(*d*) *Applications and further developments.*—In view of the turning tendency of machines fitted with high powered engines, it is important that the flow of air behind a propeller should be more fully investigated. Where the fin and rudder are in the slipstream an aeroplane cannot be balanced so as to fly straight at all speeds without the use of the rudder. Perfect balance at all speeds can only be secured with the fin and rudder outside the slip stream, though a good approximate balance can be obtained with the fin and rudder in the centre of the slipstream.

1. From the results of the exploration of the slipstream on an F.E. 2 machine, which were described in R. & M. 266, it was found that the slipstream could be regarded as a cylinder whose outer radius was 0·8 times and inner radius 0·2 times that of the propeller. Investigations now carried out on another type of pusher machine serve to determine the rotation of the slipstream and the position of its centre line. The instrument used was a small double vane (Fig. 1) fitted to the king post on the front spar of the tail plane, the fin being removed and a balanced rudder fitted, in order to avoid interference with the vane. The height of the vanes could be adjusted from the

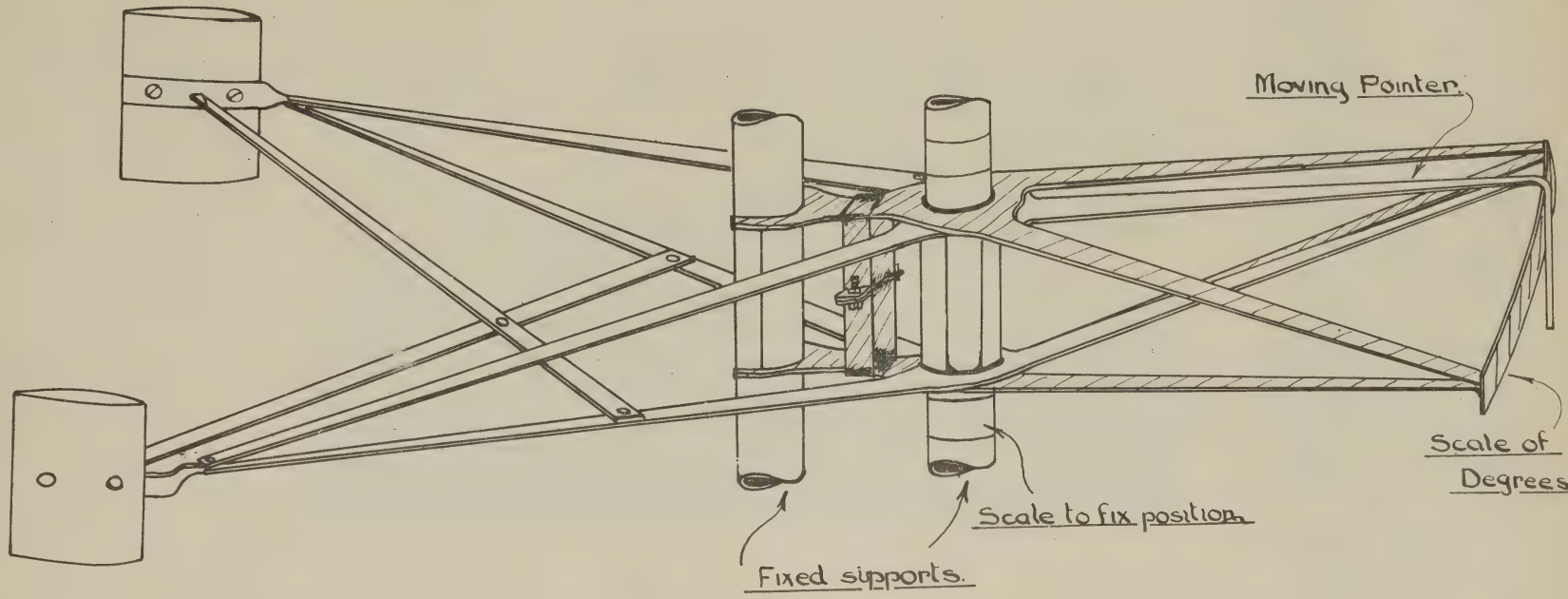
Moving Pointer.
Scale of Degrees.
Scale to fix position.
Fixed supports.

FIG 1.

ANGLE OF YAW OF THE PROPELLER SLIP STREAM.

——— 70 M.P.H.

– – – 60 M.P.H.

—·—·— 50 M.P.H.

—·—·—·— 85 M.P.H. THROTTLED.

NOTE. No importance can be attached to results within 10" of the centre line of the slip stream.

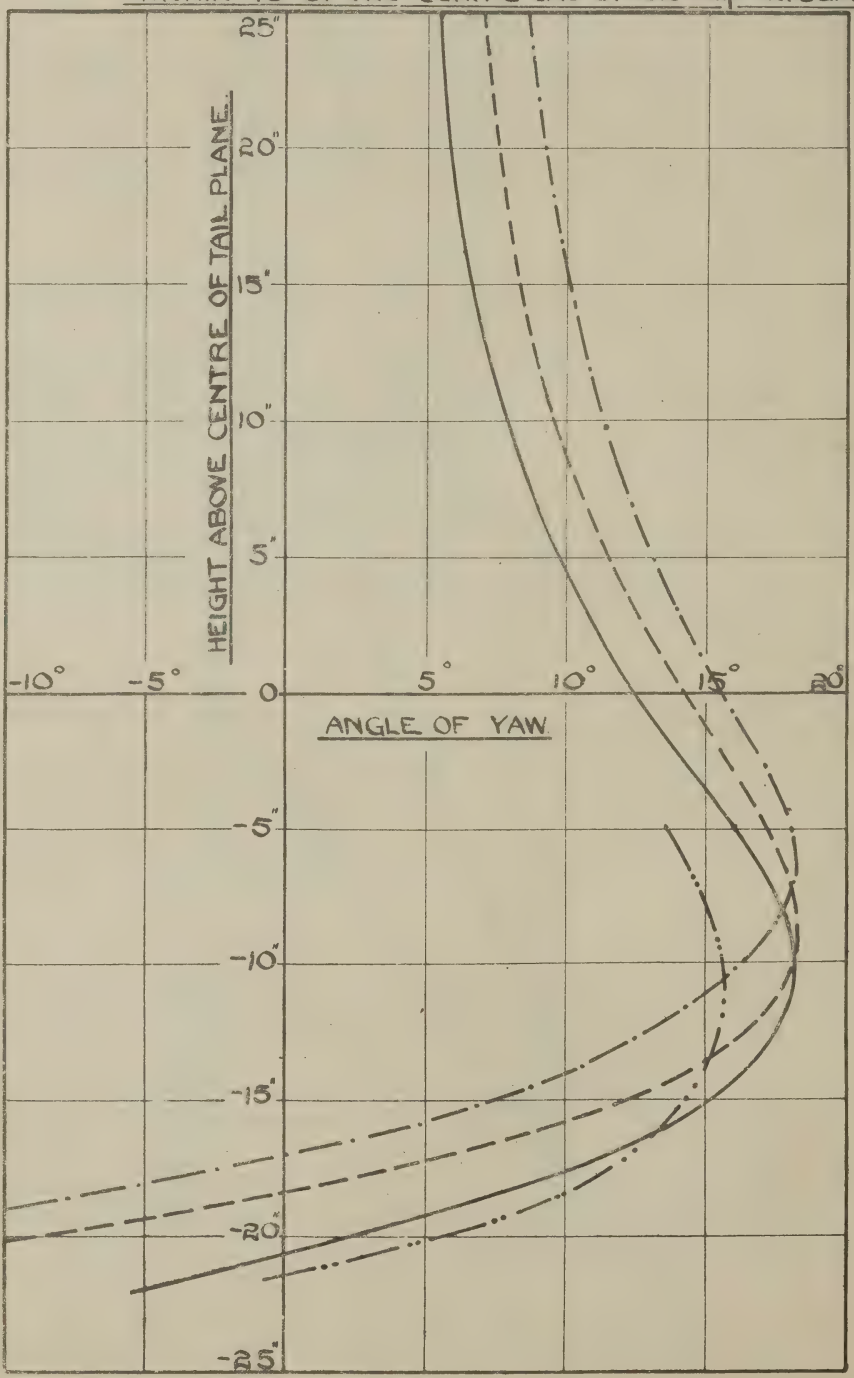

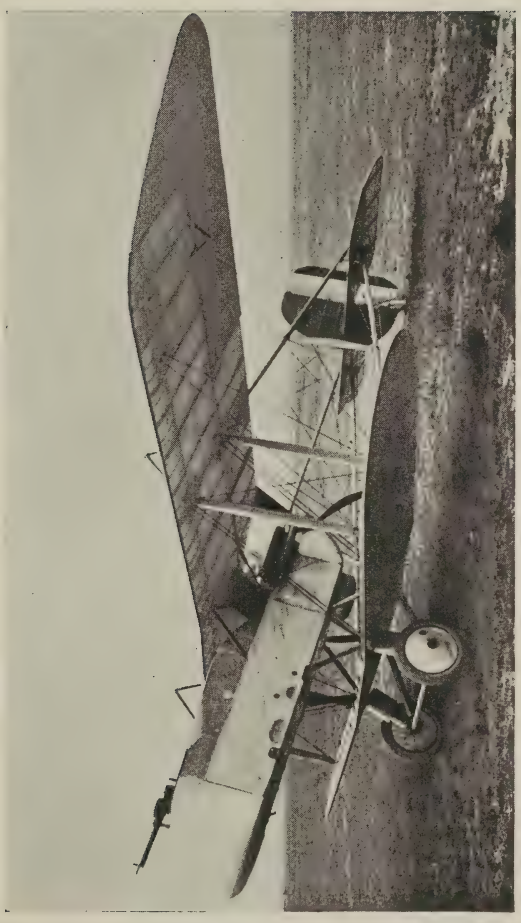

observer's compartment, and in this way readings were obtained at different airspeeds over a range of about 2 feet above and below the tail plane. The results of these experiments are shown in Fig. 2. It should be noted that, owing to the size of the instrument, it is impossible to obtain the angle of yaw of the slipstream near its centre line, but from the symmetrical form of the results it appears that the position of the centre line is determined satisfactorily.

2. The measurements were taken at a distance of 125″ behind the propeller, and the zero point on the centre line of the tail plane was 5·2″ above the propeller axis. From the depth (d) of the axis of the slipstream below the propeller axis it is possible to deduce the mean angle of downwash between the propeller and the tail plane by means of the formula

$$m + \alpha - \theta = 57{\cdot}3 \times \frac{d}{125}$$

where θ is the angle of incidence, m is the mean angle of downwash, and α is the angle between the propeller axis and the wing chord. The values of m are given in Table 1, and in the next column are the angles of downwash at the tail plane derived from full scale experiments with the same wing section on a tractor machine and corrected for the effect of the propeller. It appears that the mean angle of downwash m is uniformly 20 per cent. larger than the estimated angle at the tail plane. This is in reasonable agreement with model tests which show a similar flattening out of the downwash towards the tail plane (R. & M. 156). The model tests give for this ratio the value 1·2 when the tail plane is on a level with the upper wing, while a maximum of 1·5 is reached a little below the mid-point. On the aeroplane used in these experiments the tail plane was just below the level of the upper wing.

3. The actual angles of yaw as observed are shown in Fig. 2 and for distances of more than 15″ from the centre line of the slipstream, the angle of yaw is approximately inversely proportional to the speed and to the radius. From the results of the earlier experiments, described in R. & M. 266, the slipstream would be expected to end at a distance of 35 inches from the centre line, since the diameter of the propeller was 87 inches. This figure was based on the exploration of the velocity and the results of the present series of experiments indicate either that the rotation extends over a larger cylinder than the increased velocity or that the cross section of the slipstream has increased in size, the exploration of the slipstream velocity having been made nearer to the propeller (0·76 and 1·09 diameters) than in the present case. The true explanation is probably a combination of both of these. It is evident that eventually the slipstream will increase in diameter as the surrounding air slows

it up and mixes with it, but it was not thought that this would occur to such an extent as these experiments suggest at a distance of 1·46 diameters.

4. Experiments are being undertaken to explore the velocity in this region as well as the direction.

5. A photograph of the aeroplane (F.E. 9, No. 4818), in which the experiments were made, is attached.

TABLE 1.

Indicated Airspeed. m.p.h.	Angle of Incidence. θ.	Depth below Propeller Axis. d.	Mean Angle of Downwash. m.	Angle of Downwash at Tail Plane. e.
	°	″	°	°
50	12·2	11·8	11·6	9·8
60	8·0	13·2	8·0	6·6
70	5·3	15·4	6·3	4·9
80	2·9	16·2	4·3	3·8

TABLE 2.

Distance from Axis of Slipstream.	Angle of Yaw of Slipstream.		
	50 m.p.h.	60 m.p.h.	70 m.p.h.
	°	°	°
10″	18·2	18·3	18·3
20″	14·0	13·3	12·8
30″	10·5	9·2	8·0
40″	8·8	7·4	6·0

EXPLORATION OF THE SLIPSTREAM VELOCITY IN A PUSHER MACHINE.

By D. H. Pinsent.

Presented by the Director-General of Aircraft Production.

Reports and Memoranda, No. 444. *April,* 1918.

Summary.—(a) *Introductory.* (*Reasons for inquiry.*)—Experiments had been carried out to determine the angle of yaw of the slipstream of an F.E.9 machine at points up and down a vertical line in the plane of the fin; these experiments are reported in R. and M. 408. It was then found that, as regards yaw, the slipstream effect extended to a surprising distance upwards. It was decided, therefore, to measure the velocity of the slipstream at the same points, in order to find whether the effect of the slipstream as regards increased velocity also extended to an equal distance upwards.

(b) *Range of experiment.*—The air speed was measured by means of eight pitot heads set up at intervals along the line in which the yaw had been measured, and yawed to the direction of the stream indicated in the previous experiment. The pressure and static sides of each head were connected to manometer tubes, and simultaneous readings were taken photographically of all the sixteen tubes, using the apparatus described in R. and M. 438. Sixteen of such records were taken at various air speeds and throttle positions.

(c) *Conclusions.*—The region of increased velocity behind the airscrew does not appear to extend upwards to the same extent as the region of yaw does. On the whole, the measurements of air speed described in this report confirm the conclusions arrived at in R. and M. 382 (airspeed exploration in the slipstream of an F.E.2b machine), namely, that as regards increased velocity, the slipstream may be taken roughly as a hollow cylinder with outside diameter 0·8, and inside diameter 0·2 times the airscrew diameter.

The measurements of the downwash of the slipstream agree with R. and M. 408.

1. The aeroplane used for these experiments was the same as that used for the experiments reported in R. and M. 408, and was fitted with the same fin and rudder as on that occasion, and with the same engine and airscrew (T.28105, No. 18964). Eight pitot heads were erected in a vertical line about 12 ins. in front of, and in the plane of, the fin, their positions being as follows :—

No. 1	$29\frac{3}{4}$ inches	Above the centre line of the tail plane.
No. 2	$20\frac{3}{4}$,,	
No. 3	$12\frac{3}{4}$,,	
No. 4	... ,,	

No. 5	5 inches	Below the centre line of the tail plane.
No. 6	$9\frac{3}{4}$,,	
No. 7	$15\frac{3}{4}$,,	
No. 8	$21\frac{1}{2}$,,	

Each pitot head was fixed pointing in the direction of airflow given at its position by the experiments of R. and M. 408. The air speeds at all of these eight points were simultaneously measured photographically. Records were taken at 50, 60, 70 and 75 m.p.h., with three different settings of the throttle at each, namely, fully open, three-quarters open, and half open. With each record observations were also made of the height, temperature, and engine revolutions.

2. For each pitot head the value of

$$\left(\frac{\text{Indicated air speed in the slipstream}}{\text{Indicated air speed of the machine}}\right)^2$$

was plotted against the advance per revolution of the airscrew. These values should be functions of advance per revolution only, except in so far as they are also affected by changes of incidence, downwash, &c., due to changes in indicated air speed. (The indicated air speed may differ at the same advance per revolution, if the engine is throttled or if observations are made at different heights.) The results are shown in Fig. 1. For pitot heads Nos. 1, 2, 3, 4, 5 and 8 the points are reasonably good and give well-defined mean curves, functions of advance per revolution only, but with Nos. 6 and 7 the points are more scattered, and there are different curves for different throttles. It appears that at Nos. 6 and 7 the slipstream is a function not only of advance per revolution, but also of indicated air speed—at Nos. 1, 2, 3, 4, 5 and 8 it appears to be a function of advance per revolution only. From the mean curves drawn through these points (using the full throttle curves for Nos. 6 and 7) the distribution of velocity in the slipstream was plotted up and down the line along which the pitot heads were erected, separate curves being drawn for various different advances per revolution.

3. These curves are shown in Fig. 2, curves being drawn for advance per revolution, 3·8, 4·2, 4·6, and 5·0 ft. The exact air speed with full throttle to which these advances per revolution correspond depends upon the height. At 5,000 ft. (density $87\frac{1}{2}$ per cent.) they would correspond as follows :—

Advance per revolution.	Indicated air speed.
3·8	55 m.p.h.
4·2	61 m.p.h.
4·6	67 m.p.h.
5·0	73 m.p.h.

THE LIBRARY
OF THE
UNIVERSITY OF ILLINOIS

FIG. Nº 2

UPPER HALF OF SLIP STREAM IN F.E.9.

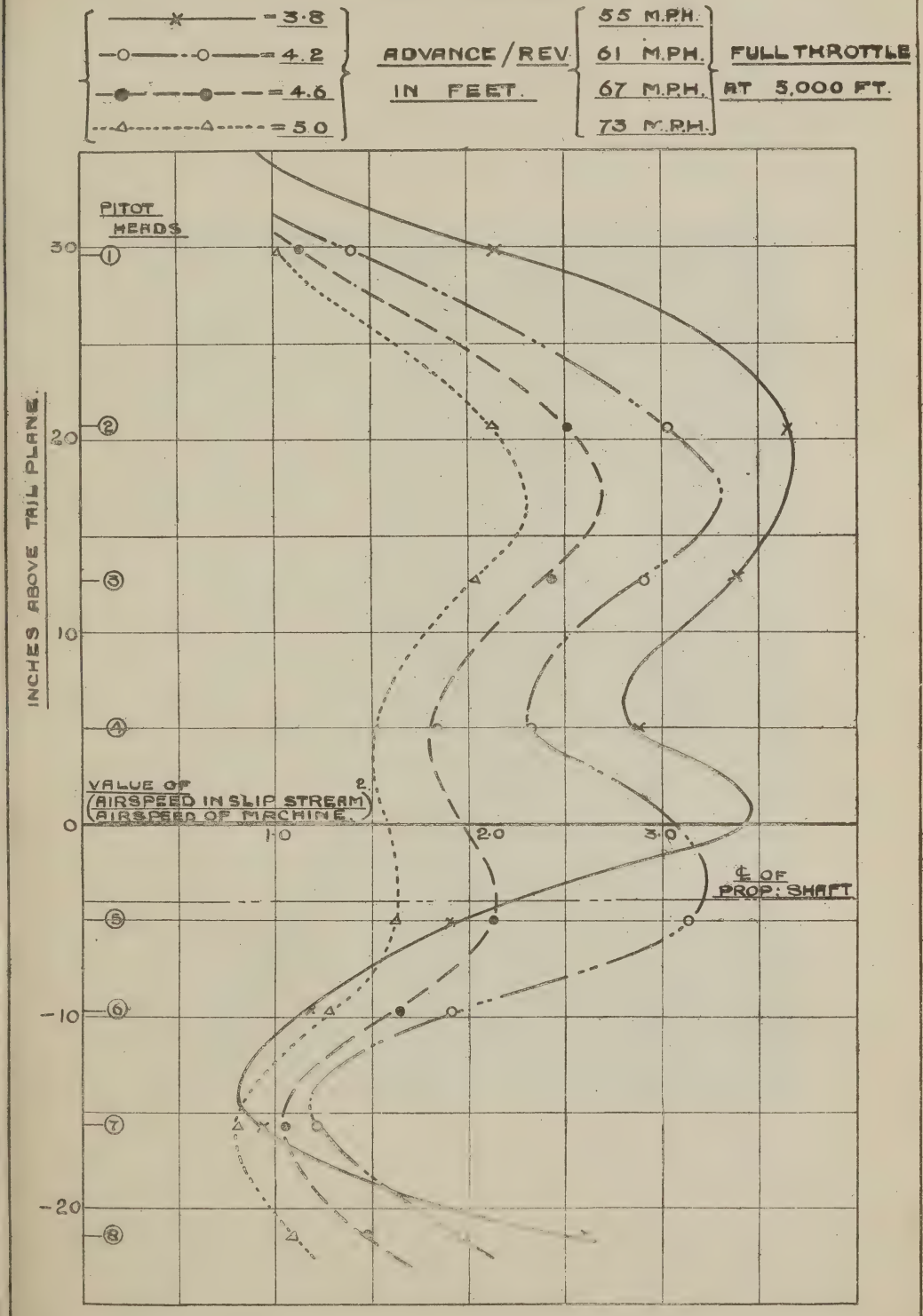

THE LIBRARY
OF THE
UNIVERSITY OF ILLINOIS

F.E.9. Rudder and Arrangement of Pitot Heads.

SUE LIBRARY
OF THE
UNIVERSITY OF ILLINOIS

4. The curves in Fig. 1 show the top half of the slipstream. It will be seen that—

(1) The larger the advance per revolution ratio the more the curves become shifted downwards. This would be expected, since a large ratio means high speed, and this means small incidence.

(2) The region of increased velocity does not extend upwards above about 32 ins. above the tail plane.

(3) There is a "hole" in the middle of the slipstream, about 10 ins. in diameter, with its centre about 15 ins. below the tail plane.

(4) All the curves show a region of less velocity about 6 ins. above the tail plane. It is probable that this is due to shielding by the top wing. It will be noticed that this region is lower down the greater the advance per revolution ratio, which follows from the fact that the incidence is then smaller.

(5) The centre line of the slipstream is from 10 to 12 ins. below the line of the propeller shaft. This must be due to downwash. From the measurements of yaw (R. and M. 408) the centre line appeared to be about 14 ins. below the line of the propeller shaft.

(6) The diameter of the airscrew was 7·25 ft. The measurements indicate that the region of the slipstream within which a large increase of velocity exists, has an outside radius of about 40 ins. and an inside radius of about 5 ins.; this is an outside diameter about 0·9, and an inside diameter about 0·1, of the airscrew diameter. This is in fair agreement with the measurements on an F.E.2.B. machine (R. and M. 382), in which the figures were 0·8 and 0·2 respectively.

5. A photograph of the machine in which the experiments were made, showing the fin and rudder fitted, and the arrangement of pitot heads, is attached (Fig. 3). (N.B.—In the photograph given in R. and M. 408 the fin and rudder shown are not those fitted during the present experiments; the fin and rudder shown in the photograph attached to this report were fitted during both series of experiments.)

AN INVESTIGATION OF THE MUTUAL INTERFERENCE OF AN AIRSCREW AND BODY OF THE "TRACTOR" TYPE OF AEROPLANE.

By A. Fage, A.R.C.Sc., D.I.C., and H. E. Collins.

Reports and Memoranda (*New Series*), *No.* 344. *August*, 1917.

Summary.—The maximum efficiency of the airscrew is increased by 4 per cent., from 75·5 per cent. to 78·5 per cent., by the presence of the body. The efficiency when climbing is increased by 1 or 2 per cent.

The effect of the presence of the body is to slow up the air, so that to develop the same thrust and torque at any given rotational speed, the translational speed of the airscrew relative to the undisturbed air has to be increased by about 3 — 5 per cent., the percentage increase being smaller at the higher values of $\frac{V}{nD}$.

The drag of the model body as measured in a 4-ft. channel at a wind speed of 40 ft. per second was 0·1455-lbs.

With airscrew interference $R/R_o = 0{\cdot}87 + 2{\cdot}18 \left(\frac{T}{\rho V^2 D^2}\right)$, where $\left(\frac{R}{R_o}\right)$ is the ratio of the resistance of the body with interference, to its resistance without interference.

The efficiency of the combination of airscrew and body, as calculated from the data of the "interference" experiments, is in close agreement with the efficiency as calculated from the ordinary experiments on the body in which no allowance is made for the effect of the slip stream, and from the airscrew when not affected by the presence of the body.

The experiments described in this report on the mutual interference of the airscrew and body in an aeroplane of the tractor type constitute a repetition of earlier experiments (T. 585), on the interference between airscrew and body of B.E.2c. A recent communication from the Royal Aircraft Factory called attention to the low value found in the earlier experiments for the efficiency of the airscrew, and to other points of difficulty with regard to the values found for the thrust and torque of the screw when tested with the body.

Description of the Models.—A sketch of the two-bladed airscrew for B.E.2c (R.A.F. drawing No.T. 4966) is given in Fig. 1. The diameter of the full-size airscrew is 9′ 6″, the angles of the blade varying from 17° 0′ at the tip to 39° 10′ at the boss.

The model airscrew was made in wood at the National Physical Laboratory and had a diameter of 1′ 6″.

A sketch of the model body of B.E.2c which had no rudder, fin, and engine cowling is given in Fig. 2. The principal dimensions of the model are given in the drawing, the scale of the model being approximately one-sixth full size.

Description of the Experiments.—The experiments were made in the 4-ft. wind channel, the thrust and torque of the airscrew being measured with the airscrew balance, which has been described in previous reports. In the present experiments the top of the balance was rotated through 180° so that the airscrew was about 10″ behind the vertical shaft of the balance. By enclosing this vertical shaft in a cylindrical guard and the bottom of the balance in a streamline body, any air forces acting on the balance, other than those due directly to the airscrew, were almost completely eliminated. It was fully realised that the balance and guards which were in the stream of air flowing into the airscrew would somewhat modify the performance of the airscrew, and accordingly the velocity distribution of the air in the plane of the airscrew—with the airscrew removed—was investigated. It was found that the velocity distribution was not constant through the disc that would be described by the airscrew during the experiments, but that the mean velocity of the air through the disc had the same value as the mean velocity of air in the channel. From a comparison between the airscrew experiments on the balance and the experiments on the whirling table, the effect of this obstruction in the inflowing stream of air on the performance of the airscrew was found to be small. For experiments with tractor bodies, this arrangement of the airscrew balance has the great advantage that the measurements of thrust or torque, with or without the interference of the body, may be made without disturbing the measuring apparatus. The order of experimenting was to obtain the thrust performance curve of the airscrew without any interference from the body, then to mount the body in position behind the airscrew, and measure the thrust performance curve with the interference of the body, and finally to take the body away and repeat the thrust performance previously measured. It was thus possible to measure very accurately the interference effect of the body even if there were small inaccuracies in the measuring apparatus. A similar procedure was followed in the case of the torque. The performance curves got from the airscrew balance without any body interference were in close agreement with those from the whirling arm, corrections obtained from this comparison being made to all the airscrew performances as measured on the balance. The correction applied to the balance measurement of the thrust was of the magnitude of 2·5 per cent., whilst the corrections were of the order of + 2 per cent. to — 2 per cent. in the case of the torque.

The results of the airscrew experiments are given in terms of absolute coefficients, and the calculation of the thrust and torque from these coefficients may be performed as follows :—

The thrust $T = T_c' \rho n^2 D^4$
and torque, $Q = Q_c' \rho n^2 D^5$

where the thrust T, torque Q, diameter of the airscrew D, the rotational speed n, and ρ the mass density are all expressed in any system of consistent units, and T_c' and Q_c' are non-dimensional coefficients.

The absolute thrust and torque coefficients of the tables are to be taken for a standard atmosphere of temperature 15·6° C. and barometer 760 mm.

Different absolute coefficients are introduced in the present report, $\frac{T}{\rho n^2 D^4}$ and $\frac{Q}{\rho n^2 D^5}$ instead of $\frac{T}{\rho V^2 D^2}$ and $\frac{Q}{\rho V^2 D^3}$, because the effect of the body may be regarded as causing a slowing up of the air in the neighbourhood of the airscrew, so that employing the new coefficients, the body interference is clearly shown by a shift of the thrust and torque curves parallel to the axis of $\left(\frac{V}{nD}\right)$, and the interference effect may be expressed as a percentage of V.

The measurements of the resistance of the body, with and without the airscrew running, were made with the balance of the 4-ft. channel, the airscrew shaft being mounted in a tube of 2″ diameter, supported by wires from the channel. With this method of supporting the airscrew the obstruction in front of the airscrew was very small.

Discussion of the Results of the Experiments.—The results of the experiments on the airscrew are given in Tables 1 and 2 and shown graphically in Fig. 3. The maximum efficiency is increased by 4 per cent., that is, from 75·5 per cent. to 78·5 per cent., by the interference of the body, whilst when climbing the efficiency is increased by 1 or 2 per cent. At any given values of the translational and rotational speeds of the airscrew, both the thrust and the torque are increased by the presence of the body. Generally speaking, to develop the same thrust and torque at the same rotational speed, the translational speed of the airscrew relatively to undisturbed air has to be increased about 3 to 5 per cent., the percentage increase being smaller at the higher value of $\left(\frac{V}{nD}\right)$.

The resistance of the model body was measured at several wind speeds in the 4-ft. wind channel. The data of these experiments are given in Table 3, from which it is seen that the drag is proportional to the square of the wind speed. The drag at

a wind speed of 40 ft./sec. was 0·1455 lbs. Owing to the blocking up of the channel by the body the values of the drag are probably about 1 per cent. too great. The curve of Fig. 4, which has been plotted from the data of Table 4, gives the relationship between $\left(\frac{R}{R_o}\right)$ and $\left(\frac{V}{nD}\right)$, $\left(\frac{R}{R_o}\right)$ being the ratio of the resistance coefficient of the body with interference from the airscrew, to the resistance coefficient of the body without interference. From Fig. 5 it is seen that the relationship between $\left(\frac{R}{R_o}\right)$ and $\left(\frac{T}{\rho V^2 D^2}\right)$ may be expressed approximately by the linear law $\left(\frac{R}{R_o}\right) = 0{\cdot}87 + 2{\cdot}18\ \frac{T}{\rho V^2 D^2}$.

It is of some interest to compare the value of $\left(\frac{R}{R_o}\right)$ as measured experimentally with the value calculated from theoretical considerations of momentum. Regarding the velocity of the slip stream as uniform and of magnitude s, this velocity is taken relatively to still air, and assuming the cross sectional area of the slip stream to be 0·60 of the area of the airscrew disc, this being the value given in Report T. 858, the thrust of the airscrew $T = \frac{0{\cdot}6\pi}{4}\rho D^2(V + s)s$.

Also, since the body is considered to be in this slip stream

$$\left(\frac{R}{R_o}\right) = \left(1 + \frac{s}{V}\right)^2$$

so that

$$2{\cdot}13\ \frac{T}{\rho V^2 D^2} = \left[\sqrt{\frac{R}{R_o}} - 1\right]\sqrt{\frac{R}{R_o}}$$

The curve given by this equation has been plotted in Fig. 5, from which it is seen that for any value of the thrust, the theoretical calculation over-estimates the value of $\left(\frac{R}{R_o}\right)$. The velocity of the region of the slip stream in which the body is placed is probably lower than that of the calculation, and also the body is to some extent shielded by the boss of the airscrew.

It has been shown in the present report that a tractor body increases the thrust and efficiency of an airscrew, but at the expense of an increase of the resistance of the body, so that a fair statement of the effect of mutual interference may be made only when both factors are taken into consideration.

Accordingly, regarding the airscrew and the body as a combination, the efficiency of this combination as calculated from the experiments involving mutual interference has been compared with that calculated from the non-interference experiments on the airscrew and body, in which the effect of the slip

stream on the body and the effect of the body on the airscrew are both ignored. From Table 3 it is seen that the drag of the body may be expressed as $0{\cdot}017\ \rho\ D^2V^2$, so that with interference the value of the thrust coefficient for the combination is

$$\left[T_c' - 0{\cdot}017\,\frac{R}{R_o}\left(\frac{V}{nD}\right)^2\right]$$

and the efficiency

$$\frac{0{\cdot}159\left(\frac{V}{nD}\right)}{Q_c'}\left[T_c' - 0{\cdot}017\,\left(\frac{R}{R_o}\right)\cdot\left(\frac{V}{nD}\right)^2\right]$$

The coefficients T_c' and Q_c' are taken from experiments with interference.

Similarly, for the combination without interference, the thrust coefficient of the combination is

$$\left[T_c' - 0{\cdot}017\,\left(\frac{V}{nD}\right)^2\right]$$

and the efficiency of the combination is

$$\frac{0{\cdot}159\left(\frac{V}{nD}\right)}{Q_c'}\left[T_c' - 0{\cdot}017\,\left(\frac{V}{nD}\right)^2\right]$$

where the absolute coefficients of the airscrew T_c' and Q_c' are obtained from the experiments without interference.

The results of these calculations have been collected in Table 5, and are shown graphically in Fig. 6.

From the curves of Fig. 6, it is seen when a comparison is made at the same value of $\left(\frac{T}{\rho n^2 D^4}\right)$, that the efficiency as calculated from the interference experiments is greater by about 2 per cent. at the low values of the thrust coefficient and smaller by about 2 per cent. at the high values of the thrust coefficient, whilst the translational speed is also greater.

From the present investigation it would appear that calculations based on the data of ordinary non-interference experiments on an airscrew and tractor body, in which no allowance is made for the effect of the slip stream on the body, and for the interference of the body on the airscrew, are of sufficient accuracy for nearly all practical purposes.

Table 1.

AIRSCREW FOR B.E.2c MACHINE (R.A.F. DRAWING No. T.4966).

Diameter of model airscrew = 1·5 feet.
Scale of model airscrew = 1/6·3 full size.

V in feet per second.
n in revolutions per second.
D diameter in feet.

Without Interference.		With Interference of B.E. 2cBody.		Without Interference.		With Interference of B.E. 2cBody.	
$\frac{V}{nD}$	Thrust Coefficient. T_c' $(=T/\rho n^2D^4)$	$\frac{V}{nD}$	Thrust Coefficient. T_c' $(=T/\rho n^2D^4)$	$\frac{V}{nD}$	Torque Coefficient. Q_c' $(=Q/\rho n^2D^5)$	$\frac{V}{nD}$	Torque Coefficient. Q_c' $(=Q/\rho n^2D^5)$
0·469	0·1041	0·475	0·1064	0·423	0·01262	0·416	0·01280
0·513	0·0975	0·485	0·1046	0·451	0·01245	0·442	0·01268
0·523	0·0960	0·518	0·0998	0·462	0·01240	0·474	0·01249
0·535	0·0941	0·542	0·0961	0·489	0·01219	0·494	0·01236
0·546	0·0924	0·565	0·0930	0·508	0·01202	0·512	0·01222
0·559	0·0903	0·588	0·0895	0·529	0·01185	0·534	0·01203
0·570	0·0885	0·611	0·0861	0·558	0·01157	0·562	0·01181
0·578	0·0873	0·638	0·0818	0·574	0·01141	0·585	0·01158
0·590	0·0853	0·661	0·0778	0·599	0·01114	0·606	0·01138
0·600	0·0836	0·676	0·0754	0·611	0·01100	0·630	0·01107
0·610	0·0820	0·705	0·0699	0·630	0·01074	0·647	0·01086
0·615	0·0813	0·738	0·0637	0·640	0·01060	0·672	0·01051
0·632	0·0784	0·760	0·0586	0·662	0·01027	0·696	0·01015
0·650	0·0752	0·796	0·0502	0·682	0·00997	0·734	0·00954
0·662	0·0730	0·805	0·0479	0·712	0·00950	0·755	0·00915
0·677	0·0702	0·840	0·0395	0·735	0·00909	0·783	0·00862
0·685	0·0687			0·756	0·00870	0·813	0·00803
0·736	0·0581			0·777	0·00828	0·880	0·00652
0·747	0·0555			0·800	0·00781		
0·764	0·0516			0·823	0·00732		
0·770	0·0500			0·854	0·00661		
0·781	0·0475						
0·810	0·0400						
0·829	0·0349						

TABLE 2.

AIRSCREW FOR B.E.2c MACHINE (R.A.F. DRAWING No. T.4966).

Diameter of model airscrew = 1·5 feet.
Scale of model airscrew = 1/6·3 full size.

V in feet per second.
n in revolutions per second.
D diameter in feet.

Without Interference.		With Interference of B.E. 2c Body.	
$\frac{V}{nD}$	Efficiency. (Percentage.)	$\frac{V}{nD}$	Efficiency. (Percentage.)
0·46	62·0	0·46	63·0
0·50	65·3	0·50	66·0
0·54	68·0	0·54	69·2
0·58	70·5	0·58	71·7
0·62	72·8	0·62	74·5
0·66	74·5	0·66	76·5
0·70	75·6	0·70	78·3
0·74	74·5	0·74	78·7
0·78	72·0	0·78	77·2
0·82	65·7	0·82	73·5
0·86	55·5	0·86	66·0

TABLE 3.

DRAG OF B.E.2c BODY AT SEVERAL SPEEDS AS MEASURED IN 4-FT. CHANNEL (No. 1).

Scale of model body = 1/6th full size (about).

Wind Speed. (Feet per Second.)	Drag of Body in Lbs.
25	0·0579
30	0·0836
35	0·1105
40	0·1432
45	0·1924

Drag of model body = 0·0000908 V^2 lbs.
Drag of body at 40 ft./sec. = 0·1455 lbs.

MUTUAL INTERFERENCE OF AIRSCREW AND BODY.

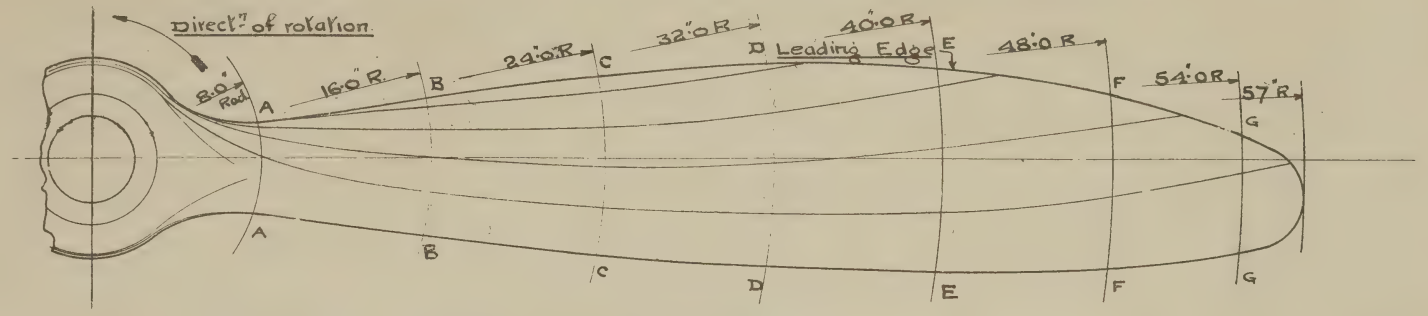

0 2 4 6 8 10 12 14 16 18

Scale in ins.

R.A.F. Drawing No. T. 4966.

REPORT No. 344.

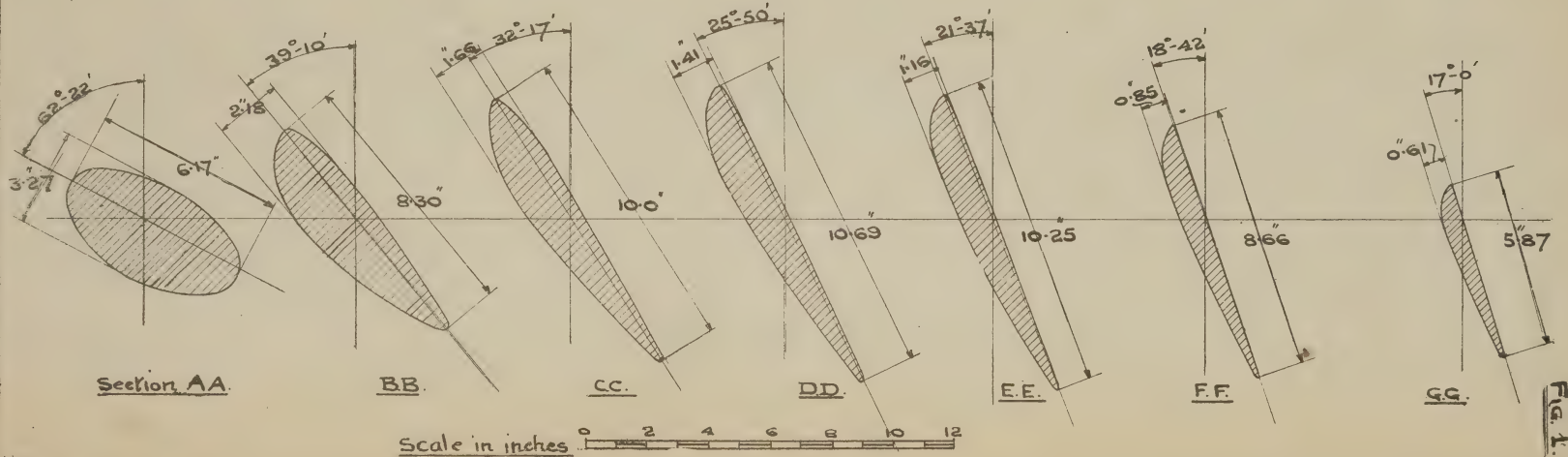

Scale in inches 0 2 4 6 8 10 12

Fig. 1.

PLT

MUTUAL INTERFERENCE OF AIRSCREW AND BODY.

REPORT No. 344.

Sketch of the model body of B.E.2c

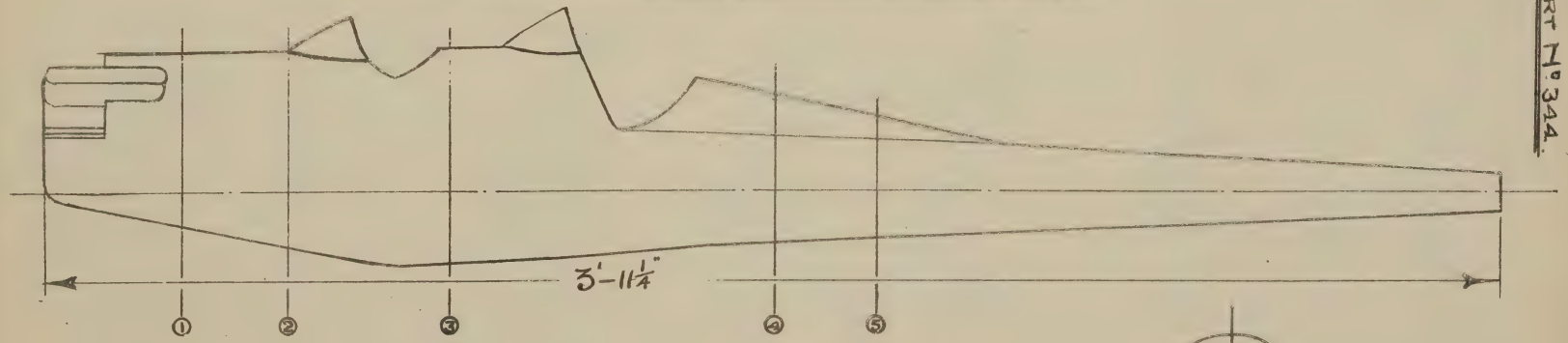

Dimensions of Model as shewn in sketch.

Scale of Drawing = ¼th full size.

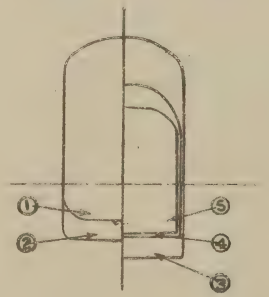

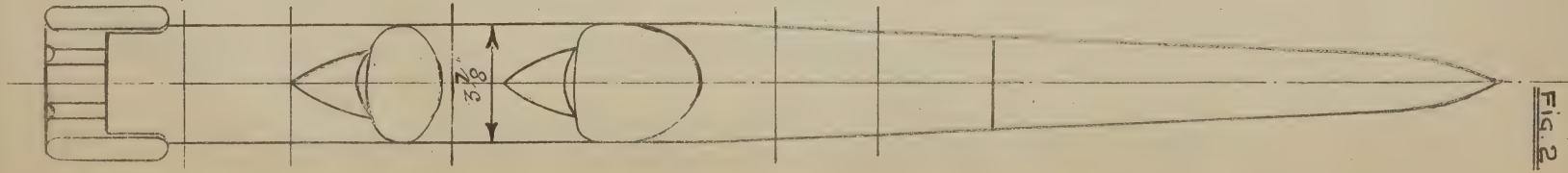

FIG. 2

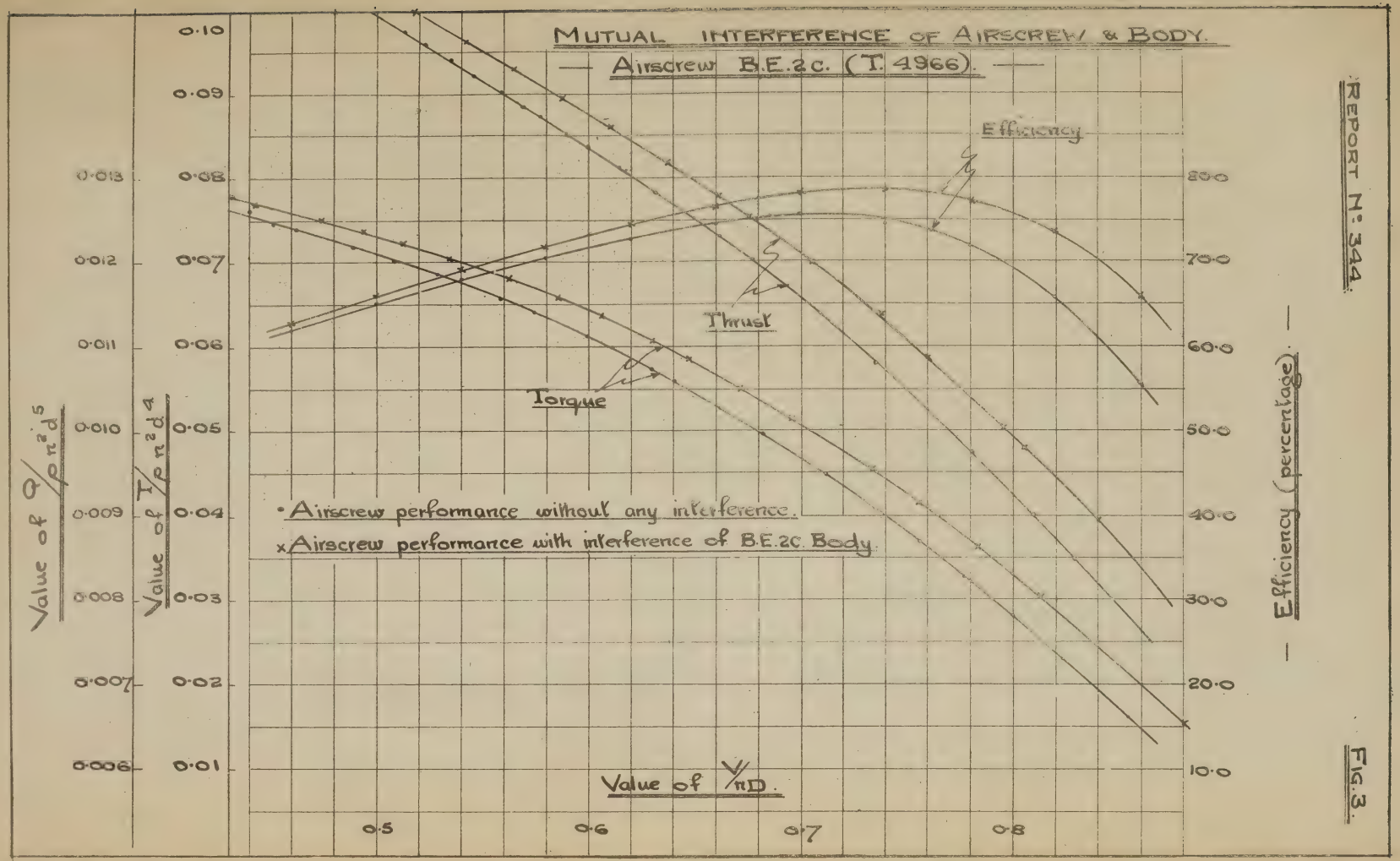

REPORT No. 344.

FIG. 3.

MUTUAL INTERFERENCE OF AIRSCREW AND BODY.

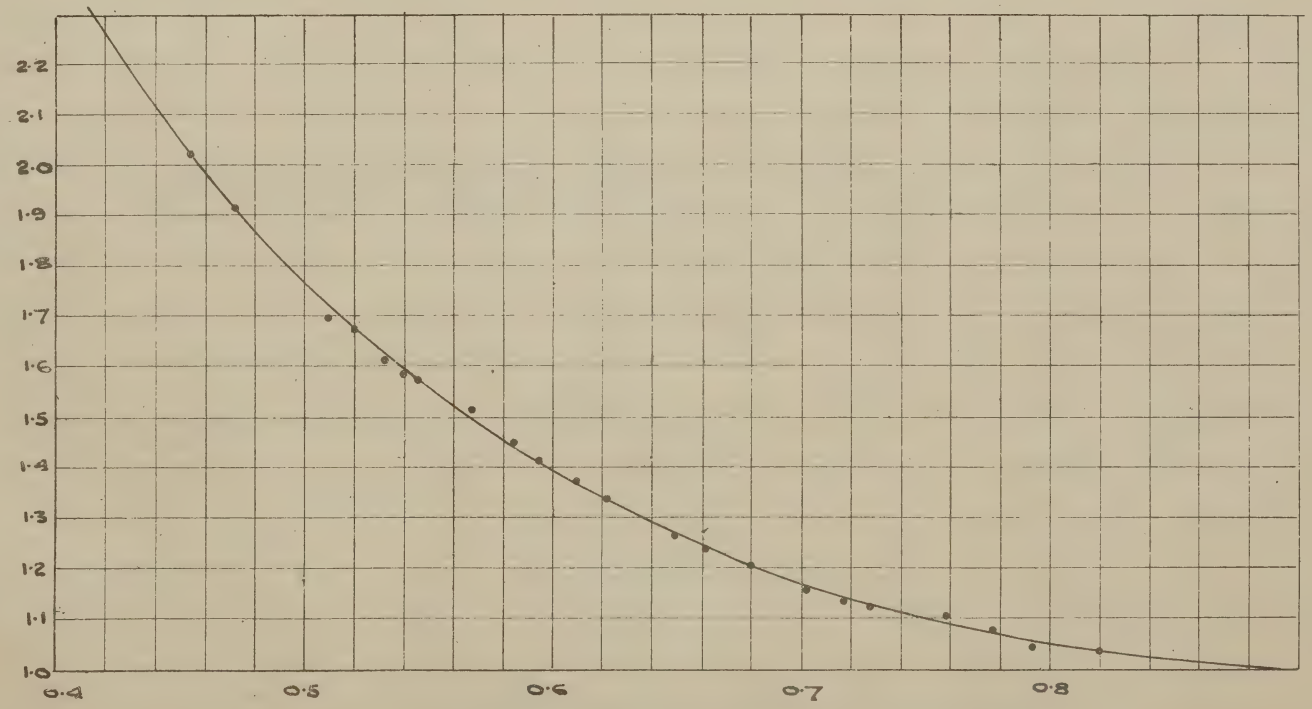

FIG. 4.

MUTUAL INTERFERENCE OF AIRSCREW AND BODY.

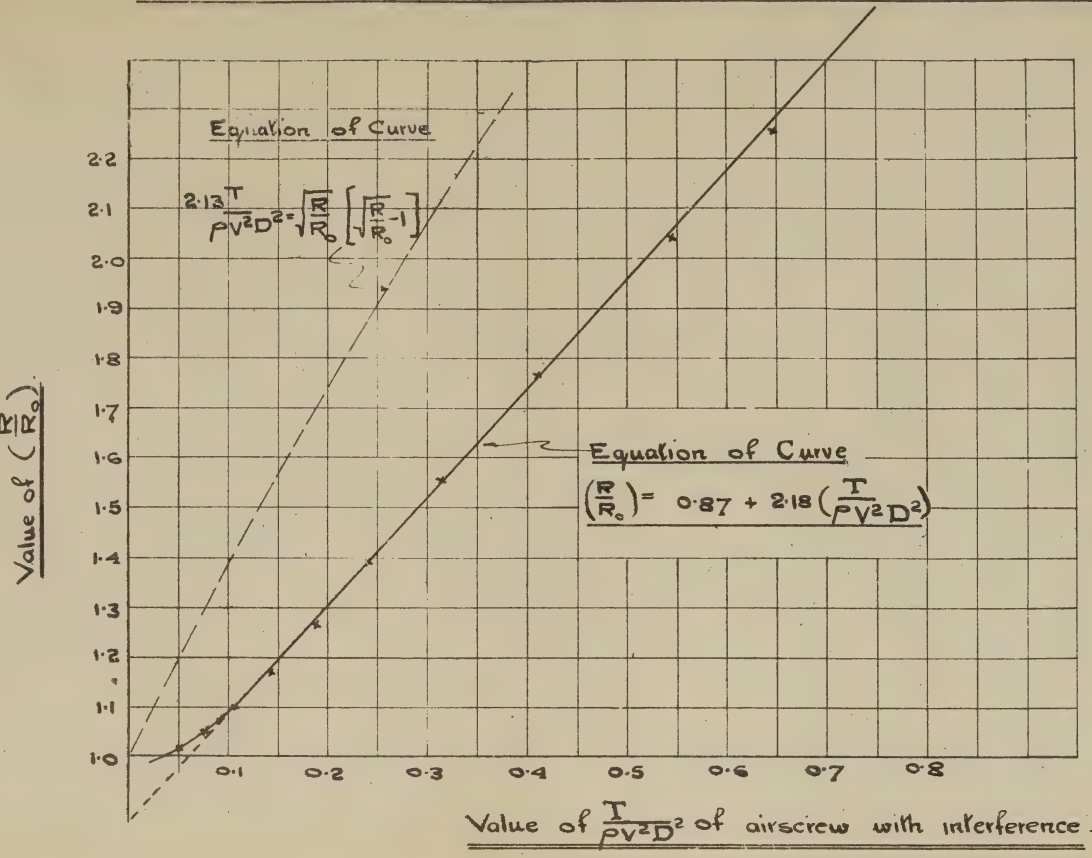

REPORT No. 344.

FIG. 5.

MUTUAL INTERFERENCE OF AIRSCREW AND BODY.

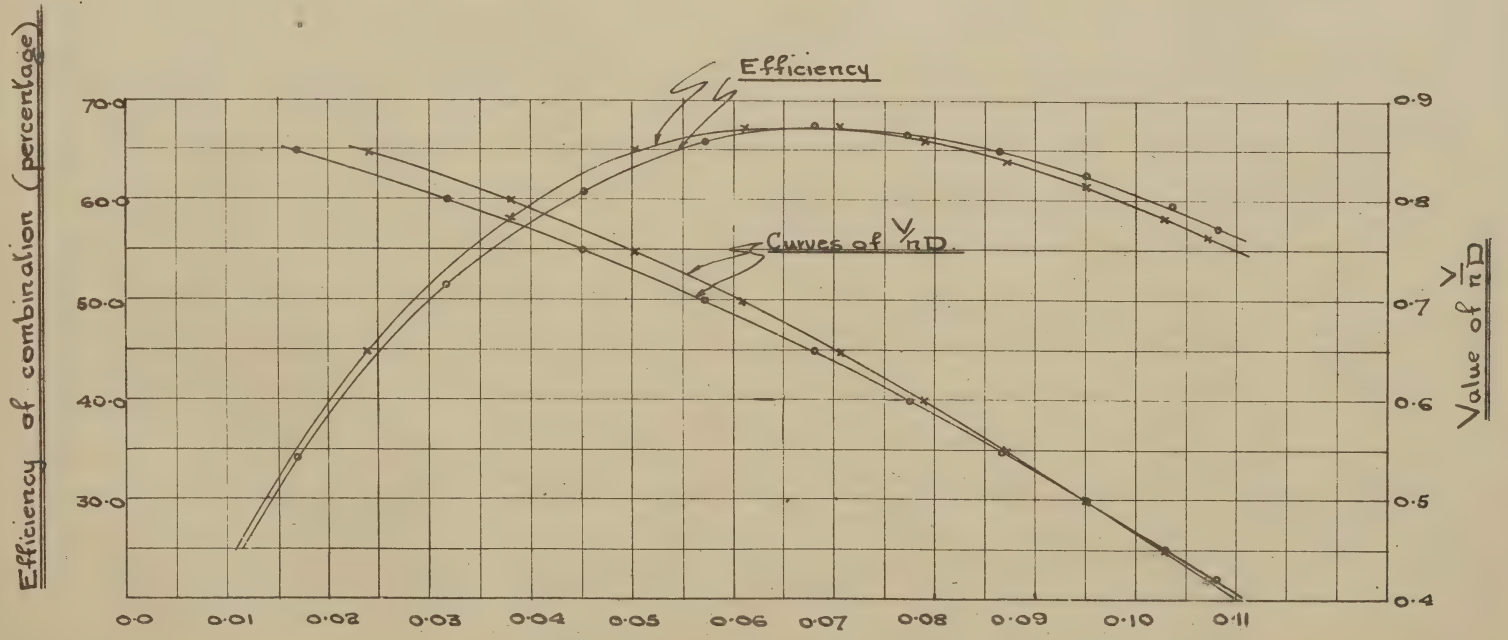

• As calculated from experiments without interference.
× As calculated from interference experiments.

FIG. 6.

Table 4.

INTERFERENCE OF AIRSCREW B.E.2c. (R.A.F. DRAWING No. T.4966) UPON B.E.2c BODY.

Scale of model body about 1/6th full size.

R_o = Resistance coefficient of body *without* interference from airscrew.

R = Resistance coefficient of body *with* interference from airscrew.

V/nD for Airscrew.	Value of R/R_o.
0·454	2·020
0·472	1·914
0·510	1·698
0·520	1·671
0·532	1·612
0·540	1·584
0·546	1·572
0·568	1·518
0·585	1·450
0·595	1·416
0·610	1·345
0·622	1·340
0·649	1·264
0·662	1·238
0·680	1·207
0·702	1·152
0·717	1·137
0·728	1·127
0·758	1·106
0·777	1·073
0·793	1·048
0·820	1·031

TABLE 5.

A COMPARISON OF THE EFFICIENCY OF THE COMBINATION OF B.E.2c BODY AND AIRSCREW, AS CALCULATED FROM EXPERIMENTS INVOLVING MUTUAL INTERFERENCE, WITH THAT CALCULATED FROM EXPERIMENTS WITHOUT INTERFERENCE.

Value of V/nD.	With Interference.		Without Interference.	
	Value of T_c' for the Combination.	Value of Efficiency (Percentage.)	Value of T_c' for the Combination.	Value of Efficiency (Percentage.)
0·42	0·1072	56·2	0·1080	57·0
0·45	0·1029	58·2	0·1036	59·5
0·50	0·0950	61·4	0·0951	62·6
0·55	0·0871	64·0	0·0864	64·7
0·60	0·0789	65·9	0·0774	66·5
0·65	0·0706	67·5	0·0682	67·4
0·70	0·0611	67·5	0·0573	66·0
0·75	0·0503	65·0	0·0451	61·0
0·80	0·0380	58·4	0·0316	51·5
0·85	0·0240	44·9	0·0169	34·2

AN INVESTIGATION OF THE MUTUAL INTERFERENCE OF THE AIRSCREW, BODY AND WINGS OF THE TRACTOR AEROPLANE, B.E. 2E.

By A. FAGE, A.R.C.Sc., and H. E. COLLINS.

Reports and Memoranda, No. 393. *January,* 1918.

SUMMARY.—(a) *Introductory.* (*Reason for inquiry.*)—A large number of full-scale experiments have been made on the B.E. 2E machine at the Royal Aircraft Factory. The objects of the present investigation were to obtain data needed in the reduction of the full-scale experiments, and also to obtain further information of the mutual interference between the airscrew and body.

Other investigations dealing with the mutual interference of the body and airscrew are given in R. & M. Nos. 305 and 344.

(b) *Range of the investigation.*—Experiments were made with the airscrew balance on models of 1/6th scale. The model body had engine cowling, landing gear, but no rudder, fin or elevator. The interference of the body, and also of the wings on the airscrew were measured. Measurements of the resistance of the body alone, and also with the interference of the wings, were made in both 4-ft. and 7-ft. channels at several wind speeds. The resistance of the body alone, and also of the body with the interference of the wings, with the airscrew running, were measured in the 4-ft. channel.

(c) *Conclusions.*—The reduction of the results was somewhat complicated by the "*vl*" effect of the model airscrew. (See R. & M. 390.) To develop the same thrust at the same rotational speed, the forward speed needs to be increased by 4·0 per cent. due to body alone, and 5·0 per cent. due to combined interference of body and wings. The same torque is expended at the same rotational speed, when the body is behind the airscrew, if the forward speed is increased by 3·0 per cent. at the higher values of the ratio of the forward speed to the product of the diameter and the rotational speed (V/nD), and about 8·0 per cent. at climbing. The wings seem to have no additional interference effect on torque.

The values of the maximum efficiency of the airscrew alone, the airscrew with body interference, and the airscrew with body and wing interferences, are 75·5 per cent., 74·0 per cent., and 76·0 per cent. respectively. At climbing the efficiency with interference of body is about 2 per cent. lower than that of the airscrew alone. At the lower values of (V/nD) the efficiency is practically unaffected by the combined interference of body and wings.

The drags of the body as measured in the 4-ft. and 7-ft. channels differ because of the "blocking-up" effect, and also of an interference from the wall of the 4-ft. channel. The drag of the body alone is proportional to the square of the wind speed, at the speeds of the experiment,

but with interference of wings the drag of the body is not proportional to the square of the wind speed. If (R/R_0) be the ratio of the drag of the body with airscrew running, to the drag without any interference,

$$(R/R_0) = 0{\cdot}855 + 1{\cdot}32\ (T/\rho V^2D^2)$$

in the case of no interference from wings, and

$$(R/R_0) = 0{\cdot}83 + 1{\cdot}18\ (T/\rho V^2D^2)$$

with interference from wings.

These values of (R/R_0) are much lower than would be calculated from considerations of momentum. The resistance of the body alone has a high value, owing to the flow of air around the engine and through the cowling, and the experiments show that the air flow at the *front* of the body is appreciably modified by the working of the airscrew. The additional interference of the wings influences both the speed and the direction of the slip stream, but does not interfere with the flow of air through the cowling.

Finally, the airscrew and body are regarded as a combination, and the efficiency of this combination as calculated from the experiments involving mutual interference—with and without the additional interference of the wings—is compared with that calculated from the non-interference experiments, in which the effect of the slip stream on the body, and the effect of the body on the airscrew are both neglected. From these calculations the conclusion previously reached in reports R. & M. 305 and 344, "that calculations based on the ordinary non-interference experiments on an airscrew and body in which no allowance is made for the effect of the slip stream on the body and for the interference of the body on the airscrew, are of sufficient accuracy for nearly all practical purposes" is supported, but not so strongly as in previous reports.

(d) *Applications and further developments.*—The present investigation forms a part of a rather extensive research made to obtain the mutual interference of airscrews and bodies of both tractor and pusher machines.

Further investigations, other than reports Nos. R. & M. 344, R. & M 305 and the present report, are necessary to explain why tractor machines are better than pusher, as these reports show that the mutual interferences of the airscrew and body are approximately the same in the two cases.

The experiments described in the present report on the mutual interference between the airscrew, body and wings of a model aeroplane of the B.E. 2E type were made at the request of the Royal Aircraft Factory.

Full scale experiments on this machine have been made at the R.A.F., and the primary objects of the present investigation were to obtain data which would facilitate the reduction of the results of the full scale experiments, and at the same time to obtain some evidence of the value of model experiments in the estimation of the performance of a full-size machine.

Description of the models.—A sketch of the airscrew for B.E. 2E, R.A.F. Drawing No. T. 7850, is given in Fig. 1. The airscrew has four blades, a diameter of 9′ 1″, and is rather full at the tip in plan form. The angles of the blade vary from 20° 39′ at the tip section to 68° 54′ at the base. The model airscrew of scale one-sixth, was made in aluminium at the R.A.F. The reduction

of the results of the experiments with this model airscrew was somewhat complicated by a " scale-speed " effect. (See Report R. & M. 390.)

A sketch of the body and wings is given in Fig. 2, the scale of the models being one-sixth. A representation of the R.A.F. engine and cowling was fitted at the front of the body. The landing gear was attached to the body, but the rudder, elevator and fin were not mounted. The model wings, section R.A.F. 14, with the struts in place, extended to the walls of the channel, the chord of a wing section making an angle of 4° with the longitudinal axis of the body.

Description of the experiments.—All the airscrew experiments were made in the No. 1 4-ft. channel, the measurements of torque and thrust being made with the airscrew balance in the manner described in Report R. & M. 344, in which the airscrew is mounted behind the vertical shaft of the balance. As pointed out in the report, measurements of the thrust and torque may thus be made, with or without the interference of body and wings, without any disturbance of the measuring apparatus, and so the " interference " effect of the body, &c., may be measured very accurately. Experiments were made to find the interference on the performance of the airscrew of the body alone, and also of the combination of body and wings. Following the customary practice, the measurements of thrust and torque have been expressed in absolute coefficients. Thus the thrust T and the torque Q may be calculated directly from the relationships,

$$T = T'_c \rho n^2 D^4$$

and

$$Q = Q'_c \rho n^2 D^5$$

where the diameter of the airscrew D, the rotational speed n, the mass density ρ, T, and Q are all expressed in any system of consistent units, T'_c and Q'_c being non-dimensional coefficients.

The absolute thrust and torque coefficients of the tables are to be taken for a standard atmosphere of temperature 15·6° C. and barometer 760 mms. Measurements of the resistance of the body alone, and also with the interference of the wings, were made in both the 4-ft. and 7-ft. channels, at several wind speeds.

The resistances of the body alone, and of the body with the interference of the wings, with the airscrew running, were measured in the 4-ft. channel, the airscrew shaft running in a tube of 2″ diameter supported by wires from the channel, so as to reduce the obstruction in front of the airscrew to a minimum.

Discussion of the results of the experiments.—As stated earlier in the report, this airscrew has a " scale-speed " effect of some magnitude. Accordingly, for consistency, the appropriate " *vl* " corrections were applied to all the experimental measurements to reduce them to a wind speed of 45-ft./sec. The experiments

definitely established the magnitude of the " scale-speed " effect described in Report R. & M. 390, from which it can be seen that the effect was not completely eliminated at the highest translational speed of the experiments, namely, 45-ft./sec.

The results of the airscrew experiments are given in Tables 1-3, and shown graphically in Figs. 3-5. The presence of the body and wings slows up the air in the neighbourhood of the airscrew, resulting as shown in Figs. 3 and 4 in a shift of the thrust and torque curves parallel to the axis of (V/nD). To develop the same thrust at the same rotational speed, the translational speed of the airscrew relatively to the undisturbed air needs to be increased by about 4·0 per cent. due to the presence of the body alone, and about 5·0 per cent. due to the combined interference of body and wings. The airscrew has the rather high value of 1·29 D for the experimental mean pitch. The effect of the interference of the body is to increase, at any value of (V/nD), the value of the torque coefficient by about 0·0018, or expressing the interference in a similar manner to the thrust, the same torque will be developed at the same rotational speed, when the body is behind the airscrew, if the translational speed be increased by 3·0 per cent. at high values of (V/nD) and about 8·0 per cent. when climbing. Within the limits of accuracy of the experiments, the combined interference of the body and wings on the torque agrees with that due to the body alone.

The values of the maximum efficiency for the airscrew alone, for the airscrew with the interference of the body, and for the airscrew with the combined interference of body and wings are 75·5 per cent., 74·0 per cent., and 76·0 per cent. respectively. It is expected that the maximum efficiency of the full-size airscrew will be somewhat higher than that of the model, because a small " *vl* " effect was present at the higher speeds of the experiment. At climbing speeds, the efficiency of the airscrew with the interference of the body alone is about 2 per cent. lower than that of the airscrew without any interference. The efficiency at the lower values of (V/nD) is practically unaffected by the combined interference of the body and wings. The drag of the body alone, and also with the interference of the wings and struts, was measured in both the 4-ft. and 7-ft. channels at several speeds. The data from these experiments are given in Table 4 and also shown graphically in Fig. 6. The drag of the body without any interference from the wings was found to be proportional to the square of the wind speed, from both series of experiments, but the values at any wind speed are not in agreement, the drag measured in the 4-ft. channel being the lower. The " blocking-up " effect of the body is greater in the 4-ft. channel, so that a discrepancy between the drag measurements would be expected, but not in the direction found from the experiments. A probable explanation is that, in addition to the " blocking-up," there is a decided " wall-interference " effect,

since the wheels of the landing gear are only about 6″ from the wall of the 4-ft. channel, and consequently are in a region of low velocity. At the speeds of the experiment the drag of the body with the interference of wings and struts is not proportional to the square of the wind speed. The agreement between the measurements of drag in the two channels, making no correction for the "blocking-up" due to the model and the interference from the walls, is closer when the body is subjected to the interference of the wings and struts.

The results of the second series of experiments from which was measured the interference of the airscrew on the body, with and without the interference of the wings, are given in the Tables 5 and 6 and in Figs. 7 and 8. In Fig. 7 the values of (R/R_0) for the body are plotted against the corresponding values of (V/nD) of the airscrew; (R/R_0) is the ratio of the resistance of the body with the airscrew running to the resistance of the body without any airscrew interference. The curves of Fig. 8 show that the relationship between (R/R_0) and $(T/\rho V^2D^2)$ may be expressed approximately by a linear equation, that is

$$\left(\frac{R}{R_0}\right) = 0{\cdot}855 + 1{\cdot}32\left(\frac{T}{\rho V^2D^2}\right)$$

in the case of no interference from the wings, and

$$\left(\frac{R}{R_0}\right) = 0{\cdot}83 + 1{\cdot}18\left(\frac{T}{\rho V^2D^2}\right)$$

with the additional interference of the wings. It is shown in Report R. & M. 344 that the theoretical relationship between (R/R_0) and $(T/\rho V^2D^2)$ calculated directly from consideration of momentum is

$$2{\cdot}13\left(\frac{T}{\rho V^2D^2}\right) = \left(\sqrt{\frac{R}{R_0}} - 1\right)\sqrt{\frac{R}{R_0}}$$

The curve given by this latter equation is represented by the dotted line of Fig. 8, which clearly shows that at any value of the thrust, the theoretical calculation considerably over-estimates the value of (R/R_0). The velocity of the air in the neighbourhood of the body would probably be lower than that calculated, but it is expected that the larger part of the discrepancy between the theoretical and experimental resistances is due to the "blocking-up" of the front of the body by the boss of the airscrew. The resistance of the body alone has a high value, owing to the flow of air round the engine and through the cowling, and the conclusion which may be drawn from the interference experiments is that the air flow at the front of the body is appreciably modified by the working of the airscrew. In fact it would seem that up to quite moderate values of the thrust

a smaller quantity of air is flowing over the engine and through the cowling than when the airscrew is not running. At the same value of $(T/\rho V^2D^2)$, the value of (R/R_0) is reduced by the interference of wings, the wings influencing both the speed and direction of the slip stream, but it is not expected that they would interfere with the flow of air through the cowling.

The separate statements of body and airscrew interferences which are given below do not in themselves convey a complete idea of the mutual interference. Accordingly, the airscrew and the body have been regarded as a combination, and the efficiency of this combination as calculated from the experiments involving mutual interference between the airscrew and body, with and without wing interference, have been compared with that calculated from the non-interference experiments, in which the effect of the slip stream on the body and the effect of the body on the airscrew are both neglected. Thus, considering the experiments in which there is no interference from the wings, it is seen from Table 4 that the drag of the body may be expressed as $0{\cdot}0391\ \rho V^2D^2$, so that the value of the thrust coefficient for the combination is

$$\left[T'_c - 0{\cdot}0391\left(\frac{R}{R_0}\right)\left(\frac{V}{nD}\right)^2\right]$$

and the efficiency is

$$\frac{15{\cdot}9\left(\frac{V}{nD}\right)}{Q'_c}\left[T'_c - 0{\cdot}0391\left(\frac{R}{R_0}\right)\left(\frac{V}{nD}\right)^2\right] \text{ per cent.}$$

The coefficients T'_c and Q'_c are taken from experiments with interference.

For the combination without interference, the thrust coefficient is

$$\left[T'_c - 0{\cdot}0391\left(\frac{V}{nD}\right)^2\right]$$

and the efficiency of the combination is

$$\frac{15{\cdot}9\left(\frac{V}{nD}\right)}{Q'_c}\left[T'_c - 0{\cdot}0391\left(\frac{V}{nD}\right)^2\right] \text{ per cent.}$$

The results of the calculations are given in Table 7.

General conclusions.—The curves of Fig. 9 which have been plotted from the data of Table 7 show that calculations based on the results of the separate experiments on the body and the airscrew would tend to under-estimate at high forward speeds,

and to over-estimate at climbing speeds, the efficiency of the combination. The conclusion made at the end of the previous reports dealing with the subject of mutual interference, "that calculations based on the data of ordinary non-interference experiments on an airscrew and body, in which no allowance is made for the effect of the slip stream on the body and for the interference of the body on the airscrew, are of sufficient accuracy for nearly all practical purposes," is supported, perhaps not so strongly, by the experiments of the present investigation.

TABLE 1.

FOUR-BLADED AIRSCREW FOR B.E. 2E (R.A.F. DRAWING No. T.7850).

DIAMETER OF MODEL AIRSCREW = 1·515 FT.
(Scale 1/6th full size).

V in feet per second.
n in revolutions per second.
D diameter in feet.
The thrust $T = T'_c \rho n^2 D^4$.

Before calculating the following coefficients all the experimental data were reduced to a uniform wind speed of 45 ft./sec. by applying the appropriate "scale-speed" corrections from R. & M. 390.

$\left(\frac{V}{nD}\right)$	Value of T'_c for Airscrew alone.	$\left(\frac{V}{nD}\right)$	Value of T'_c with Interference of Body.	$\left(\frac{V}{nD}\right)$	Value of T'_c with Interference of Body and Wings.
1·280	0·0030	1·274	0·0177	1·295	0·0182
1·200	0·0289	1·238	0·0305	1·250	0·0312
1·143	0·0493	1·166	0·0513	1·183	0·0526
1·095	0·0660	1·117	0·0689	1·123	0·0695
1·017	0·0930	1·067	0·0824	1·077	0·0835
0·957	0·1130	1·031	0·0951	1·042	0·0972
0·922	0·1235	0·998	0·1068	1·003	0·1075
0·888	0·1335	0·937	0·1255	0·971	0·1180
0·872	0·1390	0·930	0·1254	0·938	0·1280
0·828	0·1495	0·890	0·1384	0·908	0·1360
0·794	0·1570	0·852	0·1481	0·898	0·1395
0·735	0·1670	0·816	0·1552	0·862	0·1498
0·692	0·1735	0·787	0·1624	0·788	0·1650
0·654	0·1780	0·758	0·1670	0·726	0·1724
0·618	0·1820	0·726	0·1718	0·676	0·1795
0·586	0·1850	0·677	0·1800	0·630	0·1870
		0·632	0·1848	0·599	0·1900
		0·597	0·1894		

Table 2.

FOUR-BLADED AIRSCREW FOR B.E. 2E (R.A.F. DRAWING No. T.7850).

DIAMETER OF MODEL AIRSCREW = 1·515 Ft.

(Scale 1/6th full size).

V in feet per second.
n in revolutions per second.
D diameter in feet.
The torque $Q = Q'_c \rho n^2 D^5$.

Before calculating the following coefficients all the experimental data were reduced to a uniform wind speed of 45-ft./sec. by applying the appropriate "scale-speed" corrections.

$\left(\frac{V}{nD}\right)$	Value of Q'_c for Airscrew alone.	$\left(\frac{V}{nD}\right)$	Value of Q' with Interference of Body.	$\left(\frac{V}{nD}\right)$	Value of Q'_c with Interference of Body and Wings.
1·245	0·0089	1·281	0·0094	1·266	0·0092
1·238	0·0088	1·260	0·0092	1·245	0·0117
1·175	0·0129	1·246	0·0117	1·190	0·0133
1·126	0·0149	1·231	0·0114	1·171	0·0153
1·010	0·0206	1·222	0·0113	1·065	0·0198
0·947	0·0229	1·005	0·0222	1·050	0·0200
0·916	0·0244	0·974	0·0240	1·028	0·0213
0·900	0·0251	0·970	0·0240	0·990	0·0231
0·853	0·0264	0·948	0·0246	0·952	0·0247
0·786	0·0281	0·942	0·0257	0·942	0·0252
0·748	0·0288	0·894	0·0263	0·915	0·0259
0·713	0·0293	0·878	0·0280	0·871	0·0274
0·673	0·0297	0·808	0·0289	0·831	0·0283
0·582	0·0302	0·806	0·0296	0·828	0·0290
		0·778	0·0302	0·762	0·0303
		0·770	0·0300	0·755	0·0298
		0·715	0·0306	0·703	0·0306
		0·700	0·0313	0·644	0·0307
		0·645	0·0309	0·628	0·0313
		0·633	0·0313	0·590	0·0315
		0·605	0·0319	0·576	0·0312
		0·572	0·0312		

TABLE 3.

FOUR-BLADED AIRSCREW FOR B.E. 2E (R.A.F. DRAWING No. T.7850).

DIAMETER OF MODEL AIRSCREW = 1·515 FT.
(Scale 1/6th full size).

V in feet per second.
n in revolutions per second.
D diameter in feet.

Before calculating the following coefficients all the experimental data were reduced to a uniform wind speed of 45-ft./sec. by applying the appropriate "scale-speed" corrections.

$\left(\frac{V}{nD}\right)$	Value of Efficiency for Airscrew alone. Percentage.	$\left(\frac{V}{nD}\right)$	Value of Efficiency with Interference of Body. Percentage.	$\left(\frac{V}{nD}\right)$	Value of Efficiency with Interference of Body and Wings. Percentage.
1·25	30·8	1·25	48·3	1·25	58·7
1·20	51·7	1·20	60·0	1·20	67·9
1·15	61·7	1·15	67·6	1·15	72·2
1·10	68·8	1·10	71·1	1·10	75·2
1·05	73·6	1·05	73·6	1·05	76·4
1·00	75·0	1·00	74·2	1·00	76·4
0·95	75·5	0·95	73·6	0·95	75·5
0·90	74·5	0·90	72·7	0·90	74·4
0·85	73·1	0·85	71·6	0·85	73·0
0·80	71·0	0·80	69·5	0·80	71·4
0·75	68·4	0·75	67·0	0·75	67·8
0·70	65·2	0·70	63·8	0·70	64·3
0·65	61·9	0·65	60·5	0·65	61·2
0·60	58·0	0·60	57·5	0·60	58·0

Table 4.

DRAG OF B.E. 2E BODY.

(Scale of model body 1/6th full size.)

Wind Speed. Ft./sec.	Body alone without Interference of Wings.		Body with Interference of Wings and Struts.	
	Drag in Lbs.		Drag in Lbs.	
	4-ft. Channel.	7-ft. Channel.	4-ft. Channel.	7-ft. Channel.
25	0·131	0·137	0·143	0·145
30	0·187	0·196	0·207	0·206
35	0·250	0·261	0·280	0·281
40	0·330	0·341	0·356	0·364
45	0·414	0·430	0·445	0·454

Drag of model body alone at 40-ft./sec. = 0·341 lbs.

Drag of model body alone = 0·000213 V^2 lbs.

Drag of model body at 40-ft./sec. with interference of wings and struts = 0·366 lbs.

Drag of model body with interference of wings and struts = 0·00029 V^2 lbs.

TABLE 5.

INTERFERENCE OF AIRSCREW B.E. 2E (R.A.F. DRAWING No. T.7850) ON THE BODY OF B.E. 2E.

(Scale of model body 1/6th full size.)

R_0 = Resistance coefficient of body *without* interference from airscrew.

R = Resistance coefficient of body *with* interference from airscrew.

The values of the table have been corrected for the "scale-speed" effect of airscrew.

Value of $\left(\frac{V}{nD}\right)$	Value of $\left(\frac{T}{\rho V^2 D^2}\right)$	Value of $\left(\frac{R}{R_0}\right)$
1·208	0·027	0·890
1·160	0·040	0·900
1·133	0·049	0·907
1·130	0·050	0·920
1·127	0·051	0·935
1·089	0·066	0·925
1·065	0·075	0·948
1·055	0·079	0·970
0·930	0·148	1·060
0·848	0·209	1·120
0·790	0·260	1·208
0·740	0·313	1·265
0·695	0·367	1·342
0·660	0·418	1·415
0·615	0·494	1·500
0·590	0·548	1·565
0·570	0·594	1·645

REPORT No

FIG. 1.

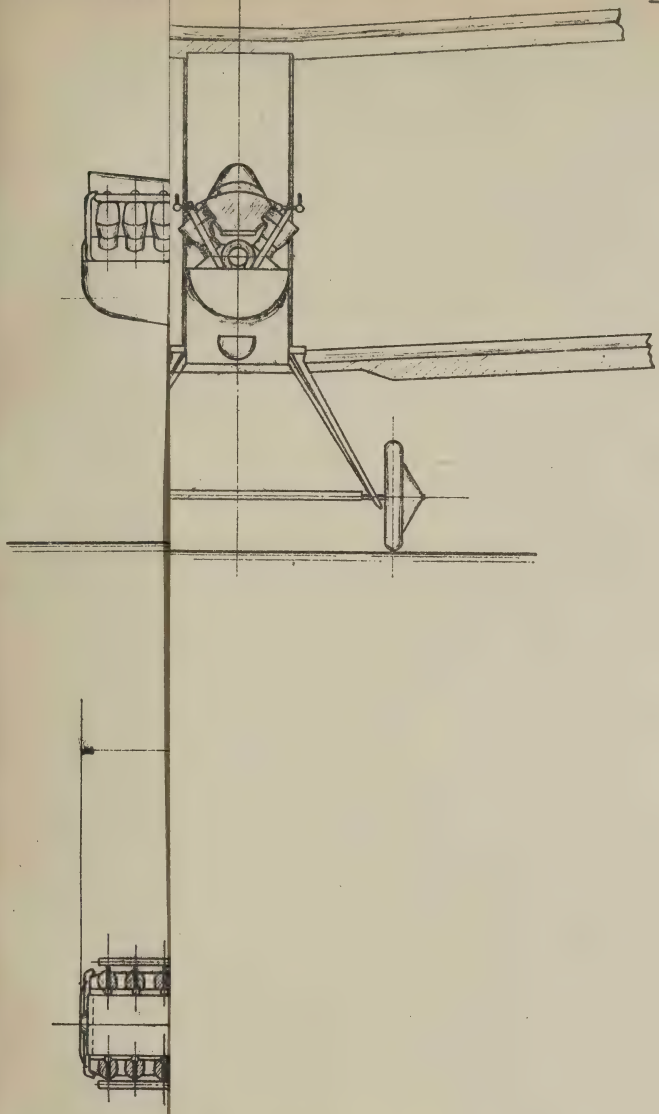

E AIRSCREW BODY

. AEROPLANE. ——

e. aeroplane. ——

18"

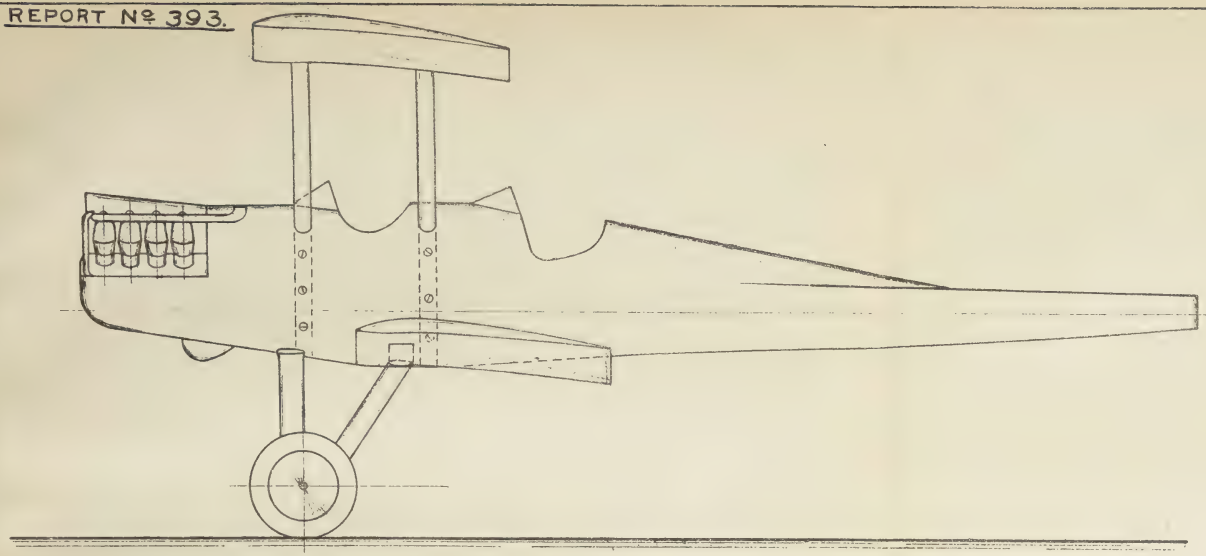

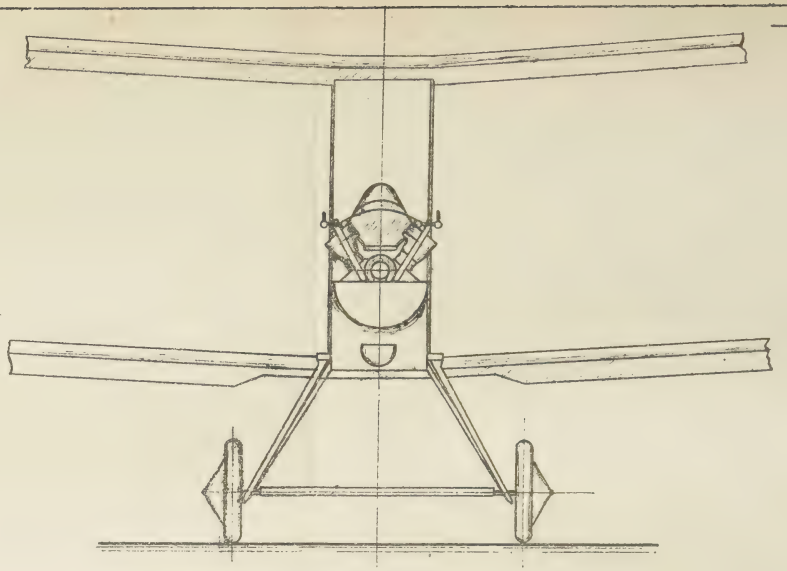

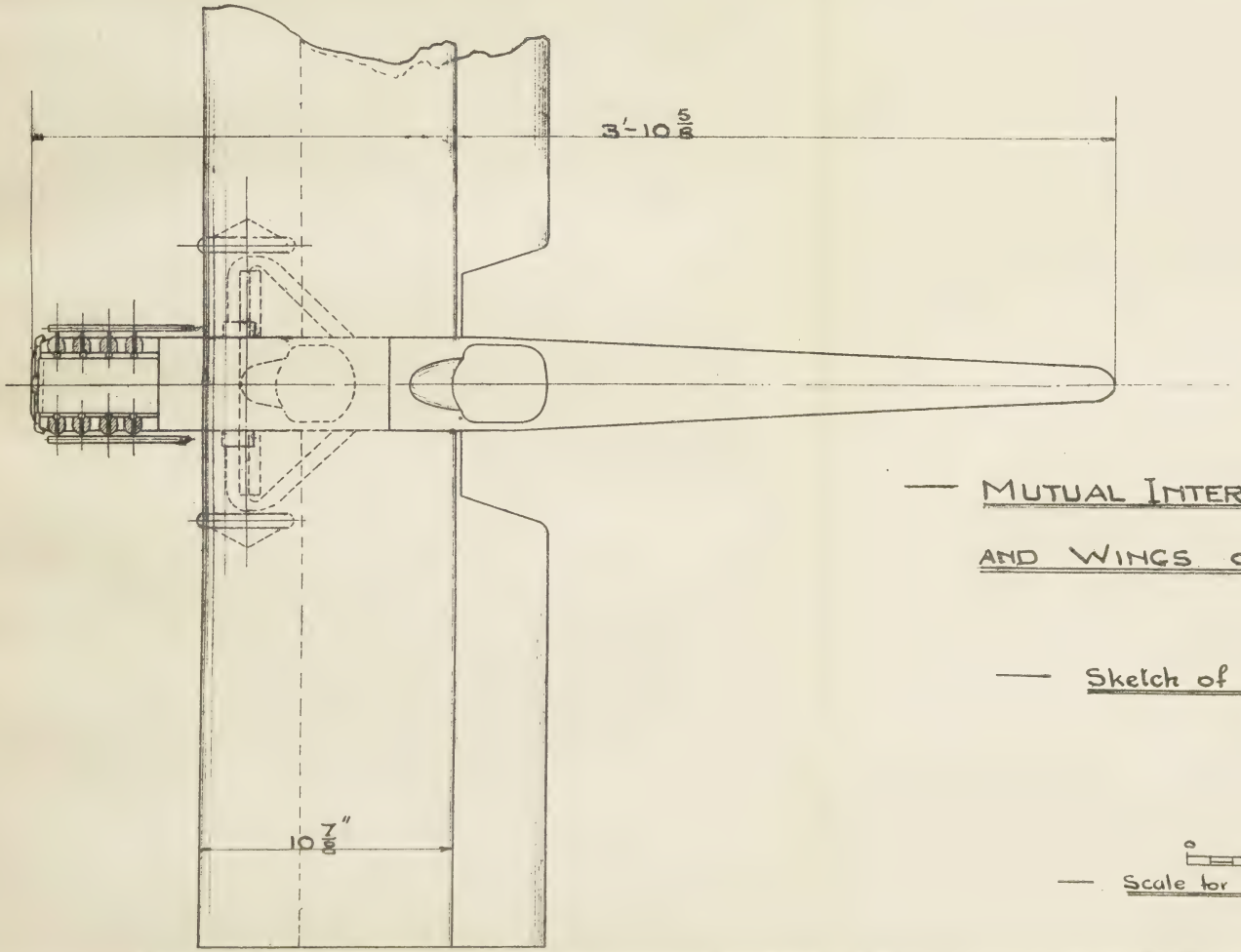

— MUTUAL INTERFERENCE OF THE AIRSCREW BODY AND WINGS OF THE B.E. 2e. AEROPLANE. —

— Sketch of model of B.E. 2e. aeroplane. —

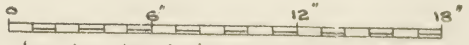

— Scale for drawing in inches. —

MUTUAL INTERFERENCE OF AIRSCREW & BODY.

R.A.F. Drawing No. T.785c.

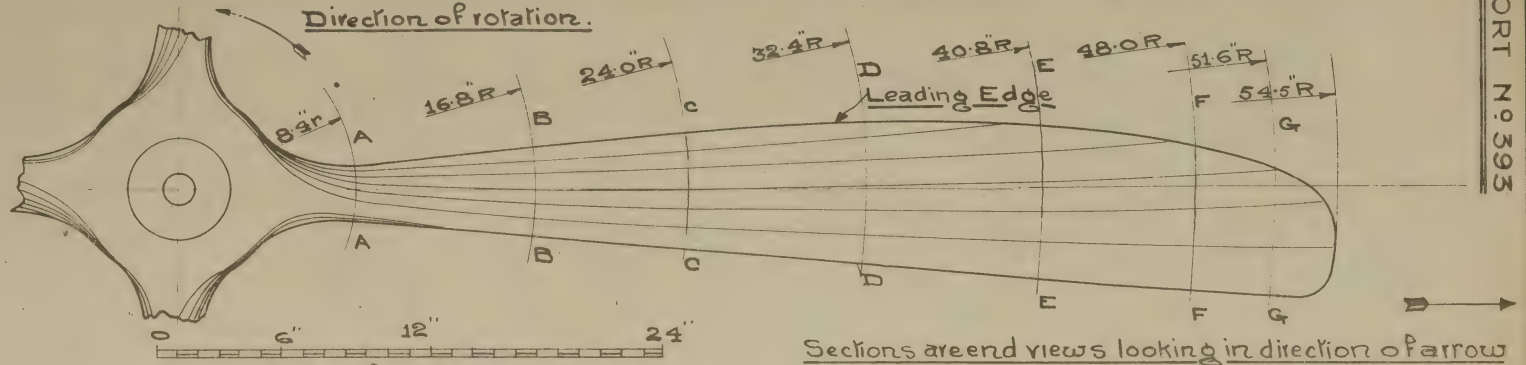

Scale in inches for plan view.

Sections are end views looking in direction of arrow

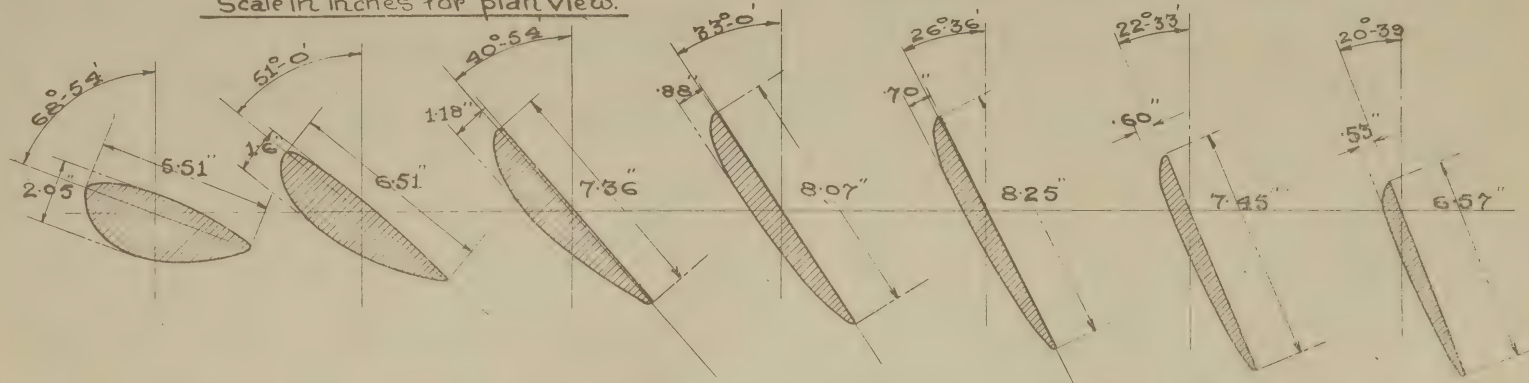

Section A.A. Section B.B. Section C.C. Section D.D. Section E.E. Section F.F Section G.G.

FIG. 2.

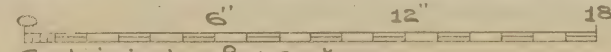

Scale in inches for sections.

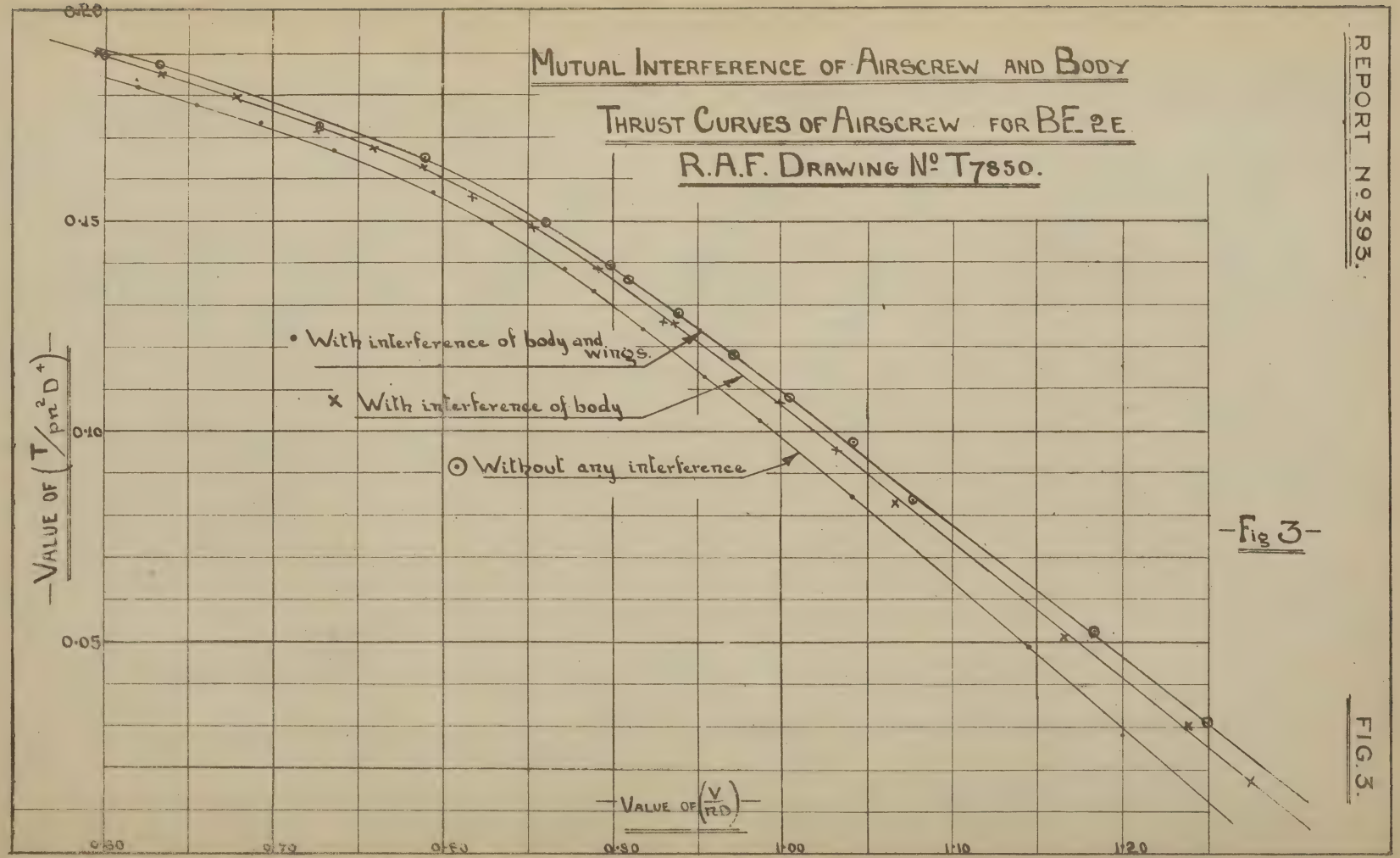

REPORT No. 393.

FIG. 3.

-Fig 3-

Mutual Interference of Airscrew and Body.

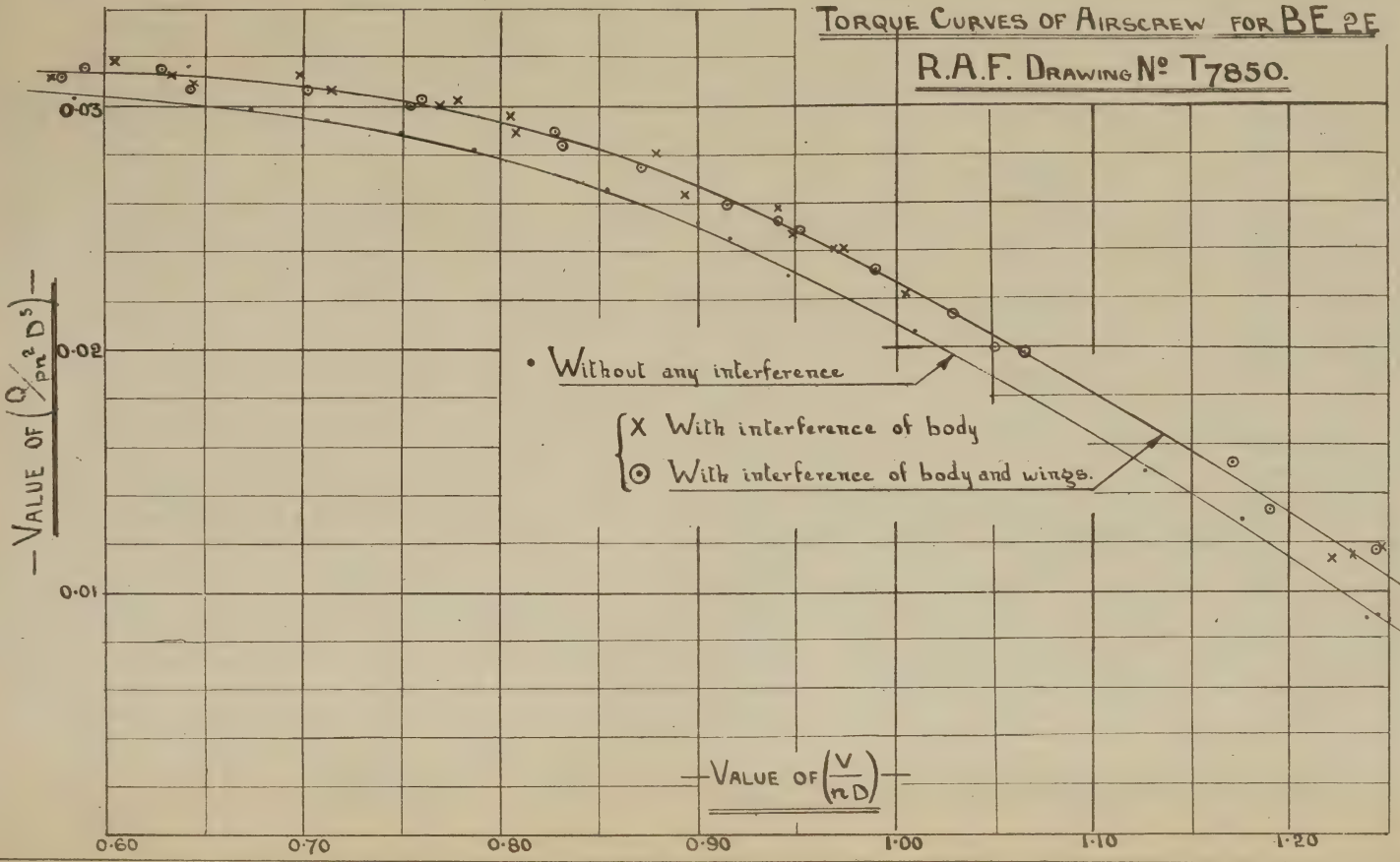

— Fig. 4 —

FIG. 4.

MUTUAL INTERFERENCE OF AIRSCREW & BODY.

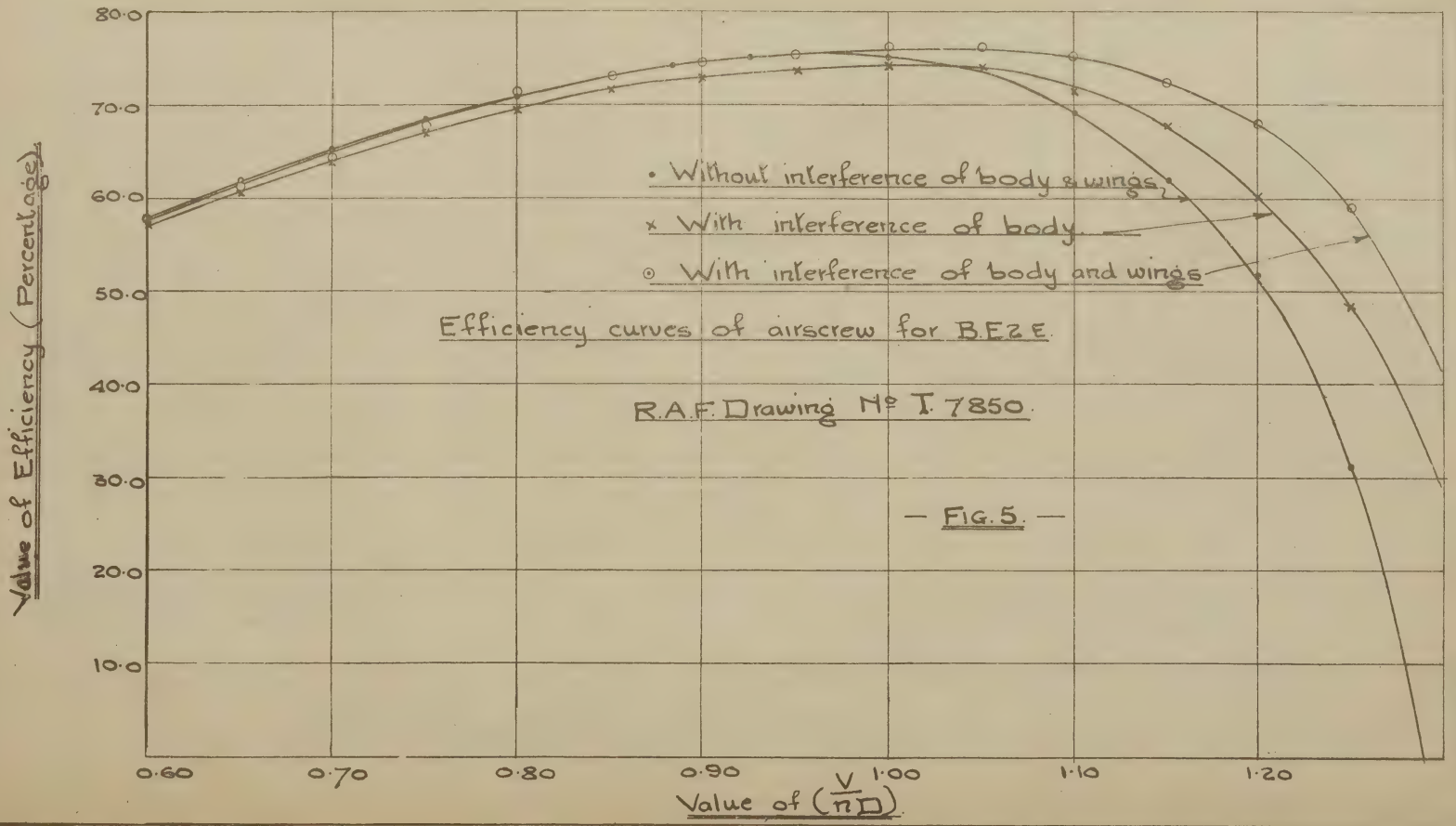

Efficiency curves of airscrew for B.E.2.E.

R.A.F. Drawing No. T. 7850.

— FIG. 5. —

MUTUAL INTERFERENCE OF AIRSCREW & BODY.

Drag of model body of B.E2e machine

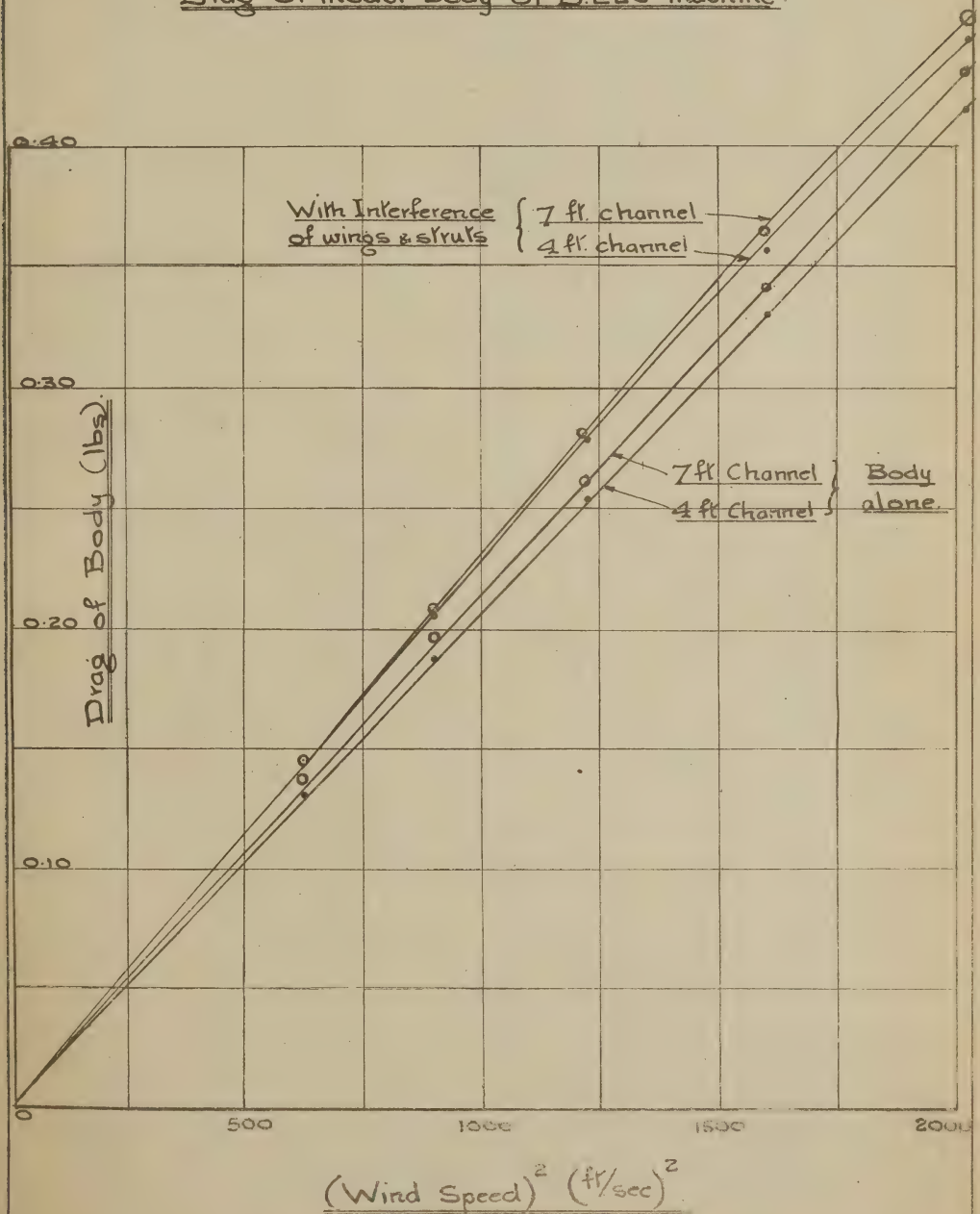

MUTUAL INTERFERENCE OF AIRSCREW AND BODY.

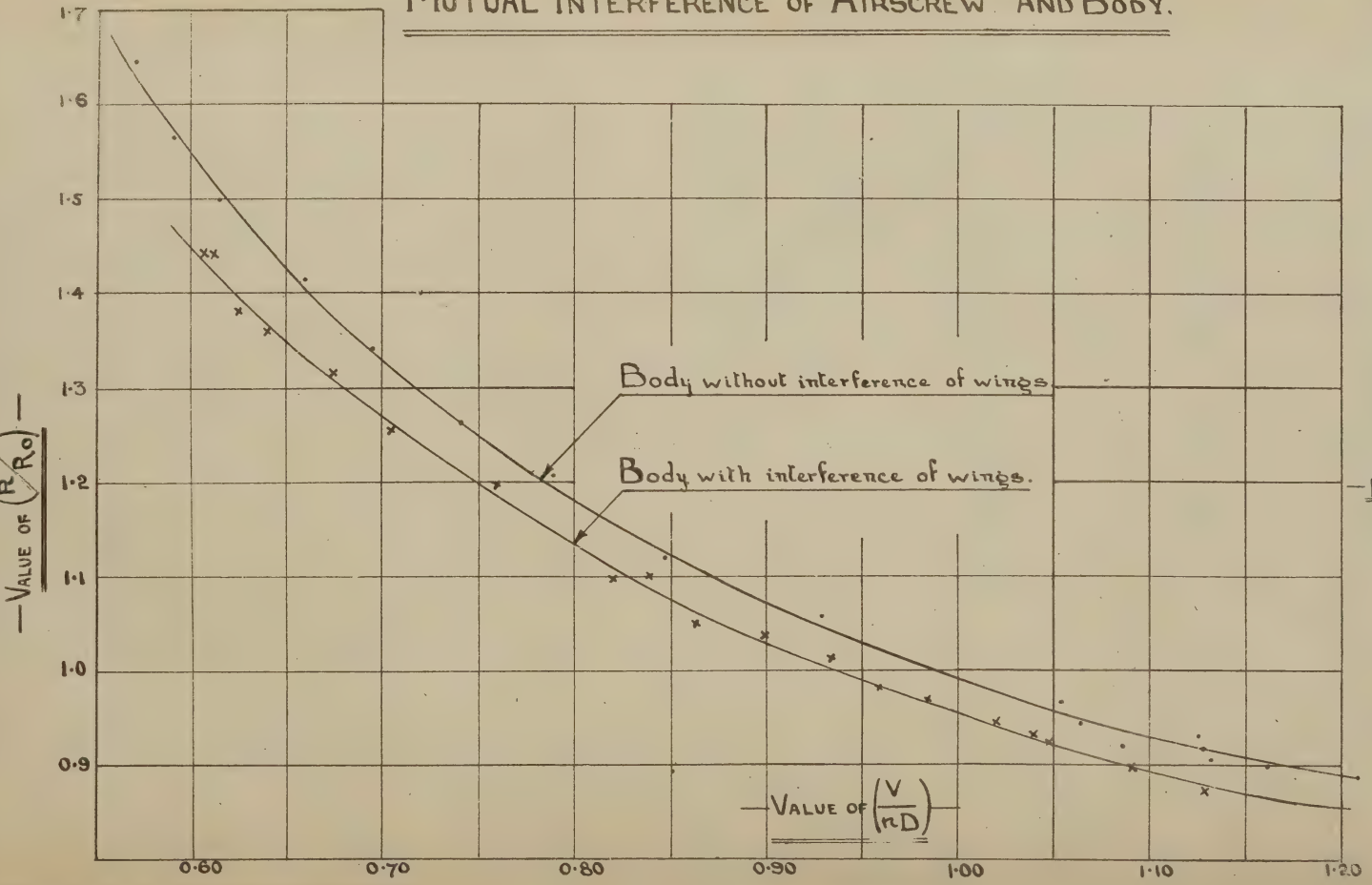

—Fig. 7.—

FIG. 7.

MUTUAL INTERFERENCE OF AIRSCREW AND BODY.

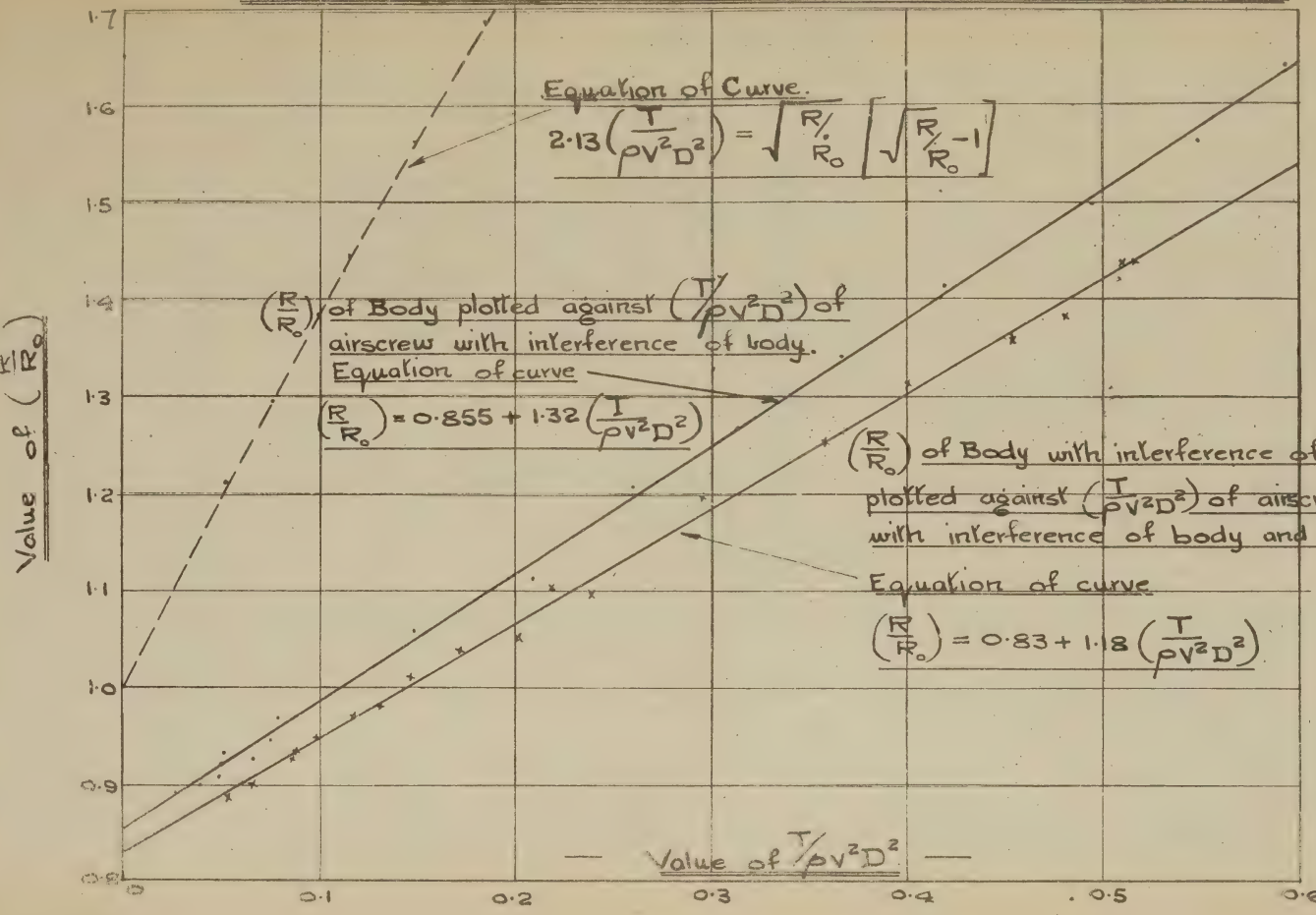

— FIG. 8 —

FIG. 8.

REPORT No. 393

MUTUAL INTERFERENCE of AIRSCREW & BODY.

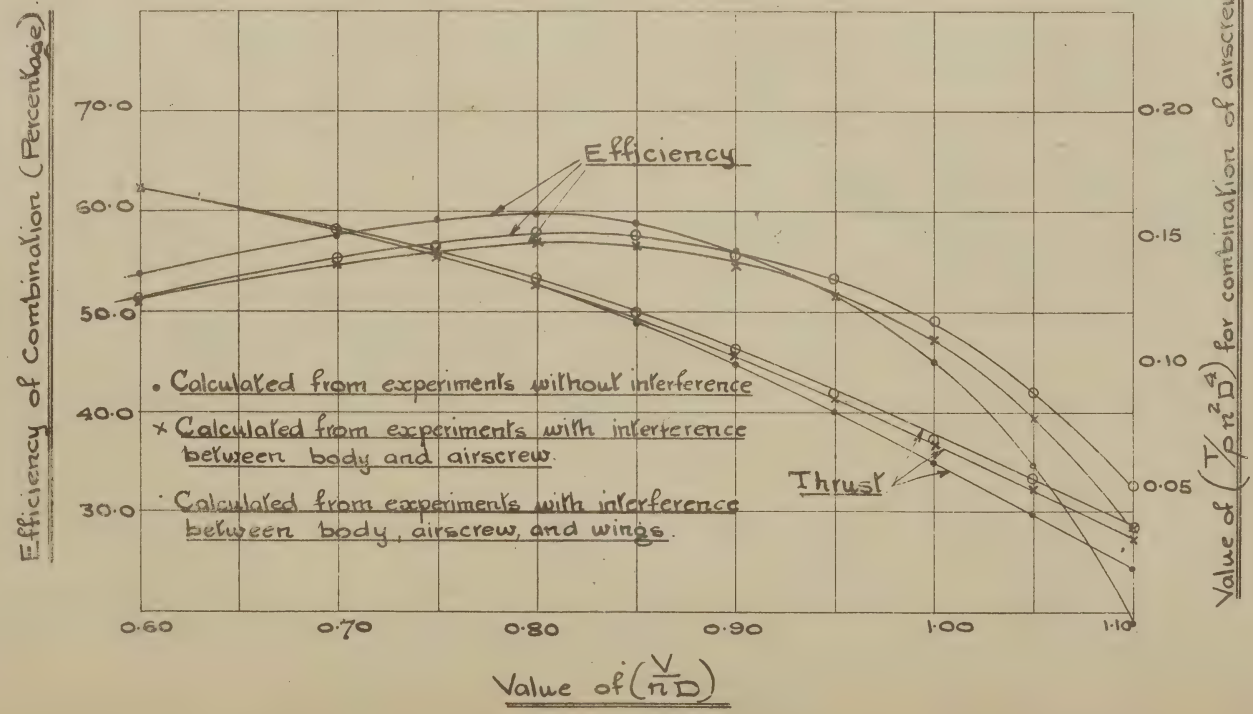

FIG. 9.

Table 6.

INTERFERENCE OF AIRSCREW B.E. 2E (R.A.F. DRAWING No. T.7850) ON THE BODY OF B.E. 2E, WITH THE WINGS MOUNTED IN POSITION BUT NOT ATTACHED TO THE BODY.

(Scale of model body 1/6th full size.)

R_0 = Resistance coefficient of body *without* interference from airscrew.

R = Resistance coefficient of body *with* interference from airscrew.

The values of the table have been corrected for the "scale-speed" effect of the airscrew.

Value of $\left(\frac{V}{nD}\right)$	Value of $\left(\frac{T}{\rho V^2 D^2}\right)$	Value of $\left(\frac{R}{R_o}\right)$
1·130	0·054	0·875
1·092	0·067	0·900
1·048	0·086	0·926
1·040	0·090	0·935
1·020	0·099	0·948
0·985	0·118	0·971
0·960	0·132	0·983
0·935	0·147	1·014
0·900	0·172	1·039
0·863	0·201	1·050
0·840	0·219	1·102
0·820	0·237	1·098
0·760	0·295	1·198
0·705	0·358	1·255
0·675	0·400	1·315
0·640	0·454	1·360
0·625	0·481	1·382
0·610	0·509	1·440
0·606	0·517	1·440

Table 7.

A COMPARISON OF THE EFFICIENCY OF THE COMBINATION OF B.E. 2E BODY AND AIRSCREW, AS CALCULATED FROM EXPERIMENTS INVOLVING MUTUAL INTERFERENCE WITH THAT CALCULATED FROM EXPERIMENTS WITHOUT INTERFERENCE.

Value of $\left(\frac{V}{nD}\right)$	Without Interference between Airscrew and Body.		With Interference between Airscrew and Body.			
			Without Interference of Wings.		With Interference of Wings.	
	Value of $\left(\frac{T}{\rho n^2 D^4}\right)$ for the Combination.	Value of Efficiency. Percentage.	Value of $\left(\frac{T}{\rho n^2 D^4}\right)$ for the Combination.	Value of Efficiency. Percentage.	Value of $\left(\frac{T}{\rho n^2 D^4}\right)$ for the Combination.	Value of Efficiency. Percentage.
1·10	0·017	18·5	0·029	28·2	0·034	32·5
1·00	0·059	45·0	0·067	47·2	0·070	49·0
0·95	0·080	51·5	0·085	51·4	0·088	53·2
0·90	0·098	56·0	0·102	54·5	0·104	55·8
0·85	0·116	58·8	0·118	56·5	0·120	57·6
0·80	0·131	59·7	0·131	57·0	0·133	58·0
0·75	0·143	59·2	0·142	56·2	0·144	56·7
0·70	0·153	57·5	0·151	54·6	0·153	55·3
0·60	0·170	53·7	0·167	51·0	0·170	51·5

A PRELIMINARY INVESTIGATION OF THE MUTUAL INTERFERENCE OF AN AIRSCREW AND A TRACTOR BODY, AS AFFECTED BY THE FAIRING OF THE NOSE OF THE BODY.

By A. Fage, A.R.C.Sc., and H. E. Collins.

Reports and Memoranda, No. 401. *January*, 1918.

Summary. — (*a*) *Introductory.* (*Reasons for inquiry.*) — The present experiments were made at the request of the Air Board to determine the effect of fairing the nose of a tractor body, the fairing being made either behind the airscrew, or the shape of the body being continued in front by a nose-piece attached to, and rotating with, the airscrew. The investigation is intended to be of a preliminary character. At the beginning of the report it is pointed out that the desirability and applicability of fairing will depend on the type of engine mounted.

(*b*) *Range of the investigation.*—A tractor body was used having the general form of the old B.E.2C body, the nose of the body being faired by means of a detachable nose-piece ; the airscrew used was a model, $\frac{1}{8}$th full size, of the R.E.7 airscrew (R.A.F. Drawing T.5014).

The investigation covered the following combinations :—

(1) The mutual interference of the airscrew and the " faired " body, *i.e.*, the body with the " faired " nose-piece attached.

(2) Mutual interference of the airscrew and the " unfaired " body, *i.e.*, with the " faired " nose-piece detached.

(3) Mutual interference of the airscrew, to which was attached the " faired " nose-piece, and the " unfaired " body.

(*c*) *Conclusions.*—No advantage was found in the use of a " faired " body behind the airscrew as compared with an " unfaired " body— " unfaired " is to be given the meaning of the present report. There is, however, a material gain of efficiency to be expected by the use of a faired nose-piece rotating with the airscrew, in conjunction with an " unfaired " body, the increase in efficiency in the present investigation as compared with the previous combinations being about 4 per cent. over the working range of V/nD.

The present experiments were made at the request of the Air Board to determine the effect of fairing the nose of a tractor body, the fairing being made either behind the airscrew, or the shape of the body being continued in front by a nose-piece attached to, and rotating with, the airscrew. As no experimental data on this problem were available, it was thought that the preliminary investigation should be of a general character. Accordingly the

present experiments were made with a model body of B.E.2C type, modified at the nose so as to facilitate the attachment of a fairing piece, whilst at the same time retaining a shape characteristic of an aeroplane body. The need for, and the nature of, the fairing at the front of the body will of course greatly depend on the type of engine mounted. Thus, in the case of the stationary air-cooled engine it may be of greater importance to make the air flow around the engine and so obtain more efficient cooling, rather than to attempt to reduce the resistance by making the flow conformable to the lines of the body.

The advisability of fairing in the case of a rotary engine often needs consideration, because the attachment of a circular fairing piece to the airscrew can usually be made very satisfactorily. With a machine driven by a water-cooled engine much depends on the position of the radiator. Obviously fairing would not be desirable if the radiator were mounted at the nose of the body, but unfortunately the flow of air through the radiator would probably greatly increase the drag of the body. In this connection it is worth noticing that a smaller radiator situated well out in the slip stream away from the body would probably suffice for the efficient cooling of the engine, whilst at the same time the body could be given a more efficient streamline shape.

Description of models.—The airscrew used in the present investigation was a model of the two-bladed airscrew for R.E.7 (R.A.F. Drawing No. T.5014). The model, of scale $\frac{1}{6}$th, was made in wood at the Royal Aircraft Factory. A drawing of the airscrew is given in Fig. 1, from which it is seen that the diameter of the full-sized airscrew is 9 feet 2 inches and that the blade-angles vary from 14° 22′ at the section next to the tip to 52° at the section next to the boss.

In Fig. 2 is given a drawing of the model body which resembles the old B.E.2C body (R. & M. 344), but with the forward end modified so as to adapt it to receive a faired nose-piece of circular section. The nose-piece of length $2\frac{7}{8}$ inches was made so as to be detachable. From the side elevation of Fig. 2 it is seen that the faired outline of the nose-piece runs into that of the body. The body with the faired nose-piece attached is hereafter referred to as the "faired body," and with the nose-piece detached as the "unfaired body." The principal dimensions of the model body are given in the drawing. A second nose-piece was made, of the same dimensions as that described above, but adapted to fit round and to rotate with the airscrew as shown in Fig. 3.

Description of the experiments.—The experiments were conducted in the No. 1 4-ft. wind channel, the thrust and torque of the airscrew being measured with the airscrew balance (described in previous reports). In the present experiments the balance was arranged so that the airscrew was about 17 inches behind the

vertical shaft of the airscrew balance, the driving belt being between the shaft and the airscrew. The usual cylindrical guard and streamline guard-body were used as described in previous reports.

In order to ascertain whether there was any appreciable interference between the guards of the balance and the airscrew, the balance as a whole was rotated through an angle of 180°, thus bringing the plane of rotation of the airscrew about 17 inches in front of the vertical shaft of the balance. The airscrew was accordingly tested in this position, in which it is thought that the interference effects of the guards, &c., are very small. It was found that the performances measured with the airscrew in these two positions were identical within the limits of experimental error.

The following experiments were then made :—

(1) The airscrew alone was tested for thrust and torque.

(2) The airscrew was tested for thrust and torque with the " faired " body in place behind the airscrew.

(3) The airscrew was tested for thrust and torque with the " unfaired " body in place behind the airscrew.

(4) The airscrew, to which was attached the faired nose-piece, was tested for thrust and torque.

(5) The airscrew with the faired nose-piece attached was tested for thrust and torque with the " unfaired " body in place behind the airscrew.

The combinations of airscrew and body set out in (2), (3), and (5) above are illustrated diagrammatically in Fig. 4 ; the arrangement of (4) is illustrated in Fig. 3.

In the experiments (4) and (5) the faired nose-piece came rather close to the guard of the balance, so that it was considered advisable to determine the effect of the faired nose-piece on the performance of the airscrew with the airscrew balance rotated as a whole through an angle of 180°, in which position the plane of rotation of the airscrew is about 17 inches *in front* of the vertical shaft of the balance, and the faired nose-piece is well in front of the guard body. It was found that the performance of the airscrew was unaffected, within the limits of experimental error, by the attachment of the nose-piece. This result is probably only a characteristic of this particular combination and not generally applicable to all combinations of airscrew and faired boss, although it is not expected that the performance of an airscrew will be greatly affected by the presence of a faired boss.

The airscrew performances (thrust and torque) are in all cases presented in the form of absolute coefficients, from which the thrust and torque may be calculated as follows :—

$$\text{Thrust} = \mathrm{T} = \mathrm{T}'_c \rho n^2 \mathrm{D}^4,$$
$$\text{Torque} = \mathrm{Q} = \mathrm{Q}'_c \rho n^2 \mathrm{D}^5,$$

where the thrust T, torque Q, diameter of airscrew D, rotational speed n, and mass density ρ are all expressed in any system of consistent units, and T'_c and Q'_c are non-dimensional coefficients, taken for a standard atmosphere of temperature = 15·6°C. and barometer = 760 mm.

The resistances of the bodies were measured in the No. 1 4-ft. wind channel. In the measurements of resistance of the body when in the slip stream of the airscrew, the latter was supported in the channel by means of a tube, 2-inch diameter, attached to the channel walls by means of wires.

Discussion of the results of the experiments.—The results of the experiments on the airscrew alone (as in (1) above) and in combinations (2) and (3) are given in Tables 1-3 and Figs. 5-7 ; those of the airscrew in combinations (4) and (5) are given in Table 4 and Fig. 8.

(*a*) *Combination* (2).—It will be seen that the proximity of the " faired " body to the airscrew does not greatly affect the efficiency of the airscrew, the effect being greatest, at low values of V/nD, where the efficiency is raised by about 2 per cent.

The thrust and torque of the airscrew, at given values of the translational velocity V and the rotational velocity n, are both increased by the presence of the body, the percentage increase being about the same for both thrust and torque in the region of maximum efficiency.

(*b*) *Combination* (3).—With the " unfaired " body situated behind the airscrew, it was found that the thrust of the airscrew, at given values of V and n, was increased to a greater extent than in the case of combination (2), whilst the torque curve (see Fig. 6), though raised at the higher values of V/nD, will be seen to cross the curve for combination (2) at a value of V/nD of about 0·59.

The maximum efficiency of the airscrew is thus increased in the case of the combination (3) from 66 per cent. for the airscrew alone to a maximum of 69 per cent. with the body in place.

(*c*) *Combination* (5).—In this case, the effect of the presence of the body on the performance of the airscrew is much more marked than in either of the combinations (2) or (3). Thus the maximum efficiency is increased from 66 per cent. for the airscrew as in (4) to a value of 72 per cent. when in combination (5). This increase is mainly brought about by the fact that whereas, at given values of V and n, the thrust is increased by about the same percentage as in combination (3), the increase in torque is very much smaller ; this will be clearly seen from a comparison of the curves of Figs. 6 and 8.

The resistance of the " faired " body at a wind speed of 40 feet per sec. was found to be 0·0626 lbs. With this body a small " scale-speed " effect was observed which almost disappeared at a wind speed of 40 ft. per sec.

Values of R/R_o, where R is the resistance of the body when in the slip stream of the airscrew, and R_o is the resistance of the body as unaffected by the airscrew, for various values of V/nD, are given in Table 6.

The resistance of the " unfaired " body at a wind speed of 40 ft. per sec. was found to be 0·113 lbs.; values of R/R_o for this body in combinations (3) and (5) are also given in Table 6; the figures given in this table are plotted in Fig. 9.

Fig. 10 gives the values of R/R_o for the three combinations (2), (3) and (5) plotted against corresponding values of the thrust coefficient T_c $(= T/\rho V^2 D^2)$ for the airscrew as affected by the interference of the body; it will be seen that in all cases the values of R/R_o lie approximately on straight lines, the slopes being different, however, with the different combinations.

The curves of Figs. 9 and 10 are probably at first sight somewhat misleading, since although for combination (2), " faired " body, the values of R/R_o are higher than those for combination (3), " unfaired " body, the actual values of both R_o and R are higher for the " unfaired " body than for the " faired " body, thus at a value of V/nD of about 0·67, the ratio

$$\left(\frac{\text{resistance of " unfaired " body in slip stream}}{\text{resistance of " faired " body in slip stream}}\right) = 1{\cdot}25 \text{ (approx.)},$$

and the ratio

$$\left(\frac{R_o \text{ for " unfaired " body}}{R_o \text{ for " faired " body}}\right) = 1{\cdot}80 \text{ (approx.)}.$$

With regard to the curve for combination (5) the low values of R/R_o are due to the fact that the value of R_o here taken is the relatively high resistance of the " unfaired " body, whilst the values of R are low because the body is shielded by the faired nose-piece attached to the airscrew. At a value of V/nD of 0·67, the value of the ratio

$$\left(\frac{\text{resistance of " unfaired " body in slip stream, as in combination (3)}}{\text{resistance of " unfaired " body in slip stream, shielded by faired nose-piece as in combination (5)}}\right)$$

is equal to about 3·1.

As pointed out in R. & M. Nos. 305 & 344, it is necessary in order to take account completely of the mutual interference of the airscrew and body, to treat these as a combination, the efficiency of which may be calculated firstly from non-interference experiments on the airscrew and on the body, and secondly from experiments involving mutual interference.

In the case of combination (2) the resistance of the body may be expressed in the form $0{\cdot}0071\rho V^2D^2$ so that for the combination without interference, the thrust coefficient is

$$\left[T'_c - 0{\cdot}0071\left(\frac{V}{nD}\right)^2\right]$$

and the efficiency of the combination is

$$\frac{15{\cdot}9}{Q'_c}\left[T'_c - 0{\cdot}0071\left(\frac{V}{nD}\right)^2\right]\cdot\frac{V}{nD} \text{ per cent.}$$

T'_c and Q'_c are the thrust and torque coefficients of the "non-interference" experiments. For the combination with mutual interference, the thrust coefficient is

$$\left[T'_c - 0{\cdot}0071\,\frac{R}{R_o}\left(\frac{V}{nD}\right)^2\right]$$

and the efficiency of the combination is

$$\frac{15{\cdot}9}{Q'_c}\left[T'_c - 0{\cdot}0071\,\frac{R}{R_o}\left(\frac{V}{nD}\right)^2\right]\cdot\left(\frac{V}{nD}\right) \text{ per cent.}$$

In this case T'_c and Q'_c are the thrust and torque coefficients of the "interference" experiments.

Similarly for combinations (3) and (5), since the resistance of the "unfaired" body is $0{\cdot}0128\rho V^2D^2$, the thrust coefficient for the combination without interference is given by

$$\left[T'_c - 0{\cdot}0128\left(\frac{V}{nD}\right)^2\right]$$

and the efficiency by

$$\frac{15{\cdot}9}{Q'_c}\left[T'_c - 0{\cdot}0128\left(\frac{V}{nD}\right)^2\right]\cdot\left(\frac{V}{nD}\right) \text{ per cent.}$$

and for the combination with interference, the thrust coefficient of the combination is

$$\left[T'_c - 0{\cdot}0128\,\frac{R}{R_o}\left(\frac{V}{nD}\right)^2\right]$$

and the efficiency

$$\frac{15{\cdot}9}{Q'_c}\left[T'_c - 0{\cdot}0128\,\frac{R}{R_o}\left(\frac{V}{nD}\right)^2\right]\cdot\left(\frac{V}{nD}\right) \text{ per cent.}$$

The results of these calculations are given in Table 7 and are shown graphically in Figs. 11 and 12. A comparison of the results for the three combinations (2), (3), and (5), with mutual inter-

ference, is given in Fig. 13. From Figs. 11 and 12 it will be seen that with

Combination (2).—The values of the efficiency obtained when interference is neglected are very nearly the same (for corresponding values of T'_c for the combination) as those obtained by taking into account the mutual interference.

Combination (3).—The efficiencies as calculated by the two methods are nearly equal, for corresponding values of T'_c up to a value of $T'_c = 0{\cdot}03$; for higher values of T'_c, however, taking account of mutual interference gives an efficiency about 3 per cent. higher than that obtained by neglecting interference, *i.e.*, at $T'_c = 0{\cdot}06$, the efficiency is raised from 61·5 per cent. to 64·5 per cent.

Combination (5).—The values of the efficiency calculated from the experiments involving mutual interference are uniformly higher than those obtained by neglecting interference, by amounts varying from about 14 per cent. at $T'_c = 0{\cdot}025$ to about 4 per cent. at $T'_c = 0{\cdot}08$.

From an examination of the efficiency curves of Fig. 13 it will be seen that there is no advantage in the use of the " faired " body, as in combination (2), as compared with the " unfaired " body as in combination (3) ; actually the " faired " body, combination (2), shows a small disadvantage at the higher values of T'_c. With combination (5) in which the nose-piece is attached to the airscrew, as compared with either combination (2) or (3), it will be seen that there is an appreciable gain of efficiency over the whole of the working range of T'_c, *e.g.*, at a value of $T'_c = 0{\cdot}03$, the efficiency is raised from 55 per cent. to 67 per cent., whilst at a value of $T'_c = 0{\cdot}08$ the efficiency is raised from values of 61 per cent. and 62 per cent. respectively, to 64 per cent.

To complete the analysis of the results obtained from the calculations, both with and without mutual interferences, some reference should be made to the torque of the combination. Accordingly, the curves of Figs. 14 and 15 have been drawn, which give the relationships between T'_c, Q'_c, and (V/nD), so supplying the additional data necessary for the complete comparison of the several combinations of airscrew and body.

Conclusions.—The conclusions to be drawn from the investigation may now be briefly summarised. With the particular bodies and airscrew of the present experiments the best combination is that in which the airscrew, having attached to it the faired nose-piece, rotates in front of the " unfaired " body. Further, it would appear that no appreciable advantage is to be expected by fairing the nose of a body behind an airscrew. At this stage of the investigation it is thought to be unwise to generalise unduly, but it would seem that where possible, fairing the nose of the body by the use of a nose-piece attached to and rotating with the airscrew, is to be recommended.

TABLE I.

AIRSCREW FOR R.E.7.

(R.A.F. Drawing No. T.5014.)

Diameter of model airscrew, 1·53 ft.

Scale of model airscrew = $\frac{1}{6}$th full size.

V in feet per second.

n in revolutions per second.

D diameter in feet.

Thrust coefficient $T'_c = \frac{T}{\rho n^2 D^4}$ (T = Thrust in lbs.).

Airscrew without interference.		Airscrew with interference of "faired" body.		Airscrew with interference of "unfaired" body.	
Value of $\frac{V}{nD}$.	Value of T'_c.	Value of $\frac{V}{nD}$.	Value of T'_c.	Value of $\frac{V}{nD}$.	Value of T'_c.
0·376	0·0900	0·381	0·0922	0·382	0·0923
0·398	0·0860	0·402	0·0881	0·405	0·0892
0·423	0·0810	0·430	0·0839	0·432	0·0845
0·456	0·0751	0·463	0·0779	0·465	0·0784
0·494	0·0690	0·495	0·0720	0·494	0·0720
0·523	0·0620	0·543	0·0627	0·535	0·0651
0·534	0·0606	0·556	0·0597	0·540	0·0649
0·554	0·0562	0·563	0·0579	0·559	0·0601
0·578	0·0510	0·596	0·0504	0·583	0·0552
0·606	0·0448	0·636	0·0411	0·610	0·0491
0·624	0·0403	0·647	0·0384	0·639	0·0415
0·639	0·0375	0·660	0·0351	0·652	0·0391
0·652	0·0342	0·682	0·0297	0·655	0·0346
0·673	0·0289	0·705	0·0233	0·690	0·0302
0·693	0·0225	0·721	0·0184	0·716	0·0241
0·711	0·0179	0·725	0·0187	0·732	0·0190
0·728	0·0128	0·742	0·0134	0·751	0·0136
0·745	0·0072	0·758	0·0074	0·770	0·0076
0·769	0·0009	0·762	0·0075	0·793	0·0010

Table 2.

AIRSCREW FOR R.E.7.

(R.A.F. Drawing No. T.5014.)

Diameter of model airscrew = 1·53 ft.

Scale of model airscrew = $\frac{1}{6}$th full size.

V in feet per second.

n in revolutions per second.

D diameter in feet.

$$\text{Torque coefficient} = Q'_c = \frac{Q}{\rho n^2 D^5} \quad (Q = \text{Torque in lbs.-ft.})$$

Airscrew without interference.		Airscrew with interference of "faired" body.		Airscrew with interference of "unfaired" body.	
Value of $\frac{V}{nD}$.	Value of Q'_c.	Value of $\frac{V}{nD}$.	Value of Q'_c.	Value of $\frac{V}{nD}$.	Value of Q'_c.
0·342	0·00938				
0·363	0·00920				
0·383	0·00913	0·361	0·00926	0·389	0·00922
0·385	0·00920	0·386	0·00922	0·414	0·00908
0·447	0·00882	0·417	0·00923	0·447	0·00879
0·486	0·00835	0·450	0·00898	0·451	0·00896
0·508	0·00816	0·491	0·00858	0·495	0·00864
0·512	0·00825	0·515	0·00830	0·511	0·00829
0·532	0·00788	0·526	0·00828	0·515	0·00828
0·542	0·00778	0·551	0·00804	0·538	0·00796
0·589	0·00694	0·574	0·00758	0·552	0·00804
0·619	0·00600	0·605	0·00715	0·605	0·00716
0·629	0·00619	0·620	0·00678	0·620	0·00683
0·661	0·00512	0·643	0·00628	0·644	0·00640
0·672	0·00495	0·680	0·00543	0·674	0·00590
0·725	0·00330	0·721	0·00443	0·695	0·00540
0·752	0·00230	0·739	0·00420	0·723	0·00458
0·769	0·00244	0·785	0·00251	0·763	0·00367

TABLE 3.

AIRSCREW FOR R.E.7.

(R.A.F. Drawing No. T.5014.)

Diameter of model airscrew = 1·53 ft.
Scale of model airscrew = $\frac{1}{6}$th full size.

V in feet per second.
n in revolutions per second.
D diameter in feet.
Values of efficiency (η).

Airscrew without interference.		Airscrew with interferenee of "faired" body.		Airscrew with interference of "unfaired" body.	
Value of $\frac{V}{nD}$.	Value of η (percentage).	Value of $\frac{V}{nD}$.	Value of η (percentage).	Value of $\frac{V}{nD}$.	Value of η (percentage).
0·37	57·7	0·37	59·2	0·37	60·1
0·40	59·7	0·40	61·7	0·40	62·4
0·44	62·0	0·44	63·8	0·44	64·9
0·48	63·9	0·48	65·3	0·48	66·9
0·52	65·1	0·52	66·5	0·52	68·3
0·56	65·7	0·56	66·6	0·56	68·9
0·60	65·9	0·60	66·0	0·60	68·7
0·64	65·0	0·64	64·5	0·64	66·8
0·68	61·0	0·68	60·1	0·68	62·8
0·72	49·6	0·72	49·6	0·72	53·4
0·76	17·4	0·76	26·6	0·76	34·2

Table 4.

AIRSCREW FOR R.E.7.

(R.A.F. Drawing No. T.5014.)

Airscrew with faired nose-piece attached, *with* and *without* interference of " unfaired " body. (See Figs. 3 and 4.)

Diameter of model airscrew = 1·53 ft.

Scale of model airscrew = $\frac{1}{6}$th full size.

V in feet per second.

n in revolutions per second.

D diameter in feet.

Thrust coefficient $T'_c = \frac{T}{\rho n^2 D^4}$. Torque coefficient $Q'_c = \frac{Q}{\rho n^2 D^5}$.

Value of $\frac{V}{nD}$.	Value of Thrust coefficient T'_c.		Value of Torque coefficient Q'_c.		Value of efficiency η (percentage).	
	Without interference of body.	With interference of body.	Without interference of body.	With interference of body.	Without interference of body.	With interference of body.
0·37	0·0906	0·0948	0·00925	0·00921	57·7	60·5
0·40	0·0855	0·0897	0·00910	0·00908	59·7	62·8
0·44	0·0785	0·0829	0·00886	0·00889	62·0	65·3
0·48	0·0711	0·0759	0·00850	0·00859	63·9	67·5
0·52	0·0633	0·0685	0·00805	0·00820	65·1	69·2
0·56	0·0550	0·0604	0·00747	0·00767	65·7	70·1
0·60	0·0462	0·0518	0·00670	0·00696	65·9	71·0
0·64	0·0368	0·0428	0·00577	0·00606	65·0	71·5
0·68	0·0263	0·0328	0·00467	0·00502	61·0	70·8
0·72	0·0150	0·0217	0·00347	0·00381	49·6	65·4
0·74	0·0091	0·0158	0·00285	0·00322	37·5	58·0

Table 5.

Resistance of " faired " body at a wind speed of 40 feet per second = 0·0626 lbs.

Resistance of " unfaired " body at a wind speed of 40 feet per second = 0·113 lbs.

Table 6.

Interference of Airscrew on "Faired" Body and on the "Unfaired" Body, and Interference on the "Unfaired" Body of Airscrew with Faired Nose-piece attached.

Scale of model airscrew = $\frac{1}{6}$th full size.
„ „ „ body = $\frac{1}{6}$th „ „

R_o = Resistance coefficient of body *without* interference of airscrew.

R = Resistance coefficient of body *with* interference of airscrew.

Airscrew and "faired" body. Combination (2).		Airscrew and "unfaired" body. Combination (3).		Airscrew with faired nose-piece attached and "unfaired" body. Combination (5).	
$\frac{V}{nD}$ for airscrew.	Value of $\frac{R}{R_o}$.	$\frac{V}{nD}$ for airscrew.	Value of $\frac{R}{R_o}$.	$\frac{V}{nD}$ for airscrew.	Value of $\frac{R}{R_o}$.
0·378	3·040	0·375	1·960	0·380	1·356
0·404	2·650	0·396	1·767	0·397	1·206
0·427	2·410	0·417	1·590	0·404	1·133
0·472	1·940	0·450	1·430	0·425	1·000
0·476	1·870	0·472	1·300	0·459	0·792
0·509	1·672	0·508	1·160	0·489	0·658
0·518	1·615	0·532	1·072	0·530	0·525
0·527	1·585	0·562	1·002	0·540	0·492
0·538	1·505	0·570	0·935	0·557	0·440
0·542	1·505	0·603	0·855	0·570	0·400
0·572	1·360	0·612	0·866	0·621	0·301
0·597	1·230	0·643	0·800	0·668	0·243
0·634	1·135	0·670	0·752	0·690	0·208
0·652	1·080	0·696	0·723	0·710	0·183
0·668	1·022	0·708	0·705	0·750	0·140
0·722	0·905	0·746	0·660	0·788	0·099
0·750	0·852	0·786	0·619	0·840	0·071
0·816	0·776	0·816	0·600		
0·828	0·740				

EFFECT OF FAIRING THE NOSE OF A TRACTOR BODY.

TWO BLADED TRACTOR FOR R.E.7.

R.A.F. DRAWING,
T5014.

REPORT No 401.

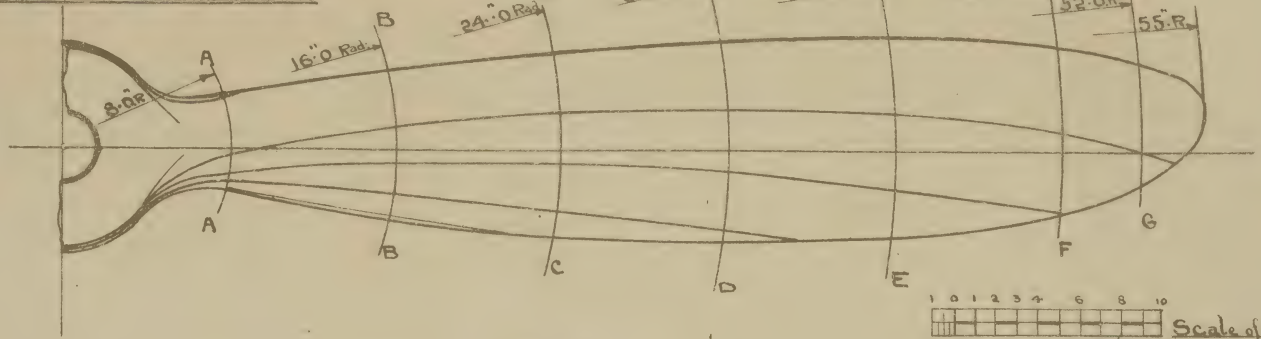

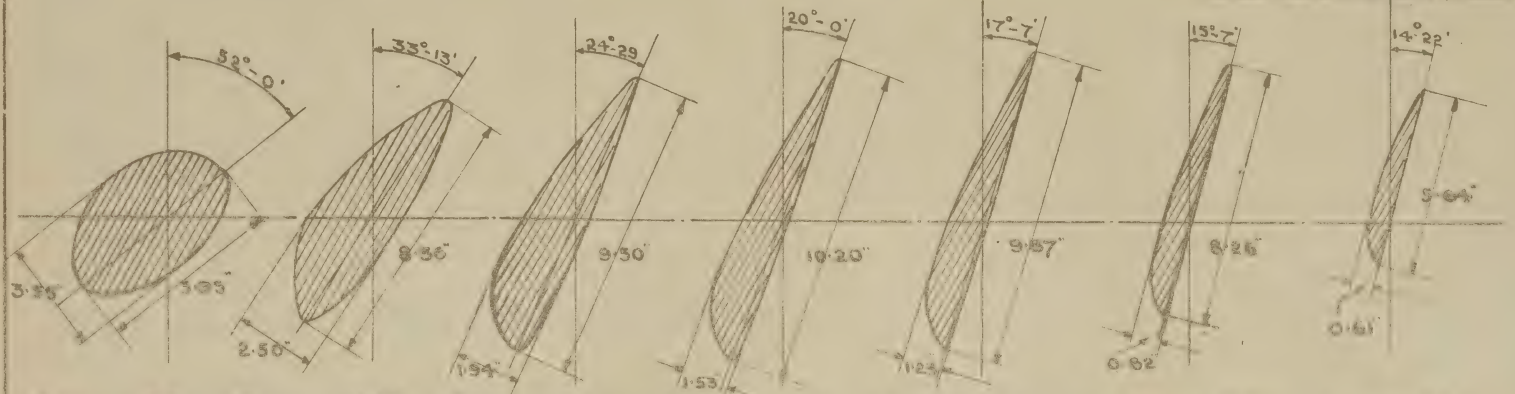

SECTION AA. SECTION BB. SECTION CC. SECTION DD. SECTION EE. SECTION FF. SECTION GG.

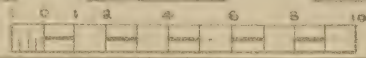

FIG. 1.

EFFECT OF FAIRING THE NOSE OF A TRACTOR BODY.

SKETCH OF MODEL BODY.

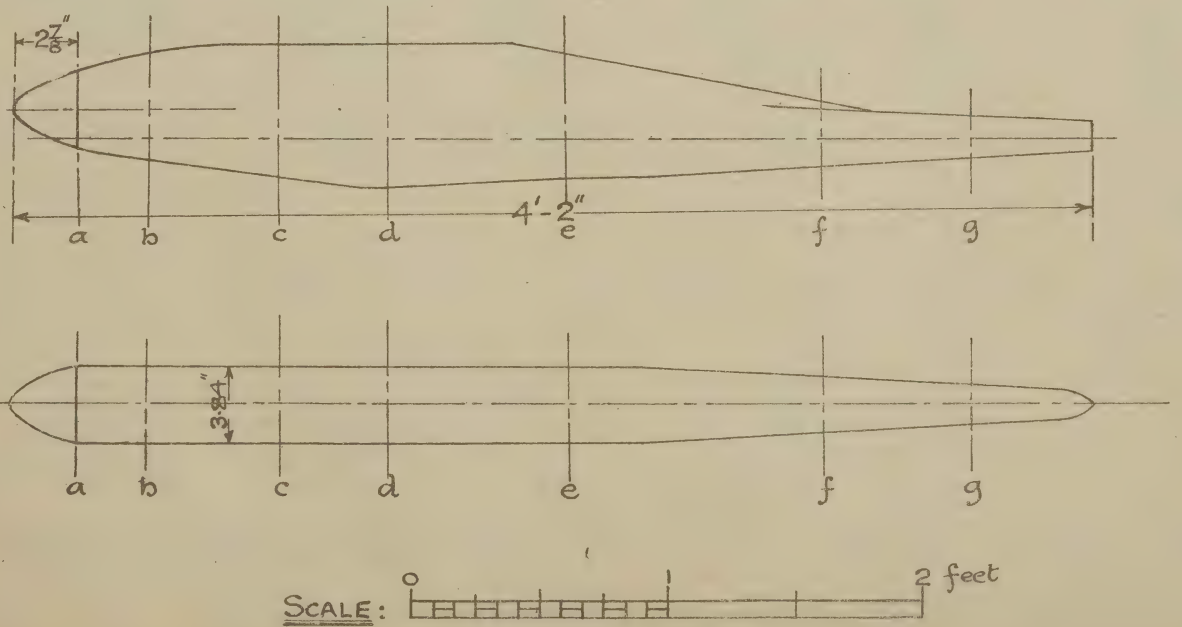

SCALE: 0 — 2 feet

REPORT Nº 401.

FIG. 2.

EFFECT OF FAIRING THE NOSE OF A TRACTOR BODY.

FIG. 3

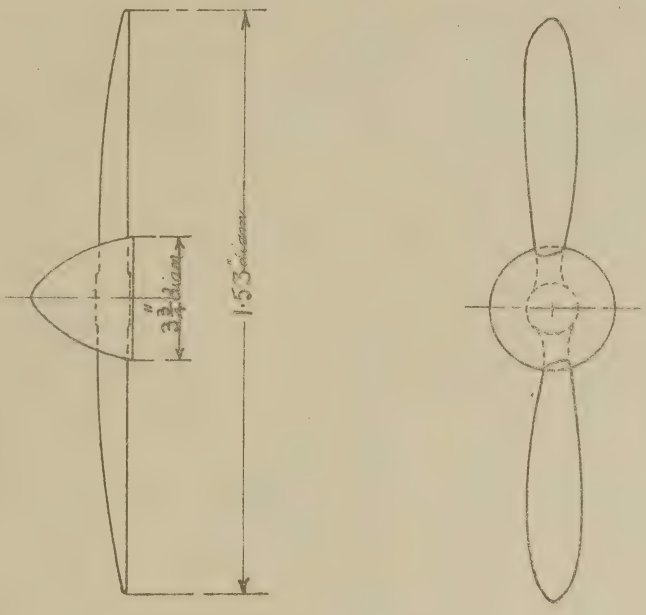

FIG. 4

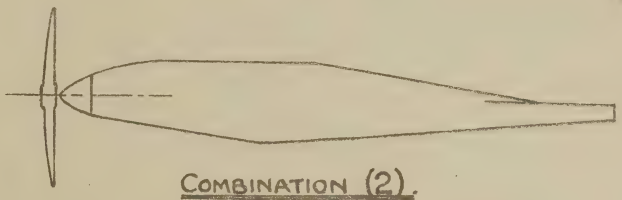

COMBINATION (2).

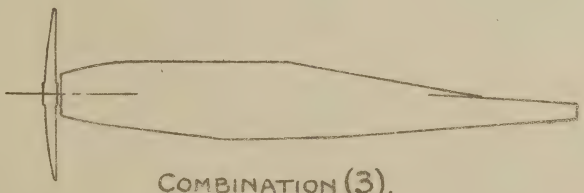

COMBINATION (3).

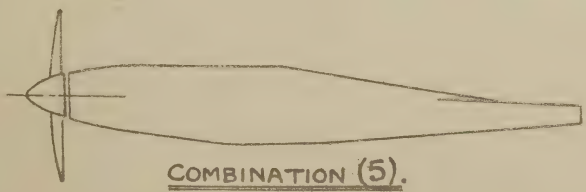

COMBINATION (5).

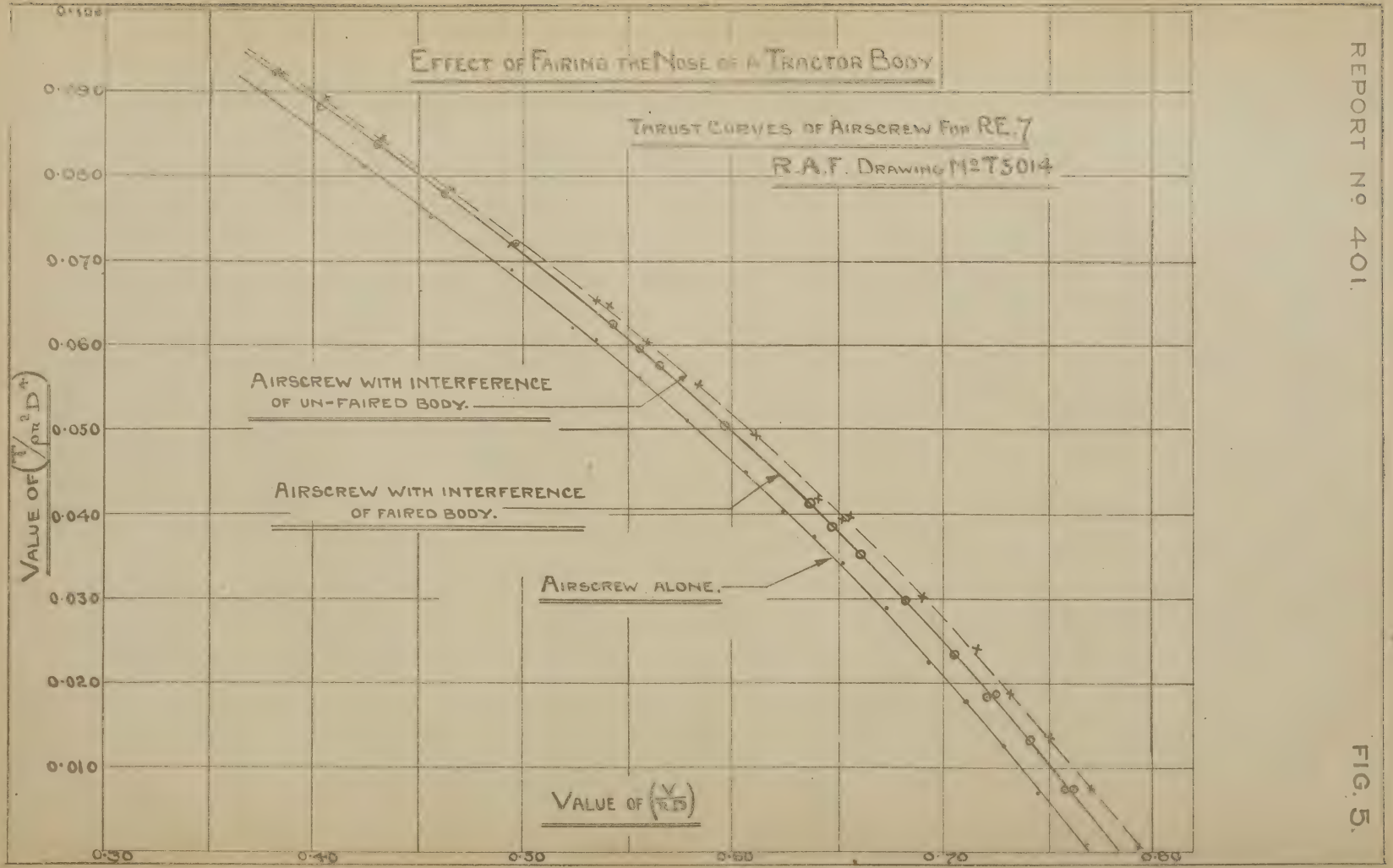

REPORT No. 401.

FIG. 5.

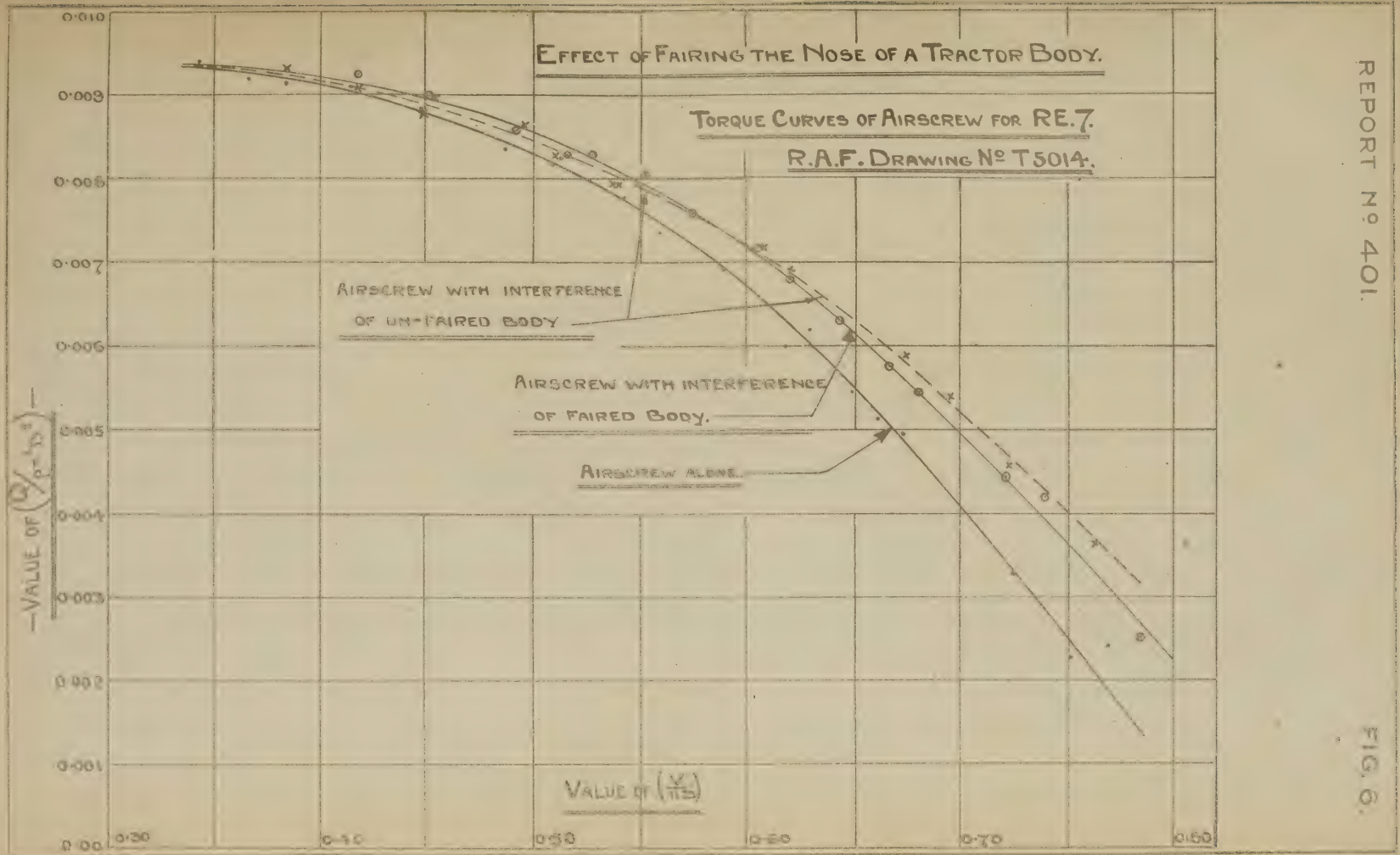

REPORT Nº 401.

FIG. 6.

Effect of Fairing the Nose of a Tractor Body.
Efficiency Curves of Airscrew for R.E.7.
R.A.F. Drawing No. T5014.

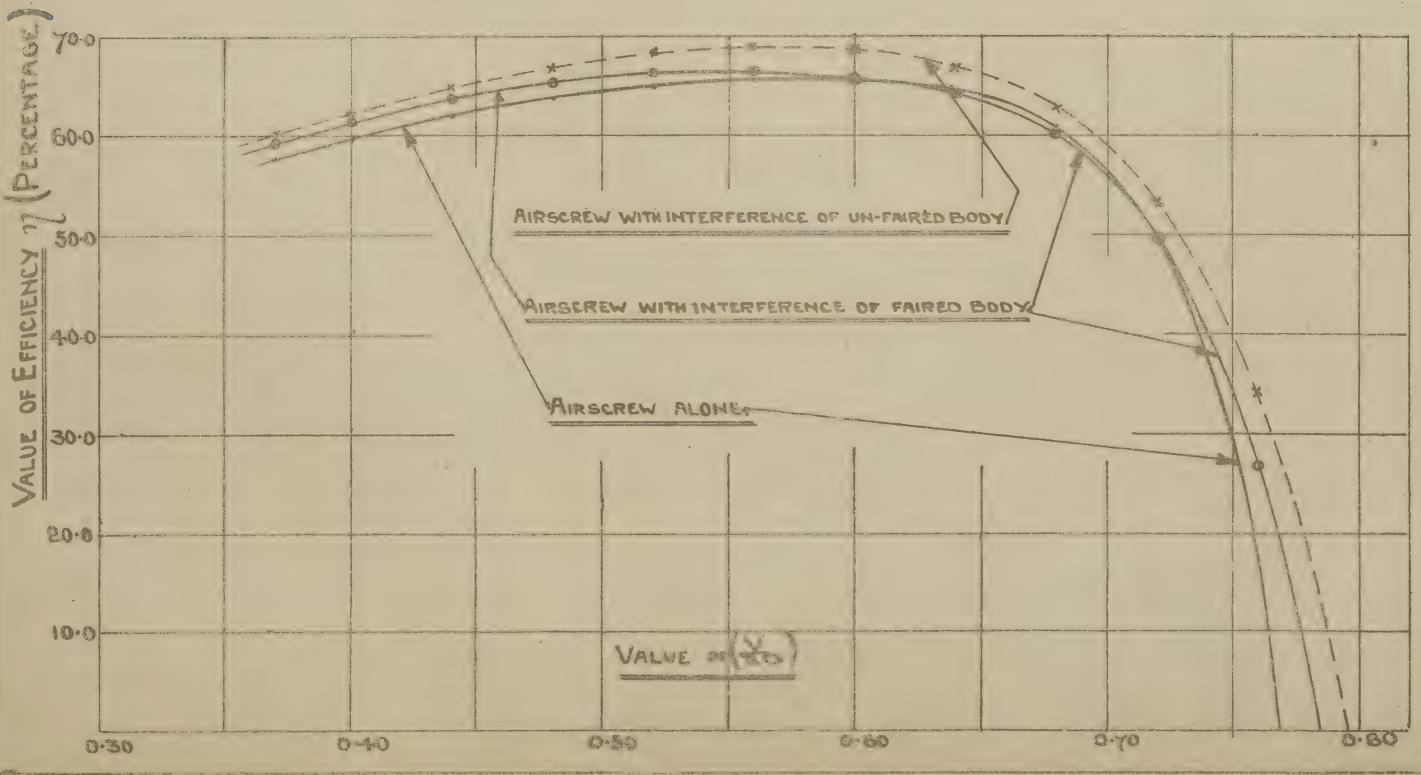

REPORT No. 401.

FIG. 7.

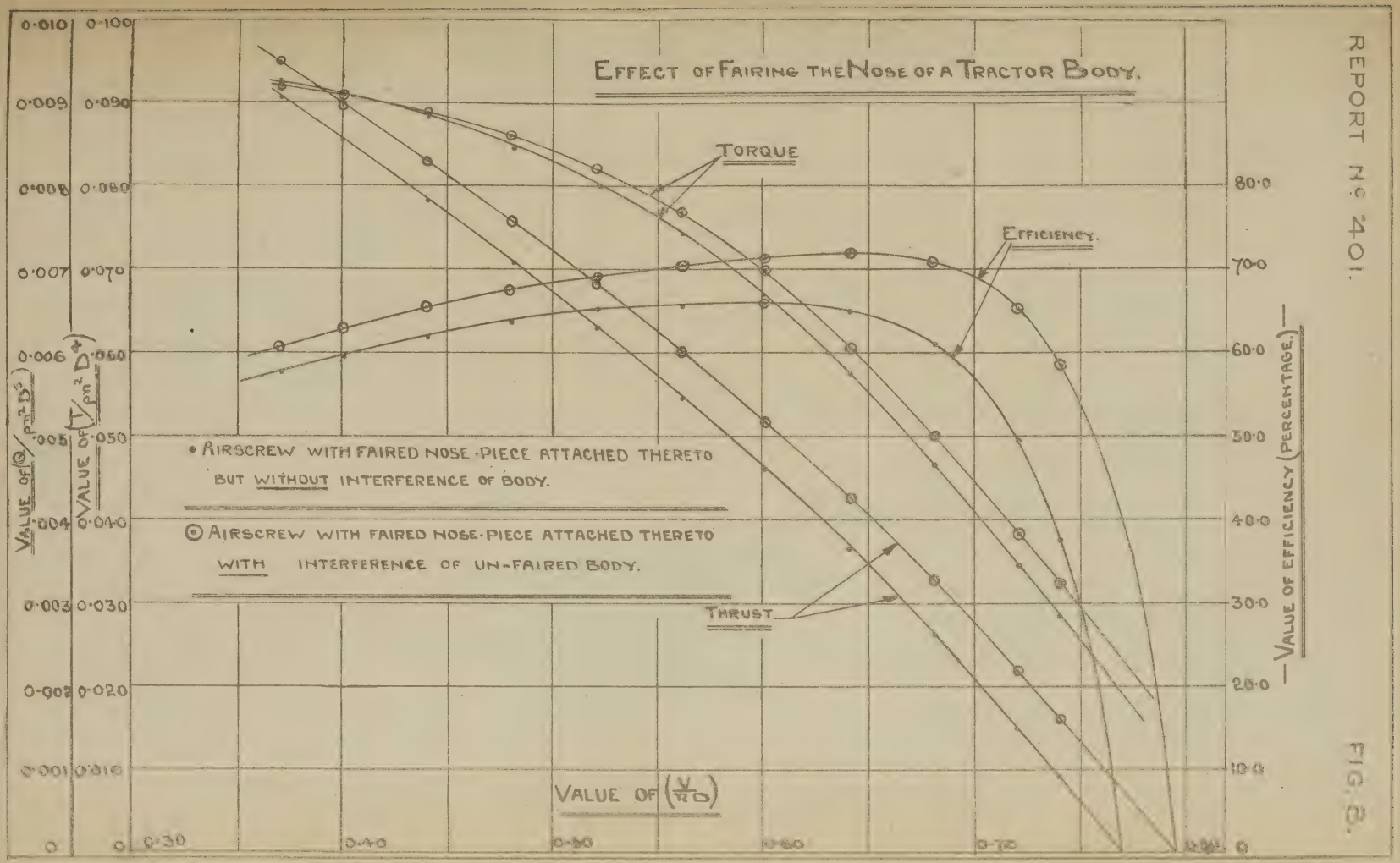
EFFECT OF FAIRING THE NOSE OF A TRACTOR BODY.
TORQUE
EFFICIENCY.
THRUST.
* AIRSCREW WITH FAIRED NOSE-PIECE ATTACHED THERETO BUT WITHOUT INTERFERENCE OF BODY.
⊙ AIRSCREW WITH FAIRED NOSE-PIECE ATTACHED THERETO WITH INTERFERENCE OF UN-FAIRED BODY.
VALUE OF $(\frac{V}{nD})$
VALUE OF $(\frac{Q}{\rho n^2 D^5})$
VALUE OF $(\frac{T}{\rho n^2 D^4})$
VALUE OF EFFICIENCY (PERCENTAGE.)
0·010 0·009 0·008 0·007 0·006 ·005 ·004 0·003 0·002 0·001 0
0·100 0·090 0·080 0·070 0·060 0·050 0·040 0·030 0·020 0·010 0
0·30 0·40 0·50 0·60 0·70 0·80
80·0 70·0 60·0 50·0 40·0 30·0 20·0 10·0 0

REPORT No 401.

FIG. 2.

EFFECT OF FAIRING THE NOSE OF A TRACTOR BODY

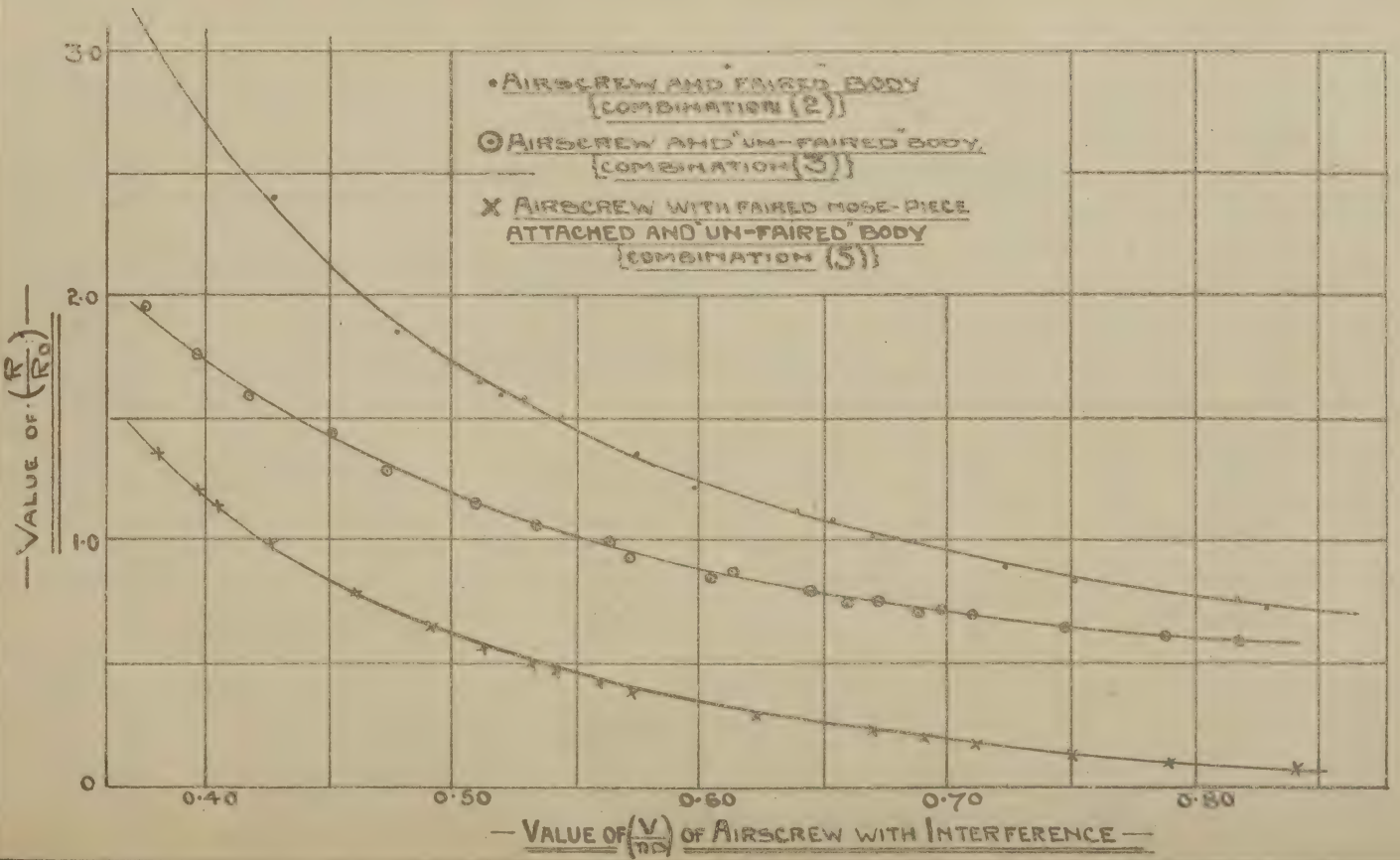

REPORT No 401.

FIG. 9.

EFFECT OF FAIRING THE NOSE OF A TRACTOR BODY

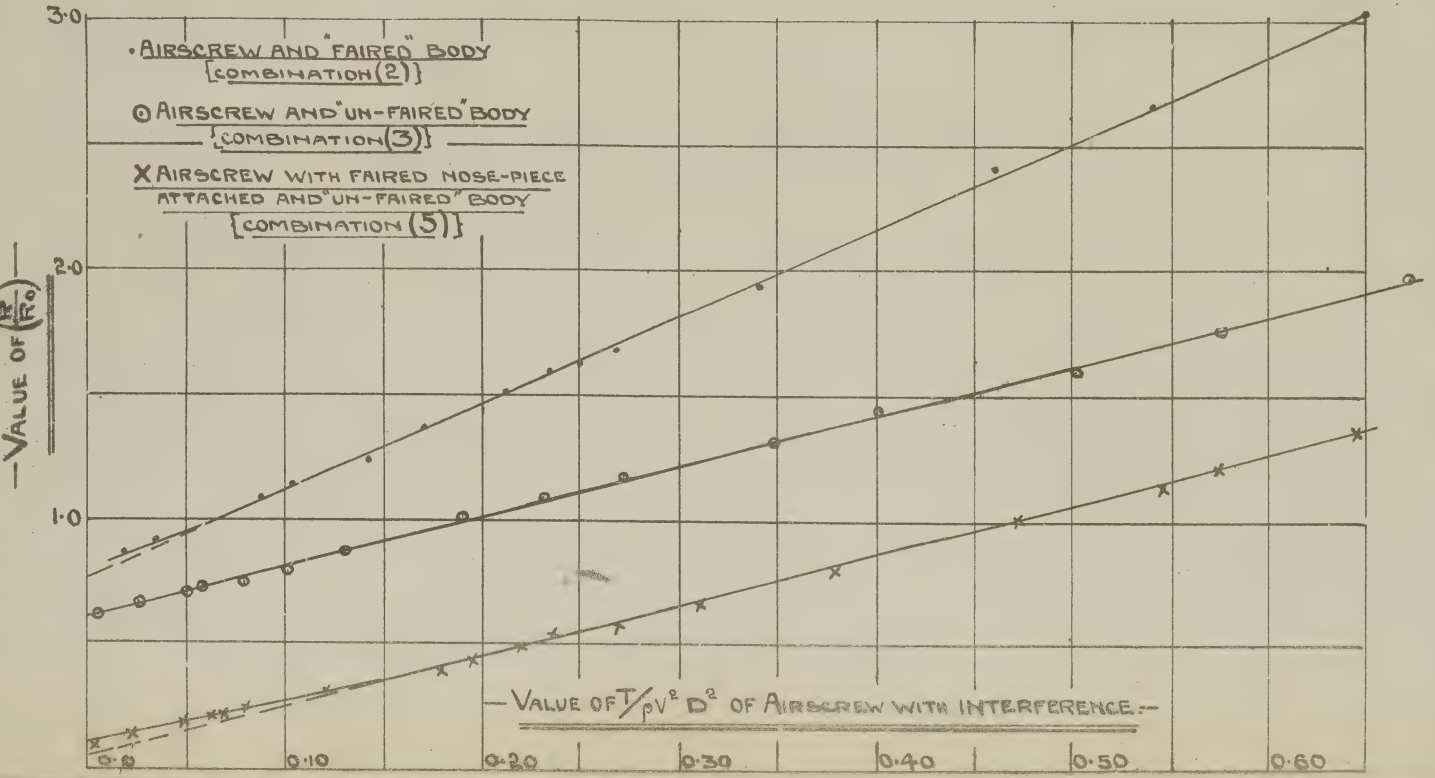

REPORT No 401.

FIG. 10.

EFFECT OF FAIRING THE NOSE OF A TRACTOR BODY.

MUTUAL INTERFERENCE OF AIRSCREW AND BODY.

COMBINATION (2).

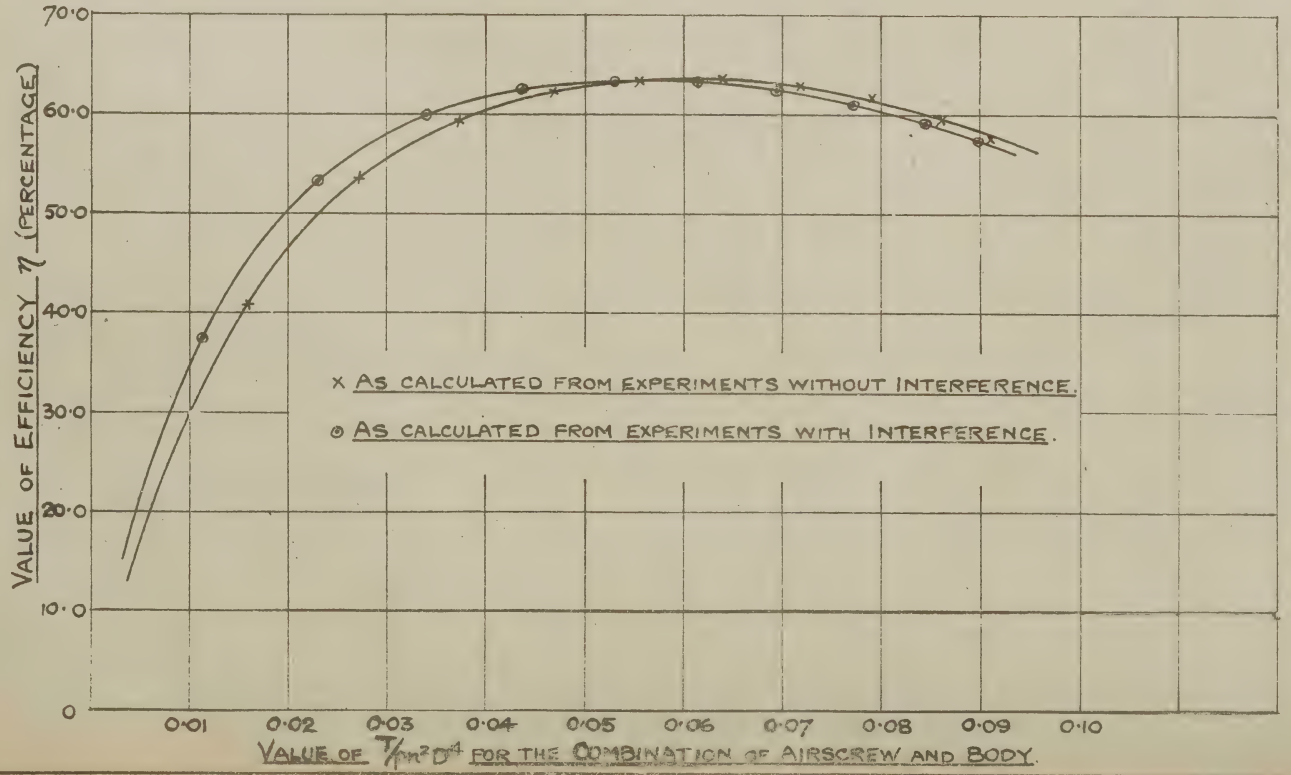

FIG. 11.

REPORT No 401.

FIG. 12.

EFFECT OF FAIRING THE NOSE OF A TRACTOR BODY.

MUTUAL INTERFERENCE OF AIRSCREW AND BODY.

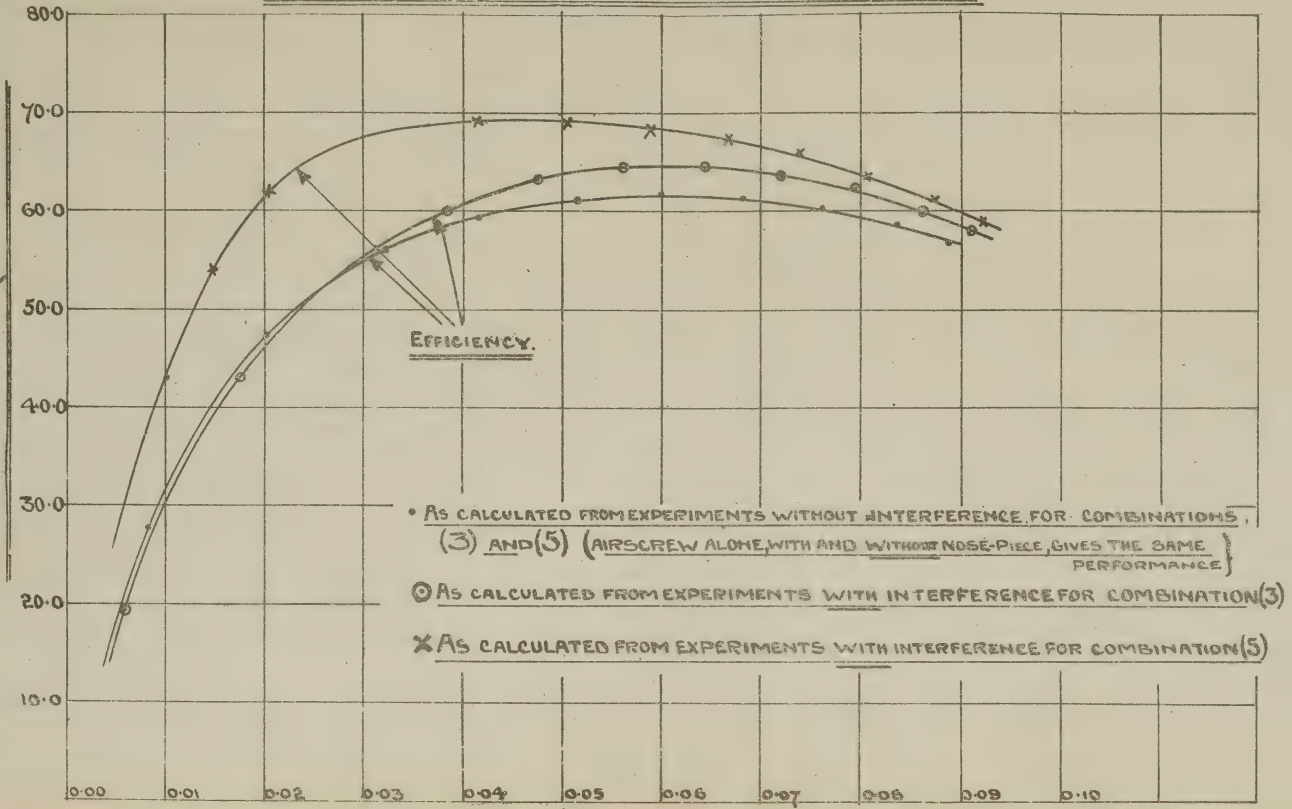

REPORT No 401.

FIG. 13.

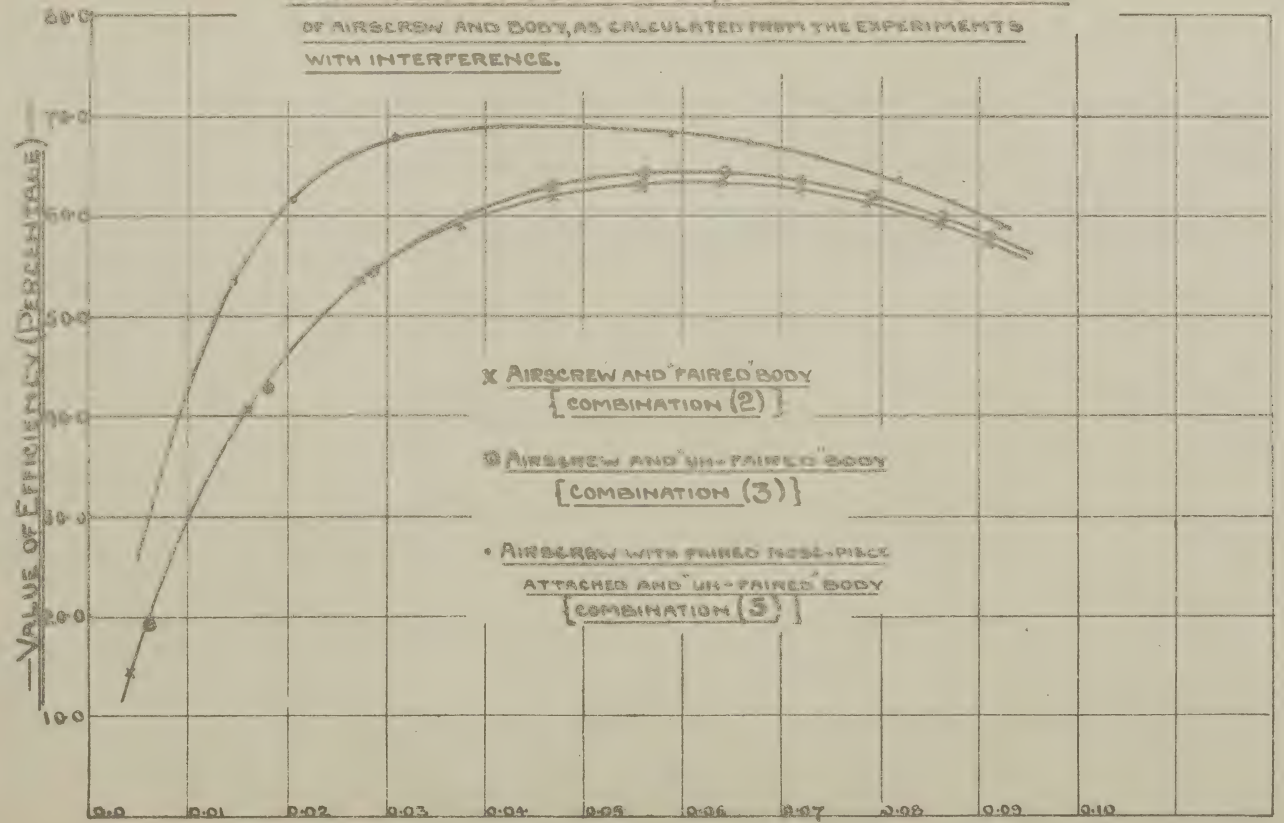

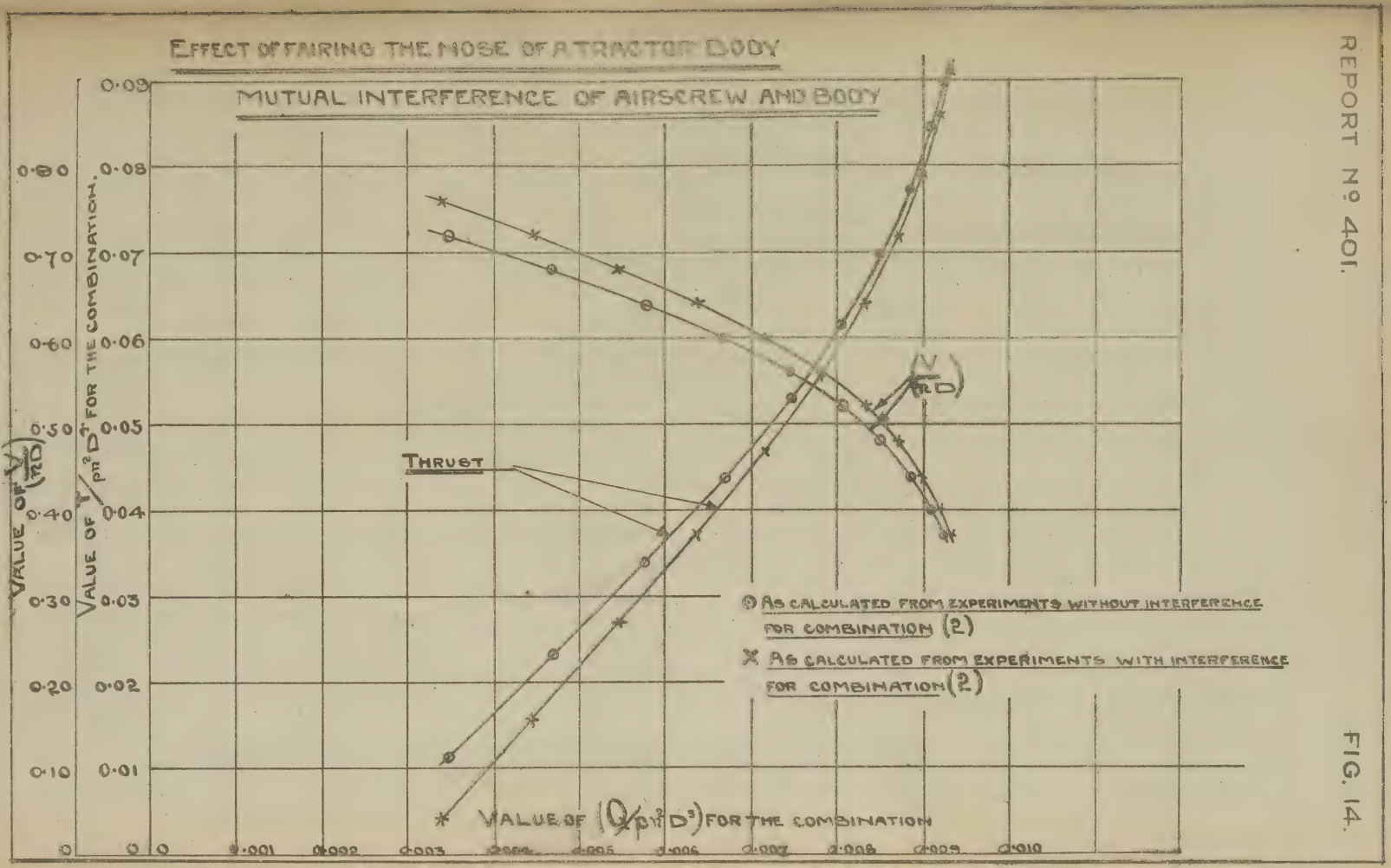
EFFECT OF FAIRING THE NOSE OF A TRACTOR BODY
MUTUAL INTERFERENCE OF AIRSCREW AND BODY
VALUE OF $\frac{V}{nD}$
VALUE OF $\frac{T}{\rho n^2 D^4}$ FOR THE COMBINATION.
THRUST
$\frac{V}{nD}$
0·80
0·70
0·60
0·50
0·40
0·30
0·20
0·10
0
0·09
0·08
0·07
0·06
0·05
0·04
0·03
0·02
0·01
0
0·001
0·002
0·003
0·004
0·005
0·006
0·007
0·008
0·009
0·010
VALUE OF $\frac{Q}{\rho n^2 D^5}$ FOR THE COMBINATION
⊙ AS CALCULATED FROM EXPERIMENTS WITHOUT INTERFERENCE FOR COMBINATION (2)
× AS CALCULATED FROM EXPERIMENTS WITH INTERFERENCE FOR COMBINATION (2)

FIG. 14.

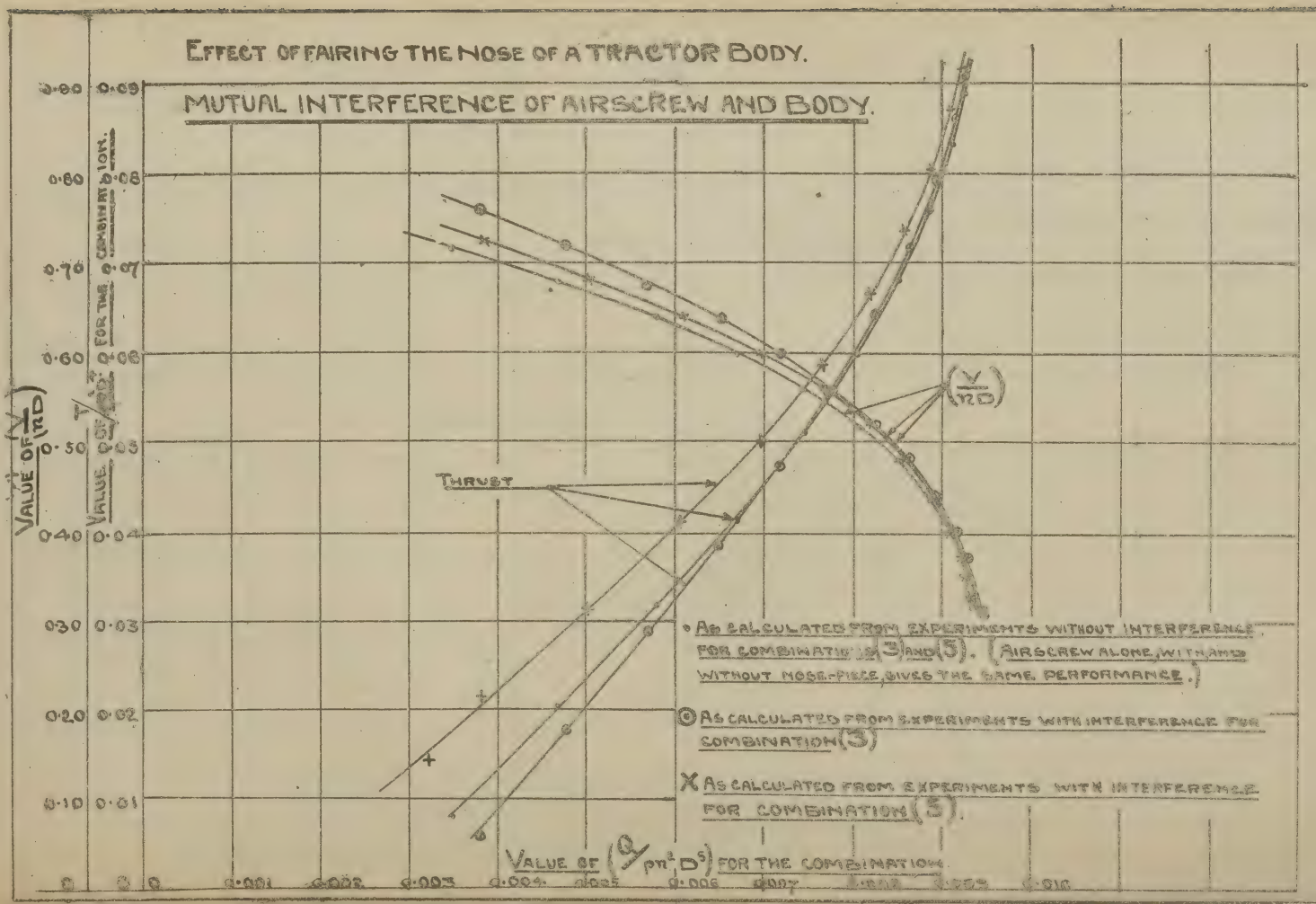
EFFECT OF FAIRING THE NOSE OF A TRACTOR BODY.
MUTUAL INTERFERENCE OF AIRSCREW AND BODY.
VALUE OF $\frac{V}{nD}$
VALUE OF $\frac{T}{\rho n^2 D^4}$ FOR THE COMBINATION
VALUE OF $\frac{Q}{\rho n^2 D^5}$ FOR THE COMBINATIONS
THRUST
$\frac{V}{nD}$
* AS CALCULATED FROM EXPERIMENTS WITHOUT INTERFERENCE FOR COMBINATIONS (3) AND (5). (AIRSCREW ALONE, WITH AND WITHOUT NOSE-PIECE, GIVES THE SAME PERFORMANCE.)
⊙ AS CALCULATED FROM EXPERIMENTS WITH INTERFERENCE FOR COMBINATION (3)
X AS CALCULATED FROM EXPERIMENTS WITH INTERFERENCE FOR COMBINATION (5).

FIG. 15.

Table 7.

A Comparison of the Efficiency of the Combination of the Airscrew and Body as Calculated from Experiments involving Mutual Interference with that Calculated from Experiments without Interference for the following Combinations (see Fig. 4) :—

(2) Airscrew and "faired" body.

(3) Airscrew and "unfaired" body.

(5) Airscrew with faired nose-piece attached and "unfaired" body.

With Mutual Interference.

Value of $\frac{V}{nD}$	Airscrew and "faired" body. Combination (2).		Airscrew and "unfaired" body. Combination (3).		Airscrew with faired nose-piece attached and "unfaired" body. Combination (5).	
	Value of T'_c for the combination.	Value of efficiency. Percentage.	Value of T'_c for the combination.	Value of efficiency. Percentage.	Value of T'_c for the combination.	Value of efficiency. Percentage.
0·37	0·0909	57·3	0·0911	58·0	0·0922	58·9
0·40	0·0859	59·4	0·0862	60·0	0·0873	61·2
0·44	0·0790	61·5	0·0793	62·1	0·0807	63·7
0·48	0·0717	62·7	0·0718	63·5	0·0739	65·8
0·52	0·0639	63·3	0·0642	64·5	0·0666	67·3
0·56	0·0555	63·2	0·0560	64·3	0·0587	68·0
0·60	0·0467	62·0	0·0475	63·0	0·0502	68·8
0·64	0·0372	59·4	0·0384	60·6	0·0411	69·0
0·68	0·0270	53·6	0·0286	54·3	0·0315	67·8
0·72	0·0159	40·9	0·0177	42·6	0·0216	61·9

Without Interference.

0·37	0·0896	57·2	0·0888	56·6	0·0888	56·6
0·40	0·0844	59·0	0·0835	58·6	0·0835	58·6
0·44	0·0711	60·9	0·0760	60·1	0·0760	60·1
0·48	0·0695	62·5	0·0682	61·3	0·0682	61·3
0·52	0·0614	63·1	0·0599	61·5	0·0599	61·5
0·56	0·0528	63·0	0·0510	60·8	0·0510	60·8
0·60	0·0436	62·2	0·0415	59·2	0·0415	59·2
0·64	0·0339	59·9	0·0316	55·8	0·0316	55·8
0·68	0·0230	53·3	0·0203	47·1	0·0203	47·1
0·72	0·0113	37·3	0·0083	27·4	0·0083	27·4

WINDAGE EXPERIMENTS WITH A MODEL OF THE ROTARY ENGINE B.R. 1.

By A. Fage, A.R.C.Sc., and H. E. Collins.

Reports and Memoranda, No. 448. *May,* 1918.

Summary.—(a) *Introductory.* (*Reasons for inquiry.*)—The present experiments were made at the request of the Technical Department of the Air Ministry to obtain data from which to calculate the windage losses in flight of the B.R. 1 engine mounted on the Sopwith " Camel."

The dependence of the windage horsepower on the area of the circular opening at the front of the cowling at the ordinary conditions of flight was also investigated.

Finally, the model engine was tested under conditions similar to those of the test-bed experiments at the Royal Aircraft Establishment.

(b) *Range of investigation.*—The experiments were made in No. 1 7-ft. channel, the scale of the models—engine, cowling, airscrew, and body—being one-third. The method of measuring the windage torque is given in detail in Report T. 1153. Experiments were made with the engine rotating (1) in a uniform wind, (2) in no wind, with and without the airscrew rotating, (3) in a uniform wind, with and without the airscrew rotating. In all three cases the windages were measured both with and without cowling, with the engine mounted in front of the body. The variation of the windage torque with the area of the circular opening at the front of the cowling was investigated over the working range of (V/n) where " V " is the forward speed of the machine and " n " the rotational speed of the engine or airscrew. Finally, experiments were made with the engine model under conditions similar to those of the test-bed experiments at the Royal Aircraft Establishment.

(c) *Conclusions.*—It was found that the cowling reduces the windage torque of the engine, both with and without the airscrew rotating, the windage with the cowling being about 67 per cent. of the value without the cowling. At any forward speed the windage of the engine, both with and without the cowling, is reduced when the airscrew is mounted on the engine shaft. The windage losses when climbing and for maximum horizontal flight speed of the machine are 15·4 H.P. and 24·5 H.P. respectively at ground level, and are greater by about 12 per cent. and 37·5 per cent. than the values calculated from experiments in which the forward speed is zero.

The interference of the wings on the windage torque of the engine is practically negligible. Small changes of the circumferential shape of the cowling affects only slightly the windage torque. If the translational and the rotational speeds are constant, the windage losses increase fairly rapidly with the area of the circular opening at the front of the cowling up to a diameter of about 16 ins., above which the losses are not greatly affected by the area of this opening. By a suitable adjustment of the area of the circular opening it is possible to maintain the windage losses—and also the cooling—constant at all flying speeds. The windage losses, forward speed being zero, are reduced about 50 per cent. by closing the openings at the circumference and at the back of the cowling. The interference of the testing tunnel of the R.A.F. on the windage losses is small, when the engine is tested without any wind blast.

(d) *Applications and further developments.*—Experiments of a similar nature are to be made with a model of the B.R. 2 engine mounted in front of a model of the Sopwith " Snipe."

At the present time the windage losses of a rotary engine on an aeroplane in flight are of uncertain magnitude, and accordingly the present experiments were made, at the request of the Technical Department of the Air Ministry, to measure the windage losses on a model of the B.R. 1 engine, mounted in front of a model of the Sopwith "Camel" body, when rotating under conditions similar to those of practice. An investigation was also made of the dependence of the windage horsepower on the areas of the circular opening at the front and the air ducts at the back of the cowling. Finally the model engine was tested in place in a model of the engine testing tunnel of the Royal Aircraft Establishment.

Descriptions of the models and of the method of measuring the windage torque.—Experiments were made in the No. 1 7-ft. channel on the B.R. 1 engine mounted in front of the Sopwith "Camel" body, the scale of the models being one-third full size. The engine has nine cylinders, each of bore 120 mms., an overall diameter of 42 ins., and develops 150 H.P. at 1,250 r.p.m. A photograph of the model engine, which was made at the Royal Aircraft Establishment, is given in Fig. 6. The model was made almost entirely of wood. To take the high centrifugal loading each cylinder head was made of aluminium attached by a long steel bolt passing through the centre of the cylinder to a steel ring in the crankcase. All the experiments were made with the engine mounted in front of the Sopwith "Camel" body. A sketch of the model body which has air ducts at the bottom and at the sides is given in Fig. 2. A modified form of the body with air ducts at the sides of triangular shape, as shown in Fig. 2a, was used in some of the experiments. The model body was fitted with detachable wings. A sketch of the two-bladed airscrew, Drg. No. A.D. 644, mounted on the Camel machine is given in Fig. 1. It will be seen that the airscrew has a diameter of 2,590 mms. and also that the blade angles vary from 20° at the tip to 46° 40′ at the boss. The shape of the model cowling used in the experiments is shown by the sketches of Fig. 3. A large part of the undersurface at the back of the cowling was cut away. To allow sufficient clearance between the valve rocker supports at the head of each cylinder the cowling had a slight "bulge" at the circumference. The diameter of the circular hole at the front of the model cowling was 9·65 ins., the diameter at the back where the attachment to the body was made being $11\frac{5}{16}$ ins. A second cowling of slightly different shape, of which a sketch is given in Fig. 4, was used in a preliminary experiment. Experiments were also made to find the interference effect on the windage measurements of a model of the R.A.F. engine testing tunnel. A sketch of this model which was made of tin plate is given in Fig. 5, from which it will be seen that the overall length is 25·75 ins. and the diameters at the inlet and outlet 18·33 ins. and 12 ins. respectively.

It is not proposed to give a detailed description in the present report of the method of measuring the windage torque of the engine. This method is of general applicability, and accordingly,

to facilitate future reference, a full description of the apparatus and of the method of measurement are given in a separate report, T. 1153, to which reference should be made in the present instance. It should perhaps be mentioned that the electric motor driving the model engine was completely encased in the model body, and was supported in such a manner as to allow a slight rocking motion about an axis parallel to the centre line of the channel. A spindle attached to the cradle carrying the electric motor was connected by a strut and "C" spring to the top of the channel balance, with which the measurements of the windage torque were made. The airscrew was mounted in front of the model engine on a separate shaft, which was driven independently from a second electric motor mounted on the top of the channel. The rotational speed of the airscrew was kept constant by a frequency meter working from the airscrew shaft.

Experiments were made with the engine rotating (*a*) in a uniform wind, (*b*) in no wind with and without the airscrew, (*c*) in a uniform wind with the airscrew rotating, the values of (V/n) being similar to those of flight, where "V" is the forward speed of the machine and "n" the rotational speed of the airscrew or engine. In all cases the engine was mounted in front of the body, and the experiments were made with and without the engine cowling.

The variations of the windage torque with change in the area of the openings at the front and at the back of the cowling, and in the circumferential shape, were also investigated. Finally, the interference on the windage torque of a model of the engine testing tunnel of the R.A.E.—with no wind blast—was measured. The data of the tables at the end of the report are for the full-sized engine. The windage torque, Q in lbs./ft., may be calculated directly from the coefficient $(Q/\rho n^2)$ where ρ is the mass density of the air in slugs per cubic foot, and is equal to 0·00237 at normal temperature and pressure, and n the rotational speed is expressed in revolutions per second. With the values of (V/n) of the report the forward speed V of the machine should be measured in feet per second.

Discussion of the results of the experiments.—The data calculated from the experiments made with the engine both with and without the cowling, (1) when rotating in a uniform wind without the airscrew, (2) when in a wind, rotating at the same speed but detached from the airscrew, and (3) when detached from and rotating at the same speed as the airscrew without any wind in the channel, are given in Tables 1 and 2 and shown graphically in Fig. 7.

From a comparison of the curves of Fig. 7 it will be seen that the windage torque of the engine with the cowling, both with the airscrew running and with no airscrew mounted, is about 67 per cent. of that without the cowling. Also at any forward speed of the machine there is a blocking-up effect due to the airscrew—

that is, the windage torque, both with and without the cowling is reduced when the airscrew is rotating in front of the engine. The airscrew has, however, only a small blocking-up effect when the forward speed of the machine is zero. The most important curve of Fig. 7 is perhaps No. 4, which shows how the windage torque of the engine varies with the forward speed of the aeroplane and the rotational speed of the airscrew and engine. The data of Table 5 give the windage horsepower of the engine, with and without cowling, when the machine is held stationary on the ground, when climbing and at maximum horizontal flight speed. It will be seen that the windage horsepower of the engine at ground level at maximum horizontal flight—the value of (V/n) is taken to be 8·45, that is, when V = 120 miles per hour and n = 1,250 r.p.m.—and at climbing where $(V/n) = 5{\cdot}35$ (V = 70 miles / hour and n = 1,150 r.p.m.) are 24·5 and 15·4 respectively. The windage losses at these rotational speeds, calculated from experiments in which no airscrew was mounted and in which the forward speed of the machine was zero, are 17·8 and 13·8 H.P. respectively.

It follows, then, that the windage losses of the engine at the maximum horizontal flight and at the climbing conditions of the machine are 37·5 per cent. and 12 per cent. greater than would be calculated from the ordinary test-bed experiments, with no wind blast.

The curves of Fig. 8 were plotted from the data of columns 4-7 of Tables 1 and 2, and show the variation of the windage torque $(Q/\rho n^2)$ with (V/n) with the following arrangements of cowling and models. With these experiments the airscrew was not mounted in front of the engine.

Arrangement 1.—With cowling, wings and air ducts at the rear of cowling as in practice.

Arrangement 2.—With cowling and air ducts at the rear of cowling as in practice, but no wings mounted.

Arrangement 3.—With cowling and no wings as in the previous arrangement, but with additional triangular side openings in body as shown in Fig. 2a.

Arrangement 4.—Body with triangular side openings and no wings, but with the cowling, of which a sketch is given in Fig. 4. These are the only experiments in which this cowling was used.

Comparing the windage curves of arrangements (1) and (2) it will be seen that the interference of the wings on the windage torque of the engine is practically negligible. Also the additional triangular openings at the bottom of the sides of the body reduce the windage torque on an average by 2 per cent. over the range of (V/n). Lastly, from the results of the experiments with the arrangements (3) and (4) it will be seen that the windage of the

engine in the cowling of Fig. 4 is about 3 per cent. less than with the cowling of Fig. 3 which was used in all the other experiments, and which has a slightly different shape at the circumference.

A series of experiments was made to measure the dependence of the windage losses on the area of the circular opening at the front of the cowling. The areas of the circular openings of the model were such as to correspond with diameters of 29·0 ins., 22·2 ins., 18·0 ins., 12·0 ins., 9·0 ins. and 5·7 ins. on the full-sized cowling. The openings at the back of the cowling and in the body were the same as in practice and the measurements were made with the airscrew rotating at the same speed as the engine. The results of these experiments are collected in Table 3. In Fig. 9 the values of $(Q/\rho n^2)$ are plotted against the corresponding values of (V/n). The data of Table 6, which were calculated from the curves of Fig. 9, show how the windage horsepower varies with the area of the circular opening at the front of the cowling, at the maximum horizontal flight at climbing, and at zero forward speed of the machine. The calculations were made for air density at ground level. The curves of Fig. 10 have been plotted from the data of Table 6. From Fig. 9 it will be seen that with circular openings of diameter 5·65 ins. and 9 ins. the windage torque is practically independent of the forward speed of the machine. In the latter case the opening is almost completely covered by the airscrew boss.

At constant values of V and n the windage horsepower varies appreciably with the area of the circular opening at the front of the cowling up to a diameter of about 16 ins., but with openings of greater diameter the windage horsepower tends to become constant (see Fig. 10). It would seem, then, that there is a certain area of the circular opening which admits just the volume of air which can be conveniently dealt with by the engine. The quantity of air flowing through the circular opening appears to be limited with a small diameter to the area of the opening, but with a larger diameter to the " drawing in " capacity of the engine. With the present arrangement of engine and cowling it would seem that the cooling of the engine will not be greatly increased with any increase of the diameter from about 16 ins., if it be assumed that there is a definite connection between the cooling and windage losses of a rotary engine. Assuming the present engine can be efficiently cooled when the windage losses are 14 H.P. then the areas of the circular openings at maximum horizontal flight and at climbing would need to be 62 and 200 sq. ins. respectively.

The windage of the engine was measured under conditions similar to those of the test-bed experiments at the R.A.E. The results of these experiments are given in Table 4, from which it will be seen that when $V = 0$ the windage losses are reduced 50 per cent. if the openings in the circumference and at the back of the cowling are covered in so that the only opening is the circular

hole of diameter 29 ins. at the front. With the additional interference due to the testing tunnel of the R.A.E. the windage losses are increased by about 3 per cent.

Summary of the conclusions of the investigations.—(*a*) The cowling reduces the windage torque of the engine. With the B.R. 1 engine the windage with the cowling is about 67 per cent. of the value without the cowling, both with and without the air-screw rotating.

(*b*) At any forward speed there is a blocking-up effect due to the rotating airscrew.

(*c*) At any rotational speed, the windage losses increase with an increase of the forward speed of the machine. With the engine of the present experiments the windage losses at maximum horizontal flight and at climbing are greater by about 37·5 per cent. and 12 per cent. respectively than the values calculated from experiments in which the forward speed is zero.

(*d*) The interference of the wings on the windage torque of the engine is practically negligible.

(*e*) The circumferential shape of the cowling does not greatly affect the windage torque.

(*f*) Keeping the values of the forward speed of the machine and rotational speed of engine and airscrew constant, there appears to be a certain area of the circular hole at the front of the cowling, below which the windage losses are dependent on the area of the circular opening, but above which the losses remain fairly constant, and depend on the " drawing-in " capacity of the engine.

(*g*) By varying the area of the circular opening at the front of the cowling the windage losses can be maintained constant at all speeds of flight.

(*h*) If the forward speed be zero, closing the openings at the circumference and at the back of the cowling so that the only opening is the circular hole at the front reduces the windage losses by about 50 per cent.

(*i*) The interference of the testing tunnel at the R.A.E. on the windage losses is very small when the engine is tested without any wind blast.

Table 1.

WINDAGE LOSSES ON B.R. 1 ENGINE. ENGINE MOUNTED IN FRONT OF "CAMEL" BODY.

Forward speed of machine zero ($V = 0$).
Q = Windage torque of engine in lbs./ft.
n = Rotational speed of engine in revs./sec.
ρ = Density of the air in slugs/cu. ft.
(= 0·00237 slugs per cubic foot at a temperature of 15°·6 C. and a pressure of 760 mms.)

The data of the table are for the full-size engine.

Engine alone. No cowling. No airscrew. No wings on body.		Engine without cowling. With airscrew rotating at the same speed as engine. With wings.		With cowling. With airscrew rotating at same speed as engine. Air ducts at rear of cowling as in practice. With wings on body.		With cowling. No airscrew. Air ducts at rear of cowling as in practice. With wings on body.		With cowling. No airscrew. Air ducts at rear of cowling as in practice. No wings on body.		With cowling. No airscrew. With triangular openings in place of the side air ducts at rear of cowling. No wings on body.		With a cowling of slightly different shape. (See Fig. 4.) No airscrew. With triangular openings in place of the side ducts at rear of cowling. No wings on body.	
Value of n.	Value of $Q/\rho n^2$.	Value of n.	Value of $Q/\rho n^2$.	Value of n.	Value of $Q/\rho n^2$.	Value of n.	Value of $Q/\rho n^2$.	Value of n.	Value of $Q/\rho n^2$.	Value of n.	Value of $Q/\rho n^2$.	Value of n.	Value of $Q/\rho n^2$.
16·0	104·0	15·4	98·0	18·35	68·2	22·3	72·6	11·2	71·1	11·4	69·6	23·6	64·5
18·7	102·0	12·5	99·6	16·15	69·5	13·6	73·7	14·0	69·0	16·1	69·5	22·1	64·7
19·7	103·5	9·1	101·2	15·10	69·1	15·8	71·8	16·0	70·4	17·9	69·7	20·5	64·1
22·1	101·0	—	—	12·70	69·1	19·2	73·2	17·7	72·0	19·7	69·5	18·5	65·4
23·0	102·0	—	—	8·40	67·9	20·8	73·0	19·5	71·3	21·3	69·6	19·5	64·8
23·4	103·5	—	—	—	—	22·4	71·7	21·0	70·9	22·7	69·4	—	—
Mean value = 102·5		Mean value = 99·6		Mean value = 68·7		Mean value = 72·6		Mean value = 70·9		Mean value = 69·6		Mean value = 64·7	

Table 2.

WINDAGE LOSSES ON B.R. 1 ENGINE. ENGINE MOUNTED IN FRONT OF "CAMEL" BODY.

V = Forward speed of machine in feet per second. Q = Windage torque of engine in lbs./ft.
n = Rotational speed in revolutions per second. ρ = Density of the air in slugs per cu. ft.
(= 0·00237 slugs per cubic foot at a temperature of 15°·6 C. and a pressure of 760 mms.)

The data of the table are for the full-size machine.

Engine alone. No cowling. No airscrew. No wings on body.		Engine without cowling. With airscrew rotating at same speed as engine. With wings.		With cowling. With airscrew, Drg. No. A.D. 644 rotating at same speed as engine. Air ducts at rear of cowling as in practice. With wings on body.		With cowling. No airscrew. Air ducts at rear of cowling as in practice. With wings on body.		With cowling. No airscrew. Air ducts at rear of cowling as in practice. No wings on body.		With cowling. No airscrew. With triangular openings in place of side air ducts at rear of cowling. No wings on body.		With cowling of slightly different shape. (See Fig. 4.) No airscrew. With triangular openings in place of air ducts at rear of cowling. No wings on body.	
Value of V/n	Value of $Q/\rho n^2$.	Value of V/n.	Value of $Q/\rho n^2$.	Value of V/n.	Value of $Q/\rho n^2$.	Value of V/n.	Value of $Q/\rho n^2$.	Value of V/n.	Value of $Q/\rho n^2$.	Value of V/n.	Value of $Q/\rho n^2$.	Value of V/n.	Value of $Q/\rho n^2$.
0·0	102·5	0·0	99·6	0·0	68·7	0·0	72·6	0·0	70·9	0·0	69·6	0·0	64·7
4·2	134·5	5·40	121·6	4·9	78·6	3·8	84·0	3·9	84·0	4·1	84·4	4·0	80·2
5·1	145·5	5·90	130·9	5·4	81·4	4·9	91·2	4·5	88·2	4·4	86·5	4·3	82·5
6·0	157·5	7·25	145·0	5·95	84·3	6·0	101·0	5·3	95·7	4·8	90·3	4·6	83·2
6·5	160·0	9·90	175·1	7·20	90·6	6·6	109·0	6·0	101·0	5·4	95·3	5·9	97·5
7·0	164·5	10·80	188·0	10·75	118·0	7·2	116·0	6·2	105·0	6·0	99·5	6·4	103·5
8·5	182·0	—	—	—	—	8·2	125·2	7·3	118·0	8·9	131·5	7·1	111·0
10·4	199·0	—	—	—	—	9·6	143·0	9·6	143·0	—	—	7·6	116·0
11·9	221·0	—	—	—	—	10·6	158·0	11·8	173·0	—	—	8·2	124·5
—	—	—	—	—	—	11·8	172·5	—	—	—	—	9·5	141·0
—	—	—	—	—	—	—	—	—	—	—	—	11·8	173·0

Table 3.

DEPENDENCE OF WINDAGE ON THE SIZE OF THE CIRCULAR OPENING AT THE FRONT OF THE COWLING.

Engine mounted in front of "Camel" body. Airscrew mounted in front of and rotating at the same speed as the engine. Openings at the back of the cowling the same as in the machine.

V = Forward speed of machine in feet per second. Q = Windage torque of engine in lbs./ft.
n = Rotational speed in revolutions per second. ρ = mass density of air in slugs per cubic feet.
(= 0·00237 at a temperature of 15°·6 C. and a pressure of 760 mms.)

The data of the table are for the full-sized engine.

With 29″ diameter opening.*		With 22″·2 diameter opening.		With 18″ diameter opening.		With 12″ diameter opening.		With 9″ diameter opening.		With 5″·65 diameter opening.	
Value of V/n.	Value of $Q/\rho n^2$.	Value of V/n.	Value of $Q/\rho n^2$.	Value of V/n.	Value of $Q/\rho n^2$.	Value of V/n.	Value of $Q/\rho n^2$.	Value of V/n.	Value of $Q/\rho n^2$.	Value of V/n.	Value of $Q/\rho n^2$.
0·0	68·7	0·0	69·0	0·0	69·2	0·0	62·8	0·0	55·4	0·0	51·7
4·92	78·6	5·42	76·7	4·92	74·3	5·46	63·0	5·36	56·3	5·52	53·5
5·41	81·4	5·92	77·6	5·34	75·2	5·91	63·8	5·92	56·5	8·81	53·3
5·96	84·3	7·14	82·8	5·91	77·0	7·17	65·4	7·15	56·0	9·96	53·5
7·20	90·6	9·80	93·7	7·11	80·8	9·80	70·4	9·85	56·2	—	—
10·74	118·0	10·75	99·1	8·78	87·5	10·78	73·0	10·70	57·5	—	—
—	—	—	—	10·74	93·0	—	—	—	—	—	—

* This is the diameter of the opening in the cowling as fitted in the machine.

TABLE 4.

EXPERIMENTS WITH A MODEL OF THE ENGINE TESTING TUNNEL OF THE R.A.E.

Tunnel mounted in place in front of the B.R. 1 engine.

n = rotational speed of engine in revolutions per second.

Q = windage torque of engine in lbs./ft.

ρ = mass density of air in slugs per cubic foot.

(= 0·00237 at a temperature of 15°·6 C. and a pressure of 760 mms.)

V = 0. No airscrew.

The data of the table are for the full-sized engine.

	Value of $Q/\rho n^2$.	Horsepower at ground level.	
		n = 1,150 r.p.m.	n = 1,250 r.p.m.
(*a*) Without testing tunnel. Cowling as in practice with air ducts at the rear and at the bottom of the cowling.	70·9	13·5	17·4
(*b*) Without testing tunnel. Cowling completely enclosing the engine with the exception of the opening at the front of diameter 29 ins. No hole in the periphery of the cowling and blocked up at the back.	31·5	6·0	7·8
(*c*) With testing tunnel, but otherwise as in (*b*) above.	32·5	6·2	8·0

TABLE 5.

CALCULATIONS OF WINDAGE HORSEPOWER AT GROUND LEVEL FOR VARIOUS CONDITIONS OF FLIGHT.

Engine mounted in front of " Camel " body.

	Forward speed V of machine zero.		Climbing.	Horizontal Flight.
			V = 70 miles per hour.	V = 120 miles per hour.
	n = 1,150 r.p.m.	n = 1,250 r.p.m.	n = 1,150 r.p.m. $\left(\frac{V}{n}\right)$ = 5·35.	n = 1,250 r.p.m. $\left(\frac{V}{n}\right)$ = 8·45.
Engine with no cowling. Without airscrew. No wings on body.	19·55	25·2	28·1	44·5
Engine with no cowling. With airscrew running. With wings on body.	18·95	24·4	23·4	38·8
Engine with cowling. Without airscrew. With wings on body.	13·8	17·8	18·1	31·6
Engine with cowling. With airscrew running. With wings on body.	13·1	16·9	15·4	24·5

- WINDAGE MEASUREMENTS of B.R.1 ENGINE -

Two bladed airscrew A.D. 644

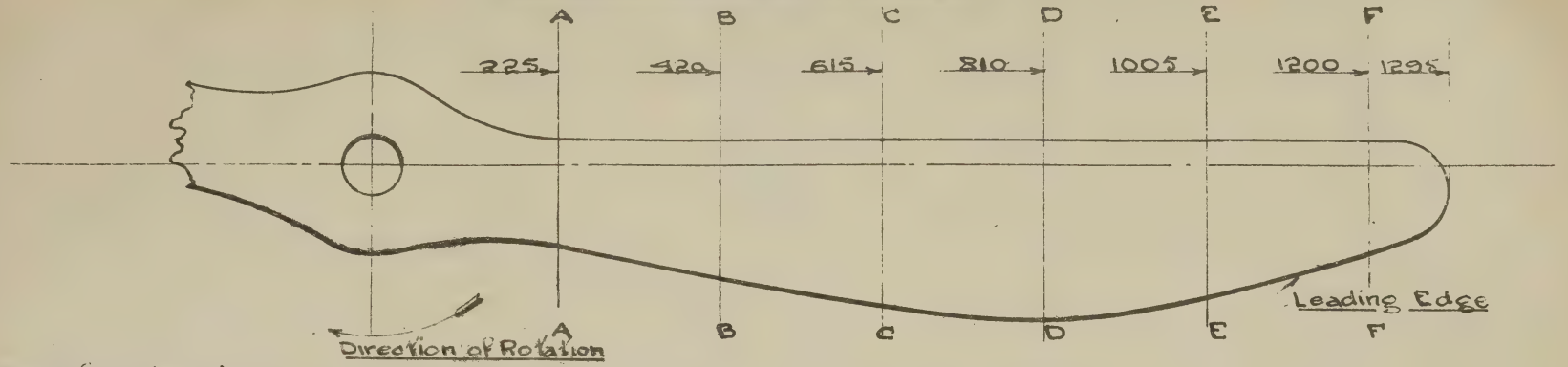

Scale for Plan View

0 60 120 240 360 420 M/M

Scale of Model 1/8 Full Size

Sections are views thus

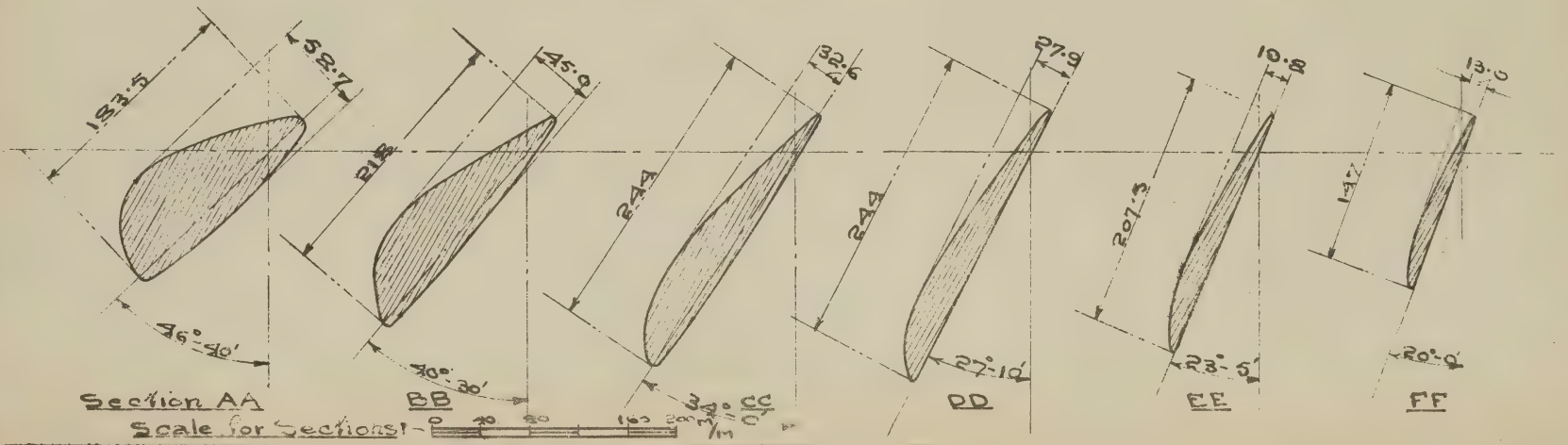

REPORT N° 448.

FIG. 1

- WINDAGE MEASUREMENTS of B.R.1. ENGINE -

Sketch of 1/3 scale model of Sopwith "Camel" Body

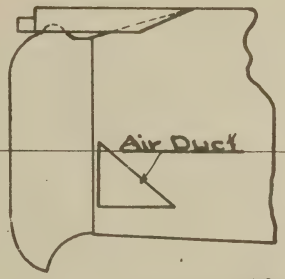

FIG 2(a)

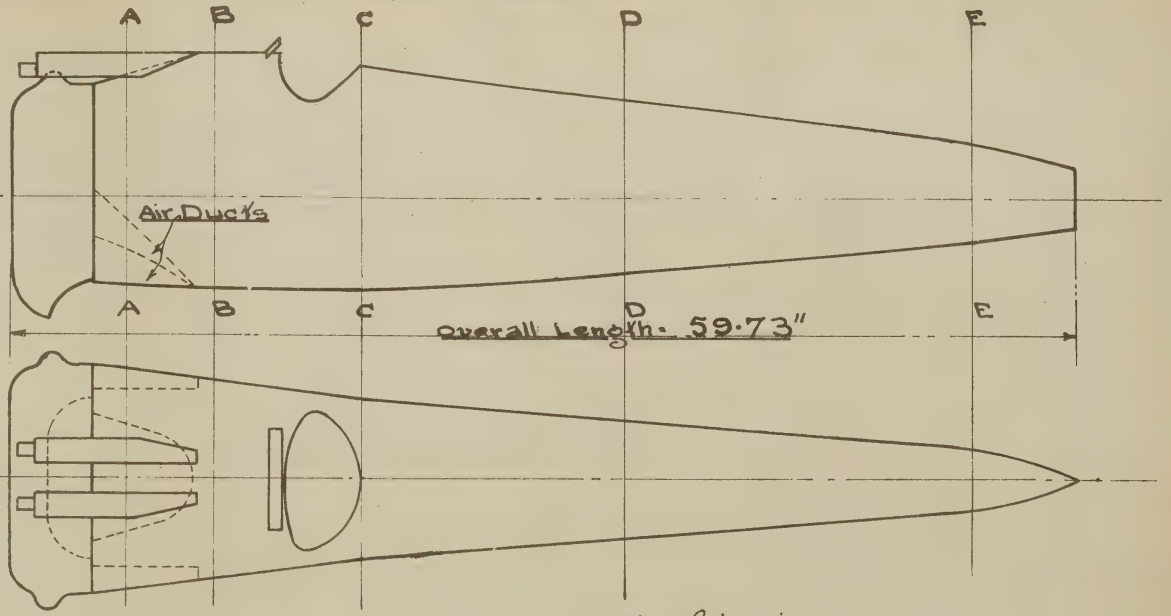

Dimensions refer to the model

Scale of drawing:-

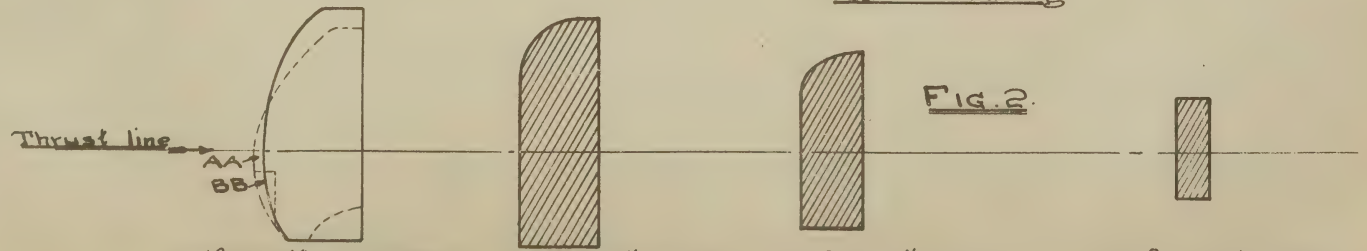

FIG. 2.

REPORT No. 448.

FIGS. 2 & 2a.

— WINDAGE MEASUREMENTS of B.R.1 ENGINE —

Sketch of a model of the cowling mounted on the Sopwith Camel.

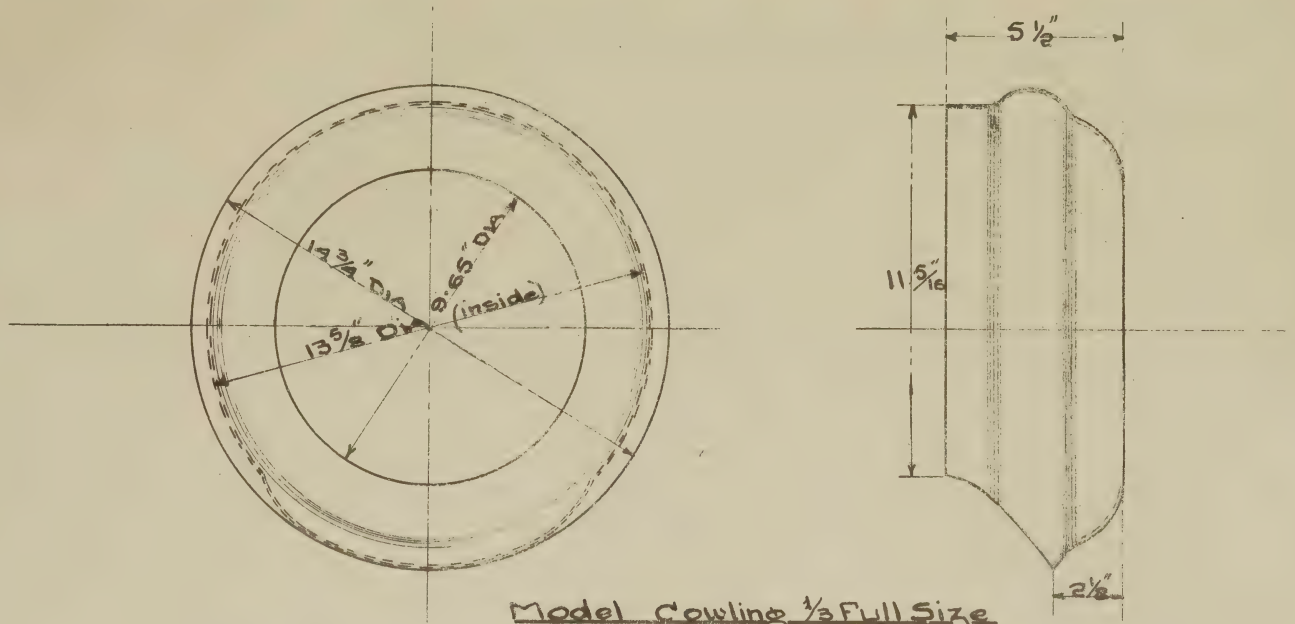

Model Cowling 1/3 Full Size

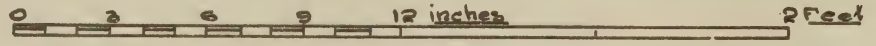

Scale for drawing:- 3" = 1 foot

REPORT No 448.

FIG. 3.

— WINDAGE MEASUREMENTS of B.R.1. ENGINE —

Sketch of model cowling used in preliminary experiments

Results of experiments with this cowling are given in the last columns of Tables 1 & 2. All other experiments made with the cowling of Fig 3.

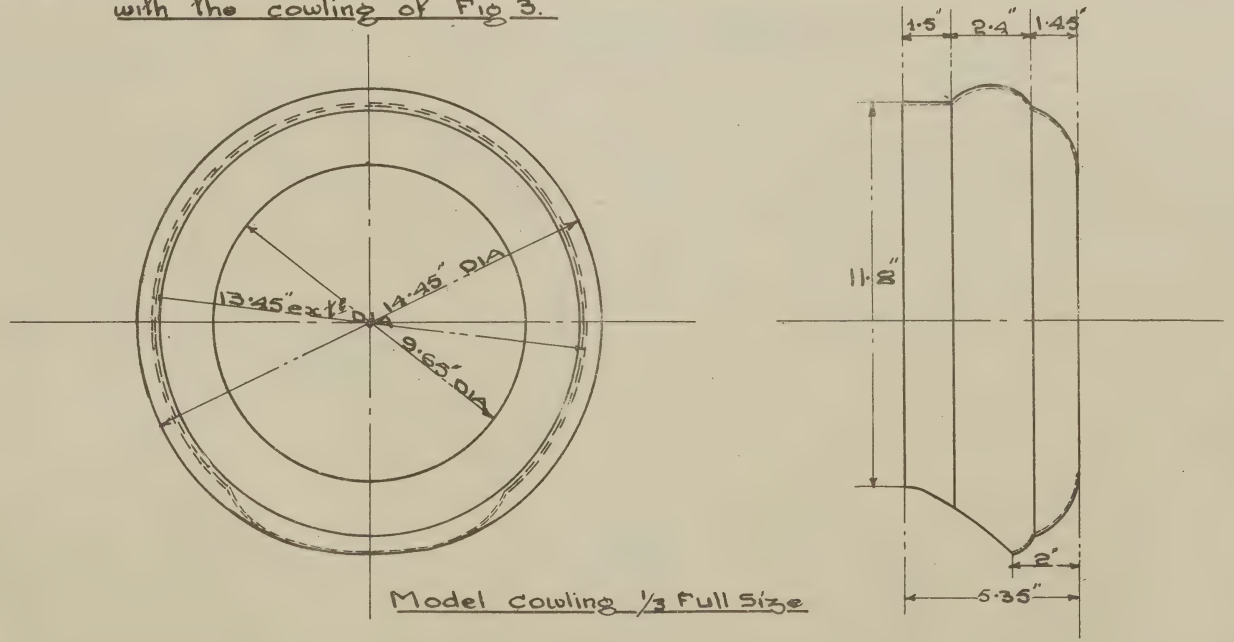

Model cowling 1/3 Full Size

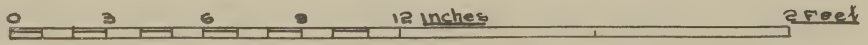

REPORT No 448.

FIG 4.

—WINDAGE MEASUREMENTS of B.R.1 ENGINE—

SKETCH of MODEL of R.A.F ENGINE TESTING TUNNEL

Scale of model = 1/3 Full Size

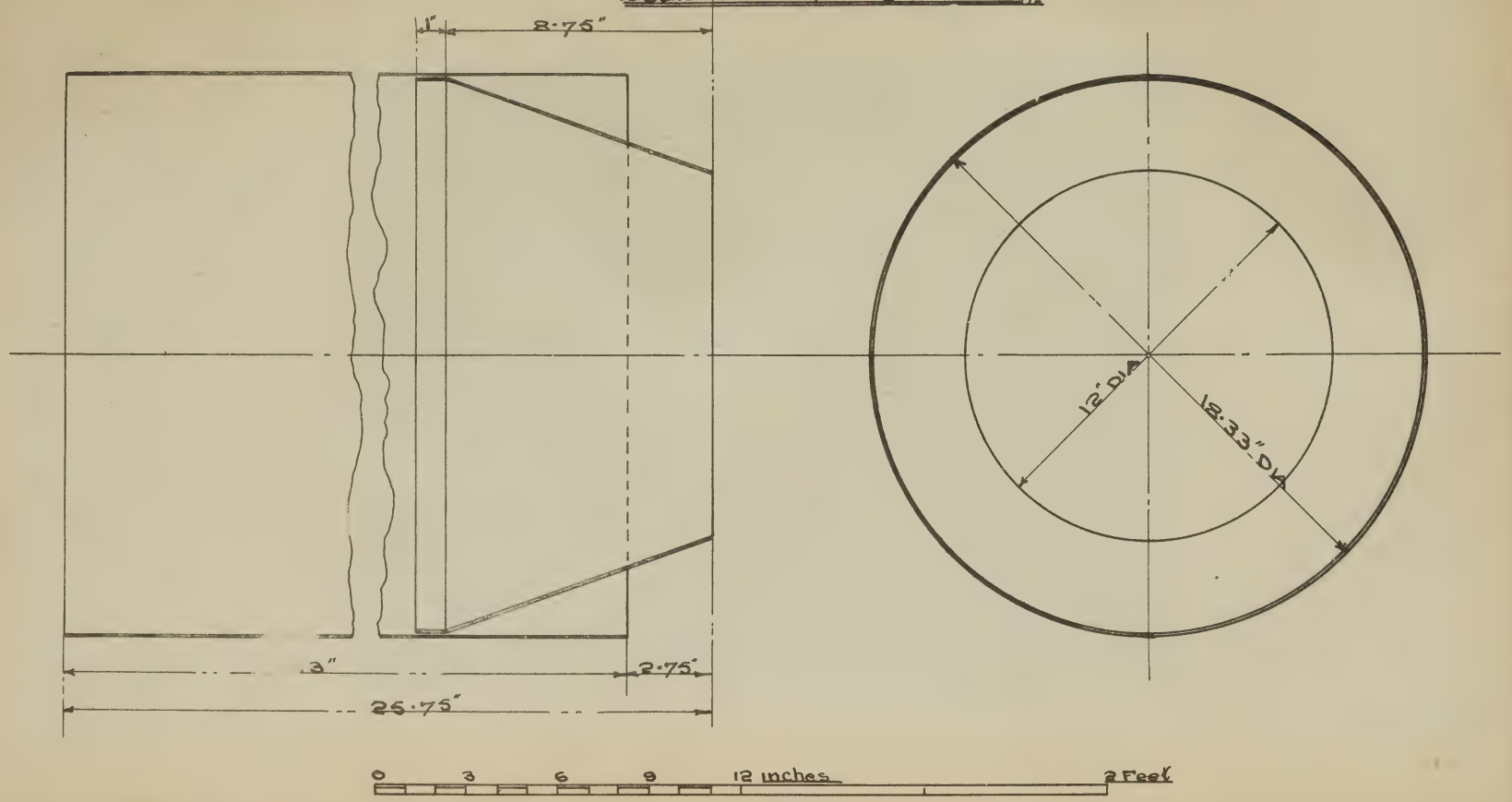

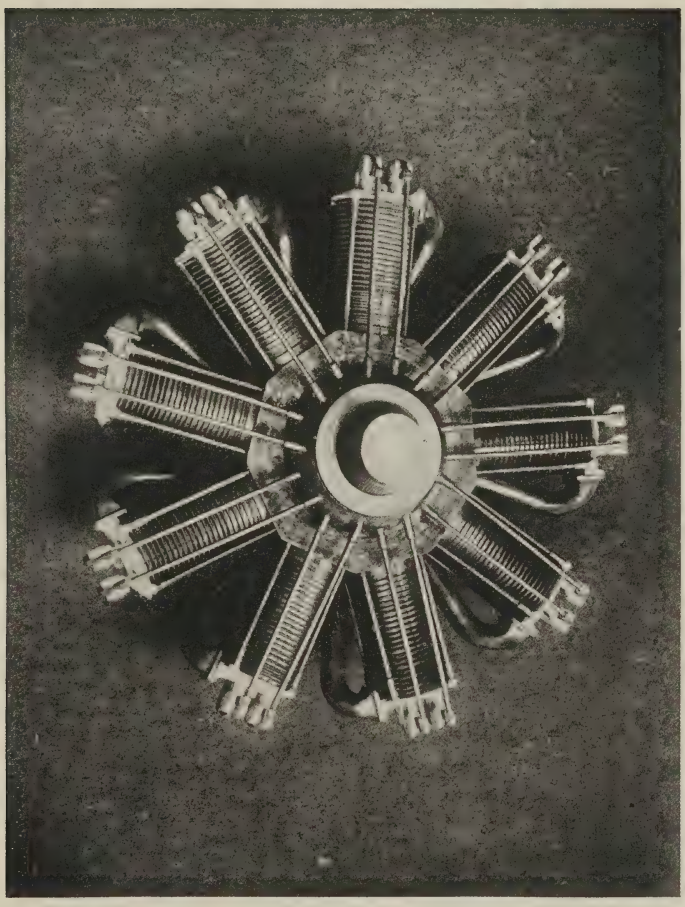

Photograph of Model BR. 1 Engine.

THE LIBRARY
OF THE
UNIVERSITY OF ILLINOIS

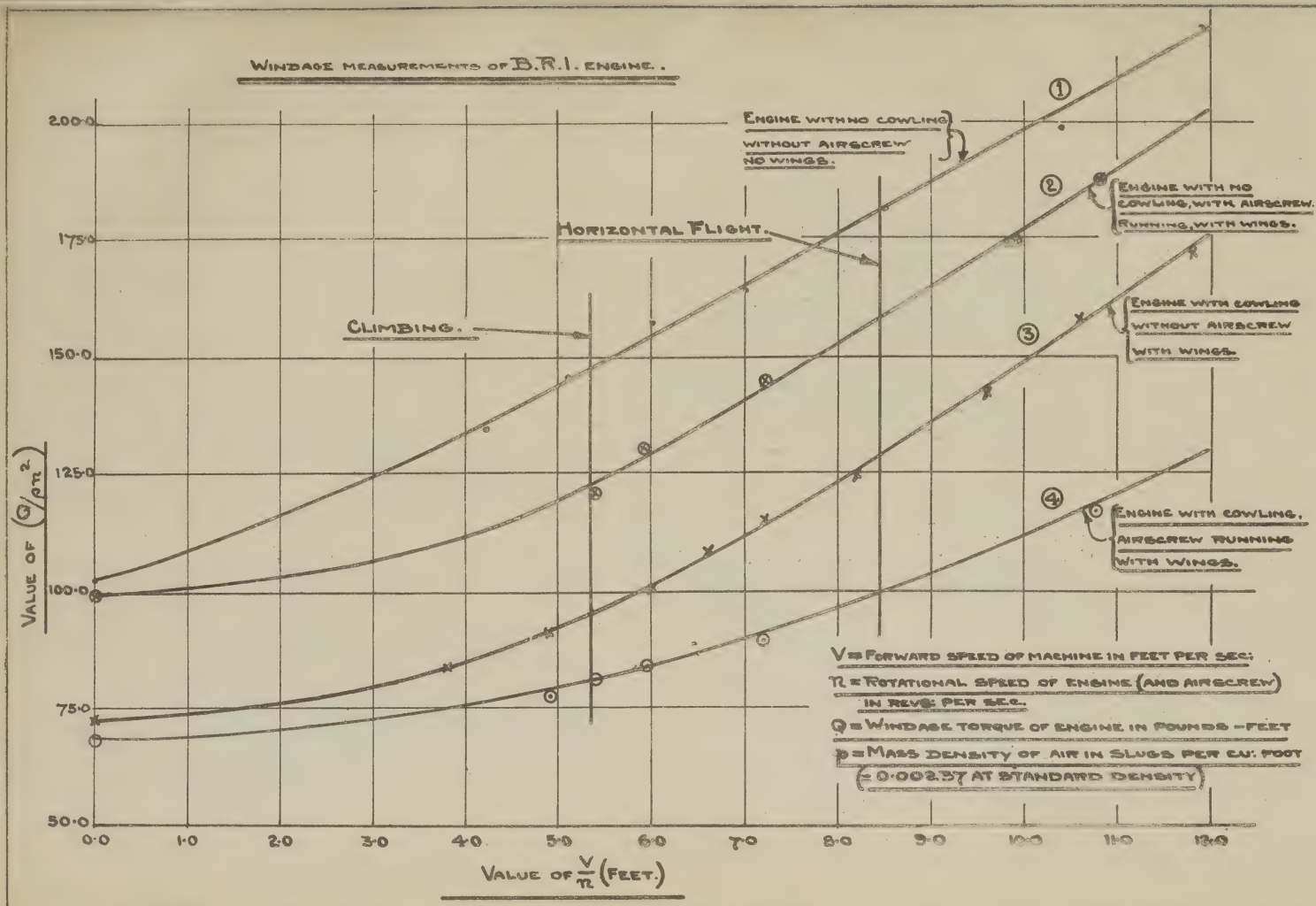
WINDAGE MEASUREMENTS OF B.R.1. ENGINE.
ENGINE WITH NO COWLING WITHOUT AIRSCREW NO WINGS.
HORIZONTAL FLIGHT.
CLIMBING.
1
2
ENGINE WITH NO COWLING, WITH AIRSCREW RUNNING, WITH WINGS.
3
ENGINE WITH COWLING WITHOUT AIRSCREW WITH WINGS.
4
ENGINE WITH COWLING, AIRSCREW RUNNING WITH WINGS.
200·0
175·0
150·0
125·0
100·0
75·0
50·0
VALUE OF (Q/ρn²)
0·0
1·0
2·0
3·0
4·0
5·0
6·0
7·0
8·0
9·0
10·0
11·0
12·0
VALUE OF V/n (FEET.)
V = FORWARD SPEED OF MACHINE IN FEET PER SEC.
n = ROTATIONAL SPEED OF ENGINE (AND AIRSCREW) IN REVS. PER SEC.
Q = WINDAGE TORQUE OF ENGINE IN POUNDS – FEET
ρ = MASS DENSITY OF AIR IN SLUGS PER CU. FOOT (= 0·002377 AT STANDARD DENSITY)

FIG 7.

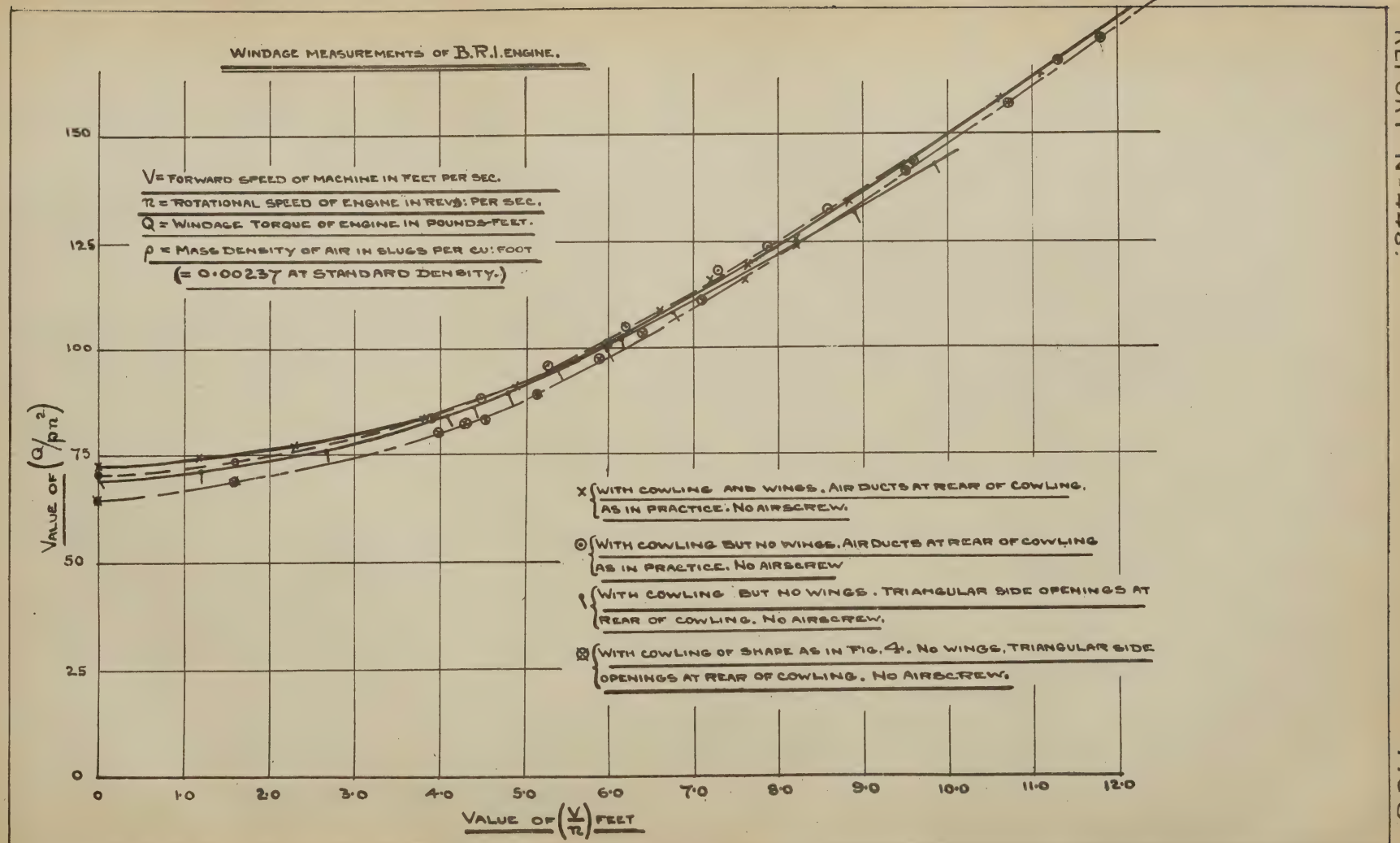
WINDAGE MEASUREMENTS OF B.R.I. ENGINE.
V = FORWARD SPEED OF MACHINE IN FEET PER SEC.
n = ROTATIONAL SPEED OF ENGINE IN REVS: PER SEC.
Q = WINDAGE TORQUE OF ENGINE IN POUNDS-FEET.
ρ = MASS DENSITY OF AIR IN SLUGS PER CU: FOOT
(= 0·00237 AT STANDARD DENSITY.)
X WITH COWLING AND WINGS. AIR DUCTS AT REAR OF COWLING. AS IN PRACTICE. NO AIRSCREW.
⊙ WITH COWLING BUT NO WINGS. AIR DUCTS AT REAR OF COWLING AS IN PRACTICE. NO AIRSCREW
WITH COWLING BUT NO WINGS. TRIANGULAR SIDE OPENINGS AT REAR OF COWLING. NO AIRSCREW.
⊠ WITH COWLING OF SHAPE AS IN FIG. 4. NO WINGS, TRIANGULAR SIDE OPENINGS AT REAR OF COWLING. NO AIRSCREW.
VALUE OF (Q/ρn²)
VALUE OF (V/n) FEET
0
2·5
50
75
100
125
150
0
1·0
2·0
3·0
4·0
5·0
6·0
7·0
8·0
9·0
10·0
11·0
12·0

FIG 8

WINDAGE MEASUREMENTS OF B.R.1. ENGINE.

DEPENDENCE OF WINDAGE ON THE SIZE OF THE CIRCULAR OPENING AT THE FRONT OF THE COWLING.

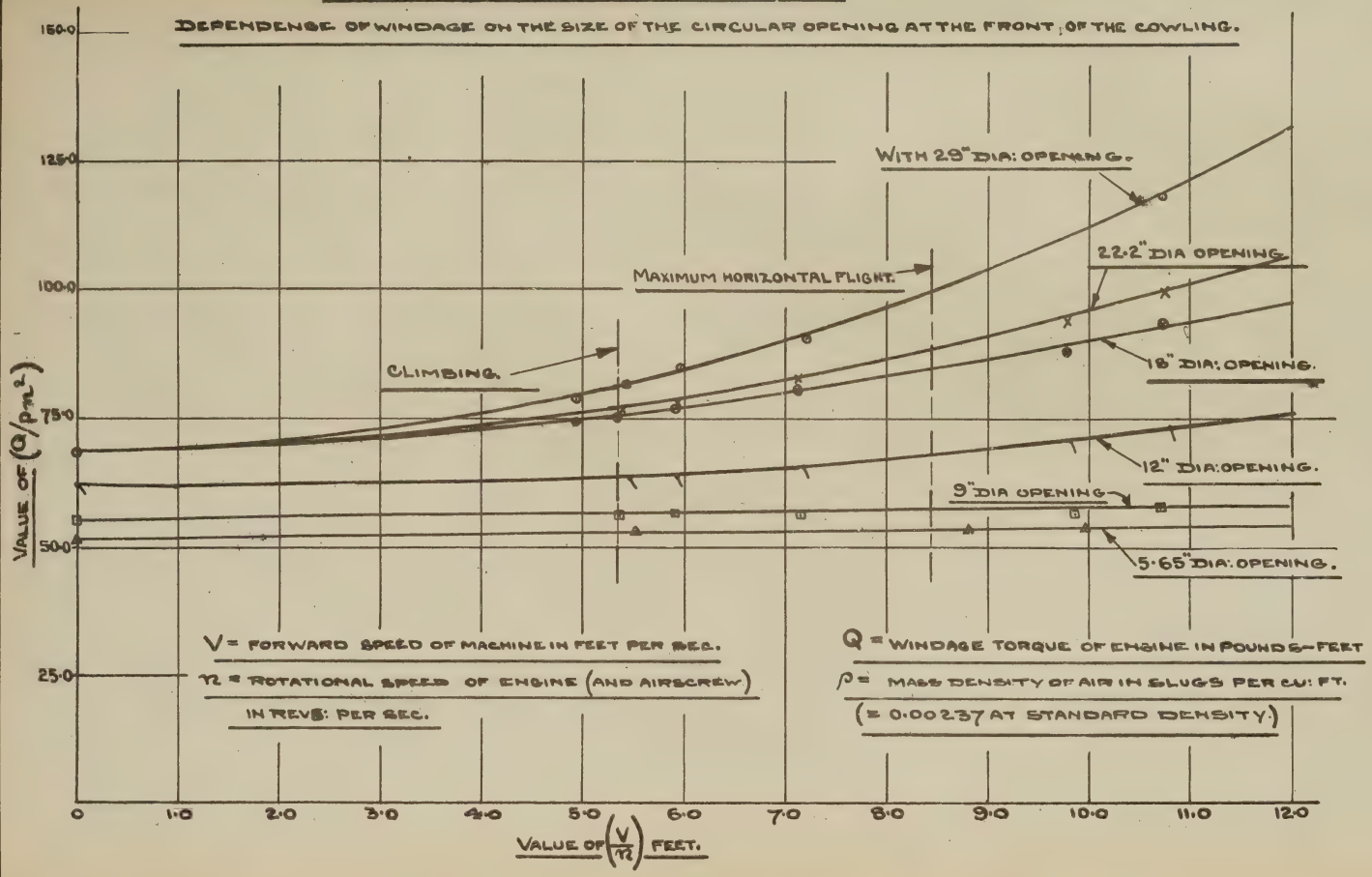

WINDAGE MEASUREMENTS OF B.R.I. ENGINE.

VARIATION OF WINDAGE HORSE-POWER WITH THE AREA OF THE CIRCULAR OPENING AT THE FRONT OF THE COWLING.

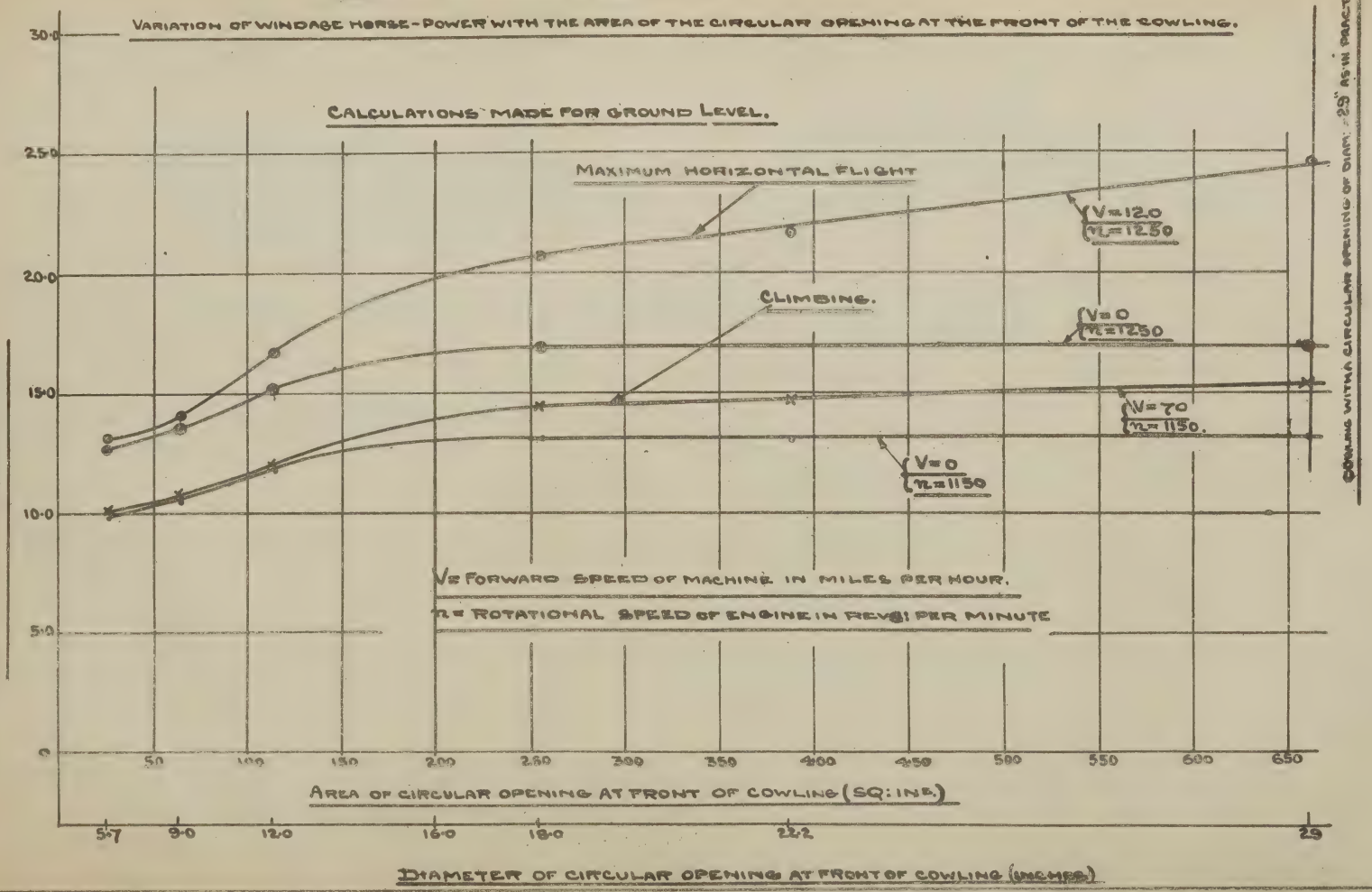

TABLE 6.

VARIATION OF THE WINDAGE HORSEPOWER WITH THE AREA OF THE CIRCULAR OPENING AT THE FRONT OF THE COWLING.

Calculations made for the full-sized engine at the ground level.

Engine mounted in front of "Camel" body.

Airscrew mounted in front of and rotating at the same speed as the engine.

Diameter of circular hole.	Area of circular hole.	Forward speed zero.		Climbing.	Maximum horizontal flight.
		Rotational speed $n = 1,150$ r.p.m.	Rotational speed $n = 1,250$ r.p.m.	Forward speed 70 m.p.h. Rotational speed = 1,150 r.p.m.	Forward speed 120 m.p.h. Rotational speed = 1,250 r.p.m.
Ins.	Sq. ins.				
29·0	660	13·1	16·9	15·4	24·5
22·2	387	13·1	16·9	14·7	21·6
18·0	255	13·1	16·9	14·4	20·7
12·0	113	11·9	15·2	12·1	16·7
9·0	63·5	10·6	13·6	10·8	14·0
5·7	25·2	9·9	12·7	10·1	13·1

DEPENDENCE OF THE EFFICIENCY OF AN AIRSCREW ON THE SPEED OF ROTATION AND THE DIAMETER, WITH A DIRECT REFERENCE TO THE QUESTION OF ENGINE GEARING.

By A. Fage, A.R.C.Sc., and H. E. Collins.

Reports and Memoranda, No. 442. *May,* 1918.

Summary.—(a) *Introductory* (*Reasons for inquiry*).—The question of the advisability of employing reduction gearing is now of some importance, in view of the development of the engine of large horse-power. From the point of view of engine design, gearing is not desired. On the other hand, the efficiency of an airscrew, driven directly from the engine, may be greatly reduced. The subject has been considered theoretically by Mr. Bairstow in Report I.C.E. 199. The present investigation—made at the request of the Technical Department of the Air Ministry—shows how the ratio of the reduction gearing modifies the design and the performance of an airscrew when mounted on an engine which was assumed to develop 300 horse-power at 1,800 r.p.m. at an altitude of 10,000 ft., the forward speed of the machine being 125 miles per hour.

(b) *Range of investigation.*—The airscrews were designed on the basis of the theory of R. & M. 328. Account is therefore taken of the velocity of the inflowing air as affecting both the pitch angle and the efficiency. Eight airscrews were designed, four of diameter 9 ft. and four of diameter 10 ft., the ratios of reduction gearing ranging from 1 to 2. The airscrews were of equal strength. The tip speed in the case of the fast running airscrew was limited to 850 ft. per second.

(c) *Conclusions.*—It was found that an airscrew mounted directly on the engine of 1,800 r.p.m. should have only two blades. With a four-bladed airscrew at this speed the blades will be long and narrow and working at a small angle of incidence. On the other hand, even with a four-bladed airscrew, the blades will be wide and will be working at a large angle of incidence if the rotational speed be lower than 900 r.p.m. The larger the diameter of the airscrew, the smaller the reduction of the efficiency due to the velocity of the inflowing air. For purposes of comparison, the ordinary performance curves of the airscrews may be misleading. Accordingly, the performances of the several combinations of engine and airscrew were compared. It was assumed that the torque of the engine had a constant value over the working range of the rotational speed and that the engine developed 300 horse-power at 1,800 r.p.m. Also that the efficiency of the reduction gearing was 97 per cent. It was found that at forward speeds of 125 m.p.h. and 75 m.p.h. the thrusts of the best geared airscrew were 10 lbs. and 22 lbs. greater than those of the ungeared airscrew. Applying these results to the calculation of the performance of a machine, it was found that if the weight of the gearing, &c., be taken as 50 lbs. and the efficiency of gearing 97 per cent., the climb at 75 m.p.h. will be 2 per cent. faster with the geared engine, the performances at the maximum horizontal flight speed of 125 m.p.h. being equal. It would seem, then, that reduction gearing is not necessary with this particular engine if the maximum diameter be limited to 10 ft.

(*d*) *Application and further developmenis.*—It is considered that a more important investigation, which anticipates the future development of both engine and aeroplane, would be the case of the large bombing machine, in which each engine is assumed to develop 600 h.p. at 1,600 r.p.m. at an altitude of 10,000 ft., the speed of the machine being 100 m.p.h. This case is under investigation.

With the development of the engine of large horse-power the question of engine gearing, as affecting the overall performance of an aeroplane, is of some importance. The subject has been considered theoretically by Mr. Bairstow in Report I.C.E. 199, in which it is shown how the efficiency of an airscrew depends on the speed of the aeroplane, on the revolutional speed of the airscrew, and on the horse-power of the engine. The present investigation, which is of a somewhat limited character, shows how the ratio of the reduction gearing modifies the design and the performance of an airscrew when mounted on an engine which was assumed to develop 300 h.p. at 1,800 r.p.m. at an altitude of 10,000 ft., the forward speed of the machine—of the scout class—being 125 miles per hour. A second particular case, which probably anticipates somewhat the future development of both engine and aeroplane, is now under consideration at the National Physical Laboratory, namely, that of the large bombing machine in which each engine is assumed to develop 600 h.p. at 1,600 r.p.m. at an altitude of 10,000 ft., the speed of the machine being 100 miles per hour. The latter investigation is probably the more important, but in view of the fact that the subject of engine gearing is now under immediate consideration, it is thought not desirable to withhold the first part of the investigation until the completion of the second.

The method of airscrew design.—The airscrews were designed on the basis of the theory of R. & M. 328, in which an attempt is made to bring the aerofoil and momentum theories into close agreement. Account is therefore taken of the velocity of the inflowing air—which is directly due to the working of the airscrew. This inflowing velocity modifies both the pitch angle and the efficiency of the airscrew and is therefore of importance in the design. In view of the large number of variables involved when designing an airscrew, the final characteristics will depend, more or less, on the experience and bias of the designer. When, however, each airscrew of a series is designed to absorb the same horse-power at the same forward speed the " personal " factor, if consistent, is negligible, in so far as comparative results are concerned. In order that the present report may not be overburdened, the details of each design are not given. It should, however, be mentioned that an endeavour was made to maintain a constant standard of consistency by adjusting the variables so as to obtain the best airscrew for the given data of design. As stated previously, each airscrew absorbs 300 h.p. at an altitude of 10,000 ft. and a forward speed of 125 miles per hour, the rotational speed depending on the ratio of the reduction gearing of the engine.

The blades of each airscrew were constructed from the same two types of aerofoil shape. For any blade section the ratio of the maximum thickness to the chord or camber, denoted by σ, will depend on the diameter of the airscrew and the load grading

curve, since each airscrew was designed for equal strength. The maximum stresses were approximately 1,500 lbs. per sq. in. compressive, and 2,500 lbs. per sq. in. tensile. The corresponding ordinates of all blade sections of the same type are the same proportion of the maximum ordinate. The shapes of the two types of blade section are shown in Fig. 5, the first shape, which is used for the outer part of the blade having a flat undersurface, and the second shape of a convex undersurface is used at the boss of the airscrew.

The curves of Figs. 1-4 give the aerodynamic data for the blade sections and show how the absolute lift coefficient L_c, and the aerodynamic efficiency (L_c/D_c) vary with σ, and with the angle of incidence, α. The same aerodynamic data are therefore used in the design of each airscrew. A correction was made for the resistance of the boss of which the diameter was taken to be $\frac{1}{12}$th of that of the airscrew. In view of the absence of any experimental data it was not possible to make any correction for the effect of compressibility at the tip of a blade. The maximum tip speed has been taken at 850 ft./sec., and it is thought that at this speed the compressibility effect will probably be small. Also since the angle of incidence at the blade tip is small it is anticipated that there will not be any breakdown of the aerodynamic flow.

The efficiency of an airscrew may probably be slightly improved by lifting the tip of the blade forward relatively to the boss and so balancing the bending moment due to the thrust by an opposite bending moment due to the centrifugal force. By so doing the blade may be made thinner and of a better aerodynamic shape for the same value of the maximum stress. In the present investigation it was not thought necessary to adopt this method of improving the design, since only the comparative performances of the several airscrews are needed. There is reason to believe that the performances, as calculated in the present report—the method of R. & M. 328—approximate very closely with those which would be obtained in practice.

Discussion of the airscrew performances.—Eight airscrews were designed to be driven by the same engine—with and without gearing. They may be conveniently divided into two series.

(*a*) Airscrews S_1, S_2, S_3, and S_4, of diameter 9 ft. Airscrew S_1, which has two blades, is mounted directly on the engine. The remaining airscrews—S_2, S_3 and S_4—of this series have four blades, the ratios of the gearing reduction—that is, the ratio of rotational speeds of engine and airscrew—being $\frac{1,800}{1,800}$, $\frac{1,800}{1,400}$ and $\frac{1,800}{1,000}$ respectively.

(*b*) Four airscrews each of diameter 10 ft. The first two airscrews, S_5 and S_6, have two blades and gearing reduction ratios of $\frac{1,800}{1,600}$ and $\frac{1,800}{1,200}$ respectively. The remaining two airscrews, S_7 and S_8, have four blades and gearing reduction ratios $\frac{1,800}{1,200}$ and $\frac{1,800}{900}$ respectively.

In Table 1 are given the descriptive data and performance data of each airscrew. The relative proportions of the airscrew are shown clearly by the sketches of Fig. 5.

The performance data of airscrews S_1, S_3, S_4, S_6, S_7 and S_8 are shown graphically in Figs. 6, 7 and 8. It was found that the other two airscrews, S_2 and S_5, were, from comparison, very inefficient, and accordingly their performances are not plotted. From the data of Table 1 it can be seen that the performance of the four-bladed airscrew S_2 is very poor as compared with the two-bladed airscrew S_1 of the same diameter and rotational speed, because with this diameter and high speed of rotation a four-bladed airscrew with blades of reasonable shape can only absorb 300 h.p. when the angle of incidence of the blade is small. Airscrew S_1 may be regarded as the best airscrew of diameter 9 ft. for the *ungeared* engine. Airscrew S_4 is the best airscrew of series (*a*), although a modification of its performance will be needed when gearing is taken into consideration. Unfortunately the efficiency of airscrew S_4 falls somewhat rapidly at climbing because to absorb the given horse-power at the rotational speed of 1,000 r.p.m. the blades, even if of a wide plan form, need to be working at a large angle of incidence.

If an airscrew of the series (*b*) was mounted directly on an engine of 1,800 r.p.m. it would have a tip speed of 940 ft. per second. Accordingly all the airscrews of series (*b*) are geared, the maximum rotational speed being 1,600 r.p.m. if the upper limit of tip speed be 850 ft. per second. The two-bladed airscrew S_5 of rotational speed 1,600 r.p.m. has a poor performance, partly because of the low pitch. Hereinafter no mention will be made of this airscrew. There is not a great difference in the overall performance of the two-bladed airscrew S_6 and the four-bladed airscrew S_7 of the same rotational speed. It would seem at this rotational speed (1,200 r.p.m.) that with a diameter of 10 ft. a change should be made from two blades to four blades, since the angle of incidence of the blade of S_6 is rather too high and that of the blade of S_7 rather too low for good efficiency of working. The four-bladed airscrew S_8 of rotational speed 900 r.p.m. is the best of the second series, although there is a tendency for the efficiency to fall somewhat rapidly at the climb because of the large angle of incidence at which the blades work in order to absorb the given horse-power. For this reason it is undesirable to put more than about 300 h.p. into a four-bladed airscrew of this diameter rotating at 900 r.p.m.

The "theoretical" efficiency of each airscrew in which the modification due to the velocity of the inflowing air is ignored is given in the last column of Table 1. The discrepancy between the "theoretical" and practical values of the efficiency is sufficiently large to emphasise the need of taking into consideration the velocity of inflow.

The conclusions of the investigation in so far as the airscrews alone are concerned—it should here be noted that the airscrews were designed for a particular engine—are summarised below.

(*a*) The efficiency curves on a (V/nD) base may be somewhat misleading. A method of comparing the performances of the airscrews is given later.

(*b*) If the tip speed be limited to 850 ft. per second—this may be a rather high value—the maximum rotational speeds of airscrews of diameters 9 and 10 ft. are 1,800 r.p.m. and 1,600 r.p.m. respectively.

(*c*) The larger the diameter of the airscrew, the smaller the reduction of the efficiency due to the velocity of the inflowing air.

(*d*) An airscrew mounted directly on the engine of 1,800 r.p.m. should have only two blades. With a four-bladed airscrew the blades will be long and narrow and working at a small angle of incidence. On the other hand, even with a four-bladed airscrew, the blades will be wide, and will be working at a large angle of incidence if the rotational speed be lower than 900 r.p.m.

Comparison of the performances of the combinations of engine and airscrew.—Curves which give the relationships between the thrust, the efficiency, and the value of V/nD, whilst completely defining the performance, are not in a suitable form for a comparison of the relative merits of the airscrews when mounted on the same engine. Accordingly, it is necessary to compare the performances of the several combinations of engine and airscrew. It is assumed that the torque of the engine had a constant value—875 lbs./ft.—over the working range of the rotational speed, so that the engine is developing 300 h.p. at 1,800 r.p.m. The assumption of constancy of torque will not diminish the value of the comparison. Also the efficiency of the reduction gearing is taken as 97 per cent. The relationship between the thrust of each airscrew when driven by this engine and the forward speed of the machine has been calculated from the performance curves of Figs. 6-8. The data of these calculations are given in Table 2 and shown graphically in Fig. 9, from which a comparison of the performances may be made. It is further assumed that the reduction gearing does not alter the external shape of the machine, but only the weight, so that at the same attitude and the same forward speed the resistance will be unaffected by gearing. The effect on the performance of the machine of the extra weight due

to gearing is considered later. From Fig. 9 it will be seen that the best geared airscrew is S_8, and also that the performance of this airscrew is better over the whole of the working range of the forward speed than that of the ungeared airscrew S_1. The extra weight due to the gearing will modify the relative performances of these two airscrews when mounted on a machine. It is well to point out that whilst the above comparison is the one which is of interest to the designer it is not a comparison of the relative merits of the airscrews taken alone. The engine, although giving a constant torque, is not giving the same horse-power to the several airscrews at the same forward speed. The relationship between the horse-power of the engine and the forward speed of the machine in the cases of airscrews S_1 and S_8 are given by the curves AA and BB respectively of Fig. 10, from which it will be seen that because of the different characteristics of the two airscrews the engine is running about 1 per cent. slower at the same forward speed with airscrew S_8. A comparison between the airscrews taken alone—this is perhaps of theoretical interest only—may be made if the engine develops the same horse-power at the same forward speed of the aeroplane, adjustment if necessary being made on both rotational speed and torque. Thus, if the airscrews S_1 and S_8 are assumed to be mounted on an engine of which the relationship between the horse-power and the forward speed of the machine is given by the curve AA of Fig. 10, then the relationships between the thrust and forward speed are as shown by the two curves, CC and DD, of Fig. 11. (See also Table 3.) From these two curves a true comparison of the merits of the airscrews may be made, but for practical purposes the comparison should be between the curves of Fig. 9.

Application of the preceding to the question of engine gearing.—The desirability of engine gearing may now be considered from the standpoint of the preceding data of airscrew design. It has been shown that the best geared airscrew is S_8, and the best ungeared airscrew S_1. Performances of these two airscrews when mounted on the same engine, working all out over the working range of the forward speed, are shown by the full lines YY and XX of Fig. 9. When calculating the performance curve for airscrew S_8 the efficiency of the reduction gearing was taken as 97 per cent., but no allowance was made for the weight of the gearing. From the curves of Fig. 9 it will be seen that at a forward speed of 125 miles per hour the thrust of airscrews S_1 and S_8 are 671 lbs. and 681 lbs. respectively. Assuming this speed to be the maximum horizontal flight speed, and that the lift/drag of the machine at this attitude is 5, the weights of the machine for equal performances are 3,355 lbs. and 3,405 lbs. respectively. Hence, assuming the weight of gearing, &c., as 50 lbs.—a very low estimate—the machine driven by either S_1 or S_8 will have the same performance at the maximum horizontal flight speed of 125 miles per hour. It is now proposed to consider the case of climbing at 75 miles per hour. The thrusts of airscrews S_1 and S_8 at this speed are

854 lbs. and 876 lbs. respectively, the weights of the machines—which are equal aerodynamically—being 3,355 lbs. and 3,405 lbs. respectively. If the lift/drag of the machine be taken as 10, it can be easily shown that at the forward speed of 75 miles per hour, the rates of climbing, when driven by airscrew S_1 or S_8, will be 1,030 or 1,045 ft. per minute.

Hence, assuming the weight of the gearing, &c., to be 50 lbs., and the efficiency of the gearing 97 per cent., the machine will climb 1·5 per cent. faster when driven by the geared engine, the performances of the machine at the maximum horizontal flight being equal for both the geared and the ungeared airscrews.

It would appear, then, from the standpoint of airscrew design, that if the maximum diameter be limited to 10 ft. reduction gearing is not necessary in the case of an engine developing 300 horse-power at 1,800 r.p.m. at an altitude of 10,000 ft., the forward speed of the machine being 125 miles per hour.

Table 1.

AIRSCREWS DESIGNED FOR AN ENGINE OF 300 B.H.P. GIVING A TORQUE OF 875 LBS.-FT. AT 1,800 REVS. PER MIN. AT AN ALTITUDE OF 10,000 FT. ($\rho = 0{\cdot}001754$ SLUG/FT.^{3}), THE FORWARD SPEED OF THE MACHINE BEING 125 MILES PER HOUR.

Maximum stresses of each airscrew about 1,500 lbs./sq. in. compressive and 2,500 lbs./sq. in. tensile.

Airscrew.	Diameter of airscrew (ft.).	Number of blades.	Ratio of gearing reduction.	Descriptive data of airscrew.						Performance data of airscrew.				
				Radius r (ft.).	Chord length c (ft.).	Maximum thickness σc (ft.).	Value of σ.	Blade angle θ (degs.).	Approximate angle of incidence when V=125 m./hr. and N=revs./min.	Value of V/nD.	Value of T'_c $(T/\rho n^2 L^4)$.	Value of Q'_c $(Q/\rho n^2 D^5)$.	Efficiency η (per-centage).	Efficiency neglecting inflow velocity of air.
S_1	9	2	1,800 / 1,800						N = 1,800					
				4·22	0·545	0·0409	0·075	15·50	1·5					
				3·66	0·743	0·0772	0·105	17·50	1·5	0·679	0·0643	0·00937	73·9	79·5
				3·10	0·795	0·1190	0·150	20·25	1·5	0·602	0·0766	0·01034	70·9	81·5
				2·53	0·775	0·1510	0·195	24·05	1·5	0·511	0·0913	0·01115	66·8	78·5
				1·69	0·680	0·2045	0·300	33·40	2·0					
S_2	9	4	1,800 / 1,800						N = 1,800					
				4·22	0·308	0·0238	0·075	13·60	—0·4					
				3·66	0·594	0·0535	0·090	15·60	—0·4	0·681	0·0618	0·00938	71·5	76·9
				3·10	0·673	0·0808	0·120	18·35	—0·4	0·595	0·0840	0·01135	70·0	79·0
				2·53	0·713	0·1083	0·152	22·15	—0·4	0·490	0·1122	0·01335	65·7	81·0
				1·69	0·634	0·1520	0·240	31·50	—0·4					

TABLE 1 (*continued*).

Airscrew.	Diameter of airscrew (ft.).	Number of blades.	Ratio of gearing reduction.	Descriptive data of airscrew.						Performance data of airscrew.				
				Radius r (ft.).	Chord length c (ft.).	Maximum thickness σc (ft.).	Value of σ.	Blade angle θ (degs.).	Approximate angle of incidence when V=125 m./hr. and N=revs./min.	Value of V/nD.	Value of T'_c $(T/\rho n^2 D^4)$.	Value of Q'_c $(Q/\rho n^2 D^5)$.	Efficiency η (per-centage).	Efficiency neglecting inflow velocity of air.
									N = 1,400					
				4·22	0·575	0·0431	0·075	18·70	1·0					
			1,800	3·66	0·792	0·0712	0·090	21·25	1·0	0·870	0·1090	0·0200	75·5	81·6
S_3	9	4	———	3·10	0·808	0·0960	0·120	24·50	1·0	0·751	0·1475	0·0243	72·5	82·5
			1,400	2·53	0·783	0·1191	0·152	29·10	1·0	0·603	0·1920	0·0274	65·2	81·9
				1·69	0·692	0·1590	0·230	39·60	1·0					
									N = 1,000					
				4·22	0·567	0·0425	0·075	30·10	6·0					
			1,800	3·66	0·783	0·0705	0·090	33·25	6·0	1·215	0·2210	0·0548	78·0	84·5
S_4	9	4	———	3·10	0·800	0·0880	0·110	37·35	6·0	1·050	0·2660	0·0606	73·5	82·8
			1,000	2·53	0·775	0·1161	0·150	42·70	6·0	1·018	0·2740	0·0613	72·6	82·8
				1·69	0·685	0·1506	0·220	54·10	6·0	1·000	0·2795	0·0623	71·3	81·8
									N = 1,600					
				4·70	0·342	0·0258	0·075	15·60	1·5					
			1,800	4·10	0·642	0·0675	0·105	17·50	1·5	0·694	0·0555	0·00788	75·8	80·6
S_5	10	2	———	3·40	0·792	0·1174	0·150	20·60	1·5	0·574	0·0715	0·00925	70·5	78·8
			1,600	2·60	0·775	0·1625	0·210	25·85	1·5	0·484	0·0828	0·00970	65·7	77·6
				1·80	0·683	0·2050	0·300	36·20	1·5					

TABLE 1 (*continued*).

Airscrew.	Diameter of airscrew (ft.).	Number of blades.	Ratio of gearing reduction.	Descriptive data of airscrew.						Performance data of airscrew.				
				Radius r (ft.).	Chord length c (ft.).	Maximum thickness σc (ft.).	Value of σ.	Blade angle θ (degs.).	Approximate angle of incidence when V=125 m./hr. and N=revs./min.	Value of V/nD.	Value of T'_c $(T/\rho n^2 D^4)$.	Value of Q'_c $(Q/\rho n^2 D^5)$.	Efficiency η (per-centage).	Efficiency neglecting inflow velocity of air.
S_6	10	2							N = 1,200					
				4·70	0·542	0·0406	0·075	24·40	6·0					
			1,800	4·10	0·809	0·0725	0·090	26·85	6·0	0·916	0·1008	0·01873	79·0	84·4
			———	3·40	0·884	0·1109	0·125	30·60	6·0	0·809	0·1174	0·02045	74·0	81·3
			1,200	2·60	0·842	0·1600	0·190	35·95	5·0	0·760	0·1245	0·02100	72·0	80·5
				1·80	0·759	0·2050	0·270	45·90	5·0					
S_7	10	4							N = 1,200					
				4·70	0·388	0·0292	0·075	19·90	1·5					
			1,800	4·10	0·692	0·0588	0·085	22·35	1·5	0·918	0·0990	0·01870	77·3	82·4
			———	3·40	0·813	0·0900	0·110	26·10	1·5	0·799	0·1314	0·02230	74·9	83·3
			1,200	2·60	0·804	0·0963	0·160	32·45	1·5	0·677	0·1620	0·02540	69·7	79·0
				1·80	0·675	0·1550	0·230	42·40	1·5					
S_8	10	4							N = 900					
				4·70	0·525	0·0392	0·075	28·60	4·7					
			1,800	4·10	0·788	0·0634	0·080	31·60	4·7	1·222	0·1790	0·0442	78·7	84·0
			———	3·40	0·858	0·0941	0·110	36·05	4·7	1·076	0·2145	0·0484	76·3	84·2
			900	2·60	0·821	0·1350	0·165	43·40	4·7	0·992	0·2350	0·0507	73·0	82·5
				1·80	0·742	0·1675	0.225	53·80	4·7					

TABLE 2.

COMPARISON OF THE PERFORMANCES OF ENGINE AND AIRSCREW.

Variation of the thrust of the airscrew with the forward speed of the machine.

Torque of engine assumed constant at 875 lbs./ft.

Efficiency of reduction gearing assumed to be 79 per cent.

Altitude of machine, 10,000 ft.

Airscrew S_1. Constant torque of airscrew 875 lbs./ft.		Airscrew S_2. Constant torque of airscrew 1,090 lbs./ft.		Airscrew S_3. Constant torque of airscrew 1,527 lbs./ft.		Airscrew S_5. Constant torque of airscrew 1,271 lbs./ft.		Airscrew S_7. Constant torque of airscrew 1,271 lbs./ft.		Airscrew S_8. Constant torque of airscrew 1,696 lbs./ft.	
Forward speed of machine. Mls./hr.	Thrust of airscrew. Lbs.	Forward speed of machine. Mls./hr.	Thrust of airscrew. Lbs.	Forward speed of machine. Mls./hr.	Thrust of airscrew. Lbs.	Forward speed of machine. Mls./hr.	Thrust of airscrew. Lbs.	Forward speed of machine. Mls./hr.	Thrust of airscrew. Lbs.	Forward speed of machine. Mls./hr.	Thrust of airscrew. Lbs.
125·0	670	127·0	648	128·0	673	129·0	675	127·2	662	129·3	665
113·5	698	119·4	668	120·0	691	118·6	695	120·1	683	117·0	706
101·5	735	111·2	689	111·0	719	107·8	723	113·0	704	105·0	748
86·5	790	103·0	710	102·4	736	89·3	776	103·0	735	91·5	794
78·5	834	88·5	765	91·5	778	76·3	805	95·0	764	85·5	818
		78·6	813	83·8	808			86·0	795		
								73·2	828		

Aerodynamic Data for Sections of Type 'A' (see Fig 5)

The figures on the curves give the angle of incidence

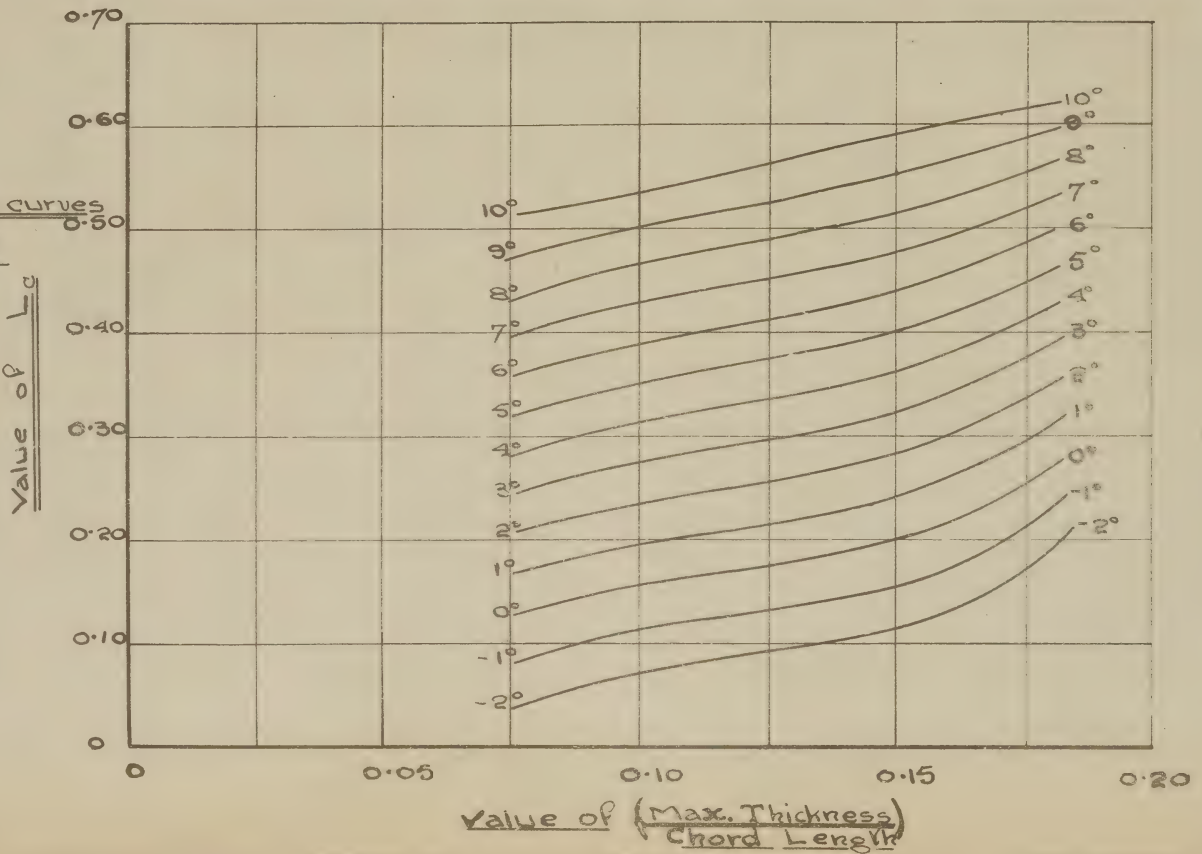

AIRSCREW EFFICIENCY and ENGINE GEARING—

Aerodynamic Data for Sections of Type 'A' (see Fig 5)

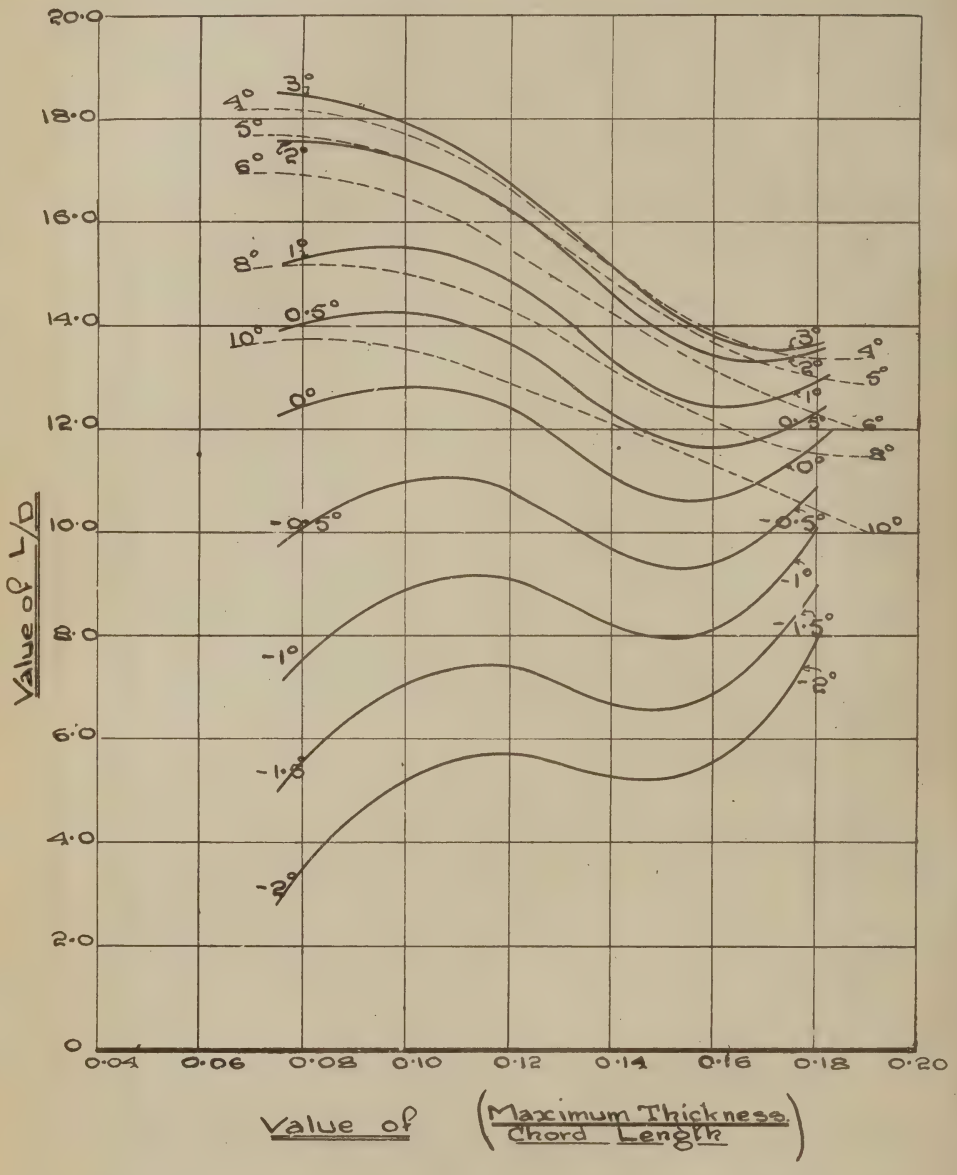

The figures on the curves give the angle of incidence

– AIRSCREW EFFICIENCY and ENGINE GEARING –

Aerodynamic Data for Sections of Type 'B' (see Fig 5)

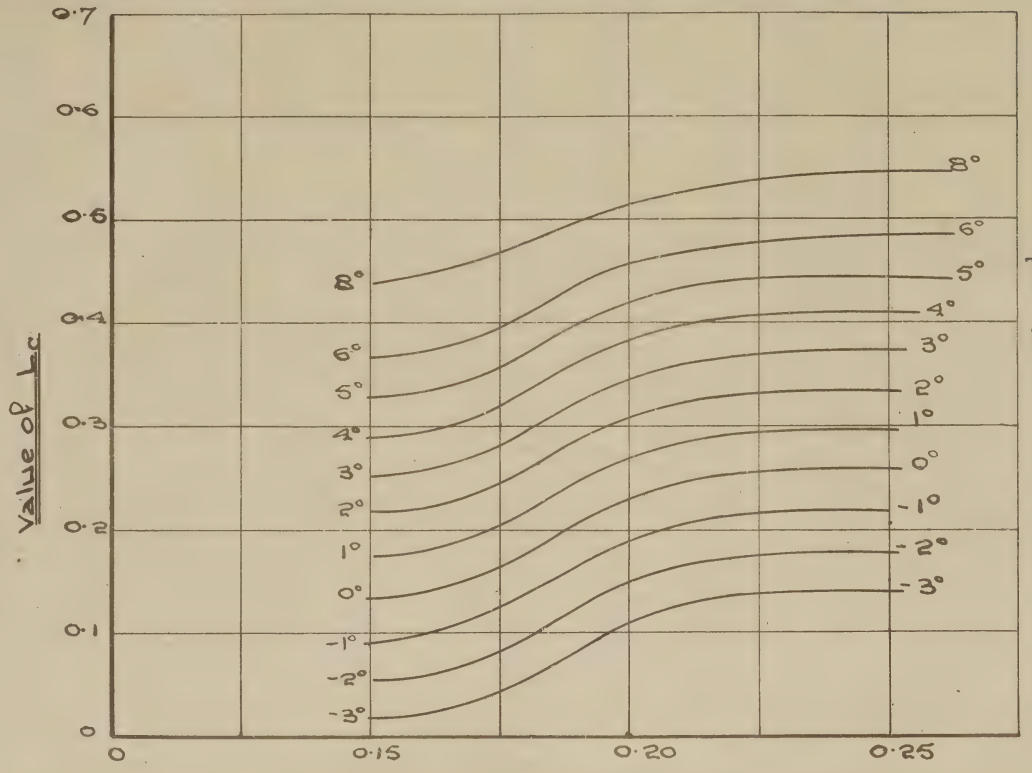

The figures on the curves give the angle of incidence.

- AIRSCREW EFFICIENCY and ENGINE GEARING -

Aerodynamic Data for Sections of Type 'B' (see Fig 5)

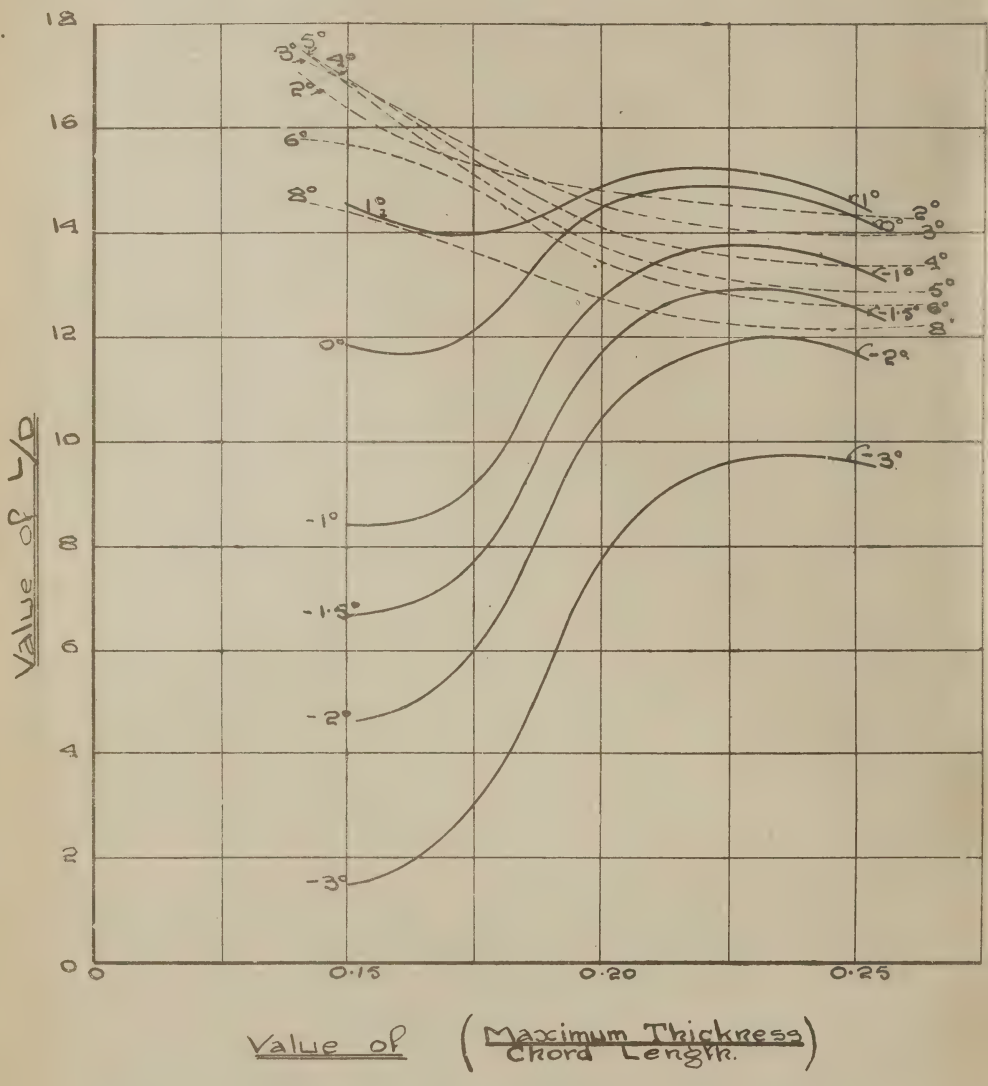

The figures on the curves give the angle of incidence.

The Airscrew

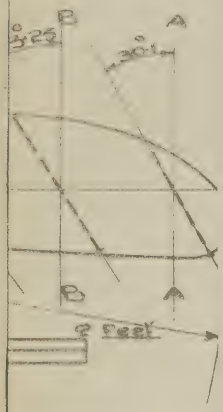

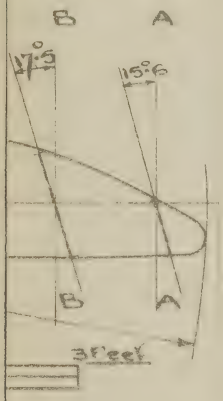

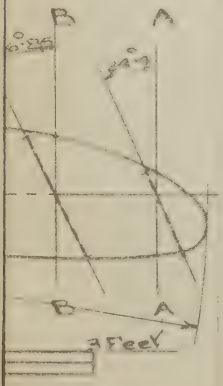

AIRSCREW EFFICIENCY and ENGINE GEARING

– Sketches Showing the Relative Proportions of the Airscrews –

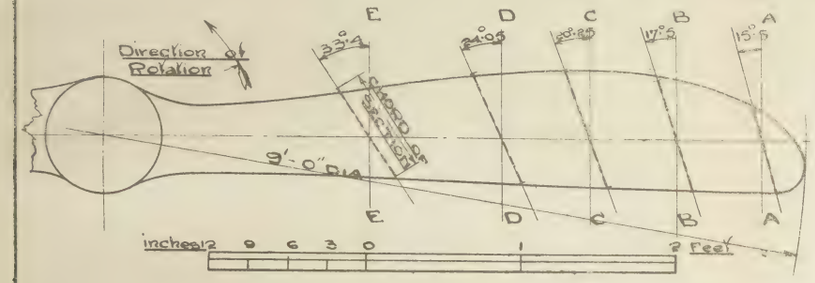

Airscrew S.1.

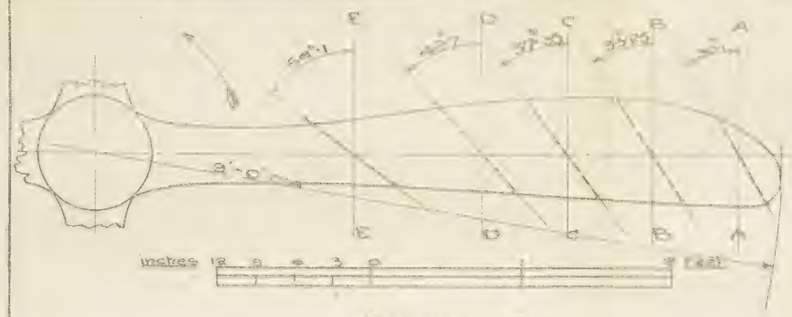

Airscrew S.4.

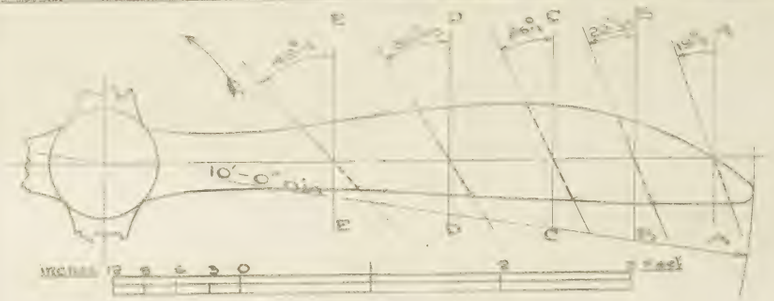

Airscrew S.7.

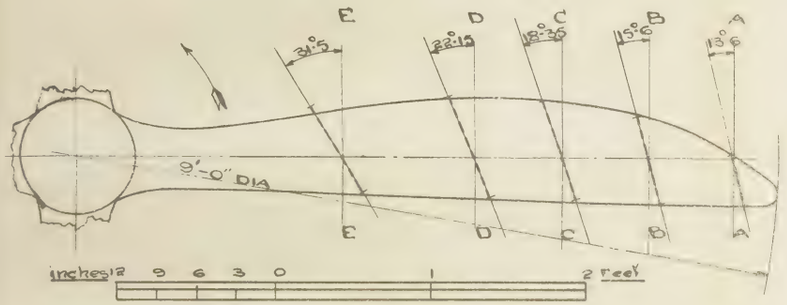

Airscrew S.2.

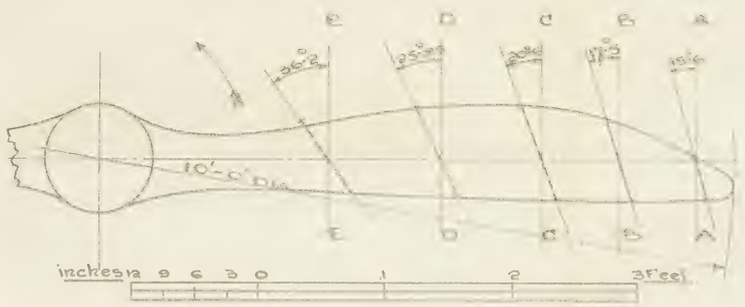

Airscrew S.5.

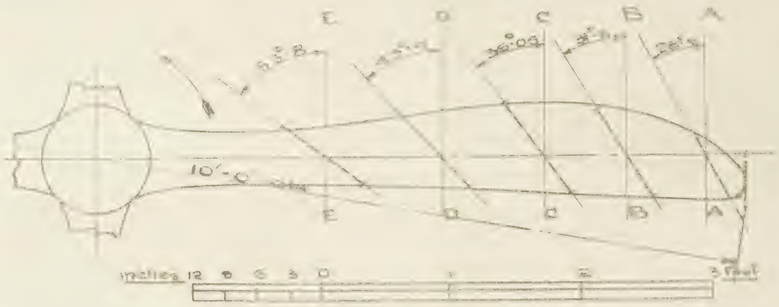

Airscrew S.8.

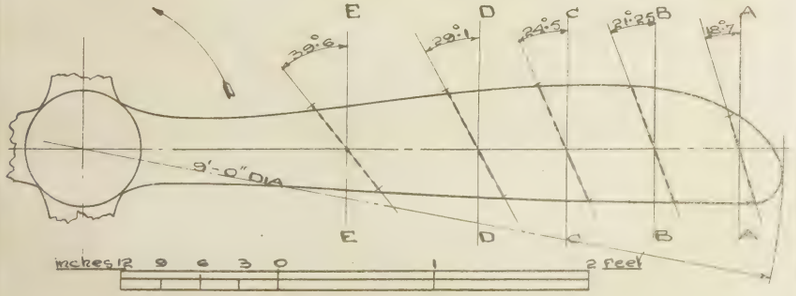

Airscrew S.3.

Airscrew S.6.

Type A.

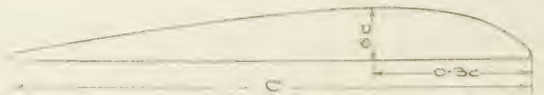

Sketch showing proportions of Blade Sections AA – DD

The corresponding ordinates in all Blade Sections are the same proportion of the max° ordinate (c)

Type B

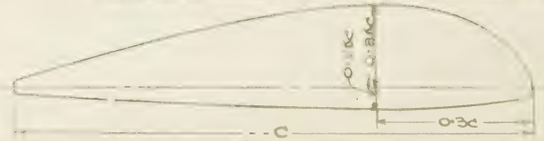

Sketch showing proportions of Blade Sections EE

AIRSCREW EFFICIENCY and ENGINE GEARING

Performance Curves of Airscrew, S1.

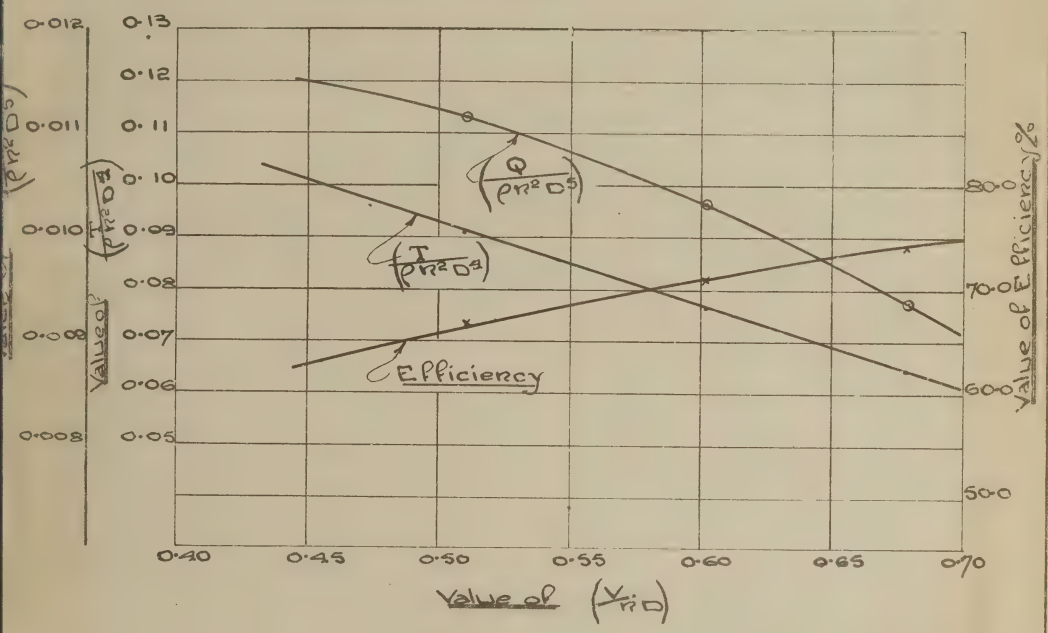

Performance Curves of Airscrew, S2.

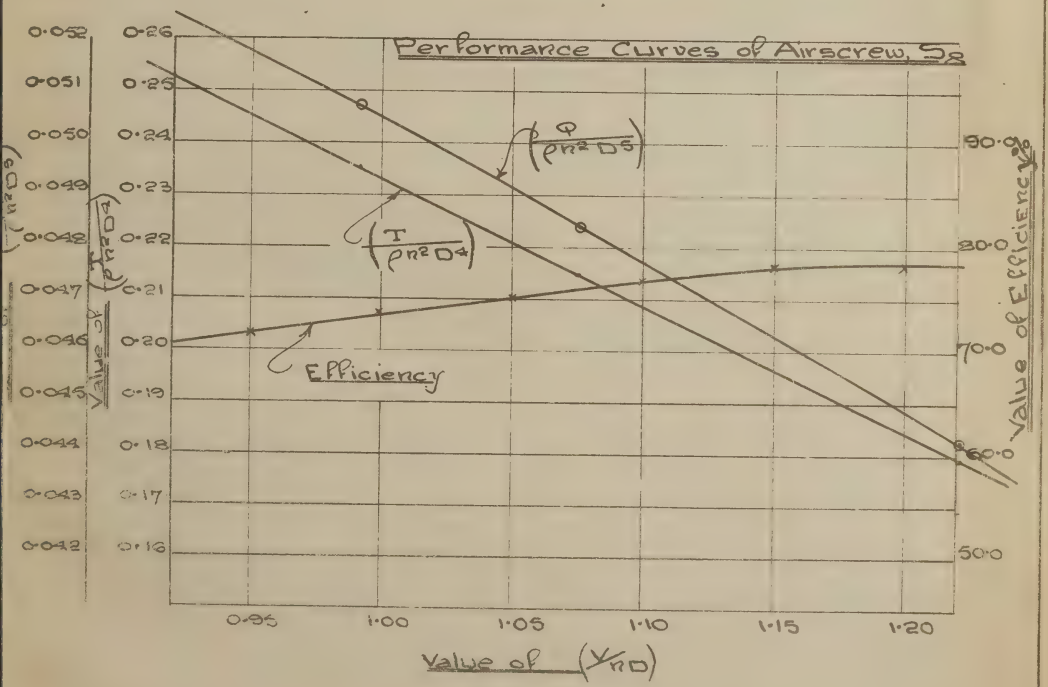

AIRSCREW EFFICIENCY AND ENGINE GEARING.

Performance Curves of Airscrew S_3

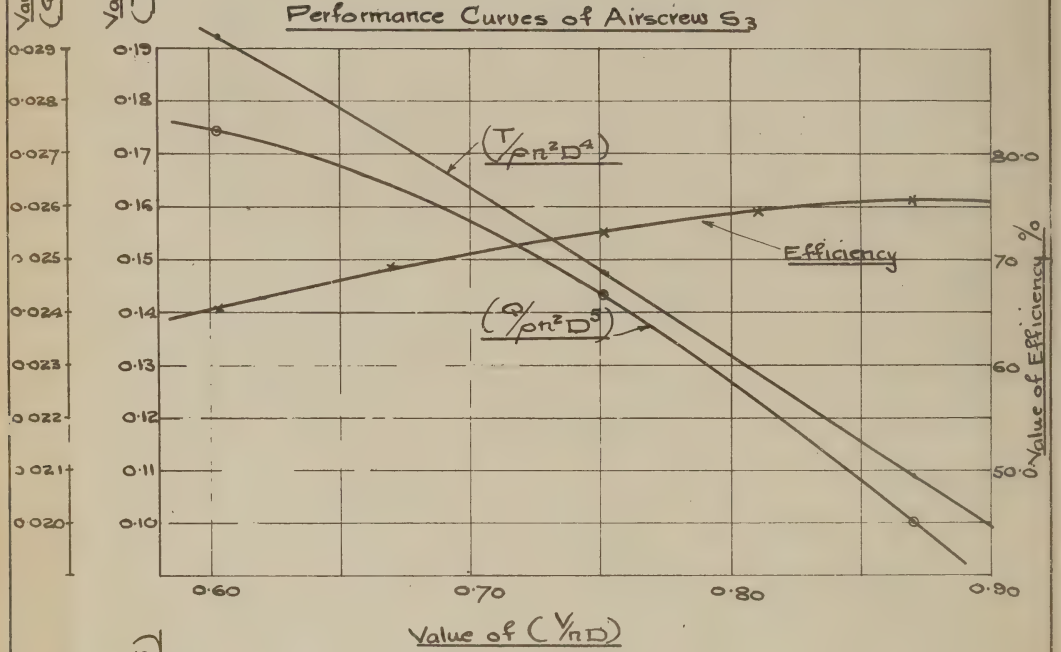

Performance Curves of Airscrew S_4.

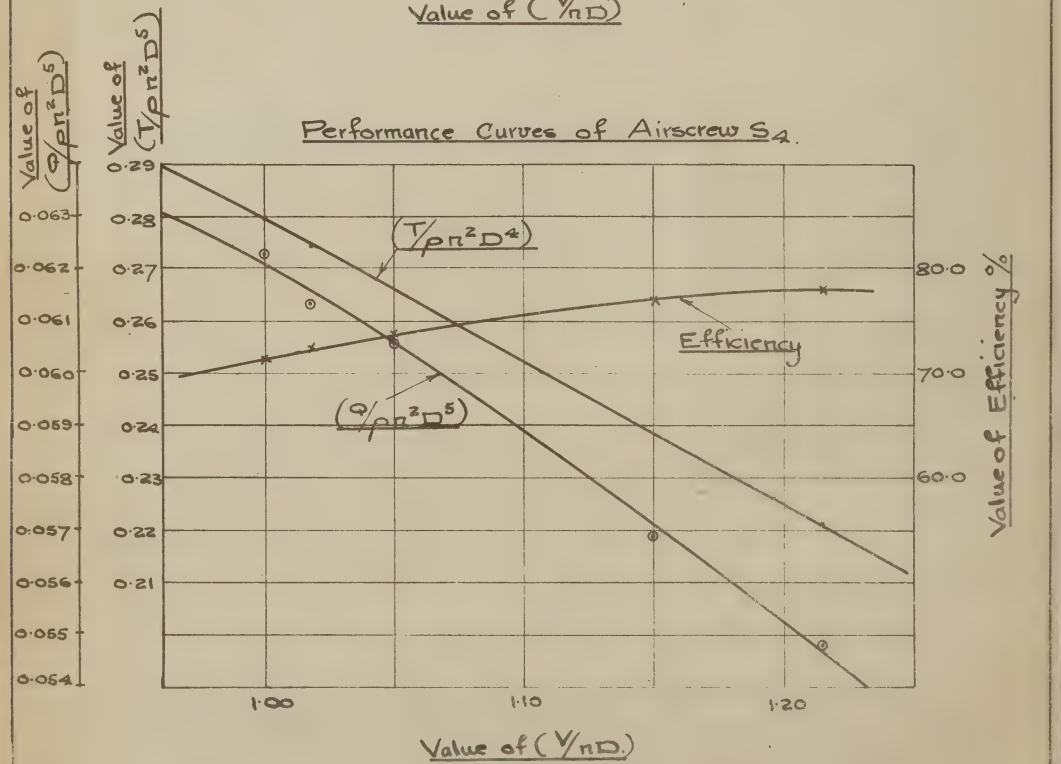

AIRSCREW EFFICIENCY AND ENGINE GEARING.

Performance Curves of Airscrew S6.

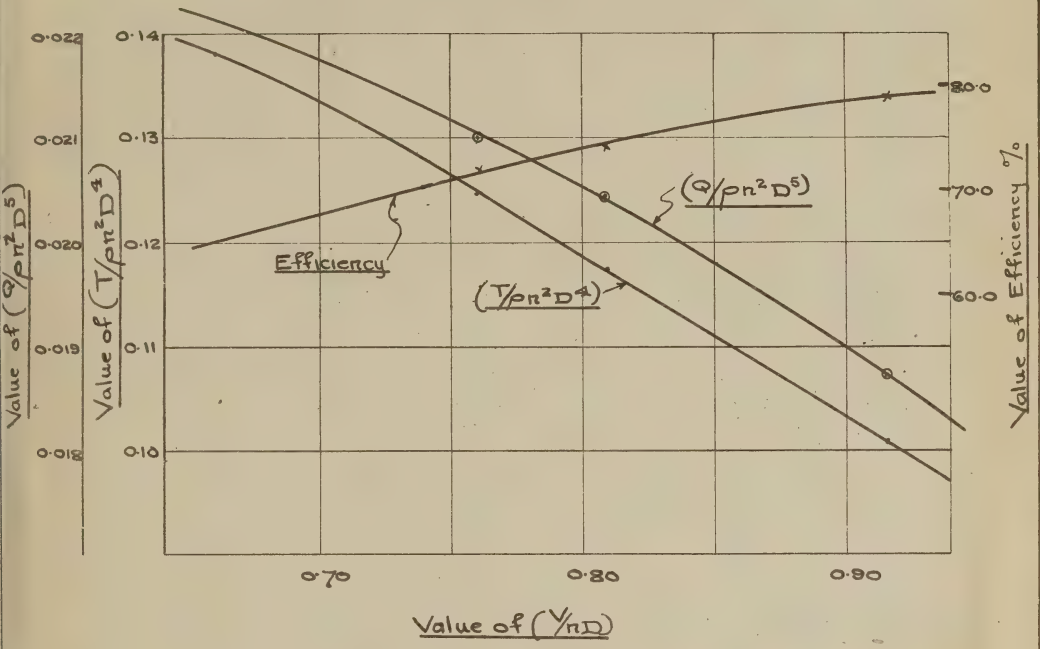

Performance Curves of Airscrew S7.

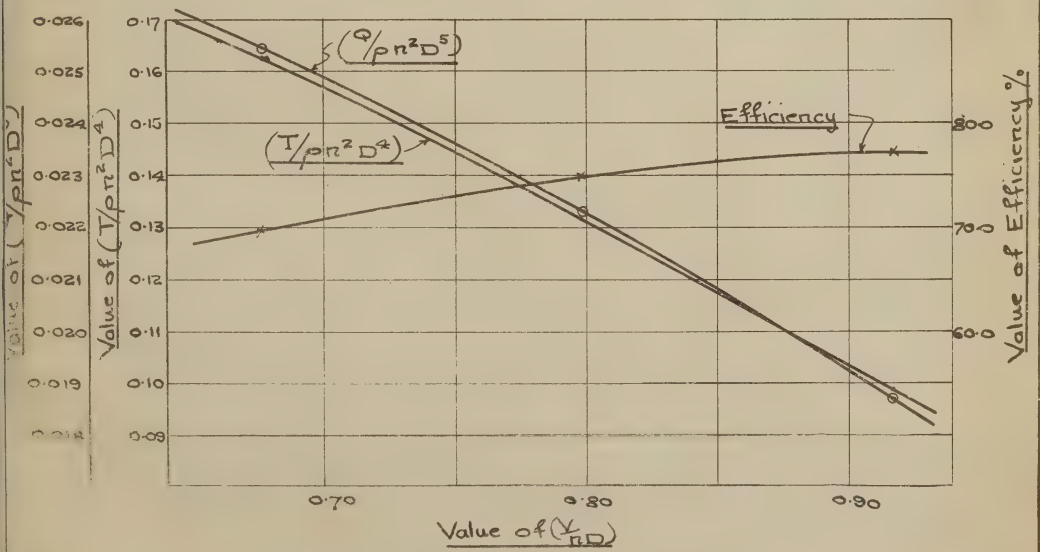

- AIRSCREW EFFICIENCY and ENGINE GEARING -

Comparison of the Combinations of Engine and Airscrew

Variation of the Thrust of airscrew with the Forward speed of the machine

Torque of engine assumed constant at 875 lbs. ft

Efficiency of reduction gearing assumed to be 97%

Altitude of machine, 10,000 ft

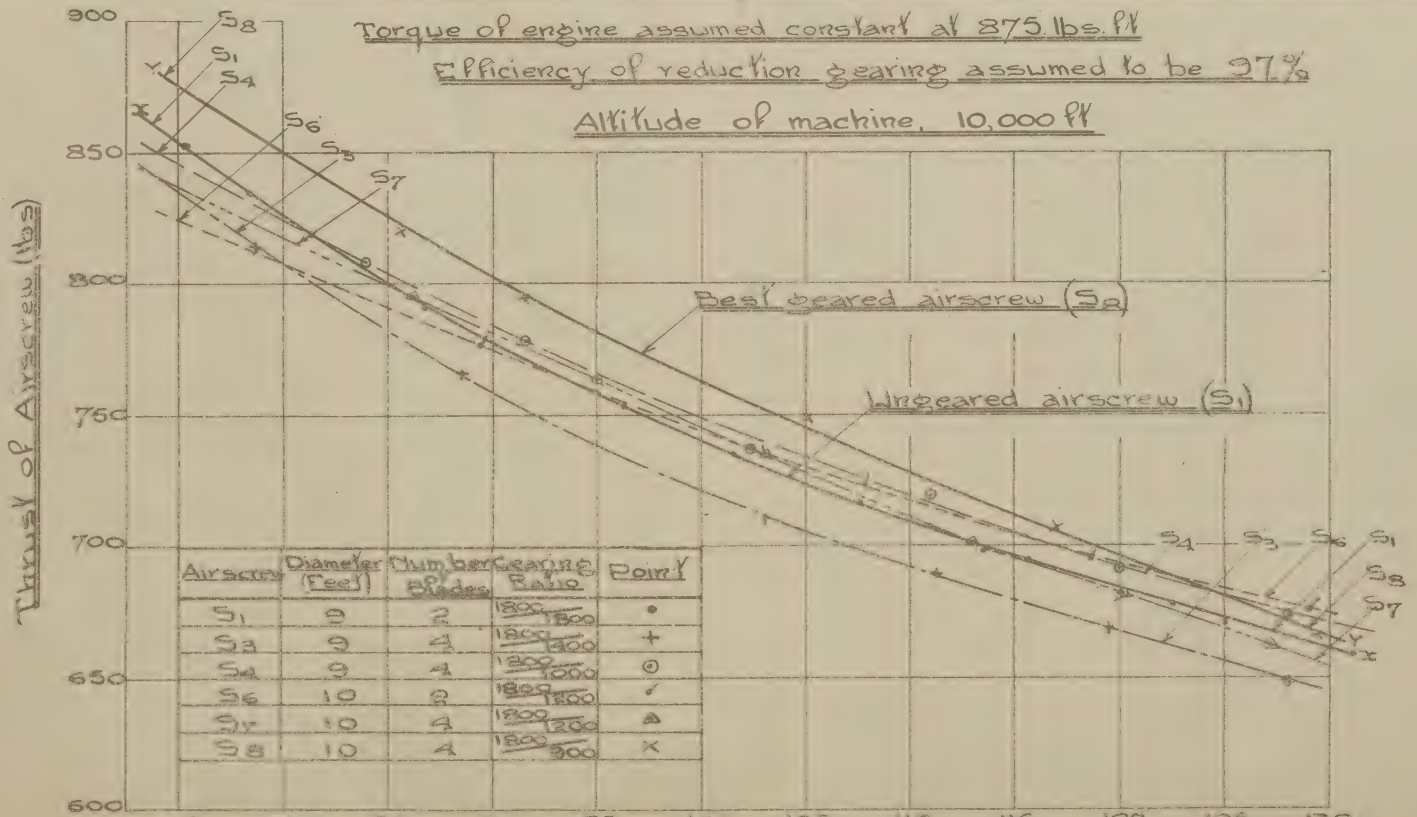

Airscrew	Diameter (Feet)	Number of Blades	Gearing Ratio	Point
S1	9	2	1800/1800	•
S3	9	4	1800/1800	+
S4	9	4	1800/1000	⊙
S6	10	2	1800/1800	✓
S7	10	4	1800/1200	▲
S8	10	4	1800/900	×

REPORT No 442.

FIG. 9

Figs.10&11.

AIRSCREW EFFICIENCY AND ENGINE GEARING.

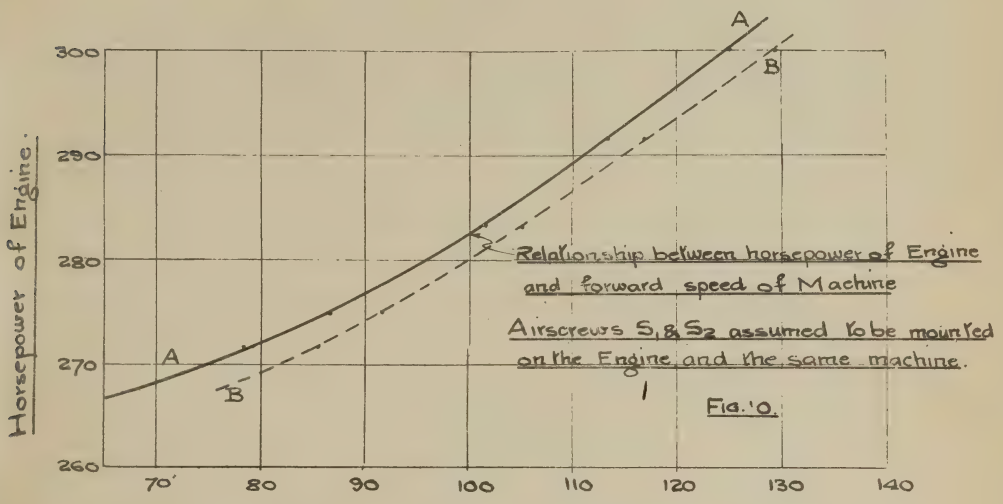

Comparison of the performances of Airscrews S_1 & S_8.

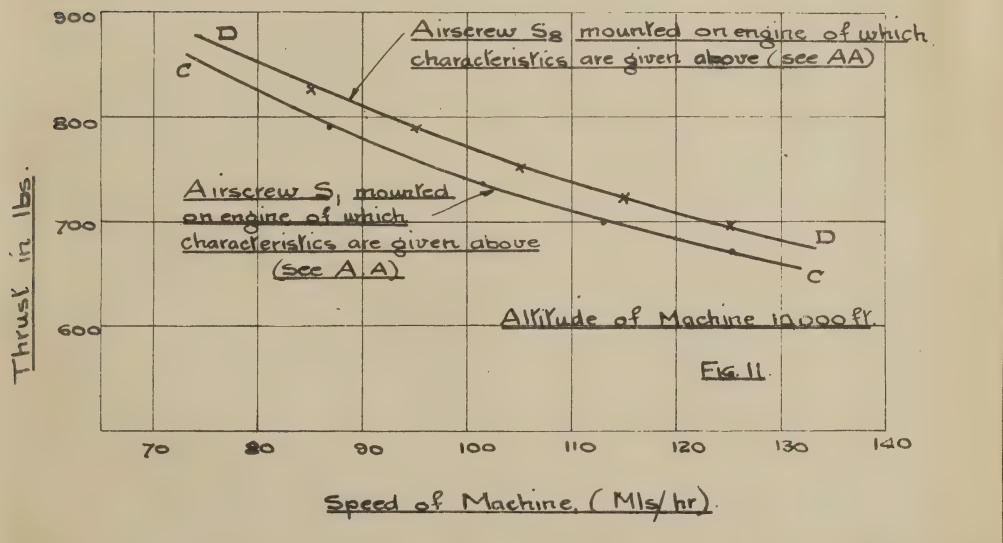

When considering the question of engine gearing use curves of Fig 9.

THE LIBRARY
OF THE
UNIVERSITY OF ILLINOIS

TABLE 3.

COMPARISON OF THE PERFORMANCES OF AIRSCREWS S_1 AND S_8 WHEN MOUNTED ON AN ENGINE OF WHICH THE CHARACTERISTICS ARE GIVEN IN FIG. 11.

At the same forward speed the airscrews absorb equal power.

Altitude of machine, 10,000 ft.

Efficiency of reduction gearing of aircrew, $S_8 = 97$ per cent.

Airscrew S_1.		Airscrew S_8.	
Forward speed of machine. Miles per hour.	Thrust. Lbs.	Forward speed of machine. Miles per hour.	Thrust. Lbs.
125·0	670	125·0	695
113·5	698	115·0	721
101·5	735	105·0	750
86·7	790	95·0	789
78·3	834	85·0	825

THE EFFECT OF THE INFLOWING VELOCITY OF THE AIR ON THE EFFICIENCY OF AN AIRSCREW, WITH A SPECIAL REFERENCE TO THE CASE OF TANDEM AIRSCREWS OF LARGE MACHINES.

By A. Fage, A.R.C.Sc., D.I.C.

Reports and Memoranda, No. 385. *December,* 1917.

Summary.—(a) *Introductory* (*Reasons for Inquiry*).—With a view to using a large h.p., with the types of engine at present available, trial was made on a Handley Page bombing machine, of substituting four Hispano Suiza engines for two Rolls Royce engines of higher power. Practical experience suggested the advisability for ease of construction of using tandem airscrews. The present report is a theoretical investigation of the loss of efficiency inherent in such tandem combinations. The method of investigation is a natural development following from R. & M. No. 328, in which the amount of the inflow velocity and the effect on the efficiency in the case of a single airscrew are considered.

(b) *Range of the Investigation.*—Summaries of the "aerofoil" and "momentum" theories for the cases of single and tandem airscrews are given. Combinations of tandem airscrews of several different diameters, the airscrews of any one combination having the same diameter, were designed to give the same thrust at a forward speed of the machine of 100 m.p.h., the rotational speed being adjusted so that each airscrew gave the same thrust. Calculations of the performances of each combination at this speed and at a climbing speed of 60 m.p.h. were made.

(c) *Conclusions.*—It is shown that the efficiency depends on two factors, the first related to the aerodynamic efficiency of the blade section and the effective pitch angle; the second, to the inflow velocity of air. The first factor was practically the same for all the combinations, but the second factor varied appreciably with the diameter and according to whether the airscrew was in the front or rear. Increase in the inflow velocity reduces the efficiency of an airscrew, especially at low forward speeds of the machine, as in climbing. In other words, it is an advantage when dealing with a large mass of air to use an airscrew of large diameter. The efficiency of an airscrew working in the slip stream of another will always be relatively low. The efficiency of the back airscrew in the case considered is about 0·9 of the front airscrew at ordinary horizontal flight speeds and about 0·75 when climbing. These results are confirmed by some full-scale experiments at the R.A.F.

The present investigation shows in a general manner how the efficiency of working of an airscrew depends on the velocity of the inflowing air, particular attention being given to the case of tandem airscrews, in which one airscrew is working in the slip stream of another. The subject has been treated theoretically on the lines of both the "aerofoil" and "momentum" theories of an airscrew, and for convenience of reference summaries of both these theories are prefaced to the present report.

It should be noted that with the conditions of airscrew design outlined in R. & M. 328, the "momentum" theory is used to obtain a thrust equal to that obtained from the aerofoil theory with a suitable inflow velocity, and, further, that the efficiency of the final design is then deduced entirely from the aerofoil theory.

Application of the "aerofoil" theory to the case of a single airscrew.—It is shown in R. & M. No. 328 that in the case of a single airscrew, the thrust on any element of a blade is $\rho . L_c . C . dr\ (2\pi rn)^2 \sec \phi \left(1 - \frac{D_c}{L_c} \tan \phi\right)$ and that the efficiency of working of the element is

$$\frac{1}{(1 + a)} \cdot \frac{\tan \phi}{\tan (\phi + \beta)},$$

where

$V \equiv$ the translational speed of the airscrew.
$n \equiv$ the rotational speed of the airscrew.
$C \equiv$ the blade width at a radius r.
$D \equiv$ the diameter of the airscrew.
$aV \equiv$ the inflowing velocity of the air due to the thrust.
$L_c =$ the absolute lift coefficient of the section.
$D_c =$ the absolute drag coefficient of the section.
$\theta =$ the blade angle of the section.
$\alpha =$ the angle of attack of the section.

$$\tan \phi = \frac{(1 + a)V}{2\pi rn}.$$

$$\tan \beta = \frac{D_c}{L_c}, \text{ and } \theta = \alpha + \phi.$$

Application of the "aerofoil" theory to the case of an airscrew working in the slip stream of another.—If aV represents the inflow velocity of air into the front airscrew, then it is shown in the Report previously quoted, that the velocity of the slip stream may be taken as $2aV$ approximately.

Assuming the back airscrew to be completely in the slip stream of the front airscrew, then the thrust of an element is $\rho C dr\ (2\pi rn)^2 L_c \sec \phi \left(1 - \frac{D_c}{L_c} \tan \phi\right)$, and the efficiency of working

$$\frac{1}{(1 + 2a)\,(1 + a_1)} \cdot \frac{\tan \phi}{\tan (\phi + \beta)}$$

where

$$\tan \phi = \frac{(1 + 2a)\,V\,(1 + a_1)}{2\pi rn}$$

and

$$a_1\,(1 + 2a)V$$

the inflowing velocity of the air due to the thrust of the airscrew.

Application of the "momentum" theory to the case of a single airscrew.—The thrust of the airscrew T, as calculated according to Froude's hypothesis is

$$\frac{\pi D^2}{4} \cdot \rho (1 + a) 2aV^2.$$

The kinetic energy of slip stream wasted

$$= \frac{\pi D^2}{4} \rho (1 + a) 2a^2V^3.$$

The efficiency of working

$$= \frac{VT}{VT + \frac{\pi D^2}{4} \rho (1 + a) 2a^2V^3}$$

$$= \frac{1}{(1 + a)}$$

Application of the "momentum" theory to the case of an airscrew working in the slip stream of another.—As before, the rear airscrew is assumed to be working completely in the slip stream, of magnitude $2a$V, of the front airscrew.

The velocity of the inflowing air due to the thrust of the airscrew $= a_1 (1 + 2a)$ V.

Mass of air flowing through the airscrew

$$= \frac{\pi D^2}{4} \rho (1 + 2a) (1 + a_1)V.$$

Assume the velocity of the air in the slip stream to be $(2a$V $+$ S). Accepting Froude's hypothesis, the thrust of airscrew

$$= \frac{\pi D^2}{4} \rho (1 + 2a) (1 + a_1)VS$$

$$= \frac{\pi D^2}{4} \frac{\rho}{2} [(2aV + V + S)^2 - (2aV + V)^2].$$

Hence

$$S (2a + 1) V + \frac{S^2}{2} = (1 + 2a) (1 + a_1) VS,$$

that is

$$S = 2a_1 (1 + 2a) V.$$

The velocity of the slip stream then becomes $(1 + 2a)$ V.$2a_1$. The kinetic energy of translation of slip stream due to the thrust of the airscrew

$$= \frac{1}{2} \frac{\pi d^2}{4} \rho (1 + 2a) (1 + a_1) V [(2aV + S)^2 - (2aV)^2]$$

$$= \frac{\pi d^2}{8} \rho (1 + 2a) (1 + a_1) V.S (4aV + S).$$

The efficiency of working

$$= \frac{VT}{VT + \frac{\pi d^2}{8}\rho\,(1+2a)\,(1+a_1)\,V.S\,(4aV+S)}$$

$$= \frac{1}{(1+2a)\,(1+a_1)}.$$

Explanation of the method and design.—Combinations of tandem airscrews of diameter ranging from 7·5 ft. to 9·5 ft. were designed to give the same thrust at a translational speed of the machine of 100 miles per hour, the variations of diameter being accounted for by a change of the rotational speed. The width and the shape of the blade section at corresponding radii were the same for all the airscrews. The front and rear airscrews of any one combination were of equal diameter and gave the same thrust at the same speed of rotation, when the translational speed of the aeroplane was 100 miles per hour. A calculation of the performance of each combination of tandem airscrews was also made for a climbing speed of 60 miles per hour of the machine, the rotational speeds being so adjusted that each airscrew gave the same thrust, the thrust of the combination at this climbing speed being 1·55 times the thrust at the horizontal flight speed of 100 miles per hour. The performance of a section of the blade at a distance of 0·8 of the radius from the axis of rotation was taken to be representative of the performance of each airscrew. The section taken had a maximum value of L/D of 20 at an angle of incidence of 2·5°, the angle of incidence of the section at the speed of translation of the design namely, 100 miles per hour, being 1°. The value of L/D of the section at the climbing speed of 60 miles per hour was about 19·0, the angle of incidence for the several airscrews ranging from 3·5° to 5·0°. The value of L/D at angles of incidence 1°, 2°, 3°, 4°, and 5° were 18, 20, 20, 19 and 18 respectively. The relationship between the lift coefficient, L_c, and the angle of incidence, α, of the section, may be expressed by $L_c = 0{\cdot}039\,(\alpha + 3{\cdot}2)$ over the working range of α.

The interference of the back airscrew on the front has not been considered. Also the rotational motion of the slip stream of the front airscrew has been neglected.

It was assumed that the whole of the rear airscrew was in the slip stream of the front airscrew, and that the velocity of the slip stream was $2a$V, where aV is the inflow velocity of the air into the front airscrew created by the thrust of this airscrew. It was realised that the velocity and the area of the slip stream of the front airscrew, in so far as the rear airscrew is concerned, will depend on the distance between the two airscrews. The assumption made will not, however, affect the general conclusions of the report.

As previously stated, the thrust of each airscrew—front and back—had the same value at the translational speed of the machine of 100 miles per hour, the changes of diameter being taken into account by a suitable adjustment of the rotational speed. Assuming the velocity of inflow of air into a front airscrew of diameter 7·5 ft. were 10 miles per hour—this corresponds roughly to a total thrust of 1,000 lbs. for each combination of tandem airscrews—then at the same speed of the machine and the same thrust the value of the inflow coefficient " a " for the other front airscrew can be calculated from the expression

$$6{\cdot}19 = a\,(1 + a)\,\mathrm{D}^2.$$

Also the " aerofoil " expression for thrust is to have a constant value for all the front airscrews—no matter what diameter—so that since the blade widths at proportional radii are equal it follows that

$$r^3n^2\mathrm{L}_c \sec\phi\,(1 - \frac{\mathrm{D}}{\mathrm{L}}\tan\phi),$$

that is

$$r^3n^2\mathrm{L}_c\,(1 + 0{\cdot}5\tan^2\phi)\left(1 - \frac{\mathrm{D}}{\mathrm{L}}\tan\phi\right)$$

has a constant value.

Assuming a rotational speed of 1,620 r.p.m. for the front airscrew of diameter 7·5 ft., keeping the above two expressions constant, the rotational speeds of the other front airscrews were calculated, and the airscrews were then designed to give the same thrust.

Since the diameters of the front and rear airscrews of any combination are equal, the coefficient of inflow velocity a_1 for the rear airscrew may be calculated from the expression

$$a\,(1 + a) = a_1\,(1 + a_1)\,(1 + 2a)^2$$

Also the thrusts of the front and rear airscrews, as calculated from the " aerofoil " theory, are equal, so that

$$n^2\mathrm{L}_c\,(1 + 0{\cdot}5\tan^2\phi)\left(1 - \frac{\mathrm{D}}{\mathrm{L}}\tan\phi\right) =$$

$$\left[n^2{}_1\mathrm{L}'_c(1+0{\cdot}5\tan^2\phi_1)\right] = \left(1 - \frac{\mathrm{D}_1}{\mathrm{L}_1}\tan\phi_1\right)$$

where

$$\tan\phi_1 = \frac{(1 + 2a)\,(1 + a_1)\,\mathrm{V}}{2\pi r n_1}$$

The rear airscrew was thus designed to give the same thrust as the front one.

In this manner combinations of tandem airscrews of different diameters, the airscrews of any one combination having the same diameter and rotating at such speeds as to give the same thrust at a forward speed of the machine of 100 miles per hour,

were designed. Calculations of the performance of the combinations at a climbing speed of 60 miles per hour were then made, each airscrew rotating at such a speed that the thrusts of all the airscrews were the same. The thrust of each airscrew during the climb was 1·55 times the thrust at the forward speed of 100 miles per hour. The velocity of inflow of air into a front airscrew of diameter 7·5 ft. during the climb was 21 miles per hour, from which the inflow velocity for all the other airscrews both front and rear may be calculated. The rotational speed at which any airscrew should rotate, if the thrust is to be constant at this climbing speed, can easily be calculated from the "aerofoil" expression for thrust.

The results of the calculations are given in Tables 1-4 and shown graphically in Figs. 1 and 2.

Conclusions of the investigation.—It will be noticed that the airscrews were so designed that $\frac{\tan \phi}{\tan (\phi + \beta)}$ has practically a constant value, the actual range of the variation being from 0·81 to 0·85. The value of $\frac{\tan \phi}{\tan (\phi + \beta)}$ is the factor of the efficiency expression which depends on the shape of the blade section, the angle of incidence, and the effective pitch angle, so that whether the machine is in horizontal flight or climbing, the efficiency of any airscrew (front or rear) when the "inflow" factor is ignored will be more or less constant at 83 per cent. It will be at once apparent from the tables, where the largest value of the efficiency of an airscrew is 79·7 per cent. and the smallest value is 44 per cent., that the "inflow" factor of the efficiency expression is very important.

From the curves of Fig. 1 it is seen that at a constant value of the thrust the efficiency increases with the diameter, for the obvious reason that the larger the area of the disc of the airscrew, the smaller is the velocity of inflow of air due to the thrust, and so the greater the "inflow" factor of the efficiency expression. For any one airscrew the "inflow" factor increases with the thrust, the value of $\left(\frac{1}{1 + a}\right)$ at climbing being of the order of 0·75. It is important to realise that even if an airscrew be designed with good aerofoil sections so as to give its maximum efficiency at the climbing speed of the machine, the value of this maximum efficiency will be small, if the climbing thrust be large, the diameter of the airscrew small, and the speed of climbing small.

The efficiency of an airscrew working in the slip stream of another will always be low, since the "inflow" factor is now $\frac{1}{(1 + 2a)\,(1 + a_1)}$. This is especially the case during the climb,

when the value of this factor is of the order of 0·55. During climbing it is extremely unlikely that the efficiency of a rear airscrew working completely in the slip stream of the front airscrew will be considerably greater than 50 per cent., even if the blade sections are very efficient aerodynamically, and are working at their best angles of incidence. Of course, the problem is slightly modified if the rear airscrew is only partly in the slip stream of the front, but it would seem that the efficiency of such an air-screw during climbing must be low.

The ratio of the efficiencies of the front and rear airscrews is about 0·9 at the maximum horizontal flight speed, and about 0·75 at the climbing speed.

Application of the foregoing conclusions to the case of the large aeroplane.—It is of interest to compare the performances of a large bombing machine—of weight about 12,000 lbs.—when driven by (*a*) two combinations of tandem airscrews, (*b*) two single airscrews of large diameter. Suppose each airscrew of the combination, of diameter 8′ 6″, gives the same thrust at the maximum horizontal flight speed of the machine. Then a similar airscrew of diameter 12′ 0″ rotating at the same tip speed and the same forward speed will give twice the thrust with the same "inflow" factor of the efficiency expression, and hence with the same efficiency as the *front* airscrew of the tandem combination. The efficiency of the large airscrew will, however, be about 5 per cent. greater than the efficiency of the tandem combination. Thus if the engines are giving the same horse-power at this horizontal flight speed, the weight of the machine carrying the two large airscrews may be approximately 12,600 lbs. The L/D of the machine in the slightly different attitude will probably be a little greater, so that 12,600 lbs. is a conservative estimate. Further, if it be assumed that the whole of the extra 600 lbs. is completely used in the construction of the machine—weight of gearing, extra weight and resistance of landing gear, &c.—then the heavier machine with the large airscrew will show a distinct advantage at the climb, because then the efficiency of the large airscrew is about 1·12 of that of the combination of tandem airscrews.

The problem may be viewed in a somewhat different manner. If a machine of weight W lbs. has the efficiency of its propelling mechanism increased in the ratio of 1 to 1·12—such an increase of efficiency is probable at the climb by substituting large air-screws for a tandem combination of small airscrews—the load carried can be increased by 0·08 W, and the speed and rate of climbing by 4 per cent. if the attitude of the machine remain the same. It would follow then that for the same rate of climbing the extra useful load carried by a machine for which W equals 12,000 lbs. would be over 1,000 lbs. Practical considerations may, of course, modify the comparison.

EFFICIENCY OF TANDEM AIRSCREWS.

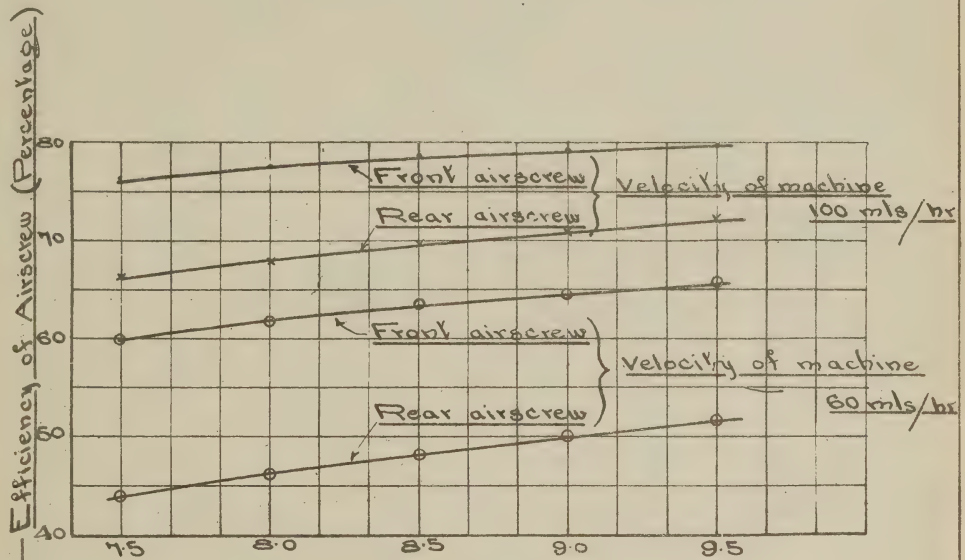

FIG. 1.

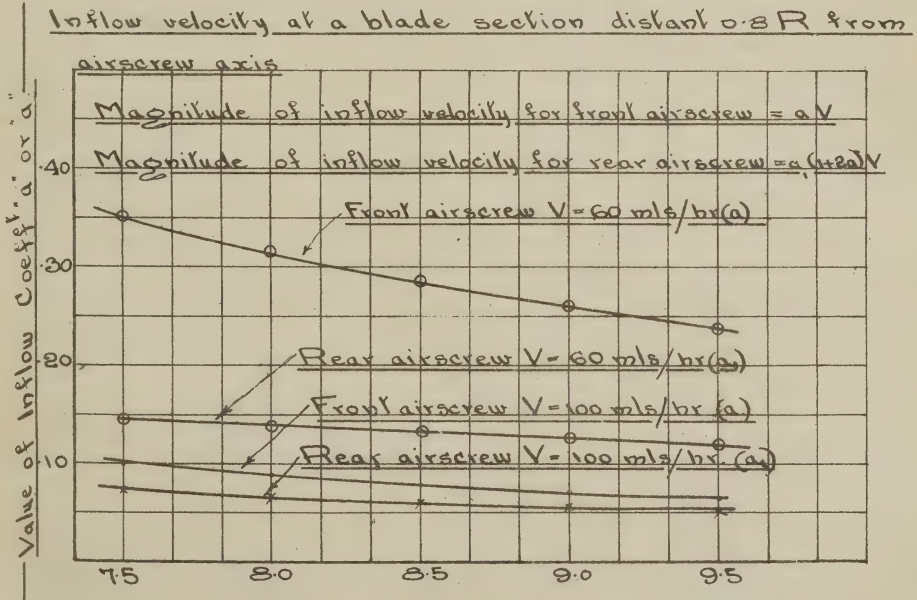
Inflow velocity at a blade section distant 0·8 R from airscrew axis
Magnitude of inflow velocity for front airscrew = a V
Magnitude of inflow velocity for rear airscrew = a(1+a) V
Value of Inflow Coeff. 'a' or 'a'
40
30
20
10
Front airscrew V = 60 mls/hr (a)
Rear airscrew V = 60 mls/hr (a)
Front airscrew V = 100 mls/hr (a)
Rear airscrew V = 100 mls/hr (a)
7·5
8·0
8·5
9·0
9·5
Diameter of Airscrew in feet

FIG. 2.

TABLE 1.

PERFORMANCE OF A FRONT AIRSCREW AT A FORWARD SPEED OF MACHINE OF 100 MILES/HOUR.

Thrust of each airscrew constant.

Inflow velocity of air into front airscrew $= aV$. $(V = 100$ m.p.h.)

Efficiency of an element of blade of front airscrew $= \dfrac{1}{(1+a)} \cdot \dfrac{\tan \phi}{\tan (\phi + \beta)}$.

Diameter of Airscrew. (Ft.)	Distance of Element from Axis. (Ft.)	Rotational Speed. (r.p.m.)	Value of "a."	Blade Angle of Section. ($\theta°$.)	$\tan \phi$.	$\phi°$	$\tan \beta$.	$\dfrac{\tan \phi}{\tan (\phi + \beta)}$	Efficiency calculated from Aerofoil Theory. (%.)
7·5	3·0	1,620	0·100	18·50	0·316	17·50	0·055	0·839	76·2
8·0	3·2	1,470	0·089	18·95	0·324	17·95	0·055	0·842	77·5
8·5	3·4	1,340	0·079	19·30	0·331	18·30	0·055	0·845	78·5
9·0	3·6	1,225	0·071	19·70	0·339	18·70	0·055	0·847	79·1
9·5	3·8	1,125	0·064	20·10	0·346	19·10	0·055	0·847	79·7

TABLE 2.

PERFORMANCE OF A REAR AIRSCREW AT A FORWARD SPEED OF MACHINE OF 100 MILES/HOUR.

Thrust of each airscrew constant and same as that of front airscrew.

Inflow velocity of air into rear airscrew $= (1 + 2a)\, V a_1$. $(V = 100$ m.p.h.)

Efficiency of an element of blade $= \dfrac{1}{(1+2a)\,(1+a_1)} \cdot \dfrac{\tan \phi}{\tan (\phi + \beta)}$.

Diameter of Airscrew. (Ft.)	Distance of Element from Axis. (Ft.)	Rotational Speed. (r.p.m.)	Value of "a."	Value of "a_1"	Blade Angle of Section. ($\theta°$.)	$\tan \phi$.	$\phi°$.	$\tan \beta$.	$\dfrac{\tan}{\tan (\phi + \beta)}$	Efficiency calculated from Aerofoil Theory. (%.)
7·5	3·0	1,620	0·100	0·072	21·35	0·371	20·35	0·055	0·854	66·4
8·0	3·2	1,470	0·089	0·066	21·50	0·374	20·50	0·055	0·855	68·0
8·5	3·4	1,340	0·079	0·060	21·65	0·377	20·65	0·055	0·856	69·7
9·0	3·6	1,225	0·071	0·056	21·85	0·381	20·85	0·055	0·857	71·0
9·5	3·8	1,125	0·064	0·051	22·05	0·385	21·05	0·055	0·857	72·3

TABLE 3.

PERFORMANCE OF A FRONT AIRSCREW AT A FORWARD SPEED OF THE MACHINE OF 60 MILES/HOUR.

Thrust of each airscrew constant and 1·55 times the thrust at a machine speed of 100 m.p.h.

Inflow velocity of air into front airscrew $= aV$. $(V = 60$ m.p.h.)

Efficiency of an element of blade of front airscrew $= \frac{1}{(1+a)} \cdot \frac{\tan \phi}{\tan (\phi + \beta)}$.

Diameter of Airscrew. (Ft.)	Distance of Element from Axis. (Ft.)	Rotational Speed. (r.p.m.)	Value of "a."	Blade Angle of Section. ($\theta°$.)	$\tan \phi$.	$\phi°$	$\tan \beta$.	$\frac{\tan \phi}{\tan (\phi + \beta)}$	Efficiency calculated from Aerofoil Theory. (%.)
7·5	3·0	1,508	0·350	18·50	0·251	14·10	0·0535	0·810	60·0
8·0	3·2	1,350	0·315	18·95	0·256	14·35	0·0540	0·813	61·8
8·5	3·4	1,215	0·285	19·30	0·261	14·60	0·0540	0·815	63·5
9·0	3·6	1,115	0·260	19·70	0·264	14·80	0·0555	0·812	64·5
9·5	3·8	1,025	0·236	20·10	0·267	14·95	0·0555	0·813	65·7

TABLE 4.

PERFORMANCE OF A REAR AIRSCREW AT A FORWARD SPEED OF THE MACHINE OF 60 MILES/HOUR.

Thrust of each airscrew constant and 1·55 times the thrust at a machine speed of 100 m.p.h.

Inflow velocity of air into rear airscrew $= (1 + 2a)\, V a_1$. $(V = 60$ m.p.h.)

Efficiency of an element of blade $= \frac{1}{(1+2a)\,(1+a_1)} \cdot \frac{\tan \phi}{\tan (\phi + \beta)}$.

Diameter of Airscrew. (Ft.)	Distance of Element from Axis. (Ft.)	Rotational Speed. (r.p.m.)	Value of "a."	Value of "a_1."	Blade Angle of Section. ($\theta°$.)	$\tan \phi$.	$\phi°$.	$\tan \beta$.	$\frac{\tan \phi}{\tan (\phi + \beta)}$	Efficiency calculated from Aerofoil Theory. (%.)
7·5	3·0	1,650	0·350	0·143	21·35	0·330	18·25	0·0500	0·855	44·0
8·0	3·2	1,475	0·315	0·137	21·50	0·329	18·20	0·0500	0·855	46·2
8·5	3·4	1,335	0·285	0·132	21·65	0·329	18·20	0·0513	0·855	48·0
9·0	3·6	1,210	0·260	0·126	21·85	0·330	18·25	0·0513	0·855	50·0
9·5	3·8	1,105	0·236	0·120	22·05	0·331	18·30	0·0513	0·855	51·7

SOME EXPERIMENTS WITH TANDEM COMBINATIONS OF AIRSCREWS.

By A. Fage, A.R.C.Sc., and H. E. Collins.

Reports and Memoranda (New Series), No. 421. *March,* 1918.

Summary.—(a) *Introductory (reasons for inquiry).*—The present investigation was made with a view to testing the general conclusions of R. & M. No. 385 in which the efficiency of a tandem combination of airscrews has been considered from a theoretical standpoint. Experiments were made with tandem combinations, in which :—

(*a*) Airscrews of different diameter rotated in the same direction.

(*b*) Airscrews of the same diameter rotated (1) in the same direction, (2) in the opposite direction.

(b) *Range of the investigation.*—Experiments were made with six airscrews $A_1 - A_6$, arranged in four tandem combinations as follows :—

Combination No. 1.—Airscrews of equal diameter, rotating in the opposite direction—forward airscrew A_1, rear airscrew A_3.

Combination No. 2.—Airscrews of equal diameter, rotating in the same direction—forward airscrew A_2, rear airscrew A_3.

Combination No. 3.—Airscrews rotating in the same direction, but with the airscrew of smaller diameter at the front—forward airscrew A_4, rear airscrew A_6.

Combination No. 4.—Airscrews rotating in the same direction, but with the airscrew of larger diameter at the front—forward airscrew A_5, rear airscrew A_6. In each combination a model of the tandem engines, suitably faired, was mounted between the airscrews. The scale of the models was taken as one-sixth full size, and the models of the engines were made accordingly.

The experiments were made more especially to show how the performance of an airscrew is modified when working in the slipstream of another, rather than to obtain the over-all performance of the complete tandem combination. The performances of each rear airscrew were measured when the forward airscrew was stationary, and when the thrust of the rear airscrew was 0·8, 1·0 and 1·2 times that of the forward airscrew.

(c) *Conclusions.*—The general results of the investigation may be conveniently summarised as follows :—

(1) The efficiency of working of the rear airscrew is reduced by the slipstream of the forward airscrew ; thus, over the working range, the efficiency of the rear airscrew is about 84 per cent. of its value when the forward airscrew is not working, this value being the mean taken from the four combinations when the forward and rear airscrews are developing equal thrusts.

(2) The efficiency of the tandem combination is increased by rotating the airscrews in opposite directions, thus, with the particular airscrews of the present investigation, the efficiency of the *tandem combination* at

climbing was increased by about 4 per cent., assuming the airscrews to be giving the same thrust and that the performance of the forward airscrew is not appreciably affected by the working of the rear airscrew.

(3) The performance of the forward airscrew was only slightly modified by the working of the rear airscrew.

(4) It would appear advantageous to use airscrews of different diameters, the larger airscrew being at the front.

(5) The rotational motion in the slipstream of the forward airscrew appears to be of appreciable magnitude, and if possible, should be allowed for when designing the rear airscrew.

The efficiency of a tandem combination of airscrews has been considered from a theoretical standpoint in R. & M. No. 385, and it was thought desirable to test the general conclusions of that report by some experimental evidence. Accordingly, the investigation described in the present report was made. The experiments, which are admittedly of a somewhat general character, were conducted more especially with a view to measuring the performance of an airscrew as affected by the slip stream of another, rather than of finding the over-all performance of the complete tandem combination. There is, however, some experimental evidence that the interference of the rear airscrew on the performance of the forward one is small. Experiments were made with tandem combinations in which

(*a*) airscrews of different diameter rotated in the same direction, and

(*b*) airscrews of the same diameter rotated (1) in the same direction, (2) in the opposite direction.

Range of the investigation.—To obtain some general experimental data with the minimum of delay, the tandem combinations were constructed from model airscrews which were at the Laboratory. Experiments were made with six airscrews, arranged in four tandem combinations, and for convenience of reference the following nomenclature is adopted.

Airscrew A_1 (*see Fig.* 1).—Airscrew designed for B.E.2c machine. R.A.F. drawing No. T.4966. Diameter of model = 1·5 feet. Right-handed direction of rotation. Two blades. The direction of rotation is obtained by looking from behind the airscrew in the direction of forward motion.

Airscrew A_2 (*see Fig.* 1).—Airscrew same as A_1, but with a left-handed direction of rotation. Two blades.

Airscrew A_3 (*see Fig.* 1).—Same shape of blade sections, diameter, and plan form as airscrew A_1, but the blade angles are smaller. Left-handed direction of rotation. Two blades.

Airscrew A_4 (*see Fig.* 2).—Airscrew designed for B.E.2e machine. R.A.F. drawing No. T.7850. Diameter of airscrew 1·515 feet. Left-handed direction of rotation. Four blades.

Airscrew A_5 (*see Fig.* 3).—Airscrew B of the "blade-interference" experiments of R. & M. No. 316. Diameter of airscrew 2·25 feet. Four blades. Left-handed direction of rotation.

Airscrew A_6 (*see Fig.* 4).—Airscrew designed for F.E.8 machine. R.A.F. drawing No. T.7143. Diameter of airscrew 2·0 feet. Four blades. Left-handed direction of rotation.

The four combinations of tandem airscrews were :—

Combination No. 1.—Forward airscrew—A_1; rear airscrew—A_3.

Hence airscrews of equal diameter, but rotating in the opposite direction.

Combination No. 2.—Forward airscrew—A_2; rear airscrew—A_3.

Hence airscrews of equal diameter, but rotating in the same direction.

Combination No. 3.—Forward airscrew—A_4; rear airscrew—A_6.

Here the diameter of the forward airscrew is smaller than that of the rear airscrew, but with the same direction of rotation.

Combination No. 4.—Forward airscrew—A_5; rear airscrew—A_6.

Here the diameter of the forward airscrew is greater than that of the rear airscrew, and both airscrews rotate in the same direction.

In each combination a model of the tandem engines with suitable engine fairing was mounted between the airscrews. A sketch of this model is given in Fig. 5. From the sketches of Fig. 6 may be found some idea of the relative sizes of the two airscrews and engines of each combination. If the scale of any combination be taken as one-sixth full size—this was the scale chosen for the model of the engines—then the diameters of the full size airscrews, taken in order, would be 9′, 9′, 9′, 9′ 1″, 13′ 6″ and 12′ respectively.

The experiments were made in the 4-ft. channel, the forward airscrew being driven by the airscrew dynamometer, whilst the thrust and the torque of the rear airscrew were measured on the airscrew balance. Ordinarily, the thrust of the airscrew acts as a pull along the shaft of the dynamometer, but with these particular experiments it was necessary to mount the airscrew so that its thrust acted as a push. By a slight modification of the thrust measuring apparatus of the dynamometer it was possible to measure the thrust of a forward airscrew, but no measurements of torque were obtained. The measurements of thrust and torque were made at a rather low wind speed of 25 ft./sec. in the channel, in order to develop the thrust of the

rear airscrew at a low (climbing) value of (V/nD). The performances of each rear airscrew were measured when the forward airscrew was stationary, and when the thrust of the rear airscrew was 0·8 1·0, and 1·2 of that of the forward airscrew. It is not convenient when dealing with combinations of several different types of airscrews to present the results of the experiments in terms of absolute coefficients, and, accordingly, the actual measurements of the thrust and torque are given for the corresponding value of the rotational speed, the forward speed of the model airscrew being 25 ft./sec.

Discussion of the results of the experiments.—The experiments of the present report show how the performance of an airscrew is modified when working in the slip-stream of another ; that is, comparisons are made between the performance of the airscrew alone and the performance of the same airscrew when mounted at the rear of a tandem combination. In some respects it would have been better, perhaps, to have made a comparison between the performance of an airscrew designed to develop a given thrust at a given rotational speed and another airscrew, of the same plan form and the shape of blade sections, designed to absorb an equal torque at the same value of the rotational speed, when working in the slip stream of a forward airscrew, the translational speed of the machine being the same in both cases. In the latter case the blade angles of the airscrew would be increased to take account of the additional translational velocity of the slip stream from the front. The general results of such an investigation would be of the same character as those of the present, but it is thought desirable to point to the slight difference between experiments on tandem combinations—where the rear airscrew is especially designed for such a combination—and experiments made to measure how the performance of any airscrew is affected by the slip stream from another. To avoid undue reiteration the thrust of the forward airscrew and the thrust of the rear airscrew will hereafter be referred to as T_f and T_r respectively.

Combination No. 1.—The performance of the rear airscrew A_3 when ($T_f = 0$, $T_r = 0{\cdot}8T_f$, $T_r = T_f$, and $T_r = 1{\cdot}2T_f$) are given in Tables 1 and 2 and Figs. 7 and 9. As would be expected, to develop a given thrust on the airscrew A_3 the rotational speed must be increased with an increase of the thrust of the forward airscrew A_1, since the augmented translational velocity diminishes the angle of incidence of the blade sections. At the same rotational speed of the rear airscrew A_3, the slip stream of airscrew A_1 does not greatly affect the torque. It will be seen from Fig. 9 that the maximum efficiency of the rear airscrew alone ($T_f = 0$) is 84·5 per cent., and that the efficiency at climbing is about 75 per cent. When ($T_r = T_f$) the maximum value of the efficiency is 75·5 per cent., and then the efficiency at climbing is roughly about 85 per cent. of the value when $T_f = 0$.

Combination No. 2.—The performance curves of the rear airscrew A_3 of this combination are given in Figs. 10–12, and the experimental data in Table 3. The shifts of the thrust and torque curves of this airscrew in the direction of the increasing value of rotational speed—due to the slip stream from the forward airscrew A_2—are more pronounced than with the forward airscrew A_1, which is only to be expected, since the airscrews of this combination are rotating in the same direction. When ($T_r = T_f$) the maximum efficiency falls to the rather low value of 65 per cent. At climbing when ($T_f = T_r$) the efficiency may be taken as about 77·5 per cent. of the value when $T_f = 0$.

The effect of the relative directions of rotation on the performance of a tandem combination.—The only difference between combinations No. 1 and No. 2 is that the forward airscrews A_1 and A_2 have opposite directions of rotation, the airscrews A_1 and A_2 being equal in all respects and the rear airscrew A_3 being common to both combinations. It is possible, then, from a direct comparison of the performance of these two combinations to determine the effect of the direction of rotation of the forward airscrew on the efficiency of working of the rear airscrew. To facilitate the comparison, the performance curves of airscrew A_3, when working as the rear airscrew of both combinations No. 1 and No. 2, with ($T_f = T_r$) and ($T_f = 0$), are re-drawn in Figs. 13–14.

It will be seen from Fig. 13 that the shifts of the thrust and torque curves of airscrew A_3, parallel to the axis of the rotational speed, are appreciably affected by the direction of rotation of the forward airscrew, these shifts being, of course, quite distinct from those due to the translational velocity of the slip stream from the forward airscrew. It would follow then that when designing the rear airscrew of a tandem combination some allowance should be made for the direction of rotation of the forward airscrew. A gain of efficiency of the rear airscrew is obtained when the airscrew rotates in the opposite direction (*see* Fig. 14) for the reason that at any rotational speed the larger fall of thrust of airscrew A_3 of combination No. 2, as compared with combination No. 1, is accompanied by a relatively smaller fall of torque. The values of the maximum efficiency of airscrew A_3 of combination No. 1 and No. 2 (when $T_f = T_r$) are 75·5 per cent. and 64·5 per cent. respectively, although perhaps the merits of the combinations are more correctly obtained from a comparison of the efficiencies at climbing. At the same rotational speed and when ($T_f = T_r$) the efficiency of the rear airscrew A_3 at climbing is about 8 per cent. greater in the case of combination No. 1. It should be noticed that at the same rotational speed airscrew A_3 is absorbing a greater torque in combination No. 1. Also the over-all efficiency of the tandem combination will only be increased by about 4 per cent. by rotating the airscrews in the opposite direction, as it is expected that the efficiency of the

forward airscrew will not be appreciably affected by the direction of rotation of the rear airscrew and presuming that ($T_r = T_f$).

Combination No. 3.—The performances of the rear airscrew A_6 when ($T_f = 0$, $T_r = 0{\cdot}8T_f$, $T_r = T_f$ and $T_r = 1{\cdot}2T_f$) are given in Figs. 15–17 and Tables 4 and 5. From Fig. 17 it will be noticed that the maximum efficiency of the rear airscrew A_6 falls from 83·5 per cent. to 63·5 per cent. when ($T_r = T_f$), and also that the efficiency at climbing when ($T_r = T_f$) is 85 per cent. of the value when $T_f = 0$.

Combination No. 4.—The experimental data for the rear airscrew A_6 of this combination are given in Table 6, and shown graphically in Figs. 18–20. The maximum efficiency is reduced by a smaller amount than in combination No. 3, that is from 83·5 per cent. when $T_f = 0$ to 75 per cent. when ($T_f = T_r$). At climbing ($T_f = T_r$), the efficiency of airscrew A_6 is reduced to about 90 per cent. of its value when $T_f = 0$.

The dependence of the performance of a tandem combination on the relative diameters of the two airscrews.—The experiments with combinations No. 3 and No. 4 were made to determine whether a higher efficiency is to be expected with the larger airscrew at the front or at the rear of the combination. It will be noticed that the three four-bladed airscrews A_4, A_5 and A_6 have the same direction of rotation. The rear airscrew A_6, which is common to both combinations, has the larger diameter in combination No. 3. A comparison of the performances of the rear airscrew A_6 of combinations No. 3 and No. 4 can most conveniently be made by reference to Fig. 21, which gives the thrust and torque curves when $T_f = 0$ and $T_f = T_r$, and to Fig. 22 which gives the corresponding efficiency curves. It will be noticed that when ($T_f = T_r$) the rear airscrew A_6, when in combination No. 4, has a greater thrust and a smaller torque over the greater part of the experimental range of the rotational speed. The maximum value of the efficiency of airscrew A_6 in combination No. 4 is 75 per cent. and in combination No. 3 is 63·5 per cent., but the discrepancy between the values of the efficiency diminished with an increase of the rotational speed, becoming zero at a rotational speed of 22 r.p.s. From these experiments it would seem advantageous to mount the larger airscrew at the front of the combination.

Interference of the rear airscrew of a tandem combination on the performance of the forward airscrew.—No measurements of the complete performance of a forward airscrew were made during the present experiments, but at a constant value of the thrust the rotational speed of a forward airscrew was measured as the thrust of the rear airscrew varied from 0 to $1{\cdot}2T_f$. The experimental data for the forward airscrews A_4 and A_5 of combinations No. 3 and No. 4 are given in Tables 7 and 8 and shown graphically in Figs. 23 and 23*a*. From the curves of these figures it will be seen that at a constant thrust T_f and a constant translational

speed, the rotational speed of either the forward airscrew A_4 or the forward airscrew A_5 is practically unaffected as the thrust of the rear airscrew changes from 0 to $1{\cdot}2T_f$.

A similar result was obtained with the forward airscrews A_1 and A_2 of combinations No. 1 and No. 2. It would seem then, that the performance of a forward airscrew of a tandem combination is only slightly affected by the working of the rear airscrew.

The conclusions of the present investigation may be summarised thus.

(*a*) When the forward and rear airscrews of a tandem combination are developing equal thrusts, the maximum efficiency of the rear airscrew is about 83 per cent. of the value when the forward airscrew is not working. At climbing ($T_f = T_r$), the efficiency of the rear airscrew is about 85 per cent. of the value when the thrust of the forward airscrew is zero.

(*b*) The efficiency of the tandem combination is increased by rotating the airscrews in opposite directions. With the particular airscrews of the present investigation, the efficiency of the tandem combination at climbing was increased by about 4 per cent. when the airscrews rotated in the opposite direction, assuming the airscrews to be giving the same thrust and that the working of the rear airscrew does not appreciably affect the performance of the forward airscrew.

(*c*) When designing the rear airscrew of a tandem combination some allowance should be made, if possible, for the rotational motion in the slip-stream from the forward airscrew, in addition to that made for the translational motion.

(*d*) It would appear advantageous to mount the larger airscrew in front of the tandem combination, and in the case where the two engines are of unequal horsepower, to drive the forward (and larger) airscrew by the engine having the higher horsepower. In the particular case which led to the present investigation the engines were both of the same horsepower, though in the circumstances in which the tests were made this condition could not be definitely attained.

(*e*) The working of the rear airscrew appears to affect only slightly the performance of the forward airscrew.

Table 1.

PERFORMANCE OF AIRSCREW A_3 WHEN UNAFFECTED BY THE SLIP-STREAM OF THE FORWARD AIRSCREW (*i.e.* $T_f = 0$), BUT WITH INTERFERENCE OF FAIRED ENGINES.

Translational speed of airscrew = 25 ft. /sec.

Thrust.		Torque.		Efficiency.	
n (revs. /sec.).	T. (lbs.).	n (revs. /sec.).	Q (lbs.-ft.).	n (revs. /sec.).	η (percentage)
21·10	0·305	20·10	0·06	20·0	75·0
23·20	0·457	23·00	0·09	22·0	82·8
25·20	0·609	26·00	0·12	24·0	84·5
27·40	0·761	28·70	0·15	26·0	84·0
28·90	0·913	31·20	0·18	28·0	82·0
30·65	1·065	33·00	0·21	30·0	79·5
32·30	1·216	35·20	0·24	32·0	77·0
33·40	1·368	37·30	0·27	34·0	75·0
34·80	1·520	—	—	36·0	72·4
36·70	1·720	—	—	38·0	70·4

Table 2.

PERFORMANCE OF THE REAR AIRSCREW (A_3) OF COMBINATION No. 1.

Translational speed of airscrew = 25 (ft./sec.).
Rotational speed of airscrew = n (revs./sec.).
Thrust of forward airscrew = T_f (lbs.).
Thrust of rear airscrew = T_r (lbs.).
Torque of rear airscrew = Q_r (lbs.-ft.).

Model of faired engines in place.

$T_r = 0{\cdot}8T_f$.			$T_r = T_f$.			$T_r = 1{\cdot}2T_f$.			Efficiency (percentage).			
T_r (lbs.).	n (revs./sec).	Q_r (lbs.-ft.).	T_r (lbs.).	n (revs./sec.).	Q_r (lbs.-ft.).	T_r (lbs.).	n (revs./sec.).	Q_r (lbs.-ft.).	n (revs./sec.).	$T_r = 0{\cdot}8T_f$.	$T_r = T_f$.	$T_r = 1{\cdot}2T_f$.
0·320	22·0	0·080	0·40	23·35	0·096	0·660	27·4	—	20·0	65·0	66·0	66·7
0·440	24·4	0·100	0·55	25·90	0·121	0·852	29·7	0·162	22·0	72·6	73·5	75·5
0·568	26·4	0·155	0·71	28·05	0·138	0·996	31·5	0·190	24·0	74·5	75·6	77·6
0·664	27·9	0·134	0·83	29·70	0·162	1·092	32·6	0·189	26·0	72·1	74·2	76·2
0·728	29·0	0·145	0·91	30·80	0·177	1·370	36·0	0·239	28·0	70·8	72·0	73·6
0·912	31·8	0·174	1·14	33·90	0·206	1·610	38·1	0·278	30·0	68·2	69·5	71·0
1·070	33·3	0·194	1·34	35·70	0·236	1·705	38·8	0·290	32·0	65·4	67·0	68·0
1·135	34·4	0·214	1·42	36·60	0·252	—	—	—	34·0	63·2	65·0	65·8
									36·0	61·0	62·8	63·3
									38·0	58·5	60·3	60·9

Table 3.

PERFORMANCE OF THE REAR AIRSCREW (A_3) OF COMBINATION No. 2.

Translational velocity of the airscrew = 25 (ft. /sec.).
Rotational speed of airscrew = n (revs. /sec.).
Thrust of forward airscrew = T_f (lbs.).
Thrust of rear airscrew = T_r (lbs.).
Torque of rear airscrew = Q_r (lbs.).

Model of faired engines in place.

$T_r = 0{\cdot}8T_f$.			$T_r = T_f$.			$T_r = 1{\cdot}2T_f$.			Efficiency (percentage).			
T_r (lbs.).	n (revs. /sec.).	Q_r (lbs.-ft.).	T_r (lbs.).	n (revs. /sec.).	Q_r (lbs.-ft.).	T_r (lbs.).	n (revs. /sec.).	Q_r (lbs.-ft.).	n (revs. /sec.).	$T_r = 0{\cdot}8T_f$.	$T_r = T_f$.	$T_r = 1{\cdot}2T_f$.
0·344	24·00	0·089	0·43	25·30	0·154	0·515	26·5	0·118	20·0	55·0	56·0	56·8
0·472	26·60	0·115	0·59	28·10	0·136	0·640	28·7	0·144	22·0	62·5	63·0	63·5
0·624	29·20	0·136	0·78	31·15	0·163	0·936	33·1	0·190	24·0	63·5	64·5	65·8
0·769	31·50	0·161	0·96	33·75	0·195	1·150	36·0	0·229	26·0	63·5	64·0	65·2
0·880	33·30	0·177	1·10	35·70	0·218	1·320	38·1	0·248	28·0	62·5	62·8	63·5
1·215	37·60	0·226	1·52	40·70	0·274	1·825	43·8	0·318	30·0	61·0	61·0	62·0
1·264	38·60	0·228	1·58	41·70	—	—	—	—	32·0	60·3	59·5	59·8
1·310	39·10	0·237	1·64	42·30	0·288	—	—	—	34·0	58·8	58·4	58·5
—	—	—	—	—	—	—	—	—	36·0	57·7	57·4	57·5
—	—	—	—	—	—	—	—	—	38·0	56·6	56·1	56·0
—	—	—	—	—	—	—	—	—	40·0	55·5	54·8	54·5

TABLE 4.

PERFORMANCE OF AIRSCREW A_6 WHEN UNAFFECTED BY THE SLIP-STREAM OF THE FORWARD AIRSCREW (*i.e.*, $T_f = 0$), BUT WITH INTERFERENCE OF FAIRED ENGINES.

Translational speed of airscrew = 25 ft. /sec.

Thrust.		Torque.		Efficiency.	
n (revs. /sec.).	T. (lbs.).	n (revs. /sec.).	Q (lbs.-ft.).	n (revs. /sec.).	η (percentage)
12·25	0·204	11·60	0·060	11·4	0
13·25	0·407	13·10	0·150	13·0	78·0
14·95	0·812	13·60	0·180	14·0	83·0
15·85	1·015	14·20	0·213	15·0	82·6
16·70	1·217	15·60	0·300	16·0	80·3
17·35	1·419	16·05	0·330	17·0	77·3
18·15	1·621	17·70	0·450	18·0	75·5
18·70	1·822	19·75	0·600	19·0	73·0
19·45	2·023	20·45	0·660	20·0	71·4
—	—	21·20	0·720	21·0	69·8
—	—	—	—	22·0	67·0

Table 5.

PERFORMANCE OF REAR AIRSCREW (A_6) OF COMBINATION No. 3.

Translational speed of airscrew = 25 (ft. /sec.).
Rotational speed of airscrew = n (revs. /sec.).
Thrust of forward airscrew (A_4) = T_f (lbs.).
Thrust of rear airscrew (A_6) = T_r (lbs.).
Torque of rear airscrew (A_6) = Q_r (lbs.).

Model of faired engines in place.

$T_r = 0{\cdot}8T_f$.			$T_r = T_f$.			$T_r = 1{\cdot}2T_f$.			Efficiency (percentage).			
T_r (lbs.).	n (revs. /sec.).	Q_r (lbs.-ft.).	T_r (lbs.).	n (revs. /sec.).	Q_r (lbs.-ft.).	T_r (lbs.).	n (revs. /sec.).	Q_r (lbs.-ft.).	n (revs. /sec.).	$T_r = 0{\cdot}8T_f$.	$T_r = T_f$.	$T_r = 1{\cdot}2T_f$.
0·32	14·20	—	0·40	14·45	—	0·48	14·55	—	11·4	0	0	0
0·52	15·75	0·230	0·65	16·20	0·260	0·78	16·95	0·312	13·0	52·2	56·7	62·0
0·72	16·80	0·287	0·90	17·60	0·340	1·08	18·20	0·382	14·0	58·0	62·0	66·2
0·92	18·10	0·327	1·15	18·85	0·385	1·38	19·55	0·438	15·0	59·1	63·0	67·8
1·12	19·25	0·386	1·40	20·10	0·454	1·68	20·90	0·515	16·0	60·2	63·5	67·3
1·28	20·10	0·435	1·60	21·10	0·520	1·92	21·90	0·588	17·0	61·3	63·5	67·1
1·44	20·80	0·465	1·80	21·90	0·565	2·16	22·90	0·653	18·0	61·2	62·5	65·5
1·60	21·50	0·515	2·00	22·80	0·630	2·40	23·80	0·720	19·0	60·5	62·2	64·2
—	—	—	—	—	—	—	—	—	20·0	59·6	60·5	62·3
—	—	—	—	—	—	—	—	—	21·0	58·4	59·2	60·6
—	—	—	—	—	—	—	—	—	22·0	57·1	57·6	59·1

Table 6.

PERFORMANCE OF THE REAR AIRSCREW (A_3) OF COMBINATION No. 4.

Translational speed of airscrew = 25 (ft. /sec.).
Rotational speed of airscrew = n (revs. /sec.).
Thrust of forward airscrew (A_5) = T_f (lbs.).
Thrust of rear airscrew (A_6) = T_r (lbs.).
Torque of rear airscrew (A_6) = Q_r (lbs.).

Model of faired engines in place.

$T_r = 0{\cdot}8T_f$.			$T_r = T_f$.			$T_r = 1{\cdot}2T_f$.			Efficiency (percentage).			
T_r (lbs.).	n (revs. /sec).	Q_r (lbs.-ft.).	T_r (lbs.).	n (revs. /sec.).	Q_r (lbs.-ft.).	T_r (lbs.).	n (revs. /sec.).	Q_r (lbs.-ft.).	(revs. /sec.).	$T_r = 0{\cdot}8T_f$.	$T_r = T_f$	$T_r = 1{\cdot}2T_f$.
0·32	13·85	0·130	0·40	14·15	0·145	0·48	14·45	0·160	11·4	0	0	0
0·52	15·30	0·185	0·65	15·85	0·225	0·78	16·35	0·257	13·0	65·0	71·0	75·0
0·72	16·55	0·250	0·90	17·30	0·295	1·08	17·90	0·325	14·0	70·5	73·5	78·4
0·92	17·90	0·307	1·15	18·70	0·365	1·38	19·40	0·418	15·0	72·3	75·0	78·8
1·12	19·05	0·382	1·40	19·85	0·445	1·68	20·80	0·521	16·0	70·2	73·2	76·8
1·28	19·95	0·400	1·60	20·90	0·492	1·92	21·90	0·592	17·0	67·0	70·6	74·4
1·44	20·70	0·470	1·80	21·80	0·575	2·16	22·90	0·680	18·0	65·0	68·8	71·6
1·60	21·60	0·520	2·00	22·80	0·638	—	—	—	19·0	63·0	65·5	68·6
—	—	—	—	—	—	—	—	—	20·0	60·6	63·5	65·4
—	—	—	—	—	—	—	—	—	21·0	58·6	60·2	62·0
—	—	—	—	—	—	—	—	—	22·0	56·9	57·8	59·2

TABLE 7.

THE EFFECT OF THE THRUST OF THE REAR AIRSCREW OF COMBINATION No. 3 ON THE FORWARD AIRSCREW (A_4), AS SHOWN BY MEASUREMENT OF THE THRUST AND ROTATIONAL SPEED OF THE FORWARD AIRSCREW.

Translational speed of airscrew = 25 (ft. /sec.).
Thrust of forward airscrew (A_4) = T_f (lbs.).
Thrust of rear airscrew (A_6) = T_r (lbs.).

Model of faired engines in place.

Value of T_f (lbs.).	Rotational Speed of the Forward Airscrew (A_4) (revs. /sec.) when :			
	$T_r = 0 \times T_f$.	$T_r = 0{\cdot}8T_f$.	$T_r = 1{\cdot}0T_f$.	$T_r = 1{\cdot}2T_f$.
0·65	18·90	19·00	19·00	19·00
0·90	20·95	20·20	20·20	20·20
1·10	22·80	22·70	22·60	22·60
1·45	24·70	24·70	24·80	24·80
1·60	26·15	26·00	25·90	26·10
1·80	27·70	27·40	27·40	27·50
2·00	29·10	28·30	28·50	28·50

TABLE 8.

THE EFFECT OF THE THRUST OF THE REAR AIRSCREW OF COMBINATION No. 4 ON THE FORWARD AIRSCREW (A_5), AS SHOWN BY MEASUREMENTS OF THE THRUST AND ROTATIONAL SPEED OF THE FORWARD AIRSCREW.

Translational speed of airscrew = 25 (ft. /sec.).
Thrust of forward airscrew (A_5)=T_f (lbs.).
Thrust of rear airscrew (A_6) = T_r (lbs.).

Model of faired engines in place.

Value of T_f (lbs.).	Rotational Speed of the Forward Airscrew (A_4) (revs. /sec.) when :			
	$T_r = 0 \times T_f$.	$T_r = 0{\cdot}8T_f$.	$T_r = 1{\cdot}0T_f$.	$T_r = 1{\cdot}2T_f$.
0·40	—	13·10	13·00	13·10
0·65	13·80	14·10	14·00	14·00
0·90	14·60	14·70	14·70	14·60
1·15	15·40	15·50	15·55	15·60
1·40	16·12	16·20	16·05	16·15
1·60	16·70	16·75	16·75	16·70
1·80	17·20	17·15	17·15	17·25
2·00	17·75	17·80	17·90	17·60

EXPERIMENTS on TANDEM AIRSCREWS

Sketch of Model Airscrew A_2 (Diam. 18 ins) Two blades.

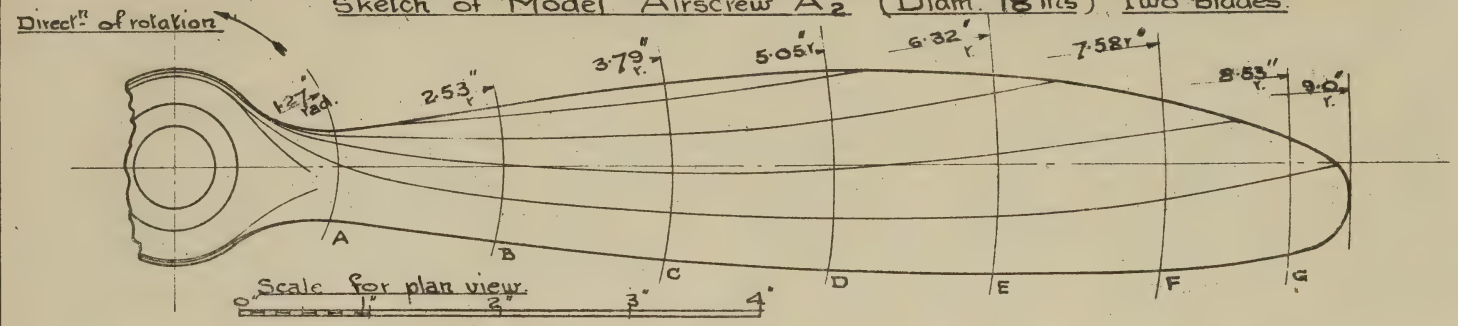

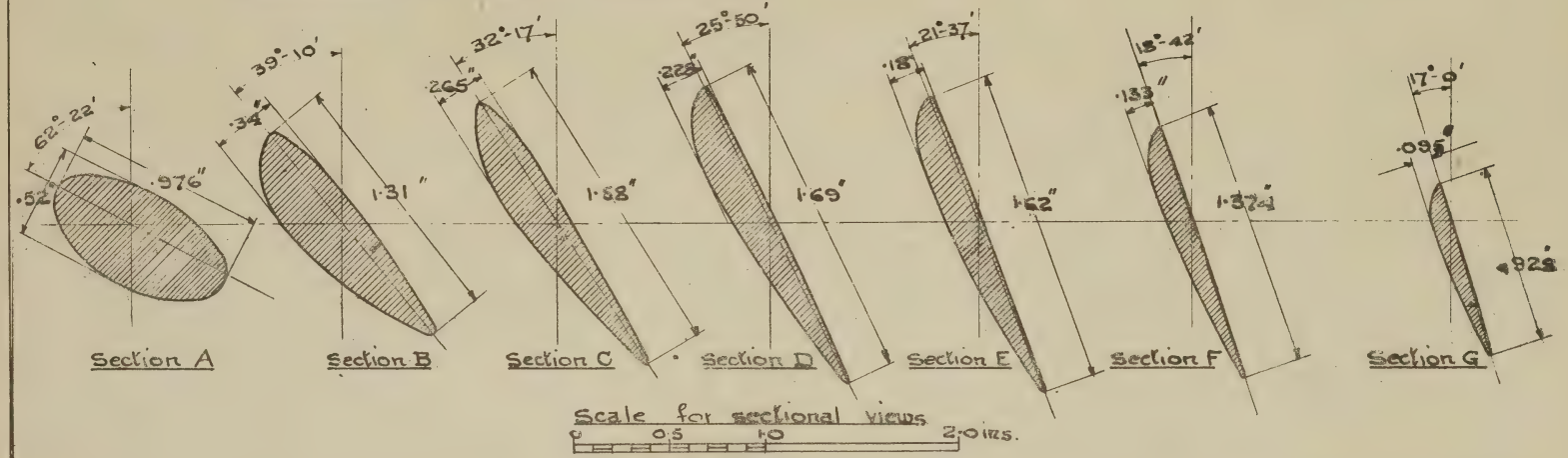

Note. Airscrew A_1 has same plan form & sections as airscrew A_2, but rotates in the opposite direction.

Airscrew A_3 has same plan form, sections, and direction of rotation as A_2, but has slightly smaller blade angles.

EXPERIMENTS on TANDEM AIRSCREWS.

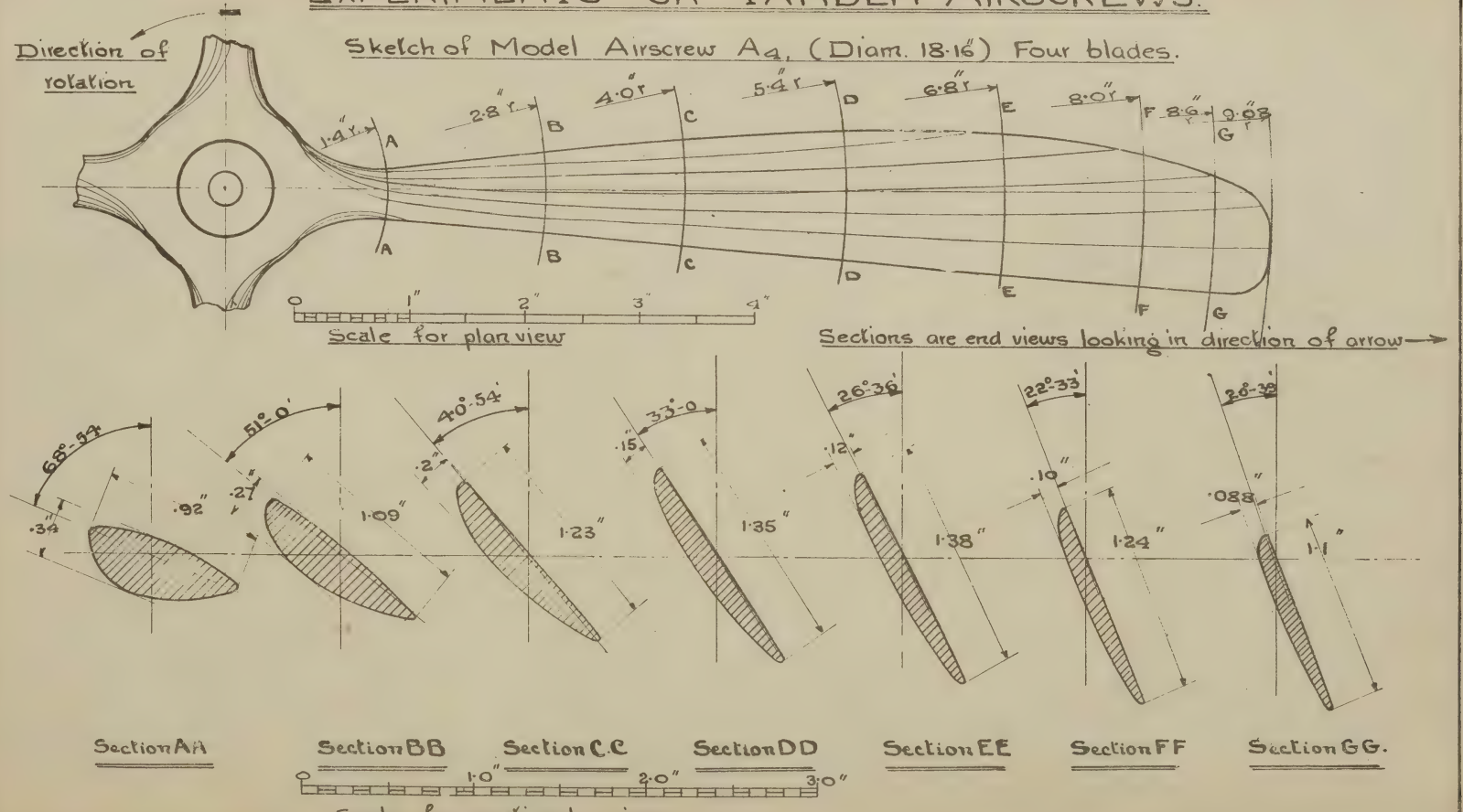

EXPERIMENTS ON TANDEM AIRSCREWS.

Sketch of Model Airscrew A_5, (Diam. 27") Four blades.

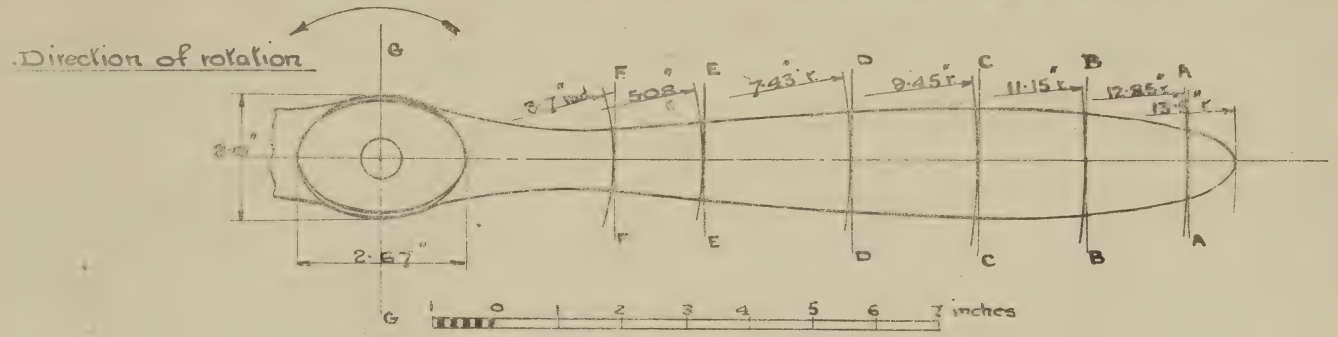

Scale for plan view.

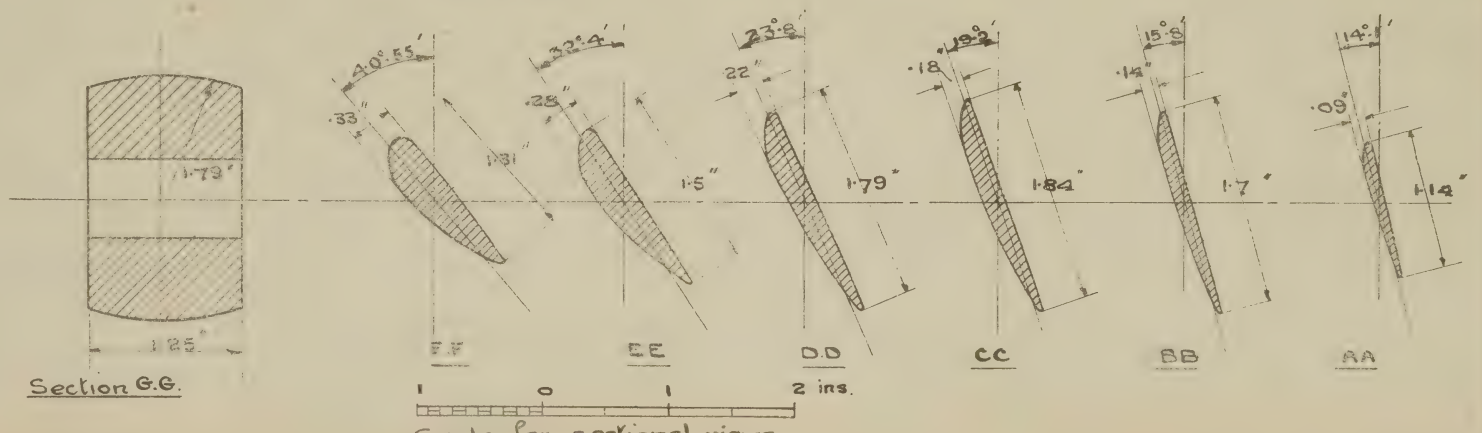

Scale for sectional views.

REPORT No 421.

FIG. 3.

EXPERIMENTS ON TANDEM AIRSCREWS.

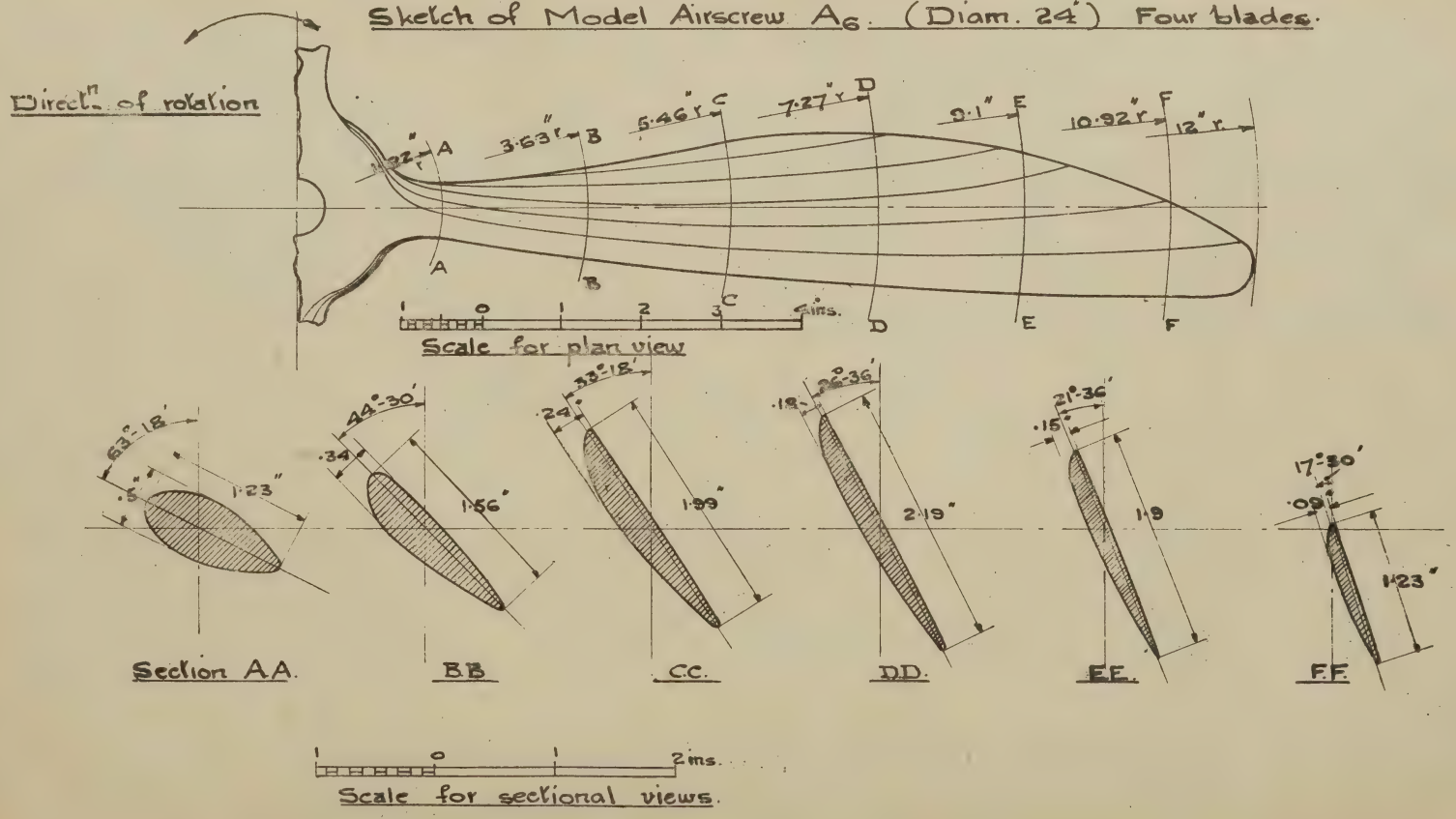

REPORT No 421.

FIG. 4.

—EXPERIMENTS ON TANDEM AIRSCREWS.—

Sketch of model of faired engines.

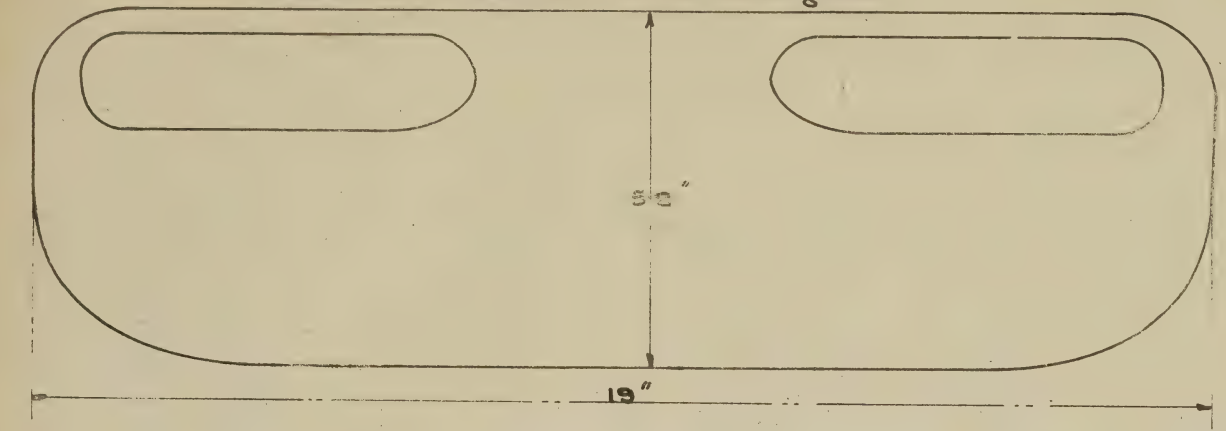

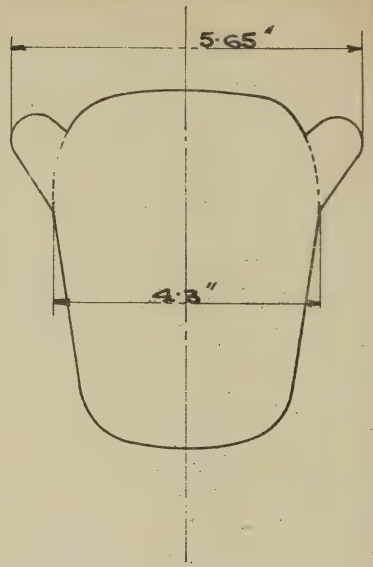

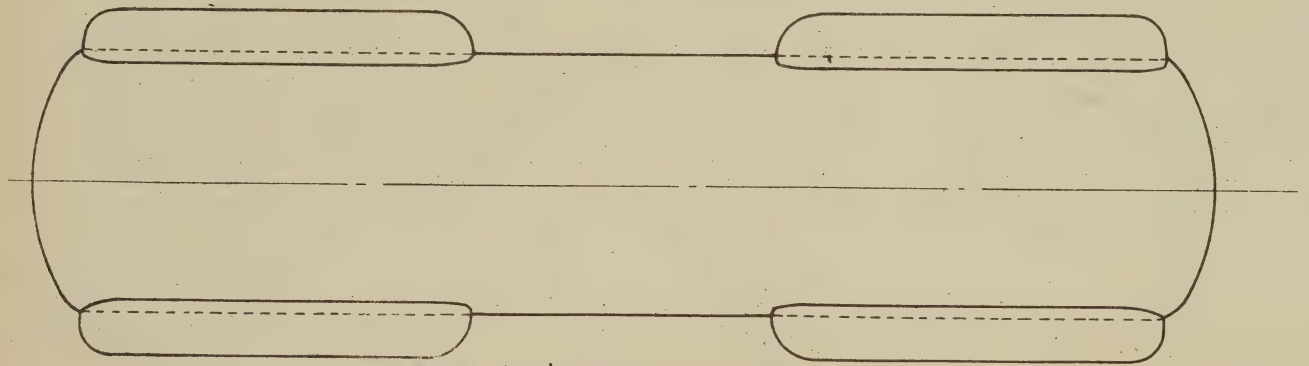

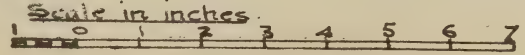

FIG. 5.

EXPERIMENTS ON TANDEM AIRSCREWS.

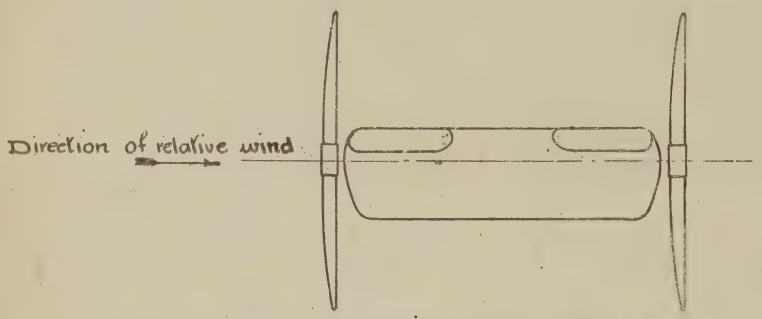

Combinations Nos 1 & 2.

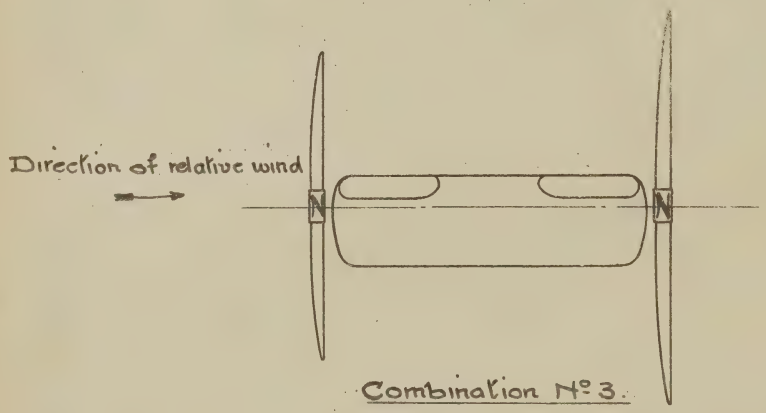

Combination Nº 3.

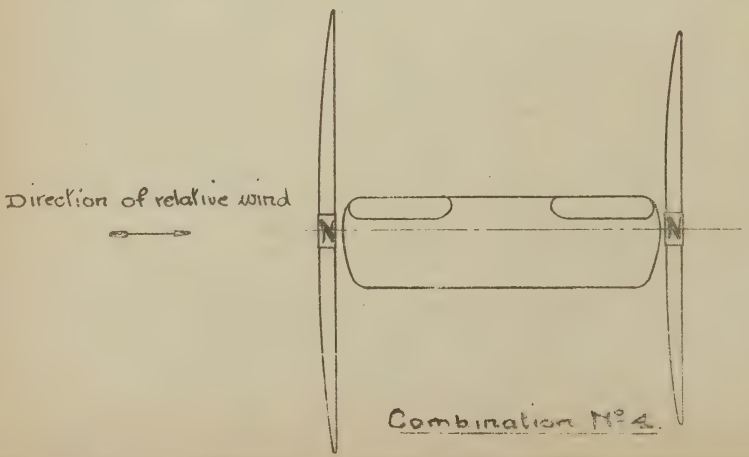

Combination Nº 4.

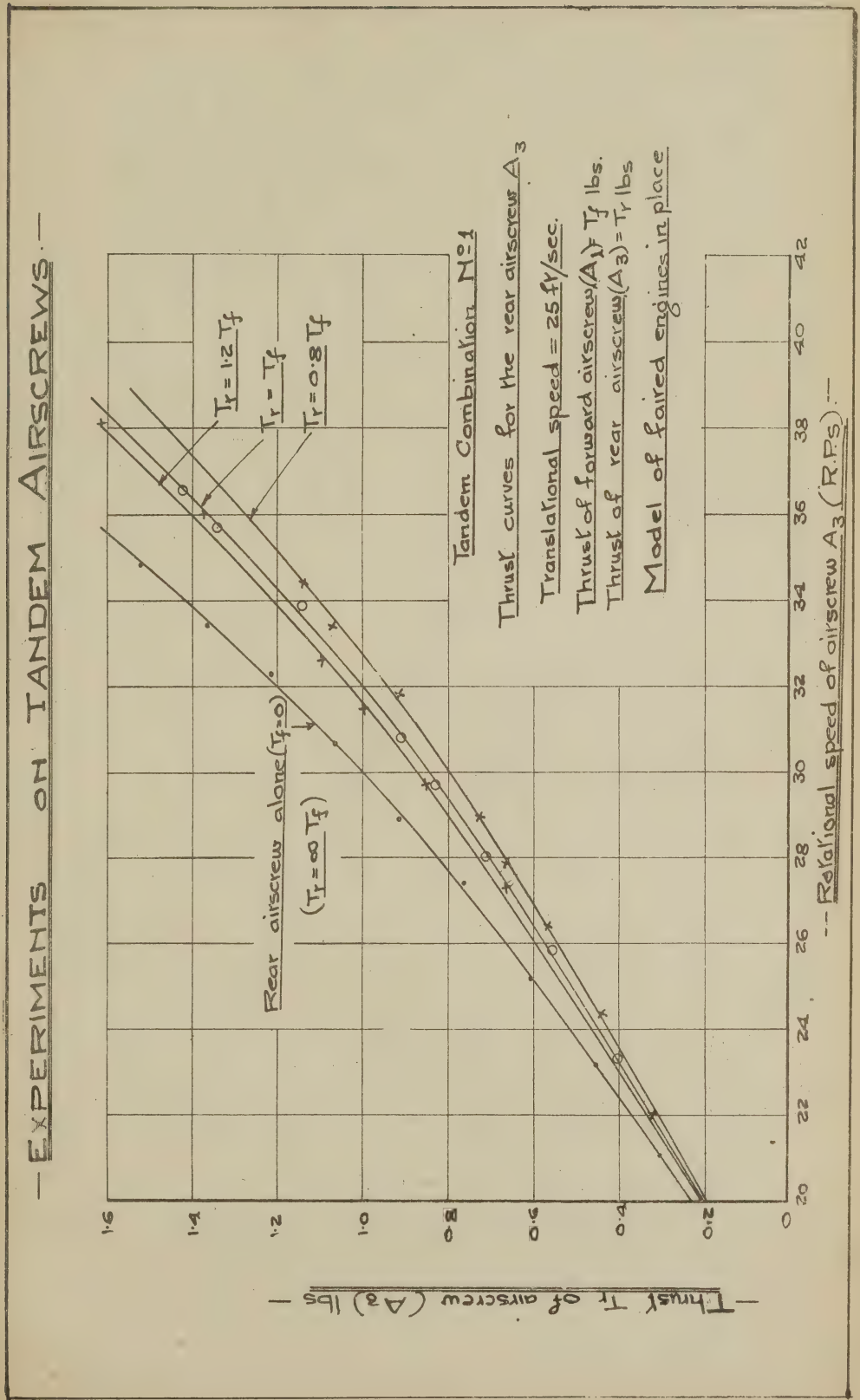
— EXPERIMENTS ON TANDEM AIRSCREWS —
Tandem Combination Nº1
Thrust curves for the rear airscrew A3
Translational speed = 25 ft/sec.
Thrust of forward airscrew (A1) Tf lbs.
Thrust of rear airscrew (A3) = Tr lbs
Model of paired engines in place
Tr = 1·2 Tf
Tr = Tf
Tr = 0·8 Tf
Rear airscrew alone (Tf = 0)
(Tr = ∞ Tf)
— Thrust Tr of airscrew (A3) lbs —
— Rotational speed of airscrew A3 (R.P.S.) —
0
0·2
0·4
0·6
0·8
1·0
1·2
1·4
1·6
20
22
24
26
28
30
32
34
36
38
40
42

— EXPERIMENTS ON TANDEM AIRSCREWS —

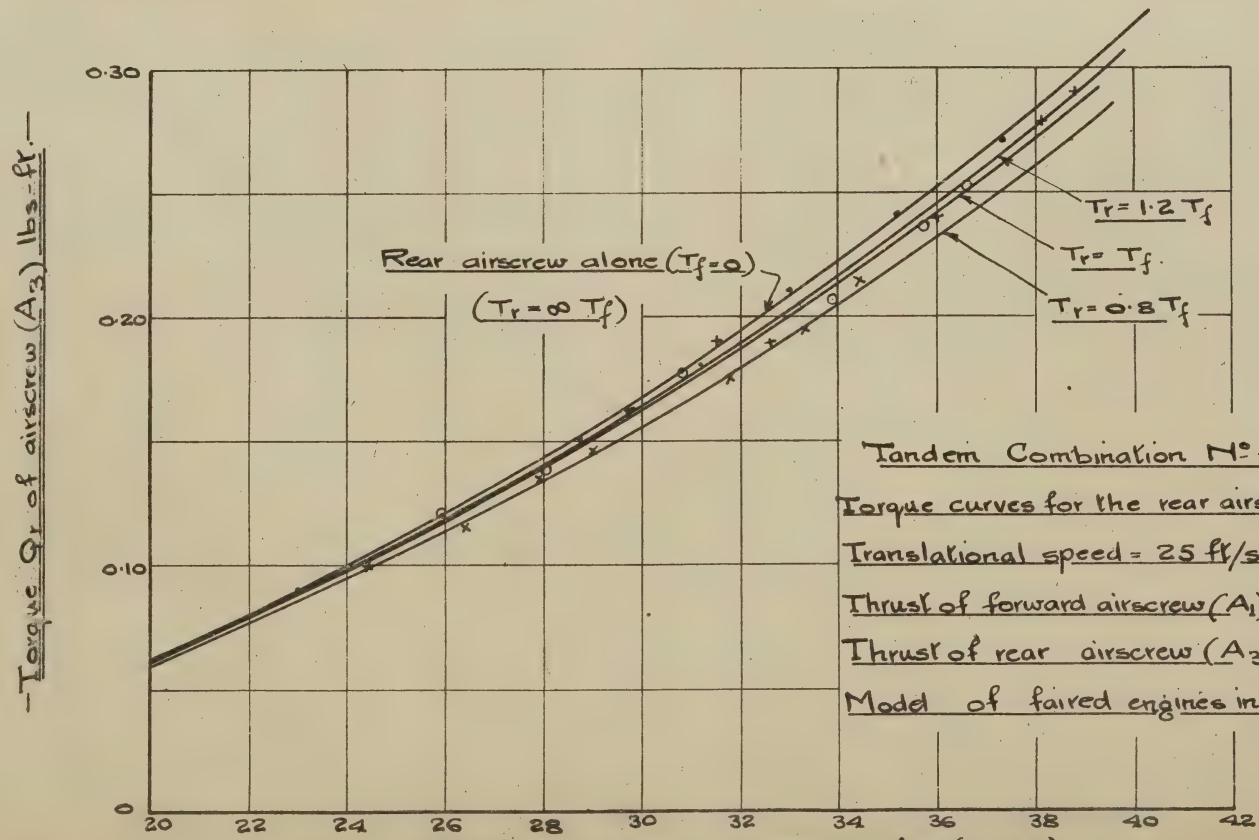

Tandem Combination Nº 1.

Torque curves for the rear airscrew A_3.

Translational speed = 25 ft/sec.

Thrust of forward airscrew (A_1) = T_f lbs

Thrust of rear airscrew (A_3) = T_r lbs.

Model of faired engines in place.

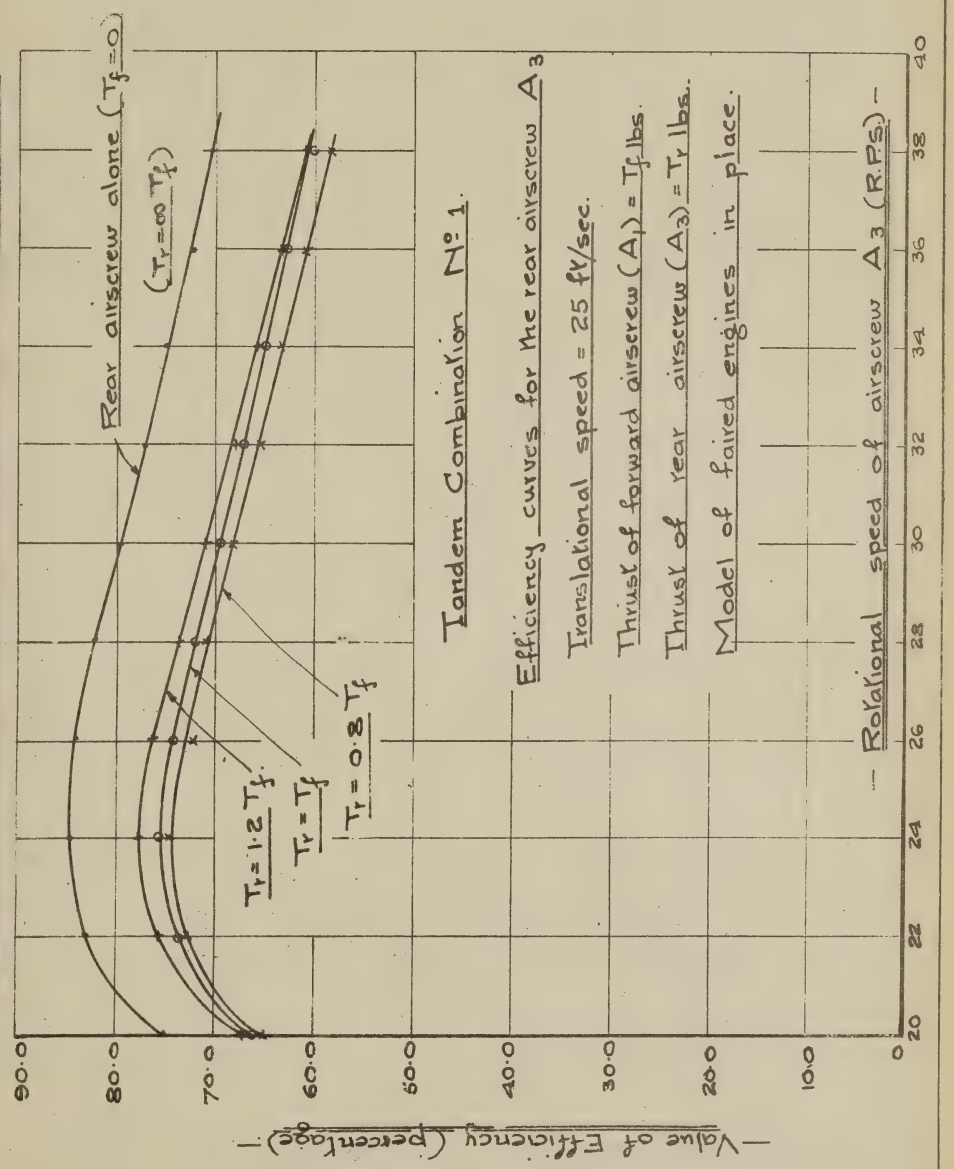
- EXPERIMENTS ON TANDEM AIRSCREWS. -
Tandem Combination Nº 1.
Efficiency curves for the rear airscrew A3
Translational speed = 25 ft/sec.
Thrust of forward airscrew (A1) = Tf lbs.
Thrust of rear airscrew (A3) = Tr lbs.
Model of faired engines in place.
Rear airscrew alone (Tf=0)
(Tr=∞ Tf)
Tr = 1·2 Tf.
Tr = Tf
Tr = 0·8 Tf
— Value of Efficiency (percentage) —
— Rotational speed of airscrew A3 (R.P.S.) —
90·0
80·0
70·0
60·0
50·0
40·0
30·0
20·0
10·0
0
20
22
24
26
28
30
32
34
36
38
40

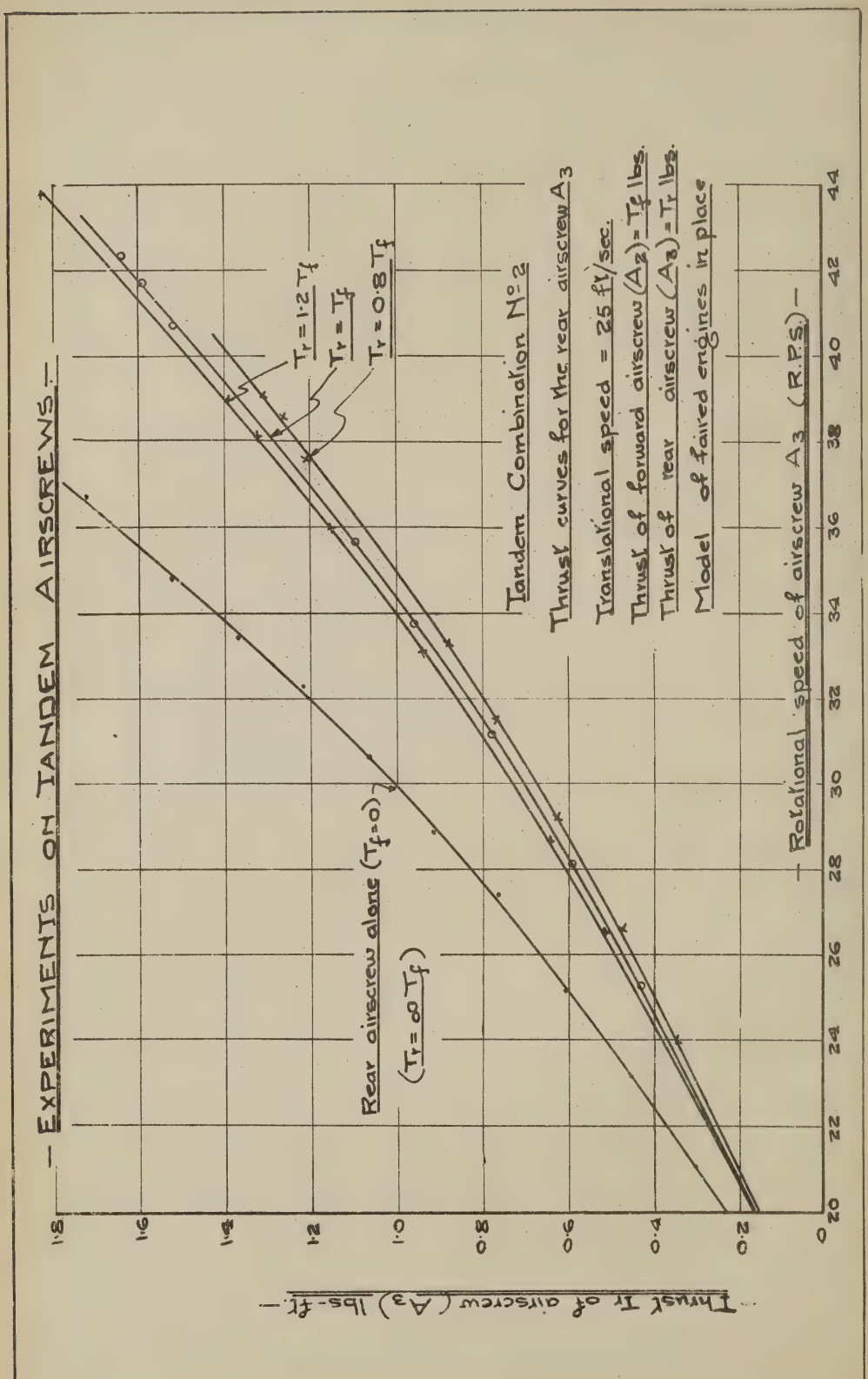
— EXPERIMENTS ON TANDEM AIRSCREWS —
Tandem Combination Nº 2
Thrust curves for the rear airscrew A3
Translational speed = 25 ft/sec.
Thrust of forward airscrew (A2) = Tf lbs.
Thrust of rear airscrew (A3) = Tr lbs.
Model of faired engines in place
Rotational speed of airscrew A3 (R.P.S.)
Thrust Tr of airscrew (A3) lbs-ft.
Tr = 1·2 Tf
Tr = Tf
Tr = 0·8 Tf
Rear airscrew alone (Tf = 0)
(Tr = ∞ Tf)
0·2
0·4
0·6
0·8
1·0
1·2
1·4
1·6
1·8
20
22
24
26
28
30
32
34
36
38
40
42
44

—EXPERIMENTS ON TANDEM AIRSCREWS—

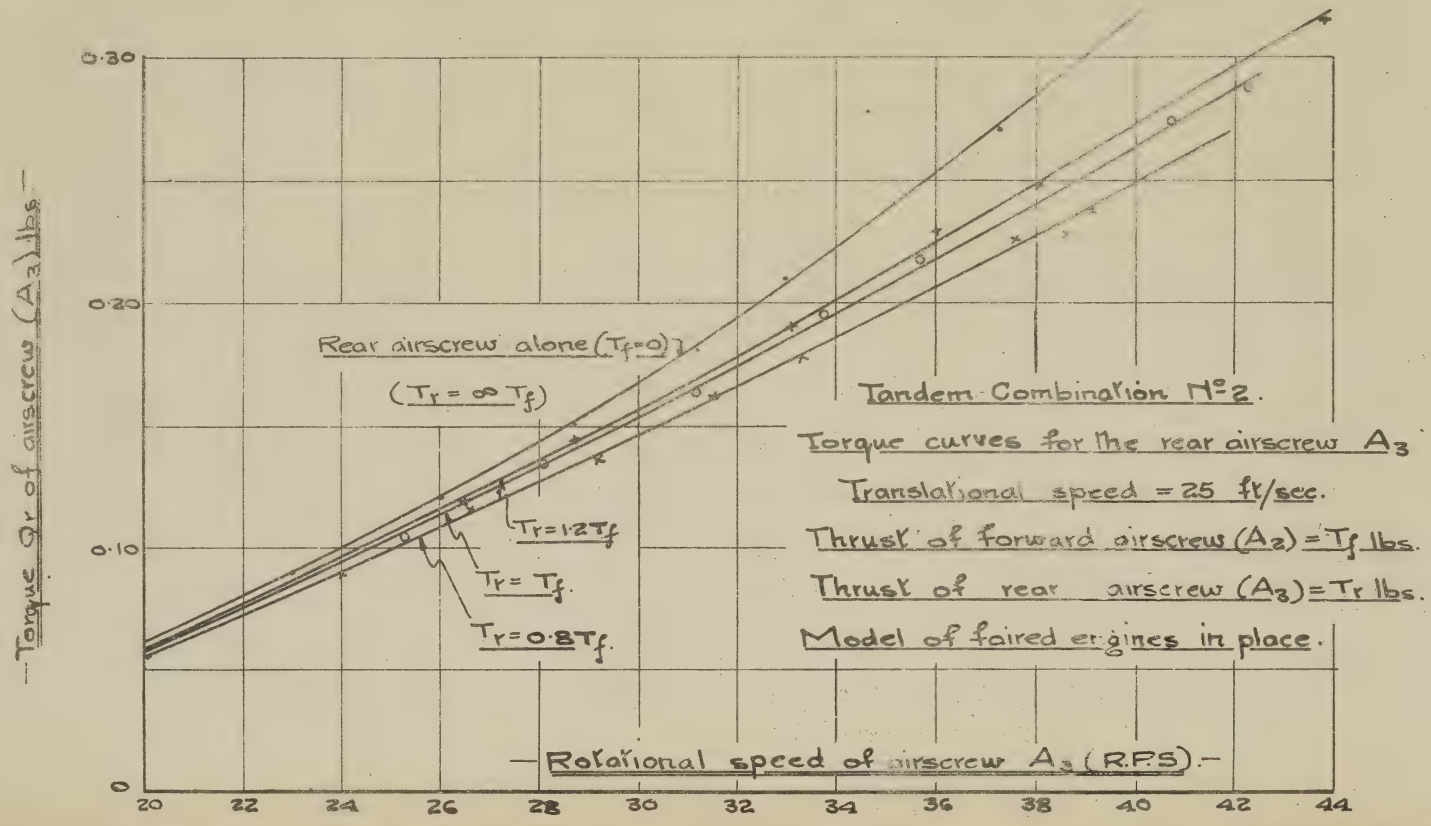

— EXPERIMENTS ON TANDEM AIRSCREWS —

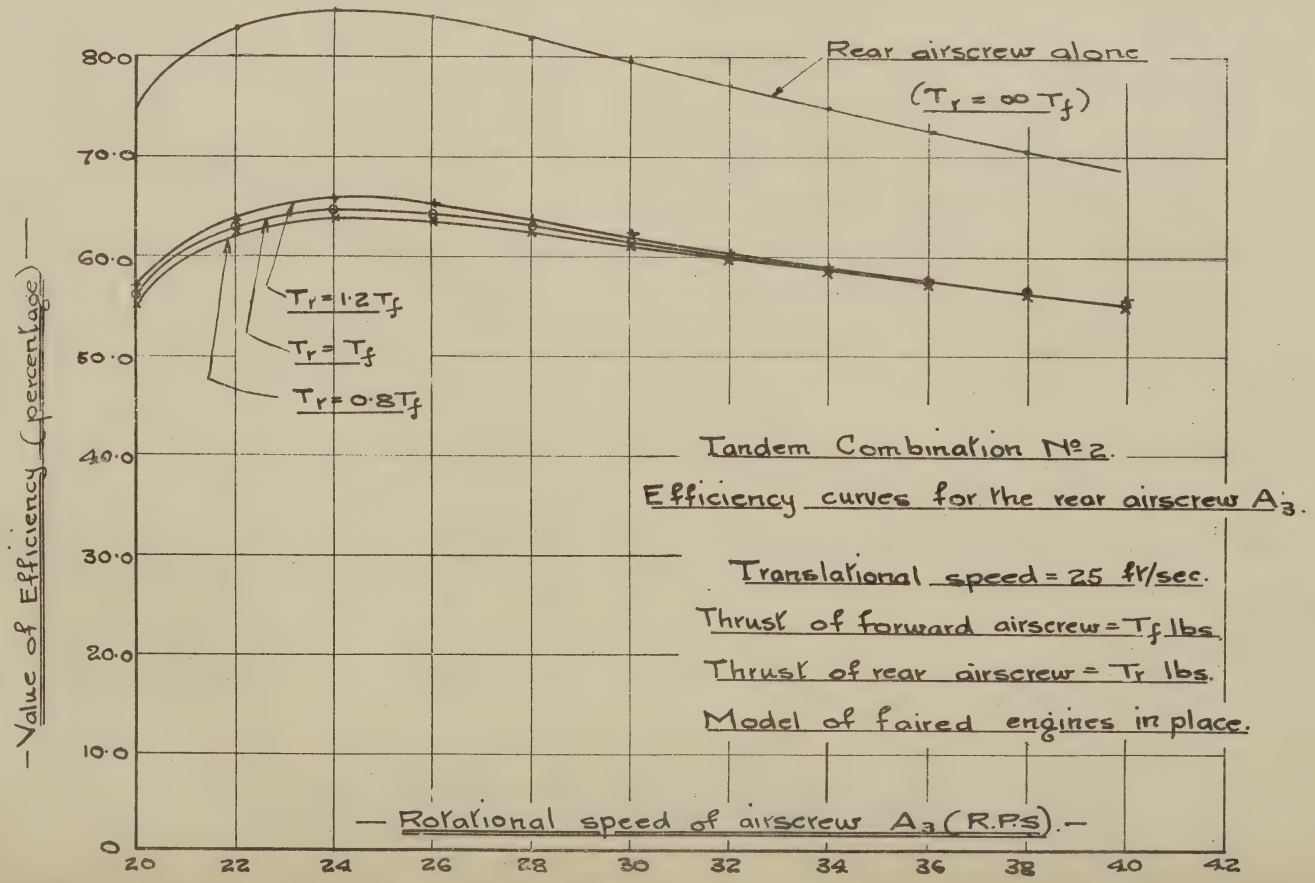

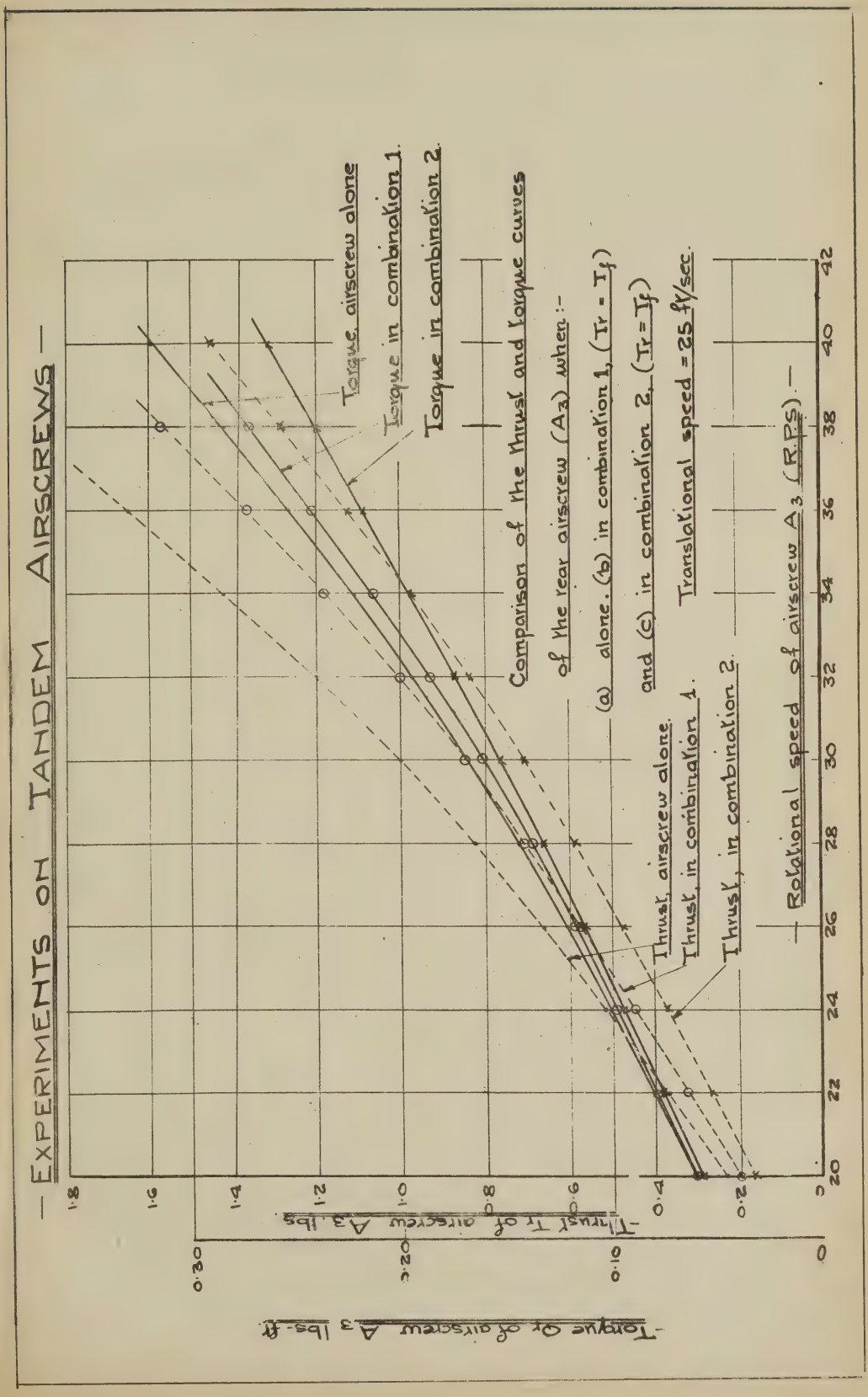
— EXPERIMENTS ON TANDEM AIRSCREWS —
Comparison of the thrust and torque curves of the rear airscrew (A_3) when :-
(a) alone. (b) in combination 1, ($T_r = T_f$) and (c) in combination 2. ($T_r = T_f$)
Translational speed = 25 ft/sec.
Torque, airscrew alone
Torque in combination 1.
Torque in combination 2.
Thrust, airscrew alone.
Thrust, in combination 1.
Thrust, in combination 2.
— Rotational speed of airscrew A_3 (R.P.S) —
Torque Q of airscrew A_3 lbs-ft
Thrust T of airscrew A_3 lbs
0·30
0·20
0·10
0
1·8
1·6
1·4
1·2
1·0
0·8
0·6
0·4
0·2
0
20
22
24
26
28
30
32
34
36
38
40
42

— EXPERIMENTS ON TANDEM AIRSCREWS —

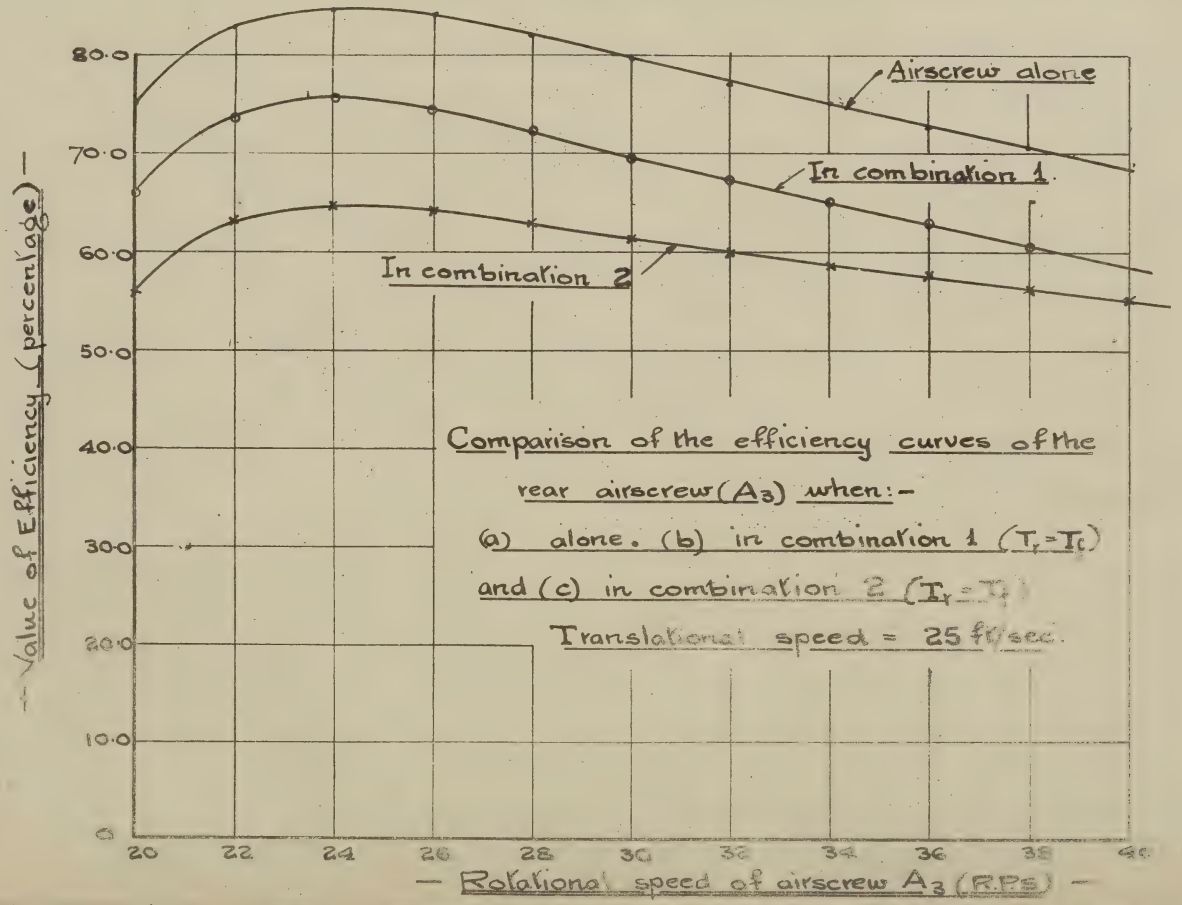

Comparison of the efficiency curves of the rear airscrew (A_3) when:-

(a) alone. (b) in combination 1 ($T_r = T_f$) and (c) in combination 2 ($T_r = T_f$)

Translational speed = 25 ft/sec.

— EXPERIMENTS ON TANDEM AIRSCREWS —

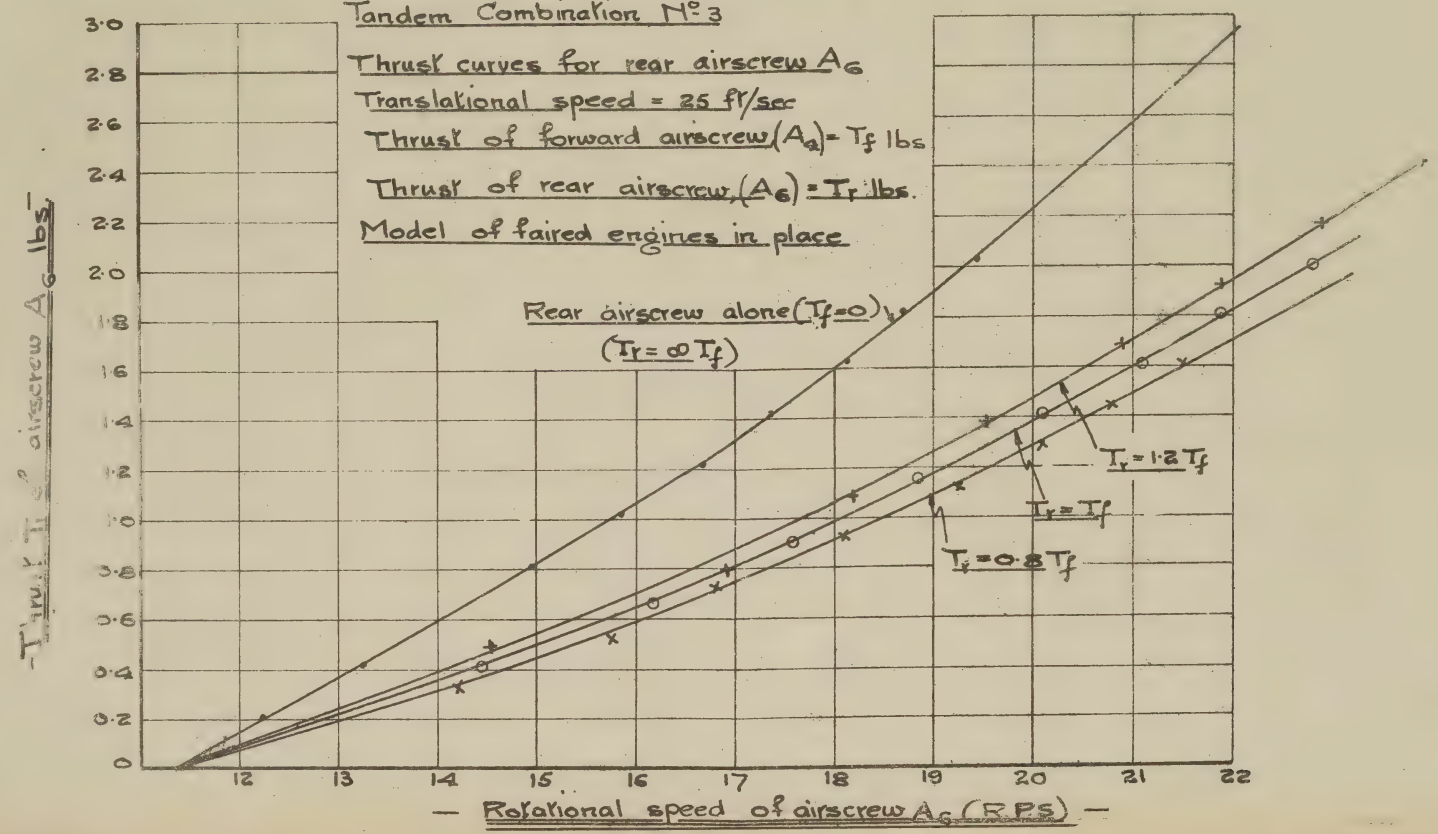

— EXPERIMENTS ON TANDEM AIRSCREWS —

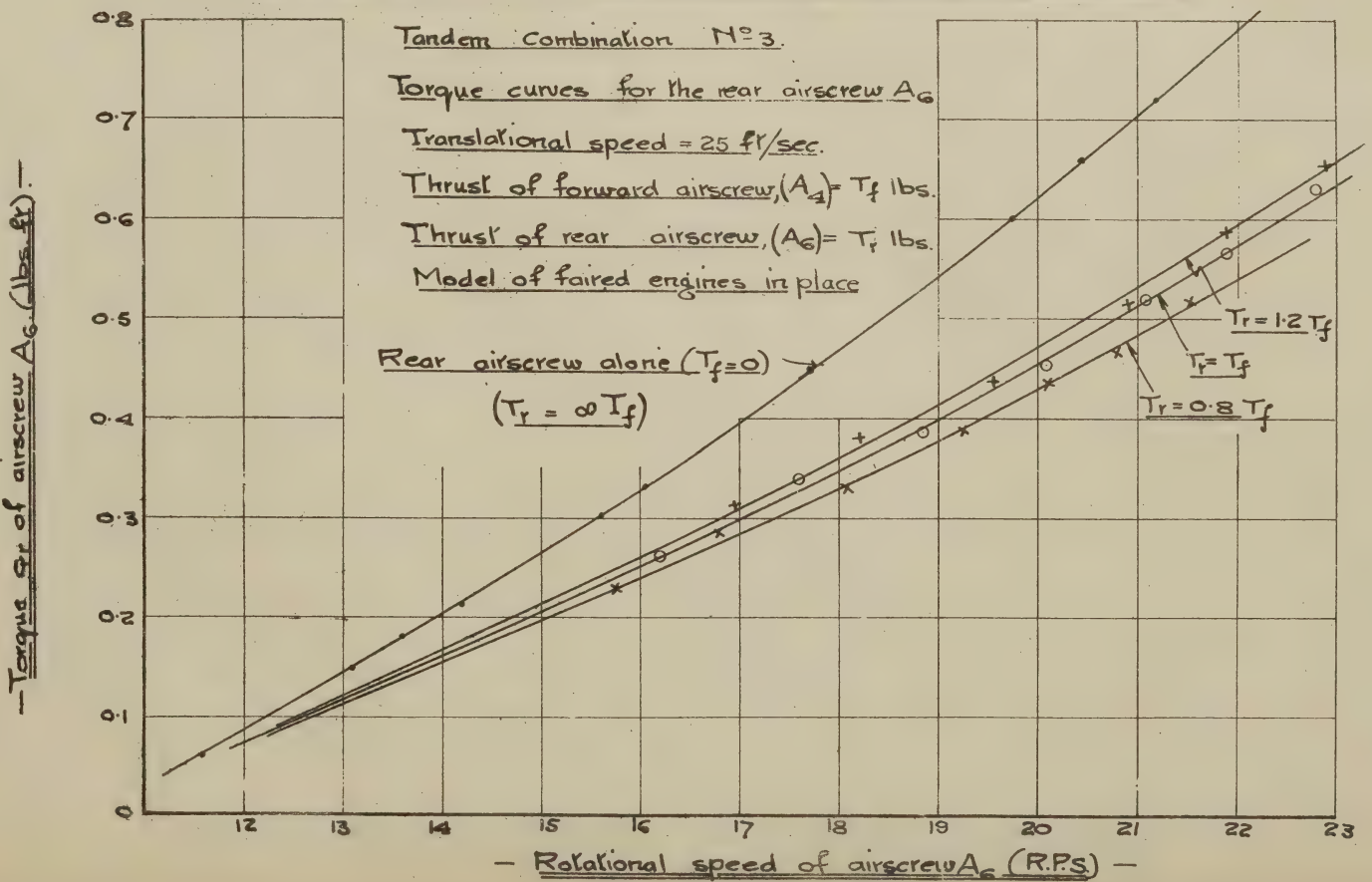

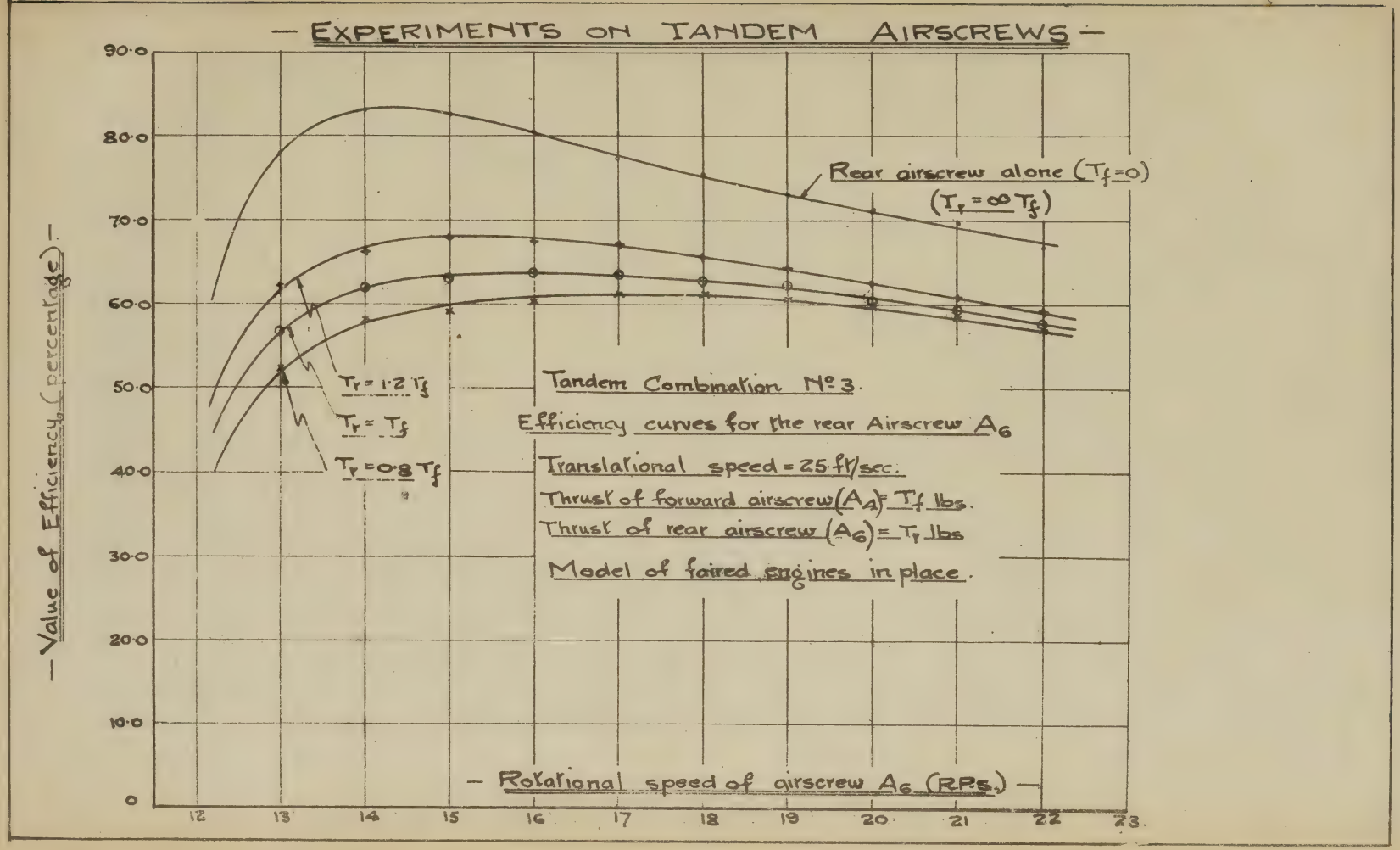
— EXPERIMENTS ON TANDEM AIRSCREWS —
— Value of Efficiency (percentage) —
90·0
80·0
70·0
60·0
50·0
40·0
30·0
20·0
10·0
0
12
13
14
15
16
17
18
19
20
21
22
23
Rear airscrew alone ($T_f = 0$)
($T_r = \infty T_f$)
$T_r = 1{\cdot}2\ T_f$
$T_r = T_f$
$T_r = 0{\cdot}8\ T_f$
Tandem Combination Nº 3.
Efficiency curves for the rear Airscrew A_6
Translational speed = 25 ft/sec.
Thrust of forward airscrew (A_4) = T_f lbs.
Thrust of rear airscrew (A_6) = T_r lbs
Model of faired engines in place.
— Rotational speed of airscrew A_6 (RPS.) —

- EXPERIMENTS ON TANDEM AIRSCREWS -

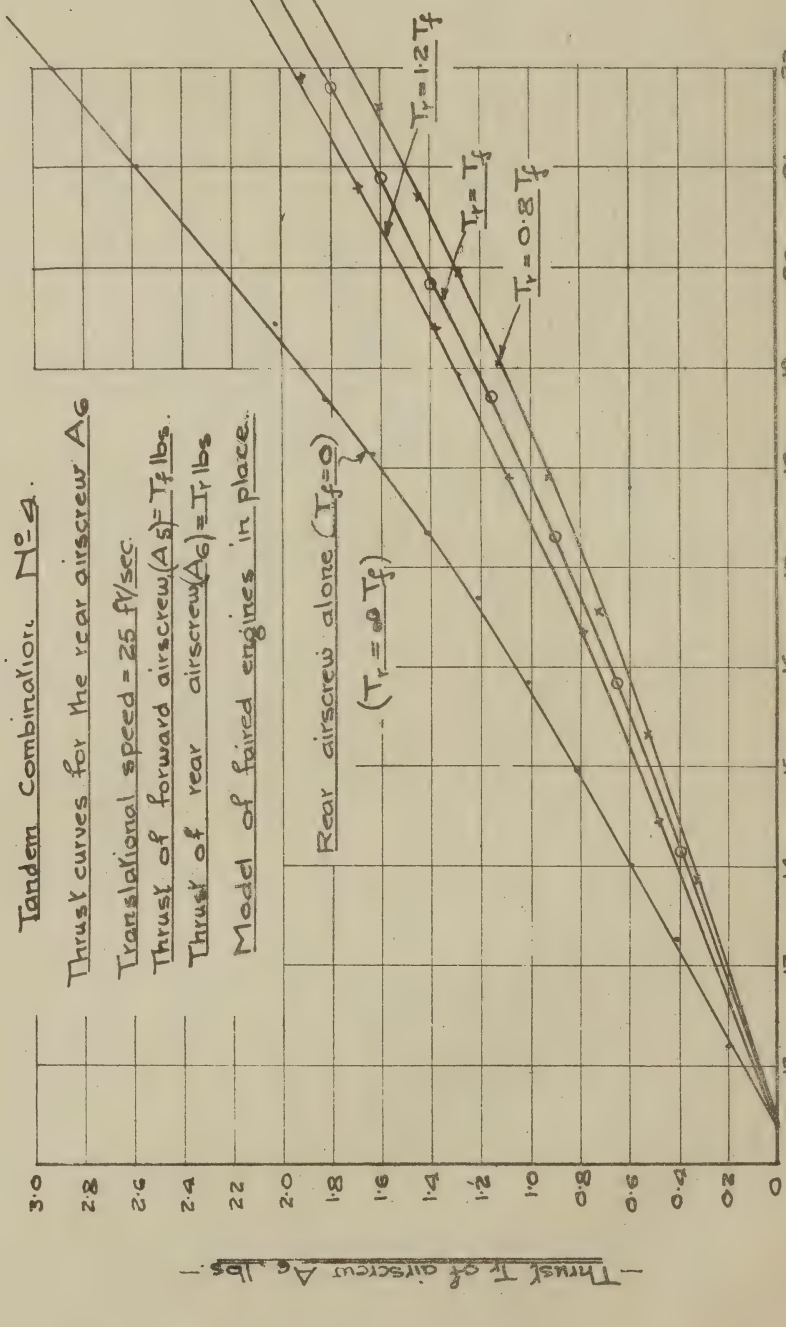
Tandem Combination Nº 4.
Thrust curves for the rear airscrew A6
Translational speed = 25 ft/sec.
Thrust of forward airscrew (A5) = Tf lbs.
Thrust of rear airscrew (A6) = Tr lbs
Model of paired engines in place.
Rear airscrew alone (Tf = 0)
(Tr = 0 Tf)
Tr = 1·2 Tf
Tr = Tf
Tr = 0·8 Tf
— Thrust T of airscrew A6 lbs. —
— Rotational speed of airscrew A6 (R.P.S.) —

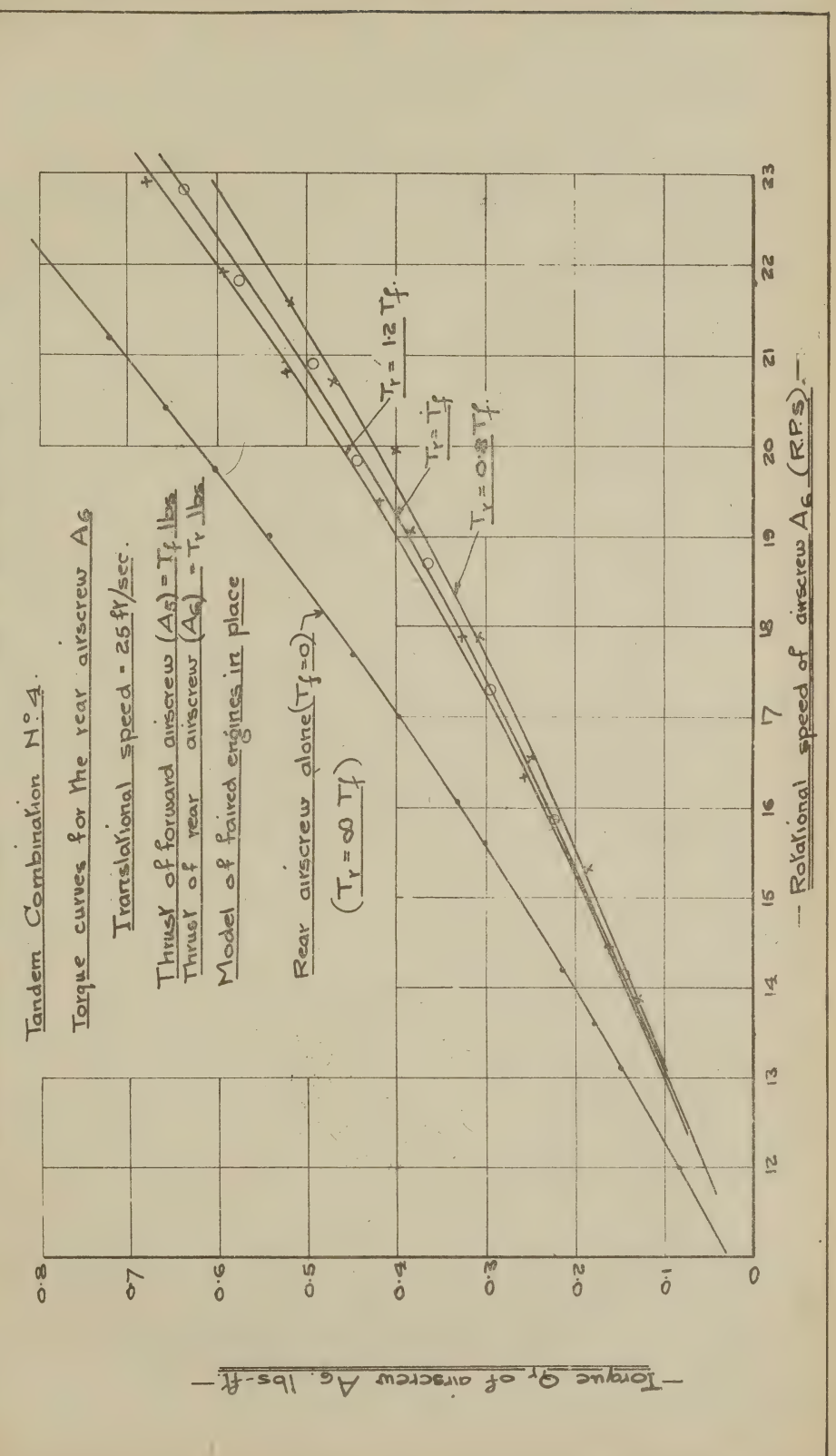
— EXPERIMENTS ON TANDEM AIRSCREWS —
Tandem Combination N°4.
Torque curves for the rear airscrew A_6
Translational speed - 25 ft/sec.
Thrust of forward airscrew $(A_5) = T_f$ lbs.
Thrust of rear airscrew $(A_6) = T_r$ lbs.
Model of paired engines in place
Rear airscrew alone $(T_f = 0)$
$(T_r = 0.0\ T_f)$
$T_r = 1.2\ T_f$
$T_r = T_f$
$T_r = 0.8\ T_f$
— Torque Q_r of airscrew A_6 lbs-ft —
— Rotational speed of airscrew A_6 (R.P.S.) —
0·8
0·7
0·6
0·5
0·4
0·3
0·2
0·1
0
12
13
14
15
16
17
18
19
20
21
22
23

EXPERIMENTS ON TANDEM AIRSCREWS.

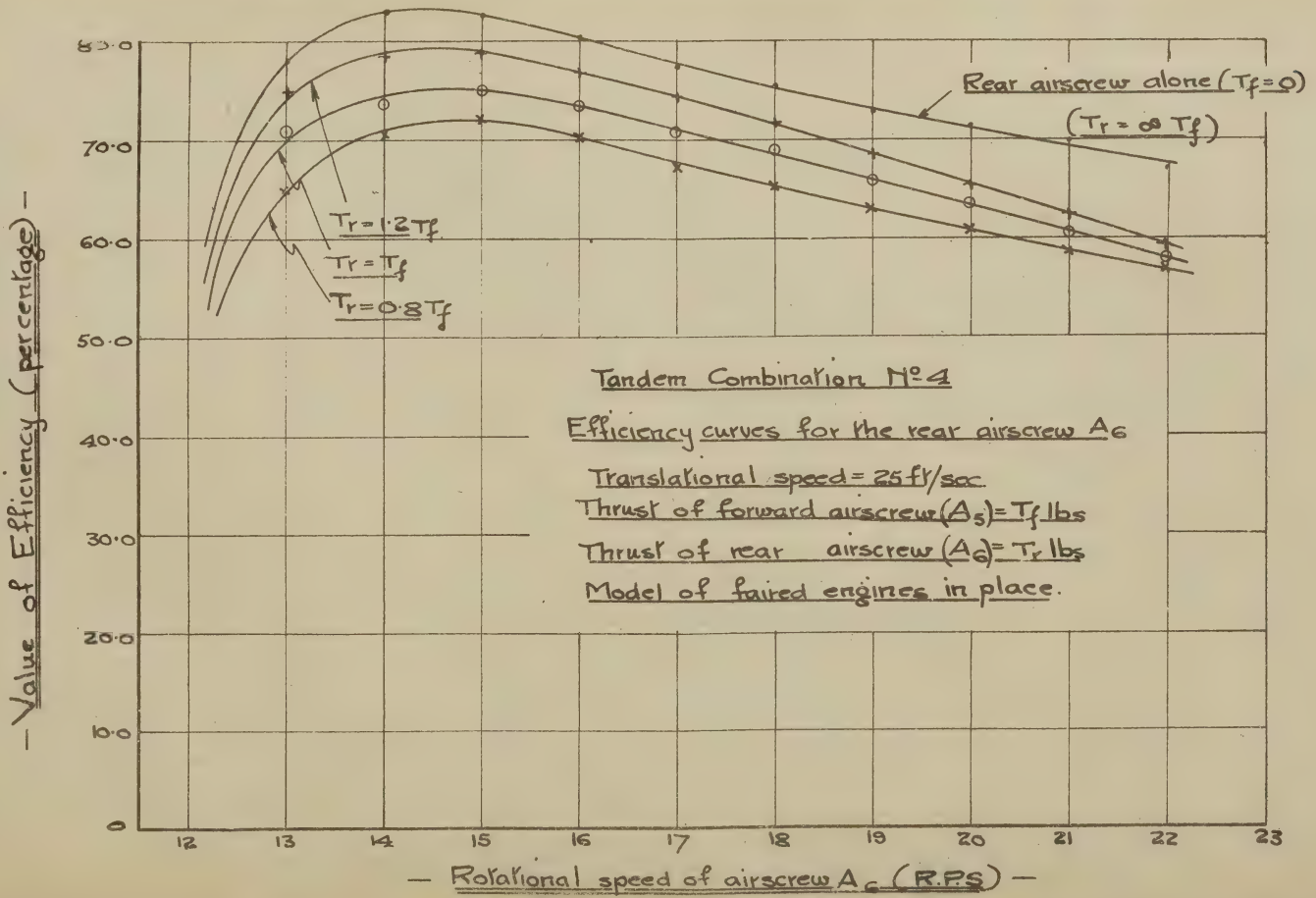

— EXPERIMENTS ON TANDEM AIRSCREWS —

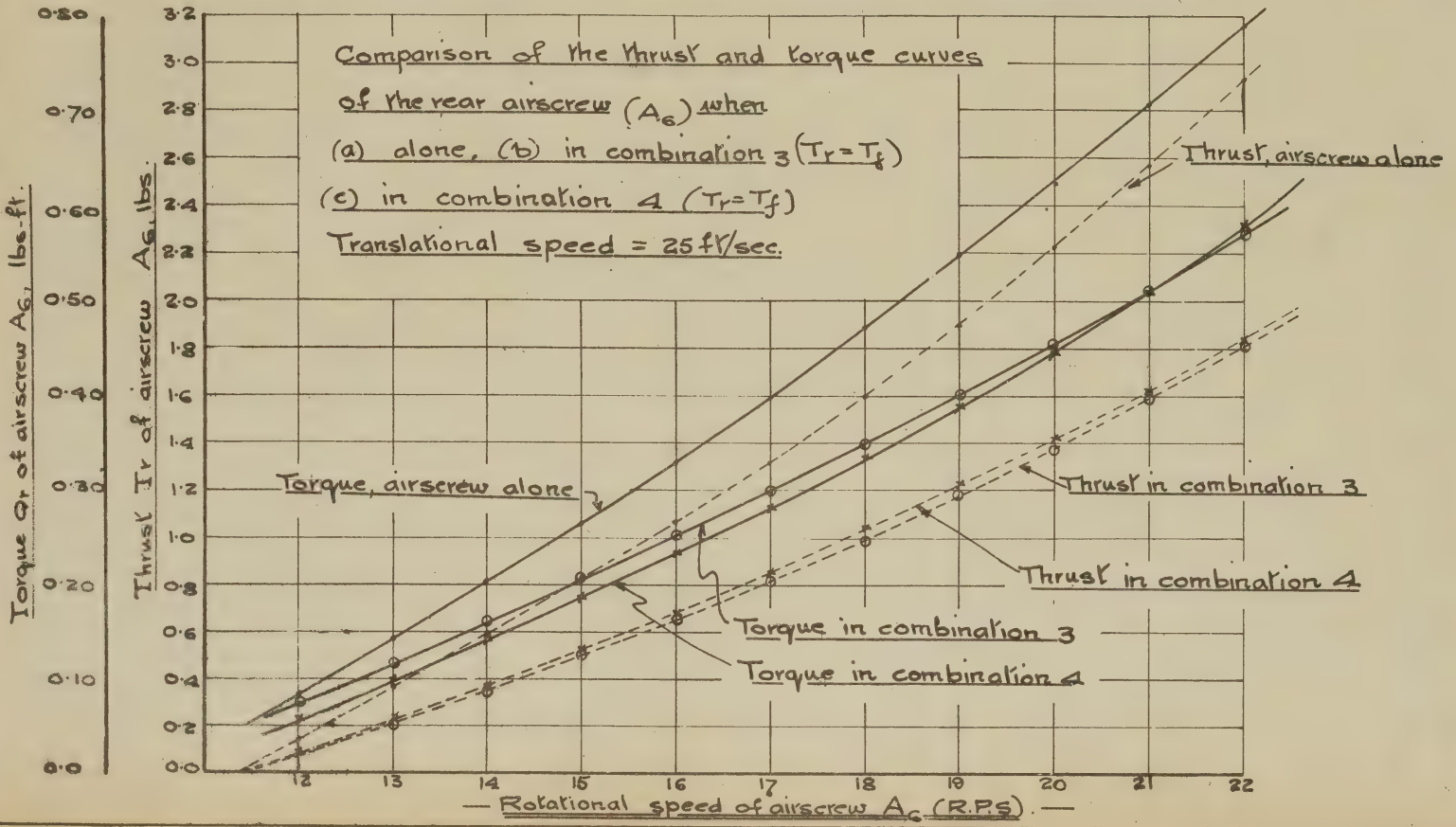

— EXPERIMENTS ON TANDEM AIRSCREWS —

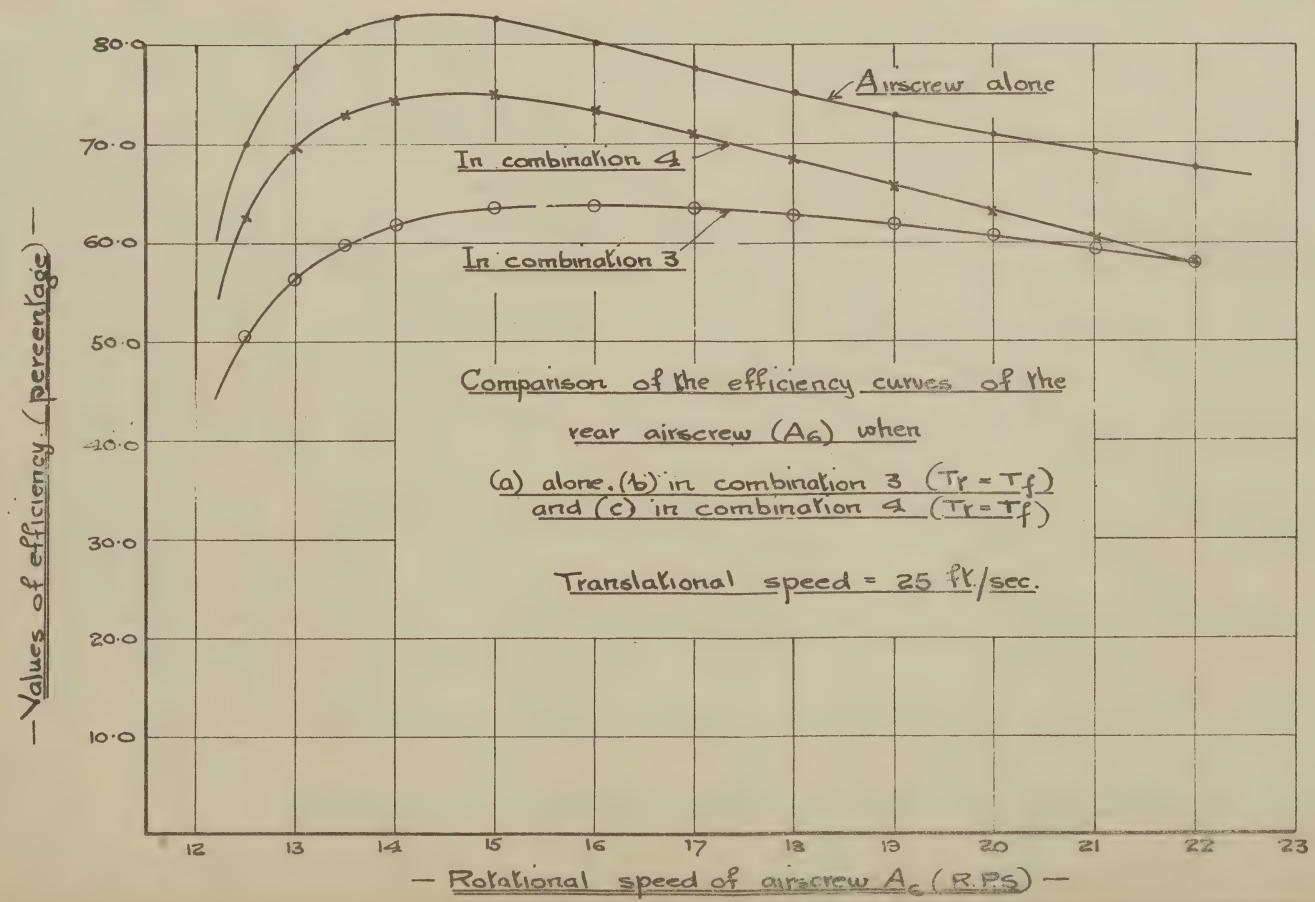

EXPERIMENTS ON TANDEM AIRSCREWS

Curves showing interference of the rear airscrew on the thrust of the forward airscrew.

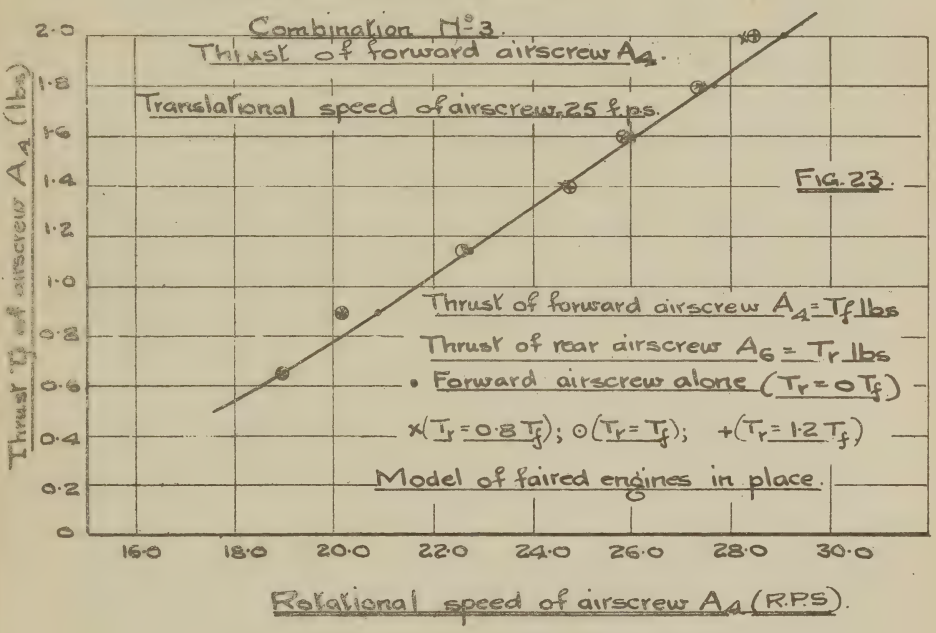

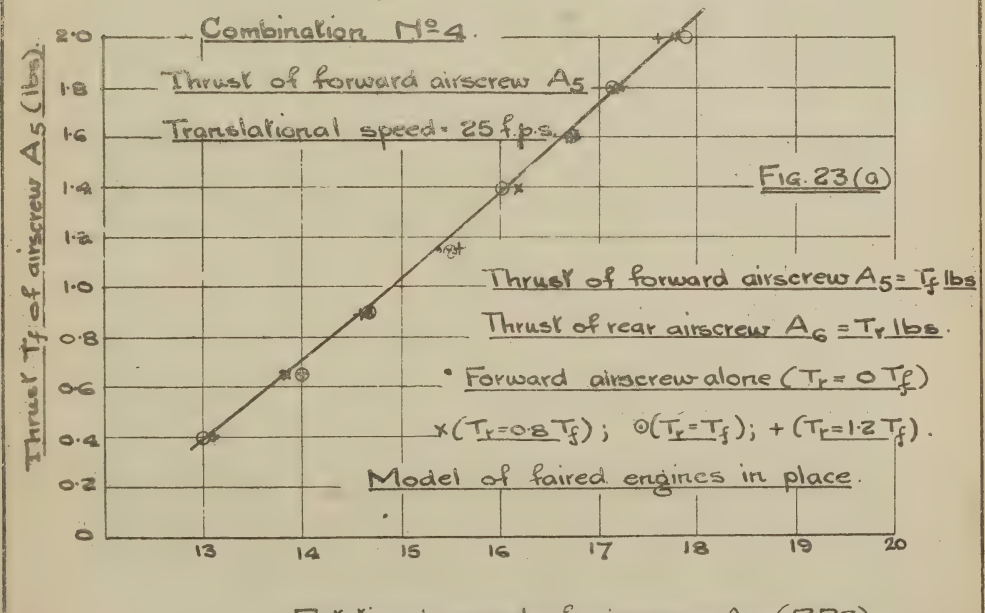

THE LIBRARY
OF THE
UNIVERSITY OF ILLINOIS

AN ANALYSIS OF THE ENERGY ACCOUNT OF AN AIRSCREW WITH AN APPLICATION TO THE CASE OF THE TANDEM AIRSCREW. (WITH APPENDIX.)

By A. Fage, A.R.C.Sc., D.I.C.

Reports and Memoranda, No. 429. *January,* 1918.

Summary.—(a) *Introductory* (*reasons for inquiry*).—It was suggested by the Aerodynamics Sub-Committee that the work of R. & M. 385, which is a theoretical investigation of the efficiency of a tandem combination of airscrews, should be further extended to consider the case of airscrews absorbing equal power, and rotating in opposite directions.

(b) *Range of investigation.*—An analysis of the energy account of an airscrew is made, which gives some idea of the probable magnitude of the reconvertible energy of the slip stream. It is shown that the energy put into an airscrew reappears in several forms—useful work, kinetic energies of translation and rotation, potential energy, mechanical energy absorbed in any vibration of the airscrew, heat and sound energy. An application of the energy analysis is then made to the special problem under consideration.

(c) *Conclusions.*—For the particular airscrew for which the calculations were made it was found that the ratio of the efficiency as calculated from considerations of momentum to the actual efficiency is about 0·82. About 15 per cent. of the total energy put into the airscrew was not directly calculable. The energy of rotation—which is calculated from the angular momentum of the air, and the reaction of the torque—is about 3 per cent. of the total energy put into the airscrew. The magnitude of any regular vortex motion is probably small. The conclusion is drawn that the efficiency of a tandem combination may be increased by about 3 per cent. if the airscrews are rotated in the opposite direction.

(d) *Applications and further developments.*—Owing to the difficulties of a theoretical investigation, it is considered desirable that experiments should be made with tandem combinations of airscrews, with a view to finding how the efficiency of a combination depends (*a*) on the relative directions of rotation, (*b*) on the relative diameters of the airscrews.

The present report should be regarded as a continuation of R. & M. 385, which is a theoretical investigation of the effect of the inflowing velocity of the air on the efficiency of a single airscrew, and also of a tandem combination of airscrews of equal diameter. The problem here considered is whether the efficiency of a tandem combination can be appreciably increased if the airscrews are rotated in the opposite direction. It has been suggested that the rotational energy of the slip-stream of the tandem combination may be somewhat reduced, with some advantage to the efficiency, if the two airscrews are rotated in

the opposite direction. Accordingly, an analysis of the energy account of an airscrew is made, which gives some idea of the probable magnitude of the reconvertible energy of the slip-stream

An analysis of the energy account of an airscrew.—Of the total energy put into an airscrew a large proportion is converted into useful work, the greater part of the remainder being carried away in the slip-stream.

The useful work done is a quantity which can be measured with considerable accuracy, but of the various other forms of energy co-existing in the slip-stream, there is no exact quantitative knowledge.

Any attempt, therefore, to analyse the energy account of an airscrew must, by virtue of the complexity of the problem, be of a somewhat speculative character. On the other hand, however, although the various forms of energy—kinetic, potential, heat, sound—are inextricably mingled, some by their very nature are negligibly small, whilst of the others the magnitudes of those which have a direct connection with the forces of the airscrew can be calculated.

Making a qualitative and quantitative analysis of the energy account, it would seem that the total energy E put into the airscrew in unit time eventually re-appears in one or other of the following forms. The usual airscrew notation is adopted.

(*a*) Useful energy E_1. A quantity which can be readily calculated from the thrust T and forward speed V.

Thus

$$E_1 = \frac{VT}{550} \text{ HP.}$$

(*b*) Kinetic energy of translation E_2, a function of both the thrust and the mass of air flowing into the airscrew. Working on the lines of the "momentum" theory of Froude, it is easily seen that

$$E_2 = \int_{r=0}^{\left(r=\frac{D}{2}\right)} \frac{(dM)\ (2v)^2}{2 \times 550} = \int_{r=0}^{\left(r=\frac{D}{2}\right)} \frac{(dT)\ v}{550}$$

where v is the inflowing velocity of air into an annulus of radius r and width dr, so that $dM = \rho\ (V + v)\ 2\pi r dr$. It is shown in Reports and Memoranda No. 328 that the velocity of this mass of air is approximately $2v$ at the minimum section of the slip-stream, so that $dT = dM\ .\ 2v$. E_2 obviously has a minimum value for the given thrust, since the air flowing through the airscrew disc is here assumed to be unaccompanied by any motions extraneous to the régime.

(*c*) Kinetic energy of rotation E_3, a concomitant effect of the torque. Since the torque is a measure of the angular momentum of the air, it would follow that the air in the vicinity of the airscrew has a kinetic energy of rotation, E_3 where

$$E_3 = \int_{r=0}^{r=\frac{D}{2}} \frac{(dQ)^2}{2r^2\,dm.} \times \frac{1}{550} = \int_{r=0}^{r=\frac{D}{2}} \frac{v\,(dQ)^2}{r^2\,(d\Gamma)} \times \frac{1}{550}.$$

This kinetic energy E_3 is due to a regular angular rotation about the axis of the airscrew, although such motion will be somewhat hidden by the various irregular motions of the slip-stream.

(*d*) The remaining energy E_4, most of which is in the slip-stream, represents a collection of energy of various forms, but chiefly the energy of confused motion. It is necessary for the object of the present report to attempt to sub-divide E_4 into its constituent parts, although it is fully realised that no marked partition between these forms of energy is possible.

(E_4a.) Energy dissipated as sound waves. Magnitude not calculated, but probably small.

(E_4b.) A mechanical loss due to any vibrational working of the airscrew.

(E_4c.) A loss due to the friction of the air on the surface of the blade. This would probably be about 1 per cent. or less, of the total energy put into the airscrew.

(E_4d.) Heat energy due to irregular eddying motion. It is to be expected that due to the eddying motions at the tip of an airscrew, and also because of the viscosity of the air, the loss of energy due to the eddying motions at the surface of discontinuity is quite appreciable.

(E_4e.) Kinetic energy of translation due to *irregular* linear motions, principally "centrifugal" flow.

(E_4f.) Pressure energy. This is probably negligible by the time the air has reached the minimum diameter of the slip-stream.

(E_4g.) Energy of any regular vortex motion.

Of the various form of energy collected under the heading of E_4, the energy of the vortex motion (E_4g)—of which the direction of rotation will depend on that of the airscrew—is of chief concern in the present report.

With the object of finding the relative magnitude of E, E_1, E_2, E_3 and E_4, calculations of the energy account have been made for a fairly representative airscrew. The airscrew had a diameter of 9 feet and was driven through a reduction gearing of $\left(\frac{35}{59}\right)$ by a 210 h.p. Hispano Suiza engine. Calculations of the

energy accounts were made for the two principal working conditions of the airscrew: firstly, at the maximum horizontal flight of 100 miles per hour, at which the airscrew is assumed to have a rotational speed of 1,250 r.p.m., a thrust of 575 lbs., and a torque of 860 lbs. ft.; and, secondly, at a climbing speed of 60 miles per hour and a rotational speed of 1,200 r.p.m., the corresponding values of the thrust and torque being 810 lbs. and 880 lbs. ft. respectively. The data of the calculations for the maximum horizontal flight speed are given in Table 1 and Fig. 1, and the data for the climbing speed in Table 2 and Fig. 2. For convenience of reference the energy accounts for each forward speed are collected together in Table 3.

Discussion of the energy account.—The efficiency of the airscrew is, of course, $\frac{E_1}{E}$, whereas the efficiency calculated according to the momentum theory is

$$\frac{E_1}{(E_1 + E_2)}.$$

The ratio of the two efficiencies is $\frac{(E_1 + E_2)}{E}$, that is about 0·82 for both climbing and horizontal flight. It was shown in R. & M. 385 that the value of this ratio depends on the aerodynamic efficiency and the effective pitch angle of the blade sections. The energy of rotation E_3, due directly to the torque, is only about 3 per cent. of the total energy put into the airscrew.

The energy losses which are not directly calculable, E_4, are about 15 per cent. of the total energy, E. The value of the ratio $\frac{(E_4 + E_3)}{E}$ appears to be more or less independent of the working conditions of the airscrew.

A tandem combination with the airscrews rotated in opposite directions.—As stated earlier in the report, a commonly accepted opinion is that the efficiency of a tandem combination may be increased if the two airscrews are rotated in opposite directions, the rear airscrew taking out of the slip-stream of the front airscrew some of the rotational energy. From the analysis of the energy account of the airscrew it is shown that the energy in the slip-stream which is due to more or less regular rotational motion is of two forms, (*a*) kinetic energy (E_3) due to a regular rotational motion about the axis of the airscrew, and (*b*) the energy of regular vortex motion (E_4g). Viscosity will degrade, both in character and magnitude, these two motions, the breakdown increasing with the distance from the airscrew. Also the two engines which are immediately behind the front airscrew will further disturb any regular rotational motion. At the region of the slip-stream of the front airscrew in which the rear airscrew is working it is to be expected that the kinetic energy

of rotation, as calculated from the torque, will not be greater than 3 per cent. of the total energy put into the front airscrew, so that, assuming the whole of this energy to be absorbed and balanced by the rotational energy of the slip-stream of the rear airscrew, the resulting increase of the efficiency of the combination would be greater by about 3 per cent. than that of a combination in which the airscrews rotate in the same direction. The magnitude of the energy of any regular vortex motion ($E_4 g$) of the slip-stream of the front airscrew, at the vicinity of the rear airscrew, cannot be calculated with any accuracy. It is shown in the energy analysis that of the total energy put into an airscrew about 15 per cent. is dissipated in several forms, such as sound, heat, frictional, mechanical, pressure, eddying motion, vortex motion, the energy of any of these distinct forms not being a calculable quantity. The energy of the eddying motions would probably account for a large part of this 15 per cent., the various other forms of energy of group E_4—including any regular vortex motion—making up the remainder. A matter of some significance is that it is unlikely that the whole of the vortex motion from the front airscrew will be taken away from the slip-stream by the superposition of equal and opposite vortices from the rear airscrew.

It would appear then, that the efficiency of a tandem combination may be increased by about 3 per cent. if the airscrews are rotated in the opposite direction.

APPENDIX.

Since the present paper was written, the publication of R. & M. No. 371—an investigation into the nature of the flow in the neighbourhood of an airscrew—has supplied some experimental data from which an analysis of the energy account of an airscrew may be made.

The energy of translation, due to axial motion in the slip-stream, and the energy of rotation at a section of the slip-stream situated about one diameter behind the disc of the airscrew were calculated from the measured velocities of translation and rotation, at climbing speeds of the airscrew ($V/nD = 0{\cdot}63$).

Summarising the results of the calculation, as in Table 3, it was found :

Energy put into the airscrew	E
Useful energy	0·67E
Energy appearing as kinetic energy of translation in the slip stream	0·11E
Energy appearing as kinetic energy of rotation in the slip-stream	0·035E
Other energy losses	0·185E

The general conclusions of this report are therefore substantiated by this experimental evidence. It was also found that the ratio of the kinetic energy of rotation to the total energy put into the airscrew decreases with an increase of V/nD.

Table 1.

ANALYSIS OF THE ENERGY ACCOUNT OF AN AIRSCREW. AIRSCREW PERFORMANCE AT THE MAXIMUM HORIZONTAL FLIGHT SPEED.

V = 100 miles per hour. N = 1,250 r.p.m. T = 575 lbs.
Q = 860 lbs.-ft. Diameter of airscrew = 9 ft.

Efficiency, 74·9 per cent.

r (feet).	Value of $\left(\frac{dT}{dr}\right)$ for Airscrew (lbs./ft.)	Value of $\left(\frac{dQ}{dr}\right)$ for Airscrew (lbs.)	Value of $\frac{v}{V}$	$\left(\frac{dE_2}{dr}\right)$ h.p./ft.	$\left(\frac{dE_3}{dr}\right)$ h.p./ft.
4·25	199·0	287·0	0·069	3·64	0·42
4·00	223·0	325·0	0·081	4·80	0·64
3·50	238·0	353·0	0·097	6·13	1·10
3·00	228·0	341·0	0·108	6·55	1·63
2·50	186·0	277·0	0·104	5·15	1·84
2·00	130·0	192·0	0·093	3·22	1·75
1·00	33·0	47·0	0·049	0·43	0·86

E = 205 h.p. E_1 = 153·4 h.p. E_2 = 14·2 h.p. E_3 = 4·6 h.p.
E_4 = 32·8 h.p.

Table 2.

ANALYSIS OF THE ENERGY ACCOUNT OF AN AIRSCREW. AIRSCREW PERFORMANCE AT CLIMBING.

V = 60 miles per hour. N = 1,200 r.p.m. T = 810 lbs.
Q = 880 lbs.-ft. Diameter of the airscrew = 9 ft.

Efficiency = 64·5 per cent.

r (feet).	Value of $\left(\frac{dT}{dr}\right)$ for Airscrew (lbs/ft.)	Value of $\left(\frac{dQ}{dr}\right)$ for Airscrew (lbs.)	Value of $\frac{v}{V}$	$\left(\frac{dE_2}{dr}\right)$ h.p./ft.	$\left(\frac{dE_3}{dr}\right)$ h.p./ft.
4·25	300·0	315·0	0·246	11·80	0·72
4·00	330·0	356·0	0·280	14·80	1·08
3·50	340·0	379·0	0·319	17·20	1·77
3·00	310·0	349·0	0·337	16·70	2·36
2·50	247·0	276·0	0·324	12·80	2·57
2·00	173·0	188·0	0·292	8·10	2·38
1·50	98·0	102·0	0·232	3·64	1·73
1·00	40·0	39·0	0·153	0·98	0·93

E = 201 h.p. E_1 = 129·5 h.p. E_2 = 37·5 h.p. E_3 = 6·5 h.p.
E_4 = 27·5 h.p.

ANALYSIS OF THE ENERGY ACCOUNT OF AN AIRSCREW.

CASE I AIRSCREW PERFORMANCE AT THE MAXIMUM HORIZONTAL FLIGHT SPEED.

V = 100 MILES PER HOUR N = 1250 R.P.M. T = 575 LBS Q = 860 LBS-FT.

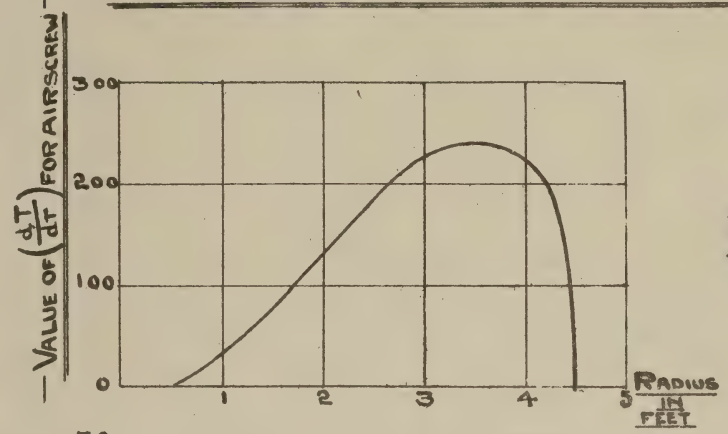

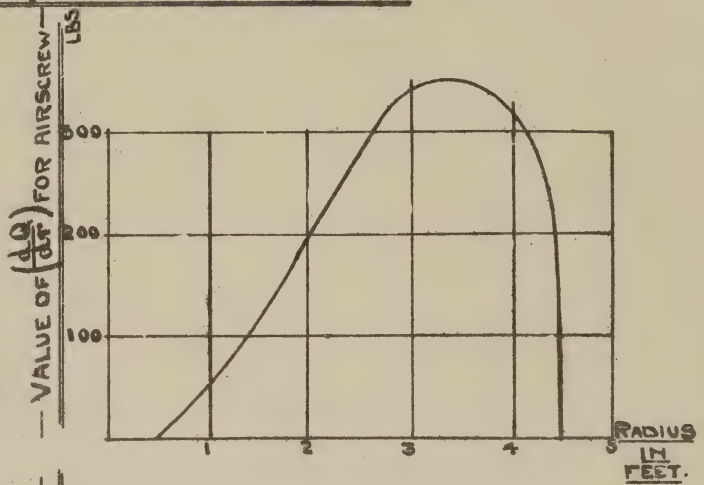

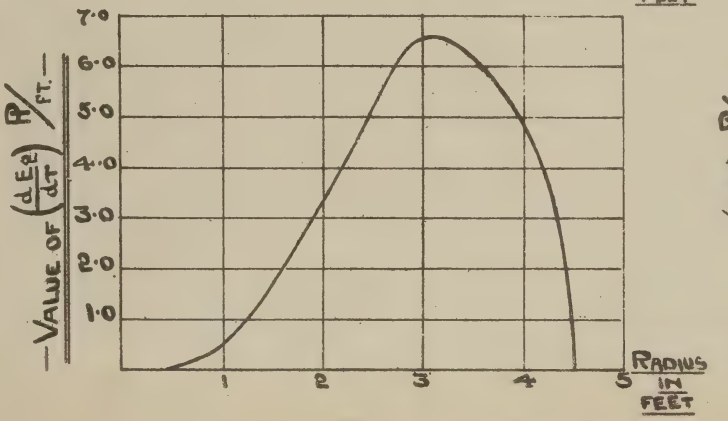

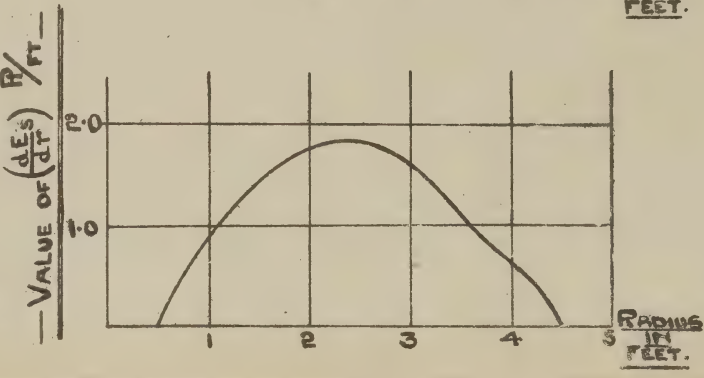

REPORT No. 429.

FIG. 1

ANALYSIS OF THE ENERGY ACCOUNT OF AN AIRSCREW

CASE II. AIRSCREW PERFORMANCE AT CLIMBING.

V = 60 MILES PER HOUR. N = 1200 R.P.M.

T = 810 LBS Q = 880 LBS - FT.

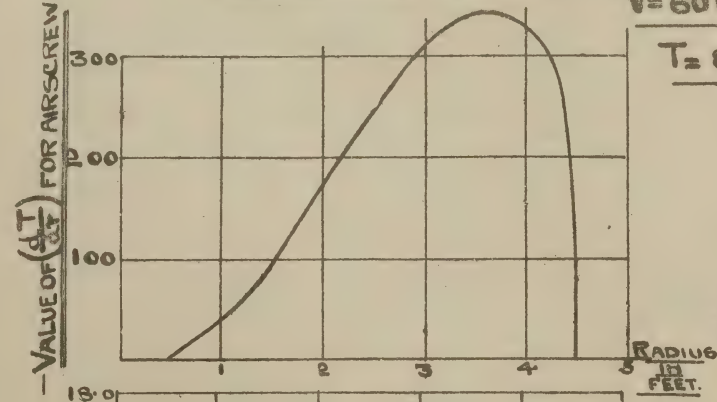

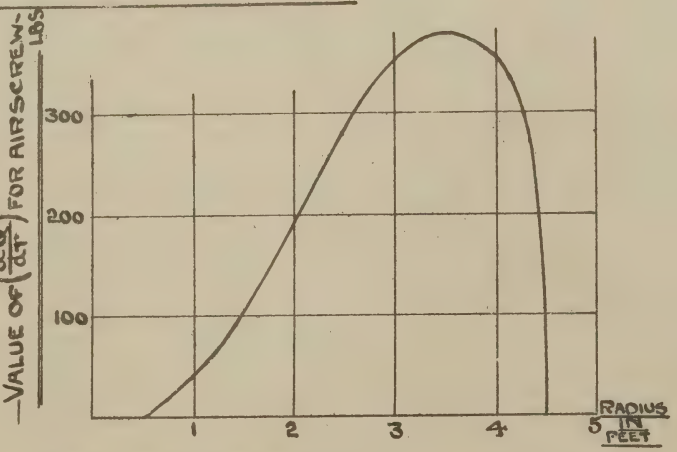

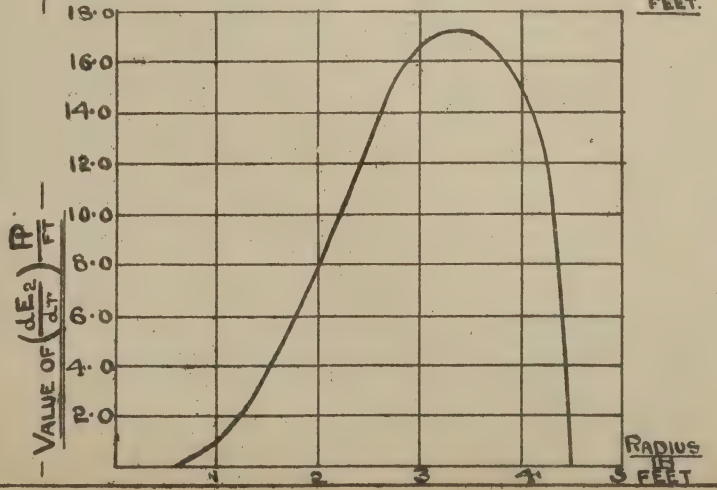

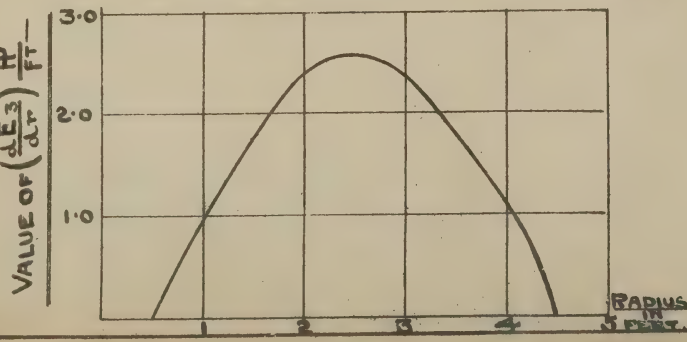

TABLE 3.

ENERGY ACCOUNT OF AIRSCREW.

	Horizontal Flight.	Climbing.
Energy put into airscrew ...E	205·0 = 1·00E	201·0 = 1·00E
Useful energy ... ...E_1	153·4 = 0·749E	129·5 = 0·645E
Energy appearing as kinetic energy of translational in slip-stream E_2	14·2 = 0·069E	37·5 = 0·186E
Energy appearing as kinetic energy of rotational in slip-stream ...E_3	4·6 = 0·022E	6·5 = 0·032E
Other energy losses ... ...E_4	32·8 = 0·160E	27·5 = 0·137E

FORCES ON A PROPELLER DUE TO SIDESLIP.

By R. G. Harris.

Presented by the Superintendent, Royal Aircraft Factory.

Reports and Memoranda, No. 427. *February,* 1918.

Summary.—(a) *Introductory (reasons for inquiry).*—The problem of the lateral force on a propeller due to a sidewind has been studied previously in Reports and Memoranda Nos. 80 and 123 (Technical Reports of the Advisory Committee, 1912–13 and 1913–14). The former report arrives at a formula which has been used in practice for the case of full throttle. The latter report proceeds to graphical integration. Both methods are based on model aerofoil forces, and are liable to errors due to interference, inflow, air rotation, &c.

(b) *Range of investigation.*—The present method gives formulæ in terms of full-scale data, viz., thrust (T), torque (Q), revolutions per second (n), and advance per revolution (P). It is applied to the three forces and the three moments on the propeller.

(c) *Conclusions.*—In the case of lateral force it is found necessary to make an assumption as to torque grading. This involves the above mentioned errors, and therefore implies a correcting factor. The final formula agrees accurately with the experimental observations over the whole range of values of revolution speed in Advisory Committee Report 123. It has the advantage that it can be used under all conditions of flight, *e.g.*, with engine throttled. The formula shows that the lateral force is proportional to the revolutions (n), to the sideslip(v_0), and to the radius of the propeller (r_1).

Pitching moment does not involve a grading assumption. It is proportional to n, v_0, and r_1^2.

Thrust and torque are constant, while yawing moment and normal force are always zero, except in the case of a two-bladed propeller, when they oscillate about zero.

(d) *Applications and further developments.*—Calculations are being made on similar lines to determine the effect on the revolutions (n) of a change of forward speed (V). This makes it possible to calculate the longitudinal stability derivative X_u from full-scale data, and affects both longitudinal and lateral stability.

1. *Method of calculation.*—Axes are chosen as follows :—The x axis is along the propeller axis, while the y and z axes are at right angles to each other in the propeller plane, as shown in Fig. 2. The y axis is horizontal, parallel to the y axis of the machine, while the z axis is the intersection of the propeller plane with the vertical plane through the propeller axis.

r is the distance of a blade element from the centre of the boss.

C is the angle between the z axis and the blade at the moment under consideration.

n is the number of propeller revolutions per second.

V is the speed of translation of the propeller along its own axis (ft./sec.).

W is the circumferential speed of the element at r.

T and Q are thrust and torque respectively on the whole propeller.

$t.dr$ and $q.dr$ are thrust and torque respectively on the element under consideration.

$s.dr$ is the circumferential force on the element, producing torque. Thus $q = rs$.

σ is the percentage density of the air.

Let

$$\frac{V}{n} = P \text{ (advance per revolution).}$$

$$\frac{T}{\sigma n^2} = F \text{ and } \frac{Q}{\sigma n^2} = G$$

where F and G are functions of P only.

Let $t.dr = a$, $s.dr = b$. Also

$$\frac{t}{\sigma n^2} \text{ and } \frac{q}{\sigma n^2}$$

are assumed to be functions of P only for a particular element. The increment in a due to any cause may be divided into two parts :—

(1) due to the resulting change in revolution speed,

(2) due to the resulting change in advance per revolution.

Thus

$$da = \frac{\delta a}{\delta P} dP + \frac{\delta a}{\delta n} dn = \frac{\delta a}{\delta P} dP + \frac{2a}{n} dn$$

Similarly

$$db = \frac{\delta b}{\delta P} dP + \frac{\delta b}{\delta n} dn = \frac{\delta b}{\delta P} dP + \frac{2b}{n} dn.$$

The corresponding increments in thrust, torque, lateral force, normal force, yawing moment, and pitching moment are da, $r.db$, $-\cos C.db$, $\sin C.db$, $r \sin C.da$, and $-r \cos C.da$ respectively (Fig. 2). Let one of these quantities be $X.dr$. Then the

present method consists in expressing the following integral in terms of the quantities F, G, n, and P, viz. :—

$$\frac{m}{2\pi}\int_{o}^{2\pi}\int_{o}^{r_1} \mathrm{X}\, dr\, d\mathrm{C}$$

where m is the number of blades in the propeller, and r_1 is the radius of the propeller blade.

This gives the *average* value of a force (or a moment) per revolution. In many cases $\sum_{o}^{m} \mathrm{X}.dr$ is independent of C; in other words, the force or moment concerned is constant throughout a revolution, and it is only necessary to evaluate

$$\int_{o}^{r_1} \Sigma\, \mathrm{X}.dr.$$

2. *Effect of side slip.*—Let v_0 be the velocity of side slip of the propeller. Then the increment in W is $d\mathrm{W} = v_0 \cos \mathrm{C}$.

Assume that a change in W can be replaced in all respects by a change in n, so far as a blade element is concerned. Thus the increments in inflow, interference, and air rotation are assumed to be the same for the change dn as for the change dW. This is the only permissible assumption on this point in the present state of knowledge, and is implied, though not stated, in Reports and Memoranda Nos. 80 and 123. It will not give strictly accurate results, but is probably much nearer the truth than the assumptions that are usually made in calculating thrust grading, &c. Thus

$$da = \frac{dn}{n}\left(-\mathrm{P}\frac{\partial a}{\partial \mathrm{P}} + 2a\right) = \frac{v_0 \cos \mathrm{C}}{\mathrm{W}}\left(-\mathrm{P}\frac{\partial t}{\partial \mathrm{P}} + 2t\right).\, dr \quad (1)$$

Similarly

$$db = \frac{v_0 \cos \mathrm{C}}{r\mathrm{W}}\left(-\mathrm{P}\frac{\partial q}{\partial \mathrm{P}} + 2q\right).\, dr \quad . \quad . \quad (2)$$

The effect of the radial component $v_0 \sin$ C is ignored. This effect corresponds to the lateral force due to an angle of yaw on an aerofoil of no dihedral, whereas the effect of $v_o \cos$ C corresponds to the lift and drag due to increments in forward speed and in angle of incidence.

3. *Thrust and torque.*—The increments of thrust and torque are seen from equations (1) and (2) to be of the form $k_1 \cos$ C, and $k_2 \cos$ C where k_1 and k_2 are constant for any particular element throughout a revolution. For any number of blades, $\Sigma \cos$ C is zero. Thrust and torque are therefore always constant.

The conclusion is that v_0 does not affect V or n, which simplifies the subsequent work.

4. *Pitching moment* (4-blader).—The increment in pitching moment is

$$dM = -r \cos C \, da = -\frac{v_o \cos^2 C}{2\pi n}\left(-P\frac{\partial t}{\partial P} + 2t\right) dr.$$

For four elements, one in each blade, at the same radius r, $\Sigma \cos^2 C = 2$. Also

$$\int_o^{r_1} t.dr = \frac{T}{4}, \text{ and } \int_o^{r_1} \frac{\partial t}{\partial P}\, dr = \frac{1}{4}\cdot\frac{\partial T}{P}.$$

$$\therefore -M = \frac{v_o}{4\pi n}\left\{-P\frac{\partial T}{\partial r} + 2\Gamma\right\} = \frac{\sigma n v_o}{2\pi}\left(F - \frac{P}{2}\cdot\frac{dF}{dP}\right) \quad . \quad (3)$$

If ψ is the angle of yaw of the machine, the above equation is equivalent to :—

$$-M = \frac{\sigma V^2 \tan \psi}{2\pi}\left(\frac{F}{P} - \frac{1}{2}\cdot\frac{dF}{dP}\right) \quad . \quad . \quad . \quad (4)$$

If ψ is small and is given in degrees, this is approximately equal to

$$\frac{\sigma V^2 \psi}{360}\cdot\left(\frac{F}{P} - \frac{1}{2}\frac{dF}{dP}\right)$$

Obviously equations (3) and (4) can also be interpreted as the yawing moment due to the propeller being pitched.

Sign of M.—Equations (3) and (4) assume $dW = +v_0 \cos C$, *i.e.*, clockwise rotation of propeller as viewed by a person in front of the machine. With such a propeller the pitching moment has the opposite sign to v_0, since

$$F - \frac{P}{2}\frac{dF}{dP}$$

is positive over the flying range of values of P. If the propeller rotates in the opposite direction the sign of M is changed, since in that case $dW = -v_0 \cos C$. The sign can perhaps be more readily remembered as follows :—In Fig. 2, v_0 increases the total value of W in the upper semi-circle, thereby increasing the thrust. Hence the pitching moment is numerically increased throughout the upper semi-circle and decreased throughout the lower, these changes being symmetrical about the origin. Thus the "centre of thrust" moves towards the point at which the side slip is parallel to the propeller's own motion in the circumference of its circle. For example, in a tractor machine, with propeller rotating counter-clockwise, as viewed from the pilot's seat, the propeller moves to the left at the top of its circle. Hence left side slipping raises the centre of thrust and *vice versa*. If this propeller is pitched upward, as for low speeds,

it has a component velocity along the negative direction of OZ; this is the direction of the propeller's motion at the left of its circle, hence the thrust moves to the left. This tends to turn the machine to the right.

$$\mathrm{F} - \frac{\mathrm{P}}{2} \cdot \frac{d\mathrm{F}}{d\mathrm{P}}$$

is of the order 6 for the propeller T.6296, hence M is of the order nv_0, say, 30 lbs./ft. per 1° yaw when engine revolutions are 1,800 per minute, gearing ratio 2 : 1, and speed is 80 m.p.h.

Since F is proportional to r_1^2, it follows that M varies as n, v_0, and r_1^2.

5. *Pitching moment* (m — blader).—For m blades, the value of $\Sigma \cos^2 \mathrm{C}$ is not constant throughout a revolution, but periodic, unless m is a multiple 4. The average value of $\cos^2 \mathrm{C}$ for each blade per revolution is

$$\frac{1}{2\pi} \int_o^{2\pi} \cos^2 \mathrm{C}\, d\mathrm{C} = \tfrac{1}{2}.$$

Hence the average value of M for one blade is

$$- \frac{v_o}{4m\pi n} \left(2\mathrm{T} - \mathrm{P} \frac{\partial \mathrm{T}}{\partial \mathrm{P}} \right), \text{ since } \int_o^{r_1} t\, dr = \frac{\mathrm{T}}{m}.$$

For m blades the average value of M is thus

$$- \sigma \frac{nv_o}{2\pi} \cdot \left\{ \mathrm{F} - \frac{\mathrm{P}}{2} \frac{d\mathrm{F}}{d\mathrm{P}} \right\}$$

which is the same expression as for the constant moment of a four blader.

For a two blader the maximum value of M is twice the above expression, and occurs twice throughout a revolution, at the instants when the propeller is "vertical."

6. *Lateral force.* (4 blader.)—The increment in lateral force is

$$- d\mathrm{Y} = \cos \mathrm{C}\, db = \frac{v_o \cos^2 \mathrm{C}}{r\mathrm{W}} \left(- \mathrm{P} \frac{\partial q}{\partial \mathrm{P}} + 2q \right) . dr.$$

For four elements, one in each blade, at radius r,

$$- d\mathrm{Y} = \frac{2v_0}{\pi n r^2} \left(q - \frac{\mathrm{P}}{2} \frac{\partial q}{\partial \mathrm{P}} \right) . dr.$$

Thus the lateral force is constant throughout a revolution. Before this equation can be integrated, q must be expressed in terms of r, *i.e.*, a torque grading curve must be assumed. Assume that q/r, the circumferential resistance per foot run is zero from $r = 0$ to $r = r_0$, and is constant from $r = r_0$ to $r = r_1$, where r_1 is the total radius of the propeller. q/r varies as shown in Fig. 3.

With this assumption

$$\int_o^{r_1} \frac{q}{r^2}\,dr = 2Q_1 \cdot \frac{\log\,(r_1/r_0)}{r_1^2 - r_0^2}$$

and

$$\int_o^{r_1} \frac{1}{r^2}\,\frac{\delta q}{\delta P}\,.\,dr = 2\,\frac{\delta Q_1}{\delta P}\,\frac{\log\,(r_1/r_0)}{r_1^2 - r_0^2}$$

where Q_1 is the torque on one blade. Thus $4Q_1 = Q$. The lateral force on the whole propeller is therefore :—

$$-Y = \frac{\sigma n v_0}{\pi}\,\frac{\log\,(r_1/r_0)}{r_1^2 - r_0^2}\left\{G - \frac{P}{2}\,\frac{dG}{dP}\right\} \quad . \quad . \quad (5)$$

$$= \frac{\sigma V^2 \tan\psi}{\pi}\,\frac{\log\,(r_1/r_0)}{r_1^2 - r_0^2}\left\{\frac{G}{P} - \frac{1}{2}\,\frac{dG}{dP}\right\} \quad . \quad . \quad (6)$$

If ψ is expressed in degrees, Y is approximately

$$\frac{\sigma V^2 \psi}{180}\cdot\frac{\log\,(r_1/r_0)}{r_1^2 - r_0^2}\left\{\frac{G}{P} - \frac{1}{2}\,\frac{dG}{dP}\right\} \quad . \quad . \quad . \quad (7)$$

Obviously this force can also be interpreted as the lift on a propeller due to an angle of pitch. In each case the force is measured perpendicular to the propeller's axis.

The force is in the direction of the relative lateral wind. When the propeller rotates as in Fig. 2, dY is equal to $-\cos C.db$, where db is proportional to $+ v_0 \cos C$. If the propeller rotates in the opposite direction, dY is equal to $+\cos C.db$, and db is proportional to $- v_0.\cos C$. Thus Y has always the opposite sign to v_0. The propeller therefore acts like a fin, so long as

$$G - \frac{P}{2}\,\frac{dG}{dP}$$

is positive, as is usually the case.

A similar expression holds for the average lateral force in the case of m blades, but the force is periodic instead of constant. For a two-blader, the maximum is twice the average, and occurs twice per revolution, when the blades are " vertical."

7. *Value of* (r_0/r_1) *from experiments.*—The value of (r_0/r_1) may be obtained by comparing the calculated results with experiments. National Physical Laboratory experiments are described in Reports and Memoranda No. 123, 1913-14, p. 287. Table 4 of the report gives the measured lateral force at various angles of yaw, when the wind speed is 30 ft./sec., while the first part of

Table 1 gives the torque for various values of n at 30 ft./sec. The torque is given in the form of a torque coefficient b; thus the torque in lbs./ft. is

$$Q = 0{\cdot}00237 \times 2^3 \times 30^2 b = 17{\cdot}1\, b.$$
$$\therefore G = 17{\cdot}1\, b/n^2.$$

The values of G, as calculated in this way, are shown plotted against P (advance per revolution) in Fig. 4. From this diagram Table 1 below is obtained.

For purposes of comparison, the results for 5° yaw are plotted against n (at 30 ft./sec.), as in Fig. 9 of the above-mentioned report. It is evident from Fig. 5 below that the calculated curve agrees well with the observed values if (r_0/r_1) is taken as 0·175. This gives the formula

$$-Y = 1{\cdot}8\,\frac{\sigma n v_0}{\pi r_1^2} \cdot \left\{ G - \frac{P}{2}\,\frac{dG}{dP} \right\} \quad . \quad . \quad . \quad (8)$$

If q were estimated as for torque grading, the ratio of

$$\tfrac{1}{2}Q \text{ to } \int \frac{q}{r^2}\,dr$$

would probably differ from 1·8, owing to the errors in the assumptions made in estimating q. Thus the value 1·8 includes a correction factor to the theory.

In Fig. 6,

$$\frac{2 \log \frac{r_1}{r_0}}{1 - \left(\frac{r_0}{r_1}\right)^2}$$

is plotted against $\frac{r_0}{r_1}$, indicating the percentage difference that would be made in the estimated value of Y if a different value of (r_0/r_1) were adopted.

The value of $G - \frac{P}{2}\,\frac{dG}{dP}$ is roughly constant at various values of the advance per revolution. For propeller T.6296 it is of the order 7, hence Y is of the order $\frac{4 n v_0}{r_1^2}$, or, say, 5 lbs. per 1° yaw when the engine revolutions are 1,800 and the air speed is 80 m.p.h. It will be noted from formula (8) that the lateral force is directly proportional to the diameter of the propeller (since G involves r^3), to the density, to the speed of revolution, and to the speed of side slip.

8. *Values of* (r_0/r_1) *from calculations.*—Values of r_0/r_1 have also been found from torque grading for propellers T.6296 (R.E.8) and T.28,066 (S.E.5), and are as follows :—

T.6296, $r_0/r_1 = 0{\cdot}282$ at top speed $(V/n = 9{\cdot}2)$.
$r_0/r_1 = 0{\cdot}280$ climbing at 60 m.p.h. $(V/n = 6{\cdot}8)$.
T.28,066, $r_0/r_1 = 0{\cdot}250$ at top speed $(V/n = 5{\cdot}9)$.
$r_0/r_1 = 0{\cdot}260$ climbing at 60 m.p.h. $(V/n = 3{\cdot}5)$.

These values, of course, have still to be corrected for errors in assumptions. The corresponding values of the numerical factor in equation (8) would be :

1·38, 1·38, 1·48 and 1·44 respectively.

This shows that, for the same propeller, these factors are approximately the same under the very divergent conditions of climbing and flying level at top speed. This agrees with the fact that the constant factor 1·8 in equation (8) produces good agreement between experimental and calculated results for the model propeller. Moreover, the uncorrected factor is very nearly the same (say, 1·42) for the two very different propellers mentioned above.

It will be assumed meantime that the true factor is also the same (1·8) for different propellers. This involves a correction factor of about 27 per cent. for the two propellers mentioned above. Further experimental evidence may modify this assumption.

9. *Normal force and yawing moment.*—The increment of normal force on an element is

$$dZ = \sin C\, db = \frac{v_0 \sin C \cos C}{rW} \cdot \left(2q - P\frac{\delta q}{\delta P}\right) \cdot dr.$$

The increment of yawing moment is

$$dN = r \sin C.da = \frac{v_0 \sin C \cos C}{2\pi n}\left(2t - P\frac{\delta t}{\delta q}\right) \cdot dr.$$

Except in the case of a two-blader, $\sum_{o}^{m} \sin C \cos C$ is zero, *i.e.*, there is no normal force or yawing moment at any time. In the case of a two blader, both these quantities oscillate about an average zero value, which occurs when the blades are horizontal or "vertical." The maximum and minimum values of $\Sigma \sin C \cos C$ are numerically equal to the average value of $\Sigma \cos^2 C$ per revolution ; therefore, the maximum and minimum values of Z and N are numerically equal to the average values of Y and M (*see* equations (5) and (3) above). Two maxima and two minima occur in each revolution, when the blades are in a diagonal position.

10. *Collected results.*—

Let θ be the angle of incidence of the wings,

,, α be the angle between wings and propeller,

and ,, $A = \theta - \alpha$.

Let X, Y, Z, L, M, N, represent the propeller forces and moments with respect to the usual stability axes, viz., axes through the C.G. along and perpendicular to the wind direction when the angle of yaw is zero. Let x_1 and z_1 be the co-ordinates of the propeller's centre with respect to the C.G. measured along and perpendicular to the propeller's axis. Then the co-ordinates of the same point with respect to the stability axes are :—

$$x = x_1 \cos A + z_1 \sin A.$$
$$z = z_1 \cos A - x_1 \sin A.$$

Let K represent

$$\frac{k\sigma n V}{\pi {r_1}^2} \cdot \left\{ G - \frac{P}{2} \frac{dG}{dP} \right\}$$

where k is the numerical factor of equation (8) taken meantime as 1·8. Let J represent

$$\frac{\sigma n V}{2\pi} \cdot \left\{ F - \frac{P}{2} \frac{dF}{dP} \right\}$$

Then, when the angle of yaw is zero, the propeller forces and moments are T, Q, lift = K tan A perpendicular to the propeller's axis, and yawing moment = $\pm$ J tan A about an axis in the propeller plane. When there is an angle of yaw ψ, there are, in addition, a lateral force = $-$ K tan ψ, and a pitching moment = $\mp$ J tan ψ. When these are compounded about stability axes, the following results are obtained. Where a double sign is given, the upper sign refers to the case when the propeller rotates clockwise, as seen from the front of the aeroplane. (T and Q are the *numerical* values of thrust and torque).

	Angle of Yaw Zero.	Additions when Angle of Yaw is ψ.
X	$\frac{1}{\cos A}$ (K $\sin^2 A$ $-$ T $\cos^2 A$)	0
Y	0	$-$ K tan ψ.
Z	sin A (K + T)	0
L	$\frac{1}{\cos A}$ ($\pm$ Q $\cos^2 A$ $\pm$ J $\sin^2 A$)	z K tan ψ.
M	$-$ Tz_1 $-$ K tan A x_1	$\mp$ J tan ψ
N	sin A ($\mp$ Q $\pm$ J)	$-$ x K tan ψ

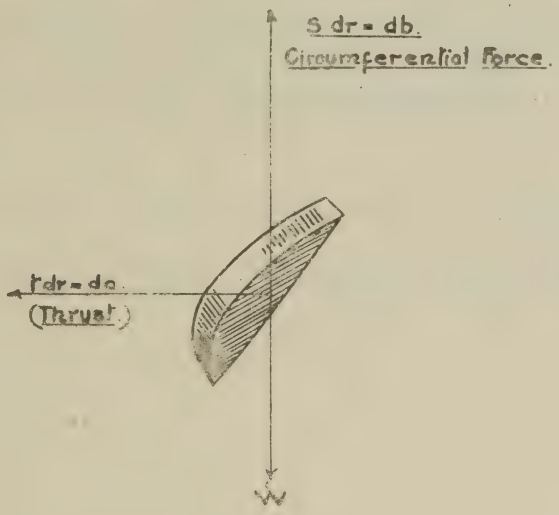
S dr = db.
Circumferential Force.
T dr = dQ.
(Thrust)
W

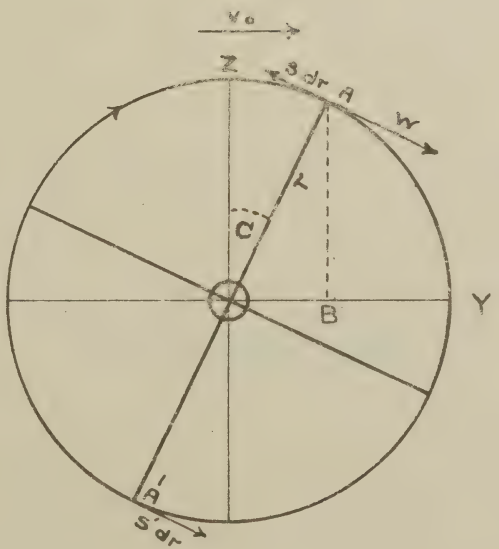
Vo
Z
S dr
A
W
T
C
B
Y
A'
S dr

CIRCUMFERENTIAL FORCE

(T. 6296, $\frac{V}{n}$ = 9·2.)

Full curve : calculated from torque grading

Dotted curve : assumed in calculating lateral force.

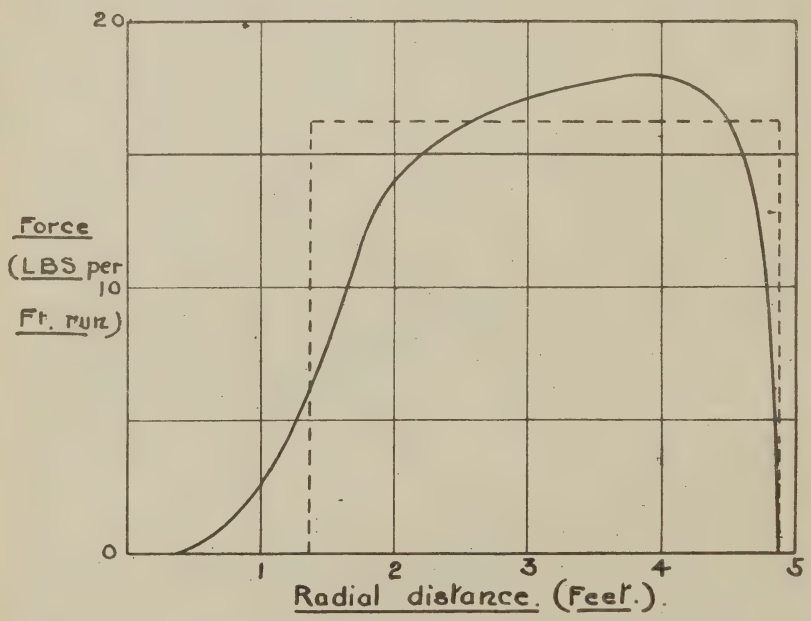

Report Nº

EXPERIMENTAL TORQUE CURVE

For a model B.E.2. propeller, from tests described in „R. and M. 123.

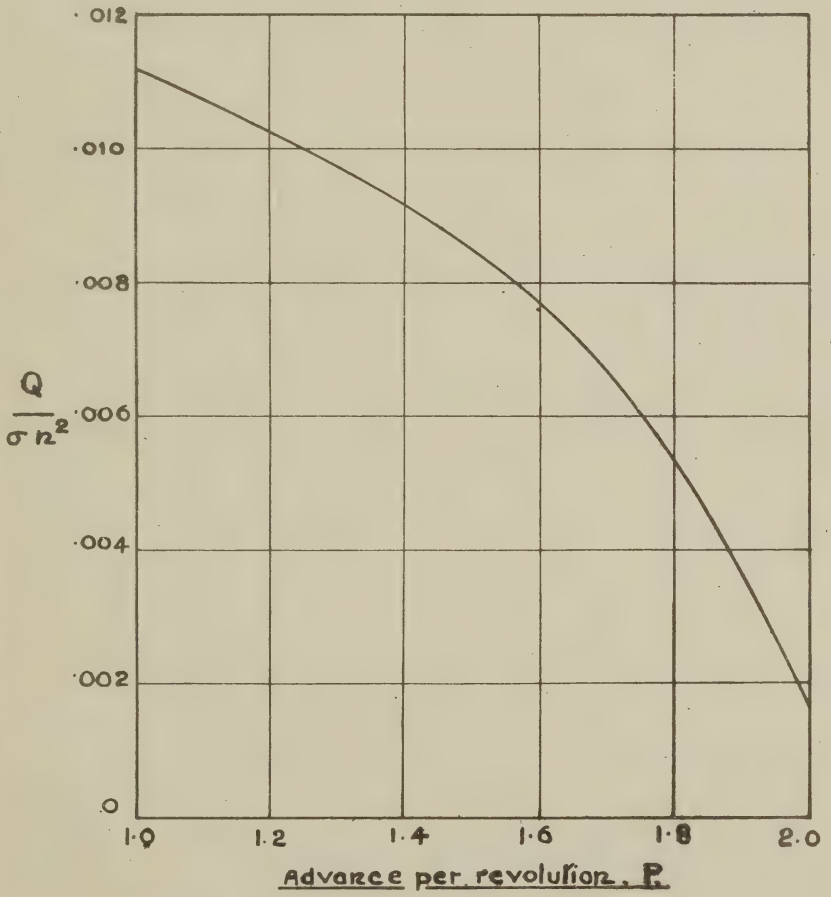

LATERAL FORCE AT 5° YAW.

× Calculated points.

○ Observed points from R and M 123.

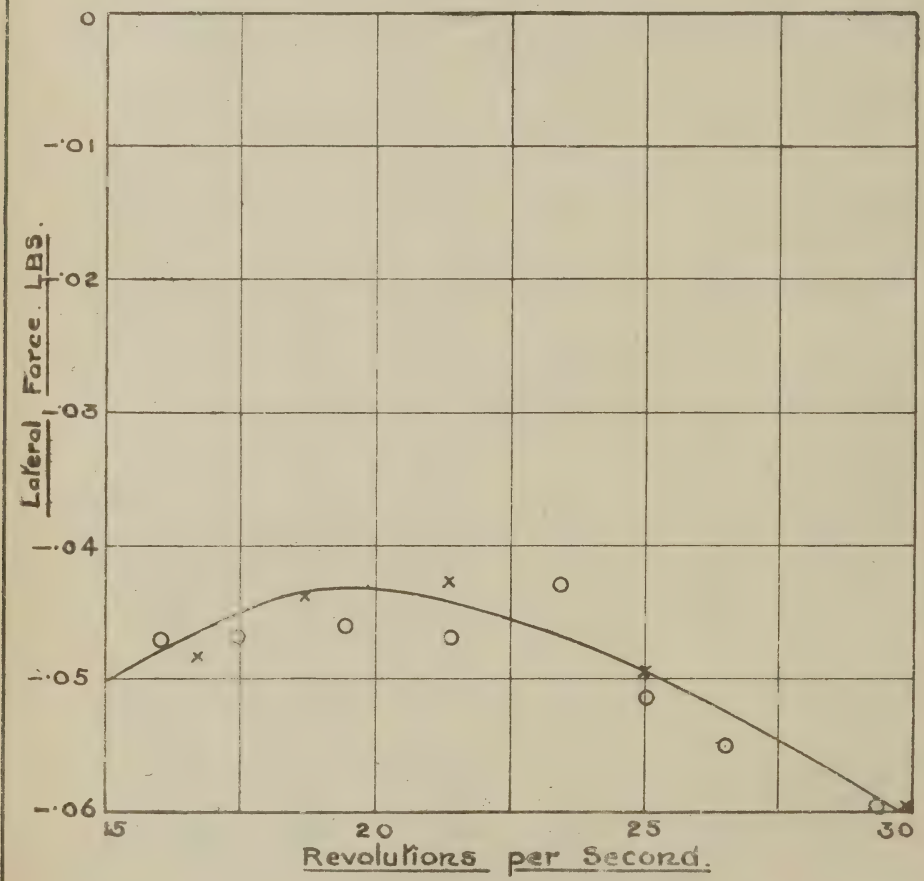

VALUES OF r_o/r_1

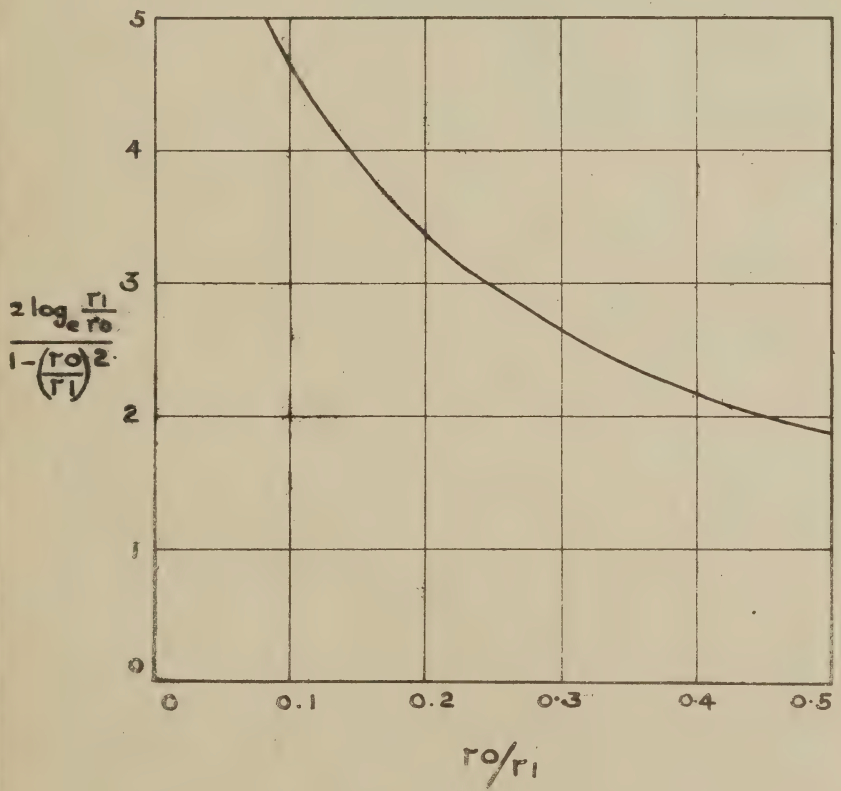

THE LIBRARY
OF THE
UNIVERSITY OF ILLINOIS

TABLE 1.

CALCULATED VALUES OF LATERAL FORCE FOR THE PROPELLER DESCRIBED IN REPORTS AND MEMORANDA No. 123 (DIAMETER 2′).

Angle of Yaw 5°. Wind speed 30 ft. per sec.

$$\frac{1{\cdot}8\ v_0}{\pi {r_1}^2} = \frac{1{\cdot}8 \times 30 \times \tan 5^\circ}{3{\cdot}14}$$

$$= 1{\cdot}504.$$

P	n	$G - \frac{P}{2}\frac{dG}{dP}$	Lateral Force $= 1{\cdot}504\ n \left\{ G - \frac{P}{2}\frac{dG}{dP} \right\}$
1	30·0	0·001,33	0·0600
1·2	25·0	0·001,32	0·0495
1·4	21·4	0·001,33	0·0429
1·6	18·7	0·001,56	0·0439
1·8	16·7	0·001,92	0·0483
2·0	15·0	0·002,16	0·0489

SOME NOTES ON THE CALCULATION OF THE WORKING STRESSES OF AN AIRSCREW.

By A. Fage, A.R.C.Sc., and H. E. Collins.

Reports and Memoranda (New Series), No. 420. *March,* 1918.

Summary.—(a) *Introductory (reasons for inquiry).*—The calculation of the working stresses of an airscrew is a matter of some importance in view of the large aeroplane engines now in use. Unfortunately, the problem is of great complexity and is further complicated by the heterogeneity of the physical properties of the material from which the airscrew is constructed. An endeavour is made in the present paper to illustrate the limitations of the ordinary theory of bending and to demonstrate the need for a rigid investigation of the subject.

(b) *Range of the investigation.*—Assuming the engineer's theory of bending to be applicable—the uncertain character of such an assumption is fully recognised—a general method of calculating the stresses, which is suitable for the drawing office, has been evolved. The " approximate " method commonly used in the drawing office is considered. The theory is illustrated by an application to a particular airscrew. The method of reducing the maximum compressive and tensile stresses by inclining the tip of the blade forward relatively to the boss of the airscrew is considered in some detail.

(c) *Conclusions.*—It is shown that an accurate calculation of the bending moment stresses cannot be made on the basis of the engineer's theory of bending. Regarding the method of stress calculation of the paper as a standard—the method is admittedly inaccurate—the " approximate " method of the drawing office may occasionally give very misleading results, especially when the resultant bending moment makes an angle of about 90° with the chord of the blade section. It is shown that the maximum stresses at any blade section may be considerably reduced by lifting the tip of the blade forward relative to the boss so as to introduce such a bending moment due to centrifugal force that the resultant bending moment on the section is at right angles to the chord. Such an adjustment is, of course, only possible at one value of the ratio of the translational and rotational speeds. Also the desirability of adopting such a method of reducing stresses must depend largely on practical considerations.

(d) *Applications and further developments.*—The need for a more rigid and complete investigation of the distribution of stress in the blade of an airscrew is demonstrated. Such an investigation would be of great utility if a reliable approximate method of stress calculation, of sufficient flexibility as to be readily adaptable to drawing office methods, could be extracted.

The calculation of the working stresses of an airscrew is of some importance, in view of the large horsepowers which are absorbed in some modern airscrews. Unfortunately, a rigid solution of this problem is a matter of extreme difficulty, even if the want of homogeneity of the physical properties of the

material from which the airscrew is constructed, were ignored. The calculations of the present paper have been made on the basis of the engineer's theory of bending, although the doubtful character of such assumptions, when applied to such a complex problem, is fully recognised. In fact a direct application of the ordinary theory of bending illustrates its limitations, and demonstrates the need of a further investigation of the subject. In spite of the time and labour involved, it is thought that a complete investigation could be made with advantage, especially if a reliable approximate method of stress calculation, of sufficient flexibility as to be readily adaptable to drawing office methods, could be extracted. Moreover, when the difficulty of the problem is fully realised, there is a certain amount of antipathy to "approximate" methods, unless the degree of approximation has been definitely established from a comparison with more rigid methods.

In a complete investigation of the stresses of an airscrew consideration would need to be given to (1) the aerodynamic loading, the magnitude of which is a function of the speed and the attitude with which the blades meet the air; (2) the centrifugal loading, which depends on the rotational speed, shape, and size of the airscrew; (3) the inertia loading due to any unsteady motion of the aeroplane, *e.g.*, linear and rotational accelerations, and gyroscopic vibrations.

In the present paper the field of investigation has been limited to the steady rectangular flight of the aeroplane, and so only the aerodynamic and centrifugal loadings are considered. Regarding the blade of an airscrew as a cantilever, the resultant force at any section, due to the loading on the outer part of the blade can be completely expressed by three forces and couples, defined with reference to rectangular axes. Figs. 1 and 2 give a sketch of a section of the blade with the principal axes OX_o, OY_o and OZ_o shown in position—the axis OZ_o passes through the C.G. of the section at right angles to the plane of the paper. A second set of rectangular axes is OX, OY and OZ, where OX passes through the C.G. of the section and is parallel to the chord. The direction of rotation is given by OA and the direction of translation by OC.

The aerodynamic loading at the section may be completely represented by:—

(*a*) A bending moment, M_T, about the axis OA due to the thrust.

(*b*) A bending moment, M_Q, about the axis OC due to the torque.

(*c*) A twisting moment, M_A, about the axis OZ (or OZ_1) due to the resultant of the air force on the outer part of the blade not passing through OZ. The twisting moment M_A is difficult to calculate, but can be made

small by suitably designing the airscrew. Even if the value of M_A were known the torsional stresses of such an irregular shaped body could only be approximately calculated with some difficulty. No account is taken of M_A in the present investigation.

(*d*) A shearing force, F_A, across the section. This shearing force is probably small, but it is worth noting that as a consequence of F_A there is a shearing stress in the plane of the glue joints.

(*e*) An air force acting at right angles to the section. This force is due to any radial air flow along OZ, and is the result of any divergence from a two dimensional airflow. No further account need be taken of this force which is very small.

If the line passing through the C.G. of the outer portion of the blade at right angles to the axes of rotation does not coincide with the radial line OZ, the centrifugal loading at the section may be completely defined by :—

(*a*) Bending moments M_F and M'_F about the axes OA and OC respectively, and a twisting moment about OZ. The twisting moment will always be small, especially for the sections at the tip, and can be neglected.

(*b*) A tensile force, F, acting along OZ.

(*c*) A shearing force, F_o, acting across the section. This shearing stress is small and may be neglected at the outset of the investigation.

Calculation of the Stresses at a Section. (*Method A.*)—The loading at a section has therefore been reduced to a bending moment $(M_T + M_F)$ about the axis OA, a bending moment $(M_Q + M'_F)$ about the axis OC, and a tensile force F acting at right angles to the section. The methods of calculating the values of M_T, M_Q, M_F and F are given later.

The resultant bending moment M on the section is :—

$$\sqrt{(M_T + M_F)^2 + (M_Q + M'_F)^2},$$

the axis of the moment making an angle Ψ with OA where $\tan \Psi = \frac{(M_Q + M'_F)}{(M_T + M_F)}$, and an angle λ with the principal axis OX_o, where $\lambda = (\Psi - \theta - \Phi)$, and

θ = blade angle of the section, that is the angle which the chord of the section OX makes with the direction of rotation OA ;

Φ = the angle between the principal axis OX_o and the chord of the section OX.

To find the neutral axis of the section.—The resultant bending moment M is first resolved into the two components M.cos λ, and M.sin λ, about the principal axes OX_o and OY_o.

If

I_{x_o} = moment of inertia of the section about the principal axis OX_o,

and

I_{y_o} = moment of inertia of the section about the principal axis OY_o,

then, according to the ordinary theory of bending, the stress at any point P of the section, of which the co-ordinates are x_o and y_o will be

$$\frac{M.\cos\lambda.y_o}{I_{x_o}} - \frac{M.\sin\lambda.x_o}{I_{y_o}}$$

The stress at any point on the neutral axis will be zero, so that the equation of the neutral axis is

$$y_o = \left(\frac{I_{x_o}}{I_{y_o}}\right)\tan\lambda.x_o$$

Hence, the neutral axis is inclined at an angle δ to the principal axis where $\tan\delta = \frac{I_{x_o}}{I_{y_o}}\tan\lambda$.

It should be noticed that the neutral axis of the section can only be found by resolving along the principal axes. For any other axes the stresses due to the bending moment about one axis will produce a bending moment about the other axis, because the product of inertia about such axes is not zero. The maximum tensile and compressive stresses of the section will occur at those points which are the greatest distances from the neutral axis, such distances being obtained directly by inspection. If y_c and y_t are the maximum distances from the neutral axis of points on the periphery of the section, y_c being measured on the left-hand side of the axis of the bending moment looking in the direction of the arrow (*see* Fig. 1), then the maximum compressive and tensile stresses due to the resultant bending moment M are

$$\frac{M.\cos(\lambda-\delta)\,y_c}{(I_{x_o}\cos^2\delta + I_{y_o}\sin^2\delta)} \text{ and } \frac{M\cos(\lambda-\delta)\,y_t}{(I_{x_o}\cos^2\delta + I_{y_o}\sin^2\delta)}$$

respectively. If A represent the area of the section, the tensile stress across the section due to the centrifugal force, F, is $\left(\frac{F}{A}\right)$, so that the maximum compressive and tensile stresses on the section are

$$\left\{\frac{M\cos(\lambda-\delta)\,y_c}{(I_{x_o}\cos^2\delta + I_{y_o}\sin^2\delta)} - \frac{F}{A}\right\} \text{ and } \left\{\frac{M\cos(\lambda-\delta)\,y_t}{(I_{x_o}\cos^2\delta + I_{y_o}\sin^2\delta)} + \frac{F}{A}\right\}$$

respectively.

It can easily be shown that the bending stresses as calculated above are those which would be called into being by the total

bending moment M. It has already been shown that the stresses will produce a bending moment $M.\cos(\lambda - \delta)$ about the axis ON. It is now proposed to show that they will produce a bending moment $M.\sin(\lambda - \delta)$ about the axis ON_1.

Thus, if n and n_1 be the co-ordinates of a point in the section referred to the axes ON and ON_1, the stress at the point as calculated above is

$$\frac{M.\cos(\lambda - \delta)\, n_1}{(I_{x_o}\cos^2\delta + I_{y_o}\sin^2\delta)}$$

The bending moment about the axis ON_1 of the stresses in the section is

$$-\int \frac{M.\cos(\lambda - \delta)\, n_1 . n . dA}{(I_{x_o}\cos^2\delta + I_{y_o}\sin^2\delta)}$$

but

$$n_1 = (y_o.\cos\delta - x_o.\sin\delta)$$

and

$$n = (x_o.\cos\delta + y_o.\sin\delta)$$

so that the bending moment about ON_1

$$= -\frac{M.\cos(\lambda - \delta)}{(I_{x_o}.\cos^2\delta + I_{y_o}.\sin^2\delta)}\int[(y_o^2 - x_o^2)\sin\delta\cos\delta + x_o y_o\cos 2\delta]\,dA$$

$$= -\frac{M.\cos(\lambda - \delta)\,(I_{x_o} - I_{y_o})\sin\delta\cos\delta}{(I_{x_o}.\cos^2\delta + I_{y_o}.\sin^2\delta)}$$

$$= -\frac{M.\cos(\lambda - \delta)\left(\frac{I_{x_o}}{I_{y_o}} - 1\right)}{\left(\frac{I_{x_o}}{I_{y_o}}\cos\delta + \tan\delta\right)}$$

$$= -M.\cos(\lambda - \delta)\tan(\delta - \lambda) = M.\sin(\lambda - \delta)$$

since $\tan\delta = \left(\frac{I_{x_o}}{I_{y_o}}\right)\tan\lambda$.

Hence the stresses as calculated above would be produced by a bending moment M, the axis OB of the bending moment making an angle λ with the principal axis OX.

The above method of calculating the stresses will be referred to as "Method A."

A second method of calculating the stresses. (Method B.)—The present paper considers the merits of a simpler method of stress calculation—Method B—in which the stresses are calculated from the component of the resultant bending moment about the axis through the centre of gravity of the section parallel to the chord.

In this case the maximum compressive stress

$$= \left(\frac{M.\cos(\Psi - \theta)\, y'_c}{I_x} - \frac{F}{A}\right)$$

and the maximum tensile stress

$$= \left(\frac{M.\cos(\Psi - \theta)\, y'_t}{I_x} + \frac{F}{A} \right)$$

where

I_x = moment of inertia of the section about an axis OX through the C.G. parallel to the chord ;

and y'_c and y'_t are the maximum distances of points on the periphery of the section from this axis, y'_c being measured on the left-hand side of the axis of the bending moment,

$$M.\cos(\Psi - \theta),$$

looking in the direction of the arrow. (*See* Figs. 1 and 2.)

A detailed calculation of the stresses of an airscrew.—It is now proposed to illustrate the general theory by a detailed calculation of the stresses of an airscrew. A sketch of the two-bladed airscrew on which the calculations are made is shown in Fig. 3. The airscrew has a diameter of 9 ft., the blade angle varying from 14°·1 at the top to 40°·55 at the section next to the boss. The blade is so shaped that the tip sections as viewed from the tail of the machine are lifted forward relatively to the boss, so that the bending moment at any section due to the thrust is partly balanced by a bending moment due to the centrifugal force acting on the blade. The centre of gravity of each blade section is in a plane passing through the axis of rotation, so that the bending moment M'_F about the axis OC and also the twisting moment about the axis OZ—both due to centrifugal force—are each zero. With this design of airscrew the twisting moment M about OZ at any section of the blade, due to the air force acting on the outer portion of the blade, is probably small at the working speeds of the airscrew and has been neglected in the present investigation.

A collection of data calculated from the shape of the blade sections is given in Table 1.

If c = length of the chord of a blade section
σc = maximum thickness of the section
A = area of the section
I_x = moment of inertia of the section about an axis through the C.G. parallel to the chord
I_y = moment of inertia of the section about an axis through the C.G. at right angles to the chord.
D = product of inertia of the section about these axes.
$\overline{Z}$ = height of the C.G. of the section above the chord.

With good accuracy,

$$A = 0{\cdot}72\sigma c^2$$
$$I_x = 0{\cdot}049\sigma^3 c^4$$
$$I_y = 0{\cdot}043\sigma c^4$$
$$\overline{Z} = 0{\cdot}40\sigma c$$
$$D = 0{\cdot}01\sigma^2 c^4$$

so that the moment of inertia of the section about any line passing through the C.G. and making an angle θ_1 with the chord of the section is I where

$$I = 0{\cdot}049\sigma^3c^4\cos^2\theta_1 + 0{\cdot}043\sigma c^4\sin^2\theta_1 - 0{\cdot}01\sigma^2c^2\sin 2\theta_1.$$

From the above equation the position of the principal axes and the magnitude of the principal moments of inertia I_{x_o} and I_{y_o} can be calculated.

Calculations of stress were made for two conditions of loading :—

(*a*) At the maximum horizontal flight speed of an aeroplane of 95 miles per hour, the rotational speed of the airscrew being 1,375 r.p.m., the thrust 350 lbs., and the torque 470 lbs.-ft.

(*b*) At a climbing speed of 57 miles per hour at which the values of the rotational speed, thrust and torque are 1,230 r.p.m., 500 lbs., and 490 lbs.-ft. respectively.

The stress calculations for the case of the maximum horizontal flight speed are given in detail, but in order that the report may not be overburdened only a table of the airscrew stresses when the machine is climbing is appended.

The calculation of the values of M_T, M_Q, M_F *and* F.—The thrust grading curve for the airscrew blade at the forward speed of 95 miles per hour is given in Fig. 4. The thrust-grading curve gives the intensity of loading due to the thrust $\left(\frac{\partial T}{\partial r}\right)$ and is constructed from the aerodynamic data of the blade sections. The thrust on the part of the blade outside the radius R is $\int_R^{\frac{D}{2}} \frac{\partial T}{\partial r}\, dr$ and is directly obtained from an integration of the thrust-grading curve, *see* Fig. 5. In a similar manner since $M_T = \int_R^{\frac{D}{2}} T dr$, the bending moment of any point of the blade is obtained from the integration of the curve of Fig. 5. The bending moment curve is given in Fig. 6. The bending moment due to the torque M_Q may be obtained in a similar manner, although at the outset a load-intensity curve—the loads being due to the torque—should be constructed from the torque-grading curve. The diagram of M_Q is given in Fig. 10.

The centrifugal force at any section distance R feet from the airscrew axis $= \int_R^{\frac{D}{2}} Ardr \,.\, w \,.\, \left(\frac{2\pi N}{60}\right)^2$, where N is the rotational speed in revs. /min. and w is the mass density of wood. In the present paper w is assumed to have the value of $\frac{42}{32{\cdot}2}$ slugs per cubic foot.

Hence the centrifugal force, F lbs., at the section distance R from the axis of rotation $= 0{\cdot}01425\ N^2 \int_R^{\frac{D}{2}} Ardr$. The curve of Fig. 11 gives the value of (Ar) plotted against r, from which the values of F have been calculated. (*See* Fig. 12 and Table 2.) The bending moment, M_F lb.-inches, at a section, due to the centrifugal force acting on the outer part of the blade $= -0{\cdot}01425\ N^2 \int_R^{\frac{D}{2}} A \,.\, r \,.\, dr \,.\, x_1$ where x_1 is the distance, in inches, of the centre of gravity of the section at the radius r, from the plane passing through the centre of gravity of the section at radius R at right angles to the axis of the airscrew. The method of calculating the value of M_F for the section R = 1·23 feet is illustrated by the curves of Figs. 13 and 14. (*See* also Table 3.)

Discussion of the data of the stress calculations made on the airscrew.—Calculations based on methods A and B were made of the maximum compressive and tensile stresses at a section due to the combined effect of the centrifugal force and the resultant bending moment—the latter being compounded of the bending moments due to the thrust, torque and centrifugal force. The data of these calculations are collected in Tables 4 and 5.

No attempt has been made in the present paper to calculate the distribution of shearing stress in the blade. The shearing force at any section of the blade is balanced by a shearing stress across that section, which will also be accompanied by a shearing stress in a plane at right angles to the section, whence it follows that the glue between the laminæ is in shear. Shearing stress may be of some importance in an airscrew which is vibrating considerably under load ; the fluctuations of the shearing stress introducing sliding between the laminæ will result in the heating of the glue, and occasionally in the fracture of the airscrew.

The following conclusions may be drawn from a study of the data of the stress calculations of Tables 4 and 5.

(*a*) An accurate calculation of the bending moment stresses cannot be made on the basis of the engineer's theory of bending.

This conclusion may perhaps be partly substantiated by a reference to Figs. 15 and 16, which give isometric sketches of the neutral surface of the blade for the two working conditions of the airscrew for which the calculations were made. If the engineer's theory of bending were applicable to the present problem, then the neutral surfaces would be as shown in these figures, but with such twisted surfaces as these it is extremely difficult to imagine the blade bending in a manner which could be specified completely by such a simple law. The problem is further complicated when the want of homogeneity of the

physical properties of the material from which the airscrew is made, is taken into consideration. The sinuosity of the neutral surfaces of the figures is such that they must occasionally cut across the wood fibres, that is the stress in such fibres must change from tensile to compressive at the neutral surface—an indication of the existence of a somewhat complex state of stress.

Unfortunately, the inaccuracies of the simple theory of bending as applied to the present problem can only be determined from a comparison with a more rigid method.

(*b*) The magnitude of the resultant bending moment may be considerably reduced by inclining the tip of the blade forward in the direction of translational motion, and so balancing the bending moment due to the thrust by a bending moment due to the centrifugal force.

At any section of the blade the value of the ratio of the bending moment due to the thrust to the bending moment due to the centrifugal force will vary with the value of V/n at which the airscrew is working, so that a complete balance between these two bending moments is only possible at one value of V/n. Whether it is desirable to incline the tip of the blade forward relatively to the boss will largely depend on practical considerations.

(*c*) The discrepancy between the stresses as calculated from the two methods A and B may be large, especially when the angle between the principal axis OX_o and the axis of the resultant bending moment is large.

The conclusions (*b*) and (*c*) are considered in more detail below.

The accuracy of the stress calculation of method B as compared with method A.—It has already been pointed out that there is no accurate, and at the same time, simple, method of calculating the working stresses of an airscrew. It is believed that the method of stress calculation commonly used in the drawing office is similar to method B, in which the resultant bending moment is resolved in the direction of the chord, and the moment of inertia is taken about an axis through the centre of gravity of the section parallel to the chord. Assuming the simple law of bending to be applicable to the case of an airscrew blade, then the method A may be regarded as a standard with which to compare the accuracy of "approximate" methods, such as the method B.

Accordingly, to obtain some idea of the relative merits of the methods A and B, calculations of the maximum tensile and compressive stresses were made on two types of blade sections, for which the values of the ratio of the maximum thickness to the chord length were 0·10 and 0·25, these two shapes representing sections of the blade at the tip and boss respectively.

Sketches of these two blade sections are given in Fig. 17. The data of these calculations are given in Tables 6 and 7 and are shown graphically in Figs. 18 and 20, in which are plotted the values of the ratio of the stresses—both tensile and compressive —as calculated from both methods against the value of $(\psi - \theta)$, the value of ψ, which is the angle between the direction of the resultant bending moment and the direction of rotation, varying from 0° to 180°. It is seen that for certain values of the angle $(\psi - \theta)$ the method B gives results which are greatly different from those of method A, the percentage discrepancy being greatest of course when $(\psi - \theta) = 90°$, since the resultant bending moment is at right angles to the chord of the section, so that the stress calculated according to the method B has a zero value. The values of the maximum stresses are small, however, when $(\psi - \theta) = 90°$. When the axis of the resultant bending moment makes an angle ranging from, say, $-20°$ to $+30°$ with the chord of the section, and the method B of stress calculation is used, the maximum compressive stresses will be in good agreement with those calculated from the more accurate method A, whilst the maximum tensile stresses will be under estimated by about 20 or 30 per cent. It will be noticed that for the values of $(\psi - \theta)$ outside the range, the method B when compared with method A, may be very misleading.

The variation of the stresses in the blade with the bending moment due to the centrifugal force.—It is now proposed to show how the maximum values of the compressive and tensile stresses of a blade may be reduced by lifting the tip of a blade forward relative to the boss, and so balancing the bending moment due to the thrust by a bending moment due to the centrifugal force acting on the outer portion of the blade. Calculations were made on the two types of blade section shown in Fig. 17, assuming in each case appropriate values of M_Q, M_T and θ. The variation of the bending moment due to centrifugal force M_F was such that the angle Ψ, that is $\tan^{-1}\left(\frac{M_Q}{M_T + M_F}\right)$, ranged from about 20° to 150°. The data of the calculations are given in Tables 8 and 9, from which the curves of Figs. 19 and 21 were constructed. It will be seen from the figures that the maximum stresses—assuming, of course, the validity of method A—may be considerably reduced by suitably designing the air-screw so as to introduce such a bending moment due to centrifugal force that the resultant bending moment on the section is at right angles to the chord, such an adjustment of the relative values of M_Q, M_T being only possible at one value of the ratio of translational and rotational speeds. Whether such a method of reducing the working stresses is of value can only be fully determined when the magnitude of the inaccuracy of the present method of stress calculation is known and practical considerations of design and manufacture are taken into account.

Table 1.

Name of Section.	Distance of Section from Airscrew Axis R. (Inches.)	Type of Section.	Value of "x." (Inches.)	Chord Length c (Inches.)	Maximum Thickness σc (Inches.)	Area A (Sq. ins.)	Height of C.G. of the Section above Chord Z.	Moment of Inertia I_x of Section about Axis through C.G. Parallel to Chord.	Moment of Inertia I_y of Section about Axis through C.G. at Right Angles to Chord.	Angle of Blade Section (Degrees.)
AA	51·3	F	1·85	4·55	0·36	$0{\cdot}73\sigma c^2$	$0{\cdot}415\sigma c$	$0{\cdot}051\sigma^3 c^4$	$0{\cdot}043\sigma c^4$	14·1
BB	44·6	F	1·50	6·75	0·54	$0{\cdot}72\sigma c^2$	$0{\cdot}400\sigma c$	$0{\cdot}047\sigma^3 c^4$	$0{\cdot}043\sigma c^4$	15·8
CC	37·8	F	1·10	7·35	0·73	$0{\cdot}71\sigma c^2$	$0{\cdot}405\sigma c$	$0{\cdot}049\sigma^3 c^4$	$0{\cdot}043\sigma c^4$	19·2
DD	29·7	F	0·76	7·15	0·89	$0{\cdot}72\sigma c^2$	$0{\cdot}400\sigma c$	$0{\cdot}049\sigma^3 c^4$	$0{\cdot}043\sigma c^4$	23·8
EE	20·3	F	0·30	6·00	1·13	$0{\cdot}71\sigma c^2$	$0{\cdot}400\sigma c$	$0{\cdot}047\sigma^3 c^4$	$0{\cdot}043\sigma c^4$	32·4
FF	14·8	C	0	5·25	1·30	$0{\cdot}71\sigma c^2$	$0{\cdot}425\sigma c$*	$0{\cdot}043\sigma^3 c^4$	$0{\cdot}042\sigma c^4$	40·6

"x" is the height of the C.G. of a section above a plane passing through the C.G. of the section at the boss and at right angles to the airscrew axis.

F = Flat under-surface. C = Concave under-surface.

* This height is taken above a line touching bottom surface and parallel to the chord.

TABLE 2.

Distance of Section from Airscrew Axis. R. in ft.	$\int_{R}^{\frac{D}{2}} AxDr$ (Ft.)⁴	Centrifugal Force at Section (lbs.). N = 1,375 r.p.m.	Centrifugal Force at Section (lbs.). N = 1,230 r.p.m.	Bending Moment due to Centrifugal Force (lb.-ins.). N = 1,375 r.p.m.	Bending Moment due to Centrifugal Force (lb.-ins.). N = 1,230 r.p.m.
3·72	0·036	972	778	179	143
3·15	0·081	2,170	1,740	745	596
2·48	0·135	3,650	2,920	1,940	1,550
1·69	0·190	5,130	4,120	4,100	3,280
1·23	0·211	5,700	4,560	5,470	4,370

TABLE 3.

CALCULATION OF BENDING DUE TO THE CENTRIFUGAL FORCE FOR SECTION. R = 1·23 FT.

Rotational Speed = 1,375 R.P.M.

Distance of Element from Axis of Airscrew. (Feet.)	$\left(\frac{dF}{dr}\right)$ (Lbs./ft.)	Value of x_1. (Inches.)	$\left(\frac{dM_F}{dr}\right)$ (Lbs.)
1·23	1,115	0	0
1·50	1,380	0·15	17
1·69	1,530	0·25	32
2·00	1,785	0·45	67
2·25	1,975	0·59	97
2·48	2,130	0·73	130
2·75	2,240	0·90	168
3·15	2,250	1·12	210
3·50	2,080	1·35	234
3·72	1,840	1·50	230
3·90	1,620	1·60	216
4·10	1,350	1·75	197
4·28	960	1·85	148
4·50	0	2·00	0

Table 4.

STRESSES IN THE AIRSCREW DURING HORIZONTAL FLIGHT CONDITIONS OF THE AEROPLANE.

Translational speed of the machine = 95 miles per hour. Rotational speed of the airscrew = 1,375 r.p.m.
Thrust of the airscrew = 350 lbs. Torque of the airscrew = 470 lbs.-ft.

Distance of the Section from the Airscrew Axis (R. in ft.)	M_T (lbs.-ins.).	M_F (lbs.-ins.).	M_Q (lbs.-ins.).	M (lbs.-ins.).	ψ (degrees).	I_{x_0} (ins.)^4	I_{y_0} (ins.)^4	Φ (degrees).	θ (degrees.)	λ (degrees).	δ (degrees).	y_c (ins.)	y_t (ins.)
3·72	228	— 179	60	78	50·7	0·048	7·25	1·05	15·8	33·85	0·25	0·31	0·29
3·15	660	— 745	216	232	111·5	0·133	12·31	1·35	19·2	90·95	147·00	2·29	1·69
2·48	1,464	—1,940	528	711	132·0	0·234	14·08	1·70	23·8	106·50	176·65	0·47	0·58
1·69	2,796	—4,100	1,080	1,694	140·3	0·385	10·44	2·60	32·4	105·30	172·30	0·74	0·79
1·23	3,648	—5,470	1,440	2,330	141·7	0·477	8·03	3·55	40·6	97·55	155·80	1·37	1·08

Distance of the Section from the Airscrew Axis. (R. in ft.)	Moment of Inertia of Section about Neutral Axis. I_N (ins.)^4.	M. cos (λ — δ) (Lbs.-ins.)	Method A. Stress due to Bending. Moment M. lbs. /sq. in		Method B. Stress due to Bending Moment M.					Stress due to Centrifugal Force. (Lbs. /sq. in.)
					I_x (ins.)^4.	y'_c ins.	y'_t ins.	Lbs. /sq. in. Compressive f'_c	Lbs. /sq. in. Tensile f'_t	
			Compressive f_c	Tensile f_t.						
3·72	0·048	65·0	420·0	390·0	0·050	0·31	0·23	395·0	290·0	370·0
3·15	3·720	130·5	80·5	59·5	0·140	0·30	0·43	20·0	28·5	570·0
2·48	0·282	242·0	405·0	500·0	0·246	0·35	0·54	315·0	490·0	795·0
1·69	0·570	665·0	865·0	925·0	0·406	0·45	0·68	375·0	870·0	1065·0
1·23	1·750	1225·0	960·0	760·0	0·497	0·56	0·74	485·0	640·0	1185·0

Angles with a positive sign are measured in an anti-clockwise direction.

y_c and y_t are the maximum distances from the neutral axis of points in the periphery of the section, y_c being measured on the left-hand side of the axis of bending looking in the direction of the screw.

I_{x_0} and I_{y_0} are the principal moments of inertia of a section.

I_x is the moment of inertia of the section about an axis through the C.G. parallel to the chord.

y'_c and y'_t are the maximum distances from the axis through the C.G. parallel to the chord, of points on the periphery of the section, y'_c being measured on the left-hand side of the axis of the bending moment, M. cos (ψ — θ), looking in the direction of the arrow.

Table 5.

STRESSES IN THE AIRSCREW DURING CLIMBING CONDITIONS OF THE AEROPLANE.

Translational speed of the machine = 57 miles per hour. Rotational speed of the airscrew = 1,230 r.p.m.
Thrust of airscrew = 500 lbs. Torque of airscrew = 490 lbs.-ft.

Distance of the Section from the Airscrew Axis (R. in ft.)	M_T (lbs.-ins.).	M_F (lbs.-ins.).	M_Q (lbs.-ins.).	M (lbs.-ins.).	ψ (degrees).	I_{x_o} $(ins.)^4$	I_{y_o} $(ins.)^4$	Φ (degrees).	θ (degrees.)	λ (degrees).	δ (degrees).	y_c (ins.)	y_t (ins.)
3·72	504	− 143	60	365	9·4	0·048	7·25	1·05	15·8	− 7·45	0	0·30	0·28
3·15	1,332	− 596	240	775	18·0	0·133	12·31	1·35	19·2	− 2·55	0	0·43	0·37
2·48	2,772	−1,550	564	1,345	24·8	0·234	14·08	1·70	23·8	− 0·70	0	0·53	0·41
1·69	4,824	−3,280	1,140	1,940	36·2	0·385	10·44	2·60	32·4	+ 1·2	0	0·65	0·57
1·23	6,108	−4,370	1,524	2,310	41·3	0·477	8·03	3·55	40·6	− 2·85	−0·2	0·72	0·62

Distance of the Section from the Airscrew Axis. (R. in ft.)	Moment of Inertia of Section about Neutral Axis. I_N $(ins.)^4$.	M. cos $(\lambda - \delta)$ (Lbs.-ins.)	Method A. Stress due to Bending. Moment M. lbs./sq. in		Method B. Stress due to Bending Moment M.					Stress due to Centrifugal Force. (Lbs./sq. in.)
								Lbs./sq. in.		
			Compressive f_c	Tensile f_t	I_x $(ins.)^4$.	y'_c ins.	y'_t ins.	Compressive f'_c	Tensile f'_t	
3·72	0·048	362	2,260	2,110	0·050	0·31	0·23	2,245	1,670	295
3·15	0·133	774	2,500	2,160	0·140	0·43	0·30	2,380	1,660	460
2·48	0·234	1,345	2,050	2,360	0·246	0·54	0·35	2,950	1,910	635
1·69	0·385	1,938	3,270	2,870	0·406	0·68	0·45	3,240	2,140	855
1·23	0·477	2,308	3,480	3,000	0·497	0·74	0·56	3,440	2,600	945

Angles with a positive sign are measured in an anti-clockwise direction.

y_c and y_t are the maximum distances from the neutral axis of points in the periphery of the section, y_c being measured on the left-hand side of the axis of bending looking in the direction of the screw.

I_{x_o} and I_{y_o} are the principal moments of inertia of a section.

I_x is the moment of inertia of the section about an axis through the C.G. parallel to the chord.

y'_c and y'_t are the maximum distances from the axis through the C.G. parallel to the chord, of points on the periphery of the section, y'_c being measured on the left-hand side of the axis of the bending moment, M. cos $(\psi - \theta)$, looking in the direction of the arrow.

Table 8.

THE VARIATION OF THE STRESSES IN A BLADE SECTION WITH THE BENDING MOMENT DUE TO CENTRIFUGAL FORCE, M_F.

Calculations made on an aerofoil section for which

$$\left(\frac{\text{maximum thickness}}{\text{chord length}}\right) \text{ is } 0{\cdot}10.$$

Length of chord taken to be 7″·3. Value of θ taken to be 20°.

I_{x_o} of section = 0·130 (inch)⁴. I_{y_o} of section = 12·23 (inch)⁴.

Φ of section = 1·35°.

Value of M_Q assumed to be 200 lbs.-ins.

Value of M_T assumed to be 800 lbs.-ins.

$$\tan \psi = \frac{M_Q}{(M_T + M_F)}$$

Value of ψ.	Value of $(M_T + M_F)$	Value of M_F.	Value of M.	Maximum Stresses due to M. lbs. per sq. inch.	
(Degrees.)	(Lbs.-ins.)	(Lbs.-ins.)	(Lbs.-ins.)	Compressive.	Tensile.
10	1,135	+ 335	1,150	3,650	3,260
20	550	− 250	585	1,900	1,700
30	350	− 450	400	1,280	1,150
45	200	− 600	285	835	775
75	+ 54	− 746	205	375	375
90	0	− 800	200	230	250
100	− 35	− 835	205	125	165
106	− 57	− 857	208	65	105
110	− 73	− 873	215	70	70
114	− 89	− 889	220	90	60
120	− 115	− 915	230	125	135
130	− 170	− 970	260	215	300
145	− 285	−1085	350	480	660

A COM

A COMPARISON OF THE STRESSES AS CALC
F

Calculations made on an ae

Length of the chord taken to be 5″·2.

I_{y_o} of section = 7

Moment of inertia of the

$\psi°$	$(\theta - \psi)°$
0	−20
5	−15
10	−10
15	− 5
20	0
25	+ 5
30	10
45	25
60	40
75	55
90	70
100	80
106	86
110	90
114	94
120	100
130	110
145	125
160	140
180	160

Ψ	$(\theta - \Psi)°$	$\lambda° = (\theta - \Psi) - 43·4$	$\delta°$	$\cos(\lambda - \delta)$	y_c (in.).	y_t (in.).	Moment of Inertia of Section about the Neutral Axis I_N. (In.)^4.	S
0	− 40	− 43·6	− 3·65	0·767	0·790	0·520	0·559	
10	− 30	− 33·6	− 2·65	0·858	0·780	0·565	0·543	
20	− 20	− 23·6	− 1·70	0·928	0·770	0·595	0·536	
25	− 15	− 18·6	− 1·30	0·955	0·760	0·605	0·525	
30	− 10	− 13·6	− 0·95	0·976	0·750	0·620	0·533	
35	− 5	− 8·6	− 0·60	0·990	0·750	0·630	0·532	
40	0	− 3·6	− 0·25	0·998	0·745	0·645	0·531	
45	+ 5	+ 1·4	+ 0·10	0·999	0·735	0·665	0·531	
50	10	6·4	0·45	0·995	0·735	0·675	0·532	
60	20	16·4	1·10	0·965	0·725	0·700	0·534	
75	35	31·4	2·35	0·874	0·715	0·740	0·544	
90	50	46·4	4·05	0·739	0·705	0·805	0·567	
105	65	61·4	7·00	0·582	0·690	0·910	0·641	
120	80	76·4	15·50	0·486	0·740	1·190	1·056	
125	85	81·4	23·95	0·538	1·050	1·455	1·749	
135	95	91·4	110·00	0·948	2·890	1·950	1·020	
140	100	96·4	149·90	0·595	1·720	1·250	2·382	
150	110	106·4	167·15	0·488	0·965	0·920	0·897	
180	140	136·4	176·35	0·767	0·520	0·790	0·559	

Angles with a positive sign are measured in an anti-clockwise di

y_c and y_t are the maximum distances from the neutral axis of bending looking in the direction of the arrow.

I_{x_o} and I_{y_o} are the principal moments of inertia of a section.

I_x is the moment of inertia of the section about an axis throug

y'_c and y'_t are the maximum distances from the axis through t on the left-hand side of the axis of the bending moment M cos (Ψ −

Table 6.

A COMPARISON OF THE STRESSES AS CALCULATED FROM METHOD A WITH THOSE CALCULATED FROM METHOD B.

Calculations made on an aerofoil for which $\left(\frac{\text{maximum thickness}}{\text{chord length}}\right)$ is 0·10.

Length of chord taken to be 7″·3. Value of θ taken to be 20°. I_{x_o} of section = 0·130 (inch)⁴.
I_{y_o} of section = 12·23 (inch)⁴. Φ of section = 1·35°. Moment of inertia of section about chord, I_x = 0·136 (inch)⁴.
M represents the total bending moment at a Section.

ψ°	(ψ − θ)°	λ° = (ψ − 21·35)	δ°	cos (λ − δ)	y_c (in.).	y_t (in.).	Moment of Inertia of Section about the Neutral Axis I_N. (In.)⁴.	Method A. Stress due to Bending Moment M. (Lbs./sq. in.) Compressive. Value of $\frac{f_c}{M}$ or $\left(\frac{y_c \cos(\lambda-\delta)}{I_N}\right)$ (1)	Method A. Stress due to Bending Moment M. (Lbs./sq. in.) Tensile. Value of $\frac{f_t}{M}$ or $\left(\frac{y_t \cos(\lambda-\delta)}{I_N}\right)$ (2)	cos (ψ − 20°)	Method B. Stress due to Bending Moment M. (Lbs./sq. in.) Compressive. Value of $\frac{f'_c}{M}$ or $\left(\frac{y'_c \cos(\psi-20°)}{I_x}\right)$ (3)	Method B. Stress due to Bending Moment M. (Lbs./sq. in.) Tensile. Value of $\frac{f'_t}{M}$ or $\left(\frac{y'_t \cos(\psi-20°)}{I_x}\right)$ (4)	Ratio of the Stresses Calculated from Methods A and B. Compressive. Col. 3 / Col. 1	Ratio of the Stresses Calculated from Methods A and B. Tensile. Col. 4 / Col. 2
0	−20	−21·35	− 0·25	0·933	0·43	0·360	0·130	3·09	2·59	·940	3·04	2·00	0·99	0·77
5	−15	−16·35	− 0·20	0·959	0·42	0·375	0·130	3·10	2·77	·966	3·12	2·06	1·00	0·75
10	−10	−11·35	− 0·10	0·980	0·42	0·375	0·130	3·17	2·83	·985	3·19	2·10	1·00	0·74
15	− 5	− 6·35	0	0·994	0·42	0·375	0·130	3·22	2·88	·996	3·23	2·12	1·00	0·74
20	0	− 1·35	0	0·999	0·42	0·375	0·130	3·23	2·89	1·000	3·24	2·13	1·00	0·74
25	+ 5	+ 3·65	0	0·998	0·42	0·375	0·130	3·23	2·89	·996	3·22	2·12	1·00	0·73
30	10	8·65	+ 0·10	0·989	0·42	0·375	0·130	3·19	2·85	·985	3·19	2·10	1·00	0·74
45	25	23·65	0·30	0·918	0·42	0·390	0·130	2·96	2·75	·906	2·94	1·92	0·99	0·70
60	40	38·65	0·50	0·786	0·42	0·395	0·130	2·54	2·38	·766	2·48	1·63	0·98	0·69
75	55	53·65	0·80	0·604	0·41	0·410	0·132	1·87	1·87	·574	1·86	1·22	0·99	0·65
90	70	68·65	1·55	0·389	0·405	0·442	0·138	1·14	1·25	·342	1·11	0·73	0·97	0·58
100	80	78·65	3·00	0·248	0·405	0·520	0·162	0·62	0·80	·174	0·56	0·37	0·91	0·46
106	86	84·65	6·50	0·205	0·445	0·720	0·286	0·32	0·51	+·070	0·22	0·15	0·70	0·29
110	90	88·65	24·30	0·433	0·64	1·610	2·190	0·32	0·32	0	0	0	0	0
114	94	92·65	167·05	0·269	1·12	0·770	0·742	0·41	0·28	−·070	0·15	0·22	0·36	0·80
120	100	98·65	176·00	0·219	0·475	0·505	0·189	0·55	0·58	−·174	0·37	0·56	0·67	0·97
130	110	108·65	178·00	0·349	0·330	0·460	0·140	0·82	1·15	−·342	0·73	1·11	0·89	0·97
145	125	123·65	179·10	0·567	0·320	0·435	0·132	1·38	1·87	−·574	1·22	1·86	0·89	0·99
160	140	138·65	179·50	0·756	0·345	0·430	0·130	2·00	2·50	−·766	1·63	2·48	0·82	0·99
180	160	158·65	179·75	0·933	0·36	0·430	0·130	2·58	3·09	−·940	2·00	3·05	0·78	0·99

Angles with a positive sign are measured in an anti-clockwise direction.

y_c and y_t are the maximum distances from the neutral axis of points in the periphery of the section, y_c being measured on the left-hand side of the axis of bending looking in the direction of the arrow.

I_{x_o} and I_{y_o} are the principal moments of inertia of a section.

I_x is the moment of inertia of the section about an axis through the C.G. parallel to the chord.

y'_c and y'_t are the maximum distances from the axis through the C.G. parallel to the chord, of points on the periphery of the section, y'_c being measured on the left-hand side of the axis of the bending moment, M cos (ψ − θ), looking in the direction of the arrow.

I 38281

TABLE 7.

A COMPARISON OF THE STRESSES AS CALCULATED FROM THE METHOD A WITH THOSE CALCULATED FROM METHOD B.

Calculations made on an aerofoil for which $\left(\frac{\text{maximum thickness}}{\text{chord length}}\right)$ is 0·25.

Length of the chord taken to be 5″·2. Value of θ taken to be 40°. I_{x_o} of section = 0·53 (inch)⁴.
I_{y_o} of section = 7·91 (inch)⁴. Φ of section = 3·6°.
Moment of inertia of the section about the chord, I_x = 0·56 (inch)⁴.

Ψ	(Ψ − θ)°	λ° = (Ψ − 43·6)	δ°	cos (λ − δ)	y_c (in.).	y_t (in.).	Moment of Inertia of Section about the Neutral Axis I_N. (In.)⁴.	Method A. Stress due to Bending Moment M. (Lbs./sq. in.) Compressive. Value of $\frac{f_c}{M}$ or $\left(\frac{y_c \cos(\lambda-\delta)}{I_N}\right)$ (1)	Method A. Stress due to Bending Moment M. (Lbs./sq. in.) Tensile. Value of $\frac{f_t}{M}$ or $\left(\frac{y_t \cos(\lambda-\delta)}{I_N}\right)$ (2)	cos (Ψ − 40°)	Method B. Stress due to Bending Moment M. (Lbs./sq. in.) Compressive. Value of $\frac{f'_c}{M}$ or $\left(\frac{y'_c \cos(\Psi-40°)}{I_x}\right)$ (3)	Method B. Stress due to Bending Moment M. (Lbs./sq. in.) Tensile. Value of $\frac{f'_t}{M}$ or $\left(\frac{y'_t \cos(\Psi-40°)}{I_x}\right)$ (4)	Ratio of the Stresses Calculated from Methods A and B. Compressive. Col. 3 / Col. 1	Ratio of the Stresses Calculated from Methods A and B. Tensile. Col. 4 / Col. 2
0	− 40	− 43·6	− 3·65	0·767	0·790	0·520	0·559	1·030	0·715	0·766	1·070	0·715	0·99	1·00
10	− 30	− 33·6	− 2·65	0·858	0·780	0·565	0·543	1·230	0·895	0·866	1·200	0·805	0·98	0·90
20	− 20	− 23·6	− 1·70	0·928	0·770	0·595	0·536	1·330	1·030	0·940	1·310	0·875	0·98	0·95
25	− 15	− 18·6	− 1·30	0·955	0·760	0·605	0·525	1·380	1·000	0·966	1·340	0·900	0·97	0·82
30	− 10	− 13·6	− 0·95	0·976	0·750	0·620	0·533	1·370	1·130	0·985	1·370	0·915	1·00	0·81
35	− 5	− 8·6	− 0·60	0·990	0·750	0·630	0·532	1·400	1·170	0·996	1·390	0·930	0·99	0·79
40	0	− 3·6	− 0·25	0·998	0·745	0·645	0·531	1·400	1·210	1·000	1·390	0·930	0·99	0·77
45	+ 5	+ 1·4	+ 0·10	0·999	0·735	0·665	0·531	1·380	1·250	0·996	1·390	0·930	1·00	0·74
50	10	6·4	0·45	0·995	0·735	0·675	0·532	1·380	1·260	0·985	1·370	0·915	0·99	0·73
60	20	16·4	1·10	0·965	0·725	0·700	0·534	1·310	1·260	0·940	1·310	0·875	1·00	0·69
75	35	31·4	2·35	0·874	0·715	0·740	0·544	1·115	1·195	0·819	1·140	0·760	0·99	0·64
90	50	46·4	4·05	0·739	0·705	0·805	0·567	0·919	1·105	0·643	0·895	0·600	0·97	0·54
105	65	61·4	7·00	0·582	0·690	0·910	0·641	0·625	0·825	0·423	0·590	0·395	0·94	0·48
120	80	76·4	15·50	0·486	0·740	1·190	1·056	0·340	0·545	0·174	0·240	0·160	0·71	0·29
125	85	81·4	23·95	0·538	1·050	1·455	1·749	0·325	0·450	0·087	0·120	0·080	0·37	0·18
135	95	91·4	110·00	0·948	2·890	1·950	1·020	0·390	0·265	−0·087	0·080	0·120	0·21	0·45
140	100	96·4	149·90	0·595	1·720	1·250	2·382	0·430	0·310	−0·174	0·160	0·240	0·37	0·78
150	110	106·4	167·15	0·488	0·965	0·920	0·897	0·525	0·500	−0·342	0·320	0·475	0·61	0·95
180	140	136·4	176·35	0·767	0·520	0·790	0·559	0·715	1·080	−0·766	0·715	1·070	1·00	0·99

Angles with a positive sign are measured in an anti-clockwise direction.

y_c and y_t are the maximum distances from the neutral axis of points in the periphery of the section, y_c being measured on the left-hand side of the axis of bending looking in the direction of the arrow.

I_{x_o} and I_{y_o} are the principal moments of inertia of a section.

I_x is the moment of inertia of the section about an axis through the C.G. parallel to the chord.

y'_c and y'_t are the maximum distances from the axis through the C.G. parallel to the chord, of points on the periphery of the section y'_c being measured on the left-hand side of the axis of the bending moment M cos (Ψ − θ), looking in the direction of the arrow.

REPORT No 420.

— SOME NOTES ON THE STRESSES OF AN AIRSCREW —

— Sketch of Airscrew —

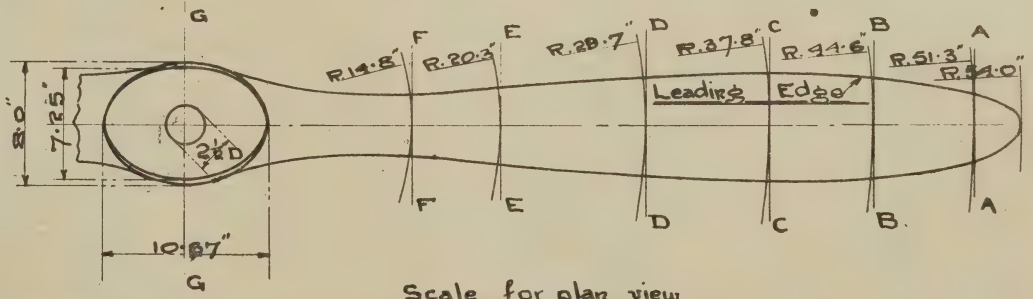

Lines "OO" all in one plane normal to axis of airscrew

Scale for plan view

0 1' 2 3 FT

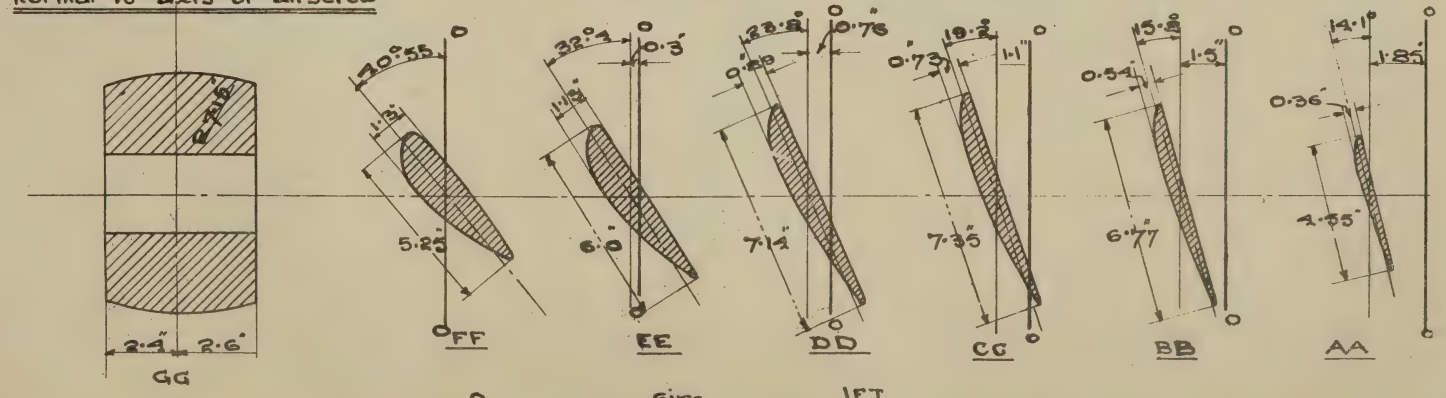

Scale for sectional views

FIG. 3.

SOME NOTES ON THE STRESSES OF AN AIRSCREW.—

—Figs. 4, 5 & 6.—

CALCULATION OF THE BENDING MOMENT DUE TO THE THRUST.

TRANSLATIONAL SPEED OF THE AIRSCREW = 95 MILES/HR.

ROTATIONAL SPEED OF THE AIRSCREW = 1375 R.P.M.

THRUST OF THE AIRSCREW = 3501bs.

Fig 4

Fig 5

Fig 6

SOME NOTES ON THE STRESSES OF AN AIRSCREW

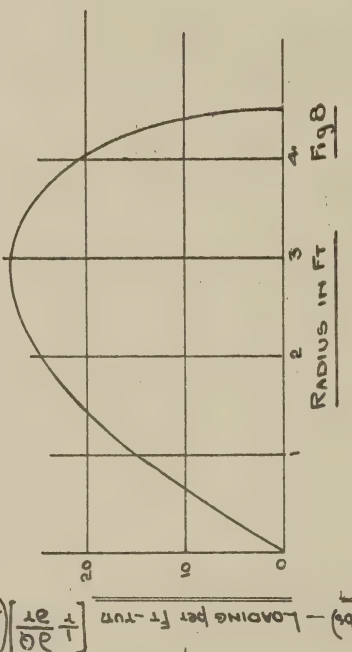

Fig 8

— LOADING PER FT-TWT $\left[\frac{1}{r}\frac{\partial Q}{\partial r}\right]\left(\frac{\text{lbs}}{\text{Ft.}}\right)$

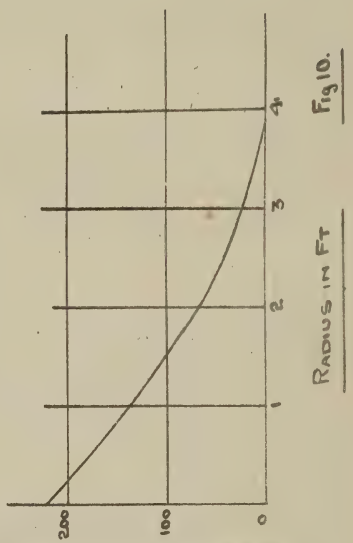

Fig 10.

— BENDING MOMENT DUE TO Q (Ft.-lbs)

CALCULATION OF BENDING MOMENT DUE TO THE TORQUE.

TRANSLATION SPEED OF AIRSCREW = 85 MILES/HR

ROTATIONAL SPEED OF AIRSCREW = 1375 R.P.M.

TORQUE OF AIRSCREW = 4701bs-FT.

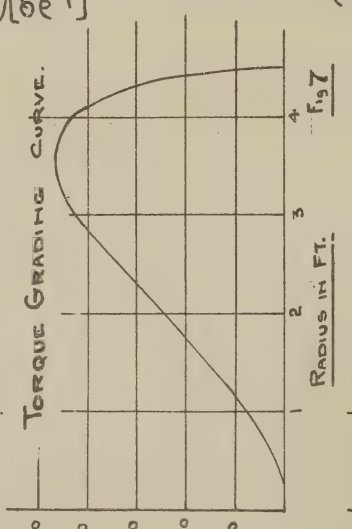

Fig 7

— VALUE OF $\left(\frac{\partial Q}{\partial r}\right)$ lbs —

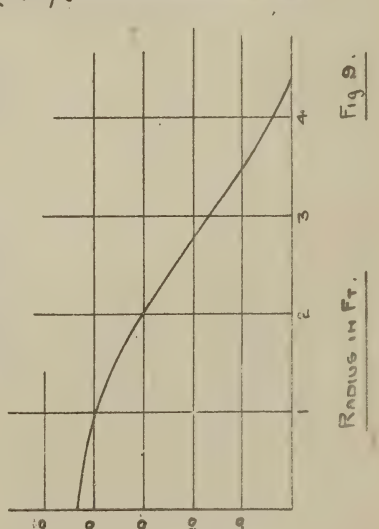

Fig 9.

— VALUE OF $\left[\int_R^{\text{TIP}} \left(\frac{\partial Q}{\partial r}\right) dr\right]$ lbs —

SOME NOTES ON THE STRESSES OF AN AIRSCREW. —

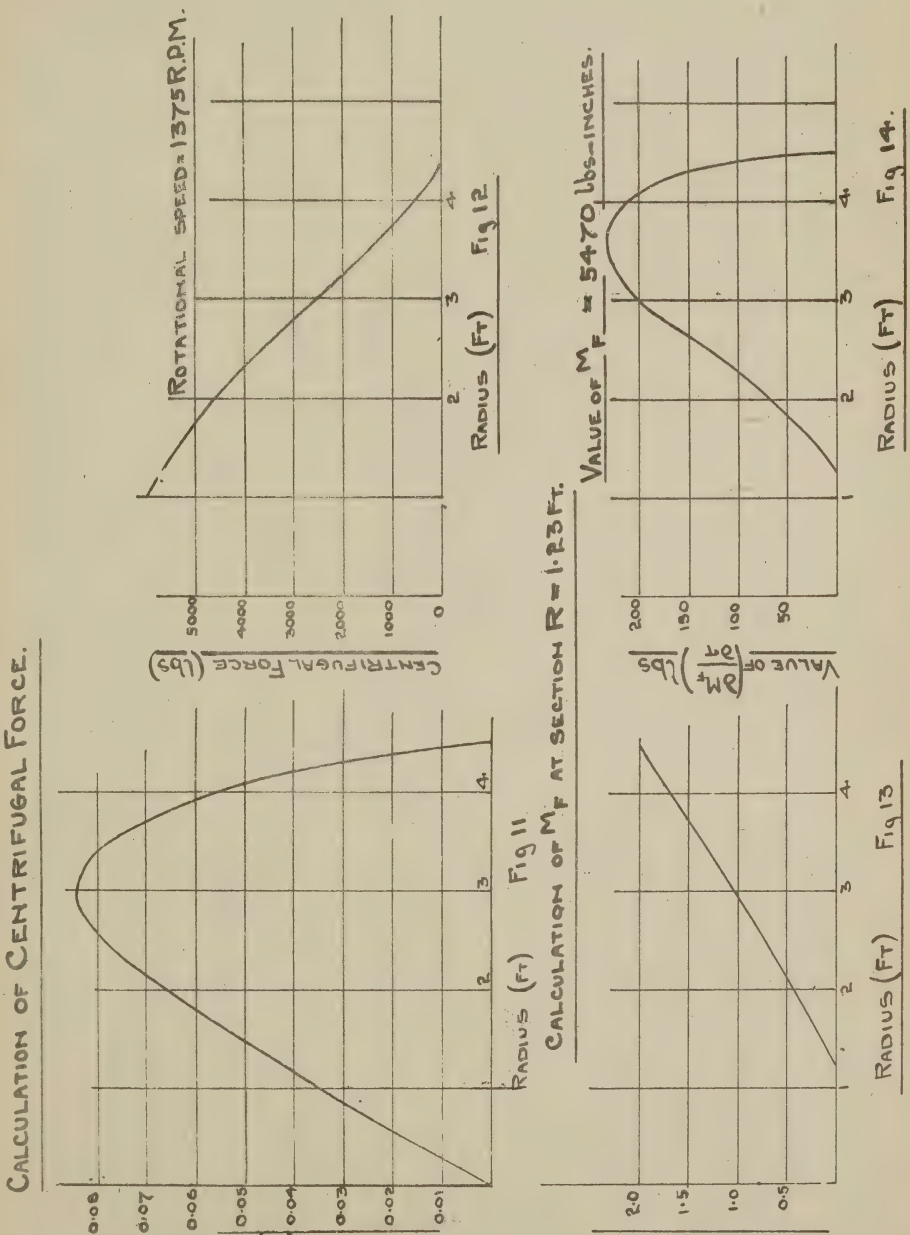

—SOME NOTES ON THE STRESSES OF AN AIRSCREW—

ISOMETRIC VIEW OF THE NEUTRAL SURFACE OF THE AIRSCREW BLADE.

TRANSLATIONAL SPEED V = 85 MILES/HR.

ROTATIONAL SPEED N = 1375 R.P.M.

THRUST T = 350 LBS

TORQUE Q = 470 LBS-FT.

ISOMETRIC VIEW OF THE NEUTRAL SURFACE OF THE AIRSCREW BLADE.

TRANSLATIONAL SPEED	V = 57 MILES/HR.
ROTATIONAL SPEED	N = 1230 R.P.M.
THRUST	T = 500 LBS
TORQUE	Q = 490 LBS – FT.

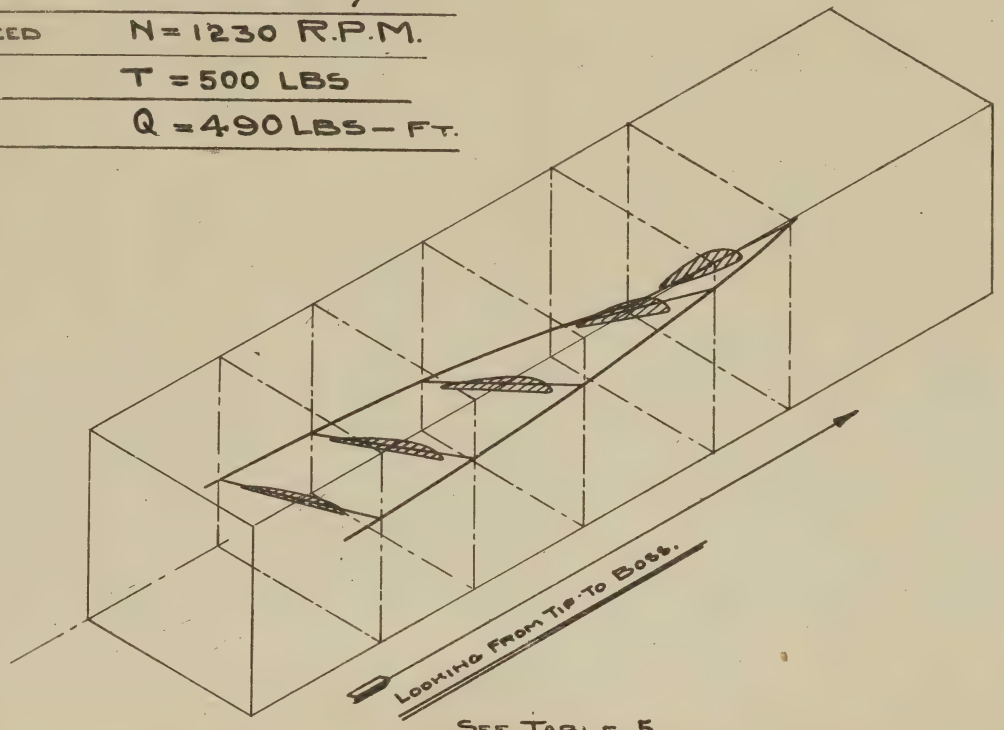

SEE TABLE 5.

SOME NOTES ON THE STRESSES OF AN AIRSCREW.

SHAPE OF BLADE SECTION FOR WHICH THE CALCULATIONS OF TABLE 6 WERE MADE.

$$\left[\frac{\text{MAXIMUM THICKNESS}}{\text{CHORD LENGTH}}\right] = 0.10$$

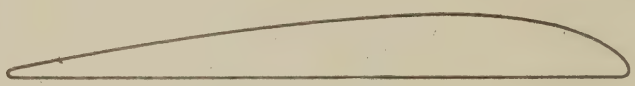

SHAPE OF THE BLADE SECTION FOR WHICH THE CALCULATIONS OF TABLE 7 WERE MADE.

$$\left[\frac{\text{MAXIMUM THICKNESS}}{\text{CHORD LENGTH.}}\right] = 0.25.$$

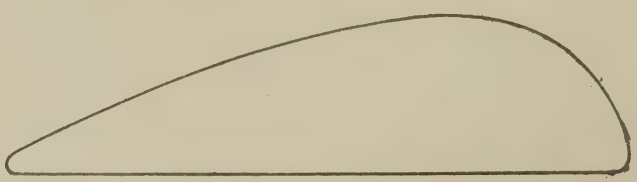

SOME NOTES ON THE STRESSES OF AN AIRSCREW.

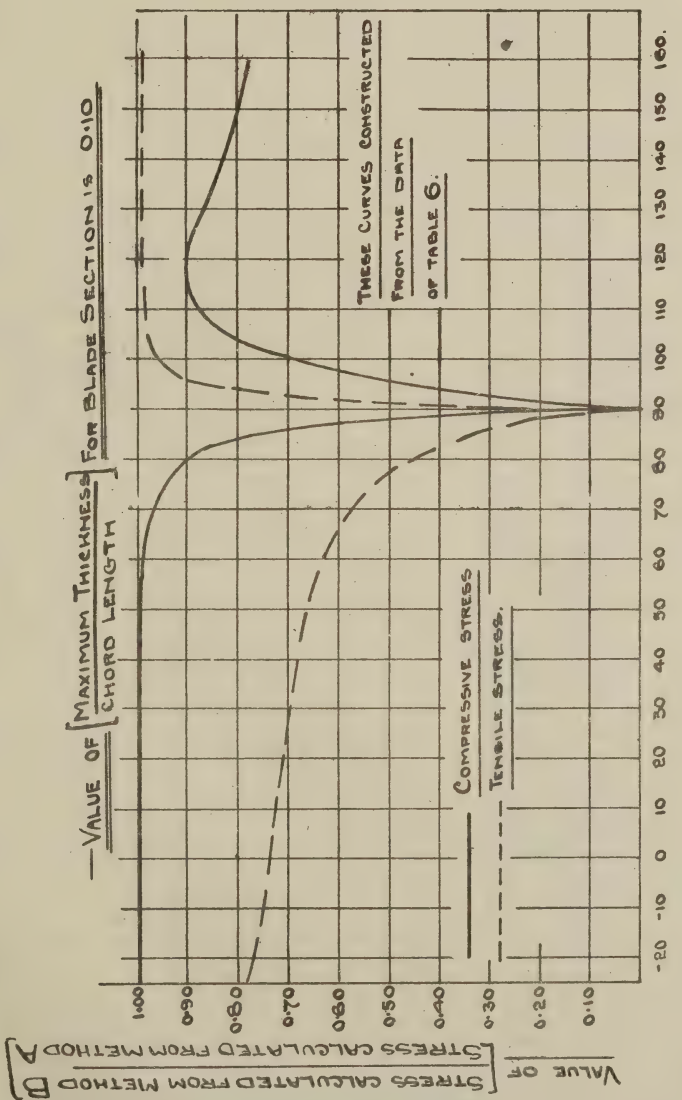
VALUE OF [STRESS CALCULATED FROM METHOD B / STRESS CALCULATED FROM METHOD A]
1·00
0·90
0·80
0·70
0·60
0·50
0·40
0·30
0·20
0·10
-20 -10 0 10 20 30 40 50 60 70 80 90 100 110 120 130 140 150 160
—VALUE OF (Ψ-θ) (DEGREES)—
—VALUE OF [MAXIMUM THICKNESS / CHORD LENGTH] FOR BLADE SECTION IS 0·10
COMPRESSIVE STRESS
TENSILE STRESS.
THESE CURVES CONSTRUCTED FROM THE DATA OF TABLE 6.

SOME NOTES ON THE STRESSES OF AN AIRSCREW.—

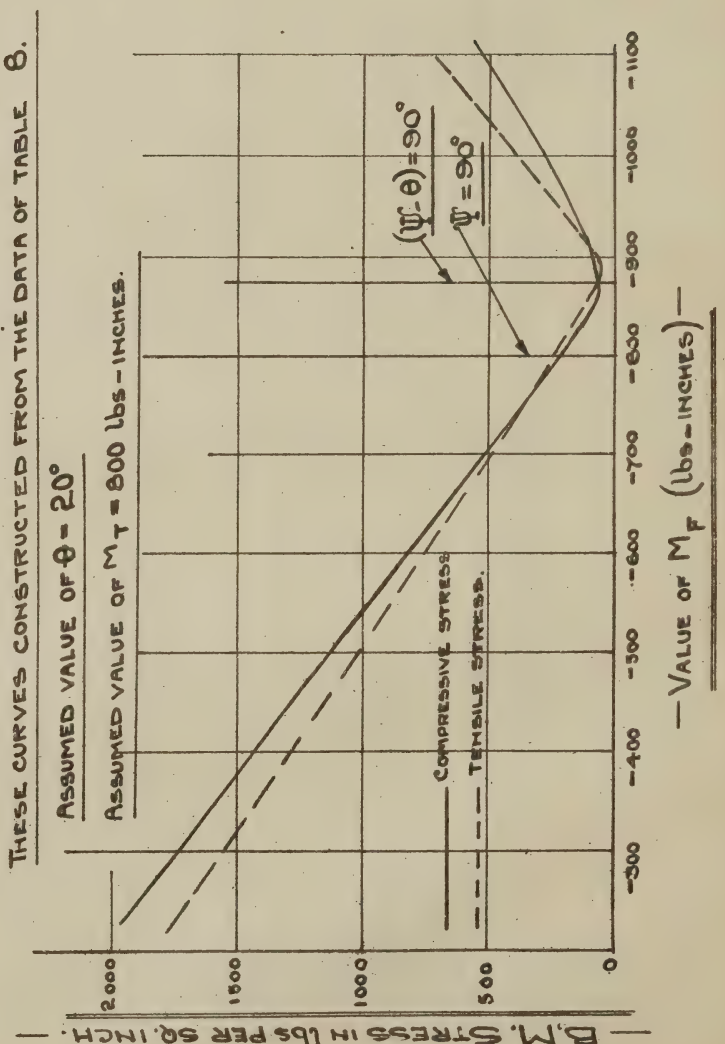

SOME NOTES ON THE STRESSES OF AN AIRSCREW.

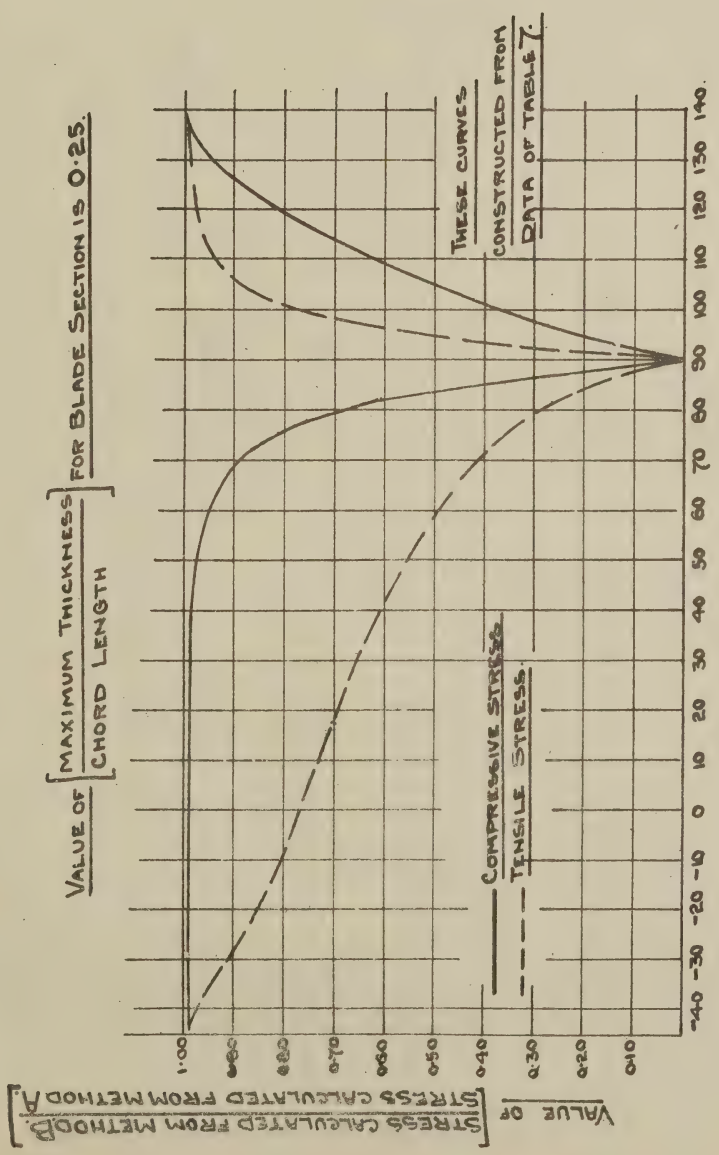
VALUE OF [MAXIMUM THICKNESS / CHORD LENGTH] FOR BLADE SECTION IS 0·25.
THESE CURVES CONSTRUCTED FROM DATA OF TABLE 7.
COMPRESSIVE STRESS.
TENSILE STRESS.
— VALUE OF (Ψ-θ) (DEGREES) —
VALUE OF [STRESS CALCULATED FROM METHOD B / STRESS CALCULATED FROM METHOD A]
1·00
0·90
0·80
0·70
0·60
0·50
0·40
0·30
0·20
0·10
-40 -30 -20 -10 0 10 20 30 40 50 60 70 80 90 100 110 120 130 140

SOME NOTES ON THE STRESSES OF AN AIRSCREW.

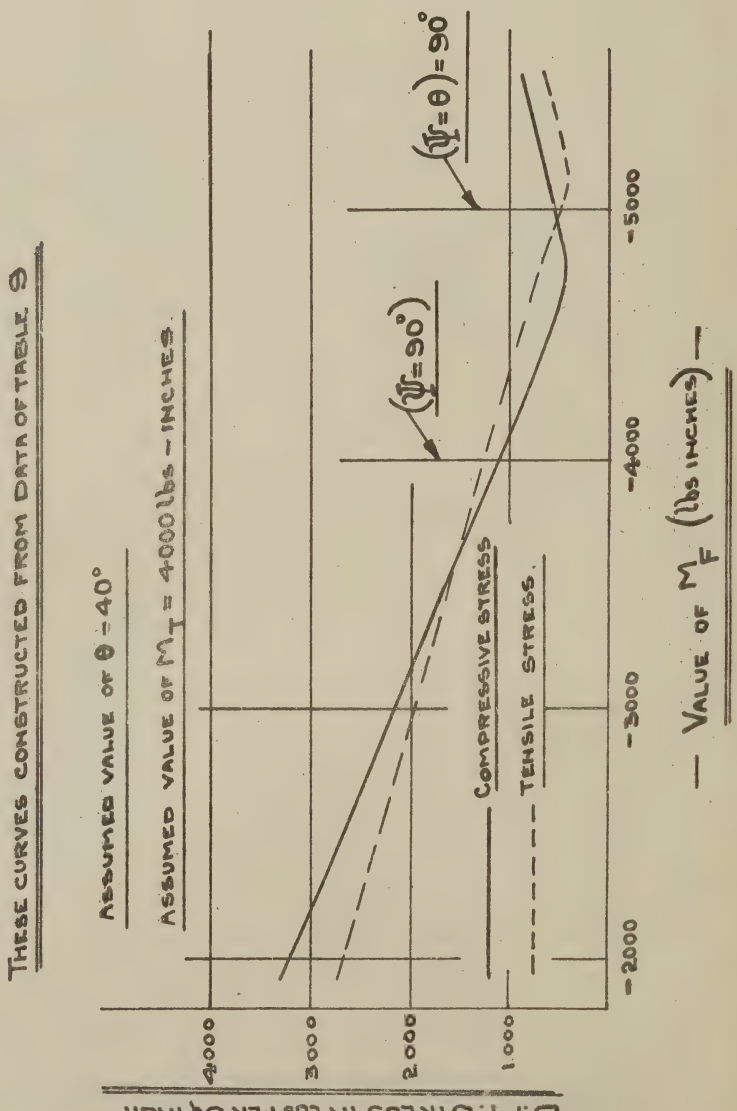

TABLE 9.

THE VARIATION OF THE STRESSES IN A BLADE SECTION WITH THE BENDING MOMENT DUE TO CENTRIFUGAL FORCE, M_F.

Calculations made on an aerofoil section for which

$$\left(\frac{\text{maximum thickness}}{\text{chord length}}\right) \text{ is } 0{\cdot}25.$$

Length of chord taken to be 5″·2. Value of θ taken to be 40°

I_{x_o} of section = 0·53 (inch)⁴. I_{y_o} of section = 7·91 (inch)⁴.

Φ of section = 3·6°.

Value of M_Q assumed to be 1,200 lbs.-ins.

Value of M_T assumed to be 4,000 lbs.-ins.

$$\tan \psi = \frac{M_Q}{(M_T + M_F)}$$

Value of ψ.	Value of $(M_T + M_F)$	Value of M_F.	Value of M.	Maximum Stresses due to M. lbs. per sq. inch.	
(Degrees.)	(Lbs.-ins.)	(Lbs.-ins.)	(Lbs.-ins.)	Compressive.	Tensile.
20	3,300	− 700	3,510	4,660	3,620
30	2,080	−1,920	2,400	3,290	2,720
40	1,430	−2,570	1,865	2,610	2,250
50	1,005	−2,995	1,565	2,160	1,975
75	+ 320	−3,680	1,240	1,430	1,480
90	0	−4,000	1,200	1,105	1,330
105	− 320	−4,320	1,240	770	1,025
120	− 695	−4,695	1,385	470	755
125	− 840	−4,840	1,465	475	660
135	−1,200	−5,200	1,700	665	450
140	−1,430	−5,430	1,865	805	580
150	−2,080	−6,080	2,400	1,260	1,200

THE WHIRLING AND TRANSVERSE VIBRATIONS OF A ROTATING AIRSCREW AND ITS SHAFT.

By A. Fage, A.R.C.Sc.

Reports and Memoranda, No. 502. *June,* 1917.

Summary.—The present paper gives the general mathematical theory of the transverse vibrations of a rotating airscrew and its shaft. The investigation is an interesting application of Lagrange's Equations for small oscillations. Calculations have been made for a two-bladed airscrew, when the transverse vibrations are in a plane parallel to both the axis of the airscrew blades and the axis of rotation, and also when in a plane at right angles to the axis of the airscrew blades and parallel to the axis of rotation. It was found that the whirling speed of a modern airscrew and its shaft was very high, and much greater than the bursting speed of the airscrew.

The general conclusions of the investigation are :—

(*a*) The air damping of an airscrew is negligible in so far as the frequency of the transverse vibrations is concerned.

(*b*) The whirling speed may be calculated with very good accuracy by assuming the effect of the shaft to be the equivalent of a mass ($78/210\ M_1$) at the end, where M_1 is the mass of the shaft.

(*c*) Neglecting the mass of the shaft makes the whirling speed too high, the discrepancy increasing with the length of the shaft.

(*d*) Even when the moment of inertia of the airscrew is small it should not be neglected in the calculation of the whirling speed.

(*e*) The critical speed of an airscrew and its shaft increases with the moment of inertia of the airscrew.

A simple formula from which may be calculated the whirling speed of an airscrew and its shaft is given at the end of the paper.

The present paper gives the mathematical theory of the transverse vibrations of a rotating airscrew and its shaft, and also an application of the method to several practical problems.

For generality, the calculations have been made for a two-bladed airscrew, when the transverse vibrations are in a plane parallel to both the axis of the airscrew blades and the axis of rotation, and also when in a plane at right angles to the axis of the airscrew blades and parallel to the axis of rotation.

The dependence of the frequency of the transverse vibrations on the length of the shaft, and also on the speed of rotation has also been determined.

Finally, by the elimination of quantities which only slightly influence the value of the frequency of the transverse vibrations, a moderately accurate working formula has been evolved, from which the whirling speed of a rotating airscrew and shaft may be readily calculated.

The whirling speed of a modern airscrew as now mounted on the engine of an aeroplane is very high and very much greater than the bursting speed of the airscrew.

The mathematical theory of the transverse vibrations of rotating systems is given by Dr. Chree in the "Proceedings of the Physical Society of London" (1903-5).

In order that the present paper may be complete, it is desirable at the outset to indicate the relationship between the frequency of the lateral transverse vibrations and the whirling speed.

Taking the simple case of a shaft of negligible mass fixed at one end and carrying a mass M at the other, it can easily be shown, if $\frac{p}{2\pi}$ be the frequency of the transverse vibrations of the mass M when the shaft is not rotating, and $\frac{q}{2\pi}$ the frequency of the transverse vibrations when the shaft is rotating with an angular velocity ω, that $q^2 = p^2 - \omega^2$.

The elastic forces of the shaft tend to restore the mass to its equilibrium position, but the centrifugal force acting on the mass has the opposite tendency, and by reducing the magnitude of the righting force diminishes also the frequency of vibration of the rotating mass and shaft. If ω be equal to p, the frequency of the transverse vibrations is zero, so that the mass is in neutral equilibrium no matter what the value of the lateral displacement may be, and hence if the lateral displacement be sufficiently great the shaft will fracture. A shaft in such a state is said "to whirl," the righting force due to the elasticity of the system having been reduced to zero by the centrifugal force called into being by deflection. For this particular instance the frequency of rotation when the shaft is whirling, and the frequency of the transverse vibrations when the shaft is not rotating, have equal values, but this is not the case with a rotating airscrew and shaft in which moments of inertia and damping need consideration.

To find the frequency of the transverse vibrations of a rotating airscrew and shaft.—The following investigation is an application of Lagrange's Equations for small oscillations.

An instantaneous position of the rotating and vibrating airscrew and shaft is shown in Fig. 1, the plane of vibration of the shaft being coincident with the plane of the paper. It is assumed that the airscrew shaft is fixed in direction at the end O, so that the line OX represents the main position of the vibrating shaft, and also the axis about which the rotation is taking place.

The following symbols are used in the investigation :—

L = length of the shaft in feet.

M = mass of the airscrew in slugs.

m = mass of the shaft in slugs per foot run.

I_1 = moment of inertia of the airscrew about the axis CA in slug/ft.^{2}

I_2 = moment of inertia of the airscrew about an axis through C at right angles to the plane of bending.

I_3 = moment of inertia of the airscrew about an axis through C in the plane of bending and at right angles to CA.

ω = speed of rotation of the airscrew in radians per sec.

E = Young's modulus of elasticity in lbs. per sq. foot.

I = moment of inertia of a cross-section of the shaft about a diameter measured in (ft)^4.

x = distance from O, in feet, of any point P on the axis of the shaft.

y = deflection in ft. of the point P from the line OX.

At any time t the free end of the shaft is displaced a distance "z" from its mean position, and the plane of the airscrew has an angular displacement "θ" from its mean position.

The equations of motion are expressed in terms of the variables θ and z.

From the above remarks it follows that

$$\text{when } x = 0, \frac{dy}{dx} = 0 \text{ and } y = 0,$$

$$\text{when } x = \mathrm{L}, \frac{dy}{dx} = \theta \text{ and } y = z.$$

So that the equation of the curve of the centre line of the shaft is

$$y = \left(\frac{3z - \theta\mathrm{L}}{\mathrm{L}^2}\right)x^2 - \left(\frac{\theta\mathrm{L} - 2z}{\mathrm{L}^3}\right)x^3$$

Lagrange's equations for a damped vibrating system in which there are two variables θ and z are

$$\frac{\delta}{\delta t}\left(\frac{\delta \mathrm{T}}{\delta \dot{\theta}}\right) - \frac{\delta \mathrm{T}}{\delta \theta} + \frac{\delta \mathrm{V}}{\delta \theta} + \frac{\delta \mathrm{F}}{\delta \dot{\theta}} = 0$$

$$\text{and } \frac{\delta}{\delta t}\left(\frac{\delta \mathrm{T}}{\delta \dot{z}}\right) - \frac{\delta \mathrm{T}}{\delta z} + \frac{\delta \mathrm{V}}{\delta z} + \frac{\delta \mathrm{F}}{\delta \dot{z}} = 0$$

where T = kinetic energy of the whole system.

V = potential energy of the whole system.

and F = half the rate at which energy is being dissipated.

For the case of a vibrating airscrew and shaft, the kinetic energy of the whole system is equal to the sum of the kinetic energy of the shaft and the kinetic energy of the airscrew

$$= \left(\int_o^L \frac{1}{2} m dx [\dot{y}^2 + (y\omega)^2]^2 \right) + \frac{M}{2}(\dot{z}^2 + \omega^2 z^2) + \frac{I_1}{2}\omega^2 \cos^2\theta + \frac{I_3}{2}\omega^2 \sin^2\theta + \frac{I_2}{2}\dot{\theta}^2$$

$$= \left\{ \begin{aligned} &\frac{m\omega^2 L}{2}\left[\frac{1}{5}(3z - \theta L)^2 + \frac{1}{3}(3z - \theta L)(\theta L - 2z) + \frac{1}{7}(\theta L - 2z)^2\right] \\ &+ \frac{mL}{2}\left[\frac{1}{5}(3\dot{z} - \dot{\theta} L)^2 + \frac{1}{3}(3\dot{z} - \dot{\theta} L)(\dot{\theta} L - 2\dot{z}) + \frac{1}{7}(\dot{\theta} L - 2\dot{z})^2\right] \\ &+ \frac{M}{2}(\dot{z}^2 + \omega^2 z^2) + \frac{I_1\omega^2}{2} + \frac{I_2}{2}(\dot{\theta}^2 - \omega^2\theta^2) \end{aligned} \right\}$$

since $I_1 = I_2 + I_3$ and $\sin\theta = \theta$ nearly.

The potential energy, V, of the system is equal to the potential energy of the shaft

$$= \int_o^L \frac{EI}{2}\left(\frac{d^2y}{dx^2}\right)^2 dx$$

$$= \int_o^L \frac{EI}{2}\left[\frac{2}{L^2}(3z - \theta L) + \frac{6x}{L^3}(\theta L - 2z)\right]^2 dx$$

$$= \frac{2EI}{L^3}[3z^2 - 3z\theta L + \theta^2 L^2]$$

Owing to the vibratory motion of the airscrew blades through the air, energy is dissipated, the rate of such dissipation—2F—being equal to $K\dot{\theta}^2$, where K is a constant. The value of the damping factor "K" can be readily calculated when the aerodynamic data of the blade sections of the airscrew and also the working conditions of the airscrew are known, but it may be of some interest to explain in general language why the rate at which energy is dissipated is proportional to the square of the angular speed of vibration.

Consider the vibratory motion of the blades about an axis through C (Fig. 1) at right angles to the axes of the airscrew and of the airscrew blades, the airscrew having the forward translational speed of the aeroplane and a rotational speed about the axis OX of ω radians per second. For any positive value of the angular velocity $\dot{\theta}$, the thrust on the blade CF, which is moving into the air with a velocity greater than that due to the motion of the aeroplane alone, is diminished, whilst the thrust on the blade CE is increased, the change of thrust of an aerofoil section of the blade being roughly proportional to the change of angle of incidence of the section relatively to the air. As a first approximation, the change of the angle of incidence of a blade section is proportional to $\dot{\theta}$, so that the change of thrust of the blade and therefore also the damping moment on the airscrew is proportional to $\dot{\theta}$. Writing the damping moment as $K\dot{\theta}$, the rate at which energy is dissipated becomes $K\dot{\theta}^2$. It will be shown later that the damping moment does not appreciably influence the frequency of the transverse vibrations.

Hence

$$F = \frac{K\dot{\theta}^2}{2} \text{ where K is a constant.}$$

Substituting the above values of T, V and F in the Lagrangean Equations we get

$$I_2\ddot{\theta} + \frac{mL^2}{210}(2L\ddot{\theta} - 11\ddot{z}) - \frac{m\omega^2L^2}{210}(2L\theta - 11z) + I_2\omega^2\theta + \frac{2EI}{L^3}(2\theta L^2 - 3zL) + K\dot{\theta} = 0$$

and

$$M\ddot{z} + \frac{ML}{210}(78\ddot{z} - 11L\ddot{\theta}) - \frac{m\omega^2L}{210}(78z - 11L\theta) - Mz\omega^2 + \frac{2EI}{L^3}(6z - 3\theta L) = 0$$

Which when collected in a convenient form become

$$\left[\left[\left(I_2 + \frac{2}{210}mL^3\right)D^2 + KD + \left(I_2\omega^2 - \frac{2}{210}m\omega^2L^3 + \frac{4EI}{L}\right)\right]\theta - \left[\frac{11}{210}mL^2D^2 + \left(\frac{6EI}{L^2} - \frac{11}{210}m\omega^2L^2\right)\right]z\right] = 0$$

and

$$\left[-\left[\frac{11}{210}mL^2D^2 + \left(\frac{6EI}{L^2} - \frac{11}{210}m\omega^2L^2\right)\right]\theta + \left[\left(M + \frac{78}{210}mL\right)D^2 + \left(\frac{12EI}{L^3} - M\omega^2 - \frac{78}{210}m\omega^2L\right)\right]z\right] = 0$$

So that the complete motion is given by the solution of the differential equation

$$\left\{\begin{array}{c}\left[\left(I_2 + \frac{2}{210}mL^3\right)D^2 + KD + \left(I_2\omega^2 - \frac{2}{210}m\omega^2L^3 + \frac{4EI}{L}\right)\right] \times \\ \left[\left(M + \frac{78}{210}mL\right)D^2 + \left(\frac{12EI}{L^3} - M\omega^2 - \frac{78}{210}m\omega^2L\right)\right] \\ - \left[\frac{11}{210}mL^2D^2 + \left(\frac{6EI}{L^2} - \frac{11}{210}m\omega^2L^2\right)\right]^2\end{array}\right\}\theta = 0$$

Owing to the large number of algebraic terms—several of them having negligible values—no advantage is to be gained by attempting to solve the differential equation of the fourth order in its present form. By the substitution of the numerical values of the symbols, the equation may be written in the form

$$(D^4 + A_1D^3 + A_2D^2 + A_3D + A_4)\,\theta = 0$$

where A_1, A_2, A_3, A_4 are numerical constants. It will be shown later that for all practical purposes the values of A_1 and A_3 are equal to zero so that the equation is reduced to

$$(D^4 + A_2D^2 + A_4)\,\theta = 0$$

The airscrew and shaft commence to whirl when the frequency of one of the transverse vibrations just becomes zero, so that at the whirling speed the solution of the equation

$$(D^4 + A_2D^2 + A_4)\,\theta = 0$$

becomes

$$\theta = B_1 + B_2\,t + B_3 \sin \beta t + B_4 \cos \beta t$$

where B_1, B_2, B_3, B_4 are arbitrary constants depending on the initial conditions. For a rotational speed less than the whirling speed, the motion consists of two vibrations, whilst at a rotational speed greater than the whirling speed the motion is compounded of a vibration, a divergence and a subsidence, so if the divergence is allowed to persist the shaft fractures.

Application of the preceding theory to several practical problems.—With the object of simplifying the differential equation of the motion of the vibrating airscrew and shaft a systematic series of calculations has been made to ascertain how the frequency of the vibrations depends upon the damping, the mass and the length of the shaft, the mass and the moment of inertia of the airscrew.

The following data which are needed in the calculations have been taken from a modern two-bladed airscrew which, rotating at about 1,300 r.p.m., would give a machine weighing one ton a forward speed through the air of 75 miles per hour, the corresponding thrust being 300 lbs. approximately.

Diameter of the airscrew ... = 9·5 ft.

Mass of the airscrew and metal fittings at the boss, M ... = 1·0 slug.

Outside diameter of the airscrew shaft ... ... = 2 ins.

Inside diameter of the airscrew shaft ... ... = 0·9 in.

Whence moment of inertia of a section of the airscrew shaft about a diameter ... ... = $0{\cdot}362 \times 10^{-4}(\text{ft})^4$.

Length of the airscrew shaft, L = 0·5 ft.

Mass of 1 ft. length of the airscrew shaft, m ... ... = 0·26 slug.

Modulus of elasticity, E ... = $4{\cdot}17 \times 10^9$ lbs/sq. ft.

Moment of inertia of the airscrew about an axis passing through the centre of the boss at right angles to both the airscrew axis and the blade axis ... ... = 3·5 slug-ft^2.

Moment of inertia of the airscrew about the blade axis ... = 0·02 slug-ft^2.

Hence $I_2 = 3{\cdot}5 \sin^2 \alpha + 0{\cdot}02 \cos^2 \alpha$

where α = angle between the blade axis and an axis passing through the centre of the boss at right angles to the plane of vibration.

Only the two extreme values of I_2 were taken, namely, 3·5 when $\alpha = 90°$ and 0·02 when $\alpha = 0°$.

The rate at which energy is dissipated for this airscrew is $1500\dot{\theta}^2$ ft-lbs. per second, when $\alpha = 90°$.

The damping when $\alpha = 0°$ can be neglected at the commencement of the investigation.

The calculations are quite straightforward, although somewhat laborious, and it has been considered not desirable to overburden the paper with the complete figures, so that only a summary of the results is given in the tables and shewn graphically in the diagrams. It will be noted that the frequency of the transverse vibrations of the airscrew as mounted in practice is very high, much higher than the bursting speed of the airscrew, which is about 3,500 r.p.m., and accordingly calculations were made for the airscrew mounted at the end of a shaft of length 2·5 ft. As stated at the commencement of the investigation it is assumed that the airscrew shaft is rigidly fixed at one end, but it is uncertain how far such a condition holds in practice, much depending on the rigidity of the engine frame and the method of mounting the airscrew shaft. Any want of rigidity at the end of the shaft will reduce, at the same speed of rotation, the frequency of the transverse vibrations.

If the end conditions are different from those postulated in the present paper, but are definitely defined, the same method of calculating the frequency of the transverse vibrations may be employed, although the equation of the centre line of the shaft will be different.

The solution of the biquadratic

$$D^4 + A_1D^3 + A_2D^2 + A_3D + A_4 = 0$$

was greatly facilitated by the fact that the terms A_1 and A_3 are of small importance compared with A_2 and A_4, so that the biquadratic could be readily split into two quadratic equations by the method of trial and error. Of course, the solution of the biquadratic equation, when the damping terms A_1 and A_3 are neglected, is a matter of no difficulty.

TABLE 1.

SUMMARY OF THE RESULTS OF THE CALCULATIONS MADE ON A MODERN TWO-BLADED AIRSCREW, MOUNTED AS IN PRACTICE ON A SHAFT OF LENGTH 0·5 FT.

Case 1.—Transverse vibrations in a plane parallel to the axis of rotation and to the blade axis.

$\alpha = 90°$ and $I_2 = 3{\cdot}5$ slug-ft^2.

Bursting speed of airscrew about 3,500 r.p.m.

Assumptions made in Calculations.	Rotational speed of the Shaft. (r.p.m.)	Number of Vibrations per Minute.	
Complete solution, making no assumptions.	0	2,770	35,800
	5,000	5,900	35,600
	10,000	10,100	34,200
	15,000	14,800	31,600
	20,000	19,000	29,700
	25,000	21,700	28,800
	30,000	17,800	31,400
	34,000	9,000	34,900
	35,000	0	35,800
Neglecting damping only	Results same as with no assumptions.		
Neglecting damping and assuming effect of shaft to be equivalent of a mass $\left(\frac{78}{210}mL\right)$ at its end.	0	2,785	35,800
	28,700	19,400	30,300
	35,100	0	35,600
Neglecting damping and also the inertia of the shaft ($m = 0$).	0	2,755	36,700
	4,000	5,100	36,700
	9,000	9,200	36,000
	14,000	13,900	33,800
	19,000	18,200	31,700
	24,000	21,500	30,200
	29,000	19,800	30,900
	34,000	12,000	34,900
	36,000	0	36,700

TABLE 2.

SUMMARY OF THE RESULTS OF THE CALCULATIONS MADE ON A MODERN TWO-BLADED AIRSCREW, MOUNTED AS IN PRACTICE ON A SHAFT OF LENGTH 0·5 FT.

Case 2.—Transverse vibrations in a plane parallel to the axis of rotation and at right angles to the blade axis.

$\alpha = 0°$ and $I_2 = 0{\cdot}02$ slug-ft^2.

No damping in this case.

Bursting speed of airscrew about 3,500 r.p.m.

Assumptions made in Calculations.	Rotational speed of the Shaft. (r.p.m.)	Number of Vibrations per Minute.	
Complete solution, making no assumptions.	0	16,600	78,800
	4,000	16,400	79,000
	10,000	14,400	80,000
	16,000	9,300	81,600
	19,000	3,800	82,700
	19,500	0	82,900
Assuming effect of the shaft to be equivalent to a mass $\left(\frac{78}{210}mL\right)$ at its end.	0	16,400	Not calculated.
	19,300	0	
Neglecting I_2, which is very small in this case, and assuming effect of the shaft to be equivalent to a mass $\left(\frac{78}{210}mL\right)$ at its end.	0	17,750	
	17,750	0	
Neglecting I_2 and also the mass of the shaft ($m = 0$).	0	18,150	
	18,150	0	

TABLE 3.

SUMMARY OF THE RESULTS OF THE CALCULATIONS MADE ON A MODERN TWO-BLADED AIRSCREW, MOUNTED AT THE END OF A LONG SHAFT OF LENGTH 2·5 FT.

Case 1.—Transverse vibrations in a plane parallel to the axis of rotation and to the blade axis.

$\alpha = 90°$ and $I_2 = 3{\cdot}5$ slug-ft^2.

Assumptions made in Calculations.	Rotational speed of the Shaft. (r.p.m.)	Number of Vibrations per Minute.	
Complete solution, making no assumptions.	0	1,000	3,640
	500	1,020	3,630
	1,000	1,060	3,620
	1,400	1,070	3,620
	1,800	950	3,650
	2,200	490	3,750
	2,290	0	3,770
Neglecting damping makes practically no difference to the frequency.			
Neglecting damping and assuming effect of the shaft to be the equivalent of a mass $\left(\frac{78}{210}mL\right)$ at its end.	0	990	3,720
	1,910	760	3,770
	2,220	0	3,780
Neglecting damping and also the inertia of the shaft ($m = 0$).	0	1,020	Not calculated.
	1,910	1,095	
	2,590	0	

TABLE 4.

SUMMARY OF THE RESULTS OF THE CALCULATIONS MADE ON A MODERN TWO-BLADED AIRSCREW, MOUNTED AT THE END OF A LONG SHAFT OF LENGTH 2·5 FT.

Case 2.—Transverse vibrations in a plane parallel to the axis of rotation and at right angles to the blade axis.

$\alpha = 0°$ and $I_2 = 0{\cdot}02$ slug-ft^2.

No damping in this case.

Assumptions made in Calculations.	Rotational Speed of the Shaft. (r.p.m.)	Number of Vibrations per Minute. Frequency of the Higher Vibration not calculated.
No assumptions	0 1,565	1,500 0
Assuming effect of the shaft to be the equivalent of a mass $\left(\frac{78}{210}mL\right)$ at its end.	0 1,510	1,480 0
Neglecting I_2, which is very small, and assuming effect of the shaft to be the equivalent of a mass $\left(\frac{78}{210}mL\right)$ at its end.	0 1,460	1,460 0
Neglecting I_2 and mass of shaft ($m = 0$).	0 1,620	1,620 0

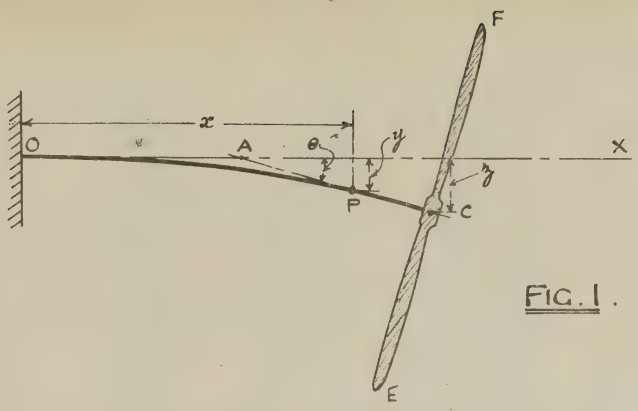

FIG. 1.

DIAGRAMMATIC SKETCH OF THE VIBRATING AIRSCREW.
PLANE OF VIBRATION COINCIDENT WITH PLANE OF PAPER.

E.F. = Axis of Airscrew Blades.

TRANSVERSE VIBRATIONS IN A PLANE PARALLEL TO THE AXIS OF ROTATION AND TO THE BLADE-AXIS. $L = 0{\cdot}5$ FT. $I_2 = 3{\cdot}5$ SLUG-(FT.)^2.

FIG. 2.

TRANSVERSE VIBRATIONS IN A PLANE PARALLEL TO THE AXIS OF ROTATION AND AT RIGHT-ANGLES TO THE BLADE AXIS $L = 0.5$ FT. $I_2 = 0.02$ SLUG-(FT.)^2

HIGHER FREQUENCY NOT PLOTTED.

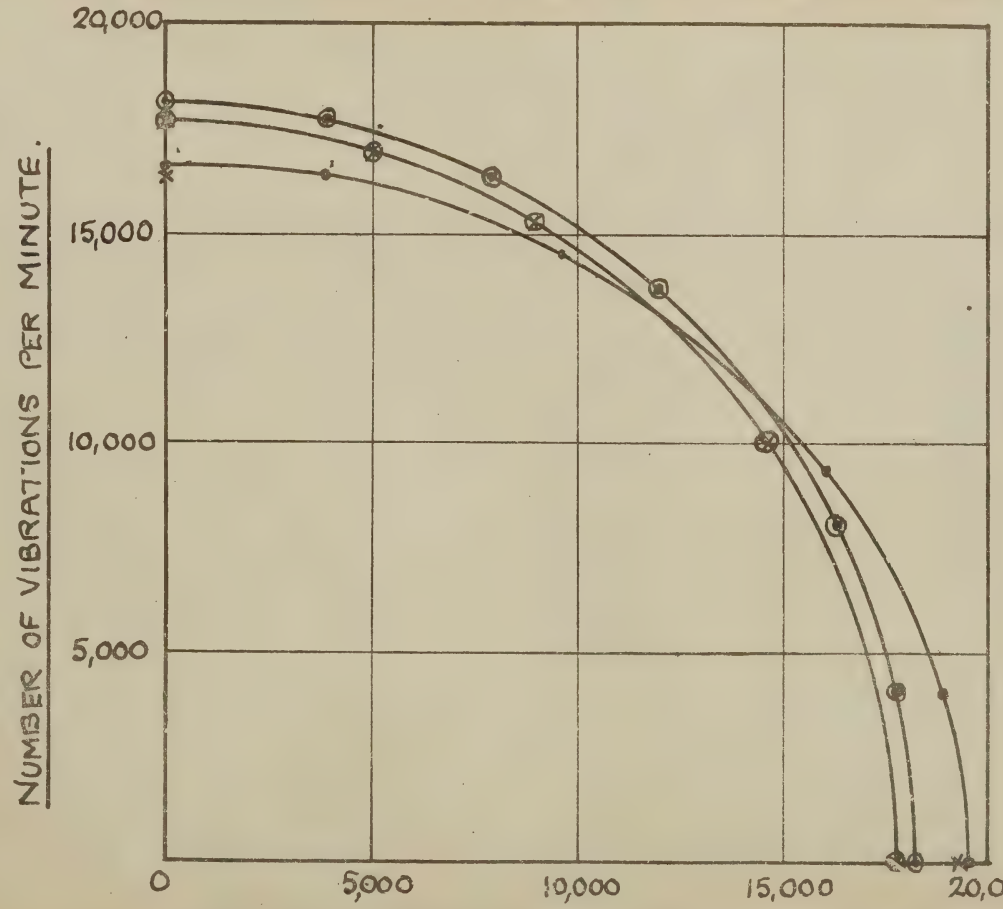

• CORRECT SOLUTION

× REPLACING SHAFT BY A MASS $\left[\frac{78}{210} mL\right]$ AT END.

⊗ NEGLECTING I_2 OF AIRSCREW AND REPLACING SHAFT BY A MASS $\left[\frac{78}{210} mL\right]$ AT END.

⊙ NEGLECTING I_2 OF AIRSCREW AND INERTIA OF SHAFT. $(m = 0)$

FIG. 3.

TRANSVERSE VIBRATIONS IN A PLANE PARALLEL TO THE AXIS OF ROTATION AND TO THE BLADE-AXIS. $L = 2{\cdot}5$ FT. $I_2 = 3{\cdot}5$ SLUG-(FT.)^2 HIGHER FREQUENCY NOT PLOTTED

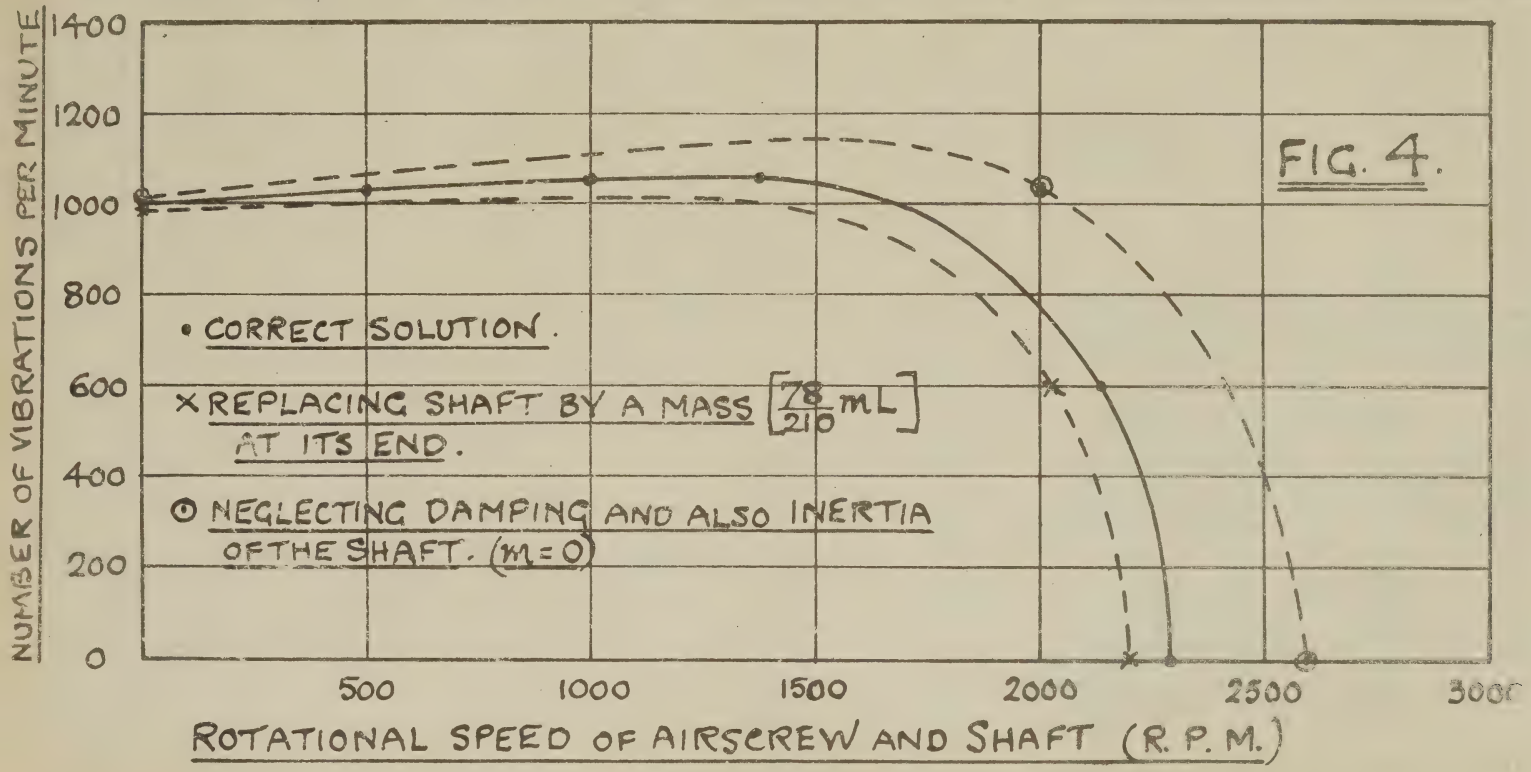

TRANSVERSE VIBRATIONS IN A PLANE PARALLEL TO THE AXIS OF ROTATION AND TO THE BLADE-AXIS. $L = 2{\cdot}5$ FEET. $I_2 = 0{\cdot}02$ SLUG-(FT.)^2 HIGHER FREQUENCY NOT PLOTTED.

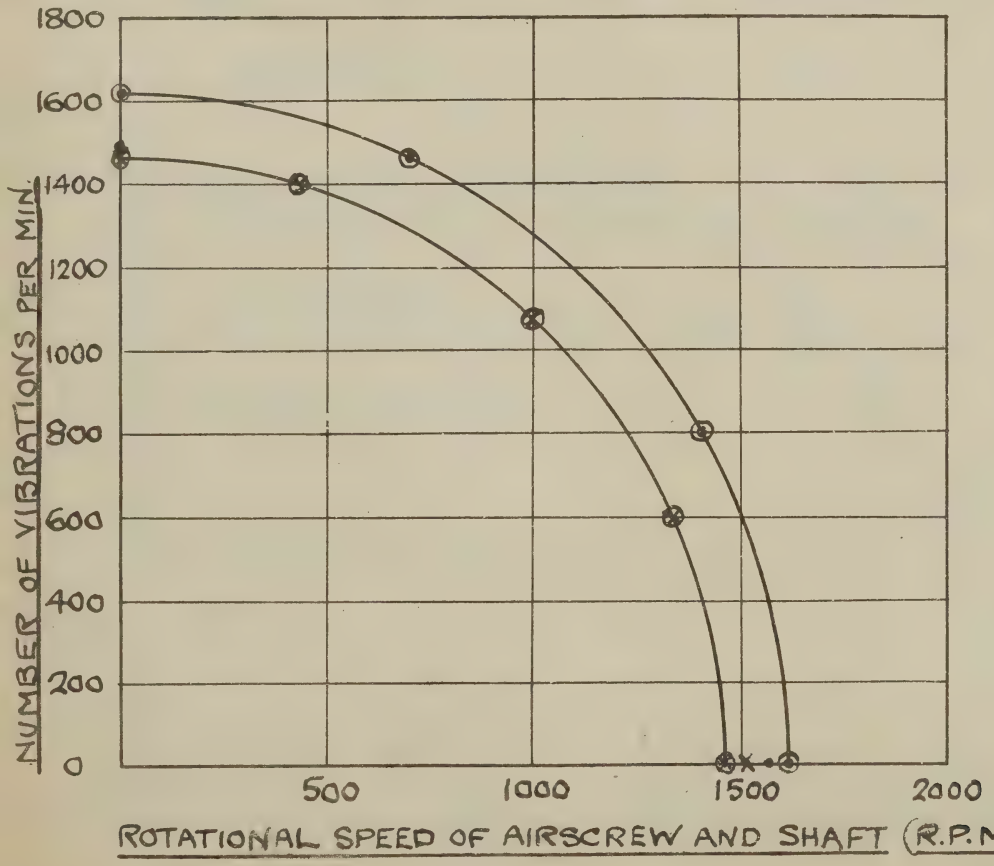

• CORRECT SOLUTION.

× REPLACING SHAFT BY A MASS $\left[\frac{78}{210} mL\right]$ AT END.

⊗ NEGLECTING "I_2" OF AIRSCREW AND REPLACING SHAFT BY A MASS $\left[\frac{78}{210} mL\right]$ AT END.

⊙ NEGLECTING "I_2" OF AIRSCREW AND INERTIA OF SHAFT ($m = 0$)

FIG. 5.

From the data of Tables (1-4) and Figures (2-5) it will be seen that the following conclusions may be drawn :—

(*a*) The air damping of an airscrew is negligible, in so far as the frequency of the transverse vibrations is concerned.

(*b*) The whirling speed may be calculated with very good accuracy by assuming the effect of the shaft to be the equivalent of a mass $\left(\frac{78}{210}\ mL\right)$ at its end. In this case the whirling speed is overestimated, the inaccuracy increasing with the length of the shaft. The maximum error due to this assumption is only about 3·5 per cent. of the true value of the whirling speed.

(*c*) As would be expected, neglecting the mass of the shaft makes the whirling speed too high, the discrepancy increasing with the length of the shaft, the maximum error due to the assumption being 13 per cent. of the true value of the whirling speed.

(*d*) It is seen from Figs. 3 and 5 that even when the moment of inertia I_2 of the airscrew is small—0·02 slug /ft^2. in this particular case—it should not be neglected in the calculation of the whirling speed.

(*e*) The critical speed of an airscrew and shaft increases with the moment of inertia of the airscrew.

(*f*) When the moments of inertia of the airscrew—I_2 in this case—and of the shaft are zero, the whirling speed has the same frequency as the natural period of transverse vibration when not rotating.

A simple formula from which may be calculated the whirling speed of rotation of an airscrew and its shaft.—It has been shewn that the air damping of an airscrew may be neglected, and also that the effect of the inertia of the shaft is equivalent, for all practical purposes, to a mass $\left(\frac{78}{210}\ mL\right)$ placed at its end.

The differential equation for the motion of the airscrew and shaft then becomes

$$\left\{\left[D^2+\omega^2+\frac{4EI}{LI_2}\right]\left[D^2-\omega^2+\frac{12EI}{L^3\left(M+\frac{78}{210}mL\right)}\right]-\left[\frac{36E^2I^2}{I_2L^4\left(M+\frac{78}{210}mL\right)}\right]\right\}\theta=0$$

that is

$$\left\{D^4+D^2\left(\frac{4EI}{LI_2}+\frac{12EI}{L^3\left(M+\frac{78}{210}mL\right)}\right)\right.$$

$$\left.+\left(\omega^2+\frac{4EI}{LI_2}\right)\left(\frac{12EI}{L^3\left(M+\frac{78}{210}mL\right)}-\omega^2\right)-\frac{36E^2I^2}{I_2L^4\left(M+\frac{78}{210}mL\right)}\right\}\theta=0$$

The whirling speed, that is, the rotational speed at which the frequency of one of the transverse vibrations becomes zero, is then got from the expression

$$\left[\omega^2 - \frac{12EI}{L^3\left(M + \frac{78}{210}mL\right)}\right]\left[\omega^2 + \frac{4EI}{LI_2}\right] + \frac{36E^2I^2}{I_2L^4\left(M + \frac{78}{210}mL\right)} = 0$$

which may be written

$$\omega^4 + \omega^2\left[\frac{4EI}{LI_2} - \frac{12EI}{L^3\left(M + \frac{78}{210}mL\right)}\right] = \frac{12E^2I^2}{I_2L^4\left(M + \frac{78}{210}mL\right)}$$

If the above equation be solved for ω^2 it will be found that there is one positive and one negative value.

The whirling speed may be got by taking the square root of the positive value ω^2.

The result of the present investigation may be summarised as follows :—

The whirling speed, ω, of a rotating airscrew and shaft, the shaft being a cantilever fixed in direction at one end, may be calculated by taking the square root of the positive value of ω^2 got from the solution of the equation

$$\omega^4 + \omega^2\left(\frac{4EI}{LI_2} - \frac{12EI}{L^3\left(M + \frac{78}{210}mL\right)}\right) = \frac{12E^2I^2}{I_2L^4\left(M + \frac{78}{210}mL\right)}$$

where ω = rotational speed in radians per second.

M = mass of the airscrew in slugs.

I_2 = moment of inertia of the airscrew about an axis passing through the centre of the airscrew at right angles to the plane of the transverse vibrations (slug-ft^2).

L = length of the shaft in feet.

m = mass of one foot length of shaft in slugs.

E = Young's modulus in lbs. per square foot.

I = moment of inertia of a cross-section of the shaft about a diameter in (feet)^4.

If $I_2 = 0$ the whirling speed may be calculated from the equation

$$\omega^2 = \frac{3EI}{L^3\left(M + \frac{78}{210}mL\right)}$$

ON THE SHAPE OF PROPELLER BLADES.

By A. A. Griffith, M.Eng., and B. Hague, B.Sc. Presented by the Director-General of Aircraft Production.

Reports and Memoranda, No. 452. *June,* 1918.

Summary.—(a) *Introductory.* (*Reasons for Inquiry*).—The ordinary methods of calculating the strength of propeller blades by considering end-grain stresses only does not appear to give an explanation of the frequent breakages of their trailing edges.

(b) *Range of the Investigation.*—The present paper deals with the design of propeller blades as affected by their elastic properties. The standard method of stressing and designing propeller blades is reviewed in the light of the theory put forward in reports R. & M. Nos. 454 and 455.

Several other points of importance in design are discussed, and among them the question of critical speeds.

The final section deals with examples and experiments bearing on the matter contained in the body of the paper.

(c) *Conclusions.*—It is shewn that previous estimates are incomplete in that they fail to take account of the torsional and cross bending strains, which may be, and in current practice frequently are, of major importance. It is further shown that the conditions for least (longitudinal) bending and least torsion are mutually exclusive, and a comparative analysis of the alternative methods of design thus presented indicates that the balance of advantages is usually in favour of the latter. The former method may, however, be preferable in special cases.

(d) *Applications.*—It is hoped to deduce from further work certain working rules which may be applied to drawing office practice, thereby ensuring adequate strength for the propeller blades.

1. *General.*

The design of aircraft propellers may be divided for convenience into two parts, aerodynamic and elastic.

It is probable that, given sufficient knowledge regarding the action of a propeller blade, the best blade-widths and angles, and the form of the cross-sections, could be determined from aerodynamic considerations. The present discussion relates only to the second or elastic part of the design, and it will therefore be assumed that these features have been fixed.

To solve the problem it is necessary to determine the plan and elevation of the blade and the blade thicknesses. In order to secure maximum aerodynamic efficiency the working part of the blades should be as thin as possible, and it is also desirable,

of course, to make the weight of the propeller a minimum. The design is subject to the conditions that the stress must be everywhere below the safe limit under any possible working conditions, while none of the natural vibration frequencies of the blade must coincide with any speed at which the propeller may be required to work.

Since the blade-widths and angles are fixed, the plan and elevation of the blade may be specified by the shape of the line joining the centroids of the cross-sections, which may be termed the central line.

In addition to the necessary centrifugal tension, and the flexure of the blade about axes perpendicular to the central line, there must, in general, be torsion and transverse flexure about axes parallel to the central line. It is obvious that the stresses due to the latter strains must depend on the shape of this line, and hence one of the objects of the design must be to determine the shape of central line which leads to minimum values of these stresses. The torsion especially is important, apart altogether from stress considerations, because it alters the blade angles, probably the most important of the three aerodynamic features of the blade.

Hitherto it has been usual in stressing propeller blades to consider only the longitudinal (end-grain) tensions and compressions due to the air-load and the centrifugal force, on account of the very great difficulties attendant on the estimation of the transverse stresses. The plan and elevation forms obtained by this method have, of course, no direct relation to those which would result from consideration of the transverse strains. The method would, however, be justifiable from the stress standpoint if the fractures in actual propeller bursts always corresponded with failure in longitudinal tension or compression, since it would then be legitimate to assume that the transverse stresses were unimportant.

As a matter of fact, a large proportion of propeller failures exhibit longitudinal cracks, which can hardly be explained on the hypothesis of rupture under maximum radial stress. Further, the breakages do not, in general, occur at the estimated positions of the maxima of the latter stresses.

It would appear, then, that the standard method of design fails to take account of stresses which may determine fracture, and that it should therefore be supplemented by a more rational theory.

Similar considerations apply to the calculation of blade angles. It would be fair to work these out, as is done at present, on the assumption that they would remain unchanged under running conditions, provided that the actual performance of a propeller could always be predicted by the designer. Here again, however, the simple theory breaks down in certain cases.

For instance, the performance of a backward-tilted* propeller is materially different from that of an otherwise identical forward-tilted one. No plausible aerodynamic hypothesis has been advanced to explain this difference, but an examination of the twist curves provided a perfectly adequate account of the phenomenon. It has been urged as an argument for the use of forward-tilted blades that they can be made materially narrower than back-tilted ones for a given power. The explanation given in the present report suggests that precisely the same results could be obtained with back-tilted blades by increasing the angles. Although it would then appear, at first sight, that the latter blades were nearer the burble-point than the former, yet this would not really be so, since the difference would be annulled by the twisting of the blades in flight.

2. *Preliminary Discussion.*

It is convenient to consider the blade in relation to rectangular axes of reference *ox*, *oy* and *oz*. The system of notation adopted in previous reports† (see Fig. 12, R. & M. No. 454), will be adhered to in the present discussion.

As regards the stresses and strains in the thinner or working part of the blade, it is sufficiently accurate for most purposes to assume that the blade is flat, as is done in the reports referred to above. The inclination of this portion to the plane of rotation may be taken to be the angle of the chord at the point of maximum air-load per unit length of the blade. Conformably with the notation of R. & M. No. 454 the axis of *y* must be taken parallel to this chord. *oz* must be taken perpendicular to the axis of rotation, and should run parallel to the projection of the general direction of the grain on the *yz* plane.

It is convenient for the purpose of elastic analysis to define the shape of the central line by means of two projections on the *xz* and *yz* planes respectively, rather than by the plan and elevation as usually understood. In the present report, the slope of the *xz* projection, relatively to *oz*, will be called the "tilt" of the blade, and it will be termed forward or backward tilt according as it is in the direction of pressure on the blade or in the opposite direction. The slope of the *yz* projection will be referred to as the "sweep," specified as leading or trailing sweep, according to its direction in relation to the leading and trailing edges.

In the case of the thicker part of the blade near the boss, the surface tractions and body forces are negligible and the stresses may be found by the standard beam methods, supplemented by the soap-film method of calculation described in R. & M. No. 399, hence no further discussion is necessary.

---

* *Vide* § 2, *infra*.

† R. & M. Nos. 454 and 455.

Turning, then, to the thinner part, the chief distorting forces which have to be considered are the centrifugal forces and the bending moments about axes parallel to *oy*, which give rise to the longitudinal tensions and compressions Z_z and shear stresses X_z and Y_z; the twisting couples about *oz* which involve the shears X_z and Y_z; and the transverse bending moments about axes parallel to *oz*. The latter have their source in the difference between the distributions of the applied moments and the flexural and torsional rigidities of the blade. They give rise to Y_y tensions and compressions and X_y shears.

The Z_z stresses depend on the tilt of the blade, while the twist, and hence the Y_z stresses, depend on the sweep. The Y_y and X_y stresses are determined partly by the sweep and partly by the shape of the cross-sections.

In addition to the attainment of maximum strength with minimum weight, &c., it is of interest to consider the possibility of controlling the twist in such a way as to secure a high all-round efficiency.

Evidently it is not to be expected that a propeller can be designed so as to be completely satisfactory in both respects, or that a shape which is best in regard to one sort of stress leads to minimum values of the other stresses.

It is proposed to illustrate these points by means of a comparison of various possible methods of design, but first the question of calculating the stresses will be dealt with.

3. *Methods of Calculating Stresses and Strains.*

The method of finding the bending moments due to the centrifugal force is well known. A similar process may be used to find the couples about *oz* due to the same force, which are of importance in connection with torsional strains.

The theory of the twisting of propeller blades under their air-load was discussed in R. & M. Nos. 454 and 455, and, of course, the same method applies in the case of the normal components of the centrifugal force.

On paper the theory put forward in these reports could be extended so as to yield the values of the transverse stresses Y_y and X_y, but as the practical application of the equations would involve a double graphical differentiation, it is not thought that the results would be sufficiently accurate to justify the excessive labour which would be necessary to obtain them.

It is possible, however, to get a general idea of the factors which determine the magnitude of these stresses. Consider a plank cut with the grain at an angle θ with its central line, and let it be bent by couples M applied to its ends about axes perpendicular to the central line. The couples may be resolved into components N cos θ and M sin θ respectively parallel and perpendicular to the grain. Evidently the component M sin θ gives rise to cross-grain flexure, and hence sets up the type of

stress under discussion, namely, Y_y. It may be inferred that, other things being equal, the cross-grain stresses are larger the greater the sweep of the blade. This conclusion is substantially confirmed by experiments which have been made on actual propeller blades under various conditions of loading.

The cross-stresses depend also on the lateral distribution of the load. Turning to the general equations (Appendix A, Eq. (1), (2) and (3), R. & M. No. 454), if the torsion is zero and the pressure P is everywhere balanced by the term $\delta^2 M_z / \delta z^2$, then the transverse stresses vanish.

The actual distribution of P over propeller blades is not very accurately known, but so far as it is possible to make an estimate, it appears that this condition is sufficiently nearly fulfilled, in blades of small sweep, to render it legitimate to neglect the cross-stresses in these cases. There is no justification whatever for supposing that they can be neglected in blades of large sweep; indeed, it is more than probable that some of the fractures which have occurred in blades with excessive trailing sweep have been due to this cause.

In addition, certain second order stresses have to be taken into consideration. A report on these is in preparation, but it may be stated here that their only influence on the argument of the present paper is to emphasise the importance of the transverse stresses.

4. *Examination of some Methods of Design.*

The following alternatives will be discussed:—

(*a*) Employment of a forward tilt such that the bending moments due to the centrifugal force are balanced by the corresponding bending moments due to the air-load.

(*b*) Adoption of a shape which twists so as to give a smaller angle of incidence when climbing than when racing, in order to improve the all-round efficiency of the screw.

(*c*) Adjustment of the initial tilt in such a way as to make the tilt under the average air-load zero, the sweep being arranged so as to make the twist zero under these conditions.

(*d*) A compromise between the preceding methods of design.

(*a*) The object of designing for zero bending moment is to enable the blades to be made of minimum thickness, and hence to obtain maximum aerodynamic efficiency with minimum weight. It is obvious that it is impossible actually to design on the assumption that the bending moment is exactly zero, on account of the widely varying conditions under which a propeller is required to work. A different design should, in fact,

be used for each condition of working, but it is possible nevertheless to reduce the bending moments very considerably by this means.

Since, however, the elements of centrifugal force act through the centroids of the sections, whereas the corresponding elements of air-load act through the centres of pressure, it is evident that each section must be subjected to a resultant couple about *oz*, and it is impossible to eliminate these couples by adjusting the sweep.

It is found, as a matter of fact, that blades of this type which are sufficiently thick to withstand the residual bending moments are by no means strong enough to support the twisting couples, and hence the apparent saving due to balancing the bending moments is largely illusory.*

Moreover, the comparatively large twist which is inherent in this type of blade is a disadvantage from the drawing office standpoint, as it must be allowed for in the calculations.

(*b*) A method of calculating the sweep of a propeller blade for zero twist under air-load was explained in R. & M. No. 455 (§ 2, Eq. 16). A similar method applies in the case of the centrifugal force.

It is found on applying this method that slight trailing sweep is required in the first case and slight leading sweep in the second. As a working rule, then, it may be said that in backward-tilted blades the twist decreases the angle of incidence if there is trailing sweep and increases it if the blades have leading sweep, in both cases. With forward-tilted blades the twist due to the centrifugal component is reversed in sign, that due to the air-load remaining unchanged.

For greatest all-round efficiency, the angle should diminish with increasing air-load. It is found that the attainment of this condition requires leading sweep in the case of the centrifugal force and trailing sweep in that of the air-load. Hence the two effects are necessarily opposite, and the desired end can only be obtained by making one of them large compared with the other. It follows that a blade having a large sweep is required. Unfortunately the Y_z and Y_y stresses in this type of blade are very high, and hence adequate strength can only be secured by using excessively thick blades. Not only does this reduce the possible range of angle variation, but it also probably involves a loss of efficiency which more than counterbalances the gain due to the twisting of the blades.

In view of these considerations, it would not appear to be feasible to control the twist in accordance with aerodynamic requirements. Hence it is advisable to make it as small as possible.

* *Vide* § 6 (*b*), *infra*.

(*c*) Since the sweep for zero twist under air-load is not quite the same as in the case of the centrifugal force, it is not possible to design a blade having zero twist under all flying conditions, but if the twist is made zero under mean conditions, it cannot be large in extreme cases.

A convenient procedure is to make the initial backward tilt such that the tilt in the strained position under the average air-load is zero. In these circumstances the centrifugal bending moment vanishes and the shape of the blade for zero twist may be deduced from the air-load distribution.

Figs. (1), (2) and (3) show the shapes which have been deduced by this method in the cases of three typical propellers, together with the shapes now in use. The calculation has been performed in each instance for the extreme conditions of climbing and racing. The line termed " j line " is the locus of the " flexural centres " of the cross-section of the blade (see R. & M. 399, § 2, and Appendix, Eq. 52). These centres are about 0·04 to 0·05 of the blade-widths forward of the centroids.

It is practically certain that the X_y and Y_y stresses, as well as the Y_z ones, are negligible in this type of blade, and hence the sections need be no thicker than is indicated by a consideration of the bending moments, provided, of course, that the necessary conditions as regards vibration frequencies can be satisfied.

(*d*) A comparison of the two methods of design, (*a*) and (*c*), for least flexure and least torsion respectively shows that (*a*) leads to a blade thinner near the root than (*c*), whereas near the tip the reverse is true.* The total weight probably comes out less in the case of (*a*), but (*c*) has the advantage in most other respects. The smaller thickness of the important part of the blade conduces to greater efficiency, and the chief stress is an end-grain compression as opposed to a shear. Moreover, as will be seen later, the range of safe speeds, from the vibration standpoint, appears to be greater in a blade of type (*c*) than in one of type (*a*).

Finally, the calculation of the blade thicknesses from the bending moments is a perfectly simple and straightforward process, whereas in the case of torsion they must be obtained from a differential equation of such complexity that trial and error is the only practicable means of evaluation (see R. & M. No. 455, § 2, Eq. 9).

There is, nevertheless, no reason to suppose that (*c*) is a better method of design than one intermediate between (*a*) and (*c*), in which the air-load bending moments are partially balanced by those due to centrifugal force. It is theoretically possible, in any such case, to calculate (from Eq. (16), R. & M. No. 455), the sweep which the blade must have for zero twist, the only case which is mathematically excluded being (*a*) itself, where the equation would indicate infinite sweep. Since the Z_z stresses

* § 6 (*b*), *infra*.

decrease progressively as we pass from (*c*) to (*a*), it is reasonable to suppose that some intermediate blade should be materially more economical than (*c*).

It is found, however, that the requisite sweep increases rapidly as (*c*) is approached, and the calculated plan-forms soon assume such extreme shapes as to have no practical interest. We have seen that there is reason to suppose that the Y_y and X_y stresses are important, and may determine fracture in blades with large sweep, and it is probable that the extent to which the air-load can usefully be balanced against the centrifugal force in blades of this type is definitely limited by these stresses. There is probably some form of blade intermediate between (*a*) and (*c*) which is more economical than (*c*), but there is no simple way of finding it, partly on account of the difficulty of estimating the transverse stresses and partly because of our present ignorance of the safe limits of these stresses in propeller timber.

An alternative method of designing between (*a*) and (*c*) is to keep the Y_y and X_y stresses small by retaining the blade form of approximately zero sweep, which yields no twist under the air-load, while giving the blade a slight forward tilt in the deflected position. This diminishes the bending moments, but it involves torsion of the blade by the centrifugal force. Here the designer is on surer ground, the aim being to adjust matters in such a way that the safe stress limits are reached simultaneously in torsion and bending. So far as present information regarding shear stress renders it possible to make an estimate, this condition holds when the centrifugal bending moments are 30–40 per cent. of those due to the air-load, so that this design yields a blade about 20 per cent. thinner than (*c*). It may be doubted whether this saving is adequate compensation for the introduction of twist and the attendant torsional stresses.

5. *Other Considerations.*

Besides the pure stress-strain questions discussed above, it is necessary in practical design to take account of several other points, the chief of which are :—

(a) *The Shape of the Laminations.*

These should be as straight and as straight-grained as possible. It frequently happens that the shape of blade indicated by the theory cannot be used because the laminations are very badly curved.

(b) *The Effects of Variations in the Average Modulus of the Timber.*

If, for instance, the actual E of the wood is appreciably different from that assumed in the calculations, then the tilt in the strained position is not the same as the estimated value. In some cases, notably when the sweep is large and the bending moments are nearly balanced, a small change in the tilt may involve a large change in the most important stresses. In such

a case the factor of safety must be made sufficiently large to cover any possible variations of modulus.

(c) *The effects of Elastic Heterogeneity in the Material of Individual Blades.*

Such variation may make the properties of the blade quite different from those of a uniform propeller, and allowance must be made for this in calculating the maximum stresses.

If j is the y — co-ordinate of the flexural centre of a section (if E is variable it is equal to $\int Eyt^3dy \Big/ \int Et^3dy$) then the position of the principal flexure point (see R. & M. No. 454) which determines the twisting couple in any given condition of loading, is

$$j + \frac{M}{S}\frac{dj}{dz}$$

where M is the bending moment and S the shear force at the section.

Consider the effect on this expression of a lamination having an abnormal value of E. The change in j depends on the position of the lamination in the blade-sections, but it is found by trial that the change in j is not very large even in extreme cases.

Considering now the term in $\frac{dj}{dz}$, it will be observed that this depends not only on the position of the lamination, but also on the rate of change of its flexural rigidity with z. Other things being equal, this is proportional to the rate of change of some power of the sectional area of the lamination, which may vary from 1·5 to 2 according to the shape of the blade. Investigation shows that the change in this term may be several times the change in j in extreme cases, and hence it is important to minimise it if possible.

An examination of the drawings of actual propellers indicates that the magnitude of the effect depends very largely on the sweep, so that, for instance, in blades having the very large trailing sweep, which is a familiar feature of current practice, the possible variation in $\frac{dj}{dz}$ is from five to seven times as great as it would be in blades of the more symmetrical form indicated by the present theory.

Minimum variation appears to be secured in blades of zero sweep, and, as has been seen, this shape is almost identical with that yielded by the condition for zero twist.

It will be seen that the influence of a lamination is in any case negligible if it be placed at the flexural centre. Hence if any form of timber grading is used, abnormal laminations may be utilised with perfect safety provided they are placed near the middle of the propeller.

(d) *The Effect of Cracks and other Defects.*

Longitudinal cracks have but little influence on the strength of wooden members subjected to pure end-grain stresses. If, however, cross-grain stresses are present, such defects almost invariably connote very high local strains, and are usually sufficient ultimately to determine fracture.

Since propellers are peculiarly liable to be slightly damaged when on service, it would appear to be advisable, from this point of view, to make the transverse stresses as small as possible. Here, again, the method of design (*c*), § 2, is indicated.

(e) *The Vibration Periods of the Propeller.*

The vibrations may be either torsional or flexural, or they may involve combined torsion and flexure. If the blade calculated by the selected method of design has a period which synchronises with any of the engine periods at a normal running speed, it must be thickened up until this no longer occurs.

The method of calculating the periods of pure flexural vibrations is mathematically identical with that of finding the whirling speeds of non-uniform shafts, and hence the well-known method of calculation employed in that problem, which consists in assuming a deflection curve and integrating, may be used here. It is convenient to take for this purpose the deflection curve which results from applying the air-load to the blade.

A similar process may be used in the case of pure torsion, but here the equation to be solved is the general linear equation of the fourth order, with the independent term only absent, and it is not, therefore, probable that the first approximation yielded by this method would be sufficiently accurate.

Usually, however, the vibrations must consist of torsion combined with both longitudinal and transverse flexure. The equations are then much more difficult, and so far no progress whatever has been made with their solution.

A certain amount of information may nevertheless be obtained from general considerations. If a blade vibrate flexurally without twisting, the acceleration forces must act through the centroids of the cross-sections, and hence the form of the blade must be such that it does not twist under a load applied through those points. Usually this means that the blade must have very slight forward sweep. The same condition must hold if the blade is to vibrate torsionally without flexure. Further, it appears to be legitimate to infer that the frequency is a maximum when a blade has this shape, since the deflection of the central line, under given loads applied along it, must be greater in any other type of blade than it is in this one. That is to say, a blade with large sweep has a lower flexural vibration speed than any otherwise identical one of small sweep. This deduction appears to be confirmed by some experiments which are described below.*

* See § 6 (*c*), *infra*.

If, however, the blade can execute pure flexural vibrations, then it must also have a period corresponding with pure torsion. Ordinarily, however, the frequency of the latter is at least three or four times that of the former, so that it is hardly likely, in general, to become a controlling factor in design.

Generally speaking, the above remarks apply only to the gravest modes of vibration. It is obviously much more difficult to draw general conclusions regarding the higher modes, and they are also much less amenable to calculation, on account of the difficulty of assuming an appropriate displacement curve.

If it should be found, after working out a design, that the first vibration speed is too low, it may be possible, as an alternative to thickening the blades, to run between the first and second speeds. The decision in such a case must be governed chiefly by the likelihood or otherwise of a protracted run at or near the first critical speed.

It is found in those cases of the vibration of cantilevers which can be subjected to rigorous analysis that the intervals between frequencies increase considerably with increase in the rate of diminution of thickness towards the free end; from this point of view, the method of design (*c*), § 4, has a distinct advantage over (*a*), since the usefulness of a propeller may be largely determined by its range of safe speeds.

(f) *The Nature of the Timber.*

The method of design to be used evidently depends on the relative values of the stresses which can be allowed in the various directions. For instance, padouk is remarkable in having an abnormally high elastic limit in longitudinal compression, and yet when tried in a standard propeller of the customary trailing-sweep type it did not give very satisfactory results. An examination of its behaviour under Y_z and Y_y stress shows that this is not surprising, since it is characterised in these respects by high moduli and low strengths. Undoubtedly, if padouk is to be employed in propeller work, method (*a*) of § 4 should be used in designing, so that full advantage may be taken of its peculiar properties.

On the other hand, if it be desired to use wavy-grained timber, having a low or variable longitudinal strength, method (*c*) would probably be preferable.

(g) *The Effects of a Burst.*

Many cases are on record of accidents having been caused or narrowly averted when propellers have burst in flight, owing to the carrying away of a strut or tail-boom by the detached piece of the propeller. The probability or otherwise of this evidently depends very largely on the shape of the blade. If there is large trailing sweep, it is almost certain that the starting

of a longitudinal crack must be followed by the complete separation of the trailing edge. If, however, the sweep is small, there seems to be no reason why such a mishap should involve anything more serious than loss of power.

6. *Examples and Experiments.*

(a) *Effect of Tilt on Performance.*

Ordinarily, R.A.E. propellers are designed with such a degree of backward tilt that the elevations of the trailing edges are straight in the undeflected position, and, in general, the performance of such propellers are in agreement with the calculated ones. This does not necessarily mean that the twist of the blades is negligible; it is possible that there are errors in the design data which approximately balance the effect of the twist. When, however, the same data are applied to the analysis of screws having forward tilt such that the leading edges are straight in elevation, it is found that agreement cannot be obtained, the angles of incidence being apparently too small to account for the observed performances.

There seems to be no aerodynamic reason for this discrepancy, but an examination of the torsional properties of the two types of blade shows that whereas in the former case the centrifugal force tends to decrease the angles of incidence, in the latter it tends to increase them, and this is therefore a possible explanation of the phenomenon. Further, an estimate of the difference in twist in any given instance should agree with the increase in angle indicated by the calculation data as being necessary to account for the observed performance, independently of possible errors in the data, since any such error should be cancelled in taking differences.

This has been done in the case of propeller No. T.28181 (S.E.5, H. C. H. S. Viper). It was estimated that a mean increase in the blade angles of 4° would bring the calculated performance into agreement with the actual one, while elastic analysis showed that the change of twist, due to altering the tilt so as to make the trailing edge, instead of the leading edge, straight in elevation, could vary from 3·5° to 5·5°, according to the values chosen for the elastic and other constants of the timber. Thus the present theory is capable of giving a quantitative as well as a qualitative explanation of the difference between forward and backward-tilted blades.

(b) *Comparison between Methods of Design* (*a*) *and* (*c*).

§ 4. The ratio of blade thicknesses necessary to support the twisting couples in the case of (*a*) to those required to withstand the bending moments in case (*c*) has been determined for a series of points along the blades of propeller T.28086, which has a radius of 47″. The ratio of safe stresses in bending and torsion has been taken to be (A) 15 and (B) 25. So far as is known,

DEVELOPED PLAN-FORMS OF BLADE HAVING ZERO TORSION.

PROPELLER SE5. DRG. T28086.

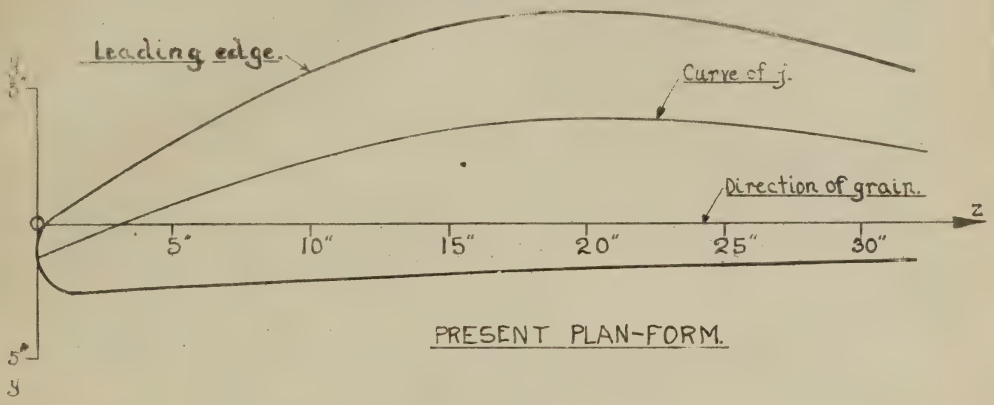

PRESENT PLAN-FORM.

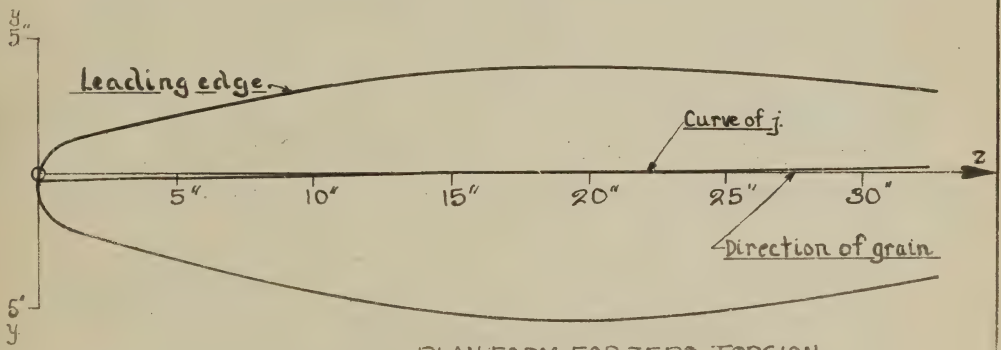

PLAN-FORM FOR ZERO TORSION.
(RACING).

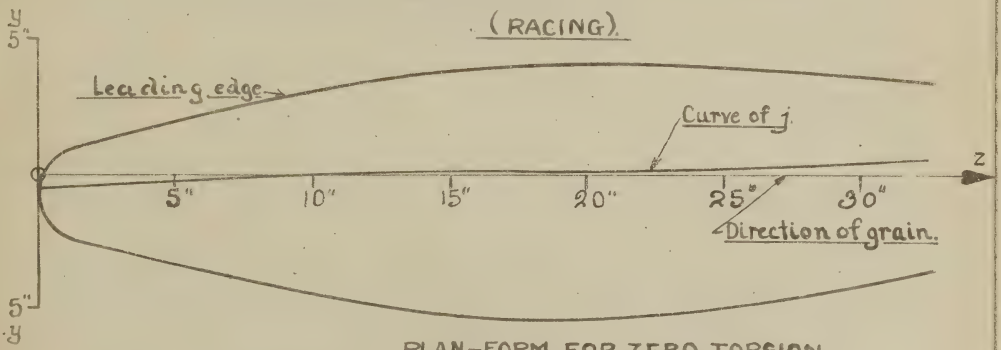

PLAN-FORM FOR ZERO TORSION.
(CLIMBING).

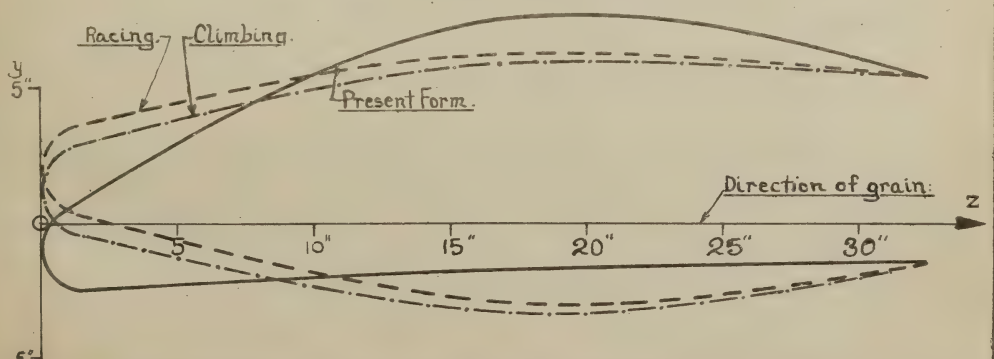

DEVELOPED PLAN-FORMS OF BLADE HAVING ZERO TORSION.

PROPELLER NE 1. DRG T28126

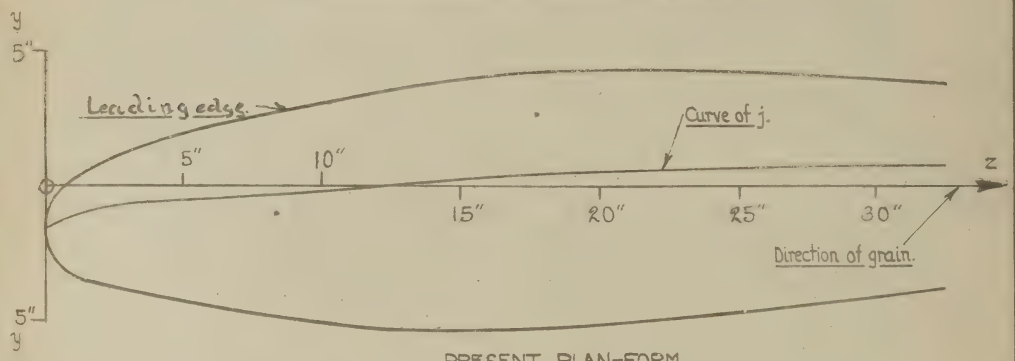

PRESENT PLAN-FORM.

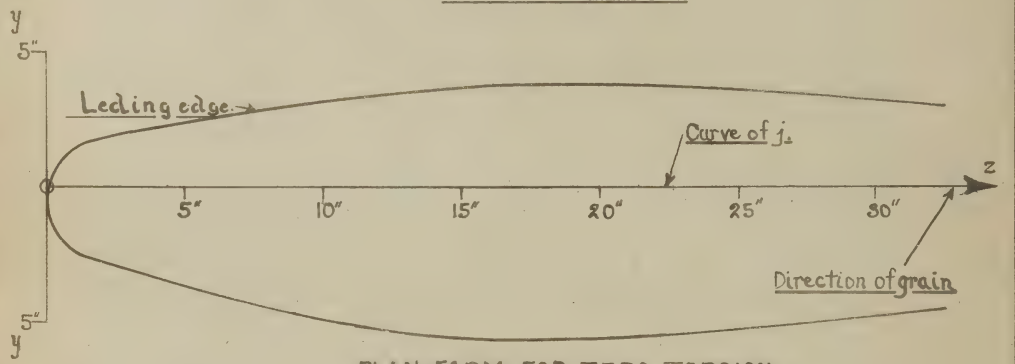

PLAN-FORM FOR ZERO TORSION.
(RACING).

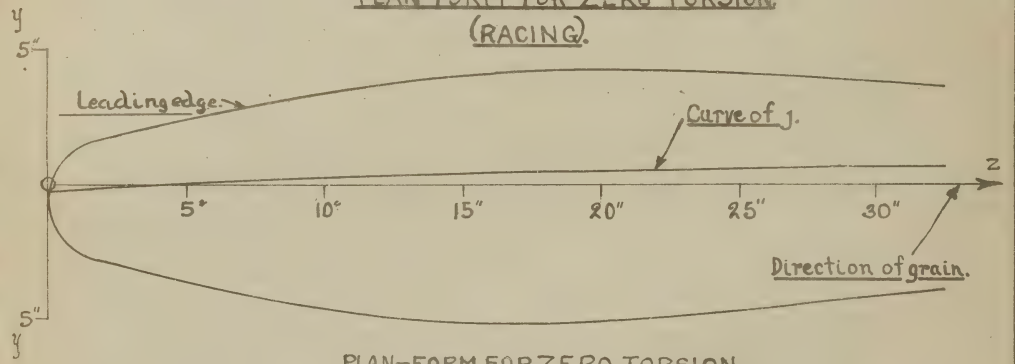

PLAN-FORM FOR ZERO TORSION.
(CLIMBING).

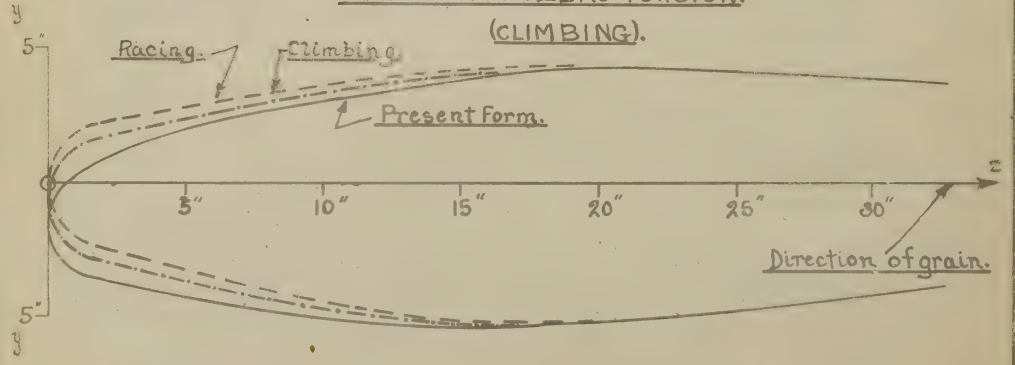

DEVELOPED PLAN-FORMS OF BLADE HAVING ZERO TORSION.

PROPELLER SE 5A. DRG. T28098.

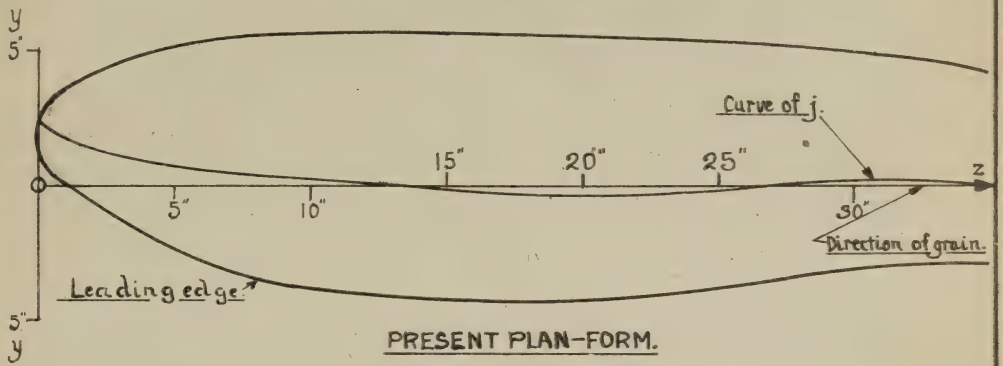

PRESENT PLAN-FORM.

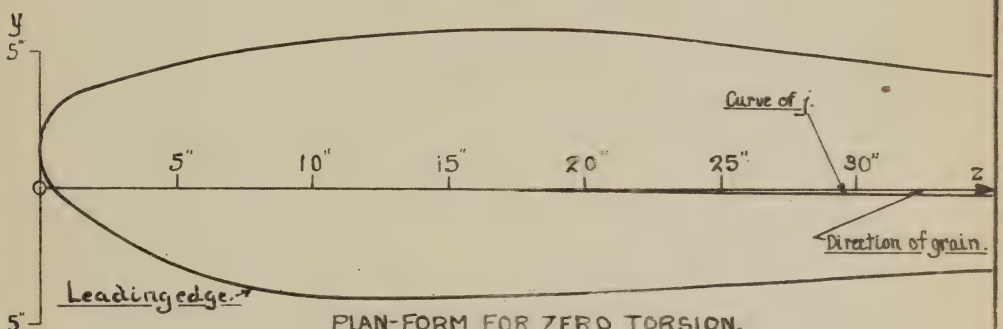

PLAN-FORM FOR ZERO TORSION.
(RACING)

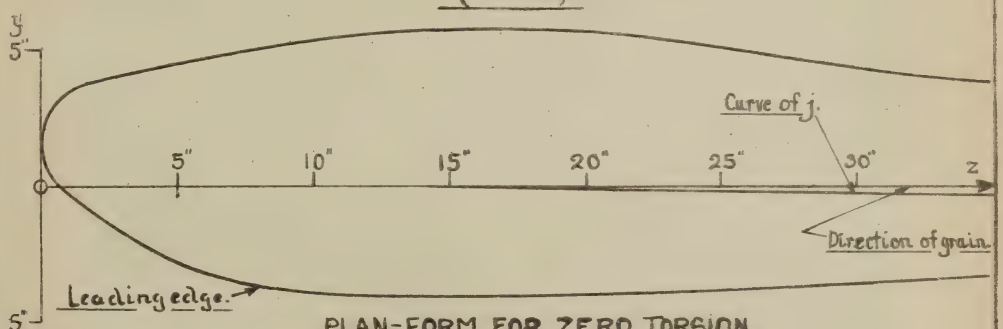

PLAN-FORM FOR ZERO TORSION.
(CLIMBING).

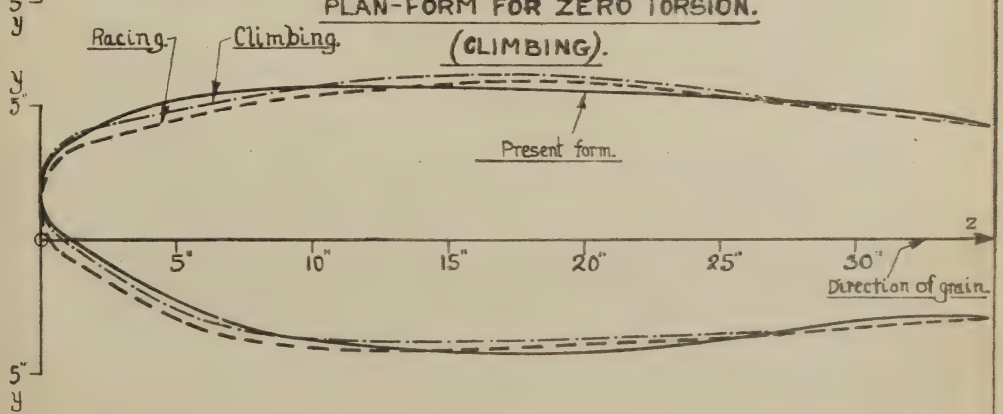

(A) is probably a representative value for walnut and mahogany, while (B) is nearer the truth in the case of padouk. The results are given in the subjoined table :—

Distance from tip. (ins.)	*ta'te*	
	A	B
3	1·75	2·26
10	1·26	1·68
15	1·12	1·45
20	1·01	1·30
25	0·95	1·23
30	0·90	1·16
35	0·84	1·08

It will be seen that, in case (A), (*c*) is definitely superior to (*a*) in the more important portion of the effective part of the blade, but that (*a*) gives thinner sections near the boss. In case (B) the superiority of (*c*) is still more marked. It is extremely doubtful whether the reduction of thickness in the boss sections is a real advantage, as it must involve a lowering of the vibration frequencies, and it probably also reduces the interval between the first two periods.

(c) *Experiments on Vibration Frequencies.*

The first flexural period of a propeller blade having very pronounced trailing sweep was calculated from data obtained from the blade itself, and was found to correspond with a speed of 1,824 r.p.m. The actual frequency of the gravest mode of the blade was found by experiment to be 1,412 per minute, so that in this case calculation gave a result 29 per cent. high.

As another example, two half-scale blades, A and B, were constructed. A had a slight leading sweep and B a large trailing sweep ; otherwise they were identical. Their periods were found experimentally and by calculation. In case A the calculated result was 5 per cent. above the actual, while in case B the figure was 19 per cent.

As a provisional rule, then, it may be taken that the usual method of estimating the first critical speed, without considering twist, yields a result which may be as much as 30 per cent. high. The error depends on the sweep and it is probably zero in blades of zero sweep.

An attempt to measure torsional periods experimentally failed to give definite results, probably on account of the very large hysteresis damping.

In all these experiments the method employed was to clamp a thin steel blade to the propeller so that its free length could be adjusted until maximum resonance was obtained when the propeller blade was set vibrating in a definite manner, *e.g.*, by dropping a weight on it from a given height. In these circumstances, the period was equal to or a sub-multiple of that of the resonator, which could be calculated.

PRELIMINARY REPORT ON THE TWISTING OF PROPELLER BLADES.

By A. A. Griffith, M.Eng., and B. Hague, B.Sc.

Presented by the Superintendent, Royal Aircraft Factory.

Reports and Memoranda, No. 454. *January,* 1918.

Summary.—In the present report a discussion is given of an attempt to apply the results of the soap-film method, for the torsion and flexure of cylindrical beams of any section, to the problem of finding the twist of propeller blades in flight.

It is shown that a simple extension of the theory of long cylindrical beams is quite inadequate to account for the observed phenomena in the case of tapering blades. Further, it has been found that the twisting of a wooden blade differs essentially from that of an otherwise similar metal one of the same stiffness.

A theory is developed, in an Appendix, which assumes that the blade is thin and its neutral surface plane. It is shown by comparison with the results of direct experiment that this theory is capable of representing satisfactorily the torsional properties of tapering propeller blades; but, though much useful information can be obtained from it, there are difficulties attendant on the practical application of the equations. It is hoped to remove these in a later report.

A circumstance which was disclosed in the course of the experimental verifications, is that the twist curves of opposite blades of a propeller, made in accordance with modern practice, may differ by an amount which may be as much as six times the usual manufacturing limits on the balance of angles. This appears to be due chiefly to the elastic heterogeneity of the timber employed, and it is suggested that some method of grading the wood might greatly improve propeller practice without involving the scrapping of any timber save that which is quite unsound. Also the twist of the blades could be minimised by this means.

It is further pointed out that unequal twisting of the blades may account for much of the noise which is emitted by propellers under flying conditions.

Lists of formulæ and symbols, definitions and tables of experimental and calculated results, are appended to the end of the report.

1. *General Statement of Problem.*

The blades of a propeller are tapering beams of completely unsymmetrical form, and, therefore, the strain due to their air-load must, in general, include torsion as well as flexure. The aerodynamic properties of the propeller are determined, not by the unstrained shape of the blades, but by their form under

flying conditions. Hence it is necessary for the designer to know the magnitude of the torsional strain, and, if it is greater than the usual manufacturing limits on angles, to take it into account in preparing his drawings. The nature of the twist is also of interest from the standpoint of vibration, which plays an increasingly important part in modern propeller practice.

Experiments have been made, from time to time, with a view to discovering an extension of the ordinary theory of bending and twisting of long beams which would represent adequately the behaviour of propeller blades, but the result has always been unsatisfactory, so much so, indeed, that it has usually been necessary to express the unknown quantities by means of a number of empirical constants at least equal to the number of experiments.

The accurate determination, by means of soap-films,* of the torsional and flexural properties of cylindrical beams of propeller section furnished, for the first time, a means of calculating these constants independently and so applying a rigorous test to this "beam" theory, as it may be called. Briefly, this theory consists in assuming that each element of the length of the blade behaves, both torsionally and flexurally, as though it were part of a cylindrical beam of the same section, and treating the blade, in the ordinary way, as a long beam having a curved central line, or rather, "line of flexural centres."†

For the purpose of checking the theory, it is quite unnecessary to reproduce the actual air-load. It is equally satisfactory to compare the calculated and observed twist‡ curves when the blade is loaded with a single concentrated load in any convenient position.

When this test was applied to the old theory, it was found that, while the two curves were accidentally in fair agreement in one instance, in general the calculated and observed results were entirely at variance. For example, Fig. 1 (Table 1, Appendix D) shows the twist‡ calculated on these assumptions for two opposite blades of an F.E.2D propeller (Drawing No. T.28020) for a concentrated load of 58·88 lbs. in the position shown in the developed plan-form, together with the corresponding curves found by experiment in the manner described later in the report. It will be seen that in this example the theory fails completely as the calculated line does not agree with either of the observed curves or with their mean. When torsions are plotted instead of twists the divergence is even more obvious. It may be mentioned here that preference was given to this example because it illustrates another point in

* See Reports Nos. R. & M. 333, 334 and 399.
† See Report No. R. & M. 399.
‡ *See* Appendix C for definitions of "twist" and "torsion."

connection with propellers, namely, that, owing to the heterogeneity of material, the twist curves of opposite blades may be entirely different. This will be referred to later.

In view of this and similar evidence, the problem was then attacked by the method given in the appendix. Briefly, this method consists of an application of the theory of flexure of a thin plate under a load applied normally to its surface. It is assumed primarily that the neutral surface of the plate is plane, and it is probable that this is substantially justified so far as the thinner parts of a propeller blade are concerned ; in any case, the twist of the thicker parts is negligible, owing to their much greater torsional stiffness.

As the Appendix shows, the general equations were much too complicated for practical use, but simplifications were introduced by assuming that the values of Young's modulus for the wood, in a direction across the grain, was small in comparison with that along the grain. The problem was still further simplified by making the torsion zero. The solution of the equations then gave the unique distribution of load which could be applied to the blade without causing any part of it to twist.* The position of the line of action of the resultant shear force on every section of the blade was found for this case, and a line joining the two points through which these shear-force resultants passed was drawn on the plan view of the blade. It is proposed to call this line the " line of principal flexure," since it specifies the type of bending in which strain-curvatures of the surface of the blade in the planes zx and xy are principal curvatures. Conformably with this nomenclature, the point where this line cuts any section may be referred to as the " principal flexure point " of that section.

On account of the intractability of the general form of the equations of equilibrium, it was sought to estimate the torsion, under any assigned load, by assuming that the couple acting on any section was given by the product of the actual resultant shear force into its perpendicular distance from the principal flexure point.

An initial difficulty was, however, encountered. In applications of this method to problems relating to thin curved rods of isotropic material, sections are taken normal to the central line. In the case of wood it was thought that the sections should be perpendicular to the grain. To test this, recourse was had to experiment. Two blades of propeller plan form and constant thickness were prepared, one of well annealed aluminium and the other of walnut, and the torsion measured along each when it was set up horizontally and loaded with a single concentrated

* When the curve of bending moment against length had any assigned form.

load of suitable magnitude. The measured curves are shown in Fig. 2 (Table 2, Appendix D), together with the plan form of the blade. It is obvious that for a blade of uniform thickness, the line of principal flexure and the centroid of the xy sections, are both coincident with the locus of the points of bisection of the chords. The calculated curves shown in the same diagram were obtained by the following methods.

In the case of the aluminium plate, which was probably approximately isotropic, sections were taken normal to the central line and the arm of the couple acting on any section was taken to be the perpendicular distance of the principal flexure point from a line drawn through the load normal to the section. The procedure adopted for the wooden plank was equivalent to this, save that the sections were all taken normal to the grain.

Fig. 2 shows the calculated and observed torsion curves for these two beams. It will be seen that, though there is a marked difference between the two experimental curves, each agrees well with the appropriate calculation, and hence the hypothesis regarding the difference between the treatment necessary for wood and metal is substantiated.

Naturally, this method of finding the torsion is open to several objections, which necessitate modifications of the simple theory outlined above. In the first place, the torsion is a function of y as well as of z, whereas in this method of treatment it is assumed to be constant over any section, z = constant. The result obtained is probably more or less accurately the mean torsion at any section, or, say, the torsion at the centroid, and for this reason all experimental determinations of torsion have been made at the centroids of the sections.

Further, it is shown in the Appendix that a tapering beam is, at any section, stiffer than a cylinder of similar cross-section, by an amount which depends on the actual magnitude of the torsion and its rate of change with respect to z. Although this increase in stiffness of the sections of a tapered beam is probably small for blades of isotropic material, it is certainly not so in the case of wooden blades.

Lastly, it is shown that if the torsion varies with z, there is a distribution of shear force over the section which depends on the rate of change of torsion and is additional to the ordinary distribution of shear force due to torsion.

Both these effects are of great importance in the case of a propeller blade, and it is necessary to know the actual torsion curve before it is possible to take them into account. This does not matter as far as checking the theory and the validity of the assumptions, by comparison with torsions measured on an actual blade, is concerned, since the requisite data for the calculation of these effects can be taken from the measured torsion

curves. The position is, however, otherwise when it is desired to employ the theory in the estimation of the twist curve of a new propeller. In that case the only direct course is to assume, from previous experience and the uncorrected torsion curve, a probable form for the actual torsion curve and work back from that ; this would have to be continued as a process of successive approximation until the corrected curve coincided sufficiently nearly with the assumed one. It is hoped that it will be possible subsequently to develop an indirect or empirical method of overcoming this difficulty. In any event, as will be seen later, the uncorrected torsion curve is capable of yielding much of the information required by the designer.

2. *Description of experimental results and corresponding calculations.*

All the experimental results and the corresponding data calculated by means of the theory were obtained for the case of a blade bent by a single concentrated load, and the following three types of blade have been dealt with in this way :—

(*a*) A special walnut plank having a flat top surface and trapezoidal cross-sections, as shown in Fig. 3.

(*b*) The blades of a B.E.2c, 4-bladed propeller (thrust meter), Fig. 4.

(*c*) The blades of a two-bladed S.E.5 propeller (T.28086), Fig. 5.

The general procedure of calculation and experiment is the same in all cases.

It is shown in the Mathematical Appendix (*see* Fig. 12 for the directions of axes) that the line of principal flexure passes through the centroid of the curve of the function $\frac{\partial}{\partial z}\left(\frac{Mt^3}{2I}\right)$ against y for any value of z = constant. Thus the y co-ordinate of the line of principal flexure is

$$\int_o^b \frac{\partial}{\partial z}\left(\frac{zt^3}{I}\right).\, y\, dy. \Big/ \int_o^b \frac{\partial}{\partial z}\left(\frac{zt^3}{I}\right) dy$$

for concentrated load. This quantity can be readily found if the function

$$\frac{W}{12}\cdot\frac{\partial}{\partial z}\left(\frac{zt^3}{I}\right) = \frac{W}{12}\left\{\frac{3zt^2}{I}\cdot\frac{\partial t}{\partial z} + t^3.\ \frac{\partial}{\partial z}\left(\frac{z}{I}\right)\right\},$$

is calculated. For this purpose it is necessary to know the thickness t of the blade at every point. This was found for the propeller blades concerned by mapping out contour lines of constant thickness upon the surface of the blade with the aid of a micrometer caliper. A tracing of this contour map was then taken (*see* the developed plan forms in Figs. 4 and 5) and from it was constructed a series of curves giving the thickness as a

function of z for various constant values of y. From these curves t^2, t^3 and, by graphical differentiation $\partial t/\partial z$, were calculated and set out in tabular form for various constant values of z. Further, $I = \frac{1}{12}\int_o^b t^3 dy$ was also found by integrating curves of t^3 plotted as a function of y for constant values of z, and hence z/I and its differential with respect to z were determined. It was then a simple arithmetical process to complete the calculation of $\frac{W}{12}\frac{\partial}{\partial z}\left(\frac{zt^3}{I}\right)$. From the table so prepared the positions of the principal flexure points were found by plotting $\frac{W}{12}\frac{\partial}{\partial z}\left(\frac{zt^3}{I}\right)$ as a function of y for various constant values of z, and determining the centroid of the resulting curves.

By this means the line of principal flexure was obtained and plotted out on the plan view of the blade, together with the line parallel to the grain through the point of application of the load, and from the two curves the couple arm was found in the manner described above; these couple arms, when multiplied by the value of the load gave the couple T. The "cylindrical torsional stiffness" C was calculated from the expression $C = 4I\Big/\left(1 + \frac{4I}{Ab^2}\right)$*, and the average value of modulus of rigidity was found from a series of experiments carried out upon test specimens cut from the blade. Then the value of τ, the uncorrected torsion, was given by $\tau = T/NC$, and is shown in the uncorrected curves of Figs. 3, 4 and 5 (Tables 3, 4, 4*a*, 5 and 5*a*, Appendix D).

When the torsion curve had been actually measured, it was possible to calculate the two effects dependent on the rate of change of torsion, namely, the increase of stiffness due to the taper of the blade and the additional distribution of shear force due to the variation of torsion with z. The observed torsion curve was differentiated graphically with respect to z, and the actual stiffness, C′, of the tapered beam calculated from the expression

$$C' = C\left(1 + 0{\cdot}14\frac{b^2}{{\tau_m}^2}\cdot\left(\frac{\partial\tau_m}{\partial z}\right)^2\right),\dagger$$

wherein τ_m is the measured torsion. The calculation of the additional shear force distribution is very similar to that employed above for the principal flexure shear force. The expression for this additional shear force (*see* Equation 16 in Appendix) is

$$\frac{\partial}{\partial z}\left(\frac{Et^3}{12}\cdot y_1\frac{\partial\tau_m}{\partial z}\right) = \frac{E}{12}\left\{3y_1\cdot t^2\frac{\partial\tau_m}{\partial z}\cdot\frac{\partial t}{\partial z} + y_1 t^3\cdot\frac{\partial^2\tau_m}{\partial z^2}\right\},\ddagger$$

* *See* R. & M. 334.
† Appendix A, §2.
‡ Appendix A, §3.

when E is taken as constant ; $\partial\tau_m/\partial z$ and $\partial^2\tau_m/\partial z^2$ were found graphically from the measured curve ; and $y_1 = y - Y$, where Y is adjusted so as to make the total bending moment due to this shear force equal to zero : it is shown in the Appendix that Y must be the y co-ordinate of the centroid of the curve of t^3. The same tabular form of calculation was employed, and the result added to the previously determined shear force, $\frac{W}{12} \cdot \frac{\partial}{\partial z}\left(\frac{zt^3}{I}\right)$. The centroid of the curve of total shear force as a function of y (z constant) was found as before. The couple T_c, is found from the curve through the points so obtained on the developed plan form of the blade and the line through the load parallel to the grain, in a manner precisely similar to that just described, and hence the curve of corrected torsion $\tau_c = T_c/C'$, shown in Figs. 3, 4 and 5 (Tables 3, 4, 4*a*, 5 and 5*a*, Appendix D) is obtained. It is seen from these diagrams that the final corrected curve is in good agreement with the measured curve, especially in the case of the flat wooden plank, Fig. 3. The theory assumes that the neutral surface is plane, which is substantially true in this case, but not so in the case of the propeller blades of Figs. 4 and 5. Further, the plank consisted of one piece of wood, whereas the blades were laminated, and it is probable that much of the discrepancy between the calculated and observed results is due to these two causes. In the case of Fig. 3 it should be noted that the drooping of the measured curve over the calculated curves for the large values of z may be largely due to additional stiffening given to the end sections of the plank by their proximity to the thick part by which it was fastened to the bench when under test.

The experiments may be conveniently considered under two headings :—

(*a*) measurements of twist and torsion to check with the calculations ; and

(*b*) measurements of the elastic constants, E and N, for use in calculating the torsion curve.

(*a*) Dealing with the first of these sub-divisions, the experimental arrangements were as illustrated in Fig. 6 and briefly described below. The propeller to be tested, A, was firmly fixed by means of a nut and plate to the cast iron table B, and tilted over to such an angle as would make the part of the blade to which the load was applied truly horizontal. The load was applied by means of a slotted shackle C, a hanger D whose position on the shackle was adjustable, and disc weights E. The edge of the shackle bearing on the pressure face of the blade was shaped up to a blunt knife-edge in order to give approximate line distribution of the load, interference with the natural anticlastic curvature of the blade when bent being prevented as far as possible by the interposition of a piece of soft felt between the shackle and the blade. The torsion on the blade when the

load was applied was found by mounting two small mirrors upon needle points which were pressed into the blade on the line of centroids at a distance of 1 inch apart. The images of a distant scale in the mirrors were observed by means of a telescope, and the angle of relative rotation between the two mirrors, due to the application of the load, was noted. Obviously, this angle was very nearly equal to the torsion midway between the two mirrors. By this means, with the scale 1·5 metre from the mirrors it was possible to estimate the scale reading to 1/10 mm., corresponding to an angle of 1/30,000 radian relative rotation between the mirrors.

The mirror method just described is the simplest and most direct way of obtaining the torsion experimentally, but another and indirect method is to measure the twist and then graphically differentiate the curves obtained—a matter of no little difficulty when accuracy is desired, owing to the irregularity of the measured twist curves. The twist can obviously be found by the mirror method by determining the rotation of a mirror mounted at the centroid of a section, relatively to that of a second mirror mounted on the stiff part of the blade near the boss. A second method is to employ a sensitive clinometer, such as F, in Fig. 6, which can be applied in turn before and after the application of the load, to a series of geometric mounts G set centrally over the line of centroids. Such a clinometer has been employed extensively for the measurement of twist and was capable of measuring to within $0{\cdot}15 \times 10^{-3}$ radian.

(*b*) Experiments for the determination of the elastic constants of the blades were carried out by cutting from them a large number of cylindrical specimens, from which the values N and E were found by the usual torsion and bending tests. Flexure tests were made by observing the curvature directly by means of a special spherometer which is shown applied to a propeller blade at H in Fig. 6, and in general detail in Fig. 7. Briefly, this instrument consists of a frame standing on three steel points and supporting a fixed mirror. A second and movable mirror is attached to an L-shaped mount which is supported on a steel point pressed into the specimen under test, two points on the upper surface of the L resting respectively in a slot and on a plane on the under face of the frame. It is clear that when flexure takes place the points of support of the frame will move vertically (in the plane of flexure) relatively to the point which is supporting the movable mirror, and thereby tilt the latter. Curvatures of 1/16,000″ could be measured with this instrument with ease, and quantities 1/10th of this magnitude estimated.

Other effects.—The theory described above and developed in the Appendix was, of course, based on the assumption that the strains and displacements were everywhere so small that their squares could be neglected. When they cannot be so neglected,

it is necessary to consider certain secondary effects, and two of these may be of importance in the bending and twisting of a propeller blade under flying conditions.

In the first place, if a beam suffer a finite deflection under a load which is not parallel to one of the principal axes of its cross-section, the beam twists slightly so as to make the axis of minimum moment of inertia more nearly perpendicular to the load. This twist is additional to that due to symmetry of loading and initial curvature of the central line.

Secondly, if the axis of flexure be not an axis of symmetry of the cross-section, there is a tendency for the latter to distort, by means of transverse bending, so as to make it more nearly symmetrical. This transverse bending must have some influence on the distribution of shear force.

Both these effects are proportional to the square of the load, and hence it is always possible, in experiments such as the present ones, to reduce them to negligibly small dimensions by suitably reducing the load.

It is proposed to discuss these second order effects fully in a later report. It is merely necessary to mention here that the conditions of the experiments described above were so adjusted as to make the effects sufficiently small to be neglected.

3. *General conclusions.*

Difference of twist of opposite blades.—A point of no little practical importance, which has been disclosed in the course of the experimental work carried out in connection with the present report is that, under present manufacturing conditions, differences in shape and elastic properties of individual blades of a given propeller may be responsible for their twist curves, under flying conditions, being quite dissimilar. This is strikingly illustrated in Fig. 1, where it is seen that the twist curves of two opposite blades under a concentrated load do not even possess the same general characteristics, and less markedly in the case of two other propellers, whose twist curves are shown in Figs. 8 and 9 (Tables 6 and 7, Appendix D).

An attempt has been made to estimate for the curves of Fig. 1 the probable out-of-balance twist of these two blades under flying conditions. The result is shown in Fig. 10 (Table 8, Appendix D); the error of this curve may be, perhaps, 30 per cent., but it is not probable that it is more. For the purpose of comparison, the manufacturing limits imposed on the balance of angles on opposite blades have been plotted on the same diagram. It appears that the out-of-balance twist may be five or six times as great as the manufacturing limits, for the important part of the blade near the tip.

Apart altogether from its other bad effects, it is thought that this want of balance may account for part, at least, of the noise emitted by propellers in flight.

To put the matter very roughly, let it be imagined that the cylinder of air acted on by the propeller is divided into a number of parts, equal to the number of blades, by helicoidal surfaces, so that each of these portions contains the air acted on by one blade. It seems fair to assume that the density of the air in any one portion is related in some way to the angle of attack of the corresponding blade. If, then, the angles of the blades differ, it is evident that there must be a constant stream of alternate condensations and rarefactions proceeding from the propeller, and hence sound must be produced.

Bearing of the present work on design.—It has been seen that the theory outlined in this report does not lend itself readily to the calculation of the true twist curve of a propeller blade. It is possible, however, to make useful deductions from the "uncorrected curve." Fig. 11 shows such an "uncorrected twist curve" calculated for the blades of an S.E.5 propeller under an assumed distribution of air-load; the remarkable constancy of torsion over a considerable part of the blade is particularly noticeable (*see* Table 9, Appendix D).

In the first place, the positions of the points of zero and maximum torsion are not greatly altered by the introduction of the corrections, and, secondly, in the three examples which are considered in this report, a curve which is, for many purposes, sufficiently near the measured curve, may be obtained by reducing the uncorrected values by about one-third. Pending the evolution of a more satisfactory process, this might be adopted as a working rule. It is, of course, equivalent to employing a value for the modulus of rigidity of about $0{\cdot}21$ to $0{\cdot}23 \times 10^6$ lbs./sq. in., instead of the actual figures of $0{\cdot}14$ to $0{\cdot}15 \times 10^6$.

From many points of view, it is advisable to construct propeller blades so that they shall twist as little as possible. The most obvious way of doing this is to modify the plan form of the blade until a shape is found for which the line of principal flexure coincides as nearly as possible with the actual line of shear force resultants due to the air-load. To conform to this condition, propeller blades would have to be swept back considerably less than is usual at present.

There is, however, another method of attacking the problem. In the theory outlined above, the principal Young's modulus of the wood has been assumed to be constant. By making the successive laminations of the blade of different woods, or of different grades of the same wood, it is possible, within certain limits, to make the modulus any arbitrary function of y, the transverse co-ordinate. The extension of the theory to this

case is obvious. Hence it is possible to exercise a certain amount of control over the shape of the line of principal flexure without altering the plan form.

It is proposed to defer the general discussion of the strength of propeller blades to a later report, but it may be remarked here that, in view of the great importance of torsional stresses, the observation in the preceding paragraph opens up the interesting possibility of strengthening propeller blades of certain forms by reducing the strength of the wood in the leading laminations.

The propellers mentioned in the present report were taken at random from among those made under ordinary workshop conditions at the Royal Aircraft Factory. Hence it seems fair to assume that their properties are more or less representative of average practice, yet in only one of the three cases is there approximate balance in the twists of opposite blades, while in one of the others the asymmetry is startling.

It is evident that little is to be gained by attempting to design blades so that they shall twist in a certain way, if it be possible for uncontrolled factors to account for an asymmetrical twist of about a degree. It is equally superfluous, in such a case, to impose on the balance of angles, manufacturing limits of one-fifth to one-fourth of a degree, and yet the necessity for balance of this order appears to be indisputable. It would seem, then, that some kind of control over the elastic properties of the timber used is called for.

One possible method is to introduce into the inspection routine some simple standard loading test, the balance of twist on opposite blades being limited within certain bounds. The objection to this course is that it would involve scrapping the unsatisfactory propellers for reasons over which the manufacturer had no control.

Another way which suggests itself is to subject the planks to a simple flexure test immediately after rough planing. For instance, they might be placed on supports and bent by a given load in the middle. A pointer actuated by the movement of the middle of the plank would read "Grade 1," "Grade 2," "Grade 3," &c. Two other pointers would be governed by the inclinations of the supported ends. The difference between the readings of these pointers would be subject to certain limits, as any lack of balance here would involve a corresponding asymmetry of twist in the opposite blades. Planks unsatisfactory in this respect would be rejected.

The drawing office might then direct, for example, that laminations 1, 2 and 3 of a certain propeller be drawn from grades 1, 3 and 5, or, alternatively, from grades 2, 4 and 6, and so on. It is easy to see thus how by the employment of some

process of this sort two perfectly sound propellers could be produced from timber which under the present system of random selection might easily be made into two unsatisfactory ones.

It is evident that, under present conditions, the two-bladed propeller is much likelier to have "elastic symmetry" than a four-bladed one. In the latter case it is necessary, in order to get balance and freedom from the source of noise referred to above, for each lamination to pair with the corresponding one in the other two blades. In the two-blader, all that is required is uniformity of single laminations.

MATHEMATICAL APPENDIX A.

1. *Deformation of thin wooden plank.*

It is required to find the equations of equilibrium of a thin plank when slightly deformed by a pressure P lbs. per sq. in. acting normally to its surface.

Let the axis of x be normal to the plank, the axis of y perpendicular to and the axis of z parallel to the grain of the wood (*see* Fig. 12).

Further, let

t = thickness of plank.
u = displacement of neutral surface, parallel to ox.
E = Young's modulus parallel to grain.
σ = corresponding Poisson's ratio.
E′ = Young's modulus perpendicular to grain.
σ' = corresponding Poisson's ratio.
N = Modulus of rigidity for Y_z shears.

It is assumed that t, $\frac{\partial t}{\partial y}$, $\frac{\partial t}{\partial z}$ are small everywhere and that the neutral surface of the plank is plane in its unstrained state. It is further assumed that there is no extension of the neutral surface.

Consider an elementary block of the material (*see* Fig. 12) t, dy, dz.

The edge $t\,dy$ is acted on by a shear stress resultant parallel to ox, $S_z\,dy$ say, and the flexural and torsional couples $M_z\,dy$ and $T_z\,dy$ about axes parallel to oy and oz respectively.

The edge $t\,dz$ is acted on by shear stress resultant $S_y\,dz$ and couples $M_y\,dz$ and $T_y\,dz$.

Lastly, there is a normal force P $dy\,dz$ acting on the face $dy.dz$

The three equations of equilibrium which are not satisfied identically are

$$\frac{\partial T_y}{\partial y} - \frac{\partial M_z}{\partial z} + S_z = 0 \quad . \quad . \quad . \quad . \quad (1)$$

$$\frac{\partial T_z}{\partial z} - \frac{\partial M_y}{\partial y} + S_y = 0 \quad . \quad . \quad . \quad . \quad (2)$$

$$\frac{\partial S_y}{\partial y} + \frac{\partial S_z}{\partial z} + P = 0 \quad . \quad . \quad . \quad . \quad (3)$$

From these equations we find

$$\frac{\partial^2 M_y}{\partial y^2} - \frac{\partial^2}{dy\,dz}(T_y + T_z) + \frac{\partial^2 M_z}{\partial z^2} + P = 0 \quad . \quad . \quad (4)$$

Also we have

$$M_y = \frac{E' t^3}{12(1-\sigma\sigma')} \cdot \left(\frac{\partial^2 u}{\partial y^2} + \sigma \frac{\partial^2 u}{\partial z^2}\right) \quad . \quad . \quad . \quad (5)$$

$$M_z = \frac{E\, t^3}{12\,(1-\sigma\sigma')} \cdot \left(\frac{\partial^2 u}{\partial z^2} + \sigma' \frac{\partial^2 u}{\partial y^2}\right) . \quad . \quad . \quad (6)$$

$$T_y = T_z = \frac{N\, t^3}{6} \cdot \frac{\partial^2 u}{\partial y\, \partial z} \quad . \quad . \quad . \quad . \quad . \quad . \quad (7)$$

The substitution of expressions (5), (6) and (7) in equation (4) gives the general equation for u. It is the object of the investigation to find the particular solution of this equation which satisfies the assigned boundary conditions.

It is evident that the general problem is much too difficult to solve by rigorous analysis.

We may note, however, as facts of experience that

(*a*) E′ is only about one-sixteenth of E, for the timber commonly used in propeller manufacture.

(*b*) σ' is of the order of 0·001.

(*c*) Under the load distributions usual in propellers, $\frac{\partial^2 u}{\partial y^2}$ and $\sigma \frac{\partial^2 u}{\partial z^2}$ are of opposite signs and about the same magnitudes.

In view of these considerations, it would appear legitimate, for practical purposes, to neglect certain terms and write the equation in the simpler form

$$\frac{\partial^2}{\partial z^2}\left(\frac{Et^3}{12} \cdot \frac{\partial^2 u}{\partial z^2}\right) - 2\frac{\partial^2}{\partial z \partial y}\left(\frac{Nt^3}{6} \cdot \frac{\partial^2 u}{\partial y \partial z}\right) + P = 0 \quad . \quad . \quad (8)$$

(8) may be further simplified by putting the torsion $\frac{\partial^2 u}{\partial y \partial z}$ equal to zero. The equation then determines the load under which the flexure is "principal flexure." We see that in this case $\frac{\partial^2 u}{\partial z^2}$ is constant across any section of the blade by an xy plane. If I be the moment of inertia of this section, and M the bending moment on it, we have

$$\frac{\partial^2}{\partial z^2}\left(\frac{M}{I} \cdot \frac{t^3}{12}\right) + P = 0 \quad . \quad . \quad . \quad . \quad (8a)$$

and the shear stress resultant, from (1) and (6),

$$S_z = \frac{\partial}{\partial z}\left(\frac{M}{I} \cdot \frac{t^3}{12}\right) \quad . \quad . \quad . \quad . \quad . \quad (9)$$

If the distribution of load along oz is assigned, this equation determines the unique distribution along oy which will bend the blade without twisting it.

By calculating S_z at a number of points, we can find the lines of action of the resultant shear forces on a series of sections and thence plot out the "line of principal flexure."

We may then seek, as described in the text, to deduce the twist under any other distribution by finding for each section, the distance between the principal flexure point and the line of action of the actual resultant shear force and assuming that the couple so obtained twists the blade as it would a cylindrical blade of the same section. This treatment, however, requires modification by reason of the effects dealt with in §§ 2 and 3 below.

2. *Increase of stiffness due to taper.*

If the torsion τ on a blade be not independent of z, the torque required is greater than would be necessary in the case of a uniform torsion.

Assuming the distortion of the cross-section to be the same as it is in the torsion problem of Saint-Venant, we may put it equal to $\tau\,(y - Y)x$ for any thin blade, where Y is a constant of the section.

Hence $(y - Y)x \frac{d\tau}{dx}$ represents an extension of the longitudinal filaments of the blade, and the strain energy due to this extension is

$$\tfrac{1}{2} \cdot \int \frac{E\,t^3}{12} \cdot \left[(y - Y)\frac{d\tau}{dz}\right]^2 dy \quad . \quad . \quad . \quad (10)$$

per unit of length.

The total bending moment due to these strains is

$$\int \frac{E\,t^3}{12} \cdot (y - Y) \cdot \frac{d\tau}{dz}\,dy \quad . \quad . \quad . \quad . \quad (11)$$

This must be zero, and hence

$$\int t^3 . (y - Y) . dy = 0 \quad . \quad . \quad . \quad . \quad (12)$$

or Y is the y co-ordinate of the centroid of the curve of t^3 against y.

The strain energy due to the ordinary torsional shear strains is

$$\tfrac{1}{2} N C \tau^2$$

where C is the " cylindrical " stiffness of the section.

Hence the total strain energy is

$$\tfrac{1}{2} N C\tau^2 + \tfrac{1}{2} \frac{E}{12} \left(\frac{d\tau}{dz}\right)^2 \cdot \int t^3 (y - Y)^2\,dy \quad . \quad . \quad (13)$$

Hence if C′ is the effective torsional stiffness

$$C' = C\left[1 + \frac{E \int t^3 (y - Y)^2\,dy}{12\,C\,N} \cdot \frac{1}{\tau^2} \cdot \left(\frac{d\tau}{dz}\right)^2\right] \quad . \quad . \quad (14)$$

or

$$C' = C\left[1 + k \frac{E}{N} \frac{1}{\tau^2} \left(\frac{d\tau}{dz}\right)^2\right] \quad . \quad . \quad . \quad . \quad . \quad (15)$$

where k is a known constant of the section.

It is evident that the foregoing analysis can be only approximately correct, since it assumes that the cross-sectional distortion is the same as in the case of a cylindrical blade under a uniform torque ; experiments have been made, however, which indicate that it is probably within one or two per cent of the truth.

It will be seen that the magnitude of the stiffness correction depends on the ratio $\frac{E}{N}$, and hence it is much greater for wooden members than for metal ones.

3. *Additional shear force due to variation of* τ.

If τ be not independent of z, there may be a shear stress resultant which is additional to the ordinary torsional shear stress, of magnitude

$$\frac{\partial}{\partial z}\left[\frac{E\,t^3}{12} \cdot (y - Y) \frac{\partial \tau}{\partial z}\right] \quad . \quad . \quad . \quad . \quad (16)$$

where, as is easily seen, Y must be the same as before in order that these additional forces may not affect the assigned distribution of load along oz.

Like the increase of stiffness due to taper, these forces cannot be calculated unless the torsion curve is known or can be approximated to by successive trial.

APPENDIX B.

Definitions of terms used in this Report.

Principal flexure.—That mode of flexure of a thin plank in which the strain-curvatures in the planes xy and yz are principal curvatures, or, in other words, non-torsional flexure.

Line of principal flexure.—A curve drawn on the developed plan-form of a propeller blade, passing through the lines of action of the resultant shear forces acting on the xy sections of the blade, when the flexure is principal flexure.

Principal flexure point.—That point of an xy section which lies on the line of principal flexure.

Twist.—The angular displacement of an xy section about oz.

Torsion.—Twist per unit length.

APPENDIX C.

List of symbols and formulæ.

A = Area of xy sections of a propeller blade.

C = " Cylindrical torsional stiffness," $4I \Big/ \left(1 + \frac{4I}{Ab^2}\right)$.

C' = Corrected stiffness of a tapering blade.

$$= C\left[1 + k\frac{E}{N} \cdot \frac{1}{\tau^2}\left(\frac{\partial \tau}{\partial z}\right)^2\right].$$

E = Young's modulus parallel to the grain in wood.
E' = Young's modulus perpendicular to the grain in wood.
I = Moment of inertia of xy sections of a thin blade

$$= \frac{1}{12}\int_o^b t^3\, dy.$$

M = Bending moment acting on any section of blade.
N = Modulus of rigidity for zy shears.
P = Pressure acting normal to surface of a thin blade.
S_z = Shear stress resultant for a blade under principal flexure

$$= \frac{\partial}{\partial z}\left(\frac{M}{I} \cdot \frac{t^3}{12}\right).$$

T = Torque acting on any section of a blade.
W = Magnitude of a concentrated load.
Y = y co-ordinate of the centroid of the curve of t^3 against y.
b = Chord of xy sections of a propeller blade.
k = A constant of xy sections of a propeller blade

$$\int_o^b t^3(y - Y)^2 dy \,/ 12C.$$

t = Thickness of thin plank.
u = Displacement of neutral surface of thin plank.
x = Co-ordinates normal to the blade.
y = Co-ordinates perpendicular to the grain of the wood.
z = Co-ordinates parallel to the grain of the wood.
y' = $y - Y$.
σ = Poisson's ratio corresponding to E.
σ' = Poisson's ratio corresponding to E'.
τ = Torsion of xy sections = $\partial^2 u / \partial y . \partial z$.

APPENDIX D (TABLES).

TABLE 1.

TWIST CURVES OF PROPELLER F.E.2D (DRAWING T.28020); FIG. 1.

First Blade.		Third Blade.		Calculated (Old Theory).	
Distance from Load. Inches.	Twist in Radians $\times 10^{-3}$	Distance from Load. Inches.	Twist in Radians $\times 10^{-3}$	Distance from Load. Inches.	Twist in Radians $\times 10^{-3}$
1·42	3·60	1·5	—5·77	5·0	8·00
3·50	5·24	3·5	—6·07	7·5	3·84
5·36	7·33	5·5	—3·00	10·0	+1·42
7·50	5·86	7·5	—2·62	12·5	0·00
9·30	3·68	9·5	—1·50	15·0	—0·78
11·50	2·94	11·5	—2·23	20·0	—1·10
13·24	2·36	13·0	—1·65	25·0	—1·00
15·50	1·87	15·5	—1·21	30·0	—0·66
17·18	1·68	17·0	—0·41	35·0	—0·32
19·50	1·43	19·5	—0·35	40·0	—0·14
21·12	1·13	23·5	—0·13	50·0	0·00
23·50	0·72	25·0	—0·21		
25·06	0·62	27·0	—0·57		
27·00	0·43	29·0	—0·36		
29·00	0·52	31·0	—0·54		
31·00	0·43	33·0	—0·80		
32·94	0·52	35·0	—0·74		
35·00	0·43	37·0	—0·50		
36·88	0·34	50·0	0·00		
50·00	0·00				

TABLE 2.

TORSION OF BLADES OF UNIFORM THICKNESS; FIG. 2.

Distance from Load.	Aluminium Plate.		Walnut Plank.	
Inches.	Observed Torsion Radians per Inch $\times 10^{-3}$	Calculated Torsion Radians per Inch $\times 10^{-3}$	Observed Torsion Radians per Inch $\times 10^{-3}$	Calculated Torsion Radians per Inch $\times 10^{-3}$
0	—	0·681	—	—
2	0·602	0·543	0·753	0·650
4	—	0·420	+0·072	+0·035
6	0·344	0·321	—0·217	—0·245
8	0·249	0·224	—0·448	—0·422
10	0·124	+0·100	—0·618	—0·560
12	+0·000	—0·035	—0·718	—0·679
14	—0·156	—0·180	—	—

Table 3.

TORSION CURVES FOR A WALNUT PLANK OF VARIABLE THICKNESS; FIG. 3.

Distance from Load.	Observed Curve.	Uncorrected Curve.	Corrected Curve.
Inches.	Radians per Inch $\times 10^{-3}$	Radians per Inch $\times 10^{-3}$	Radians per Inch $\times 10^{-3}$
1·0	0·400	0·620	0·319
2·0	1·320	1·575	1·100
3·0	1·550	1·890	1·400
4·0	1·490	2·000	1·390
5·0	1·430	1·930	1·300
6·0	1·350	1·800	1·243
8·0	1·160	1·441	1·048
10·0	0·880	1·130	0·810
12·0	0·540	0·815	0·568
14·0	0·200	0·630	0·309
16·0	—	0·530	0·152

Table 4.

CALCULATED TORSION CURVES OF PROPELLER B.E.2c (THRUST-METER); FIG. 4.

Distance from Load.	Uncorrected Curve.	Corrected Curve.
Inches.	Radians per Inch $\times 10^{-3}$	Radians per Inch $\times 10^{-3}$
2	−0·467	0·000
4	+2·100	1·290
6	2·865	1·850
8	2·335	1·700
10	1·842	1·395
12	1·405	1·120
14	1·161	0·900
16	0·856	0·731
18	0·641	0·513
20	0·433	0·316
22	+0·140	0·132
24	−0·004	—

TABLE 4*a*.

OBSERVED TORSION CURVE OF PROPELLER B.E.2c (THRUST-METER); FIG. 4.

Distance from Load. Inches.	Radians per Inch $\times 10^{-3}$
1·5	0·125
2·5	0·540
3·5	0·930
4·5	1·240
5·5	1·432
6·5	1·399
7·5	1·300
8·5	1·215
9·5	1·120
11·0	0·975
12·5	0·885
14·5	0·700
18·5	0·451
21·5	0·313

TABLE 5.

CALCULATED TORSION CURVES OF PROPELLER S.E.5 (DRAWING T.28086); FIG. 5.

Distance from Load.	Uncorrected Curve.	Corrected Curve.
Inches.	Radians per Inch $\times 10^{-3}$	Radians per Inch $\times 10^{-3}$
2	0·277	— 0·410
4	3·900	+ 2·250
6	4·690	2·810
8	4·230	2·140
10	3·520	1·720
12	2·750	1·309
14	1·970	1·026
16	1·190	0·750
18	0·770	0·464

TABLE 5*a*.

OBSERVED TORSION CURVE OF PROPELLER S.E.5 (DRAWING T.28086); FIG. 5.

Distance from Load. Inches.	Radians per Inch $\times 10^{-3}$
1·5	—1·375
2·5	+0·0645
3·5	1·392
4·5	2·485
5·5	2·450
6·5	2·120
7·5	1·820
11·5	1·100
15·5	0·800
20·5	0·420

TABLE 6.

OBSERVED TWIST CURVES FOR PROPELLER B.E.2c (THRUST-METER); FIG. 8.

Distance from Load.	First Blade.	Second Blade.	Distance from Load.	Third Blade.	Fourth Blade.
Inches.	Radians $\times 10^{-3}$	Radians $\times 10^{-3}$	Inches.	Radians $\times 10^{-3}$	Radians $\times 10^{-3}$
1	32·79	5·23	1	15·21	11·59
2	34·61	8·24	2	15·54	13·68
3	34·75	9·30	3	14·40	13·81
4	32·37	8·01	4	12·65	12·86
5	29·37	—	6	10·55	11·54
6	26·47	5·73	9	6·68	9·20
9	18·83	3·18	10·5	5·60	8·40
12	13·36	1·81	12	3·81	6·58
18	6·40	1·18	14	3·52	5·63
24	3·24	1·06	16	3·02	4·85
30	1·84	0·89	18	2·67	3·83
36	1·09	0·43	21	2·43	2·80
—	—	—	24	1·41	1·92
—	—	—	30	1·03	1·35
—	—	—	36	0·74	0·85

Table 7.

OBSERVED TWIST CURVES FOR PROPELLER S.E.5 (DRAWING T.28086); FIG. 9.

First Blade.		Second Blade.	
Distance from Load. Inches.	Twist in Radians $\times 10^{-3}$	Distance from Load. Inches.	Twist in Radians $\times 10^{-3}$
0	11·13	0	15·70
1·0	18·38	1·0	25·42
1·5	20·76	2·0	27·58
2·0	22·14	3·0	29·03
2·5	23·00	5·0	24·27
3·0	22·87	6·0	23·54
4·0	20·14	7·0	20·21
5·0	18·65	9·0	15·25
7·0	16·09	11·0	11·30
9·0	12·68	15·0	6·43
11·0	10·51	19·0	3·65
15·0	6·51	23·0	2·17
19·0	4·27	27·0	1·16
23·0	2·59	—	—
27·0	1·34	—	—

Table 8.

OUT-OF-BALANCE TWIST CURVE OF PROPELLER F.E.2D (DRAWING T.28020) UNDER AIR-LOAD; FIG. 10.

Out-of-balance Twist.		Limits on Balance of Angles.	
Distance from Tip of Blade. (Inches.)	Twist in Minutes.	Distance from Tip of Blade. (Inches.)	Angle in Minutes.
5·0	55·1	2·0	± 10·0
7·5	55·3	6·0	± 11·5
10·0	56·1	14·2	± 15·0
12·5	53·0	24·0	± 18·5
15·0	36·3	33·8	± 20·0
20·0	19·0	—	—
25·0	+6·6	—	—
30·0	—1·5	—	—
35·0	—2·4	—	—
40·0	—0·8	—	—

TWIST CURVES OF PROPELLER F.E.2.D. (DRG. T. 28020)

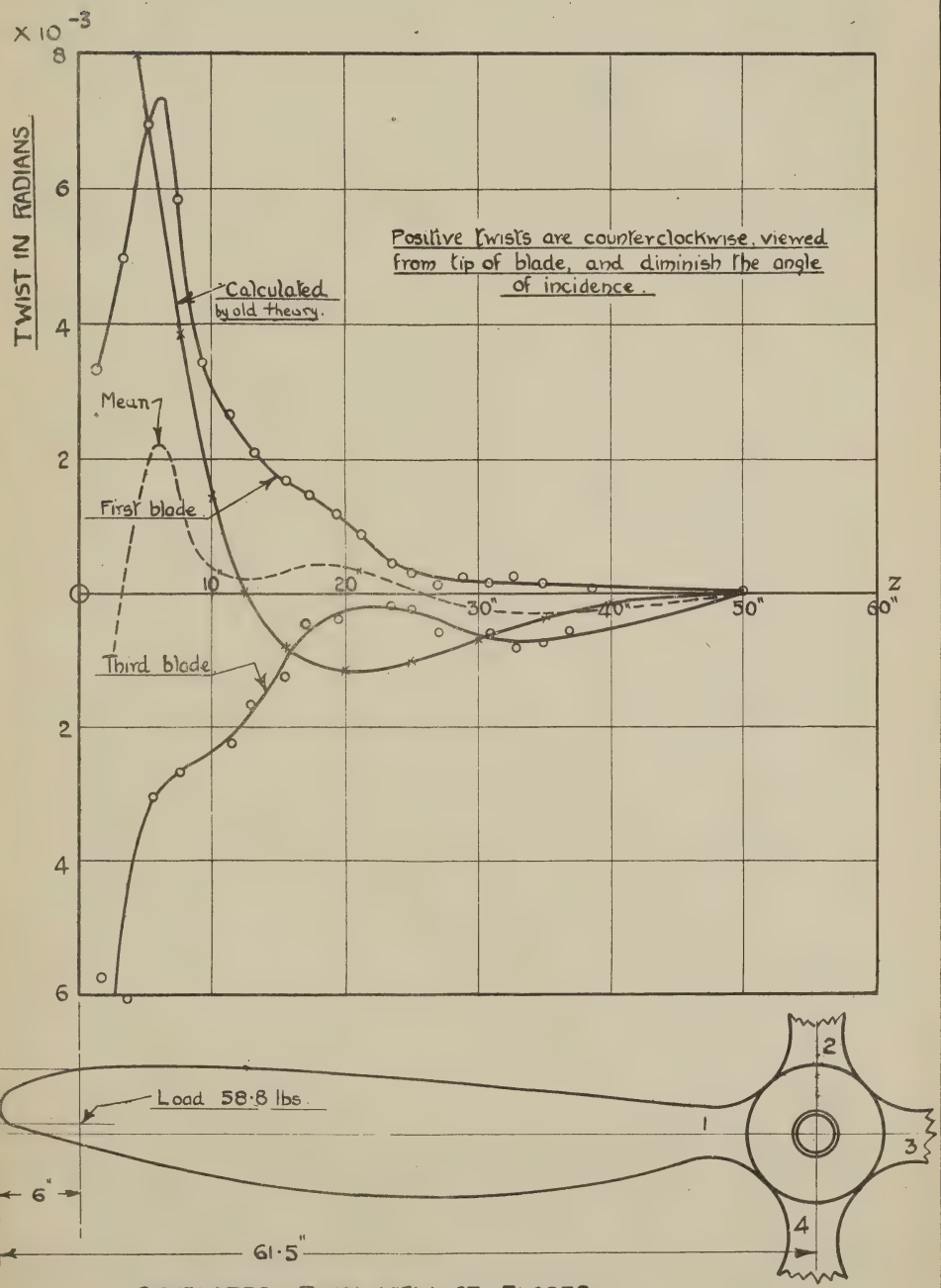

DEVELOPED PLAN VIEW OF BLADES.

TORSION CURVES OF BLADES OF UNIFORM THICKNESS.

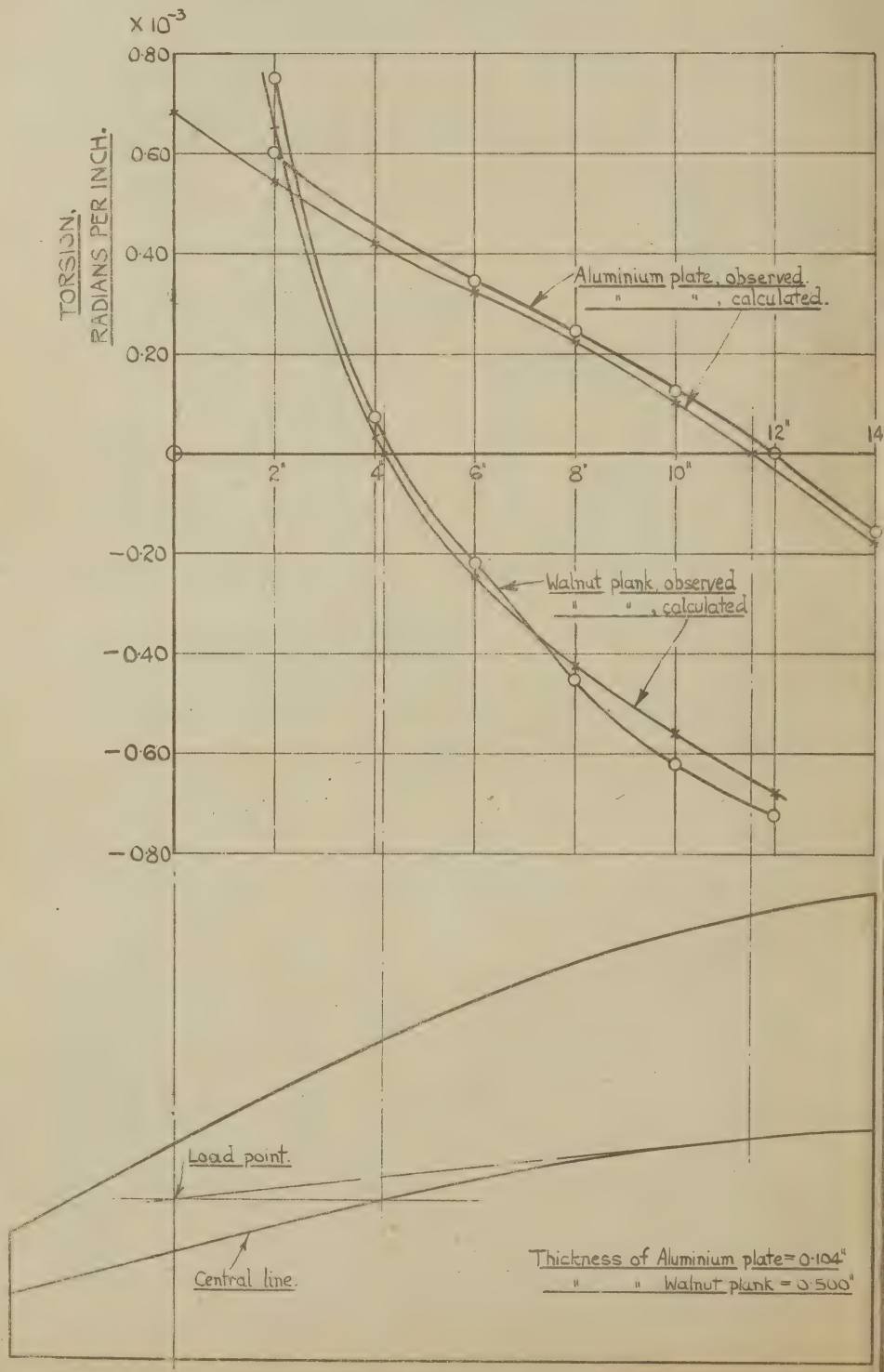

LIBRARY
OF THE
UNIVERSITY OF ILLINOIS

TORSION CURVES FOR A WALNUT PLANK OF VARIABLE THICKNESS.

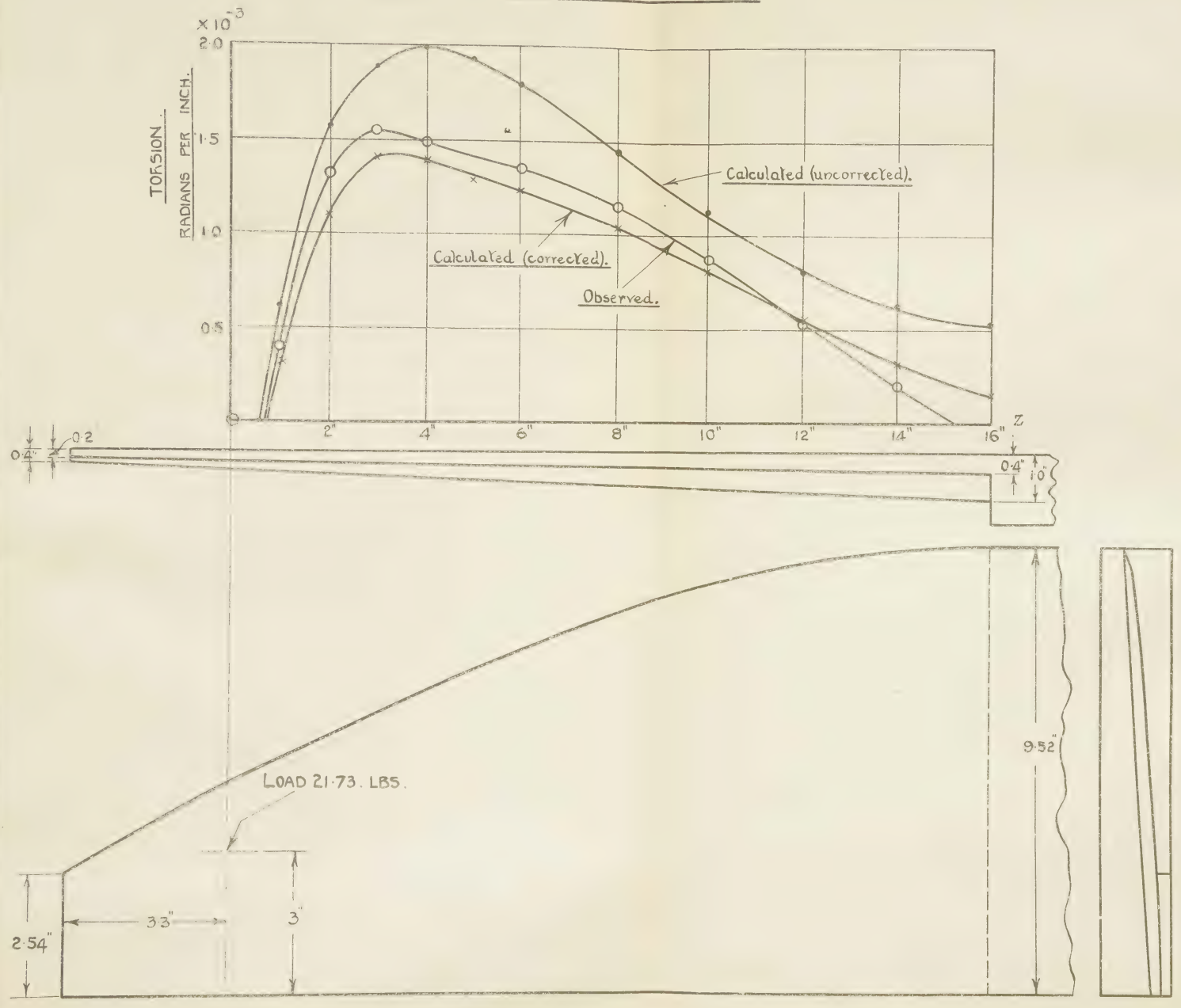

THE LIBRARY
OF THE
UNIVERSITY OF ILLINOIS

TORSION CURVES OF PROPELLER B.E 2C. (THRUST-METER)

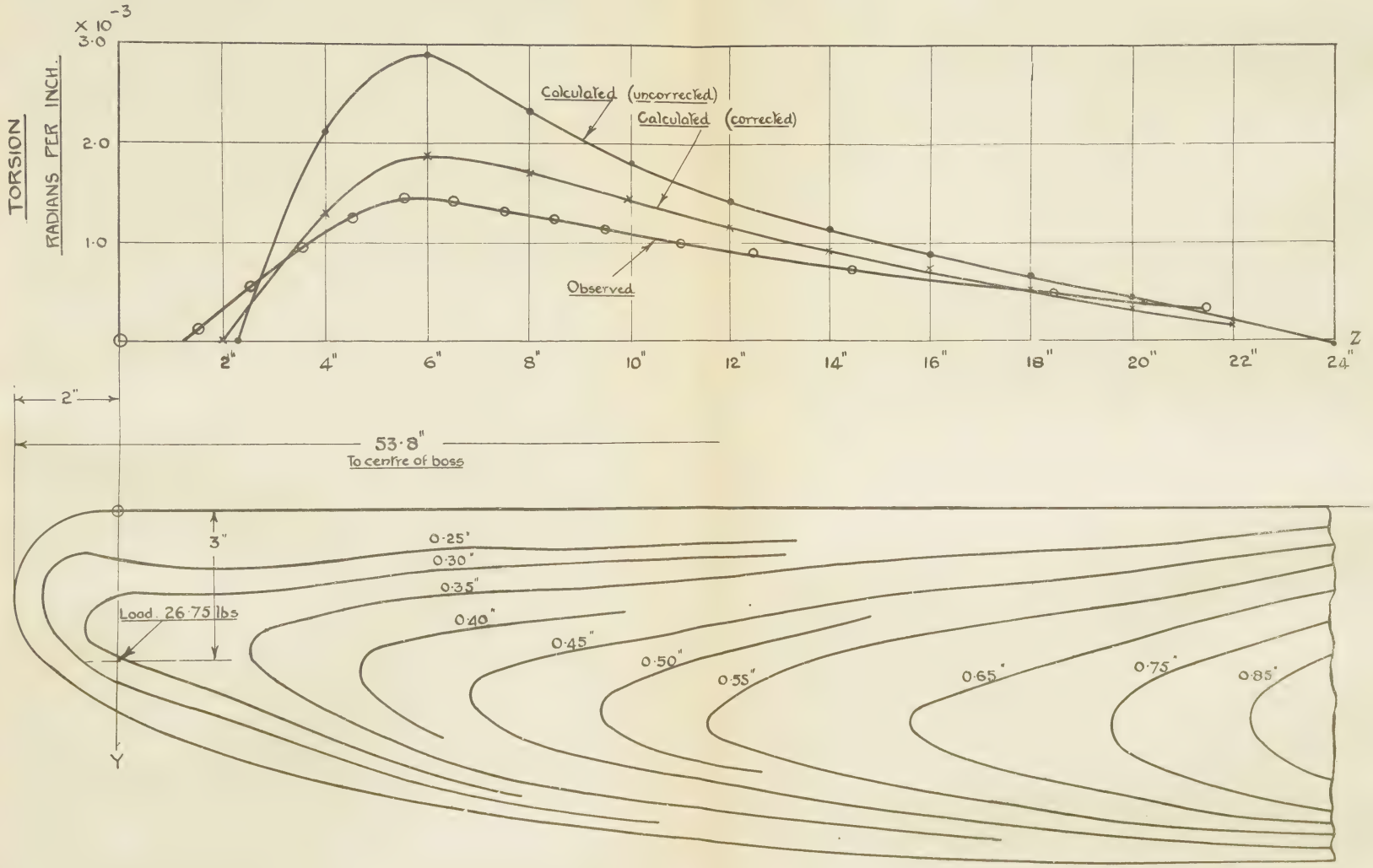

DEVELOPED PLAN VIEW WITH CONTOUR LINES OF THICKNESS.

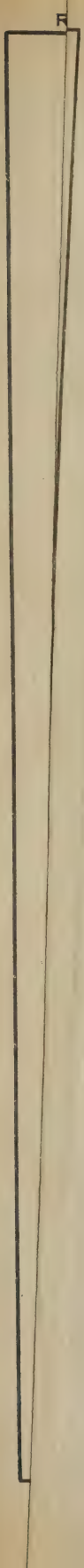
R

TORSION CURVES OF PROPELLER S.E.5. (DRG 28086).

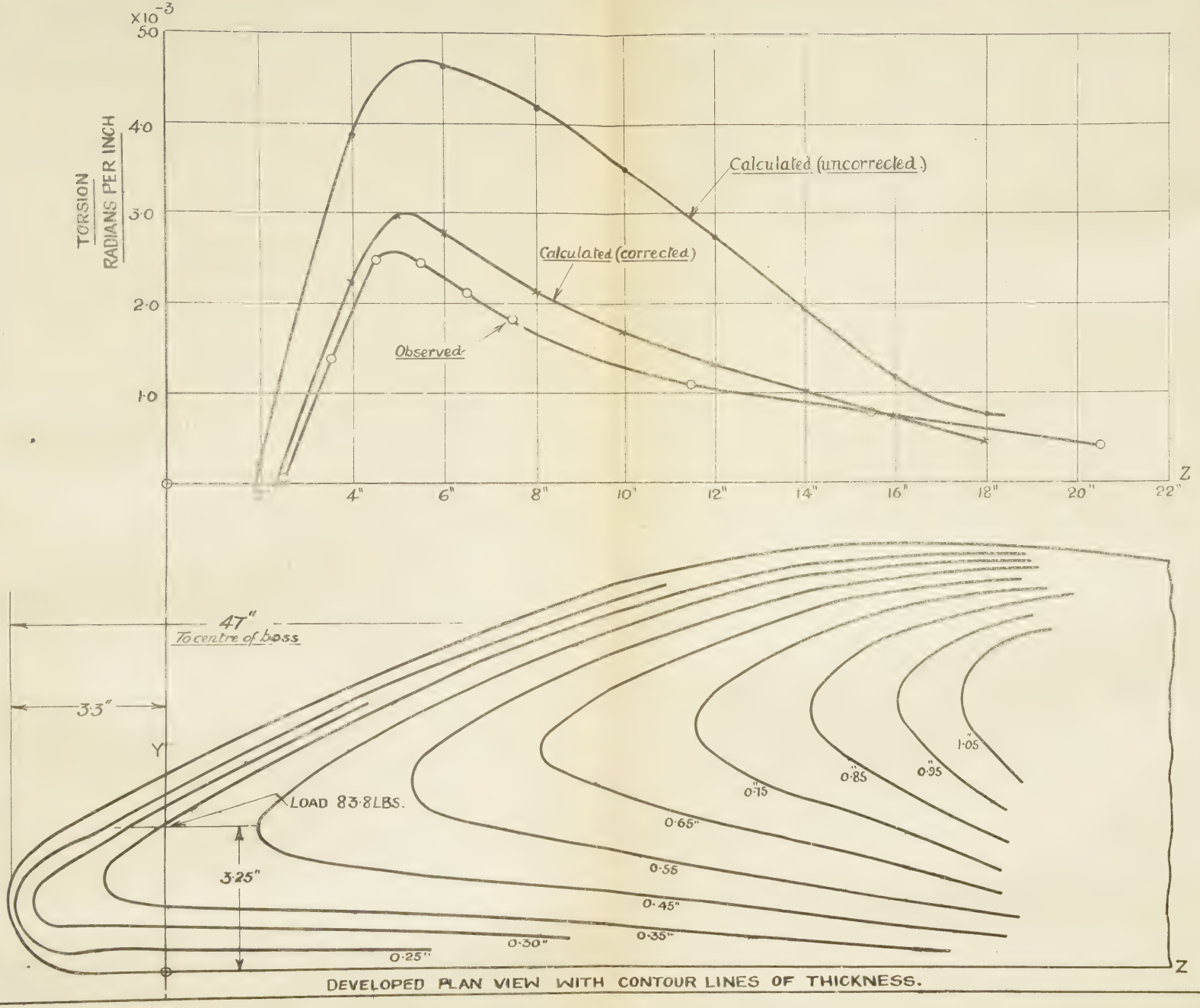

DEVELOPED PLAN VIEW WITH CONTOUR LINES OF THICKNESS.

C
D
H
E
G
F
A
B

THE LIBRARY
OF THE
UNIVERSITY OF ILLINOIS

GENERAL ARRANGEMENT OF SPHEROMETER.

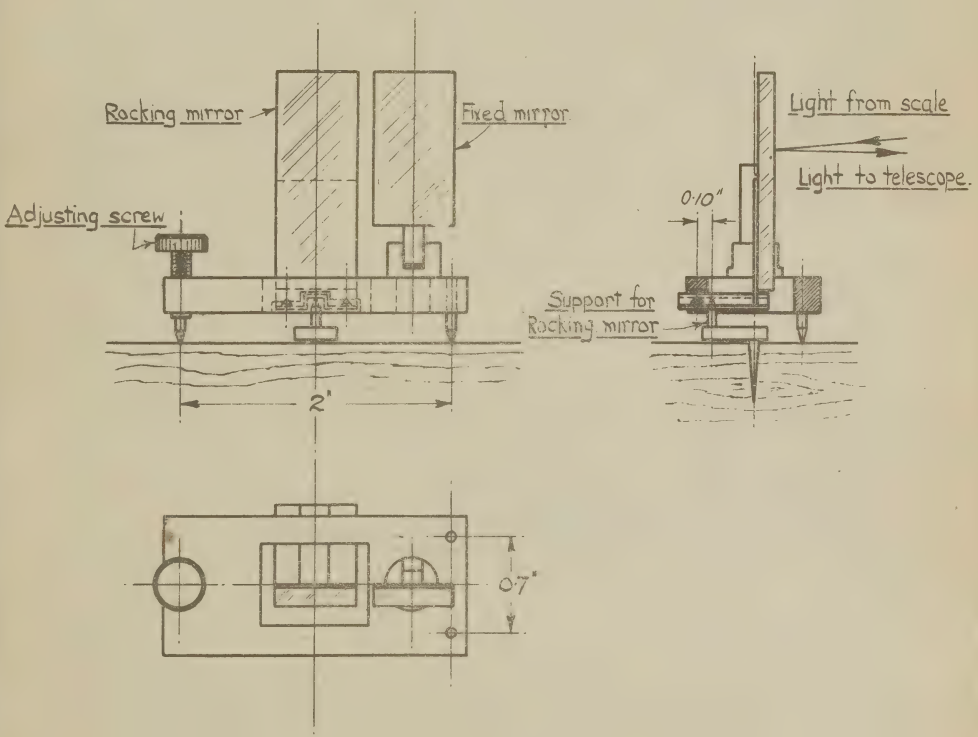

OBSERVED TWIST CURVES FOR PROPELLER B.E.2C. (THRUST-METER).

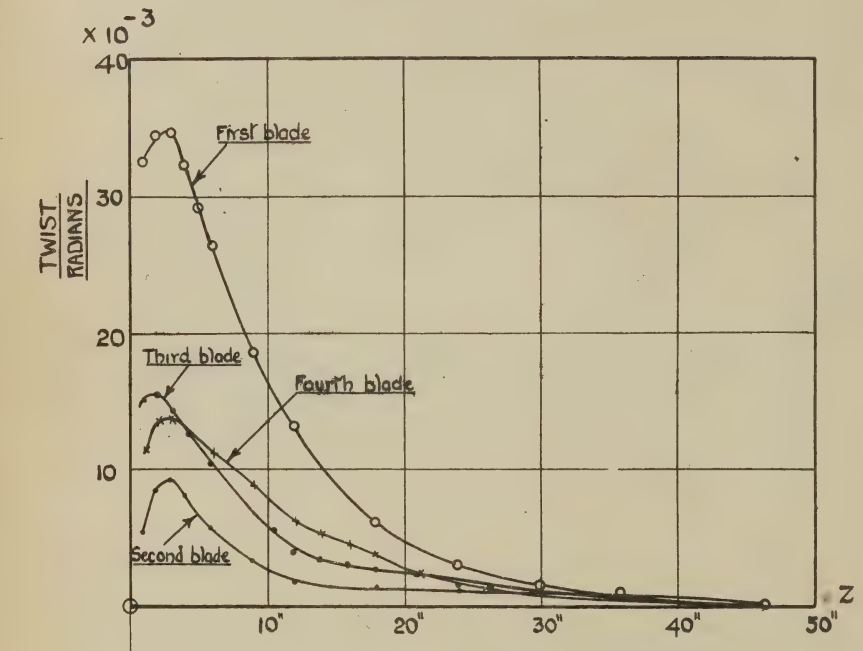

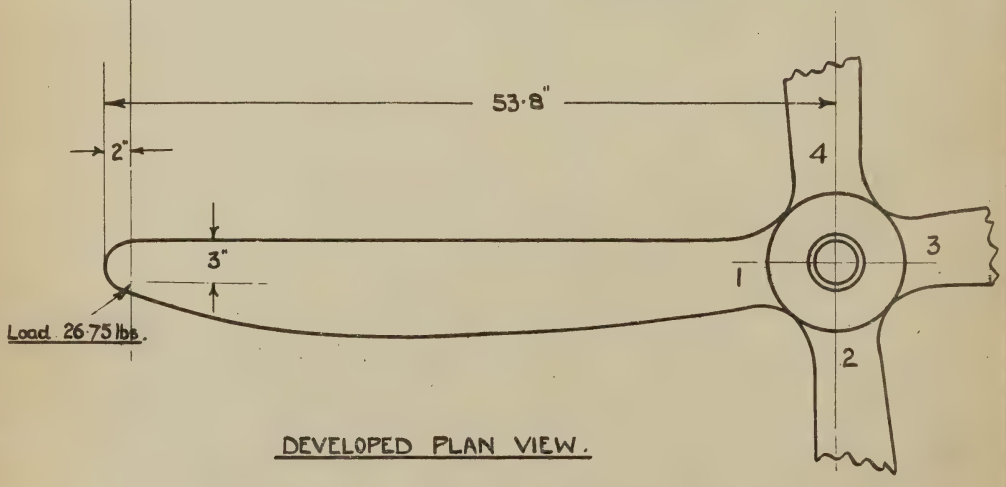

DEVELOPED PLAN VIEW.

OBSERVED TWIST CURVES FOR PROPELLER S.E.5. DRG.T.28086.

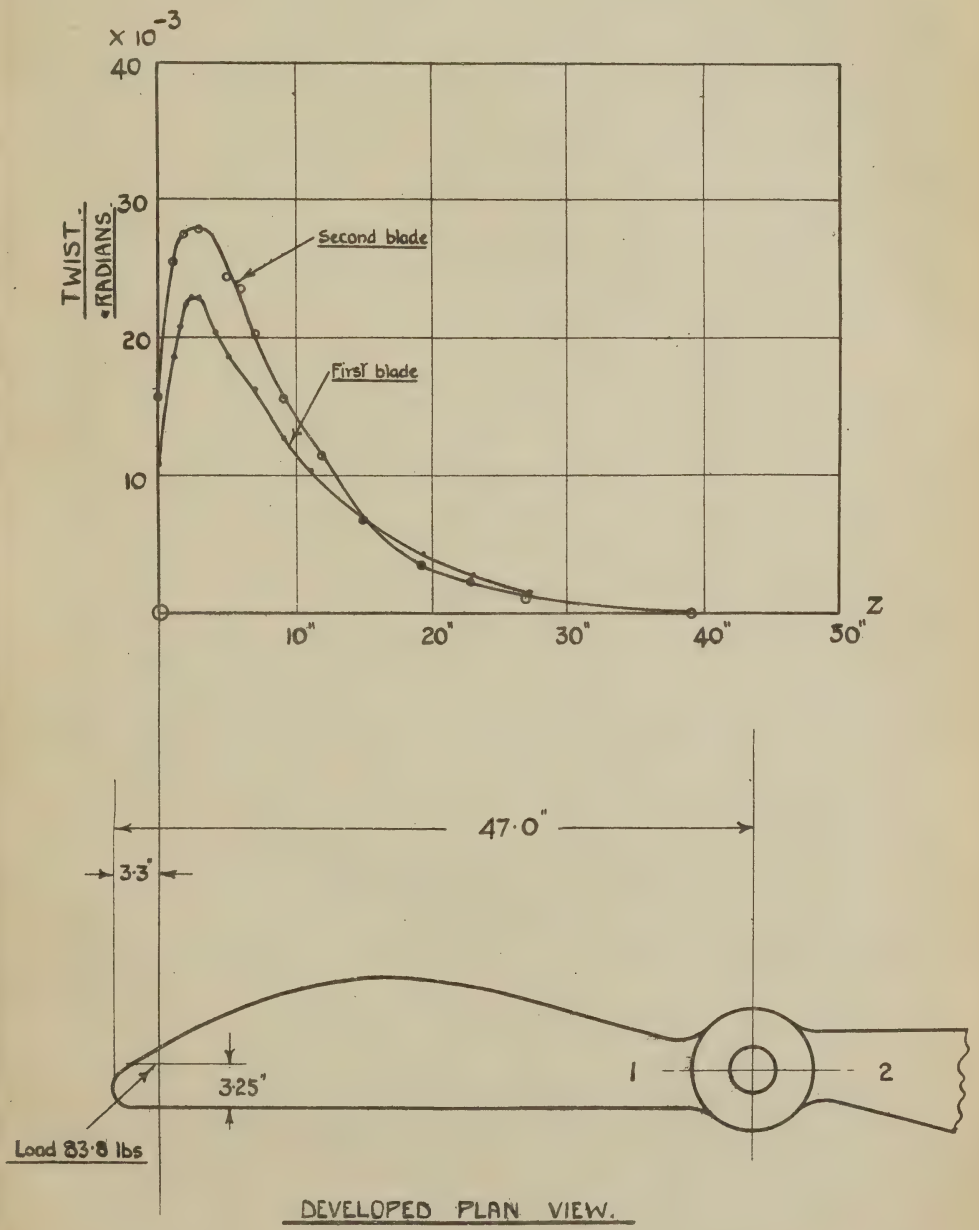

DEVELOPED PLAN VIEW.

OUT-OF-BALANCE TWIST CURVE OF PROPELLER FE.2D. (DRG. T 28020) UNDER AIR-LOAD.

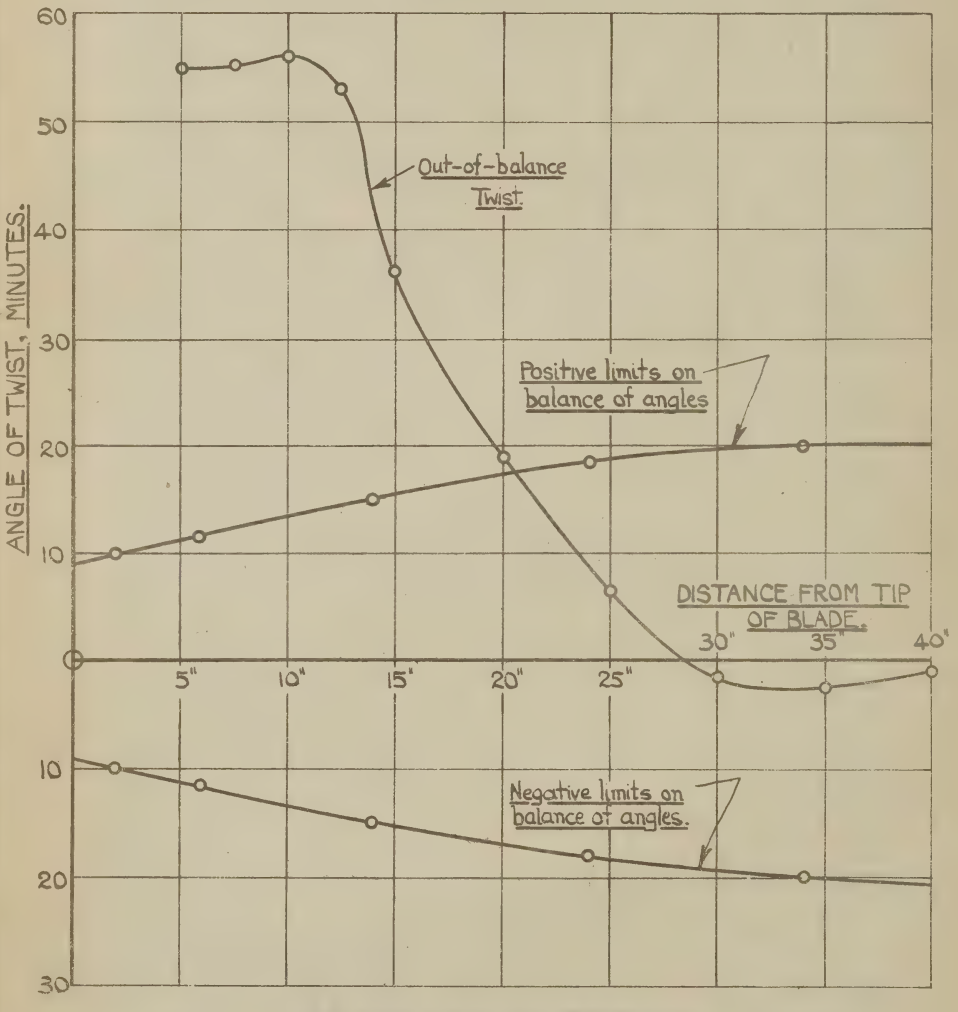

AIR-LOAD = 200 LBS PER BLADE.

CALCULATED TWIST CURVE FOR PROPELLER SE.5 (DRG. T28086).

UNDER AIR-LOAD.

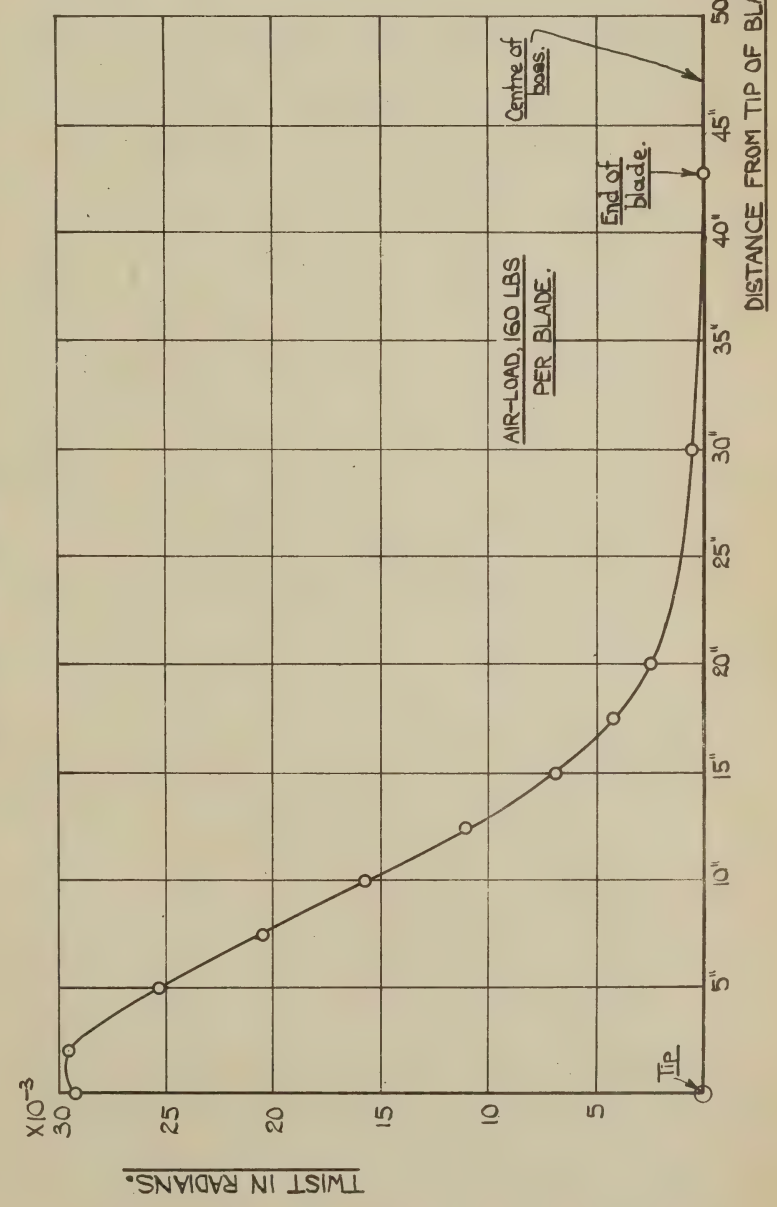

DIAGRAM ILLUSTRATING THE MATHEMATICAL

APPENDIX.

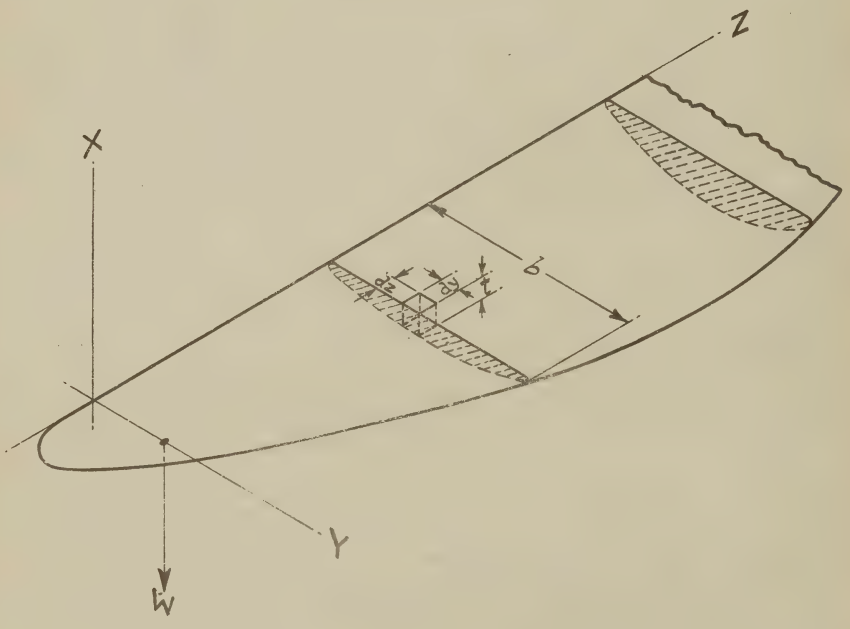

TABLE 9.

CALCULATED TWIST CURVE FOR PROPELLER S.E.5 (DRAWING T.28086) UNDER AIR-LOAD; FIG. 11.

Distance from Tip of Blade. (Inches.)	Twist in Radians $\times 10^{-3}$
0	29·3
2·5	29·5
5·0	25·2
7·5	20·5
10·0	15·9
12·5	11·1
15·0	7·1
17·5	4·2
20·0	2·5
30·0	0·5
42·75	0

SECOND REPORT ON THE TWISTING OF PROPELLER BLADES.

(Supplementary to R. & M. 454.)

By A. A. Griffith, M.Eng., and B. Hague, B.Sc.

Submitted by the Superintendent, Royal Aircraft Factory.

Reports and Memoranda, No. 455. *February,* 1918.

Summary.—The method of investigating the twist of propeller blades, which was developed in R. & M. 454, is interpreted mathematically by making a certain assumption as to the shape of the cross-sections. A general equation expressing the twist as a function of the radius is obtained, and an experimental method of solving it is evolved.

It is shown that blades of certain shapes may be peculiarly liable to torsional vibration, and that a plan form common in current practice possesses this property to an appreciable degree. It is further shown that the maximum stress due to torsion may determine fracture in this case.

A method of calculating the shape of plan form in any given case, in order that the blade shall not twist, is deduced, and it is shown that this leads to a nearly symmetrical form in one instance.

The effect of the large torsional hysteresis of timber in damping out vibrations is discussed, and it is suggested that herein may lie the reason for the comparative failure of metal propellers up to the present.

Finally, suggestions are made for the modification of current practice in accordance with the indications of the present theory.

1. *Statement of the Problem.*—In a previous report to the Committee (R. & M. 454) an approximate method of dealing with the problem of the twisting of propeller blades was discussed, and it was shown that it yielded results in fair agreement with those of actual experiments.

The application of this method involved a large amount of graphical work. In the present paper it will be shown that most of the latter can be eliminated and differential equations obtained, which express the torsion as a function of z only, by making certain assumptions regarding the shape of the cross-sections, which are substantially justified in the case of actual blades.

2. *Mathematical Analysis.*—The notation is the same as that used in R. & M. 454, save that $\dot{\gamma}$ is substituted for Y, the y-co-ordinate of the centroid of the curve of t^3, at any section.

In addition, however, to the relations

$$\left.\begin{aligned} \int \frac{t^3}{12}\,dy &= \mathrm{I} \\ \int y.\frac{t^3}{12}\,dy &= \mathrm{I}.\dot{\gamma} \\ \int y^2.\frac{t^3}{12}\,dy &= \mathrm{I}.k^2 \end{aligned}\right\} \quad . \quad . \quad . \quad (1)$$

we shall put

the integrations being taken over a section, z = constant.

It will be assumed, besides the hypotheses made in T.1075, that the blade thicknesses can be represented in the form

$$\frac{t^3}{12} = \frac{\mathrm{I}}{b} \cdot \chi\left(\frac{y-\gamma}{b}\right) \quad . \quad . \quad . \quad (2)$$

where χ is any functional form independent of z, and it will also be assumed that the values of t^3 at the edges of the blade are sufficiently small to be neglected. These are fair assumptions in the case of propellers at present in use.

In its simplified form, the equation which represents the displacement, u, of the neutral surface of the blade, is

$$\mathrm{E}\frac{\partial^2}{\partial z^2}\left(\frac{t^3}{12}\cdot\frac{\partial^2 u}{\partial z^2}\right) - 4\,\mathrm{N}\frac{\partial^2}{\partial y\,\partial z}\left(\frac{t^3}{12}\cdot\frac{\partial^2 u}{\partial y\,\partial z}\right) \quad . \quad (3)$$

In deducing this equation, it was assumed that the stress couples and stress resultants acting on the elements of the blade could be expressed in terms of t and u by means of the relations which are valid in the case of plates of uniform thickness. It is known that this involves an approximation, though means are not yet available for finding accurately the extent of the deviation of equation (3) from the truth. An attempt was made in R. & M. 454 to estimate the deviation in the case of the torsional couples on the assumption that the distortion of the cross-sections was the same as in uniform torsion, when it was found that the error might reach 10 to 15 per cent. in important cases. These are probably outside figures, as it is almost certain that the actual distortion of a tapering blade must be less than that of a cylindrical one.

The assumption made in developing the graphical method of R. & M. 454, from this equation, was that $\frac{\partial^2 u}{\partial y\,\partial z}$ or τ was independent of y. The mathematical consequences of this assumption will now be examined.

We have

$$\frac{\partial^2 u}{\partial y \partial z} = \tau \quad . \quad . \quad . \quad . \quad (4)$$

hence

$$\frac{\partial u}{\partial z} = \tau y + \psi(z) \quad . \quad . \quad . \quad (5)$$

where ψ is independent of y, substituting in (3)

$$E \frac{\partial^2}{\partial z^2} \cdot \left\{ \frac{t^3}{12} \left(y \frac{d\tau}{dz} + \frac{d\psi}{dz} \right) \right\} - 4N \frac{\partial^2}{\partial y \partial z} \left(\tau \cdot \frac{t^3}{12} \right) + P = 0 \quad . \quad (6)$$

Integrating the terms of this equation over the surface of the blade, from the tip to the section $z =$ constant, we see that the term in P becomes the resultant shear force on the section, that is, it is equal to $-\frac{dM}{dz}$ where M is the bending moment on the blade.

In performing the integrations it is to be noted that

$$\frac{\partial}{\partial z} \left(\frac{t^3}{12} \right) = \chi \left(\frac{y - \gamma}{b} \right) \cdot \frac{d}{dz} \left(\frac{I}{b} \right) + I \frac{\partial}{\partial z} \left(\frac{y - \gamma}{b} \right) \frac{d\chi}{dy} \quad . \quad (7)$$

and that, in the terms which are integrated by parts, the "integrated" terms vanish, since t^3 is zero at the edges.

We find

$$E \frac{d}{dz} \left\{ I \left(\dot{\gamma} \frac{d\tau}{dz} + \frac{d\psi}{dz} \right) \right\} = \frac{dM}{dz}$$

or

$$\frac{d\psi}{dz} = \frac{M}{EI} - \dot{\gamma} \frac{d\tau}{dz} \quad . \quad . \quad . \quad (8)$$

whence ψ is known.

Now multiply (3) by y and integrate as before. The term containing P is now the moment of the forces acting on the section, about oz. In addition to the points referred to above, it will be observed that $k^2 - \dot{\gamma}^2$ is independent of the origin of y and that $(k^2 - \dot{\gamma}^2)/b^2$ is a constant depending on χ only.

Calling T the couple resultant due to the stresses on the section, we have, as the final result,

$$\frac{d}{dz} \left(M\dot{\gamma} + EI(k^2 - \dot{\gamma}^2) \frac{d\tau}{dz} \right) + 4NI\tau = T \quad . \quad (9)$$

The quantity

$$T - \frac{d}{dz}(M\dot{\gamma}) \quad . \quad . \quad . \quad (10)$$

depends only on the applied load and the shape of the blade. It may be found directly by multiplying the resultant shear force on the section by the distance between its line of action

and the principal flexure point (*see* T.1075). The distance of the latter point from *oz* is, of course,

$$\frac{d}{dz}(\mathrm{M}\,\dot{\gamma}).\frac{d\mathrm{M}}{dz} \quad . \quad . \quad . \quad . \quad (11)$$

Putting

$$\left.\begin{aligned} \mathrm{T} - \frac{d}{dz}(\mathrm{M}\,\dot{\gamma}) &= b \\ \mathrm{E\,I}\,(k^2 - \dot{\gamma}^2) &= \mathrm{Q}^2 \\ 4\,\mathrm{NI} &= \mathrm{R} \end{aligned}\right\} \quad . \quad . \quad (12)$$

we see that (9) becomes

$$\mathrm{Q}^2\frac{d^2\tau}{dz^2} + 2\mathrm{Q}\frac{d\mathrm{Q}}{dz}\cdot\frac{d\tau}{dz} + \mathrm{R}\tau = \mathrm{G} \quad . \quad . \quad (13)$$

Put $\mathrm{U} = \tau\,\mathrm{Q}$ then (13) reduces to

$$\mathrm{Q}\frac{d^2\mathrm{U}}{dz^2} + \left(\frac{\mathrm{R}}{\mathrm{Q}} - \frac{d^2\mathrm{Q}}{dz^2}\right)\mathrm{U} = \mathrm{G} \quad . \quad . \quad (14)$$

Since the coefficients of this equation are all functions of z, its direct analytical solution presents considerable difficulties, but a certain amount of useful general information may be drawn from it. This will be referred to later.

It will be noted, however, that the coefficients depend only on the shape and size of the cross-sections of the blade, and that the independent term, G, depends only on the shape of the plan form and the nature of the load. Hence, if we have one plan form, A, given, such that the couples on it are G when it is subjected to the air load, then we can find another plan form, B, on which the couples are also G when it is bent by a single load, W, applied at the tip. Further, we can adjust the cross-sections of blade B so that its coefficients in (14) are the same as those of blade A. It follows that the twist curves of the two blades in these circumstances are identical. It will be shown subsequently that this can be made the basis of a simple experimental method of finding the twist of propellers under their air-load.

If the values of Q and R are given, it is possible to find the shape of the plan form which the blade must have in order that it shall not twist.

Let the centre of pressure of the air-load acting on a portion of the blade bounded by planes $z =$ constant, separated by a small distance δz, be at a distance c from the centroid of the t^3 curve of this portion, that is, let the y-co-ordinate of the centre of pressure be $c + \dot{\gamma}$. Then, from (13) the condition for zero, τ, is

$$\frac{d^2}{dz^2}(\mathrm{M}\,\dot{\gamma}) = (\dot{\gamma} + c)\frac{d^2\mathrm{M}}{dz^2} \quad . \quad . \quad . \quad (15)$$

where c is independent of $\dot{\gamma}$, if it be assumed that the air-load distribution is not altered by changing the shape of the plan form.

Integrating this equation, we find

$$\dot{\gamma} = \int \frac{1}{M^2} \int c\,M \frac{d^2M}{dz^2}\,dzdz \quad . \quad . \quad . \quad (16)$$

the first constant of integration being zero if the integration be started from the tip of the blade, and the second merely additive and therefore of no importance.

From (16) the curve of $\dot{\gamma}$, and hence the developed plan form, may be set out in its proper relation to the direction of the grain (axis of z).

3. *Application of the Mathematical Work.*—In equation (14) the terms in U and $\frac{d^2U}{dz^2}$ may be either of the same or opposite sign. In the former case the torsion due to the couple G is less than would have been obtained on the old theory, that is to say, the effective torsional stiffness is increased by the term in $\frac{d^2U}{dz^2}$. In the latter case the reverse is true, and if at any point the two terms should happen to be nearly equal numerically, then the effective stiffness may be very small indeed and hence a local region of very high stress is to be expected. It is also evident that a blade containing regions of this sort must be very much more susceptible to torsional vibrations than one which does not contain such regions.

Although it is difficult to solve (14) directly, yet the interest attaching to the shape of the torsion curve, more especially in view of the above observation, is so great that some method of finding it would appear to be essential to progress in design. This might be done experimentally by loading an actual blade with sand or shot in such a way as to approximate to the air-load. Naturally, this method presents considerable difficulties. We may, however, find the same twist curve experimentally by constructing another blade, whose plan form is determined from the original one by the method explained in the analytical section, and loading it with a single load at the tip. The method consists simply in adjusting the shapes of the two blades so that the equations (14) representing their torsions are identical in these different conditions of loading.

It will be seen that the technical details may be further simplified by making the sections of the auxiliary blade rectangular, since their shape is immaterial, provided that the quantities Q and R are fixed. Again, the auxiliary blade may be made on any convenient scale, and one piece of wood only need be used in its construction. Hence, from every point of view, it is far more probable that the indirect experiment will give an average result, representative of a uniform blade, than it is that such a result would be obtained by the direct method.

Another point worthy of note is that the true values of Q and R which should be used in equation (14) are greater than those given by relations (12) by an unknown amount, on account of the tapering of the blades. It is probable, in view of the nature of this factor, that these quantities are also greater in the case of the auxiliary blade by approximately the same amount.

Fig. 1 shows the twist and torsion curves of the S.E. 5 two-blader propeller dealt with in R. & M. 454, obtained by means of an auxiliary blade in the manner described above. The maximum twist is about 1·5°, and it occurs at the tip of the blade. As was generally anticipated, the twist is only important in the part between the tip and a point halfway between the tip and the centre of the boss.

On the assumption that the shear stresses due to torsion and bending are the same as they would be in a cylindrical bar under uniform torsion and a concentrated load respectively, the maximum total shear stress, in the directions yz, works out at 380 lbs. per sq. in. at a point 13 inches from the tip.

The effect on the torsion of variations in the value of E, such as are known to be possible, has been estimated, and it has been found that if the modulus vary uniformly with y, in such a way that the leading lamination is 1·8 times as stiff as the trailing one, then the maximum shear stress may be as much as 500 lbs. per sq. in.

These figures are certainly below the truth on account of the neglect of the unknown factors due to taper. It is improbable that these involve an additional stress of less than 100 lbs. per sq. in., and it is quite possible that their effect may be much greater.

Reliable figures relating to the shear strength of walnut under various types of loading have yet to be obtained. Some simple torsion experiments have been made which seem to indicate that the ultimate strength of walnut in this respect is not much greater than 2,000 lbs. per sq. in. under a unidirectional torque applied for about fifteen minutes only. Under a steady torque, applied for an indefinite period, it may be little more than half as much. Regarding the effect of vibration on the ultimate strength nothing whatever is known.

In the foregoing investigation no account is taken of the possible effect of vibration in raising the maximum stress. When this is allowed for it becomes highly probable that blades of the form under discussion are not over-designed even on the basis of ultimate strength.

At present it is usual to design propellers on the basis of the greatest longitudinal tension. It is known, however, that in propeller bursts tension failures are comparatively rare. In view of the present figures this is not surprising, and it is evident that the method of designing for maximum tension, without reference to the shape of the plan form, is inadmissible.

Fig. 2 shows the curve of U (equation 14), obtained from the experimental torsion curve of Fig. 1, for the important part of the blade. It will be seen from the form of (14) that the value of U at any place where the curve has a point of inflection should be equal to $QG/\left(R - Q \cdot \frac{d^2Q}{dz^2}\right)$. The dotted curve of Fig. 2 shows the latter quantity for all points along the blade. It will be seen that it cuts the curve of U very nearly at the points of inflexion of the latter. In calculating R, allowance has been made for the probable value of the factor due to taper. This only amounts to 5 to 10 per cent. at most parts of the curve, and therefore does not affect the general nature of the result.

At points where the U curve lies above the dotted one $\frac{d^2U}{dz^2}$ and U are of opposite signs, and hence these are portions where undue susceptibility to torsional vibrations exists. It is unfortunate that there is, in this type of blade, a well marked region of this sort in the neighbourhood of the section where the maximum stress occurs. This is evident from the diagram; in fact the torsion at the section of maximum stress is about 1·8 times as great as the value which would have been obtained if $\frac{d^2U}{dz^2}$ had been neglected.

The most satisfactory way of avoiding these sources of trouble is to choose the plan form in such a way as to make the twist as small as possible. If U is small and of the first order, then $\frac{d^2U}{dz^2}$ is a small quantity of the third order, that is, it is of the second order compared with U and hence can never be important.

Equation (16) of the mathematical discussion determines the shape of plan form of any blade in order that it shall not twist.

This equation has been applied to the blade examined above, and the resultant developed plan form is shown in Fig. 3. The dotted curve shows the present form of blade. It will be seen that the shape given by (16) is much more nearly symmetrical than the original blade. The axis of z represents, of course, the general direction of the grain.

The effect of possible variations in the value of E has been investigated in this case also, and it has been found that with the same variation as before the maximum shear stress could only be about one-fifth of its value in the previous case.

4. *The Damping of Torsional Vibrations in Propeller Blades.*—Another report to the Committee (R. & M. 528) gives an account of some torsion experiments on wood which indicate that a very large amount of hysteresis must accompany any torsional vibrations of wooden members. It is suggested that this hysteresis may be responsible for most of the damping of such

TORSION OF A PROPELLER BLADE UNDER AIR LOAD.

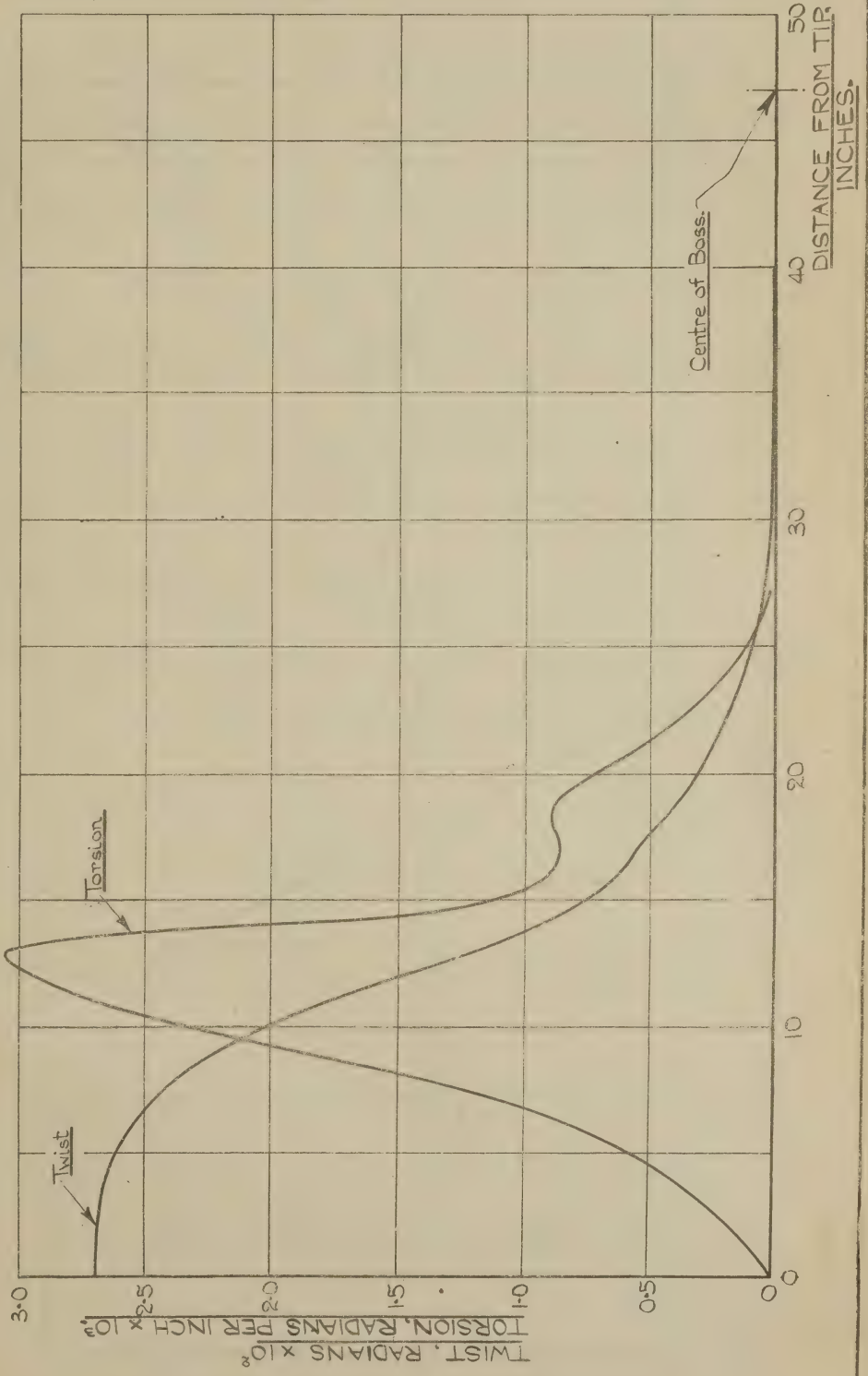

TORSION OF A PROPELLER BLADE UNDER AIR LOAD.

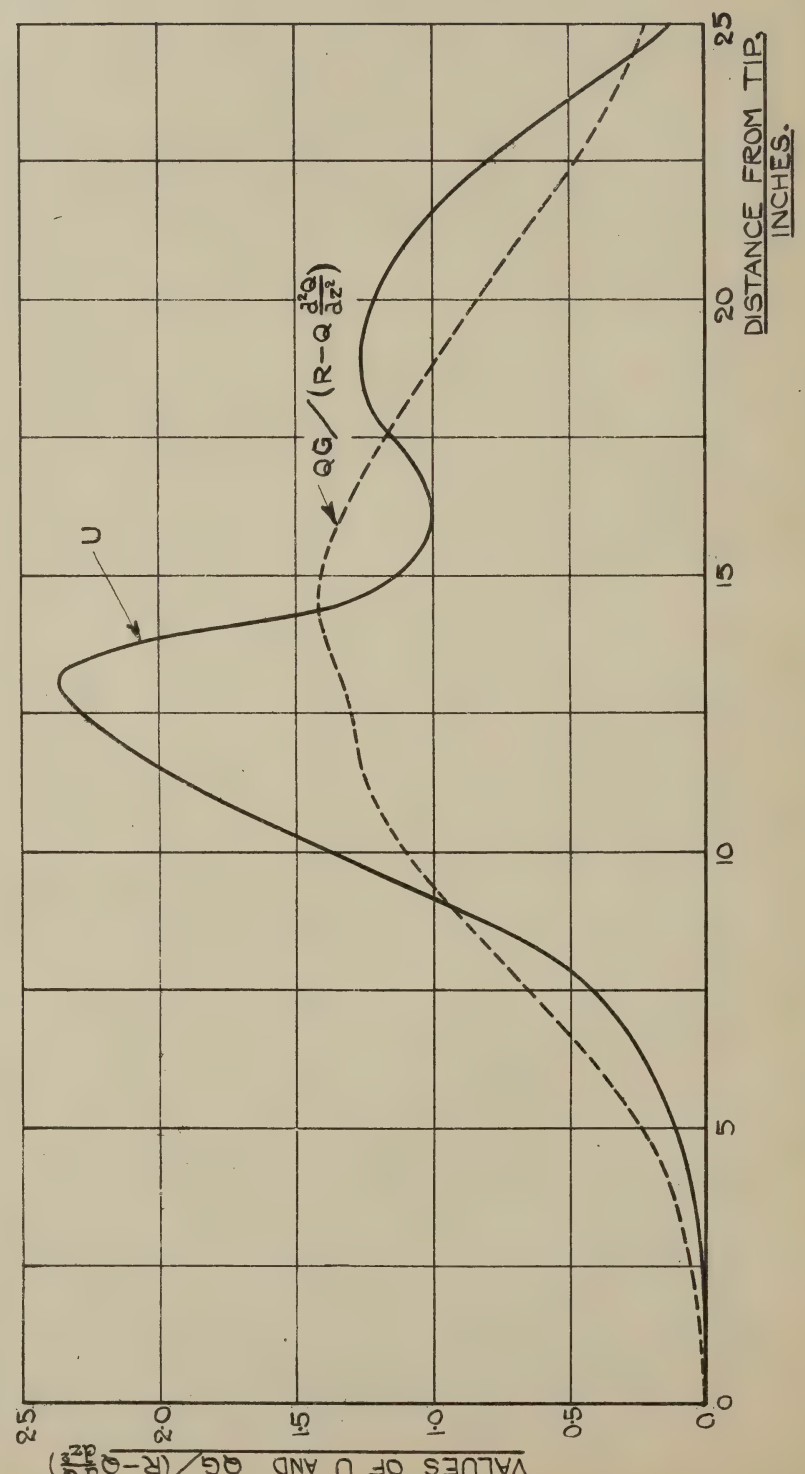

DEVELOPED PLAN FORM OF BLADE HAVING ZERO TORSION.

THE DOTTED CURVE SHOWS THE PRESENT PLAN FORM.

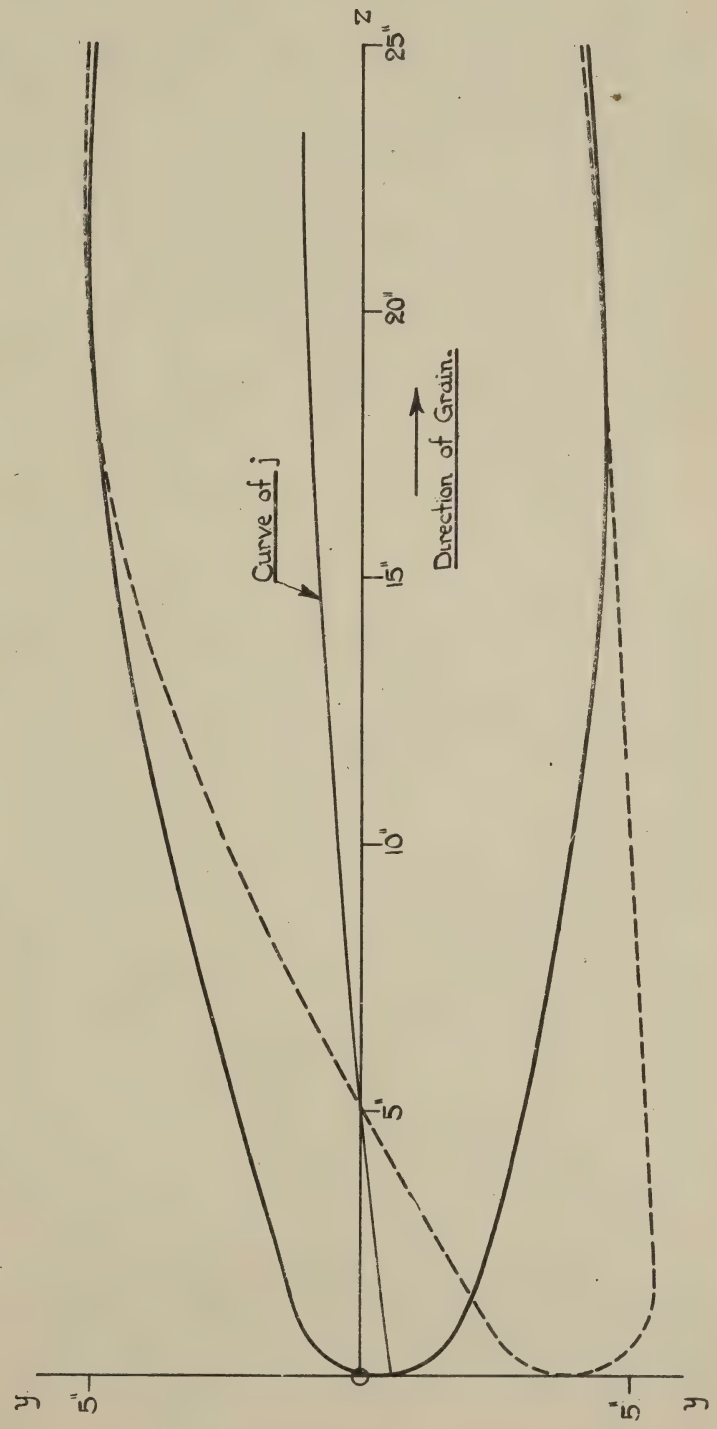

THE LIBRARY
OF THE
UNIVERSITY OF ILLINOIS

vibrations in the case of air propellers, and therefore may be one of the most valuable properties of propeller timber.

There is, in fact, a certain amount of evidence to show that the damping due to the air forces alone is insufficient in the very severe vibration conditions which subsist on aircraft. If a blade twist so as to reduce the angle of incidence (which is the direction usual with present plan forms) two things happen. In the first place the air-load is decreased, and in the second the centres of pressure move towards the trailing edge. These effects tend respectively to decrease and increase the couple G, and hence the damping moment due to them may be either positive or negative according to the shape of the plan form, or it may be positive in some places and negative in others.

More direct evidence is provided by the numerous attempts to make metal propellers. So far, none of these have been successful from the point of view of strength, although the metal construction is theoretically as strong as the wooden one on the basis of direct tension, and almost certainly considerably stiffer torsionally.

This would appear to indicate that in these cases, where damping due to elastic hysteresis must be practically negligible until the elastic limit is reached, the air-damping is insufficient to keep the torsional vibrations within safe limits.

As further evidence on this point, it may be noted that all-metal propellers have been known to fail at the boss, whereas propellers with wooden blades and metal bosses of the variable pitch type have stood up successfully.

If this should prove to be the true explanation, it implies that metal is an unsuitable material for propeller blades unless the air-damping can be largely increased by a suitable modification of the plan form and cross-sections, or unless the cyclic variations of engine torque can be largely reduced.

5. *Application to Design.*—It is suggested that the matter dealt with in this report and in R. & M. 454 points to the following as being desirable modifications in propeller practice, in the order of their probable importance :—

(1) Adoption of the shape of developed plan form given by equation (16) above.

(2) Adoption of some method of grading timber according to the value of its Young's modulus, as detailed as practical considerations will permit.

(3) Use of machine shaping in preference to hand work wherever possible in order to secure uniformity in the blade sections, since it is impossible to predict the twist curve of a blade unless the shapes of its sections are known accurately.

(4) Replacement of the electric drive usual in bursting and other propeller tests by an arrangement more nearly representative of the vibration conditions which obtain on aircraft engines. It may be noted, in this connection, that little information can be obtained, regarding the strength of propellers under flying conditions, from a test in which the motor is almost ideally free from vibration, since actual bursts on service, in the great majority of cases, occur on engines in which vibration is particularly noticeable.

(5) Introduction of some simple torsional vibration experiment into propeller timber inspection routine in order to obtain a figure for its damping efficiency.

(6) Use of two-bladers in preference to four-bladers whenever other circumstances permit.

The advisability of this course arises from the circumstance that it is much easier to get elastic balance, and the consequent comparative freedom from noise and vibration, in two-bladers than in four-bladers.

6. *Values of Section, Moduli, &c.*—The following figures, representing average values for the quantities used in the mathematical work, may be found useful in applying it to actual blades :—

b = blade width.

t_m = max. thickness of section.

Distance of centroid of t^3 curve from trailing edge = $0{\cdot}59\ b$.

$I = 0{\cdot}0434\ b^3 \cdot t_m^3$.

$R = 4\ NI$.

$Q = 0{\cdot}189\ b\ \sqrt{EI}$.

(E = Young's Modulus. N =Modulus of rigidity.)

THE VARIABLE PITCH PROPELLER—EXPERIMENTS CONDUCTED AT THE ROYAL AIRCRAFT FACTORY.

Presented by the SUPERINTENDENT of the Royal Aircraft Factory.

Reports and Memoranda, No. 402. *January,* 1918.

SUMMARY.—(*a*) *Introductory—(Reasons for inquiry).*—It is evident that some improvement in performance can be made by the use of a propeller of variable pitch, and it was desired to find the extent of this and to investigate the mechanical difficulties of the problem.

(*b*) *Range of investigation.*—A variable pitch propeller was designed and made at the Royal Aircraft Factory and fitted to a B.E.2.C., R.A.F. 1A., 100 h.p. engine. This propeller has been tested for strength on a testing tower and for performance and details of operation in flight, and compared with standard and special climbing propellers.

(*c*) *Conclusions.*—The variable pitch propeller can be made a satisfactory mechanical job for this power and speed of revolutions, and can be operated satisfactorily. It outclimbs and outdives the standard propeller and gives greater speed than the climbing propeller at all speeds above the climbing speed.

(*d*) *Applications and further developments.*—Such an improvement in performance is undoubtedly worth the small extra cost of construction.

Variable pitch propellers might also be used for brake purposes.

1. The most important criterion of performance of a fighting aeroplane is a compromise between rate of climb and speed at a height of about 15,000 ft. Reports T. 930 and 930a on "The design of aeroplanes for use at great heights" discuss the possible ways in which improvement in this performance should be sought apart from the improvement of the engine. The conclusion arrived at is (*a*) that an improvement in climb can be obtained for a very small sacrifice of speed by increasing the wing area, but that this suffers from the serious drawback of causing a decrease in manœuvrability; and (*b*) improvement in design of the airscrew gives greater possibilities. If the airscrew be designed for maximum efficiency and to hold the engine on full throttle at the maximum permissible revolutions at the level speed of the aeroplane at the height under consideration, there will be a loss of power climbing due (*a*) to decreased revolutions and (*b*) to decreased efficiency. The propeller can be designed for maximum efficiency in climbing, when there will be a loss of efficiency if flying level, or for maximum revolutions in climbing when the

engine must be throttled at higher speeds. The calculations showed that some improvement in the performance of R.E. 8 at 15,000 ft. could be obtained by designing the propeller for that height. But whatever can be done by redesigning the propeller for any one condition and purpose can be very nearly obtained by a variable pitch propeller for all purposes and conditions. The performance with a variable pitch propeller will be the envelope of the performance curves of propellers designed for special purposes.

The speed of an aeroplane along a horizontal flight path is not of much greater importance than the speed along any other flight path, climbing or diving, and the advantage of the variable pitch is increasingly apparent as the angle of climb decreases through level flight to an angle of dive. It enables the full engine power to be used on a steep dive without excessive engine revolutions.

2. Performances can best be compared on a diagram of rate of climb plotted against speed. The attached figures (1) to (3) show such curves. It will be seen generally that the use of a climbing propeller, allowing the engine to run at maximum revolutions at climbing speed, involves a serious loss of speed on the level, and still more when diving, on account of the power lost by throttling the engine down to the maximum permissible revolutions. Fig. 1 is drawn for (*a*) a theoretical variable pitch propeller for S.E. 5 at 10,000 ft.; (*b*) a theoretical "climbing" propeller; and (*c*) the Etoile propeller tested at the Royal Aircraft Factory. It will be seen that the variable pitch propeller gives the same speed as the Etoile but a greater rate of climb and higher speeds diving along a given flight path, because the full engine power can be used without excessive revolutions. The climbing propeller gives a slightly better maximum rate of climb, but much lower speeds.

3. These curves are based on curves obtained from experiments at the Royal Aircraft Factory on B.E.2.C. aeroplanes fitted with (*a*) a variable pitch propeller, (*b*) a propeller designed for climbing by allowing the engine to reach its maximum revolutions at climbing speed, and (*c*) a standard propeller (T. 7448). Figs. (2) and (3) exhibit the results of the experiments, assuming that the engine is allowed to run at 1800 and 1900 r.p.m. respectively. These are deduced from short climbs at various speeds, with various settings of the blades in the case of the variable pitch propeller. It was found for the variable pitch propeller that if the revolutions were left constant at 1,800 per minute, the thrust horse-power did not change appreciably from 50 to 100 m.p.h. It was also observed that with the gear at the limit of its adjustment on a steep dive the engine revolutions could be kept down to 1,650 r.p.m. at 115 m.p.h. The range of adjustment on the blades is 10°.

FIG. 1.

S.E. 5 WITH 170 HP. H.C. HISPANO.

RATE OF CLIMB AGAINST SPEED, AT 10.000 FT.

ESTIMATED FROM B.E.2.C. EXPERIMENTS.

A - WITH VARIABLE PITCH PROP. GIVING 2000 R.P.M. AT ALL SPEEDS

B - " CLIMBING PROP " " " " 63 M.P.H.

C - " ÉTOILE PROP " " " " 98½ M.P.H.

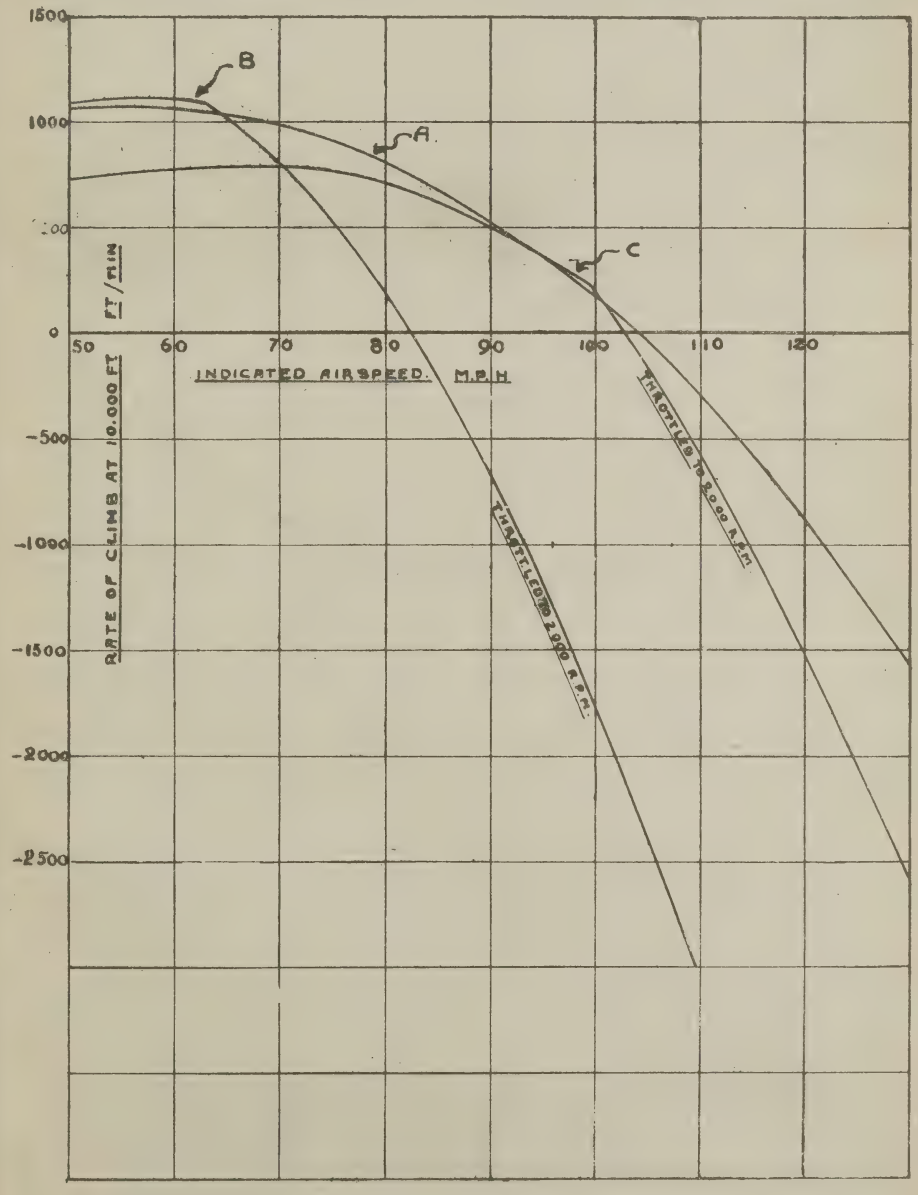

B.E.2.C. WITH R.A.F. I.A. ENGINE.

RATE OF CLIMB AGAINST SPEED, AT 10 000 FT.

A - WITH VARIABLE PITCH PROP. GIVING 1800 R.P.M. AT ALL SPEEDS.
B - " CLIMBING PROP T 2807.3 " " " " 51 M.P.H.
C - " STANDARD PROP T 7448 " " " " 98½ M.P.H.

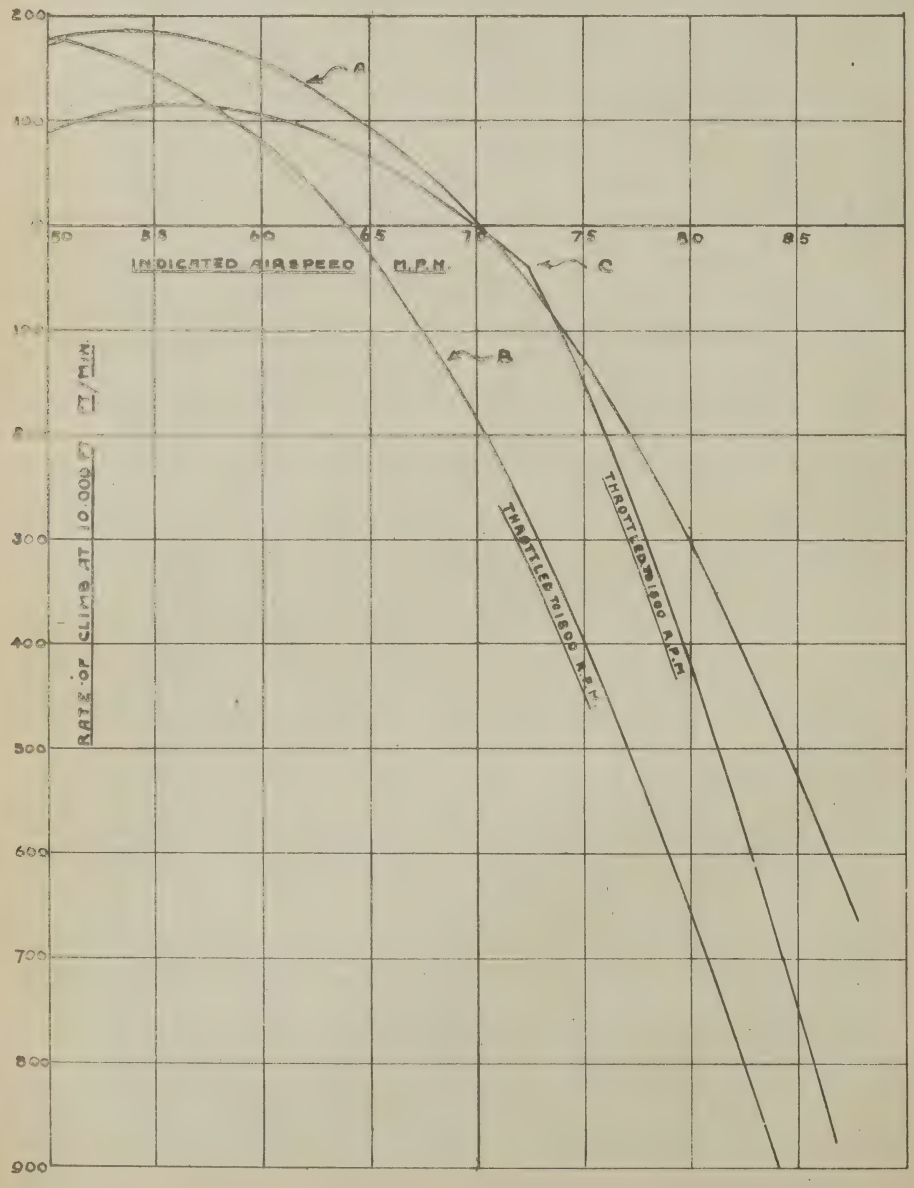

B.E.2.C. WITH R.A.F. 1A. ENGINE.

RATE OF CLIMB AGAINST SPEED, AT 10000 FT.

A. WITH VARIABLE PITCH PROP. GIVING 1900 R.P.M. AT ALL SPEEDS.
B. " CLIMBING PROP. T.28073 " " " " 51. M.P.H.
C. " STANDARD PROP. T 7448 " " " " 98½ M.P.H.

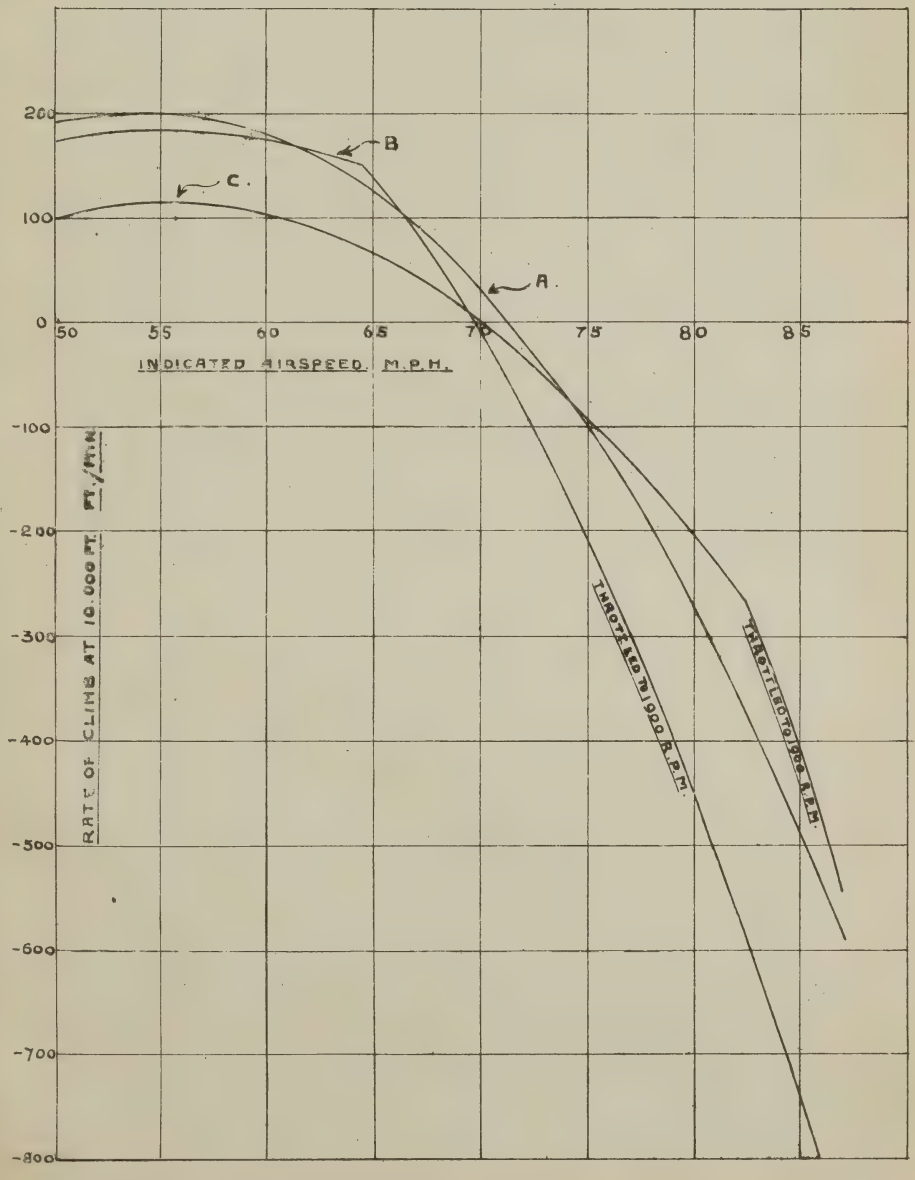

4. There can be little doubt about the aerodynamical advantage of the variable pitch propeller. These experiments show the magnitude of this advantage over a climbing and a speed propeller also designed at the Royal Aircraft Factory. The chief objections to the propeller are mechanical, but this experiment has shown that a variable pitch propeller can be designed for a 100 h.p. engine to run at 900 r.p.m. which shall be sufficiently strong and can be easily operated. The propeller has four wood blades bolted into split metal sockets which can be rotated through 10° in a metal boss by turning a handwheel in the pilot's cockpit. There has been no difficulty with the mechanical details. The propeller has been spun up to 1,100 r.p.m., taking 125 h.p. on the R.A.F. testing tower, has been also subjected to a duration test on the tower of one hour at 1,000 r.p.m. and 95 h.p., has been in flight some months, and is therefore sufficiently strong. It is the opinion of the Royal Aircraft Factory that no great difficulty will be experienced in designing a variable pitch propeller for 200 h.p. at 2,000 r.p.m. The increased weight of this propeller over the standard type is about 40 lbs. This, of course, is automatically taken account of in the performance curves.

5. Objection can be raised against the variable pitch propeller on the ground that it involves the use of a further control during a fight, and it is for fighting that the increased performance is most useful; but even if, as is probable, the pitch control would not be used during the actual encounter, it might prove very valuable for getting rapidly on to an enemy machine to attack it or to support another aeroplane either from above or below. The change of pitch would probably be more conveniently effected by a lever than by the low pitch screw and handwheel used in these experiments.

THE CONSTRUCTION OF THE R.A.E. EXPERIMENTAL VARIABLE PITCH AIRSCREW.

Presented by

THE CONTROLLER OF THE TECHNICAL DEPARTMENT, AIRCRAFT PRODUCTION.

Reports and Memoranda, No. 471. *April,* 1918.

SUMMARY.—(a) *Introductory* (*Reasons for Enquiry*).—This report, which is a description of the mechanism employed in the experiments already recorded in R. and M. 402, was written in response to a request from the Aerodynamics Sub-Committee.

(b) *Details of Design.*—The figures and drawing attached to the report indicate clearly the general design of both the airscrew itself and the hand control. Each blade, which was built up of walnut laminations in the usual manner, was held inside a split parallel steel shank by means of four bolts. These shanks were mounted radially in plain bearings with a ball thrust washer to take the centrifugal load, and were capable of rotation about their axes by the mechanism described. The weight of the airscrew complete with control gear was 85 lbs., being 50 lbs. heavier than the standard walnut tractor.

(c) *Conclusions.*—The tests show that such an airscrew can be constructed having ample strength. The most important deduction from these tests is probably the satisfactory method of attaching the metal shanks to the wooden blades. A considerable amount of backlash in the gear was experienced during the trials, but has since been almost eliminated.

(d) *Applications to future design.*—As an outcome of these experiments it was decided to design and build a two-bladed airscrew on the same principle for the direct driven Hispano-Suiza engine in S.E.5A. It is also suggested that this method of attaching wooden blades to metal shanks might well be employed on fixed pitch metal centre airscrews.

This propeller was designed for a B.E. 2c with R.A.F. 1A engine. It was fitted to B.E. 2c, No. 4122, for the experiments described in report R. & M. 402. Before flight it was tested on the spinning tower on both fine and coarse pitches taking 130 h.p. at 1,100 r. p.m. for 30 mins., and was easily operated under overload. The same casting and internal fittings except for the shanks E have since been tested on the spinning tower up to 330 h.p. at 1,050 r.p.m. for a period of 30 mins. The propeller is therefore amply strong. The weight without control gear is about 40 lbs. greater than that of the standard walnut propeller, T. 7448, which weighs 35 lbs. The control gear weighs about 10 lbs. It was found easy to operate in the air, though a lever control

FIG 1.

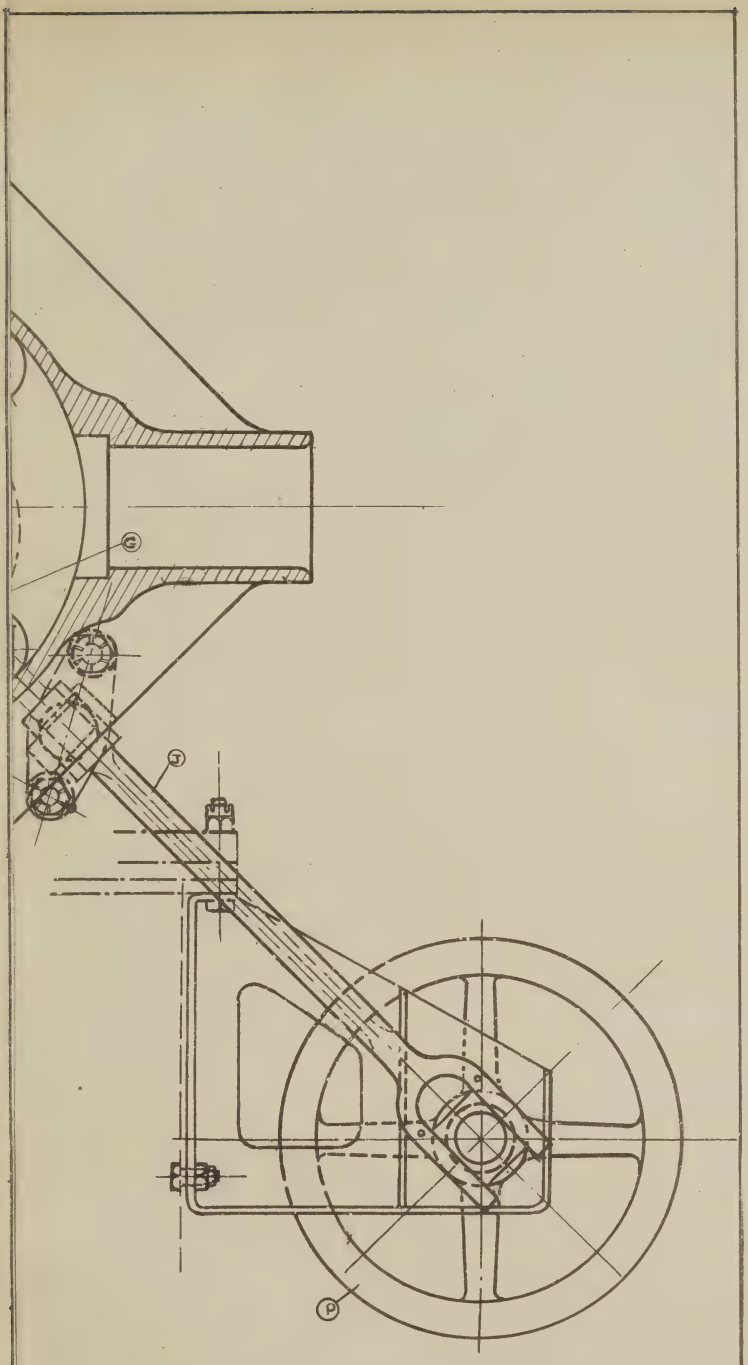

E PITCH AIR SCREW BOSS

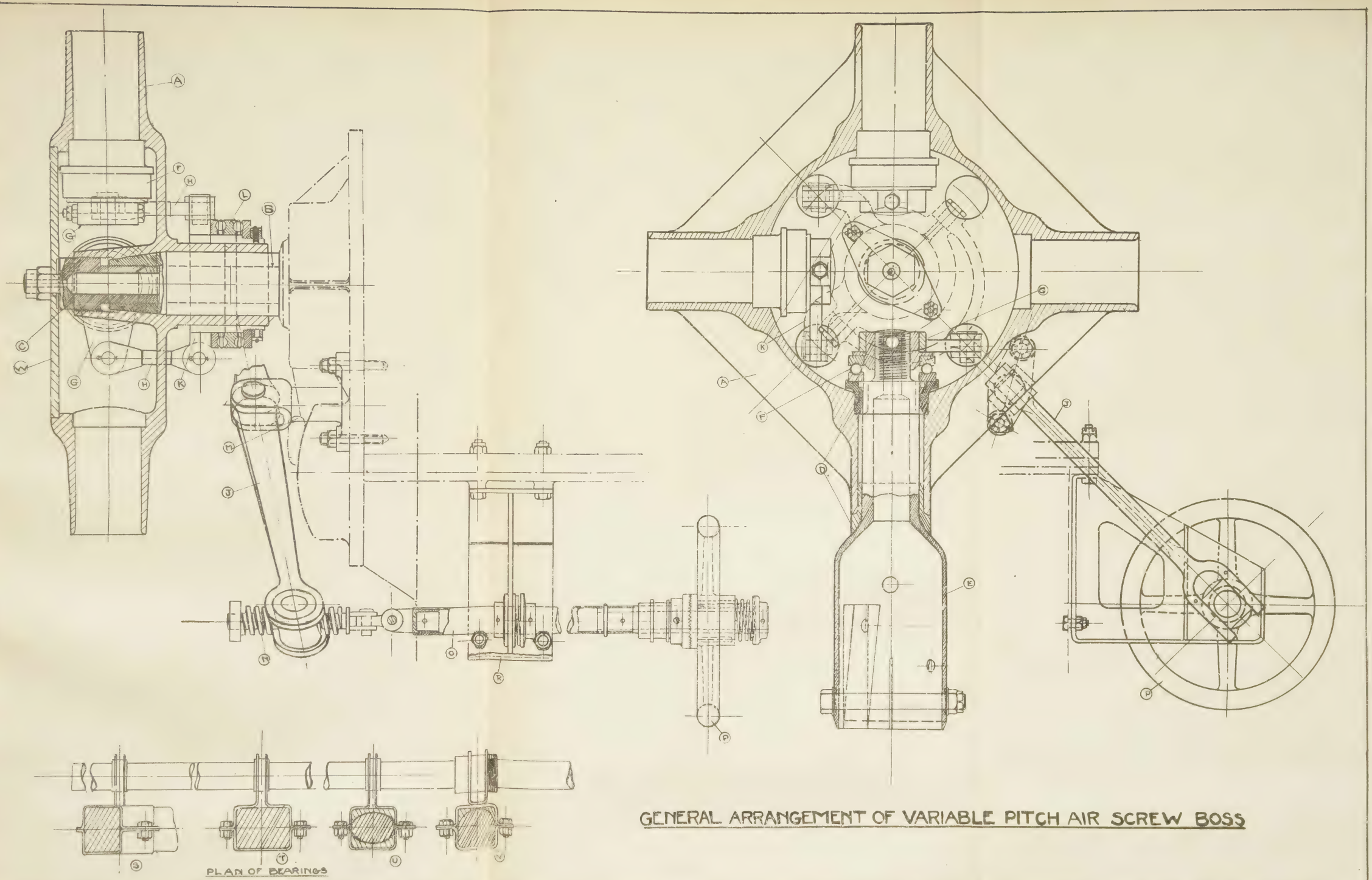

GENERAL ARRANGEMENT OF VARIABLE PITCH AIR SCREW BOSS

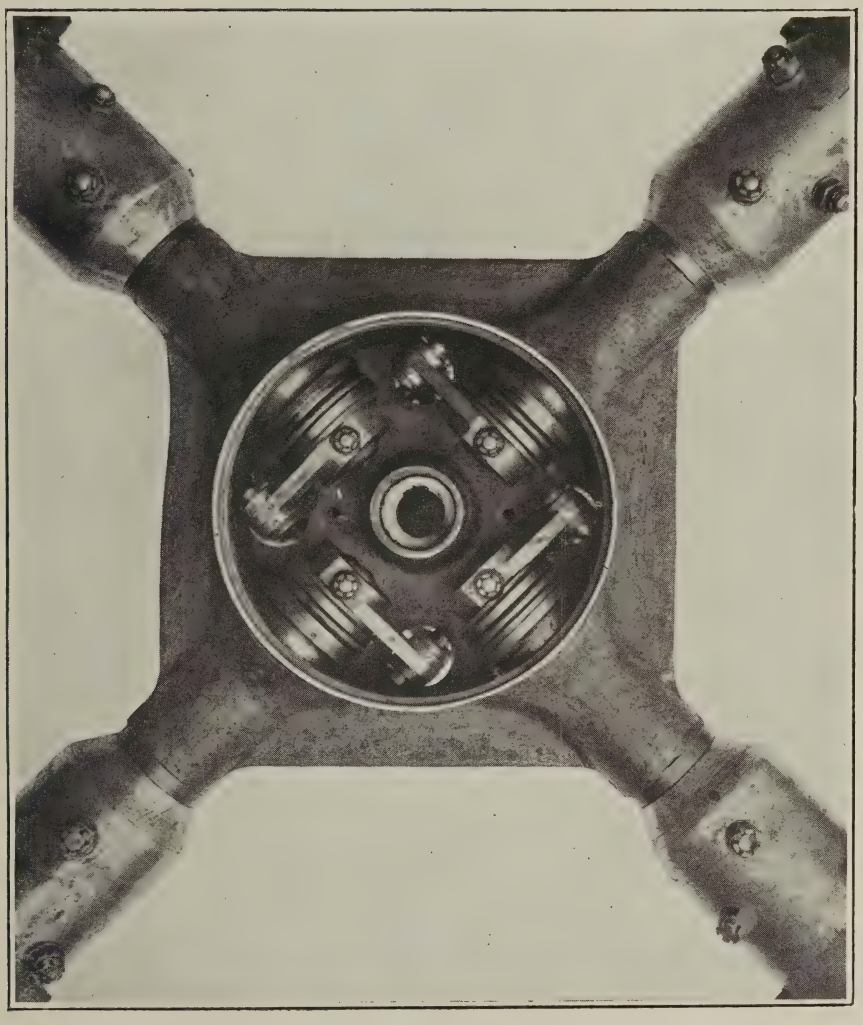

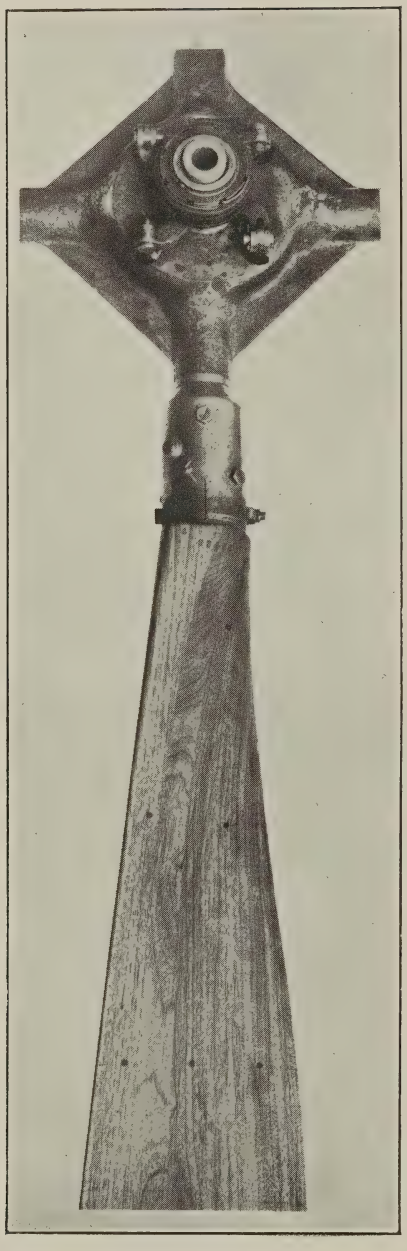

would perhaps be more convenient than the wheel fitted. There was a considerable amount of backlash in the various joints,* making it impossible to measure the actual angles at which the blades were working either by the position of the handwheel or the end of the lever J. The engine revolutions could change about 100 r.p.m. without the lever J being moved. This backlash could probably be eliminated by more careful workmanship and modification of the design, but this is a point which requires careful consideration in the design of variable pitch propellers. It was proposed to measure the blade angles optically, but pressure of other work prevented the continuation of the experiments. The gear provides a total range of angular movement of the blades of 10°.

Referring to the drawing (Fig. 1) it will be seen that the hub A which is held by nut C on the standard splined propeller shaft B, carries the four blades in plain bearings D. Each blade is bolted into a split shank E, which turns in these bearings, the centrifugal force being taken by a ball thrust race F at the inner end of the plain bearings. To the inside end of each shank is screwed and bolted the arm G, which is attached by a link H to a striking plate K, which slides on the hub and carries four arms, to which links H are attached. It is moved along the hub by lever J acting through the double thrust race L, thus rotating the blades through links H and arms G. Lever J is carried by bracket M, bolted to the front of the crankcase, and is operated by screw N through the tube O and hand wheel P. The tube O is carried by bearings R S T U V attached respectively to the crankcase and to the vertical struts of the body. It was found necessary to stay the bearing R back to the first vertical strut of the body as the walls of the crankcase were too thin to stand the strain imposed by the force necessary to operate the gear. The front plate W was removed for the photographs to be taken (Figs. 2 and 3).

* Due to lack of rigidity of the control. By fitting heavier controls this has now been entirely eliminated. Nov., 1918.

SOME EXPERIMENTS ON HELICOPTERS.

By A. Fage, A.R.C.Sc., and H. E. Collins.

Reports and Memoranda (New Series), No. 331. *June,* 1917.

Summary.—Stationary experiments were made with three types of four-bladed helicopters, and with a two-bladed and a three-bladed helicopter. Experiments were also made with a four-bladed helicopter when ascending and when descending.

The present series of experiments on helicopters was made at the request of the Munitions Inventions Department. Stationary experiments were made with three types of four-bladed helicopters, with a three-bladed and a two-bladed helicopter. Finally experiments were made with a four-bladed helicopter when ascending and when descending.

Description of the Models.—Sketches of the three types of helicopter blade are given in Figs. 1–3, from which it is seen that the plan form of each type has the same shape. The distinctive features of each type of blade are as follows :—

(1) Blade of shape " A " of Fig. 1—M.I.D. No. 12—has a flat undersurface, the chords of the blade sections being parallel to each other.

(2) Blade of shape " B " of Fig. 2—M.I.D. No. 13—has a concave undersurface over the greater portion of the blade. The chords of the blade sections were approximately parallel to each other.

(3) Blade of shape "C" of Fig. 3—M.I.D. No. 14. A partial washout of the undersurface camber, the chords of the blade sections being approximately parallel to each other.

The model blades were made in wood and were supplied by the M.I.D. The blades of any one set differed slightly from each other, this being probably due to warping.

A spider of four arms was employed to carry the blades of the four-bladed and the two-bladed helicopters, whilst a spider of three arms was similarly used in the case of the three-bladed helicopter. A sketch of the end of one of the arms of a spider is shewn in Fig. 4, the blade being clamped at any angle by a split conical bush. The overall diameter of the model helicopter when the blades were clamped in position was 2·5 feet, the proposed diameter of the full size helicopter being 40 feet.

Description of the Experiments.—All the experiments were made on the Whirling Arm. The performances were measured of helicopters of four blades, three blades and of two blades, the blades having the shape " A," the angle of the blades varying progressively from 1°·5 to 16°. The angular setting of each blade was measured from the chords CC and DD both before and after the experiment.

Ordinary stationary experiments were made on a four-bladed helicopter with blades of shape B, the angle of the blades varying from 2°·65 to 15°·5, and also experiments with the " helicopter " in translational motion, the value of $\frac{V}{nD}$ varying from $-0{\cdot}2$ to $+0{\cdot}3$ with an angular setting of the blades of 9°·9 and from $-0{\cdot}15$ to $+0{\cdot}3$ when the blade angle was 7°·5. In all cases the angular measurements were made from the chords CC and DD.

Stationary experiments were made on a four-bladed helicopter with blades of shape " C," the angle of the blade being measured from chords CC and DD, and varying progressively from 2°·5 to 12°·5.

The results of the experiments are given in terms of absolute coefficients, and the calculation of thrust and torque from these experiments may be performed as follows :—

$$\text{The thrust, } T = T_c \rho D^4 n^2,$$
$$\text{and the torque, } Q = Q_c \rho D^5 n^2,$$

where the thrust T, the torque Q, the overall diameter of the helicopter, D, the rotational speed n, and ρ the mass density of the air are all expressed in any system of consistent units, and " T_c " and " Q_c " are non-dimensional coefficients. ρ has the value 0·00237 at ground level.

The absolute thrust and torque coefficients of the tables are to be taken for a standard atmosphere of temperature 15°·6 C. and barometer 760 mms.

A ready comparison may be made between the performances of the four-bladed, three-bladed and two-bladed helicopters of blade shape " A," if the values of T_c and Q_c are given *per blade*. In presenting the results of the experiments with helicopters of blade shapes " B " and " C," the values of T_c and Q_c have been calculated *for the helicopter*. In all cases the values of T_c and Q_c given in Tables 1–7 do not take into consideration the forces acting on the supporting apparatus.

Discussion of the Results of the Experiments.—The results of the stationary experiments with helicopters of blade shape " A " are given in Tables 1–3 and shewn graphically in Figs. 5–7.

It will be noted that, at the same angle setting of the blades, the value of T_c per blade decreases with an increase of the number of blades, or in other words, if the T_c per blade and the speed of

rotation have constant values, the angle of a blade must increase with the number of blades in order to correct for the additional velocity of the inflowing air. From Fig. 7 it is seen that the maximum value of $\left(\frac{\text{Thrust} \cdot Dn}{\text{H.P.}}\right)$ for a two-bladed helicopter is 1,730 at an angle of 5°·5 and for a four-bladed helicopter 1,330 at an angle of 7°·5. Generally speaking, the increase in the angle of maximum value of $\left(\frac{\text{Thrust} \cdot Dn}{\text{H.P.}}\right)$ is due to the additional inflow velocity of the air with the increase in the number of blades, whilst the drop of the maximum value of $\left(\frac{\text{Thrust} \cdot Dn}{\text{H.P.}}\right)$ may be attributed to the fact that the angle between the direction of the relative wind and the plane of rotation is greater in the case of the four-bladed helicopter, that is, there is a bigger component of the lift force in the direction of rotation, although the blades are still probably inclined at an aerodynamically efficient angle with the direction of the relative wind. Moreover, there is also a greater direct " biplane " interference in the case of a helicopter with four blades which would also reduce the maximum value of $\left(\frac{\text{Thrust} \cdot Dn}{\text{H.P.}}\right)$.

Looking at the problem of the helicopter from the " aerofoil " standpoint, a given thrust may be most advantageously developed when for any blade section the angle between the direction of the relative wind and the plane of rotation is kept as small as possible, and it is of interest to note, in the case of the helicopter under consideration, that if there were no inflow velocity—an impossible supposition—the maximum value of $\left(\frac{\text{Thrust}}{\text{H.P.}} \cdot Dn\right)$ would probably be about 2,400. From both " momentum " and " aerofoil " considerations a given thrust may be most advantageously developed by a large diameter helicopter of low rotational speed. A helicopter is usually designed to give a certain thrust at a minimum horse-power, the diameter being as large as is consistent with constructional exigencies, the helicopter being driven from the engine through a gearing. Denoting the ratio of $\left(\frac{\text{Thrust}}{\text{H.P.}} \cdot Dn\right)$ by " K " and using the expression $T = T_c \rho n^4 D^2$, it is seen that

$$\text{Horse-power} = \frac{T^{3/2}}{T_c^{\frac{1}{2}} \cdot \rho^{\frac{1}{2}} \cdot D \cdot K.}$$

It follows then that it is advantageous to use a diameter as large as possible and also to place the blades at the angle which makes $K\sqrt{T_c}$ a maximum. Applying the above expression to the case of a four-bladed helicopter fitted with blades of type " A " and

assuming the overall diameter to be 40 feet and the thrust 1,600 lbs. —these figures were obtained from the M.I.D.—it is seen from Fig. 12 and Table 9 that the minimum horse-power needed to drive the blades is 86·5, the angle of the blades being 11°. The curves shewing the relationship between the value of $\left(\frac{\text{Thrust}}{\text{H.P.}} \cdot Dn\right)$ and the angle of the blades are somewhat misleading, if the helicopter problem be viewed from the point of view of sustaining a weight at a minimum expenditure of energy.

In Table 4 and Fig. 8 are given the results of the stationary experiments on a four-bladed helicopter with blades of shape " B," from which it is seen that the maximum value of $\left(\frac{\text{Thrust}}{\text{H.P.}} \cdot Dn\right)$ is 1,390 at an angle of the blade of 6°. Experiments were also made on this helicopter when ascending and descending, the angles of the blades being 7°·5 and 9°·9. The data of these experiments are given in Tables 5 and 6, and in Figs. 9 and 10. It is of interest to note that the maximum values of T_c and Q_c occur at a value of V/nD of about $-0{\cdot}1$, so that at particular values of the translational speed manœuvring during a descent—or when the helicopter is acted upon by an up-gust—may be somewhat difficult. The subject can only be fully investigated when the actual working conditions of the helicopter are known, but for the purpose of illustration calculations have been made for the case of a helicopter of diameter 40 feet which is sustaining a weight of 1,600 lbs., the angle of the blades being 9°·9. The results of the calculations are given in Table 10 from which it is seen that the blades will support a weight of 1,600 lbs., at a rotational speed of 97·0 R.P.M., the torque necessary to drive the blades being 4,740 lbs./ft. Assuming that for some reason the torque acting on the blades is reduced to 4,510 lbs./ft., then the helicopter will be descending with a translational speed of 9·50 ft./sec., and if the machine whilst so descending is struck by an up-gust of, say, 3·4 ft./sec. the behaviour of the machine is different from what may be expected, the helicopter falling instead of rising, since the torque on the blades remains constant at 4,510 lbs./ft. whilst the torque necessary to sustain a weight of 1,600 lbs. when descending at 12·90 ft./sec. is 4,540 lbs./ft. This is perhaps more clearly shewn by the figures of Table 11, where it is seen that if an up-gust strikes the machine when descending with a uniform velocity of 9·50 ft./sec., the thrust of the helicopter is less than the weight of the machine, so that the machine falls with increasing translational velocity.

In Table 7 and Fig. 11 are given the results of stationary experiments on a four-bladed helicopter with blades of shape " C," the maximum value of the ratio $\left(\frac{T}{\text{H.P.}} \cdot Dn\right)$ being 1,460 at an angle of the blades of 6°·5.

Table 1.

STATIONARY EXPERIMENTS ON A FOUR-BLADED HELICOPTER WITH BLADES OF SHAPE "A."

T_c = absolute thrust coefficient.
Q_c = absolute torque coefficient.
D = overall diameter of helicopter in feet.
n = rotational speed in revolutions per second.

Angle of Blade (degrees).	T_c *per blade.*	Q_c *per blade.*	$\left(\frac{\text{Thrust in lbs.}}{\text{Horse-power.}} \cdot Dn\right)$
1·55	0·00225	0·000405	488
4·10	0·00735	0·000575	1,120
6·0	0·01145	0·000772	1,300
9·75	0·02160	0·001498	1,260
12·75	0·03275	0·002740	1,050
16·0	0·04350	0·004310	884

Table 2.

STATIONARY EXPERIMENTS ON A THREE-BLADED HELICOPTER WITH BLADES OF SHAPE "A."

T_c = absolute thrust coefficient.
Q_c = absolute torque coefficient.
D = overall diameter of helicopter in feet.
n = rotational speed in revolutions per second.

Angle of Blade (degrees).	T_c *per blade.*	Q_c *per blade.*	$\left(\frac{\text{Thrust in lbs.}}{\text{Horse-power.}} \cdot Dn\right)$
3·4	0·00815	0·000527	1,348
8·0	0·0216	0·001260	1,500
12·25	0·0360	0·002630	1,200

Table 3.

STATIONARY EXPERIMENTS ON A TWO-BLADED HELICOPTER WITH BLADES OF SHAPE "A."

T_c = absolute thrust coefficient.
Q_c = absolute torque coefficient.
D = overall diameter of helicopter in feet.
n = rotational speed in revolutions per second.

Angle of Blade (degrees).	T_c *per blade.*	Q_c *per blade.*	$\left(\frac{\text{Thrust in lbs.}}{\text{Horse-power.}} \cdot Dn\right)$
2·6	0·00710	0·000445	1,395
7·75	0·02320	0·001220	1,660
12·55	0·04165	0·002955	1,230

Table 4.

STATIONARY EXPERIMENTS ON A FOUR-BLADED HELICOPTER WITH BLADES OF SHAPE "B."

T_c = absolute thrust coefficient.
Q_c = absolute torque coefficient.
D = overall diameter of helicopter in feet.
n = rotational speed in revolutions per second.

Angle of Blades (degrees).	T_c for helicopter.	Q_c for helicopter.	$\left(\frac{\text{Thrust in lbs.}}{\text{Horse-power.}} \cdot Dn\right)$
3·3	0·0283	0·00214	1,155
5·4	0·0465	0·00302	1,390
7·5	0·0740	0·00471	1,335
9·9	0·1015	0·00743	1,190
13·5	0·1485	0·01320	985
15·5	0·1735	0·01670	905

Table 5.

EXPERIMENTS ON A FOUR-BLADED HELICOPTER WITH BLADES OF SHAPE "B," WHEN CLIMBING AND WHEN DESCENDING.

V = velocity of climb or descent in feet per second.

T_c = absolute thrust coefficient.

Q_c = absolute torque coefficient.

D = overall diameter of helicopter in feet.

n = rotational speed in revolutions per second.

Angle of Blades = 7°·5.

	$\frac{V}{nD}$	T_c for helicopter.	Q_c for helicopter.	$\left(\frac{\text{Thrust in lbs.}}{\text{Horse-power.}} \cdot Dn\right)$
Descent	−0·134	0·0738	0·00466	1,380
	−0·104	0·0750	0·00466	1,415
	−0·082	0·0750	0·00457	1,435
	−0·062	0·0747	0·00470	1,385
	−0·041	0·0753	0·00470	1,400
	0	0·0719	0·00471	1,335
Climb	+0·084	0·0632	0·00425	1,300
	0·113	0·0593	0·00415	1,250
	0·266	0·0317	0·00315	880
	0·303	0·0200	0·00280	625

Table 6.

EXPERIMENTS ON A FOUR-BLADED HELICOPTER WITH BLADES OF SHAPE "B" WHEN CLIMBING AND WHEN DESCENDING.

T_c = absolute thrust coefficient.
Q_c = absolute torque coefficient.
D = overall diameter of helicopter in feet.
n = rotational speed in revolutions per second.
Angle of Blades = 9°·9.

	$\frac{V}{nD}$	T_c for helicopter.	Q_c for helicopter.	$\left(\frac{\text{Thrust in lbs.}}{\text{Horse-power.}} \cdot Dn\right)$
Descent	−0·204	0·101	0·00720	1,230
	−0·182	0·104	0·00726	1,250
	−0·159	0·105	0·00757	1,215
	−0·130	0·107	0·00736	1,270
	−0·087	0·1075	0·00765	1,230
	−0·061	0·108	0·00759	1,240
	0	0·1015	0·00743	1,190
Climb	+0·082	0·0930	0·00684	1,190
	+0·135	0·0848	0·00650	1,140
	0·269	0·0563	0·00525	940
	0·289	0·0538	0·00493	955
	0·301	0·0485	0·00479	885

Table 7.

STATIONARY EXPERIMENTS ON A FOUR-BLADED HELICOPTER WITH BLADES OF SHAPE "C."

T_c = absolute thrust coefficient.
Q_c = absolute torque coefficient.
D = overall diameter of helicopter in feet.
n = rotational speed in revolutions per second.

Angle of Blades (degrees).	T_c for helicopter.	Q_c for helicopter.	$\left(\frac{\text{Thrust in lbs.}}{\text{Horse-power.}} \cdot Dn\right)$
2·65	0·0267	0·00211	1,105
3·50	0·0332	0·00240	1,210
5·15	0·0480	0·00308	1,360
6·50	0·0639	0·00382	1,465
7·65	0·0771	0·00485	1,390
9·65	0·0973	0·00648	1,310
12·6	0·1300	0·01005	1,130

TABLE 8.

Torque of spider with four arms $= 0{\cdot}00027\rho n^2D^5$.

Torque of spider with three arms $= 0{\cdot}00021\rho n^2D^5$

where D = overall diameter of helicopter.

TABLE 9.

FOUR-BLADED HELICOPTER FITTED WITH BLADES OF TYPE "A."

Thrust of helicopter = 1,600 lbs.

Overall diameter of helicopter = 40 ft.

Density of air (ground level) = 0·00237.

Angle of Blade (degrees).	Value of K.	Value of T_r *per blade.*	Value of *n* R.P.S.	Horse-power to sustain weight of 1,600 lbs.
2	640	0·0031	4·61	461·0
3	882	0·0049	3·67	266·0
4	1,095	0·0070	3·07	180·0
5	1,225	0·0091	2·70	141·0
6	1,300	0·0115	2·40	118·0
7	1,330	0·0140	2·165	104·4
8	1,325	0·0166	1·99	96·2
9	1,300	0·0195	1·84	90·6
10	1,250	0·0226	1·71	87·5
11	1,180	0·0259	1·595	86·5
12	1,105	0·0293	1·50	86·9
13	1,039	0·0330	1·41	87·0
14	980	0·0366	1·34	87·6
15	925	0·0404	1·275	88·4
16	880	0·0441	1·225	89·0

The horse-power absorbed in driving the supporting apparatus of the blades is not included in the values given in the last column.

THE LIBRARY
OF THE
UNIVERSITY OF ILLINOIS

EXPERIMENTS ON

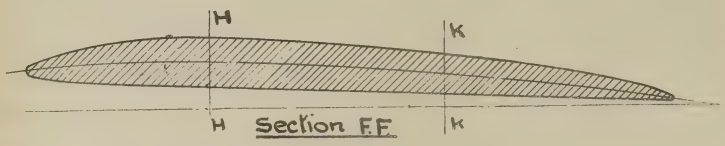

Section F.F.

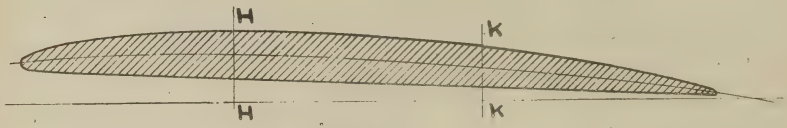

Section E.E.

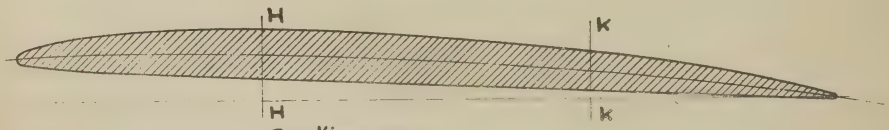

Section D.D.

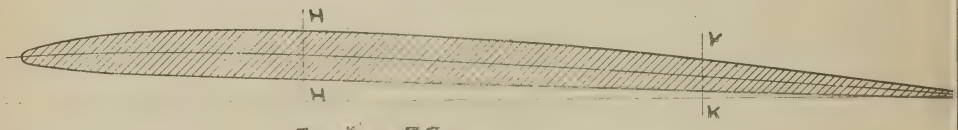

Section C.C.

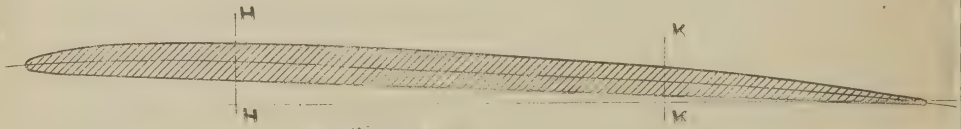

Section B.B.

Section A.A.

Section H.H.

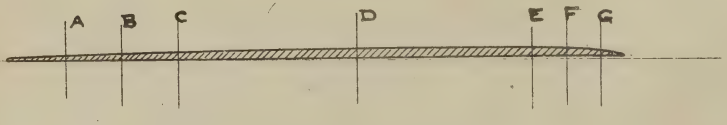

Section K.K.

— Scale fo
1'

— Scale fo
1'

Fig. 1.

HELICOPTERS.

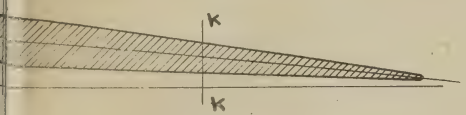

Section GG.

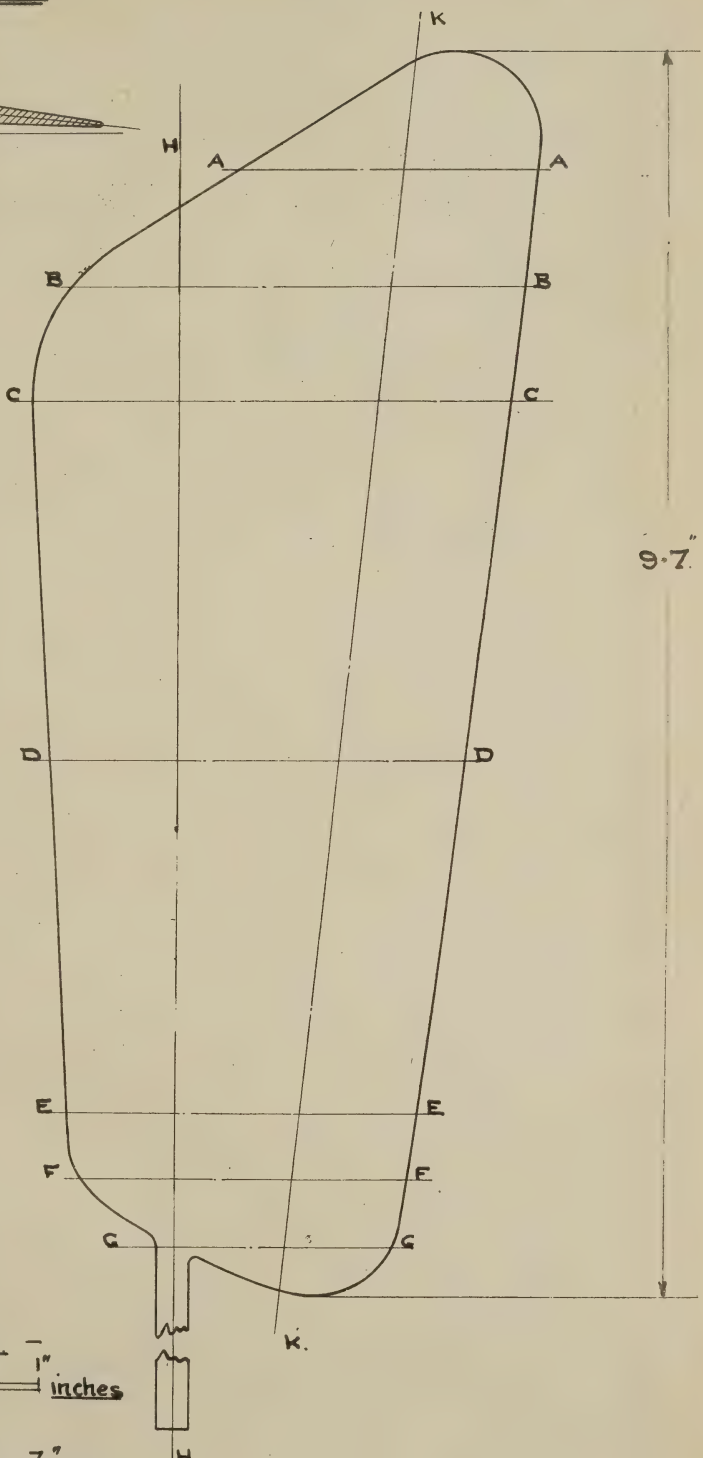

HAPE A. —

Sections A,B,C,D,E,F & G. —

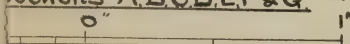

Sections H & K. —

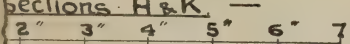

THE LIBRARY
OF THE
UNIVERSITY OF ILLINOIS

FIG. 2.

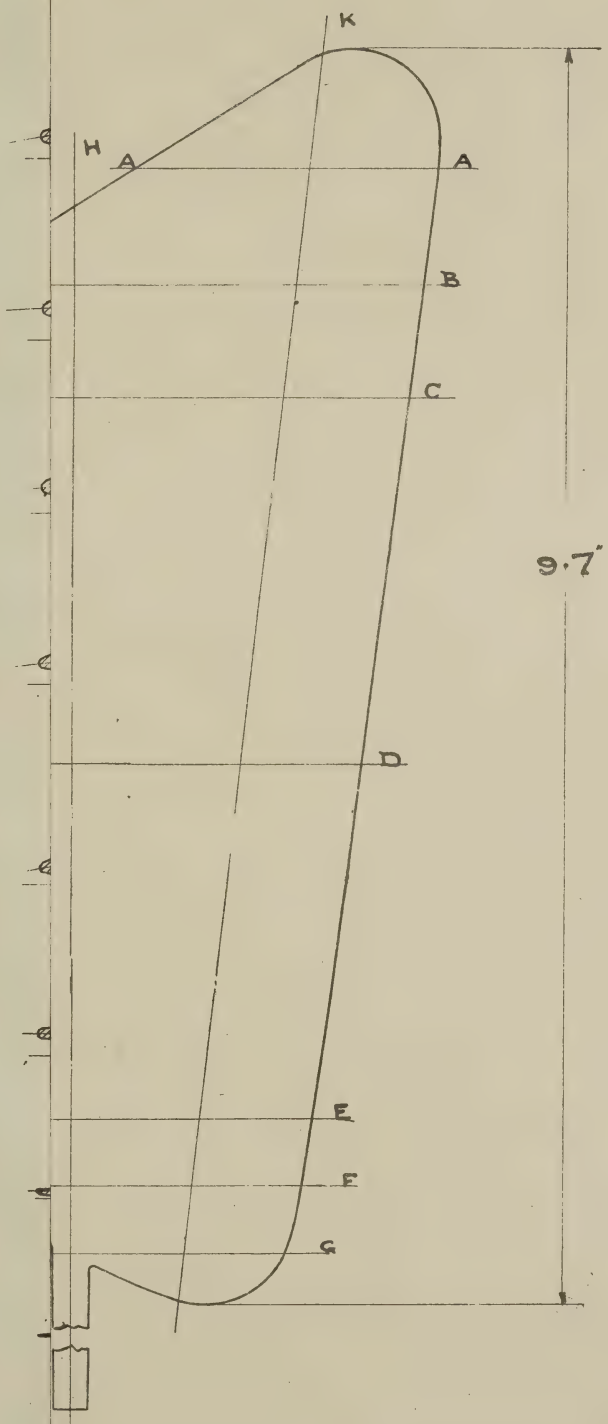

FIG. 2.

EXPERIMENTS ON HELICOPTERS.

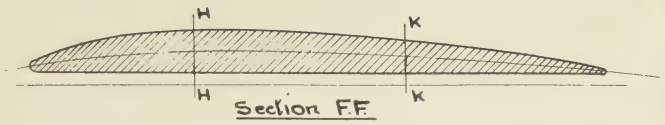

Section F.F.

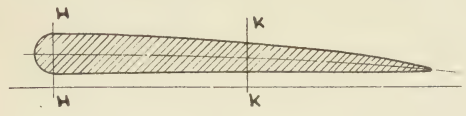

Section G.G.

Section E.E.

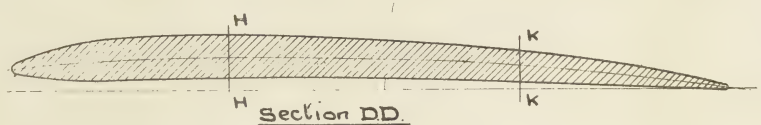

Section D.D.

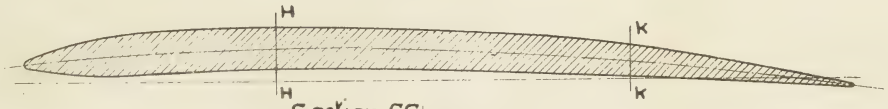

Section C.C.

Section B.B.

Section A.A.

Section H.H.

Section K.K.

— SHAPE B. —

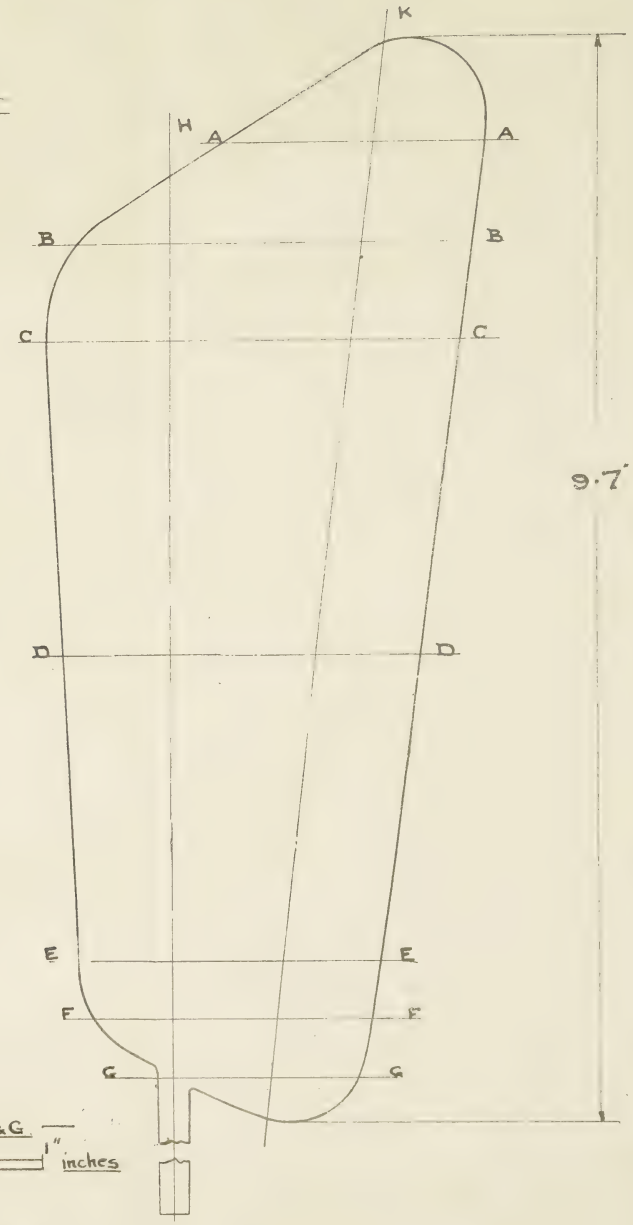

— Scale for Sections. A.B.C.D.E.F.&G. —

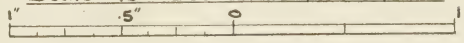

— Scale for Sections, H & K. —

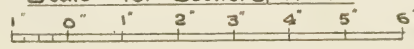

FIG. 3.

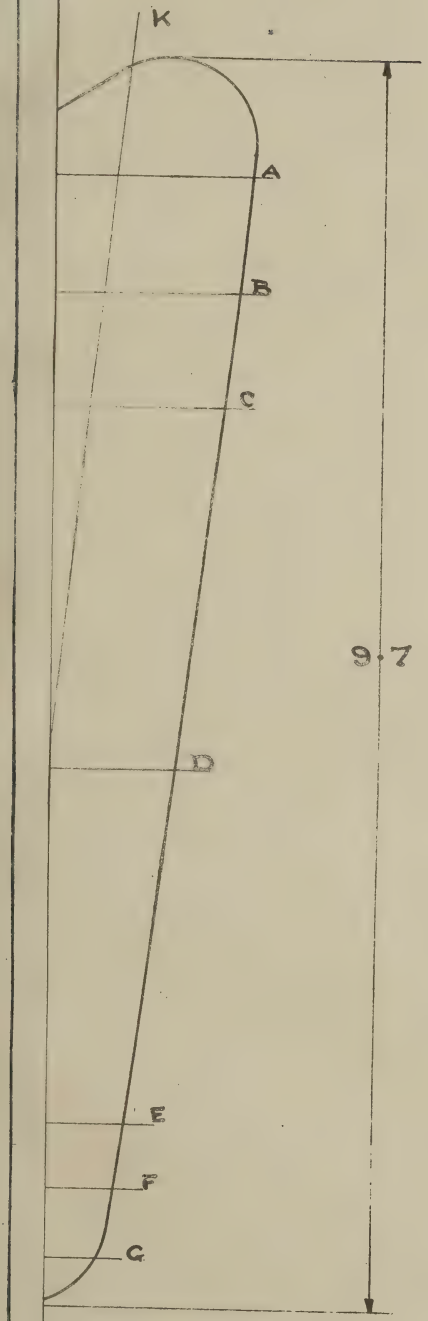

EXPERIMENTS ON HELICOPTERS

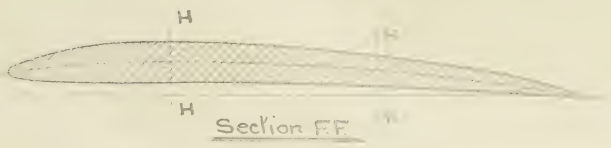

Section FF

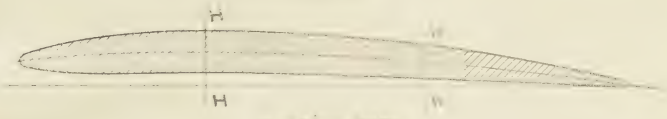

Section EE

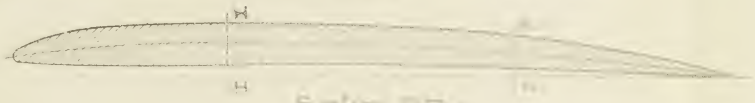

Section DD

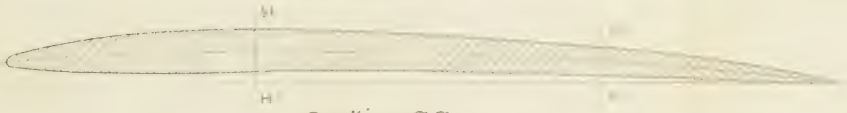

Section CC

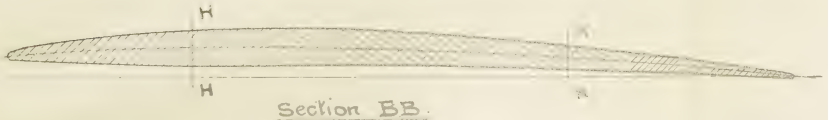

Section BB

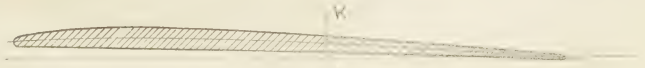

Section AA

Section HH

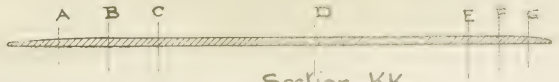

Section KK

Section GG

— SHAPE C —

Scale for Sections A B C D E F & G.

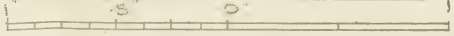

inches.

Scale for Sections H & K

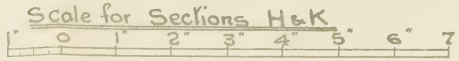

inches.

EXPERIMENTS ON HELICOPTERS.

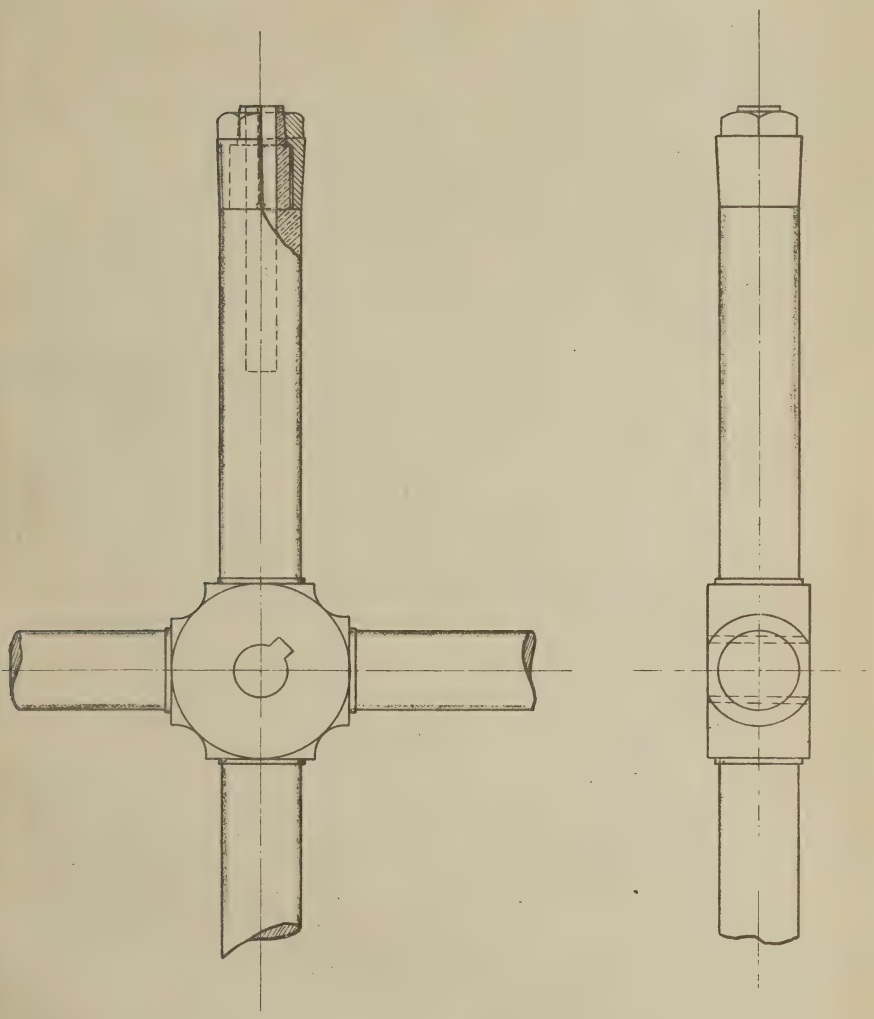

— Sketch of spider for supporting four blades. —

— Scale in inches —

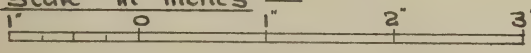

EXPERIMENTS ON HELICOPTERS.

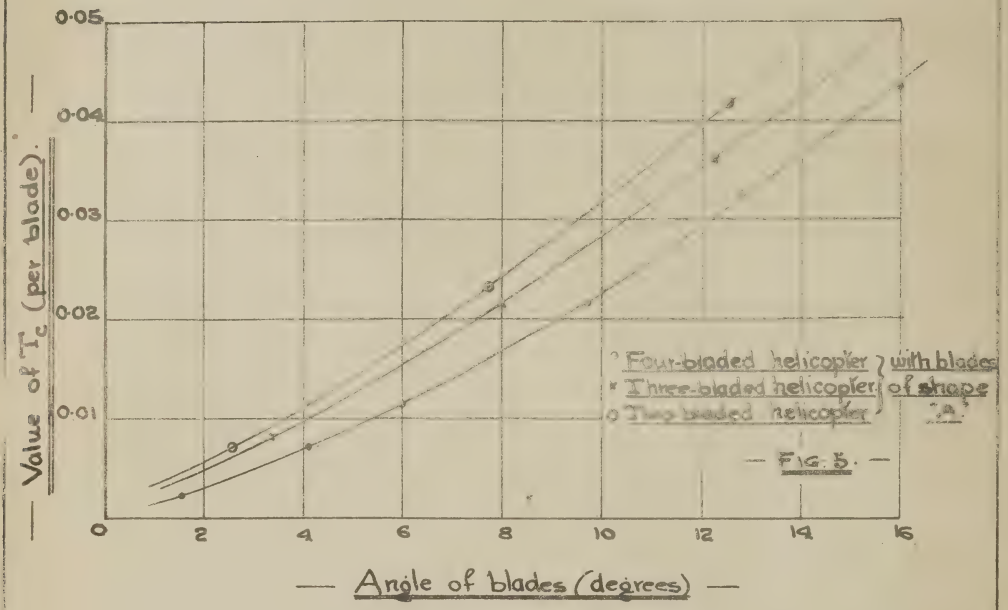

— FIG. 5. —

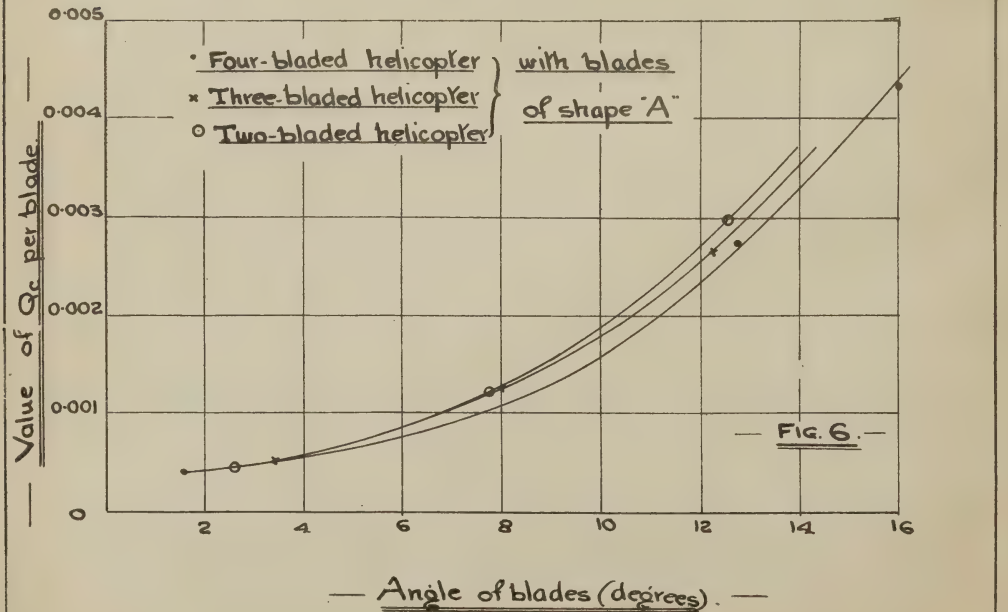

— FIG. 6. —

REPORT Nº 331. FIG. 7 & 8.

EXPERIMENTS ON HELICOPTERS.

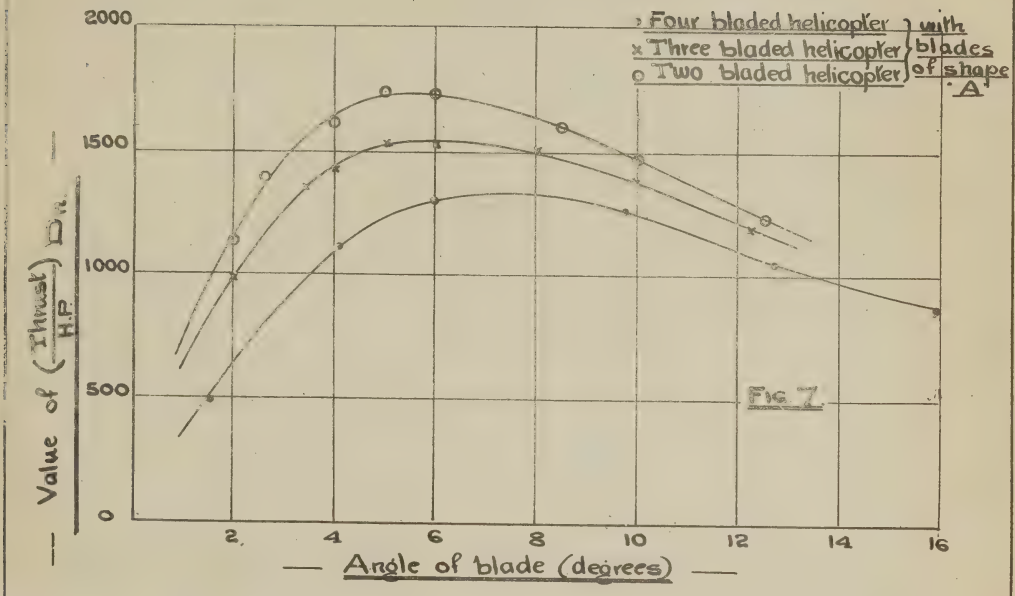

Blades of Shape "B".

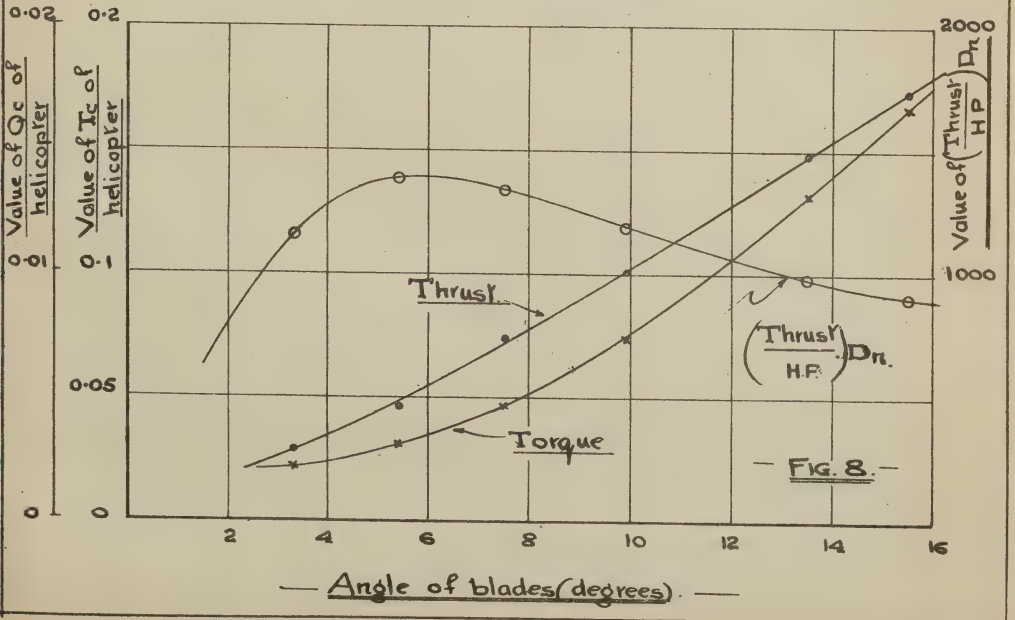

EXPERIMENTS ON HELICOPTERS.

Blades of Shape "B". Angle of Blades 9·9°.

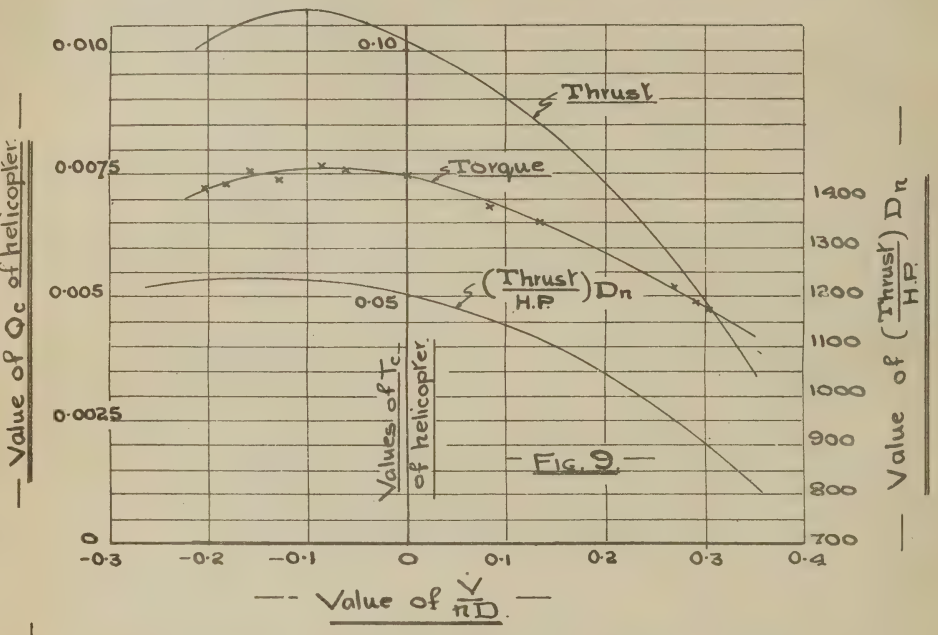

FIG. 9.

Blades of Shape "B". Angle of Blades 7·5°.

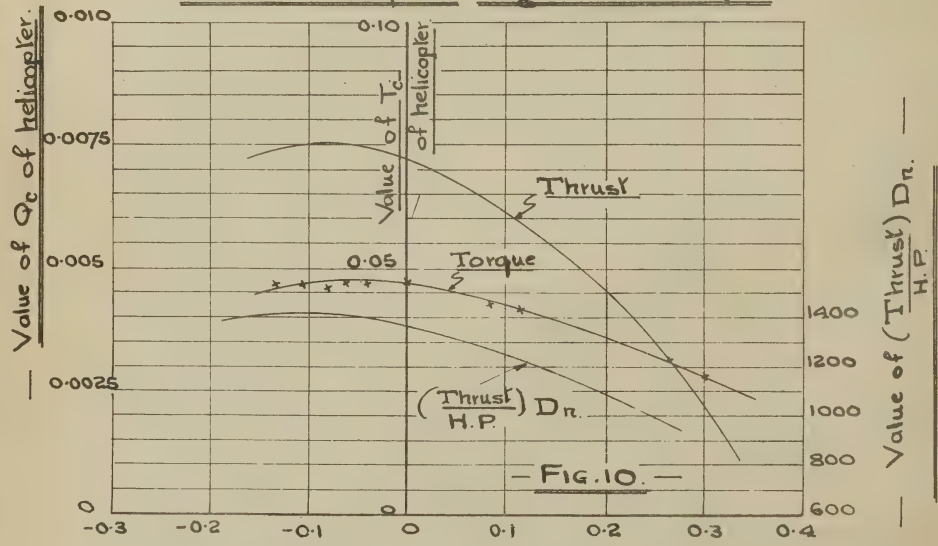

FIG. 10.

REPORT Nº 331.

FIG. 11.

EXPERIMENTS ON HELICOPTERS.

— Blades of Shape "C" —

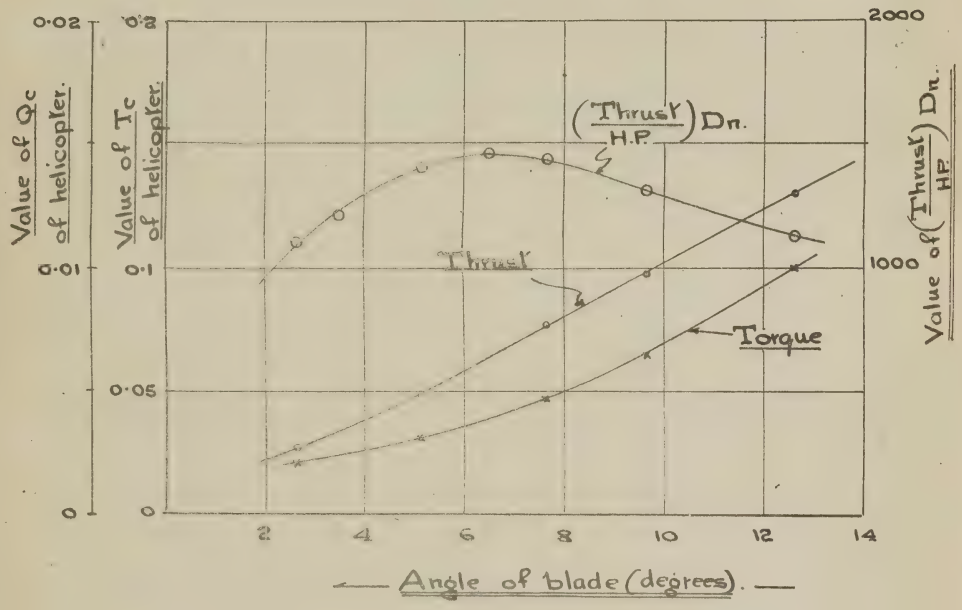

EXPERIMENTS ON HELICOPTERS.

Four-bladed helicopter with blades of shape "A"

Thrust of helicopter = 1600 lbs.

Diameter of helicopter = 40 ft.

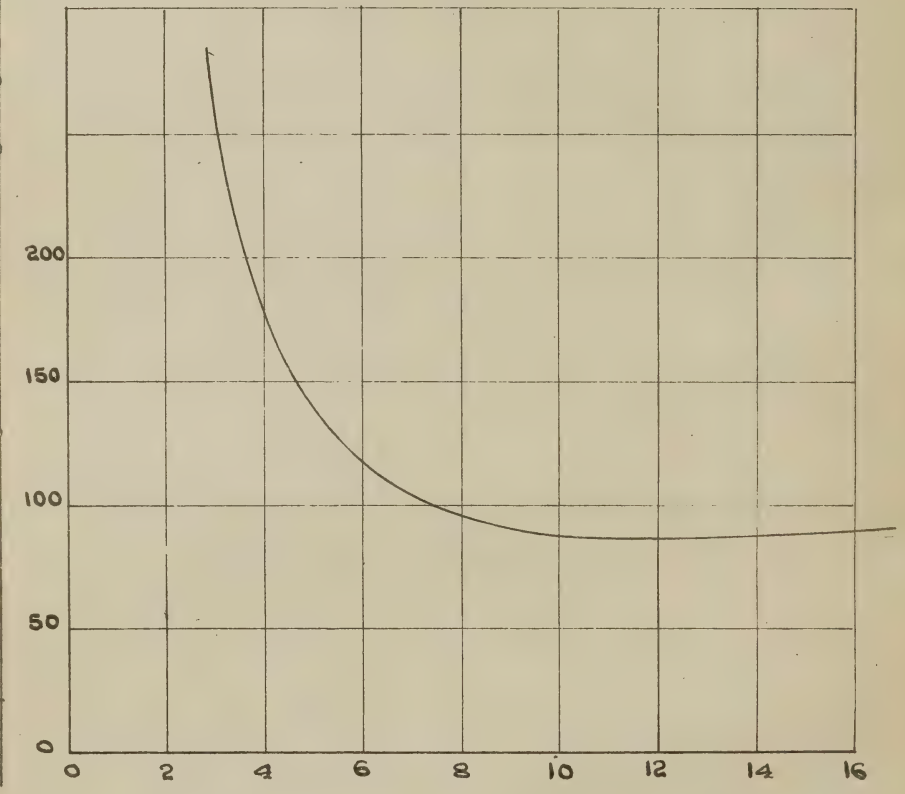

TABLE 10.

RELATION BETWEEN TORQUE OF HELICOPTER BLADES AND THE VELOCITY OF DESCENT, THE THRUST OF THE HELICOPTER BEING CONSTANT.

Blades of shape " B."
Angle of blades 9°·9.
Weight of machine 1,600 lbs.

Velocity of descent. Ft. /sec	Rotational speed of helicopter. Revs. /sec.	Torque required to drive the blades. Lbs. /ft.	Thrust of helicopter. Lbs.
0	1·62	4,740	1,600
3·15	1·58	4,630	1,600
6·25	1·56	4,515	1,600
9·50	1·58	4,510	1,600
12·90	1·61	4,540	1,600

TABLE 11.

RELATION BETWEEN THRUST OF HELICOPTER BLADES AND THE VELOCITY OF DESCENT, THE TORQUE OF THE HELICOPTER BEING CONSTANT.

Blades of shape " B."
Angle of blades 9°·9.
Weight of machine 1,600 lbs.

Velocity of descent. Ft. /sec.	Rotational speed of helicopter. Revs. /sec.	Torque required to drive the blades. Lbs. /ft.	Thrust of helicopter. Lbs.
6·25	1·56	4,510	1,600
9·50	1·58	4,510	1,600
12·85	1·605	4,510	1,570

THE "SCALE-SPEED" EFFECT ON A MODEL AIRSCREW OF SMALL DIAMETER.

By A. Fage, A.R.C.Sc., and H. E. Collins.

Reports and Memoranda, No. 390. *January,* 1918.

Summary.—(*a*) *Introductory* (*Reason for inquiry*).—A "scale-speed"* effect of appreciable magnitude was obtained during the experiments with a small aluminium model of a B.E. 2E airscrew of scale $\frac{1}{6}$th. (See Report R. & M. 393.) The effect was observed from experiments on both the Whirling Table and the Airscrew Balance. It was thought that a complete experimental investigation of this "scale-speed" effect would be of some interest.

(*b*) *Range of Investigation.*—The model airscrew was tested on the airscrew balance at translational speeds of 25, 35 and 45 ft./sec., over a large range of the rotational speed, the upper limit of the speed being fixed by the capacity of the electric motor driving the airscrew. It was not possible to eliminate the "scale-speed" effect at the highest speeds of the experiment.

(*c*) *Conclusions.*—The magnitude of the "scale-speed" effect diminishes with a decrease of the value of the ratio of forward speed to the product of the diameter of the airscrew and the rotational speed (V/nD). At the same value of (V/nD) the absolute values of the thrust, torque and efficiency increase with the speed and the diameter of the airscrew. The magnitude of the "scale-speed" effect is largest for large values of (V/nD), such large values corresponding to a small angle of incidence, and thus the result is in accordance with the data already obtained for aerofoils. (See R. & M. 148.) Small "scale-speed" effects have been noticed with two other models of a $\frac{1}{6}$th scale. A large number of model airscrews of $\frac{1}{4}$th scale have been tested at the Laboratory, but in no case has a "scale-speed" effect been observed.

The report is of importance as indicating a probable disadvantage of the employment of model airscrews of low diameter.

The present investigation of the scale-speed effect of a small model airscrew of type B.E. 2E—R.A.F. Drawing No. T.7850—was the direct outcome of the experiments described in Report R. & M. 393, which were made to determine the mutual interference between models of the body and airscrew of the B.E. 2E aeroplane. From the preliminary experiments made with the airscrew balance,

* By "scale-speed" effect is implied a change in the non-dimensional constants of an airscrew as the size of the model and the wind speed are increased.

and also on the Whirling Table, with a wooden model of the airscrew of scale $\frac{1}{6}$th, it was found that for any value of (V/nD) the values of the absolute coefficients of thrust and torque increased with the translational speed, and, therefore, with the load on the airscrew. It was thought that these discrepancies, which were much greater than could be attributed to experimental error, were largely due to the warping of the wooden model. Accordingly, to eliminate warping the experiments were repeated with an aluminium model. These later experiments confirmed those previously made with the wooden model, and so definitely established a "scale-speed" effect for this model airscrew. The report is useful as indicating a probable disadvantage of the employment of model airscrews of low diameter.

Description of Experiments.—A sketch of the four-bladed airscrew for B.E. 2E (R.A.F. Drawing No. T.7850) is given in Fig. 1. The diameter of the full-size airscrew was 9′ 1″, the angles of the blade varying from 20° 35′ at the tip to 68° 54′ at the boss. The airscrew is rather full in plan form at the tip. As previously stated the model airscrew was made in aluminium at the R.A.F., the scale of the model being $\frac{1}{6}$th.

The airscrew was tested on the airscrew balance at translational speeds of 25, 35 and 45 ft./sec., the range of the rotational speed for each translational speed being limited by the capacity of the electric motor driving the airscrew. The airscrew was arranged on the balance in the manner described in Report R. & M. 344, in which the airscrew was some distance behind the vertical shaft of the balance.

Some further corroborative evidence of the existence of the "scale-speed" effect was obtained from experiments with the airscrew mounted in front of the vertical shaft of the balance, and also from the Whirling Table. The data of these latter experiments have not been included in the report.

Following the standard method, the results of the experiments are represented in terms of absolute coefficients and the calculation of the thrust and the torque from these coefficients may be performed as follows :—

$$\text{The thrust, } T = T'_c \rho n^2 D^4,$$

$$\text{and torque, } Q = Q'_c \rho n^2 D^5,$$

where the thrust T, torque Q, diameter of the airscrew D, the rotational speed n, and ρ the mass density are all expressed in any system of consistent units, and T'_c and Q'_c are non-dimensional coefficients.

The absolute thrust and torque coefficients of the tables are to be taken for a standard atmosphere of temperature 15·6° C. and barometer 760 mms.

Discussion of the Results of the Experiments.—The results of the experiments are given in Tables 1–3 and shown graphically

in Figs. 2–4. Generally speaking the " scale-speed " effect on this airscrew is very similar to that of an aerofoil. Thus, at a value of (V/nD) of 1·20, the angle of incidence of the sections at the tip will be about – 1°, the experimental range of " vl " for a section 8″ from the axis of the airscrew being from about 6·5 to 12·0, where the values of " vl " are measured in foot-second units and " v " is the speed of the section relative to the air, and " l " the chord length. At such small values of " vl " and at this angle of incidence, the " scale-speed " effect of an aerofoil is quite appreciable so that a corresponding effect on the airscrew is only to be expected. At values of (V/nD) of 1·05 and 0·90 the angles of incidence of the tip sections are about 1° and 3° respectively, the corresponding experimental ranges of " vl " for the section under consideration being from 7·5 to 14·0 in the former case, and from 8·5 to 15·0 in the latter. It is seen from the thrust curves that the value of the experimental mean pitch increases with the speed of translation.

The " scale-speed " effect diminishes with a decrease of the value of (V/nD), that is, with an increase of the angle of incidence of the blade sections. The value of the maximum efficiency increases with the speed of translation. The value of (V/nD) at which maximum efficiency occurs also increases with the speed of translation.

It was not possible to eliminate the " scale-speed " effect of the airscrew even at the highest speeds of the experiment. It was thought that the shapes of the thrust and efficiency curves without any " vl " effect would probably be as shown by the dotted curves of the figures. Comparing similar model airscrews at the same translational speed the value of " vl " of a section of the blade is directly proportional to the diameter and inversely proportional to the values of (V/nD), at which the airscrew is working. The airscrew under consideration has both a small diameter and works at high values of (V/nD), both these factors being favourable for the appearance of a " vl " effect. The other $\frac{1}{6}$th scale airscrews which have been tested at the Laboratory are the R.E. 7 airscrew, where only a small " scale-speed " effect was noticed, probably because of the low pitch, and the F.E. 8 airscrew from which a " vl " effect was suspected, but was not definitely established. A large number of model airscrews of $\frac{1}{4}$th scale has been tested at the Laboratory, but in no case has a " scale-speed " effect been observed. In conclusion, it should be noted that the method of experiment using both the airscrew balance and the Whirling Table, where the performance of the airscrew at the higher values of (V/nD) is measured at the higher translational speeds, tends to eliminate the " scale-speed " effect at the smaller angles of incidence, where it would be greatest.

"SCALE-SPEED" EFFECT ON A MODEL AIRSCREW

R. A.F. Drawing No. T.7850.

REPORT No. 390.

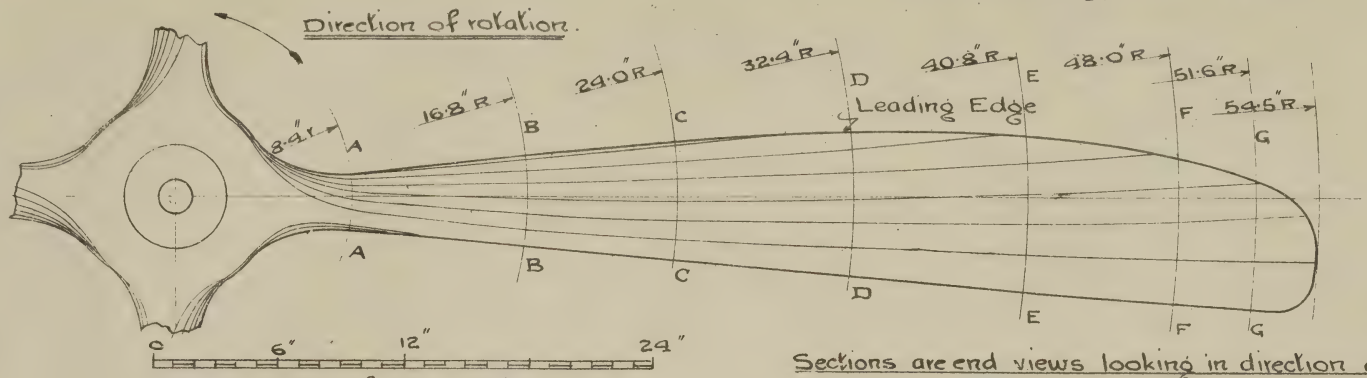

Scale in inches for plan view

Sections are end views looking in direction of arrow

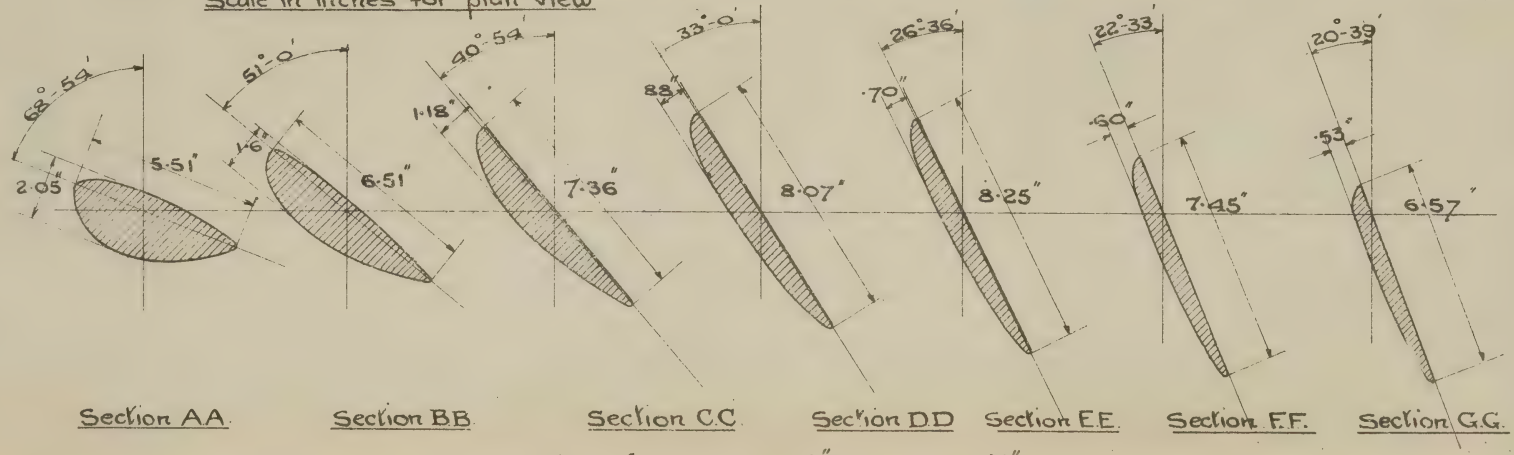

Section AA. Section BB. Section CC. Section DD. Section EE. Section FF. Section GG.

0 6" 12" 18"

Scale in inches for sections.

FIG. 1.

P.L.T.

"SCALE-SPEED" EFFECT ON A MODEL AIRSCREW.

Thrust curves of airscrew for B.E.2E. - R.A.F. Drawing No. T.7850.

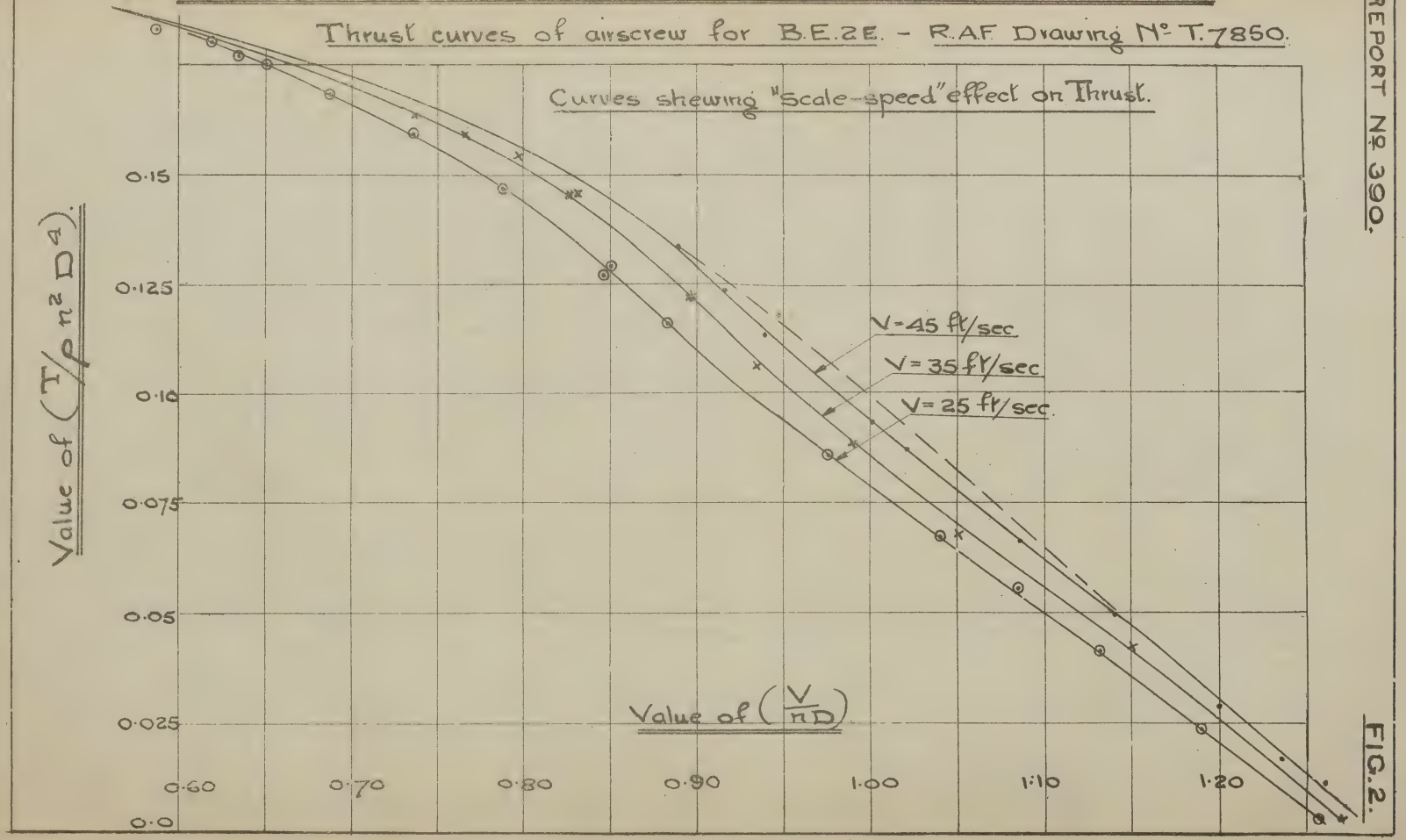

FIG. 2.

"SCALE SPEED" EFFECT ON A MODEL AIRSCREW.

Torque curves of airscrew for B.E.2E. R.A.F. Drawing No. T.7850.

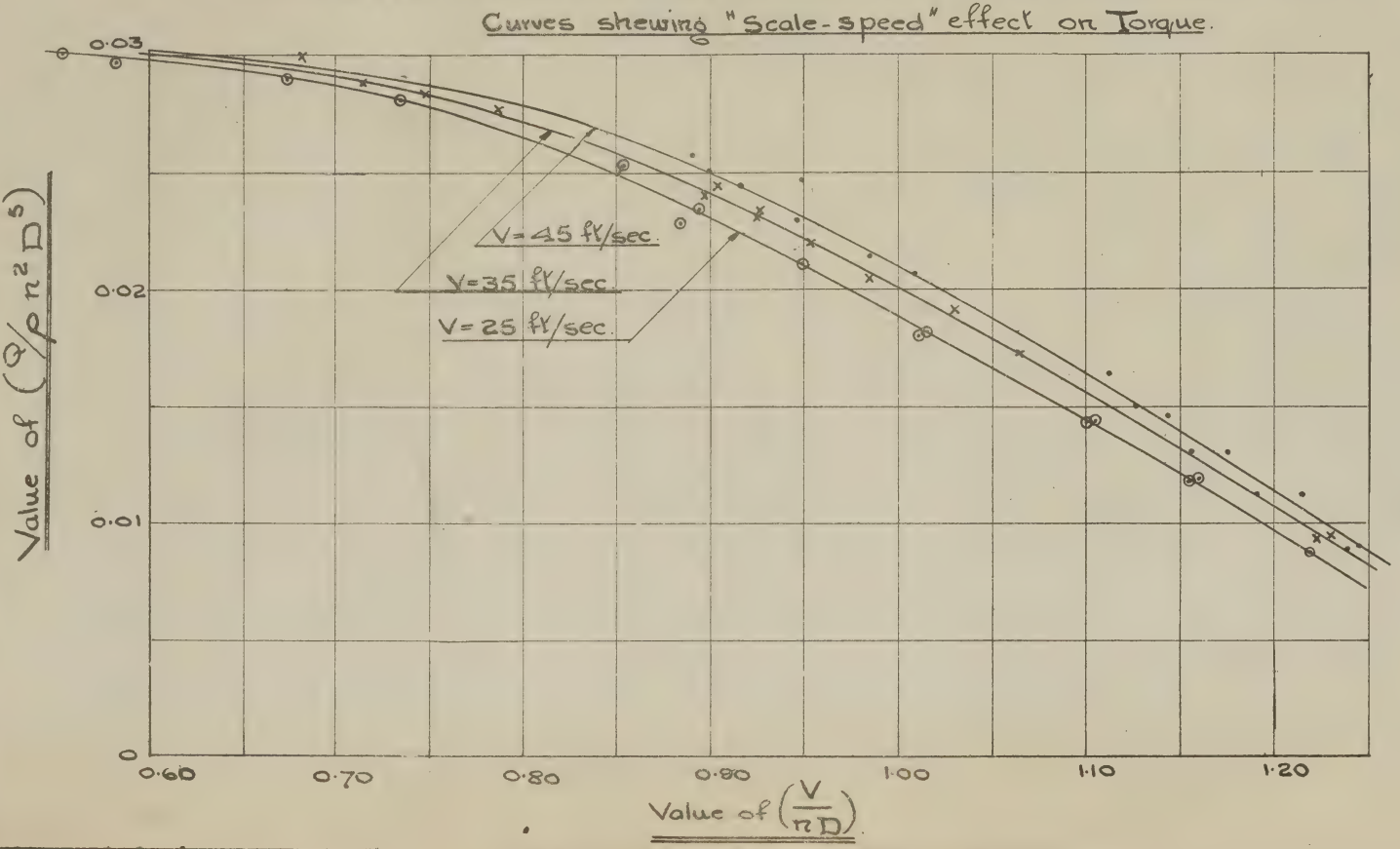

REPORT No. 390.

FIG. 3.

"SCALE-SPEED" EFFECT ON A MODEL AIRSCREW.

Efficiency curves of airscrew B.E.2E. – R.A.F. Drawing No. 7850.

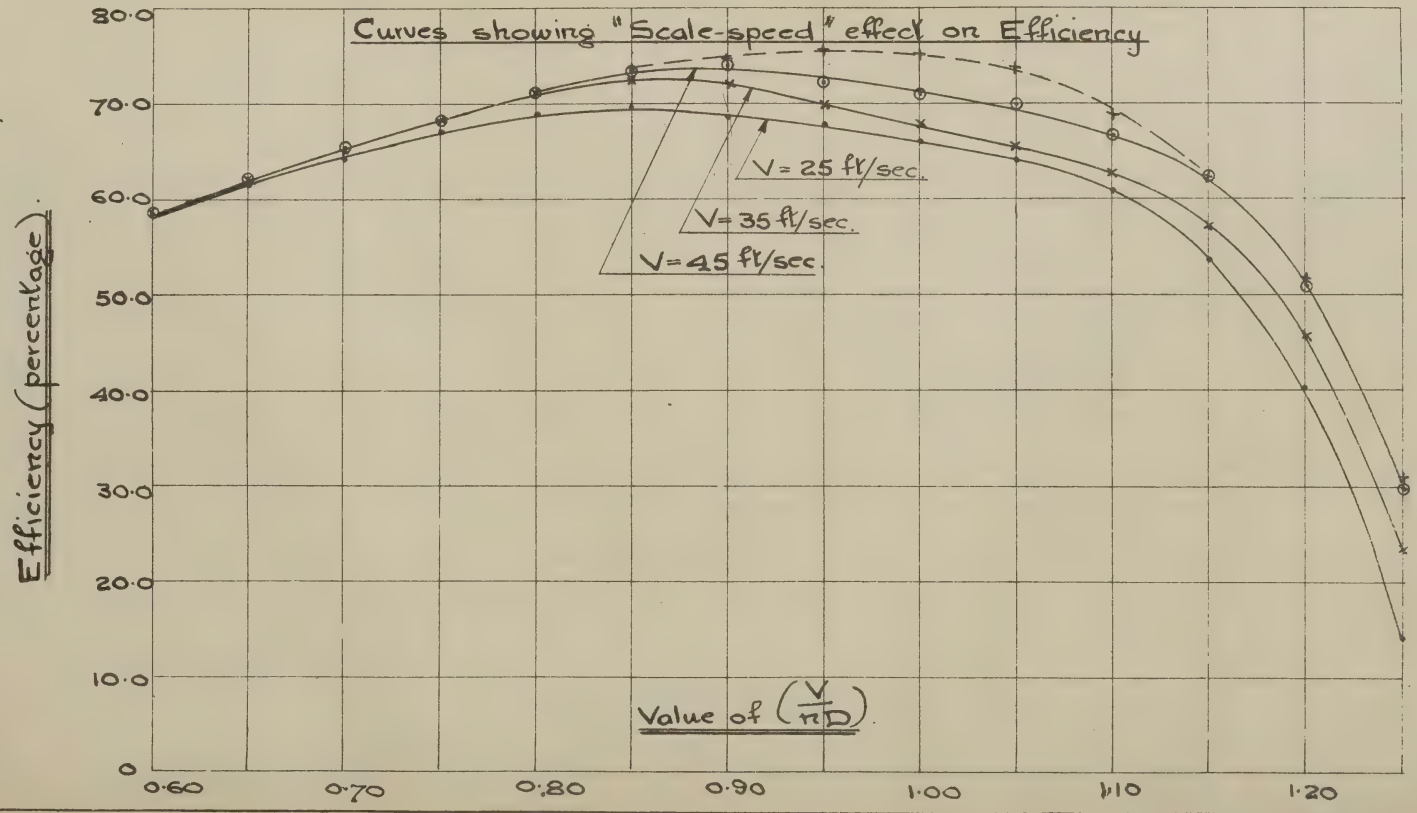

REPORT No. 390.

FIG. 4.

Table 1.

FOUR-BLADED AIRSCREW FOR B.E. 2E.
(R.A.F. Drawing No. T.7850.)

Diameter of the model airscrew = 1·515 ft.
(Scale $\frac{1}{6}$th full size.)

V in feet per second.
n in revolutions per second.
D diameter in feet.
The thrust $T = T'_c \rho n^2 D^4$.

Forward Speed in ft. /sec.	Value of (V /nD).	Value of Thrust Coeff. T'_c.	Forward Speed in ft. /sec.	Value of (V /nD).	Value of Thrust Coeff. T'_c.	Forward Speed in ft. /sec.	Value of (V /nD).	Value of Thrust Coeff. T'_c.
45·0	1·280	0·0030	35·0	1·270	0·0029	25·0	1·255	0·0028
,,	1·260	0·0101	,,	1·150	0·0422	,,	1·190	0·0233
,,	1·235	0·0166	,,	1·050	0·0678	,,	1·132	0·0410
,,	1·200	0·0289	,,	0·988	0·0881	,,	1·084	0·0554
,,	1·140	0·0493	,,	0·933	0·1058	,,	1·039	0·0672
,,	1·085	0·0660	,,	0·897	0·1219	,,	0·975	0·0855
,,	1·020	0·0870	,,	0·895	0·1220	,,	0·882	0·1158
,,	1·000	0·0930	,,	0·830	0·1455	,,	0·850	0·1290
,,	0·938	0·1130	,,	0·826	0·1455	,,	0·845	0·1270
,,	0·915	0·1235	,,	0·797	0·1540	,,	0·787	0·1470
45·0	0·888	0·1335	,,	0·765	0·1590	,,	0·735	0·1595
			35·0	0·736	0·1635	,,	0·687	0·1680
						,,	0·650	0·1750
						,,	0·633	0·1770
						,,	0·618	0·1800
						,,	0·586	0·1830
						25·0	0·568	0·1910

Table 2.

FOUR-BLADED AIRSCREW FOR B.E. 2E.
(R.A.F. Drawing No. T.7850.)

Diameter of the model airscrew = 1·515 ft.
(Scale $\frac{1}{6}$th full size.)

V in feet per second.
n in revolutions per second.
D diameter in feet. $Q = Q' \rho n^2 D^5$.

Forward Speed in ft. /sec.	Value of (V /nD).	Value of Q'_c.	Forward Speed in ft. /sec.	Value of (V /nD).	Value of Q'_c.	Forward Speed in ft. /sec.	Value of (V /nD).	Value of Q'_c.
45·0	1·245	0·0089	35·0	1·230	0·0093	25·0	1·294	0·0050
,,	1·238	0·0088	,,	1·221	0·0092	,,	1·218	0·0086
,,	1·214	0·0111	,,	1·065	0·0171	,,	1·160	0·0118
,,	1·190	0·0112	,,	1·030	0·0190	,,	1·155	0·0117
,,	1·175	0·0129	,,	0·985	0·0204	,,	1·105	0·0143
,,	1·155	0·0130	,,	0·953	0·0219	,,	1·100	0·0142
,,	1·144	0·0145	,,	0·926	0·0233	,,	1·015	0·0181
,,	1·126	0·0149	,,	0·925	0·0230	,,	1·012	0·0179
,,	1·112	0·0163	,,	0·903	0·0244	,,	0·950	0·0210
,,	1·065	0·0172	,,	0·896	0·0240	,,	0·894	0·0233
,,	1·010	0·0206	,,	0·786	0·0277	,,	0·884	0·0228
,,	0·985	0·0213	,,	0·748	0·0283	,,	0·853	0·0253
,,	0·947	0·0229	,,	0·713	0·0288	,,	0·733	0·0281
,,	0·916	0·0244	35·0	0·682	0·0299	,,	0·673	0·0290
,,	0·900	0·0251				,,	0·582	0·0297
45·0	0·890	0·0257				,,	0·552	0·0301
						,,	0·522	0·0301
						25·0	0·500	0·0305

Table 3.

FOUR-BLADED AIRSCREW FOR B.E. 2E.
(R.A.F. Drawing No. T.7850.)

Diameter of the model airscrew = 1·515 ft.
(Scale $\frac{1}{6}$th full size.)

V in feet per second.
n in revolutions per second.
D diameter in feet.

Value of V/nD.	Forward Speed = 25 ft./sec. Value of efficiency. Percentage.	Forward Speed = 35 ft./sec. Value of efficiency. Percentage.	Forward Speed = 45 ft./sec. Value of efficiency. Percentage.	Efficiency calculated from faired thrust and torque curves. Percentage.
1·25	14·0	23·3	29·7	30·8
1·20	40·2	45·7	50·7	51·7
1·15	53·4	57·2	62·2	61·7
1·10	61·0	62·5	66·5	68·8
1·05	64·2	65·3	69·7	73·6
1·00	66·0	67·7	70·6	75·0
0·95	67·8	69·6	72·2	75·5
0·90	68·2	72·1	73·6	74·5
0·85	69·5	72·3	73·2	73·1
0·80	68·8	71·2	71·C	71·0
0·75	67·0	68·3	68·2	68·4
0·70	64·0	64·8	65·3	65·2
0·65	61·5	62·0	61·8	61·9
0·60	58·5	58·5	58·2	58·0

REPORT OF THE SCALE EFFECT SUB-COMMITTEE ON THE RELATION BETWEEN MODEL TESTS AND THE FULL SCALE PERFORMANCE OF AEROPLANES.

Reports and Memoranda (New Series), No. 374. *December*, 1917.

1. In March, 1917, a Sub-Committee of the Advisory Committee was formed to consider generally the comparison between the results of experiments on models of aeroplanes, aeroplane wings, etc., as affecting the estimation of aeroplane performance, and the results obtained in full scale observations and records of performance.

In the prediction of the performance of aeroplanes it was a common practice to assume that the total resistance of any machine was the sum of the resistances of its various parts; these separate resistances were calculated from experiments on reduced or full scale models of these parts, and scale and interference corrections applied so far as known. It was brought to the attention of the Committee that the application of this method led in some cases to differences between the actual and the predicted performance which could not be accounted for by experimental errors.

2. As a result of the preliminary examination of the records and information then available, it was decided to carry out further investigations which it was hoped might improve the accuracy of the comparison. While taking into consideration all the data having a direct bearing on the question, it was thought advisable to obtain the fullest possible information with regard to one definite aeroplane. The machine chosen was a B.E. 2c, with wings of R.A.F. 14 section.

3. Full scale tests were carried out at the Royal Aircraft Factory under the direction of Captain Farren, and comprised three series of experiments :—

(i) The determination of the total drag during flight from the horse-power, speed, and propeller efficiency (*see* Appendix I).

(ii) The measurement of the pressure distribution over sections of the upper and lower wings during flight at various attitudes (*see* Appendix II, which includes also similar measurements on a section of the lower wing of a B.E. 2c with old B.E. 2c wing section).

(iii) The direct measurement of the propeller thrust during flight, by a specially designed thrustmeter. (These experiments are still in progress.)

4. The corresponding model experiments were made at the National Physical Laboratory on a complete one-tenth scale model. The work was under the direction, first, of Mr. Bairstow, and later of Dr. Stanton.

The experiments comprised :—

(i) A full determination of the forces and moments on the complete model, and an analysis of the resistances of its separate parts (*see* Appendix III).

(ii) The measurement of the pressure distribution over sections of the upper and lower wings (*see* Appendix IV, which includes also similar measurements on a section of the lower wing of a B.E. 2c with old B.E. 2c wing section).

5. A comparison between the model and full scale results is given in Figs. 1 to 8.

The results of the *pressure plotting* on R.A.F. 14 wings agree closely except with regard to the under surface of the upper wings, the pressures on this surface being consistently lower in the case of the full scale experiments (*see* Fig. 1). There is also a tendency to a higher suction on the upper surface of the upper wing of the model near the nose. It was thought possible that the effect might be due to propeller draught, or to the interference of the body ; direct experiments, however, showed that neither of these factors was responsible for the difference (*see* Figs. 2 and 3). The results on the old B.E. 2c section show more variation (*see* Fig. 4).

Integration of the pressure curves gives the lift and, neglecting viscosity, the drag on the wing surfaces. The lift may be determined in this way with considerable accuracy. For drag determinations the method is not strictly applicable, since the friction of the wings, which is appreciable at small angles of incidence, is neglected, and further at these angles a slight variation of the angle will produce large differences in the components of the forces acting in the direction of the relative wind. The results of the integration are shown in Fig. 5 for R.A.F. 14 and in Fig. 6 for old B.E. 2c section.

6. Figs. 7 and 8 give a comparison between the direct measurement of lift and drag on a model aeroplane, and their determination on the full scale by the method indicated in Section 3 (i).

The curves of lift agree closely except at the stalling angle, where the full scale experiments indicate a higher maximum of lift.

On the drag diagram every full scale experiment is marked by a separate point, and the model experiments are represented by three curves. The dotted curves show an attempt to estimate the drag from some earlier model experiments made on wings of

Comparison of Pressure Plotting on Model & Full Scale Biplane with R.A.F.14 Wings

——— Full scale.

• • • Model Points.

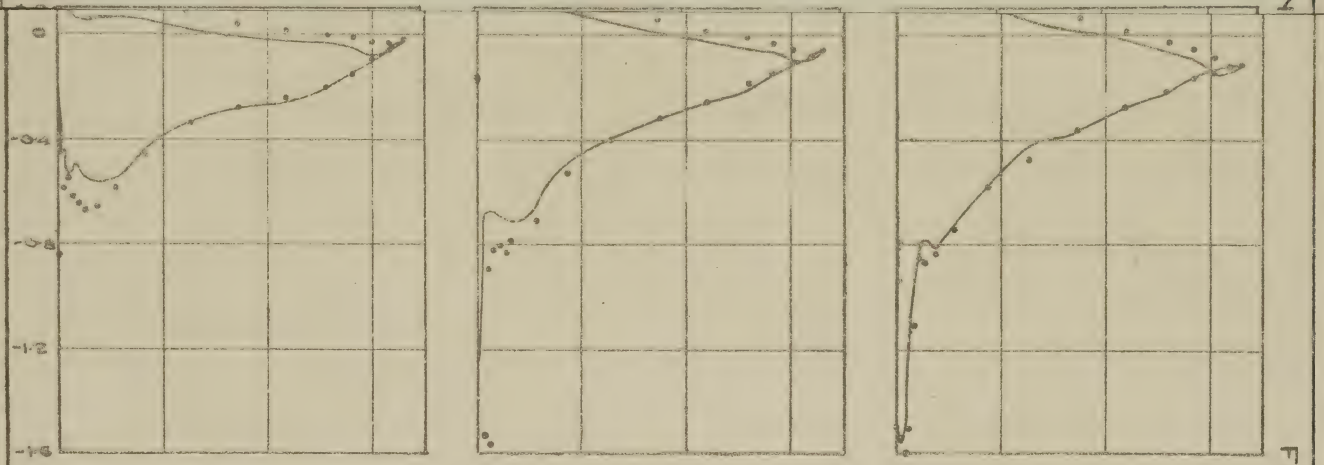

FIG. I.

Comparison of Pressure Plotting on Model & Full Scale Biplane with R.A.F.14 Wings

——— Full scale

• • • Model Points.

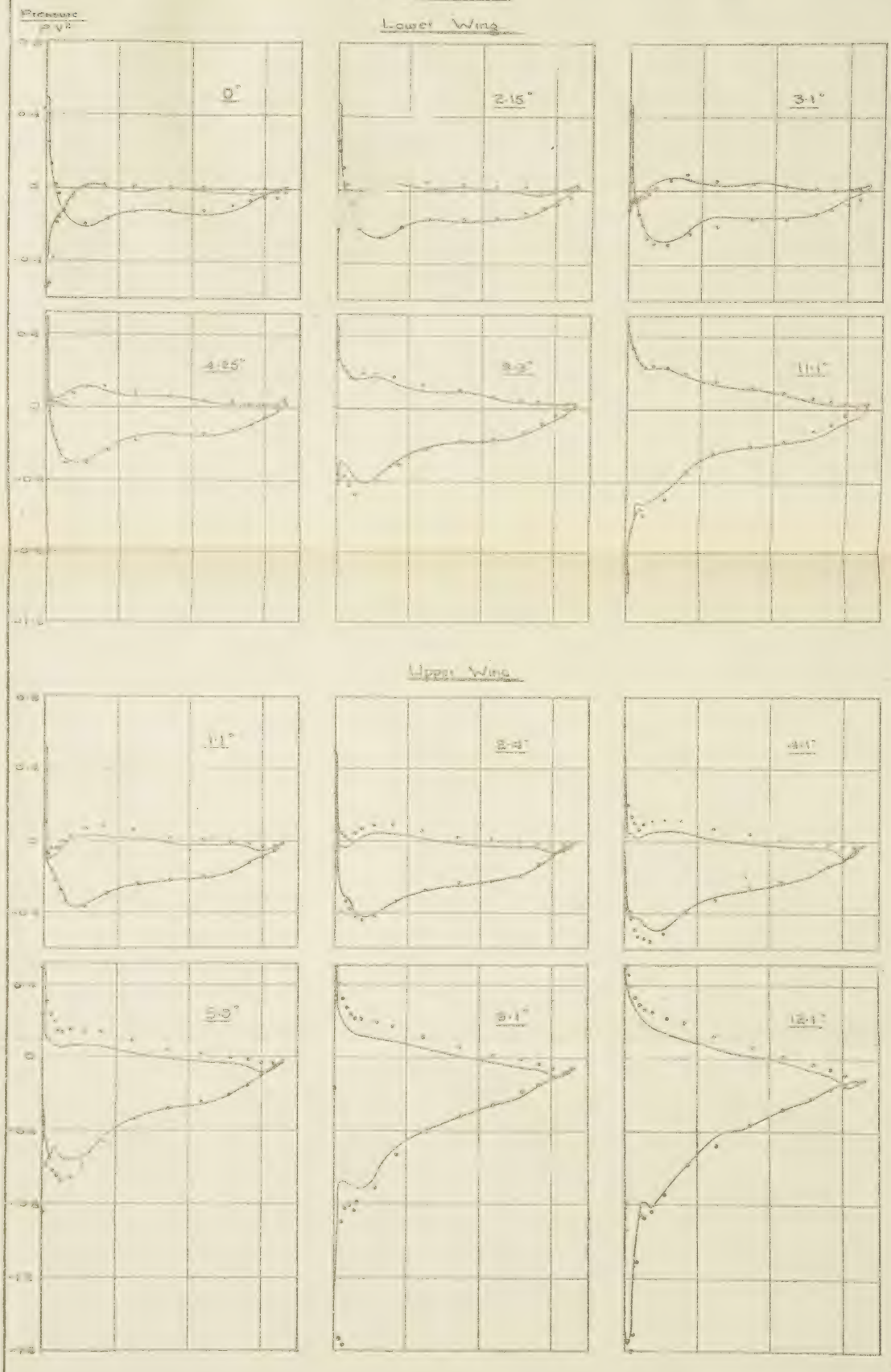

FIG. 1.

REPORT No. 374

FIG. 2

PRESSURE PLOTTING ON R.A.F. 14 WINGS ON B.E.2c MODEL.

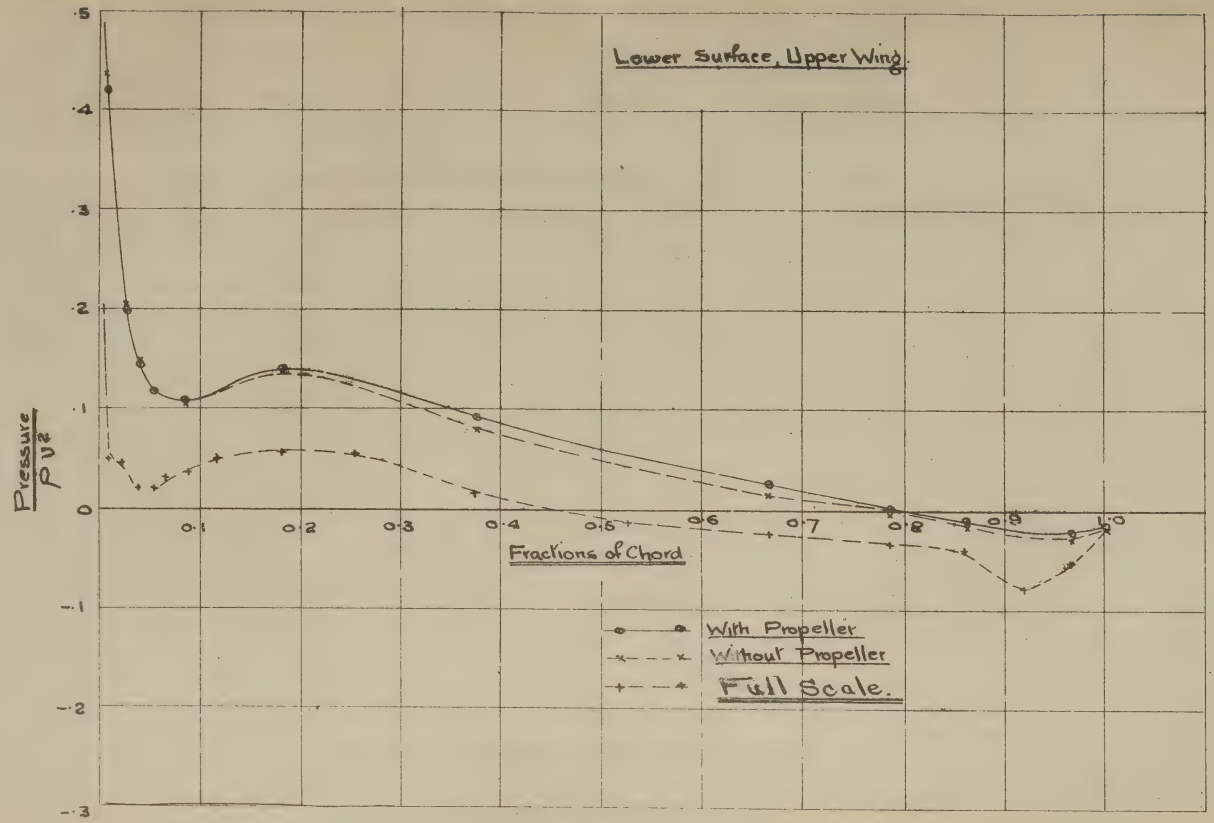

Angle of Incidence 4·1°

P.L.T.

Pressure Plotting on R.A.F 14 Wings on B.E.2c. Model.

— Lower Surface. Upper Wing —

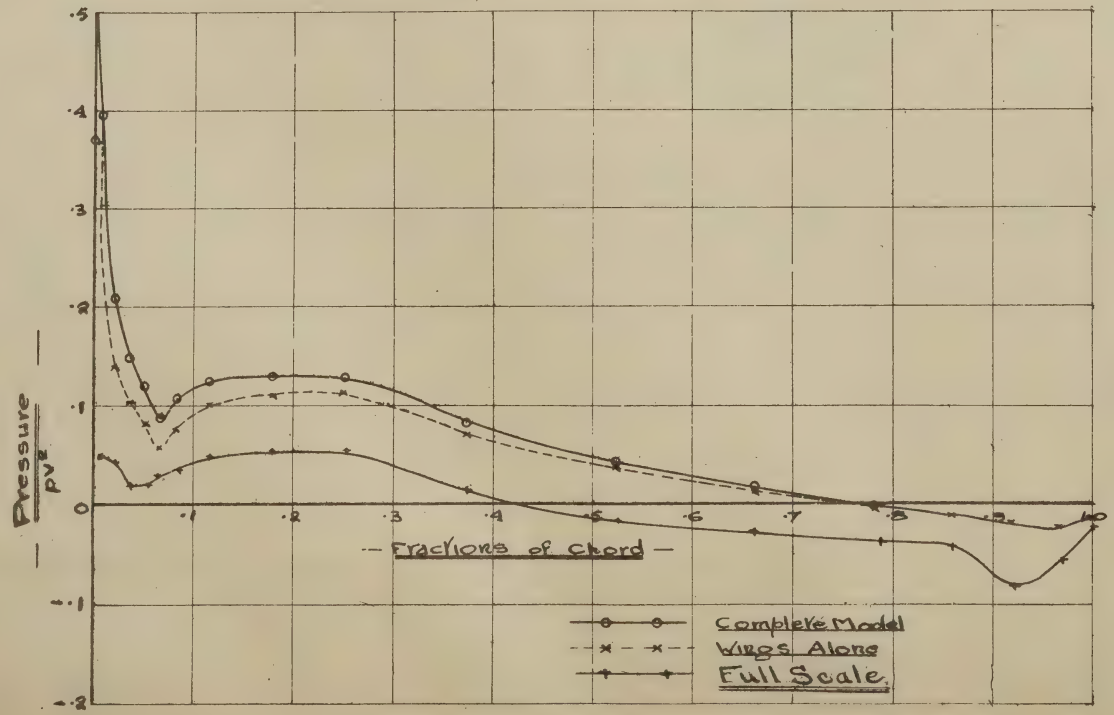

REPORT No 374

FIG. 3.

PRESSURE PLOTTING ON THE LOWER

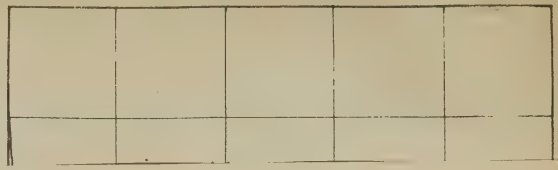

REPORT No. 374.

PRESSURE PLOTTING ON THE LOWER WING OF A B.E.2C BIPLANE WITH OLD B.E.2C WING SECTION.

—*— = MODEL.

—— = FULL SCALE

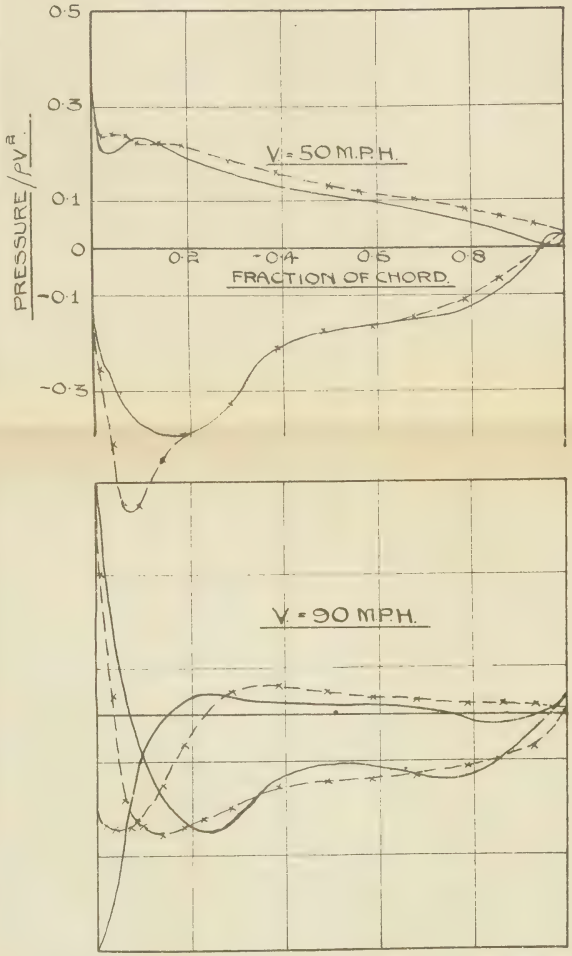

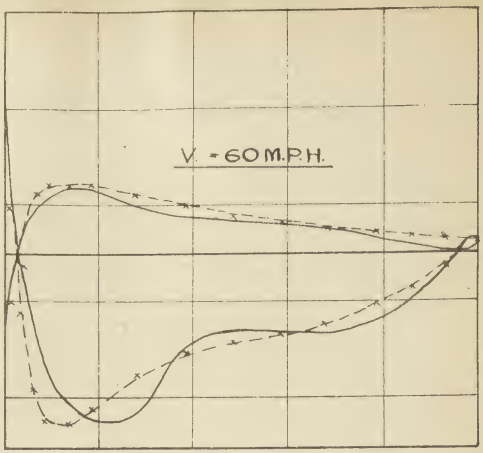

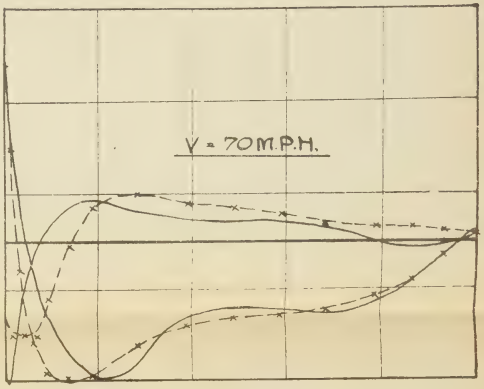

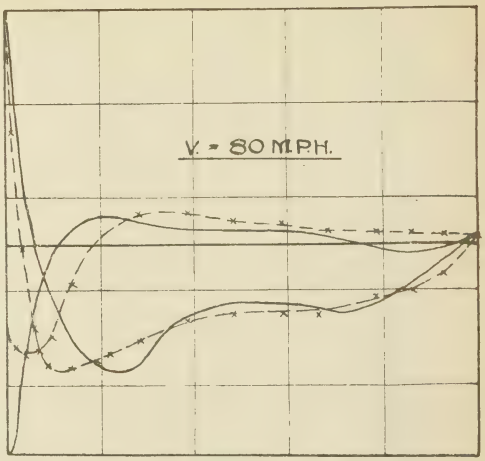

FIG. 4.

COMPARISON OF FORCES DEDUCED FROM PRESSURE PLOTTING.

R.A.F. 14 WING SECTION.

MODEL { UPPER WING ——o——o—— / LOWER WING ——×——×—— } FULL SCALE { UPPER WING ——●——●—— / LOWER WING ——■——■—— }

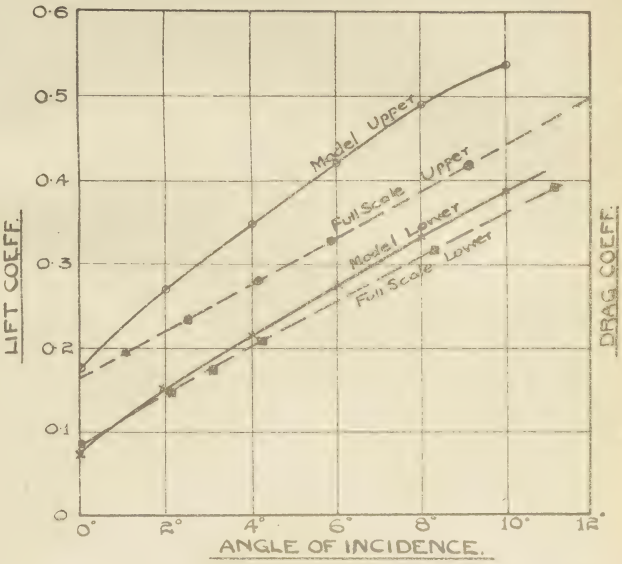

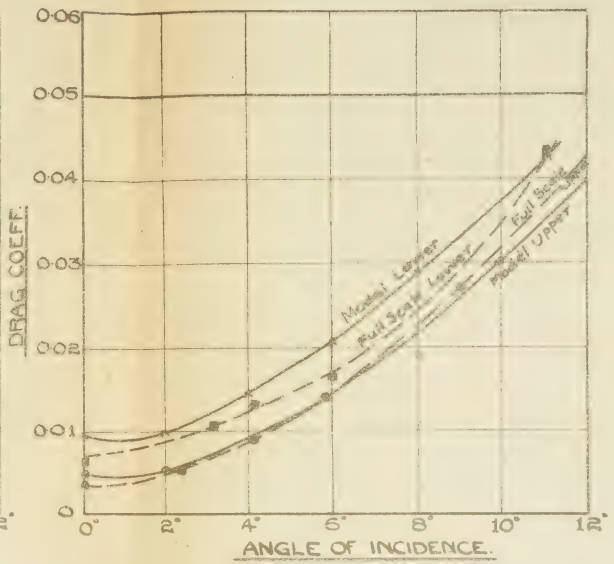

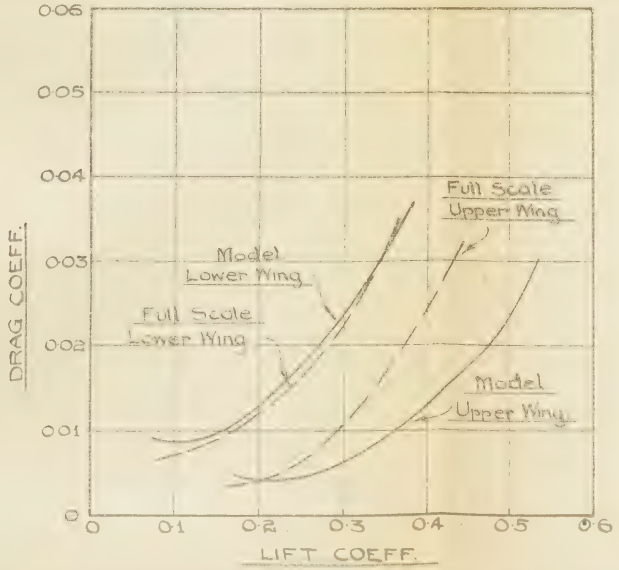

REPORT No. 374.

PRESSURE PLOTTING ON THE LOWER WING OF A B.E.2c BIPLANE WITH OLD B.E.2c WING SECTION.

-o- = MODEL.

-x- = FULL SCALE.

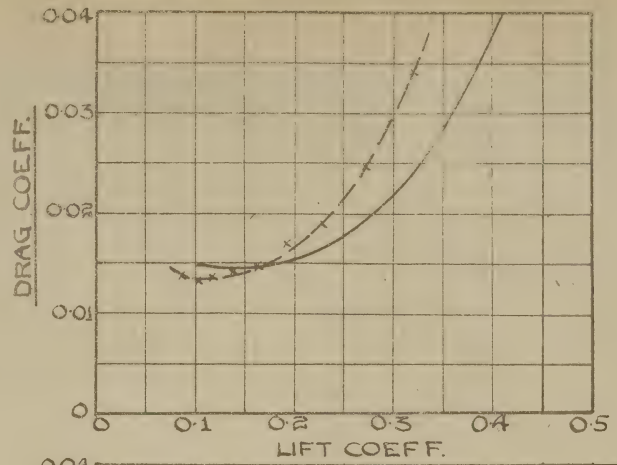

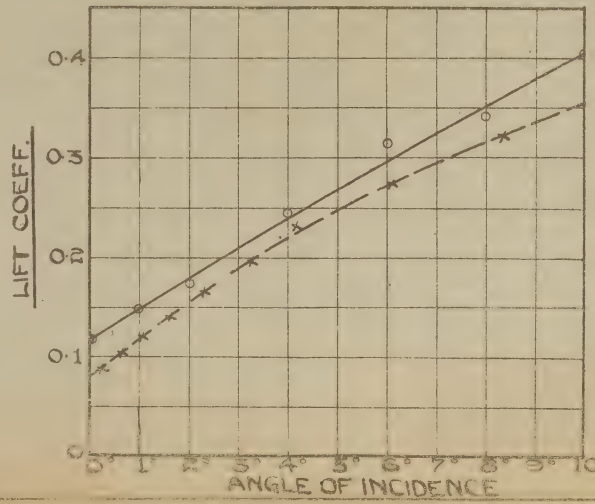

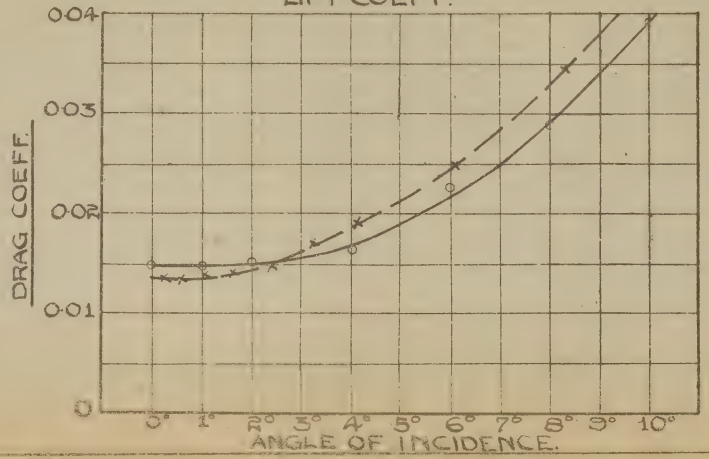

FIG 6.

THE LIBRARY
OF THE
UNIVERSITY OF ILLINOIS

R.A.F. 14 section. These wings were rectangular in plan shape, and were tested as monoplanes. Corrections (deduced from model tests on R.A.F. 6 section) have been introduced for biplane effect, stagger, and for the difference in plan shape. The investigation has shown that it is not possible to deduce with accuracy the properties of a section used as a biplane from determinations on the same section tested as a monoplane; these curves are therefore only included to indicate the order of the error which is likely to arise from this cause. The full curve gives the results deduced from the complete model, one-tenth scale.

7. The most marked difference between the full scale experiments represented in Fig. 8 and the model results is not in the absolute value of the drag coefficient, but in the rate of change of its value at low lift coefficients. A difference of the same order has been found between the full scale results for low lift coefficients shown in Fig. 8 and those obtained from the thrustmeter experiments. No explanation has been found which will account satisfactorily for these differences.

8. Careful consideration of all the available information leads to the following conclusions :—

(i) For the purpose of biplane design model aerofoils must be tested as biplanes, and for monoplane design as monoplanes. The more closely the model wing tested represents that used on the full scale machine, the more reliable will the results be. So long as the differences mentioned in paragraph 7 remain unexplained, no high accuracy can be obtained in the prediction or verification of performance at low lift coefficients.

(ii) Due allowance must be made for scale effect on parts where it is known. In the case of struts, wires, etc., the scale effect is known to be large, but these parts can be tested under conditions corresponding with those which obtain on the full scale machine.

(iii) The resistances of the various parts taken separately may be added together to give the resistance of the complete aeroplane with good accuracy, provided the parts (*e.g.*, the undercarriage) which consist of a number of separate small pieces are tested as a complete unit.

(iv) Model tests form an important and valuable guide in aeroplane design. When employed for the determination of absolute values of resistance, they must be used with discrimination and a full realisation of the modifications which may arise owing to interference and scale effect.

9. In forecasting the performance of a machine of a known type methods can be employed other than the addition of the resistance of all elementary component parts; every designer has at his disposal the full scale test results of a certain number of types of aeroplanes, and where a new design conforms to any one of these types the most satisfactory point of departure for improvement in design is probably given by these test results. For suggestion as to how improvements can be made the designer is still dependent on model tests.

It is of great importance that such information should be increased, and its use extended by further systematic full scale research.

APPENDIX I.

Description of the method of obtaining the Lift and Drag of full scale aeroplane.

(Results given by *points* on Figs. 7 and 8 above.)

I.—Lift Coefficient and Angle of Incidence.

1. The lift coefficient of the wings is derived from the relation

$$k_l = \frac{W - w}{\rho A V^2}$$

where

W = total weight of machine.

w = lift of subsidiary parts (tail, body, etc.).

ρ = air density.

A = effective wing area.

V = speed in ft./sec.

2. The angle of incidence of the wings is found by a fore and aft inclinometer attached to the aeroplane, the inclination of the flight path being found from observations of the rate of climb c. The instrument could be read to one-tenth degree.

3. The various quantities are measured as follows :—

W—by weighing, allowance being made for consumption of fuel during previous part of flight.

w—estimated from model experiments.

ρ—from observations of air pressure and temperature.

A—allowance is made for the extra velocity of the air in the slip stream over the parts of the wings affected by it, as explained below.

V—from readings of air speed indicator, corrected for instrumental error and also for error of pressure head due to interference of the aeroplane on it by doing runs at various speeds over a measured speed course.

c—(in feet per sec.) from readings of aneroid at intervals in the flight, corrected for temperature.

4. The correction for the slip stream is applied as follows :—

The force (lift or drag) on any part of the aeroplane in the slip stream *except the body* is taken to be increased in the ratio $(1 + v/V)^2$ where v is the relative slip stream speed. v is calculated by equating the momentum given to the stream per second to the total thrust, and the stream is taken to have an external diameter 0·8 and internal diameter 0·2 of the diameter of the airscrew. (These figures are obtained from full scale experiments.)

The force *on the body* is taken to be increased in the ratio 3/4 $(1 + v/V)^2$. The factor 3/4 is deduced from a model experiment, and is considered to represent the shielding of the body by the airscrew boss.

The wing area is therefore usually expressed as follows :—

$$A = A_1 + (1 + v/V)^2 A_2$$

where

A = effective wing area,

A_1 = area not in slip stream,

A_2 = area in slip stream,

and

$A_1 + A_2$ = total wing area as ordinarily measured.

5. Each point shown in Fig. 7 above was obtained as the result of about ten minutes' steady flight.

6. The maximum lift coefficient was obtained by flying at the lowest possible steady speed. The determination of this is very difficult, and the accuracy of the result is not so good as that of the other points. The experiment was, however, repeated many times.

II.—Drag Coefficient.

7. The drag coefficient is derived from the relation

$$k_d = \frac{T - \frac{Wc}{V}}{\rho A V^2}$$

where T = propeller thrust (lbs.).

This quality is determined from the relation

$$T = \frac{B \eta 550}{V}$$

where

B = engine b.h.p.

η = airscrew efficiency.

8. B was found from the observed engine revolutions, and a correction applied to the standard engine test result for the density of the air, the power at any given revolutions being taken to vary as $\rho^{1.1}$ in accordance with experiments on the same type of engine.

η was found from tests on the full size airscrew on the R.A.F. whirling arm, and the observed value of V/N.

9. It was found that the direct use of the airscrew *thrust* at the observed V/N as derived from whirling arm experiments gave points which, although consistent for different speeds in any one flight, were inconsistent from day to day, the inconsistencies being too large to be explained as due to up and down

currents. Measurements of airscrews showed that these warped from day to day sufficiently to explain the inconsistency. It can be shown, however, that, although a given warp may change the thrust at a given V/N by a large amount, the efficiency will be hardly altered, and hence the method described was used.

10. The curve of engine b.h.p. revolutions used was found by averaging the tests of a number of engines of the same type (R.A.F. 1A), as it was not at the time convenient to test the actual engines used.

Since that date, however, a number of engines used in the experimental aeroplanes have been tested, and have been found to give power curves which are very nearly parallel to the mean curve and vary above or below it up to about 3 b.h.p.

11. The spread of the points on Fig. 8 above is therefore due to :—

(i) up and down currents ;

(ii) variation in power of engine from standard (about $\pm$ 2 per cent. on the average) ;

(iii) slight effect of warp of airscrew on efficiency.

12. It may be remarked that it is assumed that the presence of the end of the whirling arm behind the airscrew produces the same effect on the efficiency, etc., as the presence of the body of the aeroplane. The resistance of the end of the arm, as now faired in, is nearly the same as the resistance of a B.E. 2c body.

APPENDIX II.

Measurement of the Pressure Distribution round sections of the top and bottom wings of an aeroplane in flight.

(*a*) R.A.F. 14 section (both wings).

(*b*) Old B.E. 2c section (bottom wing only).

SUMMARY.—Simultaneous measurements of the pressures at various points round sections of the top and bottom wings of a B.E. 2c were made by means of an apparatus which registered photographically the heights of liquid in a number of manometer tubes. Observations were made at speeds ranging from 42 to 95 m.p.h.

The pressures were integrated, and the normal and longitudinal forces and the moments, which act on the wing at the experimental sections, were found.

Inclinometer measurements of the angle of incidence corresponding to a given lift coefficient were then used to deduce the lift and drag coefficient of the sections.

The principal experiment was carried out with R.A.F. 14 section wings, but the experiment has also been done with old B.E. 2c section on the lower wing only. These two sections are shown in Fig. 23.

(*a*) EXPERIMENTS WITH R.A.F. 14 WINGS.

1. The experiments were carried out on a B.E. 2c with R.A.F. 14 section wings. Pressures were measured over ribs in the right lower plane and the left upper plane, the rib being situated in each case 7 ft. 8 in. (that is, 0·414 of the semi-span of the wings) from the centre line of the body. In each rib there were thirty-four holes (the positions of which are given in Table 1) connected by tubes to the pressure recording apparatus in the passenger's seat.

2. In order to avoid any effect due to the wing having a scalloped surface, the wing surface in the neighbourhood of the holes was made smooth, the span for about $1\frac{1}{2}$ ft. on either side of the holes being covered with sheet aluminium, and the fabric fixed to this sheet with marine glue. The holes were made by brazing the tubes to a brass rib so that they projected through this aluminium sheet, the ends being afterwards filed down flush with the outside surface.

3. The pressures at the holes were measured simultaneously by means of an apparatus shown in Fig. 9, which consisted of twenty glass manometer tubes connected at their lower ends to

a reservoir which was full of alcohol. Their upper ends were connected by means of rubber tubes with the pipes which led through the interior of the wing to the pressure holes. When the aeroplane was at rest the alcohol stood about half-way up the tubes.

4. When the aeroplane was in flight the height of the liquid in the tubes connected with the various holes registered the pressure at the holes. These heights were recorded photographically. A small electric light, some ten inches from the tubes, was used to cast shadows of the columns of liquid on to some bromide paper, which could be wound between two light-tight boxes past the tubes. The bromide paper was pressed up against the tubes by means of a back (shown leaning up against the apparatus in Fig. 9), and the whole apparatus was shut in by a hinged, light-tight door (shown open in Fig. 9). To make an exposure the small electric light was switched on for half a second.

5. Provided that the experiments were made in really calm air, and the air speed kept reasonably steady, the shadow of the meniscus at the top of the alcohol was very sharp, and it was possible to read the height of the liquid in the tube to $\frac{1}{100}$th of an inch. A specimen of the records is shown in Fig. 10.

6. The whole apparatus was hung in the aeroplane by rubber suspensions, so that it might not be affected by the vibration of the aeroplane.

7. In order to measure the height of the meniscus at the top of the fluid in each tube it was necessary to know what direction in the plane of the photograph was horizontal. For this purpose the two outside tubes in the apparatus were both connected with the static pressure side of the pitot tube. A straight line was drawn on each photograph touching the two outside meniscuses, and this was used as a base line from which the pressures in the other tubes were measured. This line is shown in Fig. 10.

8. The apparatus contains twenty manometer tubes. Of these the two outside tubes connected throughout with the static side of the pitot head, and the central tube with the pressure side. The remaining seventeen tubes were connected with the pressure holes on the planes. In all, sixty-four photographs were taken, each photograph recording the pressures over the whole of the one of the four surfaces—seventeen holes. The photographs were taken at air speeds ranging from 42 m.p.h. to 90 m.p.h.

9. From the results obtained on these photographs the pressure at any given hole was plotted as a multiple of ρV^2 against the lift coefficient, K_l, of the whole aeroplane, corrected

for tail lift only. For each photograph the depth h, below the static line in inches of the liquid in the tube connected to the pressure side of the pitot head, was measured. It was found by calibrating the airspeed indicator over a measured speed course that the pressure at the pitot head on this particular aeroplane was not exactly $= \frac{1}{2} \rho V^2$, but was equal to $\frac{1}{2} \rho V^2 / f^2$ where the factor f varied for different airspeeds, having a mean value of about 1·04. Thus the number of inches of liquid corresponding to ρV^2 for any particular photograph is equal to $2 f^2 h$ where f is appropriate to the airspeed at which the photograph was taken, and the pressure at any given hole is found as a multiple of ρV^2 by dividing the height of the liquid in its tube by $2 f^2 h$.

The value of K_l for a particular photograph depends on the airspeed. It was thought more accurate to use the value of h to determine this, and not the value observed on the airspeed indicator, since the latter cannot be read to less than $\frac{1}{2}$ m.p.h. At the time of taking each photograph, the airspeed was observed on the indicator connected with the same pitot head as that connected with the photographic apparatus. The mean value, K, was taken of

$$\frac{h}{(\text{Observed airspeed, corrected for calibration of the instrument})^2}$$

for all photographs taken in one flight. The value of ρV^2 was therefore $\frac{hf^2}{K}$.

10. Smooth curves of $\frac{\text{pressure}}{\rho V^2}$ against K_l were drawn through the experimental points obtained by measuring the photographs. The experimental points lay very close to these smooth curves—the average error not amounting to more than $0{\cdot}005 \rho V^2$.

11. In order to estimate the total forces acting on the experimental sections of the aerofoil it is necessary to integrate the pressures over it. From the smooth curves drawn through the experimental points curves were plotted showing the $\frac{\text{pressure}}{\rho V^2}$ round the aerofoil as a function of x—the distance from the leading edge parallel to the chord—and also as a function of y, the distance above and normal to the chord. These curves are shown in Figs. 11 and 12. They are drawn for different values of K_l, the lift coefficient of the whole aeroplane corrected only for tail lift. The areas of these curves, when integrated by means of a planimeter, give the total normal and longitudinal force coefficients of the experimental section of the aerofoil.

12. Curves were also plotted of $\frac{\text{pressure}}{\rho V^2} \times x$ against x. These curves are shown in Fig. 13. Their areas give that part of the moment coefficient due to the components of pressure perpendicular to the chord ; the part due to components parallel to the chord is so small as to be negligible.

13. In order to obtain the lift and drag coefficients due to the pressures on the whole rib, it is necessary to know the incidence of the wings. The mean incidence, θ, of all four wings is deduced from K_l—corrected for tail lift only—by means of the standard R.A.F. 14 lift curve compiled from inclinometer experiments. In the particular aeroplane used the right lower plane had 0°26′ less, and the left upper plane 0°28′ more incidence than the mean incidence of all four wings. Thus—for the lower wing—

$$\overline{K_l} = \overline{K_z} \cos (\theta - 0{\cdot}43)^\circ - \overline{K_x} \sin (\theta - 0{\cdot}43)^\circ$$
$$\overline{K_d} = \overline{K_z} \sin (\theta - 0{\cdot}43)^\circ + \overline{K_x} \cos (\theta - 0{\cdot}43)^\circ$$

and for the upper wing—

$$\overline{K_l} = \overline{K_z} \cos (\theta + 0{\cdot}47)^\circ - \overline{K_x} \sin (\theta + 0{\cdot}47)^\circ$$
$$\overline{K_d} = \overline{K_z} \sin (\theta + 0{\cdot}47)^\circ + \overline{K_x} \cos (\theta + 0{\cdot}47)^\circ$$

($\overline{K}$ being used where the coefficient is deduced from the pressures at the experimental holes).

14. In Fig. 14 will be found $\overline{K_l}$, plotted against $\overline{\theta}$ (the incidence of the actual rib where the holes were) both for the upper and the lower wings, and also the mean $\overline{K_l}$ against the mean $\overline{\theta}$ for the two wings together. The latter represents the lift curve of a section of both wings of a biplane taken about two-fifths way out along the span. It is seen that the lift coefficient of the upper wing is about 0·075 greater than that of the lower wing at the same angle of incidence.

15. In Fig. 15, $\overline{K_d}$ is plotted against $\overline{K_l}$ for each of the two ribs of pressure holes ; the mean $\overline{K_d}$ for the two wings is also plotted against the mean K_l. This represents the drag curve of a section of both wings of a biplane taken about two-fifths way out along the span. It will be seen that the upper wing is considerably more efficient than the lower wing as regards lift/drag ratio. (It is to be observed that $\overline{K_d}$ takes no account of skin friction, and does not therefore represent the true drag coefficient).

16. In Fig. 16 the various drag coefficients (again excluding skin friction) are all plotted against the mean K_l for the whole aeroplane corrected for tail lift only. It is seen that when the aeroplane is flying at any given mean K_l, *i.e.*, at any given mean incidence, the drag of the lower wing is greater than that of the upper wing.

17. In Fig. 17, $\overline{K_m}$, the moment coefficient, is plotted against $\overline{K_l}$ both for the upper and the lower wings ; and also the mean $\overline{K_m}$ for the two wings is plotted against the mean $\overline{K_l}$.

N.B.—It was not until the working out of these experiments was very nearly complete that the latest R.A.F. 14 model K_m curve became the standard curve in use. $(K_l - \text{Eff}.K_l)$ is therefore calculated throughout on the basis of the old R.A.F. 14 K_m curve—now out of date. In order to obtain mean incidence θ, K_l must, as a matter of fact, be so calculated, since it was so calculated in the standard R.A.F. 14 lift curve. But whenever K_l is expressly represented to be " the lift of the whole of both wings corrected for tail lift only " it should strictly be calculated on the basis of the new K_m curve, and in this report this has been done when finally the various coefficients are plotted against mean K_l (*i.e.*, in Fig. 16, but nowhere else).

(*b*) Experiments with old B.E. 2c Section Wings.

1. These experiments were carried out previously to those with R.A.F. 14 wings just described. The procedure adopted was the same, however, except for the following differences :—

(*a*) The bottom wing only was tested.

(*b*) Only nine holes were used in each surface of the experimental section instead of seventeen, the number used in the experiments just described. The positions of these holes are given in Table 2 in terms of co-ordinates x and y ; x and y are expressed as fractions of the chord.

(*c*) The surface of the wing in the neighbourhood of the experimental section was not made smooth with sheet aluminium, but was left scalloped.

(*d*) It was thought possible that rapid fluctuations of pressure would exist, and, in order to damp out resulting rapid movements of the liquid in the tubes the rubber pipes connecting these with the alcohol reservoir were constricted, so that the time taken by the liquid to come to rest after a sudden change in pressure was about 15 seconds. In the experiments with R.A.F. 14 wings these constrictions were removed, and it has been found that there was no need for them, photographs taken with as much as 4 seconds exposure giving perfectly sharp outlines.

(*e*) The $\frac{\text{pressures}}{\rho V^2}$ were plotted against indicated airspeed, instead of against K_l. This is an approximation, since it assumes a constant weight and a constant effective wing area and a constant tail lift throughout the experiments. But the error here involved is very small.

(*f*) The wing at the section tested had 0°·3 less incidence than the mean, and this correction was therefore applied in calculating the incidence of the experimental section from the indicated airspeed.

2. The results will be found plotted in Figs. 18, 19, 20, 21 and 22. Fig. 18 shows the normal force areas at various indicated airspeeds ; Fig. 19 the longitudinal force areas ; and Fig. 20 the moment areas. In Figs. 21 and 22 are shown the lift and moment coefficients and the drag coefficient of the experimental section deduced from the integrated pressures, plotted against the lift coefficient of the whole aeroplane with no corrections for tail or other subsidiary lifts. In the drag coefficients (Fig. 22) no correction is made for skin friction.

Table 1.

POSITIONS OF HOLES FOR R.A.F. 14 WINGS.

Lower Wing.

Upper Surface.			Lower Surface.		
Hole No.	x	y	Hole No.	x	y
1	0·00	0·38	1	0·70	0·03
2	0·70	1·10	2	1·65	0·00
3	1·60	1·60	3	2·55	0·00
4	2·55	2·07	4	3·50	0·00
5	3·40	2·44	5	4·35	0·03
6	4·30	2·76	6	5·85	0·16
7	5·75	3·26	7	7·90	0·38
8	7·80	3·69	8	11·80	0·69
9	11·75	4·32	9	17·80	0·84
10	17·80	4·57	10	24·80	0·78
11	24·70	4·51	11	34·80	0·72
12	34·70	4·32	12	43·70	0·53
13	43·80	3·88	13	51·80	0·28
14	51·80	3·07	14	56·80	0·19
15	56·70	2·32	15	60·80	0·12
16	60·80	1·57	16	63·80	0·06
17	63·90	0·94	17	66·00	0·38

Upper Wing.

1	0·00	0·38	1	0·80	0·06
2	0·80	1·16	2	1·70	0·00
3	1·70	1·66	3	2·60	0·00
4	2·55	2·07	4	3·45	0·00
5	3·45	2·45	5	4·40	0·03
6	4·30	2·79	6	5·90	0·12
7	5·80	3·23	7	7·90	0·34
8	7·80	3·70	8	11·90	0·66
9*	11·80	4·26	9	17·80	0·84
10	17·80	4·51	10	24·80	0·78
11	24·80	4·51	11	34·80	0·59
12	34·90	4·26	12	43·80	0·47
13	43·80	3·88	13*	51·80	0·31
14	51·80	3·04	14	56·80	0·19
15	56·85	2·26	15	60·80	0·06
16	60·80	1·60	16	63·90	0·00
17	63·90	1·10	17	66·10	0·41

* These holes were never used.

x = distance from leading edge parallel to chord, in inches.
y = height above chord, in inches.

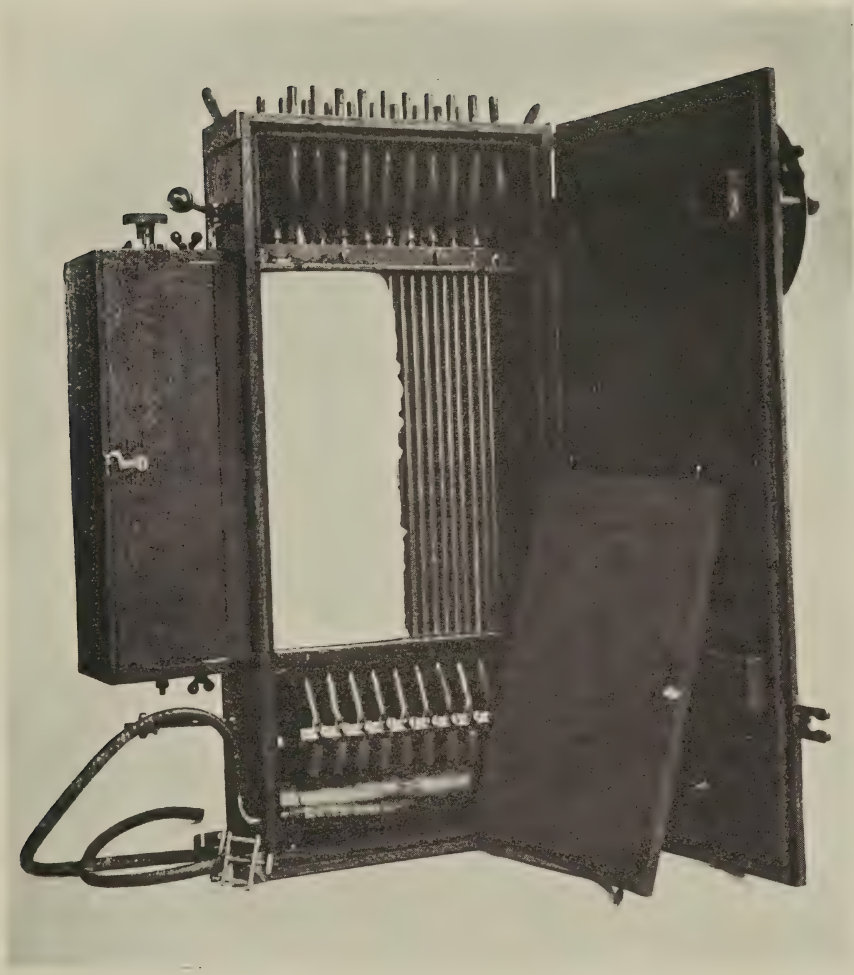

Pressure Recording Instrument.

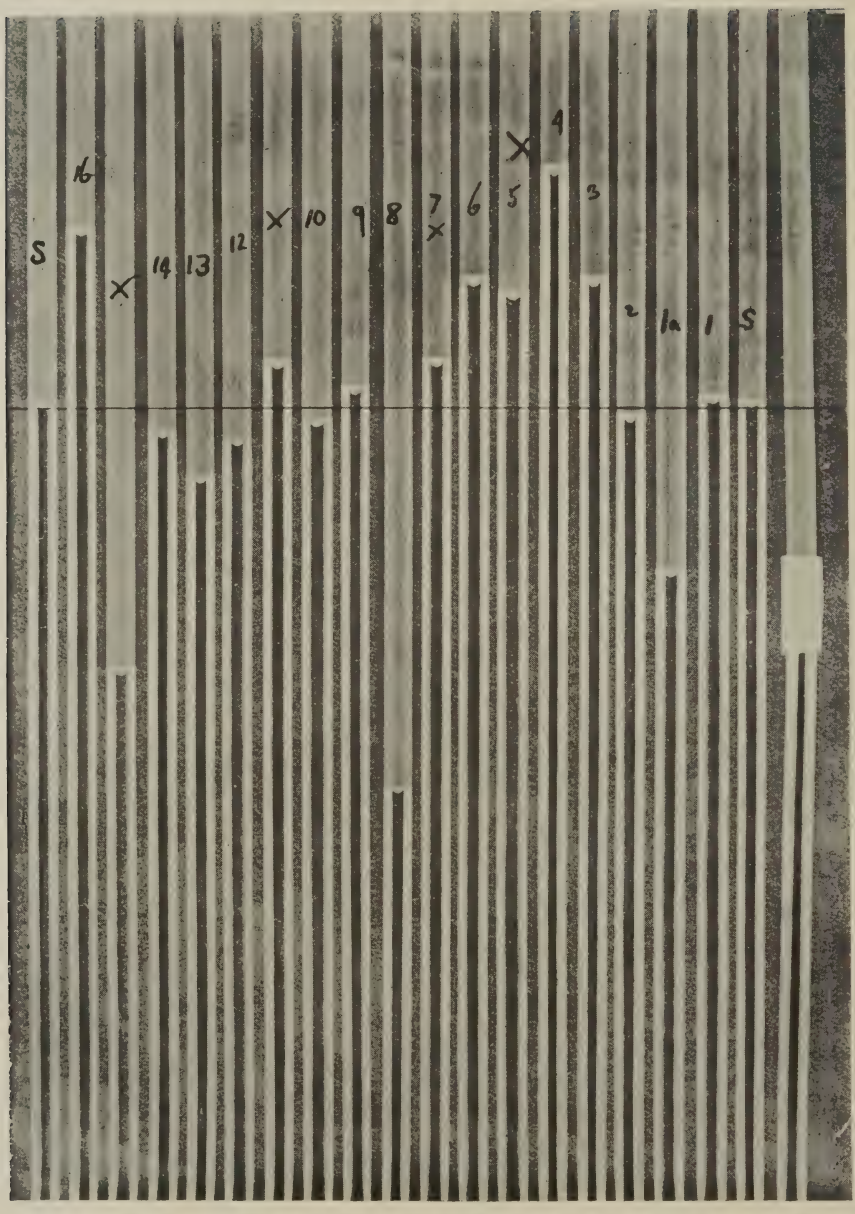

Specimen of Record.

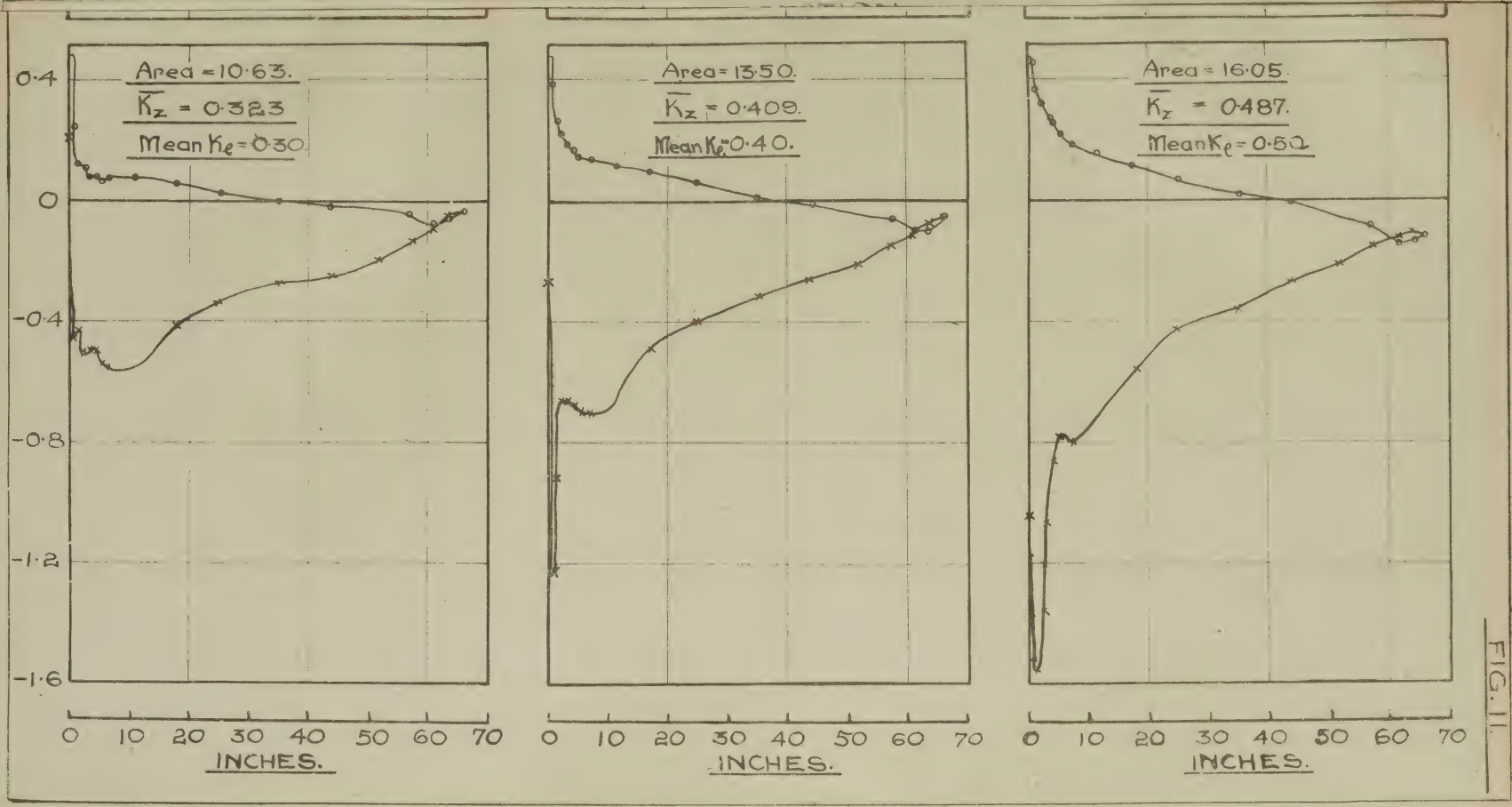
Area = 10·63.
$\bar{K}_z$ = 0·323
Mean K_e = 0·30
Area = 13·50.
$\bar{K}_z$ = 0·408.
Mean K_e = 0·40.
Area = 16·05.
$\bar{K}_z$ = 0·487.
Mean K_e = 0·50
0·4
0
-0·4
-0·8
-1·2
-1·6
0 10 20 30 40 50 60 70
INCHES.

FIG. 11.

R.A.F. 14 WING SECTION.

NORMAL FORCE AREAS.

LOWER WING.

x = UPPER SURFACE.

o = LOWER SURFACE.

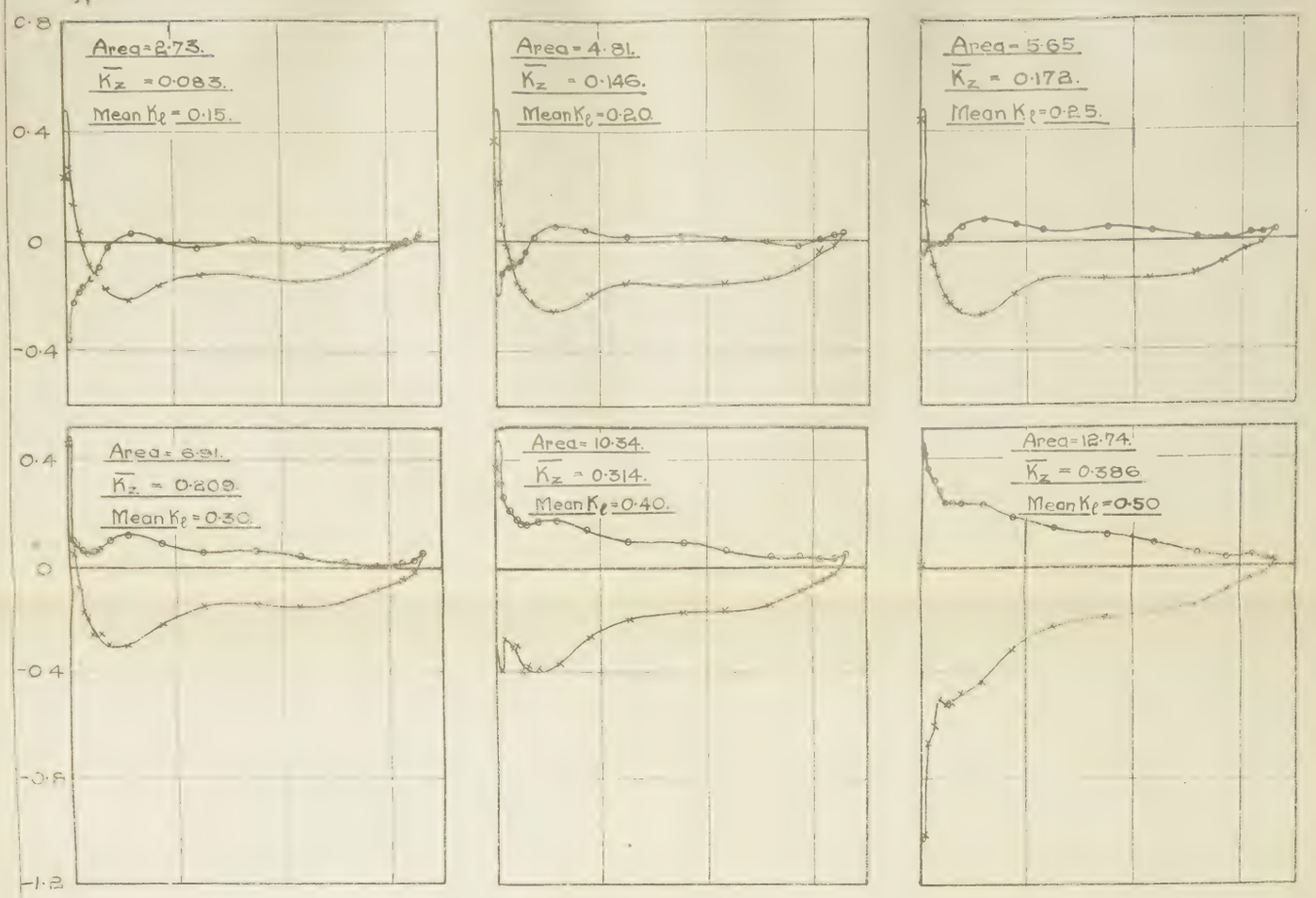

UPPER WING.

x = UPPER SURFACE.

o = LOWER SURFACE.

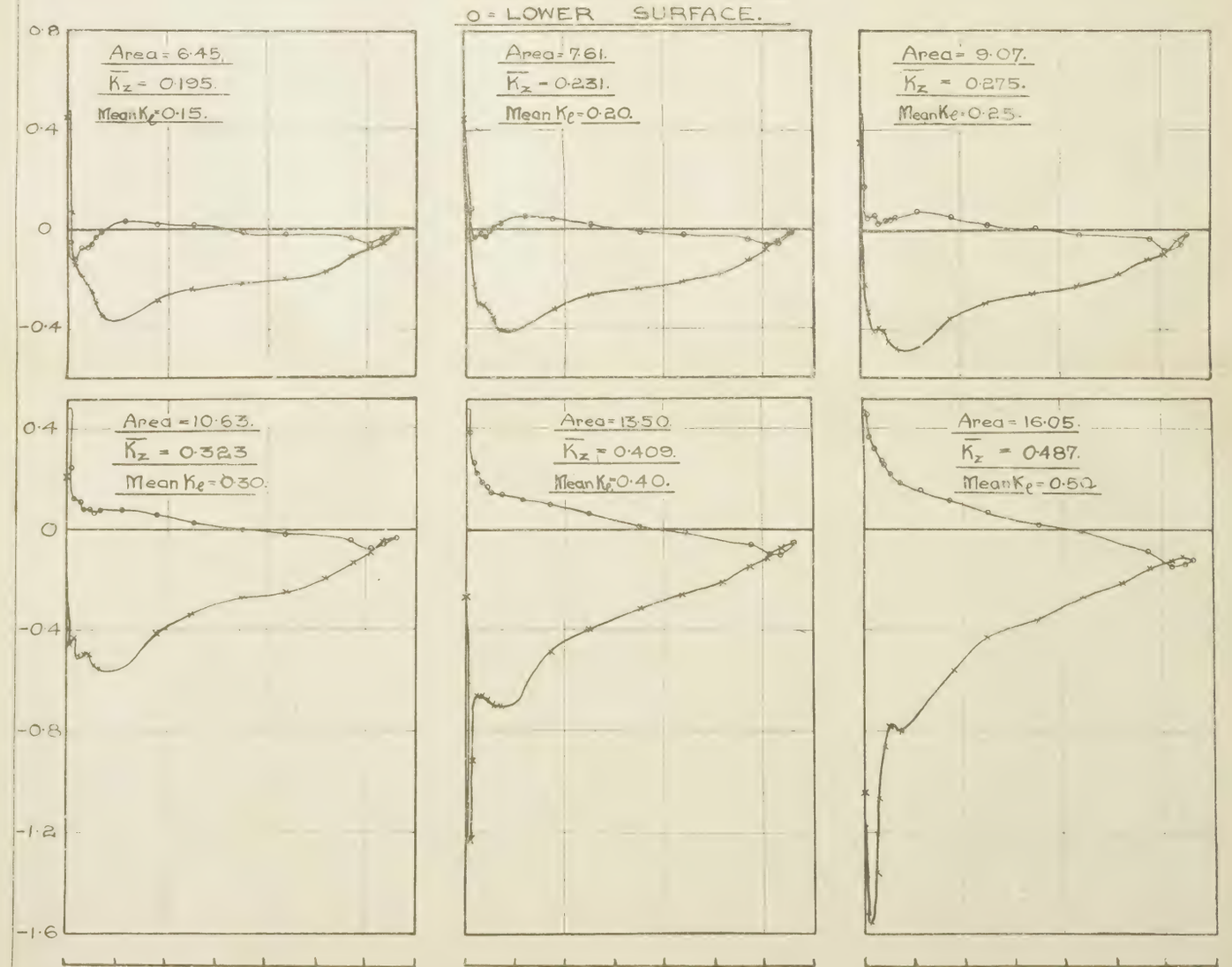

REPORT No. 374 Appendix II.

FIG. 11.

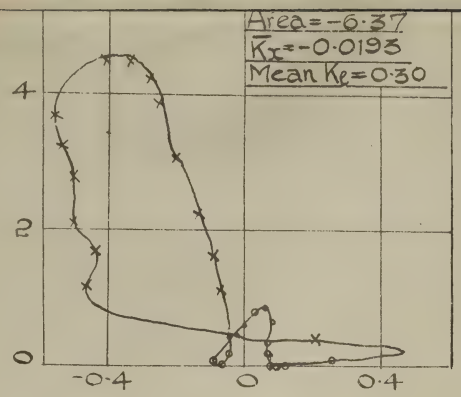

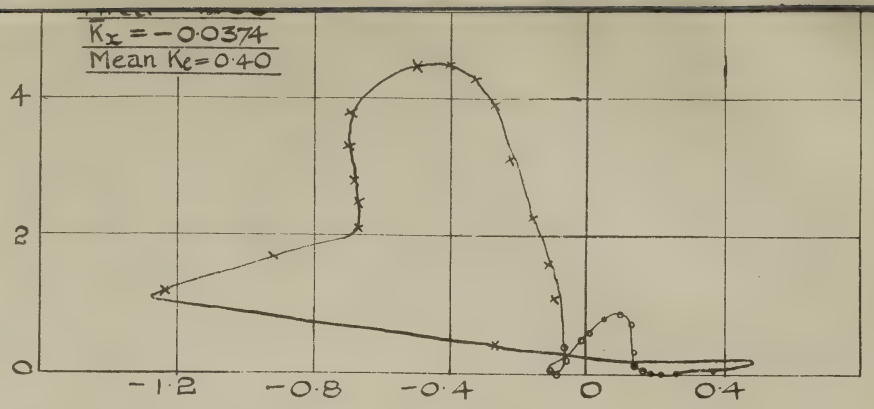

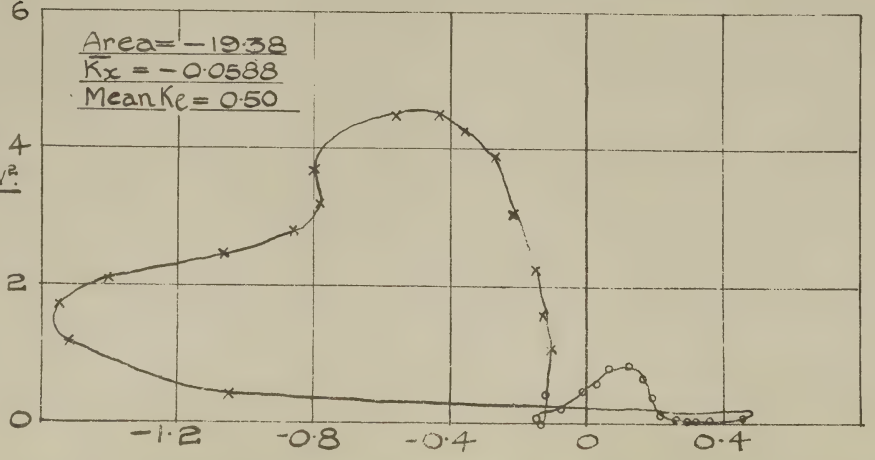

ORDINATES = INCHES.
ABSCISSAE = PRESSURE/eV^2.

FIG. 12

R.A.F. 14 WING SECTION.
LONGITUDINAL FORCE AREAS.

LOWER WING.

x = UPPER SURFACE

o = LOWER SURFACE.

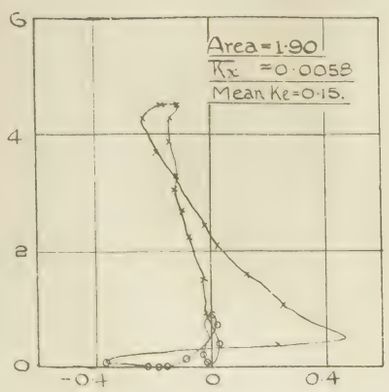

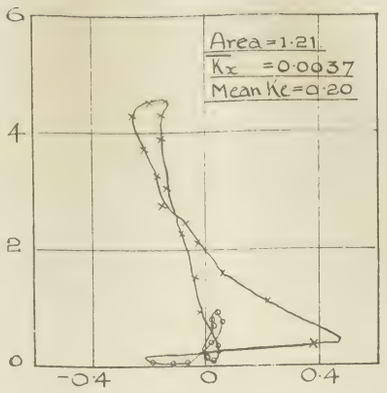

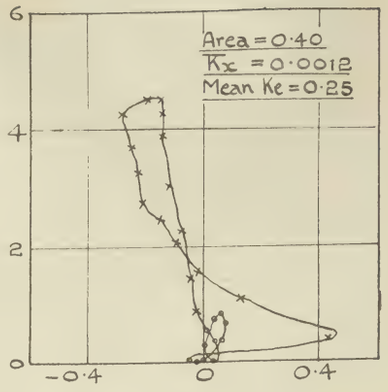

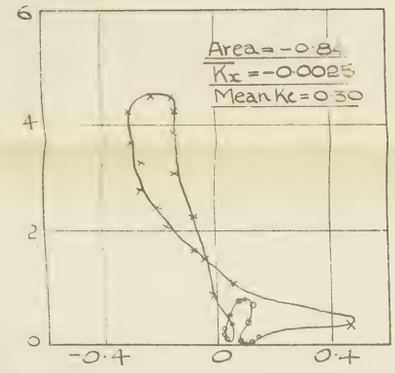

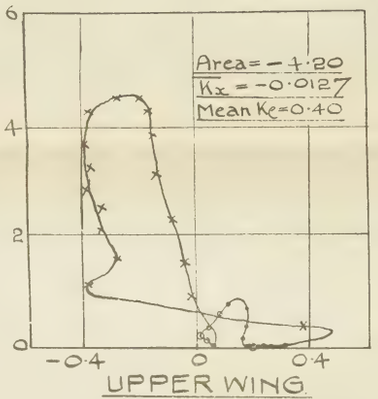

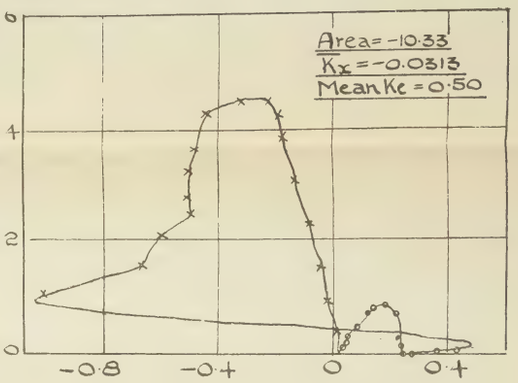

UPPER WING.

x = UPPER SURFACE

o = LOWER SURFACE.

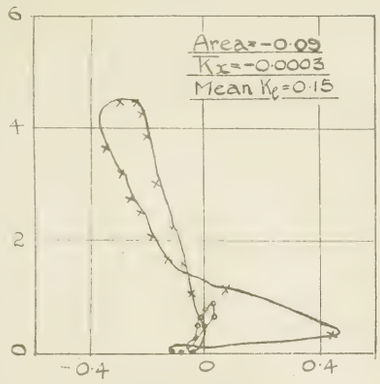

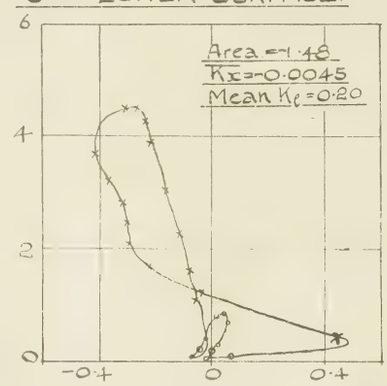

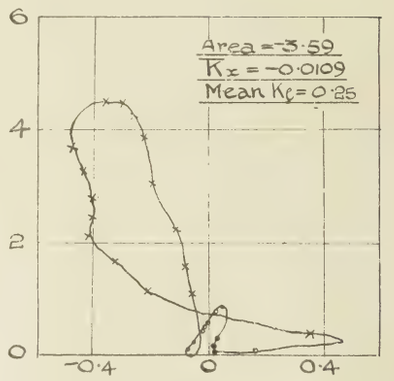

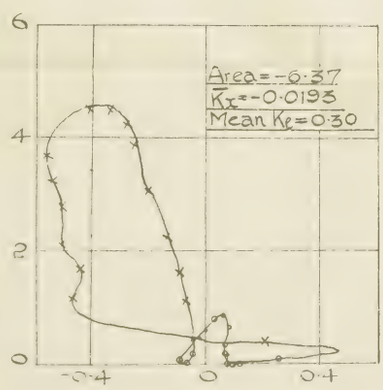

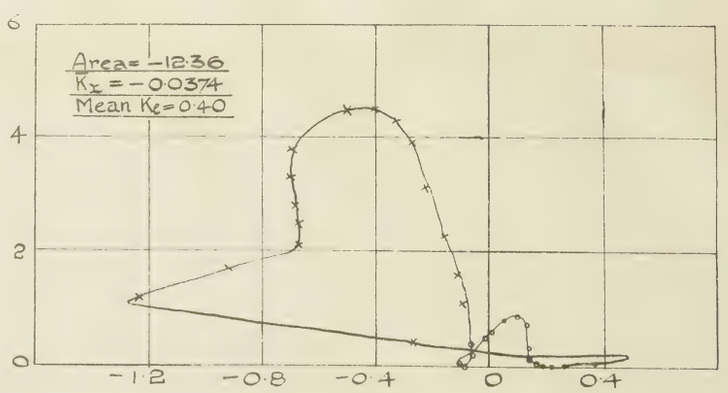

ORDINATES = INCHES.

ABSCISSAE = PRESSURE/ρV^2.

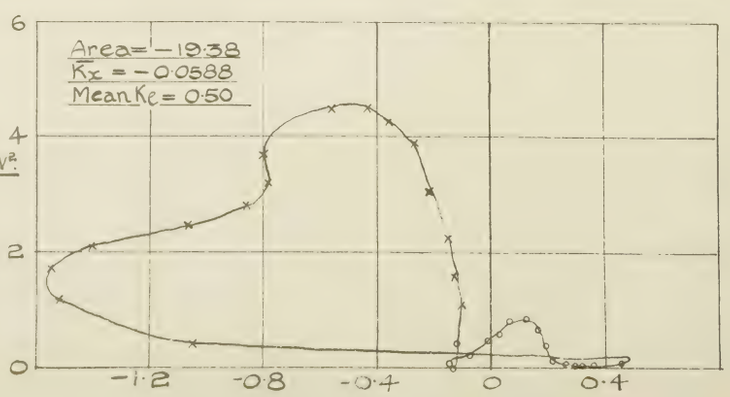

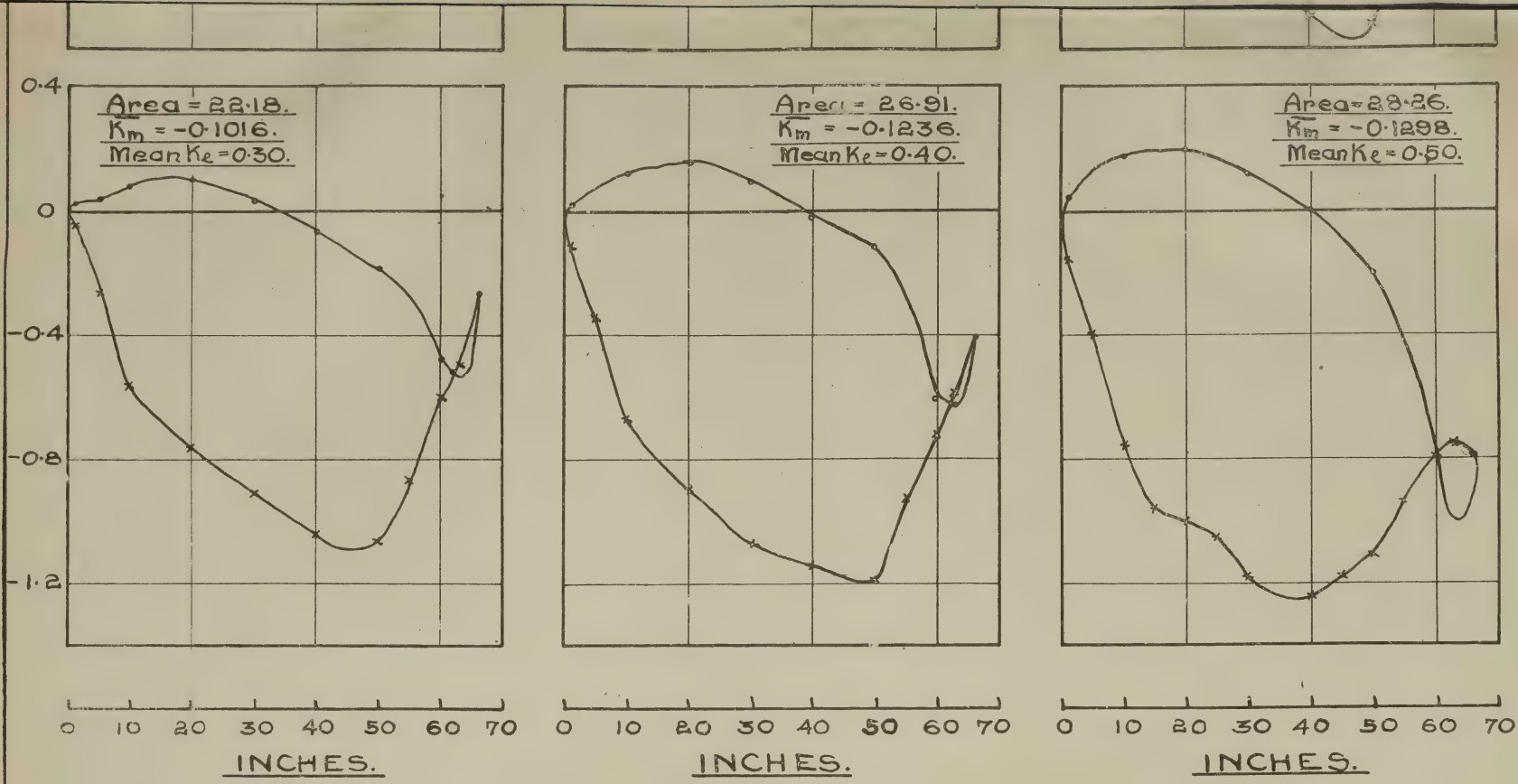
0·4
0
-0·4
-0·8
-1·2
Area = 28·18.
Km = -0·1016.
Mean Ke = 0·30.
Area = 26·91.
Km = -0·1236.
Mean Ke = 0·40.
Area = 28·26.
Km = -0·1298.
Mean Ke = 0·50.
0 10 20 30 40 50 60 70
INCHES.
0 10 20 30 40 50 60 70
INCHES.
0 10 20 30 40 50 60 70
INCHES.

FIG. 13.

R.A.F. 14 WING SECTION.
WING MOMENT AREAS.

LOWER WING.

X = UPPER SURFACE.
O = LOWER SURFACE.

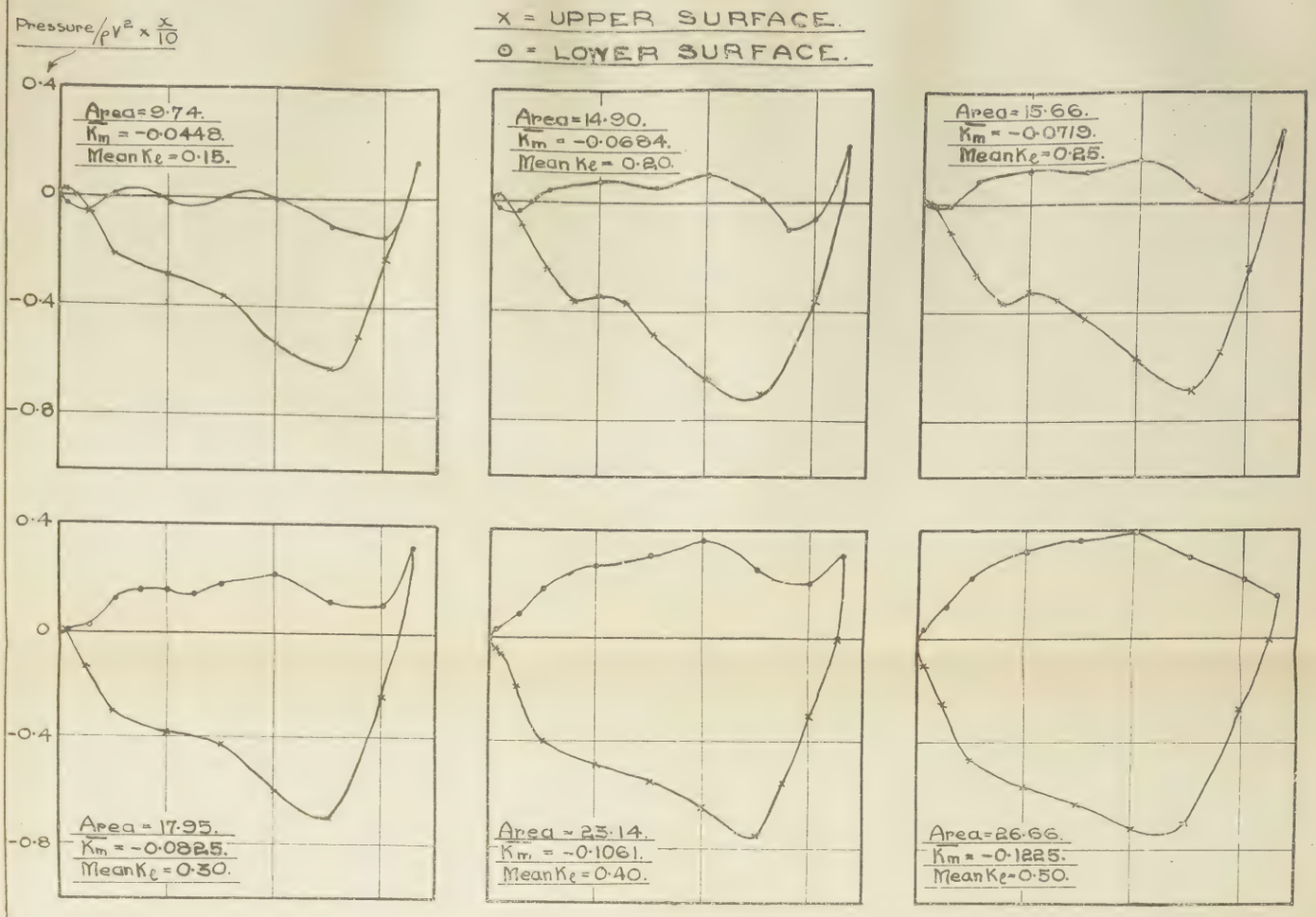

UPPER WING.

X = UPPER SURFACE.
O = LOWER SURFACE.

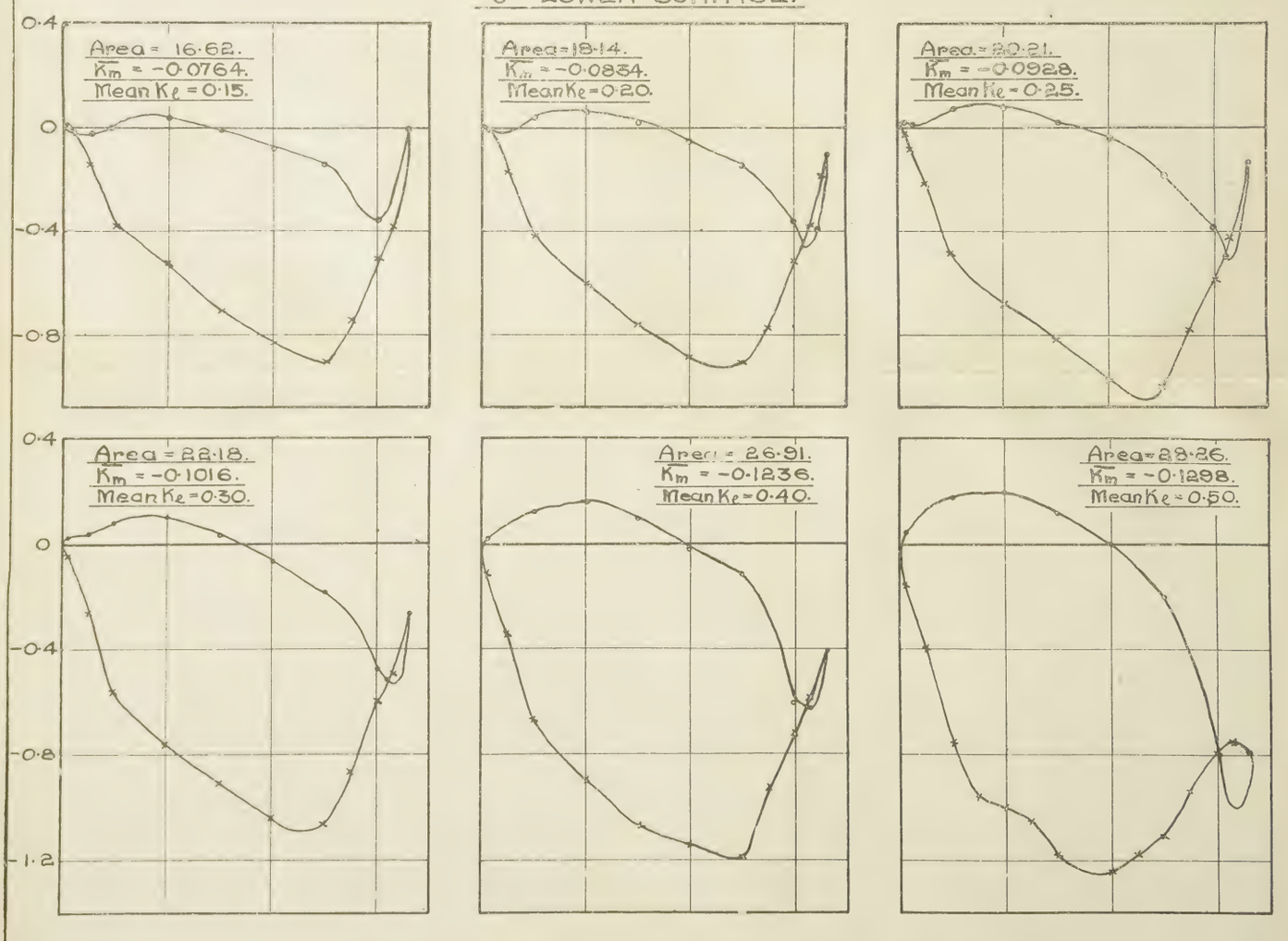

FIG. 13.

LIFT CURVES. RAF. 14 WING SECTION.

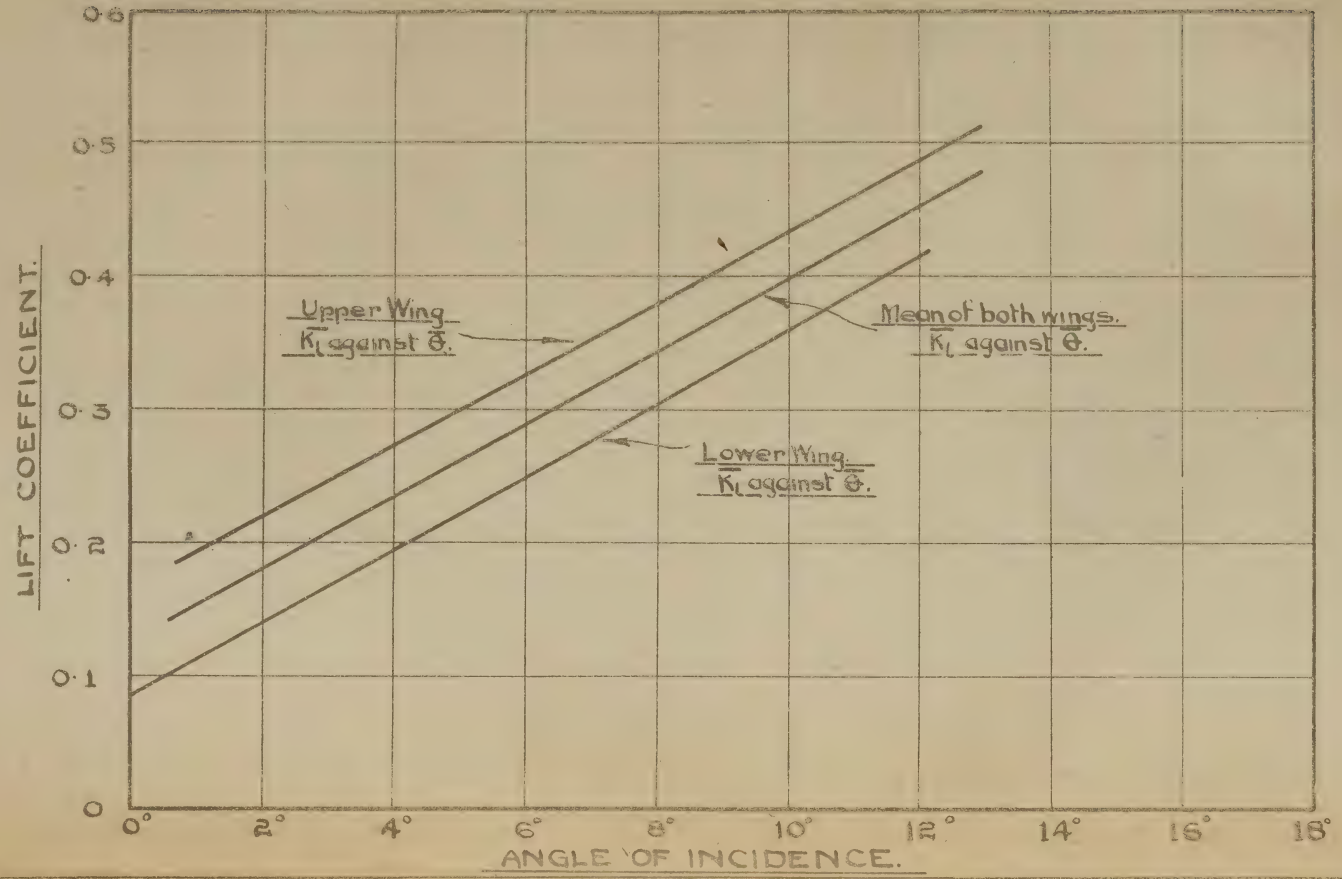

THE LIBRARY
OF THE
UNIVERSITY OF ILLINOIS

REPORT

Ap

0·0

0·0

0·03

DRAG COEFFICIENT.

0·02

0·01

0

THE LIBRARY
OF THE
UNIVERSITY OF ILLINOIS

Appendix II.

DRAG CURVES 1. R.A.F.14 WING SECTION.

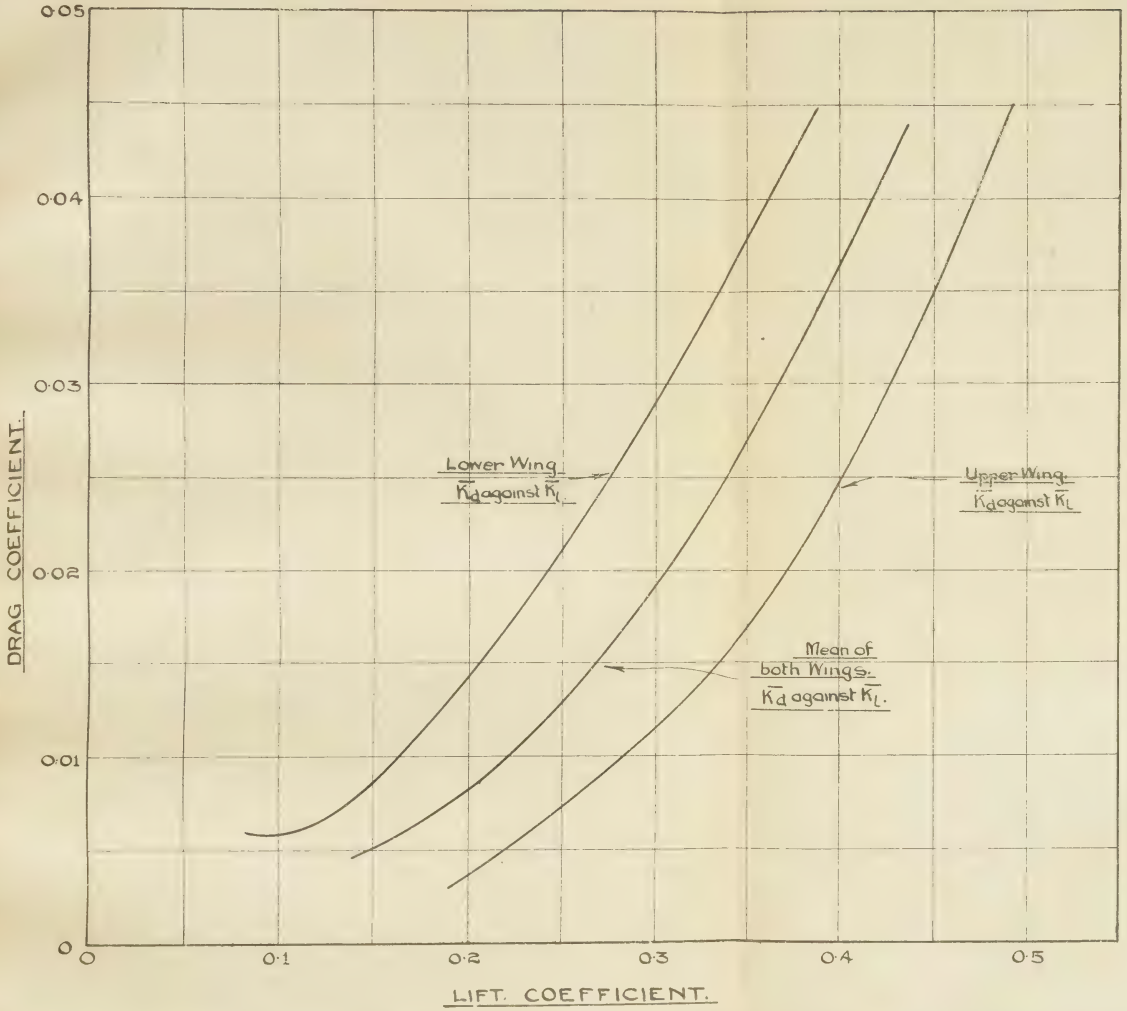

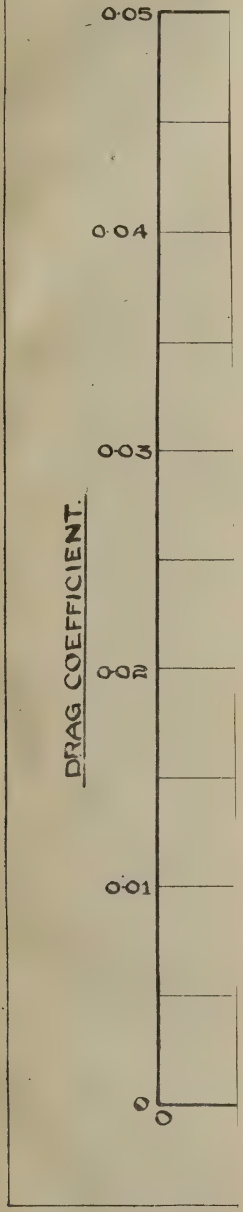

THE LIBRARY
OF THE
UNIVERSITY OF ILLINOIS

FIG. 16.

DRAG CURVES 2. RAF. 14 WING SECTION.

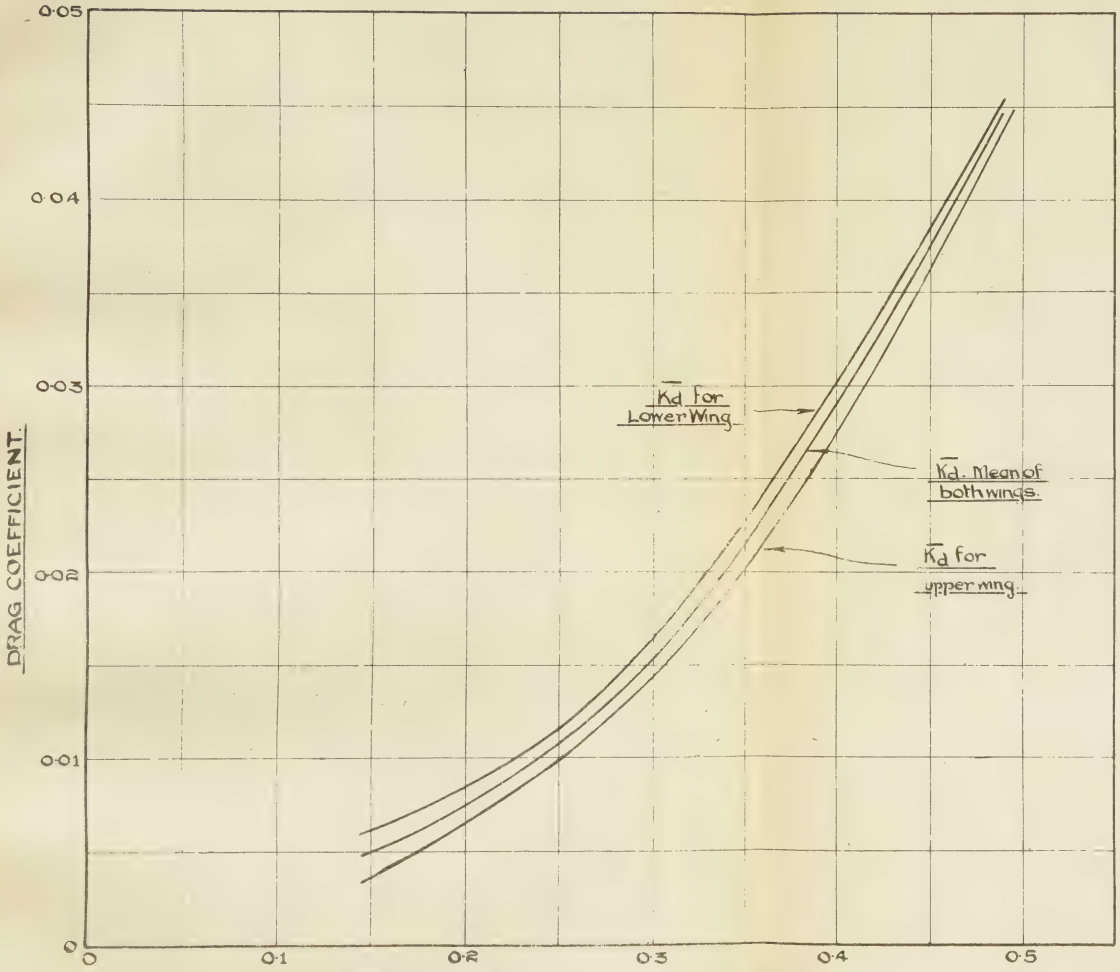

Appendix II.

MOMENT CURVES. R.A.F. 14 WING SECTION.

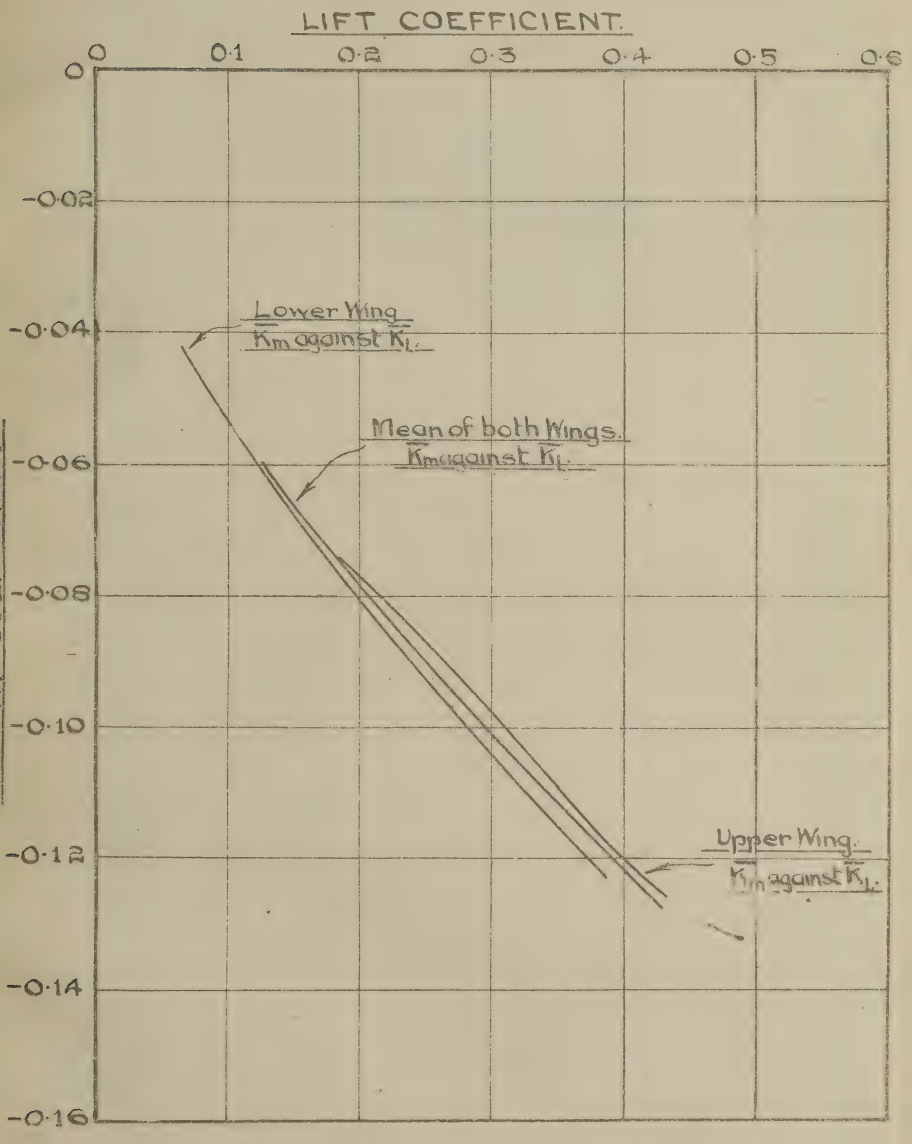

THE LIBRARY
OF THE
UNIVERSITY OF ILLINOIS

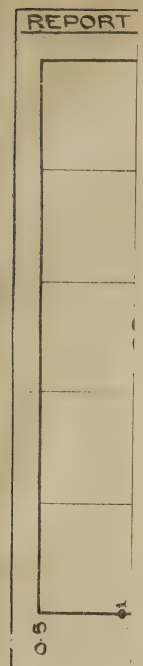

THE LIBRARY
OF THE
UNIVERSITY OF ILLINOIS

OLD B.E.2c WING SECTION.

DISTRIBUTION OF PRESSURE ALONG CHORD AT CONSTANT SPEED.

PRESSURE IN TERMS OF ρV^2 IS PLOTTED AGAINST X.

o = UPPER SURFACE.

+ = LOWER SURFACE.

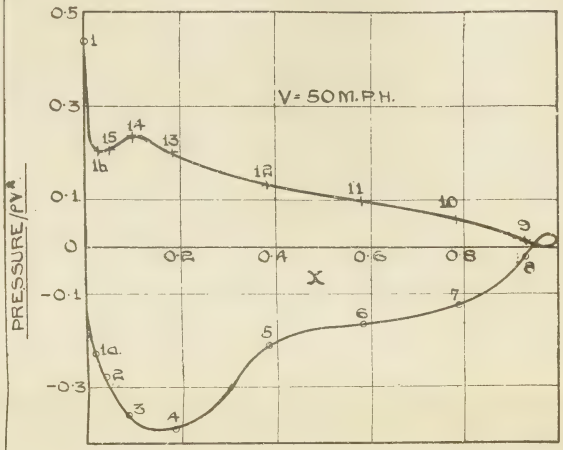

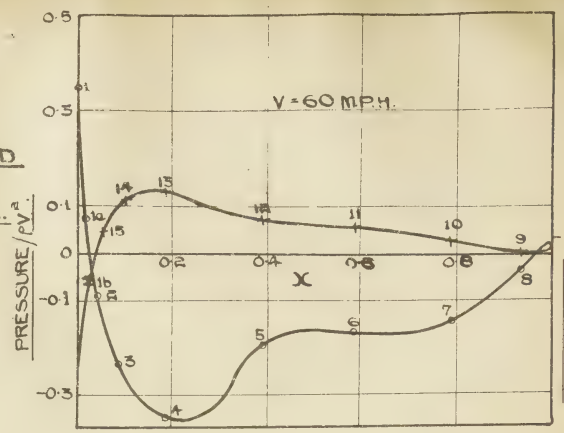

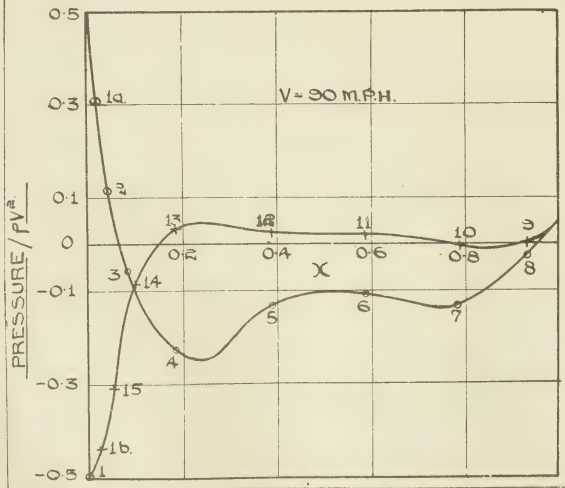

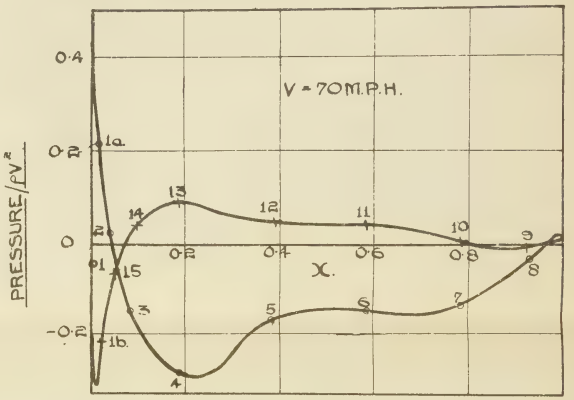

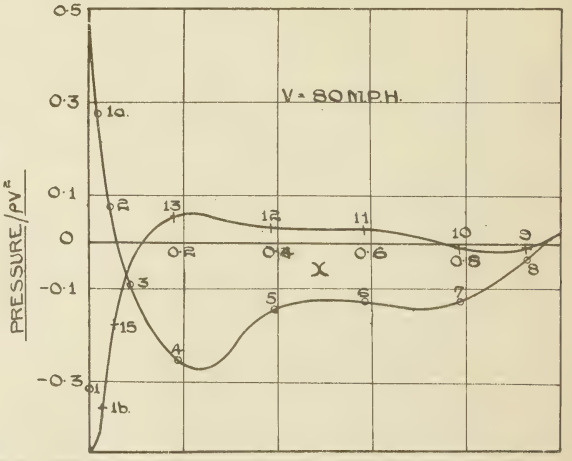

Appendix II.

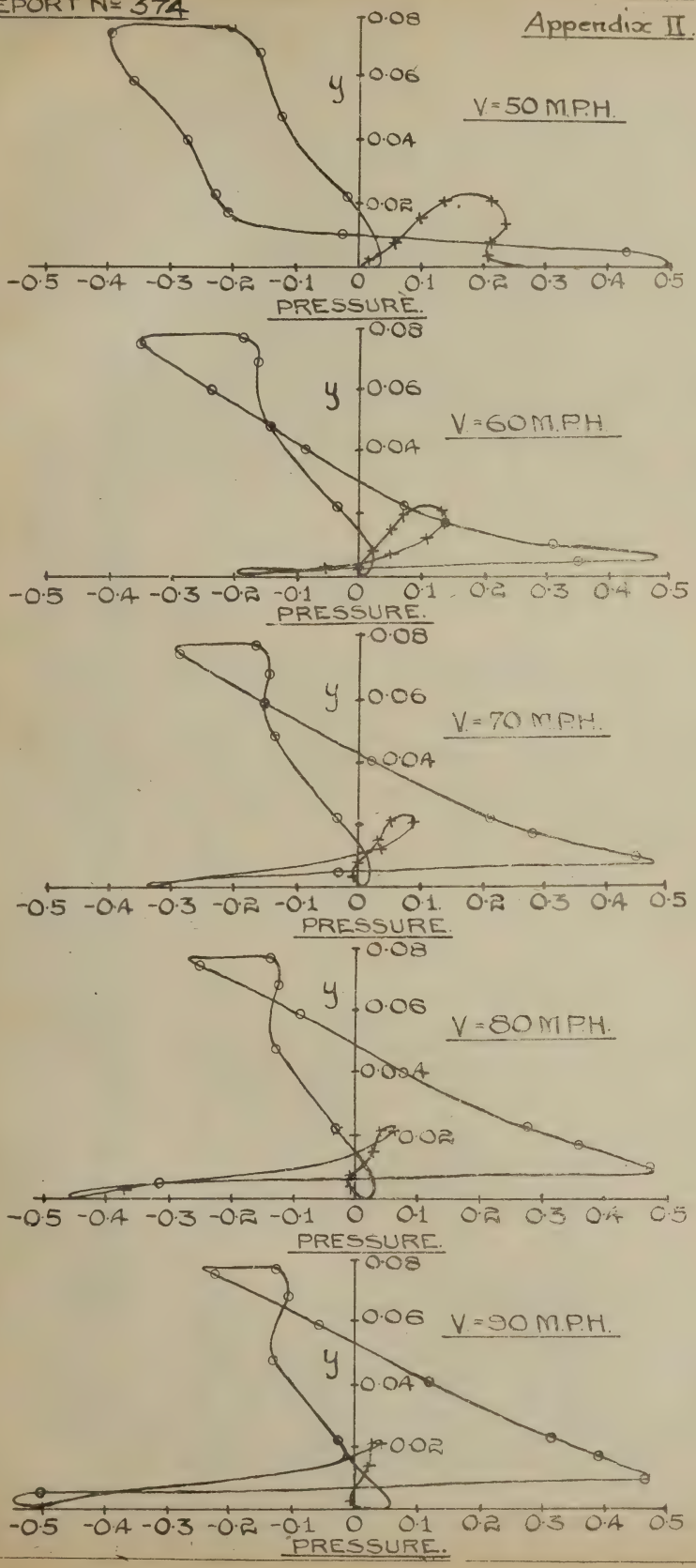

OLD B.E.2C WING SECTION.

DISTRIBUTION OF PRESSURE ALONG NORMAL TO CHORD.

PRESSURE IN TERMS OF ρV^2 IS PLOTTED AGAINST y.

FIG. 20

V = 50 M.P.H.

OLD B.E.2c WING SECTION. MOMENT COEFFICIENT DIAGRAMS.

ABSCISSAE = VALUES OF X.

ORDINATES = PRODUCTS OF (PRESSURE/ρV^2) AND X.

Appendix II.

OLD B.E.2c WING SECTION.

CURVES SHOWING LIFT COEFFICIENT —o— AND MOMENT COEFFICIENT —+— OF THE SECTION, PLOTTED AGAINST THE LIFT COEFFICIENT OF THE AEROPLANE.

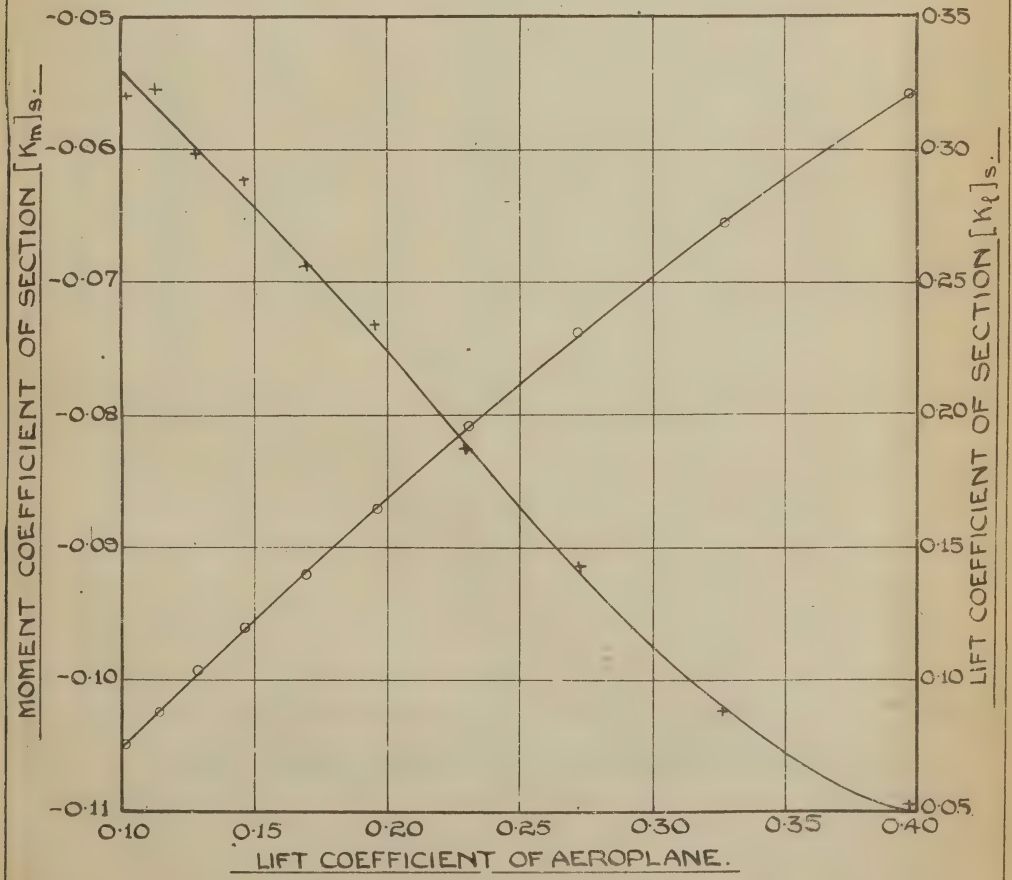

Appendix II.

DRAG CURVE. OLD B.E. 2c WING SECTION.

—o— Drag coefficient of section found by pressure integration, ($[K_D]_s$)

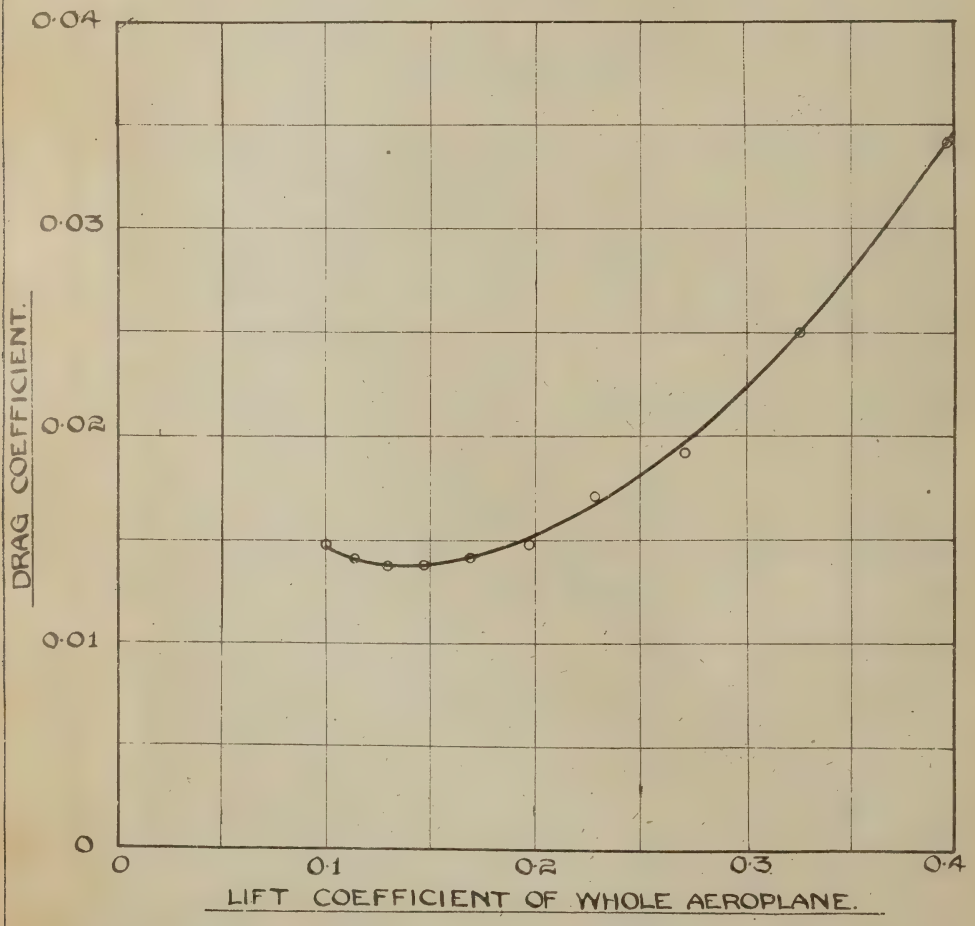

AEROFOIL SECTIONS.

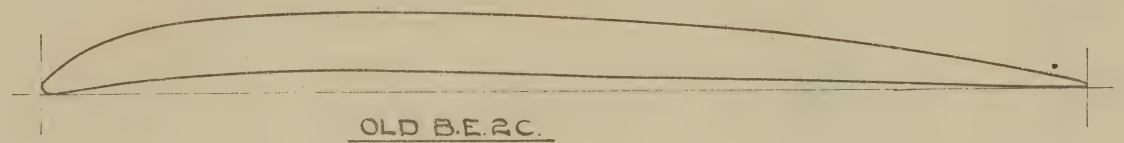

OLD B.E.2C.

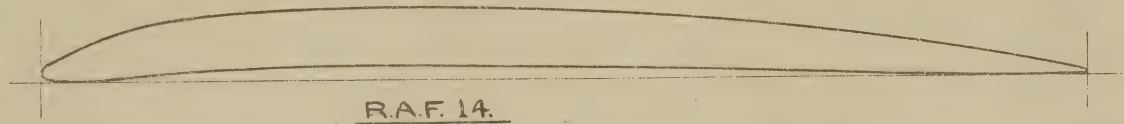

R.A.F. 14.

THE LIBRARY
OF THE
UNIVERSITY OF ILLINOIS

Table 2.

TABLE SHOWING THE x AND y CO-ORDINATES OF THE EXPERIMENTAL TUBES.

Tube.	x	y
1	0·0015	0·0052
1a	0·013	0·0230
2	0·040	0·0408
3	0·086	0·0592
4	0·185	0·0748
5	0·385	0·0772
6	0·584	0·0684
7	0·783	0·0478
8	0·930	0·0221
9	0·931	0·0025
10	0·785	0·0077
11	0·583	0·0151
12	0·387	0·0212
13	0·193	0·0215
14	0·099	0·0135
15	0·051	0·0073
1b	0·026	0·0034
a	0·0016	0·0105
β	0·0077	0·0172

APPENDIX III.

Analysis of Forces on B.E. 2c Complete Model.

By

E. F. Relf, A.R.C.Sc., and T. Lavender.

Summary.—Lift, drag, and pitching moment measured on various parts and combinations of parts. The results show that there are no large interferences, and that lift, drag, and pitching moment can be obtained with considerable accuracy for the complete model by summation of the parts, provided that biplane effect is eliminated by a test on the wings in biplane form.

The experiments described in this appendix were made mainly in order to determine the degree of accuracy with which the drags of the various parts of a machine, tested separately, can be added up to obtain the drag of the complete machine. The experiments have been arranged so as to embrace lift and pitching moment as well as drag, and they also give additional information as to the downwash on the B.E. 2c machine. The question of the addition of the values of lift and drag on parts of the machine is one of great importance, since this method of obtaining the forces on the complete machine is a very common one with designers, being a much quicker method than that of making and testing a complete model, in view of the large amount of information now available on wings, bodies and other parts of very varied types. The present report shows that the addition of the values both of lift and of drag on the various parts gives a result for the complete machines, which is accurate enough for all purposes of design, provided that the results of a test on the wings arranged as a biplane are available.

The tests have been made on the 1/10th scale model of the B.E. 2c machine with R.A.F. 14 wings, and comprise measurements upon :—

(1) Complete model.
(2) Model without tail-plane.
(3) Model without tail-plane and undercarriage.
(4) Wings as biplane with 8 wing struts.
(5) Wings as biplane with 12 wing struts.
(6) Top wing as monoplane.
(7) Body alone.
(8) Tail-plane alone.
(9) Undercarriage alone.

For tests 1 to 6 the model was supported on wires attached to the under surface of the lower plane, the model being thus held upside down in the wind channel. In the remaining tests the part under test was supported on a spindle attached to the balance, but the body drag was also measured on wires to give the spindle correction with greater accuracy.

The results of the tests are given in Tables 3 to 11, and the various deductions and comparisons which have been made from them are given in Tables 12 to 17. The results are discussed in detail below.

1. *Test on complete model.*—In the present tests the tail-plane was set parallel to the chord of the main plane, and the elevators were set at zero angle at all angles of incidence of the main planes, so that the results are not directly comparable with those on full scale machines, in which the elevator setting is different at each angle of incidence. The main object of the present experiments is to determine the accuracy with which the lifts and drags on the parts can be added up to give the forces on the complete machine, and for this purpose it is much easier to make the tests accurately if one elevator setting is used throughout.

2. *Tests on model without tail-plane.*—This test, together with test (1) and test (8) on the tail-plane alone can be used to calculate the downwash. This calculation has been made with greater care than was done in the case of R.E. 8 model (Report T.995). In the R.E. 8 model a constant leverage was assumed between C.G. of machine and C.P. of tail, and only the lift on the tail was considered. In the present calculations the lift, drag, and pitching moment on the tail-plane alone are all taken into account in the manner indicated at the head of Table 12, and the resulting equation there given has been solved by plotting the moment due to the tail forces against φ, the tail angle of incidence, and reading from the curve the value of φ for each moment difference as observed on the complete machine and on the machine without tail-plane. The downwash angle is then $\alpha - \varphi$. Measurements of downwash with the yawmeter have not yet been made on this model, but the downwash as calculated above is in reasonable agreement with that measured on the R.E. 8 model having the same wing section. These values obtained for the downwash have been used to calculate the tail lift and tail drag for various angles of incidence. It may be argued that for the purpose of building up the drag from the drags of the separate parts, an independent value of the downwash should be used, and not one based upon experiments on the complete model. Any reasonable downwash assumption will be correct to, say, 1°, and this corresponds with an error of 0·002 lb. on the tail drag between 0° and 4° angle of incidence, an amount which is less than 1 per cent. of the total drag of the complete model. It thus appears that the differences in tail drag due to

different downwash assumptions will not be large enough to affect the conclusions of this report, relating to the accuracy of the addition of the drags of the various parts as a means of obtaining the drag of the complete machine. Under these conditions the best available downwash values for the machine in question were taken, although they involve experiments on the complete model.

In Table 13 the values obtained for the tail lift and drag are compared with those obtained from the differences in the forces on the machine with and without its tail-plane. The agreement is quite reasonable on both lift and drag. The abnormal difference at 0° angle of incidence is due to the very high lift reading (1·72 lbs.) on the machine without tail-plane at this angle, and probably this is an experimental error.

3. *Tests without undercarriage.*—From tests (2) and (3) the differences on lift and drag due to the undercarriage can be found. The accuracy on these small differences is not great, but the comparison in Table 14 shows that the drag differences agree well with those on the undercarriage alone, while the lift differences are considerably greater. The values at 0° are again influenced by the above-mentioned error in the lift on the machine without tail-plane.

4. *Wings as biplane.*—The differences between these results and those in Table 5 give the forces due to the addition of the body, and these are compared with the forces on the body alone in Table 15. There is a very appreciable effect on the lift at the smaller angles of incidence. This is due to the loss of lift produced by the gap in the middle of the lower wing when the body is removed. If this gap is faired (as was done in the case of R.E. 8, T.995) the lift coefficient is increased appreciably. The accuracy with which the body lift can be added to the wing lift to give that of the combination will depend upon the condition in which the wings alone were tested. It appears from the present experiments and those on R.E. 8 that the best method is to test the biplane without gaps (*i.e.*, two complete wings) and to use the lift coefficients so obtained to give the lift on the wings with gaps, using the appropriate wing area.

The agreement on drag is good at small angles of incidence (except — 4°), but at 8° and 12° the addition gives too high a value. Even here the error is only of the order of 3 per cent. of the total drag of the machine, and it is not easy to make the drag measurement correct to 1 per cent. in the neighbourhood of the critical angle.

The results of the tests on the various combination of parts, therefore, show that there are no striking interferences between these parts, and that the direct addition of lift and drag on the parts gives in all cases a tolerably accurate estimate of the lift and drag of the combination. In Tables 16 and 17 the addition

is made for the complete machine from the four parts tabulated, viz., wings and wing struts, body, undercarriage, and tail-plane. The differences on lift are regular, the addition giving the lift too low. This, as has already been pointed out, is mostly due to the test on the biplane having been made with the central gap unfaired. If the lift coefficient on a complete pair of wings were used, the addition would give a value more nearly equal to that obtained from the complete model—possibly even a slightly higher value.

The drag comparison shows almost phenomenal agreement. Between 0° and 8° the greatest discrepancy is 1·5 per cent., and over the whole range the agreement is correct to less than 4 per cent. The slight differences of Tables 13, 14, and 15 have to a great extent cancelled out, and left differences which are within the limits of experimental error. Of course, it cannot be assumed from the present results that the forces on any two bodies placed in close proximity will be equal to the sum of those on the separate bodies, but it is fairly safe to assume that for any design of aeroplane not widely different from the B.E. 2c type, the lifts and drags on the parts may be added with a considerable degree of confidence to obtain the lift and drag on the machine. It is also safe to assume that if the scale effect correction can be applied to each of the parts separately the addition of the forces on the parts so corrected will give the forces on the full scale machine with sufficient accuracy for all practical purposes.

5. *Estimate of drag of wing struts.*—The wings having been tested as a biplane with eight wing struts ; four extra struts were added to endeavour to estimate the drag due to the struts. The results, which are exhibited in Table 7, are very peculiar. The added drag due to the four extra struts decreases as the angle of incidence increases, until at 15° the extra drag is zero. This does not mean that the four struts have no drag at this angle, but that their addition has reduced the wing drag by an amount equal to their own drag, leaving the total drag unchanged. The resistance of one strut held at an angle appropriate to 4° angle of incidence of the machine was 0·0031 lb., so that four struts would have a drag of 0·012 lb., allowing nothing for the shielding of the back strut by the forward one. The difference in Table 7 shows that four struts change the resistance of the machine by 0·018 lb. at 4° angle of incidence, so that at this angle it appears that the added resistance due to the struts is 50 per cent. greater than the drag measured on the struts alone. It is exceedingly difficult to get the requisite accuracy to establish definitely the effect of adding small members such as struts, but in the present case the values at 0° and 8° seem to show that the difference of 0·018 at 2° is reasonably correct, and that the struts on the model scale add a resistance to the machine which is greater than their drag in free air at small angles of incidence of the main planes.

It does not necessarily follow that this result will also be true for the full-sized struts on an actual machine, since there is known to be a large scale effect on struts between model and full scale sizes. Any uncertainty that may exist should be less important on the full scale than on the model, since the scale effect on struts is such that the percentage of the total drag due to struts is considerably less on the full scale than on the model.

Using the values obtained by differences for the drag of four wing struts, the drag of the eight wing struts has been subtracted from the figures of Table 6, giving the results in the last three columns of Table 7. A comparison of these results with those for the single wing (Table 8) gives an idea of the magnitude of the biplane correction for the wings under consideration. This comparison is not a fair one, because of the influence of the gap in the lower wing. A better value to use for the biplane can be obtained by subtracting the body and struts from the results of Table 5, and this has been done in plotting Fig. 25, in which the values are also given for the R.A.F. 6 monoplane and biplane with same gap and stagger, but on models 18 in. $\times$ 3 in. at 40 ft./sec. The abscissa used is the ratio of the lift coefficient to the maximum lift coefficient of the monoplane, as it was thought that this was a better basis of comparison than the value of the lift coefficient itself. The general appearance of the curves makes it seem improbable that a method of correction can be found to apply to both sections, and a further analysis shows that the lifts can be corrected fairly well, but that no simple rule can be found for the drag corrections. The whole question of biplane interferences needs more investigation, and experiments upon several wing sections as monoplane and biplane at fairly high values of vl would be well worth the time spent upon them. The experiments at present available are very limited. The only complete ones are those made upon the R.A.F. 6 section with planes 18 in. $\times$ 3 in. in plan (R. & M. 196, Sections (i), (ii), (iii)), and there is no reason to suppose that the results of these tests will apply with any considerable accuracy to a section so different as R.A.F. 14. It would, therefore, appear advisable to test any new sections in biplane form if accurate results are required, and, if the monoplane form were tested as well, valuable information as to the corrections to be applied to convert from monoplane to biplane would soon be collected.

Pitching moments.—The pitching moments about the C.G. of the machine have been plotted in Fig. 26 for the model with and without tail plane. The dotted curve shows the sum of the pitching moments on wings alone and body alone (the undercarriage was not considered). It will be seen at once that the moment due to the wings is very large compared with that due to any other member except the tail, and that the wing moment plus the body moment is a sufficiently good approximation to the moment without tail plane for all purposes of tail design.

The position of the C.G. is shown in Fig. 24 ; its co-ordinates referred to the leading edge of the lower wing chord are 0·040 ft. along the chord and 0·206 ft. perpendicular to the chord, measured on the one-tenth scale model.

Additional tests.—In Table 9a some further measurements on the body alone are given. The drag has been measured at various speeds, and the results tend to indicate a scale correction of the order of 5 per cent. between model and full scale, the full scale drag coefficient being the lower. Figures are also given for the drag of the body complete, and, after the removal of the following parts, in order—rudder, fin, aviators, and tail skid. It is worthy of note that the wind shields are so effective that the removal of the aviators does not affect the drag. All these tests have been made with the centre line of the body horizontal, *i.e.*, at 4° angle of incidence for the main planes.

General conclusion.—The results of the present report show that the lifts, drags, and pitching moments of the main parts of a model aeroplane can be added up with considerable accuracy to give the forces and moments on the complete model. Some care is needed in making the lift calculation on account of gaps cut in the wings. The wing section should be tested as a biplane, the information available as to the corrections from monoplane to biplane being insufficient to allow a general rule for the corrections to be deduced.

Table 3.

B.E. 2c ANALYSIS.

Complete Model.

Tail plane parallel to main plane chord.

Elevators at 0°.

Wind speed, 40 ft./sec.

Angle of incidence. Degrees.	Lift. Lbs.	Lift coefficient.	Drag. Lbs.	Drag coefficient.	Lift. / Drag.	Moment about C.G. Ft. Lbs.
− 4	− 0·61	− 0·046	0·485	0·0348	− 1·26	0·061
− 2	+ 0·31	+ 0·022	0·351	0·0252	+ 0·88	+ 0·002
0	1·42	0·102	0·334	0·0240	4·25	− 0·057
+ 2	2·61	0·187	0·350	0·0251	7·46	− 0·154
4	3·52	0·253	0·400	0·0287	8·80	− 0·226
6	4·53	0·325	0·490	0·0352	9·24	− 0·348
8	5·42	0·389	0·612	0·0439	8·85	− 0·497
10	6·31	0·453	0·738	0·0530	8·55	− 0·690
12	6·98	0·501	0·973	0·0698	7·17	− 0·848
15	7·91	0·568	1·55	0·111	5·10	− 1·18
20	8·19	0·588	2·68	0·192	3·06	− 1·70
25	7·80	0·560	3·79	0·272	2·06	− 2·64
30	7·27	0·522	4·60	0·330	1·58	− 2·86

Table 4.

B.E. 2c ANALYSIS.

Model without Tail Plane.

Wind speed, 40 ft./sec.

Angle of incidence. Degrees.	Lift. Lbs.	Lift coefficient.	Drag. Lbs.	Drag coefficient.	Lift. / Drag.	Moment about C.G. Ft. Lbs.
− 4	− 0·50	− 0·036	0·460	0·0330	− 1·09	− 0·214
− 2	+ 0·54	+ 0·039	0·336	0·0241	+ 1·61	− 0·210
0	1·72	0·123	0·317	0·0228	5·42	− 0·155
+ 2	2·57	0·184	0·331	0·0238	7·76	− 0·103
4	3·46	0·248	0·383	0·0275	9·03	− 0·063
6	4·36	0·313	0·450	0·0323	9·69	− 0·025
8	5·12	0·368	0·536	0·0385	9·56	− 0·002
10	5·92	0·425	0·686	0·0493	8·63	− 0·017
12	6·47	0·465	0·825	0·0592	7·84	− 0·044
15	7·20	0·517	1·40	0·101	5·13	− 0·115
20	7·19	0·516	2·49	0·179	2·88	− 0·457
25	6·80	0·489	3·24	0·233	2·10	− 0·762
30	6·65	0·470	3·91	0·281	1·70	− 0·829

Table 5.

B.E. 2c ANALYSIS.

Model without Tail Plane and Undercarriage.

Wind speed, 40 ft./sec.

Angle of incidence. Degrees.	Lift. Lbs.	Lift coefficient.	Drag. Lbs.	Drag coefficient.	Lift. / Drag.	Moment about C.G. Ft. Lbs.
− 4	− 0·47	− 0·034	0·407	0·0292	− 1·16	− 0·243
0	+ 1·51	+ 0·108	0·279	0·0200	+ 5·41	− 0·141
+ 4	3·39	0·243	0·349	0·0250	9·71	− 0·065
8	5·01	0·360	0·502	0·0360	9·98	− 0·018
12	6·37	0·457	0·796	0·0572	8·01	− 0·037
16	—	—	1·50	0·108	—	—
20	—	—	2·48	0·178	—	—

Table 6.

B.E. 2c ANALYSIS.

Wings as a Biplane with Eight Wing Struts.

Gap in Lower Wing Unfaired.

Angle of incidence. Degrees.	Lift. Lbs.	Lift coefficient.	Drag. Lbs.	Drag coefficient.	Lift. / Drag.	Moment about C.G. Ft. Lbs
− 4	− 0·77	− 0·055	0·341	0·0245	− 2·26	− 0·233
− 2	+ 0·26	+ 0·019	0·212	0·0152	+ 1·23	− 0·187
0	1·25	0·090	0·189	0·0136	6·62	− 0·132
2	2·28	0·164	0·204	0·0146	11·2	− 0·113
4	3·28	0·236	0·253	0·0181	13·0	− 0·082
6	4·08	0·293	0·335	0·0241	12·2	− 0·067
8	4·88	0·350	0·427	0·0307	11·4	− 0·058
10	5·61	0·403	0·545	0·0390	10·3	− 0·063
12	6·32	0·454	0·710	0·0510	8·90	− 0·091
15	6·84	0·492	1·25	0·0898	5·47	− 0·121
20	6·86	0·494	2·26	0·162	3·03	− 0·357

Table 7.

B.E. 2c ANALYSIS.

Angle of incidence.	Drag of wing struts.			Biplane without struts.		
	Drag with twelve struts.	Drag with eight struts.	Difference for four struts.	Drag.	Drag coefficient.	Lift. Drag.
Degrees.	Lbs.	Lbs.	Lbs.	Lbs.		
− 4	0·373	0·341	0·032	0·277	0·0199	− 2·78
− 2	—	—	—	0·164	0·0118	+ 1·59
0	0·208	0·189	0·019	0·151	0·0108	8·29
+ 2	—	—	—	0·167	0·0120	13·6
4	0·271	0·253	0·018	0·217	0·0156	15·1
6	—	—	—	0·302	0·0217	13·5
8	0·442	0·427	0·015	0·397	0·0285	12·3
10	—	—	—	0·526	0·0378	10·7
12	0·714	0·710	0·004	0·702	0·0505	9·01
15	1·249	1·25	0·00	1·25	0·0898	5·47
20	—	—	—	2·27	0·163	3·02

The resistance of a single strut at an angle appropriate to 4° angle of incidence of the machine was found to be 0·0031 lb.

Table 8.

B.E. 2c ANALYSIS.

Upper Wing as Monoplane.

Angle of incidence.	Lift.	Lift coefficient.	Drag.	Drag coefficient.	Lift. Drag.
Degrees.	Lbs.		Lbs.		
− 4	− 0·66	− 0·090	0·179	0·0244	− 3·69
− 2	+ 0·01	+ 0·001	0·085	0·0116	+ 0·12
0	0·75	0·102	0·074	0·0101	10·1
+ 2	1·44	0·196	0·076	0·0104	19·0
4	2·02	0·276	0·103	0·0140	19·6
6	2·61	0·356	0·143	0·0195	18·2
8	3·05	0·416	0·189	0·0258	16·1
10	3·44	0·469	0·252	0·0344	13·6
12	3·70	0·505	0·338	0·0461	10·9
15	3·93	0·536	0·762	0·104	5·16
20	3·44	0·469	1·21	0·165	2·82

Table 9.

B.E. 2c ANALYSIS.

Body alone, without Fin or Rudder.

Angle of incidence of wings.	Lift. Lbs.	Drag. Lbs.	Moment about C.G. Ft. Lbs.
− 4	− 0·003	0·0871	0·0092
− 2	+ 0·005	0·0866	0·0112
0	0·010	0·0859	0·0132
+ 2	0·017	0·0857	0·0160
4	0·023	0·0863	0·0180
6	0·029	0·0883	0·0212
8	0·035	0·0913	0·0228
10	0·041	0·0952	0·0223
12	0·049	0·1008	0·0216
15	0·065	0·109	0·0180
20	0·100	0·131	0·0060

Table 9a.

B.E. 2c ANALYSIS.

Drag of Body with Fin and Rudder.

Angle of Incidence of Main Planes, 4°.

Wind speed. Ft./Sec.	Drag. Lbs.	$\frac{\text{Drag}}{V^2} \times 10^5$
30	0·0520	5·78
40	0·0908	5·67
50	0·142	5·68
60	0·203	5·64
70	0·277	5·66
78·6	0·346	5·60

Analysis of Body Drag.

	Drag. (lbs. at 40 f./s.)
Body complete	0·0908
Body without rudder	0·0895
Body without fin or rudder	0·0863
Body without fin, rudder, or men	0·0863
Body without fin, rudder, men, or tail skid	0·0803

Table 10.

B.E. 2c ANALYSIS.

Undercarriage Alone.

Angle of incidence of wings. Degrees.	Lift. Lbs.	Drag. Lbs.
− 4	− 0·007	0·0428
0	− 0·003	0·0409
+ 4	+ 0·015	0·0391
8	0·030	0·0386
12	0·036	0·0425
15	0·020	0·0448
20	0·020	0·0476

Table 11.

B.E. 2c ANALYSIS.

Tail Plane Alone.

Elevators at Zero.

Angle of incidence. Degrees.	Lift. Lbs.	Drag. Lbs.	Moment about point 0·212 ft. behind leading edge of tail plane. Ft. Lbs.
0	0	0·0150	0
2	0·153	0·0186	0·0180
4	0·296	0·0272	0.0356
6	0·439	0·0418	0·0532
8	0·585	0·0658	0·0687
10	0·724	0·1035	0.0846
15	0·908	0·281	0.0568
20	0·906	0·388	0·0449
25	0·822	0·446	0.0465

B.E. 2c ANALYSIS.

Downwash Calculation.

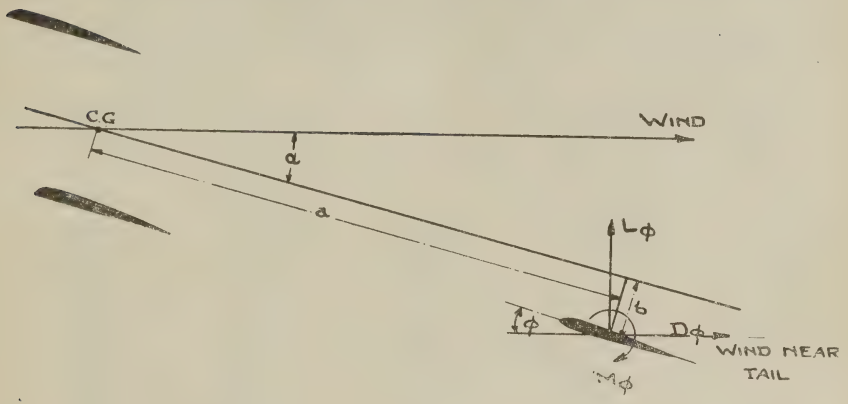

Moment about C.G. due to tail :—

$M_1 = M_\phi - L_\phi (a \cos \phi - b \sin \phi) - D_\phi (b \cos \phi + a \sin \phi)$

= (Moment on complete machine) − (Moment on machine without tail-plane).

By plotting M_1 against φ the results in the table below are obtained :—

Table 12.

Angle of incidence. α	M_1	ø	Downwash angle. α − ø	Tail lift. Lø cos (α − ø) − Dø sin (α − ø)	Tail drag. Dø cos (α − ø) + Lø sin (α − ø)
− 4	− 0·275	− 2·3	− 1·7	− 0·174	0·0243
− 2	− 0·212	− 1·7	− 0·3	− 0·130	0·0186
0	− 0·098	− 0·8	+ 0·8	− 0·062	0·0148
+ 2	+ 0·051	+ 0·4	1·6	+ 0·031	0·0159
4	0·163	1·3	2·7	0·099	0·0215
6	0·323	2·7	3·3	0·199	0·0324
8	0·495	4·1	3·9	0·302	0·0484
10	0·673	5·7	4·3	0·414	0·0700
12	0·804	6·9	5·1	0·498	0·0947
15	1·066	9·0	6·0	0·640	0·148
20	1·501	14·0	6·0	0·853	0·340

Table 13.

B.E. 2c ANALYSIS.

Comparison between tail forces calculated from downwash, and differences between models with and without tail.

Angle of incidence. Degrees.	Lift (lbs.).		Drag (lbs.).	
	Difference on model.	Calculated.	Difference on model.	Calculated.
− 4	− 0·11	− 0·17	0·025	0·024
− 2	− 0·23	− 0·13	0·015	0·018
0	− 0·30	− 0·06	0·017	0·015
+ 2	+ 0·03	+ 0·03	0·019	0·016
4	0·06	0·10	0·017	0·021
6	0·17	0·20	0·040	0·032
8	0·30	0·30	0·076	0·048
10	0·39	0·41	0·052	0·070
12	0·52	0·50	0·148	0·095
15	0·71	0·64	0·15	0·15
20	1·00	0·85	0·19	0·31

Note.—A comparison of moments will necessarily show agreement, since the moment difference was used to calculate the downwash.

Table 14.

B.E. 2c ANALYSIS.

Comparison between forces on undercarriage, and differences between model with and without undercarriage.

Angle of incidence. Degrees.	Lift (lbs.).		Drag (lbs.).	
	Difference on model.	Undercarriage alone.	Difference on model.	Undercarriage alone.
− 4	− 0·03	− 0·01	0·053	0·043
0	+ 0·21	0	0·038	0·041
+ 4	0·07	+ 0·02	0·034	0·039
8	0·11	0·03	0·034	0·039
12	0·10	0·04	0·029	0·042

Table 15.

B.E. 2c ANALYSIS.

Comparison between forces on body, and differences between biplane with and without body.

Angle of incidence. Degrees.	Lift (lbs.).		Drag (lbs.).	
	Difference on model.	Body alone.	Difference on model.	Body alone.
− 4	0·30	0	0·066	0·091
0	0·26	0·01	0·090	0·090
+ 4	0·11	0·02	0·099	0·090
8	0·13	0·04	0·075	0·095
12	0·05	0·05	0·086	0·105

Note.—The fin and rudder add 0·004 to the drag at 0°, and it has here been assumed that this small addition is independent of angle of incidence.

Table 16.

B.E. 2c ANALYSIS.

Comparison between complete model and sum of parts.

Lift.

Angle of incidence. Degrees.	Biplane and wing struts.	Body.	Under-carriage.	Tail.	Sum.	Complete machine.	Difference.
− 4	− 0·77	0·00	− 0·01	− 0·17	− 0·95	− 0·61	0·34
− 2	+ 0·26	0·01	0·00	− 0·13	+ 0·14	+ 0·31	0·17
0	1·25	0·01	0·00	− 0·06	1·19	1·42	0·23
+ 2	2·28	0·02	+ 0·01	+ 0·03	2·34	2·61	0·27
4	3·28	0·02	0·02	0·10	3·42	3·52	0·10
6	4·08	0·03	0·02	0·20	4·33	4·53	0·20
8	4·88	0·04	0·03	0·30	5·25	5·42	0·17
10	5·61	0·04	0·04	0·41	6·10	6·31	0·21
12	6·32	0·05	0·04	0·50	6·92	6·98	0·06
15	6·84	0·06	0·02	0·64	7·56	7·91	0·35
20	6·86	0·10	0·02	0·85	7·83	8·19	0·36
						Mean	0·22

The difference is largely due to the effect of the gap in the lower wing, due to removal of body. In R.E. 8 the effect of fairing this gap was to improve the lift coefficient by 0·022; the present difference on lift coefficient is 0·016.

Table 17.

B.E. 2c ANALYSIS.

Comparison between complete model and sum of parts.

Drag.

Angle of incidence. Degrees.	Biplane and wing struts.	Body.	Under-carriage.	Tail.	Sum.	Complete machine.	% error.
− 4	0·341	0·091	0·043	0·024	0·499	0·485	2·8
− 2	0·212	0·091	0·042	0·019	0·364	0·351	3·7
0	0·189	0·090	0·041	0·015	0·335	0·334	0·2
+ 2	0·204	0·090	0·040	0·016	0·350	0·350	0·0
4	0·253	0·090	0·039	0·021	0·403	0·400	0·6
6	0·335	0·092	0·039	0·032	0·498	0·490	1·5
8	0·427	0·095	0·039	0·048	0·609	0·612	0·5
10	0·545	0·099	0·040	0·070	0·754	0·738	2·1
12	0·710	0·105	0·042	0·095	0·952	0·973	− 2·1
15	1·25	0·113	0·045	0·148	1·56	1·55	0·6
20	2·26	0·135	0·048	0·31	2·75	2·68	2·6

FIG. 24.

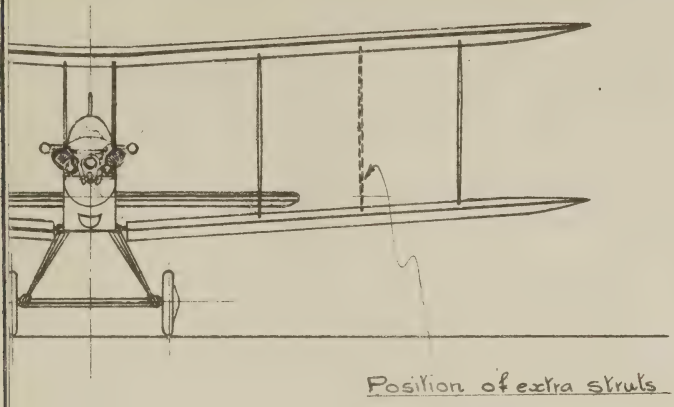

Position of extra struts

ON BE2C. COMPLETE MODEL——

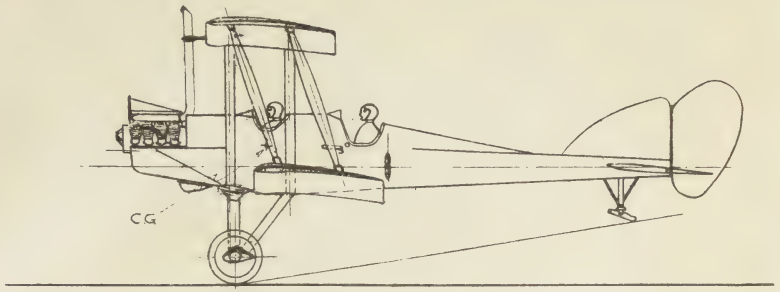

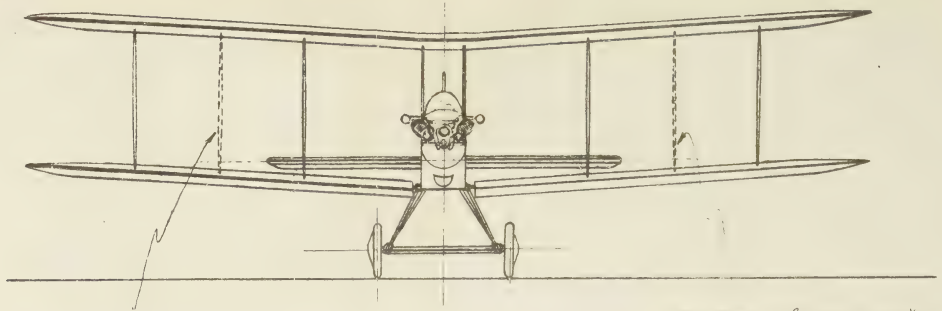

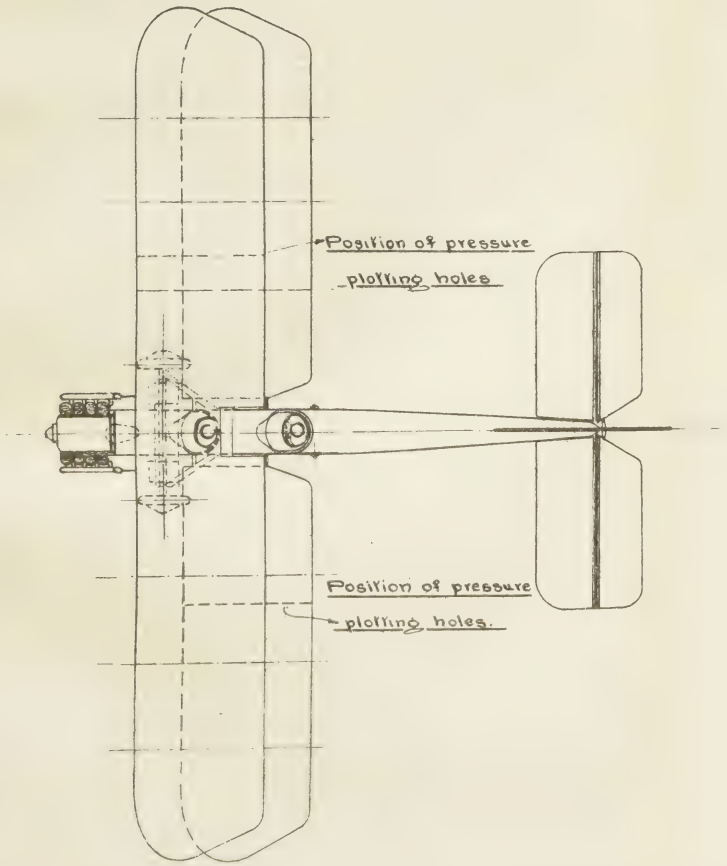

ANALYSIS OF FORCES ON B.E.2c. COMPLETE MODEL

ANALYSIS OF FORCES ON B.E.2c COMPLETE MODEL

Comparison of R.A.F. 14 with R.A.F. 6

Monoplane & Biplane

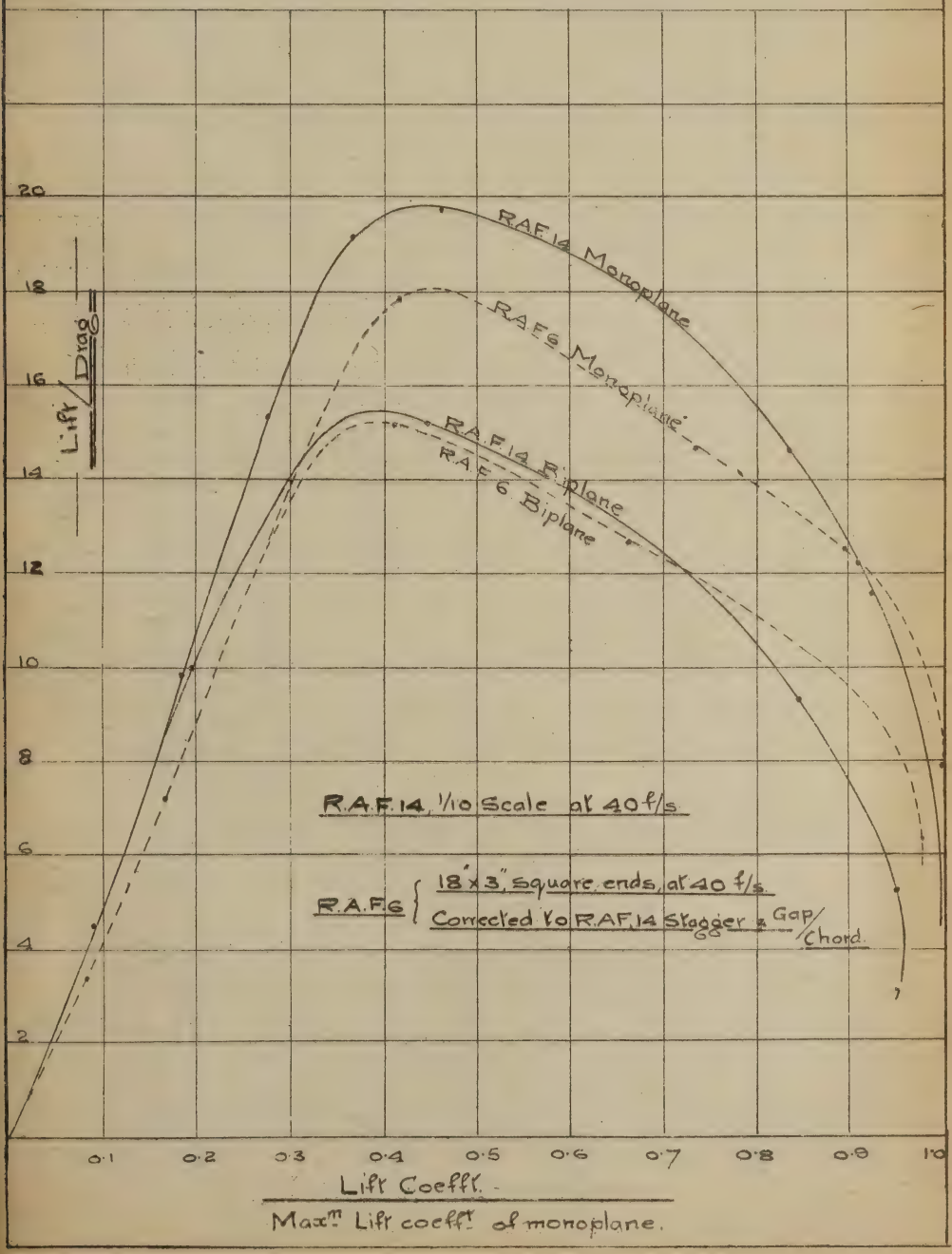

ANALYSIS OF FORCES ON B.E.2c COMPLETE MODEL

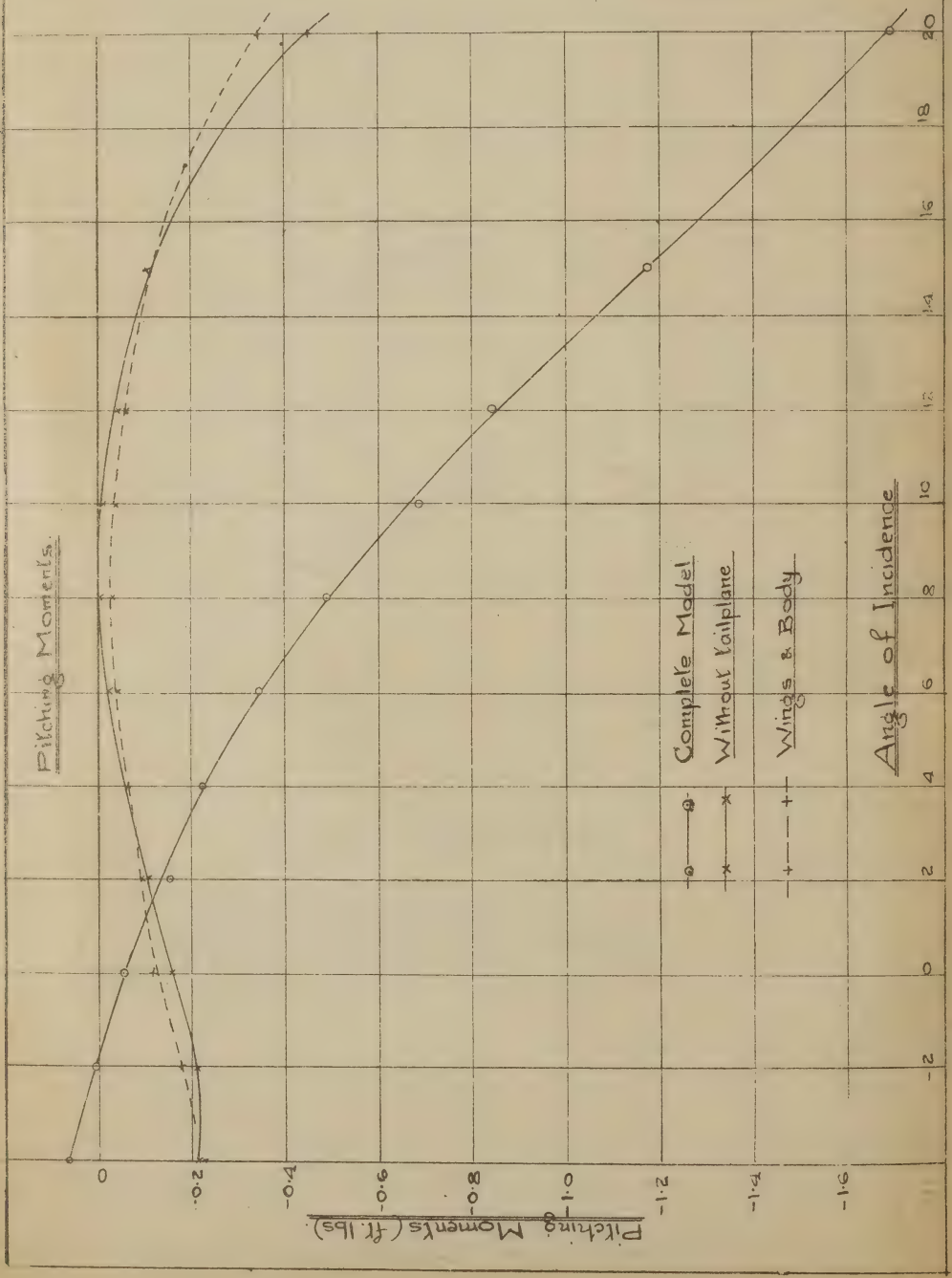

APPENDIX IV.

(i) *Pressure Plotting on sections of the Upper and Lower Wings of a Biplane with R.A.F. 14 Wings.*

(ii) *Pressure Plotting on the Lower Wing of a Biplane with B.E. 2c Wings.*

By

E. F. Relf, A.R.C.Sc., R. Jones, M.A., and T. Lavender.

(i) Pressure Plotting on Sections of the Upper and Lower Wings of a Biplane with R.A.F. 14 Wings.

The experiments of this section were carried out in continuation of the comparison of pressure plotting on model and full-scale wings. The model used was the one-tenth scale complete model of the B.E. 2c machine with wings of R.A.F. 14 section, and the pressure plotting was performed on both upper and lower wings. The sections over which the pressures were measured were in the same relative position as those used for the full-scale plotting, and the holes were intended to be in the same positions as those in the actual wing. Owing to the great difficulty of drilling these fine holes in the model wing, they do not always agree exactly in position with those of the full-scale wing, and the actual positions of the model holes were, therefore, measured after the plane was made and are recorded in Table 18. To eliminate errors due to slight differences of section the model aerofoil was measured up and corrected until it agreed very closely with the full-scale section, particulars of which were furnished from actual measurements of the pressure plotting ribs on the machine.

The model was supported on wires, as in the earlier tests on B.E. 2c wings, to make any possible interferences as small as practicable. The method of experiment is described in more detail in Section (ii) of this Appendix.

The actual pressures measured at each hole are recorded in Table 22, and the integrated results are given in Table 23. The accuracy of the integrated results is not so good on the drag as on the lift, and the exceedingly low drag coefficients at small angles on the upper wing led to a repetition of the measurements at 0° and 2° with the model the other way up in the channel, to see whether the low drags were due to any want of horizontality in the wind. The agreement between the lift coefficients shows that the wind was parallel to the channel axis

to well within one-tenth degree, and the differences in the drag figures are such as might be expected from errors of observation and integration. The means of the two results at 0° and 2° have been used in calculating lift and drag.

The pressures have been plotted in Figs. 27–34 in the forms necessary for the integration of both normal and longitudinal force. These diagrams are intended solely as a rough indication of the nature of the pressure changes round the section. The accuracy of plotting and reproduction is not great, and all figures for actual use should be taken from Table 19.

TABLE 18.

POSITION OF PRESSURE PLOTTING HOLES.

R.A.F. 14 WING.

No. of hole.	Upper plane.				Lower plane.			
	Upper surface.		Lower surface.		Upper surface.		Lower surface.	
	X.	Y.	X.	Y.	X.	Y.	X.	Y.
Leading edge	0	0·0078	0	0·0078	0	0·0070	0	0·0070
1	0·0129	0·0181	0·0071	0·0032	0·0114	0·0172	0·0118	0·0012
2	0·0248	0·0250	0·0209	0·0005	0·0225	0·0200	0·0241	0·0004
3	0·0388	0·0314	0·0364	0·0000	0·0339	0·0291	0·0361	0·0000
4	0·0523	0·0373	0·0512	0·0000	0·0508	0·0367	0·0532	0·0000
5	0·0652	0·0420	0·0656	0·0007	0·0652	0·0420	0·0695	0·0010
6	0·0896	0·0505	0·0836	0·0025	0·0888	0·0505	0·0856	0·0027
7	0·1180	0·0572	0·1177	0·0062	0·1175	0·0571	0·1175	0·0061
8	0·1755	0·0642	0·1798	0·0112	0·1742	0·0640	0·1767	0·0108
9	0·265	0·0680	0·251	0·0145	0·2645	0·0680	0·2715	0·0139
10	0·390	0·0685	0·373	0·0140	0·375	0·0685	0·3735	0·0130
11	0·529	0·0650	0·524	0·0105	0·524	0·0652	0·528	0·0098
12	0·663	0·0580	0·662	0·0070	0·662	0·0570	0·662	0·0065
13	0·784	0·0460	0·782	0·0041	0·784	0·0450	0·780	0·0037
14	0·859	0·0354	0·859	0·0020	0·852	0·0355	0·859	0·0016
15	0·915	0·0250	0·918	0·0008	0·920	0·0240	0·918	0·0008
16	0·966	0·0160	0·965	0·0000	0·968	0·0155	0·967	0·0000
Trailing edge	1·000	0·0060	1·000	0·0060	1·000	0·0060	1·000	0·0060

All dimensions are expressed as fractions of the chord.

Table 19.

PRESSURES AT HOLES ON R.A.F. 14 WINGS.

Angle of Incidence, 0°.

No. of hole.	Original test.				Repeat with model reversed.	
	Upper wing.		Lower wing.		Upper wing.	
	Upper surface.	Lower surface.	Upper surface.	Lower surface.	Upper surface.	Lower surface.
Leading edge	0·500	+0·500	0·430	+0·430	0·511	+0·511
1	0·164	−0·079	0·369	−0·541	0·199	−0·109
2	+0·046	−0·169	0·250	−0·512	+0·080	−0·217
3	−0·068	−0·131	0·142	−0·367	−0·017	−0·158
4	−0·130	−0·106	+0·036	−0·183	−0·097	−0·130
5	−0·181	−0·089	−0·025	−0·164	−0·164	−0·108
6	−0·257	−0·053	−0·120	−0·129	−0·239	−0·068
7	−0·281	−0·013	—	−0·046	−0·276	−0·034
8	−0·304	+0·034	−0·196	+0·007	−0·295	+0·031
9	−0·234	0·072	−0·163	0·020	−0·235	0·074
10	−0·195	0·044	−0·131	0·018	−0·196	0·041
11	−0·180	0·019	−0·124	0·014	−0·179	0·012
12	−0·168	+ 0·002	−0·121	0·006	−0·171	+0·001
13	−0·145	−0·003	−0·097	+0·005	−0·147	−0·007
14	−0·132	−0·010	−0·077	−0·006	−0·128	−0·015
15	−0·120	−0·018	−0·069	−0·006	−0·120	−0·023
16	−0·060	−0·018	−0·067	−0·031	−0·077	−0·030
Trailing edge	−0·010	−0·010	−0·026	−0·026	−0·016	−0·016

Angle of Incidence, 2°.

Leading edge	+0·510	0·510	0·265	+0·265	+0·360	0·360
1	−0·125	0·233	0·218	−0·237	−0·050	+0·225
2	−0·168	0·031	0·122	−0·153	−0·130	−0·009
3	−0·262	0·019	+0·038	−0·116	−0·240	−0·013
4	−0·296	0·011	−0·060	−0·086	−0·292	−0·012
5	−0·340	0·004	−0·116	−0·074	−0·325	−0·013
6	−0·393	0·031	−0·198	−0·044	−0·394	+0·014
7	−0·405	0·068	—	−0·010	−0·403	0·053
8	−0·403	0·090	−0·246	+0·051	−0·412	0·082
9	−0·314	0·095	−0·191	0·089	−0·319	0·091
10	−0·266	0·061	−0·162	0·052	−0·263	0·056
11	−0·231	0·031	−0·139	0·038	−0·230	0·026
12	−0·210	0·013	−0·135	0·030	−0·212	+0·009
13	−0·182	0·000	−0·112	0·025	−0·186	−0·003
14	−0·129	−0·008	−0·089	0·014	−0·146	−0·011
15	−0·080	−0·017	−0·080	0·013	−0·094	−0·022
16	−0·043	−0·016	−0·037	0·002	−0·049	−0·022
Trailing edge	−0·007	−0·007	+0·013	0·013	−0·013	−0·013

TABLE 19 (*continued*).

PRESSURE AT HOLES ON R.A.F. 14 WINGS.

Angles of Incidence, 4° and 6°.

No. of hole.	Angle of incidence 4°.				Angle of incidence 6°.			
	Upper wing.		Lower wing.		Upper wing.		Lower wing.	
	Upper surface.	Lower surface.	Upper surface.	Lower surface.	Upper surface.	Lower surface.	Upper surface.	Lower surface.
Leading edge	+0·378	0·378	0·515	0·515	+0·246	0·246	+0·254	0·254
1	−0·340	0·378	+0·079	0·013	−0·902	0·502	−0·115	0·209
2	−0·367	0·201	−0·005	0·014	−0·598	0·320	−0·158	0·152
3	−0·412	0·142	−0·086	0·015	−0·560	0·241	−0·206	0·133
4	−0·475	0·119	−0·165	0·017	−0·620	0·200	−0·273	0·113
5	−0·505	0·089	−0·214	0·008	−0·658	0·166	−0·311	0·092
6	−0·541	0·104	−0·295	0·028	−0·683	0·165	−0·364	0·101
7	−0·535	0·123	—	0·073	−0·664	0·173	—	0·133
8	−0·494	0·130	−0·294	0·107	−0·592	0·167	−0·343	0·155
9	−0·388	0·130	−0·226	0·113	−0·454	0·153	−0·260	0·146
10	−0·312	0·083	−0·171	0·082	−0·332	0·101	−0·194	0·114
11	−0·239	0·046	−0·148	0·064	−0·273	0·054	−0·157	0·087
12	−0·218	0·020	−0·141	0·050	−0·240	0·025	−0·141	0·067
13	−0·182	+0·002	−0·117	0·041	−0·193	+0·001	−0·107	0·055
14	−0·134	−0·010	−0·089	0·029	−0·143	−0·010	−0·076	0·042
15	−0·087	−0·020	−0·042	0·026	−0·090	−0·025	−0·024	0·036
16	−0·048	−0·023	−0·002	0·017	−0·051	−0·031	+0·005	0·024
Trailing edge	−0·014	−0·014	+0·026	0·026	−0·023	−0·023	0·032	0·032

Angles of Incidence, 8° and 10°.

	Angle of incidence 8°.				Angle of incidence 10°.			
Leading edge	−1·27	−1·27	+0·056	0·056	−1·66	−1·66	−0·300	−0·300
1	−1·31	+0·508	−0·363	0·357	−1·66	+0·510	−0·752	+0·444
2	−1·28	0·403	−0·340	0·273	−1·67	0·454	−0·733	0·357
3	−0·700	0·306	−0·344	0·237	−1·28	0·371	−0·541	0·322
4	−0·685	0·270	−0·388	0·198	−0·936	0·322	−0·463	0·272
5	−0·761	0·234	−0·415	0·170	−0·818	0·279	−0·491	0·236
6	−0·782	0·218	−0·458	0·170	−0·833	0·263	−0·535	0·230
7	−0·753	0·220	—	0·193	−0·807	0·251	—	0·241
8	−0·674	0·201	−0·391	0·195	−0·716	0·222	−0·451	0·228
9	−0·491	0·179	−0·298	0·182	−0·530	0·201	−0·322	0·214
10	−0·378	0·119	−0·222	0·141	−0·410	0·133	−0·223	0·167
11	−0·298	0·066	−0·158	0·109	−0·308	0·069	−0·169	0·132
12	−0·253	0·029	−0·148	0·085	−0·249	+0·026	−0·151	0·101
13	−0·188	+0·004	−0·113	0·069	−0·183	−0·006	−0·106	0·080
14	−0·137	−0·018	−0·073	0·053	−0·137	−0·031	−0·067	0·061
15	−0·095	−0·035	−0·022	0·045	−0·107	−0·055	−0·018	0·048
16	−0·064	−0·049	+0·009	0·028	−0·081	−0·075	+0·013	0·022
Trailing edge	−0·044	−0·044	0·035	0·035	−0·068	−0·068	0·033	0·033

TABLE 19 (*continued*).

PRESSURE AT HOLES ON R.A.F. 14 WINGS.

Angles of Incidence, 15° and 20°.

No. of hole.	Angle of incidence 15°.				Angle of incidence 20°.			
	Upper wing.		Lower wing.		Upper wing.		Lower wing.	
	Upper surface.	Lower surface.	Upper surface.	Lower surface.	Upper surface.	Lower surface.	Upper surface.	Lower surface.
Leading edge	−0·870	−0·870	−1·325	−1·325	−0·393	−0·393	−0·515	−0·515
1	−0·847	+0·514	−1·355	+0·517	−0·394	+0·526	−0·657	+0·518
2	−0·914	0·481	−1·390	0·487	−0·391	0·476	−0·663	0·500
3	−0·905	0·411	−1·390	0·439	−0·391	0·414	−0·624	0·459
4	−0·905	0·359	−1·075	0·393	−0·402	0·370	−0·629	0·418
5	−0·857	0·322	−0·816	0·357	−0·400	0·330	−0·638	0·381
6	−0·838	0·302	−0·648	0·342	−0·399	0·304	−0·634	0·364
7	−0·805	0·285	—	0·330	−0·388	0·287	—	0·350
8	−0·746	0·252	−0·526	0·304	−0·389	0·249	−0·592	0·323
9	−0·653	0·219	−0·389	0·271	−0·387	0·218	−0·552	0·288
10	−0·562	0·137	−0·282	0·221	−0·405	0·128	−0·485	0·228
11	−0·439	0·063	−0·206	0·167	−0·421	+0·029	−0·388	0·172
12	−0·360	+0·002	−0·151	0·131	−0·433	−0·049	−0·307	0·118
13	−0·288	−0·049	−0·090	0·096	−0·430	−0·125	−0·245	0·067
14	−0·255	−0·089	−0·062	0·062	−0·411	−0·187	−0·222	+0·015
15	−0·239	−0·133	−0·035	+0·037	−0·393	−0·248	−0·195	−0·030
16	−0·219	−0·180	−0·019	−0·007	−0·377	−0·317	−0·178	−0·117
Trailing edge	−0·198	−0·198	−0·012	−0·012	−0·334	−0·334	−0·158	−0·158

Table 20.

RESULTS OF FORCE INTEGRATION.

Upper Wing.

Angle of incidence. Degrees.	Normal force coefficient.	Longitudinal force coefficient.	Lift coefficient.	Drag coefficient.
0	0·178 0·170	+ 0·0042 + 0·0056	0·174	0·0049
2	0·270 0·267	− 0·0045 − 0·0035	0·269	0·0054
4	0·344	− 0·0154	0·344	0·0086
6	0·415	− 0·0271	0·416	0·0164
8	0·480	− 0·0492	0·482	0·0180
10	0·532	− 0·0631	0·535	0·0304
15	0·585	− 0·0264	0·572	0·126
20	0·480	+ 0·0004	0·451	0·165

Lower Wing.

Angle of incidence. Degrees.	Normal force coefficient.	Longitudinal force coefficient.	Lift coefficient.	Drag coefficient.
0	0·076	0·0100	0·076	0·0100
2	0·151	+ 0·0044	0·151	0·0097
4	0·212	− 0·0002	0·211	0·0146
6	0·275	− 0·0085	0·275	0·0203
8	0·332	− 0·0177	0·331	0·0287
10	0·385	− 0·0302	0·384	0·0373
15	0·503	− 0·0625	0·503	0·0701
20	0·595	− 0·0254	0·569	0·1800

(ii) Pressure Plotting on a Section of the Lower Wing of a Biplane with B.E. 2c Wings.

The experiments described in this section compare directly with the tests in Appendix II on the pressure distribution over the wing of an aeroplane in flight. The model used was the one-tenth scale complete model of B.E. 2c, with the old B.E. 2c wing section, and was as nearly as possible a scale model of the aeroplane used in the full scale tests. The pressure plotting holes were more numerous than those on the full scale machine, but many of the model holes agree in position with those of the machine, so that a direct comparison of the pressures is in many cases possible. The positions of the holes in the model wing are given in Table 21, which also defines the section.

The model was supported on wires in the wind channel, so as to minimise any possible interference due to the method of support. The pressure plotting was performed in the usual way by stopping all the holes with plasticine and then opening one at a time and measuring the pressure at the open hole by means of a tilting gauge. This process was repeated at each angle of incidence, so that the pressures at every hole at any given angle were recorded without alteration of the attitude of the model. This method differs slightly from that adopted in the older experiments, in which the pressure at one hole was measured at all angles of incidence, and then the next hole treated in like manner, and so on. The accuracy is probably slightly improved by the method adopted, since there is no error due to slight variations in angle setting for different holes as in the older method.

A preliminary set of pressure measurements was taken at an angle of incidence of + 1°, and it was found that there were considerable variations from the pressures found at corresponding holes on the full scale wing, more especially in the neighbourhood of the leading edge. It was suspected that these differences might be due to slight errors in the shape of the section. The section was measured carefully on a milling machine, and was found to depart appreciably from that given for the actual wing. It was accordingly made up to the correct section with wax, and by scraping away where necessary to accurate templates. Subsequent measurement showed that the waxed plane had the same section as that of the full scale wing within the limits of allowable errors of cutting the templates. The modified section was again pressure plotted at + 1°, and the results are compared with the original set in Fig. 35. It will be seen that the small changes of shape have only produced very small alterations in the pressures, so that it is not possible to account for the deviations from full scale by change of shape of section. In Fig. 36 the pressures at 0° angle of incidence are plotted at 40 ft./sec. and 80 ft./sec. The variation is again small, but in

the expected direction, corresponding with a higher lift coefficient at the higher speed. Any scale effect which may exist would be more marked at small angles of incidence than at larger angles and, as the differences at 0° are small, it was not considered necessary to take readings at more than one speed for the other angles of incidence.

The actual pressures observed in all the holes are given in Table 22. These were plotted in the usual way against the abscissæ and ordinates of the holes, and the areas of the resulting diagrams measured, giving the normal force coefficient and the longitudinal force coefficient. A simple resolution of these gives the lift and drag coefficients of the section. The normal and longitudinal force coefficients are given in Table 23, and also the lift and drag coefficients deduced from them.

TABLE 21.

POSITIONS OF PRESSURE PLOTTING HOLES IN B.E. 2c WING.

X and Y are the co-ordinates of the holes, along and perpendicular to the chord, measured from the leading edge, and expressed as fractions of the chord.

Hole.	Upper surface.		Lower surface.	
	X.	Y.	X.	Y.
Leading edge	0	0·0070	0	0·0070
1	0·010	0·0200	0·025	0·0034
2	0·037	0·0395	0·049	0·0070
3	0·062	0·0520	0·074	0·0102
4	0·086	0·0590	0·097	0·0133
5	0·136	0·0695	0·144	0·0182
6	0·185	0·0747	0·191	0·0215
7	0·286	0·0782	0·289	0·0230
8	0·386	0·0772	0·386	0·0213
9	0·485	0·0736	0·485	0·0187
10	0·585	0·0685	0·584	0·0152
11	0·686	0·0595	0·685	0·0117
12	0·787	0·0472	0·787	0·0076
13	0·860	0·0350	0·860	0·0050
14	0·933	0·0215	0·933	0·0024
Trailing edge	1·000	0·0040	1·000	0·0040

NOTE.—These co-ordinates were measured on the milling machine after the plane was made.

TABLE 22.

PRESSURES AT VARIOUS HOLES, EXPRESSED AS FRACTIONS OF ρV^2.

U.S. = Upper Surface. L.S. = Lower Surface.

Angle of incidence.	0°*		0°*		1°*		1°		2°	
Wind speed.	40 ft./sec.		80 ft./sec.		40 ft./sec.		40 ft./sec.		40 ft./sec.	
Hole.	U. S.	L. S.	U. S.	L. S.	U. S.	L. S.	U. S.	L. S.	U. S.	L. S.
Leading edge	0·257	0·257	0·323	+ 0·323	0·038	+ 0·038	0·375	+ 0·375	0·340	+ 0·340
1	0·318	− 0·235	0·278	− 0·244	0·287	− 0·212	+ 0·241	− 0·216	+ 0·218	− 0·211
2	+ 0·055	− 0·244	+ 0·044	− 0·256	+ 0·024	− 0·227	− 0·008	− 0·230	− 0·050	− 0·219
3	− 0·181	− 0·246	− 0·154	− 0·256	− 0·173	− 0·226	− 0·175	− 0·223	− 0·213	− 0·249
4	− 0·210	− 0·242	− 0·232	− 0·240	− 0·255	− 0·179	− 0·254	− 0·195	− 0·277	− 0·147
5	− 0·254	− 0·177	− 0·261	− 0·156	− 0·279	− 0·061	− 0·255	− 0·088	− 0·294	− 0·045
6	− 0·231	− 0·080	− 0·241	− 0·049	− 0·251	+ 0·030	− 0·250	+ 0·001	− 0·283	+ 0·055
7	− 0·193	+ 0·042	− 0·200	+ 0·059	− 0·208	0·076	− 0·204	0·067	− 0·222	0·095
8	− 0·157	0·057	− 0·160	0·061	− 0·169	0·067	− 0·167	0·068	− 0·181	0·078
9	− 0·141	0·043	− 0·145	0·047	− 0·150	0·050	− 0·148	0·054	− 0·160	0·061
10	− 0·138	0·038	− 0·140	0·036	− 0·143	0·039	− 0·151	0·042	− 0·157	0·052
11	− 0·130	0·029	− 0·138	0·027	− 0·137	0·033	− 0·140	0·034	− 0·147	0·037
12	− 0·110	0·022	− 0·122	0·025	− 0·117	0·027	− 0·115	0·028	− 0·117	0·034
13	− 0·092	0·022	− 0·091	0·027	− 0·098	0·028	− 0·100	0·027	− 0·090	0·032
14	− 0·078	0·019	− 0·044	0·028	− 0·068	0·021	− 0·056	0·023	− 0·039	0·027
Trailing edge	+ 0·008	0·008	+ 0·022	0·022	+ 0·013	0·013	+ 0·015	0·015	+ 0·019	0·019

* These columns refer to the original section: all other columns give results for section modified to agree with the full-scale wing.

TABLE 22 (*continued*).

PRESSURES AT VARIOUS HOLES, EXPRESSED AS FRACTIONS OF ρV^2.

U.S. = Upper Surface. L.S. = Lower Surface.

Angle of incidence.	4°		6°		8°		10°	
Wind speed.	40 ft. /sec.		40 ft. /sec.		40 ft. /sec.		40 ft. /sec.	
Hole.	U. S.	L. S.	U. S.	L. S.	U. S.	L. S.	U. S.	L. S.
Leading edge	0·427	+ 0·427	+ 0·491	0·491	+ 0·483	0·483	+ 0·333	0·333
1	+ 0·099	− 0·119	− 0·046	0·110	− 0·220	0·211	− 0·464	0·306
2	− 0·109	− 0·042	− 0·282	0·156	− 0·382	0·228	− 0·575	0·297
3	− 0·278	+ 0·116	− 0·409	0·173	− 0·523	0·221	− 0·633	0·278
4	− 0·341	0·128	− 0·454	0·173	− 0·519	0·212	− 0·612	0·266
5	− 0·347	0·132	− 0·412	0·177	− 0·440	0·211	− 0·522	0·257
6	− 0·318	0·138	− 0·382	0·180	− 0·385	0·209	− 0·450	0·246
7	− 0·243	0·118	− 0·370	0·155	− 0·292	0·178	− 0·364	0·214
8	− 0·208	0·098	− 0·232	0·135	− 0·218	0·149	− 0·220	0·180
9	− 0·181	0·076	− 0·175	0·107	− 0·171	0·128	− 0·181	0·155
10	− 0·170	0·062	− 0·159	0·094	− 0·161	0·109	− 0·166	0·131
11	− 0·149	0·049	− 0·146	0·076	− 0·143	0·091	− 0·151	0·111
12	− 0·110	0·045	− 0·106	0·063	− 0·107	0·074	− 0·103	0·091
13	− 0·073	0·040	− 0·061	0·055	− 0·063	0·063	− 0·060	0·076
14	− 0·026	0·033	− 0·024	0·042	− 0·018	0·048	− 0·018	0·057
Trailing edge	+ 0·025	0·025	+ 0·030	0·030	+ 0·033	0·033	+ 0·031	0·031

Pressure Plotting on R.A.F 14. Wing Sections on B.E.2c Model. Upper Wing.

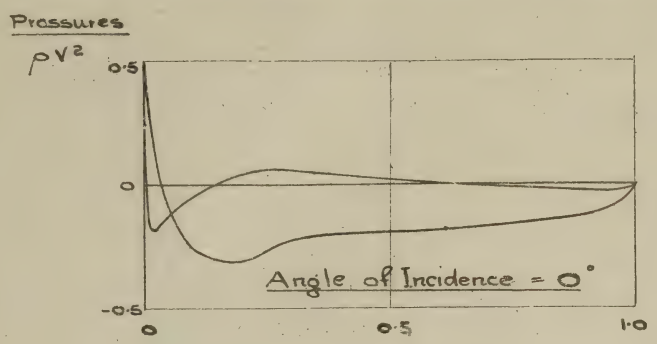

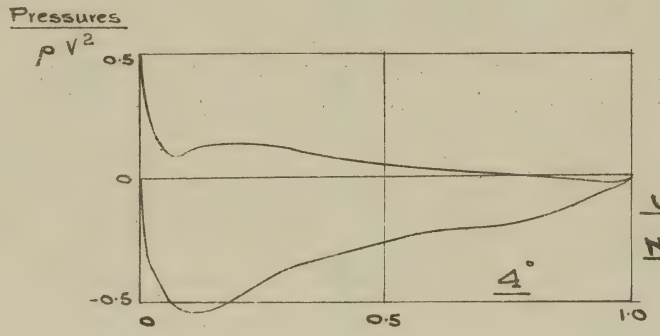

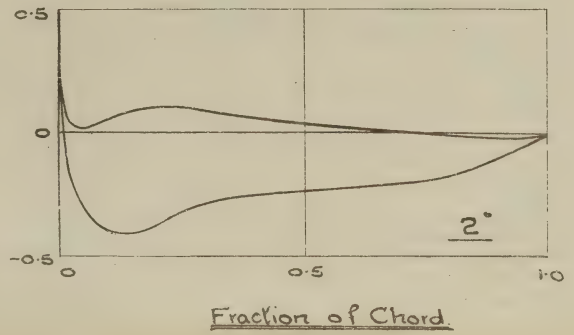

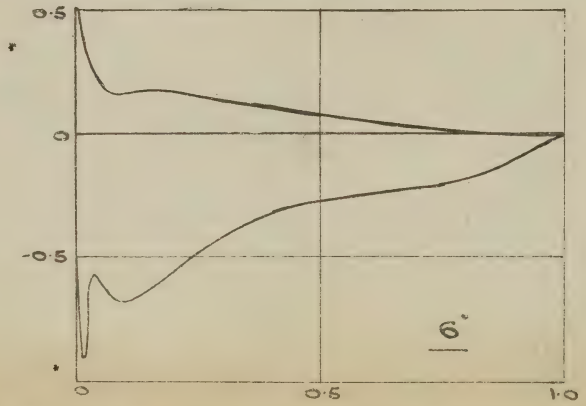

Upper wing - Normal Force

REPORT No. 374 (APPENDIX IV.)

FIG. 27.

Pressure Plotting on R.A.F. 14 Wing Sections on B.E. 2c Model. Upper Wing.

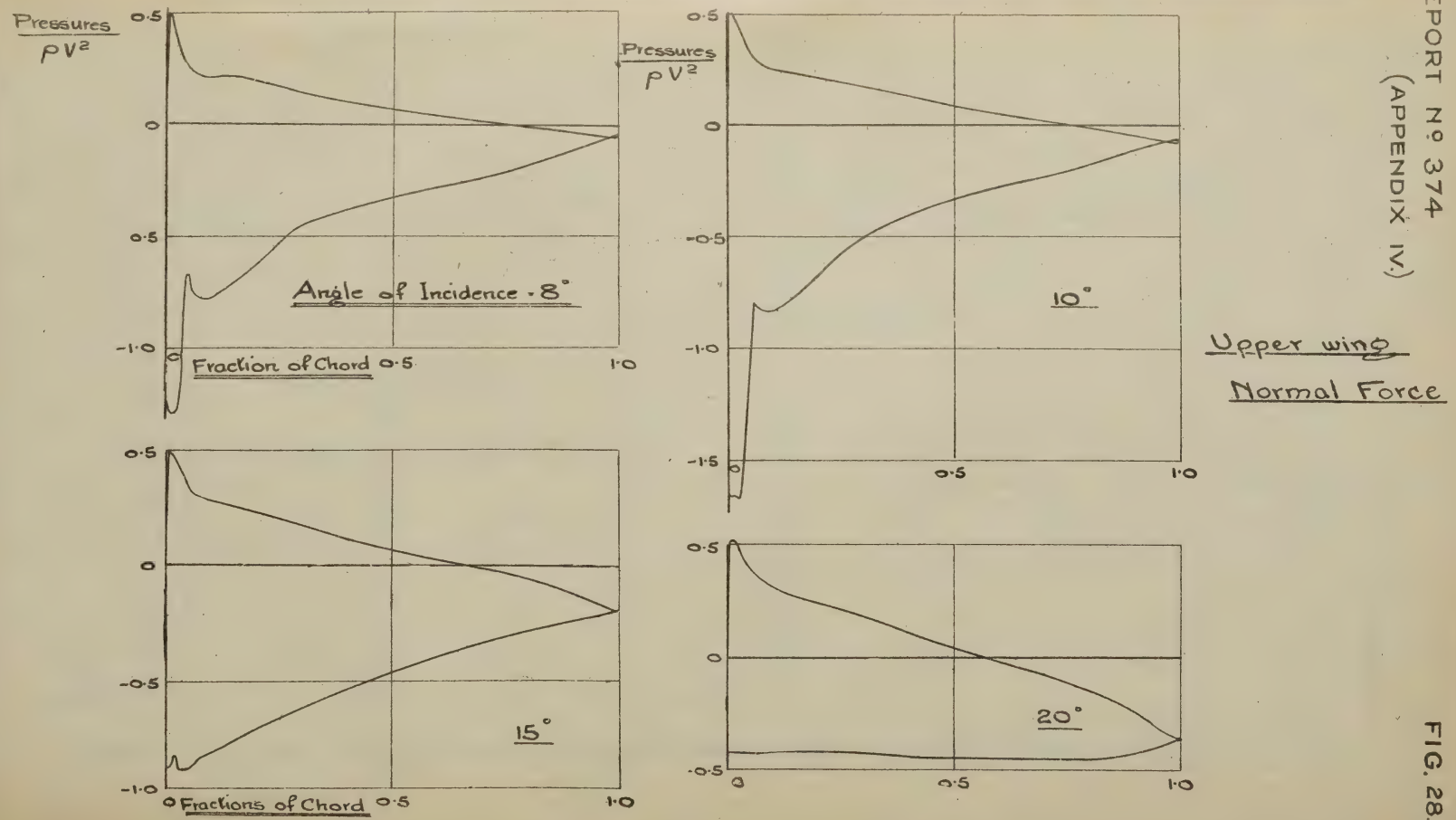

Upper wing

Normal Force

REPORT No. 374 (APPENDIX IV.)

FIG. 28.

Pressure Plotting on R.A.F 14 Wing Sections on B.E.2c Model. Lower Wing.

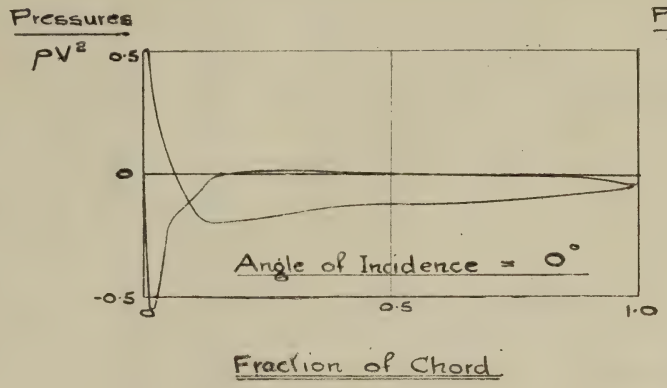

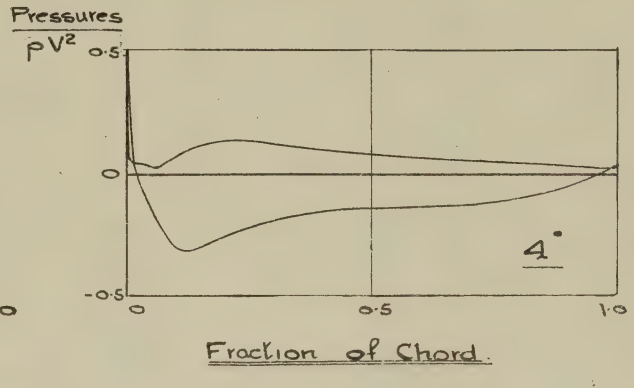

Lower wing — Normal Force

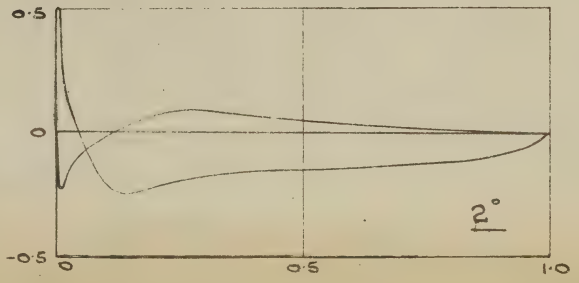

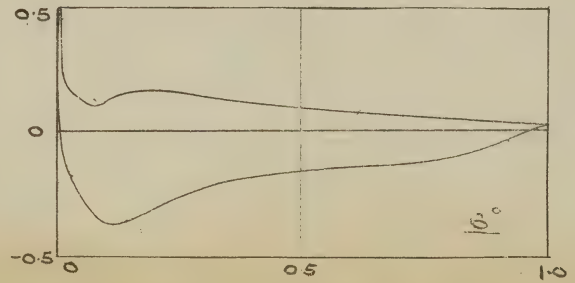

Pressure Plotting on R A F 14 Wing Sections on B.E.2c Model. Lower Wing.

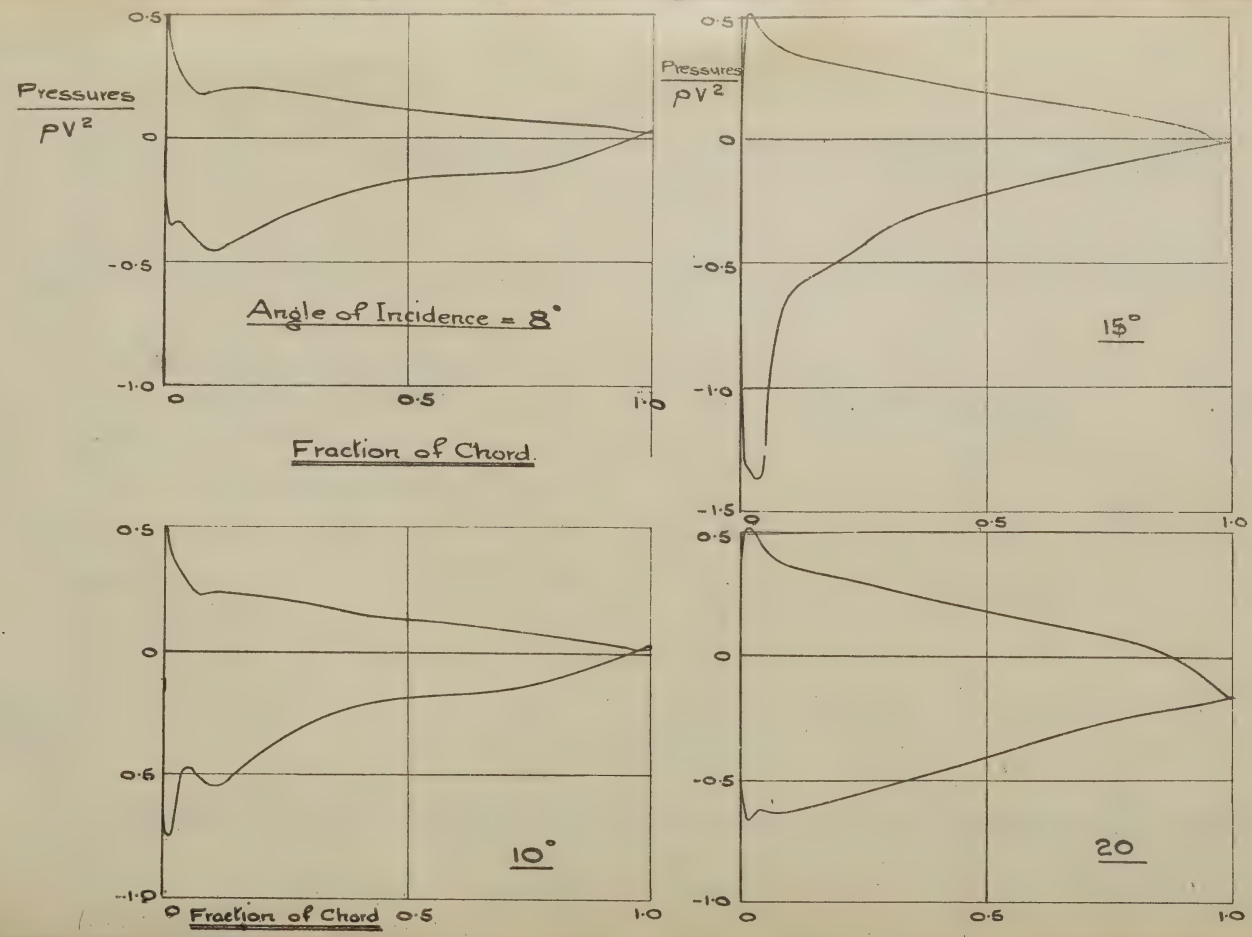

Lower wing.
Normal Force.

REPORT No 374
(APPENDIX IV.)

FIG. 30.

REPORT Nº 374 FIG. 31.

(APPENDIX IV.)

PRESSURE PLOTTING ON R.A.F.14. WING SECTION ON

B.E.2.C. MODEL

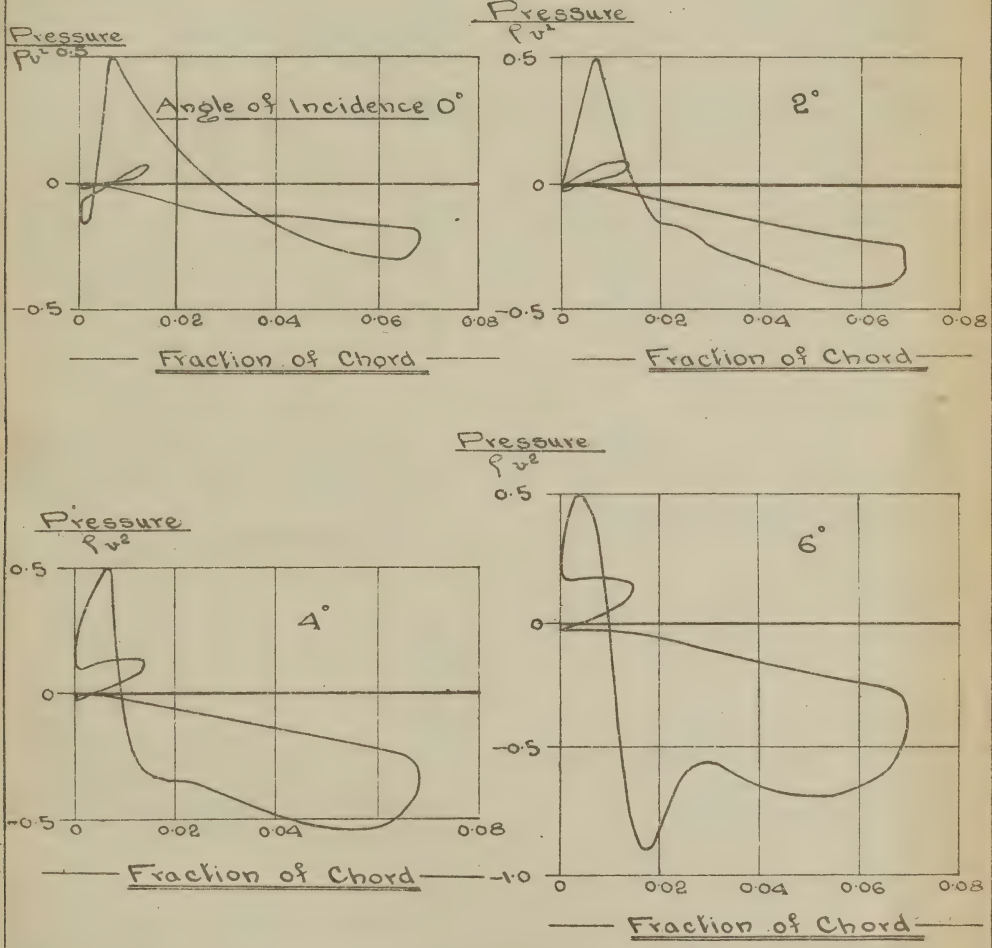

UPPER WING.

Longitudinal Force

REPORT Nº 374 FIG. 32.

(APPENDIX IV.)

PRESSURE PLOTTING ON R.A.F. 14 WING SECTION ON B.E.2.c. MODEL.

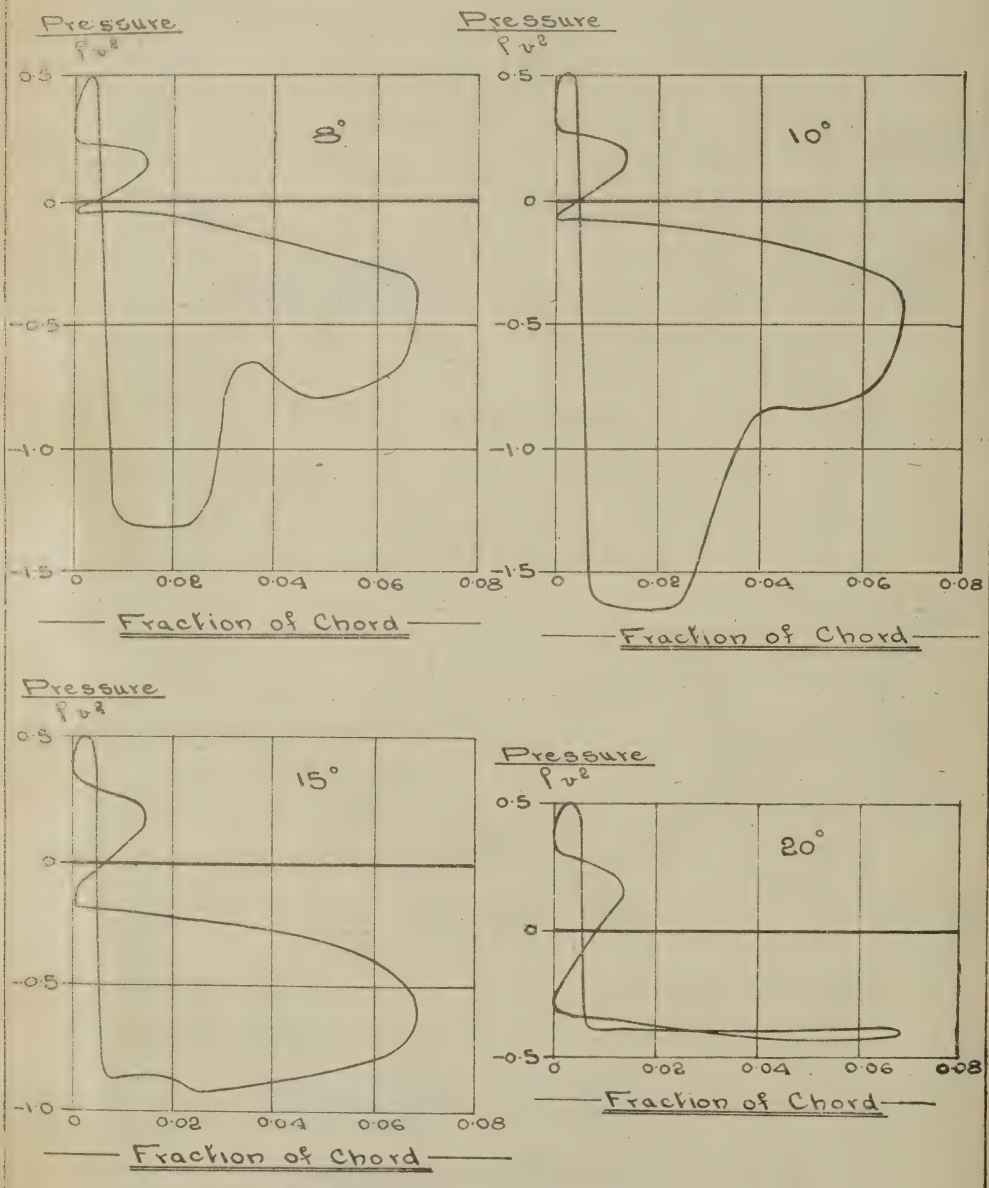

UPPER WING

Longitudinal Force

REPORT Nº 374 (APPENDIX IV.) FIG. 33.

PRESSURE PLOTTING ON R.A.F.14 WING SECTION ON B.E.2c. MODEL.

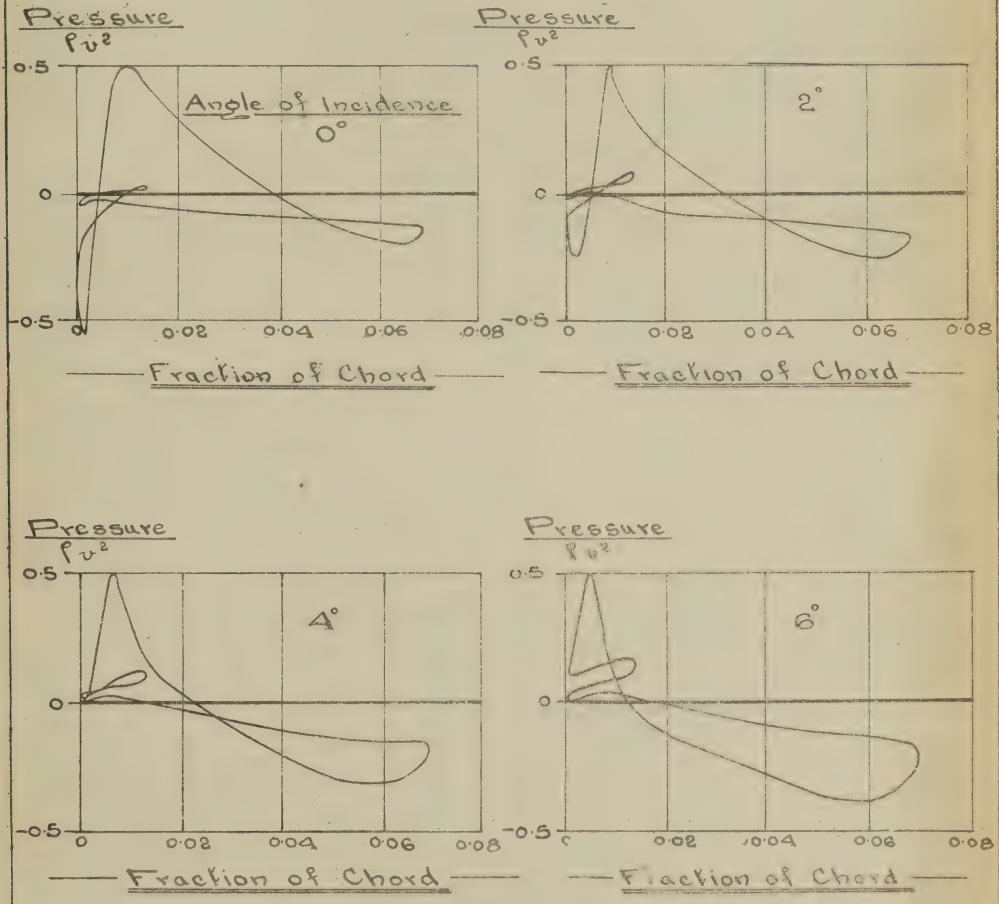

LOWER WING.

Longitudinal Force

REPORT Nº 374 FIG. 34

(APPENDIX IV.)

PRESSURE PLOTTING ON R.A.F.14. WING SECTION

ON B.E.2.c. MODEL

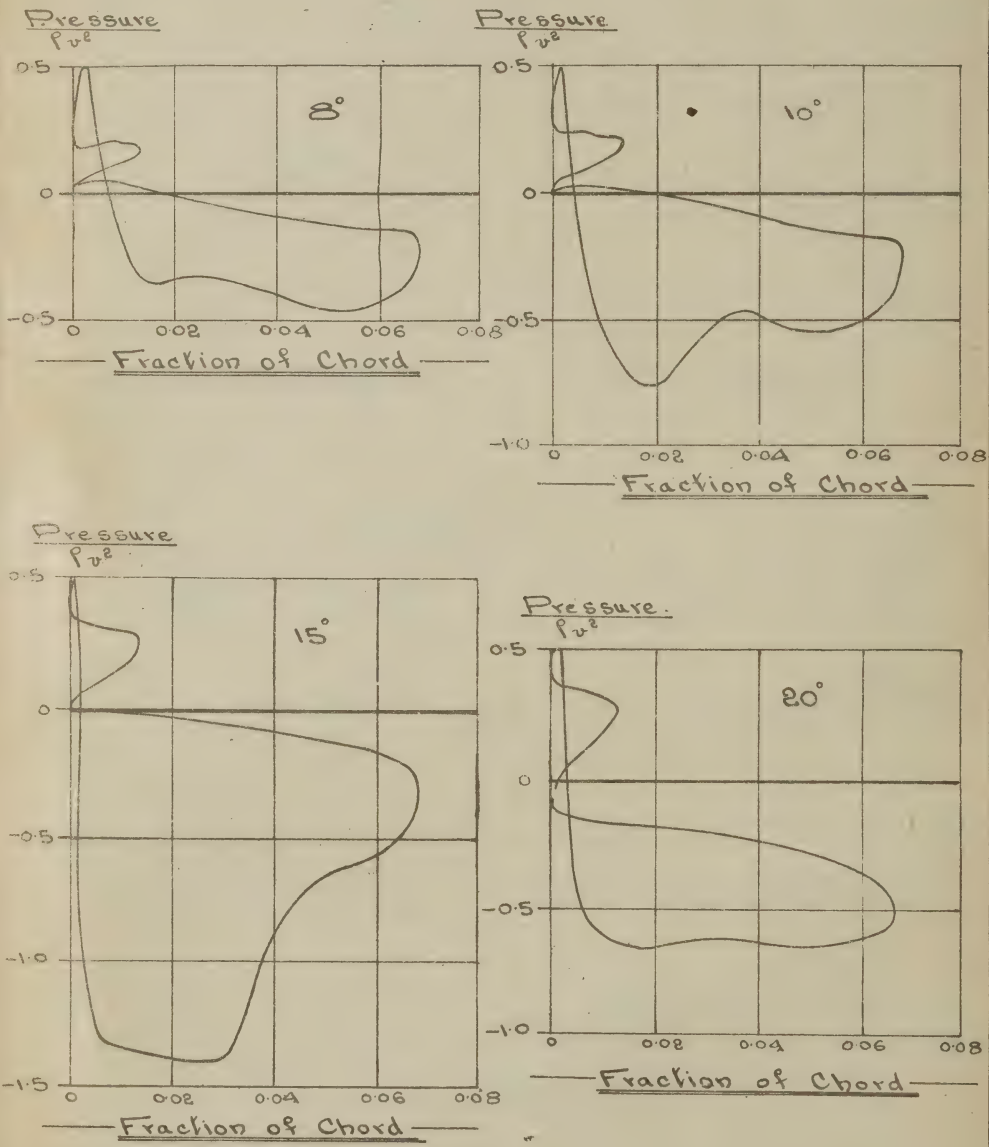

LOWER WING

Longitudinal Force

PRESSURE PLOTTING ON LOWER WING OF A BIPLANE WITH B.E.2c. WINGS.

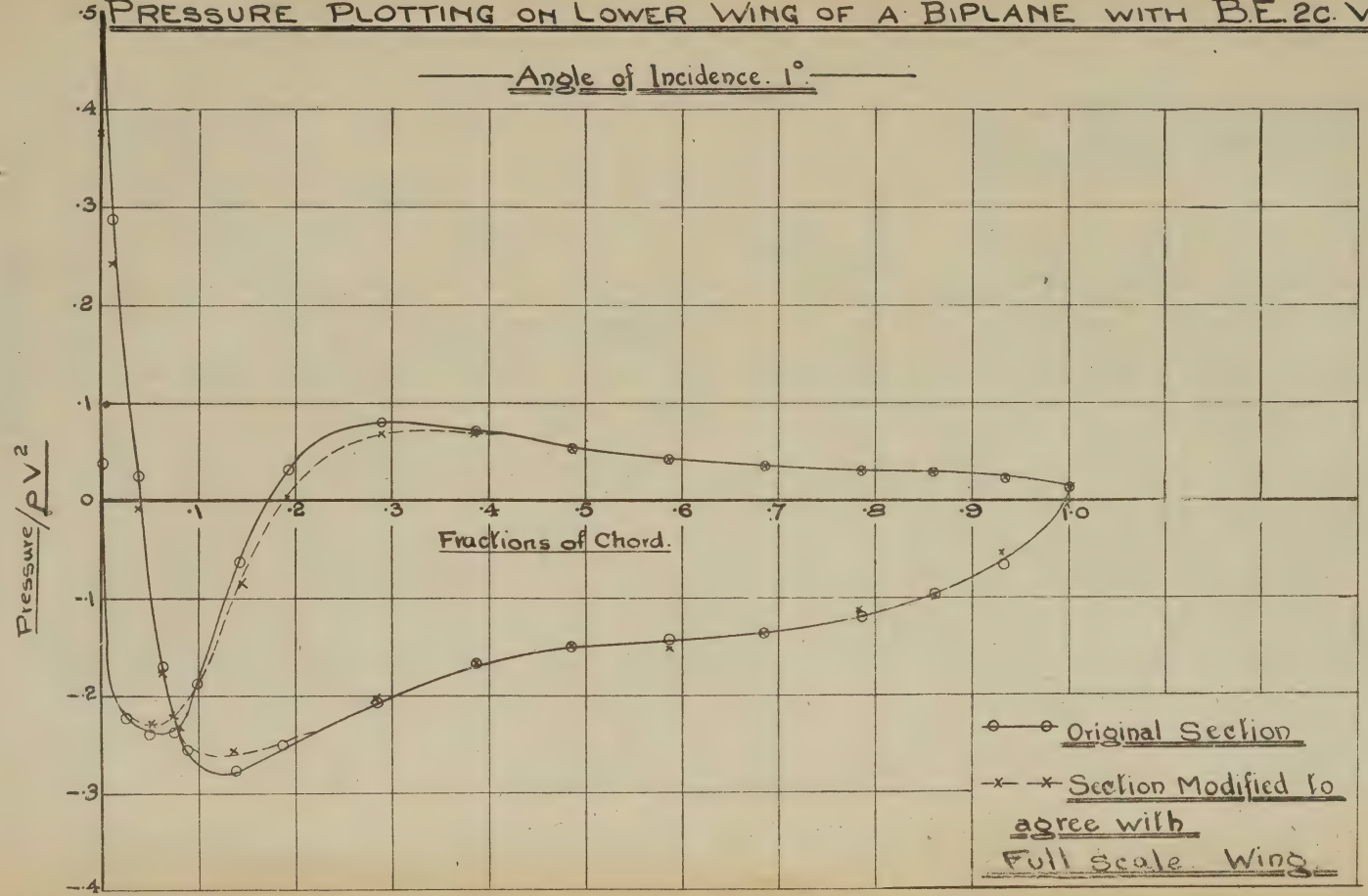

FIG. 35.

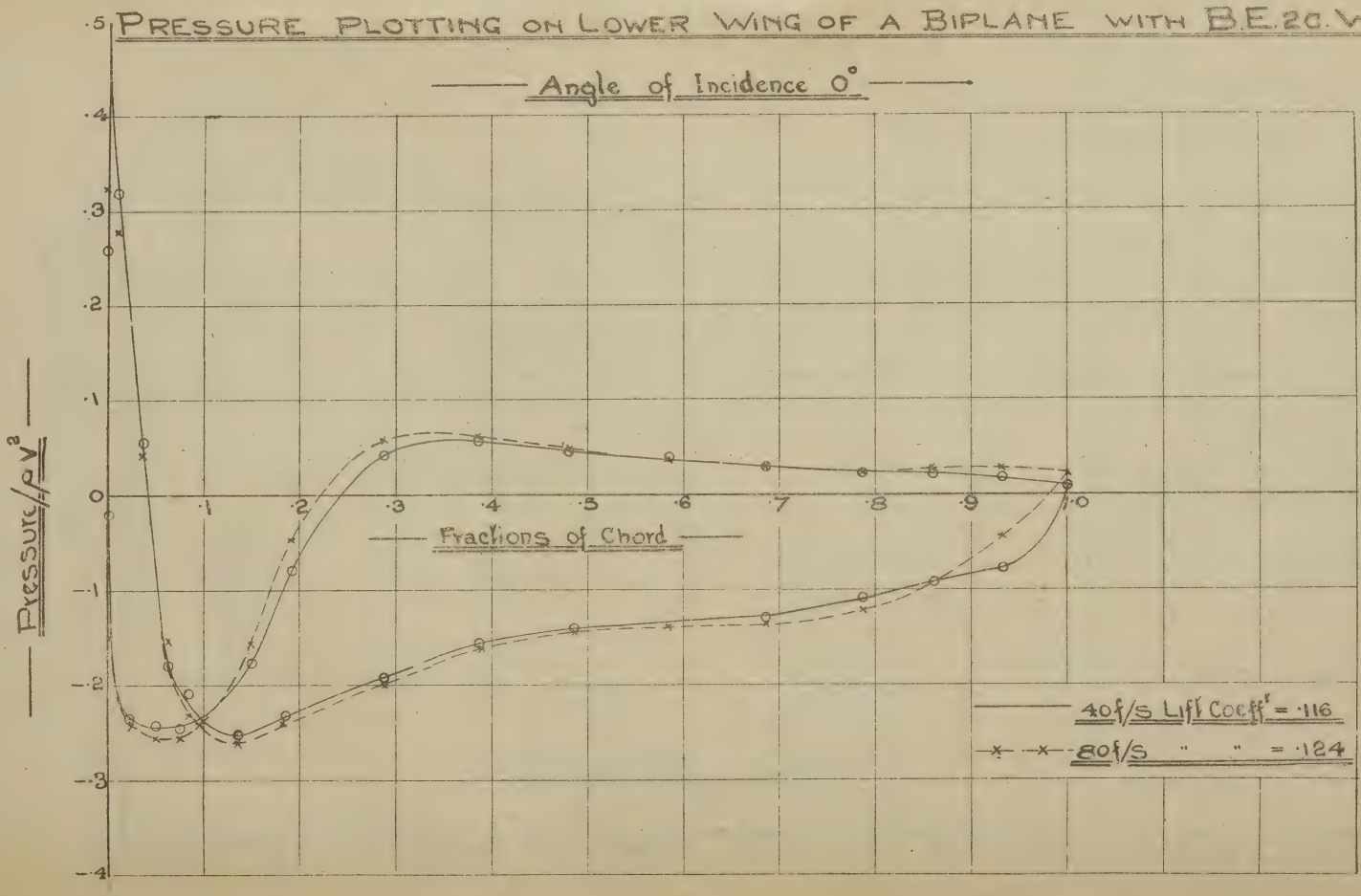
PRESSURE PLOTTING ON LOWER WING OF A BIPLANE WITH B.E.2c. WINGS.
Angle of Incidence 0°
Pressure/ρV²
Fractions of Chord
·5
·4
·3
·2
·1
0
-·1
-·2
-·3
-·4
·1
·2
·3
·4
·5
·6
·7
·8
·9
1·0
40 f/s Lift Coeff' = ·116
80 f/s " " = ·124

FIG. 36.

Table 23.

RESULTS OF FORCE INTEGRATIONS ON B.E. 2c WING SECTION.

Angle of Incidence. Degrees.	Longitudinal Force Coefficient.	Normal Force Coefficient.	Lift Coefficient.	Drag Coefficient.	Lift / Drag.
0	0·0148	0·119	0·119	0·0148	8·0
1	0·0121	0·147	0·147	0·0147	10·0
2	+ 0·0092	0·172	0·172	0·0152	11·3
4	− 0·0005	0·242	0·241	0·0164	14·7
6	− 0·0101	0·312	0·313	0·0226	13·7
8	− 0·0187	0·340	0·340	0·0289	11·7
10	− 0·0308	0·402	0·401	0·0394	10·2

PREDICTION OF THE PERFORMANCE AND LONGITUDINAL STABILITY OF AN AEROPLANE, INCLUDING THE ESTIMATION OF THE EFFECT OF SMALL CHANGES IN THE DESIGN.

By H. Glauert and S. B. Gates.

Presented by the Superintendent, Royal Aircraft Factory.

Reports and Memoranda, No. 324. *March,* 1917.

Summary.—In this report methods are developed for predicting the performance and longitudinal stability of an aeroplane. The methods are suitable for obtaining either rapid preliminary estimates, or more accurate predictions when sufficiently detailed information is available. The change in performance and stability caused by small alterations in the constants of the machine is also calculated, the analysis being based on the method of prediction previously developed.

In Part I, the time of climb to any height and the maximum height attainable are specially considered.

In Part II, the maximum speed of level flight at any height is examined.

In Part III, approximate formulæ for the period of the phugoid oscillation are developed.

Numerical examples of all the formulæ used are given for the case of a B.E.2e machine.

An Appendix, giving some details of approximations to the height density gradient, is added.

PART I. CLIMBS.

1. *Assumptions.*

Let ρ = density at height h feet, per cent. of standard.

V = true airspeed in m.p.h.

V_0 = indicated airspeed in m.p.h.

B = B.H.P. at N engine revolutions per minute.

η = airscrew efficiency.

r = head resistance at 100 m.p.h.

It will be assumed that the airspeed V_0 and the engine revs. N remain constant during the climb. Also the standard density is assumed to be related to the height by the equation

$$\rho^a = c - bh \quad \text{(See Appendix)}$$

Writing $p = \frac{V}{N} = \frac{V_o}{N}\rho^{-\frac{1}{2}}$, and regarding the curve of airscrew efficiency against V/N as a straight line for the range used in climbing, it follows that

$$\eta = \eta_o + (p - p_o)\frac{d\eta}{dp}$$
$$= \eta_o\{1 + \varepsilon(\rho^{-\frac{1}{2}} - 1)\}$$

where $$\varepsilon = \frac{p_o\, d\eta}{\eta_o\, dp}$$

and η_o, p_o are the values corresponding to the standard density of 0·00237 slugs per cubic foot.

It follows that if Z is the T.H.P. for this standard density, then at height h the T.H.P. will be

$$Z\rho^{1\cdot1}\{1 + \varepsilon(\rho^{-\frac{1}{2}} - 1)\}$$

since engine tests indicate that the variation of brake horse-power with density is approximately as $\rho^{1\cdot1}$.

It has been found by inspection of a number of airscrew efficiency curves that the quantity ε is only subject to small variations and has a mean value of 0·5.

In the calculation of r, allowance should be made for a slipstream appropriate to climbing. The variation of the slipstream during the climb will be ignored.

2. *Equations.*—The horse-power used in climbing is $\frac{W}{550}\cdot\frac{dh}{dt}$ where t is measured in seconds, and the equation of energy gives, therefore,

$$\frac{W}{550}\frac{dh}{dt} = Z\rho^{1\cdot1}\{1 + \varepsilon(\rho^{-\frac{1}{2}} - 1)\} - \frac{V}{375}\left\{W\frac{K_d}{K_l} + r\rho V^2\, 10^{-4}\right\}$$

which becomes

$$-\frac{a}{b}\rho^{a-1}\frac{d\rho}{dt} = \frac{550Z}{W}\{(1-\varepsilon)\rho^{1\cdot1} + \varepsilon\rho^{0\cdot6}\}$$

$$-\frac{550}{375}\frac{V_o\rho^{-\frac{1}{2}}}{W}\left\{W\frac{K_d}{K_l} + rV_o^2\, 10^{-4}\right\}$$

Now write,

$$\frac{V_o}{375Z}\left\{W\frac{K_d}{K_l} + rV_o^2\, 10^{-4}\right\} = \frac{H}{Z} = \alpha$$

and the equation becomes,

$$-\frac{d\rho}{dt} = \frac{b}{a}\frac{550Z}{W}\left\{(1-\varepsilon)\rho^{2\cdot1-a} + \varepsilon\rho^{1\cdot6-a} - \alpha\rho^{0\cdot5-a}\right\} \quad . \quad (1)$$

In the expression for α or $\underline{H}$ the term $W \frac{K_d}{K_l}$ is the wing drag. K_l is the "effective" lift coefficient determined by the equation,

$$W = 0{\cdot}0051\, K_l A V_o^2$$

while K_d is the drag coefficient corresponding to the true lift coefficient of the wings. For further details concerning the effective lift co-efficient see Part III of this report.

3. *Maximum possible Height.*—Equation (1) gives at once the greatest height to which the aeroplane can climb. Putting $\frac{d\rho}{dt}$ equal to zero the equation gives

$$\alpha = \varepsilon\rho^{1{\cdot}1} + (1 - \varepsilon)\,\rho^{1{\cdot}6}$$

The value of Z/H necessary to reach any height can be obtained for different values of the airscrew constant ε. It was found that the variation of ε was small and unimportant. The results are given, therefore, only for the case of $\varepsilon = 0{\cdot}5$ (Fig. 1).

For the density used in this work see Appendix to this report.

4. *Time to any Height.*—By integration, equation (1) gives the time to climb to any definite height.

$$t = \frac{a}{b}\,\frac{W}{33000Z}\int_{\rho}^{1{\cdot}026} \frac{d\rho}{\rho^{2{\cdot}1-a}(1-\varepsilon) + \rho^{1{\cdot}6-a}\varepsilon - \rho^{0{\cdot}5-a}\alpha} \text{ min.}$$

It was found that the values

$$a = 0{\cdot}30$$
$$b = 0{\cdot}4 \times 10^{-6}$$
$$c = 1{\cdot}0078$$

gave a very close representation of the standard density curve up to 10,000 feet, and quite a fair representation above this height. These values were, therefore, adopted for the evaluation of the integral.

For the purpose of calculation this expression is written as

$$t = \frac{W}{Z}\,\phi$$

and ϕ was evaluated by expanding the integral in ascending powers of $(1 - \rho)$, which may be regarded as a small quantity; for a definite value of ρ, ϕ is a function of α and ε.

Numerical values were calculated for the case of $\varepsilon = 0{\cdot}5$ and are exhibited in Fig. 2. Any deviation from this value is of small effect and can be dealt with in the method developed below. By means of the diagram (Fig. 2) it is possible to predict the climb of an aeroplane very rapidly and if care is taken in determining the head resistance r and the thrust horse-power Z, it is found that the predictions agree well with the standard performances.*

* This of course implies the use of the full scale K_l, K_d curves for the wing section. See R. and M. 321.

5. *Effect of Small Changes of Design.*—It is next proposed to examine the effect of a small change of design or of speed on the time to reach a definite height. The fundamental equations are,

$$t = \frac{W}{Z}\phi$$

$$W = 0{\cdot}0051\, K_l A V_o^2$$

$$\alpha = \frac{H}{Z} = \frac{W V_o K'_d}{375\, Z K_l}$$

where

$$K'_d = K_d + K_b \text{ and } K_b = \frac{1}{51}\frac{r}{A}$$

For the small increments we have, therefore,

$$\frac{\Delta t}{t} = \frac{\Delta W}{W} - \frac{\Delta Z}{Z} + \frac{\Delta \phi}{\phi}$$

$$\frac{\Delta K_l}{K_l} = \frac{\Delta W}{W} - \frac{\Delta A}{A} - \frac{2\,\Delta V_o}{V_o}$$

$$\frac{\Delta K_b}{K_b} = \frac{\Delta r}{r} - \frac{\Delta A}{A}$$

$$\frac{\Delta \alpha}{\alpha} = \frac{\Delta W}{W} + \frac{\Delta V_o}{V_o} - \frac{\Delta Z}{Z} + \frac{\Delta K_b}{K'_d} + (\mu' - 1)\frac{\Delta K_l}{K_l}$$

where

$$\mu' = \frac{K_l}{K'_d}\cdot\frac{dK_d}{dK_l}$$

We may also write,

$$\frac{\Delta \phi}{\phi} = X\frac{\Delta \alpha}{\alpha} - Y\frac{\Delta \varepsilon}{\varepsilon}$$

where X and Y are functions of ρ, α and ε.

On reduction the expression for Δt becomes,

$$\frac{\Delta t}{t} = \frac{\Delta W}{W}(1 - \mu' X) - \frac{\Delta Z}{Z}(1 + X) - \frac{\Delta A}{A}\left(\mu' - \frac{K_d}{K'_d}\right) X$$

$$+ \frac{\Delta r}{r} X \frac{K_b}{K'_d} + \frac{\Delta V_o}{V_o}(3 - 2\mu') X - \frac{\Delta \varepsilon}{\varepsilon} Y$$

Also since $Z = \eta B$ we can write

$$\frac{\Delta Z}{Z} = \frac{\Delta B}{B} + \frac{dB}{dN}\frac{\Delta N}{B} + \frac{\Delta \eta}{\eta} + \varepsilon\left(\frac{\Delta V_o}{V_o} - \frac{\Delta N}{N}\right)$$

and the complete expression becomes

$$\frac{\Delta t}{t} = \frac{\Delta W}{W}(1 + \mu' X) - \frac{\Delta A}{A}(\mu' - \frac{K_d}{K'_d}) X + \frac{\Delta r}{r} X \frac{K_b}{K'_d}$$

$$- \frac{\Delta B}{B}(1 + X) - \frac{\Delta \eta}{\eta}(1 + X) - \frac{\Delta N}{N}\left(\frac{N}{B}\frac{dB}{dN} - \varepsilon\right)(1 + X)$$

$$+ \frac{\Delta V_o}{V_o}\left\{(3 - 2\mu') X - \varepsilon (1 + X)\right\} - \frac{\Delta \varepsilon}{\varepsilon} Y \quad . \quad . \quad (2)$$

The values of X and Y have been calculated for a climb to 10,000 feet ($\rho = 0{\cdot}740$) when ε has the value of 0·5, and are given in Fig. 3.

6. *Numerical Values for a B.E.2e Machine.*—Typical values for a B.E.2e machine with R.A.F. 14 wing section and R.A.F. 1b. engine are

$$W = 2100, V_o = 53, N = 1575, B = 104.$$

The slipstream factor is then 2·3, and the values of the other constants become

$$A = 378, r = 425, \eta = 71{\cdot}5\ \%, \varepsilon = 0{\cdot}48$$

Effective $K_l = 0{\cdot}388$, $K_l = 0{\cdot}400$, $K = 0{\cdot}0343$

$$Z = 0{\cdot}715 \times 104 = 74{\cdot}5$$

$$H = \frac{53}{375}\left(2100 \times \frac{0{\cdot}0343}{0{\cdot}388} + 0{\cdot}0425 \times 53^2\right) = 43$$

$$\frac{W}{Z} = 28{\cdot}2 \quad , \quad \frac{Z}{H} = 1{\cdot}73 \quad .$$

Fig. 1 then shows that the maximum height attainable is 12,000 feet. For the climb we obtain the values

$h =$	3,500	6,000	10,000
$\phi =$	0·275	0·520	1·09
$t =$	7·8	14·7	31

In the above the value of $\varepsilon = 0{\cdot}50$. The correction to the true value according to the above analysis is

$$\frac{\Delta t}{t} = -Y\frac{\Delta \varepsilon}{\varepsilon}$$

$$\Delta t = 31 \times 0{\cdot}055 \times \frac{0{\cdot}02}{0{\cdot}50} = 0{\cdot}07 \text{ minutes.}$$

The percentage change in the time to 10,000 feet due to 1 per cent. change in each of the other variables is given in the table below. The values of the subsidiary variables are :—

$$X = 2{\cdot}15, Y = 0{\cdot}055, \mu' = 1{\cdot}08, K_b = 0{\cdot}022$$

and equation (2) then gives the required values.

Variable	W	A	r	B
Percentage change in t	3·3	−1·0	0·8	− 3·2
Variable	N	η	V_o	ε
Percentage change in t	−1·4	−3·2	+0·2	−0·06

It is evident from these values that no appreciable error is introduced by taking ε as 0·5 in a preliminary estimate. The quantities whose increments have most effect in changing t are the weight, horse-power and airscrew efficiency. The equal effect of the weight and horse-power is due to the value of μ' which is almost unity in the case considered. It appears also that a better climb would be obtained for a slower speed. This effect would be reversed for a larger value of Z/H which would diminish X and change the sign of this term.

PART II. LEVEL FLIGHTS.

1. *Equations.*—The equations which determine the speed of level flight of an aeroplane at any height are :

$$375\,Z\rho^{1\cdot1} = V\left(W\frac{Kd}{K_l} + r\,V_o^2\,10^{-4}\right)$$

$$W = 0\cdot0051\,K_l\,AV_o^2$$

$$Z = B\,\eta$$

where the quantities involved are as defined in Part I. It is to be noted that K_l is again the effective lift coefficient and that the resistance r will differ from its value on a climb owing to the change of the slipstream factor.

2. *Method of Solution.*—A graphical method of solution has been developed by means of subsidiary variables x, y, z, such that,

$$y = \frac{Z}{W}\frac{K_l}{K_d} \quad , \quad x = \frac{r}{W}\frac{K_l}{K_d}$$

$$375\,\rho^{1\cdot6}\,y = z = V_o + x\,V_o^3\,10^{-4}$$

These quantities are plotted in the main diagram of Fig. 4, the four quarters of which may be conveniently named NE, NW, SW, SE. In the quarters SE and SW x and y are plotted against K_l/K_d for various values of r/W and W/Z respectively. In the quarters NE and NW they are plotted against z for various values of V_o and of the height. The relation between the density ρ and the height is taken from standard density curve (Fig. 5.)

In the smaller diagrams of Fig. 4 are given curves connecting K_l and V_o for integral values of the loading W/A, and curves of K_l/K_d against K_l for the wing sections R.A.F. 14 and R.A.F. 15, derived from full scale experiments on B.E.2c and B.E.2e machines.

Starting with the value of K_l/K_d corresponding to a probable value of the lift coefficient K_l, the diagrams SE and SW serve to determine x and y. By means of NW the quantity z is next determined and the indicated airspeed V_o is then obtained from the fourth diagram NE. This value must be checked by means of the subsidiary diagrams. If the value of K_l/K_d determined from the value V_o does not agree with the value assumed at first, a second approximation should be carried out in the same way as before. The true airspeed is obtained immediately from the indicated airspeed V_o by multiplying by the factor $\rho^{-\frac{1}{2}}$.

3. *Effect of Small Changes of Design.*—For small increments to the quantities involved, we have the equations

$$\frac{\Delta K_l}{K_l} = \frac{\Delta W}{W} - \frac{\Delta A}{A} - \frac{2\,\Delta V_o}{V_o}$$

$$\frac{\Delta x}{x} = \frac{\Delta r}{r} - \frac{\Delta W}{W} + (1-\mu)\frac{\Delta K_l}{K_l} \text{ where } \mu = \frac{K_l}{K_d}\frac{dK_d}{dK_l}$$

$$\frac{\Delta y}{y} = \frac{\Delta Z}{Z} - \frac{\Delta W}{W} + (1-\mu)\frac{\Delta K_l}{K_l}$$

$$\frac{\Delta Z}{Z} = \frac{\Delta B}{B} + \frac{dB}{dN}\frac{\Delta N}{B} + \frac{\Delta \eta}{\eta} + \varepsilon\left(\frac{\Delta V_o}{V_o} - \frac{\Delta N}{N}\right)$$

$$\Delta z = \Delta x\, V_o^3\, 10^{-4} + \Delta V_o\,(1 + 3\,x\,V_o^2\,10^{-4})$$

It follows that,

$$\frac{\Delta y}{y} = \frac{\Delta z}{z} = \frac{\Delta x}{x}\left(1 - \frac{V_o}{z}\right) + \frac{\Delta V_o}{V_o}\left(3 - 2\,\frac{V_o}{z}\right)$$

and so on reduction

$$\frac{\Delta V_o}{V_o}(3 - 2\,\mu\,\frac{V_o}{z} - \varepsilon) = \frac{\Delta B}{B} + \frac{\Delta N}{N}\left(\frac{N}{B}\frac{dB}{dN} - \varepsilon\right) + \frac{\Delta \eta}{\eta}$$
$$- \frac{\Delta W}{W}\mu\,\frac{V_o}{z} - \frac{\Delta A}{A}(1-\mu)\,\frac{V_o}{z} - \frac{\Delta r}{r}\left(1 - \frac{V_o}{z}\right)$$

It is important to note that it is no longer possible to give ε the mean value of 0·5. It will be found that ε varies considerably with the speed and with the airscrew employed. The equation also deals only with the change of speed at a definite height.

4. *Numerical values for a B.E.2c. Machine.*—The values for level flight at 10,000 ft. corresponding to those used for the climb are,

$$W = 2100 \quad , \quad N = 1700 \quad , \quad B = 110 \quad ,$$

and as the slipstream factor is about 1·55 we also have

$$A = 368 \quad , \quad r = 319 \quad .$$

The efficiency will be about 85 per cent. and then,

$$\frac{W}{A} = 5{\cdot}7 \quad , \quad \frac{r}{W} = 0{\cdot}152 \quad , \quad \frac{W}{Z} = 22{\cdot}5 \quad .$$

The solution obtained by the method described above is,

Effective $K_l = 0{\cdot}206$, $K_b = 0{\cdot}218$, $K_d = 0{\cdot}0125$,

$x = 2{\cdot}50$, $y = 0{\cdot}72$, $z = 168$,

$V_o = 73\frac{1}{2}$, $V = 85$.

The percentage change in speed due to 1 per cent. change in each of the other variables is given by means of the subsidiary variables,

$$\mu = 1{\cdot}29 \quad , \quad \varepsilon = 0{\cdot}39 \quad , \quad \frac{V_o}{z} = 0{\cdot}437 \quad .$$

Variable.	B	N	η
Percentage change in V	0·68	0·26	0·68
Variable.	W	A	r
Percentage change in V	— 0·38	0·09	— 0·38

The most important terms are, of course, the horse-power and airscrew efficiency, while variation in the weight and head resistance also give a noticeable effect on the speed obtained.

PART III. LONGITUDINAL STABILITY.

1. *Notation.*—The symbols used in this investigation are defined as follows :—

V = True airspeed of machine in miles per hour.

W = Total weight of machine.

* h,k = Centre of gravity coefficients (measured respectively along and normal to the mean chord).

* b = Length of mean chord.

† l = Distance of centre of pressure of tail from centre of gravity.

A = Total wing area.

A′ = Total tail area.

‡ p = Slipstream factor for wings.

p' = Slipstream factor for tail.

e = Angle of downwash relative to wind.

---

* See Appendix I, Advisory Committee Report, R. & M. 326.

† The centre of pressure of the tail is taken, for all angles of incidence, at a distance back from the leading edge equal to one-third of the chord.

‡ If nA is area of surface in slipstream of velocity $V + v$, then

$$p^2 = 1 + n\left(\frac{v^2}{V^2} + \frac{2v}{V}\right)$$

K_l = Lift coefficient.
K_z = Normal force coefficient.
K_x = Longitudinal force coefficient.
K_m = Moment coefficient.
} of wings.

*K'_l = Nominal lift coefficient of tail with elevators loose.

E = Factor by which actual lift of tail differs from that found by using K'_l, at the same angle of the relative wind.

θ = Angle of incidence of wings.

θ' = Angle of incidence of tail to relative wind at tail.

ρ = % density, the standard being 0·00237 slugs /ft.^{3}.

2. *Equations of Equilibrium.*—The conditions of equilibrium of straight symmetrical flight, which is the motion specially considered in predictions of longitudinal stability, are :—

(1) Total pitching moment zero.

(2) Total lift = weight.

Neglecting the total pitching moment due to other parts of the machine except wings and tail, we get from (1) that the tail lift must be such as to balance the wing moment, *i.e.* :—

$$\text{Tail lift} = \frac{1}{l}(K_m + hK_z + kK_x)\, 0{\cdot}0051\, b\, \rho\, AV^2p^2$$

Now neglecting in the same way the lift of the subsidiary parts of the machine, condition (2) gives us :

$$W = \text{wing lift} + \text{tail lift}$$
$$= \left\{K_l + \frac{b}{l}(K_m + hK_z + kK_x)\right\} 0{\cdot}0051\, \rho\, AV^2p^2$$

The quantity $\frac{W}{\rho \times 0{\cdot}0051\, AV^2p^2}$ is called the effective lift co-efficient, and is related to the true lift co-efficient of the wings by the equation

$$\overline{K}_l = K_l + \frac{b}{l}(K_m + hK_z + kK_x).$$

For ordinary flight positions the tail is usually lifting negatively; hence the true lift coefficient is greater than the effective lift coefficient.

3. *Period of Phugoid Oscillation.*—A good approximate solution of the stability biquadratic gives for the long period oscillation the formula

$$p = \frac{\sqrt{2}\,\pi}{g} U \sqrt{1 + \frac{Z_w}{U}\frac{M_q}{M_w}} \text{ seconds (U in ft. per second).}$$
(See R. and M. No. 77.)

and in our notation this becomes :—

$$p = 0{\cdot}202\, V \sqrt{1 + 0{\cdot}68\, \frac{Z_w}{V}\frac{M_q}{M_w}}\ \S$$

§This is an estimate based on model experiments on T.P. 4 with 40 per cent. elevators and corrected when necessary for other proportions of elevators.

The closeness of this approximation is satisfactory at all but the extreme points of the ordinary speed range. At low speeds the formula gives too long a period, and at high speeds too short a period.

The expressions in use for the resistance derivatives are as follows :—

$$M_w \begin{cases} \text{due to wings} = -\dfrac{6{\cdot}42^*}{W}\rho A p^2 b \dfrac{dK_l}{d\theta}\left(\dfrac{dK_m}{dK_l} + h + k\dfrac{dK_x}{dK_l}\right) V \\ \text{due to tail} = \dfrac{6{\cdot}42}{W}\rho A' p'^2 l \dfrac{dK'_l}{d'\theta}\left(1 - \dfrac{de}{d\theta}\right) E V \end{cases}$$

$$Z_w \begin{cases} \text{due to wings} = -\dfrac{6{\cdot}42}{W}\rho A p^2 \dfrac{dK_l}{d\theta} V \\ \text{due to tail} = -\dfrac{1}{l}(M_w \text{ due to tail}) \end{cases}$$

$$M_q \begin{cases} \text{due to tail} = -\dfrac{l}{1 - \dfrac{de}{d\theta}} \times (M_w \text{ due to tail}) \\ \text{Total} = \dfrac{5}{3} \times (M_q \text{ due to tail.}) \end{cases}$$

In these formulæ the value of e must be determined from experiments with the propeller running. The more or less empirical expression for the total M_q is based on an N.P.L. experiment on a model B.E.2*c* with and without tail. The inaccuracy of the formula is sometimes expressed by the introduction of a correcting factor N. (See Advisory Committee Report R. & M. 326) Now write

$$a = \frac{p'^2 A'}{p^2 A}$$

$$r = \frac{l}{b}$$

$$R = \frac{p^2 A r^2 b}{W}$$

$$m = \frac{arE\dfrac{dK'_l}{d'\theta}\left(1 - \dfrac{de}{d\theta}\right)}{\dfrac{dK_l}{d\theta}} - \left(\frac{dK_m}{dK_l} + h + k\frac{dK_x}{dK_l}\right) = m_1 - m_2 \text{ say.}$$

$$Q = \frac{7{\cdot}285\, a\, RE\dfrac{dK'_l}{d'\theta}}{m}\left[1 + \frac{aE\dfrac{dK'_l}{d'\theta}\left(1 - \dfrac{de}{d\theta}\right)}{\dfrac{dK_l}{d\theta}}\right]$$

where the last term in Q, which corresponds to the rate of change of tail lift with incidence, is usually so small as to be negligible.

* 6·42 is the value of $0{\cdot}00237 \times \frac{22}{15} \times \frac{180}{W} \times g$.

Then the period P may be written :—

$$P = 0{\cdot}202\ V\ \sqrt{1 + \rho\ Q}\ \text{seconds.}$$

Conditions Affecting Stability.—From the equations developed in § 3 it is at once evident that the essential condition for longitudinal stability is that the term m shall be positive. This represents the dynamical condition that the rate of increase of the pitching moment due to the combined effect of wings and tail must be such that a restoring couple is produced. The magnitude of the quantity mQ and the speed of the aeroplane affect the period of oscillation, but cannot cause instability.

Returning to the term m, it is desirable that the first part m_1 shall be as large as is conveniently possible. This term is increased by :—

(1) An increase in the ratio of tail area to wing area.

(2) An increase in the ratio of length of machine to wing chord.

(3) A decrease in the ratio of change of downwash.

(4) An increase in the factor $\frac{dK'_l}{d'\theta}$: *e.g.* by fixing the elevators.

(5) A decrease in the factor $\frac{dK_l}{d\theta}$: *i.e.* by using a wing section with slower increase of lift coefficient with angle of incidence.

All these factors, except the first, are in general determined by considerations other than those of stability, and it remains to adjust suitably the tail area.

It is equally possible to affect the stability of the aeroplane by reducing the term m_2. This implies moving the centre of gravity forwards, or the choice of a wing section with a slow movement of the centre of pressure.

The effect of the height at which the aeroplane is flying is best seen by writing the period equation in the form

$$P = 0{\cdot}202\ V_o\ \rho^{-\frac{1}{2}}\ \sqrt{1 + \rho\ Q}$$

So long as the aeroplane flies at a constant indicated airspeed, Q will remain unaltered, and the period will vary as the term $\sqrt{\frac{1}{\rho} + Q}$. The period will therefore increase with height.

5. *Effect of Small Changes of Design.*—In this section it is proposed to consider the effect of small changes in the constants of the aeroplane, but it will be assumed that no change is made in the wing section or in the ratio of elevators to fixed tail plane. The angle of incidence will be assumed constant, the speed being adjusted according to the loading of the aeroplane.

The equations used to predict the period of longitudinal oscillation are :—

$$W = 0{\cdot}0051\, K_l\, \rho\, A V^2$$

$$P = 0{\cdot}202\, V \sqrt{1 + \rho Q}$$

$$mQ = 7{\cdot}285\, a\, RE\, \frac{dK'_l}{d'\theta}$$

$$m = \frac{ar\left(1 - \frac{de}{d\theta}\right) E \frac{dK'_l}{d'\theta}}{\frac{dK_l}{d\theta}} - \left\{\frac{dK_m}{dK_l} + h + k\frac{dK_x}{dK_l}\right\}$$

$$= m_1 - m_2 \text{ (say)}$$

and so for small increments in the quantities involved,

$$\frac{\Delta V}{V} = \frac{1}{2}\left(\frac{\Delta W}{W} - \frac{\Delta A}{A}\right)$$

$$\frac{\Delta P}{P} = \frac{\Delta V}{V} + \frac{1}{2}\frac{\rho Q}{1 + \rho Q}\frac{\Delta Q}{Q}$$

$$\frac{\Delta Q}{Q} = \frac{\Delta a}{a} + \frac{\Delta R}{R} - \frac{\Delta m}{m}$$

$$\Delta m = m_1\left(\frac{\Delta a}{a} + \frac{\Delta r}{r}\right) - \Delta h$$

neglecting any possible change in the C.G. coefficient k as small and unimportant.

Also for the subsidiary quantities a, r, R, we have

$$\frac{\Delta a}{a} = \frac{\Delta A'}{A'} - \frac{\Delta A}{A}$$

$$\frac{\Delta r}{r} = \frac{\Delta l}{l} - \frac{\Delta b}{b}$$

$$\frac{\Delta R}{R} = 2\frac{\Delta l}{l} - \frac{\Delta b}{b} - \frac{\Delta W}{W} + \frac{\Delta A}{A}$$

On eliminating the various subsidiary variables we derive :—

$$\frac{\Delta P}{P} = \tfrac{1}{2} \cdot \frac{1}{1 + \rho Q}\left(\frac{\Delta W}{W} - \frac{\Delta A}{A}\right)$$

$$+ \tfrac{1}{2}\frac{\rho Q}{1 + \rho Q}\left\{\frac{\Delta h}{m} + \frac{\Delta b}{b} + \frac{\Delta r}{r}\left(2 - \frac{m_1}{m}\right) - \frac{\Delta a}{a}\left(\frac{m_1}{m} - 1\right)\right\} \cdot \quad (1)$$

which may also be expressed in the alternative form :—

$$\frac{\Delta P}{P} = \tfrac{1}{2}\frac{1}{1 + \rho Q}\frac{\Delta W}{W} - \tfrac{1}{2}\left(1 - \frac{\rho Q}{1 + \rho Q}\frac{m_1}{m}\right)\frac{\Delta A}{A} + \tfrac{1}{2}\frac{\rho Q}{1 + \rho Q}\frac{\Delta h}{m}$$

$$+ \tfrac{1}{2}\frac{\rho Q}{1 + \rho Q}\left(\frac{m_1}{m} - 1\right)\left(\frac{\Delta b}{b} - \frac{\Delta A'}{A'}\right) + \tfrac{1}{2}\frac{\rho Q}{1 + \rho Q}\left(2 - \frac{m_1}{m}\right)\frac{\Delta l}{l} \quad (2)$$

Either of these equations may be used to determine the change in period due to small arbitrary changes in the constants of the aeroplane. It should be noted that these expressions give the change in period at a constant angle of incidence. As it is customary to connect period of oscillation with speed, it is also necessary to calculate the change in speed due to the change in loading. Curves of period against speed can then be drawn to obtain the change in period at a definite speed.

One case of special interest arises when all the dimensions of a machine are increased in the same ratio $(1 + \lambda : 1)$. The weight will increase approximately as the square of this ratio and it follows at once that

$$\frac{\Delta P}{P} = \frac{1}{2}\lambda \frac{\rho Q}{1 + \rho Q}$$

This equation shows that the period will increase with the size of the aeroplane. The maximum percentage increase in the period occurs for a machine verging on instability. Q is then large and $\frac{\Delta P}{P} \rightarrow \frac{1}{2}\lambda$.

6. *Numerical Values for a B.E.2e Machine.*—The values of the constants involved may be taken to be :—

$$\frac{W}{A} = 5{\cdot}7 \ , \ h = 0{\cdot}32 \ , \ k = 0{\cdot}38 \ , \ E = 0{\cdot}75 \ , \ a = 0{\cdot}163 \ ,$$

$$r = 3{\cdot}08 \quad , \quad R = 8{\cdot}90 \ ,$$

$$\frac{dK_l}{d\theta} = 0{\cdot}032, \frac{dK'_l}{d'\theta} = 0{\cdot}0223 \ , \frac{de}{d\theta} = 0{\cdot}50 \ ,$$

and it follows that

$$mQ = 0{\cdot}177 \quad , \quad m_1 = 0{\cdot}131.$$

The solution for ground level and 10,000 feet is given in the table below. The wing section is taken as R.A.F. 14.

K_l	V_o m.p.h.	m	Q	Period in Seconds.	
				At Ground.	At 10,000 ft.
0·15	$86\frac{1}{2}$	0·023	7·7	52	53
0·20	75	0·076	2·33	27·6	29·1
0·30	61	0·123	1·44	19·2	20·6

For the effect of small changes of design only the mean case for a speed of 75 m.p.h. will be considered. The conditions will be taken to be those at the ground, so that $\rho = 1{\cdot}0$. The results

MAXIMUM HEIGHT ATTAINABLE.

Z = T.H.P. AVAILABLE & H = DRAG H.P.

Z & H SHOULD BE CALCULATED FOR A DENSITY OF 0·00237 SLUGS PER CUBIC FOOT AND FOR THE AIRSPEED USED ON THE CLIMB.

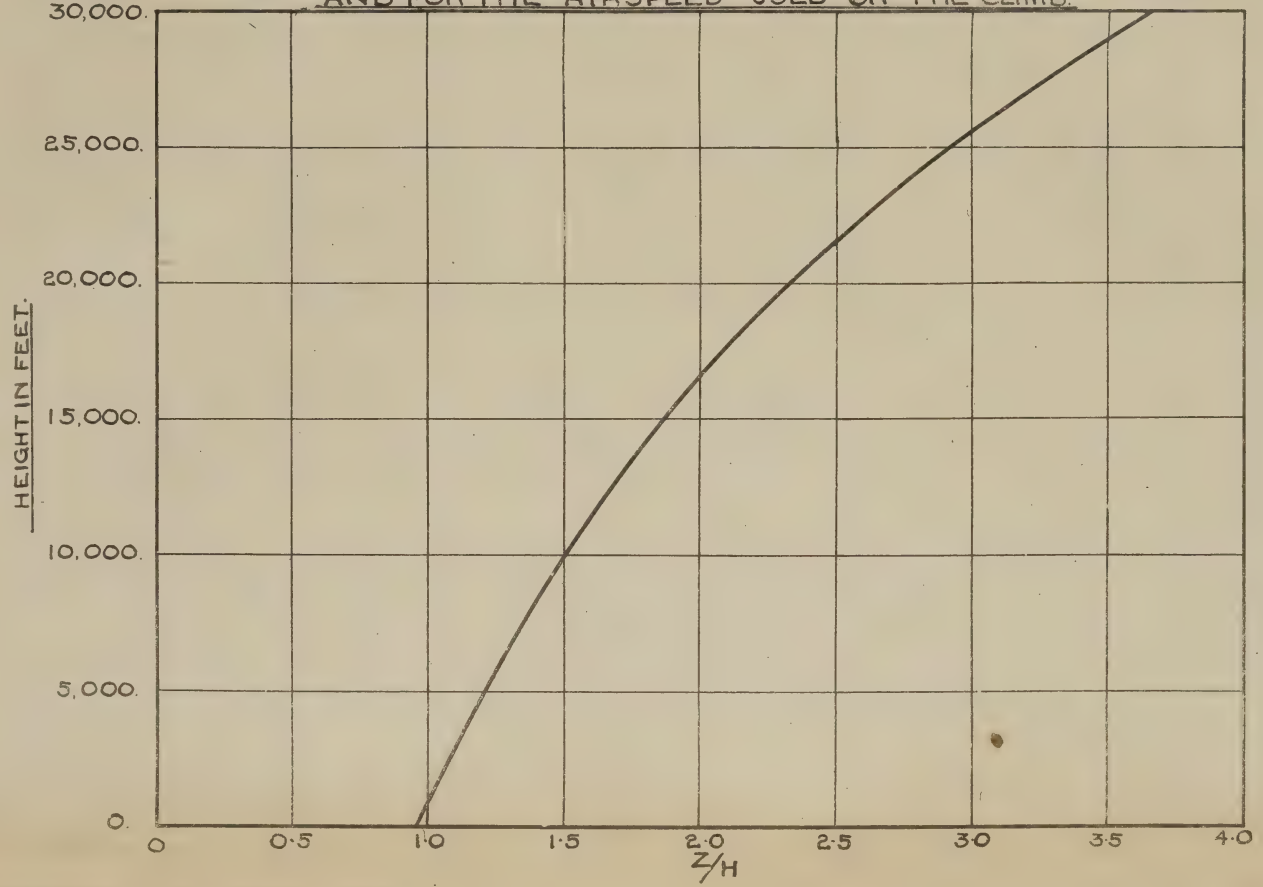

REPORT No. 324.

FIG. 1.

FIG. 2.

TIME TO HEIGHT $h = \frac{W}{Z} \Phi$ MINS.

WHERE Z = T.H.P. AVAILABLE & H = DRAG H.P.

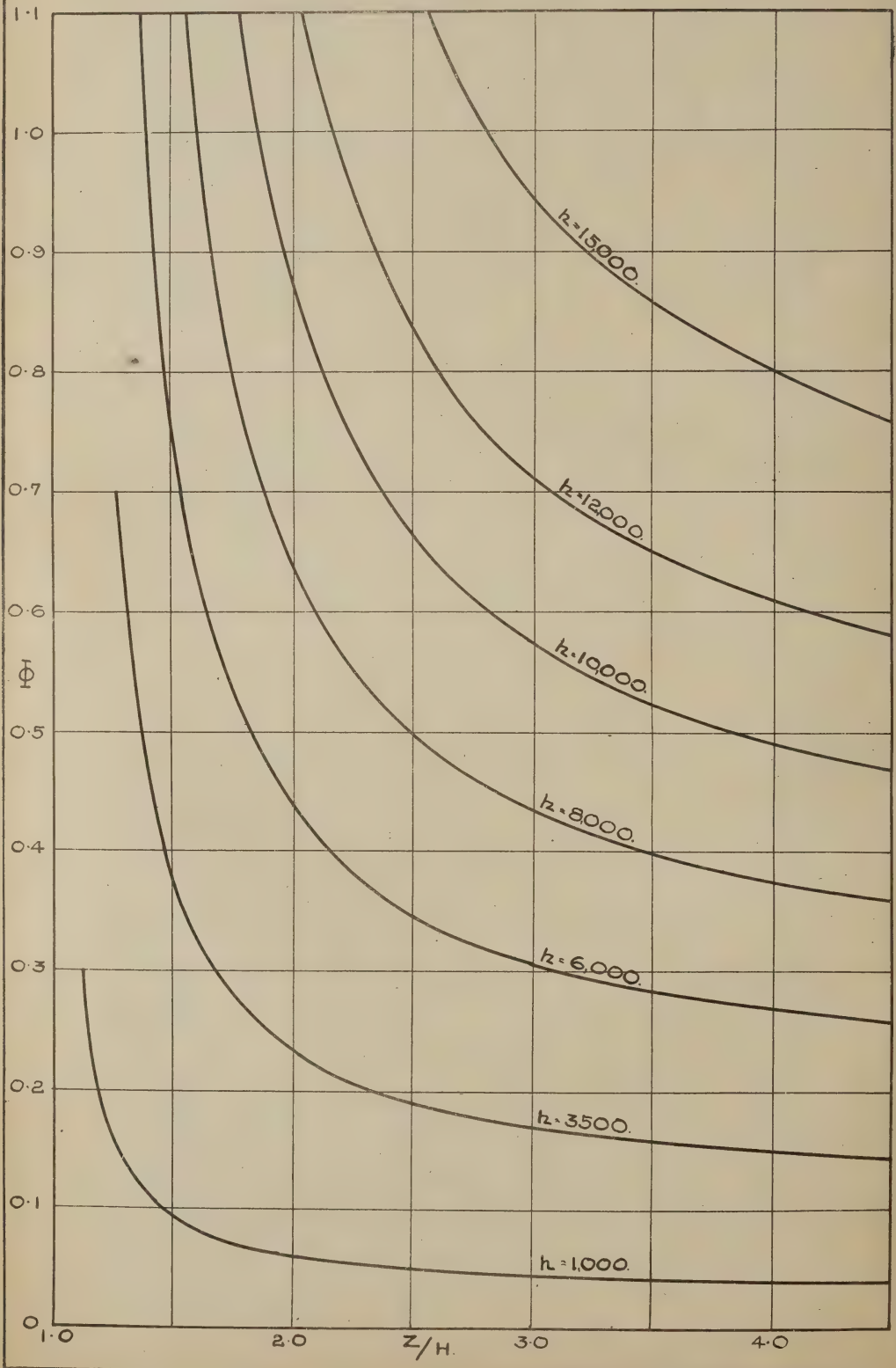

VALUES OF THE FACTORS X AND Y FOR A CLIMB TO 10,000 FT.

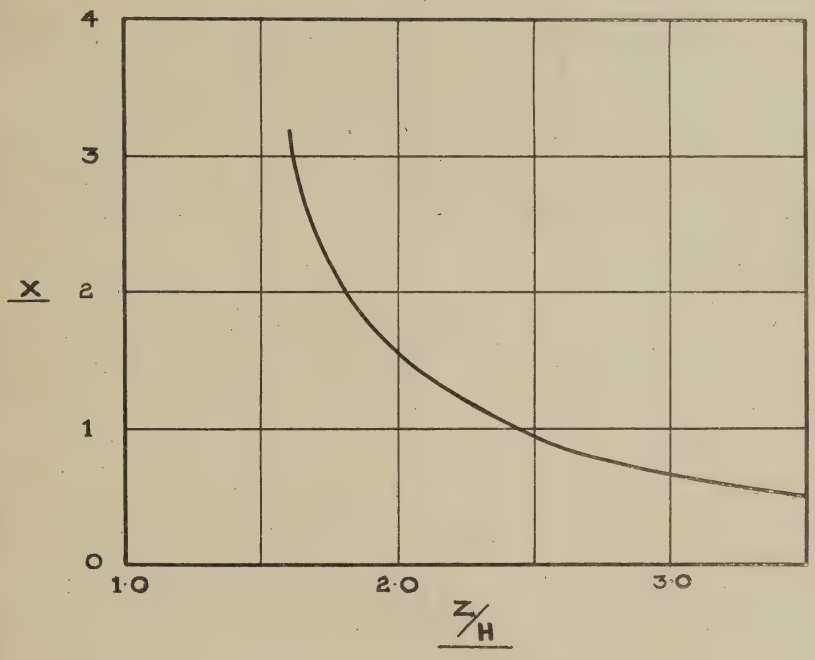

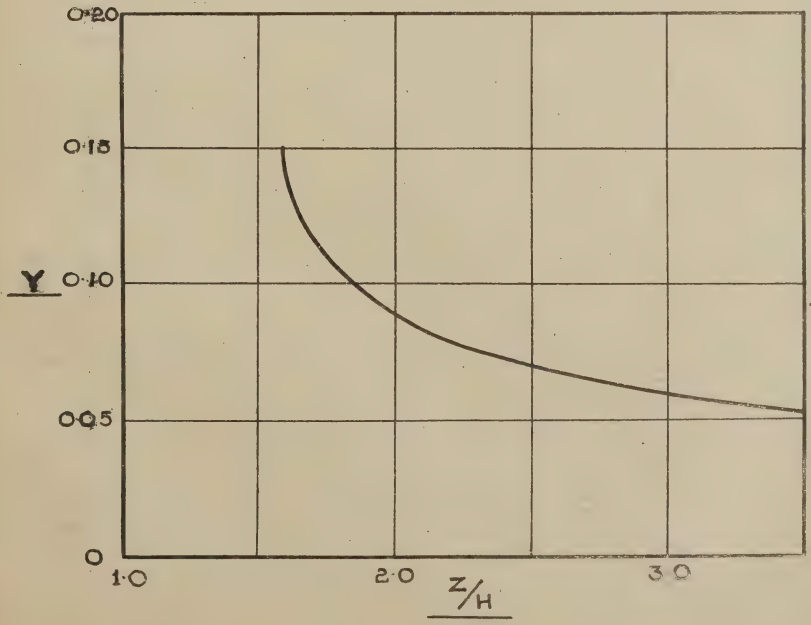

CURVE OF STANDARD DENSITY.

THE DOTTED CURVES REPRESENT THE THEORETICAL EXTENSION TO 30,000 FT.
AND THE MEAN EXPONENTIAL CURVE USED IN PREDICTING THE CLIMB TO ANY HEIGHT.

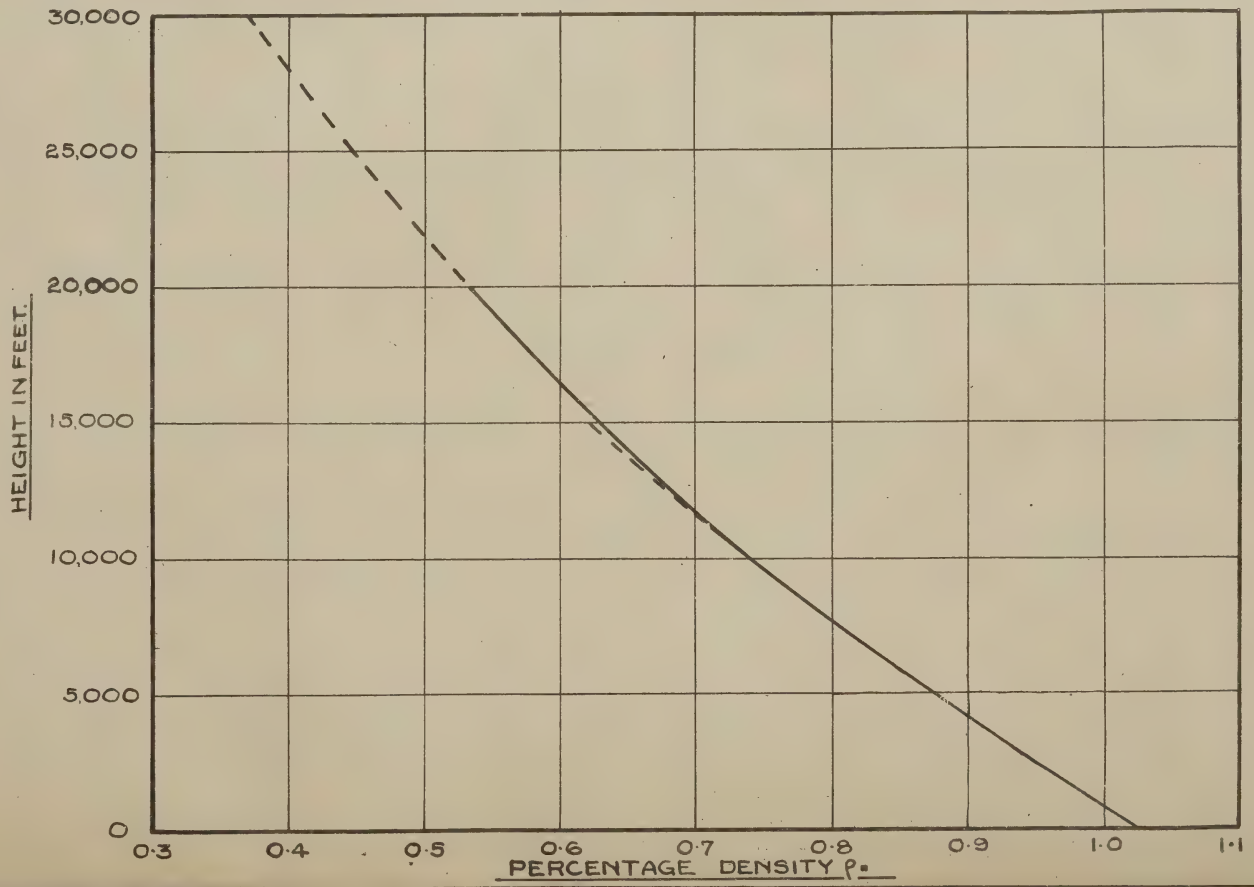

REPORT No. 324.

FIG. 5.

FIG. 4.

DETERMINATION OF SPEED AT HEIGHT.

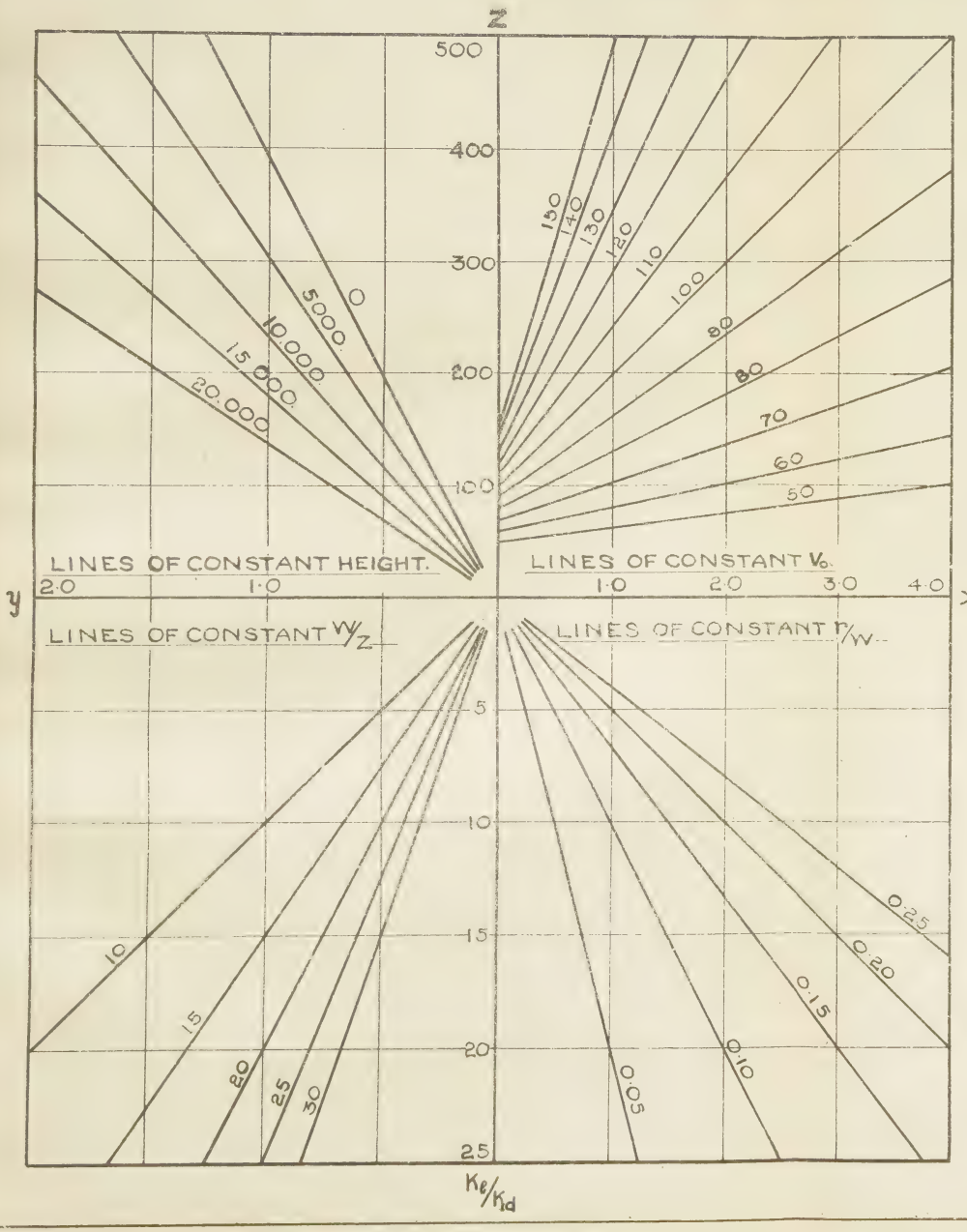

CURVES OF CONSTANT LOADING W/A

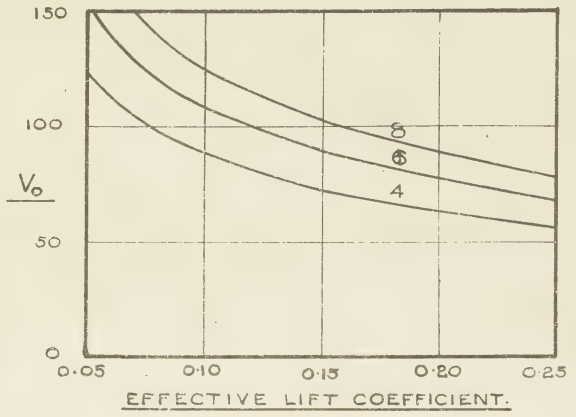

CURVES FOR K_e/K_d.

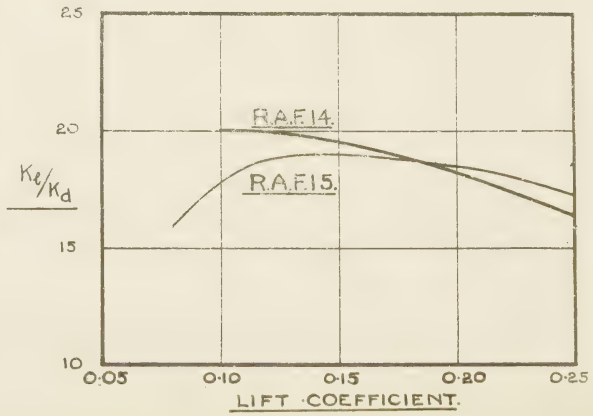

obtained from equation (2) of § 5 are given below for 1% change in each of the variables involved :—

Variable.	W	A	A′	b	l
Percentage change in P.	0·15	0·10	−0·25	0·25	0·10

The percentage change in P due to an increase 0·01 in the C.G. coefficient h is 4·6 and it is at once evident that the position of the centre of gravity and the area of the tail plane are the factors of greatest importance in determining the period.

APPENDIX.

The Variation of Density with Height.

1. In all predictions of aeroplane performance an assumption as to the nature of the fall of air density with height has to be made. The density at any point can be determined immediately barometer and thermometer readings are taken, and the Meteorological Office has supplied the results of a long series of observations of temperature and pressure up to a maximum height of about 20,000 feet. This has led to the construction of a standard density curve, the standard density at a given height being the mean value of ρ calculated from a series of observations at that height.*

It has been usual to refer all air forces in model experiments to a density of 0·00237 slugs/ft^3. All airspeed indicators are graduated to correspond with this density also. The meteorological results indicated that the true mean value at ground level is somewhat larger than this. The correcting factor 1·026, which occurs as one limit of the integral used in part I of this report to determine the time to a given height, was thus introduced in conjunction with the standardised 0·00237 The density at 10,000 feet is 74 per cent. of 0·00237.

2. The standard density curve is used directly for predictions of :—

(*a*) Maximum height for a given airspeed.

(*b*) Maximum speed at a given height.

All that is necessary in these cases is to read off the curve at the height required.

On the other hand the integration which is involved in finding the time of climb to a given height cannot be effected until the approximate equation for the density-height curve is found.

If p = pressure in lbs./ft.^{2}.

σ = density in lbs./ft.^{3}

θ = temperature in absolute centigrade units.

h = height above ground level,

then we have,

$$p = R\,\sigma\,\theta \quad . \quad . \quad . \quad (1)$$ where R is a physical constant.

and $$dp = -\sigma\,dh \quad . \quad . \quad . \quad . \quad (2)$$

If now we assume a linear temperature fall

$$\theta - \theta_o = -ah \quad . \quad . \quad . \quad (3)$$

The elimination of p and θ between these three equations leads to a result of the form,

$$\left(\frac{\sigma}{\sigma_o}\right)^b = 1 - ch \quad . \quad . \quad . \quad . \quad (4)$$

where b and c are functions of a.

Now it was found that the temperature fall with height as observed, did in fact approximate fairly closely to a linear law. It was, therefore assumed in accordance with (4) that,

$$\left(\frac{\rho}{1{\cdot}026}\right)^b = \left(\frac{\sigma}{\sigma_o}\right)^b = 1 - ch \quad . \quad (5)$$

* This standard is now in use at the Testing Squadron R.F.C. Martlesham, and also, it is believed, in the R.N.A.S.

the constants b and c being so determined as to give coincidence with the mean density curve at 6,000 feet and 10,000 feet. The values of the constants become,

$$b = 0{\cdot}30, c = 9{\cdot}32 \times 10^{-6}$$

This approximation to the standard curve is extremely close up to 10,000 feet, the consequent errors in prediction being well within the limits of other errors. It is used up to 15,000 feet, the error increasing with height.

3. The standard density curve stops at 20,000 feet. For the sake of completeness the curve has been continued beyond this to 30,000 feet by means of an assumption similar to (5). A linear temperature fall of 1·8°C. per 1,000 feet is assumed in this region, and the curve is made continuous with the standard density curve at $h = 20{,}000$. This serves to determine the constants The extension so obtained is used only for the prediction of maximum heights, which are at the best only very rough estimates, being very sensitive to small changes in engine power, etc. Hence an error in the density curve will not be of serious consequence.

NOTES ON THE PREDICTION AND ANALYSIS OF AEROPLANE PERFORMANCE.

By L. Bairstow, C.B.E., F.R.S., and Lieut. J. D. Coales, D.Sc.

Communicated by the Technical Department,
Department of Aircraft Production.

Reports and Memoranda, No. 474. *May,* 1918.

Summary.—(a) *Introductory.* (*Reasons for Inquiry.*)—The present investigation was undertaken with a view to obtaining a more rapid and accurate method of estimating aeroplane performance.

(b) *Range of the Investigation.*—A generalisation has been obtained for airscrew performance which expresses the thrust and torque of all airscrews in terms of two curves which are common to all, together with three constants which are characteristic of an individual airscrew. The common curves and their origin are dealt with in an Appendix by Miss Betts, B.Sc.

The only other fundamental change of method is in regard to the treatment of airscrew slipstream effects. By the introduction of slightly fictitious values for airscrew efficiency and aeroplane resistance the analysis is greatly simplified. In prediction there is no need to use these fictitious values if sufficient data are available. It appears that the difference between the fictitious values and the real ones is less than differences due to errors of observation but that further refinements can be made when needed.

(c) *Results.*—The greater part of these notes relates to examples. In the first of these a complete prediction of aeroplane performance is made in order to show how the details of engine revolutions, forward speed and rate of climb of aeroplane may be calculated without excessive labour. A comparison of the results with trial observations shows very clearly the general correspondence.

The second example reverses the process in the analysis of performance trials at Martlesham Heath. The records were unusually complete and suitable for analysis. It was found to be possible to deduce (1) the variation of engine power with height, (2) the efficiency of the airscrew, and (3) the resistance of the aeroplane.

A third example deals with a modification of the analysis which will sometimes cope successfully with less complete data.

(d) *Applications and further developments.*—Applications are being proceeded with, and the experience gained already warrants the statement that the results of the analysis are sufficiently accurate to be of direct value in improving aeroplanes. It is expected that appreciable improvement in analysis will occur in the course of time and with the advent of tests which will give the method its best opportunities.

Introduction—In estimating the various items of importance in the design of an aeroplane as they effect the achieved performance, it is convenient to consider an aeroplane under four main heads. The first main head consists of the estimation of

the resistance of the aeroplane as a glider without airscrew, and at the present time this estimation is built up almost wholly from experiments on models. The second main head deals with the estimation of airscrew characteristics, and this, again, is usually calculated from model experiments, with but cursory reference to any mutual effects between the aeroplane and the airscrew. The third main item is the variation of engine power with revolutions; whilst the fourth is the variation of engine power with variation of height. In connecting these four quantities with each other in the prediction of the performance of an aeroplane the first two, which deal with the aeroplane resistance and the airscrew characteristics, cannot be considered as wholly independent in a high speed Scout. The resistance of the parts of the aeroplane in the slip stream of the airscrew may be increased three or more times during a climb.

With the information at our disposal, calculations of very great accuracy are not possible, and in many cases various assumptions from general experience have been made in order to bridge gaps in the experimental data. The present notes are an attempt to outline a scheme of prediction and analysis with indications as to the best methods to be adopted with varying degrees of accuracy in the data to be analysed.

Outline of the Method.—The chief new feature in the analysis of the performance of aeroplanes is the introduction of empirical formulæ for the airscrew characteristics in such a form that individual characteristics in any one combination of aeroplane and airscrew can be taken account of by three constants to be determined during the analysis. It has been found by trial of all the airscrew results available that the curves relating the thrust and torque to the advance per revolution can be brought into fair agreement if the results are expressed as functions of the ratio of advance per revolution to the experimental mean pitch, the latter being defined as the advance per revolution at which the thrust is zero. This experimental mean pitch constitutes one of the three constants just referred to. The other constants are such that on multiplying the thrust and torque coefficients by them, the values obtained are equal to unity when the advance per revolution is equal to half the mean pitch. The constants will be referred to by the letters P, for experimental mean pitch, K_t, for the factor which makes the thrust coefficient unity when $V/nP = \frac{1}{2}$, and K_q, for the factor which makes the torque coefficient equal to unity when V/nP is one-half. The thrust and torque coefficients used throughout are defined by the expressions

$$\left.\begin{aligned} T_c &= \frac{\text{Thrust}}{\rho_m n^2 D^4} \\ Q_c &= \frac{\text{Torque}}{\rho_m n^2 D^5} \end{aligned}\right\} \quad . \quad . \quad . \quad . \quad (1)$$

where ρ_m is the mass density of the air* in slugs $\left(\frac{W}{g}\right)$ per cubic foot, n the revolutions of the airscrew per second and D the diameter of the propeller in feet, and the resulting equations for airscrew performance in terms of the three constants are as below,

$$K_t T_c = \frac{4}{3}\left\{1 - \left(\frac{V}{nP}\right)^2\right\} \quad . \quad . \quad . \quad . \quad (2)$$

$$K_q Q_c = 2\left(\frac{V}{nP}\right)^{0\cdot47} - 1\cdot772\left(\frac{V}{nP}\right)^2 \quad . \quad . \quad (3)\dagger$$

For the purpose of analysis the values of P and K_t are determined from experiments in flight near the ground during which advance per revolution is measured and from the H.P. which has been measured at atmospheric pressure on the test bed. The value of K_t is more difficult to obtain from such experiments as have been made up to the present and special arrangements are being undertaken for the purpose of more accurate determination in the future. The most suitable experiments for this purpose are the determination of the advance per revolution of the airscrew during full climb and during level flight with the engine throttled down so as to give the same speed as for climbing.

The method of dealing with the slip-stream is based on experiments at the National Physical Laboratory, where model airscrews have been run in combination with model bodies and the mutual effects on each other have been carefully measured in a number of cases. Generally speaking, the effect of the presence of a body is to increase the experimental mean pitch of the airscrew, and to increase its efficiency, whilst on the other hand, the effect of the airscrew on the body is to increase appreciably its resistance. Calculations by A. Fage have shown that with an error of the order of 5 per cent. it is possible to treat the airscrew and body combination as though the parts were operating separately. Although this assumption is convenient, and is useful in interpreting the result of analysis, it is not necessary to follow it in complete detail. The result of the analysis now proposed is to give somewhat fictitious values both to the airscrew efficiency and to the resistance of the aeroplane which will probably give correct comparisons between all aeroplanes of the same class. Within the limits of accuracy indicated in Mr. Fage's statement, the efficiency of the airscrew which is deduced and the resistance of the aeroplane both correspond with observations made on the parts separately.

* In the standard atmosphere $\rho_m = 0\cdot00237 \times \rho$, where ρ = density relative to actual density (0·00237) of air at 29·92 inches of mercury and 13° Centigrade.

† After reference to National Physical Laboratory a new formula for $K_q Q_c$ has been found which is based on a weighted mean of the observations (see Appendix) and has a wider range on V/nP. In order to avoid recalculation, equation (3) has been kept for the purposes of this report. It does not differ greatly from the new formula over the range for which it has been used.

The following more detailed statement will make the assumptions clear, and indications can be given at various stages of the degree of accuracy which may be expected.

If T be the thrust, v the rate of climb, V the forward speed, R the resistance and W the weight of an aeroplane, then

$$T = R + W\frac{v}{V} \quad . \quad . \quad . \quad . \quad (4)$$

The resistance R depends appreciably on the slip stream of the airscrew, but that fraction of it which arises from parts of the aeroplane in the airscrew slip-stream is not greatly affected by variations of the angle of incidence of the whole machine. It may be taken that the total resistance in the absence of slip-stream may be expressed in the form

$$R = R_o + R_i \quad . \quad . \quad . \quad . \quad (5)$$

R_o, that is, the part of the resistance which arises from the wings, struts, and generally the parts not in the slip-stream, is appreciably dependent on the angle of incidence and is essentially related to the lift coefficient L_c.

From all experiments in the wind channel at the National Physical Laboratory it appears that the resistance of parts in the slip-stream can be expressed as

$$R_i\left\{k_1 + k_2\left(\frac{V}{nD}\right)^{-2} T_c\right\} \quad . \quad . \quad . \quad (6)$$

k_1 is usually less than unity apparently because of the shielding of the body by the airscrew. On the whole it may be expected that k_1 will not differ by more than 10 per cent. from unity and will be nearly the same for all tractor aeroplanes. Using this expression for the total resistance, equation (4) becomes

$$T = R_o + R_i\left\{k_1 + k_2\left(\frac{V}{nD}\right)^{-2} T_c\right\} + W\frac{v}{V} \quad . \quad (7)$$

Divide through by ρAV^2 and (7) becomes after rearrangement

$$T_c\left(\frac{V}{nD}\right)^{-2}\left\{\frac{D^2}{A} - k_2(D_c)_i\right\} = (D_c)_o + k_1(D_c)_i + L_c\frac{v}{V} \quad (8)$$

The multiplying factor of $T_c\left(\frac{V}{nD}\right)^{-2}$ in equation (8) is independent of the angle of incidence to the extent mentioned above, and it is convenient to introduce an overall thrust co-efficient defined by

$$T'_c = T_c\left\{1 - \frac{A}{D^2}k_2(D_c)_i\right\} \quad . \quad . \quad . \quad (9)$$

The curve representing this overall thrust coefficient as a function of advance per revolution differs only from that of the airscrew alone in the scale of its ordinates, and the use of it in (8) leads to

$$T'_c\frac{D^2}{A}\left(\frac{V}{nD}\right)^{-2} = (D_c)_o + k_1(D_c)_i + L_c\frac{v}{V} \quad . \quad (10)$$

and eliminates the necessity for any consideration of slip-stream effects during preliminary analysis. If k_1 were strictly unity, the drag deduced from equation (10) would be the wind channel drag in the absence of airscrew. As the drag coefficient of the parts of the aeroplane in the slip-stream can be estimated with fair accuracy, and as k_1 is nearly equal to unity, a correction towards the simple wind channel resistance can be made if desired. The accuracy of reduction of present day experiments does not appear to require this refinement. Similarly, if the real thrust coefficient of the airscrew is required, an estimate must be made of the value of k_2, as well as of the resistance of the parts in the slip-stream, and the evidence as to the value of k_2 is not very great in the case of most aeroplanes. The equation for forces which corresponds with equation (10) is

$$T' = D' + W\frac{v}{V}. \quad . \quad . \quad . \quad (11)$$

where T′ and D′ may be provisionally regarded as the thrust of the airscrew and the drag of aeroplane estimated separately. It is now possible to use equation (11) to obtain the relation between the difference of the thrusts of the airscrew when climbing at two different rates and the weight of the aeroplane, its speed of flight, and the difference of the rates of climb, if the airspeed in the two cases be made the same. The condition of constant airspeed is the only condition remaining which is necessary in order to ensure that the drag of the aeroplane is the same for the two experiments. It can, therefore, be eliminated by subtraction. The difference equation required is

$$(T'_1 - T'_2) = \frac{W}{V}(v_1 - v_2) \text{ with the condition } \rho V^2 = \text{constant} \quad (12)$$

Accuracy depends on having $\frac{W}{V}(v_1 - v_2)$ large compared with D′, and this condition will be obtained if the full climb near the ground is taken for one observation and an experiment with throttled engine near the ground for the second one.

To find K_q and P resort is had to experiments near the ground with engine all out. Under these circumstances the engine power at measured revolutions is known from experiments on the test bed, and the advance per revolution of the airscrew is observed in flight. The torque coefficient of the airscrew is immediately deducible from the test bed figures and the observed revolutions, and if further accuracy in fixing the shape of the curve were necessary than is involved in the use of the empirical formula of the airscrew, such accuracy can be obtained from observations near the ground in which the full climb was not attained. It is unlikely that in the standard performance experiments on aeroplanes, the necessary range of observation will be available for analysis, and resort must be had to the empirical formulæ for airscrews.

It will be seen that equation (3) and the observations just referred to suffice to determine P and K_q and that equation (2) used in conjunction with a value of P previously found and the difference equation (12) then leads to the determination of K_t.

Details of the use of the theory for prediction.—Before using the formulæ analytically, calculations will be made on assumed data to show how they may be applied to estimate the details of prediction.

Data required.—(1) The drag coefficient D_c as a function of the lift coefficient L_c of the aeroplane, not including the effects of slip-stream.

(2) The values of the thrust and torque coefficients of the airscrew as dependent on V/nP and a knowledge of the value of P.

(3) The brake horse-power of the engine as dependent on revolutions at standard density and temperature.

(4) The variation of engine power with height. A standard atmosphere is always assumed in prediction and observations in flight are reduced to such standard atmosphere for the purposes of comparison.

The data are represented in Figs. 1, 2, 3, 4 attached and correspond in general characteristics with a high speed modern aeroplane. They do not represent any actual aeroplane.

The b.h.p. of the engine under standard conditions will be denoted by (Std. b.h.p.) whilst the variation with height will be $f(\rho)$.

At any standard height where the density is ρ the brake horse-power is given by

$$(\text{b.h.p.})_\rho = f(\rho)\{\text{Std. b.h.p.}\} \quad . \quad . \quad . \quad . \quad (13)$$

Generally, from the ordinary definition of torque coefficient

$$\text{b.h.p.} = \frac{2\pi n}{550} Q_c \rho_m n^2 D^5$$

$$\text{or } Q_c = \frac{550}{2\pi D^5} (\text{Std. b.h.p.}) \frac{f(\rho)}{n^3 \rho_m} \quad . \quad . \quad . \quad (14)$$

A form of general convenience is

$$\frac{Q_c}{f(\rho)} = \frac{550}{2\pi D^5} \frac{\text{Std. b.h.p.}}{\rho_m n^3} \quad . \quad . \quad . \quad . \quad . \quad (14a)$$

It will be noticed from (14a) that the value of $Q_c/f(\rho)$ is not dependent on the aerodynamic properties of the aeroplane.

Using equation (3) for the airscrew torque leads to

$$2\left(\frac{V}{nP}\right)^{0\cdot47} - 1\cdot772\left(\frac{V}{nP}\right)^2 = \frac{550\,K_q}{2\pi D^5} \cdot f(\rho) \frac{\text{Std. b.h.p.}}{\rho_m n^3} \quad . \quad (15)$$

as an immediate deduction from (14).

Equation (15) is one of the standard equations of the new analysis. In terms of the quantities given in Figs. 1-4 it is a simple calculation to find the relation between the speed of an aeroplane and the engine revolutions at any height if the engine is " all out."

If the empirical formula of equation (3) be not used, but a curve for Q_c is obtained in other ways equation (14) may be used directly instead of (15).

A second standard equation is obtained from (10) which is

$$T'_c \frac{D^2}{A}\left(\frac{V}{nD}\right)^{-2} = D'_c + L_c \frac{v}{V} \quad . \quad . \quad . \quad . \quad (16)$$

and becomes after use of equation (2)

$$\frac{D^4}{AP^2} \cdot \left(\frac{V}{nP}\right)^{-2} \frac{4}{3}\left\{1 - \left(\frac{V}{nP}\right)^2\right\} = K_t\left\{D'_c + L_c \frac{v}{V}\right\}$$

or after rearranging terms

$$\left(\frac{V}{nP}\right)^{-2} = 1 + \frac{3}{4}\frac{A \cdot P^2}{D^4} K_t \left\{D'_c + L_c \frac{v}{V}\right\} \quad . \quad . \quad (17)$$

As in the case of the use of equations for torque a choice may be made between equations (16) and (17) according to whether the thrust coefficient is known independently of K_t or whether this restriction must be allowed in order to examine results otherwise intractable.

It is possible to eliminate V/nP between equations (15) and (17) but there are no advantages to be gained by so doing. So far, it has been found that equations (15) and (17) are most conveniently used in the form given.

Details of the calculations of performance in the particular case cited.—In addition to the curves in Figs. 1-4 the following are needed :—

Total weight of aeroplane ...	1,900 lbs.
Loading	7 lbs. per sq. ft. Area, 272 sq. ft.
Propeller diameter	8·75 feet.
Experimental mean pitch ...	10 feet.

Equation (14) becomes

$$Q_c = 156{,}000 \frac{\text{Std. b.h.p.}}{(\text{r.p.m.})^3} \cdot \frac{f(\rho)}{\rho} \quad . \quad . \quad . \quad (18)$$

where ρ is the relative density, and is equal to unity at a height of 800 feet in a standard atmosphere.

The following table is compiled from Figs. 3 and 4 and equation (18) :—

TABLE 1.

r.p.m.	Std. b.h.p.	Std. b.h.p. / (r.p.m.)³	Q_c				
			Ground.	5,000 ft.	10,000 ft.	15,000 ft.	20,000 ft.
1,400	226·0	$8{\cdot}23 \times 10^{-8}$	0·01245	0·01215	0·01175	0·01125	0·01080
1,350	223·4	$9{\cdot}10 \times 10^{-8}$	0·01380	0·01345	0·01305	0·01245	0·01195
1,300	220·0	$10{\cdot}00 \times 10^{-8}$	0·01510	0·01475	0·0145	0·01360	0·01315
1,250	216·5	$11{\cdot}10 \times 10^{-8}$	—	—	—	0·01505	0·01460

From the values of Q_c and the curves of Fig. 2 the values of V/nP can be read off and the value of V calculated leading to Table 2.

TABLE 2.

r.p.m.	Ground.		5,000 ft.		10,000 ft.		15,000 ft.		20,000 ft.	
	$\frac{V}{nP}$	V Feet per sec.	$\frac{V}{nP}$	V Feet per sec.	$\frac{V}{nP}$	V Feet per sec.	$\frac{V}{nP}$	V Feet per sec.	$\frac{V}{nP}$	V Feet per sec.
1,400	0·692	161·5	0·705	165	0·728	170	0·750	175	0·768	179
1,350	0·611	137·5	0·635	143	0·660	148·5	0·692	156	0·717	161·5
1,300	0·420	91·0	0·496	107·5	0·545	118	0·622	135	0·652	141·5
1,250	—	—	—	—	—	—	0·430	89·5	0·520	108·5

Table 2 shows the relation between the engine revolutions and the forward speed of airscrew for all altitudes the engine being " all out." The relationship is shown in Fig. 5. The corresponding relation between V/nP and the forward speed of the airscrew is shown in Fig. 5a.

The fall of revolutions with height which is observed in level flights is deducible from these observations. The whole of the data required are shown below.

The airscrew curves of Fig. 2 correspond with $K_t = 9{\cdot}02$ and $K_q = 66{\cdot}5$ and from the data and previous equations the following are readily deduced.

Throughout the theoretical part of the analysis the units used have been the foot and second with forces measured in lbs. The unit of mass has been taken as that in a body weighing g lbs. and called the slug, thus following one of the standard engineering methods. Common language has, however, other units, speeds of flight being in miles per hour, rate of climb in feet per minute and revolutions in turns per minute and a saving of labour occurs by an early adoption of the common language.

The equation connecting W with the lift coefficient is

$$W = L_c \rho_m A V^2_{f/s} \text{ in standard units}$$

and leads to

$$L_c = \frac{W}{A} \cdot \frac{1}{\rho_m (V_{f/s})^2} = \frac{W}{A} \cdot \frac{1}{\rho 0{\cdot}00237} \frac{1}{(V_{\text{m.p.h.}} \times \frac{88}{60})^2}$$

In our instance $W/A = 7$ and

$$L_c = \frac{1{,}372}{\rho (V_{\text{m.p.h.}})^2} \quad . \quad . \quad . \quad . \quad . \quad . \quad (19)$$

$\rho^{\frac{1}{2}}V$ is often referred to as airspeed, or indicated airspeed. The advance per revolution as a fraction of the pitch of the airscrew becomes

$$\frac{V}{nP} = \frac{V_{f/s}}{n_{\text{r.p.s.}} P_f} = 88 \frac{V_{\text{m.p.h}}}{\text{r.p.m.} \times P}, \text{ or r.p.m.} = 88 \frac{V_{\text{m.p.h.}}}{V/nP} \quad (20)$$

Equation (14) is in standard units

$$Q_c = \frac{550}{2\pi D^5} \frac{(\text{Std. b.h.p.}) f(\rho)}{n^3 \rho_m}$$

If standard curves for the airscrew are used it has been found advantageous to use $\frac{1}{4} K_q Q_c \left(\frac{V}{nP}\right)^{-2}$ instead of Q_c and equation (14) becomes

$$\frac{1}{4} K_q Q_c \left(\frac{V}{nP}\right)^{-2} = \frac{1}{4} K_q \left(\frac{V}{nP}\right)^{-2} \frac{500}{2\pi D^5} \frac{(\text{Std. b.h.p.}) f(\rho)}{n^3 \rho_m} \quad . \quad (14b)$$

Changing the units and putting in numerical values for K_q, P and D leads to

$$\frac{1}{4} K_q Q_c \left(\frac{V}{nP}\right)^{-2} = 24{\cdot}35 \, L_c \frac{\text{Std. b.h.p.}}{\text{r.p.m.}} f(\rho) \quad . \quad (21)$$

Equation (19) being used to eliminate $\rho V^2_{\text{m.p.h.}}$ in terms of L_c. For thrust equation (17) is used, *i.e.*,

$$\left(\frac{V}{nP}\right)^{-2} = 1 + \frac{3}{4} \frac{AP^2}{D^4} K_t \left\{ D'_c + L_c \frac{v}{V} \right\}$$

but rearrangement has been made so as to facilitate the calculation of V. The convenient variable for use with airscrew curves is $\frac{1}{4} K_t T_c \left(\frac{V}{nP}\right)^{-2}$ and either from (17) and (2) or from (16) the equation in common units is

$$v_{f/m} = \frac{88 \cdot V_{\text{m.p.h.}}}{L_c} \left\{ 0{\cdot}0961 \left[\frac{1}{4} K_t T_c \left(\frac{V}{nP}\right)^{-2} \right] - D_c \right\} . \quad (22)$$

In level flight when $v = 0$

$$\frac{1}{4} K_t T_c \left(\frac{V}{nP}\right)^{-2} = 10{\cdot}42 \, D_c \quad . \quad . \quad . \quad . \quad (23)$$

TABLE 3.

1.	2.	3.	4.	5.	6.	7.	8.
Airspeed.	Lift Coefficient.	Drag Coefficient.	$\frac{1}{4}K_t T_c \left(\frac{V}{nP}\right)^{-2}$	$\frac{V}{nP}$	$\frac{1}{4}K_q Q_c \left(\frac{V}{nP}\right)^{-2}$	From Columns (1) and (5).	From (21).
$\rho^{\frac{1}{2}} V_{m.p.h.}$	L_c	From Standard Curve D_c	From (23).	From Curve C, Fig. 14.	Calculated from Curve B, Fig. 14.	$\rho^{\frac{1}{2}}$ r.p.m.	$\frac{\text{Std. b.h.p.}}{\text{r.p.m.}} f(\rho)$
50	0·550	0·120	1·252	0·457	1·21	962	0·0903
52	0·507	0·079	0·823	0·535	0·858	856	0·0696
53	0·489	0·070	0·730	0·558	0·773	837	0·0651
54	0·470	0·0553	0·667	0·577	0·715	826	0·0626
56	0·437	0·0492	0·577	0·606	0·635	815	0·0598
58	0·408	0·0448	0·511	0·627	0·577	815	0·0580
60	0·381	0·0370	0·468	0·646	0·535	818	0·0578
65	0·325	0·0320	0·386	0·682	0·443	838	0·0560
70	0·280	0·0270	0·334	0·707	0·405	872	0·0595
80	0·214	0·0250	0·282	0·733	0·360	960	0·0691
90	0·169	0·0244	0·261	0·747	0·340	1,060	0·0827
100	0·137	0·0240	0·254	0·757	0·330	1,163	0·0990
110	0·113	0·0240	0·251	0·759	0·325	1,280	0·1180
120	0·095	0·0240	0·251	0·759	0·325	1,395	0·1405
130	0·081	0·0241	0·251	0·759	0·325	1,510	0·1650

TABLE 4.

Height (ft.).	ρ	$f(\rho)$	$\rho^{\frac{1}{2}}$(r.p.m.).			$\frac{\text{Std. b.h.p.}}{\text{r.p.m.}} f(\rho)$ from Engine			$\rho^{\frac{1}{2}} V_{m.p.h.}$	$V_{m.p.h.}$	r.p.m.
			r.p.m. = 1,500.	r.p.m. = 1,400.	r.p.m. = 1,300.	r.p.m. = 1,500.	r.p.m. = 1,400.	r.p.m. = 1,300			
Ground	1·025	1·038	1,520	1,418	1,314	0·1582	0·1680	0·1760	129	127·5	1,472
5,000	0·874	0·842	1,402	1,309	1,216	0·1284	0·1365	0·1435	117	125	1,448
10,000	0·740	0·686	1,290	1,204	1,118	0·1046	0·1112	0·1165	105·5	122·5	1,427
15,000	0·630	0·558	1,190	1,111	1,032	0·0851	0·0902	0·0948	95	119·5	1,398
20,000	0·535	0·446	1,097	1,024	950	0·0680	0·0722	0·0758	83·5 (50·5)	114·2 (60)	1,361 (1,232)
25,000	0·445	0·352	1,000	933	866	0·0537	0·0570	0·0599	69·5 (55)	104·2 (82·5)	1,307 (1,230)

If the empirical formulæ for airscrews be used, the values of $\frac{V}{nP}$ corresponding to $\frac{1}{4}K_tT_c\left(\frac{V}{nP}\right)^{-2}$ can be read from standard curve (Fig. 14), and the values of $\frac{1}{4}K_qQ_c\left(\frac{V}{nP}\right)^{-2}$ calculated from curve B, Fig. 14A. In other cases it is advantageous to produce curves for these quantities from those for K_tT_c and K_qQ_c.

From the formulæ above Table 3 is compiled.

Columns (7) and (8) of Table 3 give a unique curve (PQ, Fig. 7) between $\rho^{\frac{1}{2}}$ (r.p.m.) and $\frac{\text{Std. b.h.p.}}{\text{r.p.m.}} f(\rho)$ for level flights. The relation between the two quantities has been derived wholly from the aerodynamics of the aeroplane and will continue to hold if the engine be throttled down. To find the top speed a graphical method of solving the equations between $\rho^{\frac{1}{2}}$ (r.p.m.) and $\frac{\text{Std. b.h.p.}}{\text{r.p.m.}} f(\rho)$ and between the engine horse-power at full throttle and revolutions appears to be most direct and the result is shown in Fig. 7 together with the figures in Table 4. Table 3, columns 1 and 7, shows a unique relation between $\rho^{\frac{1}{2}}V_{\text{m.p.h.}}$ and $\rho^{\frac{1}{2}} \times$ r.p.m., which is plotted in Fig. 8. This relation is independent of the engine and therefore applies for throttled flights level.

The last column of Table 4 is obtained from Fig. 8, the intersections there shown and marked for the appropriate height being determined from the intersections on Fig. 7, the values of $\rho^{\frac{1}{2}}$ r.p.m. being the common argument. Fig. 8 is itself plotted from the numbers in Table 3 and forms the most direct comparison between any prediction and the corresponding observations in level flights.

Maximum climb.—For various speeds the value of the rate of climb is calculated from equation (22) as below, and the results are plotted in Fig. 6 from which the maximum rate of climb is read off as well as the speed at which this climb occurs.

TABLE 5A.

Ground.

V (f/s)	L_c	D_c	$\frac{V}{nP}$ from Fig. 5a.	$0{\cdot}0961 \times \left[\frac{1}{4}K_tT_c\left(\frac{V}{nP}\right)^{-2}\right]$	$0{\cdot}0961 \times \left[\frac{1}{4}K_tT_c\left(\frac{V}{nP}\right)^{-2}\right] - D_c$	v (f/s)
90	0·356	0·0412	0·414	0·1531	0·1119	28·3
100	0·288	0·0328	0·459	0·1180	0·0852	29·6
110	0·238	0·0288	0·501	0 0940	0·0652	30·2
120	0·200	0·0264	0·542	0·0760	0·0496	29·8

After plotting it is found that
Maximum v is 30·2 f/s. at V = 110 f/s., or
1,815 feet per minute at an airspeed of 76 m.p.h. ($\rho^{\frac{1}{2}}$ $V_{\text{m.p.h.}}$)
The corresponding engine revolutions are 1,320 r.p.m.

Table 5B.

5,000 feet.

V (f/s)	L_c	D_c	$\frac{V}{nP}$ from Fig. 5a.	$0{\cdot}0961 \times \left[\frac{1}{4} K_t T_c \left(\frac{V}{nP}\right)^{-2}\right]$	$0{\cdot}0961 \times \left[\frac{1}{4} K_t T_c \left(\frac{V}{nP}\right)^{-2}\right] - D_c$	v (f/s)
90	0·417	0·0508	0·420	0·1479	0·0970	20·93
100	0·338	0·0386	0·465	0·1135	0·0749	22·15
110	0·279	0·0321	0·507	0·0910	0·0589	23·22
120	0·235	0·0286	0·548	0·0740	0·0454	23·22
130	0·200	0·0261	0·588	0·0600	0·0339	22·02

Maximum v is 23·35 f/s. at V = 115 f/s., or
1,400 feet per minute at an airspeed of 73·3 m.p.h.
Engine revolutions 1,310 r.p.m.

Table 5C.

10,000 feet.

V (f/s)	L_c	D_c	$\frac{V}{nP}$ from Fig. 5a.	$0{\cdot}0961 \times \left[\frac{1}{4} K_t T_c \left(\frac{V}{nP}\right)^{-2}\right]$	$0{\cdot}0961 \times \left[\frac{1}{4} K_t T_c \left(\frac{V}{nP}\right)^{-2}\right] - D_c$	v (f/s)
90	0·492	0·0722	0·425	0·1422	0·0700	12·79
100	0·399	0·0479	0·470	0·1109	0·0630	15·80
110	0·330	0·0379	0·514	0·0878	0·0499	16·64
120	0·277	0·0320	0·555	0·0712	0·0392	16·98
130	0·236	0·0286	0·595	0·0577	0·0291	16·03

Maximum v is 17·0 f/s. at V = 119 f/s., or
1,020 feet per minute at an airspeed of 70 m.p.h.
Engine revolutions 1,300 r.p.m.

Table 5D.

15,000 feet.

V (f/s)	L_c	D_c	$\frac{V}{nP}$ from Fig. 5a.	$0{\cdot}0961 \times \left[\frac{1}{4} K_t T_c \left(\frac{V}{nP}\right)^{-2}\right]$	$0{\cdot}0961 \times \left[\frac{1}{4} K_t T_c \left(\frac{V}{nP}\right)^{-2}\right] - D_c$	v (f/s)
100	0·468	0·0634	0·479	0·1059	0·0425	9·08
110	0·387	0·0458	0·522	0·0845	0·0387	11·00
120	0·325	0·0370	0·563	0·0681	0·0311	11·49
130	0·277	0·0319	0·603	0·0555	0·0236	11·08

Maximum v is 11·5 f/s. at V = 122 f/s., or
690 feet per minute at an airspeed of 66·1 m.p.h.
Engine revolutions 1,285 r.p.m.

TABLE 5E.

20,000 feet.

V (f/s)	L_c	D_c	$\frac{V}{nP}$ from Fig. 5a.	$0{\cdot}0961 \times \left[\frac{1}{4}K_f T_c \left(\frac{V}{nP}\right)^{-2}\right]$	$0{\cdot}0961 \times \left[\frac{1}{4}K_f T_c \left(\frac{V}{nP}\right)^{-2}\right] - D_c$	v (f/s)
110	0·458	0·0600	0·528	0·0816	0·0216	5·19
120	0·385	0·0450	0·569	0·0662	0·0212	6·62
130	0·328	0·0372	0·608	0·0535	0·0163	6·46
140	0·283	0·0322	0·647	0·0436	0·0114	5·65

Maximum v is 6·62 f/s. at V = 123 f/s., or
400 feet per minute at an airspeed of 61·2 m.p.h.
Engine revolutions 1,270 r.p.m.

TABLE 5F.

25,000 feet.

V (f/s)	L_c	D_c	$\frac{V}{nP}$ from Fig. 5a.	$0{\cdot}0961 \times \left[\frac{1}{4}K_f T_c \left(\frac{V}{nP}\right)^{-2}\right]$	$0{\cdot}0961 \times \left[\frac{1}{4}K_f T_c \left(\frac{V}{nP}\right)^{-2}\right] - D_c$	v (f/s)
125	0·427	0·0530	0·605	0·0546	0·0016	0·47
130	0·395	0·0470	0·625	0·0492	0·0022	0·74
135	0·366	0·0427	0·645	0·0442	0·0015	0·55
140	0·341	0·0391	0·663	0·0402	0·0011	0·47

Maximum v = 0·7 f/s. at V = 131 f/s., or
40 feet per minute at an airspeed of 60 m.p.h.
Engine revolutions 1,245 r.p.m.

The various items which are observed during a performance trial have been extracted from the tables and are plotted in Fig. 9.

In order to show the nature of the agreement between calculation and observation a machine has been selected from Martlesham Heath trials which has the same loading per square foot and the same horse-power per lb. The main characteristics are set out in the table below and the curves for performance in Fig. 10.

Hypothetical Aeroplane.	Martinsyde Scout. Falcon Mk. III Rolls Royce Engine.
Std. b.h.p. at climb, 272 h p. at 1,320.	Std. b.h.p. at climb, 270 h.p. at 1,950 r.p.m.
Total weight, 1,900 lbs.	Total weight, 2,260 lbs.
Wing area, 272 sq. feet.	Wing area, 323 sq. feet.
Airscrew diameter, 8·75 feet.	Airscrew diameter, 9·5 feet.
Airscrew revolutions on climb, 1,320.	Airscrew revolutions on climb, 1,150.
Loading, 7·0 lbs/sq. feet.	Loading, 7·0 lbs/sq. feet.
Lbs. per h.p. on climb, 11·7.	Lbs. per h.p. on climb, 11·9.

A comparison between Figs. 9 and 10 will show how very accurately the method used can be made to predict performance. The curves cannot be compared near the ceiling as observations rarely occur above 16,500 ft. The airscrew of the hypothetical aeroplane is of smaller diameter than that of the real aeroplane, but allowing for this difference the predictions and observations are in complete agreement.

It is now useful, before proceeding to analysis of observations, to summarise the assumptions which have led to Tables 4 and 5 and to Fig. 9.

The curve for aeroplane resistance which is given in Fig. 1 is taken directly from a model of a B.E. 2E tested in the large wind channel of the N.P.L. The model was complete with the exception of the airscrew and wires. On the other hand, no correction has been made for scale. Such evidence as exists shows a reduction of resistance with increase of size and it may happen that the omission of wires had just compensated for any scale effect.

The shapes of the airscrew curves are taken from model experiments at the N.P.L., but the numerical values given to the ordinates do not represent any particular experiment. The maximum efficiency of 78 per cent. is not unusual.

The interference between airscrew and body is dealt with on the basis of model experiments.

The engine curve does not represent any particular engine, but is typical of the results obtained on the test-bed.

The variation of engine power with height is based on an indicated horse-power which varies as the density together with the assumption of a constant mechanical loss of 15 per cent. of the standard horse-power. It is a close approximation to variations measured during flight.

The remaining factors of weight, area, &c., were chosen to represent figures for a high speed scout.

1. *Analysis of performance of an aeroplane in which level flights with throttled engine are available in addition to observation of speed and climb with the engine "all out."*—The particular aeroplane chosen for analysis was DeH. 4 with a 375 h.p. Rolls Royce engine. The airscrew was geared down in the proportion 0·6 : 1.

There appears to be some doubt as to the exact horse-power of the engine used and the effect of this appears in some uncertainty in the estimation of the airscrew efficiency but is not in other respects of any importance. The values taken for the Standard b.h.p. appear in the tables together with the observation of speed and climb.

TABLE 6.

Level Flights.			Maximum Climb.			
Relative Density.	Speed, m.p.h.	Engine, r.p.m.	Relative Density.	Speed, m.p.h.	Engine, r.p.m.	Rate of Climb. Ft /m.
0·833	134	1,935	0·963	77·6	1,700	1,265
* ,,	115	1,700	0·903	78·0	1,700	1,145
* ,,	98	1,500	0·845	79·0	1,700	1,025
* ,,	80	1,300	0·792	80·2	1,695	905
0·717	132·5	1,910	0·740	81·4	1,690	780
* ,,	115	1,720	0·695	81·6	1,685	660
* ,,	100	1,565	0·652	81·7	1,675	540
* ,,	80	1,360	0·610	82·0	1,660	420
0·611	126	1,860				
* ,,	100	1,595				
* ,,	80	1,400				
0·740	133	1,915				
0·673	130·5	1,895				
0·630	128	1,870				
0·600	125	1,855				

* These level flights were made with throttled engine.

The following further particulars apply to this aeroplane :—

Total weight . . . 3,475 lbs.
Wing area . . . . 436 sq. feet
Airscrew diameter . . 10·13 feet } . (24)

Table 6 and the particulars in (24) constitute the whole of the available data obtained during performance trials and with the power curve for the engine constitute the material to be analysed. The first illustration will ignore all questions relating to accuracy of observation in order to concentrate attention on the principles underlying the analysis.

It will be found that it is possible to deduce :—

(1) The variation of engine power with height.

(2) The efficiency of the airscrew.

(3) The resistance coefficient of the aeroplane apart from its airscrew.

(1) *Variation of engine power with height.*—From a knowledge of the standard b.h.p. at given revolutions and the use of equation (14a) it is possible to calculate directly the value of $Q_c/f(\rho)$, where Q_c is the torque coefficient and $f(\rho)$ is the factor representing variation of power with height.

The airscrew formula given in (3) may be written as

$$K_q f(\rho) \frac{Q_c}{f(\rho)} = 2 \frac{V^{0.47}}{nP} - 1{\cdot}772 \frac{V^2}{nP} \quad . \quad . \quad . \quad (25)$$

and as the advance per revolution is measured in flight, equation (25) is determined except for the values of $K_q f(\rho)$ and P. If experiments are made at the same height then $K_q f(\rho)$ is the same throughout, but the value of V/nP depends on the rate of climb. Hence if two experiments be chosen, preferably near the ground, one being a level flight with the engine "all out" and the other a maximum climb it is possible to eliminate $K_q f(\rho)$ and so lead to an equation for the determination of P. Experiments at other heights may be used, but greatest accuracy obviously goes with the observations at the least height at which steady flight is possible because the difference between the values of V/nP in the two extreme experiments then has its greatest value.

If experiments were conducted at the place where ρ is unity and where $f(\rho)$ is also defined to be unity the value of K_q would be also determined by the same two experiments. In any application, however, extrapolation to $\rho = 1$ is necessary, and this is a source of some error of prediction which must be borne in mind.

In all analyses made by this method $K_q f(\rho)$ has been found to be linear with ρ, and its value K_q where ρ is unity is reasonably certain, provided that the b.h.p. curve of the engine is accurately known.

TABLE 7.

Experiments with Engine "all out."

Height, ft.	Relative Density.	Speed, m.p.h.	Engine, r.p.m.	Standard b.h.p.	$\frac{V}{nD}$	$\frac{Q_c}{f(\rho)}$
6,500	0·833	134	1,935	354	1·005	0·0201
11,000	0·717	132·5	1,910	353	1·004	0·0242
16,000	0·611	126	1,860	351	0·978	0·0304
10,000	0·740	133	1,915	354	1·005	0·0232
13,000	0·673	130·5	1,895	353	1·000	0·0263
15,000	0·630	125	1,855	351	0·978	0·0297
16,500	0·600	128	1,870	351	0·994	0·0306
2,000	0·963	77·6	1,700	338	0·661	0·0244
4,000	0·903	78·0	1,700	338	0·664	0·0260
6,000	0·845	79·0	1,700	338	0·672	0·0278
8,000	0·792	80·2	1,695	338	0·687	0·0299
10,000	0·740	81·4	1,690	338	0·700	0·0324
12,000	0·695	81·6	1,685	337	0·701	0·0345
14,000	0·652	81·7	1,675	336	0·706	0·0373
16,000	0·610	82·0	1,660	334	0·716	0·0408

From (14a) we have for this aeroplane :—

$$\frac{Q_c}{f(\rho)} = \frac{550}{6{\cdot}28 \times (10{\cdot}13)^3} \times \frac{\text{Std. b.h.p.}}{0{\cdot}00237\rho \left(\frac{\text{r.p.m.}}{60}\right)^3} \quad \text{airscrew.}$$

$$= 73{,}600 \ \frac{\text{Std. b.h.p.}}{\rho(\text{r.p.m.})^3} \quad \text{airscrew.}$$

$$= 341{,}000 \ \frac{\text{Std. b.h.p.}}{\rho(\text{r.p.m.})^3} \quad \text{engine.} \qquad . \quad . \quad . \quad . \quad . \quad (26)$$

The values of $Q_c/f(\rho)$ calculated from (26) are given in the last column of Table 7. The figures in columns 6 and 7 are used to produce the curves of Fig. 11 showing the relation between V/nD and height and $Q_c/f(\rho)$ and height. It should be remarked that the speed during climb is an arbitrary variable at the disposal of the pilot and that a mean curve must be used with considerable caution if errors of deduction are to be avoided.

From the curves of Fig. 11 it is now possible to choose values of $Q_c/f(\rho)$ and V/nD for the same altitude and to use them in equation (25), which can be transformed to the following equation for P.

$$P^{1{\cdot}53} = 0{\cdot}886 \ \frac{\left(\frac{Q_c}{f(\rho)}\right)_2 \left(\frac{V}{n}\right)_1^2 - \left(\frac{Q_c}{f(\rho)}\right)_1 \left(\frac{V}{n}\right)_2^2}{\left(\frac{Q_c}{f(\rho)}\right)_2 \left(\frac{V}{n}\right)_1^{0{\cdot}47} - \left(\frac{Q_c}{f(\rho)}\right)_1 \left(\frac{V}{n}\right)_2^{0{\cdot}47}} \qquad . \quad (27)$$

$$\text{At 6,000 ft.} \quad \left.\begin{aligned} \left(\frac{Q_c}{f(\rho)}\right)_1 &= 0{\cdot}0196 \quad \left(\frac{Q_c}{f(\rho)}\right)_2 = 0{\cdot}0278 \\ \left(\frac{V}{n}\right)_1 &= 10{\cdot}20 \quad \left(\frac{V}{n}\right)_2 = 6{\cdot}62 \end{aligned}\right\} \qquad . \quad . \quad (28)$$

$$\text{and} \quad P^{1{\cdot}53} = 51{\cdot}4 \qquad P = 13{\cdot}1 \qquad . \quad . \quad . \quad . \quad (29)$$

At 10,000 ft., P = 13·1. At 16,000 ft., P = 12·9. Observations near the ground should be given greater weight than those at altitudes, and the value P = 13·1 will be adopted.

TABLE 8.

Height, ft.	Relative Density.	$\frac{V}{nP}$	$\frac{Q_c}{f(\rho)}$	$K_q Q_c$	$K_q f(\rho)$	$K_q = 42{\cdot}9$ See Fig. 11a.
6,500	0·833	0·777	0·0201	0·703	35·0	0·816
11,000	0·717	0·776	0·0242	0·705	29·1	0·678
16,000	0·611	0·757	0·0304	0·737	24·2	0·564
10,000	0·740	0·777	0·0232	0·703	30·3	0·705
13,000	0·673	0·774	0·0263	0·708	26·9	0·628
15,000	0·630	0·757	0·0297	0·737	24·9	0·580
16,500	0·600	0·754	0·0306	0·718	23·5	0·546
2,000	0·963	0·512	0·0244	0·994	41·8	0·974?
4,000	0·903	0·514	0·0260	0·992	38·2	0·890
6,000	0·845	0·520	0·0278	0·990	35·6	0·830
8,000	0·792	0·532	0·0299	0·982	32·9	0·766
10,000	0·740	0·542	0·0324	0·977	30·2	0·702
12,000	0·695	0·542	0·0345	0·977	28·2	0·660
14,000	0·652	0·546	0·0373	0·975	26·2	0·610
16,000	0·610	0·554	0·0408	0·970	23·8	0·554

The straight line of Fig. 11a corresponds with the formula :—

$$f(\rho) = \frac{\rho - 0{\cdot}119}{0{\cdot}881} \quad . \quad . \quad . \quad . \quad . \quad . \quad (30)$$

an equation which may be interpreted approximately as due to an indicated horse-power which is proportional to density together with a mechanical loss of 11·9 per cent. of the standard horse-power.

The preceding analysis has given in addition to the value of $f(\rho)$, the numerical value of 39·7 to K_q and the results may be summarised as :—

$$\left.\begin{aligned} P &= 13{\cdot}1 \\ K_q &= 42{\cdot}9 \\ f(\rho) &= \frac{\rho - 0{\cdot}119}{0{\cdot}881} \end{aligned}\right\} \quad . \quad . \quad . \quad . \quad . \quad (31)$$

Determination of K_t.—To determine K_t use is made of equation (17) which with numerical factors introduced becomes :—

$$\left(\frac{V}{nP}\right)^{-2} - 1 = 5{\cdot}32\, K_t \left(D_c + L_c \frac{v}{V}\right) \quad . \quad . \quad . \quad . \quad (32)$$

together with $L_c = \frac{1,570}{\rho_1 V^2_{\text{m.p.h}}}$ . . . . . (33)

Two experiments at the same airspeed $(\rho V^2)^{\frac{1}{2}}$ are used to eliminate D_c. As L_c is now an important independent variable the values of V/nP and $L_c \frac{v}{V}$ are plotted in Fig. 12 with L_c as abscissa. From the curves so drawn it will be possible to extract values of V/nP and $L_c \frac{v}{V}$ which correspond with a given airspeed. Table 9 gives the necessary data for drawing Fig. 12, &c.

TABLE 9.

Speed, m.p.h.	Relative Density.	$\frac{V}{nP}$	L_c	$L_c\frac{v}{V}$	$D_c + L\frac{v}{V}$	D_c	Airscrew Efficiency.
134	0·833	0·777	0·105	0	0·0179	0·0179	0·749
*115	,,	0·758	0·142	,,	0·0203	0·0203	0·750
* 98	,,	0·731	0·196	,,	0·0240	0·0240	0·750
* 80	,,	0·690	0·295	,,	0·0302	0·0302	0·740
132·5	0·717	0·776	0·125	0	0·0181	0·0181	0·749
*115	,,	0·749	0·156	,,	0·0215	0·0215	0·750
*100	,,	0·716	0·219	,,	0·0261	0·0261	0·746
* 80	,,	0·659	0·343	,,	0·0358	0·0358	0·731
126	0·611	0·757	0·162	0	0·0205	0·0205	0·750
*100	,,	0·702	0·257	,,	0·0283	0·0283	0·744
* 80	,,	0·640	0·402	,,	0·0398	0·0398	0·724
133	0·740	0·777	0·120	0	0·0179	0·0179	0·749
130·5	0·673	0·774	0·137	,,	0·0184	0·0184	0·749
128	0·630	0·757	0·152	,,	0·0205	0·0205	0·750
125	0·600	0·754	0·168	,,	0·0209	0·0209	0·750
77·6	0·963	0·512	0·270	0·0500	0·0775	0·0275	0·651
78·0	0·903	0·514	0·285	0·0476	0·0767	0·0291	0·653
79·0	0·845	0·520	0·297	0·0440	0·0742	0·0302	0·657
80·2	0·792	0·532	0·308	0·0395	0·0695	0·0300	0·665
81·4	0·740	0·542	0·320	0·0350	0·0659	0·0309	0·671
81·6	0·695	0·542	0·339	0·0313	0·0659	0·0346	0·671
81·7	0·652	0·546	0·361	0·0272	0·0645	0·0373	0·674
82·0	0·610	0·554	0·382	0·0224	0·0621	0·0397	0·679

* Engine throttled.

From Fig. 12 the values given below have been read off :—

$$\left.\begin{aligned} &L_c = 0{\cdot}27;\ \frac{V}{nP}\ \text{level flight} = 0{\cdot}696;\ \frac{V}{nP}\ \text{climb} = 0{\cdot}512 \\ &L_c\frac{v}{V} = 0{\cdot}0508 \\ &L_c = 0{\cdot}32,\ \frac{V}{nP}\ \text{level flight} = 0{\cdot}675;\ \frac{V}{nP}\ \text{climb} = 0{\cdot}542 \\ &L_c\frac{v}{V} = 0{\cdot}0345 \\ &L_c = 0{\cdot}37,\ \frac{V}{nP}\ \text{level flight} = 0{\cdot}655;\ \frac{V}{nP}\ \text{climb} = 0{\cdot}550 \\ &L_c\frac{v}{V} = 0{\cdot}0254 \end{aligned}\right\} \quad (34)$$

Using equation (32) these values lead to

$$\left.\begin{aligned} K_t &= \frac{1{\cdot}84}{5{\cdot}32 \times 0{\cdot}0508} = 6{\cdot}80 \\ K_t &= \frac{1{\cdot}21}{5{\cdot}32 \times 0{\cdot}0345} = 6{\cdot}59 \\ K_t &= \frac{0{\cdot}98}{5{\cdot}32 \times 0{\cdot}0254} = 7{\cdot}25 \end{aligned}\right\} \quad . \quad . \quad . \quad (35)$$

The values of K_t given in (35) are somewhat variable and it is necessary to take a mean, giving most weight to observations near the ground. The best method of weighting appears to consist of the addition of the numerators and denominators of the fractions of (35) to get

$$K_t = \frac{4{\cdot}03}{5{\cdot}32 \times 0{\cdot}1107} = 6{\cdot}85 \quad . \quad . \quad . \quad . \quad (36)$$

The maximum airscrew efficiency can be calculated from the formula

$$\eta_{\text{max.}} = 0{\cdot}583 \frac{P}{2\pi D} \frac{K_q}{K_t} \quad . \quad . \quad . \quad . \quad . \quad (37)$$

and is equal to 0·750.

More generally the airscrew efficiency can be calculated for any value of advance per revolution, the expression being

$$\eta = \frac{\left(\frac{V}{nP}\right)^{-2} - 1}{1{\cdot}5\left(\frac{V}{nP}\right)^{-2{\cdot}53} - 1{\cdot}329\left(\frac{V}{nP}\right)^{-1}} \frac{P}{2\pi D} \frac{K_q}{K_t} \quad . \quad (38)$$

The values of η for each observation are given in the last column of Table 9. It will be noticed that maximum efficiency is obtained at top-speed and that during climb the efficiency varies from 0·65 to 0·68.

Determination of D_c.—From equation (32) and Table 9 the values of $D_c + L_c \frac{v}{V}$ can be calculated and hence the values of D_c. The result of the calculation is shown in Table 9 and in Fig. 13.

The degree of consistency of the points shows what may be expected from the method apart from any systematic errors due to the method of dealing with slip-stream effect and airscrew efficiency.

In the instance of the DeH. 4 tests have been made with other airscrews and engines, though not always with the same completeness of observation.

2. *Analysis of a performance trial in which there are available only observations of level flights and climbs with the engine at full throttle.*—In the great majority of trials the only data available

for analysis are those associated with level flights at several heights and the best climb with the engine at full throttle in each case. To reduce such trials advantage is taken of the fact that when a machine is performing its best climb or level flight, the indicated airspeed diminishes continuously as the height increases, and as a consequence the lift coefficient of the machine, and its drag coefficient both increase continuously as the height increases.

When a correct analysis has been made, it is clear that the curve connecting L_c and D_c for the level flight must be continuous with the corresponding curve for the climb (see Fig. 14).

The method of reduction is best explained in connection with Tables 10 and 11, which give the analysis of the trials of DeH.4 with the 275 H.P. Rolls engine.

Columns 1 to 6 in Table 10 are the points taken from the data of the trial and engine test bed power curve.

Columns 8 to 13 are used for calculating experimental pitch P, K_q and $f(\rho)$ as explained in connection with Table 8. In short, the details of the method up to and including column 16, Table 10, are the same as those already described. For determining D_c in this case it is more convenient to use the older form of thrust coefficient,

$$t_c = \frac{\text{Thrust}}{\rho_m D^2 V^2} = \frac{T}{\rho_m D^2 V^2}, \text{ V being in feet per second.}$$

We then have $T = W \frac{D_c}{L_c} + \frac{v}{V}$

or

$$t_c \rho_m D^2 V^2 = L_c \rho_m A V^2 \left(\frac{D_c}{L_c} + \frac{v}{V} \right)$$

which reduces to $t_c \times \frac{D^2}{A} = D_c + L_c \frac{v}{V}$ or

$$\frac{1}{k_t} \times (k_t\, t_c) \times \frac{D^2}{A} - L_c \frac{v}{V} = D_c \quad . \quad . \quad . \quad (39)$$

From the values of $\frac{V \times 88}{nP}$ or $\frac{e}{P}$ in column 9 the corresponding values of $k_t\, t_c$ (column 17) are calculated from the general propeller equation $k_t\, t_c = \frac{1}{3} \left(\frac{P}{e} \right)^2 - \frac{1}{3}$, or read off the curve c for that equation in Fig. 14.

Table 11 is then begun by transferring the figures in Cols. 1, 14 and 16, Table 10, to columns 18, 19 and 25. $k_t\, t_c \frac{D^2}{A}$ is calculated from column 17, Table 10, and the figures put down in column 24, Table 11.

The next operation consists in guessing a value of k_t which will make the values of D_c when plotted against L_c lie on a continuous curve embracing the values obtained from both the level flight and climbing trials. Fig. 14 shows how this process enables the right value of k_t to be arrived at. The first guess for the value of k_t is made by assuming a probable maximum propeller efficiency and substituting this in the relation

$$\eta \text{ max.} = \frac{P^3}{8\pi D^3} \frac{(\text{new})\, K_q}{(\text{old})\quad k_t} \times 0{\cdot}583 \quad . \quad . \quad . \quad (40)$$

It will be observed from a consideration of Fig. 14 that k_t can be determined by this method to within 2 or 3 per cent. if the trials are consistent.

The values of L_c and D_c, corresponding with climbs at low altitudes, do not always fall consistently on the final curve of D_c against L_c, a result which is probably caused by bad observations at the beginning of a climb, or because the climb rate curve, as given in the trial report, has been incorrectly drawn through the individual observations.

Having finally decided on k_t, and the $D_c - L_c$ curve, the value of the maximum propeller efficiency $\eta_{\text{max.}}$ is calculated from (40) and the propeller efficiencies for all values of V/nD from the curve given in Fig. 17. It only remains to evaluate L_c/D_c in order to complete the analysis.

It is clear that considerable experience in the use of the analysis will be required before the full advantages are developed. The present notes are put forward in the hope that others may be sufficiently interested to help in the developments.

TABLE 10.

	1. Height.	2. A.S.I. m.p.h. Q	3. Speed, m.p.h. V	4. Rate of climb f/m. v	5. r.p.m. n	6. Stand. b.h.p.	7. Adv. per rev. $e = \frac{V \times 88}{n\,r}$	8. Exp. Pitch P. ft.	9. $\frac{e}{\text{mean P}}$	10. $\frac{Q_c}{f\rho}$	11. $K_q Q_c$	12. $K_q f(\rho)$	13. $f\rho$ from curve of $K_q f(\rho)$	14. L_c	15. $\frac{v}{88V}$	16. $\frac{L_c v}{88V}$	17. $k_l t_c$
Level Flight.	10,000		120·5	—	1,780	324·6	9·92	12·52	0·788	0·0160	0·695	43·4		0·147			0·201
	12,000		119·0	—	1,760	323·4	9·91	12·42	0·786	0·0175	0·698	39·9		0·161			0·205
	14,000		116·5	—	1,730	321·6	9·87	12·59	0·783	0·0195	0·703	36·1		0·179			0·209
	16,000		112·5	—	1,685	318·4	9·79	12·84	0·776	0·0224	0·713	31·8		0·205			0·217
Climb.	4,000	69·8	73·5	942	1,589	310·5	6·79		0·539	0·0176	0·987	56·0	0·880	0·323	0·146	0·0470	0·814
	6,000	69·3	75·4	840	1,585	310·1	6·98		0·554	0·0189	0·981	51·9	0·806	0·328	0·127	0·0415	0·751
	8,000	68·6	77·1	730	1,580	309·9	7·15		0·567	0·0204	0·952	46·6	0·740	0·335	0·108	0·0361	0·700
	10,000	67·5	78·5	627	1,575	309·4	7·30	12·52	0·580	0·0220	0·941	42·7	0·675	0·346	0·091	0·0314	0·657
	12,000	66·0	79·2	520	1,565	308·5	7·43	12·42	0·590	0·0237	0·932	39·3	0·617	0·362	0·075	0·0270	0·625
	14,000	64·0	79·3	418	1,553	307·3	7·49	12·59	0·595	0·0258	0·924	35·8	0·566	0·385	0·060	0·0231	0·609
	16,000	61·5	78·6	311	1,536	305·7	7·51	12·84	0·596	0·0282	0·927	32·9	0·512	0·417	0·045	0·0188	0·607

Note.—Cols. 2-6 should be filled in from faired curves.

Weight of aeroplane W = 3,502 lbs. K_q = 63·7
Wing Area A = 436 sq. ft. K_T = 10·28
Dia. of Prop. D = 11·25 ft. η max. = 0·643
Pitch ,, = 11·2 ft.
Drg. No. ,, = A.B. 732
Gear ratio r = 0·6

Mean calc. Exp. Pitch P = 12·6

$$P^3 = \frac{\left(\frac{V_l}{V_c}\right)^3 \times \frac{\text{b.h.p.}_c}{\text{b.h.p.}_l} - 1}{\left(\frac{n_l}{n_c}\right)^3 \times \frac{\text{b.h.p.}_c}{\text{b.h.p.}_l} - 1} \times e^3{}_c \times 0{\cdot}755$$

Note.—V_l, V_c, n_l, n_c are observations on level flights and climbs at the same height.

Lift coefficient $L_c = \frac{196 \cdot W}{\rho A V^2} = 1572 \times \frac{1}{\rho V^2}$

$$Q_c/f\rho = \frac{8 \times 10^8 \times \text{b.h.p.}}{D^5 \gamma^3 n^3 \rho} = 20{\cdot}5 \times 10^4 \times \frac{\text{b.h.p}}{\rho n^3}$$

$$K_q Q_c = 1{\cdot}104 - 0{\cdot}833 \left(\frac{e}{P}\right)^3; \; k_l t_c = \frac{4}{3} - \frac{4}{3}\left(\frac{e}{P}\right)^2$$

TABLE 11.

	18.	19.	20.	21.	22.	23.	24.	25.	26.	27.	28.	29.	30.	31.
			Final Values $k_t = 3{\cdot}22$.						$k_t = 3{\cdot}5$		$k_t = 3{\cdot}1$		Final $k_t = 3{\cdot}22$	
	Height from Col. 1. P. 1.	L_c from Col. 14, P. 1.	D_c	$\frac{\eta}{\eta_{\text{max.}}}$	η	$\frac{L_c}{D_c}$	$k_t t_c \times \frac{D^2}{A}$	$\frac{L_c}{88} \times \frac{v}{V}$	$\frac{k_t t_c D^2}{A\ k_t}$	$D_c = (26) - (25)$	$\frac{k_t t_c D^2}{A\ k_t}$	$D_c = (28) - (25)$	$\frac{k_t t_c D^2}{A\ k_t}$	$D_c = (30) - (25)$
Level Flight.	10,000	0·147	0·0182	0·979	0·632	8·07	0·0584	0	0·0167	0·0167	0·0188	0·0188	0·0181	0·0181
	12,000	0·161	0·0184	0·981	0·633	8·75	0·0595	0	0·0170	0·0170	0·0192	0·0192	0·0185	0·0185
	14,000	0·179	0·0188	0·983	0·634	9·52	0·0607	0	0·0174	0·0174	0·0196	0·0196	0·0188	0·0188
	16,000	0·205	0·0196	0·987	0·637	10·46	0·0630	0	0·0180	0·0180	0·0203	0·0203	0·0196	0·0196
Climb.	4,000	0·323	0·0261	0·898	0·579	12·38	0·237	0·0470	0·0676	0·0206	0·0765	0·0295	0·0735	0·0265
	6,000	0·328	0·0265	0·910	0·587	12·38	0·218	0·0415	0·0623	0·0208	0·0704	0·0289	0·0678	0·0263
	8,000	0·335	0·0271	0·922	0·595	12·38	0·203	0·0361	0·0581	0·0220	0·0655	0·0294	0·0632	0·0271
	10,000	0·346	0·0280	0·933	0·602	12·38	0·191	0·0314	0·0545	0·0231	0·0616	0·0302	0·0593	0·0279
	12,000	0·362	0·0296	0·942	0·607	12·23	0·182	0·0270	0·0519	0·0249	0·0587	0·0317	0·0564	0·0294
	14,000	0·385	0·0320	0·945	0·609	12·02	0·177	0·0231	0·0506	0·0275	0·0570	0·0339	0·0550	0·0319
	16,000	0·417	0·0359	0·946	0·610	11·61	0·176	0·0188	0·0504	0·0316	0·0567	0·0379	0·0548	0·0360

$\frac{D^2}{A} = 0{\cdot}290 \quad \eta \text{ max.} = \frac{P^3}{8\pi D^3} \times \frac{\text{(new) } K_\eta}{\text{(old) } k_t} \times 0{\cdot}583 = 0{\cdot}645$

Note.—The calculations in columns 26 to 31 are easier if the "old" thrust coefficient is used, *i.e.*, $k_t t_c = \frac{1}{3}\left(\frac{P}{e}\right)^2 - \frac{1}{3}$

If k_t = thrust constant with old $T_c \left(= \frac{T}{\rho D^2 V^2} \right)$ and K_t is constant with new $T_c \left(= \frac{T}{\rho D^4 n^2} \right)$ then

$$K_t = k_t \times \frac{4D^2}{P^2}$$

The instructions at top of columns on this sheet are for use with old $k_t t_c$.

APPENDIX.

By Miss A. D. Betts, B.Sc.

Formulæ for the Thrust and Torque Coefficients of Airscrews.

Taking T_c = Thrust $/\rho n^2 D^4$, and Q_c = Torque $/\rho n^2 D^5$, it was found by trial that the following formulæ expressed the results of tests :—

$$K_t \cdot T_c = \frac{4}{3}\left[1 - \left(\frac{V}{nP}\right)^2\right]$$

$$\text{and } K_q \cdot Q_c = 1{\cdot}104 - 0{\cdot}833\left(\frac{V}{nP}\right)^3$$

where K_t and K_q are constants such that $K_t \cdot T_c$ and $K_q \cdot Q_c$ are both equal to 1·0 when $V/nP = 0{\cdot}5$.

The above formulæ were obtained as follows :—A number of airscrew tests which were considered reliable were chosen from among those described in the reports of the Advisory Committee for Aeronautics. These airscrews were of various plan forms, and included nine two-bladed and six four-bladed airscrews. (The reports in question are R. & M. 123, Section (i), 155, Section (i), 155, Section (ii), 264, 344 and 316.)

The reports (with the exception of R. & M. 344) gave values of Thrust $/\rho V^2 D^2$ and Torque $/\rho V^2 D^3$ for various values of either V/nD or slip ratio $\left(1 - \frac{V}{nD}\right)$. The experimental mean pitch P was in most cases given, but was always tested by calculating T_c and plotting it against V/nD ; in four cases a corrected value of P, obtained by this means, was used instead of that given. In R. & M. 344, T_c and Q_c were given directly for values of V/nD, and P was found by plotting in this case.

The values of T_c and Q_c extracted from the reports were plotted against V/nP, and their values when $V/nP = 0{\cdot}5$ were then found, and used to calculate K_t and K_q. Finally, $K_t Q_c$ and $K_q Q_c$ were calculated for all observations. The points so obtained for the fifteen propellers are plotted against V/nP in the diagrams (Figs. 15 and 16). They all lie fairly closely on a single curve.

To obtain a mean curve, the points were divided into groups, taking in the first group all those with V/nP between 0·3 and 0·4 ; in the second, those with V/nP between 0·4 and 0·5 ; and so on. The values of T_c and Q_c when $V/nP = 0$ (static tests) were available in eight cases, and these constituted another group. The centre of gravity of each group of points was then found. These C.G.'s, when plotted were found to lie on fair curves passing through the C.G. of the static test points in both cases.

It was shewn that the equations of the curves must be nearly of the form $y = a + b\,x^n$; and after some adjustment the formulæ given above were arrived at.

The equation $K_Q Q_c = 1{\cdot}104 - 0{\cdot}833 \left(\frac{V}{nP}\right)^3$ represents the empirical torque curve very accurately, even in the neighbourhood of the static test point (where the formula gives 1·104, instead of 1·114 which is the actual ordinate of the C.G. of the static test points). Everywhere else the agreement is even closer. The curve $K_t T_c = \frac{4}{3} - \frac{4}{3}\left(\frac{V}{nP}\right)^2$ lies appreciably below the empirical curve for values of V/nP less than 0·3 (the formula giving 1·333 at $V/nP = 0$, as against 1·415), but is in good agreement with it elsewhere. This divergence is not important in practice, as V/n is always greater than 0·3.

Some work had been done previously (using tests of seven propellers) to obtain formulæ connecting the old form of thrust and torque coefficients (Thrust $/\rho V^2 D^2$ and Torque $/\rho V^2 D^3$) with V/nP. Calling these t_c and q_c, it was found that

$$k_t t_c = \frac{1}{3}\left[\left(\frac{nP}{V}\right)^2 - 1\right]$$

$$\text{and } k_q \cdot q_c = \frac{1}{2}\left(\frac{nP}{V}\right)^{1{\cdot}53} - 0{\cdot}443$$

as nearly as could be determined. (k_t and k_q are of course not the same as K_t and K_Q). Obviously, we may deduce the values of $K_t \cdot T_c$ and $K_q \cdot Q_c$ from these formulæ. If this is done, we find that

$$K_t \cdot T_c = \frac{4}{3} - \frac{4}{3}\left(\frac{V}{nP}\right)^2, \text{ as before;}$$

but $K_q \cdot Q_c$ is of a quite different form, and is given by

$$K_q \cdot Q_c = 2\left(\frac{V}{nP}\right)^{0{\cdot}47} - 1{\cdot}772\left(\frac{V}{nP}\right)^2.$$

This makes $K_q \cdot Q_c$ a maximum at $V/nP = 0{\cdot}42$, and zero when $V/nP = 0$, which, obviously, must be incorrect. The diagram (Fig. 17) shows the two curves

$$K_q \cdot Q_c = 2\left(\frac{V}{nP}\right)^{0{\cdot}47} - 1{\cdot}772\left(\frac{V}{nP}\right)^2$$

$$\text{and } K_q \cdot Q_c = 1{\cdot}104 - 0{\cdot}833\left(\frac{V}{nP}\right)^3$$

It will be seen that the two curves lie near together for values of V/nP between 0·5 and 0·8.

It might be objected that, though these relations hold with reasonable accuracy for airscrew models tested separately, yet they may not apply to a full-sized airscrew attached to an aeroplane, because (1) the performance of the airscrew is modified by the presence of the aeroplane parts, (2) the effect of the slip-stream on the drag of the aeroplane must be taken into account, and (3) there may be a scale-speed effect due to the considerable difference in size and airspeed between models and full-scale airscrews.

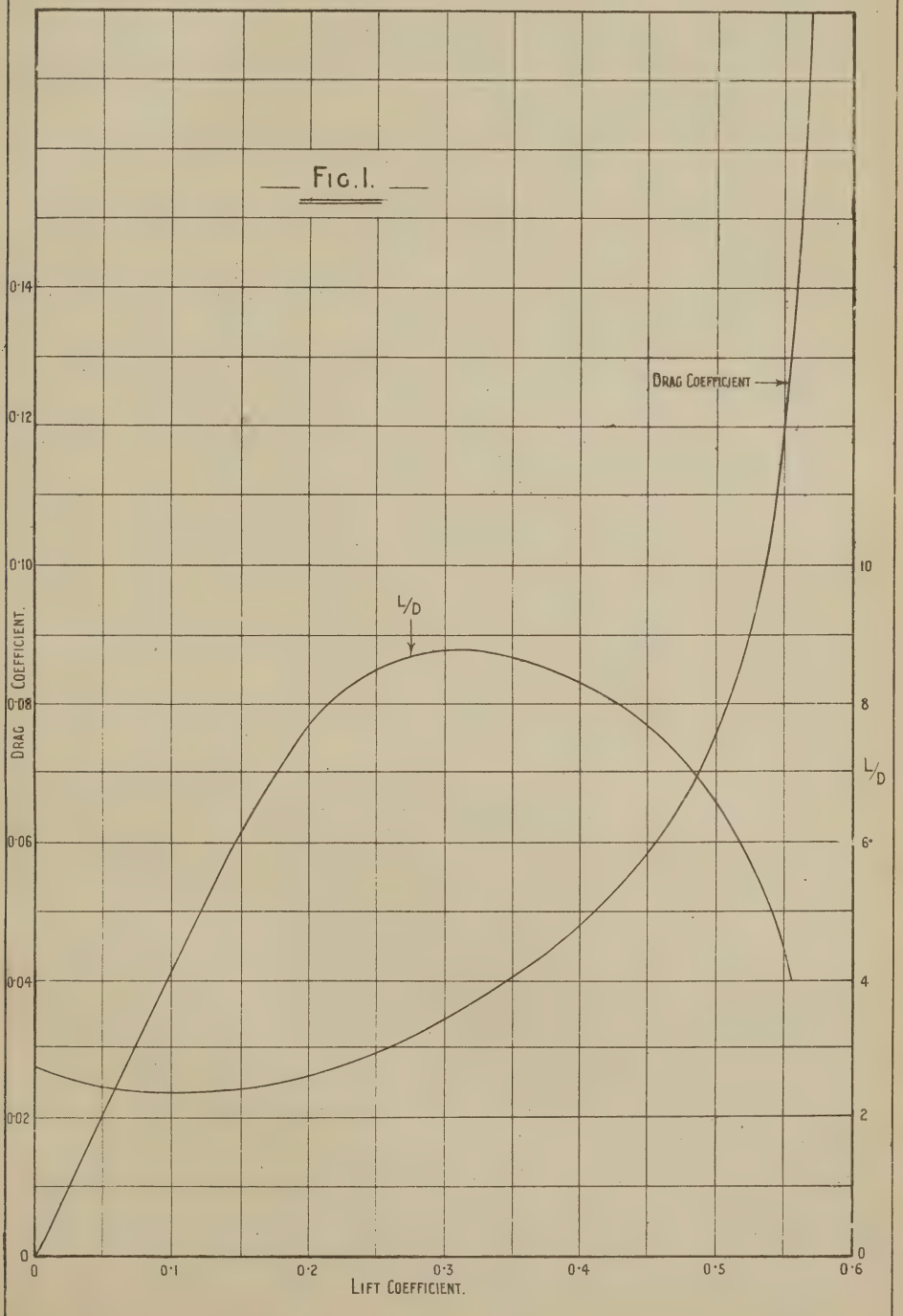
Fig. 1.
0·14
0·12
0·10
0·08
0·06
0·04
0·02
0
Drag Coefficient.
Drag Coefficient
L/D
10
8
6
4
2
0
L/D
0
0·1
0·2
0·3
0·4
0·5
0·6
Lift Coefficient.

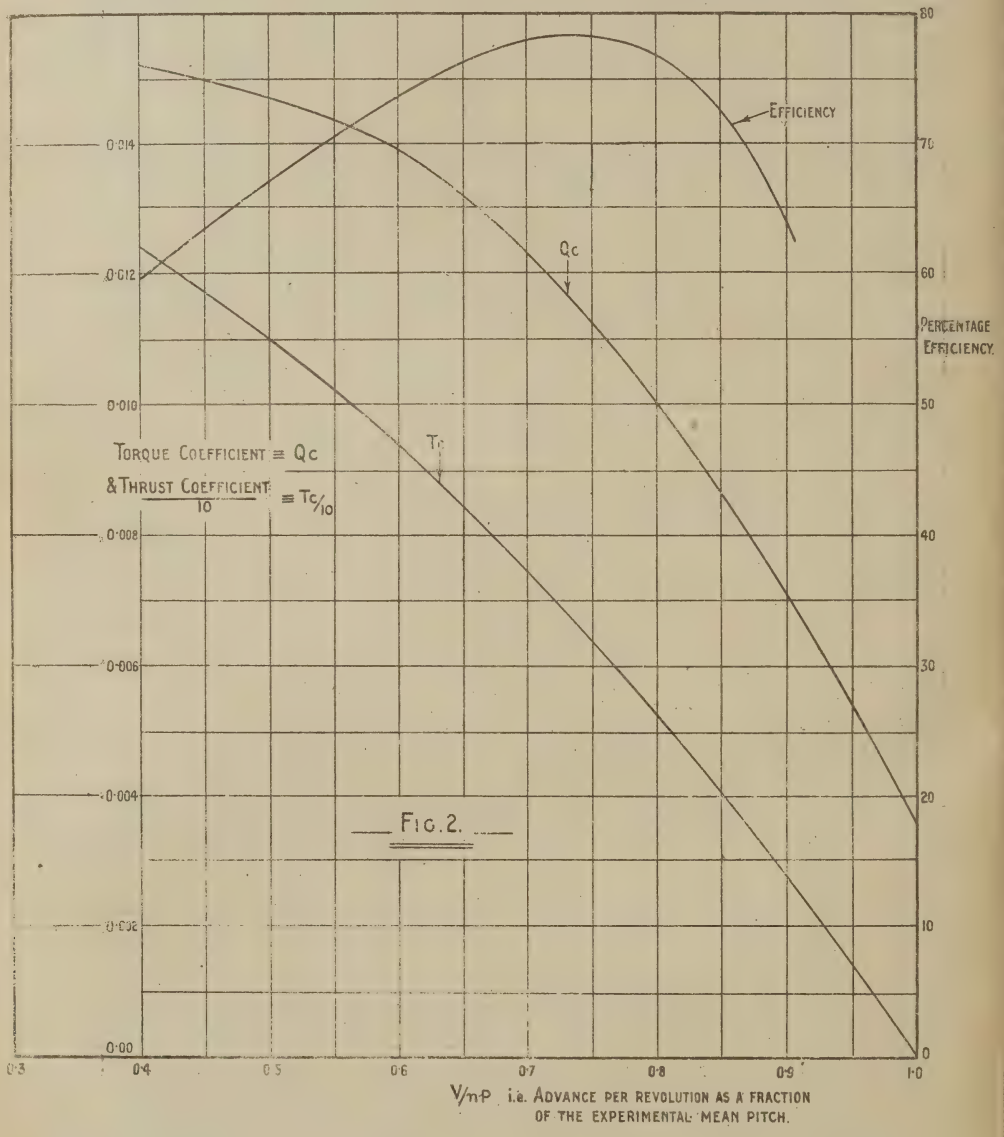
EFFICIENCY
Qc
Tc
TORQUE COEFFICIENT ≡ Qc
& THRUST COEFFICIENT / 10 ≡ Tc/10
PERCENTAGE EFFICIENCY
0·014
0·012
0·010
0·008
0·006
0·004
0·002
0·00
80
70
60
50
40
30
20
10
0
0·3
0·4
0·5
0·6
0·7
0·8
0·9
1·0
V/nP i.e. ADVANCE PER REVOLUTION AS A FRACTION OF THE EXPERIMENTAL MEAN PITCH.

FIG. 2.

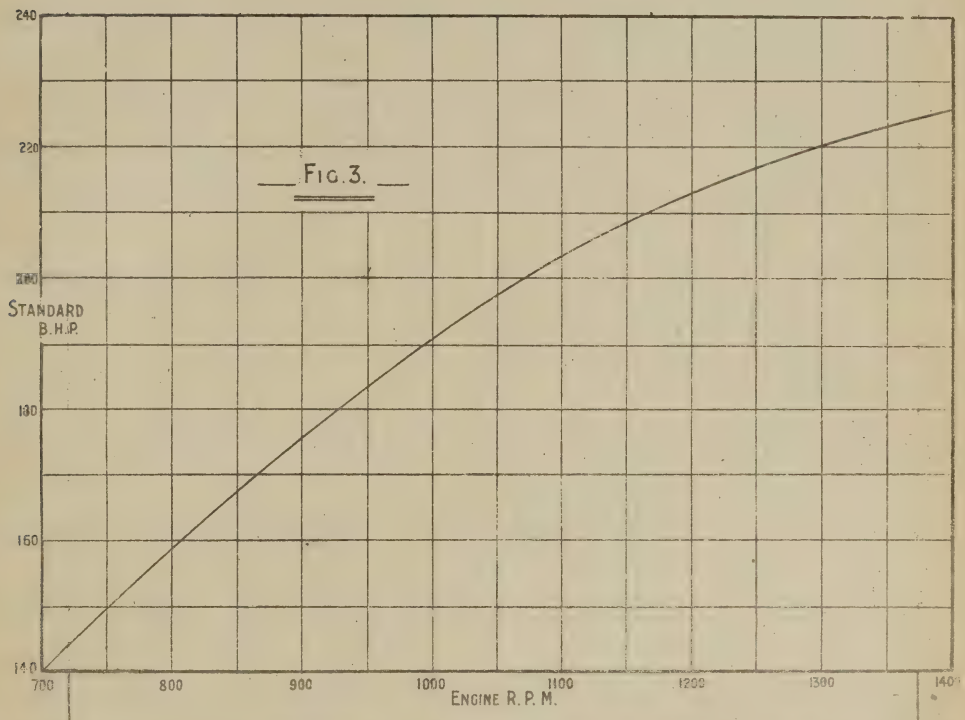
240
220
200
180
160
140
STANDARD B.H.P.
700
800
900
1000
1100
1200
1300
ENGINE R.P.M.

FIG. 3.

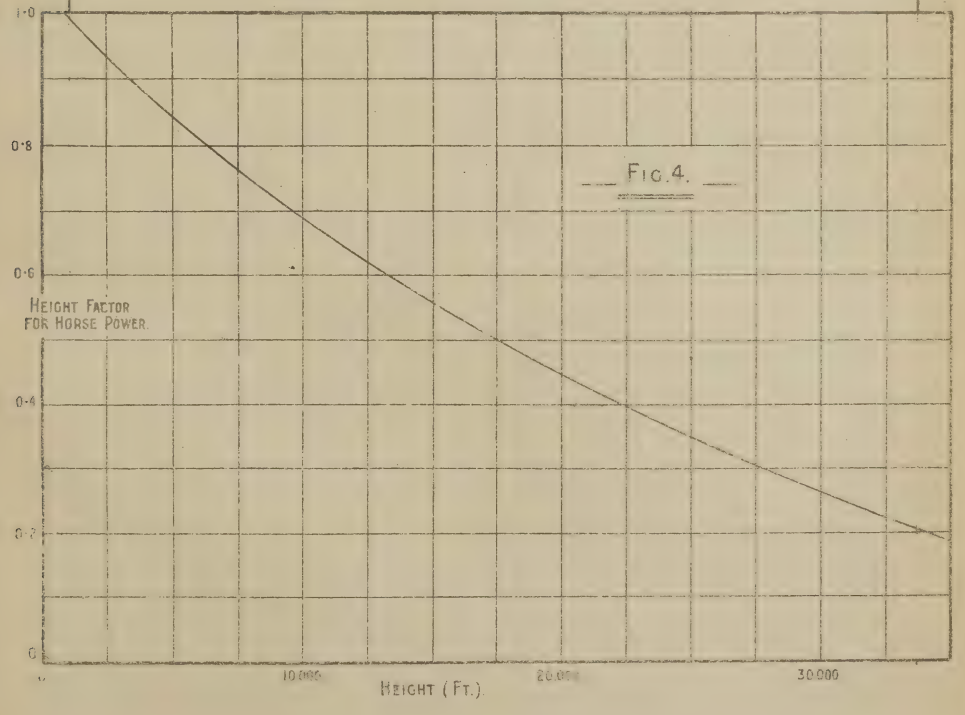
1·0
0·8
0·6
0·4
0·2
0
HEIGHT FACTOR FOR HORSE POWER.
10,000
20,000
30,000
HEIGHT (FT.)

FIG. 4.

RELATIVE DENSITY OF STANDARD ATMOSPHERE.

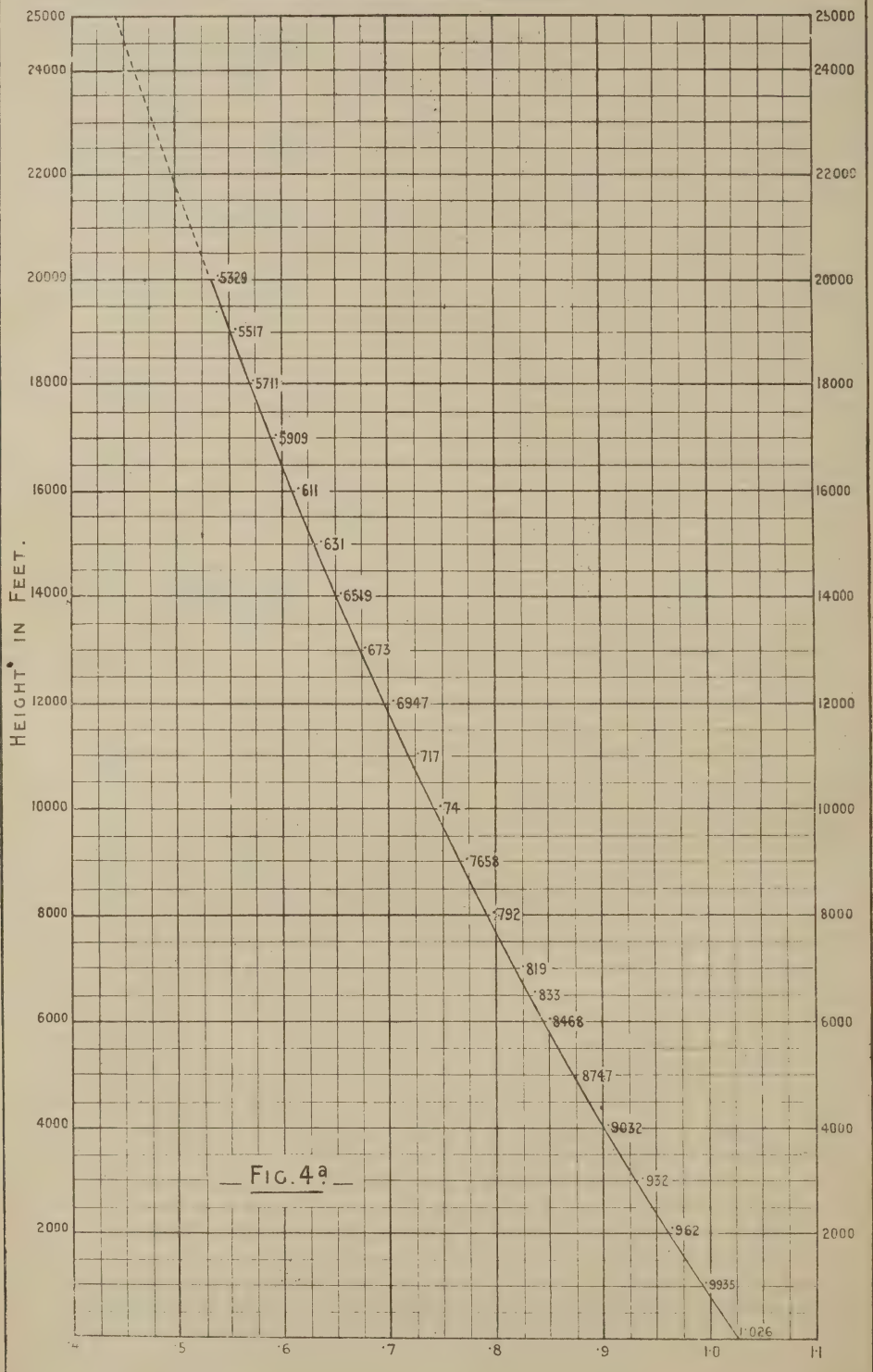

FIG. 4ª

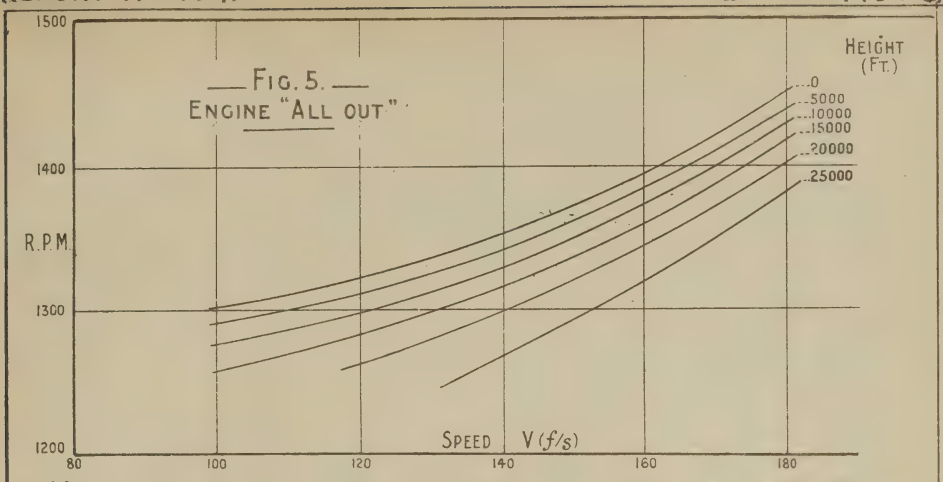

FIG. 5.
ENGINE "ALL OUT"

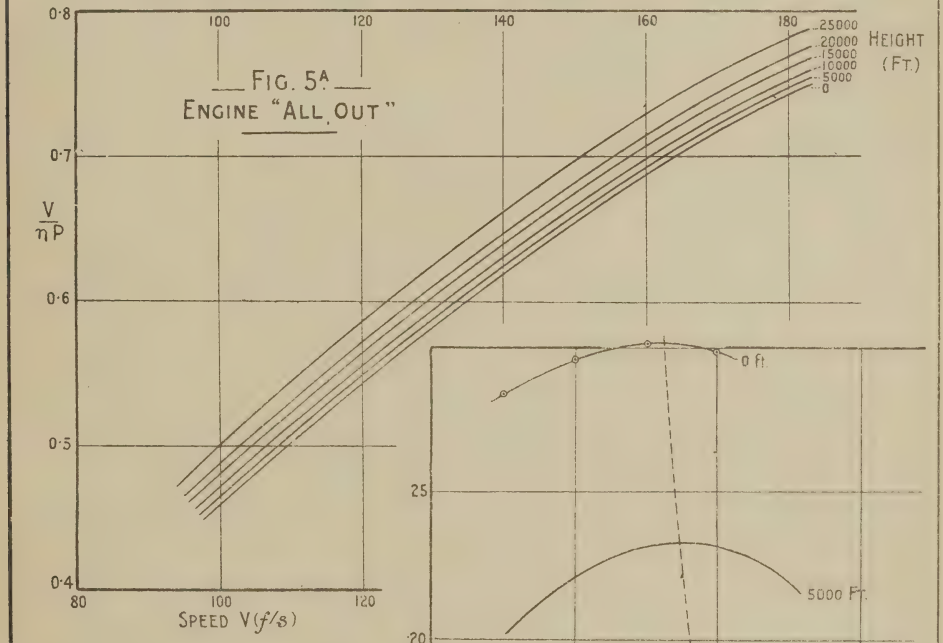

FIG. 5A
ENGINE "ALL OUT"

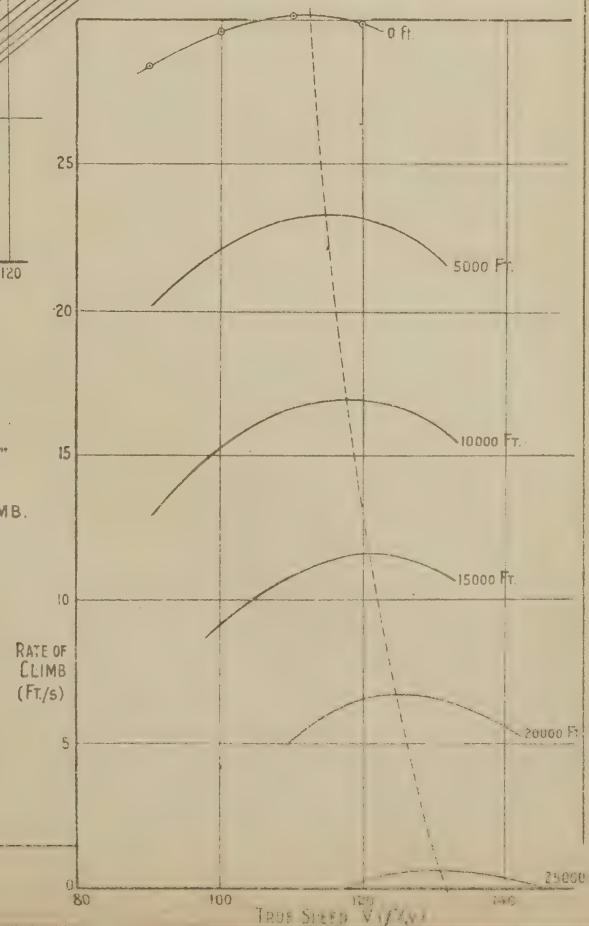

FIG. 6.
ENGINE "ALL OUT"
CALCULATION OF
MAXIMUM RATE OF CLIMB.

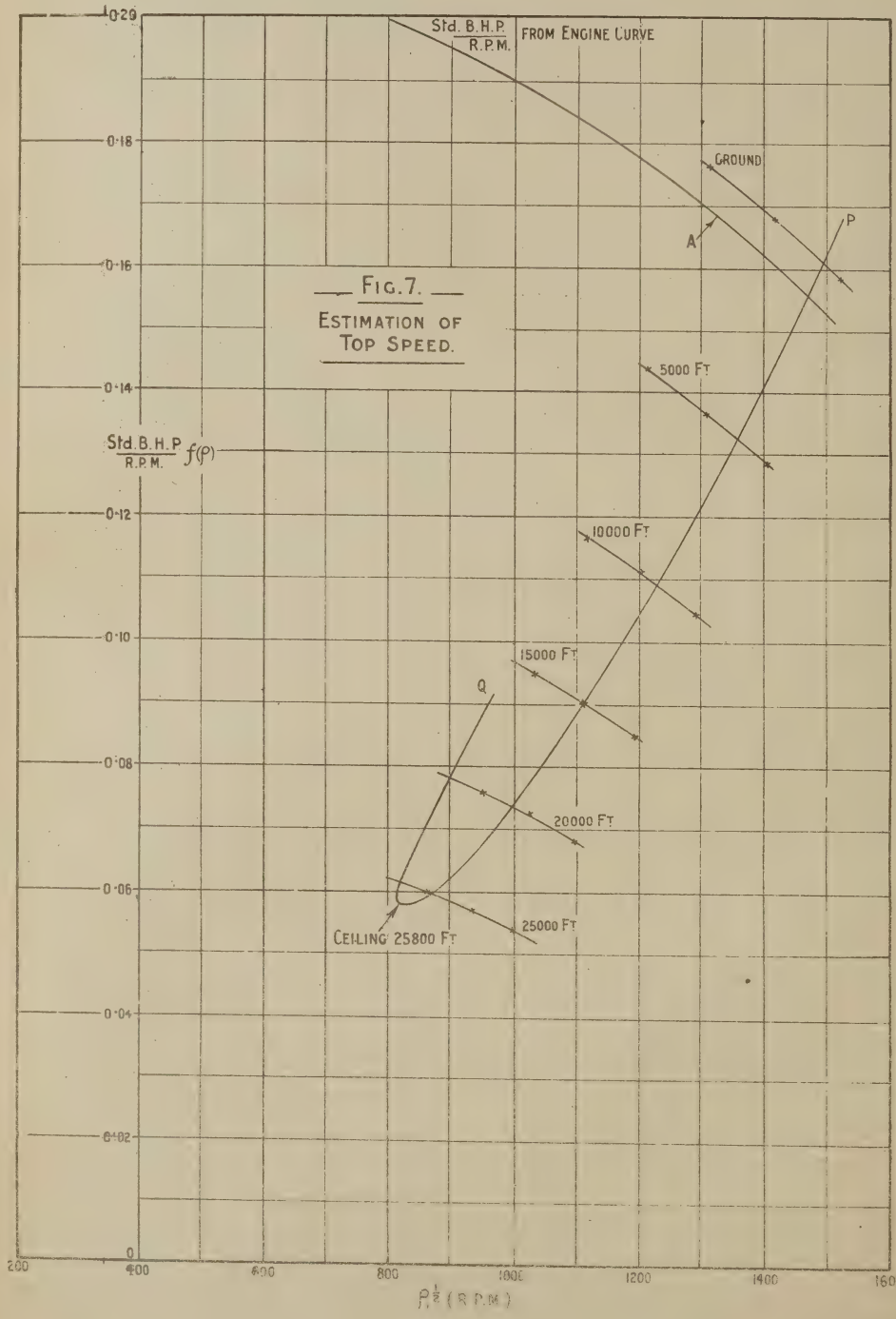

FIG. 7.

ESTIMATION OF TOP SPEED.

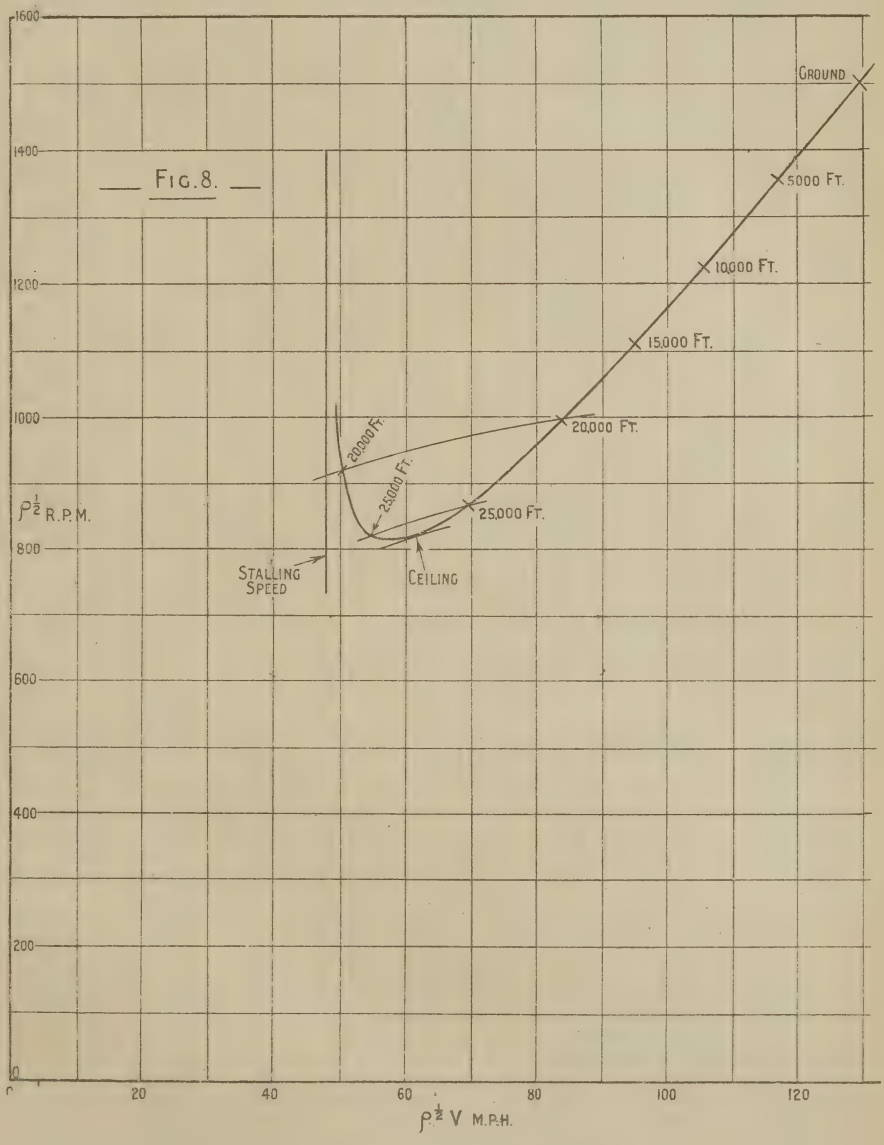
FIG. 8.
GROUND
5000 FT.
10,000 FT.
15,000 FT.
20,000 FT.
25,000 FT.
20,000 FT.
25,000 FT.
STALLING SPEED
CEILING
$\rho^{\frac{1}{2}}$ R.P.M.
$\rho^{\frac{1}{2}}$ V M.P.H.
1600
1400
1200
1000
800
600
400
200
0
20
40
60
80
100
120

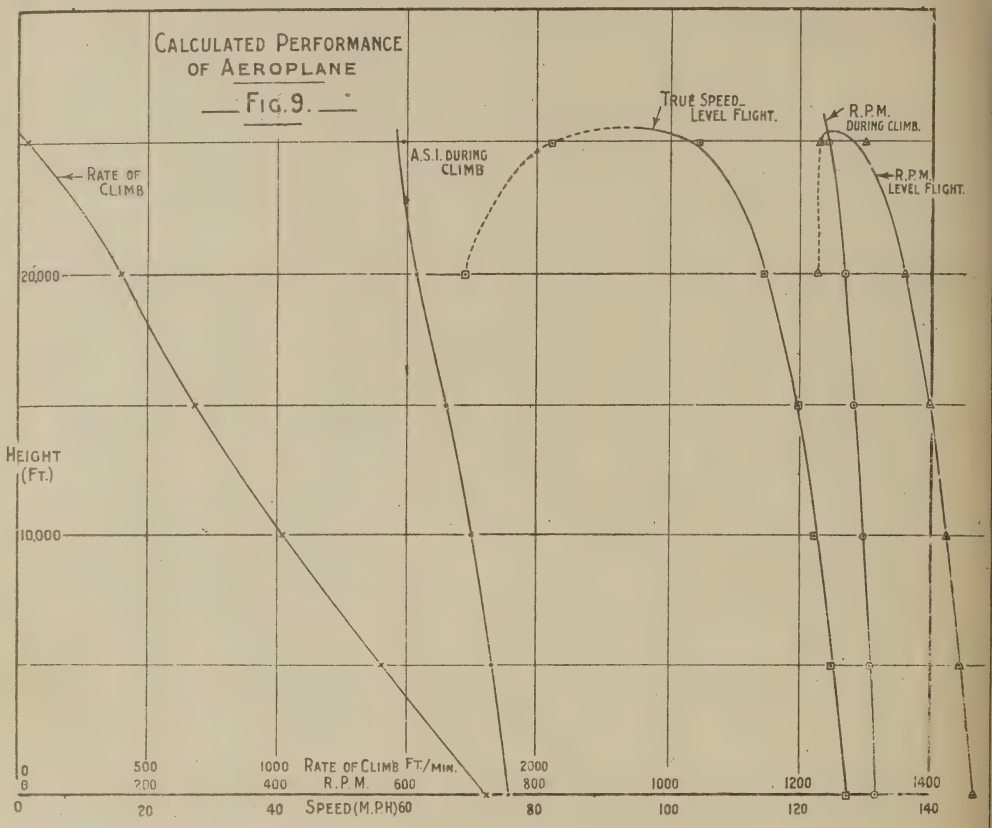
CALCULATED PERFORMANCE OF AEROPLANE
FIG. 9.
RATE OF CLIMB
A.S.I. DURING CLIMB
TRUE SPEED LEVEL FLIGHT.
R.P.M. DURING CLIMB.
R.P.M. LEVEL FLIGHT.
HEIGHT (FT.)
20,000
10,000
0
500
1000
RATE OF CLIMB FT./MIN.
2000
0
200
400
R.P.M.
600
800
1000
1200
1400
0
20
40
SPEED (M.P.H.) 60
80
100
120
140

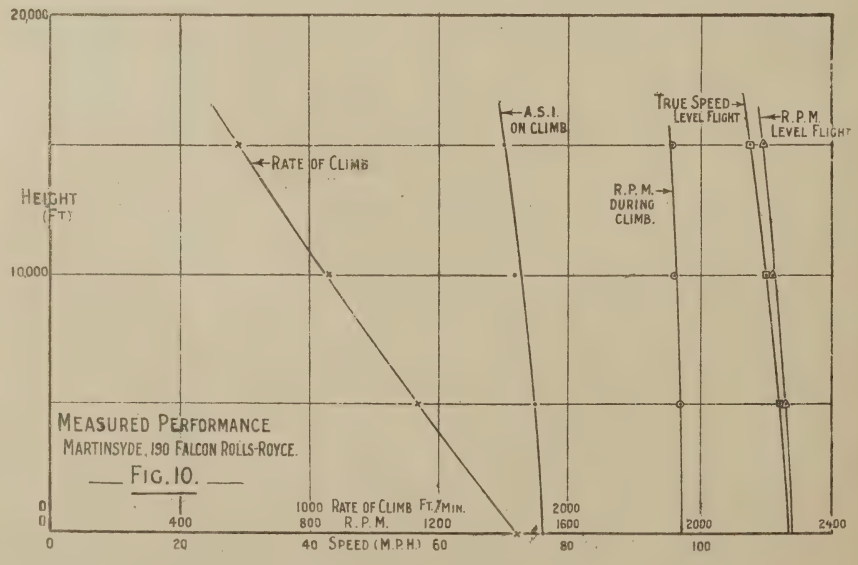
20,000
10,000
HEIGHT (FT.)
RATE OF CLIMB
A.S.I. ON CLIMB
TRUE SPEED LEVEL FLIGHT
R.P.M. LEVEL FLIGHT
R.P.M. DURING CLIMB.
MEASURED PERFORMANCE
MARTINSYDE. 190 FALCON ROLLS-ROYCE.
FIG. 10.
0
1000
RATE OF CLIMB FT./MIN.
2000
0
400
800
R.P.M.
1200
1600
2000
2400
0
20
40
SPEED (M.P.H.) 60
80
100

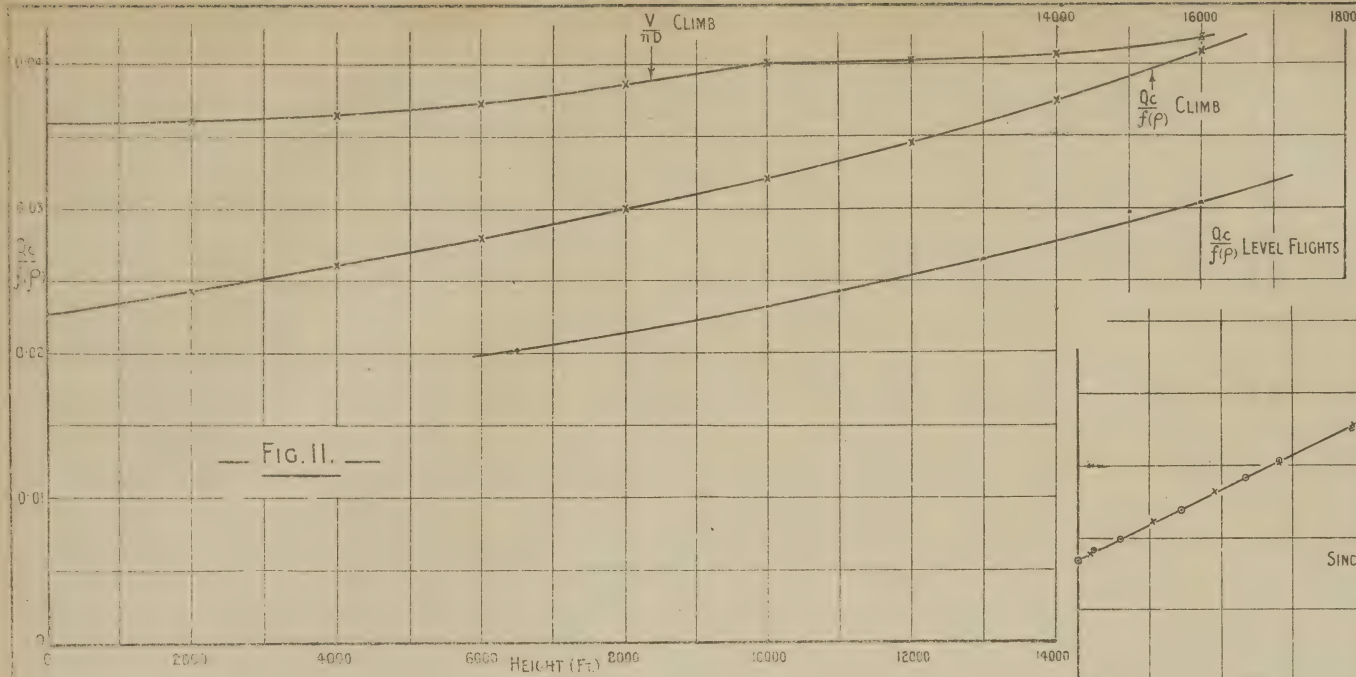

FIG. 11.

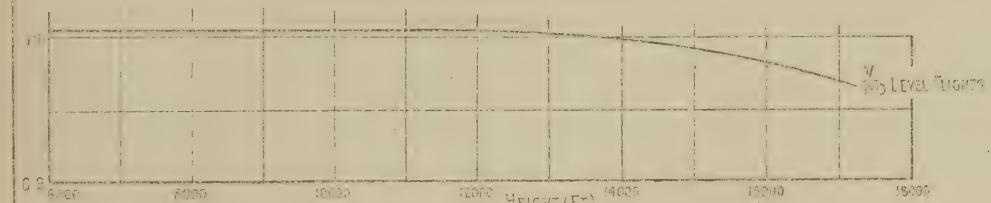

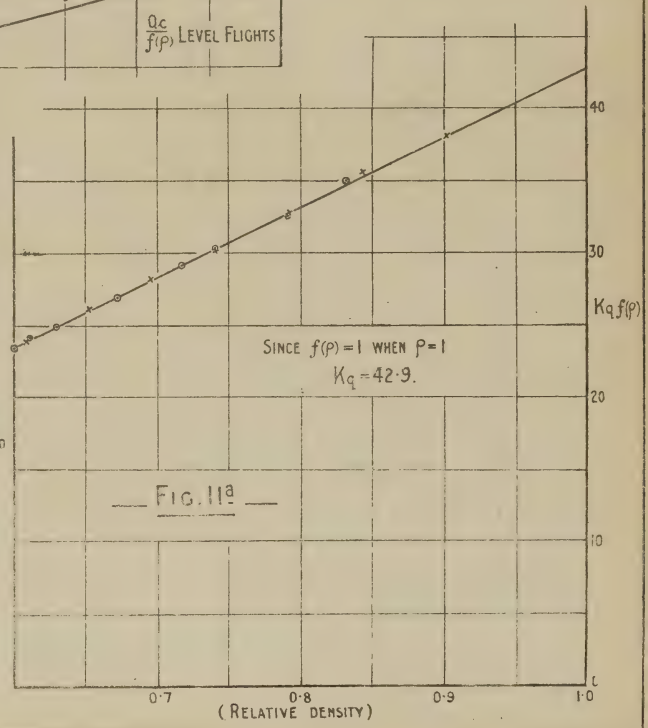

FIG. 11a.

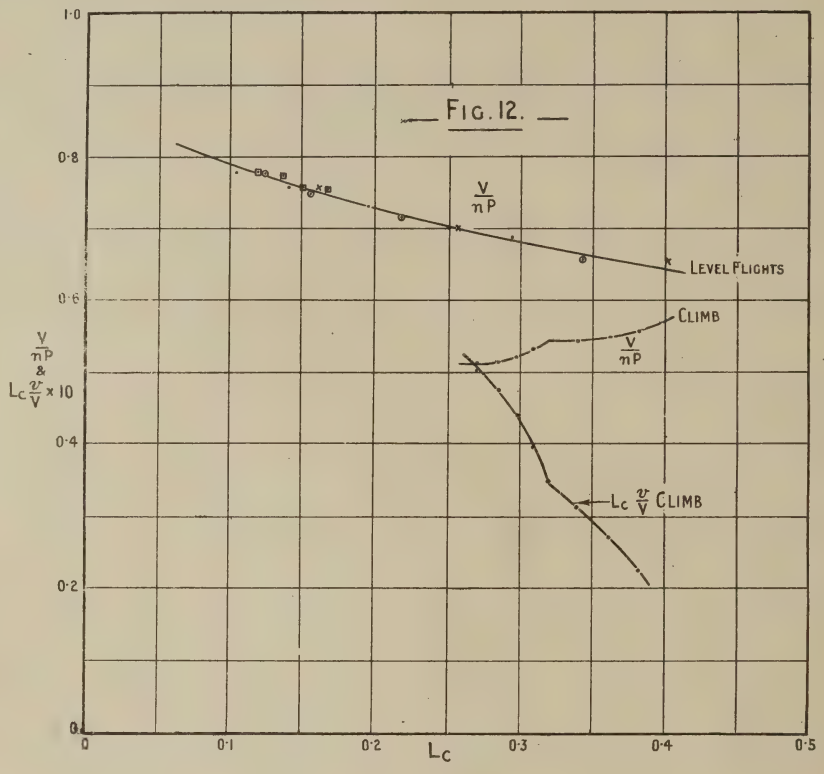
FIG. 12.
1·0
0·8
0·6
0·4
0·2
0
0·1
0·2
0·3
0·4
0·5
Lc
V/nP & Lc v/V x 10
V/nP
LEVEL FLIGHTS
CLIMB
V/nP
Lc v/V CLIMB

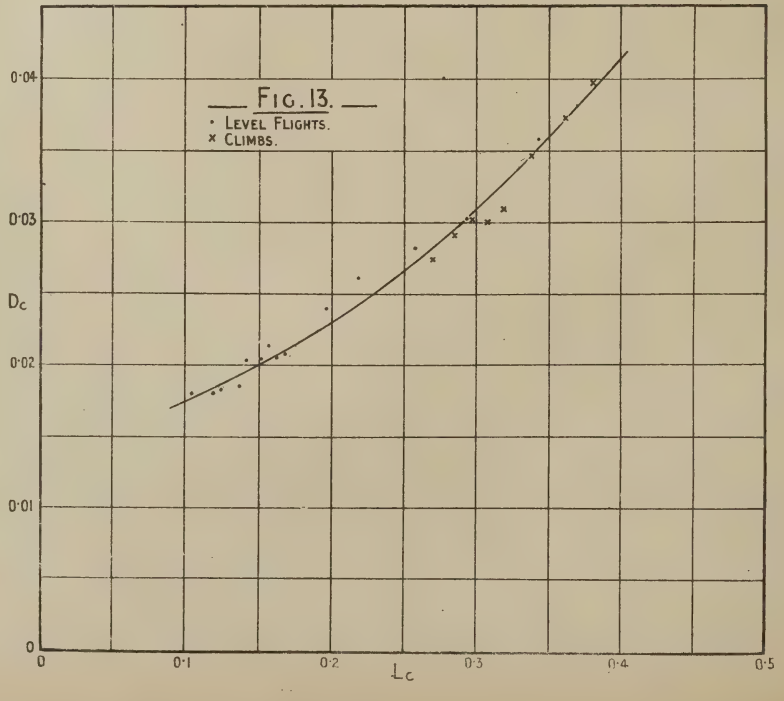
FIG. 13.
· LEVEL FLIGHTS.
× CLIMBS.
0·04
0·03
0·02
0·01
0
Dc
0
0·1
0·2
0·3
0·4
0·5
Lc

FIG. 14.

LIFT & DRAG COEFFICIENTS OF DEH4, 275 ROLLS.

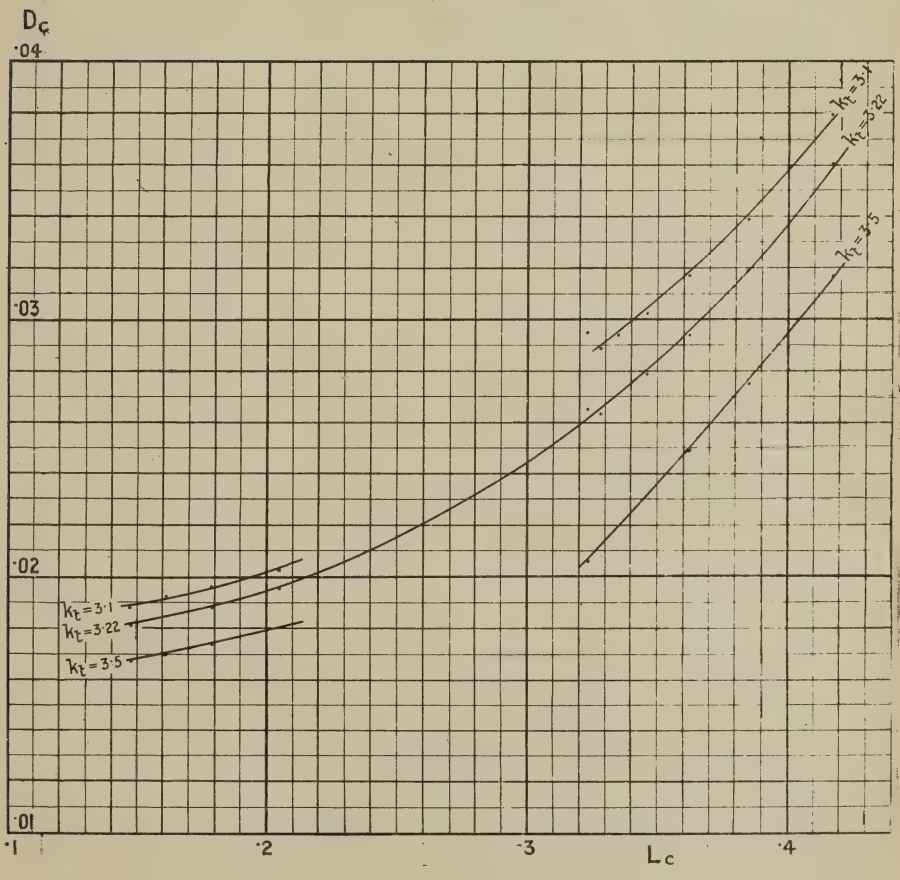

GENERAL RELATIONS BETWEEN THRUST, TORQUE, AND EFFICIENCY OF A PROPELLER.

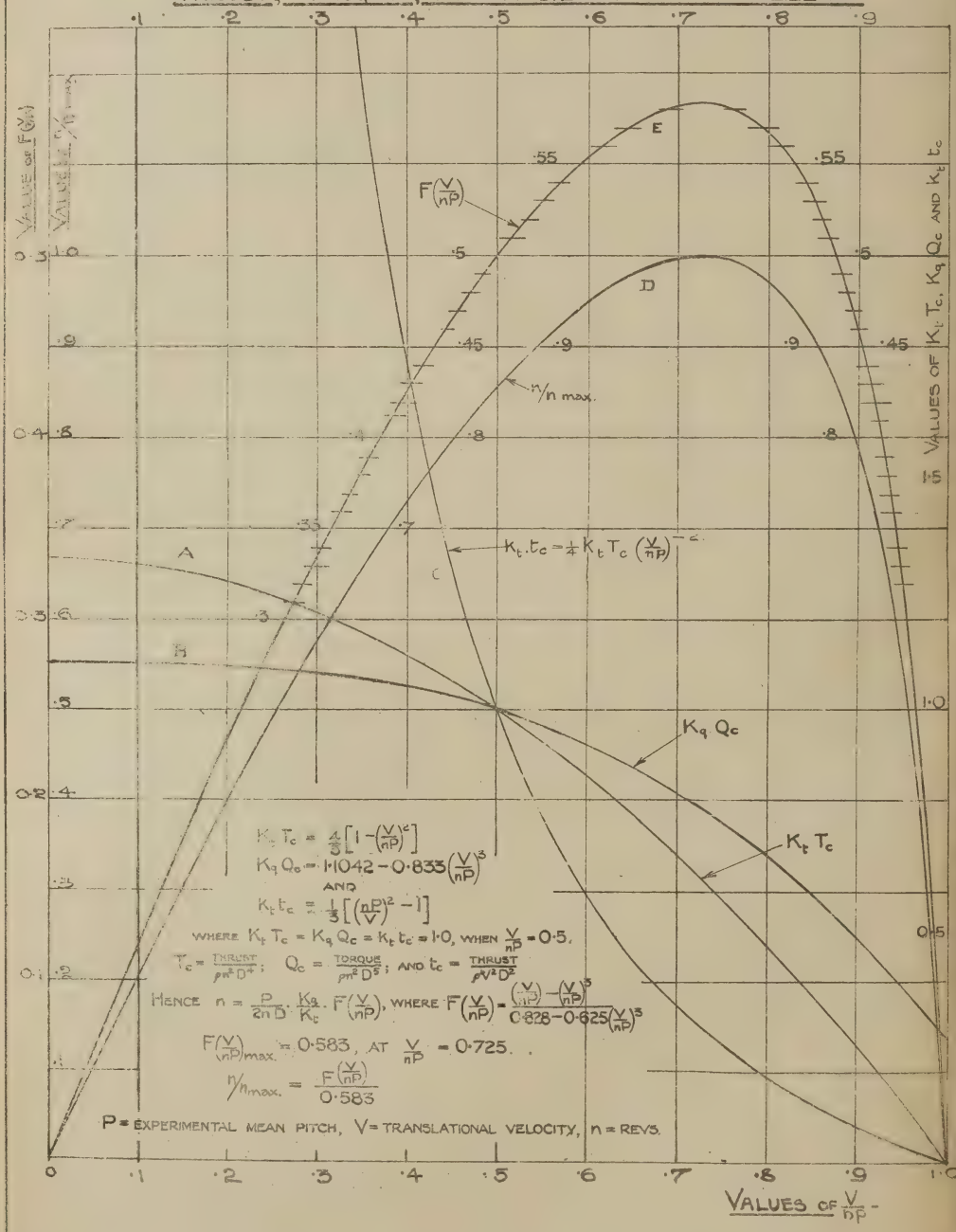

$$K_t T_c = \frac{4}{3}\left[1 - \left(\frac{V}{nP}\right)^c\right]$$

$$K_q Q_c = 1{\cdot}1042 - 0{\cdot}833\left(\frac{V}{nP}\right)^3$$

AND

$$K_t t_c = \frac{1}{3}\left[\left(\frac{nP}{V}\right)^2 - 1\right]$$

WHERE $K_t T_c = K_q Q_c = K_t t_c = 1{\cdot}0$, WHEN $\frac{V}{nP} = 0{\cdot}5$.

$T_c = \frac{\text{THRUST}}{\rho n^2 D^4}$; $Q_c = \frac{\text{TORQUE}}{\rho n^2 D^5}$; AND $t_c = \frac{\text{THRUST}}{\rho V^2 D^2}$

HENCE $n = \frac{P}{2\pi D} \cdot \frac{K_q}{K_t} \cdot F\left(\frac{V}{nP}\right)$, WHERE $F\left(\frac{V}{nP}\right) = \frac{\left(\frac{V}{nP}\right) - \left(\frac{V}{nP}\right)^3}{0{\cdot}828 - 0{\cdot}625\left(\frac{V}{nP}\right)^3}$

$F\left(\frac{V}{nP}\right)_{max.} = 0{\cdot}583$, AT $\frac{V}{nP} = 0{\cdot}725$.

$$\eta/\eta_{max.} = \frac{F\left(\frac{V}{nP}\right)}{0{\cdot}583}$$

P = EXPERIMENTAL MEAN PITCH, V = TRANSLATIONAL VELOCITY, n = REVS.

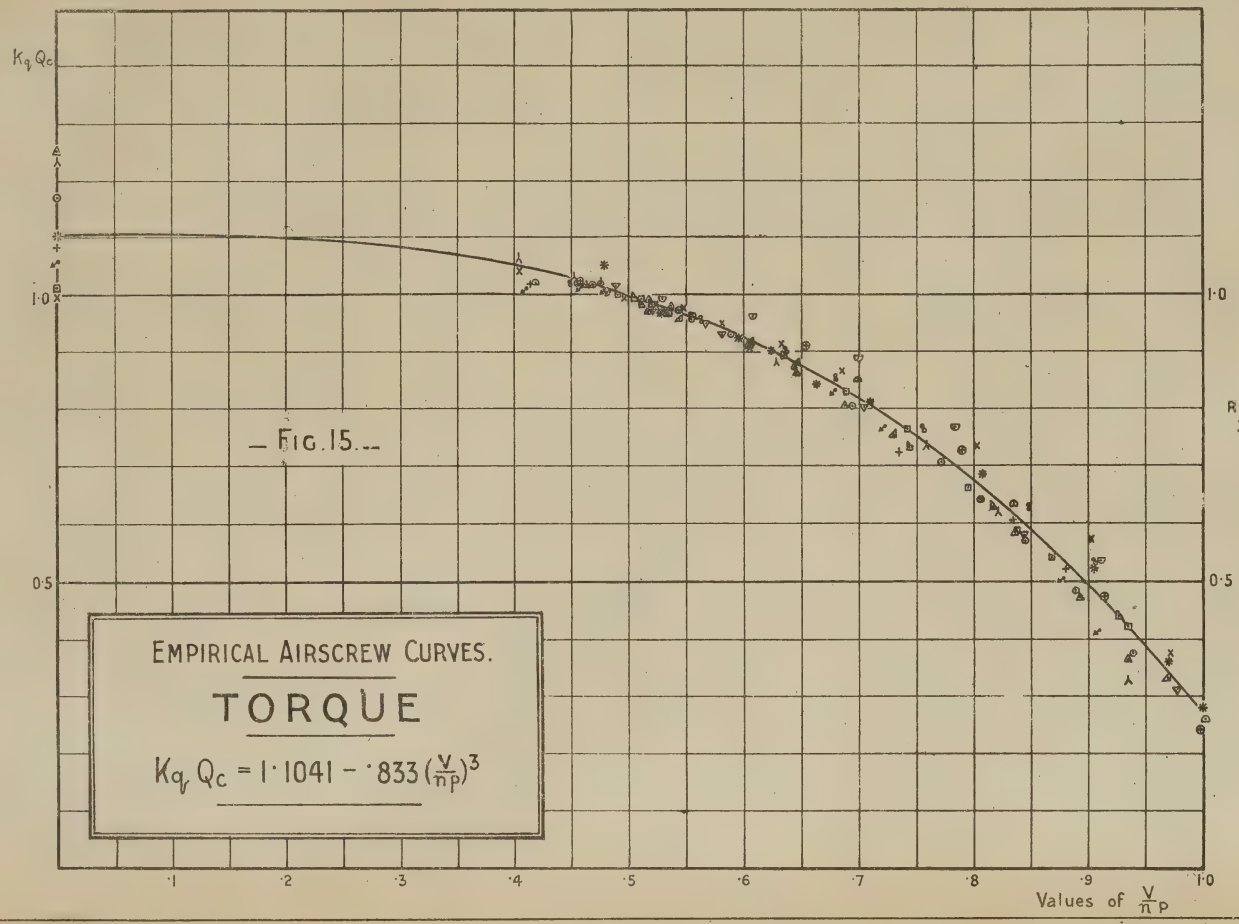

— FIG. 15. —

Δ — T.275. R.A.F.I.
⊙ — R & M.264 (i) T5291.
▲ — " T. 7143.
⊡ — " T. 5014.
↗ — T.491. FLAP AT +3°.
+ — R & M.264 (ii) T28024.
× — " T. 28033.
✱ — T.464. No1 for R.E.5.

R & M. 316.
- ◺ — A. No1.
- ◿ — A. No2.
- ▽ — A. 1 & 2, (4 BLADER).
- ⊡ — B. No1.
- ⊙ — B. No2.
- ⊕ — B. 1 & 2.

8 — R & M. 344 T. 4966.

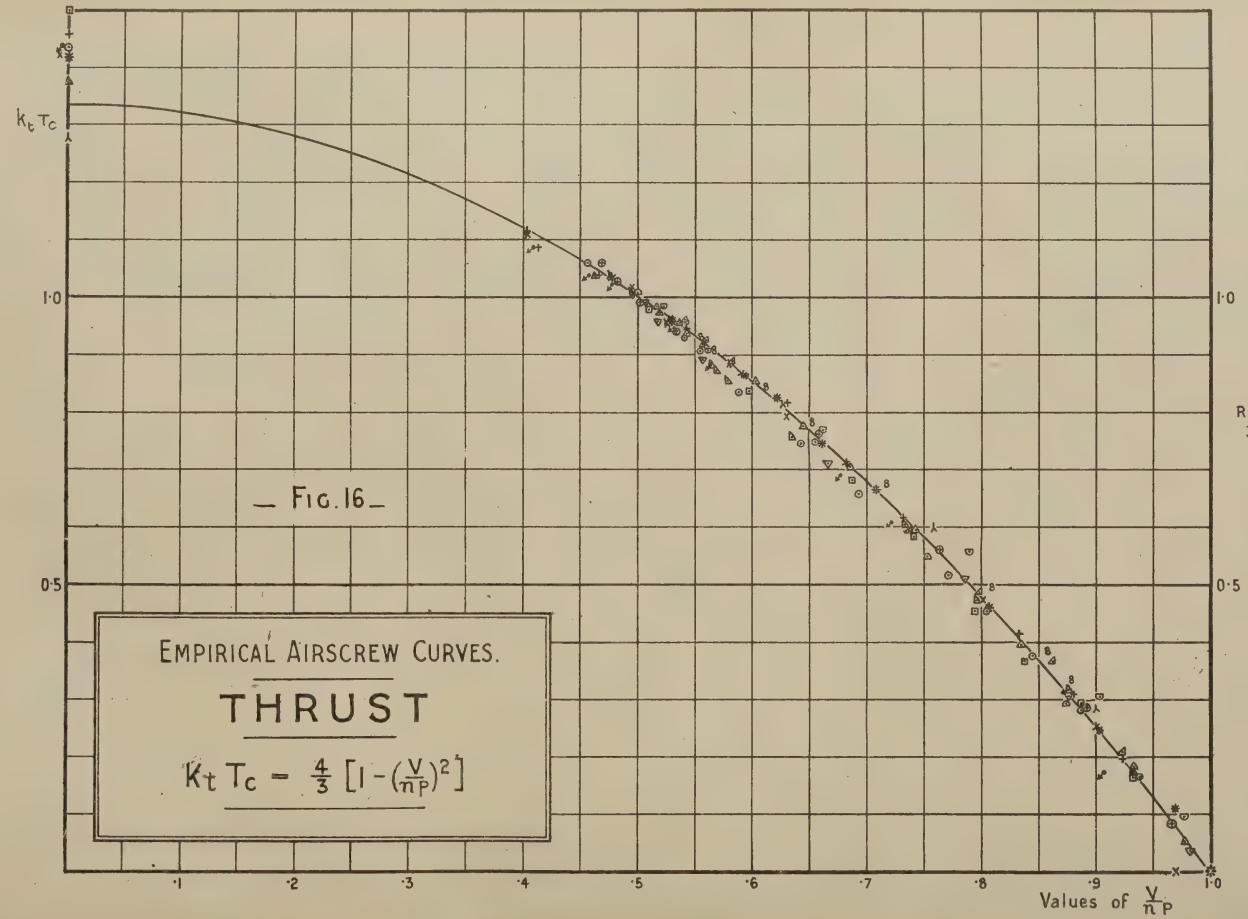

— FIG. 16 —

EMPIRICAL AIRSCREW CURVES.

THRUST

$$K_t T_c = \frac{4}{3}\left[1-\left(\frac{V}{nP}\right)^2\right]$$

λ — T.275. R.A.F.I.
⊙ — R & M.264.(i) T5291.
△ — " T. 7143.
⊡ — " T. 5014.
✓ — T.491. FLAP AT +3°.
\+ — R & M.264.(ii) T28024.
× — " T. 28033.
✱ — T.464. No1 for R.E.5.

R & M. 316.
- ◺ — A. No1.
- ◿ — A. No2.
- ▽ — A. 1 & 2. (4 BLADER).
- ⊙ — B. No1.
- ⊙ — B. No2.
- ⊕ — B. 1 & 2.

8 — R & M.344.T.4966.

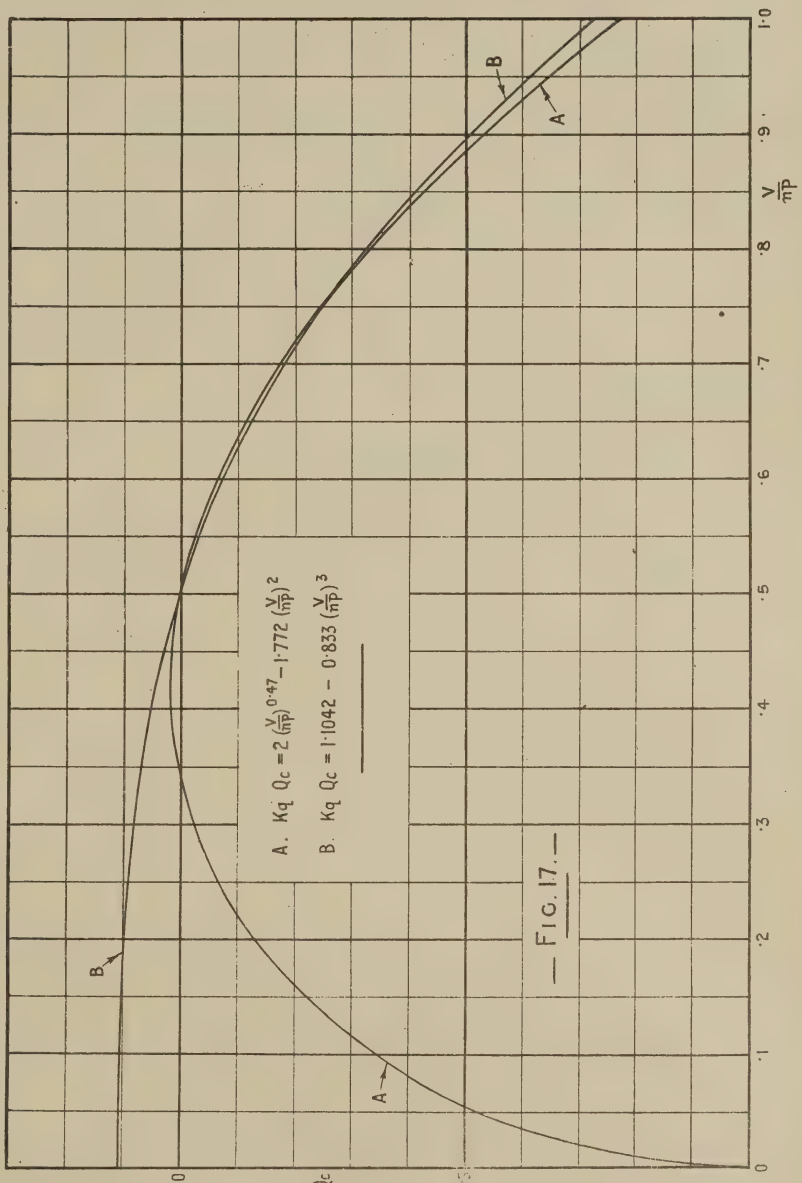
A. Kq Qc = 2 (V/mp)^0·47 − 1·772 (V/mp)^2
B. Kq Qc = 1·1042 − 0·833 (V/mp)^3
A
B
Kq Qc
V/mp
1·0
0·9
0·8
0·7
0·6
0·5
0·4
0·3
0·2
0·1
0

— FIG. 17. —

THE LIBRARY
OF THE
UNIVERSITY OF ILLINOIS

Interference and slip-stream effect.

Let D'_c = the drag coefficient of the parts of the aeroplane outside the slip-stream.

D_i = the drag coefficient of the parts of the aeroplane in the slip-stream, including the airscrew boss.

D_c = the drag coefficient of the aeroplane as a whole (including the airscrew boss) regarded as a glider.

V = the forward speed of the aeroplane in ft/sec.

v = the rate of climb in ft/sec.

A = the wing area in sq. feet.

T'_c = the thrust coefficient of the airscrew as modified by the presence of the aeroplane parts.

$\frac{R}{R_o}$ = the ratio of the resistance of the parts in the slip-stream to what the resistance of the same parts would be if there were no slip-stream.

Then, equating the airscrew thrust to the drag of the aeroplane, and the component of the weight along the airscrew axis, we obtain

$$T'_c \rho n^2 D^4 = D'_c \rho A V^2 + D_i \rho A V^2 \frac{R}{R_o} + L_c \rho A V^2 \frac{v}{V}$$

$$\text{or } T'_c \frac{n^2 D^4}{A V^2} = D'_c + D_i \frac{R}{R_o} + L_c \frac{v}{V}.$$

This reduces to

$$T'_c \left(\frac{nD}{V}\right)^2 \frac{D^2}{A} - D_i \left(\frac{R}{R_o} - 1\right) = D'_c + D_i + L_c \frac{v}{V} = D_c + L_c \frac{v}{V}$$

Hence

$$\left[T'_c - D_i \frac{A}{D^2} \left(\frac{R}{R_o} - 1\right) \left(\frac{V}{nD}\right)^2\right] \frac{D^2}{A} \left(\frac{nD}{V}\right)^2 = D_c + L_c \frac{v}{V}$$

Now (page 613), it has been shown that

$$t_c \cdot \frac{D^2}{A} = D_c + L_c \cdot \frac{v}{V} = T_c \left(\frac{nD}{V}\right)^2 \frac{D^2}{A}.$$

The quantity $\left[T'_c - D_i \frac{A}{D^2} \left(\frac{R}{R_o} - 1\right) \left(\frac{V}{nD}\right)^2\right]$, which we may call T''_c, can therefore be taken to be the thrust coefficient of the combination of the airscrew and aeroplane, for, when multiplied by $\rho D^4 n^2$, it gives the net thrust required to drive the aeroplane alone (including the airscrew boss), and $K_t \cdot T''_c$ can be calculated. This was done in the case of three of the N.P.L. tests on airscrew models with interference of bodies and wings (R. & M. 393, B.E. 2E body and wings; R. & M. 401, B.E. 2C body; R. & M. 305, F.E. 8 body with rotary engine), T'_c and R/R_o being

extracted from the reports, and T''_c calculated for several values of V/nD; The points so obtained lie closely on the curve $K_t \cdot T_c = \frac{4}{3}\left[1 - \left(\frac{V}{nP}\right)^3\right]$. particularly in the case of R. & M. 401, thus proving that the formula applies to airscrews in practice, so far as interference and slip-stream effects are concerned. The effect of these upon torque also appears to be negligible.

Scale-Speed Effect.—This was observed in the case of the airscrew tests described in R. & M. 390 and 393, and slight effects of the kind were noted at the N.P.L. in connection with two other model airscrews of $\frac{1}{6}$th scale (see R. and M. 390). As has been stated, the points calculated from R. and M. 393 lie reasonably well on the curve given by the formula, so that it may be expected that this relation will hold (even if there is a scale-speed effect) in passing from models to full-sized airscrews. This is confirmed by the results of tests made at the R.A.E. on five airscrews (on an S.E. 5 machine with 170 High Comp. Hispano-Suiza engine). $K_t \cdot T_c$ and $K_q \cdot Q_c$ were found from the data given for these five airscrews. Although the resulting points are somewhat scattered, as is to be expected in full-scale experiments, the mean curve through them is in good agreement with the formula for $K_t \cdot T_c$, but the $K_q Q_c$ curve lies somewhat higher than that from the formula for values of V/nP above 0·7.

THE DESIGN OF AEROPLANES FOR USE AT GREAT HEIGHTS.

By R. McK. Wood and H. L. Stevens.

Presented by the Superintendent, Royal Aircraft Factory.

Reports and Memoranda, No. 493.

Section (i). *General Design. April*, 1917.

Summary.—*Performance.*—A variable pitch airscrew or some other equivalent device would improve the climb at great heights and raise the ceiling while the top speed would not be appreciably reduced.

Weight is slightly more important in relation to resistance than at the ground unless climb alone is considered, when the reverse is the case. Taking climb and speed as of equal importance, then, for a typical aeroplane at the ground 1 lb. of resistance is equivalent to 5 lbs. of weight, and at 15,000 ft. to 4 lbs.

A preliminary investigation suggests that a fairly lightly loaded machine has advantages, but the problem of the " best " loading is very complicated, since it involves the characteristics of the engine and airscrew. This matter will form the subject of a further report, but from the work already done, it appears that no very radical alteration in present practice will be necessary.

Stability.—The " best margin " is so uncertain that the small effect of a change in density is negligible.

Controllability.—The radius of the smallest circle in which the machine can turn varies inversely as the density. For a given load factor the highest speed at which a turn in the smallest circle can be made varies inversely as the square root of the density. The same relation holds for the shortest time in which a turn can be made. It is doubtful how far these variations are of importance.

1. *General remarks.*—Any modification in the design of an aeroplane will in general affect more than one of its qualities. For the designer to be able to balance up the losses and the gains accurately, he must be able to express them all in commensurable units. Unfortunately, this is very seldom possible, and the real decision has to be made simply by estimation. For example, it is practically impossible to say whether a saving of 50 per cent. in the time taken to dismantle and re-assemble some component outweighs a loss of 10 ft. per min. climb. This is, however, a very common type of problem.

Even when it is easier to compare the change there is still uncertainty on account of lack of knowledge of what constitutes a gain or loss. For example, the margin of stability allowed is arbitrary and may apparently be varied 50 per cent. without appreciable effect on the aeroplane's qualities. It is evident, therefore, that the effect of a change in air density—unless very large—will generally be swamped in uncertainties of this nature. For this reason, with the exception of the variable pitch airscrew, this report does not suggest any innovation.

2. *Performance.*—In the calculations which follow, R.E.8 has been taken as the type machine, the weight being reduced slightly in order to raise the calculated ceiling to 18,000 ft. under normal conditions. It has been assumed throughout that engine torque varies as (density) $^{1.1}$. It is probable that even if a blower or equivalent device is used to make the torque roughly independent of density up to say 10,000 ft., above this height this law will hold approximately. The use of the index 1·1 is justified by experiments at the R.A.F. on engines without any form of carburetter adjustment.

In predicting the performance of R.E.8, the curves of torque, revs. per second and efficiency, against advance per rev. for airscrew T.6296 as obtained on the whirling arm and the curve of horse power against revs. per minute for the R.A.F.4A engine from test figures, have been used. The process of calculation is as follows :—A particular value of the engine revs. is chosen, the corresponding h.p. found from the engine curve, corrected for density, and Q/N^2 calculated. The corresponding figure for the airscrew is then found by correcting for the gearing and for air density. From this the airscrew curve gives the advance per rev. and the efficiency, and, therefore, the true speed, indicated speed, and thrust horse power. Curves are then plotted of h.p. available, against indicated speed at different heights. Corresponding curves of h.p. required to fly are also plotted. From the intersections of these calculated curves and the length of the maximum ordinate intercepted between them, the top speed and maximum rate of climb at any height can be predicted.

These results are exhibited in the form of curves giving the speed at any height, the best climbing speed (indicated) and the maximum rate of climb at that height. This last curve is a straight line, and the point where it cuts the axis of height gives the ceiling, which is at about 18,000 ft.

3. It will be seen that if the engine revs. could be kept up at low air speeds without a great loss of efficiency in the airscrew the rate of climb and the ceiling would be raised. At the same time the engine must not be allowed to race at top speed, and may have to be throttled to prevent this. Any loss of speed resulting from this cause must be debited against the modification.

Four methods were considered :

(1) Cutting down the blade area of the airscrew.

(2) Reducing the pitch of the airscrew.

(3) Using a variable pitch airscrew.

(4) Using a two-speed gear.

(1) *Cutting down the blade area of the airscrew.*—This, if carried at all far, involves throttling the engine at high speeds, with consequent loss of top speed. It will be seen from Fig. 2 that very little is to be gained by this method as the throttled portion of the curve is very steep and the loss in speed consequently great. A slight improvement, however, is possible if the engine is not already giving its maximum revs. at top speed. This is the case in Fig. 2, which is drawn for 15,000 ft., 2,000 revs. per minute being taken as the maximum which the engine must not exceed. In this case a blade area 0·85 of the actual would be best. The curves for different blade areas were obtained by taking the curves of T/N^2 and Q/N^2 against V/N for the airscrew, and multiplying the ordinates by the ratio of the blade areas. The efficiency curve was considered to be unaltered.

(2) *Reducing the pitch of the airscrew.*—The effect was tried of reducing the pitch of the airscrew 25 per cent. and increasing the blade area so that maximum revs. were obtained at about top speed without having to throttle the engine. It will be seen from Fig. 3 that a substantial gain in climb would be obtained at 15,000 ft. without loss of speed. The speed at the ground is reduced by about 10 m.p.h., as the engine would have to be throttled. The effect of change of pitch on the characteristics of the airscrew was deduced from an examination of all the tests of airscrews of different pitch done both at the R.A.F. and at the National Physical Laboratory.

(3) *Variable pitch screw.*—Calculations, using the ordinary theory, were made and indicated that an airscrew could be designed which, while allowing the engine to give full revs. at all air speeds would only drop about 4 per cent. in efficiency in a range of values of V/N from top speed to climbing at 15,000 ft. Fig. 4 gives the horse power curves calculated for this airscrew. The airscrew is assumed always to be adjusted so that the revs. are 2,000. Figs. 5 and 6 show the best climbing speed and the rate of climb at various heights with the ordinary screw and the variable pitch screw. The ceiling is raised about 3,500 ft., and the rate of climb increased 200 ft/min. at 15,000 ft. and 400 ft/min. at the ground. The top speed is not appreciably changed. The extra weight of the airscrew and the extra resistance (to provide the increased cooling required) will not reduce the gain very materially.

(4) *Two-speed gear.*—The mechanical difficulties in the way of this system are very great. Accordingly, it was not considered in detail. It appeared likely that about 15 h.p. could be gained for climbing at 15,000 ft. with a loss of about 3 h.p. at top speed due to the blades having to be increased in area to keep the engine revs. down to 2,000 at top speed.

4. It is evident that the variable pitch airscrew presents the most possibilities. It has, moreover, one very great subsidiary advantage. It is necessary that an aeroplane should be able to dive very steeply in fighting. With the present arrangement this often involves excessive engine revs. and excessive speeds. If a variable pitch airscrew were used, the revs. could be controlled easily and, moreover, if required, the airscrew could be used as a brake to any desired extent, making it possible to dive the machine at any angle and at practically any speed.

5. The relative importance of head resistance and weight for ground level was discussed in Report R. & M. 217. Fig. 7 gives the curves obtained, plotted as in that report. The machine taken is R.E.8, using the variable pitch airscrew at the ground and at 15,000 ft. It will be seen that weight becomes more important with regard to resistance at great heights unless climb is considered to be about twice as valuable as speed (*i.e.*, unless a gain of 1 per cent. in rate of climb is considered to be worth a loss of 2 per cent. in top speed).

6. *Stability.*—No thoroughly satisfactory criterion of stability has been found. It is usual to estimate the stability by calculating first the period of the ordinary "phugoid" oscillation, and, secondly, the range of movement of centre of gravity before instability sets in. Using the notation of R. & M. 324, these are given by

$$\text{period} = 0{\cdot}202\, U\sqrt{1 + \rho Q} \text{ approximately.}$$

range $= m =$ function of ρU^2 only, except for second order effect.

where U = true speed,

and Q = a function ρU^2 only, and is of the order of 2 for a very stable machine, and increases as the stability gets worse.

Hence, *at the same indicated speed* the period increases by about one-sixth of the percentage decrease in ρ for a very stable machine, and hardly at all for a very unstable one. m is unaffected.

Now a 10 per cent. increase in period produces no appreciable change in the aeroplane from the flying point of view, and it is safe to say that there is no need to cater specially for aeroplanes which have to fly mostly at low densities.

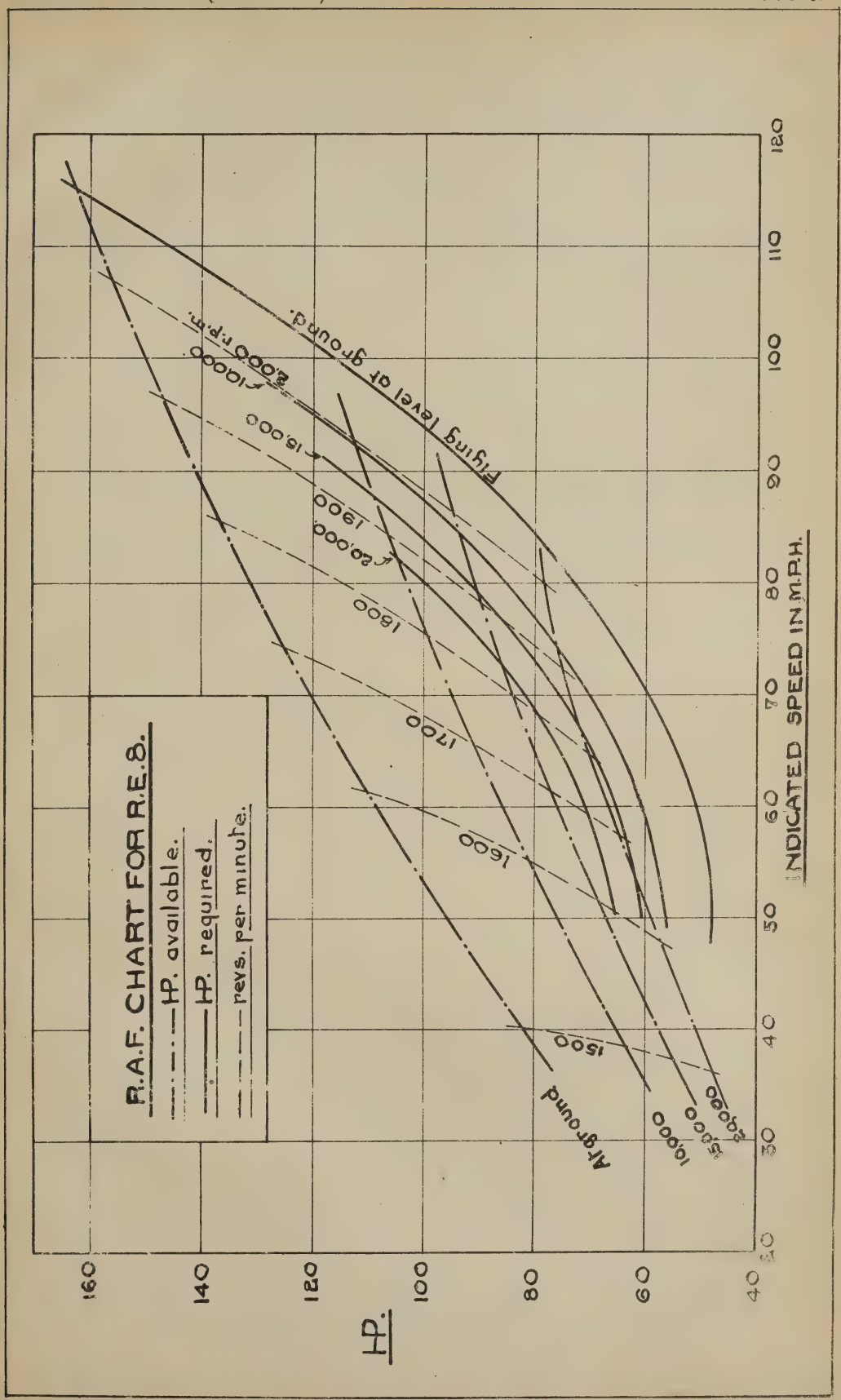
R.A.F. CHART FOR R.E.8.
H.P. available.
H.P. required.
revs. per minute.
H.P.
INDICATED SPEED IN M.P.H.
Flying level at ground.
Ground
5,000
10,000
15,000
20,000
1500
1600
1700
1800
1900
2000 r.p.m.

FIG. 2.

EFFECT OF REDUCING THE BLADE AREA OF THE SCREW ON T.H.P. AVAILABLE AT 15,000 FT.

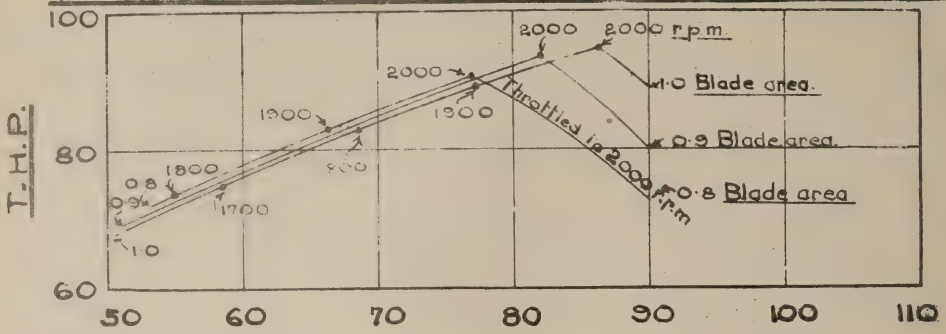

INDICATED SPEED IN M.P.H.

FIG. 3.

EFFECT OF REDUCING THE PITCH OF THE SCREW ON T.H.P. AVAILABLE.

NOTE. The blade area has been increased so that the engine revs are 2,000 r.p.m. at an indicated speed of 80 m.p.h. at 1500 FT.

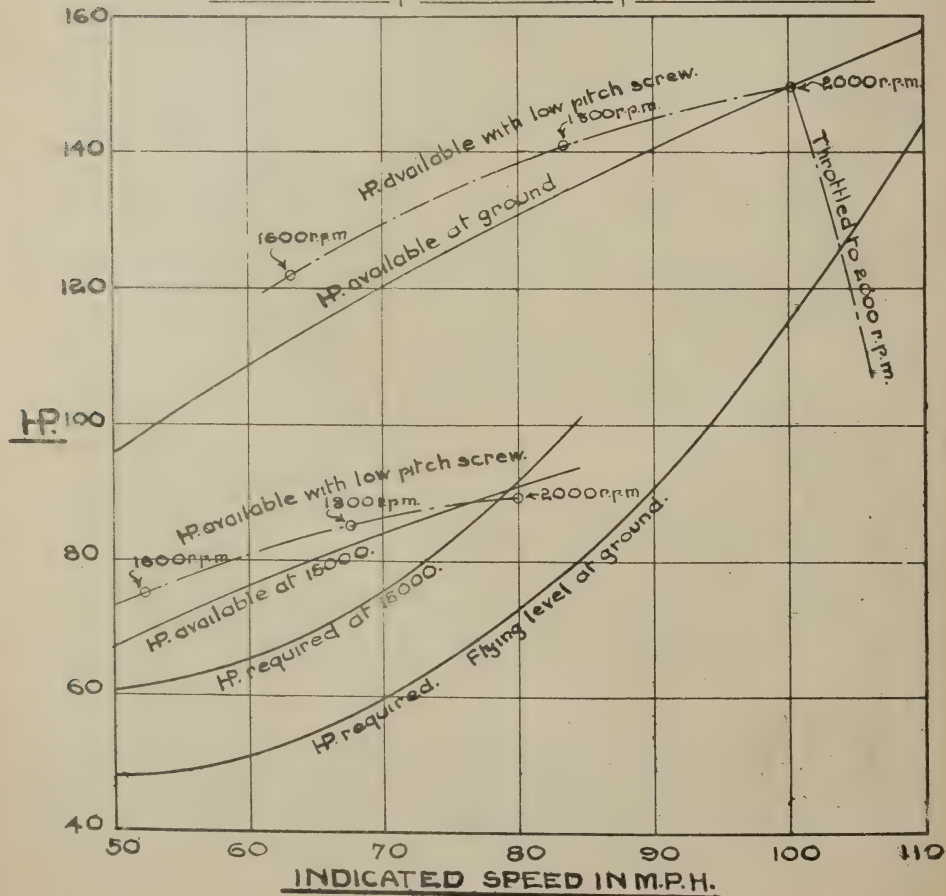

INDICATED SPEED IN M.P.H.

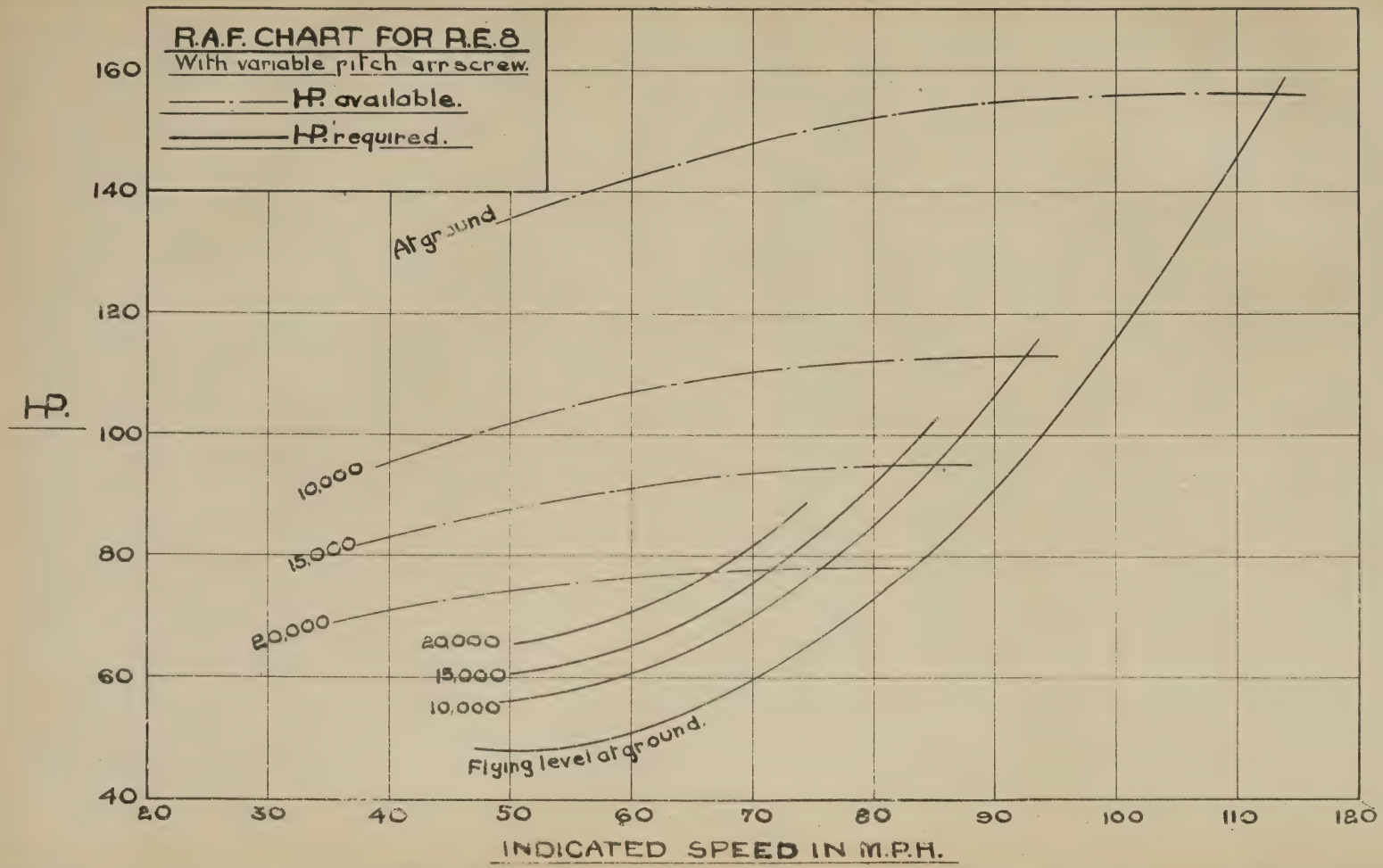
R.A.F. CHART FOR R.E.8
With variable pitch airscrew.
H.P. available.
H.P. required.
At ground
10,000
15,000
20,000
20,000
15,000
10,000
Flying level at ground.
H.P.
160
140
120
100
80
60
40
20
30
40
50
60
70
80
90
100
110
120
INDICATED SPEED IN M.P.H.

THE LIBRARY
OF THE
UNIVERSITY OF ILLINOIS

FIG. 5.

BEST CLIMBING SPEED FOR R.E. 8 AT VARIOUS HEIGHTS.

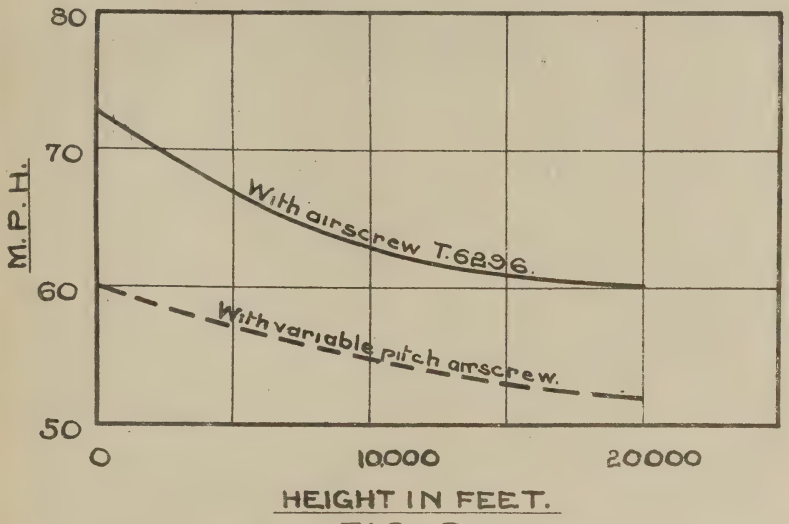

FIG. 6.

MAXIMUM RATE OF CLIMB FOR R.E. 8 AT VARIOUS HEIGHTS.

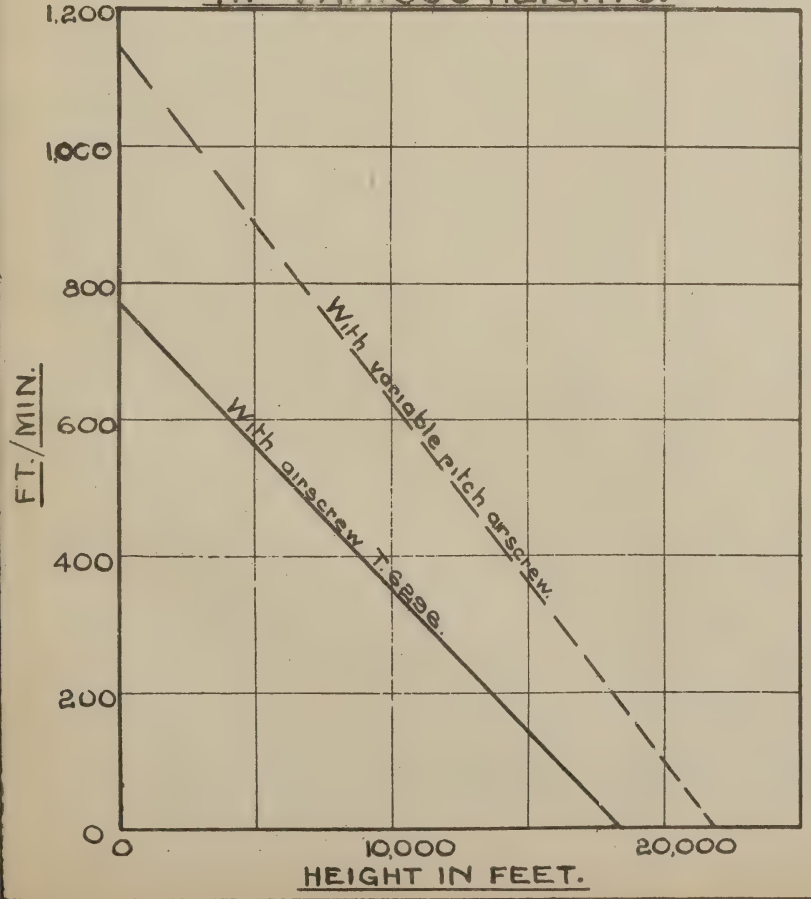

THE LIBRARY
OF THE
UNIVERSITY OF ILLINOIS

RELATIVE IMPORTANCE OF HEAD RESISTANCE AND WEIGHT FOR BEST PERFORMANCE OF R.E.8 AT THE GROUND AND AT 15,000 FEET WITH VARIABLE PITCH AIRSCREW.

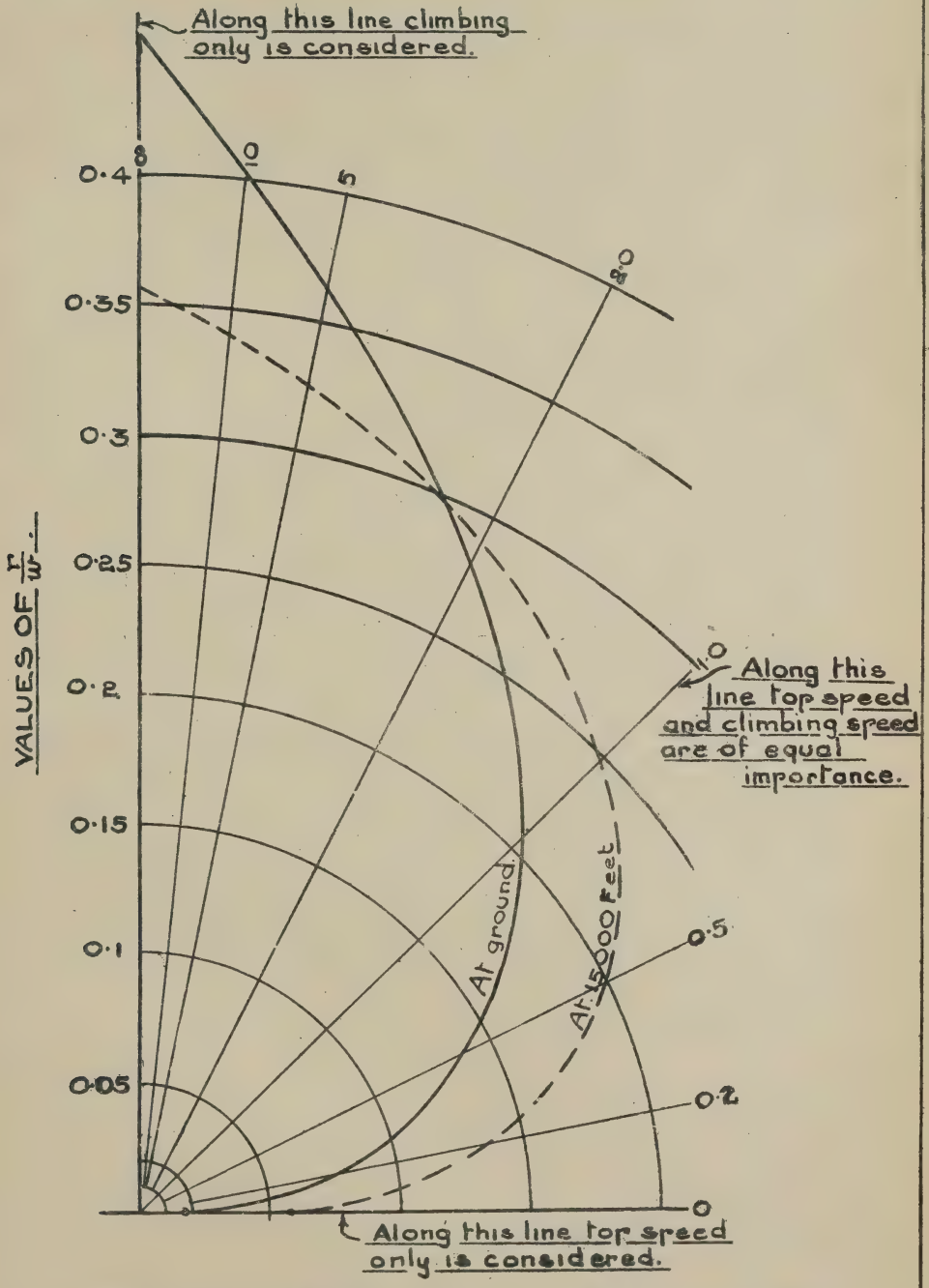

The figures 0, 0·1, 0·2, ... to ∞ on the radial lines show the relative importance of climbing speed to top speed.

THE LIBRARY
OF THE
UNIVERSITY OF ILLINOIS

7. *Controllability.*—The criteria for good controllability are rather less certain than those for stability. We have

(1) *Radius* (r) *of smallest circle.*

$$r = \frac{V_s^2}{\rho g}$$

where V_s is the stalling speed at ground level.

(2) *Highest speed* (V) *in smallest circle.*—For a load factor n

$$V = \frac{V_s \sqrt{n}}{\sqrt{\rho}}$$

(3) *Shortest time* (T) *in smallest circle.*

$$T = \frac{2\pi V_s}{g\sqrt{\rho n}}$$

Hence r, V and T all increase as ρ decreases.

The indicated speed corresponding to V (being of course $\sqrt{\rho}V$) is evidently unaffected.

The smallest circle is sometimes actually reached in practice but it is doubtful if a 30 per cent. increase in its size is very disadvantageous. To keep it to some predetermined size, the loading must be decreased as $\frac{1}{\rho}$ (ρ being the mean density at which the machine has to work). A 30 per cent. decrease of loading (say, from 8 lbs/sq. ft. to $5\frac{1}{2}$ lbs/sq. ft.) presents serious difficulties. The other limiting factors represent the "factor of safety," V being simply the highest speed at which the machine can be brought into the attitude of maximum lift without breaking. It is probably not legitimate to decrease the factor of safety in proportion to $\sqrt{\rho}$ (as (2) suggests) because the factors now used give no more than reasonable strength to resist shocks of landing, rough handling, and general wear and tear.

Section (ii) *Wing Loading for Highest Ceiling. May*, 1917.

SUMMARY.—For an aeroplane designed especially with the object of reaching the highest possible ceiling, there is a best loading (about 3 lbs /sq. ft.). This figure is not practicable for other reasons, but it appears that it would pay to reduce the loading somewhat below the values used at present for machines which are to be employed specially at very great heights.

The loss of speed entailed by using a larger area is not prohibitive. The loss of manœuvrability on account of the larger wings, &c., is a serious disadvantage.

It is assumed that the weight of the wing structure is 1 lb. per sq. ft., and that the extra to aerofoil resistance when climbing varies as the total weight, so that

$$W = W_o + A \quad . \quad . \quad . \quad . \quad . \quad . \quad (1)$$

$$r = \lambda (W_o + A) \quad . \quad . \quad . \quad . \quad . \quad (2)$$

where λ is a constant. This means that the variation of the slipstream factor R/R_o is neglected.

The ceiling depends only on Z /H and the shape of the airscrew efficiency curve, where Z is the thrust h.p. available at standard density and H is the drag h.p. under the same conditions.

We have

$$W_o + A = 0{\cdot}0051\, k_l\, A V_o^2 \quad . \quad . \quad . \quad . \quad (3)$$

and

$$H = \frac{V_o}{375}\left\{(W_o + A)\frac{k_d}{k_l} + r V_o^2\right\} \quad . \quad . \quad . \quad (4)$$

where k_l is the effective lift coefficient and k_d the true drag coefficient of the wings, and V_o is the indicated airspeed in m.p.h.

For maximum ceiling H must be a minimum, and so at any given indicated speed $\frac{\partial H}{\partial k_l} = 0$. This leads to

$$\lambda V_o^2 = \frac{W_o}{A}\left(\frac{dk_d}{dk_l} - \frac{k_d}{k_l}\right) - \frac{k_d}{k_l} \quad . \quad . \quad . \quad (5)$$

or

$$\frac{W_o}{A}\left(k_l \frac{dk_d}{dk_l} - k_d - 196\lambda\right) = 196\lambda + k_d \quad . \quad (6)$$

In this equation 196λ may be taken to have an average value of 0·003. The wing section will be assumed to be R.A.F.14.

CURVES OF Z/W_o AND H/W_o.—

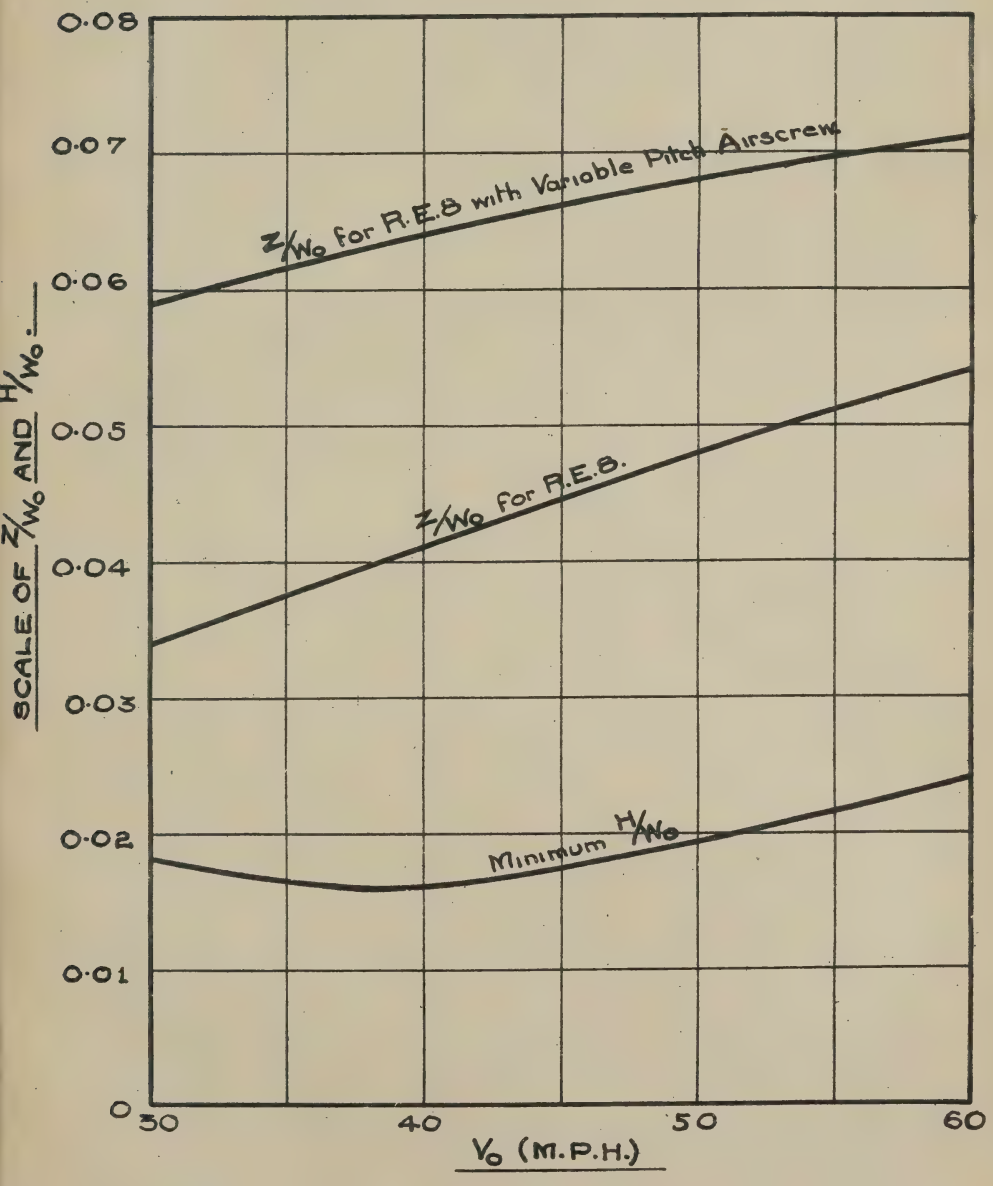

CURVE OF BEST LOADING.

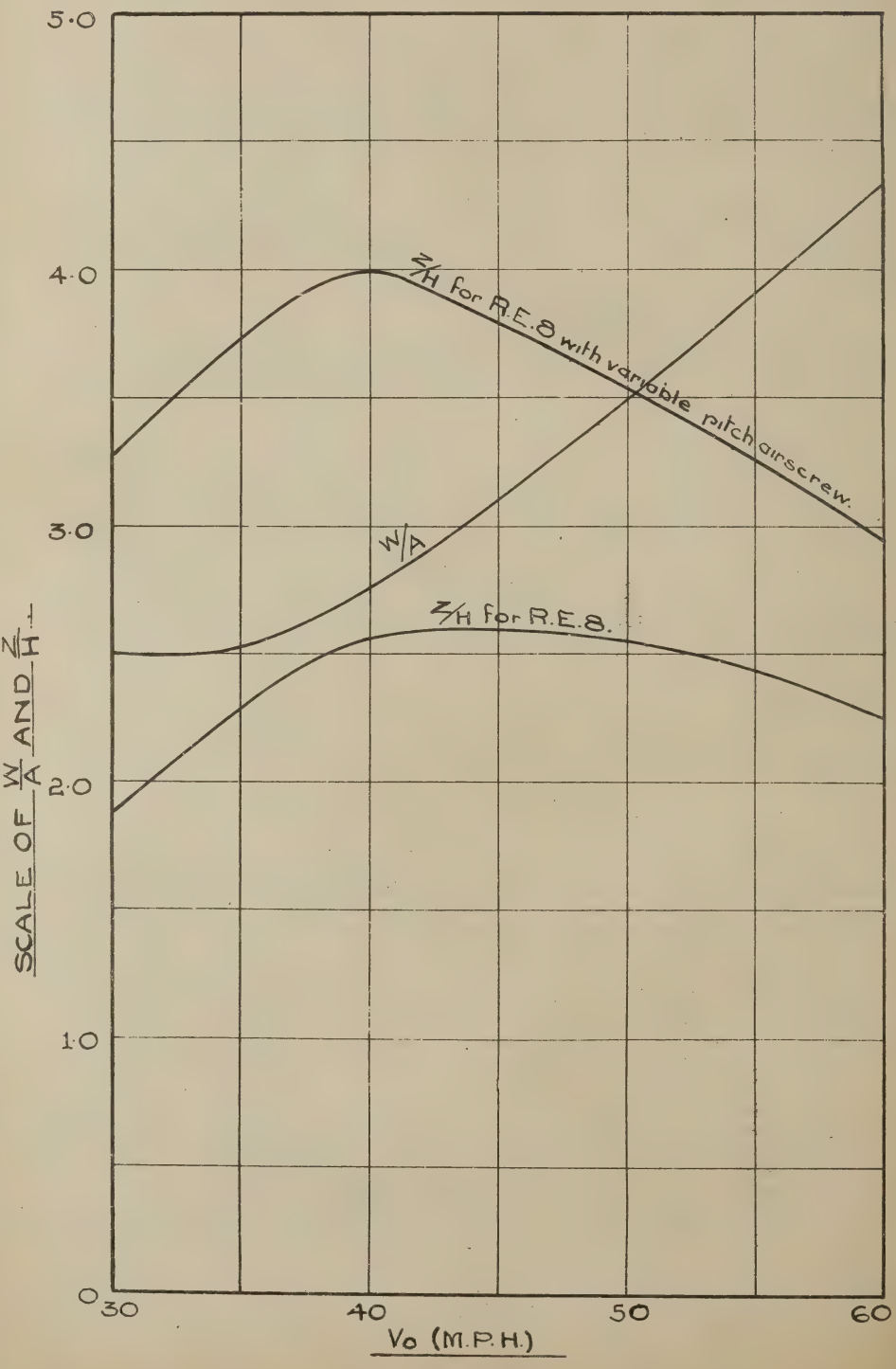

2. The solution of equations (3), (4) and (6) give the values of H/W_o and W/A for maximum ceiling at any definite speed V_o. The figures given are perfectly general except for assumptions mentioned above.

V_o.	H/W_o.	W/A.
33	0·017	2·5
36	0·0165	2·6
39	0·016	2·7
45	0·0175	3·1
56	0·022	4·0

These values (*see* also Fig. 2) give the best loading when the climbing speed is fixed. To find the best climbing speed a curve of Z/W_o against V_o is required. Values of Z/W_o have been calculated for three aeroplanes, and are given below.

V_o.	B.E.2c.	R.E.7.	R.E.8.
30	0·026	0·023	0·034
40	0·032	0·029	0·041
50	0·037	0·034	0·048
60	0·042	0·037	0·054

It appears that the values of Z/W_o for the three aeroplanes bear a constant ratio to one another, and it will be assumed that this condition holds for all aeroplanes.

The loading for maximum ceiling is now given by the speed which gives the maximum value of Z/H. The values so determined will be independent of the actual values of Z/W_o so long as the latter bear a constant ratio to the curve given in Fig. 1. The best loading appears to be approximately 3 lbs. per sq. ft., and the best climbing speed 45 m.p.h.

A curve of Z/W_o for a variable pitch airscrew on R.E.8 has also been calculated. This gives a higher maximum ceiling at a slightly lower airspeed and loading.

3. Calculations of rate of climb and speed have been made for R.E.8 with three different wing areas, and are given in the following table :—

Wing Area (sq. ft.).		400.	500.	600.
Rate of climb (ft. per min.).	Ground level ...	790	780	740
	5,000 ft.	530	525	510
	10,000 ft.	275	300	320
	15,000 ft.	65	115	125
True speed at 10,000 ft. (m.p.h.)		100	99	98½

The maximum possible rate of climb at 15,000 ft. is 195 ft. per min. with 900 sq. ft. of wing area. The effect of increasing the area is therefore to decrease the rate of climb near the ground and to increase it at heights, the increase becoming most noticeable as the ceiling is approached. The loss in speed at 10,000 ft. is small. The chief objection to the light loading is probably the loss of controllability owing to the larger wings, &c. It should be noted that secondary increases in weight due to the increase in wing area, &c., have not been taken into account. These will all reduce the advantage obtained from the reduction in loading.

PRELIMINARY REPORT ON MEASUREMENTS OF ACCELERATIONS ON AEROPLANES IN FLIGHT.

By G. F. C. Searle, Sc.D., F.R.S., and F. A. Lindemann, Ph.D.

Presented by the Superintendent, Royal Aircraft Factory.

Reports and Memoranda (*New Series*), *No.* 376. *September*, 1917.

Summary.—In order to determine the maximum "lift" force demanded from the wings of any type of aeroplane during a flight, or in any special manœuvres, an instrument was designed to give a record from which the "lift" force can be found at any instant. It is found that all the ordinary manœuvres can be carried out without this force exceeding four times the weight of the aeroplane.

1. *Introduction.*—The work described in the following pages was undertaken in order to obtain reliable information as to the factor of safety, which should be employed in the design of members taking "lift" forces in aeroplanes. An instrument was designed which records the value of the "lift" force in terms of the weight of the aeroplane at each instant. The detailed design of the final instrument is not completed, but a short description of the instrument used in the experiments here described is given, so that the results of measurements taken in actual flights may be the better understood.

Up to the present, actual measurements have been made principally in flights in a B.E.2c. Measurements in other machines are now being carried out.

2. The acceleration of a body can be calculated, when its position relative to fixed bodies can be determined at every instant, but a purely kinematical method is not available on an aeroplane in flight for the measurement of acceleration, though it is used in the "speed course" for the measurement of velocity. The acceleration of a body can, however, be found by the aid of Newton's second law of motion, according to which the acceleration of the body in any direction is proportional to the force acting upon it in that direction. The acceleration of an aeroplane in any direction can, therefore, be found, if we can measure the force required to cause a body to move with an acceleration equal in magnitude and direction to that of the aeroplane.

The simplest method of carrying this out would be to use a spring balance in the form of a massless spring AB, supporting a mass M at the end B. By the extension of the spring, the force Mf on the body can be found, and so the acceleration f, of the end A, of the spring, can be calculated.

Since, however, the acceleration will not, in general, remain constant, the position of the mass relative to the end A of the spring will not be invariable. Consequently, unless precautions are taken, there will be vibrations of the mass, which will prevent us from estimating at any given instant, the acceleration of the end A of the spring.

To make the method practical, the motion of the mass must be sufficiently damped, so that, if, for instance, the acceleration of the end A is *suddenly* changed from f_1 to f_2, the length of the spring shall change from l_1 to l_2 almost abruptly, without a series of many intervening oscillations. If the changes of acceleration to be studied occur in brief intervals of time, it is further necessary that the undamped periodic time of the system of mass and spring, when the end A is *fixed*, should be as short as possible. But a practical limit is set to the smallness of the periodic time by the fact that, the smaller this time is made, the less is the extension of the spring for a given acceleration. If the extension can be optically magnified, the periodic time can be correspondingly reduced.

3. *Description of Instrument.*—In the accelerometer designed at the R.A.F., the spring balance takes the form of a semi-circular arc of glass fibre, about 1/100 millimetre diameter, the radius of the semi-circle being about 1·3 centimetres. In the standard position of the accelerometer box, the natural plane of this semi-circular fibre is horizontal, or at least would be if the instrument were used in measuring the acceleration of a passenger lift. The position of the box in an aeroplane is described in section 9. The two ends of the fibre are fixed relative to the box, and the rest of the semi-circle is free. The fibre thus combines the functions of both the spring and the mass, in the spring balance described above.

If, now, the box has a vertical acceleration upwards, the glass fibre will lag behind, until the elasticity of the fibre is called into play sufficiently to provide the force required to produce the acceleration.

The fibre has an undamped periodic time of about 1/20 second, and its motion is highly damped by the viscosity of the air. It thus takes up very quickly a definite position corresponding to the acceleration of the box.

The volume of air in the box is, roughly, 1,500 cubic centimetres, and, as it was thought that the vibrations communicated to the box by the aeroplane engine might cause gusts in the air

inside the box, which would, in their turn, disturb the fibre, the fibre has, therefore, been mounted in a cell provided with suitable windows, and containing only a few cubic centimetres of air. This cell serves the additional purpose of protecting the fibre from injury.

Light from a metal filament electric lamp is concentrated by a condensing lens upon the vertex of the semi-circle, viz., the part furthest from the diameter, the direction of the central ray being vertical. A microscope lens, about 1·5 centimetres in focal length, whose axis is horizontal, forms an image of the illuminated fibre on a vertical plate. The image formed on this plate is a horizontal line about 1 centimetre in length. The plate has a vertical slit in it $\frac{1}{2}$ millimetre in width, and behind the slit is a kinematograph film. If the film were stationary, the illuminated fibre, if at rest, would give rise to an image on the film in the form of a very narrow horizontal line $\frac{1}{2}$ millimetre in length. But the film is drawn steadily past the slit by clockwork, and thus any motion of the fibre, due to varying acceleration, is shown as a curve on the film.

The distance of the film from the fibre is about 11 centimetres, and thus the microscope objective is used under approximately the optical conditions for which it is designed, with the result that a good image is obtained. As the distance of the image from the object is 7·33 times the focal length of the lens, the magnification is 5·14.

As a base line for measurement, a second fibre, short and straight is provided. This lies in the vertical plane which touches the horizontal semi-circular fibre at its vertex, and is illuminated by the same beam of light. The lens forms images of both fibres on the film. If measurements on the film are taken, not from the edge of the film, but from the image of the base line fibre, any error due to accidental motion of the film itself perpendicular to its length is avoided.

The current for the lamp is provided by three small accumulators giving 6 volts. A 4-volt lamp is used, but it is found necessary to overload it to obtain sufficient actinic effect to give good records when the acceleration is changing rapidly. The accumulators are attached to the box itself, but terminals are provided so that an independent battery can be used if desired. The instrument is not entirely unaffected by "vibrations," for these involve accelerations rapidly changing in direction and magnitude. But if the accelerometer box is held by an observer, or is strapped to the body of the pilot, the record of a steady horizontal flight is a line practically straight and free from sinuosities, when the air is not "bumpy," thus indicating that the vibration due to the engine does not disturb the record.

4. *Calibration.*—The instrument is easily calibrated. The box is first placed on a horizontal surface so that the natural plane of the semi-circular fibre is horizontal, and the clock is allowed to run for 5 or 10 seconds. The box is then turned upside down, and is replaced on the surface, and the clock is again allowed to run. The distance measured perpendicular to the edge of the film between the two images on the film corresponds to twice gravity. A third position in which the plane of the semi-circle is vertical, may be used. The image obtained in this position corresponds to zero acceleration in a space free from gravity.

5. *Sensitiveness.*—The deflexion, z cm., of the vertex of the fibre from the horizontal plane through its ends, due to the action of gravity, is given by

$$z = \mathrm{C}\, g\, r^4/a^2,$$

where r cm. is the radius of the semi-circle, a cm. is the radius of the section of the fibre, and C is a constant for the material of the fibre. When a fibre has been drawn (an electric heater is used), its diameter, $2a$, can be measured by a microscope, and thus the radius, r, can be chosen so as to give any required value for z. The fibres so far used in the accelerometer have given deflexions on the film of from ·25 to ·4 centimetres for gravity. The value of C, in the case of glass, is $4{\cdot}9 \times 10^{-12}$.

6. *Periodic Time.*—It can be shown that, for a fibre of diameter $2a$ centimetres bent into a semi-circular arc of radius r centimetres, the periodic time for vibrations perpendicular to its plane of equilibrium is $\mathrm{B}r^2/a$, where B is a constant for the material. By observing the deflexion due to gravity in the case (1) of a glass fibre bent into a small semi-circle, (2) of a steel wire of known diameter bent into a semi-circle of 25 centimetres radius, and by observing the periodic time of the steel wire, it was estimated that B is approximately equal to 0·000,012 for glass.

7. *Whirling Arm Experiments.*—Experiments have been made with the accelerometer attached to a small whirling arm. The natural plane of the semi-circle is parallel to the axis of revolution of the arm, and is also perpendicular to the plane containing that axis and the centre of the semi-circle. By a balance weight fixed to the other end of the arm, the centre of gravity of the system is adjusted to be on the axis. If the system revolves with uniform angular velocity about a horizontal axis, the difference in the resultant force experienced by a particle of mass m when (1) at its highest, (2) at its lowest point, is independent of its distance from the axis, and of its angular velocity, and has the value $2mg$. Thus the record will be a wave line, the height from the crests to the troughs of the wave always corresponding to $2g$. The angular velocity was varied from about 3 revolutions per second to zero, but the height from

crest to trough was found to remain constant, thus showing that, up to 3 revolutions per second, the damping of the fibre does not prevent the accelerometer from recording, on the proper scale, accelerations which go through three cycles per second.

In the second experiment the arm was made to turn about a vertical axis. The current for the lamp was brought in by one bearing and out by a brush pressing on the axle. The system was given a large initial angular velocity, which gradually diminished on account of friction and air resistance. By a key, the current was switched on for 5 revolutions of the arm, then was switched off for 5 revolutions, and so on, and the time of each motion of the switch was noted on a watch. A curve showing how the angle turned through by the arm depended upon the time was then drawn. The slope of the tangent to this curve gave A, the angular velocity. If R is the distance of the plane of the semi-circle from the axis of the whirling arm, the acceleration of the fibre is RA^2. The curve obtained on the film showed that the deflexion was proportional to A^2, and the displacement of the image on the film due to gravity was calculated to be ·42 centimetres. Calibration by the method described in (4) gave ·44 centimetres as the displacement due to gravity. Considering the difficulty of the experiment the agreement is satisfactory.

8. *Future Work.*—The designs of an instrument embodying the improvements suggested by experience are now in preparation. Two microscope lenses, with their axes pointing to the slit will be used, the angle between the axes being about 30°. One lens will be used to form an image of the accelerometer fibre on the slit. The other we propose to use for forming on the slit the image of a fibre actuated by an air speed indicator diaphragm. In this way we hope to obtain on the film simultaneous records of the acceleration and the air speed.

The use of two lenses would allow the instrument to record other pairs of quantities at the same time, as, for instance, pressure and temperature, or accelerations in two perpendicular directions.

9. *Use in Aeroplanes.*—In an aeroplane, the accelerometer box is *fixed* relative to the aeroplane so that the natural plane of the glass fibre is horizontal when the aeroplane is flying in a straight level course.

Though the instrument is called an accelerometer, and would measure accelerations if gravity did not act, it does not always measure the actual acceleration directly when gravity does act. What it actually does measure we now go on to discuss. A particle of mass m, moving with the aeroplane, is acted on by two forces ; one is mg, its weight, and the other is the force exerted on it by the aeroplane. This latter force can be equated to the resultant of three mutually perpendicular forces, viz.,

mf_1 parallel to the longitudinal axis of the aeroplane, *i.e.*, parallel to the engine crankshaft, mf_2 parallel to the wings, and mf_3 perpendicular to both mf_1 and mf_2. It is only the last of these components, mf_3, which has any appreciable effect upon the particles of glass fibre in the way of causing that deformation of the fibre which gives rise to a deflexion of its image on the film. The deflexion of the image from the line corresponding to zero acceleration in a space free from gravity (*see* 4) is proportional to mf_3. If this deflexion is z centimetres, and that due to gravity as found in the calibration is h centimetres, then $f_3 = gz/h$.

Now the wings of the aeroplane do for the aeroplane body what the aeroplane has been supposed to do for the particle. For the present purpose we may neglect the aerodynamical effect upon the body. Then, if the mass of the aeroplane body is M, the force exerted on it by the wings in a direction perpendicular to the plane of the glass fibre is Mgz/h.

Thus, to this approximation, if the deflection of the image from the line for zero acceleration and zero gravity is measured, the force exerted by the wings on the body in the specified direction can be calculated.

When an aeroplane is flying horizontally at its normal speed, its longitudinal axis is horizontal. In this case, if the mass of the body is M tons, the force exerted by the wings on the body is M tons weight in the direction corresponding to f_3. But, if the record on the film shows that, for instance, in coming out of a nose dive, there was a maximum value of z which is n times h, then we know that the maximum force which the wings exerted on the body in the direction of f_3 was nM tons weight. The records so far obtained have not given any values of n exceeding 4.

10. *Results of Measurements on a B.E.2c.*—The illustration shows a number of records from the accelerometer when recording the variations of the "lift" force on a B.E.2c during various manœuvres. The horizontal lines serve as a scale for the "lift" force, each space corresponding to g; the intervals between the vertical lines correspond to 5 seconds. All records read from left to right.

The small deflexion A is due to a turn at a bank of about 45°; B was due to a steeper turn, some 60°, C to a very slow turn at about 20° bank, and D to a very steep turn. In each case the speed was about 60 m.p.h.

Records E and F represent the effects of stalling suddenly, E at 80 m.p.h., F at 85 m.p.h. The "lift" force increased rapidly as the nose of the machine rose; it then diminished in the course of about 2 seconds to a value which remained steady at about $0{\cdot}4g$ for 12 seconds. During the latter interval the nose went down, and the machine gathered speed.

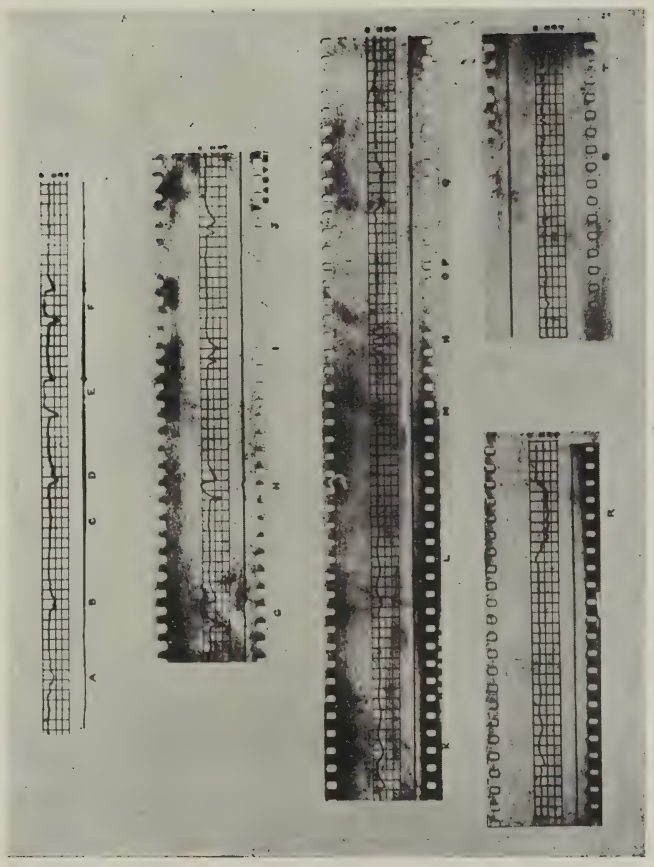

THE LIBRARY
OF THE
UNIVERSITY OF ILLINOIS

Records G and H were obtained on loops. In the first loop, started at 95 m.p.h., the "lift" force reached about $3{\cdot}2g$ at the start, then diminished to about $0{\cdot}1g$ at the top, and increased again to nearly $2g$ on the machine coming out of the loop at the end of 15 seconds. The maximum loading in H was only about $2{\cdot}8g$, and the minimum zero, but this was a slow loop, starting at 87 m.p.h.

Records I and J show the effect of rolling the machine. On a B.E.2c this manœuvre cannot be carried out very successfully, as it is difficult to prevent the nose of the machine going down. This explains the large accelerations, $2g$ and $2{\cdot}3g$, as the machine came out of the roll. The point at which the machine is upside down is well marked, and it is worthy of note that the B.E.2c can be turned over on to its back in about 3 seconds. The time for a scout machine is not much less, but the force which has to be applied to the control stick is, of course, much smaller.

Records K and L show the "phugoids" resulting from pushing the nose down at 85 m.p.h. and 75 m.p.h. respectively, and then leaving go of the controls. The damped sine curve is well marked, the period being 17 seconds.

In M and N, and also in O and P, the results of pushing the control stick rapidly backwards and forwards are shown.

The acceleration in a spinning nose dive of some 2,000 feet at 55 m.p.h. is shown in Q. It will be seen that the "lift" force never exceeded twice the weight of the machine.

Record R was obtained in an ordinary spiral; it shows that the "lift" force may be considerably greater than twice the weight of the machine. The ratio of "lift" force to weight gradually increased to about 2·8 as the spiral was made steeper; the airspeed was 70 m.p.h.

Record S shows the accelerations due to gusts of wind. These appear to be such that the "lift" force varies from ·5 to 1·5 times the weight, in ordinary bumpy weather. This means that the accelerations experienced by the aeroplane vary from $\cdot5g$ downwards to $\cdot5g$ upwards. The wind velocity was about 30 m.p.h. at 1,900 feet, at which this record was taken.

The landing is shown in T. It is seen that even a good landing with an oleo gear gives rise to considerable accelerations.

The two lines on the records, corresponding to the images of the two fibres, are clear and distinct, but the film itself shows "fogging" in places. This is due to causes which can be removed by securing better photographic conditions.

[Aug., 1919. The diagram in this Report has been prepared from a *tracing* of the original record of the *moving* fibre. Other diagrams, reproduced entirely by photography, are given in R. and M. No. 469.]

INVESTIGATION OF THE DOWNWASH BEHIND A BIPLANE.

By C. G. D. Sandison, H. Glauert, and J. H. Jones.

Presented by the Superintendent, Royal Aircraft Factory.

Reports and Memoranda, No. 426. *March,* 1918.

Summary.—(a) *Introductory (reasons for inquiry).*—Reports and Memoranda No. 156 (Section IV) contains an exploration of the downwash in the region of the tailplane of a B.E.2c machine, but, apart from this series of experiments, no data were available for determining the variation of the downwash at different points or for estimating the magnitude of the body interferences. The experiments of R. & M. 156 were also carried out at one angle of incidence only.

(b) *Range of investigation.*—The downwash has been explored behind a biplane structure in a central plane at right angles to the span at angles of incidence from $-4°$ to $+20°$ in general, and to $+40°$ in one particular case. The downwash was measured by setting the tailplane at the no lift angle. The effect of the interference of a pusher and of a tractor body has also been investigated.

(c) *Conclusions.*—The downwash is found to decrease exponentially with distance from the biplane and to have a maximum value behind the upper wing. An empirical formula has been found which is applicable throughout the region in which the tailplane is likely to be placed. The interference effect of the bodies was found to be small, except at very small distances.

(d) *Applications and further developments.*—Further experiments are needed to find out whether a change of wing section would cause any appreciable effect on the generalised conclusions of this report. The wide region through which the downwash exists seems to indicate that, for downwash measurements, $3'' \times 18''$ aerofoils are about the largest size which can be tested in a 4-ft. channel without interference from the walls.

1. This report deals with a comprehensive investigation into the distribution of the downwash behind a biplane structure with and without body interference. For this purpose two brass aerofoils ($3'' \times 18''$) of R.A.F.6A section were used, arranged as a biplane of no stagger and unit gap-chord ratio. The region investigated was the central plane at right angles to the span of the wings and extended from close up to the wing structure

to a distance of three chords behind it. The investigation was carried out over a range of wing incidence from — 4° to 20° in general, and to 40° in one position. A number of the experiments were also repeated with the addition of an F.E.2 and a B.E.2 body. In all three cases the lift curve of the combination was obtained for comparison with the downwash results. The method of determining the downwash angles was to mount a tailplane (2″·5 × 9″) on a spindle and adjust its position to that of no lift. It was considered that this method of investigation would give values which would be directly applicable to full-scale aeroplanes, as it would mean out any variation of downwash angle and curvature of the lines of flow over a region of the proper size. For points close to the wing structure a rafwire was substituted for the tailplane to eliminate interference effects. Corrections were made in all cases for the interference effect of the model stand on which the aerofoils were mounted. All experiments were made at an airspeed of 60 ft./sec. ($vl = 15$) in a 4-ft. wind channel.

2. The curves of lift coefficient against angle of incidence (Fig. 1) show that the presence of a body reduces the maximum lift coefficient very slightly, but that otherwise the effect is very small. In converting the measured lifts to absolute coefficients the same total wing area was used in all three cases. It follows that to a good approximation the lift of a tractor or pusher body can be allowed for by assuming the lift coefficient of the wings to be unaltered, while the wing area is increased by the section of the lower wing which is cut out to admit the body. This method, however, might cease to apply if any gap were left between the lower wings and the sides of the body. The addition of this fictitious wing area might also prove satisfactory as a first approximation in allowing for the increased drag of the body due to wing interference, but this point needs further investigation.

3. The values obtained for the downwash angles are given in Tables 2-4, and are exhibited in Figures 2-6. The position of the reference point is determined by the co-ordinates x and y, where x is the distances in inches behind the trailing edge of the aerofoils, measured parallel to the chord, and y is the distance in inches below the upper wing. The general form of the curves shows that the downwash is consistently higher behind the upper than behind the lower wing in all positions, but close to the biplane structure a maximum occurs between the two wings. The interference effect of the model stand is, however, more important for small distances from the biplane, and in consequence these results are less accurate than those at greater distances. The effect of the presence of the bodies is small, except quite close to the wing structure. From these results the curves of Fig. 7 have been deduced, representing the variation of the downwash with depth at a distance of 7 inches, and

the variation with distance midway between the wings. These curves show clearly that the downwash decreases as the reference point recedes from the wing structure, or passes from the level of the upper to that of the lower wing. It has been found possible to represent the variation of downwash behind the wing structure by the empirical formula

$$\varepsilon = \varepsilon_o \, 10^{-0.05\xi - 0.08\zeta}$$

where ξ and ζ are the distances x and y expressed in multiples of the wing chord and gap respectively. It is hoped that it will be possible to use this empirical formula for different biplane arrangements and for different wing sections by suitable choice of the quantity ε_o. The values of this quantity are given in Table 5. A suggested method of applying the curve to other wing sections is to change the scale of abscissæ and ordinates in the ratio of the maximum lift coefficients. This would leave unaltered the form of the curve, and also the values of ε_o at the values of k_l for which the relation between ε_o and k_l is linear. The curve drawn in Fig. 10 would form the basis for applying the results in the method suggested. The empirical formula only applies for the region directly behind, and at some distance from, the wing structure (*i.e.*, $1 > \zeta > 0$, $\xi > 1$), but this region covers all probable positions of the tailplane of an aeroplane. The empirical formula can also be used to determine the form of the streamlines, the equation obtained being

$$10^{0.08\zeta} = \mathrm{C}\, 10^{-0.0014\theta\xi} - \frac{\varepsilon_o}{35{\cdot}8 - \theta}\, 10^{-0.05\xi}$$

where C is a constant which is determined when one point of the streamline is known.

4. A wider region was investigated at a distance of $9''{\cdot}8$ from the midpoint of the wing structure. These measurements were made in a plane at right angles to the wind direction and at two angles of incidence. The results are shown in Fig. 8 and approximate to curves of the type $y = a\, e^{bx^2}$. It is of interest to note that the integrated areas over the whole plane are approximately in the ratio of the corresponding lift coefficients. The downwash angle is still noticeable (about 1°) at a distance of four times the chord or two-thirds of the span above and below the biplane. Symmetrical curves have been drawn through the observed points, and these seem to agree well, except at the apex of the curves.

The downwash was investigated up to 40° wing incidence at one point ($x = 9$, $y = 1{\cdot}5$). The form of the curve obtained (Fig. 9) bears a very close resemblance to the usual type of lift curve of an aerofoil, and its maximum occurs at the stalling incidence of the biplane.

5. It is thought that it will be possible to use the results given in this report as a standard basis of comparison for the

downwash angles found in full scale or model experiments, and that they will indicate the variation to be expected in the slope of the downwash curve for different positions of the tailplane. The empirical formula leads to the determination of the streamlines, and will give some indication of the height at which the centre line of the propeller slipstream strikes the fin and rudder. This determination is of considerable importance in estimating the turning tendency of an aeroplane.

TABLE 1.

LIFT COEFFICIENT OF THE BIPLANE.

Angle of Incidence.	Wings alone.	Wings and Pusher Body.	Wings and Tractor Body.
− 4	− 0·046	− 0·033	− 0·040
0	+ 0·094	+ 0·100	+ 0·098
+ 4	0·224	0·229	0·221
8	0·334	0·340	0·330
12	0·443	0·444	0·436
16	0·513	0·496	0·499
18	0·494	0·473	0·492
20	0·475	0·462	0·482

TABLE 2.

DOWNWASH DUE TO WINGS ALONE.

Airspeed 60 *ft./sec.*

Co-ordinates of Reference Point.		Angle of Incidence (degrees).						
x.	*y.*	− 4.	0.	4.	8.	12.	16.	20.
9″	0″	−1°·0	1°·5	3°·9	5°·7	7°·4	7°·8	6°·6
	1·30	− 0·9	1·5	3·6	5·3	6·7	7·0	6·1
	2·55	− 1·2	1·2	3·3	5·1	6·2	6·2	5·5
	3·50	− 1·2	1·2	3·1	4·4	5·4	5·7	5·1
7	0	− 0·9	1·8	3·9	6·1	7·9	8·5	7·0
	1·50	− 0·9	1·7	3·8	5·6	7·2	7·5	6·5
	3·00	− 1·2	1·5	3·7	5·2	6·5	6·7	5·9
	3·95	− 1·2	1·4	3·3	4·7	5·9	6·2	5·5
4	0	− 0·8	1·8	4·5	6·5	8·7	9·5	7·5
	2·40	− 1·3	1·6	4·0	6·0	7·8	8·0	6·4
2·35	0·06	− 1·1	1·3	5·0	6·6	9·2	10·1	9·1
	1·24	− 0·1	4·1	7·6	8·4	11·2	12·7	13·7
	3·42	0·0	2·4	4·7	7·0	9·2	9·4	7·3
1·35	−0·46	− 1·6	− 0·4	—	6·4	12·0	15·2	20·2
	+1·40	− 2·6	+ 2·6	5·3	8·4	13·2	15·3	18·2
	3·45	− 2·2	2·6	5·4	8·1	9·8	9·8	7·6

TABLE 2.—*continued.*

Experiments at different airspeeds.

Co-ordinates of Reference Points—$x = 7{\cdot}0$, $y = 1{\cdot}5$.

Airspeed ft./sec.	Angle of Incidence (degrees).						
	− 4.	0.	+ 4.	8.	12.	16.	20.
60	−0°9	1°7	3°8	5°6	7°2	7°5	6°5
55	−0·9	1·5	3·8	5·6	7·3	7·6	6·8
40	−0·9	1·3	3·8	5·6	7·2	7·7	6·7

NOTE.—x is the distance of the reference point behind the trailing edge of the wings measured parallel to the chord and y is the depth below the upper wing.

TABLE 3.

DOWNWASH DUE TO WINGS AND PUSHER BODY.

Airspeed 60 ft./sec.

Co-ordinates of Reference Point.		Angle of Incidence (degrees).						
x.	y.	− 4.	0.	+ 4.	8.	12.	16.	20.
9″	0″	−0°8	1°6	3°7	5°8	7°2	6°9	5°7
	1·28	−1·2	1·2	3·2	5·0	6·3	6·8	5·3
	3·47	−1·1	1·2	3·0	4·3	5·4	5·3	4·4
4	0	−1·2	1·2	4·1	6·6	8·5	9·2	7·2
	1·30	−1·0	1·8	3·7	5·7	7·5	8·3	6·2
	3·5	−0·9	1·7	3·6	5·4	6·9	6·3	5·1
2·35	0	−0·1	1·4	4·5	6·4	8·8	9·6	10·1
	1·30	−0·3	2·9	7·0	8·3	10·3	12·4	12·3
	3·58	−1·9	0·1	1·0	3·6	5·9	5·2	5·1
1·35	0·03	0·5	1·4	5·4	8·3	12·3	11·8	10·0
	1·70	−2·8	−0·5	4·8	10·3	14·2	15·4	17·8
	3·32	−3·8	−0·5	2·7	5·4	7·4	7·1	6·5

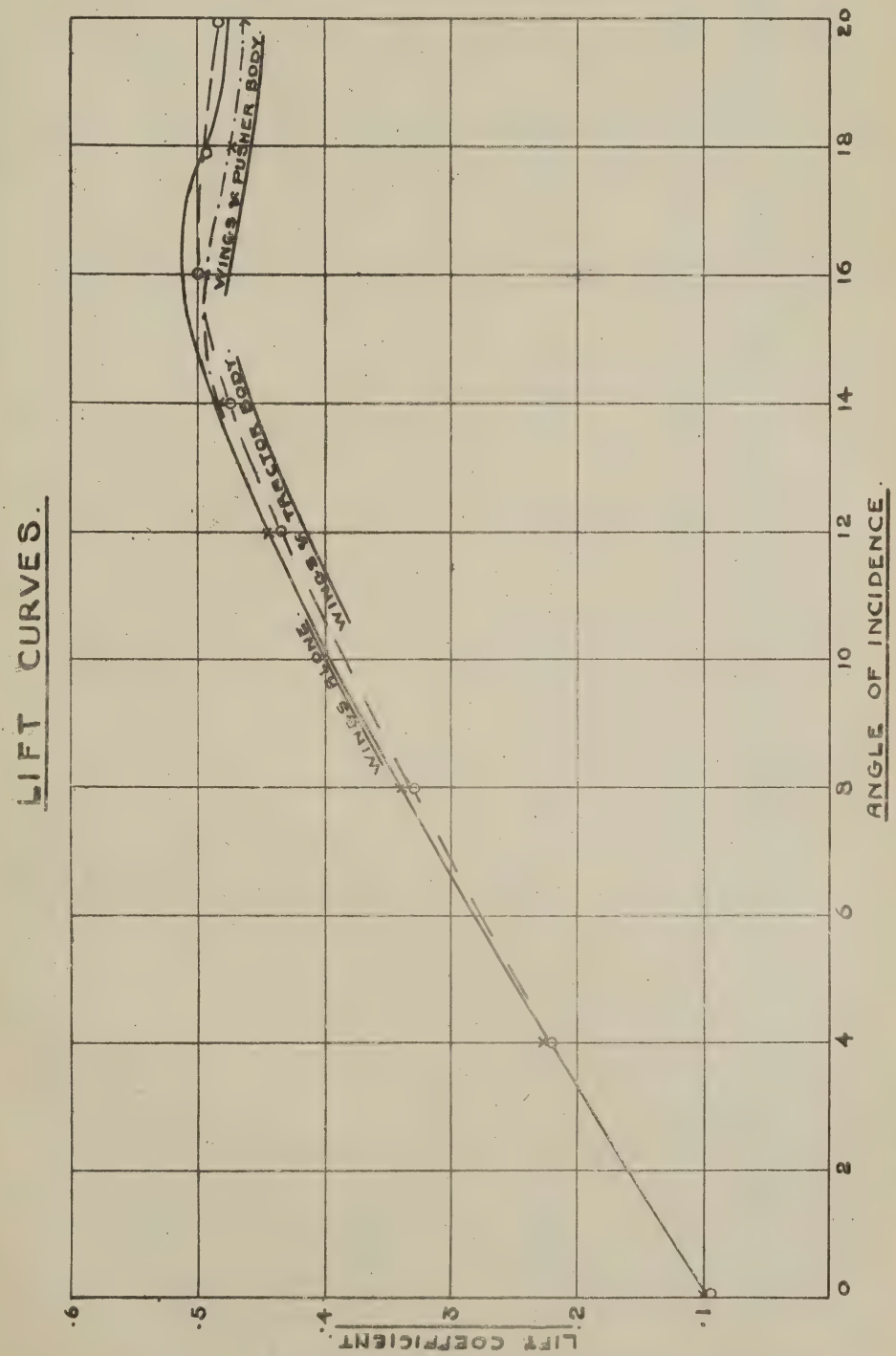
LIFT CURVES.
WINGS & PUSHER BODY.
TRACTOR & BODY.
WINGS & BODY.
WINGS ALONE.
LIFT COEFFICIENT
.6
.5
.4
.3
.2
.1
0
2
4
6
8
10
12
14
16
18
20
ANGLE OF INCIDENCE.

ANGLES OF DOWNWASH FOR 4° WING INCIDENCE

THE CURVES GIVE THE DOWNWASH OF WINGS ALONE, THE CROSSES (x) SHOW THE INTERFERENCE OF THE PUSHER BODY AND THE CIRCLES (o) THAT OF THE TRACTOR BODY.

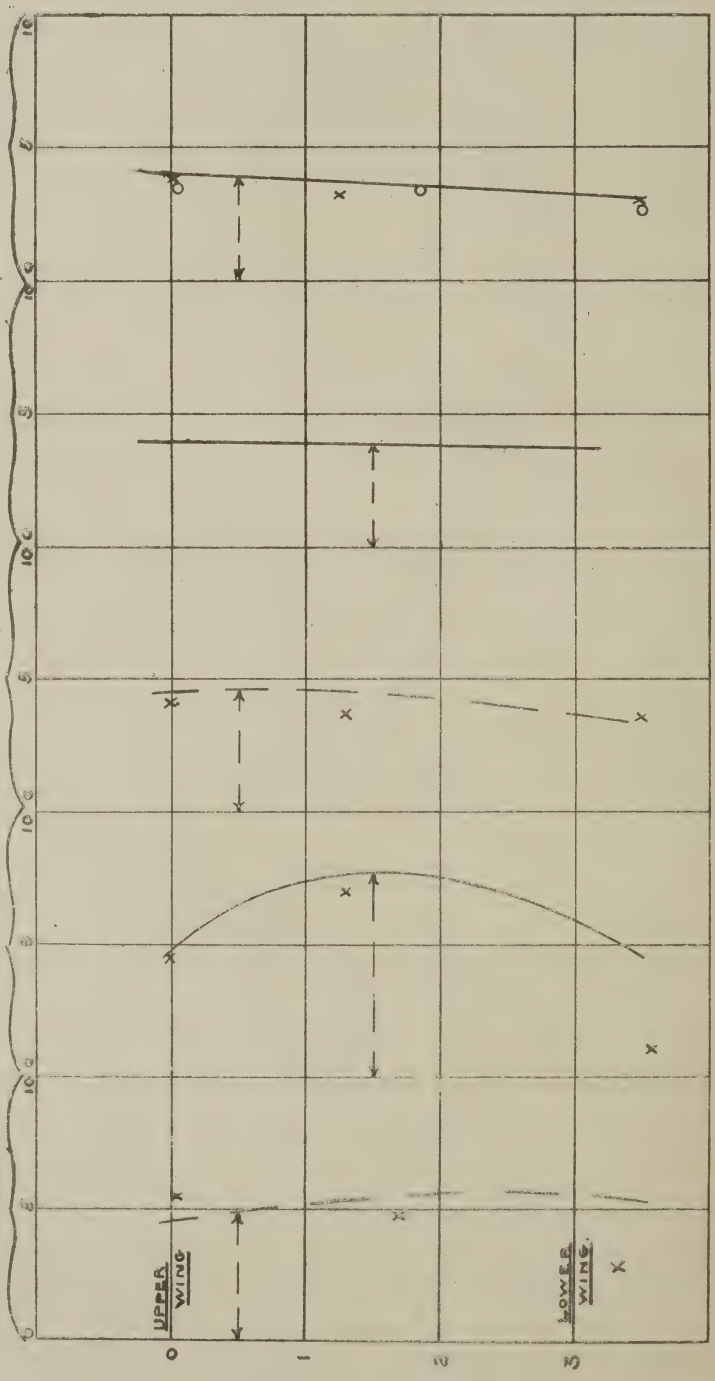

ANGLES OF DOWNWASH FOR 8° WING INCIDENCE

THE CURVES GIVE THE DOWNWASH OF WINGS ALONE, THE CROSSES (X) SHOW THE INTERFERENCE OF THE PUSHER BODY AND THE CIRCLES (O) THAT OF THE TRACTOR BODY.

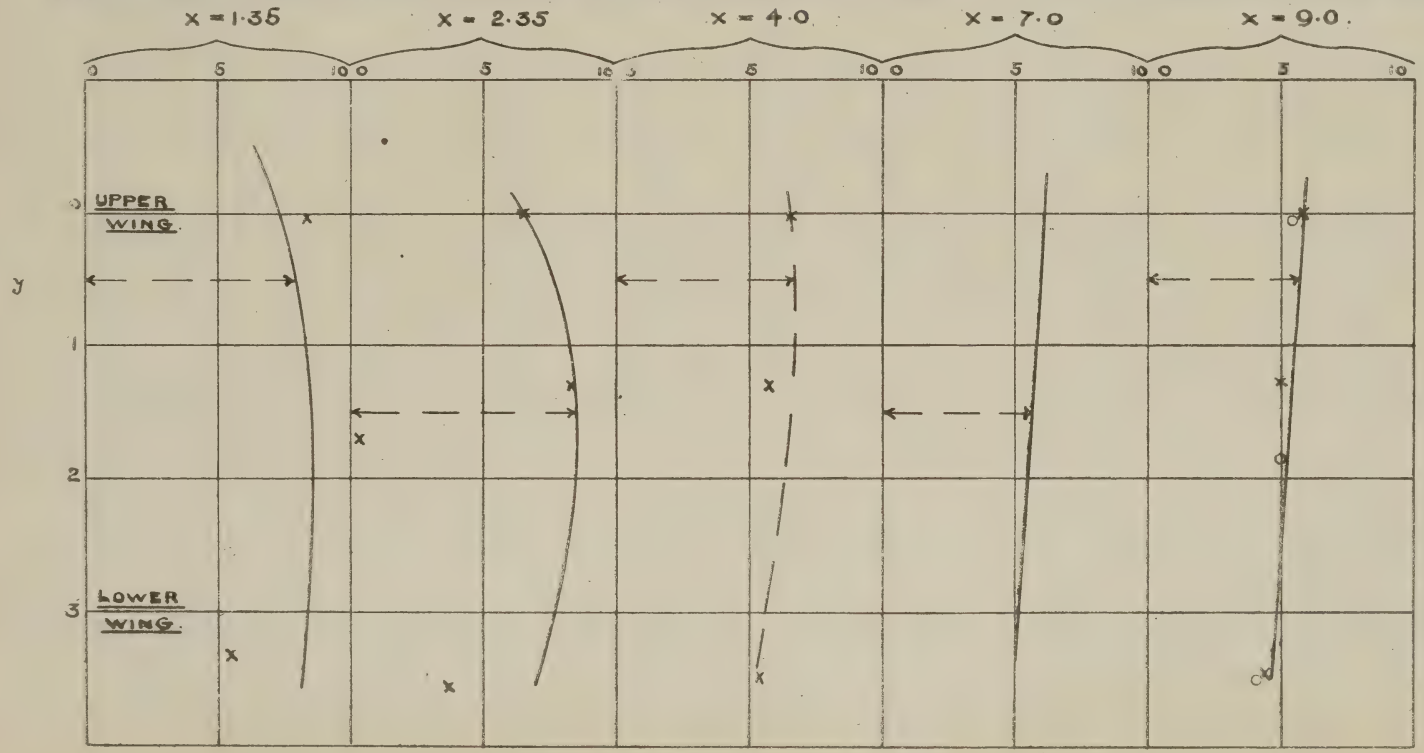

REPORT No 426.

FIG. 3.

ANGLES OF DOWNWASH FOR 12° WING INCIDENCE

THE CURVES GIVE THE DOWNWASH OF WINGS ALONE, THE CROSSES (x) SHOW THE INTERFERENCE OF THE PUSHER BODY AND THE CIRCLES (o) THAT OF THE TRACTOR BODY.

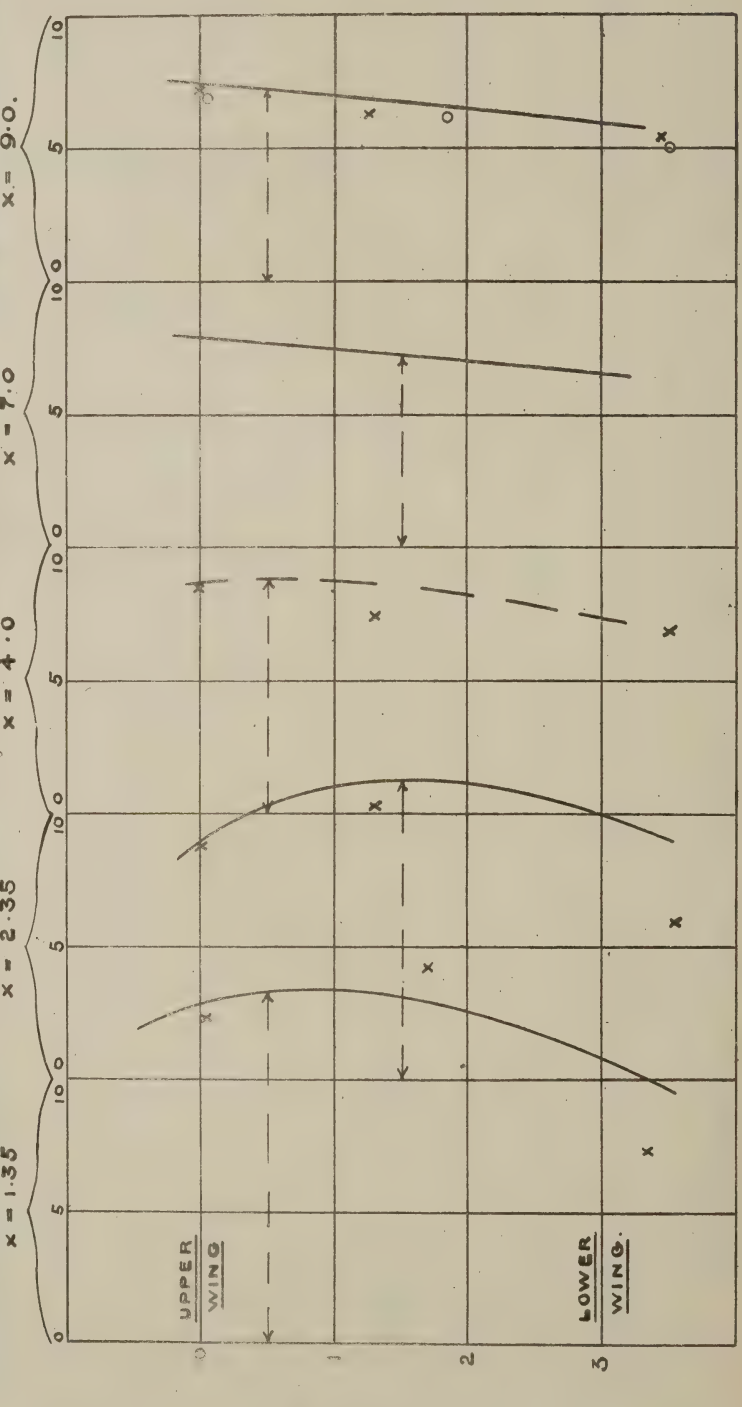

ANGLES OF DOWNWASH FOR 16° WING INCIDENCE

THE CURVES GIVE THE DOWNWASH OF WINGS ALONE, THE CROSSES (x) SHOW THE INTERFERENCE OF THE PUSHER BODY AND THE CIRCLES (o) THAT OF THE TRACTOR BODY.

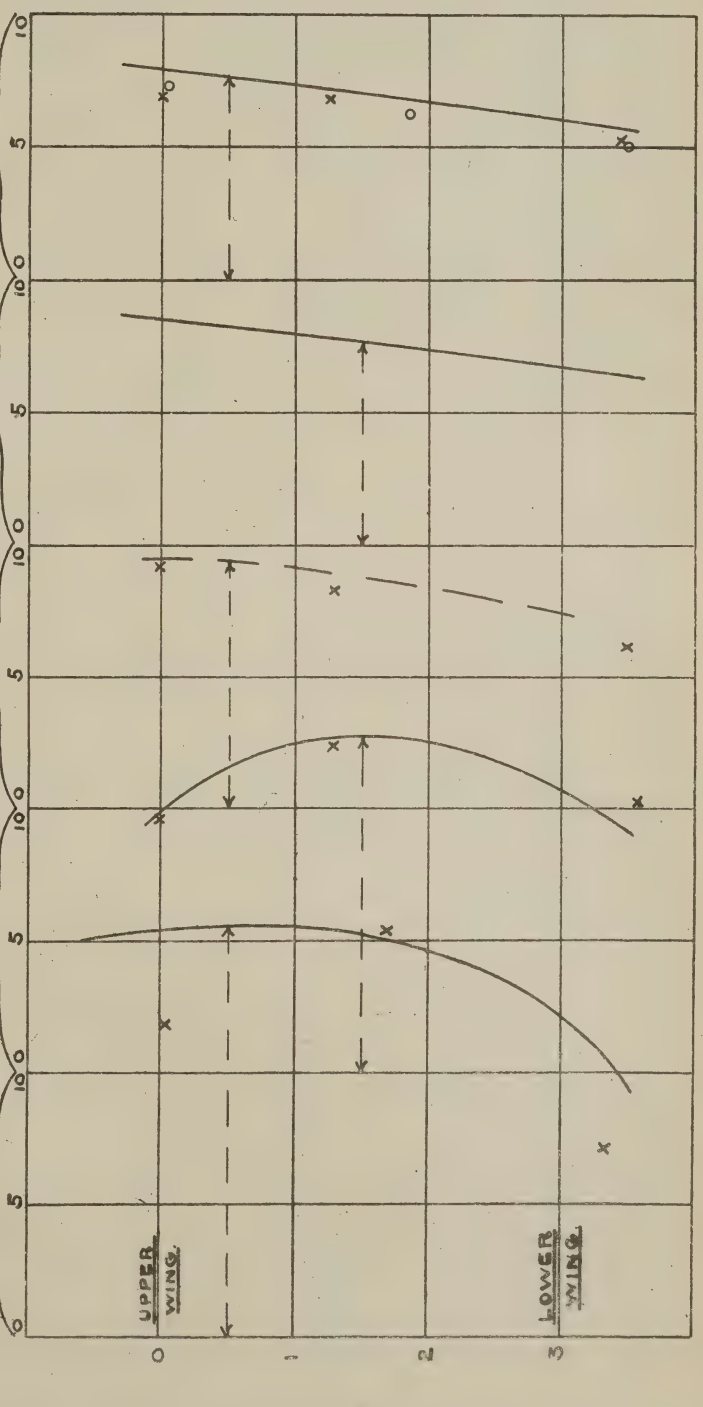

ANGLES OF DOWNWASH FOR 20° WING INCIDENCE

THE CURVES GIVE THE DOWNWASH OF WINGS ALONE, THE CROSSES (X) SHOW THE INTERFERENCE OF THE PUSHER BODY AND THE CIRCLES (O) THAT OF THE TRACTOR BODY.

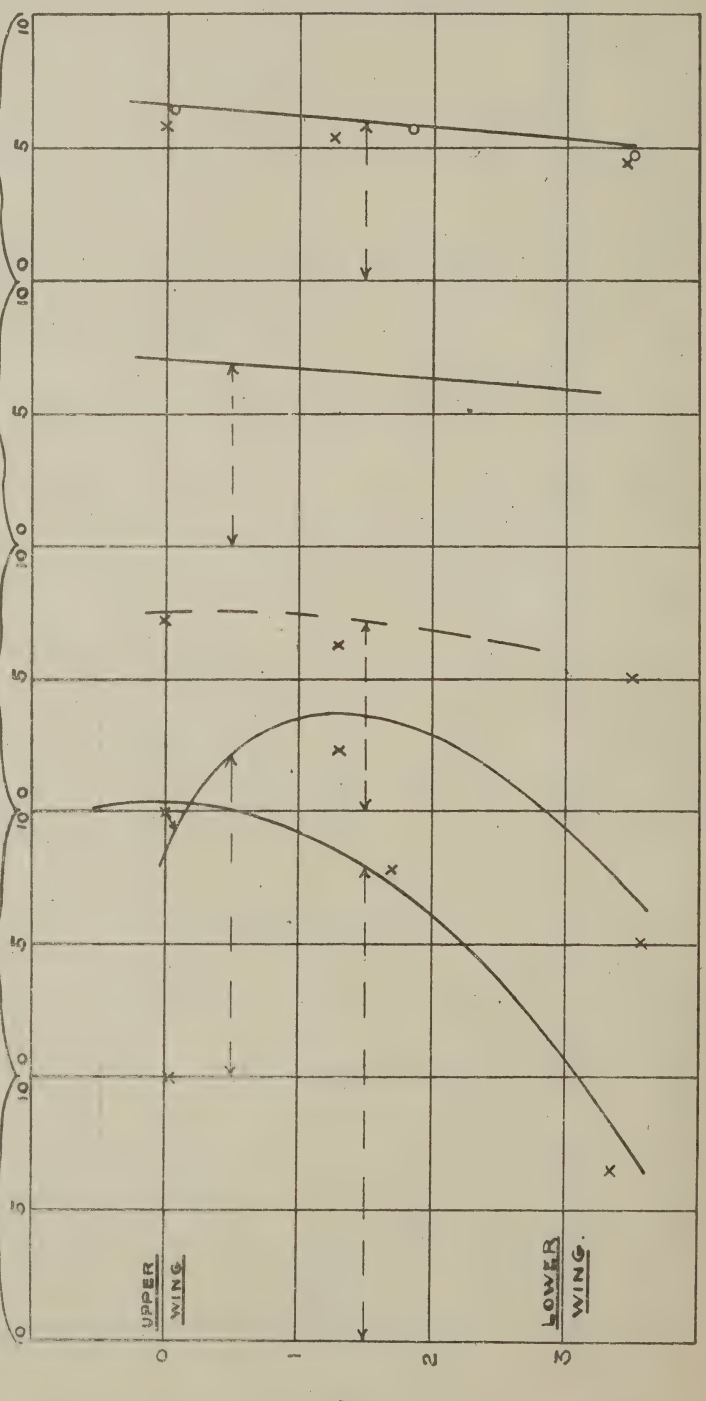

VARIATION OF DOWNWASH WITH POSITION

VARIATION OF DOWNWASH WITH DEPTH BELOW UPPER WING.

x = 7.

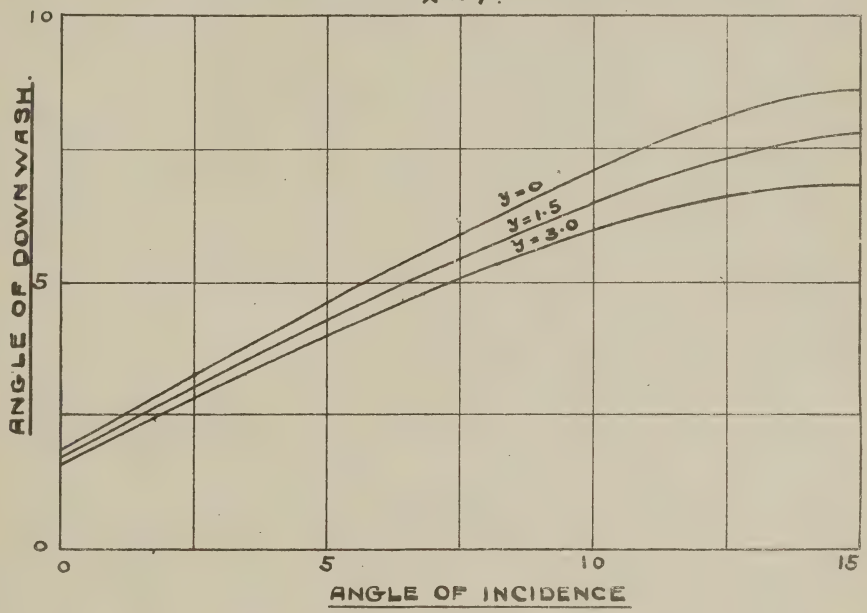

VARIATION OF DOWNWASH WITH DISTANCE FROM WINGS

y = 1·5.

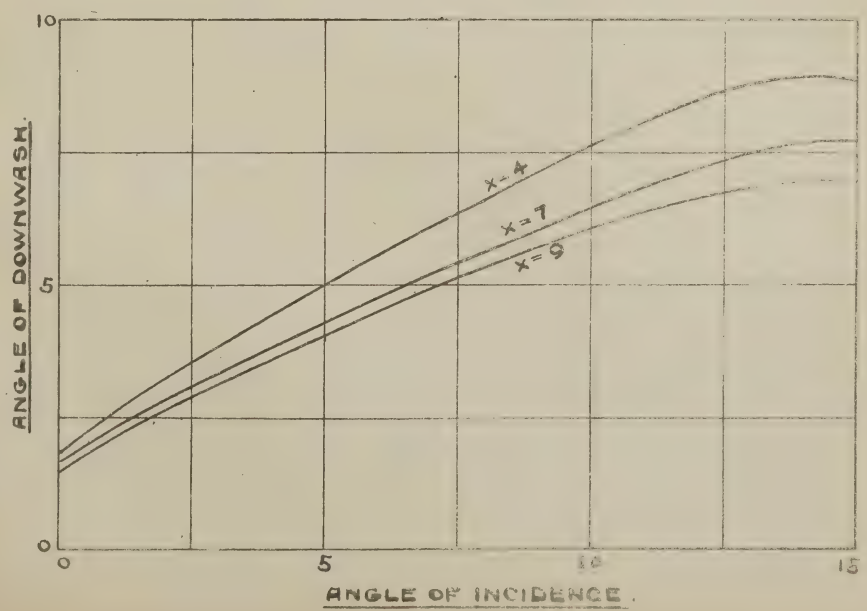

DISTRIBUTION

OF DOWNWASH OVER A LARGE AREA.

MEASUREMENTS TAKEN IN A PLANE AT RIGHT ANGLES TO THE WIND DIRECTION AS IN FIGURE.

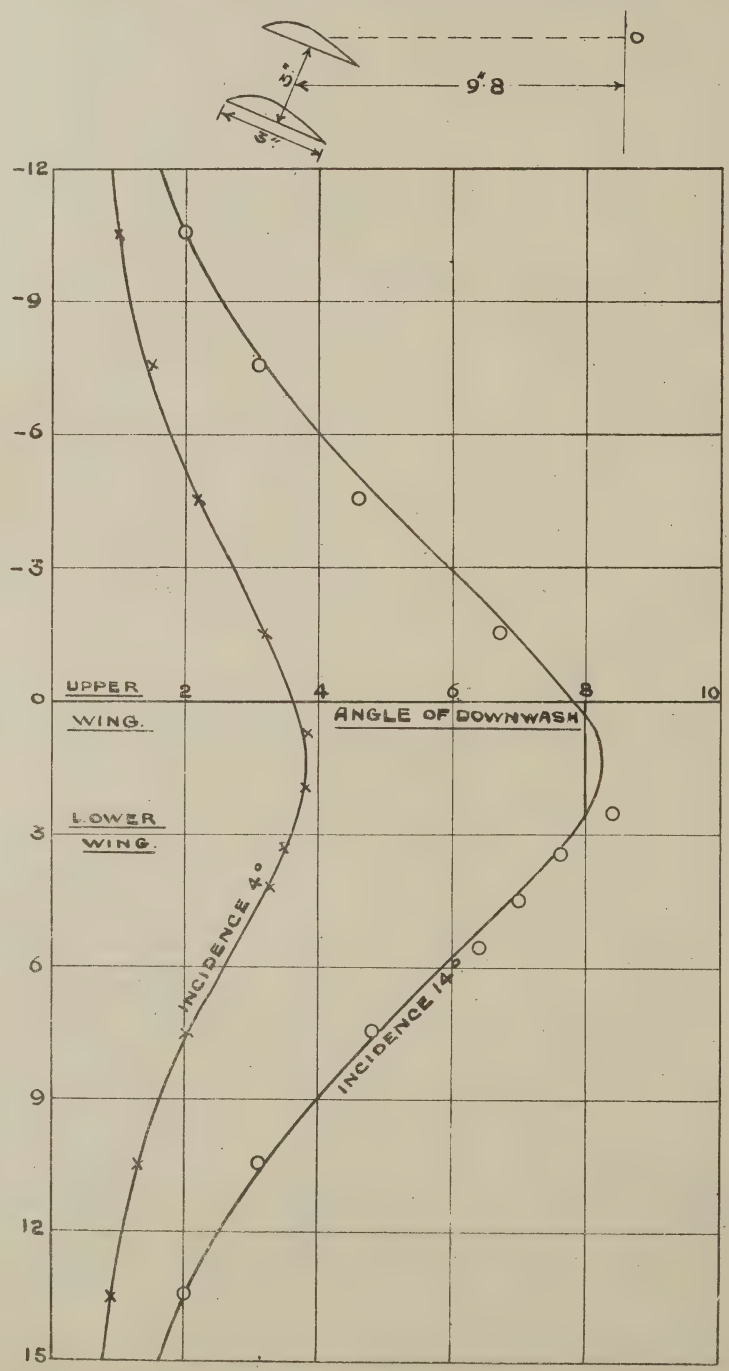

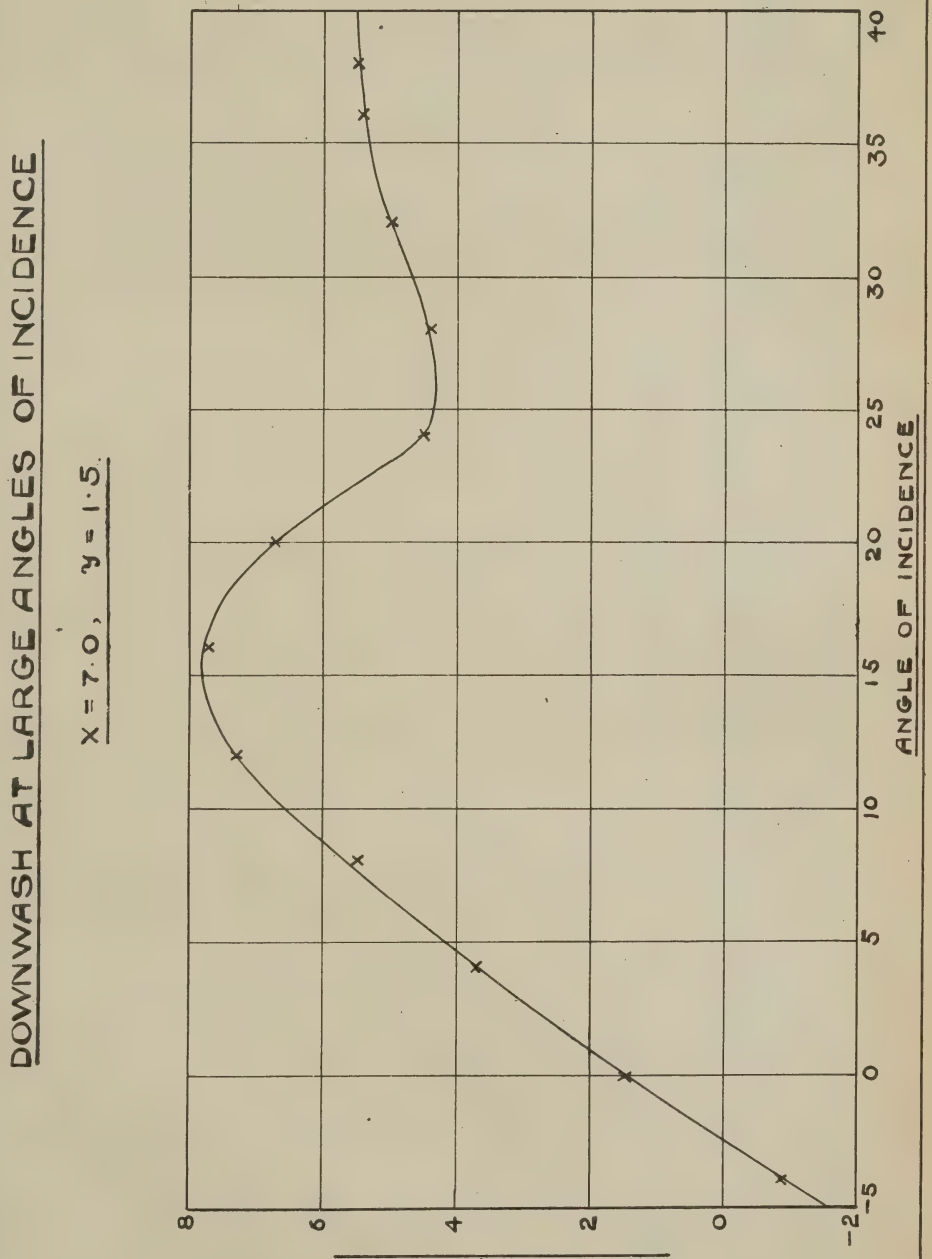
DOWNWASH AT LARGE ANGLES OF INCIDENCE
X = 7·0, y = 1·5.
ANGLE OF DOWNWASH
8
6
4
2
0
-2
-5
0
5
10
15
20
25
30
35
40
ANGLE OF INCIDENCE

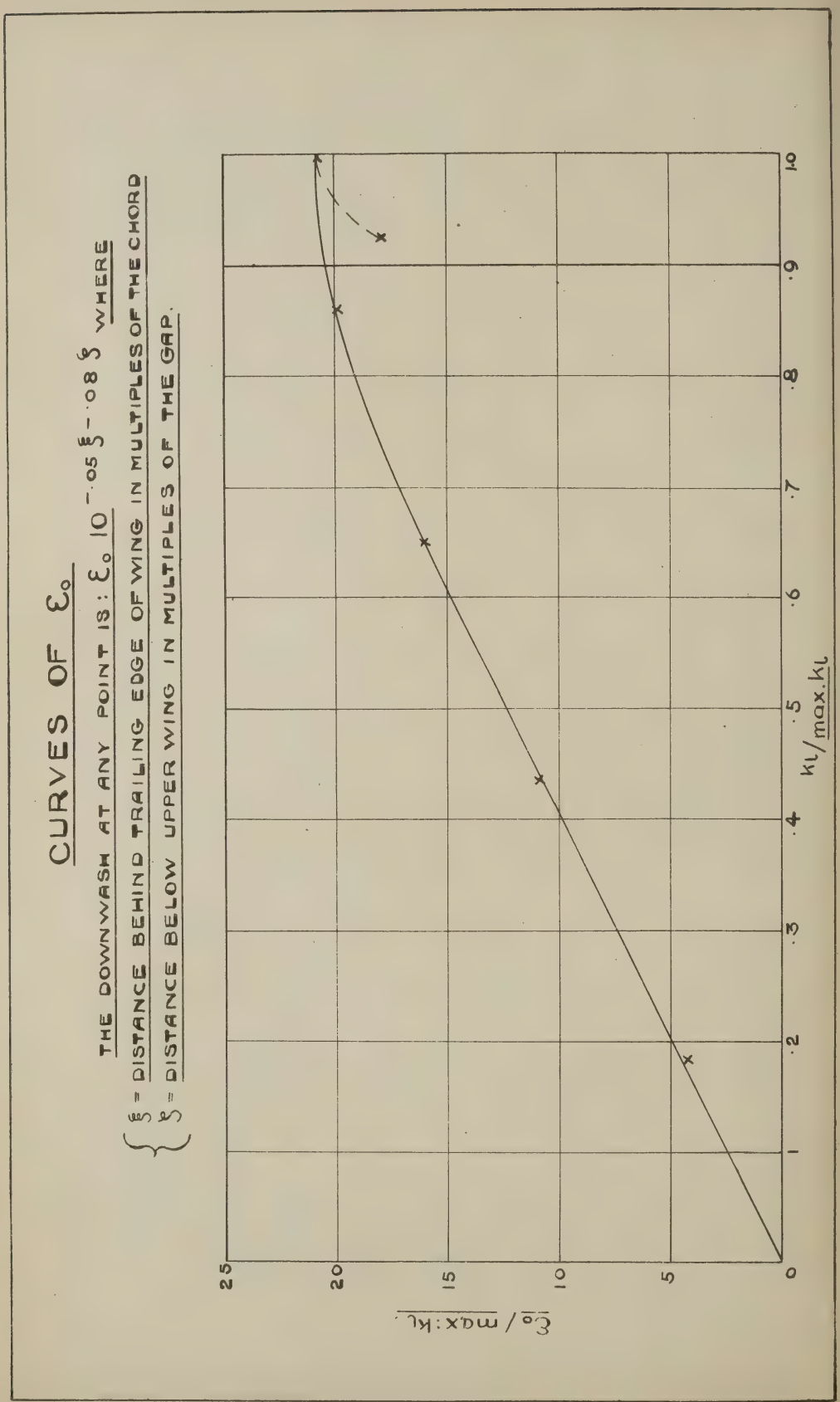
CURVES OF ϵ_0
THE DOWNWASH AT ANY POINT IS: $\epsilon_0 10^{-.05\xi - .08\zeta}$ WHERE
ξ = DISTANCE BEHIND TRAILING EDGE OF WING IN MULTIPLES OF THE CHORD
ζ = DISTANCE BELOW UPPER WING IN MULTIPLES OF THE GAP.
ϵ_0 / max. k_l
25
20
15
10
5
0
0
.1
.2
.3
.4
.5
.6
.7
.8
.9
1.0
k_l / max. k_l

Table 4.

DOWNWASH DUE TO WINGS AND TRACTOR BODY.

Airspeed 60 *ft./sec.*

Co-ordinates of Reference Point.		Angle of Incidence (degrees).						
x.	y.	− 4.	0.	+ 4.	8.	12.	16.	20.
9·0	0·04	− 0°9	1°2	3°4	5°3	6°8	7°3	6°4
	1·84	− 0·9	1·3	3·3	5·0	6·2	6·2	5·7
	3·50	− 1·2	1·1	2·7	4·0	5·0	5·1	4·7
4·95	−0·55	− 0·9	1·5	3·5	5·6	7·9	8·7	7·6
	1·98	− 1·2	1·5	3·8	5·6	7·0	7·1	6·5
	3·00	− 1·3	1·3	3·4	5·2	6·2	6·4	5·8

Note.—x is the distance of the reference point behind the trailing edge of the wings measured parallel to the chord, and y is the depth below the upper wing.

Table 5.

VALUES OF ε_0.

θ (degrees).	k_l.	k_l/max k_l.	ϵ_0.	ϵ_0/max. k_l.
0	0·094	0·183	2·1	4·1
4	0·224	0·436	5·6	10·9
8	0·334	0·65	8·2	16·0
12	0·443	0·86	10·2	19·9
16	0·513	1·00	10·6	20·7
20	0·475	0·925	9·2	17·9

THE LONGITUDINAL CONTROL OF AN AEROPLANE.

By H. Glauert, of the Royal Aircraft Establishment.

Presented by the Director General of Aircraft Production.

Reports and Memoranda, No. 470. *May,* 1918.

Summary.—(a) *Introductory.* (*Reasons for Inquiry.*)—In view of the difficulty of pulling certain types of aeroplanes out of a dive an investigation has been made into the general character of the problem of longitudinal control showing the effect of the size of the tail plane and the position of the centre of gravity on the force necessary to hold an aeroplane in different flying attitudes.

(b) *Range of the Investigation.*—Calculations were made for a fictitious aeroplane consisting of a monoplane main structure to obtain the force on the control column and the elevator angle in all attitudes. The variations considered comprised (*a*) change of position of centre of gravity, (*b*) change of tail setting, (*c*) change of tail area. Calculations were made both with engine on and gliding.

(c) *Conclusions.*—The forces necessary to control the aeroplane at high speed are large unless the tail setting is adjusted to trim it in this attitude. With the centre of gravity far back this force becomes a large pull and the aeroplane may be dangerous to fly.

The forces are all reduced if a smaller tail plane is used, but the load per square foot on the tail plane is increased proportionally. For any particular wing section it should be possible to choose the centre of gravity and the tail plane area so that the force on the control column never rises too high and that the tail plane is not unduly stressed. The effect of shutting off the engine will also be of least importance when the control forces are small.

1. The object of the work described in this report has been to obtain the variation of the force on the control column and of the elevator angle to hold an aeroplane in different attitudes with varying positions of the centre of gravity, with varying size of tail plane, and with different tail settings. For this purpose a fictitious aeroplane has been considered of weight 1,800 lbs., and wing area 240 sq. ft., so that the forces are of the same magnitude as for a scout. The wing characteristics were taken from model tests on a R.A.F. 14 monoplane wing at *lv* 10. The values used are shown in Figs. 2 and 3. Tail planes of two different sizes (40 and 25 sq. ft.) have been used, their characteristics being derived partly from model and partly from full scale tests. The

setting of the tail plane relative to the wings was varied over the range $-2°{\cdot}5$ to $+2°{\cdot}5$. The lift coefficient curves are shown in Fig. 4, and the moment about the hinge of the elevators at 100 f.p.s. (M) was taken to be

$$-1{\cdot}4\theta' - 3{\cdot}0\eta \text{ for the 40 sq. ft. tail plane,}$$

and

$$-0{\cdot}7\theta' - 1{\cdot}5\eta \text{ for the 25 sq. ft. tail plane,}$$

where θ' is the angle of incidence and η the elevator angle. The moments of the weight of the elevators were taken to be 6 and 3 lbs. ft. respectively. The tail planes were assumed to be half in the propeller slip stream.

Other numerical data used were :—

C.G. coeffts. $\begin{cases} h = 0{\cdot}3,\ 0{\cdot}4 \text{ and } 0{\cdot}5 \text{ of chord along chord.} \\ k = \frac{1}{3} \text{ of chord perpendicular to chord.} \end{cases}$

Ratio of length from C.G. to tail plane to chord of wing

$$\frac{l}{b} = {\cdot}3.$$

Resistance at 100 f.p.s., $r = 100$ lbs.

Downwash angles, from model tests as in Fig. 4.

Thrust of propeller $\begin{cases} 740 \text{ lbs. at } 80 \text{ f.p.s.} \\ 610 \quad ,, \quad 120 \quad ,, \\ 530 \quad ,, \quad 160 \quad ,, \end{cases}$

2. The notation used in the analysis is given in full in the appendix to this report. Writing K for the moment coefficent of the wings about the centre of gravity, so that

$$K = k_m + h\,k_l + k\,k_x,$$

the equations determining the motion are as follows :—

$$(1) \quad \bar{k}_l = k_l + \tfrac{1}{3}K,$$

the effective lift coefficient of the aeroplane being the sum of the lift coefficients of the wings and tail plane.

$$(2) \quad \bar{k}_l\,V^2 = 3160 \cos \alpha,$$

resolving at right angles to the flight path.

$$(3) \quad \tan \alpha = \frac{k_d + 0{\cdot}0174\,S}{\bar{k}_l} - \frac{T}{W}$$

to determine the inclination of the flight path.

$$(4) \quad \theta' = \theta + \Psi - \varepsilon,$$

to give the tail incidence in terms of the wing incidence, tail setting and downwash.

$$(5) \quad k'_t = \frac{AK}{3\ A'S}$$

to give the tail lift coefficient in terms of the moment coefficients and slipstream factor.

$$(6) \quad F = M\,S\,V^2\,10^{-4} + w\cos\alpha,$$

which determines the force on the control column from the speed and the tail plane characteristics.

V is the velocity in f.p.s. and the gearing is supposed to be such that the force on the control column in lbs. is numerically equal to the moment about the hinge of the elevators in lbs. ft.

The effect of the engine is allowed for by means of the thrust T in equation (3) and of the slipstream factor S. The lifting effect of the propeller and the effect on the downwash angles are small and are neglected.

3. *Speed and rate of climb.*—The speed and rate of climb of the aeroplane in any attitude depend slightly on the position of the centre of gravity owing to the changing tail lift, but the effect is almost negligible. The values given in Table 1 and Figs. 5 and 6 correspond to the most forward position of the centre of gravity ($h = 0{\cdot}3$). They are independent of the tail setting, as a change of tail setting only changes the distribution of load between the tail plane and elevators. The only point of interest is the rapid rise of the speed and of the loss of height gliding near no lift (angle of incidence $-2°$). This is the point where the aeroplane dives vertically at its terminal velocity.

4. *Tail settings to trim.*—Table 2 and Figs. 7 and 8 give the tail settings necessary to trim in different attitudes from 0° to 16° wing incidence with different centres of gravity and different tail areas. To trim near stalling a large negative tail setting is required, but this angle changes very rapidly with change of attitude. With the centre of gravity forward the aeroplane will dive when the engine is shut off, and with the centre of gravity back it will tend to stall. Both these effects are due to the decreased velocity over the tail plane when the engine is shut off, and appear in the equations as a change in the value of S. With the centre of gravity in its forward position there is only one trimming attitude for a given tail setting within the range considered, and this will be a position of stable equilibrium. With the centre of gravity further back two positions of equilibrium may be obtained, a stable one near stalling and an unstable one at a higher speed, *i.e.*, at a smaller angle of incidence. The effect of reducing the tail area is mainly to increase the required angles of tail setting, and has no appreciable effect on the type of the curves.

5. *Force on control column and elevator angle.*—Tables 3 to 8 and Figs. 9 to 16 give the force on the control column and the elevator angle to hold the aeroplane in different attitudes. The results are given for three positions of the centre of gravity, two sizes of tail plane and for two different tail settings in each case. The analysis is continued to large negative angles of incidence with the engine off.

The most noticeable characteristics of the force diagrams is the sharp peak which generally occurs at an incidence of — 2°. This corresponds to the terminal velocity of the aeroplane, all the forces being accentuated owing to the large velocity at this point. For a very stable aeroplane (C.G. forward) this gives a large negative force, *i.e.*, a push on the control column, so that it may be impossible to force the aeroplane into this attitude or at any rate to hold it there when the speed has risen to its full value. This condition is exemplified in many stable aeroplanes which are impossible to dive steeply for any length of time, *e.g.*, the B.E.2*c*, F.E.2*b*, De H.2. For an unstable aeroplane (C.G. back) this large force at terminal velocity may be a pull as in the case of Fig. 11, tail setting 2°·5. In this case the aeroplane may become dangerous to handle, for if the aeroplane gets into a steep dive the pilot may not have sufficient strength to prevent it turning over on its back and assuming its stable position of equilibrium at a negative angle of incidence. An example of this dangerous type of instability is the De H.6. With the smaller tail plane (Fig. 14) the necessary pull does not rise to such a high value, and so the aeroplane will be easier to handle in this respect. On the other hand, the load per sq. ft. of the tail plane will be higher for the small tail plane.

The elevator angles show no very marked peculiarity. Larger angles are required with the smaller tail plane, but these do not reach the limit usually possible on an aeroplane except quite close to the stalling attitude or at a high negative angle of incidence. An example of the large elevator angles required with a small tail plane and a forward C.G. is the R.E.9, which becomes difficult to land without a large amount of weight in the passenger's seat. It is impossible to float along just over the ground with the engine off after the speed has dropped below about 50 m.p.h. owing to the elevator control being insufficient as regards the angle obtainable. The necessary angular movements are much smaller with the engine on than when gliding.

5. The choice of the best position of the centre of gravity and of the best size of tail plane appears to be limited by the following considerations :—

(1) If the centre of gravity is far forward and the aeroplane is very stable, it will require considerable forces on the control stick to hold the aeroplane away from its trimming attitude, and there will be a considerable download on the tail plane.

(2) If the centre of gravity is far back the forces will also be considerable and the aeroplane may be dangerous to handle at high speeds, but this latter difficulty may be overcome by trimming the aeroplane at a very low speed (*cf.* Fig. 11).

(3) The forces can be reduced in all cases by fitting a smaller tail plane, but this will increase the load per sq. ft. and so can only be carried out to a limited extent.

The best arrangement of those examined in this report appears to be the case with centre of gravity at 0·4, tail area 25 sq. ft., and tail setting 0°. The aeroplane is then in trim at 57 m.p.h with engine on, and at 53 m.p.h. gliding. The force does not rise above 5 lbs. except near the stalling point where it reaches about 15 lbs. and at large negative angles of incidence. The aeroplane is in fact almost neutral throughout its flying range. The elevator movement also is not excessive, and a range of 20° on either side would be sufficient to hold the aeroplane in any flying attitude. The load per square foot on the tail plane is less than 2 lbs. over the greater part of the range and only reaches 7 lbs. at the terminal velocity. With this arrangement the aeroplane is stable gliding with a period of 11 seconds and engine on with a period of 13 secs.

6. The period of longitudinal oscillation has been estimated by the method developed in T.1038. The results are given in Table 9 and Fig. 17 shows the difference with engine on and off in one case, assuming the line of thrust of the propeller to pass through the centre of gravity of the aeroplane. With the centre of gravity at 0·3 the aeroplane is stable throughout the flying range, but in the other two positions the machine becomes unstable at high speeds. The aeroplane is stable near the stalling point for all conditions.

NOTE.—The numerical results of this report cannot be applied directly to any definite aeroplane as allowance must be made for the effects of the arrangement of the biplane structure on the position of the centre of pressure, &c., but the general conclusions as to the effect of the movement of centre of gravity and change of tail plane area on control forces still hold good.

APPENDIX.

NOTATION USED IN THE ANALYSIS.

(See also Fig. 1.)

W = total weight of aeroplane.
A = wing area.
A′ = tail area.
w = weight moment of elevators about hinge.
T = thrust.
R/R_o = slipstream factor.
S = $\frac{1}{2}(1 + R/R_o)$.
r = resistance at 100 f.p.s.
h, k = C.G. coefficients.
b = wing chord.
l = distance from C.G. to C.P. of tail plane.
k_l = lift coefficient. } of wings.
k_d = drag coefficient. } of wings.
k_z = normal force coefficient } of wings.
k_x = longitudinal force coefficient. } of wings.
k_m = moment coefficient. } of wings.
k'_l = lift coefficient of tail planes.
M = moment of air forces about elevator hinge at 100 f.p.s.
K = $k_m + h\,k_l + k\,k_x$.
$\bar{k}_l$ = effective lift coefficient of wings, allowing for tail lift.
α = angle of dive.
θ = angle of incidence.
θ' = angle of tail incidence.
ψ = angle of tail setting.
ε = angle of downwash.
η = elevator angle.

TABLE 1.

SPEED AND RATE OF CLIMB.

C.G. at $h = 0{\cdot}3$.

Angle of Incidence.	Speed, m.p.h.	Rate of climb, Engine on. Ft. per min.	Rate of climb, Engine off. Ft. per min.
− 25	62		2980
− 20	65½		2750
− 16	68		2500
− 12	71½		2200
− 8	79		2040
− 6	93½		2640
− 4	132		5580
− 2	216		18050
0	123	− 960	3270
+ 2	90	+ 890	1310
4	74	1180	790
6	65	1240	650
8	59	1210	570
12	53	1080	610
16	52	520	1130
18	52½	+ 190	1460
20	54	− 170	1770

TABLE 2.

TAIL SETTINGS TO TRIM IN VARIOUS ATTITUDES.

(1) Tail area 40 sq. ft.

Angle of Incidence.	Tail settings with engine on.			Tail settings, gliding.		
	$h = 0{\cdot}3$	$h = 0{\cdot}4$	$h = 0{\cdot}5$	$h = 0{\cdot}3$	$h = 0{\cdot}4$	$h = 0{\cdot}5$
0	− 0·5	0·6	1·7	− 0·9	0·4	1·7
2	− 1·1	0·7	2·4	− 2·0	0·5	3·1
4	− 1·6	0·5	2·7	− 3·1	0·7	4·5
6	− 2·4	+ 0·0	2·4	− 4·4	0·4	5·2
8	− 3·4	− 0·7	2·0	− 5·0	+ 0·0	5·9
12	− 6·5	− 3·4	− 0·4	− 9·1	− 1·8	5·2
16	− 11·3	− 8·0	− 4·8	− 14·8	− 7·3	0·4

(2) Tail area 25 sq. ft.

Angle of Incidence.	Tail settings with engine on.			Tail settings, gliding.		
	$h = 0{\cdot}3$	$h = 0{\cdot}4$	$h = 0{\cdot}5$	$h = 0{\cdot}3$	$h = 0{\cdot}4$	$h = 0{\cdot}5$
0	− 1·5	0·3	2·0	− 2·1	0·0	2·2
2	− 1·9	0·9	3·7	− 3·2	0·8	5·0
4	− 2·3	1·1	4·5	− 4·3	1·8	7·8
6	− 3·1	0·8	4·7	− 5·6	2·1	10·5
8	− 4·0	+ 0·3	4·7	− 7·2	2·2	—
12	− 6·9	− 1·9	+ 2·9	− 10·2	+ 1·4	—
16	− 12·2	− 6·9	− 1·7	− 16·9	− 4·8	—

Table 3.

FORCE ON CONTROL COLUMN WITH ENGINE ON.

Tail area.	C.G. coefft.	Tail setting.	Angle of Incidence. 0	2	4	6	8	12	16
40	0·3	−2·5	−30	−13	− 7	0	5	20	43
		0	7	10	12	15	19	32	55
		2·5	44	33	30	31	33	44	66
	0·4	−2·5	−45	−29	−22	−16	−10	4	26
		0	− 9	− 6	− 4	0	4	16	38
		2·5	27	16	14	15	18	28	49
	0·5	−2·5	−59	−43	−36	−30	−24	−10	11
		0	−24	−21	−18	−15	−11	2	22
		2·5	11	1	− 1	1	3	14	27
25	0·3	−2·5	− 7	− 3	− 1	2	4	11	24
		0	11	9	8	10	12	17	30
	0·4	−2·5	−20	−15	−13	−10	− 8	− 1	11
		0	− 2	− 4	− 4	− 3	− 1	5	17
	0·5	0	−14	−16	−16	−14	−12	− 7	4
		2·5	3	− 5	− 7	− 7	− 6	− 1	10

Table 4.

FORCE ON CONTROL COLUMN GLIDING.

Tail area = 40 sq. ft.

Angle of Incidence.	C.G. coefficient.	0·3		0·4		0·5	
	Tail setting.	− 2·5	0	− 2·5	0	0	2·5
	−25	—	—	—	—	−28	−26
	−20	—	—	—	−44	−28	−21
	−16	—	−62	− 47	−40	−24	−17
	−12	− 54	−44	− 38	−27	−12	− 3
	− 8	− 34	−22	− 18	− 7	+ 8	+19
	− 6	− 37	−20	− 22	− 5	9	25
	− 4	− 58	−24	− 43	−10	+ 3	36
	− 2	−115	−25	−122	−32	−39	51
	0	− 19	+11	− 34	− 5	−19	+ 8
	+ 2	− 3	12	− 18	− 3	−18	− 3
	4	+ 2	13	− 13	− 3	−17	− 8
	6	6	14	− 9	− 1	−16	− 9
	8	9	16	− 7	0	−15	− 9
	12	14	20	− 1	+ 4	−10	− 5
	16	26	31	+ 10	15	− 1	+ 4
	18	37	45	20	24	+ 9	12
	20	—	—	32	38	19	20

Table 5.

FORCE ON CONTROL COLUMN GLIDING.

Tail area 25 sq. ft.

	C.G. coefft.	0·3		0·4		0·5	
	Tail setting.	− 2·5	0	− 2·5	0	0	2·5
Angle of Incidence.	− 25	—	—	—	—	− 5	− 6
	− 20	—	—	—	− 21	− 6	− 5
	− 16	—	− 32	− 22	− 18	− 6	− 3
	− 12	− 30	− 24	− 16	− 11	0	+ 5
	− 8	− 16	− 10	− 3	2	+ 14	20
	− 6	− 16	− 7	− 4	4	16	24
	− 4	− 23	− 6	− 12	4	+ 15	31
	− 2	− 42	+ 3	− 48	− 2	− 8	37
	0	− 2	12	− 14	0	− 12	+ 3
	+ 2	+ 2	10	− 10	− 2	− 14	− 7
	4	4	9	− 9	− 3	− 16	− 11
	6	5	9	− 7	− 3	− 15	− 11
	8	6	10	− 6	− 3	− 15	− 12
	12	8	11	− 4	− 1	− 13	− 10
	16	15	18	+ 2	+ 5	− 8	− 5
	18	22	—	9	12	− 2	− 1
	20	—	—	16	—	4	5

Table 6.

ELEVATOR ANGLES WITH ENGINE ON.

Tail area.	C.G. coefft.	Tail setting.	Angle of Incidence.						
			0	2	4	6	8	12	16
40	0·3	− 2·5	4·8	4·2	3·4	2·2	0·7	− 4·3	− 12
		0	0·6	0·0	− 0·8	− 2·0	− 3·5	− 8·5	− 16
		2·5	− 3·5	− 4·2	− 4·9	− 6·1	− 7·6	− 12·6	− 20
	0·4	− 2·5	6·2	6·3	6·0	5·1	4·0	− 0·5	− 8
		0	2·0	2·1	1·8	0·9	− 0·2	− 4·7	− 12
		2·5	− 2·2	− 2·1	− 2·3	− 3·2	− 4·3	− 8·9	− 16
	0·5	− 2·5	7·5	8·1	8·6	8·0	7·2	3·1	− 41
		0	3·3	4·2	4·4	3·8	3·1	− 1·0	− 8·2
		2·5	− 0·8	0·0	0·2	− 0·3	− 1·1	− 5·2	− 13
25	0·3	− 2·5	3·6	3·1	2·5	1·4	− 0·1	− 4·8	− 13
		0	− 0·5	− 1·0	− 1·6	− 2·8	− 4·3	− 9·0	− 17
	0·4	− 2·5	5·7	6·5	6·7	6·1	5·2	1·1	− 6·7
		0	1·6	2·4	2·6	1·9	1·0	− 3·0	− 10·8
	0·5	0	3·8	5·7	6·7	6·5	6·2	2·0	− 4·6
		2·5	− 0·4	1·5	2·5	2·4	2·1	− 1·4	− 9

SKETCH OF MONOPLANE

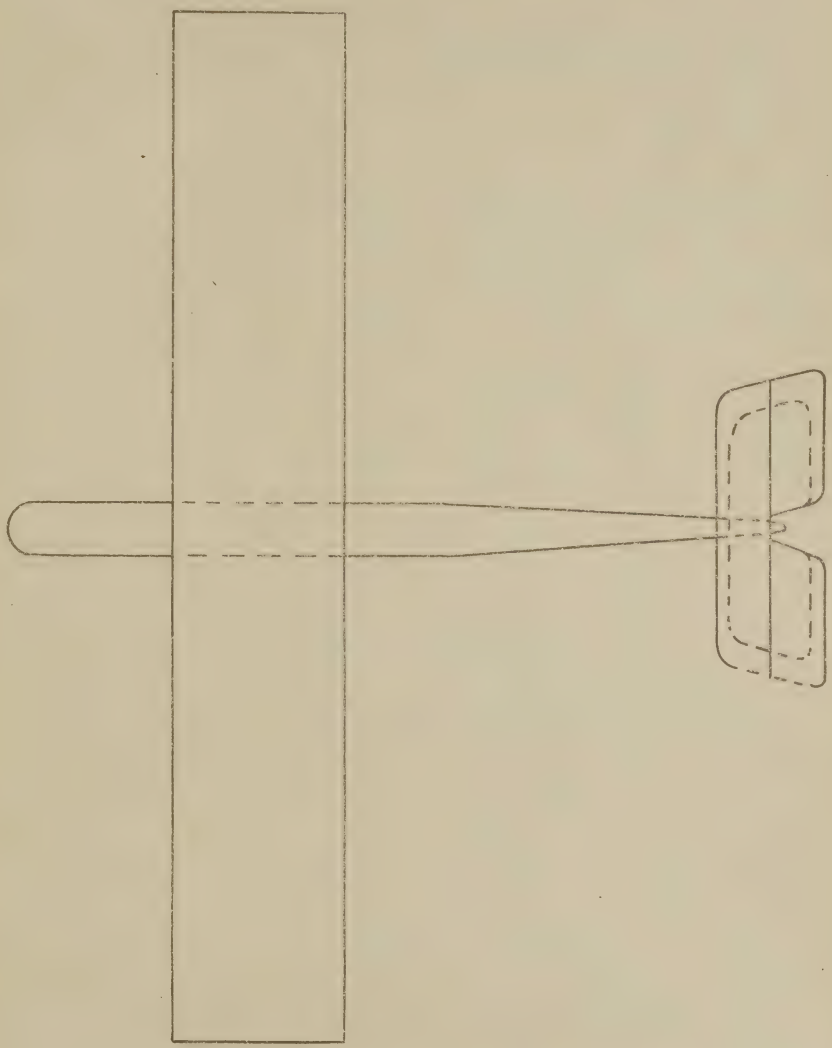

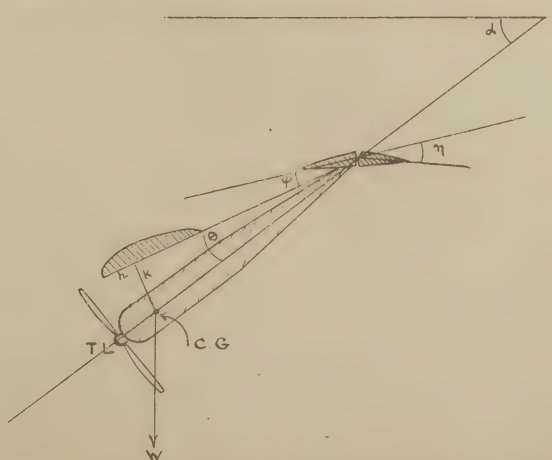

WING CHARACTERISTICS.

DRAG COEFFICIENT

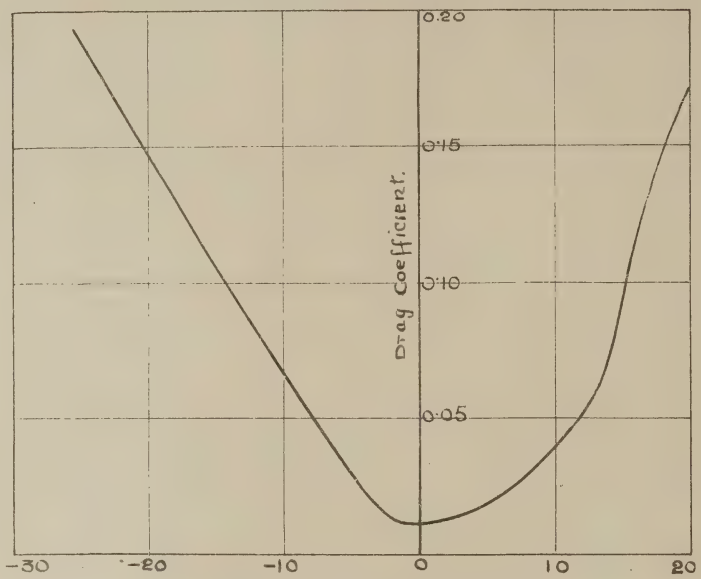

LIFT COEFFICIENT.

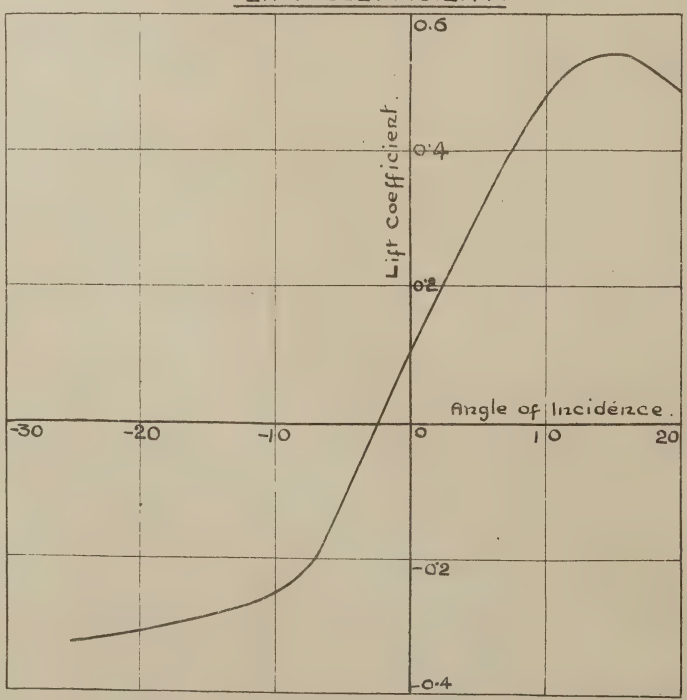

WING CHARACTERISTICS.

MOMENT COEFFICIENT.

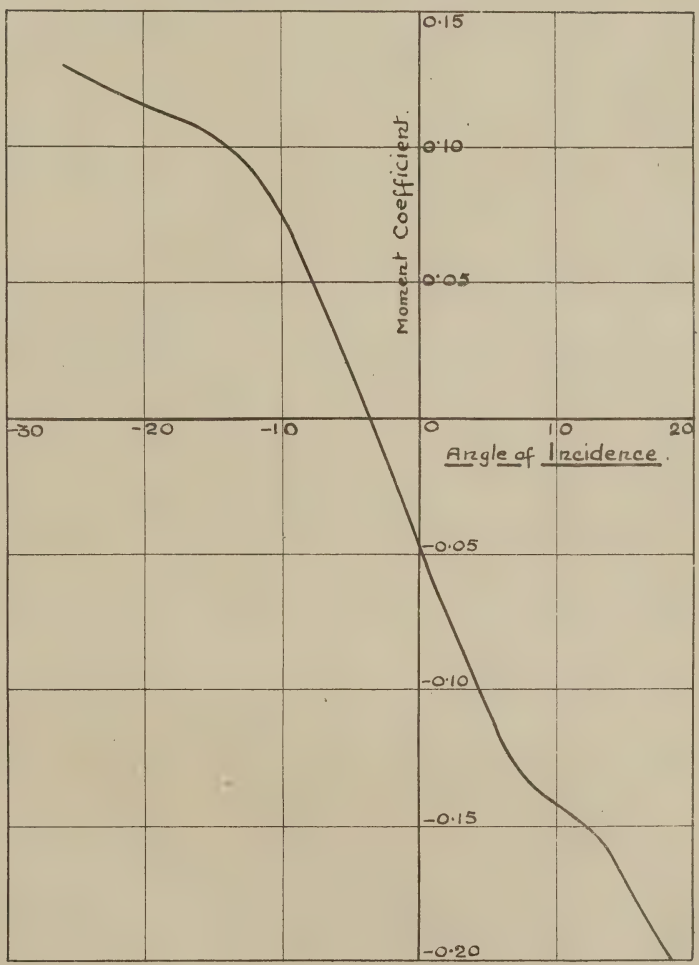

TAIL PLANE CHARACTERISTICS.

LIFT COEFFICIENT.

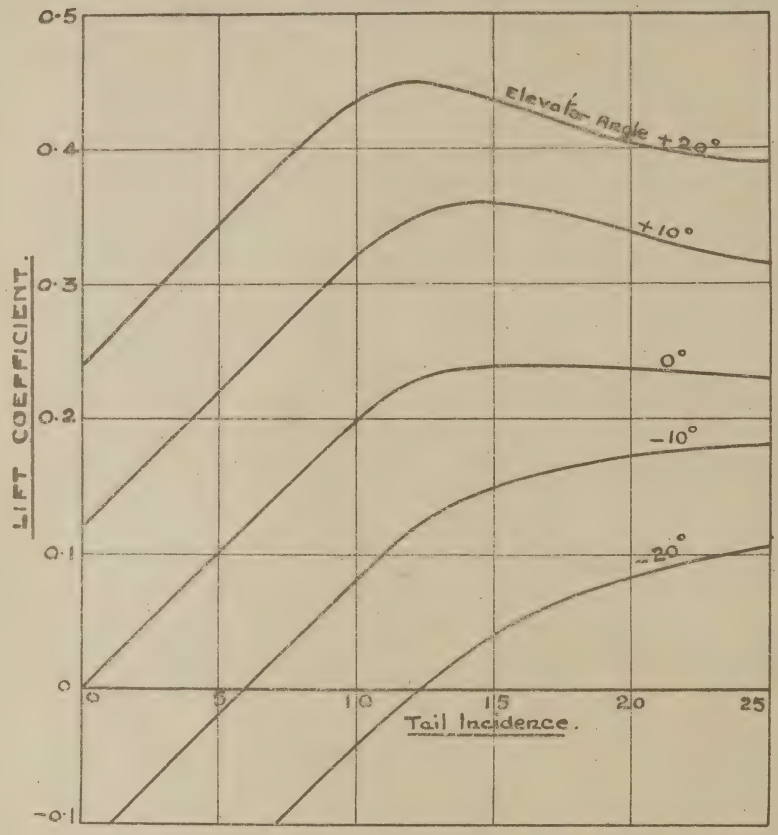

ANGLE OF DOWNWASH

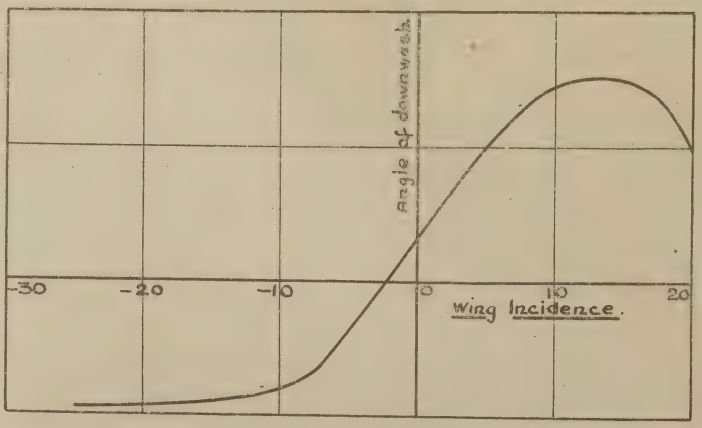

FIG: Nº 5.

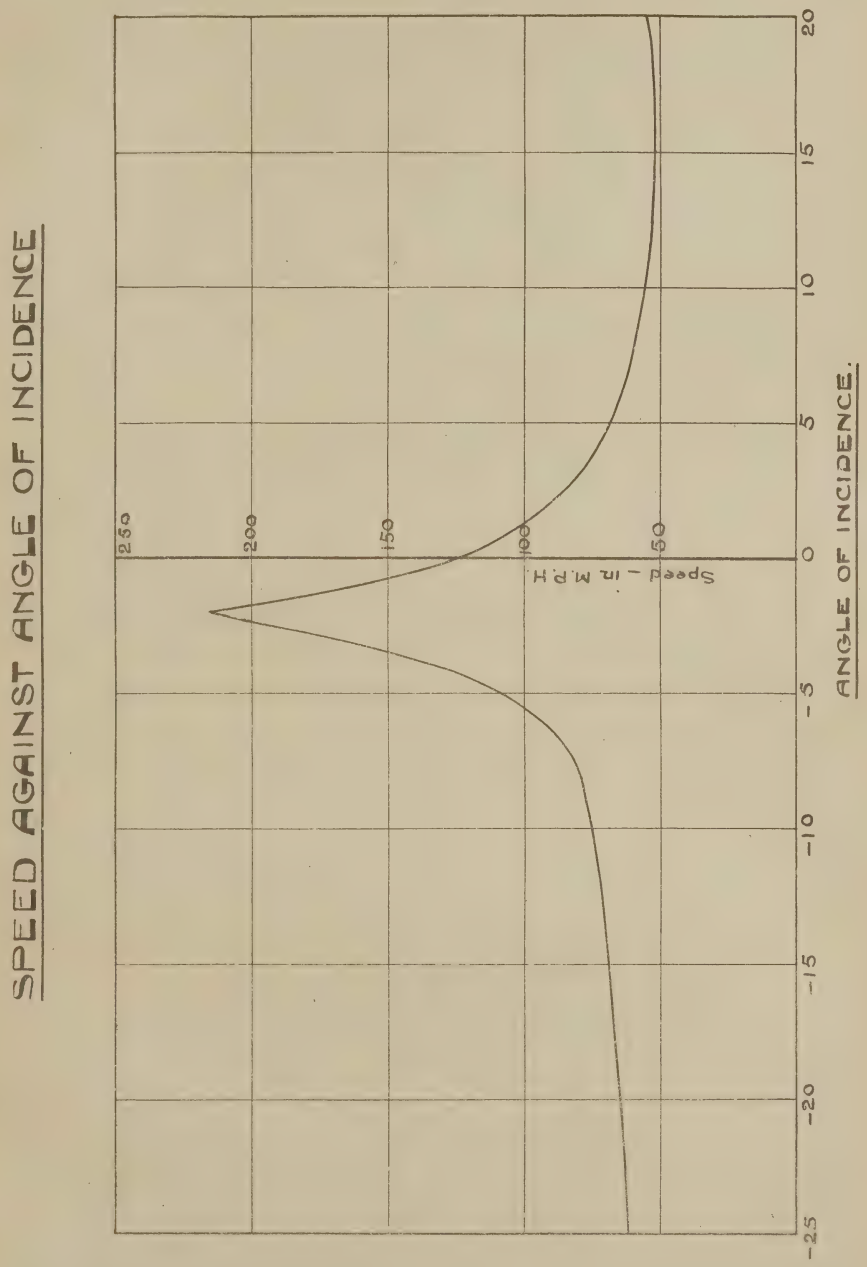
SPEED AGAINST ANGLE OF INCIDENCE
Speed - in M.P.H.
250
200
150
100
50
0
-5
-10
-15
-20
-25
5
10
15
20
ANGLE OF INCIDENCE.

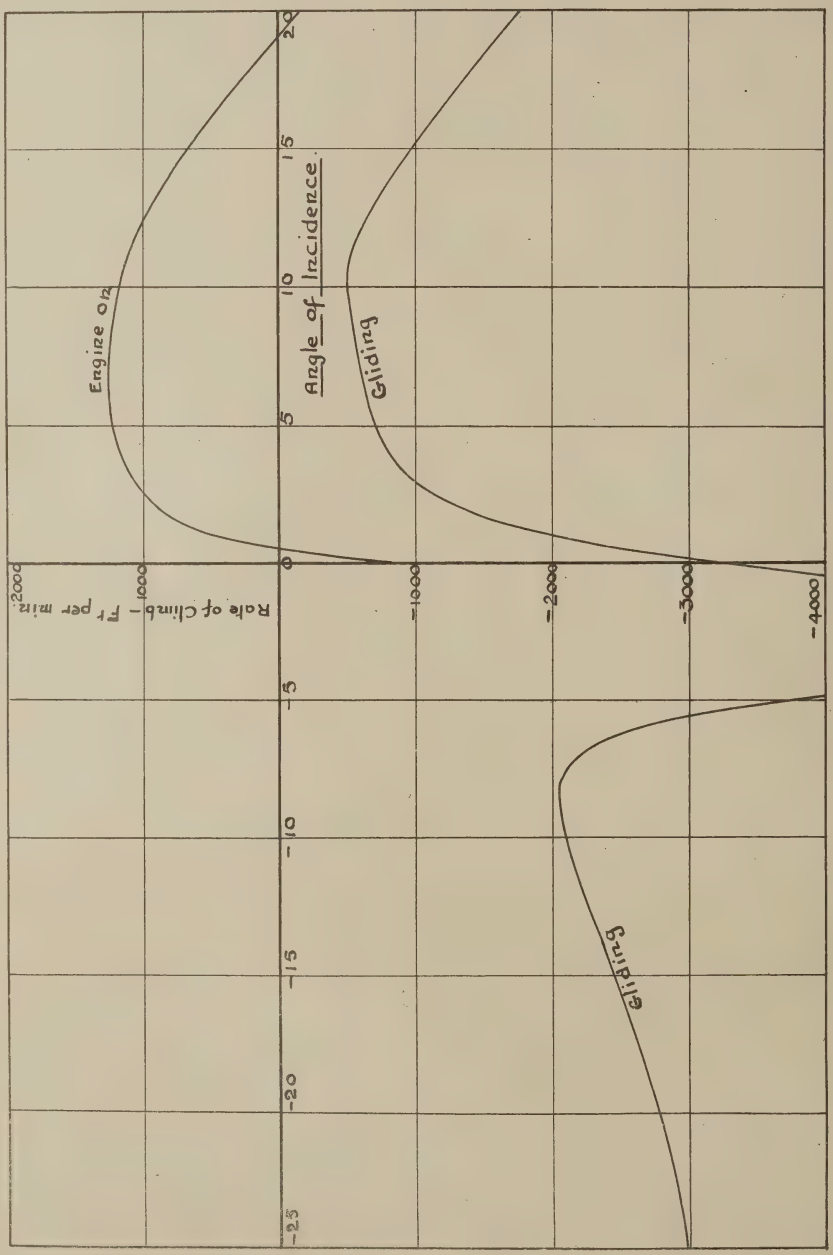
RATE OF CLIMB.
Rate of Climb – Ft per min.
2000
1000
0
-1000
-2000
-3000
-4000
-25
-20
-15
-10
-5
0
5
10
15
20
Angle of Incidence.
Engine on
Gliding
Gliding

TAIL SETTING

WITH TAIL AREA OF 40 SQ. FT.

C.G. AT 0.5.

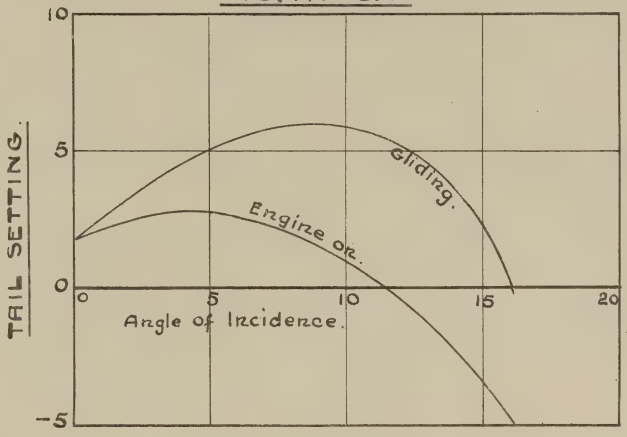

C.G AT 0.4

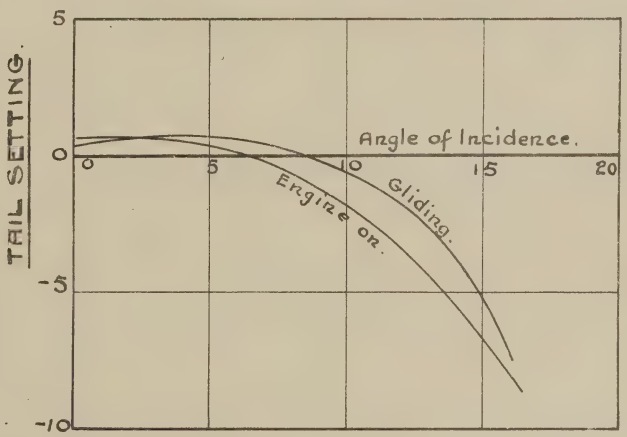

C.G. AT 0.3.

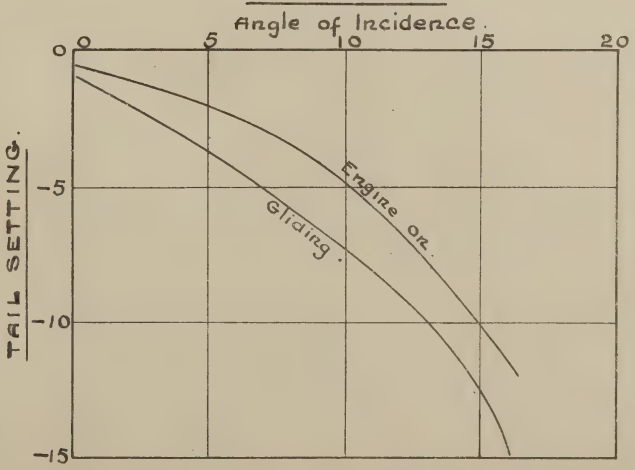

TAIL SETTING

WITH TAIL AREA OF 25 SQ. FT.

C.G. AT 0.5.

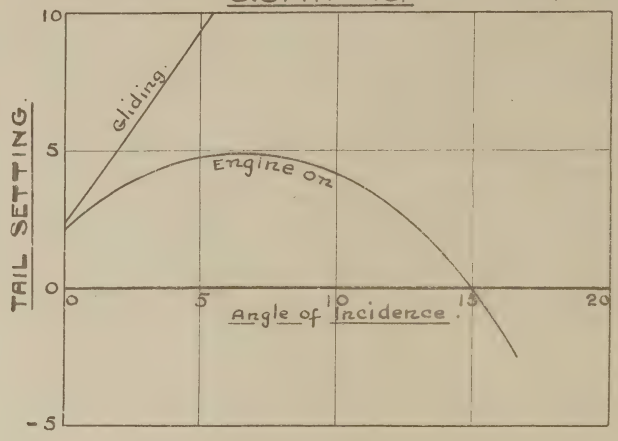

C.G. AT 0·4.

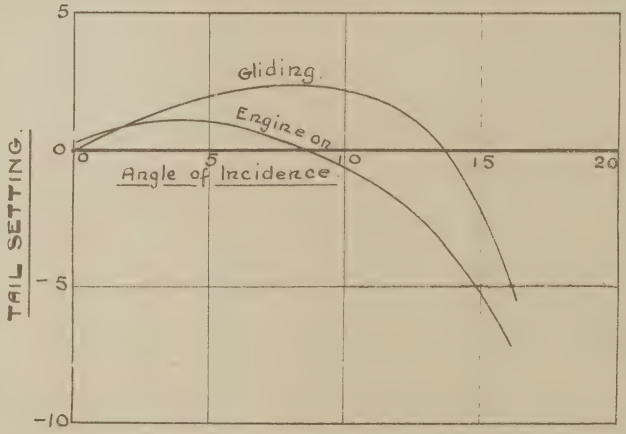

C.G. AT 0.3.

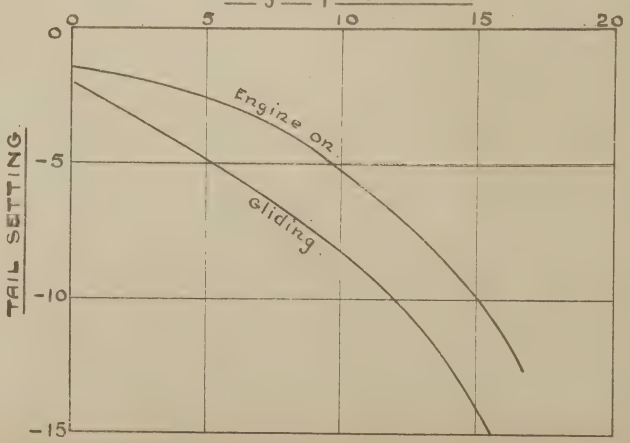

FORCE ON CONTROL COLUMN

C.G. AT 0.3 . TAIL AREA 40 SQ. FT

TAIL SETTING -2° 5

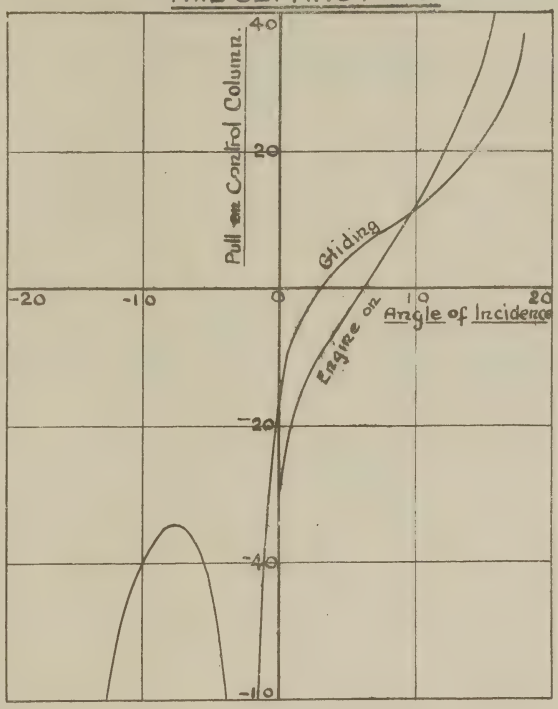

TAIL SETTING. 0°

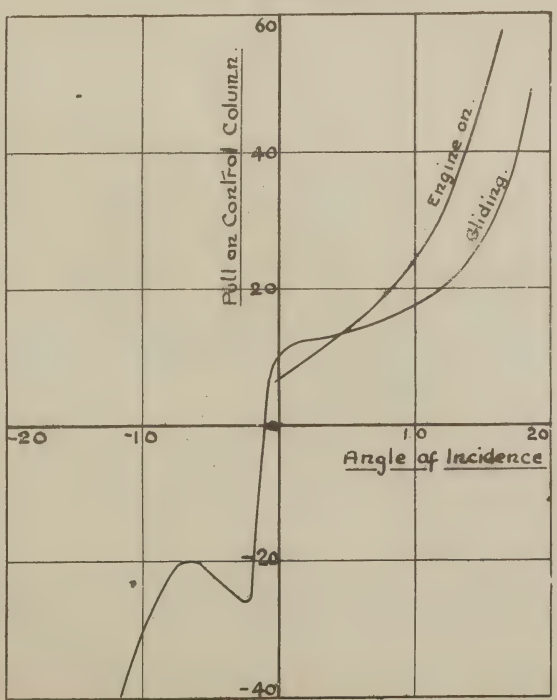

FORCE ON CONTROL COLUMN.

C.G. AT 0·4 . TAIL AREA 40 SQ. FT

TAIL SETTING -2°.5.

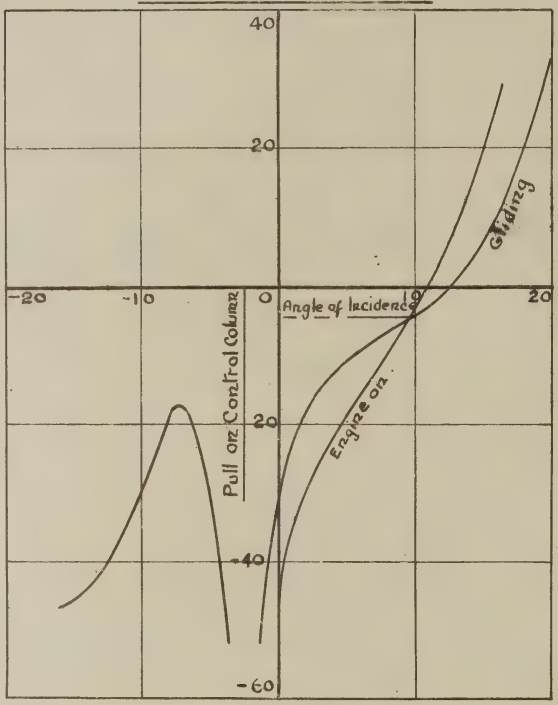

TAIL SETTING 0°.

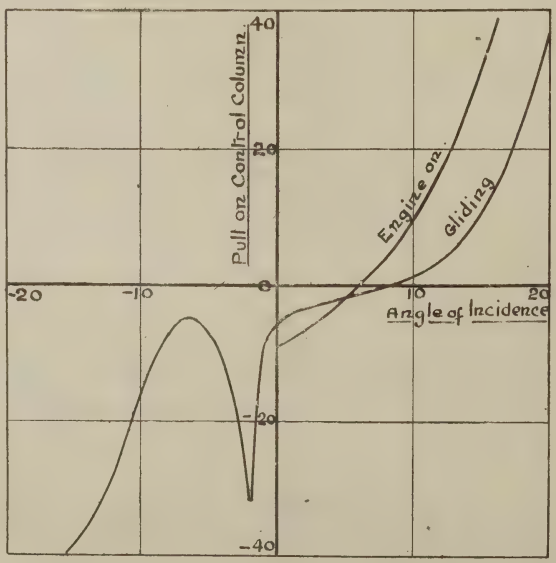

FORCE ON CONTROL COLUMN

C.G. AT 0.5 . TAIL AREA 40 SQ. FT

TAIL SETTING. 0°

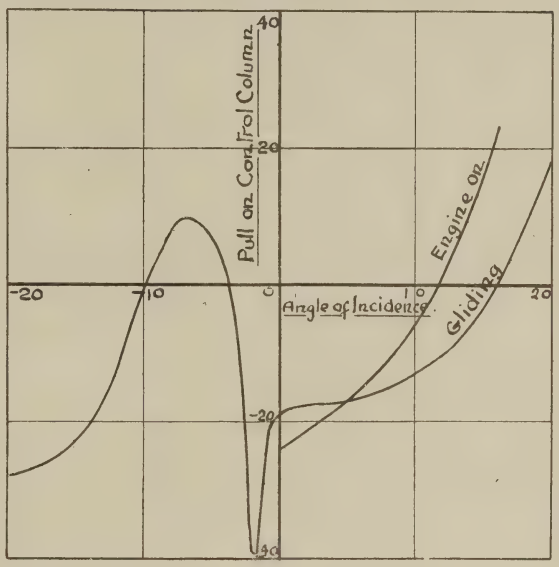

TAIL SETTING 2.5°

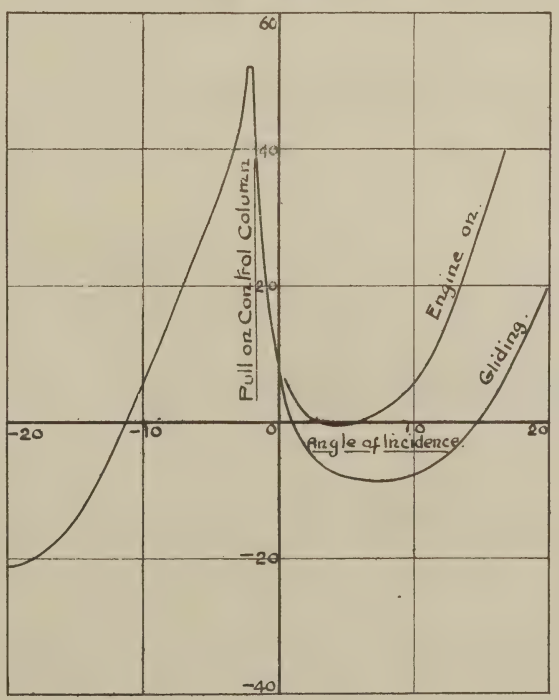

FORCE ON CONTROL COLUMN

C.G. AT 0.3. TAIL AREA 25 SQ FT

TAIL SETTING – 2°.5

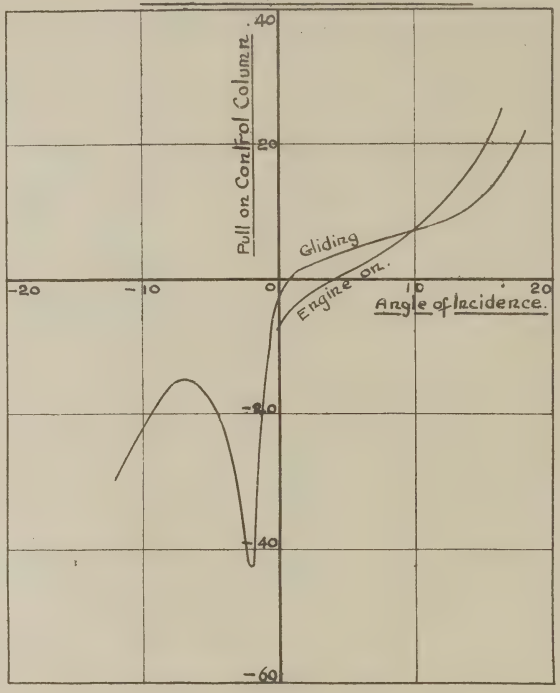

TAIL SETTING 0°

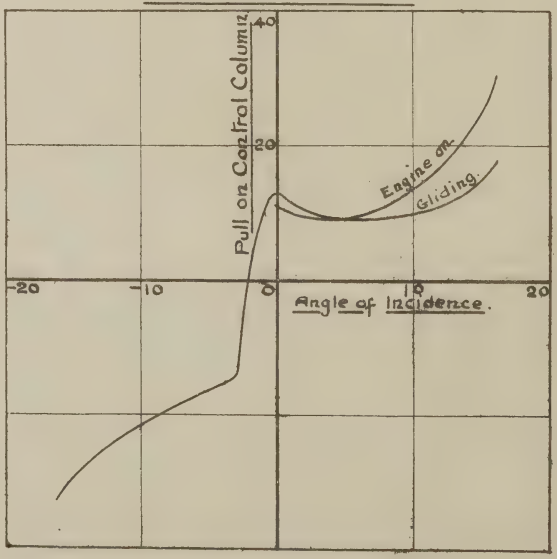

FORCE ON CONTROL COLUMN.

C.G. AT 0·4. TAIL AREA 25 SQ. FT

TAIL SETTING – 2°·5.

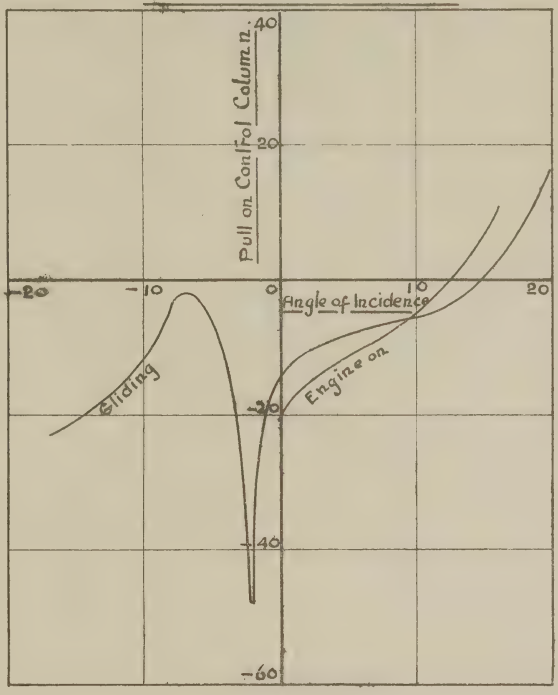

TAIL SETTING 0°

FORCE ON CONTROL COLUMN

C.G. AT 0·5 TAIL AREA 25 SQ. FT

TAIL SETTING 0°

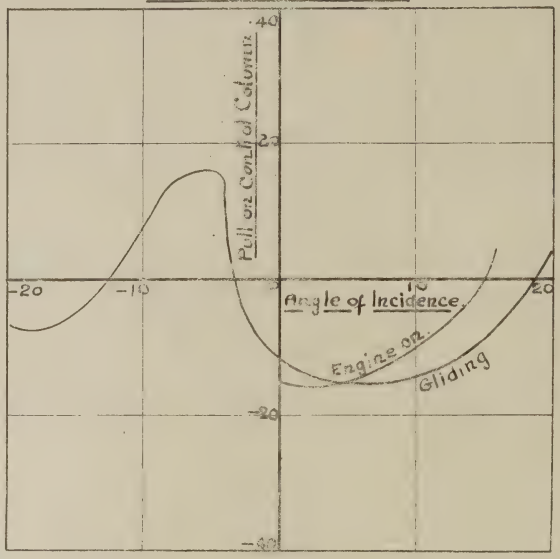

TAIL SETTING 2°.5

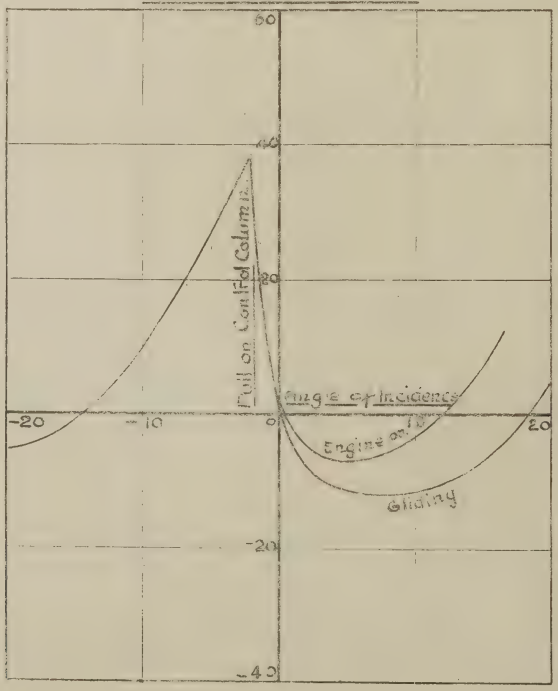

ELEVATOR ANGLES WITH ENGINE ON

TAIL SETTING. 0°

TAIL AREA. 40 SQ. FT.

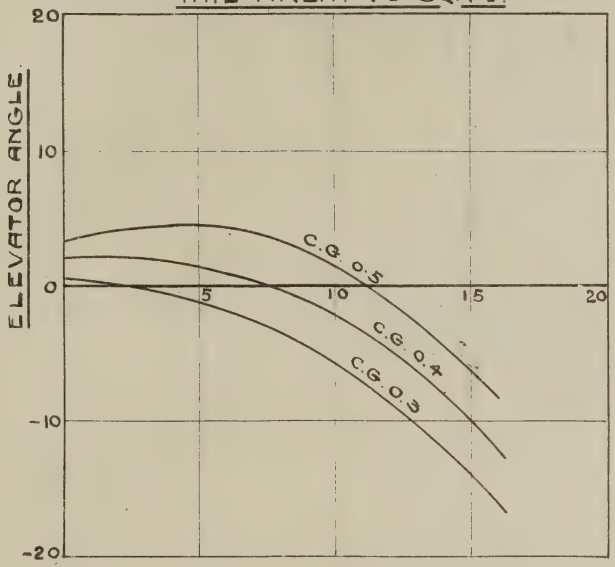

TAIL AREA. 25 SQ. FT.

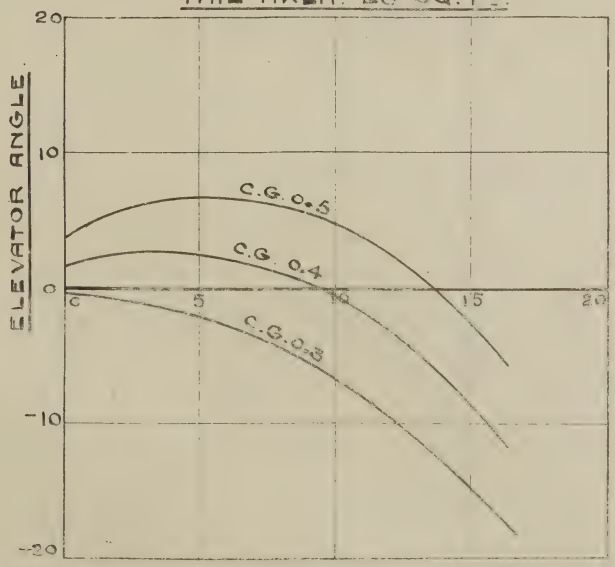

ELEVATOR ANGLES. GLIDING

TAIL SETTING. 0º

TAIL AREA. 40 SQ. FT.

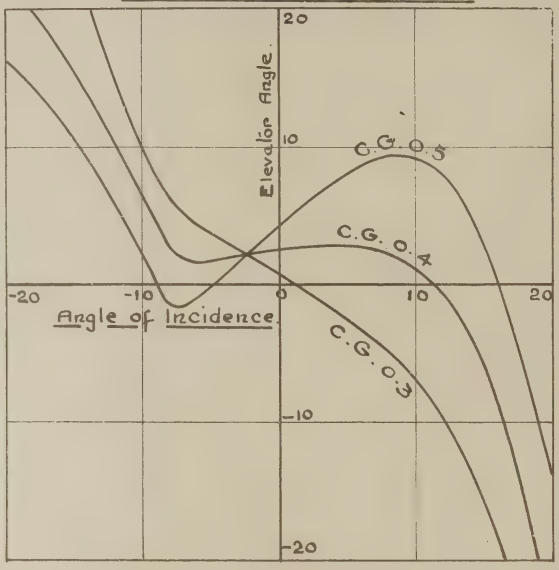

TAIL AREA. 25 SQ. FT.

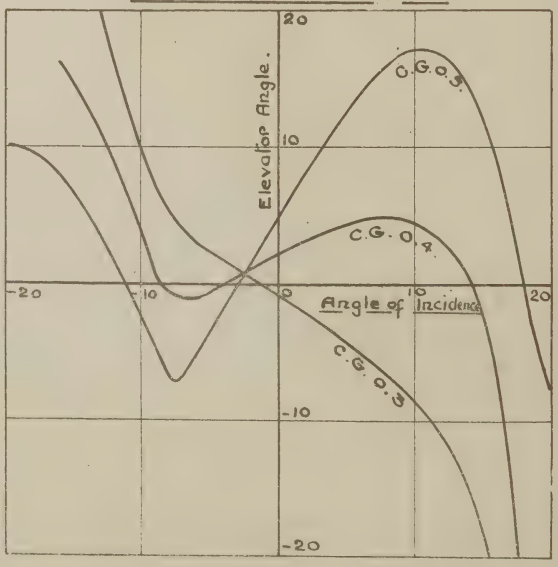

PERIOD OF LONGITUDINAL OSCILLATION.

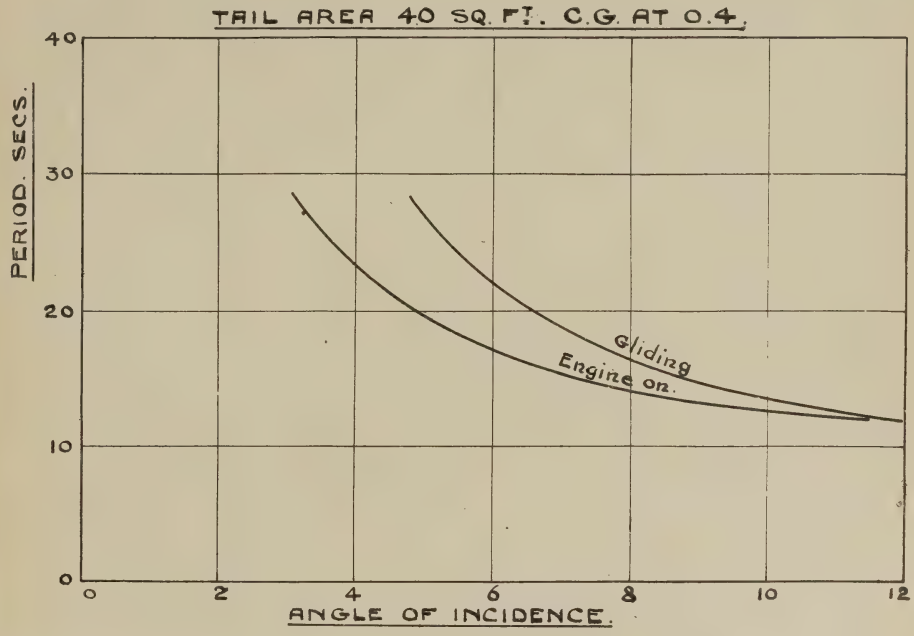

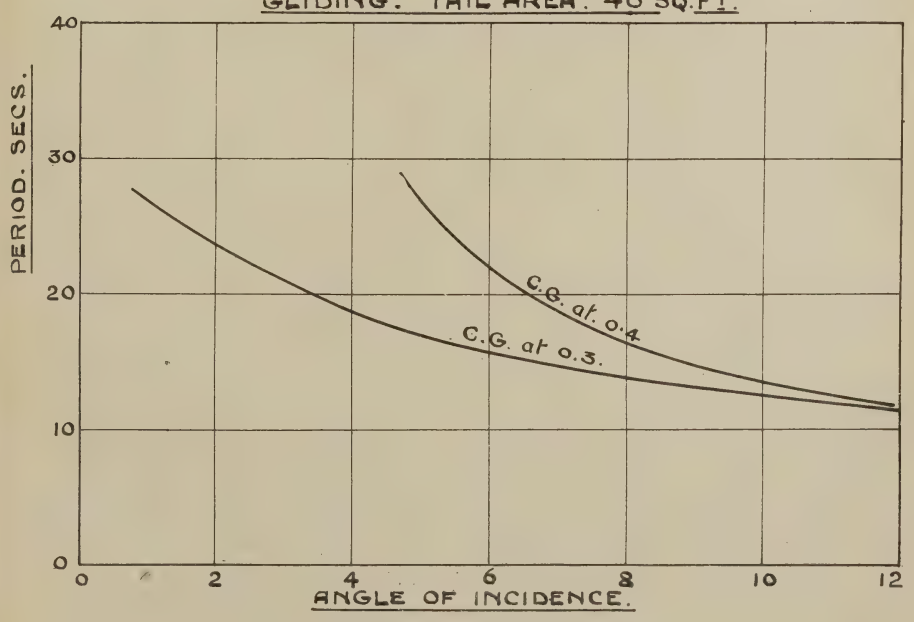

THE LIBRARY
OF THE
UNIVERSITY OF ILLINOIS

Table 7.

ELEVATOR ANGLES GLIDING.

Tail area 40 sq. ft.

	C.G. coefft.	0·3		0·4		0·5	
	Tail setting.	− 2·5	0	− 2·5	0	0	2·5
Angle of Incidence.	− 25	—	—	—	—	19	17
	− 20	—	—	—	22	16	12
	− 16	—	24	21	17	12	8·2
	− 12	19	15	15	10	5·7	+ 1·5
	− 8	10	6·1	6·5	2·3	− 1·5	− 5·7
	− 6	8·3	4·2	5·7	1·5	− 1·1	− 5·2
	− 4	7·1	2·9	5·9	1·7	0·5	− 3·6
	− 2	6·1	1·9	6·3	2·1	2·4	− 1·8
	0	4·4	+ 0·2	6·0	1·8	3·5	− 0·7
	+ 2	3·4	− 0·8	6·4	2·3	5·4	+ 1·2
	4	2·4	− 1·8	6·9	2·8	7·4	3·2
	6	+ 0·9	− 3·3	6·7	2·6	8·4	4·2
	8	− 0·7	− 4·9	6·4	+ 2·2	9·3	5·1
	12	− 5·5	− 9·7	+ 3·2	− 1·0	+ 7·7	+ 3·6
	16	− 14	− 18	− 5·1	− 9·2	0·0	− 4·0
	18	− 22	− 27	− 13	− 16	− 7·0	− 10
	20	—	—	− 20	− 24	− 14	− 16

Table 8.

ELEVATOR ANGLES GLIDING.

Tail area 25 sq. ft.

	C.G. coefft.	0·3		0·4		0·5	
	Tail setting.	− 2·5	0	− 2·5	0	0	2·5
Angle of Incidence.	− 25	—	—	—	—	11	11
	− 20	—	—	—	21	10	8
	− 16	—	25	20	16	8	+ 4·1
	− 12	21	16	13	8·9	+ 1·3	− 2·8
	− 8	9·5	5·3	3·4	− 0·8	− 6·9	− 11·0
	− 6	7·3	3·1	3·1	− 1·1	− 5·3	− 9·4
	− 4	6·0	1·9	4·1	0·0	− 1·9	− 6·1
	− 2	5·0	+ 0·9	5·4	+ 1·3	+ 1·7	− 2·5
	0	2·9	− 1·2	5·5	1·4	4·0	− 0·2
	+ 2	1·9	− 2·2	6·8	2·7	7·7	+ 3·5
	4	+ 0·8	− 3·3	8·2	4·1	11·4	7·2
	6	− 0·6	− 4·8	8·7	4·5	13·8	9·7
	8	− 2·4	− 6·6	9·0	4·8	16·1	12
	12	− 6·8	− 11	+ 7·1	+ 2·9	16·8	13
	16	− 17	− 21	− 2·1	− 6·2	+ 8·6	5
	18	− 26	—	− 11	− 22	0	− 2
	20	—	—	− 20	—	− 8	− 10

Table 9.

PERIOD OF LONGITUDINAL OSCILLATION.

(1) Gliding.

Angle of incidence.	Speed m.p.h.	Tail area 25 sq. ft.			Tail area 40 sq. ft.		
		C.G. at			C.G. at		
		0·3	0·4	0·5	0·3	0·4	0·5
− 1	160	37·5	—	—	38·6	—	—
+ 1	102	26·4	—	—	26·6	—	—
3	80	20·8	—	—	21·0	—	—
5	69	16·8	—	—	17·0	26·9	—
7	61	14·6	—	—	14·8	20·5	—
9	57	13·3	33·4	—	13·2	14·5	90
11	54	12·0	13·5	—	12·0	12·6	14·4
13	53	11·1	11·1	11·2	11·1	11·1	11·2

(2) Engine on.

Angle of incidence.	Speed m.p.h.	Tail area 25 sq. ft.			Tail area 40 sq. ft.		
		C.G. at			C.G. at		
		0·3	0·4	0·5	0·3	0·4	0·5
1	102	38·2	—	—	33·3	85	—
3	80	28·2	—	—	26·0	30·0	—
5	69	19·3	20·3	—	18·6	19·0	19·4
7	61	16·1	16·5	18·3	15·8	16·0	16·0
9	57	13·5	13·3	12·7	13·2	13·1	12·9
11	54	12·3	12·0	11·6	12·2	12·0	11·8
13	53	11·2	11·1	10·9	11·2	11·1	11·0

FULL SCALE EXPERIMENTS WITH DIFFERENT SHAPES OF TAIL PLANE.

By H. Glauert.

Presented by the Superintendent, Royal Aircraft Factory.

Reports and Memoranda, No. 532. *March,* 1918.

Summary.—(a) *Introductory.*—R. and M. 409 dealt with elevators of different size fitted to a standard R.E.8 tailplane (trailing edge longer than leading edge). This report continues the investigation by experiments on tailplanes of 40 per cent. elevator, but with square and reversed shapes.

(b) *Nature of experiment.*—The method of experiment was to determine the force on the control column and the angle at which the elevators were held to keep the machine at a definite trimming speed with different tail settings.

(c) *Conclusions.*—It was found that reversing the shape of the tailplane with 40 per cent. elevator chord was a greater improvement than reducing the elevators to 30 per cent. The square form was intermediate between the reversed and standard forms.

(d) *Applications.*—To secure lightness of control it appears desirable to have tailplanes with small elevator chord and with reduced span at the trailing edge. By analogy it would seem probable that the B.E.2C type of wing tip would secure a better lateral control than the raked tips of B.E.2E or S.E.5 type.

1. This report is a direct continuation of R. and M. 409, in which were given the results of some tests on four different sizes of elevators on R.E.8. The experiments dealt with below consisted of similar tests on two different tailplanes (Fig. 1). The former (E) was of the same area and chord as arrangement B of R. and M. 409, but with reversed shape. The latter (F) was the large square tailplane (65 square feet) which is standard for B.E.2C. The method of experiment was the same as that described in R. and M. 409, namely, to fly at some definite trimming speed with three different tail settings and to note the force on the control column and the angle at which the elevators were held. It was impossible to make the series of observations as complete as was desired owing to the breaking of the aeroplane.

2. The method of analysis is based on a linear variation of the tail lift coefficient and hinge moment with angles of incidence and elevator. These quantities are related by the equations

$$k'_l = a\theta' + b\eta.$$
$$\mathrm{M} = c\theta' + d\eta.$$

Where θ' is the angle of incidence of the tailplane.

η the elevator angle.

k'_l the lift coefficient of the tailplane.

M the hinge moment at 100 f.p.s.

The results of the analysis on these lines are given in Table 2. A table is also added on the lines of that in R. and M. 409, giving the constants as corrected for tailplanes of constant area, the results of the earlier tests being added for comparison. It should be noted that the square tailplane F does not strictly belong to the series formed by the other tailplanes, but its characteristics nevertheless appear to be intermediate between those of B and E, which have approximately the same percentage elevator chord.

3. The criterion adopted for testing the efficiency of any arrangement has been the product of the force and elevator movement required to produce a definite manœuvre when the areas of the various tailplanes are adjusted to give equal stability with elevators free. Table 4 has been prepared on these lines, and corresponds exactly to the similar table of R. and M. 409. From the figures obtained, it appears that the reversed tailplane is the most satisfactory form, and that the improvement secured over the standard R.E.8 type of the same percentage elevator chord is greater than that obtained by reducing the elevators from 40 per cent. to 30 per cent. The square tailplane, as would be expected, is intermediate between the standard and the reversed types. The values obtained from changing the trimming speed from 75 to 65 m.p.h. with engine on are less reliable than those obtained by shutting off the engine owing to the small quantities involved.

4. The conclusion derived from these results is that for the same percentage elevator chord it is advantageous to have the trailing edge shorter than the leading, so as to secure a shape of the type E. It would seem that the same form would also be preferable for wing tips. To secure lightness of control the effect of moving down a flap or elevator should be to increase the lift predominantly on the fixed part of the wing or tailplane. Any part of the control surface which projects beyond the fixed surface would therefore appear to be inefficient in this respect, and it becomes desirable to have tailplanes and wing tips which are either square in shape or cut away to a slightly shorter trailing edge. Tests are required, however, to confirm these conclusions

EXPERIMENTAL TAILPLANES.

1/12 SCALE

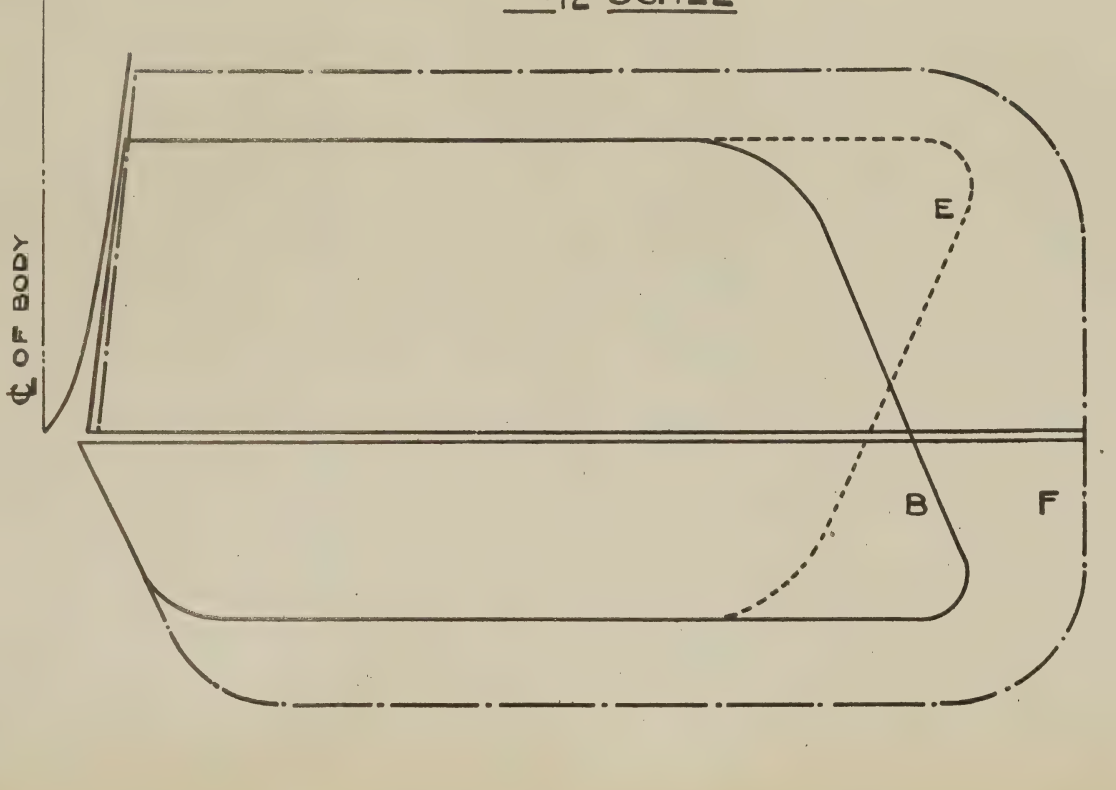

REPORT Nº 532.

FIG 1.

THE LIBRARY
OF THE
UNIVERSITY OF ILLINOIS

in the case of wing tips. The only other evidence at present available is that the original S.E.5 which had 21° raked tip was reported from Martlesham to be heavier on lateral control than the standard S.E.5*a*, which has much squarer tips.

TABLE 1.

DETAILS OF ELEVATORS.

	Total tail and elevator area. Sq. ft.	Elevator. Area. Sq. ft.	Chord. Ft.	Weight. Lbs.	Weight moment about hinge. Ft.-lbs.
B	39½	15·8	1·38	12½	5·7
E	39½	14·1	1·38	11½	4·2
F	65½	27·0	1·75	19	11·8

TABLE 2.

CHARACTERISTICS OF ELEVATORS.

$$k'_l = a\theta' + b\eta$$

$$\mathrm{M} = c\theta' + d\eta$$

Where M is the hinge moment at 100 f.p.s.

θ' is the tail incidence.

η is the elevator angle.

	$\frac{a}{b}$	$\frac{bc - ad}{a}$	$\frac{bc - ad}{d}$	b	c	d
B	1·69	1·79	−0·014	0·011	−1·1	−2·45
E	1·91	0·96	−0·019	0·010	0·0	−0·95
F	2·28	2·08	−0·0155	0·0085	−1·1	−2·55

TABLE 3.

TAILPLANES OF EQUAL AREA (46 sq. ft.).

Type.	*b*	*c*	*d*
A 22° rake, 30 per cent. elevators	0·0084	0	− 1·3
B ,, ,, 40 ,, ,,	0·0112	− 1·4	− 3·1
C ,, ,, 50 ,, ,,	0·0124	− 2·5	− 4·9
D ,, ,, 60 ,, ,,	0·0139	− 4·7	− 6·95
E type B reversed	0·0100	0	− 1·2
F square, 40 per cent. elevators	0·0085	− 0·5	− 1·2

TABLE 4.

TAILPLANES OF EQUAL STABILITY.

The machine is supposed to be trimmed at 75 m.p.h. (engine on).

Type.	To trim at 65 m.p.h.			To trim at 75 m.p.h. gliding.		
	Elevator movement.	Force Lbs.	Product.	Elevator movement.	Force Lbs.	Product.
A	− 0°·6	0·7	0·4	− 3°·8	2·5	9·5
B	− 0°·7	1·5	1·0	− 2°·4	5·3	12·7
C	− 0°·7	2·2	1·5	− 2°·0	7·4	14·8
D	− 0°·8	3·7	3·0	− 1°·5	11·5	17·3
E	− 0°·5	0·6	0·3	− 3°·2	2·2	7·1
F	− 0°·8	1·0	0·8	− 2°·8	3·0	8·4

THE FULL SCALE DETERMINATION OF THE PITCHING MOMENT OF A BIPLANE.

By S. B. Gates.

Presented by the Superintendent, Royal Aircraft Factory.

Reports and Memoranda, No. 400. *December,* 1917.

Summary.—(*a*) *Introductory.* (*Reasons for inquiry.*)—The calculation of the stability and tail setting of an aeroplane depends on a knowledge of the centre of pressure of the wings. Comparatively little information exists as to the centre of pressure of biplanes of various forms. Experiments were therefore carried out to measure this directly in flight.

(*b*) *Range of the investigation.*—By hinging the rear portion of a B.E.2e to the rest of the aeroplane, the moment about the hinge of the air forces on the rear portion was measured in flight. This enables the wing moment to be calculated independently of downwash and tail efficiency. Three wing sections—R.A.F. 14, R.A.F. 15, R.A.F. 18—were tested in this way. The results are represented as a moment coefficient about the nose of the "mean chord."

(*c*) *Conclusions.*—The results for R.A.F. 14 and R.A.F. 15 show that the method of estimating the centre of pressure of a full scale biplane from wind channel tests of model monoplanes and not from model biplanes is unsatisfactory. Application of the R.A.F. 14 results to stability experiments on R.E. 8 (which has very much the same wing arrangement as B.E.2e) gives a curve of downwash angles, which suggests that the angle of downwash is very nearly proportional to lift coefficient.

1. In the analyses of trimming speeds and of the longitudinal period which have previously appeared in Reports R. & M. No. 326, it was found that the accuracy of the experiments was not such as to provide a good determination of the wing pitching moment simultaneously with downwash and tail efficiency. Moreover, even if the accuracy could have been improved, the equations would still have remained somewhat indeterminate. The results of these calculations have, therefore, up to the present contained all the inaccuracies which follow from the use of a wing pitching moment estimated from that of a model monoplane. These errors will arise from three main causes :—

(1) Scale effect proper.

(2) Interferences on the full scale machine.

(3) Illegitimate assumptions of the mean chord theory, as explained in R. & M. 326.

From the results of the experiments to be described in the present report, the first two of these errors disappear automatically. These experiments, so far as they are now reported on, do not, it is true, throw any further light on the validity of the mean chord assumptions. In other words, there is no evidence that k_m for R.A.F. 15 wing section, as shown in Fig. 9, represents the moment coefficient about a calculable point for wings of the same shape as those here tested, but of variable stagger, gap-chord ratio and plan form. But it will be seen that the error (3) is now eliminated in the sense that the results of this report, used in conjunction with full scale lift and drag curves, do enable us to calculate with tolerable accuracy the pitching moment about any point for wings of the particular stagger, gap-chord and plan form arrangement here tested.

2. The machine used for these experiments was a B.E.2E. The device adopted was that of cutting the body into two parts at the rear of the pilot's seat and securing the rear part by means of a hinge and wires whose tension was measured from the observer's seat. The hinge was at the bottom of the body immediately behind the pilot's seat. The two supporting wires were led from the rear spar of the tail up to a bracket about 4 feet high which was attached behind the pilot's seat to the rear portion of the body, and thence down and by means of pulleys to an ordinary pointer-and-dial spring balance in the observer's seat. Two electric contacts were fitted, one on each part of the body slightly above the hinge, and were connected to two small electric lights, one on each side of the observer's balance. The observer tightened the wires by means of a turn-buckle below the balance, until contact was just established. From the balance reading then taken and the calibration of the instrument, the moment round the hinge of the air forces on the rear portion of the machine could be immediately deduced. For a discussion of the calibration see § 9. A sketch of the instrument is given in Fig. 1.

3. The actual method of experiment consists of steady flight in a straight line at speeds ranging from 40 to 110 miles per hour. It is found to be immaterial to keep either height, angle of flight path, or engine power constant from speed to speed. The reduction adopted is in fact independent of engine and propeller performance, except in so far as full scale drag curves are used. But this is a second order effect. A flight at any given speed lasts from 30 to 60 seconds. The pilot holds the machine at the speed required, keeping it as constant as possible. At the beginning of the run, height and temperature are taken; in the middle, balance reading and airspeed; and at the end, height again. The accuracy is found to be such that two, or at the most three, series of such runs are sufficient to establish the moment curve of any one section.

4. The principle of the mathematical analysis is simply that, for steady motion in a straight line, the total pitching moment on the aeroplane about any point fixed in it is zero. The pitching moment is made up of moments due to air forces, gravity, and the propeller thrust. The weight, the centre of gravity, and the air moment on the hinged part of the aeroplane are measured directly. The thrust can be calculated from the rate of climb and the known drag coefficients of the machine. For the subsidiary moments we are dependent on wind channel experiments, corrected for slip stream where necessary, and this is undoubtedly the weakest part of the determination. The wing moment is the difference between zero and all the other moments. It would, perhaps, have been most natural to reduce the experiments on a hinge moment basis, instead of working with moments round an arbitrarily chosen point, especially as the latter necessitated one or two extra wind channel tests of body lift and drag. It was found, however, that since the hinge point was at a considerable distance from the centre of pressure of the wings, the centre of gravity and the line of thrust, the quantity actually calculated was somewhat clumsily exhibited as the small difference of large quantities. The point about which the moments are calculated was therefore arbitrarily chosen on the line of thrust, and near the mean positions of the centre of gravity and the centre of pressure. It will be remarked in this connection that so far as the drag and thrust moments are concerned, the accuracy will be much the same whatever point is used. For, leaving out of account that part of the thrust which balances the resolved part of the weight along the aeroplane's path, it is roughly true that the thrust and the total drag form a couple.

5. The results for the sections R.A.F. 14, 15, 18, with which wings the aeroplane has been fitted in turn, are each exhibited in three forms. First, in Figs. 7-9, as k_m, the moment coefficient about the nose of the mean chord. This is the standard form from which moments are calculated, but it has the disadvantage in this case of giving an estimate of the accuracy of the experiment which is somewhat illusory. The reason for this is that the quantity actually measured, expressed as a moment coefficient, is never more than 0·04, which is less than half the possible value of k_m.

Next, in Fig. 10, the moment coefficient K about the arbitrarily chosen origin is plotted. This is a good criterion of experimental error, since considerably more than half of K is usually derived directly from the balance reading.

Finally, in Fig. 11, the centre of pressure is given. It cannot be too much emphasised that this is not to be taken, without further evidence, as representing with any accuracy, the centre

of pressure of a monoplane. It merely defines the point in which the resultant force on the biplane intersects a certain line, whose position and length are calculated as explained in R. & M. 326.

6. The model (monoplane) moment coefficients for R.A.F. 14 and R.A.F. 15 are plotted in Figs. 7 and 8 with the full scale values; for, although this is not a strict comparison, it shows the order of error to which previous calculations involving moments have been subject.

The broad result of comparing the various curves for R.A.F. 14 and R.A.F. 15 is that previous conceptions of their relative characteristics are confirmed, but there is a large difference in absolute values. Thus it remains true that a R.A.F. 14 biplane is more stable than R.A.F. 15 at low lift coefficients and less stable at high lift coefficients; and also that the centre of pressure, as defined in § 5, is always further from the nose of the mean chord for R.A.F. 14 than R.A.F. 15. On the other hand, all the values of k_m are now seen to be less (negatively) than the model values, as are also all the values of dk_m/dk_l. The difference in k_m has a mean value of 0·015 for R.A.F. 14 and 0·03 for R.A.F. 15, the difference in each case increasing with lift coefficient. The difference in dk_m/dk_l has a mean value of 0·03 for R.A.F. 14 and 0·055 for R.A.F. 15. Thus these wings are found to be less stable, and to have a range of movement of centre of pressure which is nearer to the nose of the mean chord than was previously supposed. The difference in stability can be demonstrated by considering it in terms of the movement of the centre of gravity of the aeroplane. At high speeds, where the differences in dk_m/dk_l are larger than those given above, the centre of gravity would have to be 2·5 inches further forward in the case of R.A.F. 14, and 5 inches further forward in the case of R.A.F. 15, to give the same degree of stability as before. No model test is available for comparison with the R.A.F. 18 curve. This lies between R.A.F. 14 and R.A.F. 15 and has much the same slope as R.A.F. 14. The shape of the section is intermediate between R.A.F. 14 and R.A.F. 15.

In R.A.F. 15 there seems to be a definite tendency for the slope to become less (negatively) at low lift coefficients, but this tendency does not occur in the other curves.

The values of k_m, dk_m/dk_l, and centre of pressure coefficient for the several sections are given in Table 8.

Tables 5, 6, 7 contain the calculations.

7. The details of the analysis are as follows, all moments being measured with the usual sign convention.

Since the moment of the hinged portion is mainly due to the tail forces, the first step is to obtain the lift T of the tail.

The calibration of the balance gives the relation between the balance reading (R) and the air moments on the rear portion (M) in the form

$$M = \alpha (R - \beta) \quad . \quad . \quad . \quad . \quad . \quad . \quad (1)$$

α and β being constants.

Then if M_r is the moment about the hinge of the rear portion of the body alone, M_t is the moment about the hinge of sundry parts attached to the hinged portion (bracket, tail skid, fin, &c.), we have

$$T = \frac{1}{11{\cdot}0} (M_r + M_t - M) \quad . \quad . \quad . \quad . \quad (2)$$

the distance between the hinge and the mean centre of pressure of the tail (taken at one-third of the chord behind the leading edge), being 11 feet.

The next step is the determination of k_l. The inclusion of as many subsidiary lifts as are at present calculable, makes this part of the work a somewhat elaborate adjustment between two equations. In addition to the tail lift, we include

L_b the lift of the whole body,
L_s the lift of the landing gear axle,

and the resolved part of the thrust along the lift axis. The latter may be written $P \cdot \pi/180 \cdot (\theta - 3{\cdot}5)$ where P is the thrust, θ the incidence, and the thrust line is inclined at 3·5° below the chord.

Then, if the inclination of the flight path to the horizontal which is calculated from the gain in height per second, be written α, the lift equation becomes

$$k_l \rho A V^2 = W \cos \alpha - \left[T + L_b + L_s P \frac{\pi}{180} (\theta - 3{\cdot}5) \right] \quad (3)$$

This equation is indeterminate until P is known, since in addition to the term containing P, L_b and A must both contain the slip stream factor R/R_o. We are therefore led to the subsidiary equation obtained by equating the thrust to the total drag plus the resolved part of the weight along the flight path.

Now P may be written in terms of the momentum theory

$$0{\cdot}6 \frac{\pi}{4} D^2 \cdot 0{\cdot}00237 \, v_o (v_o + V_o)$$

where D is the propeller diameter, and v is the slip stream speed, and the suffix o refers to indicated speed.

Now let r_1, r_2 be the head resistance respectively in and out of the slip stream at unit indicated speed, and let A_1, A_2 be the corresponding quantities for the wing area. Then we have

$$P = 0{\cdot}6 \frac{\pi}{4} D^2 \cdot 0{\cdot}00237 \, v_o (v_o + V_o) = r_1 (v_o + V_o)^2 + r_2 V_o^2$$
$$+ 0{\cdot}00237 \, l \left[A_1 (v_o + V_o)^2 + A_2 V_o^2 \right] + W \sin \alpha.$$

Reducing this, and writing

$$p = \frac{v_o}{V_o} = (R/R_o)^{\frac{1}{3}} - 1,$$

we get a quadratic in p of the form

$$p^2 (a_1 + b_1 k_d) + p(a_2 + b_2 k_d) + a_3 + b_3 k_d + \frac{W \sin \alpha}{V_o^2} = O . (4)$$

of which the positive root gives the slip stream speed, and hence P and R/R_o.

Approximating successively between (3) and (4) we can without much labour find values of

$$k_l, \theta, P, R/R_o, A, L_b, L_s,$$

to satisfy both equations.

We are now in a position to take moments about the arbitrarily chosen origin O. This is defined with respect to the mean chord by the usual co-ordinates h, k; and the centre of gravity is defined with respect to axes through O parallel and perpendicular to the mean chord, by the co-ordinates x and z (feet), z being measured positively upward. Then, if

$Kb \rho AV^2$ be the wing moment about O,
M_b be the body moment about O,
M_s be the subsidiary moment about O,

and

l the distance between O and the mean centre of pressure of the tail,

we can write

$$Kb \rho AV^2 = l T - M_b - M_s - W \left[x \cos (\theta + \alpha) + z \sin (\theta + \alpha) \right] (5)$$

Writing $W = \bar{k}_l \rho AV^2$ (so that, except for the flight path inclination, k_l is the "effective k_l"), this becomes

$$K = \frac{(lT - M_b - M_s)k_l}{bW} - \frac{k_l}{b} \left[x \cos (\theta + \alpha) + z \sin (\theta + \alpha) \right]$$
$$= X + Y \text{ (say)} \quad . \quad . \quad . \quad . \quad . \quad . \quad (6)$$

Finally, the transference from K to the more familiar k_m is effected by the equation

$$K = k_m + h k_l + k k^x \quad . \quad . \quad . \quad . \quad . \quad . \quad (7)$$

8. The various subsidiary moments and lifts which occur in the above equations were either calculated (as in the case of struts, wires, &c., and parts of the hingeing gear) from standard curves of resistance; or, as in the case of the body, they were derived from special wind channel tests.

The former, which are represented in M_t, M_s, and L_s, are easily disposed of. L_s the axle lift was taken from strut tests to be 2·6 lbs. per degree incidence at 100 f.s., and this has since been confirmed by a wind channel test.

M_t and M_s are the sums of a large number of small moments, each with its appropriate slip stream factor. Strictly speaking, these are functions of the incidence. But a calculation of their values at the extremes of the range of incidence showed them to be both roughly constant, and having regard to their relative unimportance they are taken to be represented with sufficient accuracy by the formulæ

$$M_s = -0{\cdot}0058\, V_o^2,$$

$$M_t = \quad 0{\cdot}0160\, V_o^2$$

V_o being in miles per hour. The details appear in Tables 3 and 4.

The wind channel tests on the body from which M_b, M_r, and L_s are derived, present much greater difficulty. The errors and uncertainties in this part of the work arise in two ways. It is impracticable at present to measure forces and moments in the Royal Aircraft Factory wind channel with a propeller running. The corrections which had, therefore, to be applied to the results of the model body tests to allow for slip stream effect were two, of which one could be little more than a guess. The first, which allows for the deflection of the air by the slip stream, assumes, in accordance with the theory given in R. & M. 326, that the incidence of the slip stream itself is changed from θ to $\frac{\theta + \gamma p}{1 + p}$, where γ is the inclination of the thrust line to the chord and $p = v/V$.

The second correction is to allow for the average increased velocity in the slip stream. The results of R. & M. 326 showed that the effect of the propeller slip stream on a tractor body was to increase its resistance in the ratio of about $\frac{3}{4}\, R/R_o$ (R/R_o being calculated from momentum considerations). There is no evidence as to whether the lift or the moment of the body are affected in the same way. The factor $\frac{3}{4}\, R/R_o$ seemed as likely to be true as any other, and has been applied. The measurements were made on a one-twelfth scale model and were corrected for change of incidence and for slip stream speed, as indicated above. These results are embodied in M_b. The results of the wind channel tests are given in Table 2. The error involved in k_m is discussed in the next paragraph. M_r the moment of the rear part of the body about the hinge calls for little comment. It is so small as to be almost negligible, and is corrected for slip stream in the same way as M_b.

9. The probable values of the more important errors are dealt with briefly in turn below.

(*a*) *Calibration of the balance.*—This was done by supporting the front part of the body on trestles and reading the balance at various arrangements of the signal lights and with a series of weights on the rear spar of the tail. By this means the weight moment of the hinged portion was automatically eliminated. The only difficulty to be contended with was an effect of friction at the hinge which first appeared in some of the later experiments when the bearings had rusted. It was noticed that with any given tail load, if the turnbuckle was turned until one light was just on, it required a certain number of turns of the turnbuckle in the opposite direction before the light was turned off; and that this interval increased with the tail load. In other words, the friction at the hinge was such as to stop any movement at the contacts until the wires had been considerably slackened. As was to be expected, the vibratory conditions in flight almost entirely destroyed this effect. This being so, it could not be certain that a calibration curve representing any particular arrangement of the lights would correspond exactly with readings taken under flight conditions. On the whole, the best calibration seems to be obtained by taking the mean of the four curves corresponding to each light off and each light on. Calibrations taken in this way when the tail was vibrated by hand show reduced lag and make it extremely probable that in actual flight these curves close up to the mean. These remarks only apply to R.A.F. 18. For R.A.F. 15, the first section to be tested, the effect was not noticed; and for R.A.F. 14 it was very slight. It is considered that an outside limit of this error in R.A.F. 18 is 30 ft.lbs. in M at a k_l of 0·15, and this represents a figure of 0·002 in k_m. An example of the calibration curves is given in Fig. 6.

(*b*) *The body moment.*—The uncertainty here is the correction for the propeller and slip stream. It is considered that an outside limit is obtained by assuming that the full R/R_o factor should be applied instead of $\frac{3}{4}$ R/R_o. Since the greatest value of M_b is about 170, this error would correspond to about 0·001 in k_m and would be greatest at high speeds.

(*c*) *Flap settings.*—The flights were, of course, done with the control stick central laterally, but it is impossible in practice to rig the controls so that all four flaps are level with the rest of the wing at all speeds, though the variation is slight. So long as the rigging is the same during all the tests of one wing section, we shall get the moment curve of a section which will differ only very slightly from the normal section. An opportunity was taken during the R.A.F. 18 tests of looking into this effect. In the first experiment the trailing edge of the flaps was about $1\frac{1}{2}$ inches below that of the wings. In the second, this difference

was less than $\frac{1}{2}$ inch. The effect on k_m was a constant difference of about 0·002. Since this was a rather abnormal difference, the conclusion is that ordinary differences in flap settings produce variations in k_m which are well within the order of accuracy of other parts of the experiment. Inconsistencies would occur only when the rigging was altered in the middle of a series of tests on one wing section, and this has been avoided.

(*d*) *The airspeed indicator.*—The readings of the indicated speed are corrected in the usual way in two steps, the first for the actual error of the instrument, and the second for the variation from the mean flow at the particular point of the machine to which the pitot tube is attached. Of these the first is not open to doubt, as the instruments were very carefully calibrated, but uncertainties as to the second—"the speed course factor"—led to an investigation in the case of R.A.F. 18, of the effect on k_m of the sort of error which it was then thought might occur in the speed course factor. It was assumed that the correction was wrong to the extent of about 1 mile an hour at 45 miles per hour and 3 at 100; and it was found that one and the same curve could be drawn through the points calculated on this assumption, and those calculated with the accepted speed course factor. The effect had been to move the points up and down the curve. This rendered it very unlikely that any error in the speed course factor will be seriously reflected in k_m. Further than this, the uncertainty that had remained has since been much diminished by speed course experiments which, repeated after a lapse of time, certainly show that speed course factors are not unreasonably subject to variations in weather conditions.

(*e*) *The full scale drag curve.*—The wing drag coefficient enters the calculation at two points. In equation (4) of § 7, which determines R/R_o, any error in k_d will affect the lift coefficient at a given speed,

(1) by a corresponding error in the effective wing area,

(2) by errors in those subsidiary lifts which depend on R/R_o.

These effects are both of the second order, and it is estimated that an error of 0·005 in k_d will make a difference of considerably less than 1 per cent. in K over the whole range. The other equation through which an error in k_d affects the problem is (7) of paragraph 7. The error in k_x will be of the same order as that in k_d; and, since h is about one-third the corresponding error in k_m due to an error of 0·005 in k_d is of the order 0·0015.

10. A survey of such uncertainties as these leads to the general conclusion that the error in k_m as given by these experiments may be as great as 0·003, but is probably less. Since this probable error is very much less than the difference in k_m between

any two of the sections, the comparison between the three sections is not seriously affected.

It may be remarked that the error is also much less than the difference between the model monoplane and the corresponding full scale biplane k_m curve.

As an instrument for the scientific determination of k_m, however, the method here outlined will admittedly be imperfect until the uncertainties discussed above are cleared up.

11. A rather different comparison is obtained by calculating from the full scale results the moment about the nose of a chord which differs as follows from the mean chord used in this report. It divides the gap between the equivalent chords in the ratio, not of the areas of the two planes, but of the area of the upper plane multiplied by a loading factor 5 to the area of the lower plane multiplied by a loading factor 4. If this line had been chosen as the standard mean chord, the assumption would have been that the loading ratio of upper to lower plane is 5 : 4, and is independent of stagger, &c., provided it is also assumed that the centres of pressure of the upper and lower planes are unaffected by different biplane arrangements. This ratio 5 : 4 was suggested by earlier model experiments. In this instance the comparison is as follows :—

k_l	R.A.F. 14.		R.A.F. 15.	
	Full Scale. k_m	Model Monoplane. k_m	Full Scale. k_m	Model Monoplane. k_m
0·1	− 0·0565	− 0·0616	− 0·0343	− 0·0481
0·2	− 0·0782	− 0·0850	− 0·0514	− 0·0700
0·3	− 0·0995	− 0·1065	− 0·0598	− 0·0919
0·4	− 0·1181	− 0·1270	− 0·0883	− 0·1138
0·5	− 0·1344	− 0·1470		

It will be seen that the agreement is quite close for R.A.F. 14, but it would require a much larger loading ratio to bring the R.A.F. 15 results into line.

A further comparison which is perhaps more to the point may be drawn from the full scale pressure plotting results given in R. & M. 374. The fact that the moment coefficients there given only apply to one section of the biplane (situate about 8 feet from the centre line) renders the comparison inexact, as does also the fact that the pressure plotting was done on

B.E.2c wings. The most logical comparison seems to be given by using the results of R. & M. 374 to calculate k_m about the nose of the mean chord used in this report. The result is given in the following table, k'_m being the calculated coefficient :—

k_l	k'_m	k_m
0·15	− 0·0583	− 0·0625
0·2	− 0·0646	− 0·0718
0·3	− 0·0847	− 0·0910
0·4	− 0·1036	− 0·1080
0·5	− 0·1151	− 0·1229

This divergence may very well be accounted for by the special conditions at the ribs over which the pressures were measured.

12. Perhaps the most convincing confirmation of the results of these experiments is to be found in their effect on the full scale determination of downwash. The corrected downwash curve for R.E. 8, which has very nearly the same wings as B.E.2e, pass very near the " no-lift " point, and $de/d\theta$ is of the order 0·5, agreeing very closely with model experiments.

13. A word may be said as to the further use to which these experiments may be put. The ideal procedure would be to test each new arrangement of wings on its merits, reserving the mean chord as a convenient and standard way of presenting the experimental results. This is very inconvenient for design purposes, and it is proposed to carry out a series of these tests on biplanes of varying stagger, gap and plan form, and use the results as a basis for a modified mean chord theory. Any such method evolved in this way is bound to be more or less empirical, but it will rest on a sounder basis than the present one. It may be remarked that the experiments can be done very rapidly, four or five flights being sufficient, generally, to test one arrangement. A set of B.E.2c wings, R.A.F. 14 section, are now being tested, and it is proposed to follow these with a similar set with no stagger.

TABLE 1.

GEOMETRICAL CONSTANTS.

	R.A.F. 14.	R.A.F. 15.	R.A.F. 18.
Wing area, upper ...	214 ft.²	214 ft.²	236 ft.²
,, ,, lower ...	146 ,,	146 ,,	163 ,,
,, ,, total (with slip stream).	346 + 14 R/R_o	346 + 14 R/R_o	384 + 15 R/R_o
Gap	6·15′	6·15′	6·15′
Stagger	22°	22°	22°
Span, upper	40·75′	40·75′	40·75′
,, lower	30·75′	30·75′	30·75′
Length of mean chord	5·39′	5·39′	6·02′
Nose of mean chord l_1	1·26′	1·26′	1·45′
Nose of mean chord l_2	4·14′	4·14′	4·09′
h	0·345	0·345	0·337
k	0·327	0·327	0·294

l_1 is distance in feet of nose of mean chord in front of nose of lower chord.

l_2 is distance in feet of nose of mean chord above nose of lower chord,

the axes being respectively parallel and perpendicular to the chord.

h, k are defined in § 7.

TABLE 2.

BODY FORCES AND MOMENTS.

Wind channel tests on a one-twelfth scale model B.E.2E of body lift, drag, and pitching moment. These results are in lbs. and lbs.ft. at full scale at 100 f.p.s., and are uncorrected for slip stream.

The point about which the moment M of the complete body is taken is the point (h, k).

The moment M′ of the hinged portion of the body is taken about the hinge.

Wing Incidence.	Complete Body.			Hinged Portion.
	L.	D.	M.	M′.
1·5	13	57	+ 92	+16
4·5	24	58	+ 73	+ 9
7·5	40	62	+ 33	− 2
10·5	64	65	− 38	−21
13·5	88	77	− 91	−48

TABLE 3.

MOMENTS ABOUT THE POINT (h, k) OF VARIOUS SUBSIDIARY PARTS (M_s) IN LBS.FT. AT 100 FEET PER SECOND.

Part.	0° Incidence. Moments.		10° Incidence. Moments.	
	In Slip Stream.	Out of Slip Stream.	In Slip Stream.	Out of Slip Stream.
Landing gear { Wheels, &c. ...	—	− 83·0	—	− 78·5
Landing gear { V struts ...	− 2·9	− 7·2	− 2·8	− 7·0
Landing gear { Axle	—	− 32·4	—	12·8
Exhaust pipes	1·8	1·3	2·2	1·6
Fin, rudder, &c.	2·4	1·3	− 2·3	− 1·3
Tail plane	− 0·2	− 0·2	− 8·3	− 6·6
Tail skid	− 5·1	—	− 15·0	—
Wing struts, &c.	12·6	39·8	12·0	37·8
Body struts, &c.	6·7	—	7·0	—
King posts	—	5·0	—	5·1
Hingeing gear	14·2	11·5	8·6	7·0
Totals	29·5	− 64	1·0	− 29

TABLE 4.

MOMENTS ABOUT THE HINGE OF VARIOUS ATTACHMENTS TO THE REAR PORTION OF THE AEROPLANE IN LBS.FT. AT 100 FEET PER SECOND.

Part.	0° Incidence. Moments.		10° Incidence. Moments.	
	In Slip Stream.	Out of Slip Stream.	In Slip Stream.	Out of Slip Stream.
Hinge gear	25·0	23·0	24·5	22·5
Fin and rudder	5·5	3·1	2·4	1·6
Tail plane	4·8	3·7	− 0·7	− 0·7
Tail skid	1·7	—	− 4·8	—
Totals	37	30	21·5	23·5

The formulæ given in § 8 are obtained by using these values in conjunction with an R/R_o of 1·25 at 0° incidence and 2·0 at 10° incidence.

Table 5.

R.A.F. 14 CALCULATIONS.

Number	1.	2.	3.	4.	5.
W...	1980	1979	1978	1977	1976
x	− 0·028	− 0·027	− 0·026	− 0·025	− 0·023
z	− 0·174	− 0·174	− 0·174	− 0·174	− 0·175
*V_o (observation)...	45	48	52	56	61
*V_o (calibration) ...	44·7	47·7	51·9	56·1	61·1
*V_o (speed course)	45·5	48·6	53·0	57·3	62·5
Mean height ...	4485	5150	5750	6190	6620
Temperature °C.	0	− 1·5	− 3	− 4	− 5
Percentage density	89·8	88·1	86·7	85·6	84·6
*V (true)	48·1	51·8	57·0	61·9	67·9
†Gain in height ...	470	600	420	380	320
α	6·3	7·5	4·8	4·0	3·1
M...	− 320	− 283	− 206	− 142	− 53
M_r	− 1	3	5	8	12
M_t	33	38	45	52	62
T	32	29	23	18	11
L_s	2	0	− 2	− 7	− 9
L_b	52	49	42	37	34
P	509	545	444	411	385
A	387	386	378	375	372
k_l	0·450	0·395	0·347	0·304	0·261
R/R_o	2·95	2·86	2·32	2·07	1·86
θ	10·0	8·3	6·8	5·4	4·1
M_b	37	55	64	77	91
M_s	− 12	− 14	− 16	− 19	− 23
k_l	0·487	0·426	0·365	0·315	0·267
X	0·0224	0·0170	0·0110	0·0069	0·0028
Y	0·0069	0·0058	0·0041	0·0032	0·0022
K	0·0293	0·0228	0·0151	0·0101	0·0050
k_x	− 0·0365	− 0·0238	− 0·0147	− 0·0079	− 0·0024
k_m	− 0·1140	− 0·1055	− 0·1000	− 0·0920	− 0·0844

* All speeds are in miles per hour.
† In feet per minute.

TABLE 5 (*Cont.*).

Number	6.	7.	8.	9.	10.
W...	1975	1974	1988	2007	2007
x	− 0·022	− 0·021	− 0·019	− 0·038	− 0·038
z	− 0·175	− 0·175	− 0·188	− 0·188	− 0·188
*V_o (observation)...	65	75	92	45	47
*V_o (calibration) ...	65·4	75·0	92·4	44·7	46·7
*V_o (speed course)	67·0	76·8	94·5	45·5	47·6
Mean height ...	6915	6990	6140	690	600
Temperature °C.	− 5·5	− 6	− 4	7	7
Percentage density	83·8	83·7	85·8	100·6	101·0
*V (true)	73·2	84·0	102·0	45·4	47·4
†Gain in height ...	190	20	− 640	− 120	0
α	1·7	0·2	− 4·1	− 1·7	0
M...	32	263	872	− 320	− 263
M_r	14	22	34	− 6	− 3
M_t	72	94	143	33	36
T	5	− 13	− 63	31·5	27
L_s	− 12	− 21	− 41	3·5	2
L_b	30	25	24	43	43
P	340	318	240	215	276
A	369·5	367	364	373	375
k_l	0·231	0·181	0·125	0·482	0·442
R/R_o	1·68	1·49	1·26	1·90	2·04
θ	3·2	1·6	− 0·1	11·0	9·8
M_b	102	128	174	0	19
M_s	− 26	− 34	− 52	− 12	− 13
k_l...	0·233	0·179	0·119	0·509	0·462
X...	0·0001	− 0·0053	− 0·0128	0·0244	0·0182
Y...	0·0016	0·0006	0·0001	0·0064	0·0059
K...	0·0017	− 0·0047	− 0·0127	0·0308	0·0241
k_x	0·0007	0·0044	0·0065	− 0·0447	− 0·0345
k_m	− 0·0780	− 0·0685	− 0·0579	− 0·1209	− 0·1171

* All speeds are in miles per hour.
† In feet per minute.

TABLE 5 (*Cont.*).

Number	11.	12.	13.	14.	15.
W...	2006	2005	2004	1960	1959
x	− 0·037	− 0·036	− 0·035	− 0·026	− 0·025
z	− 0·189	− 0·189	− 0·189	− 0·185	− 0·185
*V_o (observation)...	56	65	85	48·5	50·25
*V_o (calibration) ...	56·1	65·4	85·3	48·2	50·0
*V_o (speed course)	57·3	67·0	87·3	49·1	51·0
Mean height ...	780	1110	1770	5080	5590
Temperature °C.	7	6	3	0·5	0
Percentage density	100·3	99·4	98·1	87·6	86·2
*V (true)	57·2	67·3	88·2	52·5	55·0
†Gain in height ...	200	340	− 1060	463	318
α	2·3	3·3	− 7·8	5·7	3·8
M...	− 142	117	628	− 296	− 241
M_r	8	15	23	3	2
M_t	53	72	122	39	42
T	18·5	− 3	− 44	31	26
L_s	− 4	− 12	− 33	0	− 1
L_b	35	32	18	45	42
P	351	407	44	473	400
A	373	371	361	383	378
k_l	0·311	0·234	0·148	0·389	0·370
R/R_o	1·93	1·80	1·05	2·60	2·29
θ	5·7	3·2	0·3	8·1	7·5
M_b	68	110	125	52	51
M_s	− 19	− 26	− 44	− 14	− 15
k_l	0·321	0·236	0·143	0·417	0·390
X...	0·0074	− 0·0030	− 0·0104	0·0182	0·0141
Y...	0·0038	0·0025	0·0003	0·0053	0·0045
K...	0·0112	− 0·0005	− 0·0101	0·0235	0·0186
k_x	− 0·0089	0·0004	0·0061	− 0·0225	− 0·0188
k_m	− 0·0932	− 0·0813	− 0·0631	− 0·1035	− 0·1030

* All speeds are in miles per hour,
† In feet per minute.

TABLE 5 (*Cont.*).

Number	16.	17.	18.	19.	20.
W...	1958	1957	1956	1955	1954
x	− 0·023	− 0·022	− 0·021	− 0·019	− 0·013
z	− 0·185	− 0·185	− 0·186	− 0·186	− 0·186
*V_o (observation)...	52·0	56·75	61·5	65·25	70·5
*V_o (calibration) ...	51·8	56·8	61·6	65·6	70·7
*V_o (speed course)	52·9	58·1	63·1	67·2	72·4
Mean height ...	6130	6585	6980	7185	7285
Temperature °C.	− 1	− 1·5	− 2	− 2·5	− 2·5
Percentage density	84·8	836	825	821	817
*V (true)	57·5	63·6	69·5	74·1	80·1
†Gain in height ...	408	392	275	189	71
α	4·6	4·0	2·6	1·7	0·6
M...	− 227	− 138	− 65	20	150
M_r	5	9	12	15	18
M_t	45	54	64	72	84
T	25	18	13	6	− 4
L_s	− 2	− 5	− 9	− 13	− 17
L_b	40	35	32	29	27
P	430	405	363	339	312
A	378	374	371	370	367·5
k_l	0·346	0·295	0·254	0·226	0·199
R/R_o	2·28	2·02	1·80	1·67	1·54
θ	6·8	5·2	3·9	3·0	2·2
M_b	62	79	88	102	114
M_s	− 16	− 20	− 23	− 26	− 30
k_l	0·363	0·304	0·260	0·229	0·199
X...	0·0124	0·0068	0·0035	0·0005	− 0·0029
Y...	0·0040	0·0029	0·0020	0·0014	0·0010
K...	0·0164	0·0097	0·0055	0·0019	− 0·0019
k_x	− 0·0145	− 0·0066	− 0·0016	0·0012	0·0034
k_m	− 0·0982	− 0·0898	− 0·0817	− 0·0765	− 0·0716

* All speeds are in miles per hour.
† In feet per minute.

TABLE 5 (*Cont.*).

Number	21.	22.	23.	24.
W	1953	1952	1951	1950
x	− 0·017	− 0·016	− 0·014	− 0·013
z	− 0·186	− 0·186	− 0·187	− 0·187
*V_o (observation)	75·75	81·0	85·25	90·5
*V_o (calibration)	75·8	81·1	85·55	90·8
*V_o (speed course)	77·7	83·1	87·6	92·9
Mean height	7165	7075	6800	6385
Temperature °C.	− 2·5	− 2·5	− 2	− 1
Percentage density	821	824	831	840
*V (true)	85·8	91·6	96·2	101·4
†Gain in height	20	− 150	− 453	− 658
α	0·2	− 1·1	− 3·1	− 4·2
M	267	421	595	796
M_r	22	25	27	31
M_t	97	111	123	138
T	− 13	− 26	− 40·5	− 57
L_s	− 22	− 28	− 33	− 39
L_b	26	24	23	23
P	321	296	240	226
A	367	366	364	363·5
k_l	0·175	0·155	0·141	0·127
R/R_o	1·49	1·40	1·30	1·25
θ	1·4	0·8	0·4	− 0·1
M_b	131	145	152	170
M_s	− 35	− 40	− 45	− 50
k_l	0·173	0·152	0·137	0·122
X	− 0·0050	− 0·0076	− 0·0099	− 0·0121
Y	0·0007	0·0004	0·0001	0·0000
K	− 0·0043	− 0·0072	− 0·0098	− 0·0121
k_x	0·0048	0·0059	0·0063	0·0065
k_m	− 0·0663	− 0·0625	− 0·0605	− 0·0580

* All speeds are in miles per hour.
† In feet per minute.

Table 6.

R.A.F. 15 CALCULATIONS.

Number	1.	2.	3.	4.	5.
W...	1956	1952	1948	1946	1944
x	− 0·112	− 0·106	− 0·101	− 0·099	− 0·096
z	− 0·323	− 0·324	− 0·325	− 0·326	− 0·326
*V_o (observation)...	54	66	59	72	48·5
*V_o (calibration) ...	54·0	66·4	59·0	72·1	48·2
*V_o (speed course)	58·6	70·9	63·6	76·3	52·7
Mean height ...	4000	4600	5000	5100	5200
Temperature °C.	8	8	7	7	7
Percentage density	88·8	86·9	85·9	85·6	85·3
*V (true)	62·2	76·1	68·7	82·5	57·1
†Gain in height ...	200	80	200	− 130	− 60
α	2·1	0·7	1·9	−1·0	− 0·7
M	− 595	− 548	− 603	− 529	− 614
M_r	8	15	10	16	2
M_t	55	80	65	93	45
T	60	58	62	58	60
L_s	− 4	− 13	− 8	− 17	− 1
L_b	36	32	36	29	34
P	320	302	324	259	205
A	372	368	370	366	369
k_l	0·284	0·198	0·242	0·725	0·351
R/R_o	1·82	1·54	1·70	1·41	1·66
θ	5·7	3·4	4·6	2·7	7·4
M_b	67	102	83	112	36
M_s	− 20	− 29	− 24	− 34	− 16
k_l	0·300	0·207	0·255	0·179	0·372
X	0·0262	0·0169	0·0228	0·0146	0·0335
Y	0·0086	0·0049	0·0065	0·0036	0·0092
K	0·0348	0·0218	0·0293	0·0182	0·0427
k_x	− 0·0109	− 0·0011	− 0·0055	0·0010	− 0·0219
k_m	− 0·0596	− 0·0460	− 0·0524	− 0·0415	− 0·0711

* All speeds are in miles per hour.
† In feet per minute.

TABLE 6 (*Cont.*)

Number	6.	7.	8.	9.	10.
W...	1943	1940	1937	1935	1934
x	− 0·095	− 0·091	− 0·087	− 0·123	− 0·122
z	− 0·326	− 0·327	− 0·328	− 0·325	− 0·325
*V_o (observation)...	72	83	90	48·7	56·5
*V_o (calibration) ...	72·1	83·2	90·3	48·4	56·6
*V_o (speed course)	76·3	86·8	93·1	52·9	61·2
Mean height ...	4650	4300	4600	3500	4270
Temperature °C.	8	8	8	9·5	7·5
Percentage density	86·7	87·8	86·9	90·0	88·1
*V (true)	82·1	92·8	99·9	55·8	65·2
†Gain in height ...	− 50	− 250	− 2000	440	420
α	− 0·4	− 1·8	− 13·0	5·1	4·2
M...	− 517	− 408	− 459	− 570	− 580
M_r	16	23	20	5	9
M_t	93	121	139	45	60
T	57	50	56	56	50
L_s	− 17	− 26	− 33	− 2	− 6
L_b	30	31	18	42	36
P	284	284	− 125	421	401
A	366	365	358	378	373
k_l	0·1725	0·135	0·1165	0·342	0·256
R/R_o	1·45	1·35	0·85	2·26	1·93
θ	2·7	1·7	1·2	7·0	4·9
M_b	116	146	110	59	85
M_s	− 34	− 44	− 51	− 16	− 22
k_l	0·179	0·138	0·122	0·359	0·271
X	0·0142	0·0093	0·0098	0·0297	0·0231
Y	0·0036	0·0023	0·0004	0·0125	0·0088
K	0·0178	0·0116	0·0102	0·0422	0·0319
k_x	0·0010	0·0030	0·0038	− 0·0203	− 0·0072
k_m	− 0·0420	− 0·0360	− 0·0312	− 0·0690	− 0·0540

* All speeds are in miles per hour.
† In feet per minute.

TABLE 6 (*Cont.*).

Number	11.	12.	13.	14.	15.
W...	1931	1930	1927	1923	1921
x	− 0·118	− 0·116	− 0·112	− 0·107	− 0·104
z	− 0·326	− 0·326	− 0·326	− 0·328	− 0·329
*V_o (observation)...	58·25	44·0	42·5	67·5	75·5
*V_o (calibration) ...	58·2	43·6	42·1	67·8	75·5
*V_o (speed course)	62·8	48·1	46·5	72·2	79·6
Mean height ...	5650	6580	6120	5790	6180
Temperature °C.	4·5	2	3·5	4	3·5
Percentage density	84·7	82·5	83·5	84·4	83·3
*V (true)	68·3	53·0	50·9	78·6	87·3
†Gain in height ...	400	350	440	240	− 40
α	3·8	4·3	5·6	2·0	−0·3
M...	− 594	− 556	− 331	− 548	− 482
M_r	11	0	0	16	20
M_t	63	37	35	84	102
T	61	54	53	59	55
L_s	− 7	+ 1	2	− 14	− 20
L_b	36	44	47	33	30
P	389	387	438	357	302
A	372	380	383	369	366
k_l	0·246	0·404	0·420	0·188	0·157
R/R_o	1·86	2·39	2·64	1·62	1·44
θ	4·7	8·9	9·3	3·2	2·3
M_b	88	39	37	112	129
M_s	− 23	− 13	− 13	− 30	− 37
k_l...	0·258	0·430	0·456	0·196	0·1625
X	0·0227	0·0348	0·0364	0·0164	0·0124
Y	0·0079	0·0150	0·0162	0·0050	0·0035
K	0·0306	0·0498	0·0516	0·0214	0·0159
k_x	− 0·0060	− 0·0330	− 0·0364	− 0·0002	0·0019
k_m	− 0·0524	− 0·0784	− 0·0813	− 0·0433	− 0·0389

* All speeds are in miles per hour.
† In feet per minute.

TABLE 6 (*Cont.*).

Number	16.	17.	18.	19.
W	1957	1956	1955	1954
x	− 0·107	− 0·106	− 0·104	− 0·103
z	− 0·327	− 0·328	− 0·328	− 0·328
*V_o (observation)	41·0	47·0	54·0	58
*V_o (calibration)	40·6	46·7	54·0	58·0
*V_o (speed course)	44·9	51·2	58·6	62·6
Mean height...	5420	5650	6000	6570
Temperature °C.	5·75	5	4	3
Percentage density	85·0	84·4	83·7	82·3
*V (true)	48·7	55·8	64·2	69·0
†Gain in height	160	200	210	340
α	2·1	2·3	2·1	3·2
M	− 540	− 584	− 615	− 596
M_r	− 4	1	7	10
M_t	32	42	55	63
T	51	57	61	61
L_s	3	0	− 5	− 7
L_b	45	40	35	35
P	312	320	320	368
A	378	375	372	371
k_l	0·466	0·366	0·282	0·249
R/R_o	2·29	2·04	1·82	1·82
θ	10·5	7·9	5·6	4·8
M_b	16	40	67	84
M_s	− 12	− 15	− 20	− 23
k_l	0·504	0·390	0·300	0·263
X	0·0390	0·0330	0·0266	0·0230
Y	0·0164	0·0117	0·0082	0·0072
K	0·0554	0·0447	0·0348	0·0302
k_x	− 0·0478	− 0·0248	− 0·0106	− 0·0064
k_m	− 0·0900	− 0·0733	− 0·0590	− 0·0536

* All speeds are in miles per hour.
† In feet per minute.

TABLE 6 (*Cont.*).

Number	20.	21.	22.	23.
W	1952	1950	1948	1946
x	− 0·100	− 0·098	− 0·095	− 0·093
z	− 0·329	− 0·329	− 0·330	− 0·331
*V_o (observation)	64	69	79	88
*V_o (calibration)	64·3	69·2	79·1	88·3
*V_o (speed course)	68·8	73·6	82·9	91·3
Mean height...	6900	6510	5515	4680
Temperature °C.	2·5	3	5·5	8
Percentage density	81·4	82·5	84·8	86·6
*V (true)	76·3	80·9	90·0	98·1
†Gain in height	130	− 400	− 570	− 880
α	1·1	− 3·2	− 4·1	− 5·9
M	− 584	− 584	− 498	− 373
M_r	13	13	19	25
M_t	76	87	110	134
T	61	62	57	48
L_s	− 11	− 14	− 23	− 31
L_b	32	26	27	26
P	310	159	169	152
A	368	364	363	362
k_l	0·210	0·186	0·148	0·123
R/R_o	1·58	1·28	1·24	1·17
θ	3·7	3·1	2·1	1·3
M_b	95	93	122	145
M_s	− 27	− 31	− 40	− 48
k_l	0·219	0·194	0·153	0·126
X	0·0190	0·0173	0·0122	0·0081
Y	0·0052	0·0035	0·0024	0·0017
K	0·0242	0·0208	0·0146	0·0096
k_x	− 0·0022	− 0·0002	0·0024	0·0035
k_m	− 0·0476	− 0·0433	− 0·0372	− 0·0338

* All speeds are in miles per hour.
† In feet per minute.

TABLE 6 (*Cont.*).

Number	24.	25.	26.	27.
W	1944	1942	2083	2082
x	− 0·090	− 0·087	− 0·296	− 0·294
z	− 0·331	− 0·332	− 0·395	− 0·395
*V_o (observation)	98	110	42	49
*V_o (calibration)	98·4	110·5	41·6	48·7
*V_o (speed course)	100·0	110·5	45·9	53·3
Mean height	3600	—	3700	4000
Temperature °C.	10	—‡	8	775
Percentage density ...	89·5	91 ?	89·8	88·9
*V (true)	105·7	116	48·4	56·4
†Gain in height	− 1600	− 2850	200	560
α	− 9·9	− 16·0	2·7	6·5
M	− 224	− 10	− 264	− 314
M_r	28	38	− 5	4
M_t	160	196	34	46
T	37	22	26	33
L_s	− 40	− 53	3	− 1
L_b	26	15	50	48
P	47	− 113	363	510
A	361	359	380	381
k_l	0·103	0·083	0·480	0·354
R/R_o	1·04	0·90	2·42	2·48
θ	0·9	0·03	10·9	7·5
M_b	156	174	14	63
M_s	− 58	− 71	− 12	− 16
k_l	0·1055	0·087	0·510	0·377
X	0·0050	0·0021	0·0189	0·0163
Y	0·0007	− 0·0001	0·0361	0·0266
K	0·0057	0·0020	0·0550	0·0429
k_x	0·0041	0·0045	− 0·0513	− 0·0225
k_m	− 0·0311	− 0·0281	− 0·0938	− 0·0718

* All speeds are in miles per hour.
† In feet per minute.
‡ Machine descending too fast for accurate observations of height or temperature.

TABLE 6 (*Cont.*).

Number	28.	29.	30.	31.
W	2080	2079	2077	2076
x	− 0·293	− 0·291	− 0·289	− 0·288
z	− 0·396	− 0·396	− 0·397	− 0·397
*V_o (observation)	59	79	99	115
*V_o (calibration)	59·0	79·1	99·4	115·1
*V_o (speed course)	63·5	83·0	101·0	114·2
Mean height	4610	4790	4650	—
Temperature °C.	7	6	6·5	—‡
Percentage density	87·2	86·9	87·2	88 ?
*V (true)	68·0	89·0	108·1	122
†Gain in height	280	40	− 680	− 2300
α	2·7	0·3	− 4·1	− 12·3
M	− 354	− 225	41	323
M_r	7	22	34	40
M_t	65	110	163	210
T	39	32	14	− 6
L_s	− 7	− 22	− 39	− 56
L_b	40	35	32	30
P	376	353	284	45
A	371	367	364	361
k_l	0·261	0·158	0·110	0·086
R/R_o	1·82	1·48	1·26	1·04
θ	5·1	2·3	1·1	0·4
M_b	84	143	195	208
M_s	− 23	− 40	− 59	− 76
k_l	0·273	0·161	0·110	0·0865
X	0·0138	0·0059	0·0009	− 0·0018
Y	0·0174	0·0092	0·0055	0·0032
K	0·0312	0·0151	0·0064	0·0014
k_x	− 0·0079	0·0019	0·0039	0·0045
k_m	− 0·0562	− 0·0400	− 0·0327	− 0·0298

* All speeds are in miles per hour.
† In feet per minute.
‡Machine descending too fast for accurate observations of height or temperature.

TABLE 7.

R.A.F. 18 CALCULATIONS.

Number	1.	2.	3.	4.	5.
W...	1959	1958	1958	1957	1956
x	+ 0·108	+ 0·109	+ 0·109	0·110	0·111
z	− 0·416	− 0·416	− 0·416	− 0·417	− 0·417
*V_o (observation)...	44·5	46·75	51·5	57·0	61·75
*V_o (calibration) ...	44·1	46·35	51·3	57·0	61·8
*V_o (speed course)	46·5	48·8	53·9	59·7	64·6
Mean height ...	2570	2940	3315	3755	4185
Temperature °C.	7·5	7	6·5	6·5	6·25
Percentage density	93·8	92·7	91·5	90·1	88·5
*V (true)	48·0	50·8	56·4	62·9	68·7
†Gain in height ...	338	362	408	463	408
α	4·6	4·6	4·7	4·8	3·9
M...	− 566	− 531	− 488	− 425	− 367
M_r	1	3	6	11	13
M_t	35	38	47	57	67
T	55	52	49	45	41
L_s	1	− 1	− 3	− 6	− 9
L_b	43	40	38	35	35
P	400	405	406	422	408
A	422	420	417	414	412
k_l	0·391	0·360	0·299	0·248	0·215
R/R_o	2·52	2·38	2·18	2·02	1·86
θ	8·6	7·8	6·2	4·8	4·0
M_b	41	47	65	86	98
M_s	− 13	− 14	− 17	− 21	− 24
$\hat{k}_l$	0·421	0·385	0·317	0·260	0·223
X...	0·0306	0·0263	0·0199	0·0145	0·0111
Y...	− 0·0007	− 0·0011	− 0·0015	− 0·0016	− 0·0019
K...	0·0299	0·0252	0·0184	0·0129	0·0092
k_x	− 0·0288	− 0·0231	− 0·0129	− 0·0059	− 0·0022
k_m	− 0·0933	− 0·0893	− 0·0785	− 0·0690	− 0·0626

* All speeds are in miles per hour.
† In feet per minute.

TABLE 7 (*Cont.*).

Number	6.	7.	8.	9.	10.
W...	1956	1955	1954	1954	1953
$\varkappa$	0·111	0·113	0·115	0·115	0·116
z	− 0·417	− 0·417	− 0·417	− 0·417	− 0·418
*V_o (observation)...	66·5	70·75	76·0	81·75	85·5
*V_o (calibration) ...	66·8	71·15	76·3	81·9	85·8
*V_o (speed course)	69·7	74·1	79·2	84·8	88·7
Mean height ...	4510	4740	4900	4935	4750
Temperature °C.	6·25	6	5·75	5·5	6
Percentage density	87·7	87·0	86·6	86·6	87·0
*V (true)	74·5	79·5	85·2	91·2	95·2
†Gain in height ...	308	218	137	− 116	− 277
α	2·7	1·8	1·05	− 0·8	− 1·9
M...	− 296	− 233	− 116	− 14	118
M_r	16	17	22	24	26
M_t	78	88	100	115	126
T	35	31	22	14	3
L_s	− 13	− 16	− 20	− 25	− 29
L_b	33	32	32	31	31
P	387	329	367	326	305
A	409	407	407	405	404·5
k_l	0·187	0·169	0·148	0·131	0·120
R/R_o	1·69	1·55	1·53	1·42	1·36
θ	3·2	2·8	2·2	1·7	1·5
M_b	110	115	137	147	157
M_s	− 28	− 32	− 36	− 42	− 46
k_l...	0·192	0·173	0·150	$0·131_5$	0·120
X...	0·0080	0·0060	0·0032	0·0013	− 0·0006
Y...	− 0·0021	− 0·0025	− 0·0023	− 0·0024	− 0·0024
K...	0·0059	0·0035	0·0009	− 0·0011	− 0·0030
k_x	0·0004	0·0018	0·0029	0·0037	0·0042
k_m	− 0·0572	− 0·0540	− 0·0499	− 0·0463	− 0·0447

* All speeds are in miles per hour.
† In feet per minute.

TABLE 7 (*Cont.*).

Number.	11.	12.	13.	14.
W	1952	1951	1929	1928
x	0·117	0·119	0·038	0·040
z	− 0·418	− 0·418	− 0·418	− 0·419
*V_o (observation)	90·5	96·75	46·5	49·5
*V_o (calibration)	90·6	97·25	46·1	49·1
*V_o (speed course)	93·5	100·0	48·6	51·7
Mean height...	4475	3985	1750	2575
Temperature °C.	6·25	6·25	0	− 1
Percentage density	87·8	89·4	99·3	96·6
*V (true)	99·9	105·7	48·8	52·8
†Gain in height	− 378	− 705	515	545
α	− 2·45	− 4·35	6·85	6·7
M	265	443	− 353	− 357
M_r	30	34	4	6
M_t	140	160	38	43
T	− 9	− 23	36	37
L_s	− 33	− 40	0	− 1
L_b	32	32	43	41
P	215	289	476	474
A	404	403	423	421
k_l	0·1095	0·097	0·354	0·316
R/R_o	1·34	1·28	2·64	2·46
θ	1·2	0·9	7·6	6·6
M_b	175	192	56	66
M_s	− 51	− 58	− 14	− 16
k_l	0·108	0·095	0·378	0·336
X	− 0·0024	− 0·0040	0·0174	0·0157
Y	− 0·0033	− 0·0023	0·0042	0·0032
K	− 0·0047	− 0·0063	0·0216	0·0189
k_x	0·0044	0·0046	− 0·0220	− 0·0155
k_m	− 0·0429	− 0·0403	− 0·0910	− 0·0828

* All speeds are in miles per hour.
† In feet per minute.

TABLE 7 (*Cont.*).

Number	15.	16.	17.	18.
W	1927	1926	1925	1924
x	0·041	0·043	0·044	0·045
z	− 0·419	− 0·419	− 0·420	− 0·420
*V_o (observation)	53·0	56·0	61·0	66·25
*V_o (calibration)	52·9	56·1	60·0	66·55
*V_o (speed course)	55·6	58·8	63·9	69·45
Mean height...	3380	4010	4530	5000
Temperature °C.	− 2·5	− 4·5	− 5	− 6·5
Percentage density	94·4	92·8	91·3	90·2
*V (true)	57·2	60·9	66·9	73·2
†Gain in height	540	485	457	342
α	6·15	5·2	4·45	3·05
M	− 333	− 307	− 271	184
M_r	8	10	13	16
M_t	50	55	65	77
T	36	34	32	25
L_s	− 6	− 6	− 9	− 13
L_b	38	36	35	33
P	458	431	422	389
A	417·5	415	412·5	409·5
k_l	0·278	0·252	0·216	0·185
R/R_o	2·24	2·07	1·90	1·71
θ	5·6	4·9	4·0	3·2
M_b	76	85	99	110
M_s	− 18	− 20	− 24	− 28
k_l	0·293	0·263	0·224	0·190
X	0·0132	0·0110	0·0084	0·0053
Y	0·0022	0·0014	0·0007	0·0001
K	0·0154	0·0124	0·0091	0·0054
k_x	− 0·0099	− 0·0066	− 0·0023	0·0006
k_m	− 0·0754	− 0·0706	− 0·0630	− 0·0572

* All speeds are in miles per hour.
† In feet per minute.

TABLE 7 (*Cont.*).

Number	19.	20.	21.	22.
W	1923	1922	1921	1920
x	0·046	0·048	0·049	0·051
z	− 0·420	− 0·420	− 0·421	− 0·421
*V_o (observation)	70·5	75·5	81·25	85·25
*V_o (calibration)	70·9	75·9	81·35	85·55
*V_o (speed course)	73·8	78·9	84·3	88·45
Mean height	5250	5360	5405	5225
Temperature °C.	− 7	− 8	− 8	− 8
Percentage density	89·6	89·6	89·4	90·0
*V (true)	78·0	83·4	89·3	93·3
†Gain in height	183	142	− 117	− 261
α	1·5	1·1	− 0·85	− 1·8
M	− 152	− 22	78	203
M_r	17	20	23	26
M_t	87	100	114	126
T	23	13	5	− 5
L_s	− 16	− 20	− 25	− 28
L_b	32	30	30	31
P	349	358	320	312
A	408	406·5	405	404·5
k_l	0·167	0·148	0·131	0·120
R/R_o	1·58	1·51	1·42	1·37
θ	2·7	2·2	1·8	1·5
M_b	117	134	145	157
M_s	− 32	− 36	− 41	− 45
k_l	0·170	0·149	0·131	0·119
X	0·0042	0·0014	− 0·0002	− 0·0019
Y	− 0·0004	− 0·0006	− 0·0009	− 0·0010
K	0·0038	0·0008	− 0·0011	− 0·0029
k_x	0·0019	0·0029	0·0037	0·0042
k_m	− 0·0531	− 0·0500	− 0·0467	− 0·4470

* All speeds are in miles per hour.
† In feet per minute.

REPORT Nº 400.

FIG. 1.

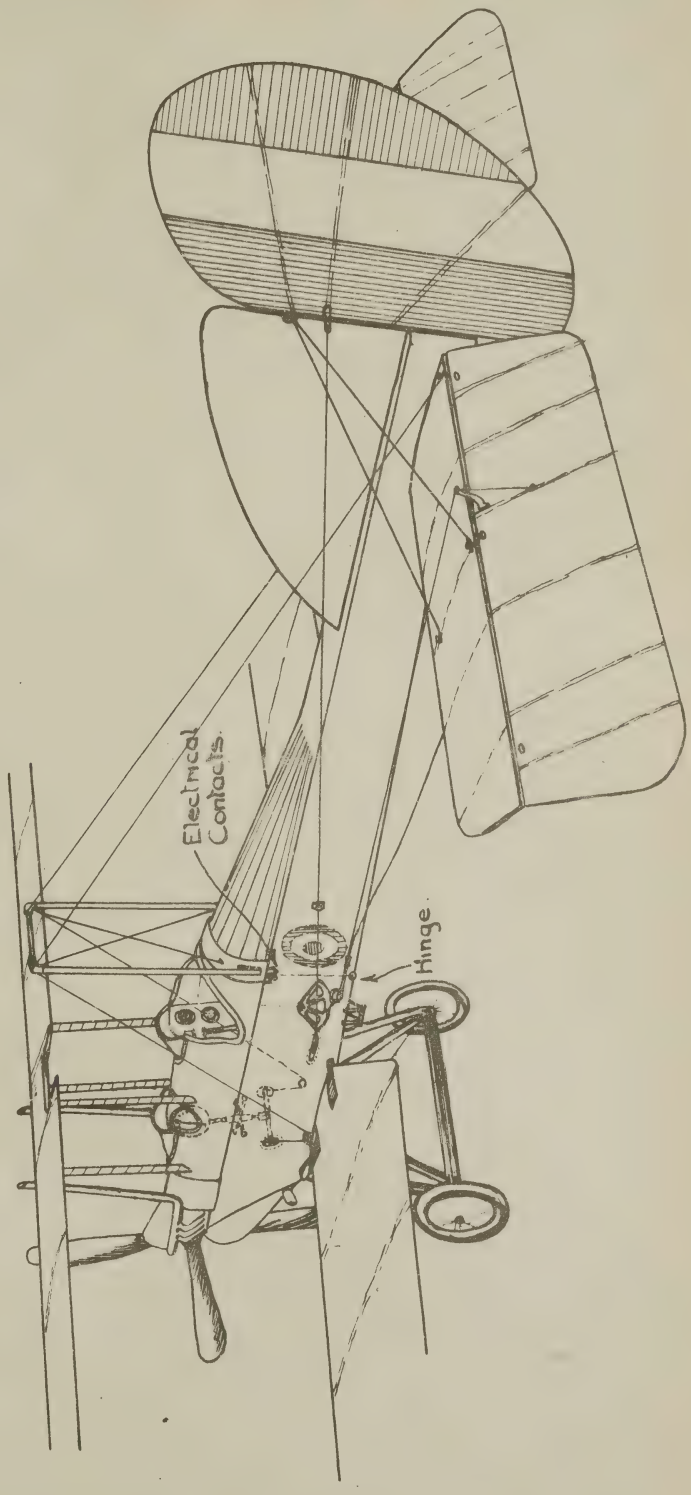

AEROFOIL SECTIONS.

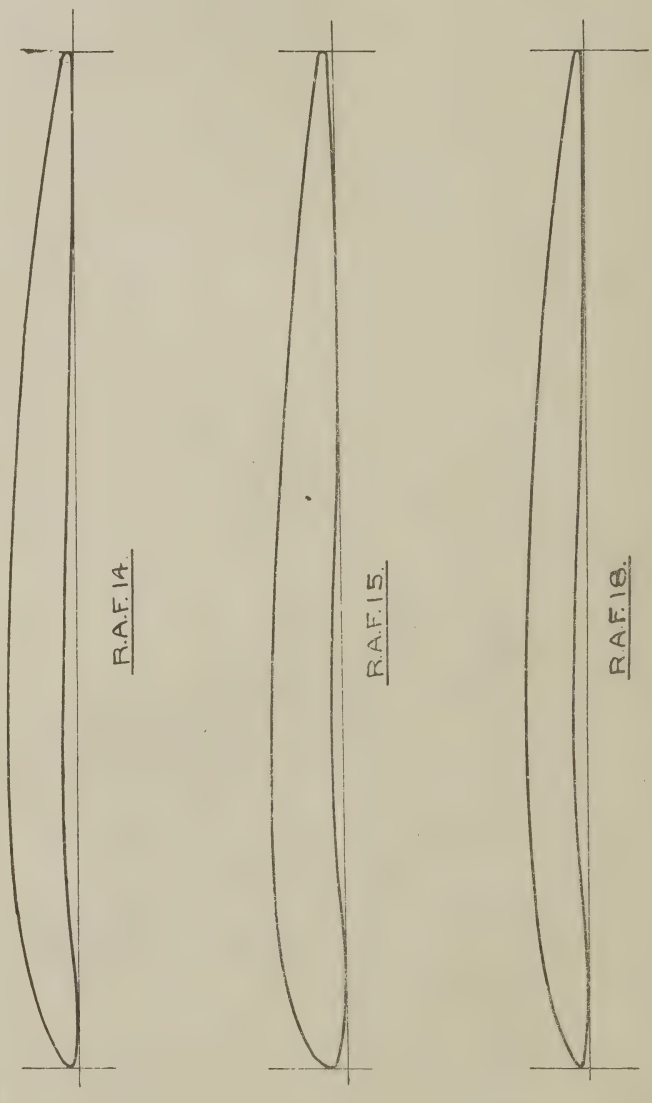

REPORT No. 400.

PLAN FORM OF B.E.2e WINGS.

THE CONTINUOUS LINE REPRESENTS R.A.F. 14 & 15 SECTIONS.

THE BROKEN LINE REPRESENTS R.A.F. 18 SECTION.

STAGGER 22°. GAP 6·26'. CHORD (R.A.F. 14&15) 5·5' (R.A.F. 18) 6·17'.

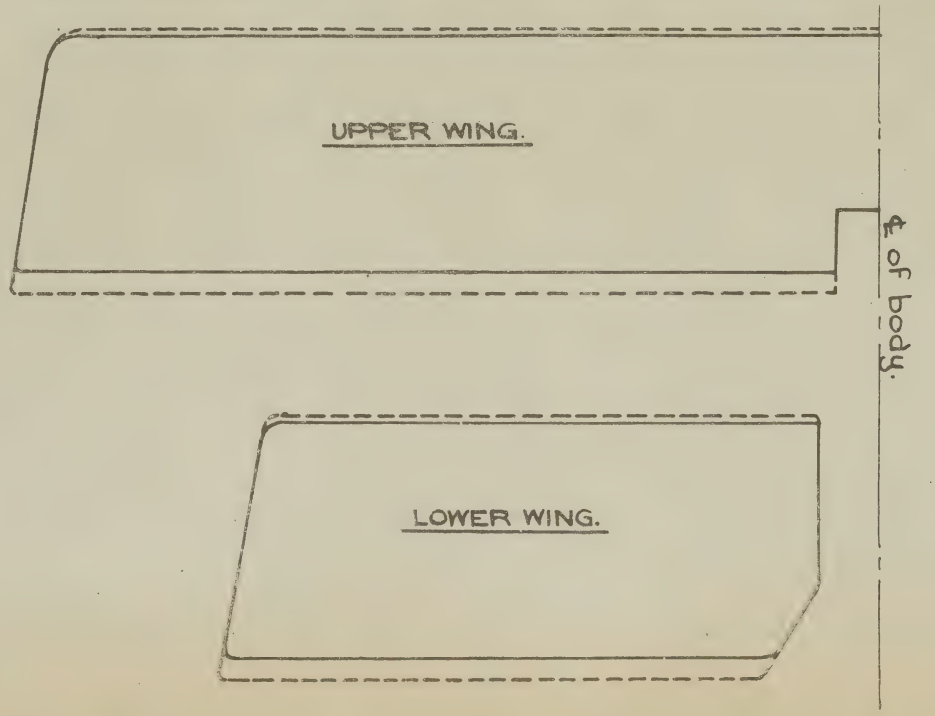

FIG. 3.

MEAN CHORD FOR R.A.F. 14 & 15 SECTIONS.

LENGTH OF MEAN CHORD = 5·39'.

MOMENTS ARE CALCULATED ABOUT THE POINT O, FOR WHICH h = 0·345, K = 0·327.

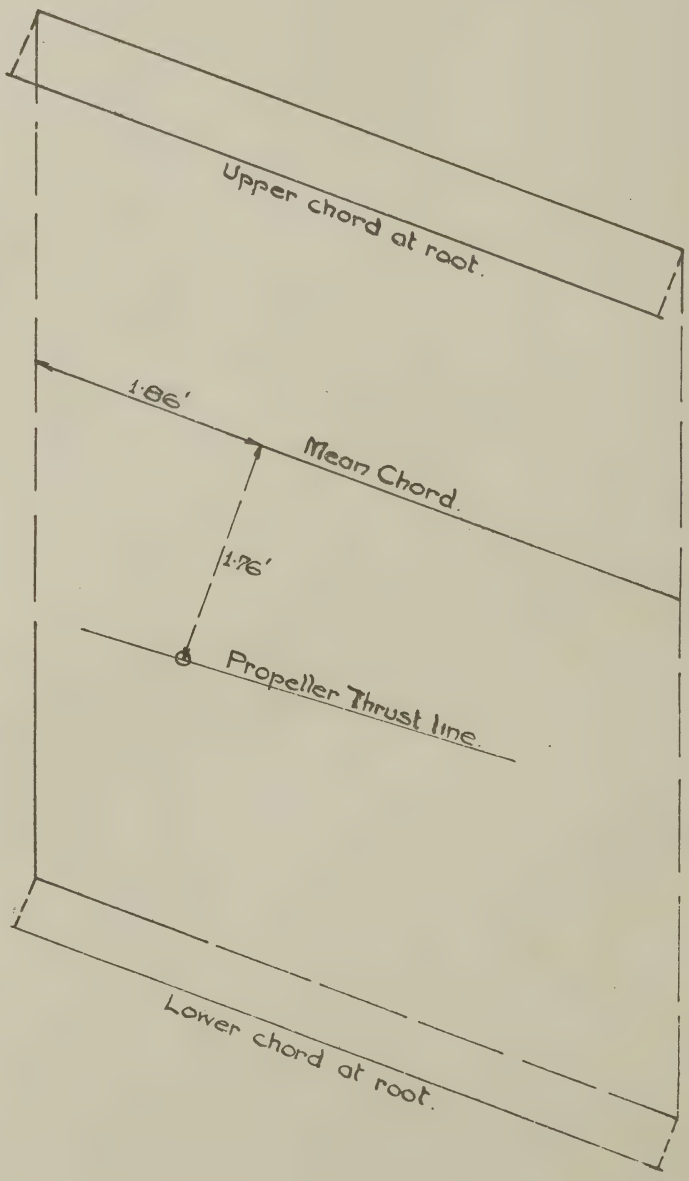

MEAN CHORD FOR R.A.F. 18 SECTION.

LENGTH OF MEAN CHORD = 6·02'.

MOMENTS ARE CALCULATED ABOUT THE POINT O, FOR WHICH h = 0·337, K = 0·294.

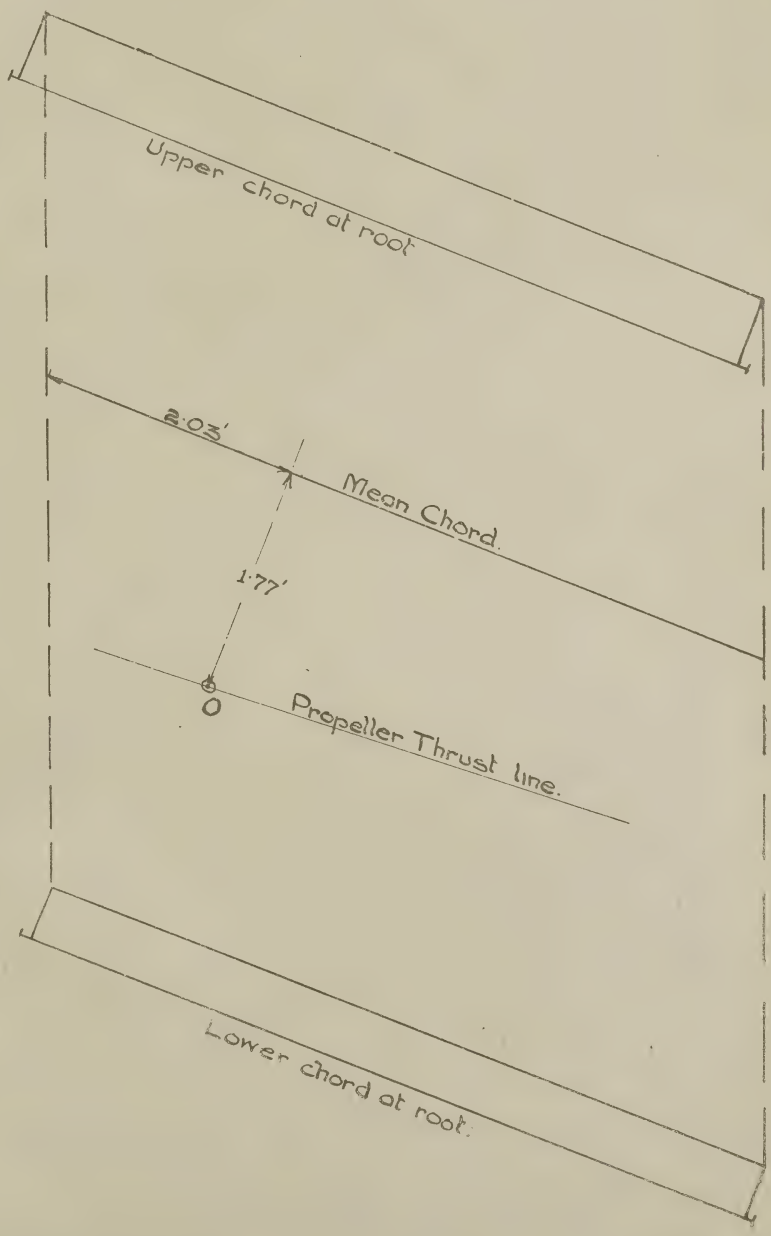

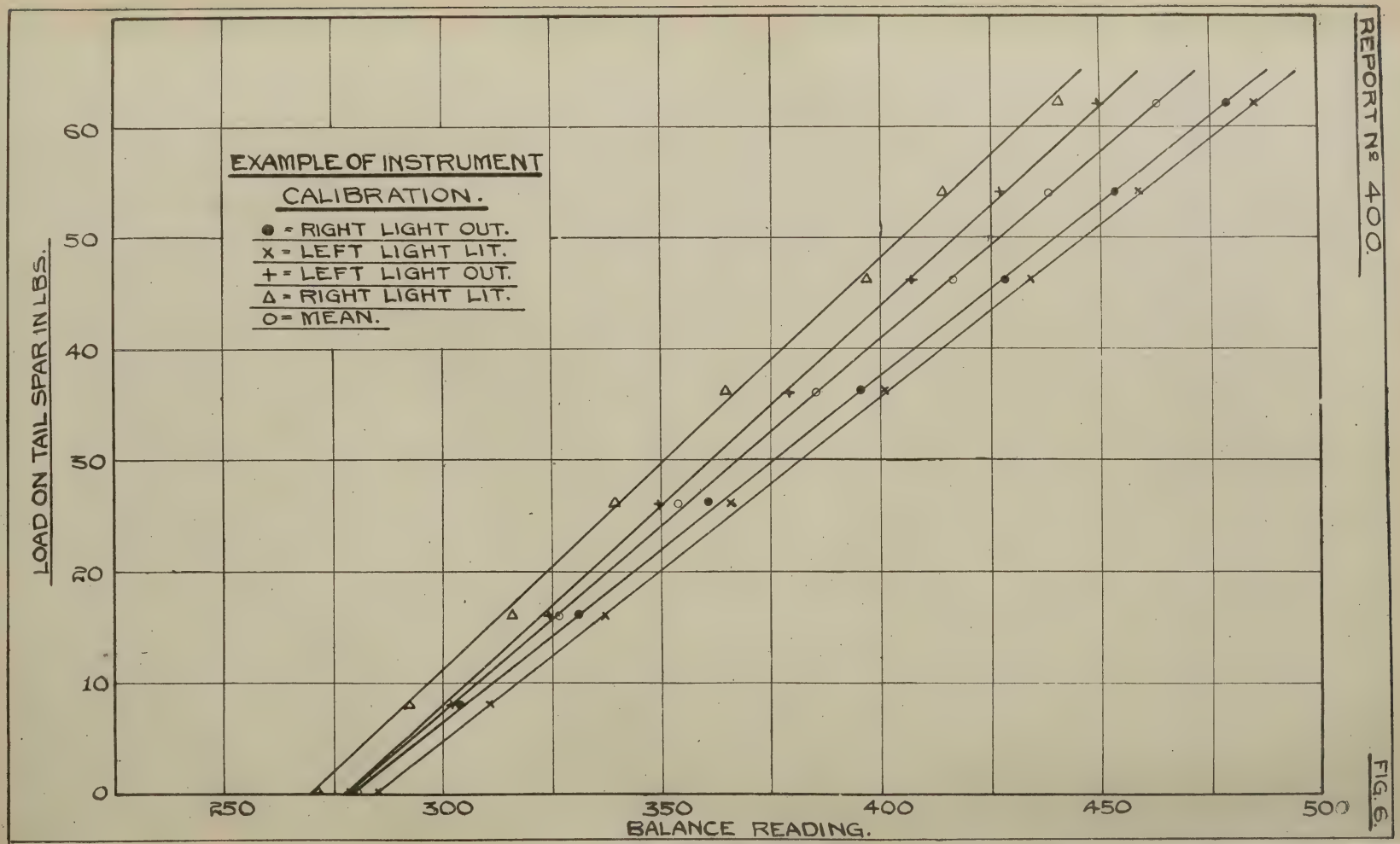

REPORT Nº 400.

FIG. 6.

RE

MOMENT COEFFICIENT. R.A.F. 14 WING SECTION.

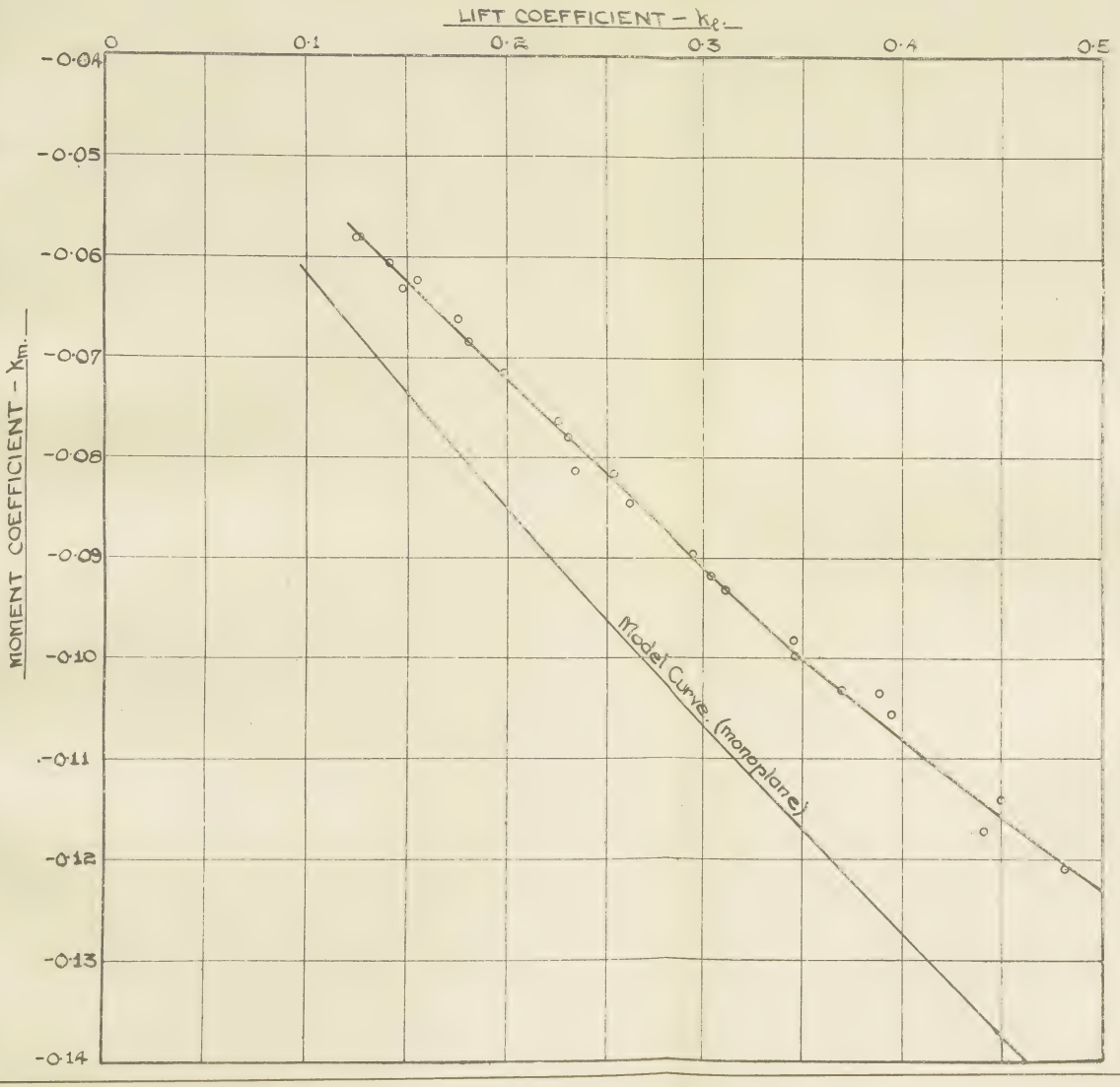

RE

MOMENT COEFFICIENT. R.A.F. 15 WING SECTION.

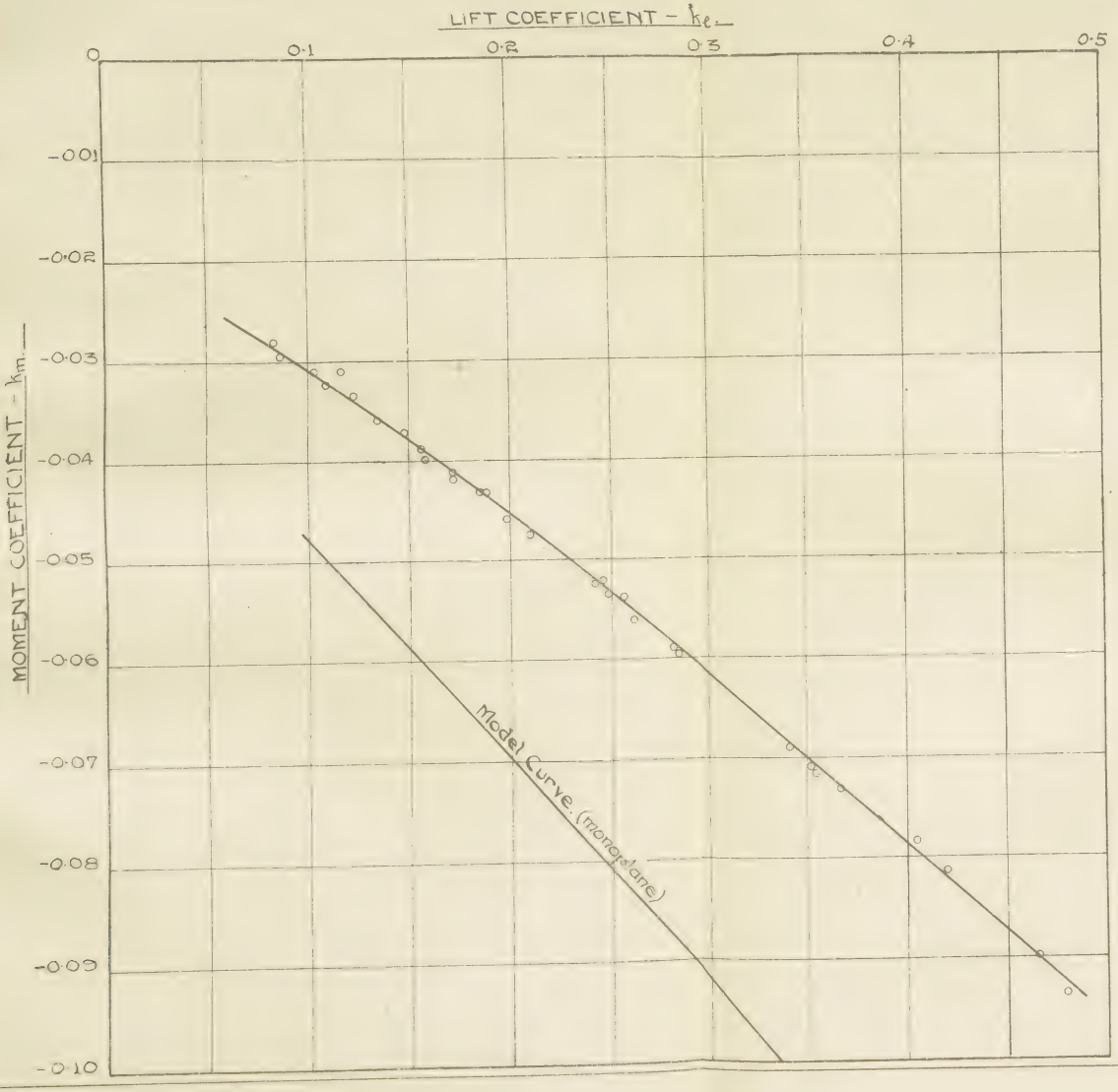

MOMENT COEFFICIENT. R.A.F. 18 WING SECTION.

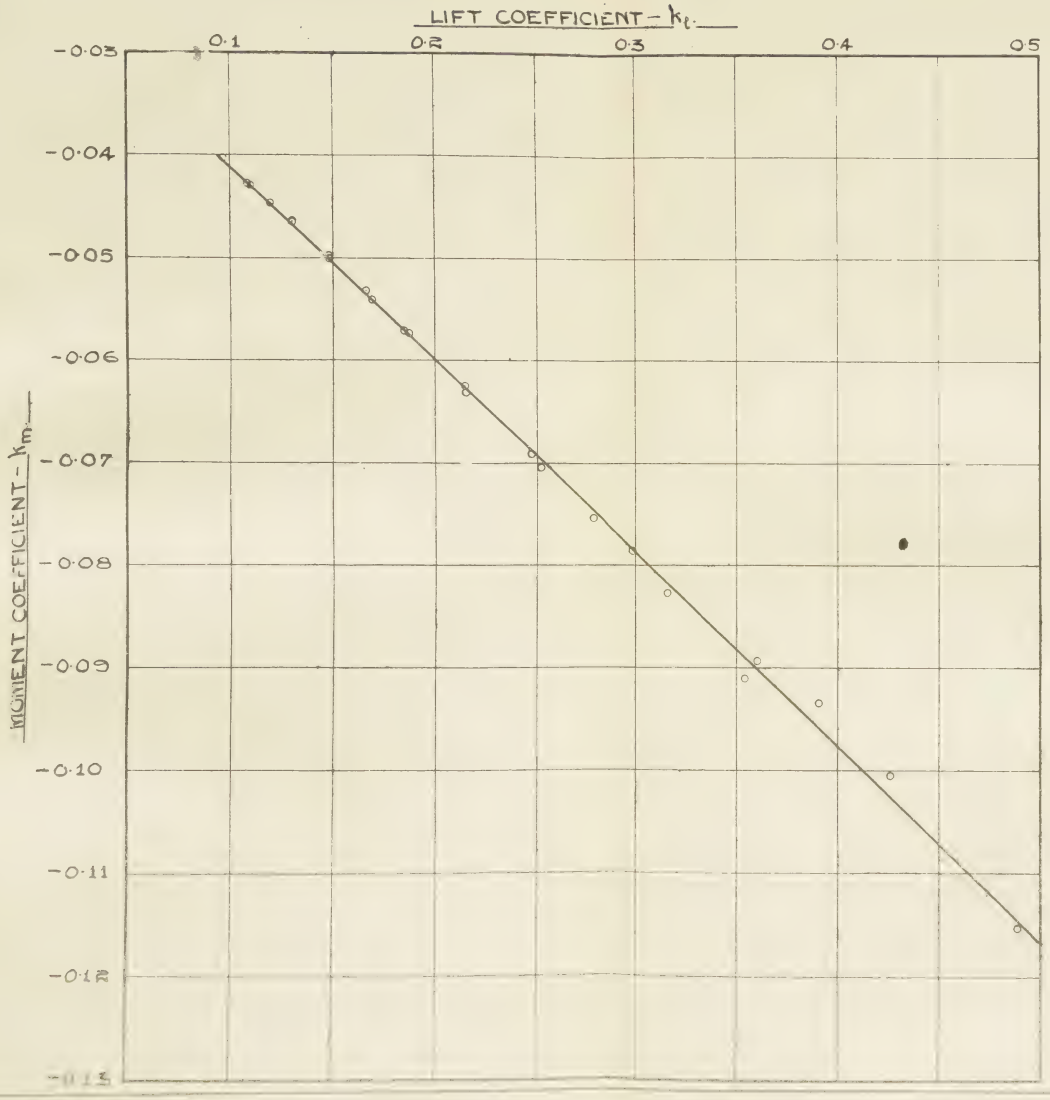

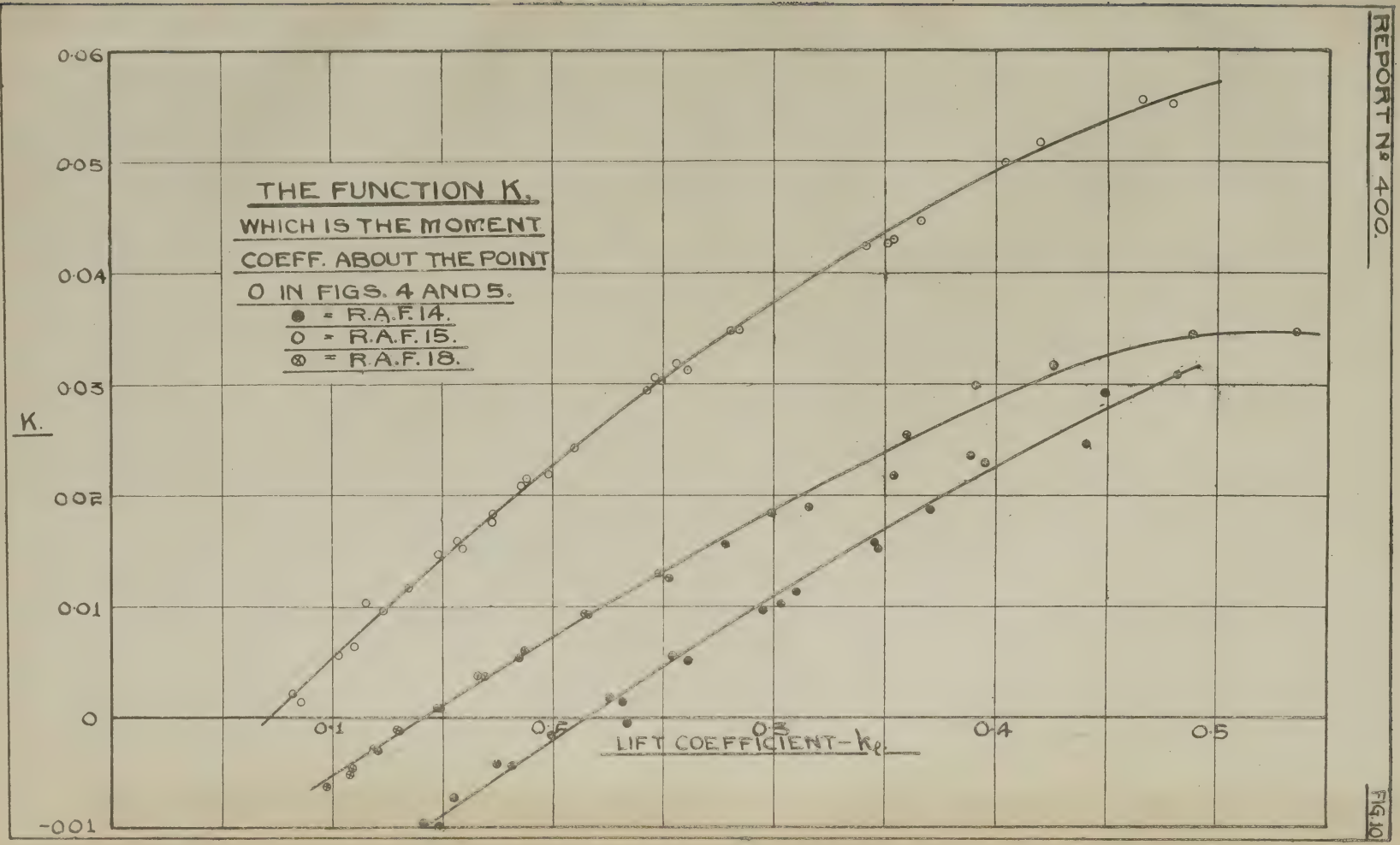

REPORT Nº 400.

FIG. 10

REPORT Nº 400.

CENTRE OF PRESSURE.

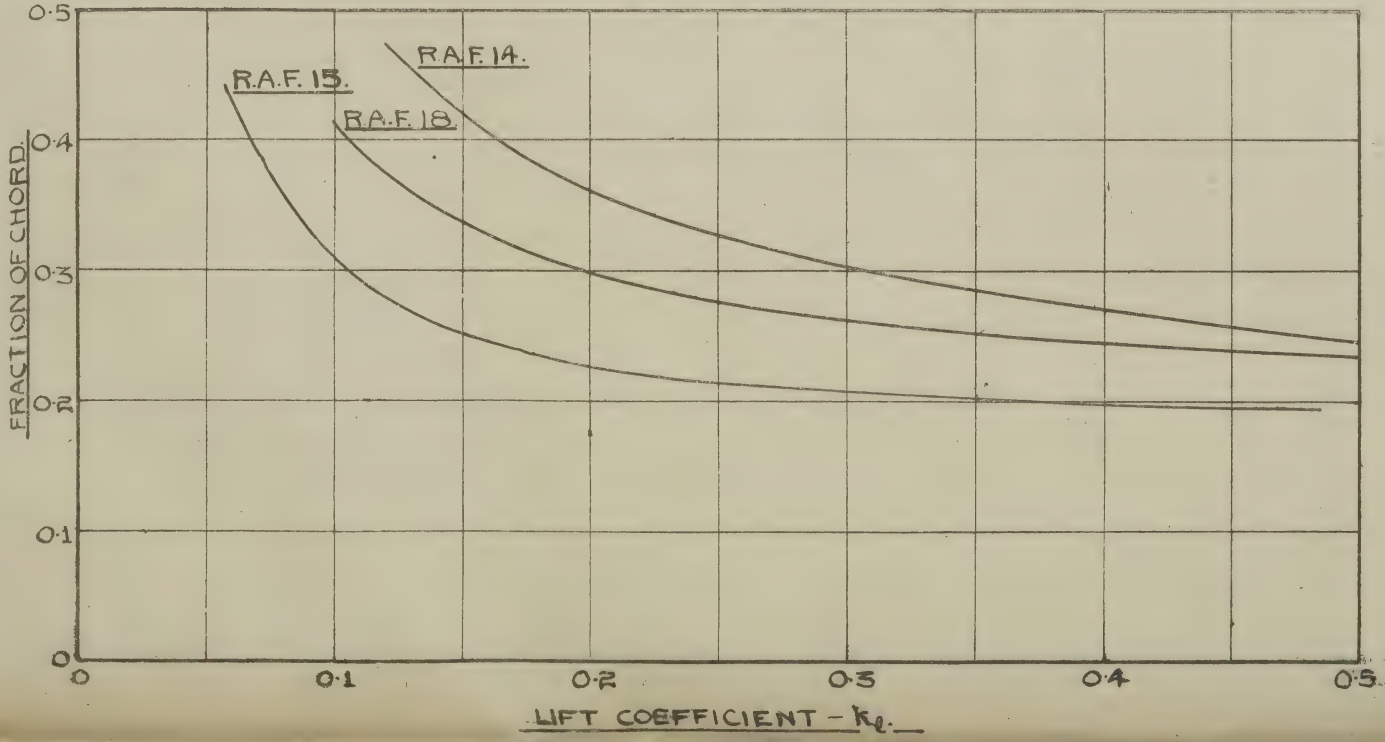

FIG. 11

TABLE 7 (*Cont.*).

Number	23.	24.	25.	26.
W	1919	2014	2013	2015
x	0·052	0·095	0·096	0·097
z	− 0·421	− 0·423	− 0·423	− 0·426
*V_o (observation)	90·5	42·0	44·0	40·0
*V_o (calibration)	90·6	41·4	43·5	39·3
*V_o (speed course)	93·5	43·7	45·7	41·1
Mean Height	4760	530	330	600
Temperature °C.	− 8	2	2	2
Percentage density	91·6	103·1	103·8	102·8
*V (true)	97·8	43·0	44·9	40·9
†Gain in height	− 500	− 360	− 200	− 400
α	− 3·3	− 5·45	− 2·9	− 6·4
M	379	− 598	− 590	− 531
M_r	29	− 7	− 4	− 10
M_t	140	31	33	28
T	− 19	56·5	56	50
L_s	− 34	4	2	4
L_b	30	29	34	30
P	284	38	118	8
A	403·5	402	407	399·5
k_l	0·108	0·488	0·426	0·546
R/R_o	1·31	1·19	1·52	1·04
θ	1·1	11·1	9·5	12·6
M_b	172	− 11	8	− 20
M_s	− 51	− 11	− 12	− 10
$\bar{k}_l$	0·1065	0·515	0·464	0·574
X	− 0·0039	0·0387	0·0349	0·0395
Y	− 0·0012	− 0·0044	− 0·0035	− 0·0048
K	− 0·0051	0·0343	0·0314	0·0347
k_x	0·0045	− 0·0495	− 0·0355	− 0·0625
k_m	− 0·0428	− 0·1153	− 0·1005	− 0·1310

* All speeds are in miles per hour.
† In feet per minute.

TABLE 8.

NUMERICAL RESULTS.

k_l	R.A.F. 14.			R.A.F. 15.			R.A.F. 18.		
	k_m.	dk_m/dk.	C.P.	k_m.	dk_m/dk_l.	C.P.	k_m.	dk_m/dk_l.	C.P.
0·06				−0·0259	−0·122	0·429			
0·08				−0·0284	−0·127	0·364			
0·10				−0·0310	−0·132	0·310	−0·0412	−0·180	0·412
0·12	−0·0568	−0·190	0·475	−0·0337	−0·137	0·280	−0·0448	−0·181	0·373
0·14	−0·0606	−0·190	0·435	−0·0365	−0·142	0·260	−0·0485	−0·182	0·346
0·16	−0·0644	−0·190	0·403	−0·0394	−0·147	0·245	−0·0522	−0·183	0·326
0·18	−0·0682	−0·190	0·379	−0·0424	−0·152	0·234	−0·0560	−0·184	0·311
0·20	−0·0720	−0·190	0·360	−0·0455	−0·156	0·227	−0·0597	−0·185	0·298
0 22	−0·0758	−0·190	0·343	−0·0486	−0·159	0·220	−0·0634	−0·185	0·288
0 24	−0·0790	−0·190	0·331	−0·0518	−0·161	0·216	−0·0671	−0·186	0·279
0 26	−0·0834	−0·190	0·320	−0·0551	−0·163	0·212	−0·0708	−0·187	0·272
0·28	−0·0872	−0·190	0·312	−0·0584	−0·165	0·209	−0·0745	−0·188	0·266
0·30	−0·0910	−0·188	0·303	−0·0617	−0·167	0·206	−0·0783	−0·188	0·261
0·32	−0·0947	−0·180	0·295	−0·0650	−0·168	0·204	−0·0821	−0·189	0·257
0·34	−0·0982	−0·170	0·288	−0·0684	−0·169	0·202	−0·0859	−0·190	0·253
0·36	−0·1015	−0·163	0·281	−0·0718	−0·170	0·200	−0·0897	−0·191	0·249
0·38	−0·1047	−0·160	0·275	−0·0752	−0·171	0·199	−0·0985	−0·192	0·246
0·40	−0·1079	−0·157	0·269	−0·0786	−0·172	0·197	−0·0973	−0·193	0·243
0·42	−0·1110	−0·154	0·264	−0·0821	−0·173	0·196	−0·1012	−0·194	0·241
0·44	−0·1141	−0·152	0·259	−0·0856	−0·174	0·195	−0·1051	−0·195	0·239
0·46	−0·1171	−0·150	0·254	−0·0891	−0·175	0·194	−0·1090	−0·196	0·237
0·48	−0·1201	−0·148	0·250	−0·0926	−0·176	0·193	−0·1129	−0·197	0·225
0·50	−0·1230	−0·146	0·246				−0·1168	−0·198	0·234

FULL SCALE EXPERIMENTS WITH ELEVATORS OF DIFFERENT SIZES.

By H. Glauert.

Presented by the Superintendent, Royal Aircraft Factory.

Reports and Memoranda (*New Series*), *No.* 409. *December*, 1917.

Summary.—(*a*) *Introductory.* (*Reasons for inquiry.*)—The size of elevators fitted to a tail plane must be chosen from two considerations, the amount of control and the force that must be exerted by the pilot. Model experiments (T. 995) indicated that a reduction in the size of the elevators from the 50 per cent. usually employed would give lighter forces without any loss of control. Experiments were made to test this, and at the same time it was desired to repeat the stability experiments carried out previously on R.E. 8, owing to the unusual values obtained for the tail efficiency and downwash.

(*b*) *Range of the investigation.*—Experiments were therefore carried out by fitting elevators of different sizes to an R.E. 8 machine, chosen so as to be respectively 30, 40, 50 and 60 per cent. of the total tail area, and measuring the force on the control column and the angle at which the elevators were held. A careful series of experiments was also made to obtain a satisfactory determination of the tail efficiency.

(*c*) *Conclusions.*—It was found that the force of the control column required to produce a definite change of tail lift increases with the size of the elevators, and that the movement of the elevators decreases. With gearing arranged to give the same total control the smaller elevators would still require smaller forces from the pilot. The determination of the tail efficiency gave a value of 0·6 and the downwash curve was approximately a straight line passing through the point of no lift. This position of the downwash curve depends on values of the moment coefficient derived from full scale experiments (R. & M. 409).

(*d*) *Applications and further developments.*—The results of these experiments showed that it is advantageous to reduce the size of elevators in general use to approximately half the chord of the fixed tail plane in order to secure lightness of control.

1. An investigation has been carried out recently on the effect of varying the size of elevator surfaces on a standard R.E. 8 machine. A series of four different elevators of the same shape were fitted to the standard fixed tail plane, and the areas were chosen so as to be respectively 30, 40, 50 and 60 per cent. of the total tail area. The form of these elevators is shown in Fig. 1, and details are given in Table 1. The positions of the tail plane and elevators in each experiment were recorded on

two scales at the side of the observers' cockpit. The method of experiment employed was to fly at some definite speed with three different tail settings, and to note the force on the control column and the angle at which the elevators were held. The experiments were carried out at three different speeds both with the engine on full throttle and gliding. Experiments were also made with each set of elevators to determine the trimming speed with free elevators for different tail settings and different positions of the centre of gravity.

2. An exhaustive series of experiments was first carried out with the standard 50 per cent. elevators to determine the tail efficiency, as defined in previous reports on longitudinal stability, and to obtain satisfactory values of the angle of downwash for different attitudes of the machine. By suitable adjustment of the loads carried in the machine it was found possible to move the centre of gravity through a distance of nearly 3 inches, and the corresponding change in tail setting, to trim at the same speed, determines the increase in lift of the tail plane for a definite increase in its angle of incidence. These experiments led to a value of 0·6 for the efficiency of the tail plane, which agrees with the results previously found for other tractor machines. The values of the angle of downwash as obtained from the present series of experiments are shown in Fig. 2, where points derived from different positions of the centre of gravity are shown in a distinctive manner. The curve derived is approximately a straight line passing through the point of no lift, and the mean slope is such that $de/d\theta = 0{\cdot}45$. The moment coefficients used in obtaining these values of e and $de/d\theta$ are derived from full scale experiments in a B.E. 2E (see R. & M. 4′0). The wing of R.E. 8 is very nearly the same as that of B.E. 2E.

3. The experimental data as to the characteristics of the different elevators has been analysed on the assumption that the lift of a tail plane and the hinge moment on the elevators are both linear functions of the angle of incidence and of the elevator angle. It is therefore permissible to write

$$k'_l = a\theta' + b\eta,$$

and

$$\mathrm{M} = c\theta' + d\eta,$$

where

θ' is the angle of incidence of the tail plane,

η is the elevator angle,

k_l' is the lift coefficient of the tail plane,

M is the hinge moment on the elevators at 100 ft./sec.,

a and b are therefore absolute coefficients, while c and d have the dimensions of a moment.

In these expressions, a, b, c, d are the four constants which have to be determined for each set of elevators. The first of these—a—expresses the rate of increase of lift with angle of incidence when the elevators are fixed, and so can be taken to be independent of the size of the elevators, except in so far as changing the chord of the elevators changes the overall section and the aspect ratio of the combination, and the ratio of its value to that derived from model test is given by the tail efficiency of 0·6. In consequence the value of a for each set of elevators is 0·0189. Two more relations between the four constants can be obtained by considering the experiments carried out at the same speed with different tail settings (ψ) and different elevator angles (η). In virtue of the fact that the attitude of the machine is unaltered, the tail lift remains the same, and so there are the following relations between the changes in the tail setting, elevator angle, and hinge moment

$$a\Delta\psi + b\Delta\eta = 0$$
$$c\Delta\psi + d\Delta\eta = \Delta M$$

which give

$$\frac{a}{b} = -\frac{\Delta\eta}{\Delta\psi}$$
$$\frac{bc - ad}{a} = -\frac{\Delta M}{\Delta\eta}$$

These two ratios can both be determined from the experimental data, since the elevator angle and tail setting are recorded by the observer, and the hinge moment (M) is derived directly from the force exerted on the control column. The probable errors of the experimental determination of these ratios were found to be 2 and 3 per cent. respectively. The results are given in Table 2.

4. The complete determination of the constants of the elevators was based on the analysis of the trimming speeds with elevators free. If w is the weight moment of the elevators the conditions when the elevators are hanging freely are

$$k_l' = a\theta' + b\eta,$$
$$-w\frac{2{\cdot}15\ V_o^2}{10^4} = c\theta' + d\eta,$$

and so

$$k_l' = \frac{ad - bc}{d}\theta' - \frac{b}{d}\frac{w\ 10^4}{2{\cdot}15\ V_o^2},$$

where V_o is the mean indicated airspeed over the elevators in m.p.h. The value of θ'_u (the angle of no lift of the tail at speed V_o, with elevators hanging freely) is

$$\frac{b}{ad - bc} \cdot \frac{w}{2{\cdot}15} \cdot \frac{10^4}{V_o^2}$$

and so can be determined from the values of the ratio of ΔM to $\Delta\psi$, as explained in the previous paragraph. The values of

θ'_u used in the analysis of the trimming speeds were determined in this manner, and the downwash was supposed to be given by the curve derived from the experiments with the 50 per cent. elevators. In this way numerous determinations were made of the quantity $\frac{ad - bc}{d}$, and the mean values given in Table 2 were found to have probable errors of only 2 per cent., but this expresses only the divergence of the experiments amongst themselves, and not the deviation from the truth of the mean values, since the analysis assumes the accuracy of the downwash curve. The values b, c, and d are shown in Fig. 3 corrected to apply to tail planes of the same total area (46 sq. ft.), and are compared with the model tests described in R. & M. 254, which have been reduced to the same basis. These model tests were made on a tail plane of different shape, but it will be seen that the results are in good agreement. The full scale values of c and d are about 90 per cent., and those of b about 60 per cent. of the model values. The latter figure is in accordance with the tail efficiency of 0·6, while the former (90 per cent.) implies that the trailing edge of the tail plane is not affected to the same extent as the leading edge. Slipstream experiments (R. & M. 438) have suggested that about one-half of the tail efficiency factor is due to the difference in the slipstreams of tractor and pusher machines. The remaining portion must be ascribed to interference of the body and to scale effect. Since a smaller proportion of the elevators is under the influence of the slipstream compared with the tail plane as a whole, and since the elevators are not in close contact with the body of the aeroplane, the factor of 0·9 instead of 0·6 appears to be quite reasonable.

5. The results have also been examined on the basis of uniform longitudinal stability. This implies that the tail plane area must be inversely proportional to the value of $\frac{dk_t'}{d\theta'}$, when the elevators are hanging freely.

Correcting the areas in this way, calculations have been made of the force on the control required to hold the aeroplane, first to 75 m.p.h. gliding, and secondly to 65 m.p.h. engine full on, the tail plane being set in each case for a trimming speed of 75 m.p.h. with engine on and elevators free. The results of these calculations are given in Table 4. In each case the force necessary increases with the size of the elevators as might be expected. When the engine is shut off, the necessary movement of the elevators is greatest with the small elevators, but to change to 65 m.p.h. with engine on, the change of elevator angle is practically independent of the size of the elevators.

The reduction in force on the control column, due to reducing the size of the elevators, could also be obtained by changing the gearing. To obtain a fair comparison of the different elevators,

REPORT Nº. 409.

EXPERIMENTAL ELEVATORS.

1/12 SCALE.

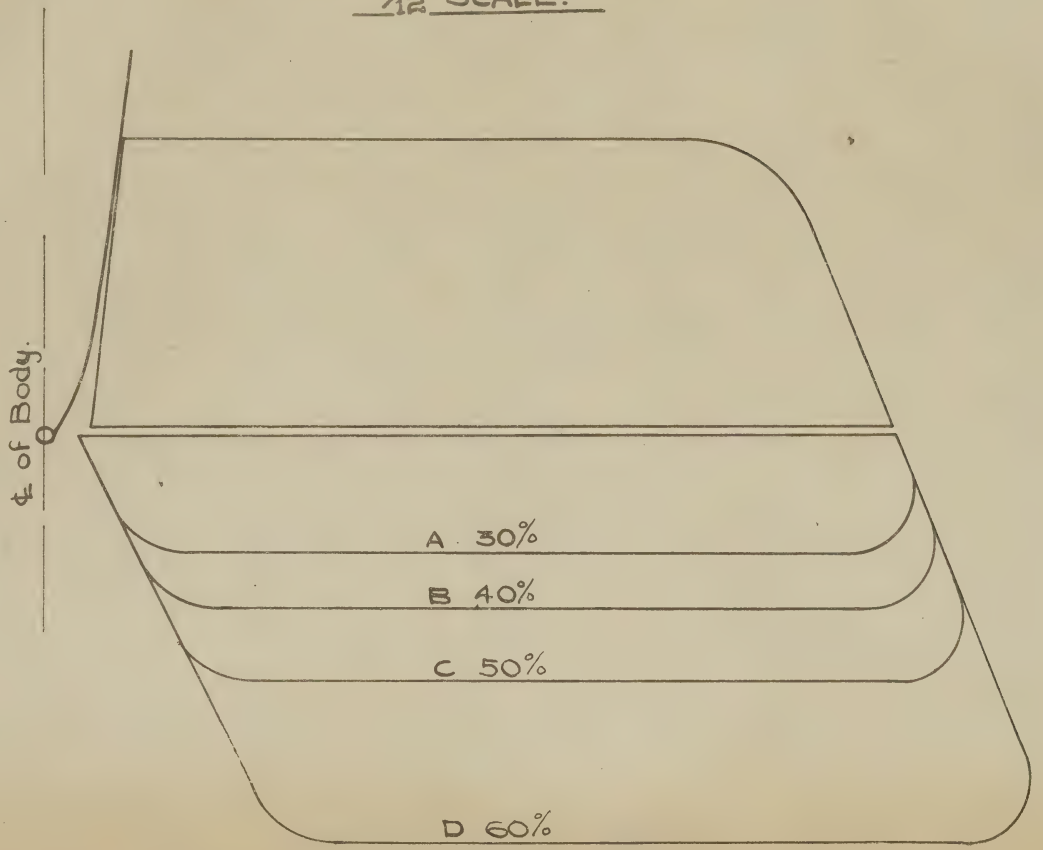

FIG. 1.

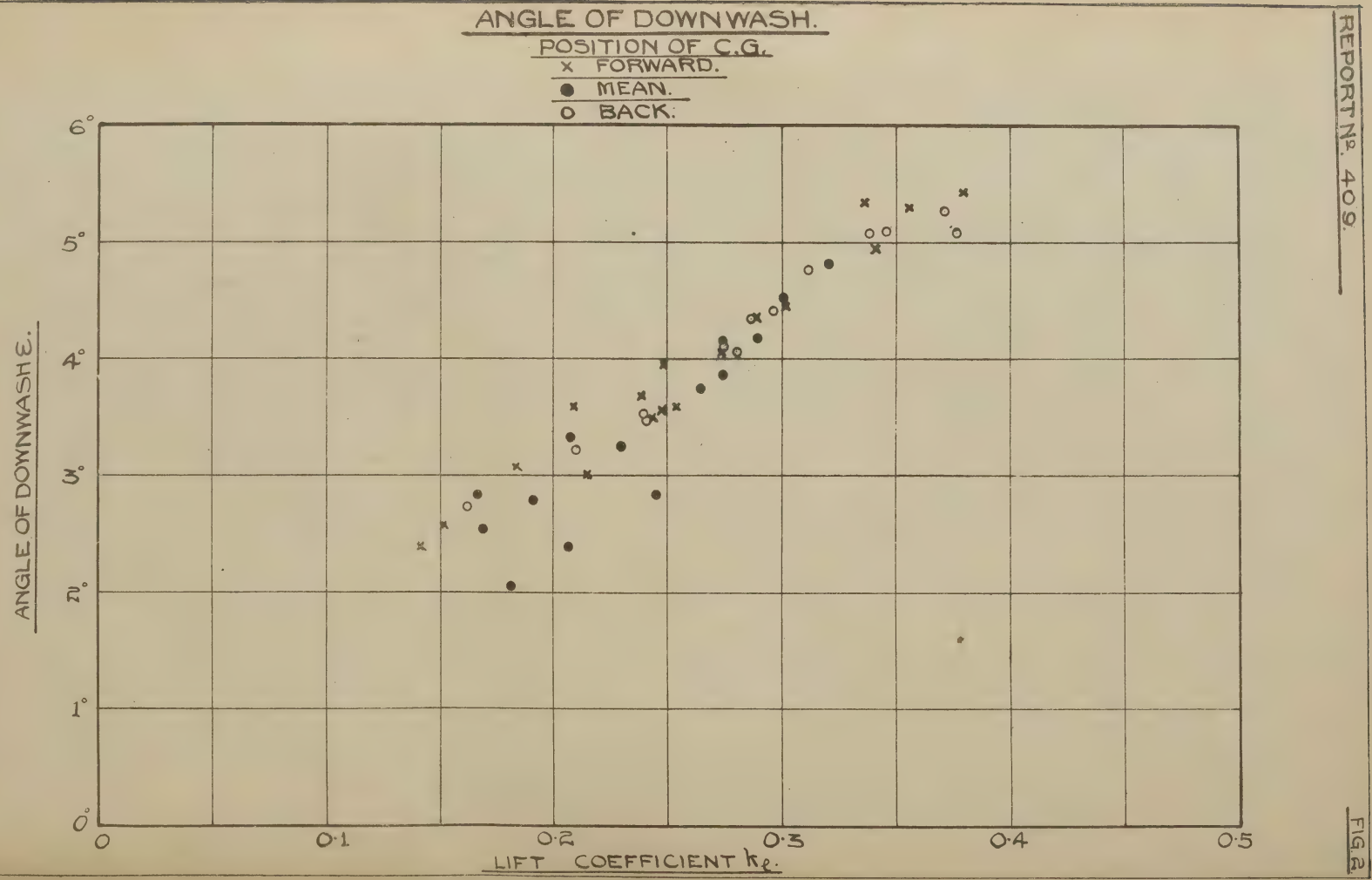
ANGLE OF DOWNWASH.
POSITION OF C.G.
× FORWARD.
● MEAN.
o BACK.
ANGLE OF DOWNWASH ε.
6°
5°
4°
3°
2°
1°
0°
0
0·1
0·2
0·3
0·4
0·5
LIFT COEFFICIENT k_L.

FIG. 2.

CONSTANTS OF ELEVATORS OF DIFFERENT SIZE.

⊙ DEDUCED FROM T.825.

× EXPERIMENTAL DETERMINATION.

The constants correspond to the equations:—

$$k_l' = a\theta' + b\eta.$$

$$m = c\theta' + d\eta.$$

where M is the hinge moment at 100'/sec. for a tailplane of 46°.

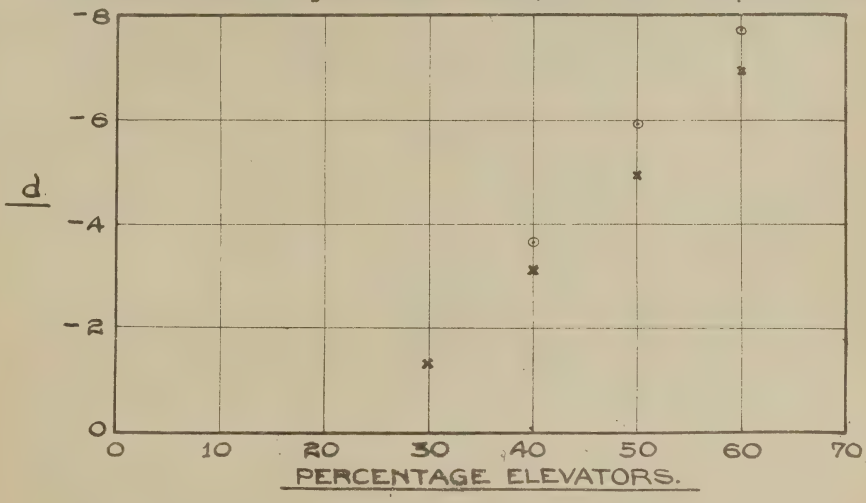

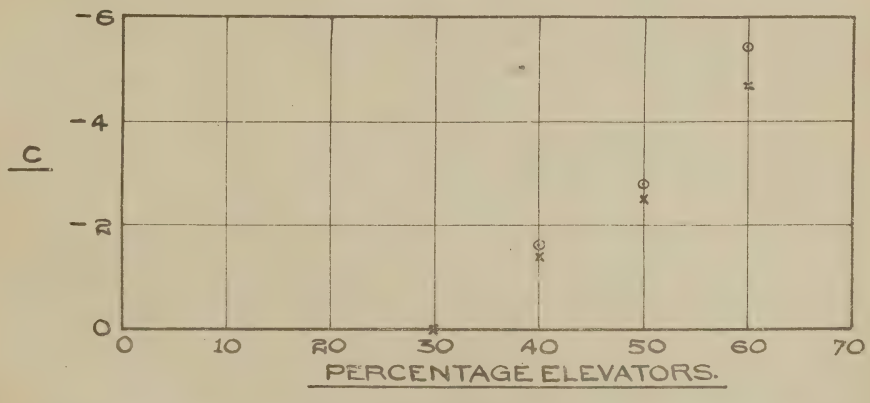

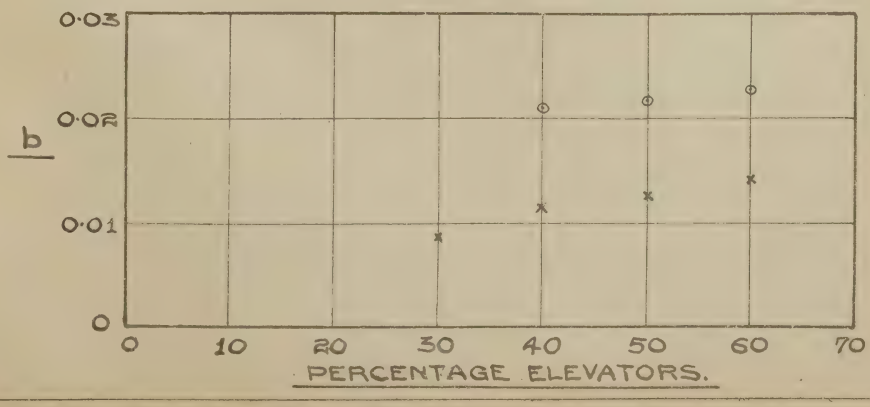

THE LIBRARY
OF THE
UNIVERSITY OF ILLINOIS

the gearing must be adjusted so that the maximum possible movement of the control column—which is limited by the size and shape of the pilot's compartment—shall give some definite change in the attitude of the machine. For the elevators used in these experiments the gearing was unaltered, and so it follows that the forces should be increased in the ratio of the elevator movement necessary for the particular manœuvre in question. The basis of comparison becomes, therefore, the product of the force, and the change of elevator angle. Using this criterion, it is found that the elevators improve steadily with decreasing size over the range tested in these experiments.

TABLE 1.

DETAILS OF ELEVATORS.

	Tail plus Elevator.	Elevator.			
	Area. Sq. ft.	Area. Sq. ft.	Chord. Ft.	Weight. Lbs.	Weight Moment about Hinge. Lbs.ft.
A	34	10·3	0·94	11½	3·2
B	39½	15·8	1·38	12½	5·7
C	46	22·3	1·88	14½	7·9
D	60	36·3	3·08	19½	17·5

TABLE 2.

CHARACTERISTICS OF ELEVATORS.

	$\frac{a}{b}$	$\frac{bc - ad}{a}$	$\frac{bc - ad}{d}$	b.	c.	d.
A	2·25	0·81	−0·0188	0·0084	0	− 0·81
B	1·69	1·79	−0·0138	0·0112	−1·12	− 2·45
C	1·52	3·28	−0·0126	0·0124	−2·50	− 4·92
D	1·36	5·20	−0·0095	0·0139	−7·00	−10·35

a and b are absolute coefficients, and c and d are constants having the dimensions of the moment. They are defined by the equations

$$k'_l = a\theta' + b\eta,$$
$$\mathrm{M} = c\theta' + d\eta,$$

where

θ' is the angle of incidence of the tail plane.
η is the elevator angle.
k'_l is the lift coefficient of the tail plane.
M is the hinge moment on the elevators at 100 ft./sec.

Table 3.

TAIL PLANES OF EQUAL AREA (46 Sq. Ft.).

% Elevators.	*b.*	*c.*	*d.*
30	0·0084	0	− 1·28
40	0·0112	− 1·41	− 3·09
50	0·0124	− 2·50	− 4·92
60	0·0139	− 4·70	− 6·95

Table 4.

TAIL PLANES OF EQUAL STABILITY.

The machine is supposed to be trimmed at 75 m.p.h.

% Elevator.	To Trim at 65 m.p.h.		To Trim at 75 m.p.h. Gliding.		
	Elevator Movement. degrees	Force. Lbs.	Elevator Movement. degrees	Force. Lbs.	Product.
30	− 0·6	0·7	− 3·8	2·5	9·5
40	− 0·7	1·5	− 2·4	5·3	12·7
50	− 0·7	2·2	− 2·0	7·4	14·8
60	− 0·8	3·7	− 1·5	11·5	17·3

LATERAL CONTROL WITH DIFFERENT TYPES OF WING FLAPS.

By H. Glauert.

Presented by the Superintendent, Royal Aircraft Factory.

Reports and Memoranda (New Series), No. 413. *February,* 1918.

Summary.—(*a*) *Introductory* (*Reasons for enquiry*).—The importance of obtaining some definite measurements of lateral control and of determining the most efficient type of wing flap has been realised for some time. Up to the present it has only been possible to judge between different types of flaps and different aeroplanes by correlating the impressions of a number of pilots, and the absence of any definite criterion of lateral controllability has been a considerable handicap in design.

(*b*) *Range of the investigation.*—The experiments described in this report consist of tests of four different types of flap on an R.E. 8 aeroplane. Measurements were made of the time to bank 45° with different forces on the control column, of the angle of flap under these conditions, and of the minimum time to come off the bank at different speeds. The variation of flap angle with movement of the control column was also obtained on the standard machine. Most of the experiments were repeated with a second pilot.

(*c*) *Conclusions.*—The general conclusion derived from the experiments is that the efficiency of a wing flap can be noticeably improved by "wash out," *i.e.*, by decreasing the incidence of the flap towards the wing tip. A further improvement of a less marked degree would be obtained by reducing the chord of the flap from 36 per cent. to 24 per cent. of the wing chord. The curves of force against flap angle gave the interesting result that the two flaps move at varying and different rates.

(*d*) *Applications and further developments.*—Further experiments are desirable with more accurate methods of measuring the rate of roll and the maximum control. It is also important that different shapes of wing tips should be examined from the same point of view and that the experiments should be extended to machines of different types.

1. *Object of the experiments.*—The lateral controllability of an aeroplane depends mainly on the shape and size of the wing flaps, other factors being the shape and arrangement of the main planes, the moment of inertia of the aeroplane, and the form of the fin and rudder. The experiments described in this report

deal with the first of these factors. Four different types of wing flap were fitted to an R.E. 8 aeroplane and measurements were made to determine the amount of control. These types were

(1) A standard flap with 24-in. chord.
(2) A similar flap with 16-in. chord.
(3) A standard flap with 9° decreased angle of incidence towards the tip.
(4) A standard flap with chord tapering to 8 ins. at the tip.

Details of the aeroplane and flaps are given in Table 1. The important factors of lateral control are the rate of banking and unbanking for a given force, the maximum rate of these movements, the lag between the application of the control and the movement of the aeroplane, and the behaviour of the flaps near the stalling speed.

Method of experiment.—To the flap strut was fixed a pointer which indicated the flap angle on a scale fixed to the front wing strut, and the force applied by the pilot was read on an indicator fitted to the head of the control column. Measurements were made of the right flap angle and the time to bank 45° corresponding to different forces on the control column, the measurement of the time being made by the observer with a stop watch. Different gearing was used in two cases, but all the results have been reduced to the basis of the standard gearing. These results were obtained with two different pilots, A and B. The relation between the flap angle and the movement of the stick was observed for the machine fitted with standard flaps. Attempts were also made to observe the maximum rate of unbanking, but the results obtained were not very satisfactory, and showed great discordance between the two pilots.

3. *Flap angle and movement of control column.*—A series of measurements were made on the machine fitted with standard flaps to determine the relation between the movement of the control column and the flap angle. A ground calibration was taken and curves were obtained in the air at speeds of 60 and 90 m.p.h., the object being to determine the stretch of the control cables under the load of the air forces. The results obtained are given in Table 2 and Fig. 1, and show a linear relation between the two measured quantities. The air calibrations show a slight increase (about 10 per cent.) in the necessary movement of the control column for a given change of flap angle as compared with the ground calibration. This increase represents a loss of efficiency due to the use of cables instead of rigid connections for operating the control surfaces.

4. *Flap angle and force on control column.*—The relation between the flap angle and the force on the control column is given in Table 3, and Figs. 2 and 3. The curves obtained show curious discontinuities of slope, and to establish this peculiarity

more definitely the calibration was made several times in the case of the tapered flaps. The results obtained were in good agreement on the whole, and showed the peculiarity quite definitely. The discontinuity was also clearly indicated in the case of the wash-out flaps, and was just noticeable with the two other types. The discontinuity occurs when the flaps are about 2° down from their equilibrium position in the air. A possible explanation of this peculiarity is that it represents the point where the left-hand flap no longer rises with a further reduction of the tension of the control wire, but has to be pulled up by the tension of the flap connecting wire which passes along the upper plane. The initial slackness of this wire in the equilibrium position might account for the observed phenomenon.

5. *Rate of bank and force on control column.*—The time to bank 45° for different forces has been obtained with two pilots for each type of flap (Table 4, Fig. 4), and although the experiment is one of considerable difficulty owing to the short intervals of time to be measured, the results of repeat experiments were found to be in good agreement. In Table 4 the mean movement of the right and left flaps from their equilibrium position is also given. These experiments were all carried out at an airspeed of 65 m.p.h. The curves of Fig. 4 show the difference in the forces with the different flaps. Although the results obtained by the two pilots are in rough agreement, it will be noticed that pilot B obtained better results with the small chord flaps and worse with the standard flaps than pilot A. This discrepancy may represent a difference in the method of applying the force or of using the rudder to assist the turn, though the elevator and rudder were always supposed to be used to keep the speed constant and to prevent sideslip. It is interesting to note in this connection that pilot B considered the small chord flaps a distinct improvement on the standard flaps, while pilot A noticed little difference. The results obtained agree with these opinions.

6. *Maximum control.*—Attempts were made to obtain a measure of the maximum control by observing the minimum time to come off a bank of 45°. The results (Table 5, Fig. 5) obtained from the two pilots are, however, very discordant, and it is impossible to attach much importance to these measurements. The series was only carried out in full by pilot A, and these observations indicate that the minimum time to unbank—limited by the strength of the pilot—is the same at all speeds above 60 m.p.h. and falls off fairly rapidly below this speed where the motion becomes analogous to that at the beginning of a spin.

7. *Efficiency of the flaps.*—Owing to the unsatisfactory nature of the measurements of the maximum control, it was decided to use a criterion similar to that used in the case of different elevators (R. & M. 409). On this theory the maximum control of a flap, whose range of movement is limited, is taken to be inversely proportional to the flap angle necessary to perform a definite

evolution, and the efficiency of the flap is then inversely proportional to the flap angle and the force applied. The lateral movement of the control column is limited by the shape and size of the pilot's cockpit. For a definite maximum control a certain flap angle is necessary, depending on the type of the flap, and the gearing can then be altered until this maximum flap angle corresponds to the limiting position of the control column. A type of flap which requires small angular movement can have its range of movement restricted in the appropriate ratio and the force on the control column correspondingly reduced. From these considerations the formula for flap efficiency given above follows at once. In Table 6 the results of the tests have been analysed in this manner (see also Fig. 6) for different rates of bank. The general conclusion to be drawn from these results is that the wash-out flaps are the most efficient over the greater part of the range considered. These flaps, however, give a linear relation between efficiency and time of bank, and it seems possible that for more rapid manœuvres involving forces greater than 20 lbs. the small chord flaps would be more efficient. The best compromise would seem to be the use of flaps whose chord was 25 per cent. of the wing chord and whose incidence decreased towards the tip. For slower movements the results obtained from the two pilots are not in good agreement, especially as regards the small chord flaps. The more rapid evolutions are, however, of the greatest importance, and in this region both agree that the wash-out and the small chord flaps are better than the other two types. The discrepancy indicated may represent a difference in the method of handling an aeroplane and give estimates of the differences of opinion of pilots as to the controllability of various types of aeroplanes.

8. *Conclusions.*—The experiments dealt with in this report indicate the advisability of using wash-out flaps of small chord. Further experiments are necessary to determine the best length of flap and shape of wing tip. The latter of these tests could probably be best dealt with in the wind channel and experiments on the former are already in progress on an R.E. 9 aeroplane. Considerable improvement in the accuracy of the results can probably be obtained by the use of a mechanical means of applying the force so as to eliminate the personal equation of the pilot and by some mechanical means (*e.g.*, a cinematograph camera) of recording the small intervals of time which occur on a rapid bank.

TABLE 1.

DETAILS OF AEROPLANE.

	Span (ft.).	*Chord* (ft.).	*Span of flap* (ft.).
Upper Wing	43	$5\frac{1}{2}$	11
Lower Wing	33	$5\frac{1}{2}$	6

Type of flap.	*Chord* (ins.).
Standard	24
Small chord	16
Wash-out	24 (with a decrease of angle of incidence along the flap = 9°).
Tapered	24 to 8.

TABLE 2.

FLAP ANGLE AND MOVEMENT OF CONTROL COLUMN WITH STANDARD FLAPS (DEGREES).

Ground.		60 m.p.h.		90 m.p.h.	
Control column.	Flap angle.	Control column.	Flap angle.	Control column.	Flap angle.
10	11·7	15	9·2	14	7·3
+ 5	8·4	12	7·3	11	5·3
0	5·0	8·5	5·3	7	3·4
− 5	+ 1·8	+ 5	3·4	+ 2	+ 0·2
− 10	− 1·3	0	+ 0·6	− 0·5	− 1·8
		− 3·5	− 1·8	− 5	− 4·0

The movement of the control column is reckoned positive to the left.

TABLE 3.

FLAP ANGLE AND FORCE ON CONTROL COLUMN.

Force (lbs.).	Flap Angle (degrees).			Force (lbs.).	Flap Angle (degrees). Tapered.
	Standard.	Small chord.	Wash-out.		
20	5·2	—	10·1	18	3·9, 2·7, 3·5.
15	3·7	7·4	8·6	15	2·8, 2·1, 3·0.
10	3·0	5·9	6·8	12	1·8, 1·9.
7·5	2·6	4·5	—	9	0, — 0·7.,
5	2·3	3·5	6·0	6	— 1·4, — 1·6.
0	1·5	—	4·5	0	— 2·6, — 2·8, — 3·3.
— 5	0·7	0·4	3·5	— 6	— 5·1, — 5·5.
— 7·5	0·2	— 0·7	—	— 9	— 6·2, — 6·2.
— 10	— 0·5	— 2·0	2·5	— 12	— 7·8, — 7·9.
— 15	— 1·4	— 4·6	1·5	— 15	— 8·6, — 8·6, — 8·6.
— 20	— 2·4	—	— 0·2	— 18	— 8·9, — 9·5, — 9·1.

The values given are the angles of the right flap at 65 m.p.h.
The forces are reckoned positive to the left.

TABLE 4.

TIME TO BANK 45° AGAINST FORCE ON CONTROL COLUMN.

Type.	Force (lbs.).	Force corrected to standard gearing (lbs.).	Flap angle (degrees).	Time to bank 45°.	
				Pilot A (secs.).	Pilot B (secs.).
Standard ..	5	5	0·8	9·0	—
	10	10	1·7	4·7	5·6
	15	15	2·5	3·6	4·5
	20	20	3·8	2·9	3·1
Small chord..	10	5	1·5	6·3	6·5
	15	7½	2·6	4·9	—
	20	10	3·9	3·8	3·6
	25	12½	5·2	3·1	—
	30	15	6·0	2·5	2·2
Wash-out ..	5	5	1·2	6·6	—
	10	10	2·1	4·3	4·6
	15	15	3·3	3·0	3·0
	20	20	5·1	2·3	2·2
	25	25	5·8	1·9	—
Tapered ..	10	6	1·9	5·3	6·7
	15	9	2·9	—	4·1
	20	12	4·8	3·1	3·3
	25	15	5·6	—	2·7
	30	18	6·3	2·6	—
	35	21	—	—	2·3

The flap angles given in this table are the mean of the movement of the right and left flaps from their zero position at this speed.

REPORT No. 413.

FLAP ANGLE AND MOVEMENT OF CONTROL COLUMN.

Measurements made with standard flaps.

Movements of control column reckoned positive to the left.

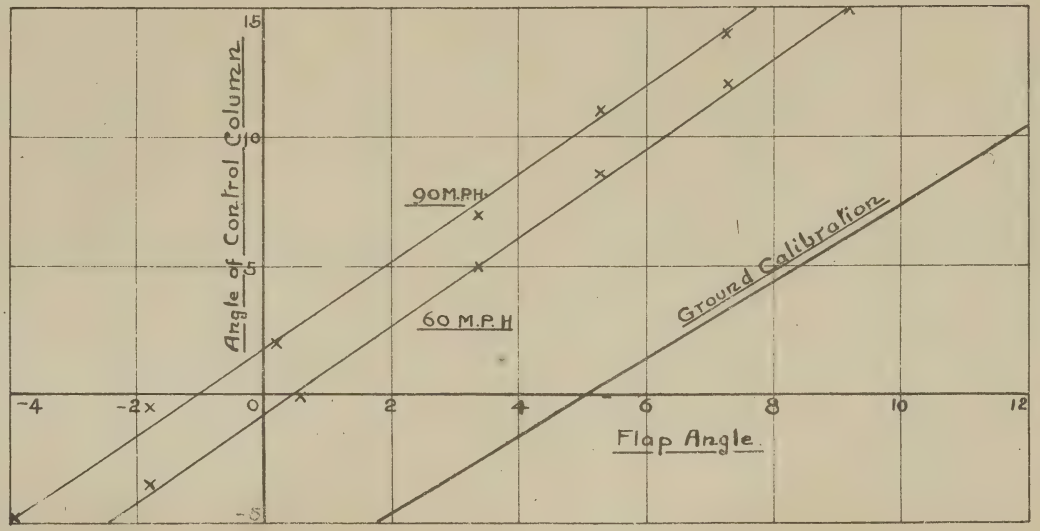

FIG. 1.

FLAP ANGLES.

Forces on the control column are reckoned positive to the left.

The flap angles correspond to a speed of 65 M.P.H.

Standard Flaps.

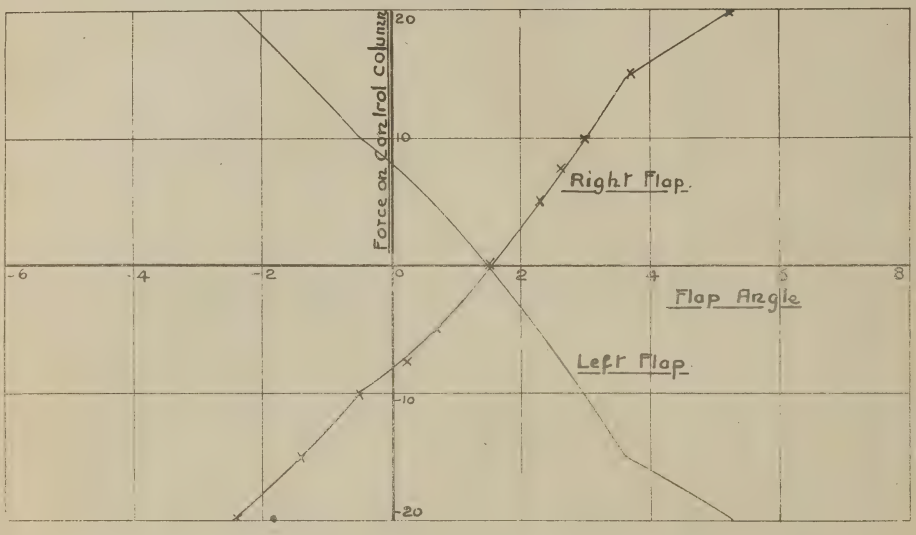

Small Chord Flaps.

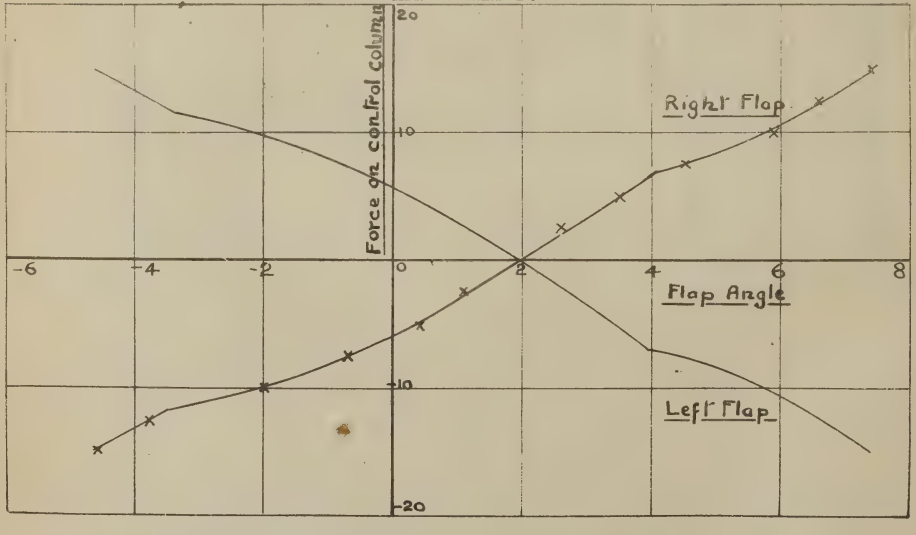

FLAP ANGLES.

Forces on the control column are reckoned positive to the left

The flap angles correspond to a speed of 65 M.P.H.

Wash out Flaps.

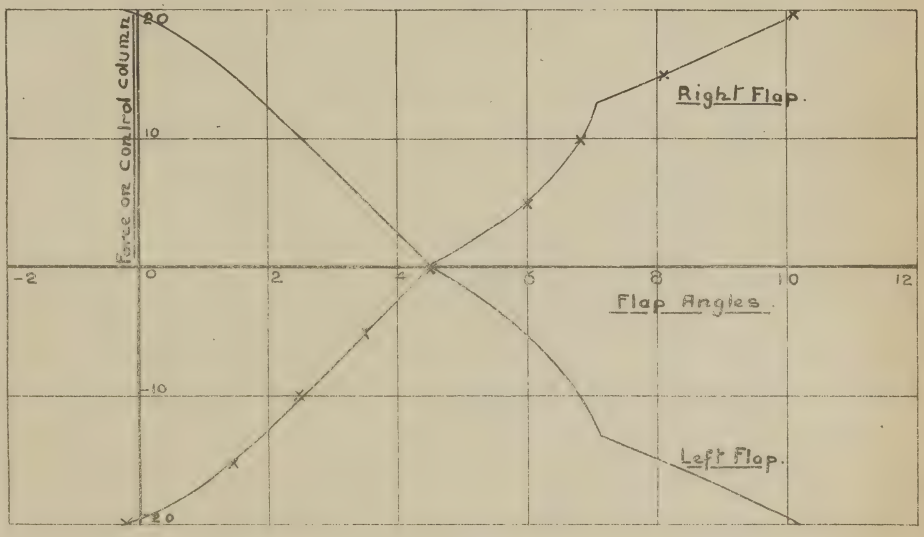

Tapered Flaps.

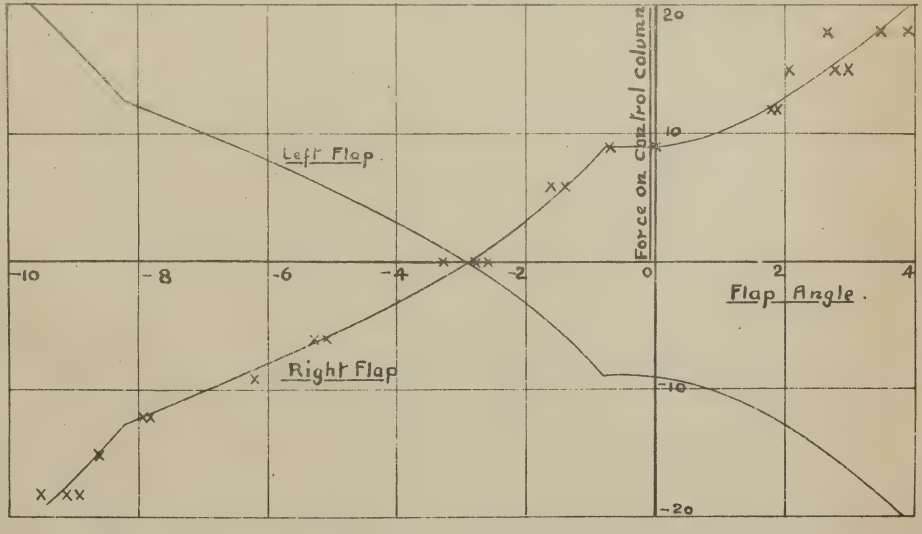

TIME TO BANK 45°

Standard ——— Wash out —·—·—

Small Chord – – – Tapered —··—··—

Pilot A.

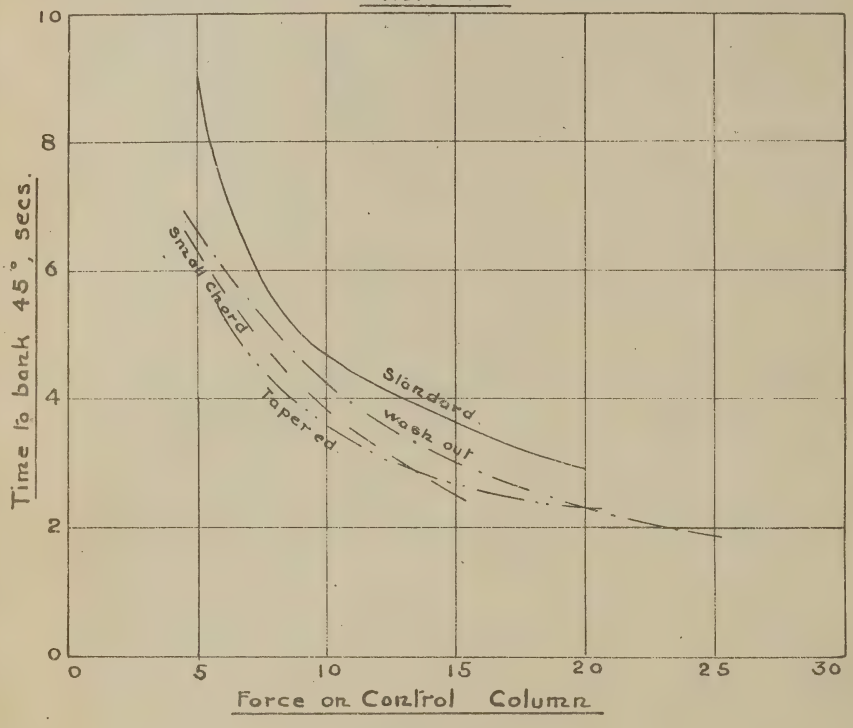

Pilot B.

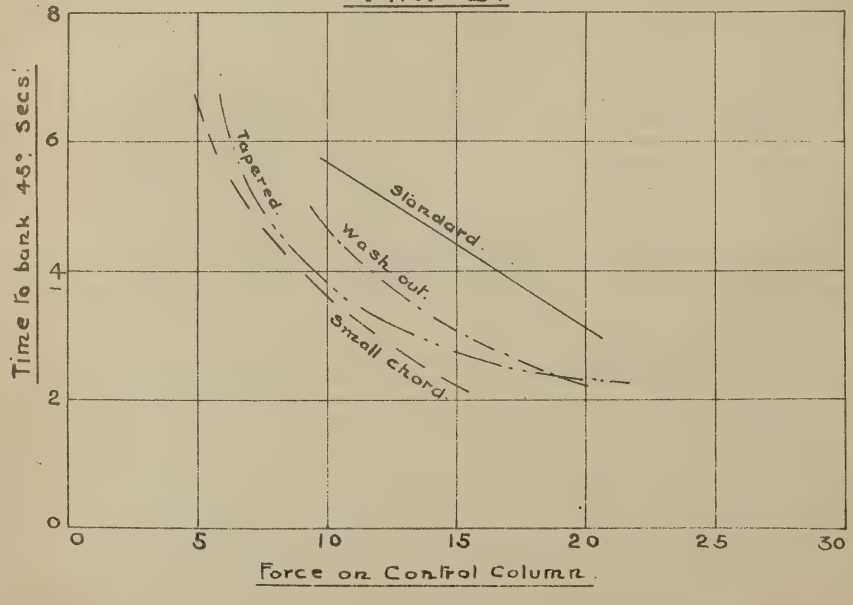

TIME TO UNBANK 45°.

Standard ——— Wash out. —·—·—

Small Chord — — — Tapered. —··—··—

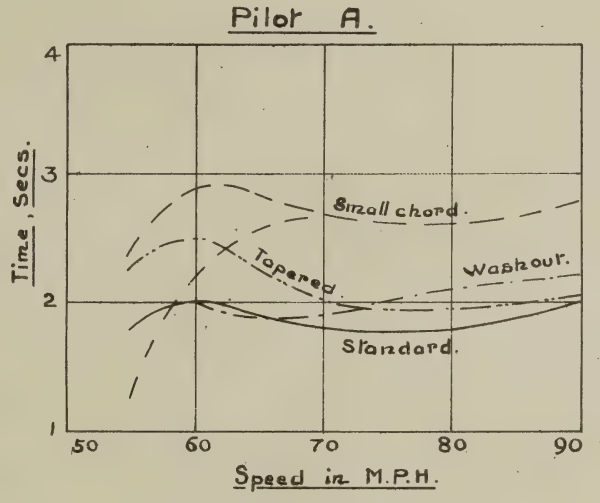

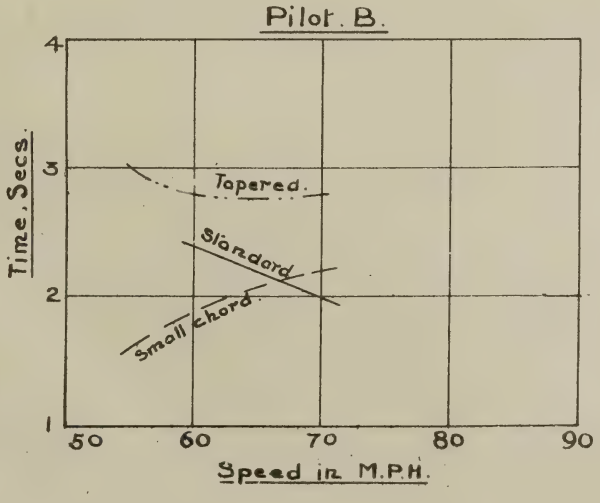

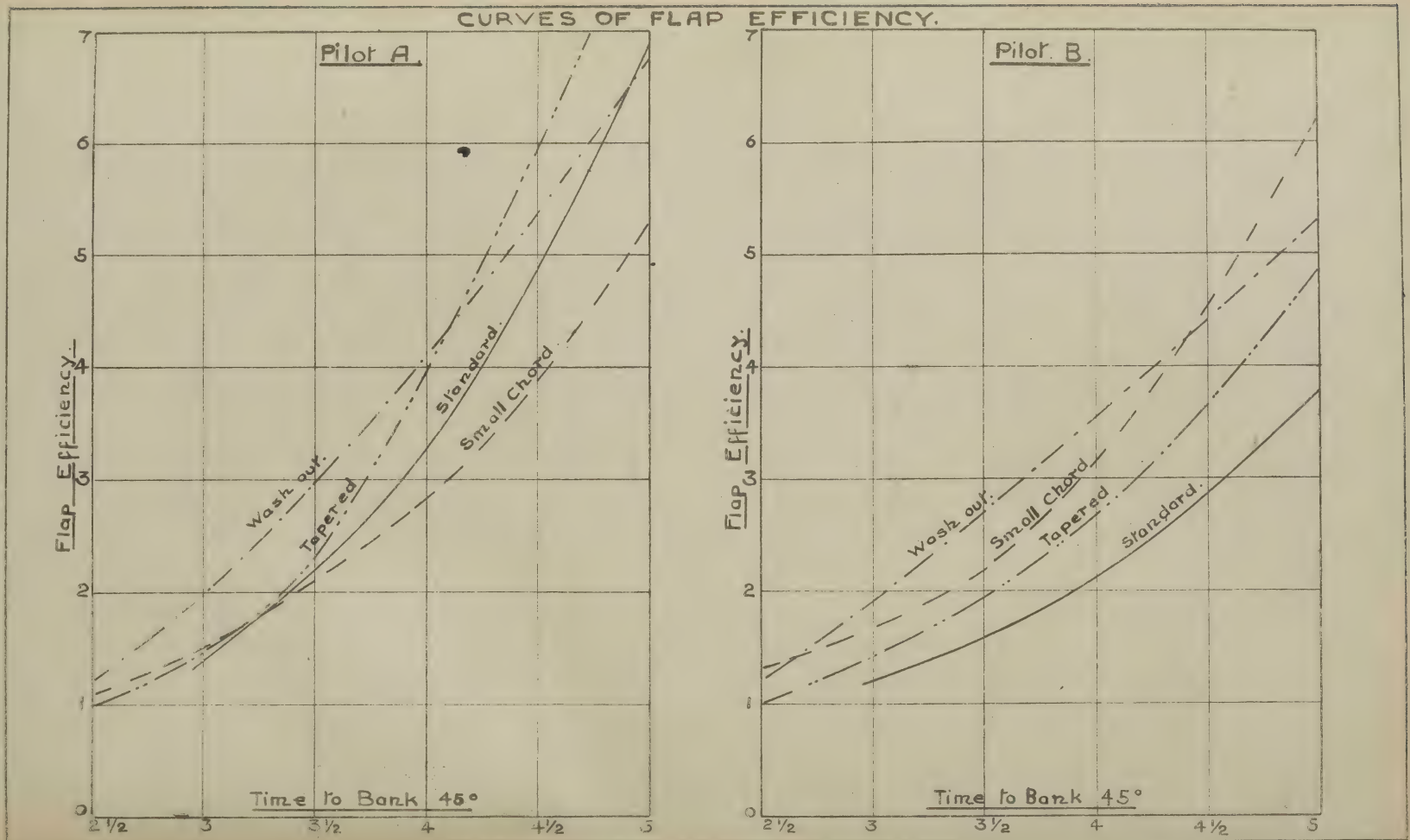
CURVES OF FLAP EFFICIENCY.
Pilot A.
Flap Efficiency.
Wash out.
Tapered
Standard.
Small Chord
Time to Bank 45°
0
1
2
3
4
5
6
7
2 1/2
3
3 1/2
4
4 1/2
5
Pilot B.
Flap Efficiency.
Wash out.
Small Chord
Tapered
Standard.
Time to Bank 45°

FIG. 6.

TABLE 5.

MINIMUM TIME TO UNBANK 45°.

Type.	Speed (m.p.h.).	Time to unbank 45°.	
		Pilot A (secs.).	Pilot B (secs.).
Standard ..	55	1·8	—
	60	2·0	2·4
	70	1·8	2·0
	80	1·8	—
	90	2·0	—
Small chord ..	55	1·3, 2·4	1·6
	60	2·2, 2·9	1·9
	70	2·7	2·2
	80	2·6	—
	90	2·8	—
Wash-out ..	55	—	—
	60	2·0	—
	70	1·9	—
	80	2·1	—
	90	2·2	—
Tapered ..	55	2·3	3·0
	60	2·5	2·8
	70	2·0	2·8
	80	1·8, 2·1	—
	90	2·0, 2·1	—

TABLE 6.

EFFICIENCY OF FLAPS.

The efficiency is taken to be inversely proportional to the force and the flap angle required for a definite rate of bank.

Time to bank, 45° (secs.).	Standard.		Small Chord.		Wash-out.		Tapered.	
	A	B	A	B	A	B	A	B
2·5	—	—	1·1	1·3	1·2	1·2	1·0	1·0
3	1·4	1·2	1·5	1·7	2·0	1·9	1·5	1·4
3·5	2·2	1·6	2·0	2·2	3·1	2·7	2·3	2·1
4	3·3	2·1	2·9	3·3	4·0	3·6	4·2	2·8
4·5	4·9	2·9	3·9	4·5	5·4	4·4	5·9	4·6
5	6·9	3·8	5·3	6·2	6·8	5·3	7·7	5·9

LATERAL CONTROL OF VARIOUS AEROPLANES.

Presented by the SUPERINTENDENT, Royal Aircraft Establishment.

Reports and Memoranda, No. 441. *March*, 1918.

SUMMARY.—(a) *Introductory (reasons for inquiry).*—The results of some measurements of lateral control with different types of wing flaps were given in R. & M. 413. The experiments have now been extended to a few different types of aeroplane.

(b) *Range of the investigation.*—Measurements were made of the flap angle and the rate of roll for different forces on the control column in the method described in R. & M. 413. The series of experiments consisted of tests on the Bristol Fighter, R.E. 9 and R.T. 1 with balanced and ordinary flaps.

(c) *Conclusions.*—Using the criterion of flap efficiency developed in R. & M. 413, the best results were obtained with the R.T. 1 aeroplane. The balanced flaps were a considerable improvement for slow movements, but the effect was hardly noticeable for rapid rates of bank. The Bristol Fighter appeared to have a better control than R.E. 8 or R.E. 9 for rapid movements, but was very bad for slow ones. However, since the gearing of the ailerons is determined by the maximum control obtainable, which has not yet been measured completely, the comparison of the aeroplanes is not necessarily a true one.

(d) *Applications and further developments.*—Mechanical means of measuring the rate of roll are being developed so as to obtain more accurate results for rapid movements, and it is hoped to attack shortly the question of maximum control with this new apparatus.

The results of R. & M. 413 and of this report can only be regarded as a rough preliminary investigation.

1. The experiments described in R. & M. 413 dealt with four different types of wing flap fitted to an R.E. 8 aeroplane. The same method of experiment has now been applied to different types of machine—R.E. 9, R.T. 1 and the Bristol Fighter—and the results are compared with those obtained on the standard R.E. 8. Details of the wing structure are given in Table 1. R.E. 9 resembles R.E. 8, except that the wings are of equal span and were fitted with 16″ chord flaps occupying a larger proportion of the span, instead of the standard 24″ chord of R.E. 8. R.T. 1 is also similar to R.E. 9, but has wings of unequal chord and flaps of 20″ chord. This machine was also fitted with balanced flaps, as shown in Fig. 1. The Bristol Fighter has wings of equal span and chord, and flaps of the same chord (24″) as R.E. 8.

2. The results obtained—flap angle and rate of bank against force on the control column—are given in Tables 2 and 3, and are shown in Figs. 2–4. The experiments were carried out with pilot A of report R. & M. 413. It will be noticed from the

figures that the relation between flap angle and force on the control column shows the same type of discontinuity of slope that was found in the earlier experiments. From the forces of Fig. 4 it is evident that the Bristol Fighter is heavy on the lateral control except when large forces are applied. This aeroplane is generally agreed to have a pleasant lateral control, though it certainly feels slow for small forces. It is also very difficult to roll, though this is probably due to the small effect of the rudder. One reason for the pleasantness of the Bristol Fighter may be suggested : it differs from the R.E. 8, R.E. 9 and R.T. 1 in that it has a more comfortably disposed cockpit ; the hinge at the bottom of the control stick is further forward, and the pilot's legs are not confined sideways, as in the other three aeroplanes ; these two facts allow greater lateral movement of the stick with comfort, consequently a greater maximum control could be obtained, other things being equal. As would be expected, the forces on the R.T. 1 with balanced flaps are small, but this is largely compensated for by the fact that the flaps have to be set over to a larger angle than the unbalanced ones to obtain a definite rate of roll. This effect must be due to the disturbance in the flow on the wing tip owing to the projecting horn of the balanced flap.

3. The criterion for comparing the efficiency of the flaps used in R. & M. 413 has been applied to these tests, and the results are given in Fig. 5. This criterion postulates that the efficiency of a flap is inversely proportional to the force and to the flap angle necessary for a definite manœuvre. This basis of comparison is obtained by realising that a flap which requires relatively small angular movements can have its range of movement restricted and so have the forces on the control column reduced by change of gearing. Until definite measurements can be made of the maximum control, this criterion seems to give the fairest basis of comparison. It must be clearly held in mind, however, that this comparison is merely the best that can be done so far, and that the comparison of the aeroplanes is incomplete and liable to be misleading, since the curves for the various aeroplanes cross each other for large forces. Maximum control essentially involves large forces, in fact, the largest forces the pilot can apply. These are of the order of 50 lbs. and the largest forces measured are only about 20 lbs., hence it is impossible to predict with any certainty the order in which the aeroplanes will appear for maximum controls. However, using the same criterion as in R. & M. 413, Fig. 5 has been prepared, and it appears that R.E. 9 is an improvement on R.E. 8 and that R.T. 1 is better than both. The balanced flaps of R.T. 1 only seem to be an improvement for slow movements. The Bristol Fighter shows peculiar characteristics, being definitely better than R.E. 9 for rapid manœuvres, but much worse for slow ones. This may be due to the smaller span of the flaps on the Bristol aeroplane.

Table 1.

DETAILS OF AEROPLANES.

	R.E. 8.	R.E. 9.	R.T. 1.	Bristol Fighter.
Span, upper wing –	43′	38′	41′	39½′
lower wing– –	33′	38′	41′	39½′
upper flap – –	11′	10·5′	9·2′	7·3′
lower flap – –	6′	10·5′	9·2′	7·3′
Chord, upper wing –	5·5′	5·5′	6·5′	5·5′
lower wing –	5·5′	5·5′	4·8′	5·5′
flap – –	24″	16″	20″	24″

Table 2.

FLAP ANGLE AND FORCE ON CONTROL COLUMN.

R.E. 9.		Bristol Fighter.		R.T. 1 Unbalanced.		R.T. 1 Balanced.	
Force (Lbs.)	Flap Angle. (Degrees.)	Force. (Lbs.)	Flap Angle. (Degrees.)	Force. (Lbs.)	Flap Angle. (Degrees.)	Force. (Lbs.)	Flap Angle. (Degrees.)
21	8·0	21	5·9	20	6·0	18	9·6
17½	6·5	17½	4·2	16	4·8	15	8·6
14	5·0	14	3·6	12	3·6	12	7·2
10½	3·4	10½	2·4	+ 8	2·3	9	5·5
+ 7	3·0	+ 7	+ 1·2	0	+ 1·1	6	4·7
0	+ 1·2	0	0·0	− 8	− 0·5	+ 3	4·1
− 7	− 1·7	− 7	− 1·4	−12	− 1·0	0	2·7
−10½	− 2·7	−10½	− 2·7	−16	− 2·4	− 3	2·1
−14	− 3·6	−14	− 3·5	−20	− 2·6	− 6	+ 0·6
−17½	− 4·8	−17½	− 4·1			− 9	− 1·2
−21	− 5·4	−21	− 5·3			−12	− 1·3
						−15	− 1·7
						−18	− 3·0

The values given are the angles of the right flap at 65 m.p.h.
The forces are reckoned positive to the left.

FORMS OF WING FLAPS.

SCALE 1/48.

R.E.8.

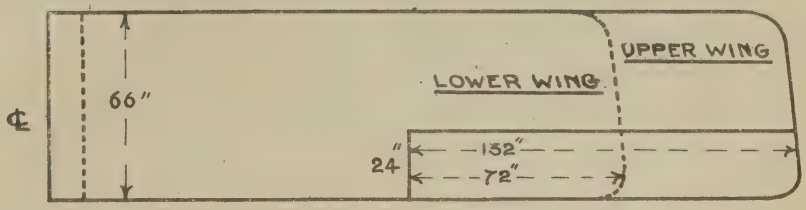

R.E.9.

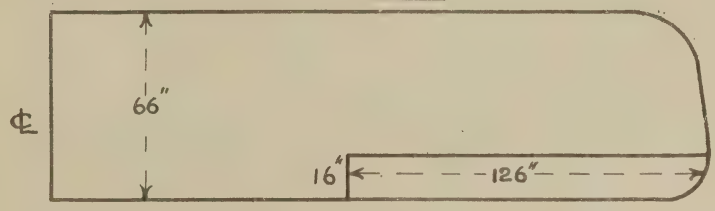

R.T.1. UNBALANCED.

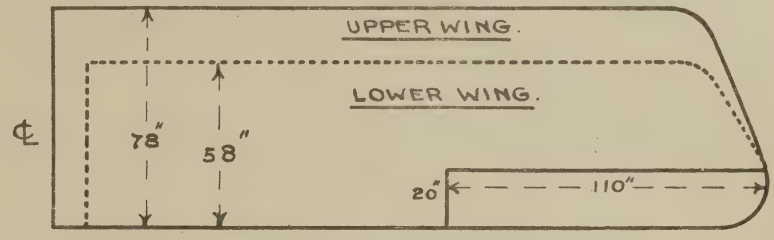

R.T.1. BALANCED.

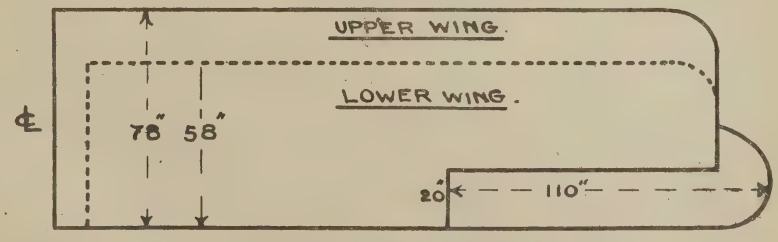

BRISTOL FIGHTER.

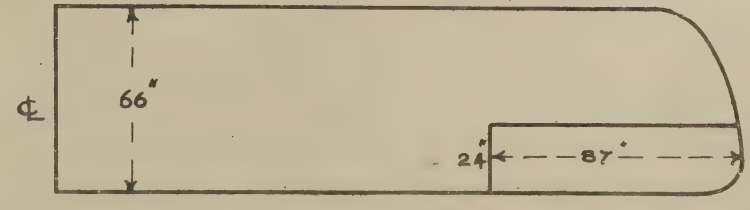

FLAP ANGLES

FORCES ON THE CONTROL COLUMN ARE RECKONED POSITIVE TO THE LEFT

THE FLAP ANGLES CORRESPOND TO A SPEED OF 85 M.P.H.

ALL FORCES ARE REDUCED TO STANDARD GEARING (R.E.8.)

R.E.8 SMALL CHORD FLAPS

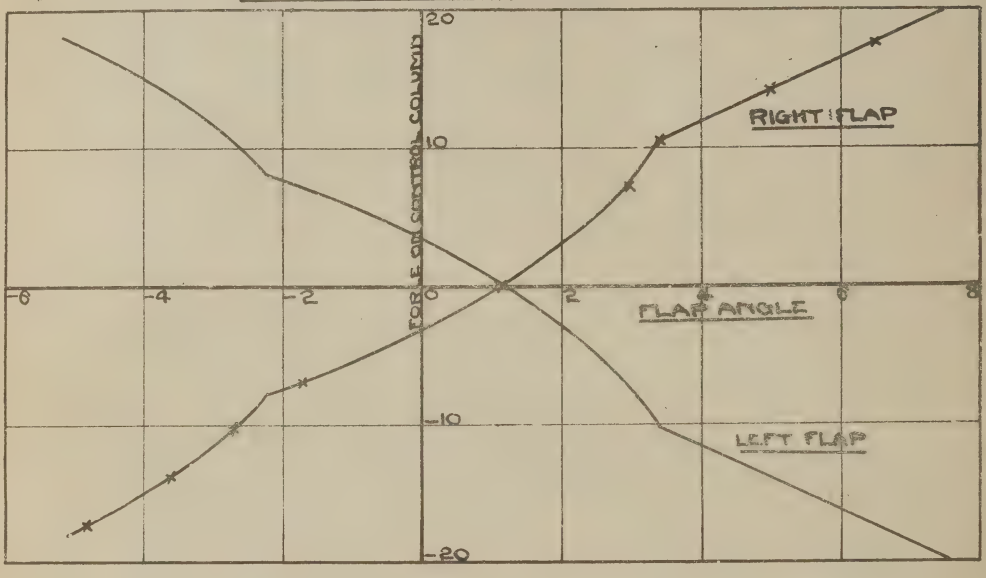

BRISTOL FIGHTER

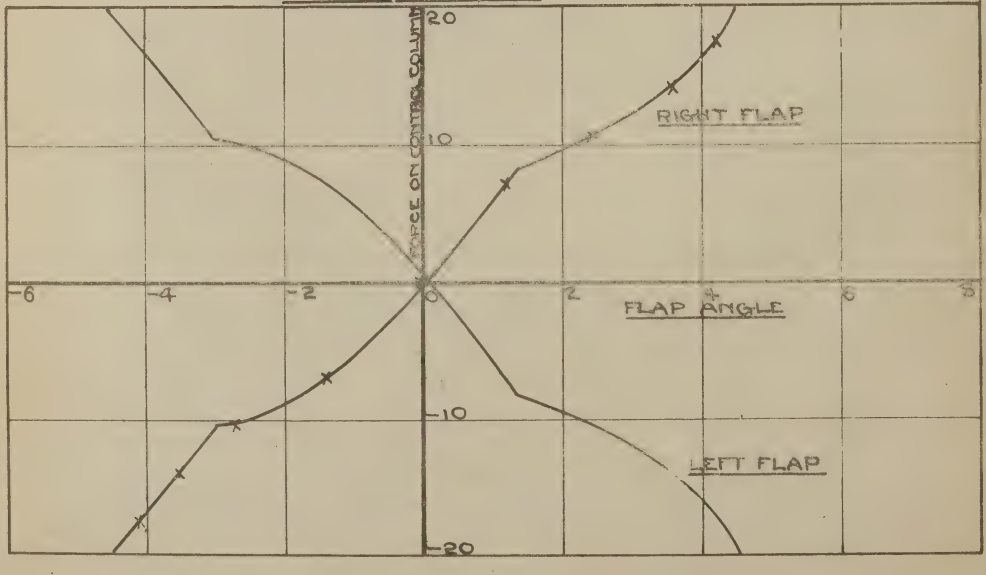

FLAP ANGLES

FORCES ON THE CONTROL COLUMN ARE RECKONED POSITIVE TO THE LEFT

THE FLAP ANGLES CORRESPOND TO A SPEED OF 65 M.P.H.

ALL FORCES ARE REDUCED TO STANDARD GEARING (R.E.8.)

R.T.1 UNBALANCED FLAPS

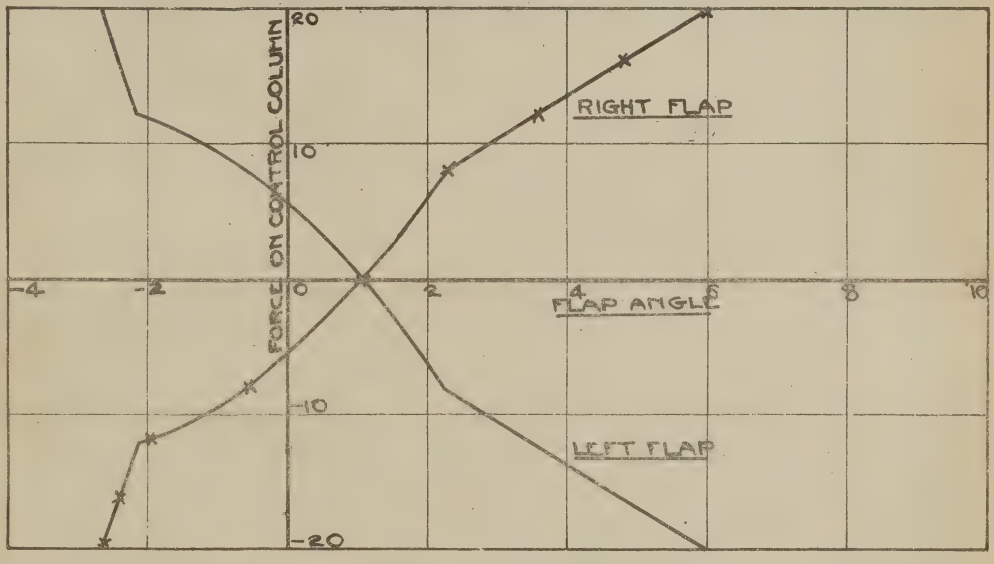

R.T.1 BALANCED FLAPS

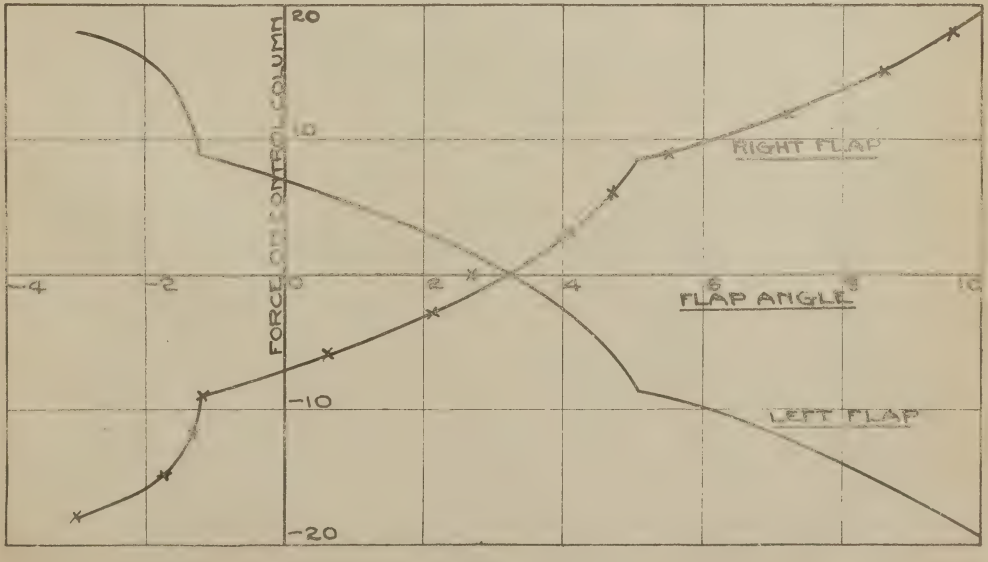

TIME TO BANK 45°

BRISTOL FIGHTER —— R.T.1. (UNBALANCED) ·····

R.E.2 (16" CHORD) —·—·— R.T.1 (BALANCED) —·—·—

ALL FORCES ARE REDUCED TO STANDARD GEARING (R.E.8)

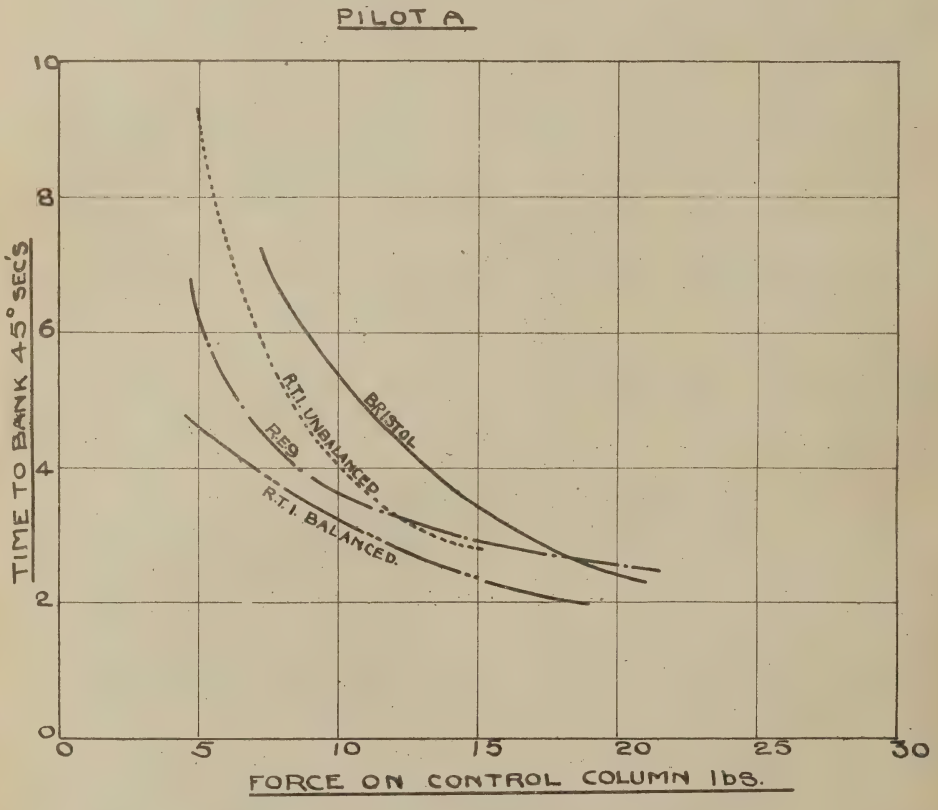

CURVES OF FLAP EFFICIENCY

THE EFFICIENCY IS TAKEN TO BE INVERSELY PROPORTIONAL TO THE FORCE AND FLAP ANGLE NECESSARY FOR A GIVEN RATE OF BANK.

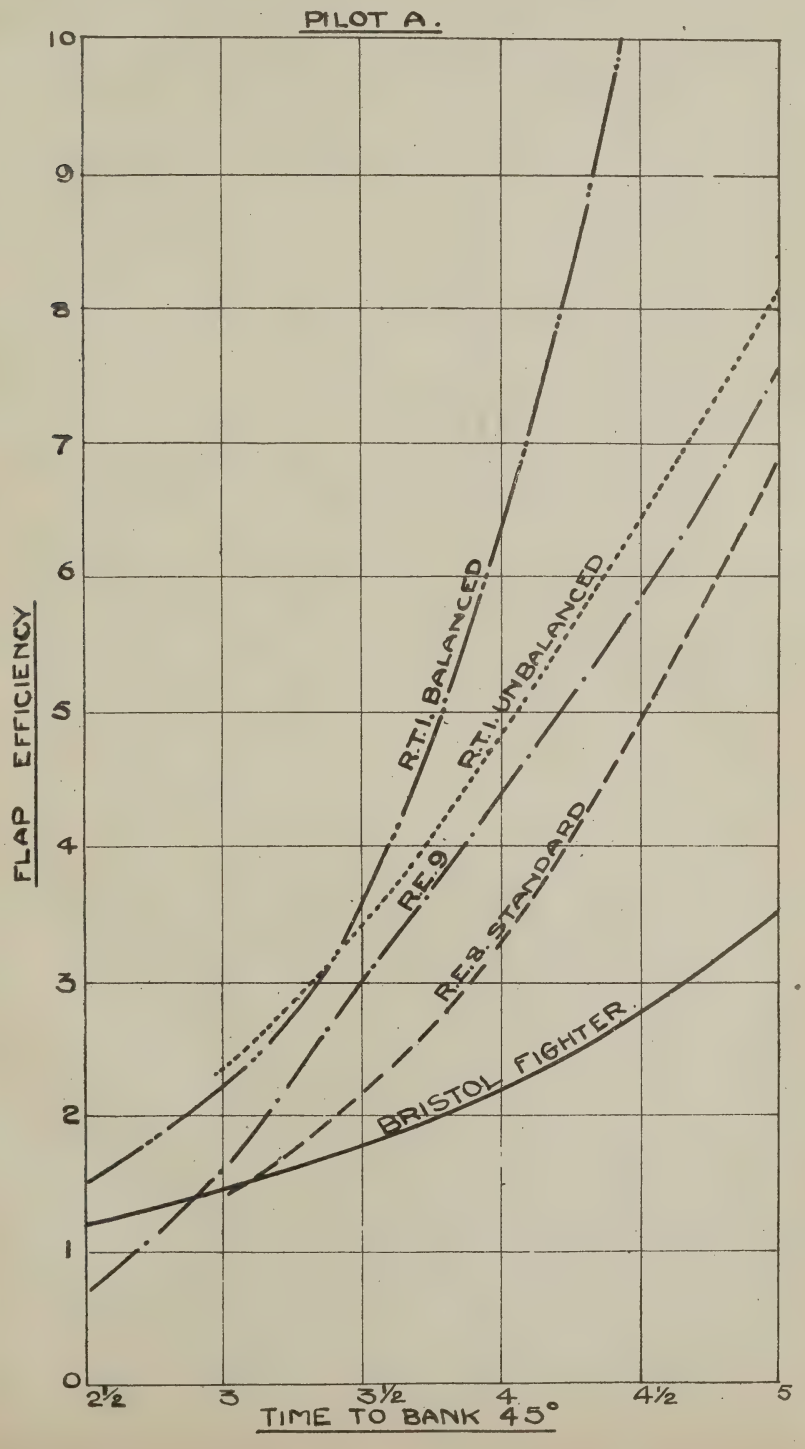

THE LIBRARY
OF THE
UNIVERSITY OF ILLINOIS

Table 3.

TIME TO BANK 45° AGAINST FORCE ON CONTROL COLUMN.

Type.	Force. (Lbs.)	Force Corrected to Standard Gearings. (Lbs.)	Flap Angle. (Degrees.)	Time. (Sec.)
R.E. 9	7	5	1·6	6·3
	10	7	2·3	4·6
	20	14	4·3	3·0
	30	21	—	2·5
Bristol Fighter	10	7	1·3	7·2
	15	10½	2·7	5·4
	20	14	3·5	3·5
	25	17½	4·2	2·8
	30	21	4·7	2·3
R.T. 1 Unbalanced	10	5	0·9	9·0
	20	10	2·1	4·0
	30	15	3·4	2·8
R.T. 1 Balanced	10	6	2·1	4·2
	20	12	4·3	2·8
	30	18	6·3	2·0

The flap angles given in this table are the mean of the measurements of the right and left flaps from their zero position at this speed (65 m.p.h.).

Table 4.

EFFICIENCY OF FLAPS.

The efficiency is taken to be inversely proportional to the force and flap angle required for a definite rate of bank.

Time to bank 45° (Secs.)	R.E. 9.	Bristol Fighter.	R.T. 1 Unbalanced.	R.T. 1 Balanced.
2½	0·7	1·2	—	1·5
3	1·6	1·5	2·4	2·2
3½	3·0	1·8	3·4	3·5
4	4·4	2·2	4·8	6·4
4½	5·8	2·8	6·4	10·7
5	7·6	3·5	8·1	—

FULL SCALE STABILITY EXPERIMENTS WITH R.A.F. 14 WING SECTION.

By H. Glauert.

Presented by the Superintendent, Royal Aircraft Factory.

Reports and Memoranda, No. 505. *June,* 1917.

Summary.—A series of experiments has been completed on an F.E.2*c* aeroplane fitted with R.A.F. 14 wing section for the purpose of determining the downwash. The tail efficiency appears to be higher than in the case of the B.E.2*e* previously tested. The downwash is in good agreement with model results.

The notation is the same as that of R. and M. 326.

1. *Experimental Data.*—The method of experiment and of the reduction of the results has been the same as in R. and M. 326, except that the results given in this report depend entirely on experiments with free elevators. A locking gear for the elevators was designed, but proved unsatisfactory owing to the slackness and length of the control cables.

2. *Analysis.*—The quantities to be determined were the angle of downwash (e), the tail efficiency (E), and the rotary derivative M_q. The equations determining these quantities are—

$$e = (\theta + \psi - \theta'_u) - \frac{72{\cdot}1}{p'^2\,\mathrm{E}}(\mathrm{K}_m + h\mathrm{K}_l + k\mathrm{K}_x).$$

$$1 - \frac{de}{d\theta} = 0{\cdot}765\,\mathrm{N}\,\frac{\mathrm{W}_o}{\mathrm{WQ}} + \frac{2{\cdot}30}{p'^2\,\mathrm{E}}\left(\frac{d\mathrm{K}_m}{d\mathrm{K}_l} + h + k\,\frac{d\mathrm{K}_x}{d\mathrm{K}_l}\right)$$

where

$$\mathrm{P} = 0{\cdot}138\mathrm{U}\,\sqrt{1 + \sigma\mathrm{Q}} \text{ and } \mathrm{W}_o = 2700.$$

In these equations $\frac{d\mathrm{K}'_l}{d\theta}$ has been given the value 0·021, which corresponds to 40 per cent. of elevators.

3. *Determination of E and N.*—The values of E and N were determined so as to bring into agreement the results obtained with different tail settings and different positions of the centre of gravity. The value found for the tail efficiency E was 0·8,

which compares reasonably with the value 0·55 found for the R.E.2*e* aeroplane (R. and M. 326). The value of the correcting factor N was not so well defined, but appeared to be approximately 0·45. This value shows, as might be expected, that the value of M_q for the body of a pusher machine is negligible.

4. *Value of the downwash.*—The values of the angle of downwash found from experiments gliding and with engine running, are in good agreement. The mean value of $\frac{de}{d\theta}$ appears to be 0·55 and the analysis of the periods gives values in the neighbourhood of this value. The effect of the airscrew on the downwash was allowed for as in R. and M. 326, the correcting equation being

$$e = \varepsilon + 0{\cdot}29\,\frac{u}{U+u}\,(\theta - \alpha - e).$$

For the aeroplane employed, α had the value 4° and the resulting values of ε gave the mean slope of 0·50.

5. *Conclusions.*—It appears from the series of experiments described in this report and in R. and M. 326 that the tail efficiency of a pusher aeroplane is of the order of 80 per cent. and that of a tractor 60 per cent., due to interference effects. The rate of change of downwash due to the wings is in both cases approximately 0·5, but this must be increased in full scale work by 15 per cent. to 20 per cent. to allow for the airscrew.

TABLE 1.

Expt.	Weight. Lbs.	C.G. Coefficient h.	Indicated airspeed m.p.h.	Density. σ	Engine Revs.	Tail Setting. ψ
1	2,750	0·437	77½	0·978	1,310	− 1·93
2	2,740	0·426	69¼	0·938	1,290	− 2·40
3	2,725	0·427	70¾	0·925	1,290	− 2·40
4*	2,725	0·427	67¼	0·969	700	− 2·40
5	2,720	0·437	66¾	0·913	1,300	− 2·40
6	2,700	0·454	63	0·862	1,270	− 2·40
7	2,680	0·454	62¼	0·917	1,270	− 2·40
8	2,680	0·454	62	0·910	1,185	− 2·40
9	2,680	0·454	61	0·911	1,095	− 2·40
10*	2,680	0·454	59	0·917	790	− 2·40
11	2,700	0·464	57	0·958	1,255	− 2·40
12	2,700	0·464	55½	0·940	1,145	− 2·40
13	2,700	0·464	54	0·941	1,040	− 2·40
14*	2,700	0·464	53	0·952	820	− 2·40
15	2,710	0·440	56½	0·888	1,260	− 3·07
16	2,710	0·440	55¾	0·872	1,170	− 3·07
17	2,710	0·440	54¾	0·881	1,000	− 3·07
18*	2,710	0·440	53½	0·898	650	− 3·07
19	2,710	0·427	59	0·851	1,260	− 3·07
20	2,710	0·427	58¼	0·821	1,155	− 3·07
21	2,710	0·427	58	0·843	1,000	− 3·07
22*	2,710	0·427	56½	0·862	710	− 3·07
23	2,685	0·454	51½	0·943	1,230	− 3·07
24	2,685	0·454	50¾	0·901	1,120	− 3·07
25	2,685	0·454	50¼	0·901	1,000	− 3·07
26*	2,685	0·454	48¼	0·920	610	− 3·07

* Denotes experiments done gliding

FIG. 1.

FULL SCALE DOWNWASH.

F.E.2c WITH R.A.F.14 WING SECTION.

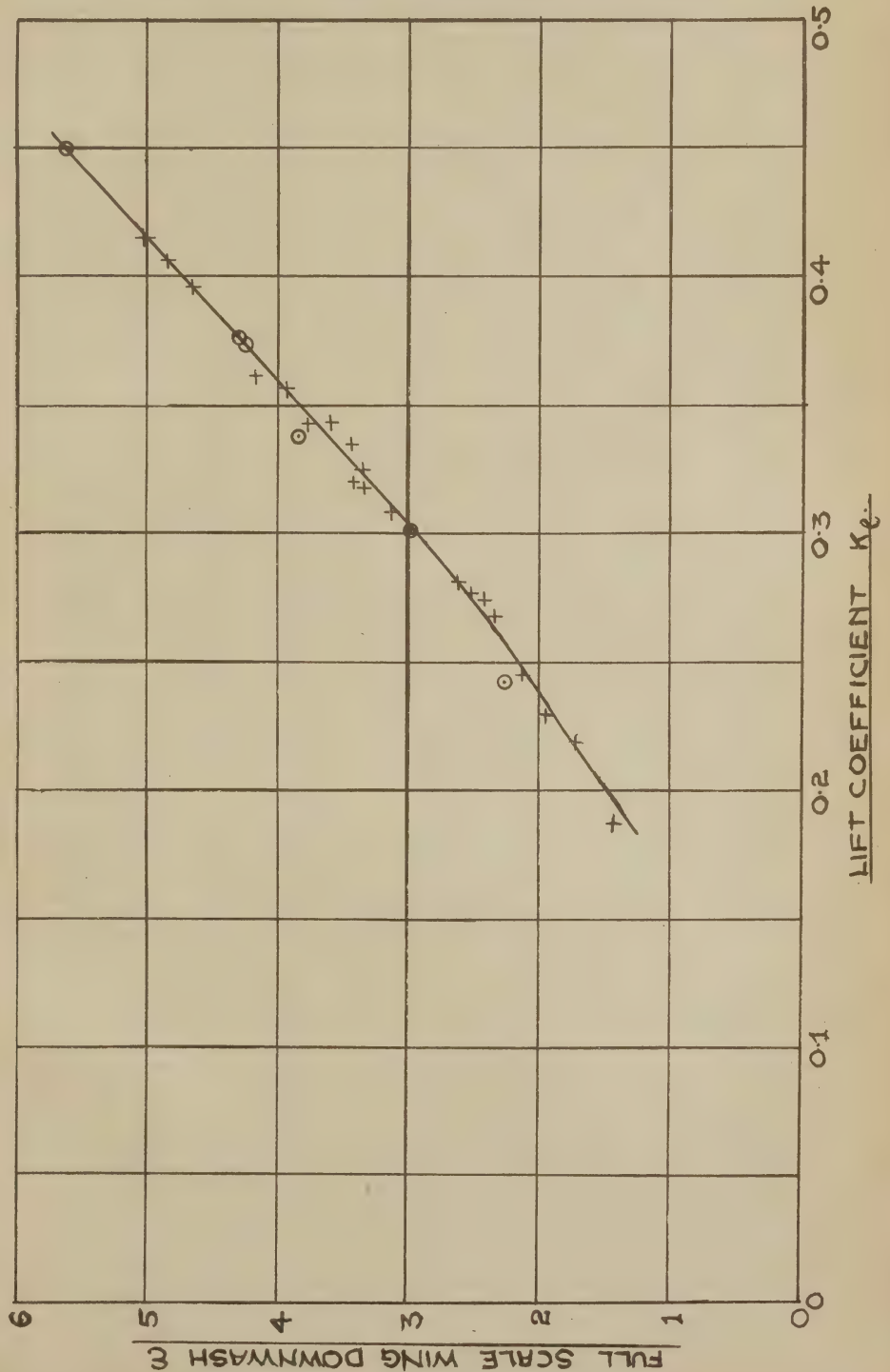

FULL SCALE WING DOWNWASH.

——— R.A.F. 14 WING SECTION ON F.E.2c (E=0·80)

– – – – R.A.F. 15 WING SECTION ON B.E.2e (E=0·55)

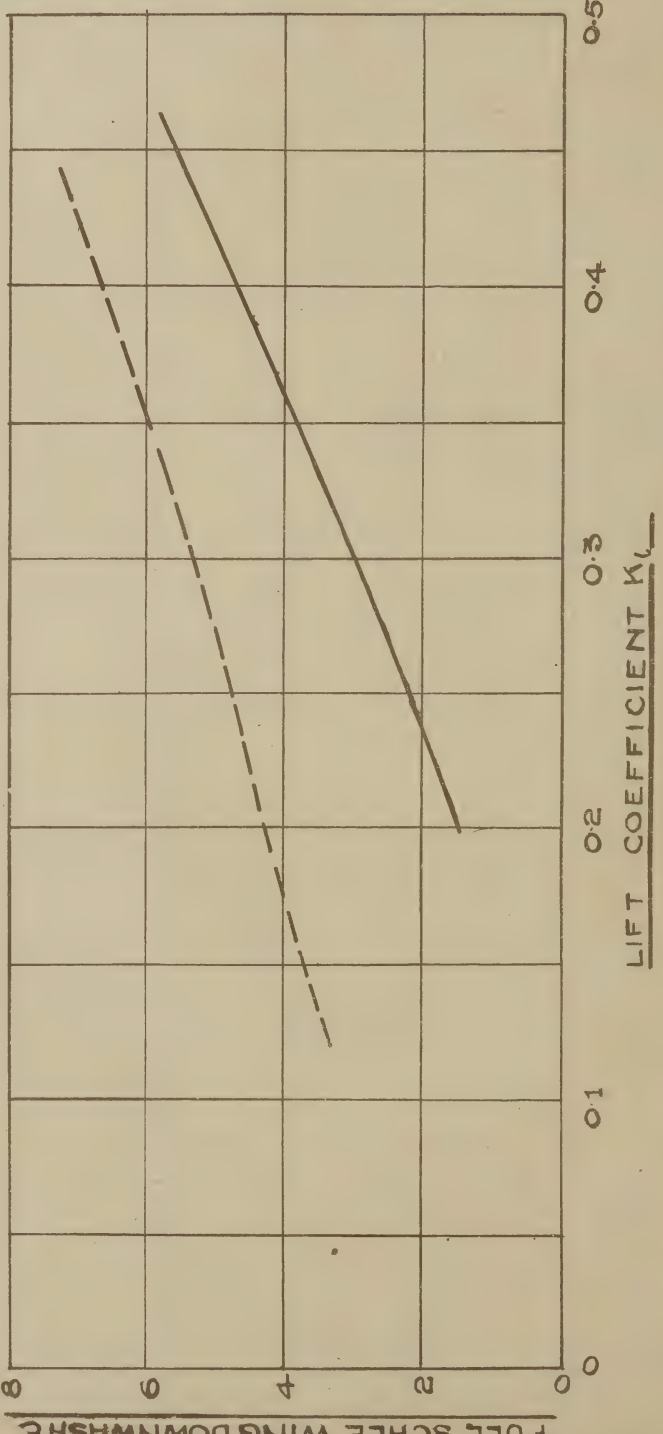

TABLE 2.

Expt.	Lift Coefficient. K_L.	Period secs.	$\frac{W_o}{W_Q}$	$\frac{d\epsilon}{d\theta}$	Downwash. ϵ.	Wing Downwash E.
1	0·187	28½	0·42	0·39	1·20	1·43
2	0·229	—	—	—	1·78	1·97
3	0·219	26	0·44	0·49	1·54	1·74
4*	0·242	23	0·54	0·38	2·38	2·28
5	0·245	26½	0·36	0·53	1·93	2·12
6	0·268	24	0·42	0·49	2·17	2·33
7	0·273	26	0·31	0·53	2·27	2·43
8	0·276	25	0·35	0·50	2·37	2·52
9	0·281	26½	0·28	0·53	2·49	2·63
10*	0·302	24	0·34	0·42	2·99	2·99
11	0·325	22¾	0·35	0·53	3·26	3·37
12	0·343	22	0·36	0·33	3·68	3·78
13	0·361	21½	0·35	0·53	4·10	4·18
14*	0·375	20	0·41	0·44	4·27	4·29
15	0·335	22½	0·36	0·58	3·35	3·44
16	0·344	21¼	0·41	0·56	3·59	3·60
17	0·356	20¾	0·42	0·55	3·87	3·94
18*	0·373	19½	0·47	0·44	4·28	4·27
19	0·309	22½	0·42	0·55	3·03	3·14
20	0·318	22	0·44	0·54	3·25	3·35
21	0·320	21	0·49	0·52	3·32	3·42
22*	0·337	20	0·52	0·45	3·86	3·84
23	0·396	18½	0·47	0·56	4·60	4·83
24	0·407	17½	0·56	0·51	4·82	4·84
25	0·415	17½	0·54	0·51	5·00	5·01
26*	0·450	16½	0·57	0·41	5·61	5·61

* Denotes experiments done gliding.

STRESSES IN AN AEROPLANE WHEN DIVING STEEPLY.

Presented by the SUPERINTENDENT, Royal Aircraft Factory.

Reports and Memoranda, No. 494. *April*, 1917.

SUMMARY.—In spite of the very high speeds which are reached in diving steeply, no part of the aeroplane is in general very highly stressed during the dive, providing certain precautions are taken in designing. The margin of strength in S.E. 5, for example, is high. The greatest stress occurs when flattening out after the dive, and the danger of breakage is increased by the comparatively small forces on the controls. This is inevitable in an aeroplane which is light on its controls.

1. It is doubtful, for reasons explained in R. & M. 492 (the terminal velocity of S.E. 5), whether aeroplanes are dived absolutely vertically for more than a few seconds. But very high speeds—of the order of 200 m.p.h.—are occasionally reached, corresponding to dives at about 60° to the horizontal. The stresses which occur in a vertical dive are dealt with below, this extreme condition being considered because it is simple, and because it appears that the stresses are likely to be more severe than in a less steep dive, so that there is in practice a certain margin of strength above that shown by the figures.

2. A vertical dive implies that the wings are at the attitude of no lift. There is some uncertainty as to their resistance in this attitude, but it does not materially alter the conclusions. At the terminal velocity, the total upward force on the aeroplane is equal to its weight, and in S.E. 5 this force is supplied by the head resistance of the various parts and is distributed in the following way :—

Body, tail, etc.	45 per cent.
Landing gear and wheels	10 per cent.
Airscrew	10 per cent.
Wings, struts, wires, etc.	35 per cent.
	100 per cent.

These figures are approximate only, but the main point is that well under half of the weight is supported by the wing structure as drag.

3. In addition to these forces the wings are in twist owing to the fact that, at no lift, there is a definite moment on the wings due to the air forces, though the resultant force at right

angles to the wind (the lift) is zero. The term "centre of pressure" has no meaning in this state, being at an infinite distance from the wing, but the moment on the wings is definite and, in general, small. This puts a down load on the front spar and an equal up load on the rear spar, and these vary as the square of the speed. In S.E. 5 at the terminal velocity (about 260 m.p.h.) these are each equal to 2·3 times the weight approximately. The factor of safety under the combined drag and twist is about 2 on the front spar and 3 on the rear spar. The stresses on the rest of the aeroplane are inconsiderable.

4. The magnitude of the load on the spars depends very much on the wing characteristics, and the best form of wing is one in which the moment at no lift is small, such as R.A.F. 15. In all modern wing sections the rate of change of moment with lift is roughly the same, and hence a small moment at no lift means small moments over the whole range, *i.e.*, that the centre of pressure is well forward. Wing sections with the centre of pressure further back will have greater moment at no lift, *e.g.*, R.A.F. 14. With this section the load on the spars of S.E. 5 at the terminal velocity would amount to about six times the weight.

5. One of the chief objections to diving at very high speeds is that intense vibration is often set up. This naturally gives the pilot cause to think that the machine is intrinsically weak, and, at any rate, continuous vibration is very bad for any structure. Much of this vibration is undoubtedly due to the high engine speed. Probably a great deal more is due to the wires, which are also responsible for much of the noise. But it is important to see if any is due to what appears as the rapid change of centre of pressure near no lift. It has been pointed out above that in this region the term "centre of pressure" has very little meaning. Although its position does change very rapidly *the moment* on the wings changes quite slowly, in fact, if anything, more slowly than at ordinary speeds, and it appears probable that very little of the vibration is due to this cause.

It is evident, of course, that if a definite moment is to be balanced a reduction can be made in the forces by increasing the distance between the spars. The forces will, in fact, vary inversely at this distance, and therefore any vibration which is really due to the wing forces could probably be reduced by increasing the spacing. But the spacing used gives a stronger structure for resisting the very high stresses produced in flattening out, and these are much more important because they also occur in sharp turns.

6. It will be seen that adequate precautions can be taken for ensuring a reasonable factor of safety even for extreme conditions. In practice, the actual factor is certainly ample.

THE TERMINAL VELOCITY OF S.E. 5.

Presented by the SUPERINTENDENT, Royal Aircraft Factory.

Reports and Memoranda, No. 492. *April,* 1917.

SUMMARY.—The terminal velocity of S.E. 5 at 10,000 ft. is 265 m.p.h. indicated with the engine on, and 255 with it off. In the former case the aeroplane acquires a velocity of 250 m.p.h. in the first 1,500 ft. of drop. These figures apply to the geared 200 h.p. Hispano engine. The effect of the engine is so doubtful that the speeds with the 150 h.p. engine have not been worked out, but they would probably be rather higher on account of the smaller breaking effect of the smaller engine and airscrew.

1. The conditions of air fighting at the present time make it necessary for pilots to dive their machines very steeply. It is stated that aeroplanes are dived "vertically" for several thousand feet. It is probable that the actual angle of the path to the horizon is nearer 45–60° (the tendency of an observer in an aeroplane is always to overestimate the steepness of a dive).

The following calculations, which refer to S.E. 5, give support to this suggestion, for they show that a speed of the order of 200 m.p.h. would soon be attained on an aeroplane capable of anything like 120 m.p.h. flying level, whereas it appears that so high a speed as this is seldom reached in practice. Some notes on the stresses which occur in diving at these speeds are given in another report (R. & M. 494).

The calculations cannot be regarded as very accurate, there being considerable uncertainty as to the resistance of the wings in the neighbourhood of no lift. The resistance (positive or negative) of the propeller is also doubtful. It is fairly certain that the engine revolutions will be so high that it will be acting as a brake even with throttle open. The error is, however, probably not more than about 10 m.p.h.

2. The assumptions made are as follows :—

(1) Weight, 1,930 lbs.

(2) Initial speed, 130 m.p.h.

(The aeroplane is supposed turned instantaneously into a vertical position when at this speed.)

(3) Wing resistance, 27 lbs. at 100 ft./sec. (drag coefficient, 0·0045).

Miscellaneous resistance, 91 lbs. at 100 ft./sec.

Propeller resistance, see below, § 3.

(4) Effect of slipstream ignored.

(5) Engine revolution, 2,500 (engine on).

(6) Torque of engine when off taken as 60 lbs./ft.
(This is deduced from a knowledge of the mechanical efficiency of similar engines.)

3. To find the resistance of the propeller or its pull when the engine is on, it is necessary to know certain data for the propeller. This particular propeller has not been tested, and so it is assumed that the ratio of the pitch to the advance per revolution at top speed is the same as for a B.E. 2c propeller. It has also been assumed that the curve of T/N^2 against advance per revolution is a straight line over the working range, as is the case with all propellers tested up to the present time. Finally, in order to find the resistance when the engine is off, it is assumed that the ratio of advance per revolution for no thrust to that for no torque is the same as for the B.E. 2c airscrew, T.5291.

4. The terminal velocity at 10,000 ft. with engine on is found to be 265 m.p.h. (indicated), while with the engine off it is 255 m.p.h. The table shows the relation between speed and height in the former case.

Ht. drop.	Speed in M.P.H. indicated.
0	130
100	157
200	175
300	187
400	192
500	206
1,000	235
2,000	257
3,000	263

It is to be noted that the *true* speed varies from about 150 to 290 m.p.h.

THE EFFECT OF A WIND GRADIENT ON THE RATE OF CLIMB OF AN AEROPLANE.

Presented by the SUPERINTENDENT, Royal Aircraft Factory.

Reports and Memoranda (New Series), No. 379. *September*, 1917.

SUMMARY.—This paper investigates the effect of a change of wind velocity on the rate of climb of an aeroplane. It is found that if the wind velocity increases with height, the aeroplane will climb best when flying up wind.

1. Consider an aeroplane flying at a constant airspeed U in a wind of varying velocity V. The horizontal and vertical components of the aeroplane's velocity relative to fixed axis will be $V + U \cos \theta$ and $U \sin \theta$ respectively, if θ is the angle of the flight path to the horizontal. The forces acting on the aeroplane are the thrust T and the drag D parallel to the flight path, the lift L at right angles to this direction and the weight $m g$ vertically downwards. The equations of motion can therefore be written in the form

$$\left.\begin{aligned} m\frac{LV}{dt}\cos\theta &= (T - D) - mg\sin\theta \quad . \quad . \quad .. \\ mU\frac{d\theta}{dt} - m\frac{dV}{dt}\sin\theta &= L - mg\cos\theta \quad . \quad . \quad . \end{aligned}\right\} \quad (1)$$

2. Now let Uc be the rate of climb of the aeroplane and v be the rate of change of wind velocity with height, then $\frac{dV}{dt} = v\,U\,c$ and the equations become

$$\left.\begin{aligned} m\,v\,U\,c\sqrt{1-c^2} &= (T - D) - m\,g\,c \quad . \quad . \quad . \\ \frac{m\,U}{\sqrt{1-c^2}}\frac{dc}{dt} - m\,v\,U\,c^2 &= L - m\,g\sqrt{1-c^2} \quad . \end{aligned}\right\} \quad (2)$$

If v is zero, these equations reduce to the ordinary expressions for the lift and drag of an aeroplane. If, again, v has same constant value other than zero, the conditions will be steady and $\frac{dc}{dt}$ will be zero. The increase in c from its value when v is zero, is given to the first order by the equation

$$g \Delta c = - v \, U \, c \quad . \quad . \quad . \quad . \quad . \quad (3)$$

When v is the rate of increase of wind velocity in m.p.h. per thousand feet, and U is expressed in m.p.h., this last equation becomes

$$\frac{\Delta c}{c} = - v \, U \, x \, 0{\cdot}0067\,\% \quad . \quad . \quad . \quad . \quad . \quad (4)$$

3. This result can also be obtained by another method. A wind gradient v is equivalent to a horizontal acceleration $v \, U \, c$, and so the resultant acceleration makes an angle $\frac{vUc}{g}$ to the vertical. An aeroplane will climb relative to this resultant acceleration, being unable to distinguish between the accelerations due to gravity and to the wind gradient. It follows at once the change Δc in the angle of flight path must be equal to the deviation of direction of the resultant acceleration from the vertical and hence $g \Delta c = - v \, U \, c$ as before.

4. It appears, therefore, that if the wind velocity increases with height, the ratio of climb of an aeroplane will be less when flying down wind than when flying against it. This effect is of chief interest close to the ground, where it attains its greatest value owing to the fact that the rate of change of wind velocity is greatest in this region. If the wind velocity is taken to increase 20 m.p.h. in the first 1,000 feet, the effect on an aeroplane flying at 60 m.p.h. will be to cause a difference of 16 per cent. in the rates of climb when flying up and down wind. The rate of change of wind velocity attains its highest value in the neighbourhood of the ground, and this might contribute to the supposed danger of turning down wind. In a steady wind without gradient there is no such effect, although, of course, the speed of the aeroplane over the ground will be proportionately increased. The real danger of turning down wind is due to the pilot wrongly estimating his speed by looking at the ground instead of at his air-speed indicator.

THE EXPERIMENTAL AND MATHEMATICAL INVESTIGATION OF SPINNING.

By F. A. Lindemann, H. Glauert, and R. G. Harris.

Presented by the Superintendent, Royal Aircraft Factory.

Reports and Memoranda (*New Series*), *No.* 411. *March*, 1918.

Summary.—This report describes the results of a series of experiments to determine the aerodynamic conditions of an aeroplane when spinning and to investigate the effect of movements of the controls. The motion is subjected to mathematical analysis and the question of the stresses in the wing structure is also considered.

Part I deals with the experimental observations obtained on a B.E. 2E. and shows that the spin is essentially a spiral glide in a very steep path with the wing incidence above the stalling point.

The stresses involved in a spin are considered in Part II and it is found that these are probably not dangerous in a proper spin, although large stresses may occur when passing from a spin to an ordinary spiral. Care must also be taken not to flatten out too abruptly from the nose dive at the end of a spin. The data for calculating the stresses are, however, insufficient and further information is required.

The mathematical analysis is contained in Parts III and IV. The former deals with the motion of the centre of gravity in its spiral path and the latter considers the balancing of the various moments by adjusting the control surfaces.

PART I.

Experimental Investigation.

1. A number of spins were performed on a B.E. 2E. machine over a camera obscura so as to obtain a full series of observations and to determine the effect of small motions of the controls. It was found that in a normal spin with full left rudder and with the stick full back to the right, the time for one complete turn was approximately four seconds, the indicated airspeed about 55 miles per hour, and the radius of the turn about 20 feet. The attitude of the machine was such that the wing struts were horizontal and there was no appreciable sideslip. This motion of spinning could be kept quite steady and appeared to be a stable motion.

Observations were taken in the aeroplane of the indicated airspeed and of the loss of height. Lateral and longitudinal spirit levels were fitted so that the direction of the resultant force could be determined, and the value of this force was also obtained by means of a spring accelerometer in the pilot's seat. The lateral

bubble was found to be one or two degrees to the left, indicating an outward sideslip, but in all probability this was due rather to the fact that the bubble was a short distance behind the centre of gravity of the machine than to any sideslip of the machine as a whole.

2. A number of spins were made with full left rudder but varying positions of the control column to observe the consequent changes in the motion. The results are given in Table 1 below. It will be noticed that as the stick is moved across, the period of rotation, the airspeed and the total force all increase. When the stick is also moved a little forward the time of turn is still further increased and the motion has developed into a steep spiral rather than a proper spin. In the last case when the stick was nearly central and a little forward, there was a considerable sideslip outwards. On another occasion it was found possible to convert a spin gradually into a spiral and back again to a spin (see Table 2).

TABLE 1.

Effect of Movement of Controls.

Position of control column.	Period of rotation. Secs.	Indicated airspeed. M.p.h.	Radius of turn. Feet.	Loss of height. Ft. per sec.	Number of times normal loading.
Full back, right ...	4·2	58	30	66	1·6
Full back, central...	4·5	70	45	83	2·6
Full back, left ...	7·5	70	115	56	2·7
Slightly forward, right.	—	70	140	47	2·0
Slightly forward, central.	10·0	75	190	—	2·2

TABLE II.

Conversion of a Spin into a Spiral.

No. of turn.	Time of turn. Secs.	Indicated airspeed. M.p.h.	No. of times normal load.	Radius of turn. Feet.
1	4·9	—	1·9	31
2	3·8	54	—	—
3	3·8	—	—	27
4	4·1	—	—	—
5	5·2	—	—	77
6	8·0	70	2·5	—
7	8·4	—	—	130
8	7·1	—	—	115
9	4·4	—	1·8	—
10	4·0	55	—	—
1	4·5	55	1·6	35
2	5·6	—	—	62
3	7·0	65	2·6	110

3. An approximate analysis* of the results has been made on the basis of no sideslip as indicated by the readings of the lateral bubble. The forces on the fin, rudder, and tail plane have been neglected as they do not appear to be large. The data used in these calculations have been the period of rotation, the total force, the indicated airspeed, and the reading of the longitudinal bubble. It is then possible to calculate the attitude of the machine, and the various wing characteristics. The results obtained show that the attitude of the machine is beyond stalling, the angle of incidence varying from 20 to 40 degrees. The wing characteristics derived are shown in Fig. 6. They are in good agreement with model tests for high angles of incidence and form continuations of the full scale curves obtained from other experiments. The radius of the turn and the loss of height as calculated agree reasonably with the observations. It is to be noted that, while the observations of the period and total force are made with considerable accuracy, the airspeed is a little uncertain owing to the pitch of the pitot head. The observations of the radius of the turn and the height drop are also rather uncertain as it is difficult to correlate them accurately with a particular turn and the latter is also affected by the lag of the aneroid.

The analysis reveals the fact that the incidence varies rapidly along the span of the wings. This point is dealt with further in Part III of this report.

TABLE III.

Details of Spins on B.E. 2E.

No.	Period of rotation. Secs.	Number of times normal loading.	Indicated air-speed. M.p.h.	Radius of turn. Ft.	Loss of height. Ft. per sec.	Angle of flight path to horizontal. °	Angle of bank. °	Angle of incidence. °	Lift coefficient of machine.	Lift Drag.
1	3·8	2·3	61	25	88	65	79	25	0·62	2·4
2	3·9	2·0	54	22	76	65	77	—	—	—
3	4·2	1·6	58	18	85	72	76	37	0·41	1·3
4	4·5	2·6	70	40	93	59	78	15	0·54	2·9
5	4·5	1·6	55	20	83	71	75	32	0·45	1·3
6	4·9	1·9	54	32	76	61	74	26	0·63	1·9
7	4·0	1·8	55	19	76	68	76	30	0·55	1·7

4. Some experiments were next carried out with streamers to measure the angle of incidence on a spin directly. For this purpose rods 12 feet long were fixed to the middle of the wing struts of the B.E. 2E. which had been used for the previous experiments. A vertical cross-piece marked in inches was fixed 7 feet in front of the front strut and a piece of tape was attached to the tip of the rod. The angle of incidence could be derived from the position of the tape as there was little likelihood of the

* See Part III for mathematical analysis.

air flow being disturbed so far ahead of the wings. The tape, however, fluttered so much that errors of 2° or 3° must be reckoned with. The airspeed was measured by a special pitot head set down at an angle of 30°, so that its pitch was inconsiderable on the spin. The subjoined table gives the results of these experiments and shows that the observations agree well with the calculated values.

TABLE IV.

Period of rotation. Secs.	No. of times normal loading.	Indicated airspeed. M.p.h.	Loss of height. F.p.s.	Angle of flight path. °	Angle of bank. °	Mean angle of incidence. °	Angle of incidence on rods. Calculated. Left. °	Calculated. Right. °	Observed. Left. °	Observed. Right. °	Mean lift co-efficient.	Mean lift/drag
3·7	1·8	55	82	71	78	30	37	17	35	15	0·55	1·6
3·5	1·7	53	84	74	79	32	41	19	38	16	0·56	1·5

5. A few spins were also carried out on an F.E. 2B. In this aeroplane the pilot and observer are both a considerable distance from the centre of gravity. This complicates the interpretation of the results considerably as both the direction and magnitude of the resultant force differ from the values at the centre of gravity. The observations of a typical spin are given below :—

TABLE V.

	Period. Secs.	Rate of fall. F.p.s.	Distance from C.G.	Loading.	Longitudinal bubble.	Lateral bubble.
Pilot	2·5	74	5′	1·0	20°	9°
Observer ...	—	—	8′	0·8	>20°	18°

It is difficult to derive the angle of the flight path to the horizontal, angle of bank, angle of incidence and radius of curvature of the path from these observations. The following values, however, would lead to results similar to those given in Table V. :—

Angle of flight path = 80°
Angle of bank = 78°
Mean angle of incidence = 35°
Radius of turn = 7 ft.

It is curious to find that the F.E. 2B. spins more rapidly and in a smaller circle than the B.E. 2E. in spite of its greater span and weight. It is possible that the extreme conditions may give rise to greater stresses than are met with in the B.E. 2E.

6. The general result of the experiments is to show that a spin is merely a spiral with a large angle of incidence on the wings. This angle is so great, usually well beyond stalling angle, that the drag is very large and a sufficient airspeed to give the necessary lift can only be maintained by losing height very rapidly. This is why the nose of the machine points downwards at such a steep angle as to have given rise to the term "spinning nose dive."

The resultant force during a spin is almost exactly at right angles to the wings. As the lift drag ratio is of the same order as the cosecant of the angle of incidence at angles of 25° to 40° such as occur in a spin, the longitudinal bubble remains near its normal position and there is no sensation of falling forward as there is in a steep dive. The lateral bubble remains very nearly central as the nose of the machine is pointing so steeply downwards that the bubble is very insensitive to the gravity control.

A spin is a state of perfectly steady and by no means violent motion at a comparatively low airspeed. Were it not for the position of the controls it might well be mistaken for an ordinary spiral by a pilot flying in a cloud. This is due to the wings being stable at an angle of incidence greater than the stalling angle owing to lift decreasing with increasing angles whilst the centre of pressure moves back. A small deviation therefore tends to correct itself. The tail plane and elevator are not necessary for stability, but together they must exert a downward moment to balance the moment due to the centre of gravity being in front of the centre of pressure. As the fixed tail plane is exerting a considerable upward force on account of the large angle of incidence, the elevator must be raised very much, *i.e.*, the stick pulled right in to counteract this effect. The wings being stalled the flap control is of course reversed, which is the reason that the stick must be held in the opposite direction to the rudder in really successful spins.

7. The methods of starting a spin and of coming out of it are obvious once its nature is realised. As the spin itself demands an angle of incidence greater than stalling angle the simplest and commonest way of starting a spin is to stall the machine and put on plenty of rudder while keeping the stick well back and preferably to the opposite side. A less usual method is to keep the airspeed low on a spiral by putting on plenty of upward rudder and pull the stick right in and gradually put the rudder over. In this way the stalling angle may be passed almost imperceptibly. In order to get out of a spin the reverse procedure may be adopted, *i.e.*, the rudder taken off gradually and the stick eased forward thus turning the spin into a spiral. A more rapid method is to take off rudder and push the stick forward enough to flatten out in the usual way without going through the spiral stage. This method requires a certain amount of care, as a spin may start in the opposite direction unless the stick is eased forward.

PART II.

Stresses on the Wing Structure.

1. The stresses on the wings of an aeroplane are abnormal for four reasons. In the first place the angle of incidence is abnormally large, 30° to 40°. Secondly the angle of incidence varies rapidly along the span of the wings, the rate being as high as 1° per foot span in the case of the F.E. 2B. Thirdly the speed of the outer wing tips is higher than that of the central portions, and lastly the centrifugal force along the wings is considerable. Apart from these four causes there does not seem to be any reason why the stresses on the wings during the spin itself should be large, as the loading is not excessive. In the course of a large number of spins on a B.E. 2E the loading was seldom found to exceed 2·5 g (2·5 times normal load), and in these cases the radius of turn was large, *i.e.*, the aeroplane was descending in a steep spiral rather than in a true spin. In a spin proper the loading should not exceed 2g, and any aeroplane should stand this amount, providing the conditions mentioned above do not introduce special stresses.

2. In the cases of the B.E. 2E the abnormal conditions do not seem to lead to any great stresses. The resultant force for any large angle of incidence is almost normal to the plane of the wings, as is indicated by model experiments and confirmed by the readings of the lateral and longitudinal bubbles during a spin. Thus according to the model experiments on R.A.F. 6 wing section the direction of the resultant force relative to the wing chord only varies some 20° for a change of incidence from 0° to 70°. The position of the centre of pressure changes from about 0·28 to 0·5 of the chord as the angle of incidence increases from 15° to 65°. Similar considerations show that the variation of the angle of incidence and of the speed along the span of the wings does not lead to undue stresses. As pointed out above the resultant force is almost at right angles to the chord and the distribution of the load is abnormal, but less so than might have been expected at first sight. According to the model tests the load at right angles to the chord of the wing only varies by some 30 per cent. if the angle of incidence varies from 15° to 65°. The variation of the angle of incidence is not often greater than this even in a very violent spin. Assuming the most unfavourable distribution of the angle of incidence actually found, with all the controls as far over as possible, which is roughly 10° to 50° from wing tip to wing tip, the bending moment on the front spar of the outer bottom wing is 400 lbs. ft. corresponding to a factor of safety of 1·9,* the loading on the machine being 1·7 times normal. The factor on the rear spar of the inner bottom wing is 2·2 and on the front spar of the outer top wing 2·3. The factors on the

* This assumes the failing strength of spruce to be 5,500 lbs. /in.^{2}.

other parts are considerably greater. The torque along the wing due to the shift of the centre of pressure is not serious. Thus from 15° to 70° the centre of pressure only moves 0·22 of the chord. The torque on a B.E. 2E wing would safely be taken up by the incidence bracing and lift wires. The fact that the speed of the wing tips is greater than at the centre increases the load on the extension, but not seriously. This effect is taken into account in the above calculations. The centrifugal force along the wings may amount to some 6*g* at the tips, but the weight of the wings is small and the total force is insignificant compared with the stresses wood will take in tension. In any case this effect will relieve the compression of the spars and strengthen the wing. The fixing of the wings to the body is normally calculated to stand compression, and tension so that there is no danger of the whole wing coming loose.

3. The only times apparently during which dangerous forces are likely to be exerted on the wings are when getting into or coming out of the spin. The stalling angle must be passed in these cases and if it is passed at a high speed the stresses will certainly be great. Thus if the spin is started from a spiral by pulling the stick in without taking care to keep the speed down with the rudder, the stalling angle is passed at a comparatively high speed. At 80 m.p.h. the loading will be 4 times normal and at 100 m.p.h. the machine might break. The same of course applies to the conversion of a spin into a spiral. Starting a spin in the usual manner, by stalling the aeroplane when flying straight and then crossing the controls, is scarcely likely to put any stress on the machine, as the speed never rises above some 60 m.p.h. Coming out of the spin by putting the controls central and converting the spin into a nose dive is probably quite safe so long as care is taken to pull out of the dive gently. The speed of course is likely to increase very rapidly during the dive and it is found in practice that the stress coming out of the dive is greater than during the spin. It might be desirable for pilots engaged on spinning tests to use an accelerometer and to avoid letting the loading rise above 3*g*. If the aeroplane spins faster than the B.E. 2E with which the experiments were carried out, the factor of safety might be less, but it does not seem likely that the conditions would be seriously aggravated.

PART III.

Motion of Centre of Gravity.

1. Two sets of axes $O\xi\eta\zeta$ and OXYZ are used. The former is fixed in space, $O\zeta$ being vertical. The latter is fixed in the aeroplane and is chosen so that OX is the projection of the line of motion of the aeroplane on to its plane of symmetry, and OY is at right angles to this plane. The axes OXYZ are derived from the axes $O\xi\eta\zeta$ by a pitch θ about $O\eta$ and a bank ϕ about OX (see Figure 1).

2. Let R be the radius of the cylinder on which the aeroplane moves, U the speed of the aeroplane, ω the angular velocity of the turn, h the height drop per second. Also let kg be the acceleration corresponding to the resultant of the air forces. The resultant of gravity and the centrifugal force will act along OG where G lies on the great circle $\eta\zeta$ and $\cos G\zeta = 1/k$. If there is no side slip G must be the intersection of XZ and $\eta\zeta$, because the air-forces consist solely of the lift at Z and the drag at X. When there is side slip the angle GT is determined by the reading of the lateral and longitudinal levels.

3. Resolving along the axes OXYZ we obtain the equations

$$\left.\begin{aligned} k_d\rho AU^2 &= mg\sin\theta \\ Y &= mg\cos\theta\sin\phi - m\omega^2 R\cos\phi \\ k_l\rho AU^2 &= mg\cos\theta\cos\phi + m\omega^2 R\sin\phi \end{aligned}\right\} \quad . \quad . \quad (1)$$

where k_l and k_d are the lift and drag coefficients of the whole machine, Y is the lateral force due to side slip, and it is assumed that the side slip is too small to effect the lift and drag. In addition there are the relations

$$\left.\begin{aligned} \omega R &= U\cos\theta \\ h &= U\sin\theta \\ k^2g^2 &= g^2 + \omega^4 R^2 \end{aligned}\right\} \quad . \quad . \quad . \quad . \quad . \quad (2)$$

4. If readings of the longitudinal and lateral bubbles (i and i') are obtained, a complete solution can be derived. The two bubbles are assumed to be fixed at the centre of gravity of the machine, and the zero of the longitudinal bubble is taken to coincide with zero wing incidence. From Fig. 2 it is then possible to deduce the relations

$$\left.\begin{aligned} \tan n &= \cos i\tan i' \\ \sin(\alpha + i) &= \frac{\sin\theta}{k\cos n} \\ k\sin n &= \sqrt{k^2 - 1}\cos\phi - \cos\theta\sin\phi \end{aligned}\right\} \quad . \quad . \quad (3)$$

Equations 1, 2, and 3 give a complete solution of the aeroplane's motion, including a determination of the angle of incidence.

5. *Case of no sideslip.*—Observation shows that in most spins the sideslip is negligible, and this case will be considered in some detail. The equations (1) reduce to

$$\left.\begin{aligned} k_d \rho A U^2 &= mg \sin\theta \\ k_l \rho A U^2 \cos\phi &= mg \cos\theta \\ \frac{k_d}{k_l} &= \tan\theta \cos\phi \\ \omega U &= g \tan\phi \end{aligned}\right\} \quad . \quad . \quad . \quad . \quad (4)$$

These equations have been used to analyse the experiments with a view to determining the attitude of the machine, the nature of its path, the angle of incidence and the wing characteristics. It was found that the incidence varied considerably along the wings, differing at times by as much as 50° between the wing tips. The coefficients k_l and k_d must therefore be regarded as mean effective values corresponding to these abnormal conditions.

6. The force equations (1) are nearly independent of details of design, such as size of fin, rudder, elevators, &c., but they involve broad characteristics such as loading and aerofoil section. Differences in body resistance, &c., are not important at high angles of incidence. It will be found, however, that the moment equations (Part IV) depend very much on details of design, particularly of control. It follows that two machines which have the same wing sections and loading can be made to spin at the same speed and in the same attitude if the controls are sufficiently powerful.

7. The third equation (4) gives a relation between θ, ϕ, and the aerofoil characteristics. This relation is shown graphically in Fig. 3 for R.A.F. 6 wing section. The drag coefficient has been increased by 0·014 to represent the body drag. An inspection of this diagram shows that ϕ is even greater than θ in spinning motion (*i.e.*, when θ is large) except when the angle of incidence is very large, say, 40° or more. The conclusion is that the angle of "bank" is always of the order of 70° to 90° during spins. This large bank is, however, not very obvious to an observer, because the outer wing tip is very little above the level of the inner, owing to the steepness of the flight path. The term bank is used in its ordinary meaning, viz., the angle through which the aeroplane must rotate about its flight path in order to obtain the symmetrical position (*i.e.*, plane of symmetry vertical).

Table 6, on which Fig. 3 is based, gives the values of R, U, ω and ϕ for various values of θ and α, the mean angle of incidence. These figures assume a machine whose wing loading is $6\frac{3}{4}$, but the relation between θ, ϕ, and α is independent of this value.

8. The resultant force on the machine is measured by the quantity k and gives a limit to the possibility of spinning from

considerations of strength. k is measured experimentally by means of an accelerometer, but the reading needs correction unless the accelerometer is fixed at the centre of gravity of the machine and in the direction of the resultant force. In the case where there is no sideslip the expression for k can be reduced to

$$k = \sin\theta \sqrt{1 + (k_l/k_d)^2} \quad . \quad . \quad . \quad . \quad (5)$$

$\sin\theta$ is of the order of 0·9 for a true spin and so k varies roughly as $\frac{k_l}{k_d}$. Thus the resultant force increases as the angle of incidence decreases so long as θ remains large. The curves of Fig. 4 show that the stress may become dangerous if a machine is held in the attitude of spinning without being stalled. This is due to the high speed under these conditions (see Table 6).

9. *Reduction of experiments.*—The quantities determined experimentally and used in analysing the results obtained were the speed U, the angular velocity ω, the resultant force k, and the readings of the two bubbles i and i'. The height drop by aneroid and the radius of turn measured by means of a camera obscura were used as a check. When the observations of k, i and i' were obtained at the centre of gravity, as in the case of experiments on a B.E. 2E, the analysis was carried out by means of equations 1, 2, and 3. The results obtained were the values of R, h, θ, ϕ, α, k_l, k_d. The values derived from a number of spins on B.E. 2E. have been given in Part I of this report (see Table 3) and showed satisfactory agreement with the check observations.

10. *Velocity and force at a distance from the centre of gravity.*—For this purpose it is useful to have axes OABC fixed in the aeroplane and with OA parallel to the wing chord and OB coinciding with OY. The equations to transform from these aeroplane axes to the fixed axes whose origin coincides with the centre of gravity of the aeroplane at that instant are

$$\left.\begin{aligned} x &= a\cos\alpha + c\sin\alpha \\ y &= b \\ z &= -a\sin\alpha + c\cos\alpha \end{aligned}\right\} \quad . \quad . \quad . \quad . \quad . \quad (6)$$

$$\left.\begin{aligned} \xi &= x\cos\theta - y\sin\theta\sin\phi - z\sin\theta\cos\phi \\ \eta &= y\cos\phi - z\sin\phi \\ \zeta &= x\sin\theta + y\cos\theta\sin\phi + z\cos\theta\cos\phi \end{aligned}\right\} \quad . \quad . \quad (7)$$

The radius of the cylinder described by the point (abc) is $\sqrt{\xi^2 + (R + \eta)^2}$ and so its velocity has components relative to the axes (XYZ).

$$\left.\begin{aligned} u_x &= -U - \omega\eta\cos\theta \\ u_y &= \omega\eta\sin\theta\sin\phi + \omega\xi\cos\phi \\ u_z &= \omega\eta\sin\theta\cos\phi - \omega\xi\sin\phi \end{aligned}\right\} \quad . \quad . \quad (8)$$

The difference of the incidence at the point of the wing from the mean incidence is given by $\tan \Delta\alpha = \frac{u_z}{u_x}$.

11. The gravity and centrifugal forces at the point (*abc*) have components parallel to the axes (ABC) of value

$$\left.\begin{aligned} A &= -g(\cos\alpha\sin\theta - \sin\alpha\cos\theta\cos\phi) \\ &\quad + \omega^2\{\xi(\cos\alpha\cos\theta + \sin\alpha\sin\theta\cos\phi) + (R+\eta)\sin\alpha\sin\phi\} \\ B &= -g\cos\theta\sin\phi - \omega^2\{\xi\sin\theta\sin\phi - (R+\eta)\cos\phi\} \\ C &= -g(\sin\alpha\sin\theta + \cos\alpha\cos\theta\cos\phi) \\ &\quad + \omega^2\{\xi(\sin\alpha\cos\theta - \cos\alpha\sin\theta\cos\phi) - (R+\eta)\cos\alpha\sin\phi\} \end{aligned}\right\} \quad (9)$$

The angles i and i' measured by the longitudinal and lateral bubbles at the point (*abc*) are now given by $\tan i = A/C$ and $\tan i' = -B/C$.

The quantity measured by an accelerometer fixed in the machine at this point is C/g.

12. The equations developed in the last two sections make it possible theoretically to analyse the observations even when the instruments are not fixed at the centre of gravity of the machine. In practice the analysis becomes far too complicated to deal with directly, but it is possible to determine the kind of variation to be expected some feet from the centre of gravity and to determine the motion corresponding to the observed quantities by trial and error.

13. *Numerical example.*—As an example of the analysis developed above, a spin on a B.E. 2E machine has been chosen in which the flaps were held in a neutral position. The data on which the analysis is based are $U = 108$, $\omega = 1{\cdot}39$, $k = 2{\cdot}6$, $i = 1{\cdot}5$, $i' = 3$.

Equations (1), (2) and (3) lead to the solution

$$R = 40, \quad h = 93, \quad \theta = 59°{\cdot}0 \quad \phi = 74°{\cdot}7$$
$$\alpha = 20°, \quad k_l = 0{\cdot}53, \quad k_d = 0{\cdot}186.$$

The variation of the speed and angle of incidence over the wings has been worked out by the method developed above. The results are shown in Fig. 5. The values refer to the middle of the wing chord. The angle of incidence as calculated is 2° higher and the speed 2 f.p.s. lower at the leading edge than at the trailing edge. There is no difference between the two wings as regards angle of incidence, but the speed differs by some 5 f.p.s.

TABLE 6.

Angle of incidence. α	Angle of flight path. θ	Angle of bank. ϕ	Speed. U. M.p.h.	Rate of spin. ω	Reduced spiral. R. Ft.
°	°	°			
15	20	66·9	72·5	0·71	141
	30	75·7	87·7	0·98	114
	40	80·2	98·2	1·28	86
	50	83·1	108·5	1·67	61
	60	85·3	115	2·33	36
	70	87·0	120	3·49	17
	80	88·6	123	7·30	4
20	40	64·9	67·7	0·69	110
	50	72·5	74·0	0·94	74
	60	78·2	78·7	1·34	43
	70	82·6	82·0	2·06	20
	80	86·4	83·8	4·16	5
30	40	42·7	54·4	0·37	164
	50	58·8	59·4	0·61	92
	60	69·1	63·2	0·91	51
	70	77·0	65·8	1·44	23
	80	83·7	67·4	2·95	6
40	40	39·4	49·7	0·36	129
	60	58·0	52·9	0·66	58
	70	70·5	55·0	1·13	24
	80	80·7	56·4	2·38	6
50	60	45·1	49·0	0·45	80
	70	63·6	50·9	0·87	29
	80	77·6	52·2	1·91	7

PART IV.

Motion about Centre of Gravity.

The axes chosen for dealing with the equations of moments are the axes AOBC defined in § 10 of Part III. The equations are

$$\left.\begin{aligned} -m\omega_b\omega_c(k^2_b - k^2_c) &= P_1 + P_3 \\ -m\omega_c\omega_a(k^2_c - k^2_a) &= Q_1 + Q_2 \\ -m\omega_a\omega_b(k^2_a - k^2_b) &= R_1 + R_3 \end{aligned}\right\} \quad . \quad . \quad . \quad (10)$$

where $\omega_a = \omega\ (\cos\alpha \sin\theta - \sin\alpha \cos\theta \cos\phi)$

$\omega_b = \omega \cos\theta \sin\phi$

$\omega_c = \omega\ (\sin\alpha \sin\theta + \cos\alpha \cos\theta \cos\phi)$

k_a, k_b, k_c are the radii of gyration about the axes, and P, Q, R are the moments of the air forces about the axes, the suffix (1) refers to the wings, (2) to the tailplane and elevators, and (3) to the fin, rudder and body. The quantities P_2, Q_3, R_2 can be neglected to a sufficient approximation.

2. Movement of the flaps affects P_1 and to a less extent R_1, the elevator angle affects Q_2 and the rudder angle R_3. Thus if the motion is determined from the previous considerations, these three equations serve to determine the necessary position of all the controls and the spin will be a possible one if these lie within the range of movement. The three moment equations will be examined in turn to see if the values obtained from the analysis of an actual spin can be made to agree with possible positions of the controls.

3. *Rolling moments.*—Taking the experimental spin considered in § 13 of Part III, the values of the constants are

$$\alpha = 20^\circ \qquad \theta = 59^\circ \qquad \phi = 74^\circ{\cdot}7 \qquad \omega = 1{\cdot}39$$

and so

$$\omega_a = 1{\cdot}06 \qquad \omega_b = 0{\cdot}69 \qquad \omega_c = 0{\cdot}59$$

The change of incidence along the wing is 0°·63 per foot and the variation of speed along the wing is shown in Fig. 5. With these values the inertia term of equation (10) has a value of 590 lbs. ft. and from model data of R.A.F. 6 wing section the value of P_1 is calculated to be 1,000 lbs. ft. The difference is accounted for partly by the rolling moment P_3 of the fin and rudder, which is estimated as 300 lbs. ft., and the remaining 110 lbs. ft. is probably due to a small flap angle or errors in the approximate data used.

4. *Pitching moments.*—The inertia moment is — 780 lbs. ft. The value of Q_1 depends on both the lift and drag of the wings, and taking the mean incidence of 20° these two parts give respectively — 5,750 and 3,050 lbs. ft. Q_2 must therefore have a value

FIG. 1.

SPHERICAL DIAGRAMS.

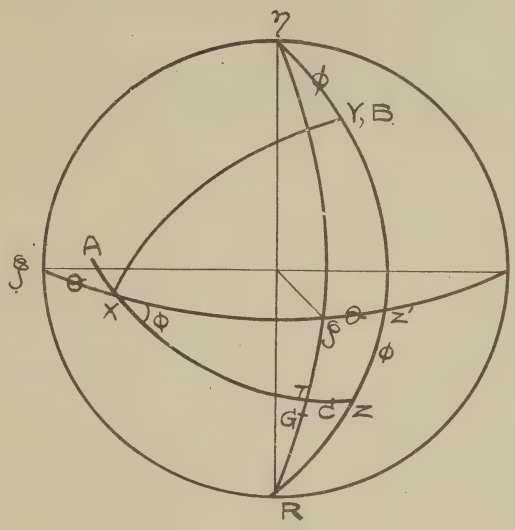

FIG. 2.

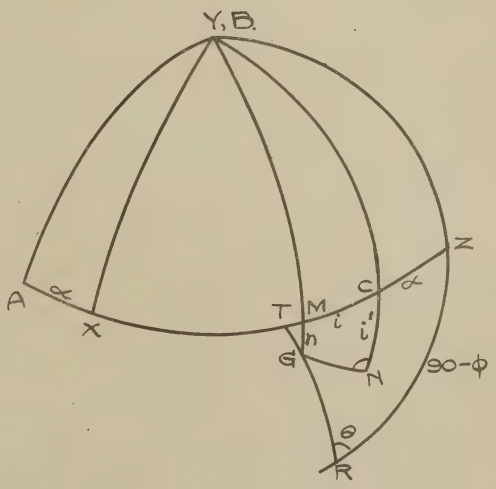

RELATION BETWEEN FLIGHT PATH, BANK, ANGLE OF INCIDENCE (α) AND RATE OF SPIN (ω) IN A SPIRAL GLIDE WITH NO SIDE SLIP

THE LOCI OF CONSTANT SPEED ARE ROUGHLY PARALLEL TO THE α CURVES WHEN THE FLIGHT PATH IS STEEP

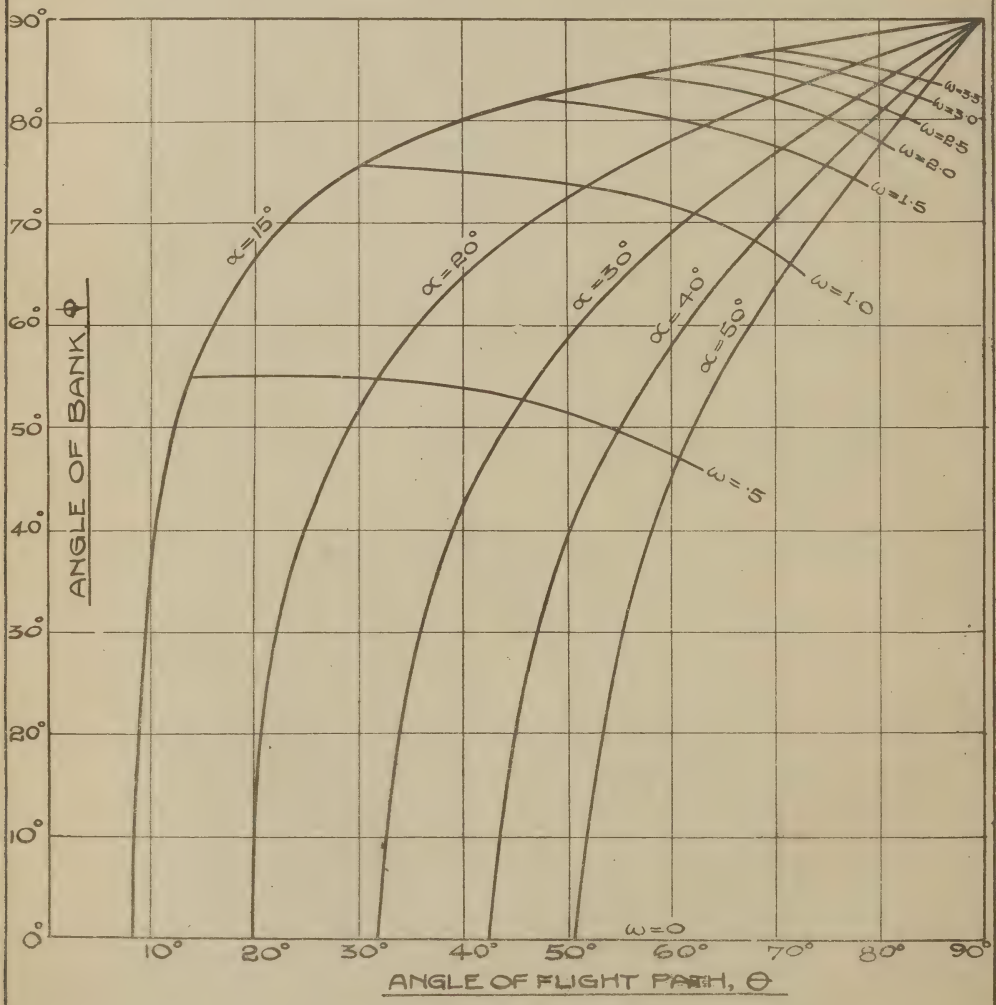

RESULTANT FORCE ON AEROPLANE WHEN PATH IS A SPIRAL AND THERE IS NO SIDE SLIP

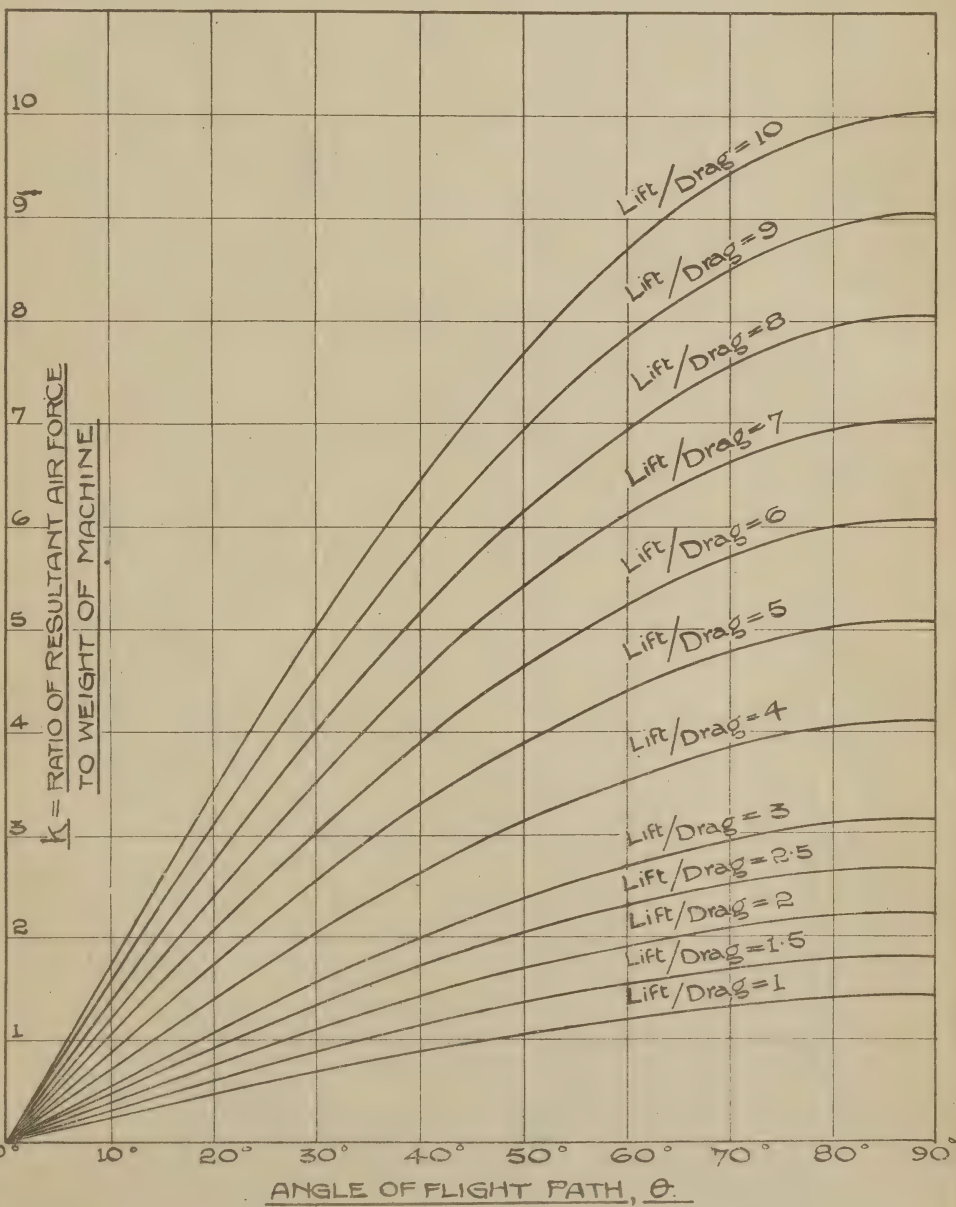

VARIATION OF SPEED AND ANGLE OF INCIDENCE OVER THE WING OF AN AEROPLANE IN A SPIN.

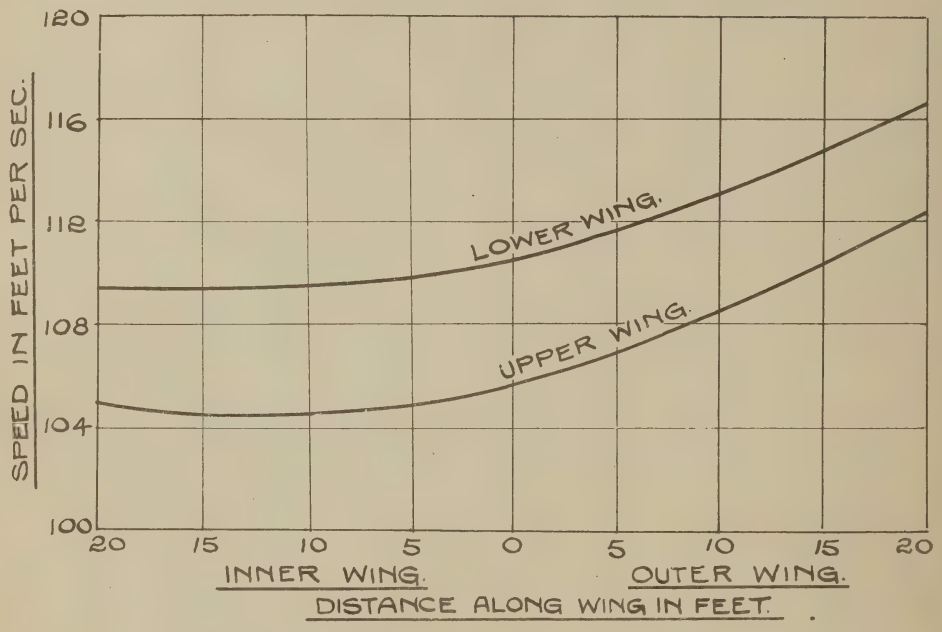

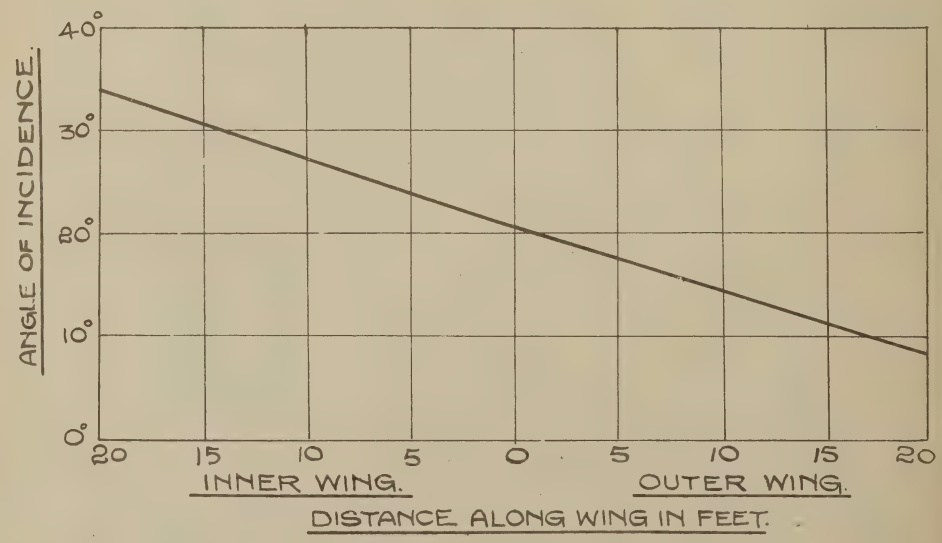

LIFT & DRAG AT HIGH ANGLES OF INCIDENCE.

FROM SPINS ON A B.E.2E MACHINE.

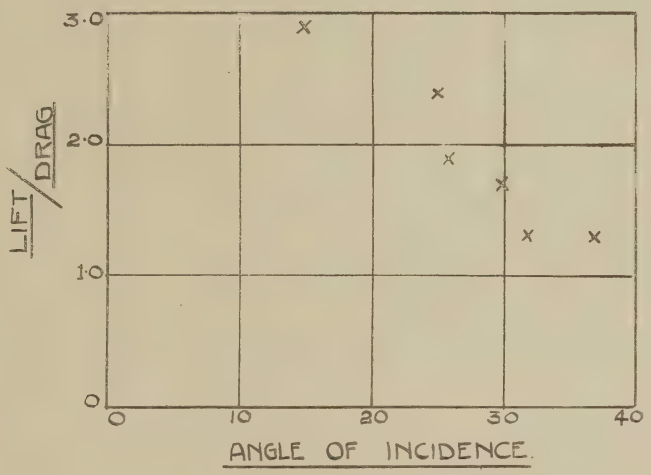

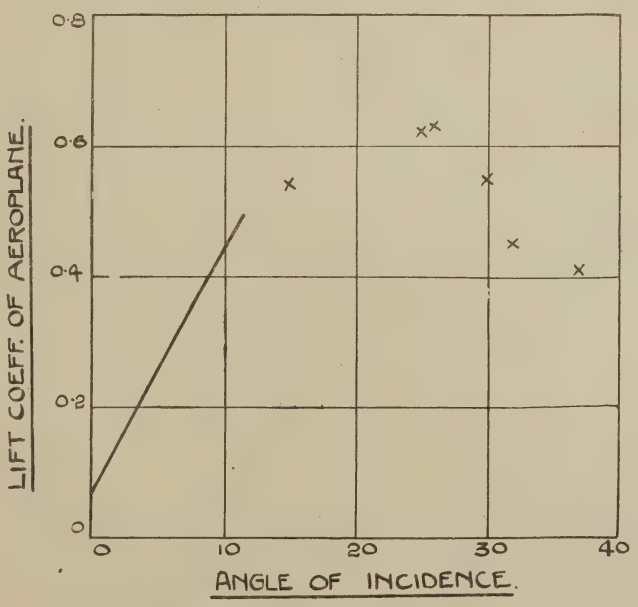

The curve drawn is the full scale lift curve of the wing section for normal flying angles.

of 1,920 lbs. ft. or a negative tail lift of 115 lbs. Allowing for the rotation and taking the downwash from model tests as 7° the effective tail incidence becomes 17°. Full scale tests on the elevators then indicate that an elevator angle of — 30°, which is the limiting position, would give a tail lift of 104 lbs. This gives excellent agreement for the pitching moments.

5. *Yawing moments.*—In this case the inertia terms are negligible as k_a is nearly equal to k_b. The yawing moment on the wings due to the longitudinal force is 2,900 lbs. ft. and is assisting the rotation. Due to the rotation the fin is yawed 5° and gives a moment of — 360 lbs. ft., but with the rudder set over to assist the turn, as in the case of a spin, this value may be changed to as much as 1,600 lbs. ft. for a rudder angle of 30°. This is a considerable discrepancy, but too much importance must not be attached to this result as the longitudinal force is rather uncertain, and a small change in the angle of incidence or a small flap angle would produce large changes in the yawing moment. The method of integrating the forces over the wing also involves considerable uncertainty in the results, as the actual distribution of the air forces may differ considerably from that obtained by assuming that the lift and drag of any section of the wing correspond to the calculated angle of incidence at that section.

6. The above analysis of a typical spin shows how the various forces are balanced. Experimental results also indicate that this is a stable form of motion. The effect of movement of the controls has been described in Part I, and it is seen that any movement of the controls from their limiting positions increases the period of rotation and the stress on the wing structure.

The chief characteristics necessary for a machine to spin rapidly are large elevator and rudder controls. A low position of the centre of gravity will enable a machine to spin with less elevator control owing to the increased pitching moment of the wing drag. The same effect is produced to a smaller degree by distributing the load along the body. A reduction of wing span and a small fin area will also aid the rudder. The total load on a machine during a spin is less than that obtained on a really sharp turn or spiral, but owing to the peculiar distribution the factor of safety is not very high.

THE OBJECT OF TABULATING ENGINE DATA.

By Lieut.-Col. Mervyn O'Gorman, C.B.

Reports and Memoranda, No. 503. *May,* 1917.

1. The utility of standardising the "dry weight" of engines which has been suggested by Commander Briggs is not to be questioned, and the only addition I would make is to suggest that an agreed symbol for this "dry weight" might be put forward at the same time.

2. The reason for defining this or any other matter, such as the agreed total loaded weight of an aeroplane, etc., is that when data are collected they shall be comparable. The use of the tabular form is the expression of this; the object is to save time on the constantly repeated references made by the administrative staff and others to the relative engine performances.

3. It has been objected that tabulation and the attendant standard definitions for one purpose cannot be precisely in the form required for another, and that is the reason urged here for considering some of the objects of producing such definitions and such tables, so that they may be as useful and as little liable to misconception as possible.

4. One of the uses of engine data tables is the ultimate one of getting good aeroplane performances, by giving to the administration a rapid and accurate indication as to which engine weight and engine power should be selected. If this view is adopted, a table which includes for some engines the weight of cooling and omits it from others requires to be supplemented by some such figure as a "Weight of the *power unit complete.*"

5. For intercomparison between water-cooled engines *alone*, the dry weight is more helpful and accurate, and therefore the dry weight as defined is not here objected to, but welcomed.

6. The weight, W, of the aeroplane loaded per h.p. (normal) being one of the most important factors in relation to performance, it is useful to consider that W is made up as follows:—

$$W = P + U + F + G$$

when

P is the power unit complete.

U is the military load, viz., pilot, passenger (if any), guns, ammunition, such mountings as are not structural to the aircraft, bombs, bombsights, armour (non-structural), bomb carriers, landing lights, etc.

F is the fuel, oil, and tanks.

G is the glider weight.

7. It is now worth discussing what can most usefully be included in the *power unit weight*, "P," and it is suggested that this should be

$$P = R + A + S,$$

viz., the cooler, the airscrew, and certain sundries to be fixed arbitrarily.

8. (*a*) *The weight of the cooler* system, with all water and pipes and sundries relating to the cooler, is probably best expressed as a function of the agreed normal h.p., say 0·65 lbs. per b.h.p. normal.

In this way any improvement of radiators is made available for the credit of all engines using radiators. In view of the wide range of speeds at which aeroplanes perform, there is an inaccuracy, but this is much less than appears because the size of the necessary radiator is determined by the worst heating condition, which occurs on climbing "all out." When radiator shutters become universal they should be included.

9. (*b*) *The weight of the airscrew.*—This also goes up with the h.p. handled and goes up as the screwshaft speed or engine speed goes down, so that the estimation of the airscrew weight for accuracy needs to be based on the data of the particular engine considered.

There exists a rough rule, which should, it is suggested, be gone into by using data of the class supplied by S.R.A.F. on 8.5.17.

$\frac{\text{H.P.}}{5}$ in lbs. for airscrew shaft of 1,600 r.p.m.

$\frac{\text{H.P.}}{4}$ in lbs. for airscrew shaft of 1,200 r.p.m.

$\frac{\text{H.P.}}{3}$ in lbs. for airscrew shaft of 900 r.p.m. (4 blades).

10. If such rough rules are used in the power unit weight they could be remodelled as the tables are brought up to date when actual experience of the engines in the air exists. But pending such experience, there is need for the just approximation to the airscrew weight, not only because the aeroplane design must carry this weight but for comparison purposes between various power units.

11. (*c*) There are certain *sundries* which should be included in making up the power unit weight. Thus, some engines definitely require two magnetos to get the requisite power; if so, the extra magneto should be added in. There are also among these sundries the throttle control, ignition control, mixture control, altitude device, petrol pipes to the tanks, etc.

These are no doubt not precisely a constant amount for all engines, but a figure should be added to represent these, when determined from existing analyses, since it ought not to be ignored. It may be about 15/20 lbs. per engine, or more.

12. The very large engines have a further weight called for in the power unit in requiring starting gear consisting of items which are not included in the dry weight. This is properly part of the power unit weight, and even if no definite size of air bottle or other device has been standardised, a suitable representative weight could be taken. What this weight is could, if the departments were to afford the information, be sufficiently closely known. It is improbable that it varies gradually with the h.p., but is more probably to be taken in steps, according to the class of engine.

13. The stationary engines all employ exhaust manifolds and exhaust pipes. A reasonable weight based upon experience should be added, probably indicated by a constant figure, or more accurately by a constant plus a variable per h.p., which should be averaged up and added to the power unit. An allowance for cowling might be added also.

14. It is to be agreed that certain inaccuracies must exist in such "power unit weight," and in any deduction made as to the "power unit weight" per h.p. because

(i) of the imperfect estimation of (*a*), (*b*) and (*c*) above ;

(ii) of the incompletely defined h.p. of rotaries when under a close fitting cowl, and the difference of head resistance of various shapes of engine ;

(iii) of the effect on carburation of altitude ;

(iv) of the effect of blowers or supercharger when introduced.

15. As regards (i), (ii) and (iii) these need not prevent the data from being very useful in their approximate form. If no such data be given, the inaccuracy of any comparison becomes even greater, since each authority making a study of the question will be obliged to estimate these matters for himself, and the unnoticed omission of some detail which may accidentally occur in one case and not in another will tend to incorrect deductions.

16. As regards (iv), the effect of the blowers. This could be practically eliminated if it were agreed that all the h.p.'s were corrected for operations supposed occurring at a good average height, say 6,500 feet (2,000 metres), or if preferred, 10,000 feet (3,000 metres approximately). Then, when the blower engines come in, or the Ricardo engine becomes a quantity to be reckoned with, it would fall correctly into the table.

If the I.C.E. Committee accepts the general idea of this recommendation it is invited to decide arbitrarily upon the data, h.p. at height and sundries included.

17. *Weight of fuel, oil, and tanks.*—It is suggested that these weights do not enter conveniently or usefully into the weight of the power unit. They are liable to rapid alteration by any change in the character of the warfare. They are different according to the class of aircraft (seaplane, scout, fighter, bomber, reconnaissance or artillery machine), and, moreover, the rate of fuel consumption is a quantity which is not fixed in relation to an individual engine type, but departs much from test results in accordance with what squadron is in charge of the particular engine and carburetter. It also varies with the climate and other matters.

18. In order to give value to the differences known to exist between the fuel and oil consumption of air-cooled rotaries, air-cooled stationaries, water-cooled stationaries, and supercharged engines like the Ricardo, it would seem best for the moment to take the joint weight of fuel and oil at some such figures as :—

0·75 lbs. per normal h.p. hour for rotaries,

0·7 lbs. per normal h.p. hour for air-cooled stationaries,

0·65 lbs. per normal h.p. hour for water-cooled stationaries,

? 0·6 lbs. per normal h.p. hour for Ricardo type engines,

and to add 10 per cent. of this weight for tanks in all cases, keeping, however, this fuel, oil and tanks item in a separate column, and I suggest for the present taking the 3-hour full power at 6,500 feet as the basis and leaving out any allowance for climbing time (save in so far as the extra half hour's fuel included in the 3 hours may be said to allow for the climbing expenditure of fuel).

19. *Military Load, U.*—It will be observed that the weight, " F," of fuel and oil and tanks is kept separate from the military load, which is entirely independent of the engine design and indeed of the aeroplane designer, but which represents the main objects which the aeroplane has to transport. The actual load imposed is not, even for one class of aeroplane, *e.g.*, single-seater fighter, strictly constant, but it is to be considered whether, in view of the enhanced value of tests which might be made truly comparable, it is not worth while to do this. Strictly equalising the loads during the actual testing—even though for certain reasons the use in the field called for the differences (which are to be noted in the existing tables)—would make the performances as measured a better index of the technical achievement of the designer, and a basis for deducing improvements in designs generally.

20. *Glider weight.*—There remains the glider weight, which should if possible be defined, and not left simply as the residuum after deducting the previous loads. This would not, however, be a matter for the I.C.E. Committee, save in collaboration with the Aeroplane Committee so as to get a consonant whole.

ON THE DISSIPATION OF HEAT FROM THE SURFACE OF AN AIR-COOLED ENGINE WHEN RUNNING AND WHEN AT REST.

By T. E. Stanton, D.Sc., F.R.S.,
Miss Dorothy Marshall, B.Sc., and E. Griffiths, D.Sc.

Reports and Memoranda, No. 520. *October*, 1917.

Summary.—The experiments described in the report are the outcome of the suggestion approved at the meeting of the Advisory Committee in January, 1917, that an investigation should be undertaken at the Laboratory with a view of obtaining further evidence on the effect of vibration on the heat dissipated from the surfaces of air-cooled engines.

Some experiments were made at the National Physical Laboratory in September and October, 1916, on the resistance of a copper tube, and the heat transmission from a platinum strip, when vibrating and when at rest. No difference due to vibration was detected in these experiments. Experiments were also made on a honeycomb radiator, and no effect of vibration on resistance or cooling was observed. It was thought that the absence of effect in these experiments might be due to the low frequency of the vibrations, but experiments in the Heat Department with a bar vibrating at a high frequency likewise exhibited no result due to the vibration.

In the present communication experiments are described on the distribution of temperature in metal rods rigidly attached to one of the cylinders of an aero engine, and in the gills of the cylinder itself, with the engine running at various speeds and with the engine at rest.

The emissivity coefficient for each metal bar and also for the cylinder gill is calculated, and its relation to the temperature difference between metal and air is examined.

The experiments afford no evidence that the thermal emissivity of the cooling surfaces is appreciably affected by vibration.

In the early part of 1917, evidence was brought before the Advisory Committee for Aeronautics which appeared to lead to the conclusion that a hot body, subject to high frequency vibrations, such as those produced in an aero engine cyclinder by the explosions, possessed a thermal emissivity from its surface considerably higher than when these vibrations were absent.

After discussion, it was agreed that, in view of the important bearing on engine design of such an increase in thermal emissivity due to vibration, experiments should be carried out at the Laboratory in order that the accuracy of the above conclusion might be investigated under more rigorous conditions than had hitherto been possible.

By the kindness of General Sir David Henderson, a 70 h.p. Renault air-cooled engine was supplied by the Royal Flying Corps for the purpose of the tests.

This engine was mounted on the test stand previously used for the engine tests in the Patrick Alexander Competitions of 1909 and 1911.

In this plant, which has been fully described in the Advisory Committee Report for 1909–10, the power is absorbed by a generator mounted on knife edges so that the torque can be measured, the current generated being dissipated in resistance mats. The air blast for cooling purposes is supplied by a motor-driven fan.

Two series of experiments were made :—

Series I.—Observations of the distribution of temperature in metal rods of circular cross section rigidly attached at one end to one of the cylinders of the engine under the following conditions,

(*a*) when the engine was running at various speeds ;

(*b*) when the engine was at rest and the root temperature of the rod maintained at the value which it had in the running test, by means of a heating coil wound round the rod at its base.

Series II.—Observations of the distribution of temperature in one of the gills of the engine cylinder,

(*a*) when the engine was running at various speeds ;

(*b*) when the engine was at rest and the root temperature of the gill maintained at the value which it had in the running test, by means of an electric heater specially designed for the purpose of the test.

Series I.

Experiments with metal rods fixed to the cylinder.—In the design of the apparatus for these tests, the essential conditions to be fulfilled were as follows :—

(1) That the rods should be attached to the cylinder in such a way that there could be no doubt that any vibration of the cylinder itself was communicated to the rod. This was not

an easy matter on account of the thinness of the walls of the cylinder, but after some consideration it was decided to use the sparking plug connection as the method of attachment for the rod.

(2) That the rod should be screened as far as possible from the radiation of the hot cylinder and from currents of hot air which might impinge on it during the running tests.

(3) That, in the stationary tests, means should be provided of maintaining the root temperature of the rod at the same value as that which was obtained in the running tests.

(4) That the position of the rod relative to the engine and the air blast should remain unchanged throughout the whole of the static and running tests.

The arrangement finally adopted to satisfy these conditions is shown in Fig. 1.

R is the experimental rod which is firmly bolted to the engine cylinder by means of the sparking plug screw. The diameter is 1·27 cms., and the total length of the cylindrical part 14·2 cms. The last 3·2 cms. at the root is wound with a heating coil of nichrome flat strip connected with the supply mains through a variable resistance so that in the stationary trials the root temperature could be maintained at the value which it had in the running trials. The experimental length is 9·7 cms., and thermo-junctions are fitted at given distances along the length. For attaching the thermo-junctions small holes were drilled in the rod, and the connections made by driving a wedge of the same metal as the rod into each hole so as to fix the junction securely. S is the screen to prevent radiation and eddy currents from the cylinders reaching the surface of the rod. This was lined on the upper surface with a layer of uralite 0·4 cms. thick.

The temperature of the air impinging on the rod was taken by a thermo-junction 10 cms. in front of the rod, and the velocity of the air by means of a Pitot tube fixed to the screen in front of the rod and at the same distance from it as the axis of the rod. The junctions used were of iron-constantan wire, and were four in number and so arranged that by means of a special switch all the readings could be taken in succession on a Paul unipivot millivoltmeter.

The method of taking the observations was to run the engine up to the required speed and to take a set of readings when the temperature conditions became steady, which was generally about 10 minutes after the speed had been obtained. A second set was then taken, and if the latter were in agreement with the former, the engine speed was increased and readings taken at the new speed. When several sets of observations had thus been obtained, the engine was stopped, the air blast being left on. The heating current was then put on, and when the temperature at the root of the rod had attained a steady value

equal to that which it had during the first of the running experiments, sets of readings were taken as before. Further sets of observations were then taken corresponding with the other engine speeds.

Results of Experiments.

No. 1 *rod.*—This was machined from a bar of cast aluminium alloy (R.A.F.B4) supplied by the Superintendent of the Royal Aircraft Factory.

The dimensions of the bar and the positions of the thermo-junctions were as follows :—

Diameter = 1·27 cms.

Distance of observation points from the cooler end :—

$x_1 = 0{\cdot}8$ cm. ; $x_2 = 3{\cdot}8$ cm. ; $x_3 = 6{\cdot}7$ cm. ; $x_4 = 9{\cdot}7$ cm.

The temperatures at crankshaft speeds of 1,800, 1,400 and 950 revolutions per minute, and when stationary, are given in Table 1.

TABLE 1.

EXPERIMENTS ON ROD PREPARED FROM BAR OF R.A.F. ALUMINIUM ALLOY.

Revolutions of crankshaft per minute.	Wind speed cms. per sec.	Temperature of air impinging on rod. (degrees C.).	Temperature of observation points (degrees C.).				Value of k at mean temperature of bar.	Calculated value of σ	
			T_1	T_3	T_5	T_6		for speed observed.	for speed 1,118 cms. per sec.
950	1,122	5	21·6	25·1	32·4	45·5	0·363	0·00295	0·00293
			20·1	23·4	30·6	44·6			
0	1,097	7	22·4	26·2	34·0	47·5	0·364	0·00303	0·00307
			22·8	26·5	34·2	47·3			
1,400	1,130	6	31·0	37·4	50·7	72·5	0·369	0·00314	0·00311
			31·6	37·4	51·0	73·1			
0	1,085	6·9	32·0	38·4	51·7	74·1	0·369	0·00319	0·00326
			32·3	38·4	52·0	73·8			
1,800	1,153	6·7	32·1	38·2	54·5	80·0	0·370	0·00351	0·00343
			32·7	39·4	54·5	80·6			
0	1,169	6·8	—	39·1	54·8	80·3	0·370	0·00339	0·00329
			33·3	40·0	55·4	80·6			

Calculated values of the emissivity coefficient from the results of Table 1.—Denoting by σ the heat abstracted by the air in calories per second, per unit surface of the rod, per degree difference of temperature between rod and air ; and assuming that in any experiment the value of σ between the observation points is practically constant, the ratio of the temperature differences θ_2 and θ_1 between metal and air at any two points will be given by the expression

$$\frac{\theta_2}{\theta_1} = \frac{\cosh mx_2 + \frac{\sigma}{km} \sinh mx_2}{\cosh mx_1 + \frac{\sigma}{km} \sinh mx_1} \quad . \quad . \quad (1)$$

where k = conductivity of metal,

r = radius of rod,

and $m = \sqrt{\frac{2\sigma}{kr}}$

Taking the observed temperature differences at the two extreme observation points, *i.e.*,

$$x_1 = 0{\cdot}8 \text{ cm. and } x_2 = 9{\cdot}7 \text{ cm.},$$

and using the value of k determined at the National Physical Laboratory for this bar, the values of σ have been calculated from the above formula and are given in the last column of Table 1. The variations of θ along the rod are also shown plotted in Fig. 2 for the three engine speeds and for the corresponding static tests.

No. 2 *rod.*—This was machined from a bar of cast copper.

The dimensions of the bar and the positions of the thermo-junctions were as follows :—

Diameter = 1·27 cms.

Distance of observation points from the cooler end

$x_1 = 0{\cdot}5$, $x_2 = 6{\cdot}5$, $x_3 = 9{\cdot}5$ cms.

The temperatures at crankshaft speeds of 1,780, 1,520 and 1,180 revolutions per minute, and when stationary are given in Table 2, together with the values of σ calculated from (1) on the assumption that the thermal conductivity of the copper was constant throughout the experiments and equal to 0·9 in C.G.S. units.

The variations of θ along the rod are shown plotted in Fig. 3.

From the calculated values of σ given in Tables 1 and 2, it will be seen that for the same temperature difference between air and metal at the base of the rod, the thermal emissivity for both copper and aluminium rods is practically the same when the engine is running and when it is at rest. This is also obvious from the close agreement in the temperature gradients plotted in Figs. 2 and 3.

TABLE 2.

EXPERIMENTS ON COPPER ROD.

Revolutions of crankshaft per minute.	Wind speed cms. per sec.	Temperature of air impinging on rod. (degrees C.).	Temperature of observation points (degrees C.). T_1	T_2	T_3	Value of k.	Calculated value of σ for speed observed.	Calculated value of σ for speed 1,118 cms. per sec.
1,180	1,058	8·3	54·7	67·7	81·5	0·9	0·00317	0·00330
0	1,080	8·2	53·6	66·3	80·3	0·9	0·00322	0·00330
1,520	1,072	8·8	61·0	75·3	91·8	0·9	0·00324	0·00334
0	1,092	8·7	62·1	77·0	93·2	0·9	0·00325	0·00331
	1,085	8·6	61·3	76·8	93·3			
1,780	1,090	9·4	78·7	97·5	118·2	0·9	0·00321	0·00327
	1,094	9·9	74·1	92·4	112·7			
0	1,063	11·6	76·3	94·5	115·0	0·9	0·00319	0·00331
	1,060	11·8	82·0	102·2	123·7			

At the suggestion of Lieutenant Gibson sets of observations of the temperature gradient in the aluminium rod were also taken under the following conditions :—

(1) With spark advanced.

(2) With spark retarded.

(3) With a mixture richer than the normal.

(4) With a mixture poorer than the normal.

In no case, however, was there any appreciable difference in the temperature distribution on the rod when the engine was running, and when it was at rest with the root temperature maintained by means of the heating coil at the same level as in the corresponding running test.

The dependence of the emissivity on the temperature.—From the results given in Tables 1 and 2 it will be seen that, in the case of the aluminium rod, when the temperature difference between metal and air at the base is increased, there is a small but appreciable increase in the value of σ, whereas for the copper rod no definite rise in σ with temperature is apparent. This latter effect, however, may be due to the smallness of the range of temperature obtained in this series of experiments, and in view of the results of other experiments, in which a small but definite rise in the value of the emissivity coefficient of a flat copper strip was detected, it was decided to determine the heat emission at a series of temperatures covering the widest range obtainable with the available heating arrangements (engine standing), and to do this both for copper and for aluminium. In the case of copper, the same bar was used that has been previously described. In the case of the aluminium alloy a new bar was made, still of 1·27 cms. diameter, but longer than the original bar and with a larger basal portion on which a more effective heating coil could be wound. This coil was made of carefully insulated flat strip nichrome alloy, and over it was fitted a brass clip by means of which the bar was secured in position. The new bar was intended for stationary tests only. Two temperature observation points were provided, one 8 mm. and the other 8 cm. from the cooler end of the bar.

Tables 3 and 4 show the values of σ calculated from the new series of observations. It will be seen that both for copper and for the aluminium alloy σ appears to increase as the mean surface temperature of the bar is raised, but that the proportional increase in σ is considerably greater for the aluminium alloy than for copper.

The results of these experiments thus confirm the conclusion that there is an appreciable rise with temperature in the value of the emissivity coefficient.

TABLE 3.

RELATION OF σ TO TEMPERATURE. (ENGINE STANDING.)

Aluminium Bar No. 2.

Wind speed cms. per sec.	Temperature of air impinging on rod (degrees C.).	Observed temperatures.		Temperature excesses.		$\frac{\theta_2}{\theta_1}$	k at mean temperature.	σ for actual wind speed.	σ for speed of 1,118 cms. per second.
		T_2	T_1	θ_2	θ_1				
1,291	16·8	52·2	32·5	35·4	15·7	2·255	0·366	0·00364	0·00328
1,277	15·3	67·9	38·7	52·6	23·4	2·248	0·369	0·00367	0·00333
1,276	16·0	67·5	38·2	51·5	22·2	2·320	0·369	0·00384	0·00348
1,274	15·0	88·9	46·8	73·9	31·8	2·324	0·374	0·00389	0·00354
1,250	17·2	117·0	61·1	99·8	43·9	2·273	0·379	0·00384	0·00354
1,254	17·5	121·0	62·9	103·5	45·4	2·279	0·380		
1,282	15·0	122·1	61·0	107·1	46·0	2·328	0·380	0·00397	0·00360
1,238	16·3	163·7	79·6	147·4	63·3	2·328	0·388	0·00405	0·00374
1,255	17·5	170·7	83·8	153·2	66·3	2·310	0·389		
1,244	18·1	225·4	108·2	207·3	90·1	2·301	0·400	0·00413	0·00383
1,234	18·3	230·6	110·8	212·3	92·5	2·295	0·401		
1,236	17·2	275·1	129·9	257·9	112·7	2·288	0·409	0·00418	0·00389

TABLE 4.

RELATION OF σ TO TEMPERATURE. (ENGINE STANDING.)

Copper Bar.

Wind speed cms. per sec.	Temperature of air impinging on rod. (degrees C).	Observed temperatures.		Temperature excesses.		$\frac{\theta_2}{\theta_1}$	k at mean temperature.	σ for actual wind speed.	σ for speed of 1,118 cms. per second.
		T_2	T_1	θ_2	θ_1				
1,054	13·3	49·8	36·9	36·5	23·6	1·545	0·9	0·00300	0·00313
1,054	13·3	50·0	37·1	36·7	23·8				
1,055	13·4	62·3	44·9	48·9	31·5	1·553	0·9	0·00305	0·00317
1,071	13·6	62·7	45·2	49·1	31·6				
1,061	13·6	77·2	54·4	63·6	40·8	1·557	0·9	0·00307	0·00319
1,059	13·6	77·0	54·4	63·4	40·8				
1,080	8·2	80·3	53·6	72·1	45·4	1·588	0·9	0·00322	0·00330
1,092	8·7	93·2	62·1	84·5	53·4	1·595	0·9	0·00325	0·00331
1,085	8·6	93·3	61·3	84·7	52·7				
1,063	11·6	115·0	76·3	103·4	64·7	1·582	0·9	0·00319	0·00331
1,060	11·8	123·7	82·0	111·9	70·2				
1,082	13·7	126·8	84·5	113·1	70·8	1·597	0·9	0·00327	0·00336
1,071	13·6	126·8	84·5	113·2	70·9				
1,078	13·9	145·5	95·8	131·6	81·9	1·607	0·9	0·00332	0·00341

Series II.

Observations of the distribution of temperature in the gills of the engine cylinder.—In the provision of the appliances required for making the tests on the cylinder gills, the essential conditions to be fulfilled were :—

(1) that the external conditions of the gills as regards situation relative to air blast and intensity of air blast should be identical in the static and in the running tests. This condition does not seem to have been fulfilled in much of the previous work, in which it has been necessary to remove the cylinder from the engine bed and erect it in a wind tunnel, so that both the speed of flow and the distribution of flow round the cylinder were different in the two cases.

(2) that in the stationary tests means should be provided of regulating the temperature of the root of the gill to the value which it had during the corresponding running test, and maintaining it at that temperature for the duration of the experiment.

In one set of experiments the temperature of the gill during the static tests was maintained by the internal heating of the cylinder by means of a blow lamp. How the regulation was effected is not described, but after some preliminary experiments with various methods the authors of the present paper came to the conclusion that the only satisfactory method of satisfying the above conditions was by means of an electric furnace fitted into the cylinder body and provided with the necessary resistances for regulation. Such a heater was accordingly designed and constructed in the Heat Department of the Laboratory.

The general arrangement of the cylinder, the gill under observation and the appliances for determining the temperatures of the gill and the velocity and temperature of the air current are shown in Fig. 4. In the same figure is shown a view of the electric heater.

In order to prevent the cooling air impinging on the experimental portion of the gill from being heated by radiation and convection from the hot cylinder, and also to shield from radiation the thermo-junction used to determine the temperature of the air impinging on the gill, a small sheet iron screening channel lined internally with asbestos was attached to a bracket and fitted close up to the cylinder in the position shown. Small Pitot and static pressure tubes were fitted as shown to measure the velocity of the air current between the gills, and a second set of tubes was fixed between the engine and the roof of the wind channel to measure the average wind speed over the engine.

The two thermo-junctions TJ_1, TJ_2 were fitted at the root and tip of the gill, distant 2·06 cms. apart. The thickness of the gill at the root was 0·241 cms. and at the tip 0·140 cms. The thermo-junction TJ_3 was used for measuring the temperature of the air.

The heating furnace rests directly on the piston, which is set so that the crank is on the inner dead point. The furnace consists of two flat circular iron electrodes provided with conducting rods and arranged horizontally in a carborundum pot cast to fit tightly into the cylinder. The central part of the pot is filled with a hollow cylindrical block of insulating material, through which passes the insulated iron rod attached to the lower electrode. The rest of the pot, above, below and all round the central block, is packed with powdered graphite which serves as the high resistance filling of the furnace. The central insulating block is merely a device for increasing the resistance of the filling. The metal rods, iron and copper respectively, attached to the electrodes project through holes drilled in the cylinder head, and carry the current leads and also a pair of voltmeter leads. The current was supplied from a storage battery, and the circuit contained also a variable resistance, consisting of an 8 per cent. solution of washing soda, of adjustable length, and an ammeter provided with a suitable shunt. Using a battery consisting of two sets of 40 cells connected in parallel, the current through the furnace and the heating of the cylinder were well under control.

By this means the temperatures recorded for the root of the gills in the running tests could be reproduced fairly accurately in the static tests.

Table 5 shows the results of experiments made at running speeds of 1,800, 1,500 and 1,200 revolutions per minute, and also of experiments made with the engine stopped and the temperatures at the root of the gill maintained by the furnace at approximately the values observed in the running tests.

For the determination of the value of the emissivity coefficient it was necessary to measure the thermal conductivity of the gill. For this purpose a small piece of the gill under test was cut away from the cylinder and machined to the dimensions $6{\cdot}0 \times 0{\cdot}5 \times 0{\cdot}18$ cms. In this way a specimen was obtained which was fairly representative of the metal of the gill from root to tip. A precisely similar strip was cut from a sample of annealed cast iron of the composition used for making cylinder castings, the conductivity of which had previously been determined by an absolute method. Each strip was securely attached to one end of a cylindrical copper bar 10 cm. long and 2·5 cm. diameter, bar and strips being supported in a horizontal position. A current flowing through a coil of insulated nichrome flat strip, wound round the copper bar, served as the source of heat. In each cast iron strip three little holes were drilled at equal distances apart, and an iron-constantan thermo-junction was pegged into each hole.

The coil having been connected through an ammeter and a variable resistance to a storage battery, time was allowed for the temperature gradients along the strips to become steady,

and the temperature readings for the given points were then taken in the ordinary way by means of a potentiometer. With a steady current and an adequate screen to shield the apparatus from draughts, the temperatures were extremely steady and could be read off with great accuracy.

If k_1 be the thermal conductivity of the gill strip and θ_1, θ_2, θ_3 be the temperature excesses of the thermo-junctions in it over the surrounding air, k_2 and θ_4, θ_5, θ_6 being the corresponding quantities for the standard strip, and writing

$$\frac{\theta_1 + \theta_3}{\theta_2} = 2\,n_1 \text{ and } \frac{\theta_4 + \theta_6}{\theta_5} = 2\,n_2 \quad .$$

then it can be shown* that

$$\sqrt{\frac{k_1}{k_2}} = \frac{\log\,(n_2 + \sqrt{n^2{}_2 - 1})}{\log\,(n_1 + \sqrt{n^2{}_1 - 1})}$$

From a series of observations by this method, the value of k for the gill strip was found to be 0·108 in C.G.S. units and to be apparently independent of temperature.

Using this value of the thermal conductivity, the values of σ for the experiments of which the results are given in Table 5 have been calculated and are tabulated in column 10 of this table.

It will be seen that, as in the case of the rods, the difference in the emissivity of the gill with the engine running at various speeds, and when at rest, is negligible.

In the whole series of experiments described in this paper there is, therefore, no evidence that the thermal emissivity of hot metal surfaces forming parts of the cylinders of petrol engines is appreciably affected by oscillations set up by the explosions in the cylinders.

---

* Preston's "Theory of Heat," p. 634.

EXPERIMENTS ON THERMAL EMISSIVITY.

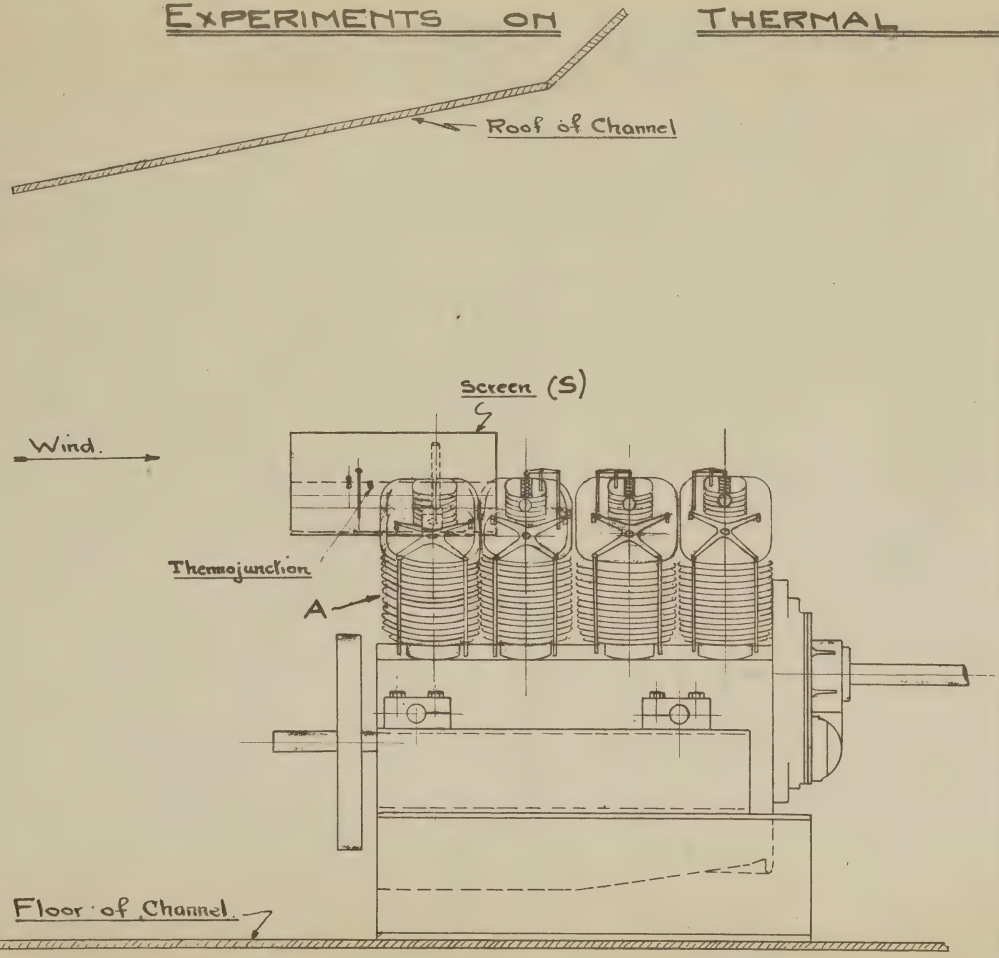

FIG. 1.

EXPERIMENTS ON THERMAL EMISSIVITY.

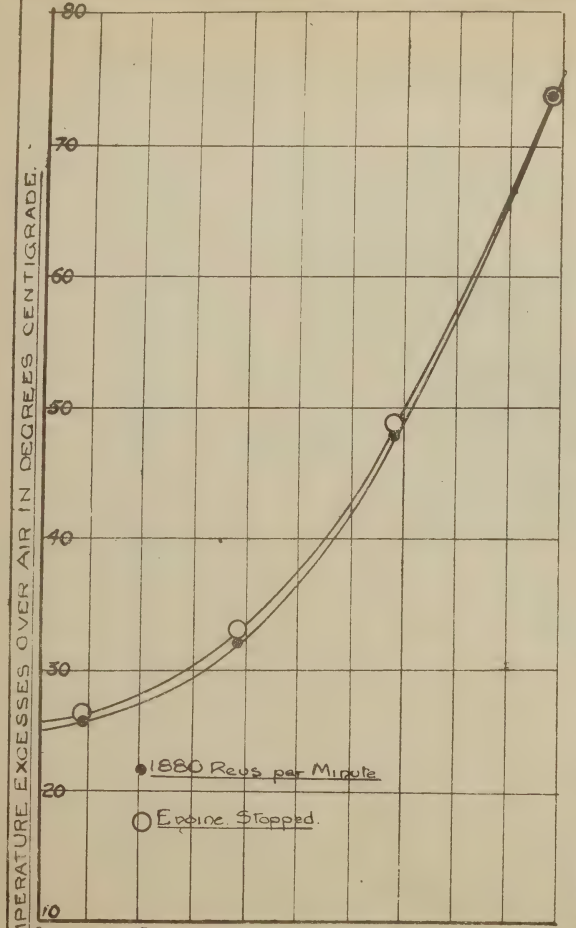

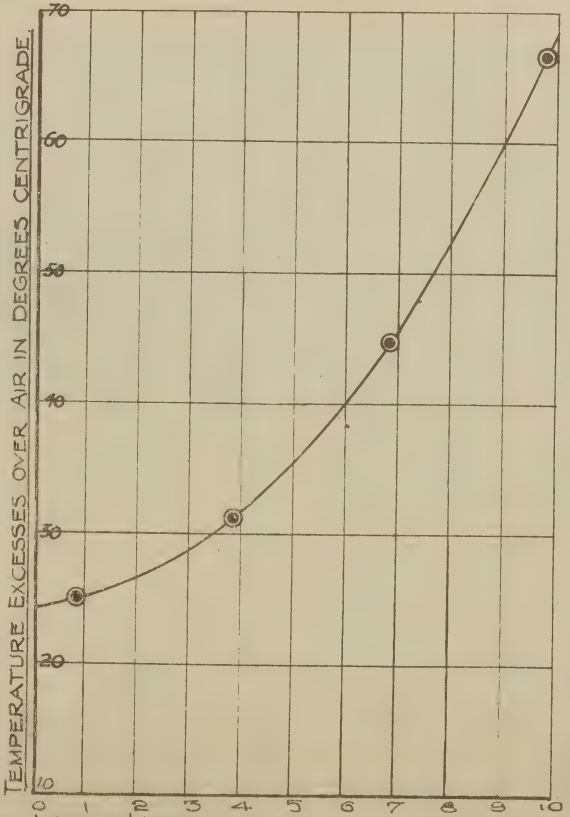

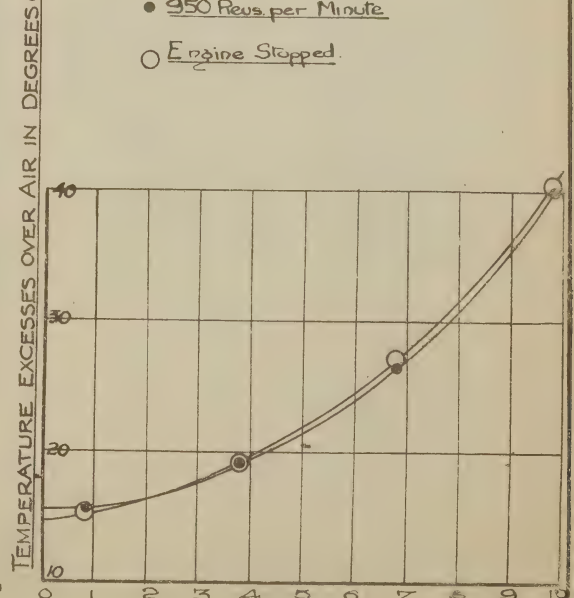

EXPERIMENTS ON ALUMINIUM ROD No 1.

FIG 2.

EXPERIMENTS ON THERMAL EMISSIVITY.

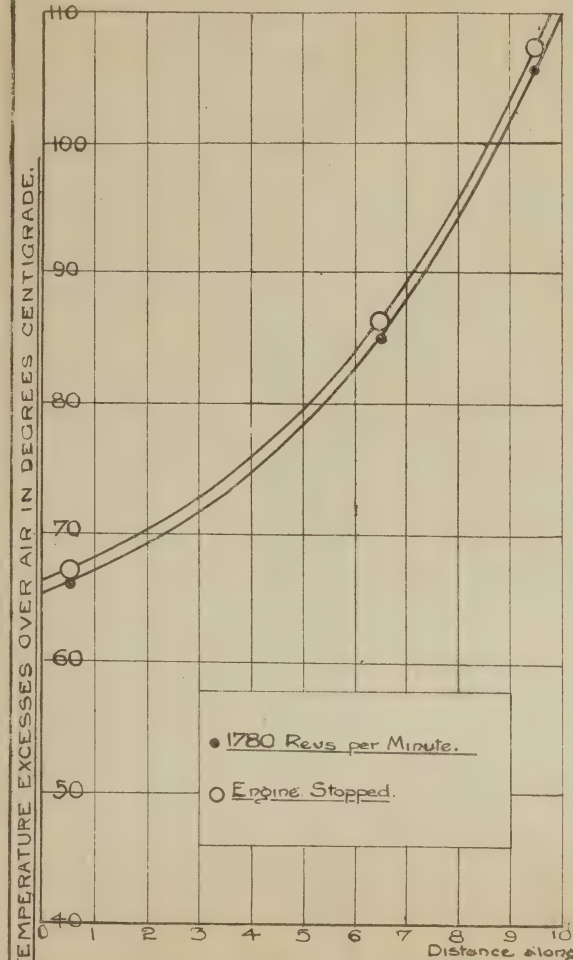

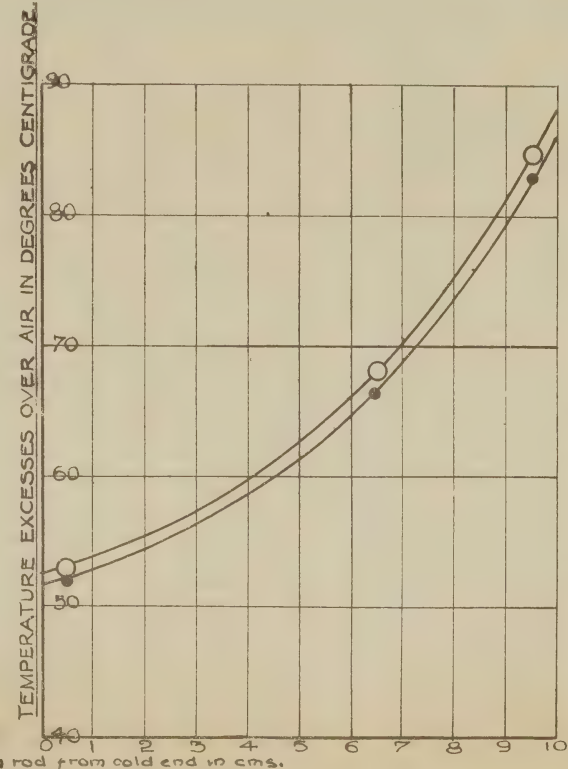

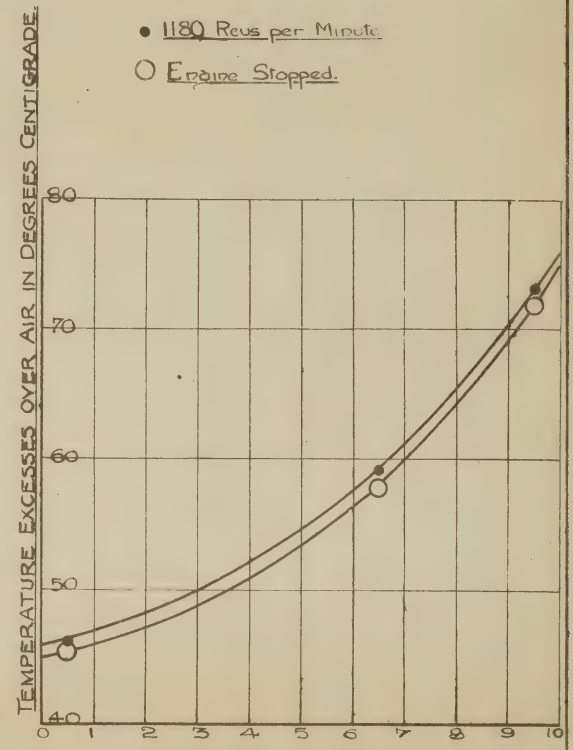

Distance along rod from cold end in cms.

EXPERIMENTS ON COPPER ROD.

EXPERIMENTS ON THERMAL EMISSIVITY.

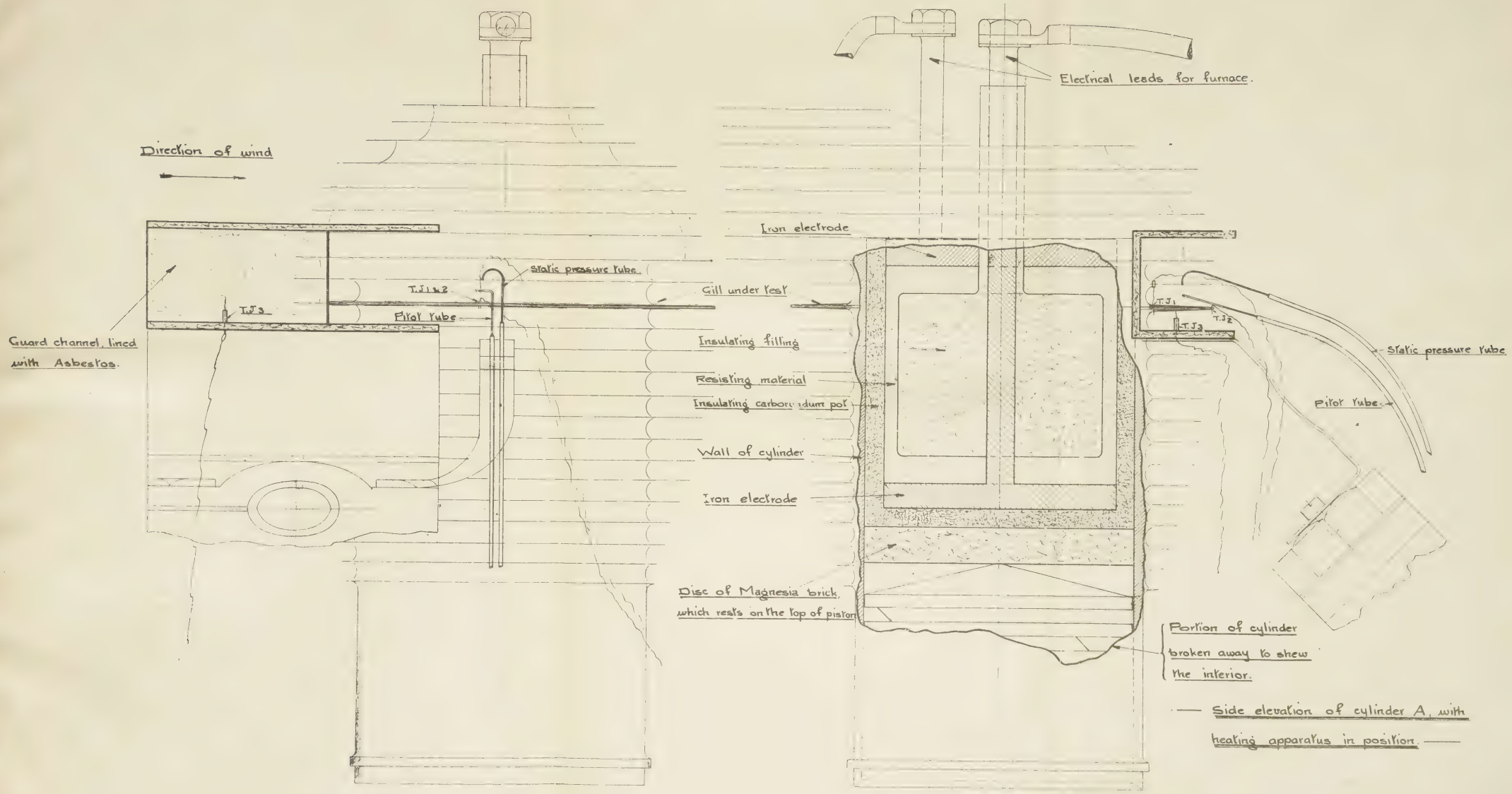

— Elevation of cylinder A on plane XX. Fig. 1. —

— Side elevation of cylinder A, with heating apparatus in position. —

TABLE 5.

COOLING OF CYLINDER GILL.

Revolutions of crankshaft per min.	Wind above engine cms /sec.	Wind between gills cms /sec.	Temperature of air impinging on gill.	Observed temperatures.		Temperature excesses.		$\frac{\theta_2}{\theta_1}$	Calculated value of σ.
				T_2	T_1	θ_2	θ_1		
1,200	1,842	1,488	15·7	116·6	65·1	100·9	49·4	2·04	0·0049
	1,842	1,476	15·7	117·8	66·2	102·1	50·5	2·02	
0	1,948	1,540	16·6	112·8	62·6	96·2	46·0	2·09	0·0050
	1,918	1,515	17·0	120·4	67·2	103·4	50·2	2·06	
1,500	1,837	1,482	15·5	122·7	69·2	107·2	53·7	2·00	0·0048
	1,848	1,490	15·3	122·2	68·7	106·9	53·4	2·00	
0	1,918	1,515	17·0	120·4	67·2	103·4	50·2	2·06	0·0050
1,800	1,818	1,455	14·6	169	93	154	78	1·97	0·0048
	1,842	1,500	14·5	172	95	157	80	1·96	
	1,856	1,482	15·0	175	95	160	80	2·00	
0	1,933	1,537	17·6	160·6	87·1	143·0	69·5	2·06	0·0050
	1,942	1,522	17·2	169·6	90·8	152·4	73·6	2·07	
	1,945	1,525	17·0	185·8	100·1	168·8	83·1	2·03	0·0049
	1,942	1,522	16·9	184·2	99·4	167·3	82·5	2·03	

THE VARIATION OF ENGINE POWER WITH HEIGHT.

By D. H. Pinsent and H. A. Renwick.

Presented by the Superintendent, Royal Aircraft Establishment.

Reports and Memoranda, No. 462. *March,* 1918.

Summary.—(a) *Introductory (reasons for inquiry).*—In a previous report (I.C.E. 168) to the Engine Sub-Committee, the manner in which engine-power decreases with height was deduced from tests on the R.A.F. 4D engine and the 170 h.p. high compression Hispano-Suiza. These tests were incomplete in that they included no considerable range of temperature at any given height, and the conclusions deduced from them appear now to be erroneous. In the present report the experiments were extended over a very considerable range of temperature, and three more types of engine were tested.

(b) *Range of the investigation.*—The following engines were tested :—

The R.A.F. 4D (200 h.p. aluminium cylinder, air-cooled, V).
The 250 h.p. Rolls-Royce (water-cooled).
The 170 h.p. high compression Hispano-Suiza (ungeared, water-cooled).
The 150 h.p. ungeared Hispano-Suiza (water-cooled).
The R.A.F. 1A engine (100 h.p., air-cooled, V).

The variation of power was measured by observing the revolutions of the engine over a range of air speeds from 50 to 100 m.p.h., with the throttle full open. Flights were made on several different days with each engine, and the temperature was varied over the largest possible range which was obtainable.

(c) *Conclusions.*—The experiments indicate in all cases that the b.h.p. can be better expressed as a function of the barometric pressure only, instead of the previous and customary method where it was assumed to be a function of density. That is to say, the power developed, at given revolutions and at a given height on the aneroid, is constant and independent of the air temperature at that height.

A possible explanation of the reason why the power should be independent of temperature is suggested.

(d) *Applications and further developments.*—The above conclusion makes it necessary to reconsider the methods at present in use of reducing climbs and speeds at heights to a standard basis for comparison. It has been customary hitherto in comparing the performances of two machines, as regards speed, to compare their true air speeds at the same density ; and as regards climb, to compare their times to climb from one given density to another. If the engine power can be better expressed as a function of pressure only, this method of comparison is unduly favourable to machines tested in warm weather, and *vice versa.* A new standard method of comparison, based on the assumption that engine power is a function of pressure only, is suggested in this report.

In illustration of the method, four climbs are compared in the new way. It is found that two climbs with the same machine which do not agree when reduced by the old method, agree remarkably well when compared by the new method.

1. *Method of Experiment and Reduction of Observations.*—The experiments are based on the use of a propeller as a torque dynamometer. The method of experiment was to take simultaneous observations of engine revolutions, indicated air speed, height, and temperature, with the throttle fully open, and the compensator adjusted so as to give the maximum revolutions. Such readings were taken, as a rule, at 3,000 ft., at 6,000 ft., at 9,000 ft., and at 12,000 ft., and also as near to the ground as possible. The observations were made at air speeds varying from 50 to 100 m.p.h., observations being made over the whole of this range at each height. The experiments were repeated on different days so as to obtain the greatest possible range of temperature at each height. In this way a temperature variation of as much as 20°C. at each height was sometimes obtained.

2. Generally speaking, the method of reducing the experiments was as follows :—The revolutions at which the engine can turn the propeller at a given density and advance per revolution are a measure of the power developed, and a comparison of revolutions under two different conditions of height and temperature will give the ratio of the powers developed under these two conditions.* Thus, the experiments give in the first instance the ratio :—

$$\frac{\text{Horse power developed at various heights and temperatures.}}{\text{Horse power developed at about 1,000 ft.}}$$

(1,000 ft. being the lowest height at which observations of revolutions could be taken).

This direct method of calculation is, however, very inconvenient in practice. From the revolutions N_1 and N_2 at the same advance/revolution, at two different conditions of height and temperature, it is easy to calculate the ratio of the power developed on these two occasions, but this will be a ratio of powers developed at two different revolutions, namely N_1 and N_2, and will not therefore give the law of variation with height. In practice therefore the following method has been used, which is in principle the same. A law of variation of power with height and temperature is found by trial and error ; from it and from the test bed power curve of the engine, and from the observations at 1,000 ft., a curve of torque $/\sigma N^2$ is deduced for the airscrew ; from this curve and from the observations at greater heights the power developed at these greater heights is in turn deduced, and the original law must be so chosen that these powers deduced at greater heights agree with it.

* For a propeller, HP = (density) × (r.p.m.)^3 × (some function of the advance per revolution).

Alternatively the following method, which amounts to the same thing, may be used. The law of variation must be so chosen that the torque $/\sigma N^2$ values deduced from it, for all heights and temperatures, give the same curve. This method is simpler than the former one, but by the former one the law of variation can be determined considerably more accurately.

3. Since the power may depend on any two of the three interdependent quantities, pressure, density and temperature, it is obvious that the law of variation cannot be ascertained unless experiments are carried out over a range of temperature at each barometric height, and this range should be as large as possible. Unless this is done, it is possible to obtain quite consistent results by assuming a wrong law of variation of power.

4. The method of experiment here used assumes only that the characteristics of the propeller do not change during test, *i.e.*, that the shape of the propeller does not alter. It does not assume any particular calibration, but simply that the calibration does not alter during test.

It has been suggested that the principal conclusion of this report, namely, that engine power varies with pressure only and not with density, may be explained by propeller distortion. The chief evidence against this suggestion is that in order to explain the conclusions of this report by propeller distortion it is necessary to assume that 10 very different propellers on 5 different aeroplanes have distorted in the same somewhat complicated way, so as to convert the density into the pressure law. It is, however, proposed to conduct experiments on variation of power during which the angle at a few points on the blade will be measured optically in flight. If there is any change of shape it will be due to (*a*) warp due to atmospheric conditions, (*b*) strain due to load variation with density. Experiments are therefore in hand to determine the effect of reduced temperature (to — 20°C.) on a propeller, the boss also being heated with boiling water.* This propeller is the one which will be used to determine the variation of power with height on the B.R. 1 engine, and it will also be tested on the whirling arm at different loads at the same advance per revolution.

5. *Tests with the R.A.F.* 4D *Engine.*—The results are plotted of observations taken on six different flights on an R.E. 8, fitted with this engine. Two trial assumptions are made in order to get a $Q/\sigma N^2$ curve from the lowest observations, namely :—

(*a*) That power varies as $\sigma^{1.0}$.

(*b*) That power varies as $p^{1.0}$.

* *Note* (*June*, 1918).—Experiments have been carried out on these lines, and the warp due to a reduction of temperature from + 20° to — 15° did not exceed $\frac{1}{10}$°.

The two $Q/\sigma N^2$ curves deduced are shown in Fig. 1. In Fig. 2 are plotted the values of (power at heights)/(power on test bed), deduced from the $Q/\sigma N^2$ curve derived from assumption (*a*) and from the observations at greater heights. Each point here plotted represents the mean value of $\frac{\text{power at height}}{\text{power on test bed}}$ deduced from observations over the whole range of air speeds, and is plotted against σ, the mean percentage density for these observations. It is seen that there are consistent differences with temperature, the points at low temperatures lying consistently high. The original assumption—that $\frac{\text{power at height}}{\text{power on test bed}} = \sigma^{1.0}$—is therefore not verified, for it should give the same curve for $\frac{\text{power at height}}{\text{power on test bed}}$ against σ for all temperatures.

6. In Fig. 3 are plotted the mean values of $\frac{\text{power at height}}{\text{power on test bed}}$ deduced from assumption (*b*), from the observations at greater heights; this is here plotted against p, the percentage pressure, and it is seen that there are no consistent differences with temperature, the points at all temperatures lying on the same mean curve. This mean curve is approximately $\frac{\text{power at height}}{\text{power on test bed}} = p^{0.95}$, and is therefore a good verification of the original assumption $\frac{\text{power at height}}{\text{power on test bed}} = p^{1.0}$. It follows that, for the R.A.F. 4D engine, the power at heights varies approximately as (percentage pressure)$^{0.95}$.

7. *Tests with the High Compression Hispano Engine.*—The data used here consists of observations made on tests of an S.E. 5A machine with six different airscrews, in order to compare their efficiencies. These tests consisted of "partial climbs" at air speeds ranging from 50 to 100 m.p.h., carried out in general from 4,000 to 5,000 feet, from 9,000 to 10,000 feet, from 14,000 to 15,000 feet. The necessary observations of height, temperature, air speed, and revolutions were made in all cases. The observations at 4–5,000 ft. with each of the six different airscrews were used, on a trial assumption that power varies as $p^{1.0}$, to obtain a $Q/\sigma N^2$ curve for each airscrew. These curves are plotted in Fig. 4. In Fig. 5 are plotted the mean values of $\frac{\text{power at height}}{\text{power on test bed}}$ deduced from these curves and from the observations at greater heights, the values being plotted against percentage pressure p. It is seen that the points show no consistent differences with temperature, and lie on a mean curve representing approximately $\frac{\text{power at height}}{\text{power on test bed}} = p^{1.05}$. The original assumption that it $= p^{1.0}$ is therefore very approximately verified. It follows

that the power of the high compression Hispano engine varies approximately as (percentage pressure)$^{1.05}$—or slightly worse than the R.A.F. 4D.

8. *Tests with the* 150 *h.p. Ungeared Hispano Engine.*—Three flights were made on an S.E. 5 fitted with this engine, and observations taken at 3,000 ft., 6,000 ft., 9,000 ft., and 12,000 ft. The three sets of observations at 3,000 ft. were used on a trial hypothesis that power varies as $p^{1.0}$ to obtain a $Q/\sigma N^2$ curve for the airscrew. This curve is plotted in Fig. 6. In Fig. 7 are plotted the mean values of $\frac{\text{power at height}}{\text{power on test bed}}$ deduced from this curve and from the observations at greater heights—the values being plotted against p. It is seen that the points show no consistent differences with temperature, and lie on a mean curve representing approximately $\frac{\text{power at height}}{\text{power on test bed}} = p^{1.04}$. Thus the original assumption that it $= p^{1.0}$ is very approximately verified, and it follows that the power of the 150 h.p. Hispano engine varies approximately as (percentage pressure)$^{1.04}$—almost exactly the same figure as that obtained for the high compression engine.

9. The same conclusion is more forcibly illustrated in Fig. 8. Here are plotted groups of $Q/\sigma N^2$ curves, each group being deduced from the three sets of observations at a given height. Each group is shown as deduced on two trial assumptions :—

(*a*) That power varies as $p^{1.04}$;
(*b*) That power varies as $\sigma^{1.40}$

($\sigma^{1.4}$ being the density law which gave the least inconsistent results). It is seen at once that for each separate group the curves deduced on the $p^{1.04}$ assumption agree amongst themselves, whereas those deduced on the $\sigma^{1.40}$ assumption show consistent differences with temperature. Also it is seen that all four groups, deduced on the $p^{1.04}$ assumption, are the same $Q/\sigma N^2$ curve. (The curves are plotted with different zeros to avoid confusion.)

10. *Tests with the* 250 *h.p. Rolls-Royce Engine.*—Three flights were made on an F.E. 2D fitted with this engine. Observations were taken at 3,000 ft., 6,000 ft., and 9,000 ft. The results are plotted in Fig. 9—the method by plotting groups of $Q/\sigma N^2$ curves being adopted. The curves are plotted on the two trial assumptions :—

(*a*) That power varies as $p^{1.0}$;

(*b*) That power varies as $\sigma^{1.2}$.

($\sigma^{1.2}$ being the density law which gave the least inconsistent results). It is seen at once that the curves deduced on the $\sigma^{1.2}$ assumption show consistent differences with temperature,

whereas those deduced on the $p^{1.0}$ assumption are all the same curve. It follows that the power of the Rolls-Royce engine varies approximately as $p^{1.0}$.

11. *Tests with the R.A.F.* 1A *Engine.*—The evidence in this case is taken from a large number of "partial" climbs carried out, in the course of tests of two different wing sections, on B.E. 2c No. 1769. These partial climbs consist of two large groups —the one group carried out in very warm weather (Summer, 1917) and the other group in much colder weather (Autumn, 1917). The same engine and airscrew were fitted to the machine on both occasions.

12. The airscrew fitted was to Drawing No. T.7448. The $Q/\sigma N^2$ curve for this airscrew is independently known, an airscrew of this type having been tested on the whirling arm. In Fig. 10 are plotted the values of $Q/\sigma N^2$, deduced from the observations taken on the two sets of partial climbs, and also the curve given by the whirling arm tests. It is seen that, when reduced on the assumption that power varies as $p^{1.0}$, the points deduced from the observations on both sets of partial climbs are in agreement with the whirling arm curve, but that when reduced on the assumption that power varies as $\sigma^{1.1}$ (the law hitherto assumed), though the points deduced from the Summer observations agree with the whirling arm, those deduced from the Autumn observations do not. It is probable therefore that the power of the R.A.F. 1A engine varies approximately as $p^{1.0}$.

13. *Possible theoretical explanations.*—Mechanical losses. It has been suggested that the fact that engine power at height varies with pressure and not with density might be accounted for by mechanical losses. This may be disproved as follows :—

Assume that the I.H.P. $= f(p, t)$, some function of pressure and temperature. The mechanical losses will consist of a constant part, and a part which varies as the I.H.P. Hence b.h.p. $= Af(p, t) - B$ where A and B are constants, from which it follows that if the b.h.p. is sensibly independent of temperature so also is the I.H.P., and conversely.

14. *Suggested explanation.*—The following theoretical explanation of the existence of a pressure, as opposed to a density law, is suggested. The I.H.P. is directly proportional to the density of the charge in the cylinder, which is therefore the sole factor determining the power at heights. But it is probable that the temperature of the charge just before the inlet valve is closed will be substantially the same, whatever the atmospheric temperature may be. It follows that the density of the charge, and therefore also the I.H.P., will vary directly as the atmospheric pressure. Thus the law I.H.P. $\propto$ density of charge just before the inlet valve closes is exactly equivalent to the law I.H.P. $\propto$ atmospheric pressure.

The B.H.P. is equal to I.H.P. less mechanical loss, and will therefore be practically proportional to (pressure)$^{1\cdot0}$, if the constant part of the mechanical losses (*i.e.*, independent of I.H.P.) is small; the effect of the constant part is to make the b.h.p. vary somewhat more rapidly than the pressure. Thus the above theory would account for the differences in pressure law which were observed with different engines, *e.g.*, with the Hispanos and the R.A.F.4.D.

15. There is considerable evidence that the absolute temperature of the charge just before the closing of the inlet valve, if not constant at all outside temperatures, is at any rate so high that its *percentage* variations, and therefore the resultant variations of percentage density, are small. Firstly, there is evidence that the charge when it reaches the cylinder and before the inlet valve is closed, has assumed an increased temperature, comparable with that of the cylinder walls, piston head and exhaust valves. This is given in a paper by Coker and Scoble (Proc. Inst. C.E. 1913–14) in which the following temperatures were measured on a 12 H.P. slow running gas engine :—

Temperature of the charge at end of suction stroke—over 200°C.

Exhaust valves—about 400°C.

Centre of piston—about 340°C.

In an aeroplane engine the temperature of the exhaust valves is about 700° C. and that of the piston top about 500°C., and it is probable, therefore, that the temperature of the charge just before the closing of the inlet valves is at least of the order 300°C. If this is so, small variations due to variations in atmospheric temperature outside, will have a very small effect upon the percentage density, and thus upon the I.H.P.

16. *High altitude test house experiments.*—This argument is confirmed by the experiments on the test bed described in Report No. I.C.E. 196. In this case an increase of 19 per cent. in the absolute temperature of the outside air produced a decrease in B.H.P. of only 5·7 per cent.—or less than one-third. These experiments were made at temperatures above + 3°C.; it is possible that at lower temperatures, such as are encountered in flight, any small increase in I.H.P. due to decrease of temperature is counterbalanced by incomplete vaporisation in the carburettor.

17. These experiments indicate that the pressure law is much more nearly true than the density law. The maximum temperature range for any one pressure in the experiments in flight described above was 20°C. The corresponding variation in power from test bed experiments would be only 2 per cent., which would be hardly measurable, whereas the variation according to the $\rho^{1\cdot0}$ law would be 7 per cent., an error of 5 per cent. which is quite appreciable. The experiments are therefore in sufficiently

close agreement, and the variation of b.h.p. with pressure independently of temperature may be assumed up to at least 15,000 ft., but the density law is demonstrated to be seriously in error.

18. *Reduction of performances to a standard basis for comparison.*—It appears therefore that the power at heights of internal combustion engines is a function of pressure only, and not, as has hitherto been supposed, a function also of temperature. It has been assumed hitherto that the engine power at heights is some function of the density, and if this were the case the same machine should do the same performance in speed and maximum rate of climb at the same density, even though on two different days this corresponded to two entirely different heights and temperatures. It has been customary therefore, when comparing the performances of two different machines, to compare their speeds and rates of climb at some given density. If, however, the engine power is a function of pressure only, it is clear that this method of comparison is unfair on machines tested in cold weather, and *vice versa*; for if the two machines were tested at the same density, the machine tested in cold weather has been tested at a greater height (*i.e.*, at lower pressure) than the machine tested in warmer weather.

19. It will be shown (*see* Appendix II) that the fair method of comparison, on the assumption that engine power is some function of pressure only, is as follows :—

(*a*) To compare speeds at heights. It is only necessary to compare the indicated air speeds, uncorrected for density, at the same height on the aneroid, *i.e.*, the same pressure. Or if it is required to compare true speeds, the indicated air speed at a given height on the aneroid must be corrected for density always by means of the same density factor, that is to say by the factor $\frac{1}{\sigma^{\frac{1}{2}}}$ where σ is the standard density at that height.

(*b*) To compare rates of climb. The rates of climb should be compared at the same height on the aneroid, after being corrected by the factor $\left(\frac{\sigma}{\sigma_o}\right)^{\frac{1}{2}}$ where σ was the actual density observed at that height, and σ_o is the standard density at that height. (In general, this factor is so nearly $= 1$ as to be negligible.) If it is desired to compare complete climbs, say, from the ground to 15,000 ft., the rates of climb in true feet per minute (*i.e.*, corrected for the temperature effect on the aneroid) must be plotted against aneroid height (or pressure), and then corrected by the factor $\left(\frac{\sigma}{\sigma_o}\right)^{\frac{1}{2}}$, and the climbs from any one pressure to any other may then be reconstructed and compared.

20. In Figs. 11 and 12 are shown examples of climbs reduced by the above methods, based upon a pressure law for engine power and also by the methods hitherto in use which are based upon a density law. Fig. 11 shows two climbs to 15,000 ft. on S.E. 5A No. C/1091, fitted with the Wolseley " Viper " engine, carried out at the R.A.F. on 28th February, 1918, and on 6th March, 1918. On 28th February, 1918, the weather was considerably colder than on 6th March, 1918, and of the two climbs, if reduced by the old method, that of 28th February, 1918, appears considerably worse than that of 6th March, 1918, as much as six minutes longer being required for climbing to 15,000 ft. If the new method of reduction is used, however, the two climbs are practically identical.

21. Fig. 12 shows two climbs to 10,000 ft. on N.E. 1 machines, with 200 h.p. Hispano engines, carried out at the R.A.F. on 13th September, 1917, and on 15th October, 1917. The weather was considerably warmer on the former date than on the latter, and on the former date the time to 10,000 ft., using the old methods of reduction, was about two minutes less than on the latter date. If the new method of reduction is used, however, the two climbs are identical. (N.B.—The climb of 15th October, 1917, was made with 56 lbs. more weight than that of 13th September, 1917, but this has been corrected for in both methods of reduction.)

Appendix I.

ANALYSIS OF METHOD OF REDUCING EXPERIMENTS.

1. For each engine tested the test-bed power curve was approximately known, and was used in reducing the observations. It will be shown later that an error in this assumed power curve makes no difference to the results obtained. Assuming such a power curve, and assuming as a trial hypothesis that the power of the engine at a percentage pressure p, and a temperature t, is some function $f(p, t)$ of p and t, times its power at the same revolutions on the test bed, it is possible from any set of observations of height, temperature, and revolutions at various air speeds to plot a torque $/\sigma N^2$ curve for the airscrew. For if Q be the airscrew torque and N the airscrew revolutions per second, and B_N the power developed at the corresponding engine revolutions on the test bed, then $Q = \lambda \frac{B_N f(p, t)}{N}$ where λ is a constant depending on the gearing of the airscrew, and therefore $\frac{Q}{\sigma N^2} = \frac{B_N f(p, t)}{\sigma N^3} \lambda$, and this quantity can be plotted against $\frac{V}{N}$, the advance per revolution of the airscrew.

2. Conversely, if the $Q/\sigma N^2$ curve for the airscrew is known or assumed, it is possible from it and from any set of observations of height, temperature, and revolutions and air speed, to deduce the power that the engine was giving at that height and temperature; in other words, to plot a function $f(p, t)$ of p and t, so that the engine power at any height or temperature is equal to $B_N f(p, t)$.

3. In the reduction of the experiments described in this report, the method adopted has been as follows:—A functional form $f(p, t)$ has been found by trial and error, so that if a $Q/\sigma N^2$ curve for the airscrew be deduced therefrom in the manner described in para. 1, using the observations at the lowest height where observations were made, this $Q/\sigma N^2$ curve, in its turn, gives, by the method described in § 2, using the observations taken at the other greater heights, values of $f(p, t)$ identical at all heights and temperatures with those originally assumed. It is also necessary, of course, that the value of $f(p, t)$ for $p = 1$ and $t = +16°C.$ (the test bed conditions) shall be unity.

4. It will now be shown that this method is determinate, that is to say, that it gives only one solution and that the true solution. First, if from any trial assumption b.h.p. $= B_N f(p, t)$, used for the lowest observations, values of the b.h.p. for greater heights are deduced, which are entirely independent of t; then, though the original assumption containing t was wrong, the true f, when found, will be independent of t. For let the observed quantities at a given Adv./Rev., α, be:—

$p_0\ t_0\ \sigma_0\ N_0$ near the ground;
$p_1\ t_1\ \sigma_1\ N_1$ higher up.

Then the value of $Q/\sigma N^2$ for Adv./Rev. α, deduced, on the trial assumption power $= B_N f(p, t)$, from the observations near the ground, will be

$$\left[\frac{Q}{\sigma N^2}\right]_\alpha = \lambda \frac{B_{N_0} f(p_0\ t_0)}{\sigma_0 N_0^3}.$$

And the value for power at pressure p_1, and temperature t_1, deduced from the observations higher up, will then be

$$\text{Power} = \frac{1}{\lambda}\left[\frac{Q}{\sigma N^2}\right]_\alpha \sigma_1 N_1^3$$

or

$$\frac{\text{Power}}{B_{N_1}} = f(p, t) = \left[\frac{f(p_0\ t_0)}{\sigma_0}\right] \left\{\sigma_1 \frac{N_1^3 B_{N_0}}{N_0^3 B_{N_1}}\right\}, \quad - \quad - \quad (a)$$

Now, if the true power law, say power $= B_N \varphi(p, t)$, had been assumed, the expression (a) above would have differed only in having $\varphi(p_0 t_0)$ instead of $f(p_0 t_0)$—*i.e.*, in the constant ratio $\frac{\varphi(p_0 t_0)}{f(p_0 t_0)}$.

5. In the case of all the engines covered by this report it was found on some trial assumption that the b.h.p. deduced from the observations at the greater heights was independent of t. Hence in all cases the true solution, when found, must be a function of p only, and the method of reduction is simplified to the following form :—A function $f(p)$—of p only—is to be found by trial and error, so that if a $Q/\sigma N^2$ curve for the airscrew be deduced therefrom from the lowest observations, this $Q/\sigma N^2$ curve, in its turn, shall, from the observations at greater heights, give values of $f(p)$ identical at all heights with those originally assumed It is also necessary that $f(1)$ shall equal unity.

6. It can now be shown that there is only one reasonable solution. For suppose $f(p)$ and $\varphi(p)$ to be two solutions, then the $Q/\sigma N^2$ values obtained from the lowest observations on the φ assumption will be $\frac{\varphi(p_0)}{f(p_0)}$ times those obtained on the f assumption. Thus so also will be the values of b.h.p. deduced in their turn from the observations at greater heights. (This is proved by exactly similar reasoning to that used in § 4 above.) That is to say, $\varphi(p) = \frac{\varphi(p_0)}{f(p_0)} \times f(p)$ for the range of p corresponding to the range of the observations at greater heights, *i.e.*, in this range the two functions will be constant multiples of each other. Thus all possible solutions will be of the type plotted below :—

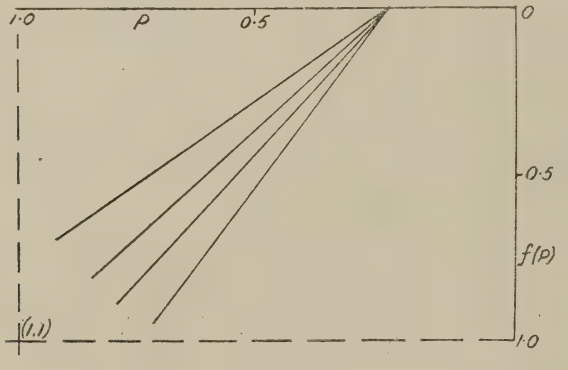

Now the true solution has to pass through the point (1, 1); and, without drawing a discontinuous distorted curve, there is only one solution which will do so. Thus there is only one reasonable solution.

7. Any solution satisfying the requirements of § 5 will clearly cover the experimental facts. In § 6 it has been shown that there is only one reasonable such solution. That solution is therefore the true one.

8. It is most important, however, if tests are made in the manner described in this report, to obtain as great as possible a range of variation of temperature at all heights. Unless this is done, the method of reduction becomes indeterminate, and there are in fact an infinity of solutions covering the facts observed. For though it is provable that there exists only one function of p covering the facts—and though it is similarly probable that there exists only one function of p and t covering the facts,

when the facts include a number of different variations of t with p—yet it is obvious that when the facts include only one variation of t with p for instance, only one flight, an infinity of functions of p and t will cover them. For let $F(p, t)$ be the true solution, and suppose the observations confined to one flight in which $t = \lambda(p)$, then there are an infinity of functions φ such that $\varphi[p, \lambda(p)] = F[p, \lambda(p)]$. For instance, let $F(p, t)$ be $= p \times t$, and let $\lambda(p) = \mu \times p$; then $F[p, \lambda(p)] = \mu p^2$, and the following $\varphi(p, t)$ will give $\varphi[p, \lambda(p)] = \mu p^2$—namely, $\varphi(pt) = \mu p^2$, or $= \frac{\mu^2 p^3}{t}$, or $= \frac{\mu^3 p^4}{t^2}$, etc.

9. In report No. I.C.E. 168 this was in fact the cause of the erroneous conclusions arrived at. The experiments here with the Hispano engine included no very great range of temperature at the same height, and with the R.A.F. 4D engine only one set of observations was made at each height. The reason why, in I.C.E. 168, it was thought that the R.A.F. 4D was so much better than the Hispano, whereas it now appears that there is not much difference between them, was as follows :—The experiments gave for both engines the ratio $\frac{\text{power at various heights}}{\text{power at the lowest height}}$ where observations were taken.

In order to express the ratio :—

$$\frac{\text{power at various heights}}{\text{power on the test bed}},$$

it was necessary to assume the ratio

$$\frac{\text{power at lowest heights where observations were made}}{\text{power on test bed}}.$$

There being insufficient data to determine this by trial and error, it was assumed that the power was some function of density, and this latter ratio was estimated on this hypothesis. Since, as a matter of fact, this ratio should have been estimated on a pressure basis, it is clear that, if estimated on a density basis, it was very much too large in cold weather, but not far wrong in warm weather. The Hispano experiments were done in very warm weather and the R.A.F. 4D experiments in cold weather, and, in consequence, the power at heights of the R.A.F. 4D was overestimated but that of the Hispano was not far wrong.

The tests upon which report No. I.C.E. 168 was founded, though they give consistent results upon a density basis when taken by themselves, are inconsistent with the later tests (upon which this report is founded) if reduced upon a density basis, but are quite consistent both taken by themselves and with the later tests if reduced upon a pressure basis.

10. An error in the assumed test bed power curve (provided the engine does not vary from day to day) makes no difference to the results obtained. Suppose the power curve assumed to be $B_N = F(N)$, and suppose that at some given Adv./Rev. the revolutions at the lowest height are N_1 and at some greater height are N_2, then the value of $Q/\sigma N^2$ for this Adv./Rev. obtained from the lowest observations is given by :—

$$[Q/\sigma N^2] = \lambda \frac{f(p_0 t_0)}{\sigma_0 N_1^3} \quad F(N_1) = \mu \frac{F(N_1)}{N_1^3} \quad \text{say.}$$

The value of $f(p, t)$ from the observations at this Adv./Rev. at greater heights is in its turn given by :—

$$f(p, t) = \frac{1}{\lambda} \sigma \frac{N_2^3}{F(N_2)} [Q/\sigma N^2]$$

i.e., by

$$f(p, t) = \frac{\mu}{\lambda} \sigma \left(\frac{N_2}{N_1}\right)^3 \cdot \frac{F(N_1)}{F(N_2)}.$$

This value will be unaffected by the form assumed for the function F, provided $\frac{F(N_1)}{F(N_2)}$ is correctly assumed. And though errors may occur in the determination of F, it is improbable that large errors will occur in the value of $\frac{F(N_1)}{F(N_2)}$, the ratio of the powers at two different revolutions, and this error is still further reduced when the mean value of $f(p, t)$ is taken of its value, deduced from all the observations (at different adv. /rev.) at a given p and t, that is to say, from the revolutions observed over the whole range of air speeds.

11. Using the method of reduction which has just been explained, two methods of presenting the results have been employed. In the one case the method has been followed exactly as detailed above, the values of $f(p, t)$ have been plotted against p, different symbols being employed for different values of t at the same p. In other cases the following method, which in principle is exactly the same, but which illustrates the results somewhat more forcibly, has been adopted. The object has been to find, by trial and error, a function $f(p, t)$, so that $f(p = 1, t = +16°\text{C.}) = 1$, and so that, from the observations at each (height and temperature) the same $Q/\sigma N^2$ curve is obtained in the manner described in § 1. If this is done, it is clear that, conversely, the conditions demanded in § 3 above will be satisfied, and the method is therefore in principle the same as the method there laid down. When this method is used it is possible to plot side by side sets of $Q/\sigma N^2$ curves, obtained by assuming two different $f(p, t)$—say $\sigma^{1.3}$ and $p^{1.0}$—and it is seen at a glance that one or the other set is by far the more consistent.

R.A.F. 4.D. ENGINE. AIRSCREW T.28093.

$Q/\sigma N^2$ CURVES DEDUCED FROM LOWEST OBSERVATIONS.

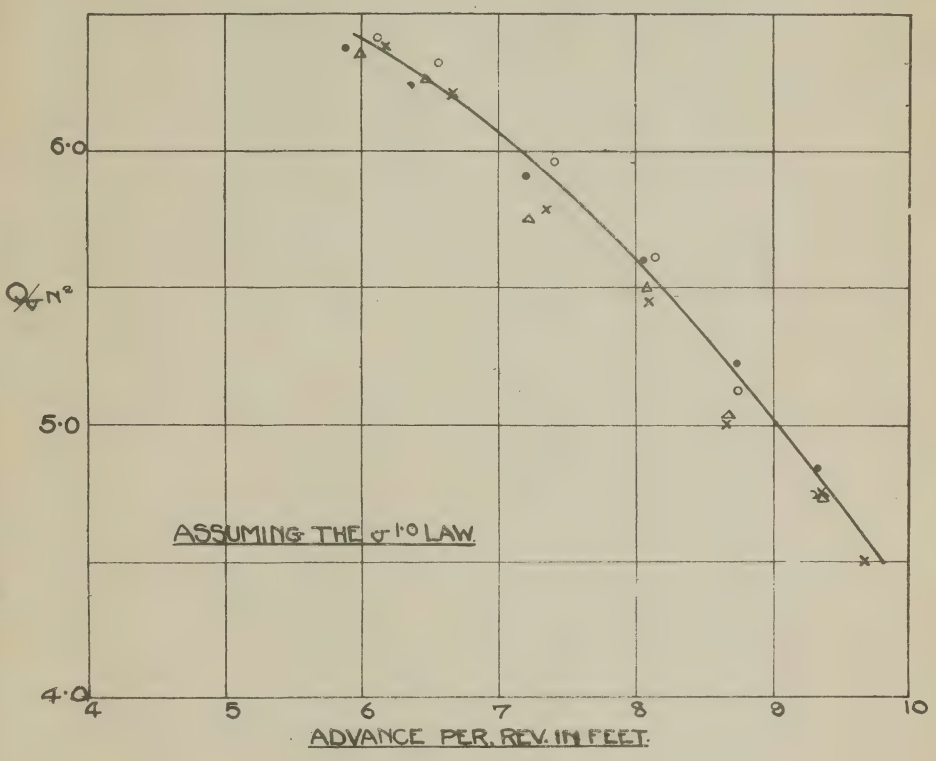

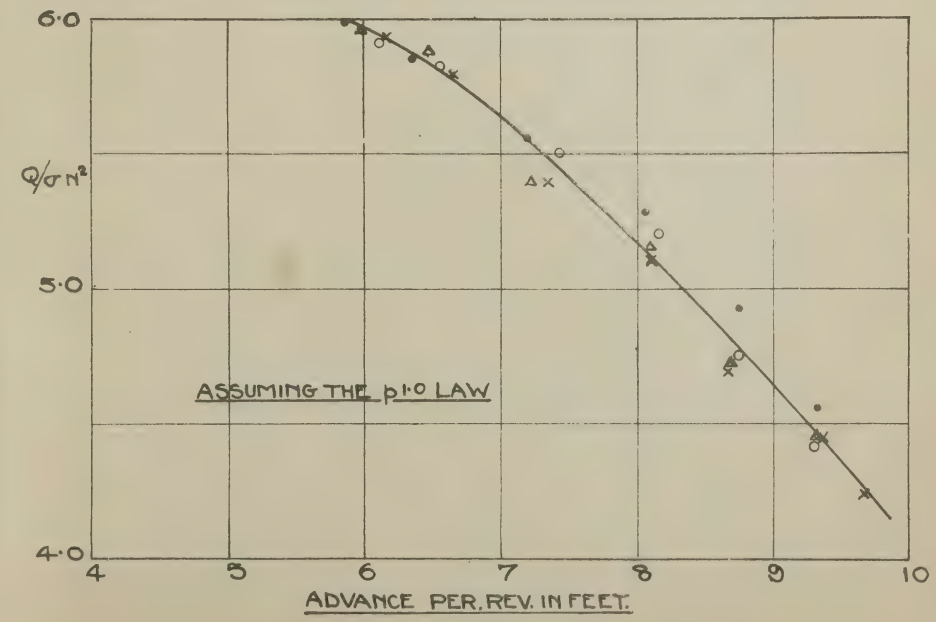

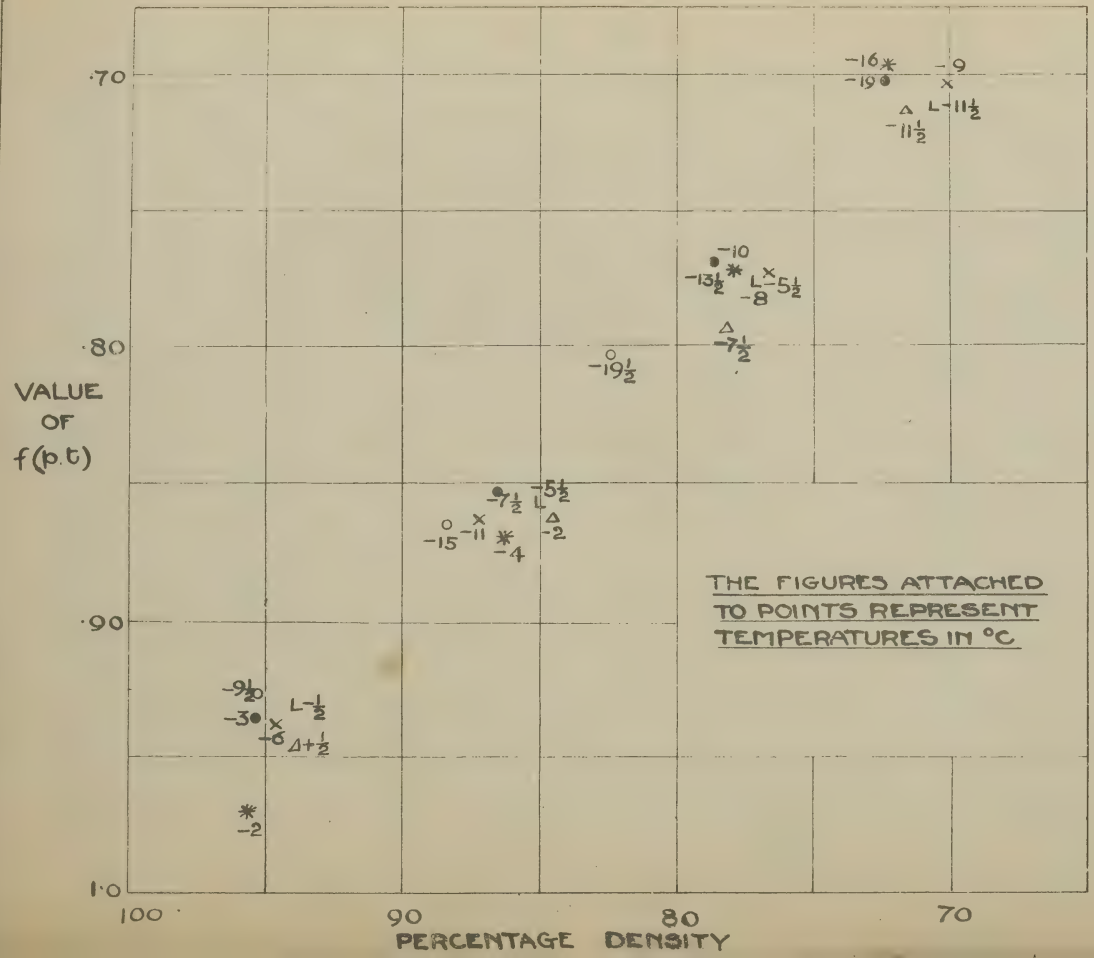

R.A.F. 4D ENGINE

REDUCTION ASSUMING A $\sigma^{1.0}$ LAW

$f(p\,t)$ IS THE RATIO OF THE POWER DEVELOPED AT PRESSURE p AND TEMPERATURE t TO THAT DEVELOPED ON THE TEST BED

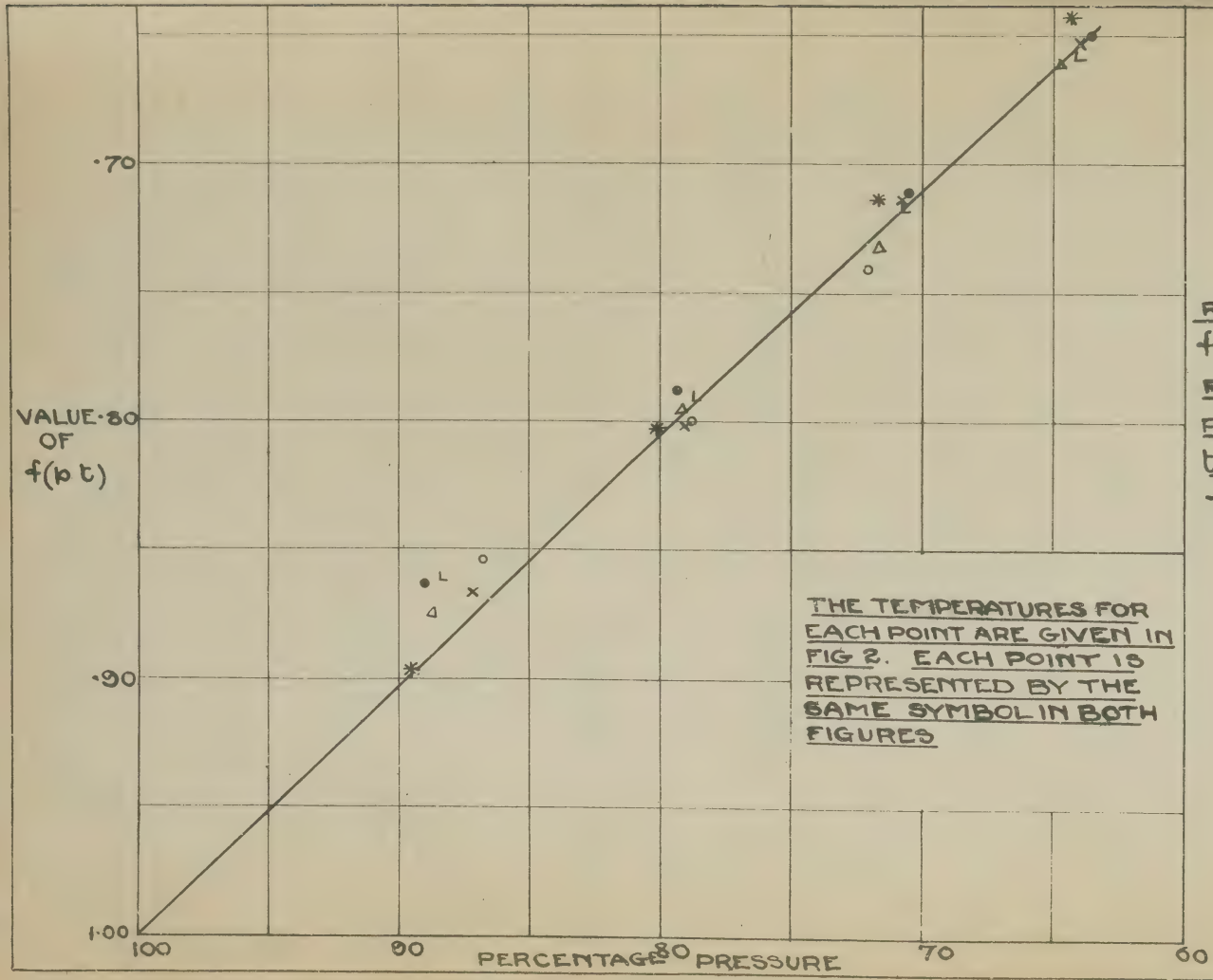

R.A.F. 4D ENGINE.

REDUCTION ASSUMING A $p^{1\cdot0}$ LAW

$f(p.t)$ IS THE RATIO OF THE POWER DEVELOPED AT PRESSURE p AND TEMPERATURE t TO THAT DEVELOPED ON THE TEST BED

THE TEMPERATURES FOR EACH POINT ARE GIVEN IN FIG 2. EACH POINT IS REPRESENTED BY THE SAME SYMBOL IN BOTH FIGURES

HIGH COMPRESSION HISPANO ENGINE

Q/N^2 CURVES

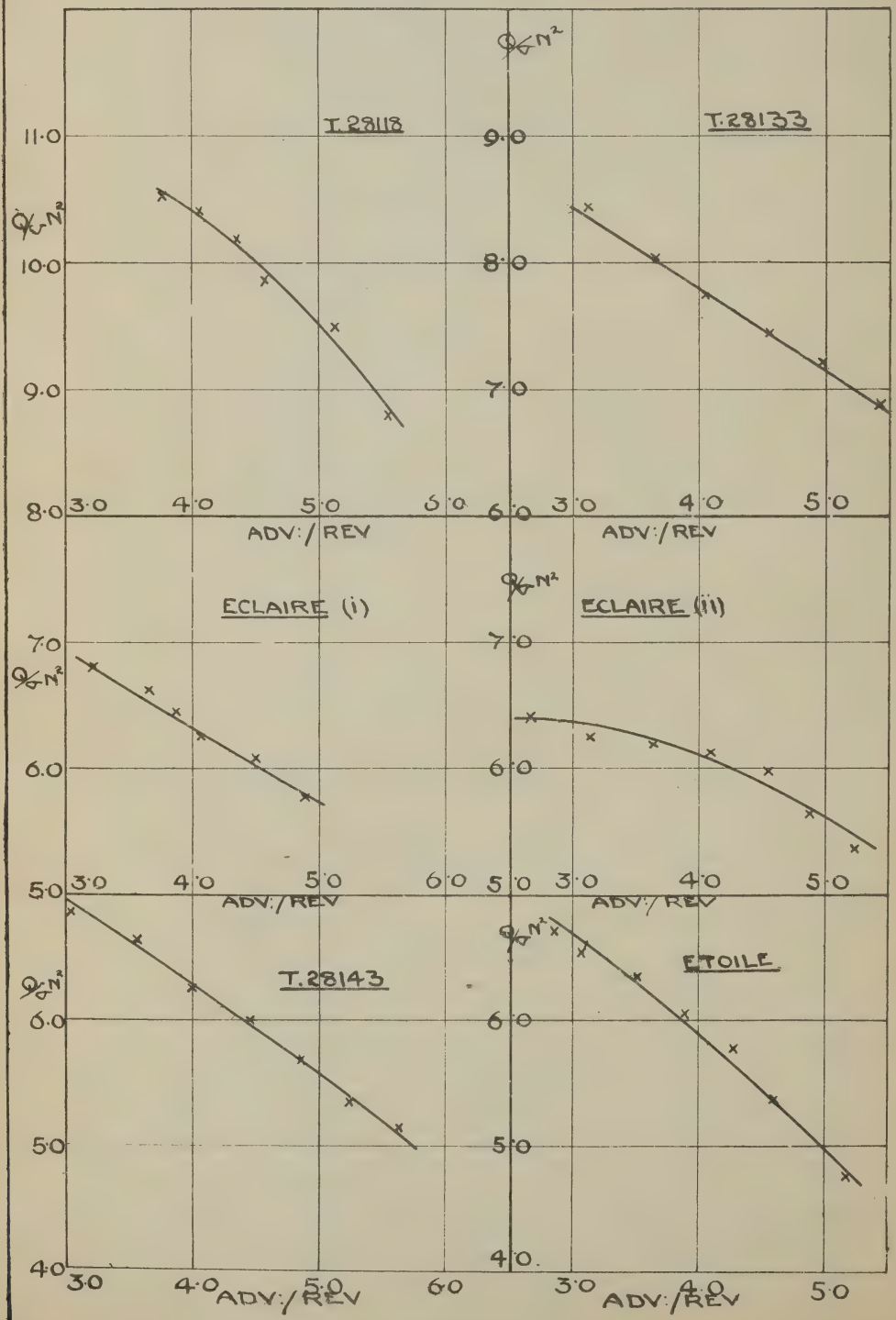

HIGH COMPRESSION HISPANO ENGINE

REDUCTION ASSUMING A $p^{1\cdot0}$ LAW

$f(p\,t)$ IS THE RATIO OF THE POWER DEVELOPED AT PRESSURE p AND TEMPERATURE t TO THAT DEVELOPED ON THE TEST BED

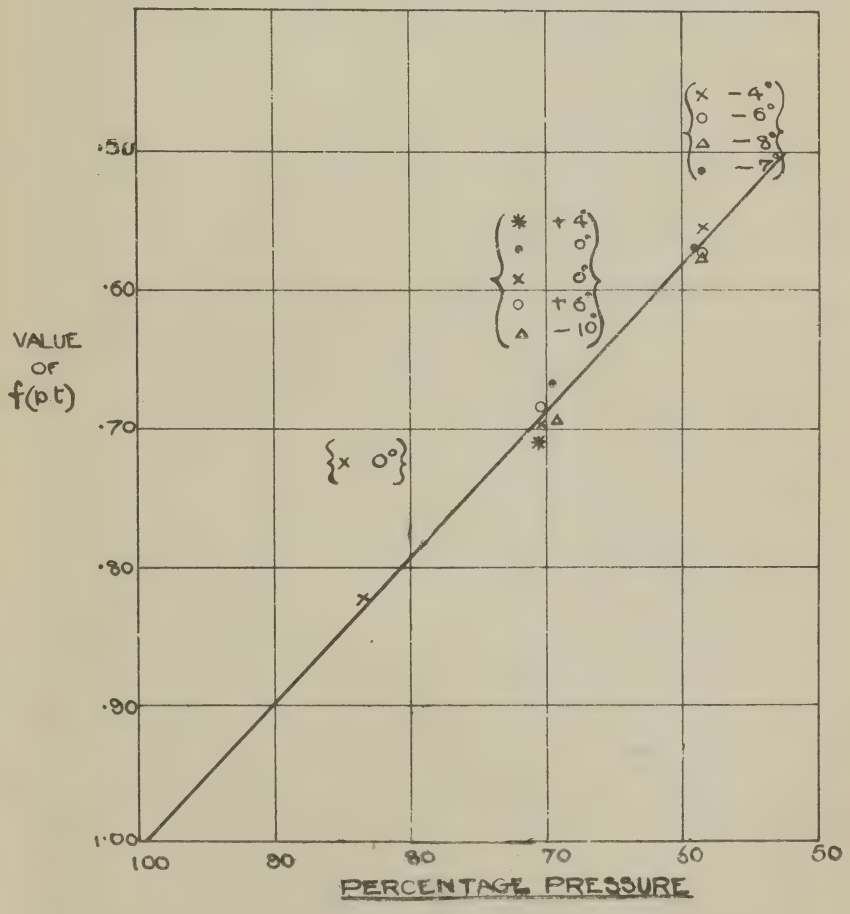

UNGEARED HISPANO ENGINE.

AIRSCREW T 28116

$Q/\sigma N^2$ CURVE DEDUCED FROM LOWEST OBSERVATIONS

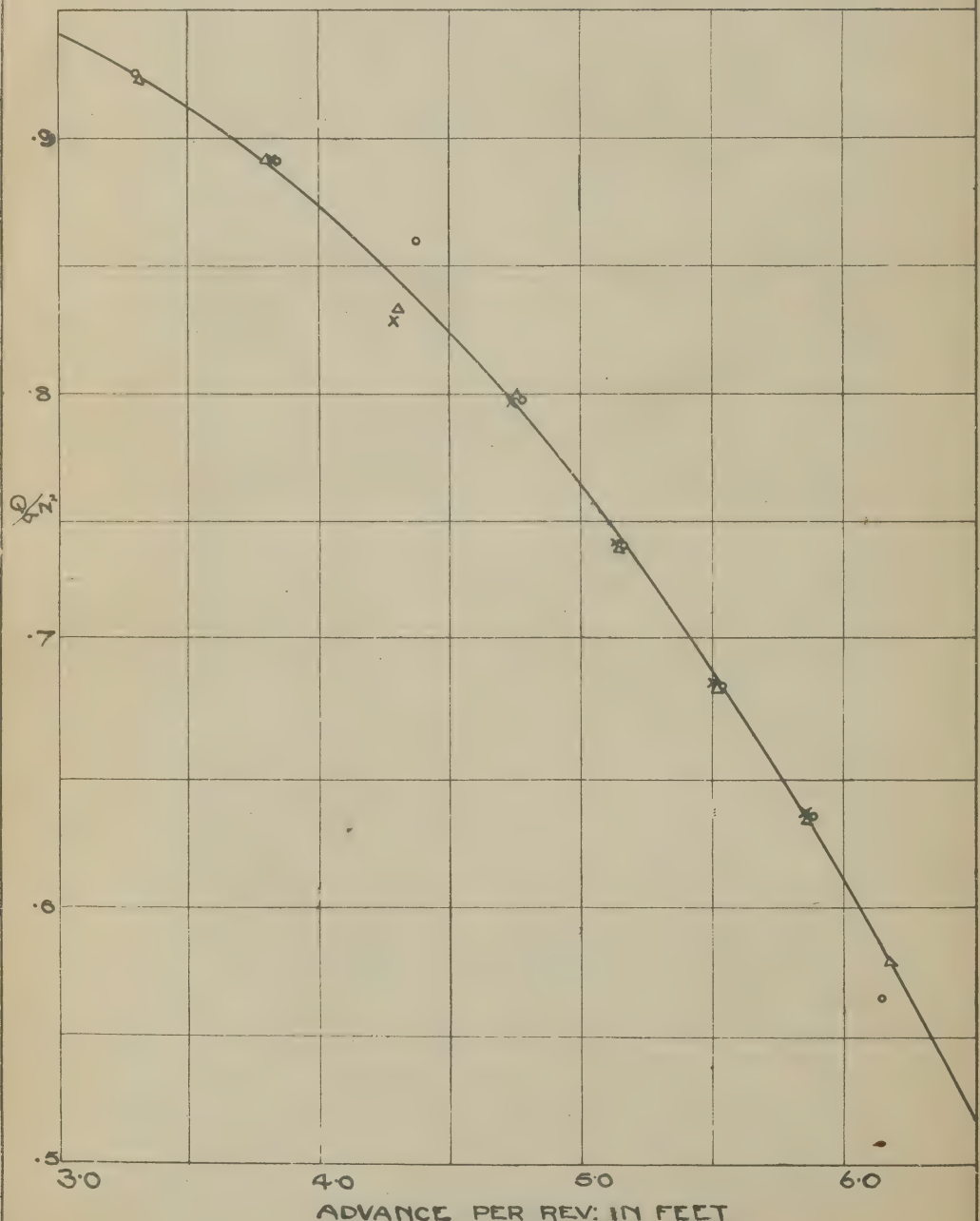

UNGEARED HISPANO ENGINE.

REDUCTION ASSUMING A $p^{1.0}$ LAW.

$f(p\,t)$ IS THE RATIO OF THE POWER DEVELOPED AT PRESSURE p AND TEMPERATURE t TO THAT DEVELOPED ON THE TEST BED

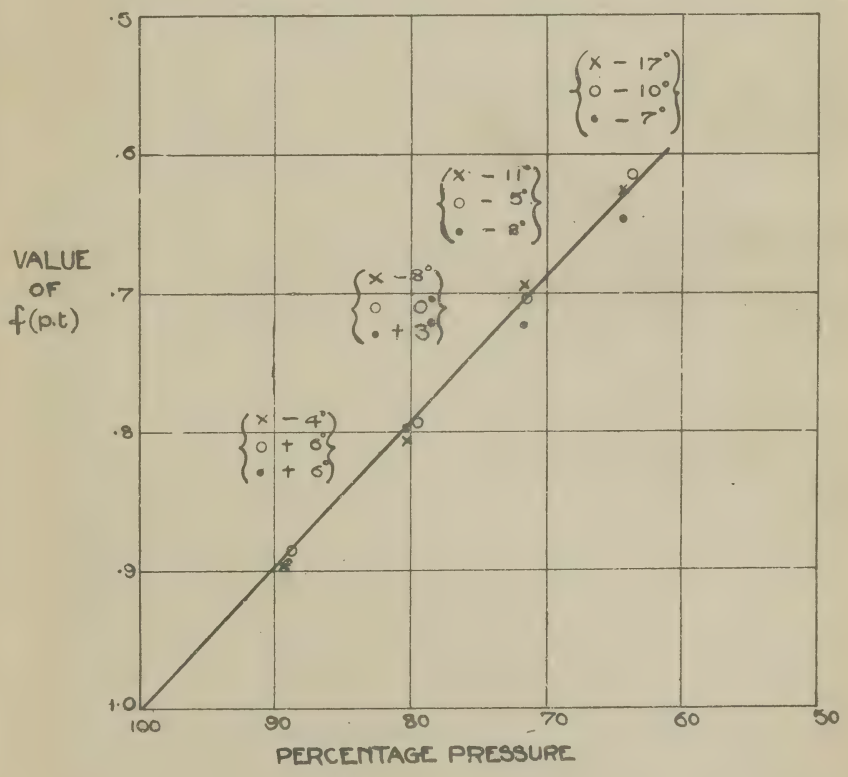

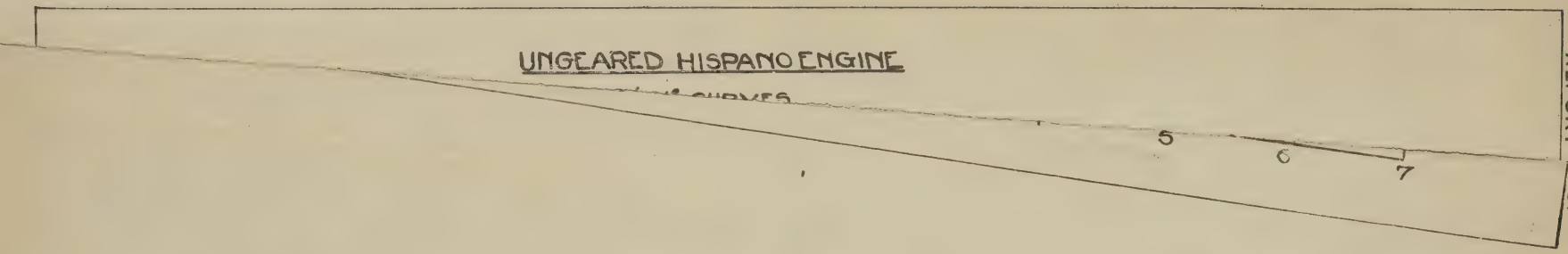
UNGEARED HISPANO ENGINE
CURVES
5
6
7

UNGEARED HISPANO ENGINE

Q/σN² CURVES

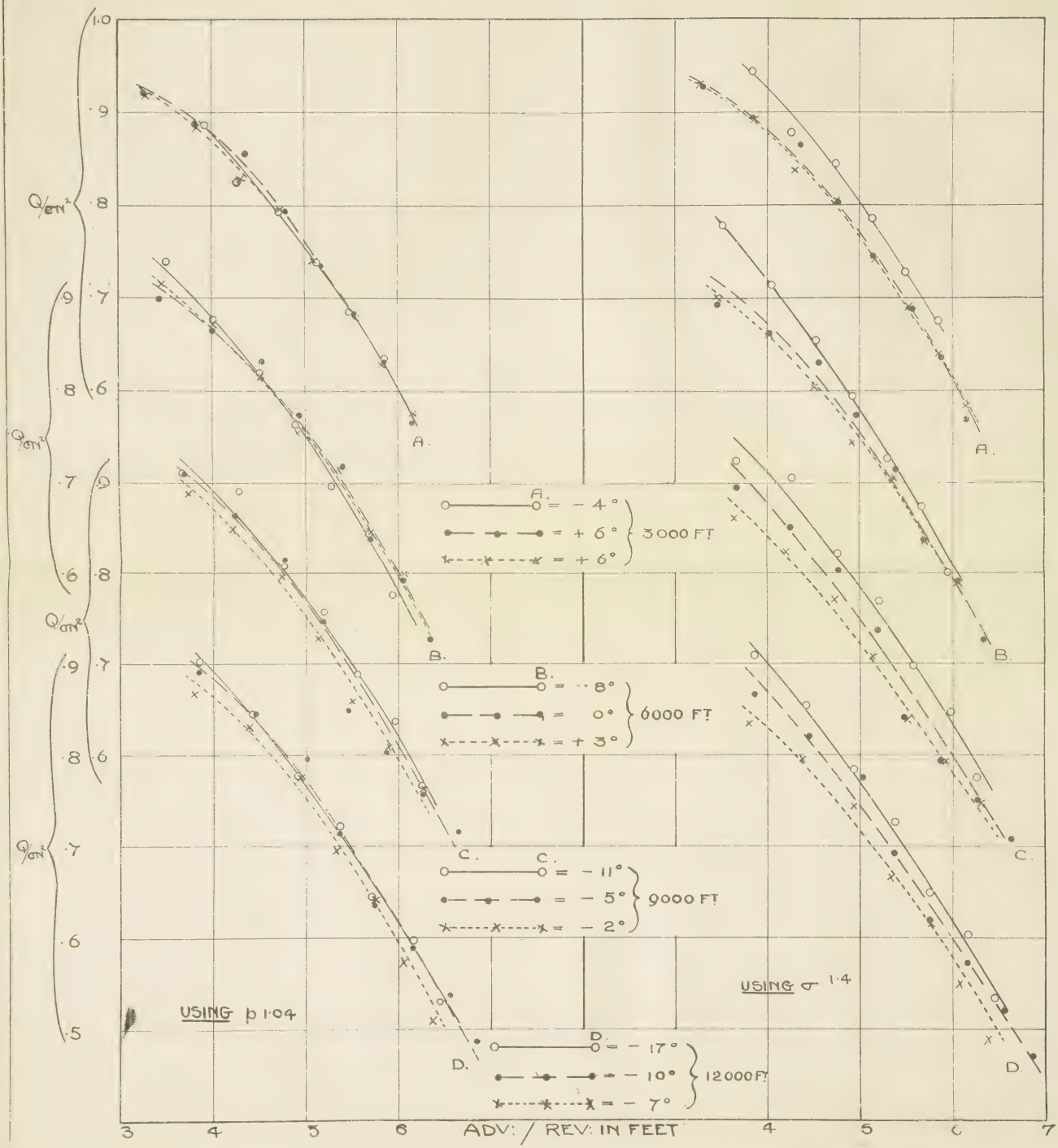

250 H.P. ROLLS ROYCE ENGINE
Q/σ N² CURVES

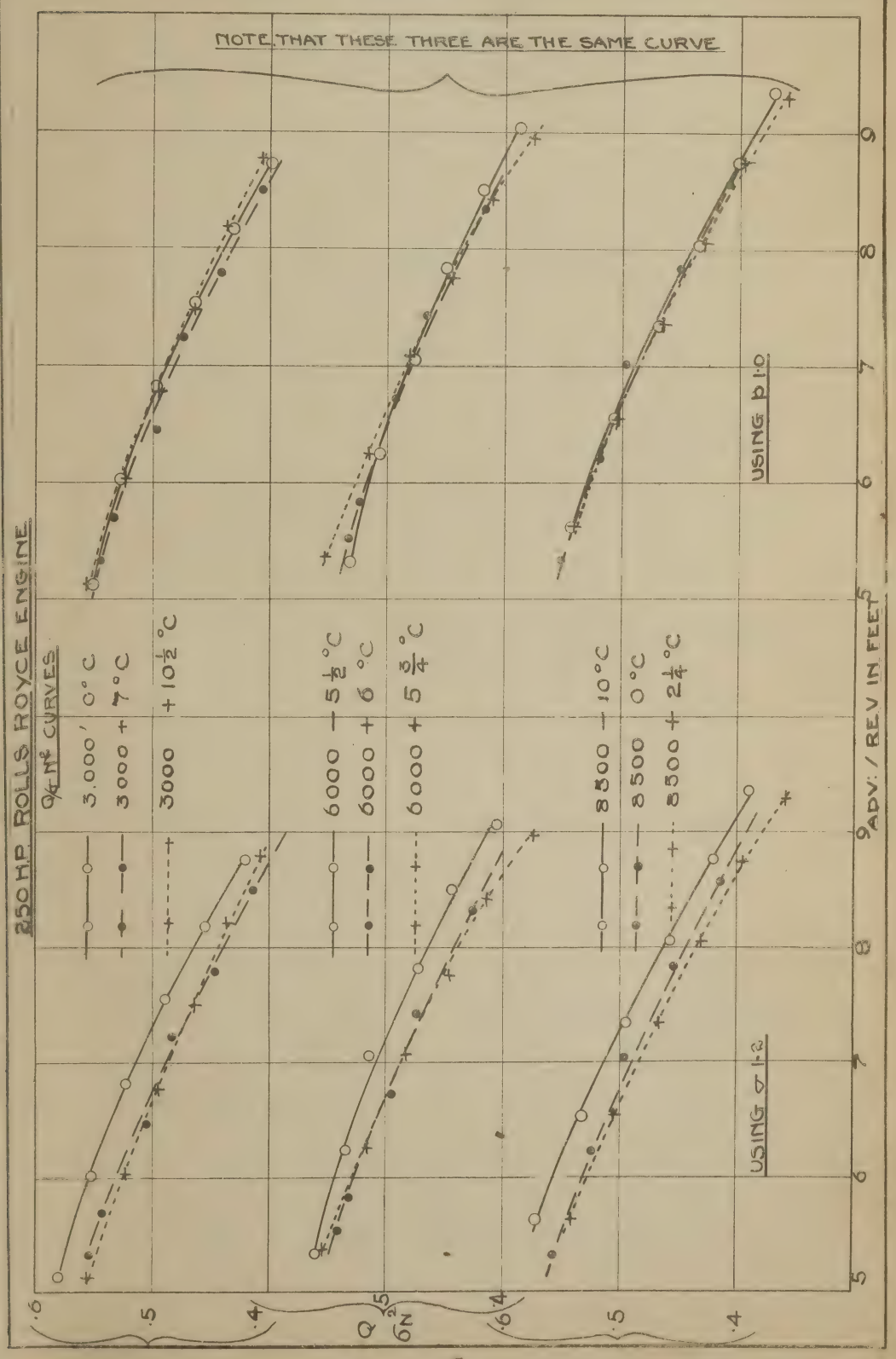

R.A.F. I.A. ENGINE AIRSCREW T.7448

$Q/\sigma N^2$ CURVES

X = EXPTS OF SUMMER 1917

O = EXPTS OF AUTUMN 1917

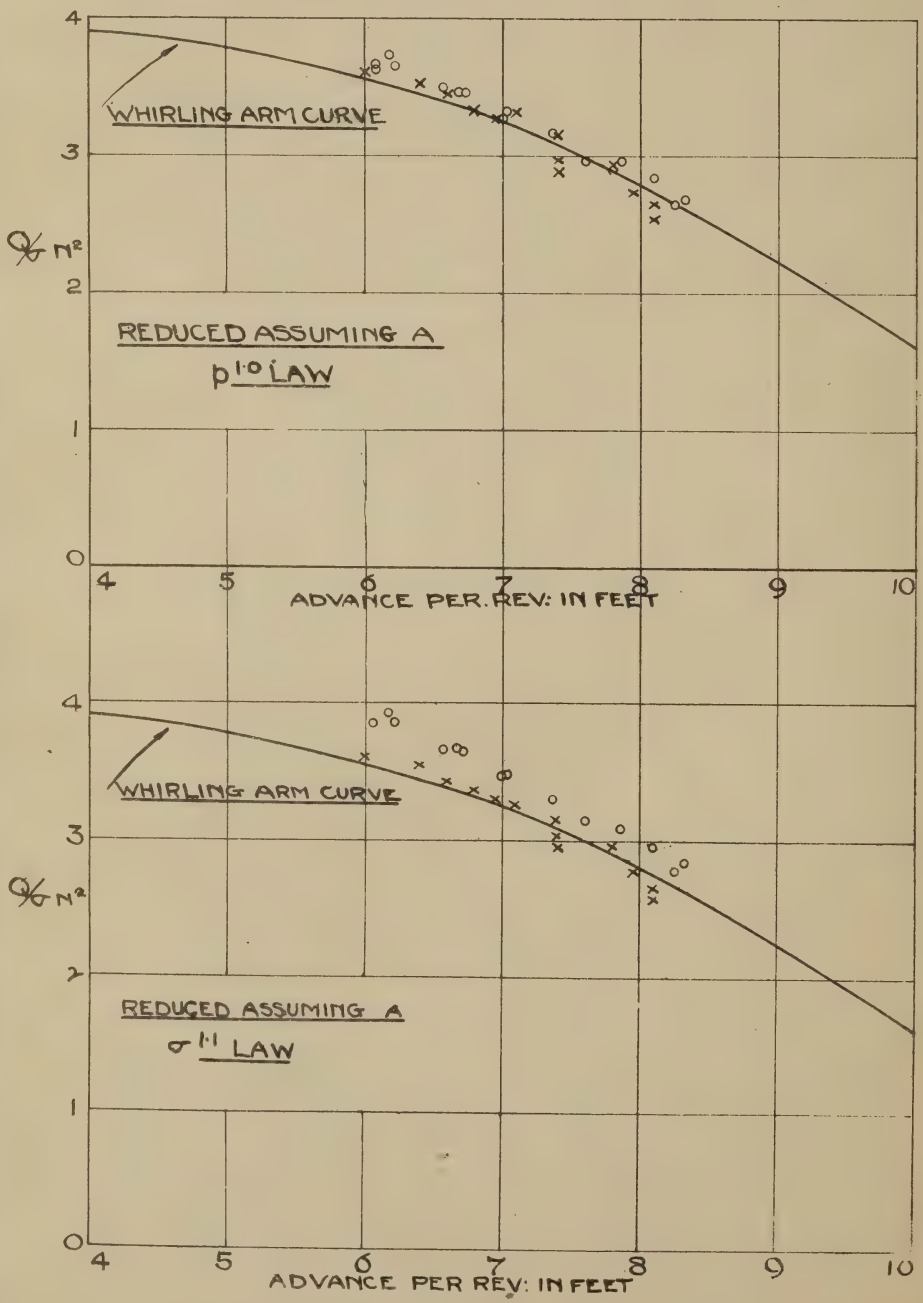

CLIMBS ON SE.5a Nº C/1091 WOLSELEY VIPER ENGINE

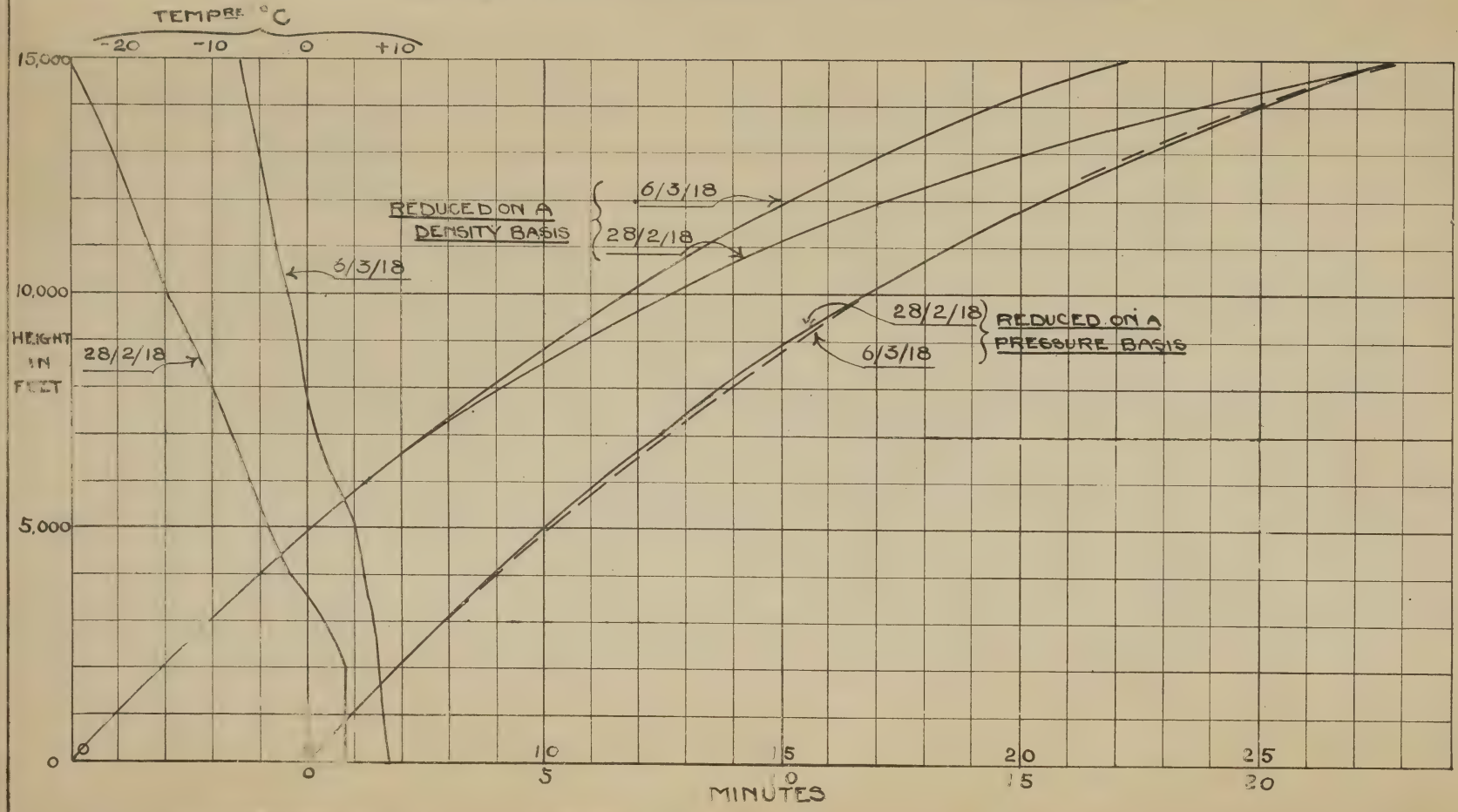

FIG 11.

CLIMBS ON N.E.1 200 HP HISPANO ENGINE

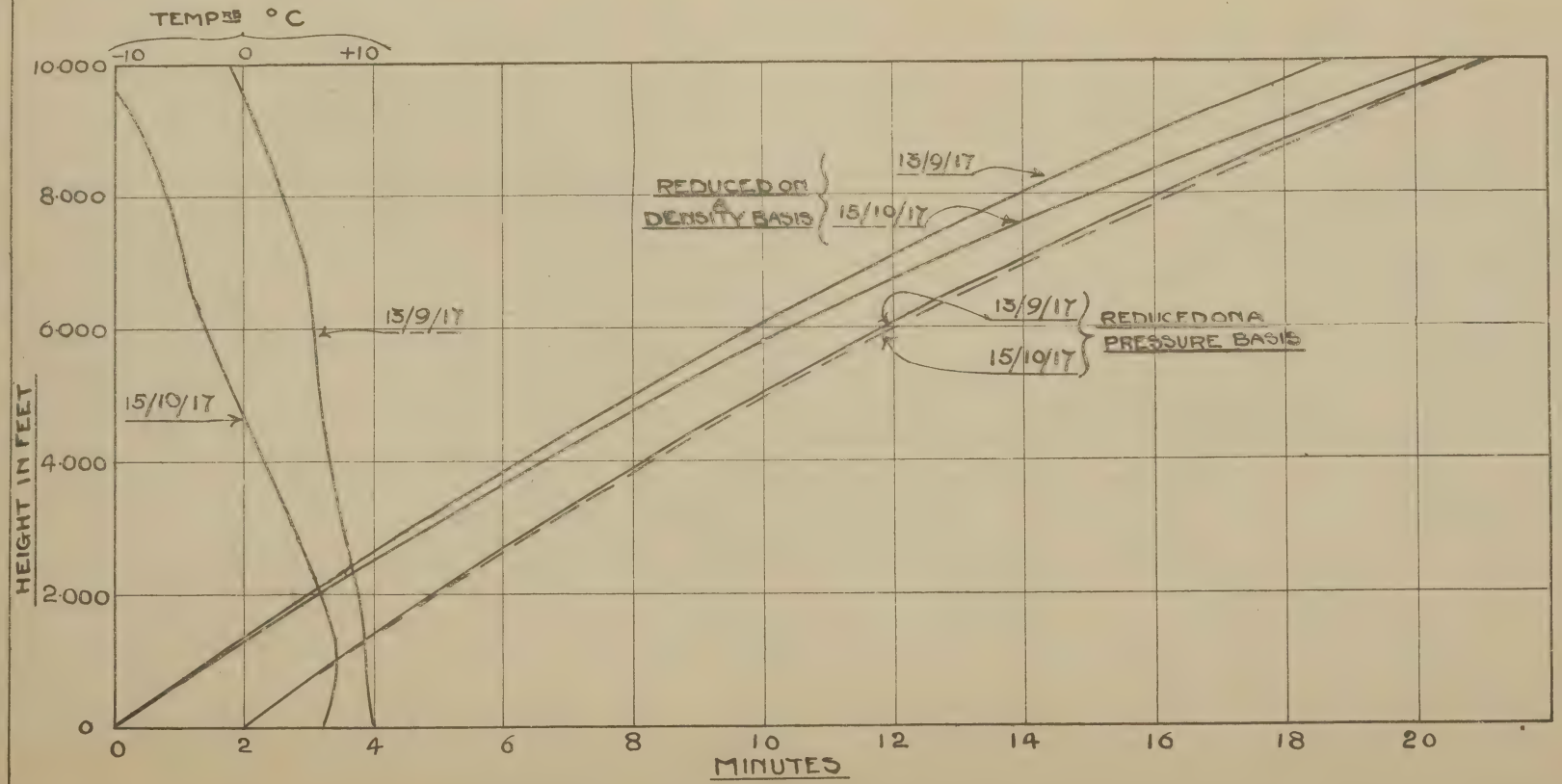

Appendix II.

REDUCTION OF PERFORMANCE TO A STANDARD BASIS FOR COMPARISON.

1. The method suggested in this report for reducing speeds at heights to a standard basis for comparison will be fair if a machine always does the same indicated air speed at the same pressure. This will be the case if

(i) the total drag in lbs. is constant at a constant pressure p, and a constant indicated air speed V_0; and

(ii) the thrust of the airscrew is constant at a constant p and a constant V_0.

As to (ii) we may write for the airscrew $Q/\sigma N^2 = F\left(\frac{V}{N}\right)$. And we may assume the test bed power curve for the engine to be b.h.p. = K.N. (This form of power curve, namely, a straight line through the origin (equivalent to a constant engine torque or constant M.A.P. at all revolutions) appears to hold approximately for all modern engines, so long as the engine is not over-revved.) Further, let the law for variation of power with height be that the power varies with $f(p)$—any given function of pressure only. Then the torque Q of the airscrew $= \lambda \frac{B_N f(p)}{N} = \lambda K f(p)$ = constant for constant p. Therefore, from the equation

$$\frac{Q}{\sigma N^2} = F\left(\frac{V}{N}\right),\ \sigma N^2 F\left(\frac{V}{N}\right) = \text{constant at constant } p,$$

that is to say,

$$F\left(\frac{V}{N}\right) \times \frac{N^2}{V^2} = \frac{\text{constant}}{\sigma V^2} = \frac{\text{constant}}{V_0^2}$$

$$= \text{constant at constant } p \text{ and constant } V_0.$$

Hence at constant p and V_0, $\frac{V}{N}$ is constant. Now $\frac{\text{thrust}}{V_0^2}$ is a function of $\frac{V}{N}$ and is therefore also constant at constant p and V_0; hence, so also is the thrust.

As to (i) the total drag at an indicated speed V_0 is equal to

$$\left[\frac{r_1 + r_2 R/R_0}{10^4} + K_d A\ (\cdot 0051)\right] V_0^2$$

where K_d is the drag coefficient of the wings = constant for a constant V_0.

A is the wing area
r_1 is the resistance at 100 m.p.h. out of the slipstream
r_2 is the resistance at 100 m.p.h. in the slipstream
R/R_0 is the slipstream factor for resistance
} (constants).

Now R/R_0 is a function of V/N, for R/R_0 is equal to $\frac{(v_0 + V_0)^2}{V_0^2}$ (where $v_0 + V_0$ is the indicated air speed in the slipstream) $= \frac{v_0(v_0+V_0)}{V_0^2} + \frac{(v_0+V_0)}{V_0}$

The former term is, from considerations of momentum $= \frac{\text{thrust}}{V_0^2} \times a$

constant depending only on the area of the slipstream, and is therefore a function of V/N; the latter term is $\sqrt{R/R_0}$. Hence, $R/R_0 =$ a function of $V/N + \sqrt{R/R_0}$. Hence, R/R_0 is a function of V/N, and therefore constant at a constant p and V_0. Thus the total drag is constant at a constant p and V_0.

2. The method suggested for reducing climbs will be fair if the rate of climb at a given p and V_0 (V_0 being the best climbing speed) for any machine is proportional only to $\frac{1}{\sigma^{\frac{1}{2}}}$. It has been proved that at a constant p and V_0 the thrust of the engine, and the total drag, are constant. Now, if α be the angle of the flight path to the horizontal, and W the weight of the machine,

$$W \sin \alpha = \text{engine thrust} - \text{total drag.}$$

Hence, $\sin \alpha =$ constant at constant p and V_0. Now $\sin \alpha = \frac{\text{rate of climb in ft./min.}}{88 \times V \text{ in m.p.h.}}$, and is therefore proportional to (rate of climb) $\times \sigma^{-\frac{1}{2}}$ at a constant V_0. Hence, at a constant p and V_0, rate of climb is proportional to $\sigma^{-\frac{1}{2}}$.

3. *Note on generality of this method.*—This argument is perfectly general. If the b.h.p. is a function only of any other variable or combination of variables φ, "p" may be replaced in the above equation by "φ"; the rate of climb at a constant φ and V_0 is then proportional to $\sigma^{-\frac{1}{2}}$, and the same holds for speeds, *i.e.*, the aeroplane will do the same indicated speed at the same value of φ.

End of Vol. II.

INDEX TO VOLUME II.

Page

Accelerometer, Description of 630

Aerofoils for Airscrew Design 277

Aeroplanes :—

Banking—Rate of Bank and Force on Control Column 697

Body Moment 664, 668, 673

Body and Airscrew, Mutual Interference of ... 340, 349, 363, 376

Centre of Gravity, Effect of changing position of 642

Best position of 645

Climbing—

Best Speed and Rate of 623

Calculations for Predicting 576, 603

Centre of Gravity, Effect of position of 644

Rate of, Effect of a Wind Gradient 714

Stresses in the Airscrew during 453

Controllability, Criteria for 625

Design—

Effect of Small Changes in 576

For Use at Great Heights 621

Diving 710, 712

Elevators of Different Sizes, Full Scale Experiments with ... 689

Equilibrium, Equations of 584

Flap Angle and Force on Control Column, Relation between ... 699

Flap Angle and Movement of Control Column, Relation between 696

Flap Settings 664

Flaps, Efficiency of 697, 701, 703, 705

Lateral Control of Various Types 701

Lateral Control with Different Types of Wing Flaps 695

Lift and Drag of Full Scale Aeroplane, Method of Obtaining ... 539

Longitudinal Control 642

Longitudinal Oscillation 646, 652

Measurement of Accelerations on Aeroplanes in Flight 629

Model Tests and Full Scale Performance, Relation between ... 535

Performance, Prediction and Analysis of 576, 592

Phugoid Oscillation, Period of 584

Power Unit Weight 731

Prediction of the Performance and Longitudinal Stability of, including the Estimation of the effect of Small Changes in the Design 576

Page

Aeroplanes—*contd.*

Pressure Distribution round Sections of Top and Bottom Wings of an Aeroplane in Flight 542

Pusher Machine—
Rotation of a Propeller, Slipstream in 344
Slipstream, Velocity in 303, 308, 337
S.E.5, Terminal Velocity of 712
Speed in Level Flight, Method of Predicting 581
Spinning, Experimental and Mathematical Investigation of ... 716
Stability. *See that Title.*
Stresses when Diving Steeply 710
Tail Area, Effect of Change of 642
Best Size of... 645

Tail Plane—
Experiments with Different Shapes of 653
Tail-setting, Effect of Change of 642, 644

Tractor Machine—
Airspeed in the Slipstream of 327
Fairing of Nose of Body, Effect on Mutual Interference of Airscrew and Body 363
Mutual Interference of Airscrew and Body 340
Mutual Interference of an Airscrew and a Tractor Body, as affected by the Fairing of the Nose of the Body 363
Mutual Interference of the Airscrew, Body, and Wings of the Tractor Aeroplane B.E.2E 349
Weight, How made up 730
Wing Flaps—Lateral Control with Different Types of 695

Air :—
Density Curve (with Variation of Height) 590

Airscrews :—
Aerofoil Theory, Application of 401
Aerofoils Suitable for Airscrew Design 277
Body of Aeroplane and Airscrew, Mutual Interference of 340, 349, 363, 376

Blades—
Shape of 471
Twisting of 484, 506
Stresses in 471
Burst, Effects of 481
Cracks and other Defects, Effects of 480
Damping of Torsional Vibrations 512
Diameter, Effect of 388

Page

Airscrews—*contd.*

Efficiency of—

Dependence on the Speed of Rotation and the Diameter, with Special Reference to the Question of Engine Gearing ... 388
Effect of the Inflowing Velocity of the Air 400
Energy Account, Analysis of 414
Flow in the Neighbourhood of 296
Increase of Stiffness due to Taper, Method of finding 497
Laminations, Shape of 478
Material of Individual Blades, Effect of Elastic Heterogeneity in 479
Model of Small Diameter—" Scale Speed " Effect on 530
Modulus of the Timber, Effect of Variations in 478
Momentum Theory, Application of 402
Pitch, Change of, Effect of 623
Stresses, Working 440
Tandem Combination 414
Airscrews Rotated in Opposite Directions, Effect of 425
Experiments with 409
Large Machines, Use on 400
Thrust and Torque Co-efficients, Formula for 617
Tilt, Effect of, on Performance 482
Timber, Nature of 481
Torsion of Blades of Uniform Thickness 500

Torsion Curves—

B.E.2c (Thrust Meter) 501, 502
F.E.2d 504, 560
S.E.5 ... ...502, 503
Walnut Plank of Variable Thickness 501

Variable Pitch, Experiments with 515, 518
Vibration Frequencies 483
Vibration Periods 480
Whirling and Transverse Vibrations of an Airscrew and its Shaft 458

Airspeed in the Slipstream of a Tractor Machine 327

Bairstow, L., and Lieutenant J. D. Coales :—

Notes on the Prediction and Analysis of Aeroplane Performance 592

B.E.2c. :—

Airspeed in the Slipstream of 327
Analysis of Forces on Complete Model of 550

Page

B.E.2E.—Mutual Interference of the Airscrew, Body and Wings ... 349

Betts, Miss A. D.—Airscrews, Formulæ for the Thrust and Torque Co-efficients of 617

Biplanes :—
Downwash behind 636
Pitching Moment, Full Scale Determination of 657
B.R.1 Windage, Experiments on 376

Climbing Rate of an Aeroplane :—
Effect of a Wind Gradient 714

Coales, Lieutenant J. D., and L. Bairstow :—
Notes on the Prediction and Analysis of Aeroplane Performance 592

Collins, H. E., and A. Fage :—
Airscrews—
Dependence of the Efficiency of an Airscrew on the Speed of Rotation and the Diameter, with a Direct Reference to the Question of Engine Gearing 388
Model of Small Diameter, " Scale Speed," Effect on 530
Tandem Combinations, Experiments with 409
Working Stresses 440
Helicopters, Experiments on 520
Mutual Interference of an Airscrew and Body of the Tractor Type of Aeroplane 340
Mutual Interference of the Airscrew, Body and Wings of the Tractor Aeroplane, B.E.2E. 349
Mutual Interference of an Airscrew and a Tractor Body, as affected by the Fairing of the Nose of the Body 363
Windage Experiments with a Model of the Rotary Engine, B.R.1 376

Controls. *See* Aeroplane, etc.

Cowley, W. L., and H. Levy :—
Aerofoils for Airscrew Designs 277

Density of Air, Table of Variation of, with Height 590

Downwash :—
Angle of 657, 707
Determination of 706
Behind a Biplane 636

Drag and Lift of Full Scale Aeroplane, Method of obtaining ... 539

Elevators of Different Sizes, Full Scale, Experiments with ... 689

Page

Engines :—
Blowers, Effect of 732
B.R.1, Windage Experiments with a Model of 376
Data, Object of Tabulating 731
Dissipation of Heat from the Surface of an Air-cooled Engine when Running and when at Rest 734
Distribution of Temperature in the Gills of the Engine Cylinder 744
" Dry weight " 730
Hispano High Compression, Variation of Power with Height ... 751
Hispano 150 h.p. Ungeared, Variation of Power with Height ... 752
Power Unit Weight 731
R.A.F. 1A, Tests with 753
R.A.F. 4D, Variation of Power with Height 750
Rolls-Royce 250 h.p., Tests with 752
Variation of Power with Height 607, 748
Analysis of Method of Reducing Experiments 758
Reduction of Performance to a Standard Basis for comparison 761

Fage, A., Airscrews :—
Effect of the Inflowing Velocity of the Air on the Efficiency of, with a Special Reference to the case of Tandem Airscrews of Large Machines 400
Energy Account, Analysis of 414

Fage, A., and H. E. Collins :—

Airscrews—
Dependence of the Efficiency of an Airscrew on the Speed of Rotation and the Diameter, with a Direct Reference to the Question of Engine Gearing 388
Model of Small Diameter, " Scale Speed," Effect on 530
Tandem Combinations, Experiments with 409
Whirling and Transverse Vibrations of a Rotating Airscrew and its Shaft 458
Working Stresses 440
Helicopters, Experiments on 520
Mutual Interference of an Airscrew and Body of the Tractor Type of Aeroplane 340
Mutual Interference of the Airscrew, Body and Wings of the Tractor Aeroplane, B.E.2E 349
Mutual Interference of an Airscrew and a Tractor Body, as affected by the Fairing of the Nose of the Body 363
Windage Experiments with a Model of the Rotary Engine B.R.1. 376

Fairing of the Nose of a Tractor Body, Effect on Mutual Interference of Airscrew and Body 363

Page

F.E.9, Rotation of a Propeller in 334

Flaps. *See* Aeroplane.

Full Scale Experiments with Elevators of Different Sizes 689

Full Scale Stability Experiments with R.A.F. 14 Wing Section ... 706

Gates, S. B.—Full Scale Determination of the Pitching Moment of a Biplane 657

Gates, S. B., and H. Glauert.—Prediction of the Performance and Longitudinal Stability of an Aeroplane, including the Estimation of the effect of Small Changes in the Design 576

Glauert, H. :—
Full Scale Experiments with Different Shapes of Tail Plane ... 653
Full Scale Experiments with Elevators of Different Sizes ... 689
Lateral Control with Different Types of Wing Flaps 695
Longitudinal Control of an Aeroplane 642

Glauert, H., and S. B. Gates.—Prediction of the Performance and Longitudinal Stability of an Aeroplane, including the Estimation of the effect of Small Changes in the Design 576

Glauert, H., F. A. Lindemann, and R. G. Harris.—Spinning, Experimental and Mathematical Investigation of 716

Glauert, H., C. G. D. Sandison, and J. H. Jones.—Investigation of the Downwash behind a Biplane 636

Griffith, A. A., and B. Hague :—
Propeller Blades, Shape of 472
Twisting of 484, 506

Griffiths, E., T. E. Stanton, and Miss Dorothy Marshall.—Dissipation of Heat from the Surface of an Air-cooled Engine when Running and when at Rest 734

Hague, B., and A. A. Griffith :—
Propeller Blades, Shape of 471
Twisting of 484, 506

Harris, R. G.—Forces on a Propeller due to Sideslip 430

Harris, R. G., F. A. Lindemann, and H. Glauert.—Spinning, Experimental and Mathematical Investigation of 716

Heat, Dissipation of, from the Surface of an Air-cooled Engine when Running and when at Rest 734

Height :—
Design of Aeroplanes for Use at Great Heights 621
Variation of Engine Power with Height 747

Page

Height—*contd.*
Analysis of Method of Reducing Experiments ... 758
Reduction of Performance to a Standard Basis for comparison 761

Helicopters, Experiments on 520

Hispano Engine, Experiments on 751

Inflow Velocity of Airscrew. *See* Airscrew.

Instruments.—Accelerometer 630

Interference :—
Mutual Interference of an Airscrew and Body of the Tractor Type of Aeroplane 340
Mutual Interference of the Airscrew, Body and Wings of the Tractor Aeroplane, B.E.2E 349
Rear Airscrew of a Tandem Combination, Interference of, on the Performance of the Forward Airscrew 414

Jones, J. H., C. G. D. Sandison, and H. Glauert.—Investigation of the Downwash behind a Biplane 639

Jones, R., and J. R. Pannell.—Flow in the Neighbourhood of an Airscrew 296

Jones, R., E. F. Relf, and T. Lavender.—Pressure Plotting on Wings of Biplanes 565

Lateral Control of Aeroplane. *See* Aeroplane.

Lavender, T., and E. F. Relf.—Analysis of Forces on B.E.2c, Complete Model 550

Lavender, T., E. F. Relf, and R. Jones.—Pressure Plotting on Wings of Biplanes 565

Levy, H., and W. L. Cowley.—Aerofoils for Airscrew Design ... 277

Lift and Drag of Full Scale Aeroplane, Method of Obtaining ... 539

Lindemann, F. A., H. Glauert, and R. G. Harris.—Spinning, Experimental and Mathematical Investigation of 716

Lindemann, F. A., and G. F. C. Searle.—Measurements of Accelerations on Aeroplanes in Flight 629

Longitudinal Control of Aeroplane. *See* Aeroplane.

Marshall, Miss Dorothy, T. E. Stanton, and E. Griffiths.—Dissipation of Heat from the Surface of an Air-cooled Engine when Running and when at Rest 734

Model Tests of Aeroplanes, Relation between, and the Full Scale Performance 535

O'Gorman, Lieut.-Colonel Mervyn.—The Object of Tabulating Engine Data 731

Page

Pannell, J. R., and R. Jones.—Flow in the Neighbourhood of an Airscrew 296

Performance of Aeroplanes. *See* Aeroplanes.

Pinsent, D. H.—Slipstream Velocity in a Pusher Machine 337

Pinsent, D. H., and H. A. Renwick.—Variation of Engine Power with Height 748

Pitching Moment of a Biplane, Full Scale Determination of ... 657

Pressure Distribution round Sections of the Top and Bottom Wings of an Aeroplane in Flight 542

Pressure Plotting on :—
Lower Wing of a Biplane with B.E.2c Wings 570
Upper and Lower Wings of a Biplane with R.A.F.14 Wings ... 565

Propeller. *See* Airscrew.

R.A.F.1A Engine, Tests with 753

R.A.F.4D Engine, Variation of Power with Height 750

R.A.F. 14 Wing Section, Full Scale Experiments with 706

Relf, E. F., and T. Lavender.—Analysis of Forces on B.E.2c, Complete Model 550

Relf, E. F., R. Jones, and T. Lavender.—Pressure Plotting on Wings of Biplanes 565

Renwick, H. A., and D. H. Pinsent.—Variation of Engine Power with Height 748

Rolls Royce 250 h.p. Engine, Tests with 752

Sandison, C. G. D., H. Glauert, and J. H. Jones.—Investigation of the Downwash behind a Biplane 636

Scale Effect Sub-Committee, Report on the Relation between Model Tests and the Full Scale Performance of Aeroplanes ... 535

"Scale-speed" Effect on Model Airscrew 530, 620

S.E.5, Terminal Velocity of 712

Searle, G. F. C., and F. A. Lindemann.—Measurements of Accelerations on Aeroplanes in Flight 629

Sideslip, Forces on a Propeller due to 430

Slipstreams :—
Airspeed in the Airscrew Slipstream of a Tractor Machine ... 327
Flow in the Neighbourhood of an Airscrew 296
Resistance of Parts in, Formulæ for expressing 595
Rotation of a Propeller Slipstream in a Pusher Aeroplane ... 344
Velocity in a Pusher Machine 303, 337

Page

Spinning, Experimental and Mathematical Investigation of ... 716

Stability of an Aeroplane 624
Full Scale Experiments with R.A.F.14 Wing Section 706
Longitudinal, Estimation of 576

Stanton, T. E., Miss Dorothy Marshall, and E. Griffiths.—Dissipation of Heat from the Surface of an Air-cooled Engine when Running and when at Rest 734

Stevens, H. L., and R. McK. Wood.—Design of Aeroplanes for Use at Great Heights 621

Stresses in an Aeroplane when Diving Steeply 710

Tail plane, Experiments on. *See* Aeroplane.

Tandem Airscrews. *See* Airscrews.

Terminal Velocity of S.E.5 712

Torsion of Airscrew Blades. *See* Airscrews.

Timber.—Equations of Equilibrium of a Thin Plank when slightly deformed by Pressure, Method of finding 496

Vibration of Airscrews. *See* Airscrews.

Wind Gradient, Effect of, on the Rate of Climb of an Aeroplane ... 714

Wing Flaps, Lateral Control with Different Types of 695

Wings, Pressure Distribution round Sections of the Top and Bottom Wings of an Aeroplane in Flight 542

Wood, R. McK., and H. L. Stevens.—Design of Aeroplanes for Use at Great Heights 621

Printed under the authority of His Majesty's Stationery Office
By Sir Joseph Causton & Sons, Limited, 9, Eastcheap, London, E.C. 3.

UNIVERSITY OF ILLINOIS-URBANA
3 0112 078746432